

Proceedings of the 15th International Symposium on District Heating and Cooling

September 4th - 7th, 2016, Seoul, South Korea



*Technology Collaboration Programme on District Heating and Cooling
including Combined Heat and Power*



Copyright

PREFACE

The 15th International Symposium on District Heating and Cooling (DHC) has over the years developed into one of the most well-reputed events world-wide for communication of academic research in the field of DHC. The first Symposium took place in Lund, Sweden in 1987. Since then the Symposium has been arranged consecutively every two years in seven different European countries, but has increasingly drawn delegates from beyond Europe. Now, under the wing of the International Energy Agency's research programme on District Heating and Cooling (IEA-DHC), the Symposium is truly global and the 15th in the sequence took place in Asia for first time.

The International Symposium on DHC has steadily been gaining greater significance particularly in relation to the environmental challenges faced by many countries around the world. In fact, DHC has positioned itself as a vital element of a sustainable energy future. DHC companies have committed themselves to cut greenhouse gas emissions and improve energy efficiency by reducing the use of fossil fuels and increase the use of new and renewable energy resources. In this light, the Executive Committee (ExCo) of IEA-DHC wishes to express their gratitude towards the Korea District Heating Corp. (KDHC) and their partners for taking on the duty to serve as the host of the 15th International Symposium on DHC.

The Symposium gave the DHC-world the opportunity to again experience a showcase of cutting edge technologies on DHC, new developments and best practices available on DHC in different countries. It is clear to the ExCo that KDHC succeeded in making the Symposium into a vibrant hub for communication and networking of DHC experts and scholars from the established and aspiring DHC-countries world-wide.

On behalf of the ExCo and the organizers of The Symposium we want to express our sincere thanks to the members of the Scientific Committee, the Local Organizing Committee and the members of the Advisory Committee for their valuable contribution. We will also thank the individual authors for their contribution with Papers and Posters and the regular participants of The Symposium.

On behalf of the ExCo of IEA-DHC, the Chairman of the Scientific Committee wants to express a special thank to the organizers for an excellent performance of The Symposium.

Rolf ULSETH, Guest Editor

Chairman of the Scientific Committee

(Senior Adviser to IEA-Technology Collaboration Programme on District Heating and Cooling, including Combined Heat and Power)

Kyung Min KIM, Co-Editor

Korea District Heating Corporation

RESEARCH TOPICS

A. Urban energy systems, planning and development

How does city planning influence the development of district heating and cooling systems and vice versa? Papers in this section explore district heating and cooling as a driving force for city planning and development including development of large or regional heat networks.

B. Resource efficiency and environmental performance

How can district heating and cooling contribute to an efficient and low carbon energy supply? Papers in this section will consider performance and environmental issues in district heating and cooling, including the integration of renewables, primary energy savings, reduction of CO₂ emissions, combined heat and power and the use of thermal storage.

C. Key elements in District Heating and Cooling systems

What are the new developments in district heating and cooling technology?

Papers in this section consider steps towards the next generation of district heating and cooling. They focus on improving current district heating and cooling solutions and key elements of the technology: for example piping systems, sub stations and metering techniques. This area includes issues regarding cost reduction, the increase of service life, demand side management and low temperature technologies.

D. Customer relations and market issues

How do customers interact with district energy companies and what is the role of the district energy customers in general? Papers in this area focus on business and infrastructure management and development. A special focus lies on how the challenges for establishing district heating and cooling in an economically viable way can be overcome.

E. Policy and regulation

What policies and regulatory framework can be deployed to assist the establishment and evolution of efficient district heating and cooling networks? How flexible is district heating and cooling to different regulatory environments? What aspects work universally and to what extent do national and regional elements affect the potential of this technology?

F. Open Arena, District Heating and Cooling

What other research can forward the success of district heating and cooling?

In line with the broad and multi-disciplinary approach needed to overcome the sector's challenges, the organizers offer the opportunity to submit abstracts that do not fit into the above categories but still bear relevance for a successful future of district heating and cooling.

COMMITTEES

Scientific Committee

Rolf ULSETH, Chairman, Adviser to IEA DHC Research Programme, NORWAY
Jianjun XIA, Tsinghua University, CHINA
Svend SVENDSEN, Technical University of Denmark, DENMARK
Lars GULLEV, West Copenhagen Heating Transmission Company, DENMARK
Andres Siirde, Tallinn Technical University, ESTONIA
Clemens FELSMANN, Technical University of Dresden, GERMANY
Ólafur Pétur PALSSON, University of Iceland, ICELAND
Yoshiyuki SHIMODA, Osaka University, JAPAN
Kyung Min KIM, Korea District Heating Corp., KOREA
Ki-Un OHN, Soongsil University, KOREA
Hoseon YOO, Soongsil University, KOREA
Natasa Nord, Norwegian University of Science and Technology, NORWAY
Louise TRYGG, Linköping University, SWEDEN
Robin Wiltshire, Building Research Establishment, UNITED KINGDOM

Advisory Committee

Ken CHURCH, Canmet Energy Natural Resources Canada, CANADA
Liu RONG, Beijing District Heating Group, CHINA
Lars GULLEV, West Copenhagen Heating Transmission Company - VEKS, DENMARK
Antti KOHOPÄÄ, Finnish Energy Industries, FINLAND
Carsten MAGASS, Project Management Jülich, GERMANY
Heiko HUTHER, German Efficiency Association for Heating and Cooling, GERMANY
Byung-Hwan UM, Hankyong National University, KOREA
Seung-Hoon YOO, Seoul National University of Science and Technology, KOREA
Jaesung KANG, Korea Energy Economics Institute, KOREA
Yong Hoon IM, Korea Institute of Energy Research, KOREA
Shin Young IM, Korea District Heating Corp., KOREA
Heidi M. JUHLER, Norsk Fjernvarme, NORWAY
Åse MYRINGER, Swedich Energy Research Centre, SWEDEN
Robert P. THORNTON, International District Energy Association, USA

Local Organization Committee

Bongkyung SEO, Korea District Heating Corp., KOREA
Hangjin KIM, Korea District Heating Corp., KOREA
Deogyong AN, Korea District Heating Corp., KOREA
Lee Jin KIM, Korea District Heating Corp., KOREA
Kyung Min KIM, Korea District Heating Corp., KOREA
Choongseek WOO, Korea District Heating and Cooling Association, KOREA

TABLE OF CONTENTS

PREFACE	i
RESEARCH TOPICS	ii
COMMITTEES	iii
TABLE OF CONTENTS	iv
 TOPIC A: URBAN ENERGY SYSTEMS, PLANNING AND DEVELOPMENT	
THE FEASIBILITY ANALYSIS FOR THE CONCEPT OF LOW TEMPERATURE DISTRICT HEATING NETWORK WITH CASCADE UTILIZATION OF HEAT BETWEEN THE NETWORKS	2
<i>M. IMRAN, M. USMAN, Y. H. IM, B.S.PARK</i>	
TECHNOLOGICAL ISSUES TO SUPPLY LOW TEMPERATURE DISTRICT HEATING	8
<i>LI, H., SVENDSEN, S., GUDMUNDSSON, O., KUOSA, M., SCHMIDT, D., KALLERT A.M., PESCH RUBEN, GUNNAR LENNERMO</i>	
EXERGY-BASED ANALYSIS OF RENEWABLE MULTI-GENERATION UNITS FOR SMALL SCALE LOW TEMPERATURE DISTRICT HEATING SUPPLY	13
<i>A. KALLERT, D. SCHMIDT, T. BLAESE</i>	
LOW TEMPERATURE DISTRICT HEATING FOR FUTURE ENERGY SYSTEMS	22
<i>D. SCHMIDT, A. KALLERT, M.BLESL, S. SVENDSEN, H. LI, N. NORD, K. SIPILÄ</i>	
DEVELOPMENT OF AN INNOVATIVE LOW TEMPERATURE HEAT SUPPLY CONCEPT FOR A NEW HOUSING AREA	31
<i>D. SCHMIDT, A. KALLERT, J. OROZALIEV, I. BEST, K. VAJEN, O. REUL, J. BENNEWITZ, P. GERHOLD</i>	
NECESSARY MEASURES TO INCLUDE MORE DISTRIBUTED RENEWABLE ENERGY SOURCES INTO DISTRICT HEATING SYSTEM	37
<i>N. NORD, SCHMIDT, D., KALLERT A.M.</i>	
TRANSITION TO LOW TEMPERATURE DISTRIBUTION IN EXISTING SYSTEMS	45
<i>M. RĂMĂ, K. SIPILÄ</i>	
PRIMARY ENERGY FACTOR FOR DISTRICT HEATING NETWORKS IN EUROPEAN UNION MEMBER STATES.....	52
<i>E.LATŮŠOV, A.VOLKOVA, A.SIIRDE, J. KURNITSKI, M. THALFELDT</i>	
THE ROLE OF DISTRICT HEATING IN ACHIEVING SUSTAINABLE CITIES: COMPARATIVE ANALYSIS OF DIFFERENT HEAT SCENARIOS FOR GENEVA.....	60

ASSESSMENT OF THE THERMAL ENERGY STORAGE IN FRIEDRICHSHAFEN DISTRICT ENERGY SYSTEMS	68
<i>B. REZAIÉ, B.V. REDDY, M.A. ROSEN</i>	
SIMULATION OF A DISTRICT HEATING NETWORK FOR A CASE STUDY IN THE CITY OF VIENNA CONSIDERING ENERGY AND EXERGY LOSSES	79
<i>M. POTENTE, K. PONWEISER</i>	
CHANCES FOR POLISH DISTRICT HEATING SYSTEMS	87
<i>K. WOJDYGA, M. CHORZELSKI</i>	
MAPPING ENERGY AND EXERGY FLOWS OF DISTRICT HEATING IN SWEDEN	96
<i>MEI GONG, SVEN WERNER</i>	
BARRIERS AND ENABLERS FOR EXPANSION OF DISTRICT COOLING IN SWEDEN	103
<i>J. PALM, S. GUSTAFSSON</i>	
THE DEMAND FUNCTION FOR RESIDENTIAL HEAT THROUGH A DISTRICT HEATING SYSTEM AND ITS CONSUMPTION BENEFITS IN KOREA	112
<i>S.-Y. LIM, S.-H. YOO</i>	
PUBLIC PREFERENCES FOR POWER GENERATION SOURCE SWITCH FROM NUCLEAR POWER TO NATURAL GAS-BASED COMBINED HEAT AND POWER WITH A VIEW TO DECENTRALIZED GENERATION.....	119
<i>H.-J. KIM, S.-Y. LIM, S.-H. YOO</i>	
SIMULATION BASED MULTI-CRITERIA EVALUATION OF DESIGN SCENARIOS FOR AN INDUSTRIAL WASTE HEAT BASED MICRO DISTRICT HEATING NETWORK SUPPLYING STANDARD AND LOW-ENERGY BUILDINGS	126
<i>C. MARGUERITE, R.R. SCHMIDT, N. PARDO-GARCIA, R. ABDURAFIKOV</i>	
ECONOMIC OPTIMIZATION OF A COMBINED HEAT AND POWER PLANT: HEAT VS ELECTRICITY	135
<i>F. MARTY, S. SERRA, S. SOCHARD, J.M. RENEAUME</i>	
RISK OF INDUSTRIAL HEAT RECOVERY IN DISTRICT HEATING SYSTEMS.....	144
<i>K. LYGNERUD, S. WERNER</i>	
DISTRICT COOLING – FUTURE DESIGN AND STANDARD	148
<i>JAN H. SÄLLSTRÖM</i>	
INTEGRATION OF SOLAR THERMAL SYSTEMS INTO EXISTING DISTRICT HEATING SYSTEMS.....	155
<i>C. WINTERSCHIED, S. HOLLER, J.-O. DALENBÄCK</i>	
STATUS OF H2020 STORM-PROJECT	161

MEASURED LOAD PROFILES AND HEAT USE FOR "LOW ENERGY BUILDINGS" WITH HEAT SUPPLY FROM DISTRICT HEATING 169

ROLF ULSETH, KAREN BYSKOV LINDBERG, LAURENT GEORGES, MARIA JUSTO ALONSO, ÅMUND UTNE

ENERGETIC AND EXERGETIC PERFORMANCE OF SHORT TERM THERMAL STORAGES IN URBAN DISTRICT HEATING NETWORKS 175

GEORG K. SCHUCHARDT(NÉE BESTRZYNSKI), STEFAN HOLLER

OPERATIONAL DEMAND FORECASTING IN DISTRICT HEATING SYSTEMS USING ENSEMBLES OF ONLINE MACHINE LEARNING ALGORITHMS 187

C. JOHANSSON, M. BERGKVIST, O. DE SOMER, D. GEYSEN, N. LAVESSON, D. VANHOUDT

ESSENTIAL IMPROVEMENTS IN FUTURE DISTRICT HEATING SYSTEMS 194

H. AVERFALK, S. WERNER

SPACE HEATING WITH ULTRA-LOW-TEMPERATURE DISTRICT HEATING – A CASE STUDY OF FOUR SINGLE-FAMILY HOUSES FROM THE 1980S 201

D. ØSTERGAARD, S. SVENDSEN

PERFORMANCE VERIFICATION OF DISTRICT COOLING SYSTEMS COMPARED WITH CONVENTIONAL COOLING SYSTEMS BASED ON MONITORED DATA 210

WENJIE GANG, SHENGWEI WANG, FU XIAO

A MINLP OPTIMIZATION OF THE CONFIGURATION AND THE DESIGN OF A DISTRICT HEATING NETWORK : STUDY CASE ON AN EXISTING SITE 218

T. MERTZ, S. SERRA, A. HENON, J.M. RENEAUME

BOTTLENECKS IN DISTRICT HEATING SYSTEMS AND HOW TO ADDRESS THEM 227

L. BRANGE, J. ENGLUND, K. SERNHED, M. THERN, P. LAUENBURG

ECONOMICALLY OPTIMAL HEAT SUPPLY TO LOW ENERGY BUILDING AREAS 235

AKRAM FAKHRI SANDVALL, ERIK O AHLGREN, TOMAS EKVALL

TECHNO-ECONOMIC ASSESSMENT OF THE IMPACT OF LOW-TEMPERATURE DISTRICT HEATING SUBNETS IN A DISTRICT HEATING NETWORK 244

J. CASTRO FLORES, J. NW. CHIU, B. LACARRIÈRE, V. MARTIN

TOPIC B: RESOURCE EFFICIENCY AND ENVIRONMENTAL PERFORMANCE

LOW-CARBON AND RESILIENT URBAN DISTRICT IMPLEMENTING A SMART ENERGY NETWORK IN THE TAMACHI STATION NORTH-EAST URBAN RENNAISSANCE PROJECT IN TOKYO 255

OSAMU KUNITOMO, MASASHI BANSAI, AKINARI TAKEDA, TOMOMI YAMAMOTO, KENICHI SASAJIMA

ANALYSIS OF THE INFLUENCE ON GREENHOUSE GAS EMISSION REDUCTION POTENTIAL BY DISTRICT ENERGY SUPPLY IN KOREA	264
<i>KYOUNG-A SHIN, JAESUNG KANG, YONGHOON IM, DAHYE KIM</i>	
CONSIDERING INVESTMENT RESOURCES WHEN ASSESSING POTENTIAL CO₂ REDUCTIONS OF CHP – A CASE STUDY	269
<i>L. NORDENSTAM, M. BENNSTAM, L. TRYGG</i>	
HEAT COLLABORATION FOR INCREASED RESOURCE EFFICIENCY: A CASE STUDY BETWEEN A REGIONAL DISTRICT HEATING SYSTEM AND A MINE	279
<i>LOUISE TRYGG, CURT BJÖRK, PETER KARLSSON, MATS RÖNNELID, DANICA DJURIC ILIC</i>	
ENERGY PERFORMANCE OF DECENTRALIZED SOLAR THERMAL FEED-IN TO DISTRICT HEATING NETWORKS.....	283
<i>PILAR MONSALVETE ÁLVAREZ DE URIBARRI, URSULA EICKER, DARREN ROBINSON</i>	
EXERGY ANALYSES ON THE USER-SIDE THERMAL FACILITIES OF KOREAN DISTRICT HEATING SYSTEM.....	291
<i>B.Y. JANG, C. LEE, H.W. PARK, H. KIM, J. Y. YI, J.S. EOM, S. Y. IM</i>	
PREDICTIVE SUPPLY TEMPERATURE OPTIMIZATION OF DISTRICT HEATING NETWORKS USING DELAY DISTRIBUTIONS	295
<i>L. LAAKKONEN, T. KORPELA, J. KAIVOSOJA, M. VILKKO, Y. MAJANNE, M. NURMORANTA</i>	
UTILIZATION OF DISTRICT HEATING NETWORKS TO PROVIDE FLEXIBILITY IN CHP PRODUCTION.....	304
<i>T. KORPELA, J. KAIVOSOJA, Y. MAJANNE, L. LAAKKONEN, M. NURMORANTA, M. VILKKO</i>	
 TOPIC C: KEY ELEMENTS IN DISTRICT HEATING AND COOLING SYSTEMS	
DETERMINATION OF ESSENTIAL PARAMETERS INFLUENCING SERVICE LIFE TIME OF POLYURETHANE INSULATION IN DISTRICT HEATING PIPES	313
<i>NAZDANEH YARAHMADI, ALBERTO VEGA, IGNACY JAKUBOWICZ</i>	
STRATIFICATION IN HOT WATER PIPE-FLOWS	316
<i>DENIS F. HINZ, SIMON GRANER, CHRISTIAN BREITSAMTER</i>	
LONG TERM PERFORMANCE OF VACUUM INSULATION PANELS IN HYBRID INSULATION DISTRICT HEATING PIPES	322
<i>A. BERGE, B. ADL-ZARRABI</i>	
CORROSION BEHAVIOR OF PIPELINE STEEL UNDER DIFFERENT IRON OXIDE DEPOSIT IN THE DISTRICT HEATING SYSTEM	329
<i>Y.-S. KIM, J.-G. KIM, W.-C. KIM</i>	

DEVELOPMENT OF A REINFORCED BEND WITH SHEAR CONTROL RING FOR DISTRICT HEATING	337
<i>JOOYONG KIM, CHONGDU CHO</i>	
ON THE INFLUENCE OF THERMALLY INDUCED RADIAL PIPE EXTENSION ON THE AXIAL FRICTION RESISTANCE	342
<i>T.GERLACH, M. ACHMUS</i>	
SENSITIVITY ANALYSIS ON THE AXIAL SOIL REACTION DUE TO TEMPERATURE INDUCED PIPE MOVEMENTS	352
<i>INGO WEIDLICH</i>	
NON-DESTRUCTIVE METHODS FOR ASSESSMENT OF DISTRICT HEATING PIPES: A PRE STUDY FOR SELECTION OF PROPER METHOD	357
<i>P.LIDÉN, B. ADL-ZARRABI</i>	
ADVANCED MONITORING TECHNOLOGY FOR DISTRICT HEATING PIPELINES USING FIBER OPTIC CABLE	363
<i>SUKYONG SONG, JOOYONG KIM</i>	
RISK MANAGEMENT FOR MAINTENANCE OF DISTRICT HEATING NETWORKS	367
<i>K. SERNHED, M. JÖNSSON</i>	
INTEGRATION OF SOLAR THERMAL SYSTEMS INTO DISTRICT HEATING – DH SYSTEM SIMULATION	376
<i>M. HEYMANN, K. RÜHLING, C. FELSMANN</i>	
COMPARATIVE ANALYSIS BETWEEN DISTRICT AND GEOTHERMAL HEAT PUMP SYSTEM	385
<i>J-S. LEE, H-C. KIM, S-Y. IM</i>	
TREND ANALYSIS TO AUTOMATICALLY IDENTIFY HEAT PROGRAM CHANGES	388
<i>S. ABGHARI, E. G. MARTIN, C. JOHANSSON, N. LAVESSON, H. GRAHN</i>	
A METHOD FOR TAKING INTO ACCOUNT SEASONAL STORAGE IN A DISTRICT ENERGY SYSTEM OPTIMISATION PROBLEM	395
<i>J. ROBINEAU, J. PAGE, F. MARÉCHAL</i>	
HYDRAULIC BALANCING OF DISTRICT HEATING SYSTEMS OPERATED ACCORDING TO A PUSH PRINCIPLE	404
<i>O. GUDMUNDSSON, J.E. THORSEN, C. THYBO</i>	
METHOD FOR ACHIEVING HYDRAULIC BALANCE AND OPTIMIZING INDOOR TEMPERATURE CONTROL IN CHINESE BUILDINGS’ HEATING SYSTEMS	411
<i>LIPENG ZHANG, JIANJUN XIA, ODDGEIR GUDMUNDSSON, JAN ERIC THORSEN, HONGWEI LI, SVEND SVENDSEN</i>	
A SYSTEM PERSPECTIVE ON ALTERED DISTRICT HEATING DEMAND IN MULTIFAMILY BUILDINGS	417

A NEW DH CONTROL ALGORITHM FOR A COMBINED SUPPLY AND FEED-IN SUBSTATION AND TESTING THROUGH HARDWARE-IN-THE-LOOP	422
---	------------

T. ROSEMANN, J. LÖSER, K. RÜHLING

ACHIEVING LOW RETURN TEMPERATURE FOR DOMESTIC HOT WATER PREPARATION BY ULTRA-LOW-TEMPERATURE DISTRICT HEATING.....	429
---	------------

XC. YANG, S. SVENDSEN

REDUCTION OF RETURN TEMPERATURES IN URBAN DISTRICT HEATING SYSTEMS BY THE IMPLEMENTATION OF ENERGY-CASCADES	437
--	------------

M. KÖFINGER, D. BASCIOTTI, R.R. SCHMIDT

INDIVIDUAL APARTMENT SUBSTATION TESTING – DEVELOPMENT OF A TEST AND INITIAL RESULTS	446
--	------------

MARTIN CRANE CENG

AN ON-OFF CONTROL STRATEGY TO REDUCE RETURN WATER TEMPERATURE.....	453
---	------------

YEMAO LI, JIANJUN XIA

TOPIC D: CUSTOMER RELATIONS AND MARKET ISSUES

ASSESING THE FEASIBILITY OF USING THE HEAT DEMAND-OUTDOOR TEMPERATURE FUNCTION FOR A LONG-TERM DISTRICT HEAT DEMAND FORECAST	460
---	------------

I. ANDRIC, A. PINA, P. FERRÃO, J. FOURNIER, B. LACARRIERE, O. LE CORRE

HEAT SOURCE SHIFTING IN BUILDINGS SUPPLIED BY DISTRICT HEATING AND EXHAUST AIR HEAT PUMP	468
---	------------

J. KENSBY, A. TRÜSCHEL, J.O. DALENBÄCK

PRACTICAL AND ACCURATE MEASUREMENT OF COGENERATED POWER	476
--	------------

A. VERBRUGGEN

TOPIC E: POLICY AND REGULATION

THE ROLE OF INTERMEDIARIES IN THE TRANSITION TO DISTRICT HEATING	483
---	------------

R.E. BUSH, C.S.E. BALE

CONSIDERATION OF HIGH EFFICIENT WASTE-TO-ENERGY WITH DISTRICT ENERGY FOR SUSTAINABLE SOLID WASTE MANAGEMENT IN KOREA.....	492
--	------------

GEUN-YONG HAM, DONG-HOON LEE

TOPIC F: OPEN ARENA, DISTRICT HEATING & COOLING

FEASIBILITY STUDY ON THE APPLICATION OF ADSORPTION COOLING TO DHC	500
<i>J.D. CHUNG, H. YOOR</i>	
SERVICE ORIENTED ARCHITECTURE ENABLING THE 4TH GENERATION OF DISTRICT HEATING.....	504
<i>JAN VAN DEVENTER, HASAN DERHAMY, KHALID ATTA, JERKER DELSING</i>	
USING PREDICTIVE ANALYTIC SOFTWARE SOLUTION FOR IDENTIFYING EQUIPMENT FAILURE IN ADVANCE; THE UNIVERSITY OF TEXAS AT AUSTIN.....	512
<i>A. ROBERTO DEL REAL, B. HO JOON SEO</i>	
THE INVESTIGATION OF FAILURE RATE REDUCTION IN HEAT METERS FOR DISTRICT HEATING.....	516
<i>W. KANG, H-M. CHOI, Y-M. CHOI, C-Y. KIM, J-S. LEE, S-Y. LIM</i>	
EFFICIENCY OF STRAINERS.....	520
<i>D. WALDOW, G. WALDOW</i>	
THE EFFECT OF CALCIUM CARBONATE FOULING IN PLATE HEAT EXCHANGERS FOR DISTRICT HEATING AND COOLING.....	525
<i>K.S. SONG, C.H. BAEK, S.K. CHOI, Y.C. KIM</i>	
REMOVAL OF INORGANIC FOULING USING ULTRASONIC AND HYDRODYNAMIC CAVITATION.....	531
<i>KYOUNG HO HAN, KWANGKEUN CHOI, DEOK-YONG AHN, KYUNG MIN KIM, DO YOUNG YOON</i>	

TOPIC A:

Urban Energy Systems, Planning and Development



THE FEASIBILITY ANALYSIS FOR THE CONCEPT OF LOW TEMPERATURE DISTRICT HEATING NETWORK WITH CASCADE UTILIZATION OF HEAT BETWEEN THE NETWORKS

M. Imran^{1,2}, M. Usman^{1,2}, Y. H. Im¹, B.S.Park¹

¹Korea Institute of Energy Research (KIER), 152 Gajeong-ro, Yuseong-gu, Daejeon (34129), South Korea

²Korea University of Science & Technology, 217 Gajeong-ro, Yuseong-gu, Daejeon (34113), South Korea

Keywords: Low temperature district heating, heat pump, cascade heat utilization

ABSTRACT

Recently, low temperature district heating networks (LTDH) have received attention in district heating and cooling market due to their benefits in terms of efficiency, greenhouse gas reduction, flexibility to use renewable energy sources and economic benefits. In this work, physical and techno-economical aspects of the new concept of cascade types with high temperature district heating (HTDH) return is utilized to supply heat at low temperature networks. The HTDH return water temperature is around 45°C and supply of LTDH can be set around 60°C. The return water temperature of HTDH return line at 45°C can be raised to 60°C with the help of heat pump. A detailed study of major components, network design, pressure drop, heat loss and power consumption was performed to formulate an annual, hourly, based energy simulation to assess the techno-economic feasibility of the systems for different types of customers (residential & commercial) The economics were also analysed in terms of internal rate of return (IRR) and the results show that IRR for residential buildings varies from 14 ~ 17%. In order for the successful realization of the proposed system in the market new sustainable systems encouragement in government level is desired to be provided in the form of renewable energy target/certificates or CO₂ reduction incentives especially at the initial stage of the commercialization of the model

INTRODUCTION

District Heating (DH) is concerned with centralized production of heat and electrical power and its distribution in such efficient way that the production and maintenance cost incurred is lower than individual production of end user [1]. District heating network has evolved over time in terms of its supply temperature and efficiency. Fig 1 presents the evolution and enhancement of efficiency of DH network with respect to the supply temperature. It is evident that the low temperature district heating networks are the best in term of efficiency and will be sustainable alternative in future of DH technology.

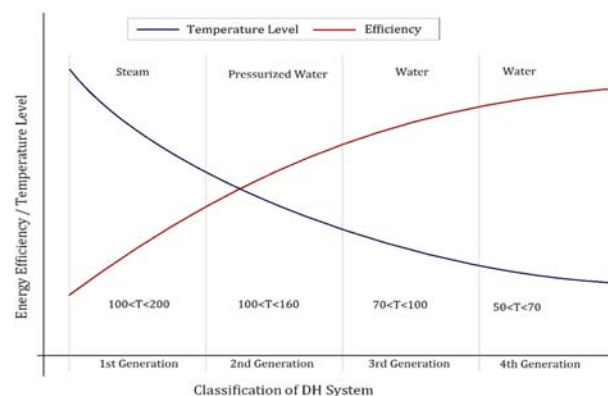


Fig. 1 Classification of DH system based on temperature

The advantages of low temperature district heating include the following

- Reduced Network heat loss
Decreasing the temperature of supply reduce the overall mean temperature difference between pipelines and ambient and thus heat loss is reduced without changing the insulation.
- Reduced Pipeline Thermal stress
Using lower supply temperature, there will be less variation in supply temperature along the pipeline. The reduced risk of pipe leakages due to thermal stress and maintenance cost will be reduced. Furthermore, different material can be considered as candidates instead of steel or copper as in HTDH.
- Reduced Risk of boiling
The Lower supply temperature reduces the risk of boiling as fluid temperature is far from saturation temperature.
- Renewable/Multiple heat source
With reduced temperatures, it is not necessary to always use high exergy heat source. Renewable or multiple heat sources can also be used with ease.
- Greater utilization of thermal storage units

Utilization of thermal storage units allow to handle the peak loads without greatly oversizing equipment and so reduce investment costs.

- Improved power to heat ratio in steam CHP system

The efficiency of CHP unit is dependent on the condensing temperature of CHP unit. Low network supply and return temperature allow more power to be extracted from steam turbines. The reduction of the electricity output can be defined by z-factor as (1):

$$Z = \frac{E_{\text{electricity,loss}}}{E_{\text{electricity,produced}}} \quad (1)$$

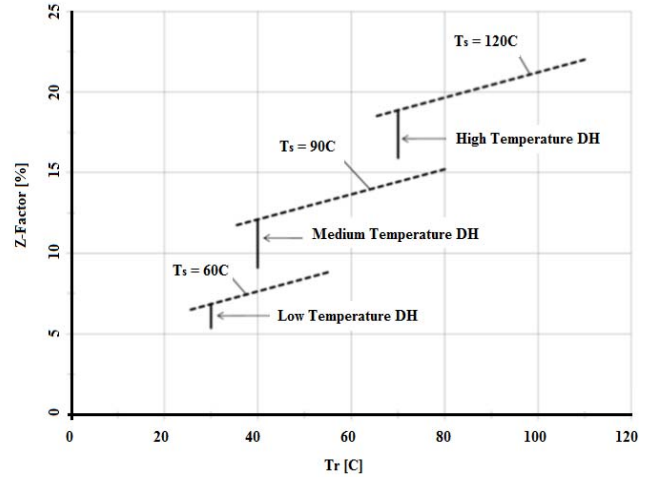


Fig. 2 Z-factor in an extraction-condensing turbine for CHP as function of DH temperature [2]

Table 1 Practical application of LTDH

Name	Year	Supply Temp.	Return Temp.	Outdoor Temp.	Heat Supplied	Heat Sold	Heat Loss
		C	C	C	GJ	GJ	GJ
Kirsehir, Turkey	1995	57	38	11	39,312	33,572	5,739
Lystrup, Denmark	2009	52	34	8	986	790	196
Okotoks, Canada	2007	39	31	4	2,705	2,564	141
Halmstad, Sweden	2010	70	38	7	920	809	111
Falkenberg, Sweden	2010	78	44	7	1,374	1,252	122
Munich, Germany	2006	59	33	10	6,534	6,379	155
Slough, UK	2010	51	34	11	178	129	49
Høje Taastrup, Denmark	2013	70	40	9	1,978	1,715	263

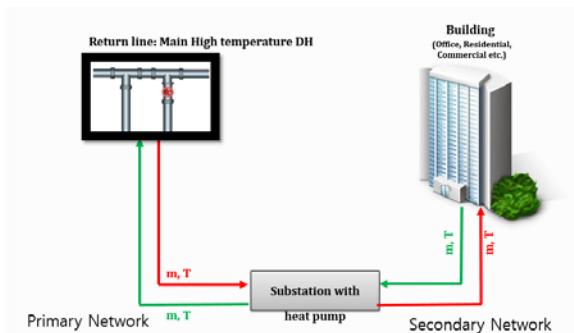


Fig 3. Utilization of HTDH return in LTDH using heat pump

Table 1 presents the practical demonstration of low temperature district heating networks. It can be believed that LTDH systems can be implemented with reliability and will be sustainable solution of future DH systems.

HTDH return cascade utilization in LTDH

Fig 3. represents the scheme where an already high temperature district heat network is operational and the return water temperature of HTDH is sent to a substation where the temperature is boosted up to 60 °C. by the utilization of heat pump.

The heating load profiles were generated by estimating the heating load for the apartment complex type of

building in Seoul. The number of houses per floor were 4 and total of 15 floors per apartment were considered. The supply and return water temperatures were kept at 60°C & 30°C, respectively. Fig 4 presents the layout of the considered building type.

Heat loss model

Heat loss in piping is considered in two parts, building pipe heat loss & underground pipe heat loss.

$$\text{Pipe Heat Loss} = Q_{\text{loss}} = UA_{p,s}(T_f - T_a) = UA_{p,s}\Delta T \quad (2)$$

$$\text{Pipe Surface Area} = A_{p,s} = 2\pi D_4 L \quad (3)$$

$$U = \frac{1}{R}; R = \frac{1}{h_t} + \frac{r_4 \ln \frac{r_4}{r_3}}{k_p} + \frac{r_4 \ln \frac{r_4}{r_2}}{k_p} + \frac{r_4 \ln \frac{r_4}{r_1}}{k_t} + \frac{r_4 \ln \frac{r_4}{r_0}}{k_c} + \frac{1}{h_o} \quad (4)$$

$$h_t = \frac{k_p}{D_1} \times 0.023 Re^{0.8} Pr^{0.4} \quad (5)$$

$$h_o = 13.79 + 0.03232\Delta T - 40.86D_4 + 0.000117\Delta T^2 + 97.3D_4^2 - 0.01388\Delta T D_4 \quad (6)$$

Table 2. Parameter of pipe material used in model

Pipes	Density [kg/m ³]	Thermal conductivity [W/mK]	Thermal capacity [kJ/kg.K]
Carrier pipe	940	0.38	2.31
Insulation	60	0.0237	1.21
Outer pipe	918	0.33	2.31

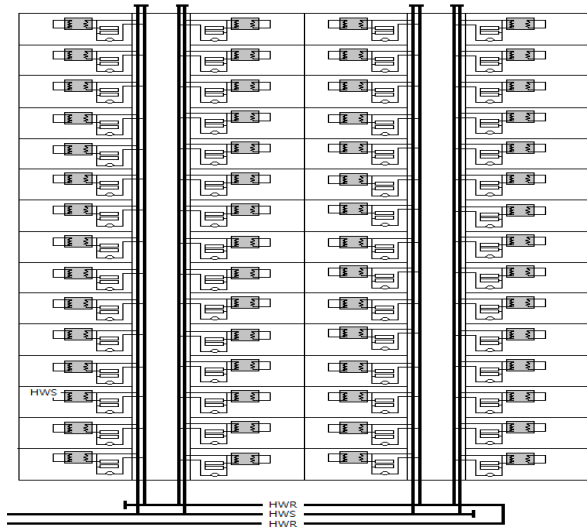


Fig 4. Layout of piping in building

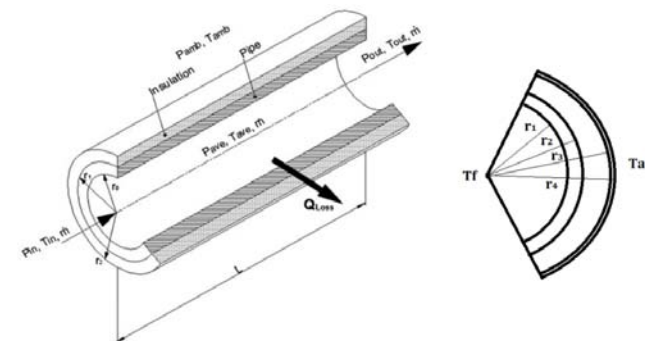


Figure 5. Layout of pipe and insulation layer

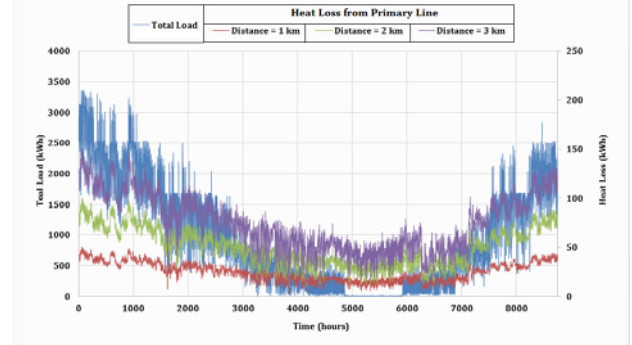


Fig. 6 Annual heat loss & total load profile of LTDH with respect to distance from HTDH network

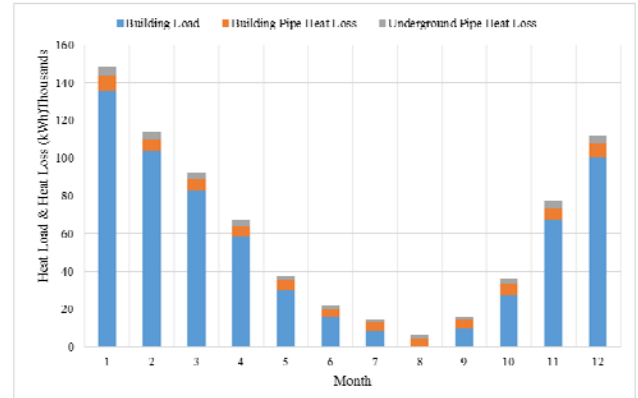


Fig. 7 Component of heat loss with respect to total load

The heat loss model formulated using equations (2)~(6) and the material and parameters used in modelling are presented in Table 2. Fig 5 presents the layout of piping scheme.

Fig. 6 presents the heat loss in terms of load if LTDH supported apartment is at 1km, 2km and 3km distance from HTDH network. The respective total heat load is also presented in Fig.6.

Fig. 7 presents the heat component of heat loss with respect to total load for every month of the year.

Heat pump model

The heat pump performance data of commercial heat pumps is used to develop an empirical correlation of COP of heat pump using regression analysis and can be reposted as eq. (7) & (8).

$$P_{\text{est}} = \frac{Q}{\text{COP}(T_{\text{e,t}}, T_{\text{c,o}}, m_{\text{c}}, m_{\text{e}})} \quad (7)$$

$$\text{COP} = C_1 T_{\text{e,t}} + C_2 T_{\text{c,o}} + C_3 T_{\text{e,t}}^2 + C_4 T_{\text{c,o}}^2 + C_5 T_{\text{e,t}} T_{\text{c,o}} + C_6 m_{\text{c}} + C_7 m_{\text{c}}^2 + C_8 m_{\text{c}} m_{\text{e}} + C_9 m_{\text{e}} + C_{10} m_{\text{e}}^2 \quad (8)$$

The coefficients of used in prediction of equation (8) are presented in table 3.

Table 3. Coefficient of regression equation

C1	0.06233097	C6	3.20265706
C2	-0.14968569	C7	-0.23095988
C3	-0.00080224	C8	0.001611807
C4	0.000555618	C9	0.069420396
C5	0.000160963	C10	-0.00442447

Economic Analysis

The project economic feasibility was assessed by considering the capital costs of equipment and electricity billing. Following assumptions were made for the analysis:

- Project life is 30 years
- Inflation rate is 5%
- Two pipe system has been selected for secondary network
- Distance of substation is 3km
- Price of pipes, heat and labor expense is based on local market of Korea

The capital investment cost includes the cost of DH pipe network, heat pump and network connection, labor and materials. The capital cost of the primary side pipe network is based on the local Korean market and the table 4 and 5 present the cost estimation of primary side and secondary side pipe.

Table 4. Capital cost of pipe for primary pipe network [3]

Type	Pipe Standard	Price ₩/m	Carrier Pipe		Insulation	Casing Pipe	
			Inner mm	Outer mm	Thickness mm	Thickness mm	Outer Dia. mm
PEX	150A	253300	154.2	165.2	38.4	4	250
	125A	163800	129.6	139.6	39.1	3.5	225
	100A	124000	104.5	114.3	39.4	3.5	200
	80A	103200	80.1	89.1	32.2	3.2	160
	65A	84300	67.3	76.3	28.7	3.2	140
	50A	67600	52.7	60.5	29.1	3.2	125
	40A	49200	41.2	48.6	27.7	3	110
	32A	38300	35.5	42.7	30.7	3	110
	25A	32990	27.2	34	25.5	2.5	90
	20A	29600	21.4	27.2	28.9	2.5	90

Table 5. Capital cost of pipe for secondary pipe network

Type	Pipe Standard	Price ₩/m	Carrier Pipe		Insulation	Casing Pipe	
			Inner mm	Outer mm	Thickness mm	Thickness mm	Outer Dia. mm
STS (SCH 10)	100A	83780	114.3	108.2	50	0	158.2
	80A	67730	89.1	83	50	0	133
	65A	51550	76.3	70.2	50	0	120.2
	50A	46040	60.5	54.9	50	0	104.9
	40A	41220	46.8	41.2	50	0	91.2
	32A	36400	42.7	37.1	50	0	87.1
	25A	32250	34	28.4	50	0	78.4
	20A	29600	27.2	23	50	0	73

The different cost quotations have been obtained and an average cost has been chosen for heat pump based on its capacity in kW.

Cost of Heat Pump = 450 \$/kW

This cost is based on the price quotations that are valid for heat pump size of 30kW to 300kW.

For comparison purpose of the LTDH with gas heating, an average price of condensing gas boiler for single family unit is also considered. The considered cost of condensing boiler is \$1200 with 90% efficiency and operating cost of 21₩/MJ.

The operating cost of the low temperature districting heating is the cost of heat supplied and heat loss, pumping power cost, and the electricity cost utilized by heat pump. For the simplification, a flat rate of 83.5 ₩/MCal has been used in the present simulation. The cost of heat loss is also based on this flat rate.

The cost of electricity is presented in table 6 as under.

Table 6. Electricity price for industrial usage

Energy charge (₩/kW)			
Time Period	Summer	Spring/Fall	Winter
Off-Peak	55.2	55.2	62.5
Mid-Peak	108.4	77.3	108.6
On-Peak	178.7	101.0	155.5

The pipe sizing for secondary network is presented in the table 7 below.

Table 7. Pipe sizing for secondary network

Pipe Description		Standard	Length (m)	
Underground	Supply	80A	160	
	Return	80A	160	
Basement	Supply	80A	42.6	
	Return	80A	85	
Vertical	Supply	1-2 Floor	65 A	5.6
		3-8 Floor	50A	16.8
		9-11 Floor	40A	8.3
		12-15 Floor	32A	11.1
	Return	1-2 Floor	65 A	5.6
		3-8 Floor	50A	16.8
		9-11 Floor	40A	8.3
		12-15 Floor	32A	11.1

The pumping power was estimated by calculating the pressure drop in the piping network. The distribution piping accessories like elbow and tee were considered to calculate the pressure drop. The pump performance curves were used to calculate the electric power requirement against the required mass flow rate and pressure drop.

The flat rate for heating is provided in section before. The same rate is considered for billing from the consumer. The capital costs, operating costs and inflation factors are summed and balanced against the incomes generated from the consumer to find the payback period which is given in Eq. 9 below.

$$\text{Payback Period} = (\text{Cost of the investment} + \text{annual operating costs}) / (\text{Annual net cash flow}) \quad \text{Eq. 8}$$

Similarly, internal rate of return was calculated by considering the mentioned 30 years of system operation and summation of incomes and expenses generated monthly.

The particulars of simulation scenarios considered in economic analysis are presented in table 4.

Table 8. Simulation Scenario for economic analysis

Case	Primary Network		Secondary Network		Heat Pump
	Heat Loss	Pumping Power	Heat Loss	Pumping Power	Electric Power
1	Included	Included	Included	Included	Included
2	Not Included	Included	Included	Included	Included
3	Included	Included	Not Included	Included	Included
4	Not Included	Included	Not Included	Included	Included

RESULTS & DISCUSSION

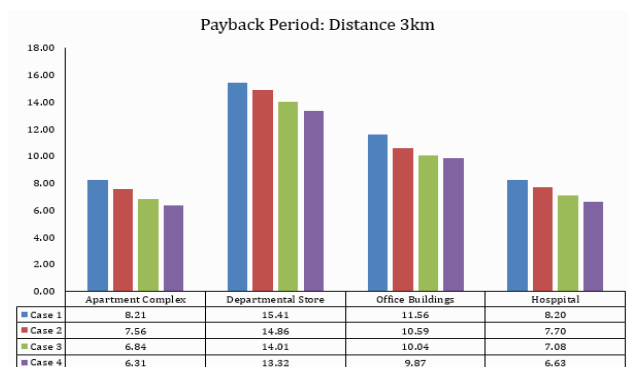


Figure 8. Payback period of system for the mentioned scenarios and type of building

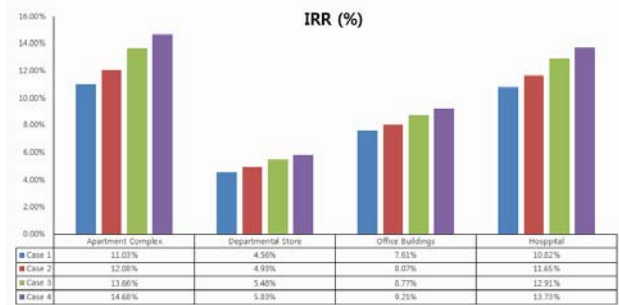


Figure 9. Internal Rate of Return of system for the mentioned scenarios and type of building

Fig 8. Presents the payback period for the system with various simulation scenarios and types of buildings. It can be observed that the payback for residential buildings is less than the other types. The major reasons is load demand. Fig 9 represents the internal rate of return and again apartment complex and hospital type buildings are suitable choices but departmental stores yield smaller IRR due to their smaller load demand. The concept of heat pump and low temperature network integration has mature technology and market. The network design for low temperature district heating have been already successfully implemented in EU.

The economic analysis of different buildings shows that economic feasibility is very high for high heat density buildings [ration of heat supplied to land area], for example apartment complex and office buildings. The fluctuation of the building heat load results in lower COP and higher electric power consumption. Therefore, buildings with high heat density and low load fluctuation are favorable for low temperature district heating.

The rate of return of residential building varies from 5~6 years, for office 9~10 years, for hospital 5~7 years, and for departmental store 12~ 14 years depending on various cases considered in economic analysis. The internal rate of return varies from 11~15% for residential building, 5~6% for departmental store, 8~10% for office building, 13~15% for hospital. Decrease of return temperature from 45C~30C results in double saving of electric power per kW of heat production. Similarly 37% reduction in heat loss, supply T reduced 90 to 60C. These benefits will definitely double the economic benefits and profit for low temperature district heating.

CONCLUSION

In this study, the concept of cascade utilization of surplus energy in district heating network is newly suggested by utilizing the return water of HTDH as a heat source for LTDH and its feasibility is assessed for different types of buildings. Especially this cascade

types of LTDH model is believed to be more favorable to propagating it into the market against the existing LTDH, i.e. isolated low temperature district heating or converting the existing HTDH model to LTDH one. The economic analysis for different types of buildings shows that economic feasibility is very high for high heat density buildings, for example apartment complex and office buildings. It is also shown that the fluctuation of the building heat load results in lower COP of the heat pump and higher electric power consumption. Consequently negative effect on techno-economic benefits of the model. Therefore, buildings with high heat density and low load fluctuation seems to be very appropriate conditions for creating new customer in the vicinity of the HTDH network. In this work, the applicability and feasibility of the model is carried out from the view point of expanding the existing DH network to a neighboring building. In forthcoming study, the feasibility analysis between the thermal networks,

i.e. to build complex connected by the low supplying temperature network, will be carried out and its result will be presented.

ACKNOWLEDGEMENT

This paper covers a topic from IEA DHC Annex TS1

REFERENCES

- [1] Bordin C, Gordini A, Vigo D. An optimization approach for district heating strategic network design. *Eur J Oper Res* 2016;252:296–307. doi:10.1016/j.ejor.2015.12.049.
- [2] Dalla Rosa A. The development of a new district heating concept 2012;R-269:238.
- [3] <http://www.pipeteckorea.co.kr/> [Feb 2015]

TECHNOLOGICAL ISSUES TO SUPPLY LOW TEMPERATURE DISTRICT HEATING

Li, H. ¹, Svendsen, S. ¹, Gudmundsson, O. ², Kuosa, M. ³, Schmidt, D. ⁴, Kallert A.M. ⁴, Pesch Ruben ⁵, Gunnar Lennermo ⁶

¹ Building Energy Section, Department of Civil Engineering

Technical University of Denmark, 2800 Kgs. Lyngby, Denmark

² Heating segment, Application Center, Danfoss A/S, Nordbrg, 6430 Denmark

³ School of Engineering, Department of Energy Technology, Aalto University, FI-00076 Aalto, Finland

⁴ Fraunhofer Institute for Building Physics, Department Energy Efficiency and Indoor Climate,
Gottschalkstrasse 28a, DE-34127 Kassel, Germany

⁵ Centre for sustainable energy technology research, Hochschule fur Technik Stuttgart, 70174, Germany

⁶ Energianalys AB, 44127, Alingsas, Sweden

Keywords: *Low-temperature, District heating, Energy system*

ABSTRACT

Current research and development shows that it is technical feasible to change high/medium temperature district heating system to low temperature district heating system for both new and existing building areas. We collect and identify promising technologies in low-temperature district heating application to meet the goals of future renewable based community energy systems. Innovative technologies and advanced system concepts in low temperature district heating are described. Technological issues to supply low temperature district heating to existing building area, supply low temperature district heating with renewables and supply ultra-low temperature district heating are discussed in this paper.

INTRODUCTION

In Europe, heating represents the largest share of end use of energy. It accounts approximately 50% of total final energy consumption. Building sector takes more than 40% of total final energy consumption and accounts for 40% of CO₂ emissions. District heating (DH) is an essential strategic tool to reach the EU 2020 and 2050 environmental and energy efficient targets.

Low temperature DH based on renewable energy can substantially reduce total greenhouse gas emissions and secure energy supply for future development of society [1]. There have large potential to transform the current 3rd generation DH (water system with $T_s < 100^\circ\text{C}$) or 2nd generation DH (water system with $T_s > 100^\circ\text{C}$) to the future low temperature DH system (also called 4th generation DH ($T_s = 50 \sim 55^\circ\text{C}$)). An IEA DHC research project (Annex TS1: Low temperature district heating for future energy system) has been developed to study low temperature DH for future energy system. In Subtask B (District heating and cooling technologies), different low-temperature DH technologies and solutions were collected which include solutions to control and operate space heating system to achieve

low supply and return temperature, solutions to supply domestic hot water at low-temperature in energy efficient and cost effective way without risk of Legionella, solutions to design energy efficient network and eliminate network bypass losses, solutions to operate district heating system at ultra-low temperature and solutions to utilize decentralized waste heat[2].

The paper focuses on several research issues in low temperature DH supply. The first issue is to supply DH to existing buildings with low network supply and return temperature. The second issue is to supply low temperature DH with renewable energy. The third issue is to supply buildings with temperature below 50°C.

SUPPLY LOW TEMPERATURE DISTRICT HEATING TO EXISTING BUILDINGS

Traditionally, DH system focuses on the production or supply side. The DH operators have limited knowledge on the consumer heating profile. The operation of DH system is to provide sufficient high temperature and differential pressure to the end users. The low temperature DH system concept switches this perspective starting from building energy conservation and minimizing supply and return temperature in the building, then the energy efficient DH network and the renewable energy supply.

Literally, the 3rd generation DH can be operated under low temperature without the need to renovate the existing buildings and their heating systems. The precondition to achieve such goal is that the problem to safety supply domestic hot water without the risk of Legionella should be firstly solved [3].

There is no need of discussion of the floor heating system as it typically requires temperature around 30-40°C, which causes no problem to operate the system at low temperature. It was also demonstrated that low temperature DH can meet the heating demand in low energy buildings. For existing buildings with radiators which were dimensioned based on the old

high/medium temperature design criteria, low temperature can be supplied when the ambient temperature becomes sufficiently high.

To illustrate the relationship between the DH supply temperature and the ambient temperature, a building simulation was performed in IDA-ICE building simulation tool. The building is a typical Danish single family house built in 1970s. The internal floor area is 142 m². The simulated annual heating load is 110 kWh/m².y and the peak heating power is 9.2 kW.

A supply temperature compensate curve is constructed based on the operational criteria which demands the annual accumulated hours in the most critical room zone should be no more than 5% of the total heating period when the room operative temperature is below 20°C.

Figure 1 illustrates the suggested temperature compensate curve. The low supply temperature at 50°C starts when the ambient temperature is above -1°C. **Figure 2** shows the operative temperature duration curve in the most critical room (except the entrance which has lower temperature) based on the compensate supply temperature curve. It can be seen that the accumulated annual total hours for room temperature below 19.9°C is around 2%. The consumer thermal comfort is satisfied with the constructed temperature compensate curve.

Assuming the heating period is from Oct 1st this year to March 31st next year. The total hours in this period is 4368 hrs. During this period, the total hours for ambient temperature above -1°C is 3455 hrs. This means low temperature DH can be supplied to the existing buildings for 80% of heating period without the need for building or heating system renovation.

The benefits of low network supply temperature is higher power to heat ratio in steam CHP plants, higher COP for heat pumps, higher utilization of low temperature renewable energy and waste heat sources, and lower network heat losses. The demand for low supply temperature is not in urgent as far as the high temperature heat source (like steam power plant) is still in dominant.

The significant benefits of low network return temperature is higher utilization of flue gas condensation and larger temperature drop in the consumer end. Flue gas condensation is particular relevant for biomass and waste incineration CHP plants, which have high moisture content fuels. To encourage low network return temperature, some Danish DH utilities use incentive tariff to regulate network return temperature. For example, 1% of variable price per 1°C is returned back to the consumers when their return temperature is below a threshold value (for example, 30°C). On the other hand,

extra payment is made for consumers who have higher return temperature than the threshold value.

The operation toward low temperature DH tries to push the limit for the lowest possible supply and return temperature. One of the barriers to operate at low temperature is that there have different errors in the consumer heating systems and substations [4]. Such errors should be identified and removed. Low temperature can then be achieved in a well-balanced and controlled hydronic circuit.

Low supply temperature needs the knowledge of building heating demand and building heat system. It can be achieved through a well-toned temperature compensative curve. To adjust the room thermal comfort and ensure low return temperature, radiator thermostatic valves should be used with a pre-setting function. The purpose of pre-setting function is to limit the maximum flow through the valve and achieve better hydraulic balance.

Due to misunderstanding of the thermostatic valve, consumers often use it as an on/off valve. In some occasions, they may leave the windows open and keep the heating system running. These result inevitable high return temperatures even the thermostatic valves are correctly installed and functioning. To ensure low return temperature, a thermostatic return limiter can be installed at the radiators. It closes the flow when the return temperature is higher than the set-point value. In this way, minimum cooling of supply water can be achieved in all situations.

Figure 3 shows an indirect connected space heating substation with thermostatic radiator valve, a return limiter and a differential pressure controller. The function of differential pressure controller is to ensure a stable differential pressure across the heating installation.

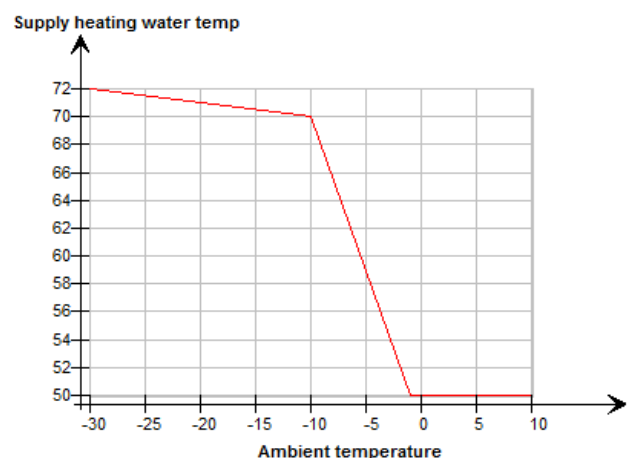


Figure 1 Supply water temperature compensate curve

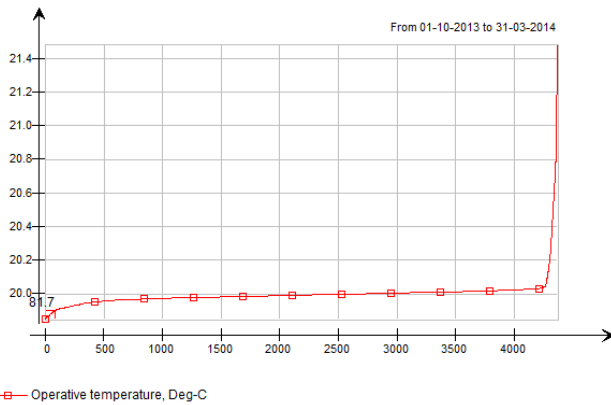


Figure 2 Duration of operative temperature in the critical room

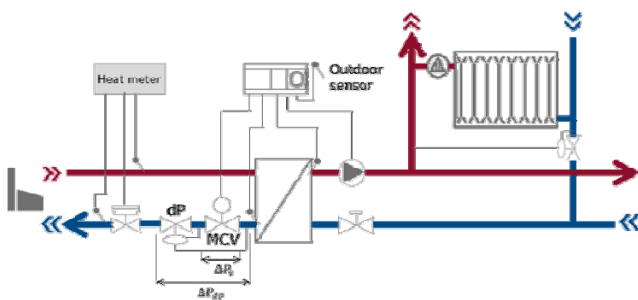


Figure 3 Control of indirect heating system

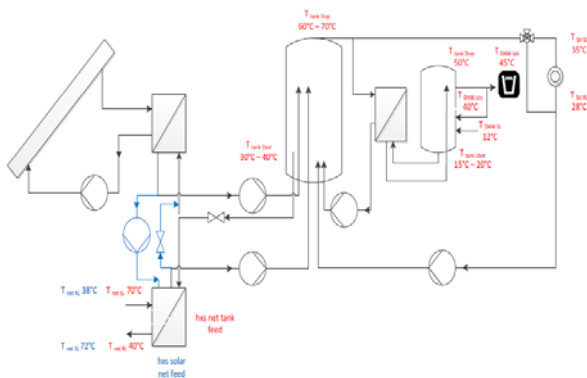


Figure 4 Hydraulic connection of decentralized solar plant to existing substation

SUPPLY LOW TEMPERATURE DISTRICT HEATING WITH RENEWABLES

The 2009/28/EC Directive sets target to achieve at least 20% of renewable share in the final energy consumption by the year 2020 within EU countries. To face the challenge of fossil fuel depletion and greenhouse gas emissions reduction, more renewable energy will be used in the power and heating sector.

The current renewable heating technologies are feasible to be implemented in different circumstances in DH [5]. Biomass has high heat content and can be

easily stored. It is an ideal replacement for fossil fuel in current CHP plants. However, long term use of biomass as the primary heat source is arguable due to competing land use with food and feed production, and the prioritised use of biomass in other sectors like in transportation and materials production which are traditionally made from petrochemical products.

Low temperature renewable energy sources can be solar energy and geothermal energy. Solar collector from flat plate produces hot water at 80-90°C. Up to 25°C can be obtained from shallow geothermal with depth less than 400m. Coupled with heat pump, it can provide the low temperature DH needs.

The use of renewables can be in centralized way or in decentralized way. Decentralized heat generation produces heat close to the users thus does not require expensive long-distance pipelines. It reduces the distribution heat loss and meanwhile increases system flexibility and the capability to use more local heat sources.

The decentralized heat sources can be solar thermal, geothermal heat, or waste heat recovered from compressor machine (as in supermarket) or city data centre, etc. The scale of decentralized heat source is typically small and the owner of the decentralised heat can also be a customer. Figure 4 shows Hydraulic connection of decentralized solar plant to existing substation as installed in Ludwigsburg, Germany for multi-family houses. The heat is transferred from the transfer station to the micro grid when there is surplus solar heat and vice versa when the solar heat is not sufficient. The simulation results indicate that during summer period, the heat delivered from the solar station is much higher than that the heat removal from the grid.

SUPPLY ULTRA-LOW TEMPERATURE DISTRICT HEATING

The minimum supply temperature in a district heating network is restricted by whether the supply temperature level is high enough to meet the space heating demand and whether the produced domestic hot water can meet the hygiene and comfort standard. For low energy buildings and buildings with floor heating, the supply temperature constrains mainly comes from the domestic hot water. In Denmark, the prevention of Legionella requires that the hot water temperature no lower than 50°C for system with circulation and 60°C for system with storage tank [DS 16355, 2012].

For a domestic hot water system which uses instantaneous heat exchanger and confines the total water volume from the heat exchanger to the tapping point within 3 litres, there is no risk of Legionella

contamination. In this case, low-temperature district heating can supply 50°C at the primary side of the domestic hot water circuit.

There exist various heat sources in the urban area which have the temperature below 50°C. Such heat sources can be sewage water, waste heat recovered from server centre or electric transformer, or shallow geothermal heat. Comparing with low-temperature district heating, such low temperature waste heat sources have temperature below 50°C which cannot be directly used for domestic hot water supply. This type of district heating is called ultra-low temperature DH or cold DH. The DH water temperature needs to be boosted on-site with auxiliary heaters that often use electric energy.

A case study was performed to investigate the performance of several different substation configurations in single-family houses supplied with ultra-low temperature district heating [7]. In the local district heating system, the waste heat recovered from a local pump factory and then boosted with a heat pump provides heating need for residential buildings. The plant supply temperature is at 46°C when the ambient temperature is above 5°C. Below this temperature, the district heating supply temperature is increased by 1 °C for every 1 °C decrease in the outdoor temperature in order to provide sufficient heat to the consumers during cold weather. With consideration of heat loss in the distribution network, the supply temperature at the consumer end is around 40°C.

Different types of domestic hot water substations were studied which include conventional storage tank with auxiliary electric heater, micro-heat pump substation, and instantaneous heat exchanger with supplementary electric heaters. Figure 5 shows the instantaneous heat exchanger substation with supplementary electric heater for kitchen water use. It has the lowest relative electricity consumption and the lowest integrated energy costs for domestic hot water production in all studied cases.

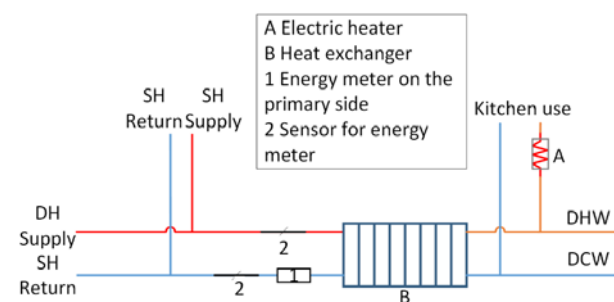


Figure 5 Instantaneous heat exchanger with supplementary electric heaters

CONCLUSION

Several technological issues to supply low temperature DH have been discussed in this paper.

When people interpret low temperature DH, some may have an understanding that either the building or the heating system should be renovated before low temperature DH can be applied in large scale. Such understanding assumes supply temperature at 50-55°C should be used all year round including cold winter period. This however hinders the development of low temperature DH. From building simulation, it can be seen that even in cold climate like in Denmark, low temperature at 50°C can be supplied in a major portion of time during the heating season for existing buildings which have high energy consumption and use radiators as the heating system. This means low temperature DH operation is possible in current DH system as far as the problem to safely supply domestic hot water at temperature close to 50°C could be firstly addressed.

Low temperature DH emphasis both low network supply temperature and low return temperature. Low supply temperature can be achieved with well-tuned temperature compensate curve. Low return temperature can be achieved through thermostatic radiator valve and thermostatic return flow limiter.

When heat sources for high temperature heat generation are still in dominant, it may be an uneasy task to persuade DH utilities to shift to low supply temperature even for low energy buildings. This is because high temperature can keep the system simple (no additional measures are required for domestic hot water system). It can also achieve larger temperature drop from the heating system thus keep smaller pipe diameters and low pumping cost.

On the other hand, low network return temperature benefits biomass or waste based CHP plant performance due to heat recovery from flue gas condensation. Therefore, the transition from current DH system to low temperature DH system can be divided into two steps. The first step is to achieve low network return temperature. Then the second step, when high temperature heat source is gradually phasing out, low network supply temperature can be the main target. It demands the low temperature supplied all year round as there has no cheap high temperature heat source available to boost the temperature in peak winter period. Deep renovation of existing buildings and their heating system are required in order to meet this target.

The share of renewable energy in heating supply will continuously increase. Comparing with biomass, solar heating and geothermal with heat pump may more suitable for low temperature district heating. Other low temperature waste heat sources which cannot be used directly in low temperature DH due to its ultra-low temperature can be recovered and supplied to consumers. Such ultra-low temperature DH can be applied when there have on-site temperature boosters installed at the consumer ends. The use of renewables and waste heat can be either centralized or

decentralized to increase the system flexibility and the possibilities to maximum recover available waste heat.

ACKNOWLEDGEMENT

The work presented in this paper is supported by The Energy Technology Development and Demonstration Program (EUDP) from Danish Energy Agency.

REFERENCES

- [1] Lund, H., Werner, S., Wiltshire, R., Svendsen, S., Thorsen, J-E., Hvelplund, F., Mathiesen, B., , 4th Generation district heating (4GDH): Integrating smart thermal grids into future sustainable energy systems, Energy, Vol 68, 2014. pp.
- [2] Li, H., Svendsen, S., Gudmundsson, O., Kuosa, M., Schmidt, D., Kallert, A.M., Ruben., Lennermo., P., IEA DHC Annex TS1, Subtask B: Low temperature district heating for future energy system: District heating and cooling technologies. 2016
- [3] Dalla Rosa, A., Li, H., Svendsen, S., Werner, S., Persson, U., Ruehling, K., Felsmann, C., Crane, M., Burzynski, R., Bevilacqua, C., Toward 4th Generation District Heating: Experience and Potential of Low-Temperature District Heating, Annex X Final Report, 2014
- [4] Frederiksen, S., Werner, S., District heating and cooling, Studentlitteratur AB, 2013
- [5] Li, H., Energy efficient district heating, chapter in Handbook of Clean Energy Systems, Wiley, 2015
- [6] DS/CEN/TR16355. Recommendations for prevention of Legionella growth in installations inside buildings conveying water for human consumption. København: CEN; 2012.
- [7] Xiaochen Yang, Hongwei Li, Svend Svendsen, Evaluation of different domestic hot water preparing methods with ultra-low temperature district heating, Submitted to Energy

EXERGY-BASED ANALYSIS OF RENEWABLE MULTI-GENERATION UNITS FOR SMALL SCALE LOW TEMPERATURE DISTRICT HEATING SUPPLY

A. Kallert¹, D. Schmidt¹, T. Blaese¹

¹ Fraunhofer Institute for Building Physics, Gottschalkstrasse 28a, DE-34127 Kassel, Germany

Keywords: Thermal Simulation; Low Exergy Communities; Low Temperature Supply Structures and District Heating

ABSTRACT

One third of the world's end energy consumption is used on heating purposes in the building sector. The larger part of energy used for heating comes from high exergetic sources (e.g. coal or gas). Since living spaces are usually heated up to around 20 °C, application of low exergetic sources (e.g. solar thermal energy or ground heat sources) is sufficient for low temperature district heating supply.

The main target of the work carried out is to demonstrate the advantages of exergy-based assessment for increased efficiency of small scale district heating supply schemes. For this reason different supply scenarios, based on fossil and renewable energy sources, are investigated. The different renewable energy supply units are regarded individually or in two- or three-way combinations. In this study renewable and fossil-based supply are compared on the one hand and on the other hand the benefits of merging several renewable energy suppliers for a small building group with a high energy standard are identified. For evaluation and identification of the best supply solution, the exergetic-based assessment method is applied. Additionally simplified aspects of operational management and estimation of investment costs are used to compare the different supply solutions. The evaluation of the scenarios clearly shows that the combination of innovative supply strategies and exergetic assessment leads to a more "holistic understanding" of the energy conversion chain and offers prospects for optimized low temperature district heating supply. Furthermore economic considerations and an analysis of emissions are to be included in the evaluation.

This paper represents modelling, simulation and exergetic analysis of renewable multi-generation units to low temperature district heating supply of a building group and covers a topic from IEA DHC Annex TS1 [1].

INTRODUCTION

The building sector is responsible for more than one third of the end energy consumption and therefore for a large amount of greenhouse gas emissions. Low temperature district heating (LTDH) supply in particular offers new possibilities for greater energy efficiency

and reduced consumption of fossil energy. On the demand side, low temperature heat is commonly available as a basis for energy efficient space heating and domestic hot water (DHW) preparation. Low temperature heat can be integrated into district heating through e.g. the use of efficient large scale heat pumps, solar thermal collectors and biomass fired - combined heat and power plants. Generally, the utilisation of lower temperatures reduces transportation losses in pipelines and can increase the overall efficiency of the entire energy chain used in district heating. To achieve maximum efficiencies, not only the district heating networks and energy conversion need to be optimal, but the demand side must also be fitted to allow the use of low temperatures supplied by the network. For this reason, the implementation of solutions based on large shares of renewable energies requires an adaptation of the technical and building infrastructure [1]. To identify potential savings and to increase efficiency of supply a holistic analysis of energy flows is necessary. In particular the application of exergy principles is especially important, allowing the detection of different available energy-quality levels and the identification of optimal contribution to an efficient community supply. From this, appropriate strategies and technologies with great potential for the use of low-valued energy sources (LowEx) and a high share of renewable energies for heating and cooling of community supply systems can be derived [2].

The main target of the work is to demonstrate advantages of exergy-based assessment for increased efficiency of small scale district heating supply. For this reason this paper is focused on modelling, simulation and exergetic analysis of renewable multi-generation units to low temperature district heating supply.

EXERGY-BASED ANALYSIS

To improve the efficiency of small scale district heating supply the physical property "exergy" is used. In accordance to thermodynamic laws, exergy is the maximum theoretical work obtainable from the interaction of a system (energy flow or a change of a system) with its environment, until a state of equilibrium is reached between them [3]. Thus exergetic assessment shows a strong dependence on the selected reference environment. In this paper the outdoor air temperature is chosen using [4]. In contrast

to energy, exergy can be destroyed. In this way the exergy content expresses the quality, respectively the ability of transformation, of an energy source or flow. This property can be used for identification and quantification of improvement potential for complex community supply systems [2], [7].

The work carried out in this paper is based on findings of the study [8]. This study deals with modelling and exergetic analysis of renewable multi-generation units of a small building group. As part of this study it is demonstrated that the combination of innovative supply strategies and exergetic assessment leads to a more "holistic understanding" of the energy conversion chain and offers prospects for optimized community supply. Furthermore it shows that the meaningfulness of the results of exergy assessment of community supply systems could be increased if simplified aspects of operational management are regarded as well. In addition it was found that additional impact factors should be considered which play an important role for assessment of small scale district heating supply technologies. As part of further work the factors CO₂ emissions and aspects of economy have been identified. For that reason the method shown in [8] has been refined and extended by analysis of CO₂ emissions and consideration of economic aspects.

Next to the choice of assessment parameters the definition of the system boundaries plays an essential role when assessing small scale district heating supply. For the analysis carried out in this study the methodology described in [6] is used and adapted to the assessment of community energy systems. This method is also known as the "LowEx"-approach, a more detailed description can be found in [2]. For evaluating the energy and exergy flows all transformation processes occurring in the community energy conversion chain need to be taken into account. The calculation of the energy and exergy demands starts at the demand side beginning at the building envelope. Supply chains are broken down into individual subsystems for analysis conducted in this paper. For each subsystem, the incoming and outgoing exergy flows are considered [6] (refer Figure).

MODELLING OF A SMALL ENERGY SYSTEM

By using the simulation tool TRNSYS [9] a small energy system is modelled. The model includes ten high energy standard residential buildings. To supply the building a local district heating (DH) network with substations, storages, and heat generation units consisting of: solar thermal collectors (ST), ground source heat pumps (GSHP) and natural gas-fired CHP are implemented. Additionally as a reference case, a common decentralized supply technology using natural gas (NG) boilers, without grid, storage and application of renewable energy sources (RES) is modelled. For both variants the ten buildings of the cluster are physically identical and are equipped with floor heating systems. To guarantee uninterrupted heat supply and to avoid undersupplying or oversupplying the emission systems, as well as the energy suppliers, are controlled by using weather forecasting. For modelling and simulation the weather data for Kassel (Germany) created by "Meteonorm" [4] is used.

Assumptions for buildings and thermal network

All buildings have a floor space area of 180 m² and are dimensioned for a specific heating demand of 45 kWh/m²a. This demand reflects the energy demand for new buildings according to EnEV 2009 [10]. Real settlements are characterized by a variation of user behaviour which results in greater deviation of each single building. For this reason the buildings are classified by different user profiles "average", "saver" and "waster" [11].

Table 1: User profiles for determination heat demand

	user type „average”	user type „saver”	user type “waster”
Room temperature	21 °C	19 °C	22 °C
Night setback	Yes	Yes	No
Air exchange rate	0,6 1/h	0,3 1/h	1,0 1/h

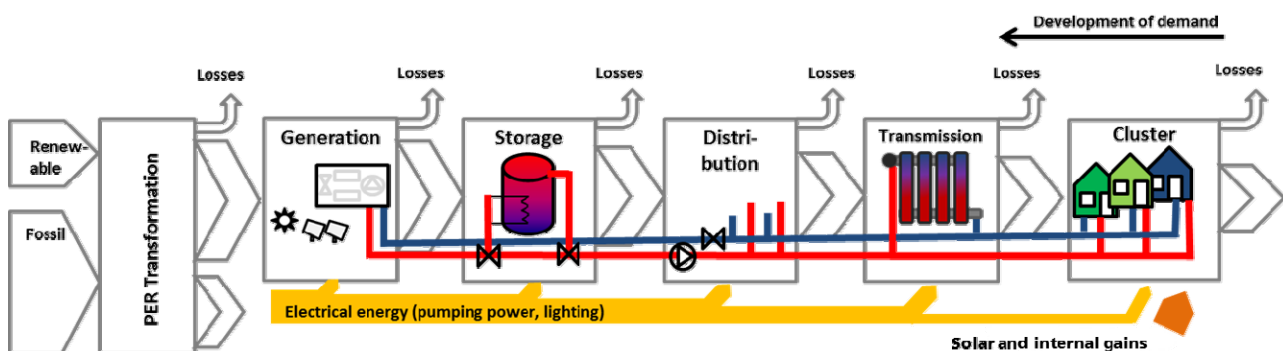


Figure 1: Energy conversion chain used for modelling of a building group [8]

For each profile internal gains are varied in order to reflect a two-person household as well as a family of four. "Average" and "saver" are equipped with night setback, which means that the room temperature is lowered by 3 °C for seven hours. In case of DHW preparation different stochastic DHW-tapping profiles were created using "DHWCalc" [12]. These profiles are classified corresponding to user profiles described above and differ in the temporal variance of tapping. The energy demand for DHW preparation is calculated using DIN V 18599 [13].

The DH network is designed as a radial network. To cover the heating demand and DHW demand simultaneously the design supply temperature is 45 °C. The thermal network is equipped by pre-insulated twin-pipes (U-Value = 0.027 (W/m²K)) with small diameters (DN50 and DN25) which leads to a highly efficient supply of the buildings. In the model a subroutine for the calculation of the ground temperature is implemented. This subroutine models the vertical temperature distribution of the ground given as the mean ground surface temperature for the year, the amplitude of the ground surface temperature for the year, the time difference between the beginning of the calendar year and the occurrence of the minimum surface temperature as well as the thermal diffusivity of the soil [14]. For determination of pressure losses and dimensioning of the required pumping power the Darcy-Weisbach-Equation is used [15]. For the modelling of the thermal distribution networks the velocity of individual fluid segments must be taken into account due to emerging thermal interactions. Furthermore, it has to be considered that the twin pipes are buried in the ground and that the media-carrying pipes are inside a common insulating layer. For dynamic simulation and determination of heat losses

the „ground buried plug-flow model“ [16] is used. This model combines „ground buried pipes“ [17] and the „plug-flow model“ [18]. For coupling of the local low temperature DH network with the heating system the buildings are equipped with a substation (HAST). In the HAST the fluid coming from the district heating supply line is divided into two flows: heating fluid and DHW fluid. The fluid for space heating is provided directly to the building service systems. To provide the required temperature level for space heating a bypass is used for admixture of return line water from the DH grid. For DHW preparation instantaneous heat exchangers are modelled taking Legionella prevention into account. In the event that the target temperature for DHW is not achieved, each building is equipped with an electric heating element.

Assumptions for the energy suppliers and storage facilities

The interconnection of energy suppliers and storage devices is shown in Figure 2. The storages act as interface between the supply line of the DH-network and centralized energy supplying units. Two storage solutions are implemented; buffer and seasonal storage. Depending on the simulation scenario, both storages can be charged or re-charged respectively and activated or de-activated using the valves (1) and (2). If e.g. high solar yields are achieved, the seasonal storage is charged. As soon as the seasonal storage is recharged, HP and CHP can be activated to guarantee the uninterrupted heat supply. For the operation of the HP and CHP a small buffer storage is available. Depending on the selected supply scenario all supply units can be operated individually or in combination. All energy suppliers can be enabled or disabled, using the pumps and the valves (1)-(4). Additionally these pumps and valves (1)-(4) regulate the mass flows. As long as the temperature level in the seasonal storage is above the return temperature of the network (6) the residual heat can be used for reheating in the buffer storage, by activating valves (2) and (4).

If the supply temperature is higher than the required supply temperature in the network the bypass valves (5) and (6) are used to control the return flow.

EXERGY-BASED ANALYSIS OF CASE STUDIES

For comparison and exergy-based analysis seven renewable scenarios (centralized) and a fossil-based (decentralized) supply scenario are investigated (refer to **Table 2**). The selection and dimensioning of case studies using renewable energy sources is based on realized projects, where a high degree of innovation was targeted (e.g. [19], [20]).

The aim of this analysis is to compare renewable on one hand and fossil-based supply and on the other

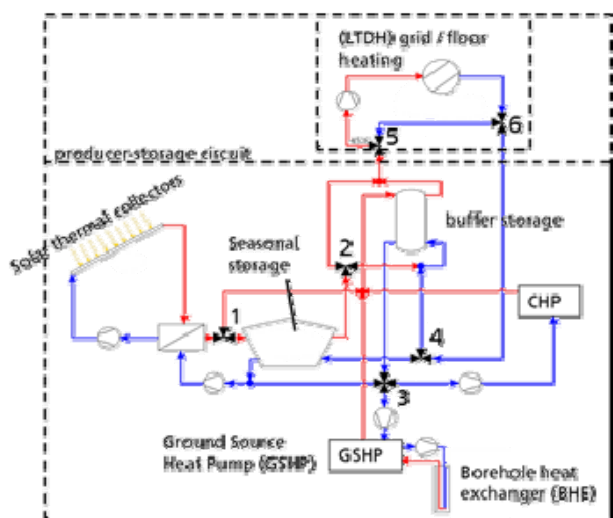


Figure 2: Principle sketch of interconnection of energy suppliers and storage devices

hand to identify benefits by merging several renewable energy suppliers for a small building group with high energy standard. The first three scenarios deal with self-sufficient renewable supply variants. In scenario 2, two energy supplying units are interconnected. For supply scenario 3 three energy supplying units are interconnected. To compare renewable and fossil fuels as well as decentralized supply technologies in the context of exergetic evaluation a NG boiler (scenario 0) is included in the evaluation.

EVALUATION AND DISCUSSION

In this section the results of exergy-based assessment is presented.

Energy and exergy Assessment

For energy and exergy assessment of energy conversion processes different benchmarking parameters can be found in literature [6]. The most common benchmarking parameter for evaluating energy systems in general is the energy conversion efficiency η . This factor describes the ratio between the useful output of an energy conversion machine and the input, in energy terms. By using this parameter different occurring qualities or the ability of transformation [6] are not taken into account.

$$\eta = \frac{E_{out}}{E_{in}} \quad (1)$$

In order to assess occurring qualities the exergy efficiency ψ is used. Different expressions and definitions of this parameter can be found in literature (e.g. [21], [22]). The so-called “overall exergy efficiency” is used in this work. The application of this exergy efficiency allows characterizing the total performance of a complete energy system. Overall exergy efficiencies of different energy systems (e.g. different supply scenarios for a building group) can be directly compared with each other, since the same reference temperature is used for exergy analysis of all supply systems [6].

$$\psi = \frac{Ex_{out}}{Ex_{in}} = 1 - \frac{Ex_{loss} + Ex_{destroyed}}{Ex_{in}} \quad (2)$$

For allocating the CHP the “Carnot method” is used in this paper. Using this method the reference temperature is taken into account. Furthermore electrical and thermal efficiency are assessed independently [23],[24],[25]. In this study the primary energy factors in accordance to national German standard [10] are used. A description of other methods could for example be found in [31].

The comparison of energy efficiency η is shown in Figure 3.

Table 2: Representation of supply variants

	Scenario	Solar thermal (ST)	Heat pump (HP)	CHP
0	NG boiler			
1.1	ST	800 m ² (100%)		
1.2	HP		60 kW	
1.3	CHP			60 kW
2.1	ST + HP	350 m ² (40%)	60kW	
2.2	ST + CHP	350 m ² (40%)		60 kW
2.3	HP + CHP		60 kW	5kW
3	ST + HP +CHP	350 m ² (40 %)	45 kW	20kW

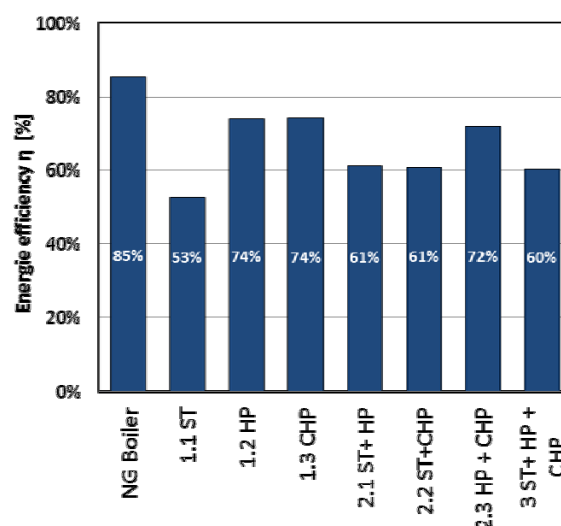


Figure 3: Assessment of energy efficiency η

Assessment of energy efficiency η leads to the conclusion that the NG boiler is the favoured solution. But particularly in new housing areas implementation of renewable energy sources (RES) is mostly targeted due to further restrictions (e.g. reduction of CO₂ emissions or the presence of an urban ventilation path) [19]. Taking this into account the HP (1.2 HP) or the CHP (1.3 CHP), or a combination of these units (2.3 HP + CHP) would be the favoured variant. The solar thermal collectors show a low degree of energy efficiency in comparison and provide little incentive for implementation. This picture changes significantly when taking exergy efficiency ψ into account (Figure4).

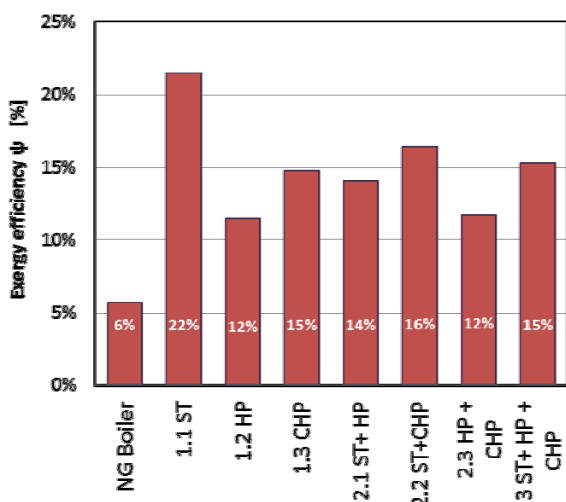


Figure 4: Assessment of exergy efficiency ψ

Table 3: Emission factors for $g\ CO_{2eq/kWhEnd}$ [27].

Energy source	Process	CO ₂ -Emmision (g CO _{2eq/kWhEnd})
Burnable fuels	Natural gas	244
	Liquid gas	263
Electricity	Electricity Mix	633
District heating	70 % CHP	219
	35 % CHP	313
	0 % CHP	407

From an exergy point of view the boiler solution is not a good option, since high quality fuels are burned and therefore the temperature level potentially available (flame temperature) to heat the room air is too high. However the supply variant using solar thermal collectors (1.1 ST) shows high potentials for demand adapted supply. But there are large limitations: the heat is mostly generated during summer where the heat demand is low and must be stored with high heat losses until the heating season. Additionally the installation of large-area solar collector-arrays, especially in urban areas (densely populated areas), is often not feasible. Self-sufficient CHP (1.3 CHP) or self-sufficient heat pumps (1.2 HP) offer another good supply option. Thus application of "Carnot Method" for allocating the CHP leads to high exergy efficiencies, although a combustion process occurs. In comparison to CHP the exergy efficiency of HP is lower, since the current German electricity mix [26], [10] is used for supplying the heat pump. In future energy systems with an increased share of renewable energy this picture might change. A restriction on the use of HP is the

space requirement if borehole heat exchangers are used. In order to exploit the exergetic advantages of solar thermal energy and to identify benefits of multi-generation supply the CHP as well as the HP are combined with solar thermal collectors. The decentralized DH solution using RES shows advantages. When comparing self-sufficient renewable energy suppliers solar heating is the most attractive heat source. Based on these interim results it can be concluded that the exergetic analysis shows optimization potential, beyond energy analysis and offers prospects for an optimized community supply. However, exergy analysis does not inherently include other objectives such as maximizing the use of renewables or minimizing emissions. For that reason the assessment of CO₂ as an indicator for global warming potential (GWP) is added to this method.

Assessment of CO₂ emissions

The choice of energy resources is also important, as the type of fuel is crucial for CO₂ emissions. In Table 3 the emission factors used for assessment of for energy sources are listed.

CO₂-emission is an indicator for GWP. For that reason it indicates the necessity of need for urgent action. The CO₂ emission is directly linked to the final energy demand which is calculated as part of this method. In this study CO₂ equivalent (CO_{2eq}) values from [27] are used. In this research the values used are for burnable fuel, Germany's electricity mix respectively and district heating because they are the only fuels considered for powering the heating units.

It should be noted that the selection of the emission factors has a significant impact on the assessment of the energy suppliers. A description and discussion of other factors can for example be found in [31] and [32].

The assessment of CO₂ emission in tons per year is shown in Figure 5. In particular supply scenario (1.1 ST) shows the most significant reduction of CO₂ emissions. However the electrical heaters for DHW preparation have negative impact on this balance since they are supplied by electrical energy. These heating rods are mainly used for pre-heating during wintertime.

A similar picture emerges in the comparison of the heat pump scenarios (1.2 HP) and (3 ST+HP +CHP). Here the electricity mix has a decisive influence as well. The emission of CO₂ will decrease if the share of renewable energies in the electricity mix is increased or the HP is supplied by wind turbines or PV. It can further be shown that in particular the combination of solar thermal and heat pump has a positive impact on the CO₂ balance (2.1 HP). A reduction of CO₂ emissions for the CHP (1.3 CHP) could possibly be reached if the plant is operated with bio methane instead of natural

gas. Based on these interim results it can be shown that the meaningfulness of the results was increased by the combination of exergy assessment and assessment of CO₂ emissions. Another important factor for the evaluation of small scale district heating supply is the consideration of economic aspects. For this reason the assessment is expanded by roughly estimation of investment costs.

Estimation of economic aspects

As part of the rough estimation of economic aspects, the operating hours of heat pump and CHP as well as the investment costs for the energy suppliers are considered.

GSHP are mostly designed for 1800-2400 operating hours per year [28]. CHP units benefit from the combined production of heat and electricity. In order to be operated economically, both electricity and heat must be generated for a long period. In [29] it is recommended to reach at least 3000-5000 operation hours per year with small and very small CHP, so that they are economically viable. Figure 6 shows a comparison and assessment of different operational times of heat pump and CHP. It is shown that the heat pump-based supply variants (1.2 HP) and (2.3 HP+CHP) achieve the minimum required operational times whereas (2.1 ST+HP) and (3 ST+HP+CHP) do not reach minimum required operational times. Under the set boundary conditions only option to be operated economically viable is (2.3 HP+CHP).

Figure 7 shows a comparison and rough estimation of the investment costs for the energy suppliers. The calculation is simplified in accordance with [30]. This determination of the investment costs represents only a rough indication of the cost ratios. As expected the decentralised reference scenario (NG Boiler) has the lowest investment costs. The reason for this lies in the absence of both storage and grid in this supply variant. Among the central supply units, the self-sufficient solar supply (ST 1.1) is front runner with regard to investment costs. This is mainly due to the reason that investment costs for storage and collector are high in comparison to the other variants. The high investment costs are considered to be less critical, since they are potentially compensated by low consumption costs. The costs of solar collectors and storage units also have an impact on all other variants in which solar heat is used. The CHP variant (1.3 CHP) has the lowest investment costs. However, it should be considered critical that economic operational times may not be achieved. In comparison, the investments for the heat pump are higher since borehole heat exchangers (BHE) are implemented. In this context it should be noted that the installation of the BHE leads to additional

costs (drilling, space requirements), which are not yet considered here in this study. These costs could possibly be lowered if air source heat pumps are used. The investment costs for the LTDH grid is equal in all centralized variants and is estimated to be 180000 €.

The investigations carried out in this study do not claim to be a full economic analysis. Instead the goal is to estimate economic aspects. In particular, the economic analysis has to be extended by consumption costs (fuel costs and costs for heat supply) and operational related costs (maintenance and repair). The consideration of national funding programs is not planned at present.

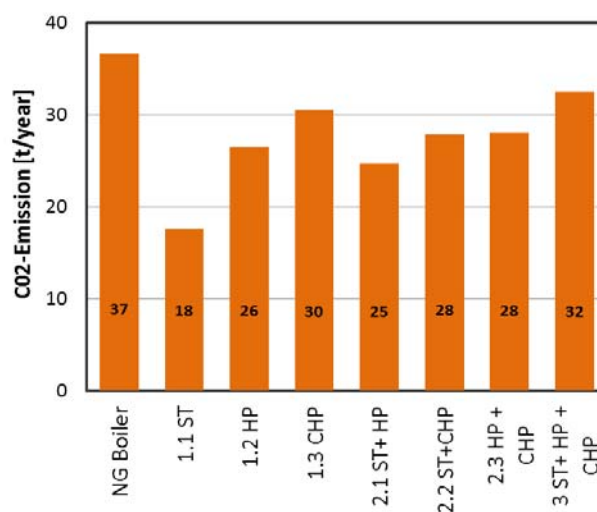


Figure 5: Assessment and comparison of CO₂ emission.

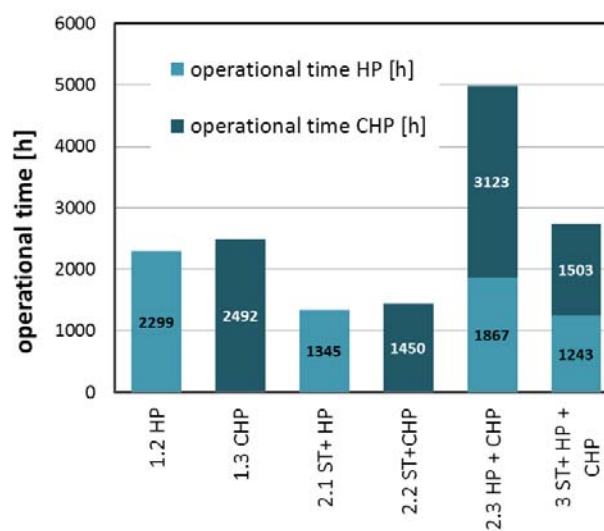


Figure 6: Operational time of heat pump and CHP (hours in full load)

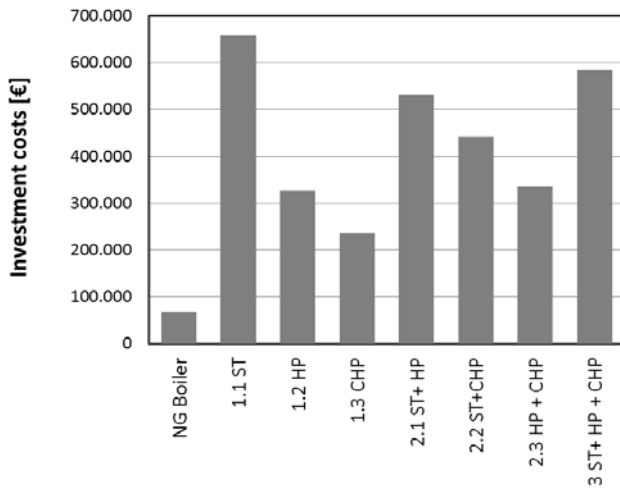


Figure 7: Estimation of the investment costs

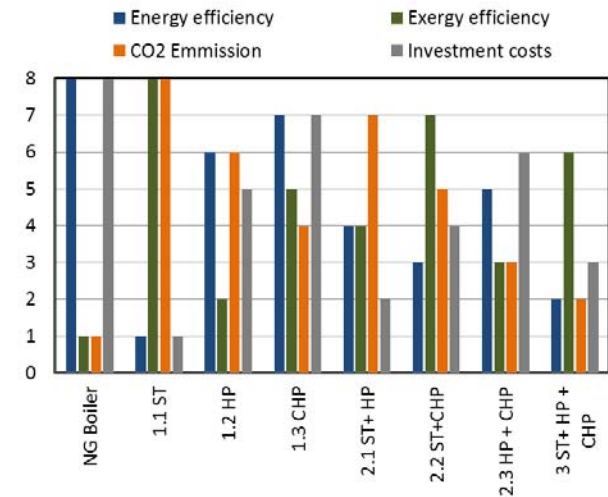


Figure 8: Comparison of supply variants

Summary

As part of the analysis of each single assessment parameter renewable and fossil-based supply are compared. Furthermore benefits of merging of several renewable energy suppliers for a small building group are demonstrated. For the comparative analysis of all parameters the results of the individual examination are ranked. The most favoured variant is rated with 8 points and least favoured variant is rated with 1 point.

Figure 8 shows the result of ranking of the supply variants. It turns out that the reference variant (NG boiler) scores well with regard to energy efficiency and investment costs whereas demand adapted supply (exergy efficiency) or low CO₂ emission are not achieved. A contrasting result is achieved by centralized supply variant of self-sufficient solar thermal supply (1.1 ST). The comparison of decentralised LTDH supply scenarios shows that supply variant (1.3 CHP) is promising with respect to all assessment parameters - only CO₂ emissions scores rather badly. For increasing the exergy efficiency and decreasing CO₂ emissions of this supply option the exergetic advantages of solar thermal energy could be exploited (2.2 ST+CHP). However, it should be considered critical that operational times are possibly not reached. The heat pump scenario (1.2 HP) is in particular limited with regard to exergy assessment. To increase the exergy efficiency the HP could potentially be combined with (3 ST+HP+CHP). Based on these finding it can be stated that the simultaneous consideration of energy and exergy efficiency as well as CO₂ emissions and consideration of economic aspects increases the meaningfulness of the results of exergy assessment. The developed approach facilitates identification of the best supply solution taking into account certain requirements (for example, reduction of CO₂ emissions).

In the course of on-going research the assessment approach presented here is constantly developed further. In particular it is necessary to extend economic analysis by consumption costs (fuel costs and costs for heat supply) and operational related costs (maintenance and repair). Furthermore, additional significant influence parameters need to be identified which have an impact on assessment. As it could be seen in the comparison of the different supply variants another important factor for example is area requirement. This has particularly been demonstrated in analysis of variants in which solar thermal or borehole heat exchangers are implemented. Another important parameter is the influence of the electricity mix in future energy systems. Moreover weighting factor needs to be introduced to highlight the influence of parameters on the final result. These weighting factors of the individual aspects do not necessarily have to be proportional. Regarding the relevance of the different indicators in relation to project focus or target group (e.g. planner, academia or research) the weighting can be varied. For planners and decision makers the economy factors would have more weight. For academia or research aspects of demand-adapted supply (using exergy as indicator), development for future energy systems or degree of innovation would have more weight. A very promising method for identification of further impact factors and weighting factors for planners and decision makers are found in [7]. As part of further investigations other relevant parameters will be examined. To reduce the use of additional heating and to increase security of supply in wintertime analysis of different supply and return temperatures need to be investigated. As part of these investigations the impact of the electrical heating elements and alternative solutions need to be analysed. Furthermore the influence of the restoration

level of buildings and plant technology on the overall efficiency of thermal networks needs to be quantified. In this context the influence of the transfer systems in the buildings (space heating and radiators) needs to be identified.

CONCLUSION

The main target is to demonstrate potentials of exergy-based assessment for increased efficiency of small scale district heating supply. For this reason this paper is focused on modelling, simulation and exergetic analysis of renewable multi-generation units for low temperature district heating supply. As part of the work a small building group of ten residential low energy buildings is modelled [9]. To supply the buildings a centralized and decentralized concept is compared. By using this model different case studies based on fossil and renewable energy sources are investigated by using the model. The supplying units using renewable energy sources are regarded individually or in groups of two or three-way combinations. On one hand the case study aims to compare renewable and fossil-based supply. Furthermore benefits by merging of several renewable energy suppliers are identified.

For evaluation and identification of the best supply solution, the exergetic assessment method is applied. As part of this paper the method introduced [8] has been expanded by CO₂ emissions [27] and aspects of economy [30]. The evaluation of the scenarios shows that the combination of innovative supply strategies and exergetic assessment leads to a "holistic understanding" of the energy conversion chain. Furthermore exergetic analysis shows optimization potential, beyond energy analysis and offers prospects for an optimized community supply. Additionally it is shown that simultaneous consideration of energy and exergy efficiency as well as CO₂ emissions and consideration of economic aspects increases the meaningfulness of the results of exergy assessment.

As part of future work the assessment approach will be further developed. In particular it is necessary to extend the economic analysis by consumption costs (fuel costs and costs for heat supply) and operational related costs (maintenance and repair). In case of evaluation of CO₂ emissions it should be noted that the selection of the emission factors has a significant impact on the assessment of the energy suppliers. A description and discussion of other factors could for example be found in [31] and [32]. For this reason, different methods of assessment of CO₂ emissions are compared as part of further investigations. Furthermore, additional influence parameters need to be identified which have an impact on assessment results (e.g.: space requirements). Moreover weighting factors need to be introduced to control the influence of parameters on the final result.

ACKNOWLEDGEMENT

The authors warmly thank the German Federal Ministry for Economic Affairs and Energy (BMWi) for the received financial support.

REFERENCES

- [1] Schmidt, D., et al., Low temperature district heating for future energy systems, The 14th International Symposium on District Heating and Cooling, 2014, Stockholm, Sweden
- [2] Schmidt, D., Kallert, A., Sager-Klauss C., (2016), Optimising Community Energy Supply with Exergy Principles, Proceedings of the 12th REHVA World congress Clima2016, Aalborg, Denmark
- [3] Moran M.J. and Shapiro H.N. (1998) Fundamentals of Engineering Thermodynamics. 3rd Edition, John Wiley & Sons, New York, USA.
- [4] METEOTEST. – URL <http://meteonorm.com/de/>. – (assessed February 15th 2015)
- [5] Sangi R., Streblow R., Müller D., (2014), Approaches for a fair exergetic comparison of renewable and non-renewable building energy systems, Proceeding of 27th international conference on ECOS 2014, Turku Finland
- [6] Torio, H., Angelotti A., Schmidt, D. (2009): Exergy analysis of renewable energy-based climatisation systems for buildings: A critical view, Int. J. Energy and Buildings, Vol. 41, pp. 248–271
- [7] Sager-Klauss, C.: Energetic Communities – Planning support for sustainable energy transition in small and medium-sized communities, Delft University of Technologies, Dissertation, 2016.
- [8] Kallert A., Schmidt D., Simulation and exergetic analysis of renewable multi-generation units, 12th REHVA World Congress; CLIMA2016, Mai 22th - 25th 2016, Aalborg , Denmark
- [9] TRNSYS - Official Website. – URL <http://sel.me.wisc.edu/trnsys/>. – (online)
- [10] EnEV 2009, Energieeinsparverordnung für Gebäude - Verordnung über energiesparenden Wärmeschutz und energiesparende Anlagentechnik bei Gebäuden, 2009.
- [11] Loga, T., Grossklos, M., Knissel, J. Der Einfluss des Gebäudestandards und des Nutzerverhaltens auf die Heizkosten. Juli 2003
- [12] DHWcalc: Program to generate domestic hot water profiles with statistical means for user defined conditions <http://solar.umwelt-unikassel.de> (assessed January 3rd 2015)
- [13] DIN V 18599-8: 2011-08. Energy efficiency of buildings – Calculation of the net, final and primary energy demand for heating, cooling, ventilation, domestic hot water and lighting Part 8: Net and

- final energy demand of domestic hot water systems.
- [14] Kasuda, T., and Archenbach, P.R. "Earth Temperature and Thermal Diffusivity at Selected Stations in the United States", ASHRAE Transactions, Vol. 71, Part 1, 1965
- [15] Herwig H.: Strömungsmechanik. Wiesbaden: Vieweg+Teubner, 2008
- [16] Dahm, Jochen: District Heating Pipelines in the Ground: Simulation Model, 2001. www.trnsys.de/
- [17] Wallentén P.; Steady-state heat loss from insulated pipes, Lund Institute of Technology, Department of building physics, 1991
- [18] TRNSYS 16 - Volume 5 Mathematical Reference Solar Energy Laboratory, University of Wisconsin-Madison, 2006
- [19] Schmidt, D., et al. Development of an Innovative Heat Supply Concept for a New Housing Area Proceedings of the 12th REHVA World congress Clima 2016, Aalborg, Denmark
- [20] E. Bollin, K. Huber und D. Mangold, Solare Wärme für große Gebäude und Wohnsiedlungen, Stuttgart: Fraunhofer IRB Verlag, 2013.
- [21] Ahern J. (1980). The Exergy Method of Energy System Analysis. Wiley Interscience Publication, John Wiley and Sons, New York.
- [22] I. Dincer, M. Rosen, Exergy—Energy, Environment and Sustainable Development, Second ed., Elsevier Publication, Oxford, UK, 2013
- [23] Hertle, H. et al.: Die Nutzung von Exergieströmen in kommunalen Strom-Wärme- Systemen zur Erreichung der CO₂-Neutralität von Kommunen bis zum Jahr 2050 / ifeu.Okttober 2014. – Umweltforschungsplan
- [24] VDI 4608 Blatt 2; Energiesysteme Kraft-Wärme-Kopplung – Allokation und Bewertung; Beuth-Verlag 2008
- [25] Rosen, M (2008): Allocating carbon dioxide emissions from cogeneration systems: descriptions of selected output-based methods, Int. J. Cleaner Production, Vol.16, pp. 171-177
- [26] Bundesministerium für Wirtschaft und Energie <http://www.bmwi.de/>. (online)
- [27] GEMIS <http://www.iinas.org/gemis-docs-de.html>
- [28] VDI 4640, Thermische Nutzung des Untergrunds. Juni 2010
- [29] Riedl K., Karsten: Exergetische und Exergoökonomische Bewertung von Verfahren der Energie- und Stoffwandlung, Martin-Luther-Universität Halle-Wittenberg, Dissertation, 2006
- [30] VDI 2067:2012 "Wirtschaftlichkeit gebäudetechnischer Anlagen - Grundlagen und Kostenberechnung"
- [31] DeWulf J et al., Exergy: Its Potential and Limitations, Environmental Science and Technology, Vol. 42, No. 7, 2008
- [32] Icha P, Entwicklung der spezifischen Kohlendioxid-Emissionen des deutschen Strommix in den Jahren 1990 bis 2015, Umweltbundesamt, 2016

LOW TEMPERATURE DISTRICT HEATING FOR FUTURE ENERGY SYSTEMS

D. Schmidt¹, A. Kallert¹, M. Bles², S. Svendsen³, H. Li³, N. Nord⁴, K. Sipilä⁵

¹Fraunhofer Institute for Building Physics, Gottschalkstrasse 28a, DE-34127 Kassel, Germany

²University of Stuttgart, Inst. of Energy Economics and Rational Use of Energy, Stuttgart, Germany

³Technical University of Denmark, Department of Civil Engineering, Lyngby, Denmark

⁴Norwegian University of Science and Technology, Dep. of Energy and Process Eng., Trondheim, Norway

⁵VTT – The Technical Research Centre of Finland, Department Energy Systems, Espoo, Finland

Keywords: *Low Exergy Communities; Low Temperature Supply Structures and District Heating*

ABSTRACT

The building sector is responsible for more than one third of the end energy consumption of societies and produces the largest amount of greenhouse gas emissions (GHG) of all sectors. This is due to the utilisation of combustion processes of mainly fossil fuels to satisfy the heating demand of the building stock. District heating (DH) can contribute significantly to a more efficient use of energy resources as well as better integration of renewable energy (e.g. geothermal heat, solar heat and biomass from waste), and surplus heat (e.g. industrial waste heat) into the heating sector. Low temperature district heating offers prospects for both the demand side (community building structure) and the generation side (properties of the networks as well as energy sources). Especially in connection with buildings that demand only low supply temperatures for space heating. The utilisation of lower temperatures reduces transportation losses in pipelines and can increase the overall efficiency of the total energy chains used in district heating. To optimise the exergy efficiency of community supply systems the LowEx approach can be utilised, which entails matching the quality levels of energy supply and demand in order to optimise the utilisation of high-value energy resources, such as combustible fuels, and minimising energy losses and irreversible dissipation (internal losses).

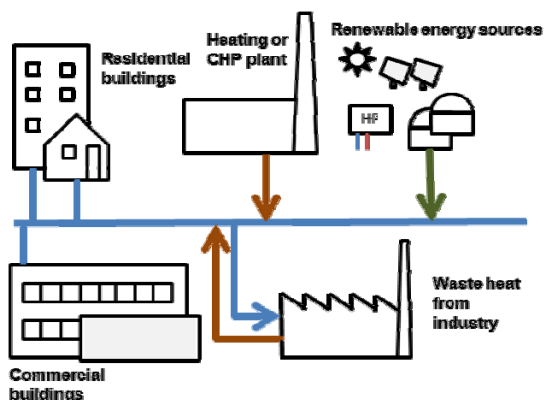


Figure 1. Schematic district heating community supply system with multiple supply options [1].

The paper presents the international co-operative work in the framework of the International Energy Agency (IEA), the Technology Cooperation Programme on District Heating and Cooling including Combined Heat and Power (DHC|CHP) Annex TS1.

INTRODUCTION

The energy demand of communities for heating and cooling is responsible for more than one third of the final energy consumption in Europe and worldwide. Commonly this energy is provided by different fossil fuel based systems. These combustion processes cause greenhouse gas (GHG) emissions and are regarded one core challenge in fighting climate change. National and international agreements (e.g. the European 20-20-20-targets or the Kyoto protocol) limit the GHG emissions of the industrialized countries respectively for climate protection. Country specific targets are meant to facilitate the practical implementation of measures. While much has already been achieved, especially regarding the share of renewables in the electricity system, there are still large potentials in the heating and cooling sector and on the community scale. Exploiting these potentials and synergies demands an overall analysis and holistic understanding of conversion processes within communities. Communities are characterized by a wide range of energy demands in different sectors, for instance heating and cooling demands, lighting and ventilation in the building stock. Different energy qualities (exergy) levels are required as heat or cold flows or as electricity and fuels.

On community scale especially low temperature district heating offers new possibilities for greater energy efficiency and lower fossil energy consumption. On the demand side, low temperature heat is commonly available as a basis for energy efficient space heating and domestic hot water (DHW) preparation. Low temperature heat can be integrated into district heating through e.g. the use of efficient large scale heat pumps, solar thermal collectors and biomass fired - combined heat and power plants.

Generally, the utilisation of lower temperatures reduces transportation losses in pipelines and can increase the overall efficiency of the total energy chains used in district heating. To achieve maximum efficiencies, not only the district heating and cooling networks and energy conversion need to be optimal, but also the demand side must be fitted to allow the use of low temperatures supplied by the network (e.g. via surface heating system). For this reason, the implementation of solutions based on large shares of renewable energies requires an adaptation of the technical and building infrastructure.

DESCRIPTION OF TECHNICAL SECTOR AND LOW TEMPERATURE DISTRICT HEATING

The application of low temperature district heating technology on a community level requires a comprehensive view of all process steps: from heat generation over distribution to consumption within the built environment. The approach includes taking primary, secondary, end and useful energy and exergy into account. This allows an overall optimization of energy and exergy performance of new district heating systems and the assessment of conversion measures (from high temperature DH to low temperature DH) for existing DH systems.

The temperature levels required to heat and cool most building types (residential and non-residential buildings) are generally low (slightly above 23 °C). In the case of the provision of domestic hot water, temperatures in the range of 50 °C should principally be sufficient to avoid the risk from the legionella bacteria. Both renewable and surplus energy sources, which can be harvested very efficiently at low temperature levels, can fulfil this energy demand. On the community scale, synergies are maximised when buildings and building supply systems are regarded as integrated components of an energy system. A number of issues need to be addressed in regard to matching the demand created by space heating (SH) and domestic hot water (DHW) on the building side with the available energy from the supply side in order to develop advanced low temperature heating and high temperature cooling networks.

Latest developments of DH tend towards low-temperature DH schemes and the integration of renewable energy sources [19]. The low-temperature DH which is in focus here, is also called the 4th generation DH.

Benefits

The use and implementation of low temperature district heating networks offers various benefits:

Utility companies benefit from low temperature district heating by having lower heat losses in the DH

networks. Also, they can use plastic piping, which can be more cost effective than conventional DH metal based pipes. The use of low temperature heat allows the integration of additional heat sources into the DH scheme, such as solar thermal collectors, deep geothermal wells and low temperature waste heat. If heat is generated by advanced CHP plants, such as combined-cycle plants, the low temperature of the used heat can lead to a higher electricity generation and therefore improved revenues from energy sales.

Customers benefit in various ways. First of all, the use of district heating ensures a secure supply. Customers do not have to worry about maintenance, fuel supply and optimal operation of heating systems. In the case of low-temperature DHW supply, the use of systems without DHW storage and pipes with small volume from heat exchanger to taps could allow the safe use of DHW at supply temperatures in the range of 50°C. In this way, the risk of legionella growth may be minimised without having to resort to higher temperatures.

From an economical point of view, relatively high price stability can be expected due to the use of locally available, renewable, or surplus heat energy sources. An additional advantage of this is a lower dependency on foreign fuel supplies. The high overall system performance that can be achieved by using low temperature DH would lead to reduced resource consumption and therefore lower costs for fuels. This would also increase price stability and could potentially provide heat at very competitive prices.

STRUCTURE OF THE DHC ANNEX TS1 ACTIVITY

To work on the field of low temperature district heating the IEA DHC activity Annex TS1 is covering work items ranging from the assessment and further development of planning tools, via the collection of suitable DHC technologies and the engagement on the field of the interfaces between the community, the DHC network and the buildings to the analyses of various case studies. Furthermore, dissemination in form of workshops and publications is also covered by the project participants [2].

The IEA DHC Annex TS1 is operated within the frame of the IEA DHC Annex X (e.g. [18]) and IEA DHC Annex XI [2], and thus benefits in highest degree from results developed with this. Furthermore the unrestricted exchange of experience and information is ensured.

RESULTS FROM INVOLVED RESEARCH PROJECTS

The goal of the research activities are primarily reducing resource consumption (including primary energy) and GHG emissions through overall system optimization and developing new ways of bringing

knowledge into practice. First of all identification, demonstration and collection of innovative low temperature district heating systems is in foreground. Here advanced technologies and the interaction between system components are to be demonstrated, as ideas and technologies for reduced network heat loss and improved thermal plant performance or innovative network topologies. Following the collection and identification of promising technologies to meet the goals of future renewable based community energy systems is accomplished.

Technologies for efficient LTDH supply

In this section selected examples for innovative technologies and advanced system concepts in LTDH are shown. They deal with the issues that need to be addressed for space heating and DHW preparation when using LTDH. Other examples deal with the limitation of higher return temperature when bypassing is avoided. At the end an example for an innovative network topology, the ring network, is discussed.

Space heating control and return temperature

To ensure consumer thermal comfort while saving energy and reducing network return temperature, the hydronic system in the SH loop need to be properly designed and operated. It was proven that LTDH can meet space heating (SH) demand for both low-energy buildings and existing buildings with floor heating. For existing buildings with old radiators, LTDH can meet SH demand for a certain amount of time of the year, while the supply temperature needs to be increased during cold winter period [11].

Radiator space heating control when applying LTDH in general is the same as when applying traditional DH but there are some points that differentiate. Due to the reduced supply temperatures, it becomes very important to achieve accurate control to limit the flow rate and achieve the design cooling of the supply. To minimize the risk of overflow in radiators thermostatic radiator valves (TRV), a pre-setting function should be used. The purpose of the pre-setting is to limit the maximum flow through the valve to the design demand. Properly set pre-set function will significantly increase the hydraulic balance in the heating loop. To ensure proper operating condition for the TRV's, it is important to install a differential pressure controller. The differential pressure controller will ensure a stable differential pressure at the correct level across the heating installation. To limit the impact of wrong setting of the TRV, a thermostatic return limiter can be installed at the radiators. The purpose of the return limiter is to ensure minimum cooling of the supply. The function of the return limiter is that it closes if the outlet from the radiator is higher than the set point. Most of the year a return temperature of 25 °C can be used but

in cold periods a higher temperature has to be accepted. Therefore it is proposed to develop new type of smart thermostatic radiator valve with a return temperature sensor. Such a TRV could secure a low return temperature even if the TRV is not used in an optimal way. In case of floor heating installation, the maximum supply temperature requirements are typically around 40 – 45 °C, which causes no problem for the application of LTDH. As with radiator controls, it is important to apply differential pressure controllers to achieve the optimum operating conditions for the floor heating installation. The flow rate is typically regulated by a room thermostat. To ensure minimum cooling of the supply return temperature limiters should be applied.

DHW preparation for LTDH

A well-designed DHW system should meet several criteria which include consumer comfort, hygiene, energy efficiency.

DHW installations should be designed as energy efficient devices. The factors which influence DHW system's energy efficiency include DH supply and return temperature, heat losses from heat exchanger, storage tank and pipes, and thermal bypass set-point.

There are two types of DHW units used for LTDH: instantaneous heat exchanger unit (IHEU) and DH storage tank unit (DHSU). Both IHEU and DHSU can work at low-temperature without the risk of Legionella. Due to the storage tank buffer effect, DHSU can reduce the connection capacity and thus apply a smaller diameter service pipe at the cost of additional heat loss from the storage tank.

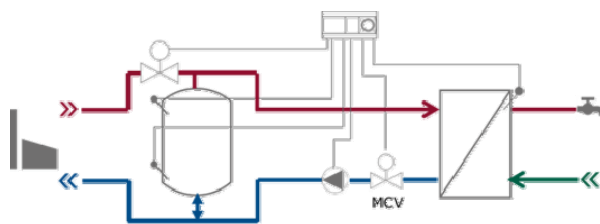


Figure 2. District heating storage unit (DHSU) [24]

On the other hand, IHEU has less standby heat loss and is more compact and less costly.

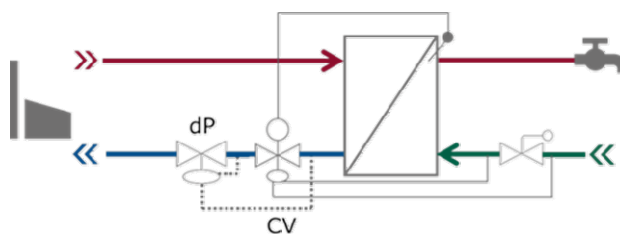


Figure 3. Instantaneous heat exchanger unit (IHEU) [24]

Both units can be applied in centralized and decentralized systems.

One of the major barriers to implementing LTDH is the increased Legionella risk with grid supply temperatures close to 50 °C. In [12] and [13] a review has been made for effective Legionella disinfection solutions to allow DHW system to operate safely at low temperature levels. In general, the Legionella treatment solutions include thermal treatment, chemical treatment, physical treatment and other alternative methods. Such treatments aim at either killing the bacteria presented in the water or prevent the spread of Legionella by limiting the bacteria multiplication within a safety margin. Alternative approaches include electric heating, electric heat tracing, or heat pump which aims to control the DHW supply temperature level. Effective treatment solution concerns not only to meet hygiene and comfort requirement but also to achieve total energy and economic cost saving.

General solutions to avoid bypass flow in service pipes

When the network heating demand becomes low, the required mass flow rate is reduced accordingly. Smaller mass flow rate causes larger water temperature drop along the pipeline due to heat loss to the ground. In non-heating season, the DHW load is low and its demand is intermittent with the total draw-off duration

less than 1 hour/day. To keep high thermal comfort, bypass valves are installed at the DHW substation. When there is no draw-off, the DH supply water is bypassed and flows back to the network return line without any cooling, it increases the network return temperature significantly and subsequently increases the network heat loss and decreases the thermal plant performance. This network performance degradation is particularly relevant for LTDH and DH supply to sparse areas. To keep low network return temperature, it should be avoided to having the DH supply water directly mixed with the return water. Several solutions have been suggested to eliminate the service pipe bypass.

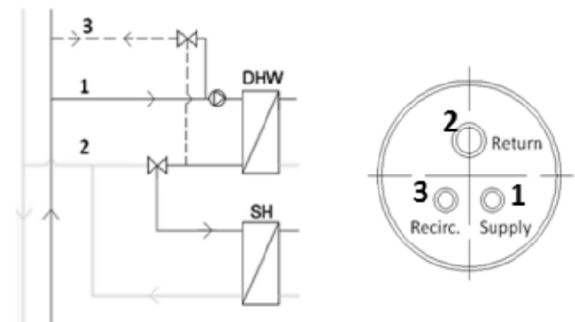


Figure 5. Minimum cooling concept with a triple service pipe [22].

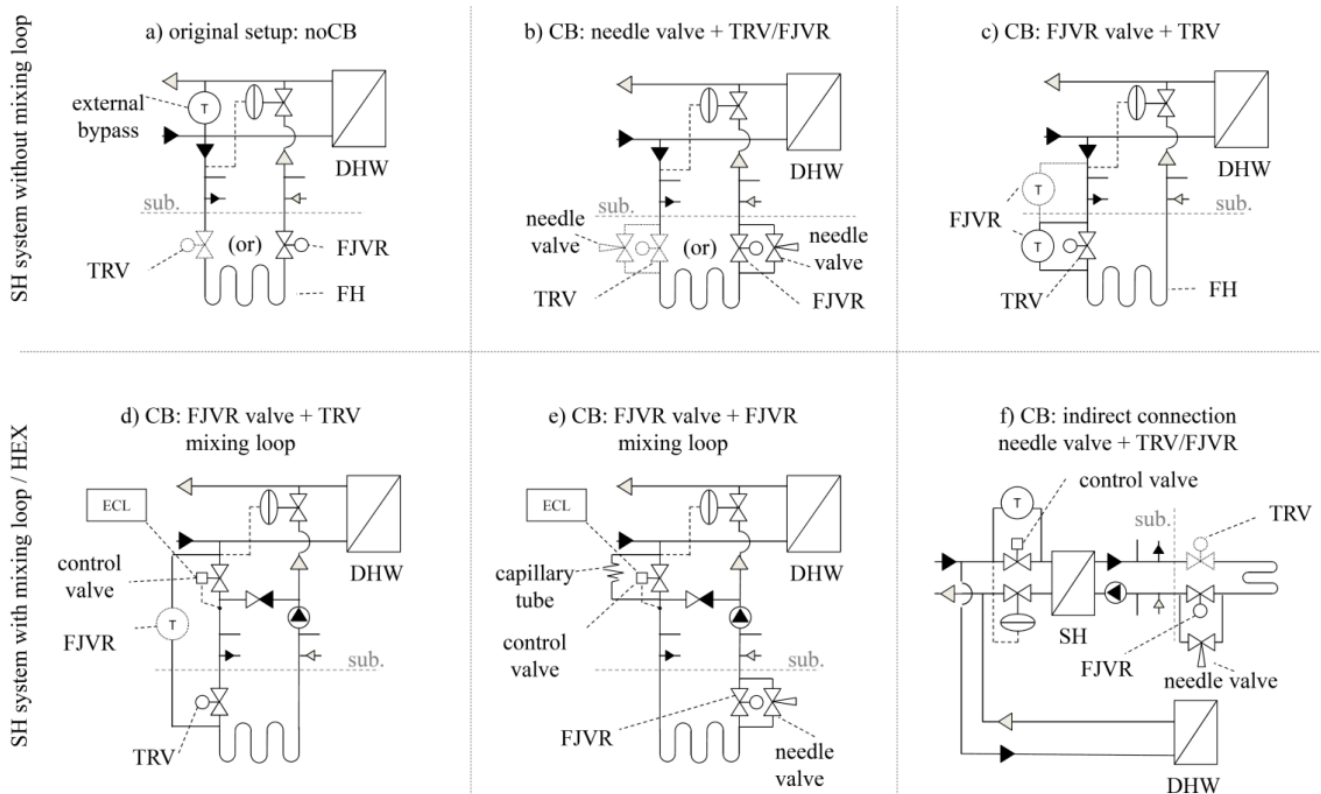


Figure 4. Technical solution for CB implementation [23]. Direct SH system without mixing loop: a) reference case without CB, with traditional external bypass; b) CB realised with a needle valve (installed in parallel to TRV valve on supply pipe or in parallel to FJVR valve on the return pipe of FH loop); c) CB realised with a FJVR bypass valve. Direct SH system with mixing loop: d) CB realised with a FJVR bypass valve; e) CB realised with a needle valve and capillary tube. Indirect SH system: f) CB realised with FJVR bypass valve.

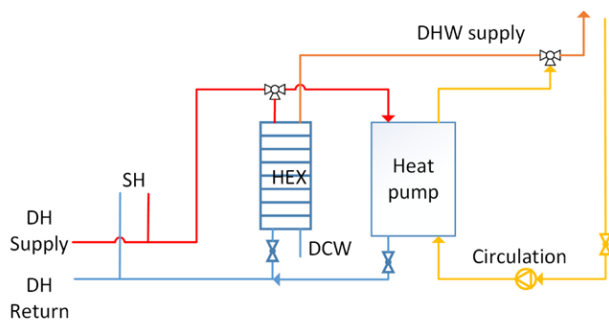


Figure 6. DHW system installing a central heat exchanger combined with heat pump [21].

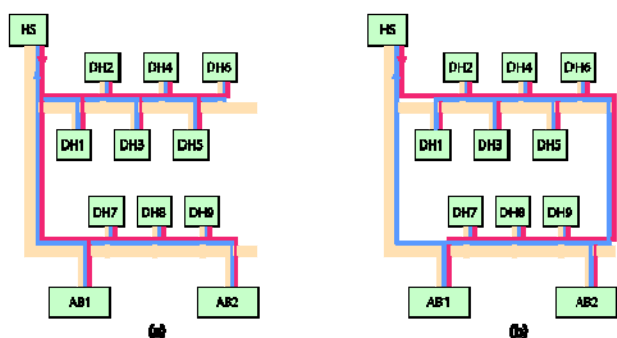


Figure 7. a) Traditional district heating network design and (b) new ring network design [14].

The 1st solution is based on the minimum cooling principle. A recirculation flow in the supply pipe warms up the service pipe and then flows back to the supply pipe in the street through a third recirculation pipe. The recirculation pipe can be a separate DH pipe or one of the pipes in a co-insulated triple pipe. This solution is however likely to create a need for a bypass flow in the street pipes.

The 2nd solution is based on the maximum cooling principle. After passing through the service pipe, the bypass water is directed to the bathroom floor heating and cooled down to 25 °C before it flows back to the return pipe. The benefit of this concept is that it uses the bypass flow continuously in the floor heating and replaces an intermittent flow due to a conventional floor heating control.

In case there is no floor heating in the bathroom a towel heater may utilize the bypass flow. Such an application is called ‘Comfort Bathroom (CB)’ concept (Figure 4). This solution is also securing a flow in the street pipes and therefore does not need a bypass flow in the street pipes.

The 3rd solution is based on electrical supplementary energy. In large buildings with DHW circulation the need to keep the circulation at a minimum of 50 °C results in a high return temperature and requires a district heating supply temperature of more than 55 °C. This can be avoided by use of a heat pump that

cools the district heating from 50 °C to 20 °C and heats the circulation loop to 55 °C. Figure 5 shows the schematic to use micro-heat pump to compensate the heat loss in the DHW circulation loop and keep the pipes temperature at 50 °C.

The benefit of this concept is that the district heating flow to the heat pump also secures the instantaneous DHW heating of the heat exchanger. This solution does not require bypass in the street pipes.

Example for an innovative district heating network typology: The ring network

In traditional DH network design, the pipe lengths between the heating plant and different consumers vary. The consumers close to the plant has larger available differential pressure, whereas the consumers away from the plant have smaller available differential pressure. In an uncontrolled pipe network, the pressure profile in the system would lead to more water flow through the consumers close to the plant and insufficient water flow through the consumers located far away from the plant. To overcome this, valves are installed in the network to increase the flow resistance and throttle the excess pressure that is available at the consumers close the heat plant until the specified flow to the consumers is achieved. One solution to reduce the valve throttling and potential hydraulic imbalance when the valves were malfunctioned is to apply a ring shape network topology.

Unlike the traditional network, a topology based on ring network equalize the pressure differences between the supply and return pipes, which reduces the impact in case of malfunctioning valves [14].

Figure 7 (a) shows the traditional and ring network in an area of nine detached houses (1-9, DH) and two apartment buildings (1-2, AB) [15]. The idea of the ring topology is to have an equal pipe length for every consumer as presented in Figure 7 (b). The supply line (red line) begins from the heat station (HS) and ends with the last customer, as in the traditional network design. However, the return line (blue line) begins from the first customer and ends at the heat station. In both the supply and return lines, DH water circulates in the same direction. On the contrary, in a traditional DH network design, the return line begins from the last customer and proceeds back to the heat station.

Methodologies and Planning Tools

Another Objective of the described project is the development of a methodology for assessment and the analysis of procedures to optimise local energy systems. Furthermore it includes the development of simplified and advanced tools for design and performance analysis of energy systems within communities, which are based on district heating.



Figure 8. Aerial view Building Exhibition - Hyvinkää (Finland) [17].



Figure 9. Terraced low energy house in Lystrup [4].

As part of the project the simulation Tool “The Low Exergy – Cluster Analysis Tool (LowEx-CAT)” has been developed. As the integration of low temperature technologies is a main focus of the model, heat grids are also considered in terms of grid temperature, design and optimization of the grid distribution. The goal of the simulation performed by LowEx-CAT is the comparison and evaluation of different energy supply strategies based on district heating technologies. The assessment method developed in the frame of the IEA DHC Annex TS1 aims toward a comprehensive, exergy based evaluation method for local energy systems. The overall objective of the work is the analysis of emerging primary energy and exergy as well as the assessment of CO₂ emissions and economy analysis [8].

Case studies

While requirements to energy performance of buildings are introduced generally on European and on national levels heat demands of buildings are decreased by applying improved building envelopes and more

efficient heat recovery for ventilation systems. Nonetheless LTDH offers a way to supply heat to buildings in an economical feasible and environmental friendly way. The case studies shown in the following are examples where a successful application of new and innovative district heating concepts has been demonstrated [3].

Example: Hyvinkää (FI)

The project at the housing fair area Hyvinkää consists of a number of very low energy buildings and so-called passive houses which are connected to a district heating network. The particular goal for this project is the estimation of the long term performance of innovative district heating systems. So the long-term goal extends to the year 2020 and beyond. A life-cycle analysis on the community-level is carried out. Consequently, an influence of solutions on the community life-cycle emissions can be shown based on these analyses. The aim is also to explore in Finnish climate the boundary conditions and opportunities for the district heating solutions for so-called “nearly zero-energy houses”.

During the course of the project energy consumption in the connected single-family houses and on the DH-system level will be monitored for several years. The results from the measurements will be used to explore short- and long-term fluctuations of power and energy consumption in buildings and to assess their impact on operation of electricity and district heating networks [5]. The project aims at the development of special district heating solutions for single-family houses with 2012- and 2021-level (Finish energy standards) of heat consumption. The approach is based on the life-cycle analysis (LCA) and lifecycle costing (LCE) of the entire energy system (i.e. extending from the indoor space services, through the new district heating network solutions up to the community level energy generation). The potential of using communal waste in energy generation will be assessed, too.

Example: Lystrup (DK)

A key challenge for achieving a competitive district heating system of today and in the future is to reduce heat loss in network while today’s building regulations demand reduction of heat consumption. So, the ratio between network heat loss and heat consumption in the connected buildings is a main issue. Low temperature district heating offers a solution and is implemented and evaluated in real scale in Lystrup close to Aarhus in Denmark [4]. The goal of this project is to reduce district heating temperature delivered to consumers to 50°C and connect the buildings in a manner that no reheating is needed to be applied - neither at consumer site nor at district heating site. For the Lystrup project, two types of low-temperature district heating substations and new district heating

twin pipes with reduced diameter were developed and tested.

The project consists out of 7 row houses with totally 40 flats where two different sizes of flats are being realised: 89 m² and 109 m² (gross area) with a resulting design heat demand for space heating of 2.2 kW and 2.6 kW respectively. All rooms - except bathrooms – are equipped with low-temperature radiators with a design supply temperature of 50°C and a return temperature of 25°C. The bathrooms are supplied with floor heating. To keep the very low supply temperatures district heating water is supplied directly into the building's heating system, no heat exchanger between building heating system and district heating system has been applied [6],[7]. The project is a show case that demonstrated that low temperature district heating can be used even in areas with low energy demand while being economically feasible and giving high comfort levels for the connected users [8].



Figure 10. Scheme of net extension in Ludwigsburg Sonnenberg [9].



Figure 11. Map of investigated planning area "Zum Feldlager"; representation of the possible supply concept based on a district heating network with central heating plant (CHP plant) [20].

Example: Ludwigsburg (GER)

The urban planning concept for the city quarter of Ludwigsburg entails the design of the local energy supply system by the extension of the main district heating network of the quarter "Sonnenberg" with the aim the use innovative network technology, a so-called low exergy (LowEx) sub grid, and to integrate thermal solar energy into the new grid section.

The project goals for the city of Ludwigsburg are to realise an energy supply concept with a gas-fired cogeneration plant (CHP) of 700 kW_{th} and with a geothermal driven heat pump of 200 kW_{th}. The decentralised heat storages are planned to be located inside the buildings and operated via a smart metering concept with a central control unit [9] The LowEx network extension is operated with supply temperature at 40°C from the return temperature of existing network of the city quarter Sonnenberg. This new district heating network, which represents about 30% of the total network length, is going to be connected to low energy/passive standard buildings. The research project focuses on the demand side management and structure (energy standard of buildings, operation of heaters), the network structure, on the chosen supply concepts and on the storage management.

Example: Kassel Feldlager (GER)

An innovative heat supply concept for the new housing area „Zum Feldlager“ of the city of Kassel in Germany with about 130 houses has been set up. The main objectives and challenges with this particular project are the minimization of primary energy consumption, the reduction of CO₂ emissions compared to common supply systems, the reduction of transmission heat losses and the usage of a high share of renewable energy sources for the supply of the about 500 persons living there in near future. So, the heat supply concept has been set up with regard to realise the supply to the entire development area without fossil fuels, such as oil (expensive, water protection area), natural gas (no gas network) or fire wood (fine dust emissions). Use of renewable energy sources such as geothermal and solar energy for low temperature supply has been elaborated [10]. The following figure 11 shows the development plan.

The supply to the different houses has been planned to be a low temperature heat supply with implementation of intelligent storage systems and thermal load shifting concepts. For the chosen energy concept the houses are supplied by a low temperature district heating grid. For the heat generation both a renewable gas powered combined CHP plant and a low temperature heat generation via a ground coupled (boreholes) central heat pump are investigated separately. For the domestic hot water preparation solar thermal systems with an additional electrical backup heater are planned.

The supply temperatures of the low temperature district heating grid is designed to be 40°C, the heat supply for space heating is preferably done via floor heating systems or via low temperature radiators. To increase the efficiency of the heating systems and to optimise the hydraulic integration of the heat generation systems the use of smaller water storage tanks in all buildings is intended. A hygienic preparation of domestic hot water is realised by fresh water stations.

EXPECTED OUTCOME AND RESULTS FROM THE PROJECT

The primary deliverable of the presented activities within the annex is an easy to understand and practical, applicable future low temperature district heating design guidebook for key people in communities. It is to contain an executive summary for decision makers. Some key questions for the targeted group of people are:

- What are arguments for taking action in regards to a possible change of the energy system within the community?
- What shall be done with regard to the community's energy system?
- And, what should not be done?
- Does our community fulfil the conditions for the implementation of low temperature district heating and, if not, what could we improve to allow for this in the future?

These questions will be answered in the guidebook, which is to be focussed at low temperature district heating from a communal, decision makers' point of view. This will cover issues on how to implement advanced low temperature district heating technology at a community level and how to optimise supply structures to ensure reduced costs for the system solution.

This guidebook will be published preferably both as a book via a publisher, and as an electronic publication. More detailed results, which will be published as appendices or separate reports via the project homepage [2] are intended to cover topics such as:

- Analysis concept and design guidelines with regard to the overall performance. This could include a possible classification of technologies in terms of performance, improvement potential and innovation prospects.
- Analysis framework and open-platform software and tools for community energy system design and performance assessment.
- A collection of best-practice examples and technologies.

- Dissemination of information on demonstration projects.
- Guidelines on how to achieve innovative low temperature systems design, based on analysis and optimisation methods, and derived from scientific studies.

The dissemination of documents and other information is to be focussed at transferring the research results to practitioners.

SUMMARY

The IEA DHC Annex TS1 is a framework that promotes the discussion of future heating networks with an international group of experts. The goal is to obtain a common development direction for the wide application of low temperature district heating systems in the near future. The gathered research which is to be collected within this Annex should contribute to establishing DH as a significant factor for the development of 100% renewable energy based communal energy systems in international research communities and in practice. The Annex TS1 is intended to provide solutions for both expanding and rebuilding existing networks and new DH networks. It is strongly targeted at DH technologies and the economic boundary conditions of this field of technology. The area of application under consideration is the usage of low temperature district heating technology on a community level. In connecting the demand side (community/building stock) and the generation side (different energy sources which are suitable to be fed in the DH grids), this technology provides benefits and challenges at various levels. The scientific basis for the development of assessment methods provides the low exergy (LowEx) approach. This approach promotes the efficient and demand adapted supply (e.g. at different temperature levels) and the use of renewable energy sources. As Annex TS1 is a task-shared annex, there will be no individual, separate research projects started within the Annex. The Annex TS1 provides a framework for the exchange of research results from international initiatives and national research projects and allows, in a novel way, the gathering, compiling and presenting of information concerning low temperature district heating. Currently 12 research institutions from 8 countries are participating [2].

ACKNOWLEDGEMENT

This cooperative research work is funded by various national sources. The authors would like to thank for the given financial support and would like to acknowledge the contributions of all their colleagues. The authors are responsible for the content of this paper.

REFERENCES

- [1] Fredriksen S, Werner S. (2013) "District heating and cooling", English Edition. Studentlitteratur, Lund, Sweden
- [2] Homepage of the IEA District heating and Cooling, including the integration of CHP, Implementing agreement: www.iea-dhc.org.
- [3] Schmidt D.(ed.) (2015) "Successful Implementation of Innovative Energy systems in Communities". Case study brochure of IEA DHC Annex TS1. Available at www.iea-dhc.org.
- [4] Thorsen, J.E., et al. (2011) "Experiences on low-temperature district heating in Lystrup – Denmark", published in proceedings of: International conference on district energy 2011, 20-22.3, Slovenia
- [5] Klobut K., "Future District Heating Solutions for Residential Districts (TUKALEN)", presentation at the IEA DHC Annex TS 1 meeting 4.9.2013, Espoo, Finland.
- [6] Brand, M, et. al. (2010) "A Direct Heat Exchanger Unit used for Domestic Hot Water supply in a single-family house supplied by Low Energy District Heating", Published at the 12th International Symposium on District Heating and Cooling, September 5 to September 7, 2010, Tallinn, Estonia.
- [7] Paulsen, O., et. al. (2008), "Consumer Unit for Low Energy District Heating Network", Published at the 11th International Symposium on District Heating and Cooling, August 31 to September 2, 2008, Reykjavik, Iceland.
- [8] Olsen, P.K., et. al. (2008) "A New Low-Temperature District Heating System for Low Energy Buildings" Published at the 11th International Symposium on District Heating and Cooling, August 31 to September 2, 2008, Reykjavik, Iceland.
- [9] Pesch, R. "Low Temperature District Heating for Future Energy Systems – DHC Technologies", presentation at IEA DHC Annex TS 1 meeting 4.9.2013, Espoo, Finland
- [10] Schmidt, D., et al. Development of an Innovative Heat Supply Concept for a New Housing Area The 15th International Symposium on District Heating and Cooling September 4-7, 2016, Seoul, Republic of Korea (South Korea).
- [11] Brand. M, Svendsen. S, Renewable-based low-temperature district heating for existing buildings in various stages of refurbishment. Energy, 2013.
- [12] Yang, X., Li, H., Svendsen, S., Analysis and research on promising solutions of low temperature district heating without risk of legionella. DHC 14 Stockholm, 2014
- [13] Yang, X., Li, H., Svendsen, S., Alternative solutions for inhibiting Legionella in domestic hot water systems based on low-temperature district heating. Building Service Engineering Research & Technology. 2015
- [14] Kuosa, M, et.al, Study of a district heating system with the ring network technology and plate heat exchangers in a consumer substation, Energy and Building, 80 (2014), pp.276-289
- [15] Laajalehto T., Kuosa M., Mäkilä T., Lampinen M., Lahdelma R., Energy efficiency improvements utilising mass flow control and a ring topology in a district heating network, Applied Thermal Engineering 69 (2014), pp.86-95
- [16] Kallert A., Schmidt D., Simulation and Exergetic Analysis of Renewable Multi-Generation Units for a Building Group, Proceedings of the 12th REHVA World congress Clima2016, Aalborg, Denmark
- [17] Picture was taken by Rakentaja.fi/Jarno Kylmänen.
- [18] S. Svendsen; H. Li; et. al; "DHC Annex X Final report Toward 4th Generation District Heating: Experience and Potential of Low-Temperature District Heating" Homepage <http://www.iea-dhc.org/home.html> accessed on 30.03.2015
- [19] Lund, H. Wiltshire, R., Svendsen, S., Thorsen, J.E., Hvelplund, F., Mathiesen, B., 4th Generation district heating (4GDH) integrating smart thermal grids into future sustainable energy systems, Energy, 68 (2014) 1-11.
- [20] Development plan Nr. IV/65 „Zum Feldlager“; Architektur+Städtebau Bankert, Linker & Hupfeld, City of Kassel- Urban planning, building supervision and monument conservation; 02 February 2013.
- [21] Li, H., Svendsen S., Gudmundsson O., Kuosa M., Schimdt D., Kallert A., Low temperature district heating technologies for future energy system, The 12th REHVA World Congress – Clima 2016, May 22nd to May 25th, 2016, Aalborg, Denmark.
- [22] Dalla Rosa, A., Li, H., Svendsen, S., Method for optimal design of pipes for low-energy district heating, with focus on heat losses, Energy 2011 (36), pp.2407-2418
- [23] Brand M., Heating and Domestic Hot Water Systems in Buildings Supplied by Low-Temperature District Heating, PhD Thesis Department of Civil Engineering 2014.
- [24] District heating application handbook, Danfoss Co. Ltd. www.danfoss.com

DEVELOPMENT OF AN INNOVATIVE LOW TEMPERATURE HEAT SUPPLY CONCEPT FOR A NEW HOUSING AREA

D. Schmidt¹, A. Kallert¹, J. Orozaliev², I. Best², K. Vajen², O. Reul³, J. Bennewitz⁴, P. Gerhold⁵

¹Fraunhofer Institute for Building Physics, Gottschalkstrasse 28a, DE-34127 Kassel, Germany

²University of Kassel, Department of Solar and Systems Engineering, Kurt-Wolters-Straße 37, DE-34109 Kassel, Germany

³University of Kassel, Department of Geotechnics, Mönchebergstr. 7, DE-34109 Kassel, Germany

⁴Staedtische Werke Kassel AG, Königstor 3-13, DE-34117 Kassel, Germany

⁵City of Kassel, Rathaus / Obere Königsstrasse 8, DE-34117 Kassel, Germany

Keywords: low temperature district heating; new housing area; ground source heat pump; solar heat

ABSTRACT

The energy demand of buildings for heating and cooling is responsible for more than one third of the world's final energy consumption. Therefore the identification of innovative heat supply concepts based on renewable energies is required. The utilization of renewable energies in combination with efficient supply technologies increases the sustainability of new housing areas.

For the new housing area "Zum Feldlager", located in Kassel (Germany), various supply concepts are investigated. Main objective is the development of an innovative and optimised heat supply concept based on renewable energies and a low temperature district heating. Central challenge in achieving this objective is the identification of the most promising and efficient technical solutions for practical implementation. In order to identify the best possible system solution, different centralised and decentralised supply strategies have been investigated and compared.

The most promising heat supply concept is based on a central ground source heat pump in combination with a low temperature district heating (40°C supply temperature) for space heating and decentralised solar thermal systems for domestic hot water preparation. The advantages of this supply variant are comparable low annual heating costs and about 60 % lower CO₂-emissions in comparison to the reference.

This project is a cooperative activity and of the Fraunhofer Institute for Building Physics (IBP) in Kassel, Institute for decentralized Energy Technologies (IdE), Kassel University, the City of Kassel and the local utility company Staedtische Werke Kassel AG.

The paper presents a description of the new housing area as well as the evaluation of the various supply concepts and covers a topic from IEA DHC Annex TS1.

INTRODUCTION

During the planning phase of new residential areas, the investigation of suitable energy sources and supply

strategies is crucial. The use of renewable energy sources (e.g. solar energy and geothermal energy) offers great potential for a sustainable and efficient supply of heat. However for optimized usage of these resources it is necessary to identify appropriate technologies to ensure efficient supply of the new housing area.

In order to identify the best possible system solution, different supply strategies have been investigated and compared. Main objective is the development of an innovative heat supply concept based on renewable energies and an optimised supply concept. Central challenges in achieving these objectives is the identification of the most promising and efficient technical solutions for practical implementation. Furthermore aspects of future network management as well as business models for distribution and operation are considered. As a result, the focus of this project is on investigations on suitable centralised or decentralised supply concepts for a new residential area using renewable energy sources in a cost efficient way.

The project is carried out in two project phases. The first project phase consists of a study in order to identify the most efficient and economical heat supply concept. In the course of the second project phase a detailed concept will be elaborated which includes selecting, dimensioning and detailed cost determination of the various components.

This paper presents the results of the first project phase.

DESCRIPTION OF THE NEW HOUSING AREA

The planning area "Zum Feldlager" is located in the city of Kassel (Germany). The area is surrounded by existing buildings of the district and is located in an urban ventilation path. For that reason combustion of oil or wood (fine dust emissions) should be avoided. Due to the location of the area a connection to the existing district heating network of Kassel is not feasible because of logistical and economic reasons.

Instead a local district scheme is implemented. The concept involves principally the use of renewable energy sources (RES) such as geothermal and solar energy for low temperature district heating supply. The additional use of a combined heat and power (CHP) plant is also investigated. Furthermore the implementation of intelligent storage systems and thermal load shifting concepts is envisaged.

The new housing estate will be characterized by a very compact and south oriented construction; 1-2 storey detached and semi-detached houses in the north, two-storey terraced houses in the centre and large three-storey apartment buildings in the south. All buildings have specific heat demands of 45 kWh/m²a and a specific domestic hot water (DHW) demand of 730 kWh/pers.a. Thus, the demand is significantly below the maximum energy demand for new buildings (< 50 kWh/m²a) according to the current German energy saving ordinance EnEV [2].



Figure 1. Map of the investigated area
Source: City of Kassel/Germany, [1]

Table 1. Assumptions for the buildings [1]

Total number of buildings	127
Dwelling units	154
Persons per dwelling unit	4
Roof shape	SFH, SDH and TH = Gable roof, MFH = flat roof
Heat emission system	surface heating

DEVELOPMENT AND COMPARISON OF VARIOUS INNOVATIVE SUPPLY CONCEPTS

For the identification of a possible supply concept in a first step DHW, heating and cooling demands are calculated. Based on the resulting energy demand suitable supply concepts are elaborated.

Determination of heat/ cool demand and DHW demand

The monthly heat and cool demand as well as DHW demand is calculated corresponding to the monthly balance method of DIN V 18599 [3] including part 2 [4], part 4 [5], part 5 [6], part 8 [7] and part 10 [8].

The total annual energy demand according to the monthly balance method DIN V 18599 [2] is calculated for a heating demand of $Q_{hd} = 1.199$ MWh/a, for cooling demand $Q_{cd} = 319$ MWh/a and for domestic hot water demand $Q_{DHW} = 365$ MWh/a. These values correspond to a very good insulation standard of the buildings.

Selection of supply variants

Based on the low determined monthly energy demand different supply options are examined. Since it has been decided to supply the district preferably with renewable energy sources the utilization of near-surface geothermal energy by means of borehole heat exchangers (BHE), the use of solar energy or the installation of a bio-methane powered CHP are eligible. For economic reasons, the use of a natural gas powered CHP is examined as well. In general two decentralised (D1 and D2) supply concepts and two centralised supply variants (C1 and C2) have been developed and compared. For the centralised supply options sub-variants have been analysed, too.

DECENTRALIZED HEAT SUPPLY VARIANTS (D1 AND D2)

As part of the first decentralized supply concept (D1) a decentralized air / water heat pump system is investigated. During the summer months, the domestic hot water is prepared by solar thermal energy. The disadvantage of this concept is the high initial cost and the noise emissions of distributed generation units. As part of the second decentralized supply concept (D2) a decentralized gas fired condensing boiler with solar DHW supply is investigated. The second supply concept D2 serves as a reference case for assessment and pre-selection of supply concepts.

Table 2. Overview of the investigated decentralised supply variants

Decentralized heat supply variants	
Decentralized (D1):	Decentralized air / water heat pump with solar DHW support
Decentralized (D2): Reference Case	Decentralized gas fired condensing boiler with solar DHW support

Table 3. Overview of the investigated centralised supply variants

Centralised heat supply variants	
Centralized (C1a)	Centralized geothermal powered HP for district heating supply at low temperature level of 20°C, decentralized heat pumps and solar thermal systems for DHW supply.
Centralized (C1b)	Centralized geothermal powered HP for district heating supply at low temperature level of 40°C. DHW preparation by solar/ heating rod
Centralized (C2a)	Centralized natural gas powered CHP for district heating supply in combination with demand-oriented power generation, a large heat storage and HP.
Centralized (C2b)	Centralized renewable-powered CHP for district heating supply in combination with demand-oriented power generation, a large heat storage and HP.

CENTRALISED SUPPLY VARIANT (C1): HEAT PUMP AND BOREHOLE HEAT EXCHANGERS

The first supply variant consists of a centralized heat pump connected to borehole heat exchangers (BHE). Depending on the supply variant, the ground acts as heat source and/or thermal storage. For the thermal regeneration of the ground unglazed solar collectors (swimming pool absorbers as a low-cost option) are intended to be used (see Figure 2). It is conceivable to use the district heating during heating period to provide (low temperature) heat.

As part of the preliminary investigation further sub-variants have been developed (e.g. regarding different temperature levels).

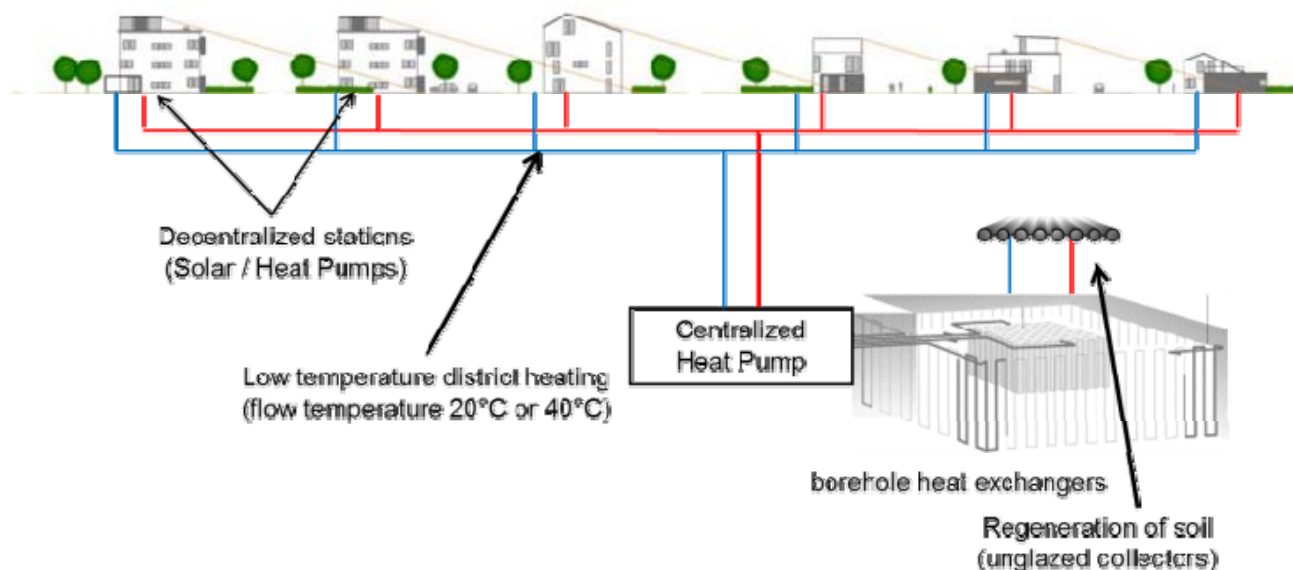


Figure 2. general description of hydraulic of centralised geothermal powered HP for district heating supply C1

Description of supply variant (C1a)

In supply variant (C1a) a centralised ground coupled heat pump feeds the district heating grid at a temperature level of 20°C. In order to supply the building for space heating and domestic hot water preparation the temperature level must be raised. For this purpose two variants, or a combination of these variants depending on the required temperature level of 45-60°C (DHW preparation or space heating) are possible. The first possibility is the application of a decentralized heat pump, which raises the temperature to the required temperature level for space heating and DHW preparation. The second possibility for decentralized reheating is to use thermal solar collectors (e.g. flat-plate collectors), wherein this variant is appropriate only during summer months. The solar collectors could be installed on the roof of each building or on carports.

The advantages of this supply variant are that heat losses in the network are very low and operation of the heat pumps is very effective. A possible weakness of the supply variant is the very low flow temperature. The lower the supply temperature the higher are the pumping costs and the high unit costs of de-central and small heat pumps.

Description of supply variant (C1b)

In supply variant (C1b) a centralised ground coupled heat pump feeds the district grid at a temperature level of 40°C. The heat for space heating is supplied directly by the district heating network through the use of heat exchangers. For preparation of DHW different variants are possible. In case of separated domestic hot water preparation thermal solar collectors (e.g. flat-plate

collectors) or a heating rod (with a preheating via district heating) could be used. The solar panels could be installed on the roof or on carports.

The advantage of this supply variant is the direct use of heat for space heating from the grid (substation required). No decentralized heat pumps must be installed and thus the investments costs are significantly lower.

Storage technologies

The DHW and the heat for space heating (variant C1a) will be stored in buffer tanks which are intended to be located in the thermal envelope of the buildings.

As storage option for heat for space heating (variant C1a and C1b) the BHE field is also available. This field is planned at the border of the development area. The thermal regeneration of the ground takes place via unglazed solar absorbers. The absorber technology is very cheap and effective (approx. 1 €ct / kWh of heat in an installation area of approximately 1.500 m²).

CENTRALISED SUPPLY VARIANT (C2): HEAT PUMP AND CHP PLANT

In the second centralized supply variant (including sub-variants C2a and C2b) a combination of a CHP plant (140kW_{el} / 207kW_{th}) and a ground coupled heat pump with 535 kW heating capacity has been investigated. According to manufacturer's instructions the heat pump can achieve a COP greater than 4.0 even if the supply temperature is higher than 35°C. As fuels for the CHP plant both fossil fuels (C2a - natural gas) and renewable energy sources (C2b - bio methane) are eligible. To increase the system efficiency a solar collector field (vacuum tube collector) is considered. Additionally a gas fired backup boiler is planned. The network operation temperature for space heating is 35°C - 50°C. For domestic hot water preparation the grid temperature will be increased to 70°C 1-2 times a day for ~ 1.5 h.

Storage Technologies

As heat storage option for heat for space heating the BHE field is available, see variant C1. For the storage of high temperature heat of 70°C-80°C (variant C2), two buffers with a volume of 25 m³ are foreseen. It has been determined that this size is sufficient for the sole heating of all decentralized DHW storage tanks located in the buildings including heating of the district heating grid.

Control strategies

Three control strategies for the operation of CHP and heat pumps are eligible. The first possible strategy is the usage of the CHP plant in case of base load and the heat pump for covering the peak load.

The second possible strategy is to run CHP and heat pump in parallel. In this variant the CHP plant charges the storage tank with high temperature heat.

The third strategy is to run the CHP plant during peak load and the heat pump during base load. The heat pump supplies the heat generated to the network or to the storage and thus covers the entire base load heat demand.

PLANNED NETWORK DESIGN AND HEAT LOSSES

Based on the investigated supply options (refer to Table 2 and Table 3), the selection of suitable district heating pipes is made. Within the project the installation of PEX twin pipes (PN 6/10 bar) is considered. These pipes are cost effective and are characterized by low heat losses. The heat loss through the district heating network are estimated to be ~ 40 MWh/a, corresponding to ~ 2,5% related to the useful heat of 1.564 MWh/a.

ASSESSMENT AND PRE-SELECTION OF SUPPLY CONCEPTS

For assessment and pre-selection of suitable supply variants different parameters and characteristics are considered. The parameters are classified into "technical", "economic" and "soft" factors; for each case a subdivision is made. The "technical" parameters include the primary energy demand, CO₂ emissions and space requirement for installed supply technology. Depending on the supply concept other parameters are taken into account indirectly. For the HP the seasonal performance factor (SPF), for CHP the coefficient of performance (COP) and for the use of solar systems the efficiency of the absorbers, solar yield and solar fraction are considered. The "economic" parameters include the annual heating costs (including investment and operating costs, maintenance costs and arising costs for the consumer) as well as price stability. Moreover the determination of the amortization period and the expected return on invest is of importance.

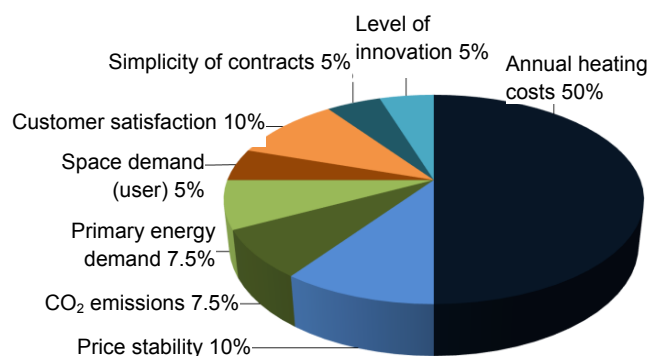


Figure 3. weighting factors for assessment of supply concepts as discussed with the partners

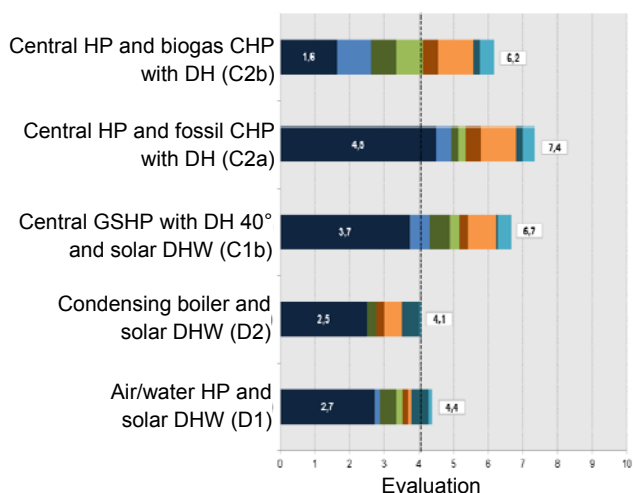


Figure 4. Assessment and pre-selection based on weighting factors (see also figure 3)

The "soft" factors include the consideration of the level of innovation and ease of use. Furthermore customer satisfaction and customer loyalty are factors that have to be considered, because they also potentially contribute to the successful implementation of the project. Both, the assessment parameters and the weighting factors have been discussed and decided by the project partners.

RESULTS

Based on preliminary studies two de-centralized (D1 and D2) supply variants and two centralized supply variants (C1 and C2) have been selected and assessed. As reference case for assessment and comparison of different supply options serves variant D2. This supply variant comprises decentralized gas fired condensing boilers with solar DHW. The annual heating costs amount to 3.207 €/a (26 Ct/kWh), CO₂ emissions are 368 t/a and the primary energy demand amounts to 1.773 MWh/a.

For assessment and pre-selection of suitable supply variants different parameters and characteristics are considered. The key evaluation parameters, which are used for comparison of the variants, are shown in Figure 4. According to the weighting factors it turned out that the variants C1b (Centralized HP, decentralized DHW preparation by solar/ heating rod – 40°C) and C2a (Centralized fossil powered CHP/HP, without boiler without solar DHW) are the most suitable and selected solutions. Since the variant C2a integrates the combustion of fossil fuels, it has not been chosen for further investigation. The first variant is economically more favourable than reference variant D2 (Gas condensing boiler with solar DHW). In comparison to reference variant D2 both variants are advantageous due to environmental issues (CO₂ emissions, primary energy demand) too. The supply

concepts differ essentially with regard to the dependency on price of electricity (C1) and natural gas (C2).

The following figure contains the comparison and the detailed assessment of the individual supply variations.

DISCUSSION

In particular renewable energy sources offer great potential for sustainable and efficient heat supply of buildings. However, for optimized utilization of these resources it is necessary to identify appropriate technologies to ensure efficient supply for the new housing area. For this reason, extensive preliminary studies were carried out to identify suitable supply options. Since, in addition to the technical aspects economic aspects play a crucial role, an evaluation was developed that combines both aspects.

It turned out that the centralized heat supply variants integrating a district heating grid are more favourable, especially because of the 5 % lower annual costs (C1b). This is in contradiction to the common opinion that district heating grids are generally not cost efficient for low energy housing areas. The investigation for this particular project shows clearly the opposite.

OUTLOOK

Within first project phase efficient and economical heat supply concepts have been identified. The next necessary step within the project consists of detailed elaboration of the selected heat supply concept. In this course the verification of information which is relevant for the design of system characteristics is intended in order to increase planning reliability. Based on knowledge gained in the first phase the second phase will be carried out. The second phase consists of elaboration of the favoured supply variant and development of a detailed concept. In the course of the second phase core drillings and Enhanced Geothermal Response Tests (EGRT) will be carried out and geotechnical investigations (for example to investigate ion the geological and hydrogeological site conditions and to establish assessment of the geothermal ground properties, implementation of drilling) will be performed. In order to select and dimension the system components Enhanced Geothermal Response Tests (EGRT) will be carried out. Subsequently the development of a business model will be carried out. The last and final step includes detailed feasibility studies and a detailed estimation of costs.

CONCLUSION

In order to identify the best possible system solution for a new housing area planned in Kassel (Germany), different supply strategies were assessed and compared. Main objective is the development of an

innovative and optimised heat supply concept based on renewable energies and low temperature district heating. Central challenge in achieving this objective is the identification of the most promising and efficient technical solutions for practical implementation. Furthermore aspects of future network management as well as business models for distribution and operation are considered. As a result, the focus of this project is investigating suitable centralised or decentralised supply concepts for a new residential area using renewable energy sources.

Based on a preliminary study an innovative centralized heat supply concept is developed and selected in a political process for realization: C1b: Solar heating and geothermal powered heat pumps in a DH grid (40°C).

This variant is economically more favourable than the reference variant D2 (Gas condensing boiler with solar DHW). The annual heating costs are 5 % lower compared to the reference variant D2. Furthermore, this variant is advantageous due to environmental issues (CO₂ emissions and primary energy demand are approx. 63 % lower).

ACKNOWLEDGEMENT

The content of the paper was developed as part of the above mentioned collaboration. The financial support given to the project by the City of Kassel and the Staedtische Werke Kassel AG is greatly acknowledged by the project partners. Furthermore, the financial support given by the German Federal Ministry of Economic Affairs and Energy under support code: 03ET1336 A, B, C & E to conduct the second phase of the project is highly acknowledged by all involved project partners. The authors are responsible for the content of this paper.

REFERENCES

- [1] Development plan Nr. IV/65 „Zum Feldlager“; Architektur+Städtebau Bankert, Linker & Hupfeld, City of Kassel- Urban planning, building supervision and monument conservation; 02 February 2013
- [2] EnEV2014 - Regulation on energy-saving insulation and energy-saving systems engineering for buildings (Energy Saving Ordinance - EnEV); 01. Mai 2014
- [3] DIN V 18599-1: 2011-08. Energy efficiency of buildings – Calculation of the net, final and primary energy demand for heating, cooling, ventilation, domestic hot water and lighting
- [4] DIN V 18599-2: 2011-08. Energy efficiency of buildings – Calculation of the net, final and primary energy demand for heating, cooling, ventilation, domestic hot water and lighting –Part 2: Net energy demand for heating and cooling of building zones
- [5] DIN V 18599-4: 2011-08. Energy efficiency of buildings – Calculation of the net, final and primary energy demand for heating, cooling, ventilation, domestic hot water and lighting –Part 4: Net and final energy demand for lighting
- [6] DIN V 18599-5: 2011-08. Energy efficiency of buildings – Calculation of the net, final and primary energy demand for heating, cooling, ventilation, domestic hot water and lighting – Part 5: Final energy demand of heating systems
- [7] DIN V 18599-8: 2011-08. Energy efficiency of buildings – Calculation of the net, final and primary energy demand for heating, cooling, ventilation, domestic hot water and lighting Part 8: Net and final energy demand of domestic hot water systems
- [8] DIN V 18599-10: 2011-08. Energy efficiency of buildings – Calculation of the net, final and primary energy demand for heating, cooling, ventilation, domestic hot water and lighting - Part 10: Boundary conditions of use, climatic data

done in the supply or in the return line of the DH system. Viborg DH in Denmark is an example where the surplus heat from the new Apple computer center will be rejected to the DH system. To provide heat for the DH system, high temperature heat pumps will be implemented, thus providing directly supply water for the DH system of approximately 55°C. To enable this, Viborg DH had a long-term plan for decreasing the DH temperature and distribution losses. Customers with the high temperature requirements will be grouped and provided with an additional heat pump for increasing the temperature level. In Trondheim, Norway, excess heat from cooling the datacenter at the university campus was utilized by connecting in the return line. The reason for this was currently high temperature level requirement for the existing buildings. To enable integration of the excess heat, the university campus separated from the main connection to the Trondheim DH by using heat exchangers and establishing own DH ring, see Figure 2. In that way, it was possible to control the supply and return water temperature in the university DH ring and utilize excess heat from the datacenter. Proper control was enabled easily because university is property owner and has own maintenance service with a powerful building energy monitoring system for the entire campus. Currently, the excess heat may provide the base heat load in the range of 1 to 1.2 MW entire year.

In this study, possibilities and necessary measures to utilize more renewables from the distributed sources in DH system in Norway were analyzed. In the study, it was assumed that the distributed sources may be connected to the building area. Therefore, analysis of the area size and their possibility to deliver heat to the central DH was analyzed too. The objectives were to (i) identify the size of the building complex able to deliver heat to the DH system and (ii) identify the typical measures that may enable a higher share of renewables delivered by building complexes. The idea was that heat pumps, solar collectors, and waste heat recovery might be installed at different buildings and contribute to the DH system. An optimization analysis was carried out in order to determine the optimal size and amount of the heat sources with respect to DH cost, electricity cost, investment cost for these components, plant performance, and total heat demand. The aim was to get low cost for heating with a low investment cost at the same time. The optimization problem was hence defined as a multiobjective optimization problem with two objective functions: heat cost and investment cost.

The article is organized as follows: first model for analysis of the DH system with distributed heat sources is presented. Potentials for heat interactions and analysis are given in the result section.

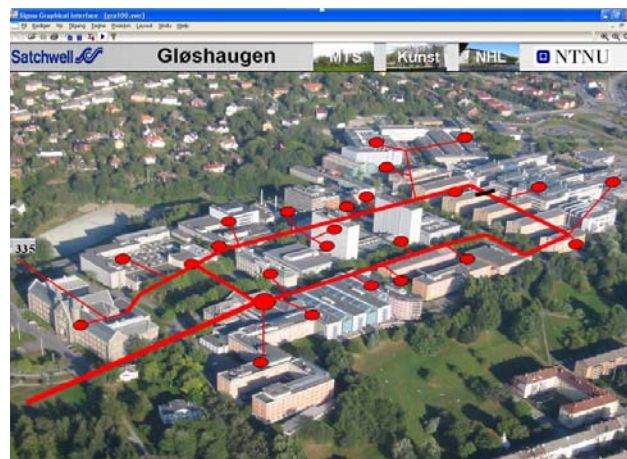


Figure 2. Use of excess heat at NTNU in Trondheim, Norway [6]

METHODOLOGY

To evaluate possibilities to utilize distributed heat sources at building complexes and their interaction to the DH system, a heat balance model for an imaginary building area with possibility for heat generation was developed. Since the aim of the study was to evaluate possibility and identify the most necessary measures in this new systems with distributed sources, the model was developed on annually basis.

For an imaginary building area, the total annual heat demand may be calculated as:

$$Q_{Tot,A} = \sum_i p_i \cdot q_i \cdot A \quad (1)$$

where p is the percentage of buildings of the certain type, q is the annual specific heat demand of the certain type, and A is the total building area. i is counting different building types.

In the case when heat pumps might produce heating and cooling for the buildings where they were located and in addition export heat to the DH grid, the total heat production from the heat pump over the year may be calculated as:

$$Q_{HP} = COP \cdot W_c \cdot n_{HP} \cdot \tau_{HP} \quad (2)$$

where $COP (-)$ is coefficient of performance for the heating mode of the heat pump, $W_c (kW)$ is the compressor power, $n_{HP} (-)$ is number of the heat pumps that might be installed in the imaginary area, and $\tau_{HP} (h)$ is the assumed operation time of the heat pump on the annual level. n_{HP} was calculated based on the number of office and commercial buildings at the area.

Heat provided from the solar collectors might be calculated as:

$$Q_{sol} = \eta \cdot q_{sol} \cdot A_{sol} \quad (3)$$

where q_{sol} (kWh/m²) was total specific annual solar irradiation, A_{sol} (m²) was area of the solar collectors, and η (-) was the average efficiency of the solar collector.

In the future DH systems, all the heat has to come from the renewables, such as waste heat, solar, and geothermal. In that case the heat delivered from the central DH system can be expressed as:

$$Q_{dhs,ren} = Q_{Tot,h} - Q_{HP} - Q_{WH} - Q_{sol} \quad (4)$$

In Equation (4), Q_{WH} (kWh) is available waste heat that might contribute to the DH system. The waste heat sources may be some industrial process or waste heat from high energy use buildings such as hospitals.

As explained before, the aim was to evaluate possibilities for a higher share of renewable energies into the DH system. Therefore, it was important to estimate additional cost for investment in the solar collectors and heat pumps as:

$$C_{additiv} = f_{HP} \cdot COP \cdot W_C \cdot n_{HP} + f_{sol} \cdot A_{sol} \quad (5)$$

where f_{HP} (EUR/kW) was the investment cost for the heat pump based on the condenser capacity and f_{sol} (EUR/m²) was the investment for the solar collectors per unit of area. The total heat cost for such DH system was calculated as:

$$C_{heat} = c_{dh} \cdot Q_{dhs,ren} + c_{el} \cdot W_C \cdot n_{HP} \cdot \tau_{HP} + c_{wh} \cdot Q_{WH} \quad (6)$$

where c_{dh} (EUR/kWh) was district heating price, c_{el} (EUR/kWh) was electricity price, and c_{wh} (EUR/kWh) was waste heat price. The specific heat cost for heat was calculated as:

$$c_{heat} = C_{heat} / Q_{Tot,h} \quad (7)$$

The total cost for the heat and additional investment was:

$$C_{Tot} = C_{additiv} + C_{heat} \quad (8)$$

The total specific cost for heat was calculated as:

$$c_{Tot} = C_{Tot} / Q_{Tot,h} \quad (9)$$

To evaluate possibilities for a higher share of renewable energies into the DH system, the objective was to decrease heat production from the central DH system, while the total specific heat cost had to be low.

Therefore, the optimization problem was defined as a multiobjective problem, where the objective function was defined as:

$$\min(Q_{dhs,ren}, C_{Tot}) \quad (10)$$

where the optimization parameters were: W_C , compressor power, n_{HP} , number of the heat pumps, Q_{WH} , available waste heat, and A_{sol} , area of the solar collectors.

RESULTS

Before the results are presented, the model and optimization input are introduced. Possible plant size, plant performance, and heat demand were assumed based on the literature review and statistical data. In this analysis, a building structure with high percentage of residential buildings was analyzed. Finally, the optimization results and the necessary measure analysis for different size of the area are given.

Model and optimization input

In this study, an imaginary area was assumed with four different building types: residential, multipurpose, office, and high energy use buildings. The high energy use buildings presented buildings such as hospitals or sport centers. Based on the national building energy use statistics and residential energy use [7], the specific heating use was defined for each building type and is given in Table . Specific heat demand was defined as 70 % of the total energy demand. This is a usual assumption for the Norwegian conditions. A building complex may consist of different percentage of the above mentioned building types. Based on the Norwegian statistics on the building stock [8], the building stock should have the structure as given in Table . This building structure presented a typical situation in a town with lots of residential buildings.

The other model input parameters are given in Table 2. These parameters were based on annual average values, because the introduced model was based on annual calculation.

Table 1. Building heat demand and area structure

Building type	Specific heat demand (kWh/m ²)	Building area structure
Residential buildings	119	66 %
Multipurpose buildings	154	20 %
Office buildings	140	12 %
High energy use buildings	280	2 %

Table 2. Model inputs

Parameter name and unit	Value
Heat pump operation time, t_{HP} (h)	3 000
COP of the heat pumps, COP (-)	3
Total specific annual solar irradiation, q_{sol} (kWh/m ²)	400
Average efficiency of the solar collector, η (-)	0.75
Investment cost for the heat pump, f_{HP} (EUR/kW)	500 [9]
Investment for the solar collectors, f_{sol} (EUR/m ²)	300 [10]
District heating price, c_{DH} (EUR/kWh)	0.08
Electricity price, c_{el} (EUR/kWh)	0.1
Waste heat price, c_{wh} (EUR/kWh)	$0.3 \cdot c_{DH}$

The parameter values in Table 2 were defined based on the literature review in [9] and data for solar thermal collectors [10]. District heating and electricity price were assumed for the Norwegian conditions. The price for the waste heat was assumed, since still there is no clear indication on the price level for the waste heat.

In order to define an optimization problem, it is necessary to define the upper and lower bounds for the optimization parameters. In this study, the upper and lower bounds were defined based on the previous analysis of the energy supply plants within the research project Interact [11] and possibility to install solar collectors. Regarding possibility for the heat export from the heat pumps, it was assumed that the office, multipurpose, and high energy use buildings might have possibility to install big heat pumps and export heat when relevant. Based on the analysis of the energy supply plants, the installed compressor rate for the heat pumps was between 150 to 450 kW. To estimate potential number of the heat pumps, it was assumed that these buildings could have an average area of 10 000 m². By dividing the total area of the

mentioned buildings, potential number of installed heat pumps was obtained. Consequently, the lower and upper bounds for the number of heat pumps were defined to be from 3 to 50. Regarding possibility for the solar collector area, it was assumed that the office, multipurpose, and high energy use buildings might get installed solar collectors on the roof. In the case that average building height is three floors, the potential area for installing solar collector was three times lower than the total building area. The lower and upper bounds for the solar collector area were defined to be from 1 000 to 11 000 m².

Possibility of building complex to deliver heat to the DH system

Firstly, an analysis on how different building area size influence amount of delivered heat to the central DH system is presented. Since building complexes may have different size as shown in [11], building area sizes from 20 000 to 100 000 m² were analyzed. In this analysis where the building complex interact with the central DH, it was assumed that only business related buildings might export heat to the central DH system. Regarding number of the heat pumps, it was assumed that on each 10 000 m² of this type of buildings, one heat pump of 100 kW compressor power would be installed.

Regarding size of the solar collector area, it was assumed that the area was three times lower than the total building area of this type. Based on these assumptions, the possible amount of heat to be delivered to the central DH system was estimated for different building complex size as shown in Figure 3.

The possible amount of heat that might be delivered to the central DH system in Figure 3 vary a lot depending of the area size. The reason for this was that one heat pump came on each 10 000 m² of business related buildings, and in the model the number of heat pump was a round number. Also, size of the solar collectors

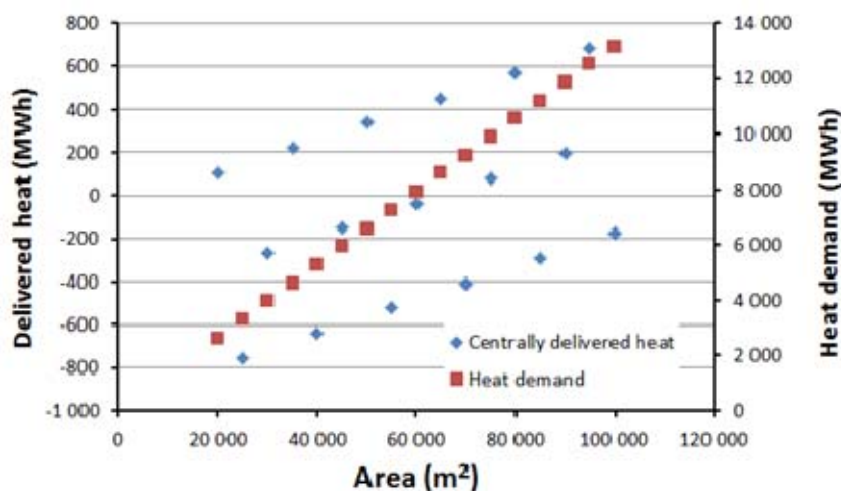


Figure 3. Possibilities of different building area structure to interact with the central DH system

was related to the size of the business related buildings. Due to the high share of the residential buildings that were not contributing to the central DH system, just using directly the DH heat, amount of heat was varying depending on the business related building sizes e.g. their possibility to produce excess heat for the central DH system. In the case, when in a building complex business buildings dominated, a building complex might deliver much more heat to the central DH system than itself might have need for heat. In that case there is no so big variation in the delivered heat. The situation with a high percent of business buildings is not presented in Figure 3. The results in Figure 3 show that the bigger the building complex, more excess heat might be produced. This meant that a building complex might be an active prosumer and deliver lots of renewable heat to the central DH system for the Norwegian conditions. In addition, due to this high amount of heat, daily and annual heat storage systems would be necessary.

Based on the heat amount that might be provided from

the building complexes, further analysis on the specific heat cost and total specific cost was performed as shown in Figure 4. To recall, the total specific cost included the additional investment for the heat pumps and solar collectors and heat cost.

The results in Figure 4 shows that the total specific cost in the area with the high share of residential buildings might achieve values lower than 0.05 EUR/kWh, which is the DH price for the solar DH, SDH Solar District Heating [12]. This meant that the solution to utilize heat from the business buildings resulted in a very favorable DH cost.

Optimization results and measure analysis

The multiobjective optimizations were performed for the building area of 20 000 m² and 100 000 m² and for building area structure with the high share of residential buildings. To recall, the objectives were to decrease the amount of heat centrally delivered and to decrease the total specific cost. The Pareto frontiers for the mentioned building areas are given in Figure 5. The

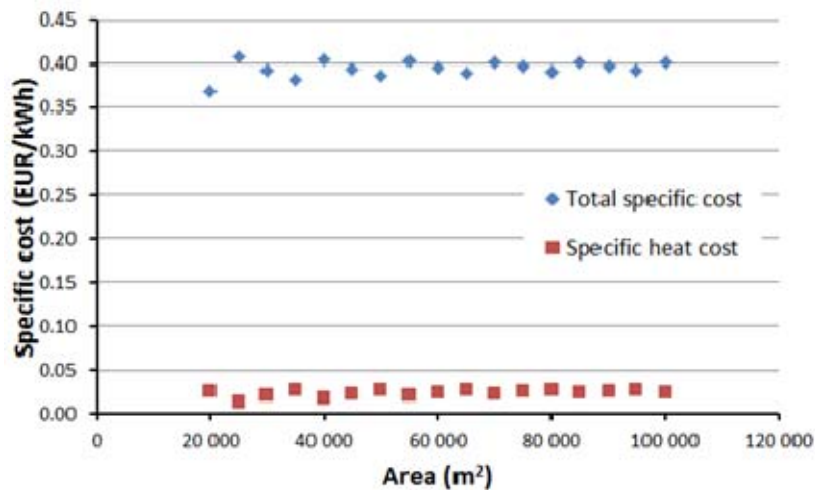


Figure 4. Specific heat and total investment cost

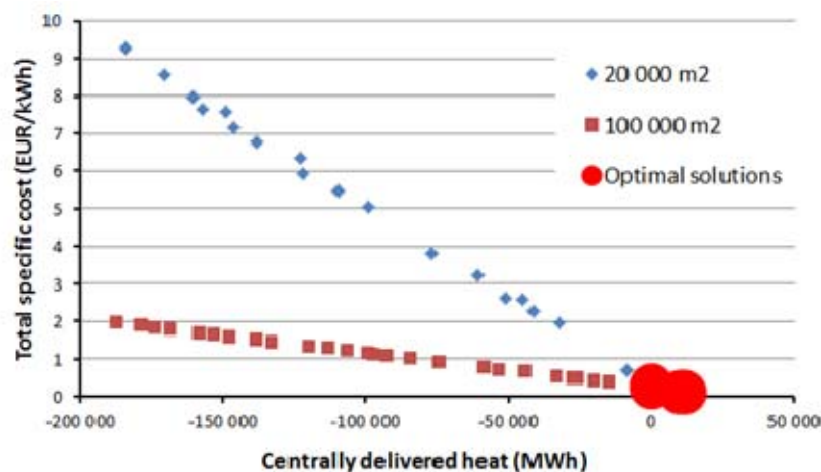


Figure 5. Optimization results for small and big building complex area

optimal solutions may be chosen from the entire range of the Pareto frontiers. In this study, it was chosen that the optimal solutions are those where the total specific cost is the lowest. This meant that the total energy cost and additional investment per kWh of heat were the lowest.

When observing the Pareto frontiers in Figure 5 for different size of the building area, it may be concluded that the bigger area had much higher possibility to produce heat with lower cost. For smaller area the investments for the heat pumps and solar collectors were high compared to the provided heat.

It is interesting to note, that the optimal solution for the 100 000 m² area was still using about 10 GWh of the DH heat centrally delivered. The reason was that use of centrally delivered heat was still cheaper than use of the heat from the heat pump and solar collectors. The big area may become a big heat prosumer, but with the current prices, see Table 2, it was still not completely favorable.

To evaluate and suggest which measures might help to a higher share of renewables, a few scenarios with different measures were suggested. The scenarios are given in Table 3.

Table 3. Measures to enable a higher share of renewables into DH

Scenario	Brief description
As input data	See Table 2
Lower investment for solar	$f_{sol} = 150 \text{ EUR/m}^2$
Heat pump advantage	COP = 4 $f_{HP} = 300 \text{ EUR/kWh}$
All the measures	COP = 4 $f_{HP} = 300 \text{ EUR/kWh}$ $f_{sol} = 150 \text{ EUR/m}^2$ $c_{el} = 0.19 \text{ EUR/kWh}$ $c_{gas} = 0.2 \text{ EUR/kWh}$

Firstly, measures to promote a single technology such as solar collectors or heat pump were suggested. Finally, a combination with different energy price, investment cost, and higher heat pump performance was suggested as the final measure, called “All the measures”. The reason to decrease the investment

cost for the renewable energy technologies was that usually the cost should be lower in the future when the technologies are well established. In addition, to promote a higher use of renewables, many governments give support for the investment. Performance of a heat pump may be significantly improved if a proper heat pump is chosen for the observed load and if the temperature levels for heating and cooling are favorable. In the case of LTDH, the temperature in the DH network will become lower, enabling that the heat pumps might achieve a good average COP values. In addition, cooling loads in office buildings and data centers is usually stable over the year, allowing good operation conditions for the heat pumps between the cooling load and the LTDH network. The final measure combined all the benefits of low investment and high performance, but considered a higher electricity price in the future.

The results how the above measures could help a higher penetration of the renewable energies into the distributed DH system are given in Figure 6 for the 20 000 m² building area and in Figure 7 for the 100 000 m² building area. Figures 6 and 7 show the Pareto frontiers when the above measures were included.

The results in Figures 6 and 7 show that when only solar collectors would be cheaper for 50 %, the total specific heat cost would not be much lower. This means that a solely measure to enable cheaper solar collectors would not help a higher share of renewables for the Norwegian conditions. The second measure, where the heat pump performance was better together with the lower investment cost, gave much faster

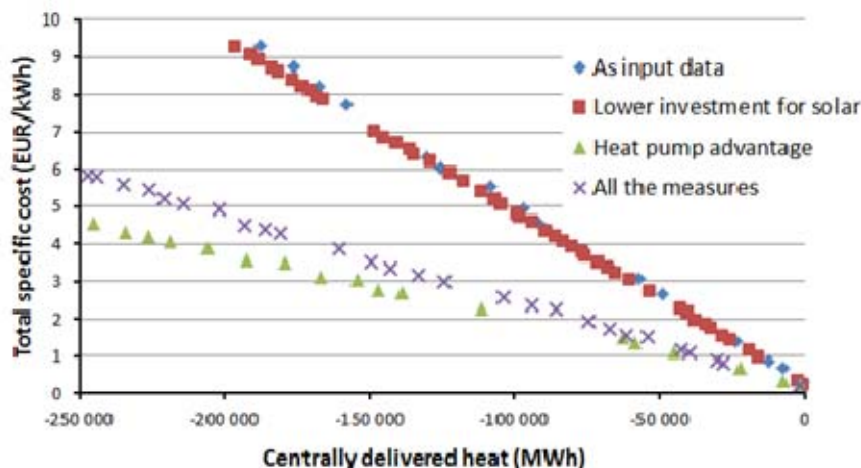


Figure 6. Results of the measures implementation in the 20 000 m² building area

decrease of the total specific heat cost.

The final measure, combining different measures, would not give significant decrease in the total specific heat cost as the measure with the heat pump. The conclusion from Figures 6 and 7 is that better performance of the heat pump and lower investment cost may enable a higher share of the renewables from the prosumers. These prosumers were related to the building complexes.

By comparing the results in Figures 6 and 7, it may be concluded that the total specific heat cost is again lower for the bigger area, see Figure 7, than for the small area. This means that the bigger area or building complexes should be considered as an active prosumer or a new partner to the central DH system.

CONCLUSION

The aim of the study was to identify some of the necessary measures to enable easier connection of the distributed heat sources such as solar and waste heat. Different sizes of building area including a high share of residential buildings were analyzed for the Norwegian conditions.

The energy balance model for the heat supply and demand on annual level was developed. The model was used for the optimization. Since the simple heat balance model was developed, heat storages were not considered in this study. Implementation of the heat storage may also increase the total specific cost.

The results showed that the building complexes might deliver a substantial amount of heat to the central DH system. The bigger the building area, the more heat might delivered. Sensitivity analysis of the results showed that the bigger area was less sensitive in the change of the parameters. All these meant that the big building complexes should be considered as an active

prosumer or a new partner to the central DH system in the future.

For the current economic conditions, it was still favorable to use a big part of the heat from the central DH plant. By analyzing different measures to enable a higher share of the renewables into the DH system, it was found out that lower investment and better performance of the heat pump gave the best results and the fastest decrease of the total specific cost. The increase in the heat pump performance might be easily achieved in the LTDH, because the temperature in the DH network will become lower, enabling lower temperature rise for the heat pump. In addition, cooling loads in office buildings and data centers is usually stable over the year, allowing good operation conditions for the heat pumps between the cooling load and the LTDH network.

Future work should consider development of energy prices and operation issues to enable reliable heat delivery from renewables in the future.

REFERENCES

- [1] On the Promotion of the Use of Energy from Renewable Sources, Directive 2009/32/28 of the European Parliament and of the Council, E. Union, Editor 2010, Official Journal of the European Communities, Brussels.
- [2] L. Brange, J. Englund, P. Lauenburg, Prosumers in district heating networks - A Swedish case study. *Applied Energy*, 2016. 164: p. 492-500.
- [3] R. Schleicher-Tappeser, How renewables will change electricity markets in the next five years. *Energy Policy*, 2012. 48: p. 64-75.
- [4] D. Menniti, A. Pinnarelli, N. Sorrentino, A. Burgio, G. Brusco. Demand response program implementation in an energy district of domestic prosumers. in *IEEE AFRICON Conference*. 2013.
- [5] U. Persson, B. Möller, S. Werner, Heat Roadmap Europe: Identifying strategic heat synergy regions. *Energy Policy*, 2014. 74(C): p. 663-681.

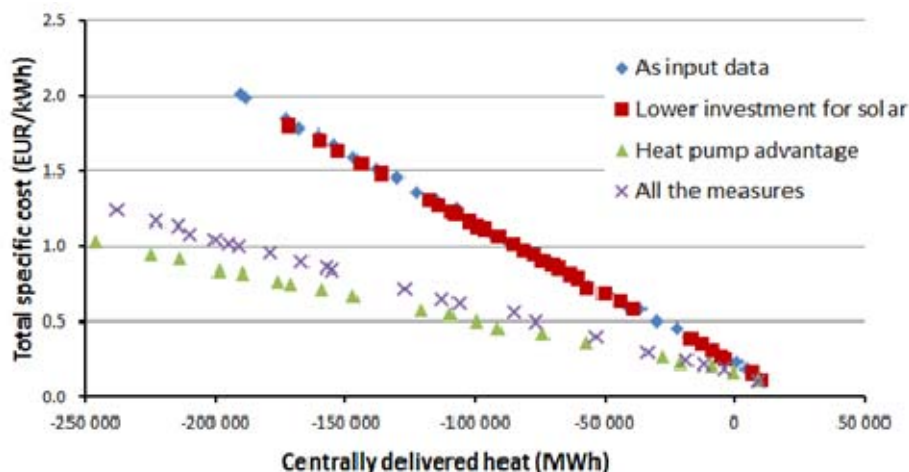


Figure 7. Results of the measures implementation in the 100 000 m² building area

- [6] NTNU Property owner, NTNU - reconstruction of the heat supply, 2012.
- [7] M.E. Ingebretsen, Possibilities for transition of existing buildings to the low temperature district heating system in Department of Energy and Process Engineering, 2014, Norwegian University of Science and Technology, Faculty of Engineering Science and Technology.
- [8] Statistics Norway. 2014; Available from: <http://www.ssb.no/>.
- [9] T. Tereshchenko, N. Nord, Energy planning of district heating for future building stock based on renewable energies and increasing supply flexibility. Energy, 2016. Accepted for publication.
- [10] S. Deutsche Gesellschaft für, Planning and installing solar thermal systems : a guide for installers, architects and engineers, 2005, London: James & James. 1844071251
- [11] Sintef Energy. Interact, 2014; Available from: <https://www.sintef.no/projectweb/interact/>.
- [12] SDH Solar District Heating in Europe - Guideline for end-user feed-in of solar heat, J.-O. Dalenback, 2015.

TRANSITION TO LOW TEMPERATURE DISTRIBUTION IN EXISTING SYSTEMS

M. Rämä¹, K. Sipilä¹

¹VTT Technical Research Centre of Finland

Keywords: 4GDH, low temperature district heating, existing systems

ABSTRACT

One key aspect of the 4th generation district heating systems [1] is low temperature solutions for distribution network – i.e. the supply temperature in the distribution network is set to lower level (30-70 °C, depending on design) than traditionally (80-115 °C). The temperature level has the most defining impact on the efficiency of the distribution due resulting heat losses. It improves the potential for integrating heat pumps and renewable energy sources such as solar heat into the system as more heat can be recovered from available heat sources. This is also favourable for utilisation of waste heat from e.g. industrial sources. Combined heat and power (CHP) production and boiler based heat production would benefit from a lower temperature level as well.

At the same time the transition to lower temperature level imposes challenges on pipe capacities within the network, heat exchanger and secondary side design. Low temperature distribution is simply a design choice for new systems, but refurbishing existing systems is much less straightforward and a current challenge in countries with developed district heating systems. Although technically feasible, required changes should be evaluated on a system level in order to confirm cost efficiency in terms of energy savings and emissions.

The needed investment and the benefits can also end up to be unevenly distributed among the parties, representing a practical barrier impeding or blocking the refurbishment.

This paper studies the effects and impacts of a transition to low temperature distribution in existing district heating systems, the needed technical solutions and the improved potential for utilising heat pumps and solar heat. A systematic method and tools for evaluating the system level benefits of the transition are described. This study lays the groundwork for a system specific case study of a major refurbishment of an existing district heating system.

INTRODUCTION

Current, ambitious greenhouse gas (GHG) emission reduction targets set by European Union (EU) pose a serious challenge for the energy systems in the member countries. Industrial heat consumption and heating and cooling of buildings corresponded to

approximately half of total final energy consumption in EU in 2013 [2], [3]. The importance of the sector is recognised in an EU Strategy on Heating and Cooling, announced 16th February 2016, setting up a framework for improving energy efficiency and sustainability within the industry, in buildings and their heating and cooling systems as well as for integrating heating and cooling into the electricity system. [4] District heating and cooling as a technological solution can clearly have a crucial role in the implementation of the strategy.

Replacing building specific heating and cooling system by expansion of district heating can potentially reduce primary energy consumption, fossil fuel consumption and CO₂ emissions in Europe by 7%, 9 % and 13 %, respectively. [5]

Using renewable energy sources as heat supply in district heating system can have a major impact due to large connected building stock. Currently, the share of renewable energy in heating sector energy supply is only 15 % [6]. Share of renewable energy in district heating in Finland reached 33 % in 2015 [7].

Integrating heating and cooling into the electricity system is an issue where district heating clearly has a potential to be one of the key solutions facilitating the integration of more variable electricity production such as wind and solar power into an energy system. [8]

District heating is currently developing towards a concept defined as 4th generation district heating (4GDH). Its main characteristics are closer connection to other long-term infrastructure planning processes, low temperature heat distribution systems within the buildings, a smart low temperature distribution network, improved waste heat and renewable heat source integration, and in overall closer integration with the surrounding energy system. [1]

One of the key aspects the 4GDH concept is the low temperature distribution, i.e. low temperature district heating (LTDH). This is typically defined as a system with supply temperatures between 30 °C and 70 °C [1].

A low temperature level in distribution greatly improves the potential for waste heat recovery, and use of renewable energy sources such as solar heat or heat pump technology utilising available, natural heat sources. It also improves the efficiency of more conventional heat supply technologies such as boilers and combined heat and power plants.

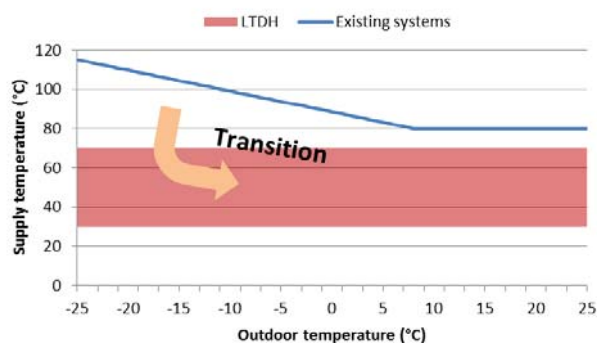


Figure 1. Supply temperature change in transition.

This paper investigates the transition process from high or medium to low temperature distribution in context of existing district heating systems. It describes the changes involved, and discusses the effects and relations between the components in a district heating system.

The barriers due unevenly distributed benefits and needed investments caused by the transition process are discussed and potential solutions presented.

The objective is to construct a framework and a systematic method for evaluating the benefits and challenges of moving towards LTDH systems. The study will lay the groundwork for a system specific case study of a major refurbishment of an existing district heating system. District heating system design in Finland is used as example where relevant and needed.

COMPONENT SPECIFIC IMPACTS

Transition to low temperature distribution will have an effect on the district heating network itself, on the heat supply and on the consumer equipment. The specific impacts on each of these are explained and their interactions discussed.

Existing systems e.g. in Finland typically use outdoor temperature dependent supply temperatures, resulting in temperature level varying from about 80 °C to 115 °C depending on the season. Transition to LTDH implementation would lower the supply temperature to a constant temperature within the region of 30 to 70 °C. This change is illustrated in the Figure 1..

This paper discusses district heating consumption for space heating point of view with less emphasis on domestic hot water (DHW) consumption. Temperature requirements for DHW production are in region of 60-65 °C depending on what temperatures for DHW are required by regulations. Loosening the sometimes strict requirements for DHW are one of the issues discussed in context of 4th generation district heating [1].

Heat supply

Lower temperature level in distribution enables more efficient heat recovery from any heat source. This includes the conventional technologies of boiler and CHP based production, heat pump based heat supply, solar collectors and utilisation of waste heat from e.g. industrial processes.

Both boilers and CHP units experience improved efficiencies due to lower distribution temperatures, especially on low supply temperature. This is due to continued heat recovery from steam and flue gasses. In CHP plants steam expansion can be continued to lower temperatures increasing power production and thus, improving the power to heat ratio of a CHP plant.

Lower supply temperature is more significant for heat pumps, solar collectors and utilisation of waste heat than for conventional heat production technologies. This is because it does not just improve the efficiency, but can actually enable the utilisation of these options at first place.

Efficiency or coefficient of performance (COP) of heat pumps depends heavily on condensation and evaporation temperatures within the heat pump process. These temperatures are in turn close to temperature of the heat sources and e.g. heated water. Lowering the temperature requirement for heat supply, i.e. supply temperature, will improve the efficiency of the process. Upper limit for the supply temperature provided by a heat pump is in the region of 80-90 °C.

Low distribution temperature increases the production potential for solar collectors. The traditional distribution temperatures of 80 °C and more are often on the maximum limit for a reasonable design. Thus the potential for solar heat in district heating systems can grow dramatically with lower distribution temperatures.

In overall, low distribution temperatures clearly represent a potential for improving the efficiency of the system from the heat production point of view.

Distribution of heat

A clear benefit of LTDH is that low distribution temperatures result in low heat losses. However, low temperatures also mean lower temperature difference between supply and return. This in turn results in either reduced transport capacity of the pipes in the network –

if the flow rate is unchanged – or higher pressure drop if the flow rate is increased to offset the effect of lower temperature difference.

Figure 2 presents the assumptions for corresponding supply and return temperatures as input for an example illustrating these effects.

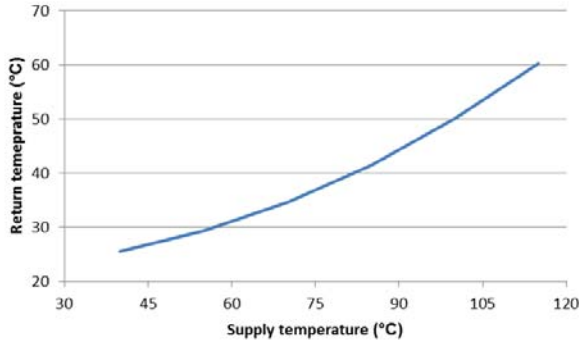


Figure 2. Assumed relation between supply and return temperatures.

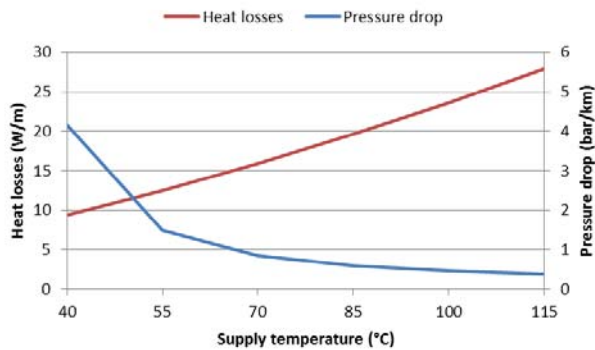


Figure 3. Heat losses and pressure drop with a fixed heat demand and varying supply temperatures.

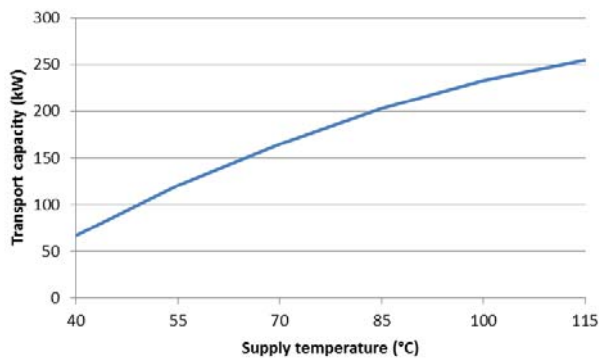


Figure 4. Transport capacity with a fixed pressure drop and varying supply temperatures.

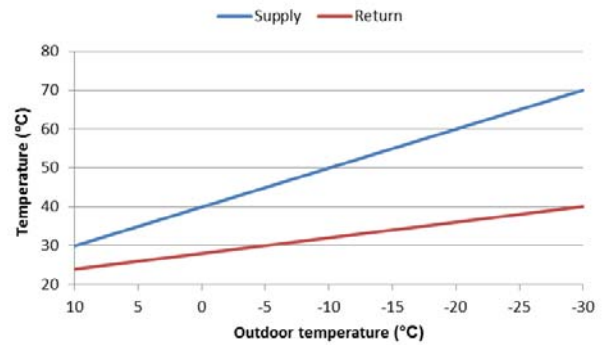


Figure 5. Typical outdoor temperature dependency for radiator based heating systems.

These temperatures and a constant heat demand of 150 kW were first used to calculate heat losses (W/m) and pressure drop (bar/km) for a DN50 size pipe (2Mpuk) with insulation according to current Finnish recommendations [9]. Average ground temperature of 5 °C is used in calculation. Figure 3 shows how heat losses and pressure drop relates to supply temperature with a defined constant heat demand.

Figure 4 shows the effects on transport capacity (kW) for the same DN50 pipe in a second calculation where the pressure drop is fixed at 1 bar/km and supply temperatures varied.

Figures 3 and 4 represent both the benefits and challenges of lower distribution temperatures from the distribution system point of view. Higher pressure drop can be compensated by additional pumping within the network.

Consumer equipment

Consumer equipment for a building connected to district heating consists of a substation and a heat distribution system within the building providing heat supply for the heated space.

The most significant elements in context of low temperature distribution are the heat exchangers both in the substation and in the heat space, i.e. radiators. Floor heating and ventilation based heating are easier to modify to enable use of lower supply temperatures. Floor heating generally requires temperatures of around 40 °C thus being a good fit for LTDH as such. Ventilation heat exchangers often require modifications only to the substation itself. Radiator based heating can require upgrade of the substation heat exchangers, but more extensive renovation is needed if the existing radiators cannot supply the required amount of heat due to lower temperatures.

In Finland, control systems set the supply (and return) temperatures within the distribution system. The temperatures are dependent on outdoor temperatures

as is the common practice at the district heating production plant. Supply and return temperatures for a typical 70/40 °C radiator system for existing buildings in Finland are presented in Figure 5 as a function of outdoor temperature.

However, high (> 50 °C) supply temperatures are used only during few hundreds of hours in a year of operation. This is illustrated in Figure 6 below as duration curves for supply temperatures according to aforementioned design temperature and outdoor temperature for a sample year in Southern Finland. It is assumed that with higher outdoor temperatures than 10 °C little or no heating is needed.

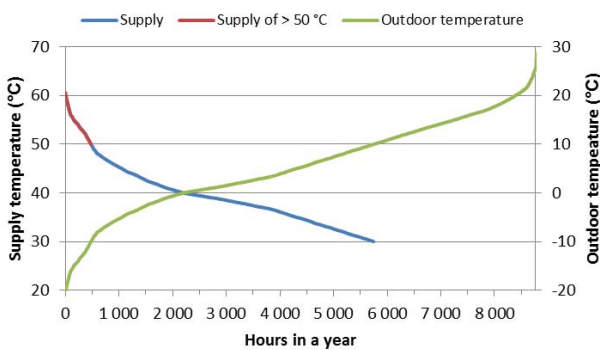


Figure 6. Typical outdoor temperature dependency for radiator based heating systems as a duration curve.

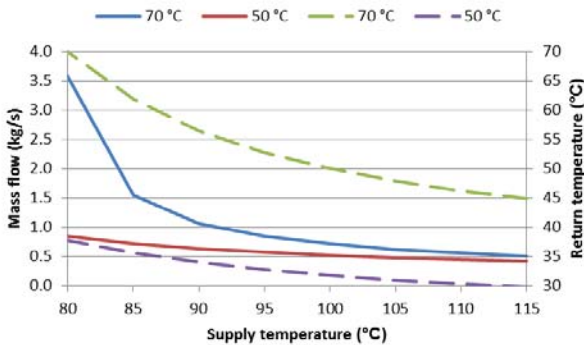


Figure 7. Comparison of mass flow and primary side return temperatures (dashed line) corresponding to 70 °C and 50 °C secondary side supply temperatures.

This example shows that high design supply temperatures on the secondary side, and thus also on the primary side are not required very often. When they are required, the increase could be offset by higher flow rate which would result in poorer cooling performance, i.e. temperature difference. Another option is to raise the supply temperature on-site by e.g. electric heaters or other heating technologies with low investment costs.

The mean logarithmic temperature difference is defined as

$$\theta_{\ln} = \frac{\theta_1 - \theta_2}{\ln\left(\frac{\theta_1}{\theta_2}\right)}, \text{ with} \quad (1)$$

$$\theta_1 = T_s - t_s \text{ and } \theta_2 = T_r - t_r \text{ where} \quad (2,3)$$

T_s Primary side supply temperature (°C)

t_s Secondary side supply temperature (°C)

T_r Primary side return temperature (°C)

t_r Secondary side return temperature (°C)

Basic heat transfer equation is defined as

$$G = \frac{Q}{\theta_{\ln}}, \text{ where} \quad (4)$$

Q Heat supply (W)

G Conductance (W/°C)

Calculating the mean logarithmic temperature difference and the conductance using equations (1-4) with design temperatures of 70/40 °C (secondary side) and 115/45 °C (primary side) and assuming that conductance of the heat exchanger remains a constant enables iterative round of calculations where primary side supply temperatures are varied from 115 °C to 80 °C with secondary side temperatures of 70/40 °C and 50/28 °C. Secondary side return temperature corresponding to a supply temperature of 50 °C is based on assumption presented in Figure 5. Using this method mass flow and primary side return temperature can be found out. Results of these calculations are presented in Figure 7. They show that with existing heat exchanger design, lower secondary side temperatures are essential.

Radiator systems of higher temperature requirements can still be commonly found in older buildings. Also, the systems are unfortunately often not balanced and require higher temperatures for longer periods of time.

Current recommendations [10] in Finland for designing radiator based heating are defined to lower temperatures, 45/30 °C (recommendation) or 60/30 °C (for exceptional cases). These are in line with long term objectives of moving towards lower distribution temperatures.

Lower distribution temperatures in the district heating network can also enable two-way connections for the consumers, i.e. concept of prosumer described and investigated in e.g. [11] that are to be considered as part of the heat supply in the evaluation process. Prosumer is a consumer with local heat production and

possibility to sell surplus heat to the district heating system.

EVALUATION OF THE TRANSITION

The transition to low temperature distribution generally improves the efficiency of the heat supply, reduces heat losses, but can cause transportation capacity problems in the distribution network and is likely to set constraints on heat exchangers located at consumer buildings. Table 1 lists the benefits and challenges. As seen from the contents, benefits are focused on heat supply and distribution, less so for consumers.

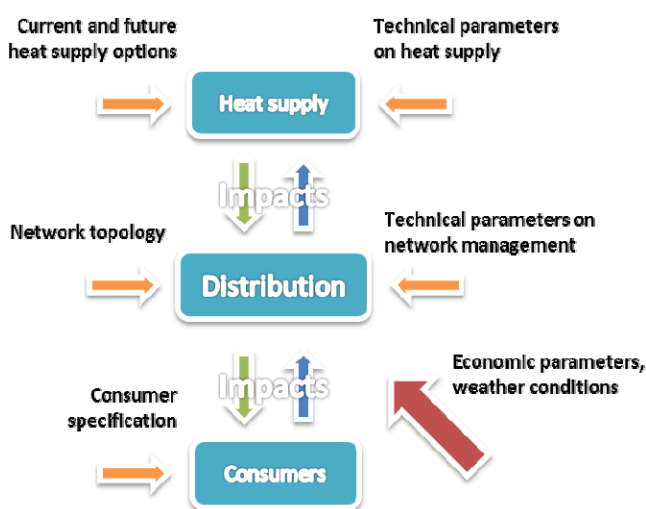


Figure 8. Input information for each component in the evaluation process.

Table 1. Benefits and challenges related to transition.

Component	Benefits	Challenges
Heat supply	Improved efficiency, opens up new possibilities for supply	Potentially negative effects on existing heat supply, more complicated operation and maintenance
Distribution	Less heat losses	Transport capacity issues, possible investment and additional management required
Consumers	Possibly reduced price of heat due to efficiency improvements in the system	Heat exchanger and internal heat distribution related capacity issues, needed investment

In order to evaluate benefits and challenges on moving to low temperature distribution and finding out what temperatures are feasible, variety of input information is needed. Table 2 to the right lists and describes the required input data.

The process of evaluation and what aspects need to be taken into account is illustrated in Figure 8.

Distribution is in a key role in the evaluation process as it connects the consumer related constraints to benefits of improved efficiency in heat supply. It can also set limitations on both supply and consumption. Simulation or other method of modelling the distribution network is needed.

Based on implications of Figure 6, if an investigated temperature level is found not to be technically feasible at the design point (e.g. peak demand) it could still be a reasonable choice if the number of hours where these conditions are present is small. Measures to address the technical limitation might exist in form of e.g. on-site heat supply if the limiting factor is secondary side temperature for a specific consumer.

Table 2. Input information required for evaluation of transition to low temperature system.

Input	Description
District heating network	Topology of the network (pipe sizes, lengths, and layout) enabling network simulations for finding out possible bottlenecks, pressure and temperature levels in design point.
Existing heat supply	Locations and technical characteristics of supply resources.
Technical parameters on heat supply	Current temperature levels and control principles, and how lower temperature level influences these, e.g. potential for heat recovery.
Plans for new heat supply options	Possible, planned options for new heat supply made possible or feasible by low distribution temperatures, e.g. heat pumps, solar collectors, waste heat.
Consumer specification	Consumer specific data on demand, heat exchanger specifications, building level heat distribution setup and control principles. Possibilities for on-site heat supply.
Economic parameters	Estimated prices of electricity, resources and fuels and investment costs for future options and needed renovation on distribution network or consumer equipment.
Weather conditions	Conditions that affect heat demand or temperatures e.g. within the building heat distribution system.

General principle of the evaluation is to lower the supply temperature level step by step, investigate on what is required from and, on the other hand, made possible by the lower temperature level, e.g. heat pump based heat production. In addition it needs to be studied that what actions are required to make the system technically feasible. Linking these actions to cost data will provide answers on whether the investigated temperature level is reasonable or not.

The investigation should be done from a system point of view, i.e. not taking into account the ownership of

different components within the system or any stakeholder involvement. It should be carried out in two parallel, but connected perspectives; economic and technical.

DISCUSSION

The studies on LTHD systems are always case specific due to the interactions between different components within the system. The district heating systems can vary significantly in terms of heat supply options, heat demand and heat demand density, pipe design and network structure. Therefore, it can be difficult and unreasonable to generalise results from any investigation. Results of any study should always be interpreted in context of the specific case. Additional studies need to be made to confirm the findings for another system.

District heating systems are often over-dimensioned; especially in distribution networks due to reduced heat demand or due to preparing for future expansion of the system, and concerning consumer equipment, i.e. larger substation heat exchangers and radiators than actually needed. However, as proposed in this paper, this is still a fact that needs to be systematically confirmed.

In order to enable integration of renewable energy sources as a heat supply option for district heating, low temperature distribution is essential. Closer integration with the electricity sector through continued utilisation of CHP production and controllable electricity based production such as heat pumps will ensure the role of district heating in the future energy system. Lower temperature level will also open up more possibilities for efficient heat storages. Combined with the connection to electricity supply, this can play a major role in addressing the issues of energy storage and flexibility needed by variable renewable electricity production based on wind and solar energy. [12]

CONCLUSION

Low distribution temperatures are an integral part of future 4th generation district heating systems, improving the system level energy efficiency. They also significantly improve the integration potential of renewable energy sources in heat supply.

Transition to low temperature distribution has both benefits and challenges. Generally, it improves the efficiency of heat supply and reduces heat losses in distribution network. However, it can result in transport capacity issues, and potentially pose challenges on the consumer equipment.

Evaluating the transition process must be carried out as a system specific study. The paper in hand gives guidelines and describes a method for evaluating the benefits of using lower temperature levels in an existing

district heating system. The proposed method is to be tested in a case study in Finland.

REFERENCES

- [1] H. Lund, S. Werner, R. Wiltshire, S. Svendsen, J. E. Thorsen, F. Hvelplund, and B. V. Mathiesen, "4th Generation District Heating (4GDH)," *Energy*, vol. 68, pp. 1–11, Apr. 2014.
- [2] N. Pardo, K. Vatopoulos, A. Krook-Riekkola, J. A. Moya, and A. Perez, "Heat and cooling demand and market perspective," 2012.
- [3] Eurostat, "Final energy consumption by sector 2013," 2016. [Online]. Available: <http://ec.europa.eu/eurostat/tgm/table.do?tab=table&init=1&language=en&pcode=tsdpc320&plugin=1>. [Accessed: 13-May-2016].
- [4] European Commission, "Communication from the Commission to the European Parliament, the Council, the European Economic and Social Committee and the Committee of the regions: An EU Strategy on Heating and Cooling (COM(2016)51/F1)," *COM(2016)51/F1*, 2016. [Online]. Available: https://ec.europa.eu/energy/sites/ener/files/documents/1_EN_ACT_part1_v14.pdf. [Accessed: 13-May-2016].
- [5] D. Connolly, B. V. Mathiesen, P. A. Østergaard, B. Møller, S. Nielsen, H. Lund, D. Trier, U. Persson, D. Nielsson, and S. Werner, "Heat Roadmap Europe 2050 - First Prestudy," 2012.
- [6] International Energy Agency, "European Union - 28: Electricity and heat for 2013," 2016. [Online]. Available: <http://www.iea.org/statistics/statisticssearch/report/?country=EU28&product=electricityandheat&year=2013>. [Accessed: 13-May-2016].
- [7] Finnish Energy, "One-third of district heat production now carbon neutral," 2016. [Online]. Available: <http://energia.fi/en/topical-issues/lehdistotiedotteet/energy-year-2014-district-heating-one-third-district-heat-producti>. [Accessed: 13-May-2016].
- [8] D. Connolly, B. V. Mathiesen, P. A. Østergaard, B. Møller, S. Nielsen, H. Lund, U. Persson, D. Nielsson, S. Werner, J. Grözinger, T. Boermans, M. Bosquet, and D. Trier, "Heat Roadmap Europe 2050 - Second Prestudy," 2013.
- [9] Finnish Energy, "Kiinnivaahdotetut kaukolämpöjohdot, suositus L1/2016 Kaukolämpö (in Finnish)," 2016. [Online]. Available: http://energia.fi/sites/default/files/suositusl1_2016_kiinnivaahdotetut_kaukolampojohdot.pdf. [Accessed: 13-May-2016].

- [10] Finnish Energy, "Rakennusten kaukolämmitys. Määräykset ja ohjeet (in Finnish)," 2014. [Online]. Available: http://energia.fi/sites/default/files/julkaisuk1_2013_20140509_0.pdf. [Accessed: 13-May-2016].
- [11] L. Brange, J. Englund, and P. Lauenburg, "Prosumers in district heating networks - A Swedish case study," *Appl. Energy*, vol. 164, pp. 492–500, 2016.
- [12] H. Lund, B. Møller, B. V. Mathiesen, and A. Dyrelund, "The role of district heating in future renewable energy systems," *Energy*, vol. 35, no. 3, pp. 1381–1390, 2010.

PRIMARY ENERGY FACTOR FOR DISTRICT HEATING NETWORKS IN EUROPEAN UNION MEMBER STATES

E.Latõšov¹, A.Volkova¹, A.Siirde¹, J.Kurnitski², M.Thalfeldt²

¹ Tallinn University of Technology, Department of Thermal Engineering, Ehitajate tee 5, Tallinn, 19086, Estonia

² Tallinn University of Technology, Department of Structural Design, Ehitajate tee 5, Tallinn, 19086, Estonia

Keywords: *primary energy factors, district heating, energy efficiency*

ABSTRACT

The use of Primary Energy Factor (PEF) was chosen by European Union policy makers as an obligatory part of methodology for comparing the primary energy consumption of products, using different energy sources.

Approaches for definition of primary energy differ in EU member states. Different methodologies and definitions of primary energy factors have impact on calculation of energy sector key indicators, including district heating (DH) sector. The aim of the research was collection, analysis and systematization of data about PEF and its calculation and definition methods for DH in EU Member states.

Method used for data collection about EU Member States with adequate share of DH in heat supply is meta-analysis systematic review methodological approach, where main data sources are legislation and standards currently in force, which are used to regulate implementation of PEF in EU Member States with adequate share of DH in heat supply.

The main criterion for the classification of DH PEF in different countries is PEF determination procedure. Based on this criterion three main groups were analysed: single fixed DH PEF, differentiated DH PEFs and DH PEF, calculated for each DH network independently.

INTRODUCTION

According to the Directive 2010/31/EU of the European Parliament and of the Council of 19 May 2010 on the energy performance of buildings [1] (hereinafter EPBD recast), the European Union (hereinafter EU) Member States should draw up national plans for increasing the number of nearly zero-energy buildings.

The national plans shall include, inter alia, the Member State's detailed application in practice of the definition of nearly zero-energy buildings, reflecting their national, regional or local conditions, and including a numerical indicator of primary energy use expressed in kWh/m² per year. Primary energy factors used for the determination of the primary energy use may be based

on national or regional yearly average values and may take into account relevant European standards.

EPBD recast determines, that the energy performance of a building shall be expressed in a transparent manner and shall include an energy performance indicator and a numeric indicator of primary energy use, based on primary energy factors (hereinafter PEF) per energy carrier, which may be based on national or regional annual weighted averages or a specific value for onsite production.

The methodology for calculating the energy performance of buildings should take into account European standards and shall be consistent with relevant Union legislation, including Directive 2009/28/EC. In the calculation positive effects of such aspects as electricity produced by cogeneration, district or block heating and cooling systems, where relevant, shall be taken into account.

Unfortunately, EPBD recast does not provide a strict definition of PEF and rigid adherence to the standard concerning how to calculate PEFs for different energy chains. This fact creates confusion in unanimous understanding of the PEFs nature.

In general PEF can be stated as [2] primary energy divided by delivered energy, where the primary energy is that required to supply one unit of delivered energy, taking account of the energy required for extraction, processing, storage, transport, generation, transformation, transmission, distribution, and any other operations necessary for delivery to the building in which the delivered energy will be used. The use of primary energy factors has influence on the accounting of such targets as energy saving and use of renewable energy sources [3].

Determination and application of district heating (hereinafter DH) PEFs is not researched as well as PEFs for electricity [4, 5, 6], however importance of DH is significant. Heating and cooling consume half of the EU's energy where DH provides 9% of the EU's heating. In some countries, district heating is seen as an attractive option for companies and consumers and as a mean of improving energy efficiency and the deployment of renewables [7]. It was estimated that DH

could help Europe reduce total European CO₂ emissions by 9.3% by 2020 [8].

Evaluating the PEF of the specific DH system give possibilities to rate and compare the performance of a different DH systems. DH PEFs take into account heat losses of the heating network as well as all other energy used for extraction, preparation, refining, processing, and transportation of the fuels to produce the heat. DH PEF also may account for power produced in cogeneration plants (hereinafter CHP) and waste heat sources. [2]

The main objective of this article is to give constructive state of the art review analysis of the data sources in a field of DH PEF for EU countries and identify main differences and gaps in implementation of DH PEFs. It is expected, that this article will give state of the art information to experts in energy efficiency research areas and will promote further research activities on this field.

METHODOLOGY

Methodology to provide constructive analysis of the data sources in a field of PEF for DH for EU Member States consists of four main steps:

- 1) Selection of EU Member States with adequate share of DH in heat supply.
- 2) Definition of methods for data collection about EU Member States with adequate share of DH in heat supply.
- 3) Data collection in accordance with defined methods.
- 4) Collected data classification, analysis and comparison.

The scope of research includes only EU Member States. Not all EU Member states are presented in this study, but only countries, where DH plays important

role in energy sector. First step is elimination of countries, where district heating sector is not presented in country energy balance for the last five years, according to database of statistical office of the European Communities (hereinafter Eurostat).

Remaining countries are compared by share of inhabitants supplied by district heating. This criterion Remaining countries are compared by share of inhabitants supplied by district heating. This criterion allows to compare the importance of district heating in countries, which vary in terms of population, size and climate. Countries, where the share of inhabitants supplied by district heating is higher, than 1% will be selected for analysis of DH PEFs.

Method used for data collection about EU Member States with adequate share of DH in the heat supply is meta-analysis systematic review methodological approach, where findings from various individual studies are analyzed and pooled. Data sources used for review are selected based on validity criteria. High priority data sources are legislation and standards currently in force, which are used to regulate implementation of PEF in EU Member States with adequate share of DH in the heat supply. This study is a status quo type, where current situation for a given DH PEFs is presented.

DATA COLLECTION AND PROCESSING

Selection of EU Member States with adequate share of DH in the heat supply

Confirming to proposed methodology first step is elimination of EU Member States, where DH is not presented in energy balance. As it is shown in Simplified Energy Balances of EUROSTAT database

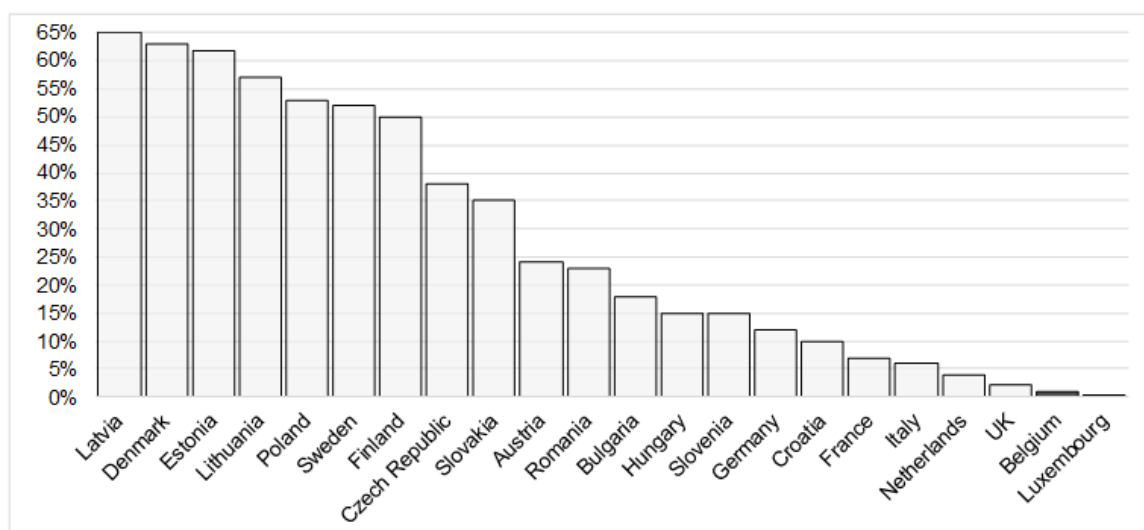


Figure 1. Share of inhabitants supplied by district heating in EU Member states [9, 10, 11]

[9] DH sector is not presented in national energy balances during last five years in Ireland, Greece, Spain, Malta, Cyprus, and Portugal. District heating sector is presented in Italy starting from 2010.

The criterion, chosen for further selection is share of inhabitants supplied by district heating. District heating has a significant role to play in energy sector of 20 EU Member States. As it can be seen from Figure 1 district heating provides heat energy for more than 1% of inhabitants in 20 Member States.

These countries are Austria, Bulgaria, Croatia, the Czech Republic, Denmark, Estonia, Finland, France, Germany, Hungary, Italy, Latvia, Lithuania, the Netherlands, Poland, Romania, the Slovak Republic, Slovenia, Sweden and the United Kingdom.

The policy, concerning primary energy factors for district heating sector will be analysed for these EU member states. Share of inhabitants supplied by district heating in Belgium and Luxembourg is not higher than 1% and they will not be considered.

Data collection and general criteria development for classification

Data about primary energy factors for district heating in EU member states was collected based on methodology described before.

During data collection it was found, that there are EU Members States in which:

- Single fixed DH PEF is used. This PEF is valid for all DH networks (for example in Finland, Estonia and Bulgaria).
- Differentiated DH PEFs are used, according to the fuels used and /or energy production technologies applied (for example, in Latvia, Czech Republic and Hungary).
- DH PEF is calculated for each DH network independently (for example, in Poland, Germany and Italy).

Consolidated data about sources applied during data collection, which define DH PEFs and information about the general types of DH PEF used (single fixed, differentiated or calculated DH PEFs) for respected EU Member States is presented in Table 1. Sources found are tentatively translated in *References / Sources* column of the Table 1.

There are EU Member States, which were not included in proposed classification structure: Croatia, Sweden, Romania and Netherlands. The reason, is that there is no use of PEF concept and/or insufficient of information obtained from various individual studies, legislation and standards to make a solid statement about situation

with DH PEFs. Description of current review results for those countries is shown below.

Sweden. According to [12, 13] the Swedish Energy Authority does not support the concept of primary energy factors. There is no information found that we should reject this statement.

Croatia. On the official webpage of Ministry of Construction and Physical Planning in the section of regulation in the field of energy efficiency, the methodology of conducting an energy audit of buildings and algorithm for calculating the energy performance of buildings are described [14]. According to the algorithm for determining energy requirements and efficiency of thermal systems in building (cogeneration and DH) are based on EN 15316-4-5 [2], which assumes calculation of DH PEFs for each DH system. Total number of DH systems in Croatia is about 110 [10].

The list with PEFs is also published on the official webpage of Ministry of Construction and Physical Planning [15]. This list consists of DH PEFs for a different regions of Croatia as well as country average value (total 18 different values which does not correspond with the number of DH networks).

Sources [14] and [15] are valid but contradictory. According to available information it is not possible to make a solid statement about situation with DH PEFs in Croatia.

Romania. There is rapid development in energy efficiency legislation in Romania. In August 2014 the Law no. 121/2014 on energy efficiency came into force. The Law transposes the European Union regulations set out under Directive 2012/27/UE regarding energy efficiency, into national legislation.

The main purpose of the Law is to establish a coherent legislative framework for the development and application of the national energy efficiency policy in order to achieve the national target for increasing energy efficiency.

Following the provisions of the Law no. 121/2014 on energy efficiency for the transposition of the Directive 2012/27/UE regarding energy efficiency, the Romanian authorities drafted the third National Energy Efficiency Action Plan (NEEAP III), government approved by Government Decision 122/2015 [16].

In [17, 18] a very good overview about implementing the EPBD in Romania is given. But after familiarization with respective legal the situation about implementation of DH PEFs was not clear enough. As an example PEFs are shown in [19] and [20] differs.

It is expected, that clarification of this topic can be possible after expanding methodology used in this

article to provide constructive analysis of the data sources (negotiations and consultations with Romanian experts in the field of energy efficiency is necessary).

Netherlands. According to [21] there are valid PEF for electricity, natural gas and heating oil. No PEFs for renewables and DH are applied or calculated. There is no information found that we should reject this statement.

Single fixed DH PEFs

There are five (5) EU Member States where single fixed DH PEFs are used. PEF values are shown in table 2.

DH PEF values differ more than two times and are in range between 0.6 (in Denmark) and 1.3 (in Belgium).

Denmark has a unique way to select and use DH PEFs. Applied DH PEFs can be different, but they do not depend on fuels or technologies used in DH area (values does not comply with differentiated DH PEFs group definition used in this article).

Table 1. Sources, references used for DH PEFs data collection and general types of DH PEFs for respective EU Member States

Type of DH PEF	Country	References / Sources
Single fixed	Bulgaria	Ordinance № E-RD-04-2 for the indicators of energy consumption and energy performance of buildings, 22.01.2016 [22]
	Denmark	Danish Building Regulations 2015 [23]
	Estonia	Minimum requirements for buildings energy performance. Revision in force: 01.07.2015 [24]
	Finland	D3 Energy management in buildings. Regulations and guidelines 2012. [25]
	France	Decree of 26 October 2010 on the thermal characteristics and energy performance requirements of new buildings and new parts of buildings [26]
Differentiated	Austria	OIB guidelines on energy savings and thermal requirements of the buildings. March 2015, OIB-330.6-009/15 [27]
	Czech Republic	Energy Performance of Buildings decree n. 78/2013 Coll. [28]
	Hungary	Ministerial Order the 7/2006. Decree of Minister without Portfolio, about Determination of Energy Efficiency of Buildings [29]
	Slovakia	Ministerial Decree n. 364/2012 Coll. on the energy performance of buildings and on the amendments to certain laws, as amended [30]
	Slovenia	Technical guideline for construction: TSG-1-004:2010 efficient use of energy [31]
	Latvia	Cabinet Regulation No. 348 of 25 June 2013 "Regulations Regarding the Methodology for Calculating the Energy Performance of Buildings" [32]
	Lithuania	Lithuanian Building Technical Regulation STR 2.01.09.2012 - Energy performance of buildings - Certification of energy performance of buildings, with amendments in 2016 [33]
	UK	The Government's Standard Assessment Procedure for Energy Rating of Dwellings 2012 editions [34]
Calculated for each DH network independently	Italy	Decree on the minimum requirements (decree 26 June 2015), Annex 1 [35], Coordinated text of decree-law 4 June 2013, n. 63 [36], UNI/TS 11300 standards [37]
	Germany	Energy Performance of District Heating - Determination of the specific primary energy factors in district heating supply. 2014. [38]
	Poland	Journal of laws of 2012, POS. 962. Regulation of the Minister of Economy dated 10 August 2012. Detailed description of the scope and method of preparation audit of energy efficiency, the design of the card auditing energy efficiency and methods for calculating energy savings [39]

Table 2. PEF values in EU Member States with a single fixed DH PEFs

Country	PEF value
Bulgaria	1.3
Denmark	0.6 – 1.0
Estonia	0.9
Finland	0.7
France	1.0

According to BR15 [23] buildings in Denmark may be erected in accordance with the energy performance frameworks (minimum requirements), or as a voluntary low-energy building according to Building Class 2020. PEF of 0.8 for DH is used for buildings erected in accordance with the minimum requirements of BR15 and of 0.6 for buildings erected according to Building Class 2020. For buildings which comply with the renovation classes, a DH PEF of 1.0 is used.

Differentiated fixed DH PEFs

There are eight (8) EU Member States where differentiated fixed DH PEFs are used. Brief description and comments about DH PEFs use in those countries is shown below. PEF values are shown in summary Table 3.

It should be mentioned, that *Austria* is unique in term of DH PEF general types used, because for heat only boilers of differentiated type are used and DH PEFs for cogeneration and utilization of waste heat are calculated. In this work context Austria is grouped as Member State with differentiated DH PEF type because not all DH networks are calculated independently.

In Austria DH PEFs for networks with heating only plants are selected based on differentiated fixed

approach. Default DH PEF can be used for networks with efficient cogeneration in accordance to Directive 2004/8/EC [40] is 0.19.

Default DH PEF for waste heat utilization is 1.0. At the same time DH PEFs for cogeneration and waste heat can be calculated in accordance to EN 15316-4-5 [2].

In Czech Republic DH PEFs are differentiated based on share of renewables. For the systems of heat supply with more than 80% share of renewables DH PEF is of 0.1. If share of renewables is 50 – 80%, than DH PEF is 0.3. Thermal energy supply systems with 50% or lower than 50% share of renewables has DH PEF of 1.0.

In Hungary different DH PEFs are given based on fuels usage (renewable or not) and share of cogenerated heat. DH PEF values for heating only plants in table 3 means, that share of cogenerated heat is less than 50%. Values for cogeneration plants in table 3 are valid for DH networks where at least 50% of heat is produced in cogeneration regime.

In Slovakia DH PEF for heat only plants based on renewables (wood chips) is of 0.15. DH PEFs for fossil fuels heat only plants vary between 1.19 and 1.4. Lower value is valid for black coal and higher for brown coal. DH PEFs for heavy fuel oil and natural gas are respectively 1.35 and 1.36.

DH PEFs for heat produced in cogeneration regime also depends on fuels used and are the same as for heat only plants. It should be mentioned, that DH PEFs for cogeneration based on renewables is not shown in regulation, but DH PEF of 1.0 for heat cogenerated in nuclear power plants is added.

Table 3. PEF values in EU Member States with a differentiated DH PEFs

Country	CHP		Heating only plants		Waste heat
	Fossil fuels	Renewable fuels	Fossil fuels	Renewable fuels	
Austria	0.19 (default value for efficient cogeneration)		1.36	0.28	1 (default value)
Czech Republic	0.1 - 1				-
Hungary	0.83	0.5	1.26	0.76	-
Slovakia	1.0 - 1.40	-	1.19 - 1.40	0.15	-
Slovenia	1.2		1		-
Latvia	0.7	0	1.3	0.1	-
Lithuania	0.91 (country average), 0.17 - 0.9 (defined for selected DH producers)				-
UK	1.06 - 1.22	1.01 - 1.10	1.06 - 1.22	1.01 - 1.10	1.34

In *Slovenia* DH PEF are differentiated for heating only plants and for heating plants with CHP. PEF don't vary in case of different fuel type and don't depend on the fact whether the energy source for DH is renewable or not. PEF for DH with cogeneration is higher, then DH without cogeneration.

In *Lithuania* DH PEF are offered for 35 separate DH producers, where total number of DH systems is about 360 [10] with renewable and non-renewable energy sources. Besides determined country average DH PEF varies for DH based on renewable and non-renewable energy sources. Those DH PEF are the same for DH with or without CHP.

In the *United Kingdom* DH PEF are defined for heat energy produced in DH systems, based on various energy sources, including fossil fuels (mains gas, LPG, oil, mineral oil), renewable fuel (biomass, biodiesel, and biogas), and geothermal sources. DH PEF are the same for DH with CHP and without it.

In *Latvia* DH PEFs are different for DH with CHP and without CHP. It is mentioned in regulation that DH with CHP means, that at least 70% of heat is supplied by CHP. PEF is provided for the non-renewable part of energy sources, and it is equal to zero for renewable energy sources for DH with CHP and 0.1 for DH without CHP. DH PEF is 1.3. When fossil fuels are used DH PEF is 0.7 for DH with CHP and 1.3 for DH without CHP.

DH PEFs calculated for each DH network

In Italy, Germany and Poland DH PEFs can be calculated for each DH network.

Italy. According to [35] the methodology of calculation of the performance energy of the buildings are regulated by the technical document No 14/2013 from the Italian Thermotechnical Committee and UNI/TS 11300 standards series [36] from Italian Organisation for Standardization. In 2016 CTI 14:2013 was replaced by a new standard UNI/TS 11300:5 2015. In turn UNI standards are aligned with the standards prepared by CEN to support the directive 2010/31/EU [37]. Default DH PEF of 1.5 is used.

Poland. Calculation of DH PEFs goes in accordance to method described in [39]. Method is based on power bonus approach which is also followed in EN 15316-4-5 [2].

Germany. According to [38] calculation of DH PEFs in general follows power bonus approach principles and EN 15316-4-5 [2].

DISCUSSION AND CONCLUSION

Present situation shows that EU Member States flexibly adopt primary energy concept according to their

features and the way how DH PEFs are defined, as well as their values differ significantly.

There are single fixed DH PEFs which are valid for all DH networks in the country, differentiated DH PEFs which are used according to the fuels used and /or applied energy production technologies, and there are also cases when DH PEF for each DH network is calculated independently.

The use of single fixed DH PEFs does not conform the PEF definition. Some of mismatches are given below:

- This solution does not take into account a combination of different fuels and technologies used for heat production in some specific DH networks. At the same time the primary energy consumption and environmental impact in DH networks with renovated DH networks (low energy losses, heat load smoothing by heat storage systems), installed flue gas condenser, implemented cogeneration and high share of renewable fuels are lower.
- Benefits from the use of waste heat are not taken into account. At the same time, the reuse of the waste heat emitted during industrial processes in DH will allow to save a fuel in quantity.

In order to conform the DH PEFs with the PEF definition, when the PEFs take into the account the use of primary energy required for the energy supplied as well as its environmental impact, it is justified either to calculate the PEFs or choose from the differentiated solution. It should be divided and promoted by assigning lower DH PEF factors to DH networks with smaller environmental impacts, i.e. renovated DH networks (low energy losses, heat load smoothing by heat storage systems), installed flue gas condenser, implemented cogeneration and a high share of renewable fuels and utilized waste heat.

Separation of the efficient DH networks with low environmental impacts would promote DH firms to move towards the use of renewable energy and the adoption of the energy efficient technical solutions.

Despite PEF being an important common EU energy policy tool for comparing various energy types, calculation approaches, its determination differs significantly in the EU member states. One possible solution to avoid this difference is the development of a common procedure to determine PEF in all the EU member states.

Methodology used for data collection (findings from various individual studies are analysed and pooled) can be improved. It is expected, that additional negotiations and consultation with experts in the field of energy

efficiency from different EU Member States will increase the accuracy and actuality of findings and allow to consider such topic as trends in PEF formation for different countries during some period of time.

REFERENCES

- [1] Directive 2010/31/EU. European Parliament and of the Council of 19 May 2010 on the Energy Performance of Buildings (recast). Official Journal of the European Union; 2010.
- [2] European standard EN 15316-4-5. Heating systems in buildings - Method for calculation of system energy requirements and system efficiencies - Part 4-5: Space heating generation systems, the performance and quality of district heating and large volume systems.
- [3] N.Surmeli-Anac, A.Hermelink, D.Jager, H.Groenberg Primary Energy Demand of Renewable Energy Carriers. Part 2 Policy Implications. Ecofys 2014 by order of: European Copper Institute. 2014, <http://www.ecofys.com/files/files/eci-ecofys-2014-pef-part-ii-policy-implications.pdf>
- [4] E. Molenbroek, E. Stricker, T. Boermans Primary energy factors for electricity in buildings Toward a flexible electricity supply; Ecofys Netherlands BV, 2011, http://download.dalicloud.com/fis/download/66a8abe211271fa0ec3e2b07/ad5fcc2-4811-434a-8c4f-6a2daa41ad2a/Primary_energy_factors_report_ecofys_29.09.2011.pdf
- [5] U. R. Fritsche, H.-W. Greß Development of the Primary Energy Factor of Electricity Generation in the EU-28 from 2010-2013. IINAS, Darmstadt, March 2015, http://www.iinas.org/tl_files/iinas/downloads/GEMIS/2015_PEF_EU-28_Electricity_2010-2013.pdf
- [6] Wilby, M.R., Rodríguez González, A.B., Vinagre Díaz, J.J. Empirical and dynamic primary energy factors (2014) *Energy*, 73, pp. 771-779.
- [7] An EU Strategy on Heating and Cooling, Communication from the Commission to the European Parliament, the Council, the European Economic and Social Committee and the Committee of the Regions, Brussels, 16.2.2016, <https://ec.europa.eu/transparency/regdoc/rep/1/2016/EN/1-2016-51-EN-F1-1.PDF>
- [8] Ma, Z., Li, H., Sun, Q., Wang, C., Yan, A., & Starfelt, F. (2014). Statistical analysis of energy consumption patterns on the heat demand of buildings in district heating systems. *Energy and Buildings*, 85, 664–672. doi:10.1016/j.enbuild.2014.09.048, <http://www.sciencedirect.com/science/article/pii/S0378778814007853#bib0010>
- [9] Simplified energy balances - annual data, EUROSTAT database, http://ec.europa.eu/eurostat/web/products-datasets/-/nrg_100a
- [10] Euroheat and Power: "District Heating and Cooling – Country by Country – Survey 2015", 2016.
- [11] J. Vansteenbrugge, G. Van Eetvelde District heating networks in the framework of spatial planning in Annual congress: from control to co-evolution, proceedings, 2014.
- [12] Molenbroek, M., Stricker, E., & Boermans, T. Primary energy factors for electricity in buildings. Toward a flexible electricity supply, 1–52, 2011.
- [13] Persson, T. (2015). Energimyndighetens syn på viktnings- och primärenergifaktorer, 1(202100), 1–5., <https://www.energimyndigheten.se/globalassets/om-oss/stallningstaganden/energimyndighetens-syn-pa-viktningsfaktorer.pdf>
- [14] Dovi, D. Algoritam za određivanje energijskih zahtjeva i učinkovitosti termo tehničkih sustava u zgradama Sustavi kogeneracije, sustavi daljinskog grijanja, fotonaponski sustavi. (2015), <http://www.mgipu.hr/doc/EnergetskaUcinkovitost/Algoritam-OdredivanjeEnergijskihZahtjeva.pdf>
- [15] Faktori primarne energije i emisija CO₂. (2014), 2014., http://www.mgipu.hr/doc/EnergetskaUcinkovitost/FAKTORI_primarne_energije.pdf
- [16] Energy Efficiency trends and policies in Romania. Romanian Energy Regulatory Authority, Energy Efficiency Department, 2015, <http://www.odyssee-mure.eu/publications/national-reports/energy-efficiency-romania.pdf>
- [17] Report on the state-of-the-art of the EPBD National implementation, describing policy mapping comprising the assessment of the existing national plans, policies and regulatory frameworks of target countries, RePublic – ZEB Project Project consortium. (2015), (April), 1–145, http://www.republiczeb.org/filelibrary/WP3/D3-1_EPBD-implementation.pdf
- [18] Implementing the Energy Performance of Buildings Directive. Featuring Country Report. Lisbon. 2015. <http://www.epbd-ca.eu/ca-outcomes/2011-2015>
- [19] Cercetare referitoare la cadrul metodologic de calcul al nivelurilor de cost optim al cerințelor minime de performanță energetică pentru clădiri și elemente de anvelopă ale acestora: Faza 2 – Raport final http://www.mdrap.ro/userfiles/ancheta_publica_ctr5_31.pdf
- [20] Metodologie de calcul al performanței energetice a clădirilor Partea a II-a - Performanța energetică a

- instalațiilor din clădiri Indicativ Mc 001/2-2006
<http://www.ce-casa.ro/wp-content/uploads/2014/01/Mc-001-2.pdf>
- [21]EPISCOPE, Inclusion of New Buildings in Residential Building Typologies: Steps Towards NZEBs Exemplified for Different European Countries, Synthesis Report No. 1.
- [22]Наредба № Е-РД-04-2 от 22.01.2016 г. за показателите за разход на енергия и енергийните характеристики на сградите, January 2016, Bulgaria,
http://www.seea.government.bg/documents/NAREDBA_ERD042_ot_22012016.pdf
- [23]The Danish Transport and Construction Agency: Danish Building Regulations 2015,
http://byggningsreglementet.dk/file/591081/br15_english.pdf
- [24]Hoone energiätõhususe miinimumnõuded, RT I, 05.06.2015, 15. In force from: 01.07.2015,
<https://www.riigiteataja.ee/akt/105062015015>
- [25]D3 Suomen rakentamismääräyskokoelma. Ympäristöministeriö, Rakennetun ympäristön osasto. Ympäristöministeriön asetus rakennusten energiatehokkuudesta. Annettu Helsingissä 30 päivänä maaliskuuta 2011,
http://www.finlex.fi/data/normit/37188-D3-2012_Suomi.pdf
- [26]Arrêté du 26 octobre 2010 relatif aux caractéristiques thermiques et aux exigences de performance énergétique des bâtiments nouveaux et des parties nouvelles de bâtiments, 2010, May 2016,
<https://www.legifrance.gouv.fr/affichTexte.do?cidTexte=JORFTEXT000022959397&dateTexte=20160508>
- [27]Österreichisches Institut für Bautechnik: Richtlinie 6 Energieeinsparung und Wärmeschutz, March 2015, Austria,
https://www.oib.or.at/sites/default/files/richtlinie_6_26.03.15.pdf
- [28]Předpis č. 78/2013 Sb.Vyhláška o energetické náročnosti budov, 22.03.2013, Czech Republic,
<https://www.zakonyprolidi.cz/cs/2013-78>
- [29]7/2006. (V. 24.) TNM rendelet az épületek energetikai jellemzőinek meghatározásáról.
http://njt.hu/cgi_bin/njt_doc.cgi?docid=101820.298307
- [30]Vyhláška č. 364/2012 Z. z.Vyhláška Ministerstva dopravy, výstavby a regionálneho rozvoja Slovenskej republiky, ktorou sa vykonáva zákon č. 555/2005 Z. z. o energetickej hospodárnosti budov a o zmene a doplnení niektorých zákonov v znení neskorších predpisov,
<http://www.zakonypreludi.sk/zz/2012-364>
- [31]Tehnična smernica TSG-1-004:2010 Učinkovitost raba energije. Ministrstvo za okolje in prostor Slovenija, 2010,
http://www.arhiv.mop.gov.si/fileadmin/mop.gov.si/pageuploads/zakonodaja/prostor/graditev/TSG-01004_2010.pdf
- [32]Ministru kabineta noteikumi Nr.348 Ēkas energoefektivitātes aprēķina metode, Rīgā 25.06.2013
<http://likumi.lv/doc.php?id=258128>
- [33]Statybos techninis reglamentas STR 2.01.09:2012 „Pastatų energinis naudingumas. Energinio naudingumo sertifikavimas“. 6.01.2016. version, Lithuania,
<https://www.etar.lt/portal/lt/legalAct/TAR.FE0988A078E5/SoYrUFIaOk>
- [34]The Government's Standard Assessment Procedure for Energy Rating of Dwellings 2012 edition,
http://www.bre.co.uk/filelibrary/SAP/2012/SAP-2012_9-92.pdf
- [35]Decreto requisiti minimi (decreto 26 giugno 2015),
<http://biblus.acca.it/download/decreto-requisiti-minimi-dm-26-giugno-2015/#>
- [36]Testo coordinato del decreto-legge 4 giugno 2013, n. 63,
<http://www.gazzettaufficiale.it/eli/id/2013/08/03/13A06688/sg>
- [37]Standard UNI/TS 11300:5 2015. Prestazioni energetiche degli edifici. Parte 5: Calcolo dell'energia primaria e dalla quota di energia da fonti rinnovabili.
- [38]Arbeitsblatt FW 309-1. Arbeitsblatt AGFW FW 309 Teil 1. Energetische Bewertung von Fernwärme. Bestimmung der spezifischen Primärenergiefaktoren für Fernwärmeversorgungssysteme. AGFW. 04.2014.
<https://www.agfw.de/erzeugung/energetische-bewertung/enev-und-fernwaerme/>
- [39]Dz.U. 2012 poz. 962. Rozporządzenie Ministra Gospodarki z dnia 10 sierpnia 2012 r. w sprawie szczegółowego zakresu i sposobu sporządzenia audytu efektywności energetycznej, wzoru karty audytu efektywności energetycznej oraz metod obliczania oszczędności energii.
<http://isap.sejm.gov.pl/DetailsServlet?id=WDU20120000962>
- [40]Directive 2004/8/EC of the European Parliament and of the Council of 11 February 2004 on the promotion of cogeneration based on a useful heat demand in the internal energy market, Official Journal of the European Union; 2004.

THE ROLE OF DISTRICT HEATING IN ACHIEVING SUSTAINABLE CITIES: COMPARATIVE ANALYSIS OF DIFFERENT HEAT SCENARIOS FOR GENEVA

L. Quiquerez¹, B. Lachal¹, M. Monnard², J. Faessler¹

¹ University of Geneva, Institute Forel & Institute for Environmental Sciences, Switzerland

² Industrial Services of Geneva, Switzerland

Keywords: District heating, renewable energy, energy modeling, heat scenarios

ABSTRACT

In many European cities, heat demand remains mostly supplied by individual fossil fuel boilers, contributing to an inefficient and non-sustainable energy system. In order to decrease the fossil fuel consumption in the heating sector, an improvement of energy efficiency and an increase of renewable energy use must be achieved. This study assesses and compares the impacts of implementing different heat strategies regarding both demand and supply side of the heating system, through a case-study in the city of Geneva, Switzerland. Different heat scenarios for 2035 were developed, based on an input/output hourly energy system model which ensures the matching between heat demand and energy resources. This model is coupled with spatial data that enable to identify the areas where district heating could be developed. The results show the impacts of the different strategies regarding the energy supply, the CO₂ emissions and the related socio-economic costs. The findings demonstrate the importance of district heating networks, which offer the possibility to use local heat sources that otherwise would be unused due to technical, spatial or economic constraints. Compared to a scenario essentially focused on very high energy savings in buildings, a more flexible scenario, combining district heating expansion and a smaller reduction in heat demand, enables to achieve the same reductions in fossil fuel consumption and CO₂ emissions, but with lower socio-economic costs.

INTRODUCTION

In accordance with the IPCC recommendations [1], the core of the Swiss government sustainability strategy is based on the concept of 1 ton of emitted CO₂ per inhabitant by the end of the 21st century [2].

In Geneva, 482,500 inhabitants in 2014, the present CO₂ emissions related to the energy sector represents 4.2 tCO₂ per capita, of which 2.2 emitted by the heating sector, 1.1 by the transport sector (not including the airport) and 0.8 by the electricity sector (considering the Swiss electricity consumption mix of 139 gCO₂/kWh) [3-4]. Consequently the main CO₂ emissions reduction potential lies in the heating sector, which represents about half of the final energy consumption in the city.

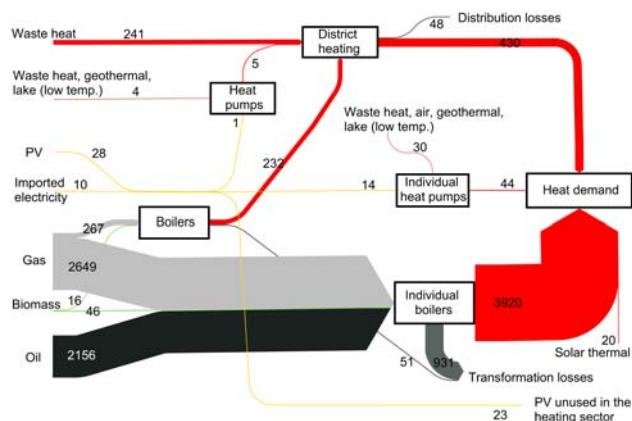


Figure 1: Energy flow chart of the heating sector in 2014. Unit: GWh/y

In 2014, the energy consumed by the heating sector in Geneva amounts to 5,444 GWh or 40.6 GJ/capita [3], mainly based on fossil fuels (figure 1). The energy targets of the state of Geneva for 2035 are to reduce this consumption to 29.0 GJ/capita, from which only 19 GJ/capita would be supplied by fossil fuels [5]. Considering an expected population of 557,000 inhabitants in 2035 [6], renewable energy resources (RES) in the heating sector should increase from the current 362 GWh to 1,543 GWh, while fossil fuels should decrease from 5,072 to 2,945 GWh.

Although it has now been demonstrated that district heating could play an essential role in order to decarbonise the European energy system [7-8], its share in the heat market is still marginal in Switzerland (4-5%) [9] and in the city of Geneva (9-10%) [3].

In this context, fundamental questions were addressed through the project REMUER [10]: What is the role of district heating in order to achieve the energy targets? Is there a synergy or a competition between the development of DH on the one hand and the investments in buildings energy renovation on the other hand? How could be designed the heating system in 2035? And how could it fit into the overall energy system?

RENEWABLE ENERGIES AVAILABILITY AND DH EXPANSION POTENTIAL

Local renewable energy resources potential for the heating sector have been estimated in Geneva and

would represent about 5,500 GWh [11] (not including the heat from the outdoor air which is difficult to quantify). The main potential resources identified are geothermal energy (1,000 GWh) and the thermal energy of the lake (4,000 GWh). Although the renewable energy resources potential is large, their integration in the energy system can be limited by: (i) their spatial availability, temporal dynamics and quality (e.g. temperature); (ii) their costs; (iii) their social acceptance.

Some of these local resources can't be used without district heating for two main reasons: (i) the spatial distance between heat source and heat demand, (ii) and the need to share investment costs on a significant number of consumers. In Geneva, the potential for DH expansion is huge, since today it represents only 10% of the heat market while most of the heat demand is located in dense urban areas (figure 2). A spatial analysis of the heat demand density indicates that 70% and 80% of the heat consumption is located in urban areas where the heat density is respectively greater than 250 and 500 MWh/hectare. In such areas, the distribution cost of DH should remain affordable to guarantee its competitiveness when supplied by low cost resources [12].

METHODOLOGY

In order to assess the role of district heating in the future energy system, different scenarios were developed in collaboration with the local energy utility company. Different variables were identified in order to make projections for 2035 regarding heat demand evolution and the implementation of different energy technologies. In order to compare the scenarios, an input-output model designed for energy system modelling at a regional scale was developed, inspired from the EnergyPLAN model [13]. The model is based on an hourly time-step which ensures the matching between resources availability, production capacities and the fluctuating heat demand. The load curve of the main DH system is used to characterize the heat demand dynamic [14]. This load curve is then adapted to take into account energy savings (reductions applied solely on space heating demand). Four different types of DH systems can be modelled. The main model outputs are energy balance, costs and CO₂ emissions.

Designing the scenarios for 2035

Four scenarios were developed. The business-as-usual scenario (BAU) extends the trends observed in the recent period. The EE&RES scenario is based on both enhancement of energy savings into buildings and integration of more renewable energy through the development of individual heat pumps, solar thermal energy and the expansion of district heating systems. Compared to the EE&RES scenario, the EE+ scenario

is more focused on heat demand reduction and less on renewable energies integration, whereas this is the opposite logic in the RES+ scenario (figure 3).

Future heat demand projection

In each scenario, two important variables that partly determine the future heat demand are identical: (i) the population growth: 557,000 inhabitants in 2035; (ii) and the decreasing heating degree-days (-13 HDD per year) as observed since 1960 [15]. Considering new buildings, it is assumed that 71m² of heated floor area (HFA) will be constructed per additional inhabitant, with a specific heat demand of 180 MJ/ m²/y.

The estimation of heat demand reduction in existing buildings is carried out from a buildings database which contains the current annual heat consumption as well as the heated floor area of about 70% of the total heated building stock [16], completed by extrapolations for the remaining buildings [17-18]. On the basis of these data, gross energy savings potentials are estimated, assuming that the specific heat demand of all buildings consuming more than 300 MJ/m²/y is reduced to a target value specifically defined in the four scenarios (figure 4 and table 1). The effective amount of saved energy subsequently depends on the refurbishment rate, which is defined here as the percentage of the annual energy savings potential to be achieved each year.

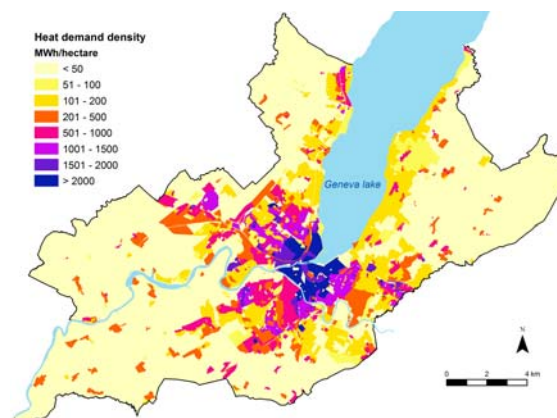


Figure 2: Heat demand density in 2014

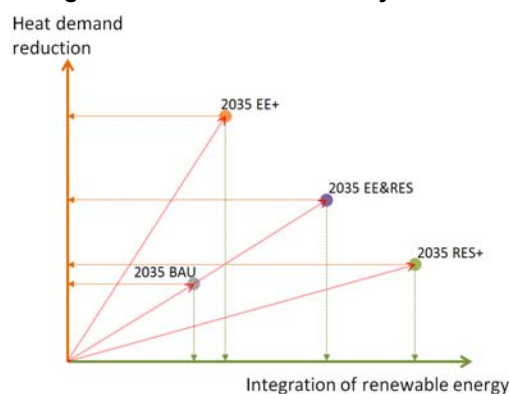


Figure 3: Conceptual positioning framework of the scenarios

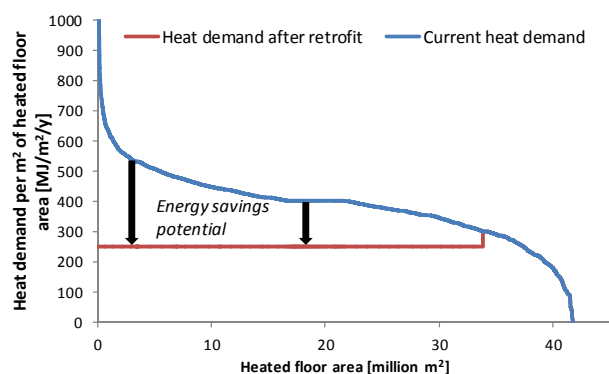


Figure 4: Gross heat savings potential. Scenario EE&RES

Table 1: Renovation rate and specific heat demand of the energy renovated buildings in each scenario

	Renova- tion rate	Specific heat demand after renovation	Heat saved (2035 vs 2014)
BAU	1.2%	350 MJ/m ² /y	205 GWh/y
EE&RES	2%	250 MJ/m ² /y	663 GWh/y
EE+	2.5%	200 MJ/m ² /y	1,072 GWh/y
RES+	1.5%	300 MJ/m ² /y	351 GWh/y

Table 2: buildings heat supply in each scenario

	DH	HP	Fossil boilers	Biomass boilers
2014	10%	1%	88%	1%
BAU	14%	5%	80%	1%
EE&RES	30%	20%	48%	2%
EE+	16%	15%	68%	1%
RES+	40%	25%	33%	2%

In the EE&RES scenario, the heat demand reduction through energy efficiency measures in the existing buildings amounts to 663 GWh/y, compared to 2014 (table 1). This saved energy represents a 17% decrease in the total current heat consumption of the existing buildings with a specific heat demand greater than 300 MJ/m²/y. This reduction is more important in the EE+ scenario (-28%), and lower in the BAU and RES+ scenarios (respectively -5 and -9%).

Future energy infrastructures

The buildings heat supply in the four scenarios is described in table 2. The energy system in the BAU

scenario doesn't differ much from the current system that is mainly based on individual fossil fuels boilers. In the EE&RES and RES+ scenarios, district heating is extended, supplying respectively 30 and 40% of the heat demand. The market share of individual heat pumps (HP) is also respectively increased to 20 and 25%. In the EE+ scenario, renewable energy technologies are slightly less developed.

It is obvious that the development of district heating is relevant when it allows recovering renewable and waste heat. The DH production, transport and storage infrastructures are described in the table 3. In scenarios with DH expansion, the main share of base loads is supplied by waste heat, medium/deep geothermal heat and large scale heat pumps. As an important development of heat pumps (individual and centralized) increase the electricity consumption, especially in winter, gas cogeneration units are also implemented in the EE&RES and RES+ scenarios. Eventually, large scale seasonal storage capacities are also integrated in those scenarios with the aim to shift a part of remaining excess heat wasted in summer.

The total network length in the different scenarios can be estimated by using a simplified method [19] which is based on the ratio between the current DH length and the road network length in the DH areas. In average, this ratio is 0.9. By knowing the total road network length, this value could be used for extrapolations.

Individual solar energy production is considered in every scenario. Hourly distributions of solar PV and solar thermal production for domestic hot water come from actual measurements [20-21]. The PV potential identified in Geneva corresponds to 550-650 MW [22-23].

Table 3: DH supply infrastructures in each scenario

	Unit	2014	BAU	EE& RES	EE+	RES+
Waste heat	MW _{th}	45	45	45	45	55
Geothermal	MW _{th}	-	10	48	10	68
Heat pump	MW _{th}	0.3	18	55	20	67
CHP	MW _{th}	-	-	40	-	65
Storage	GWh	-	-	25	-	25
Biomass boiler	MW _{th}	3	8	8	8	8
DH network	km	62	84	180	97	246

Table 4: Production, transport and storage efficiencies

Efficiencies	Unit	2014	2035
Gas boilers	$\eta\%$	90	92
Oil boilers	$\eta\%$	83	85
Biomass boilers	$\eta\%$	80	85
CHP heat	$\eta\%$	-	45
CHP electricity	$\eta\%$	-	40
Heat pumps	COP	3.3	3.5
DH storage	$\eta\%$	-	80
DH transport	$\eta\%$	90	86-89*
Solar thermal	kWh/m ²	500	500
Solar PV	kWh/m ²	160	200

*Depending on the heat savings in the 4 scenarios

In each scenario, the PV capacities installed are 400 MW (+13% each year), this value representing the 2035 objective [5]. The hourly comparison between PV production and electricity consumption of HP enables to determine the share of the PV production that can effectively be used in the heating sector. The remaining PV production is logically not considered as an energy

input for the heating sector. Regarding solar thermal, only systems supplying domestic hot water are considered in this study. The potential identified represents around 200 GWh/y [22-23]. In the BAU scenario, the total solar thermal panels' surface is multiplied by 5 compared to 2014 and represents 0.35 m² per inhabitants. This increase is doubled in the other scenarios (0.7 m²/capita).

The energy efficiencies assumed for the different energy infrastructures mentioned are indicated in the table 4. Regarding the heat transport, a small increase of distribution losses is taken into account, which is explained by a decreasing linear heat density (ratio between the heat delivered and the length of pipes) compared to 2014.

Quantifying the total economic costs

Data about investment costs related to production, storage and transport infrastructures were gathered from the main energy utility company, and are compiled in the table 5 [24]. The specific costs are generally related to average size infrastructures. In order to estimate the cost of energy efficiencies measures in buildings, a cost curve was developed based on data from [25]. This curve enables to take into account the fact that energy efficiency measures become more expensive as larger savings are achieved (figure 5). All the investment costs were annualized with an assumed 2.5% interest rate.

Table 5: Investments and O&M costs assumed in 2035 [24]

	Unit	Investments (USD million per unit)	Life time (year)	O&M (% of invest.)
Medium-Deep geothermal	MW _{th}	2	30	3.5%
DH fossil boiler	MW _{th}	0.25	25	1.5%
DH biomass boiler	MW _{th}	0.5	25	1.8%
DH heat pump	MW _{th}	2	30	1.0%
DH Storage	GWh	4	30	0.1%
DH network	km	2.5	40	0.1%
DH SST	MW _{th}	0.2	30	0.2%
CHP	MW _{el}	2	15	5.0%
PV	MW _p	1	25	1.0%
Ind. fossil boiler	MW _{th}	0.3	20	2.5%
Ind. biomass boiler	MW _{th}	0.7	20	2.5%
Ind. heat pump	MW _{th}	2.5	20	1.0%
Solar thermal	m ² ·10 ³	1.2	20	1.5%
Building retrofits	m ² (HFA)	0.2 (BAU); 0.4 (EE&RES); 0.6 (EE+); 0.27 (RES+)	40	0%

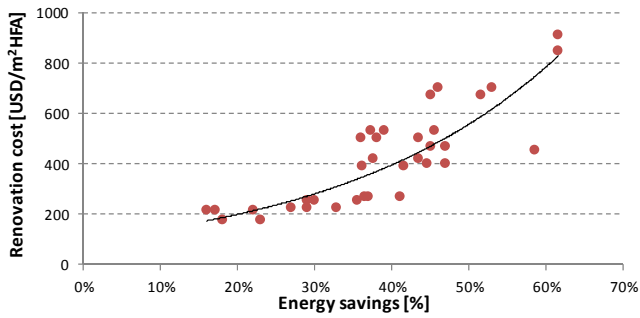


Figure 5: Energy efficiency cost curve based on [25]

Table 6: Energy and CO₂ prices assumed in 2035 [24]

	Unit	USD per unit
Gas	MWh	110
Fuel oil	MWh	110
Electricity	MWh	200
Biomass	MWh	90
Waste heat (from waste)	MWh	35
CO ₂ tax	tons	160

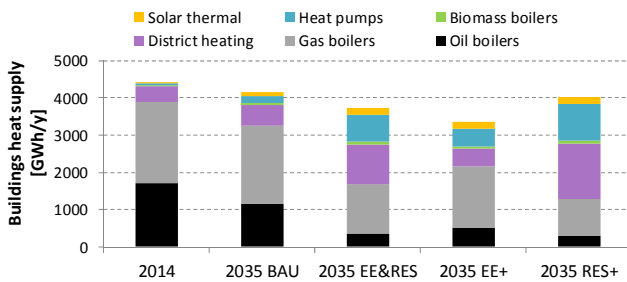


Figure 6: Buildings heat supply (useful energy)

Of course, predicting the future energy prices is very difficult. Based on some hypothesis elaborated in collaboration with the main utility company, prices in 2035 have been defined and are presented in the table 6 [24].

RESULTS

Energy balance and CO₂ emissions

The main differences in the four scenarios are the level of energy efficiency measures and the level of RES integration. As it is shown in the figure 6, the total heat demand in the four scenarios decrease between 6% (BAU) and 24% (EE+) compared to 2014, although the population is more important (+15%).

As district heating is extended in the EE&RES and RES+ scenarios, more renewable energies can be integrated, especially from geothermal energy and large scale heat pumps (figure 7).

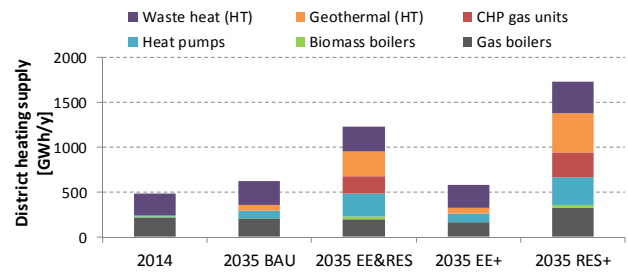


Figure 7: Annual district heating heat supply

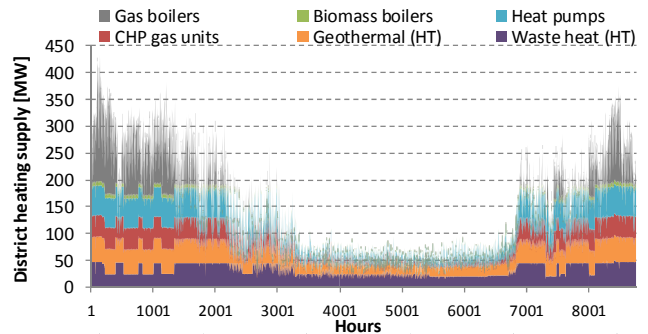


Figure 8: District heating load curve (EE&RES scenario)

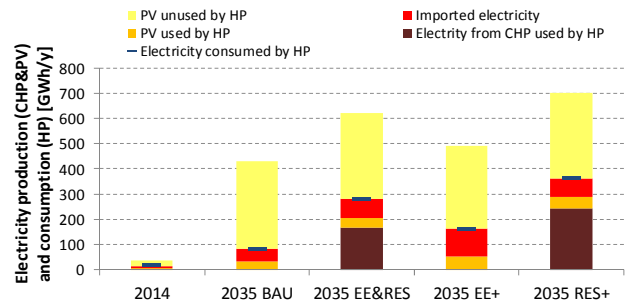


Figure 9: Electricity balance between PV, CHP and HP

In the EE&RES and RES+ scenarios, the electricity consumed by heat pumps is partly offset by the production of CHP units, which simultaneously provide heat to the DH system. Although the PV production is relatively high (380 GWh), only a small share of this renewable electricity production (8-13%) can effectively be used for heat pumps due to the temporal mismatch between heat demand and solar resource (figure 9). This is the reason why the imported electricity in the scenario EE+ is more important, especially in winter, even though fewer heat pumps are integrated.

Figure 10 illustrates the annual energy flows in the modelled heating system (EE&RES). Aside from the drop in heat demand and the increase in use of renewable energies, such a system is characterized by more interactions between the different urban energy networks (gas, electricity and district heating) in comparison to the current heating system (figure 1).

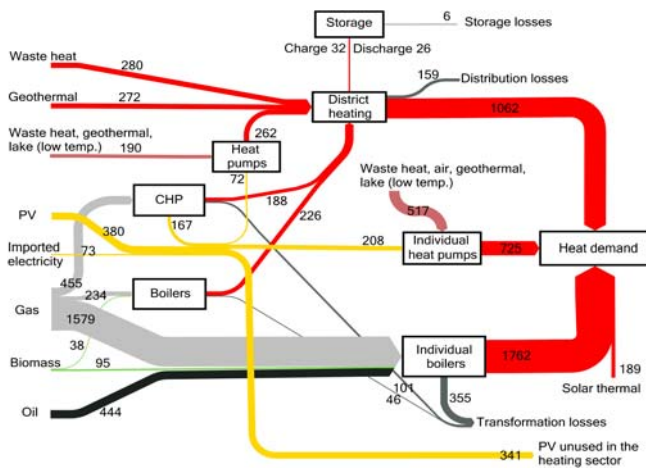


Figure 10: Energy flow chart of the heating sector in 2035 (EE&RES scenario). Unit: GWh/y

In terms of fossil fuels consumption and CO₂ emissions, the three scenarios EE&RES, EE+ and RES+ are quite similar. As it is displayed in the figure 11, the total fossil fuel consumption (gas+oil) in these scenarios decrease between -45% (EE+) and -49% (RES+) compared to 2014. Such reductions enable achieving the fossil fuel reduction target for 2035. By contrast, the BAU scenario does not allow it (figure 12).

The total energy consumption reduction target in the heating sector is only achieved in the EE&RES and EE+ scenarios. However, the BAU and RES+ scenarios are close to it: respectively +2.9 and +1.6 GJ/capita compared to the target value. It should be noticed that the imported electricity (total electricity consumed by HP minus the PV and CHP production used by HP) is not converted into primary energy in this analysis, and that the CO₂ content of this electricity is integrated and corresponds to the Swiss electricity consumption mix [4].

In the EE+, RES+ and EE&RES scenarios, CO₂ emissions in the heating sector are lowered from the current 2.2 tCO₂/capita to about 1 tCO₂/capita (figure 12).

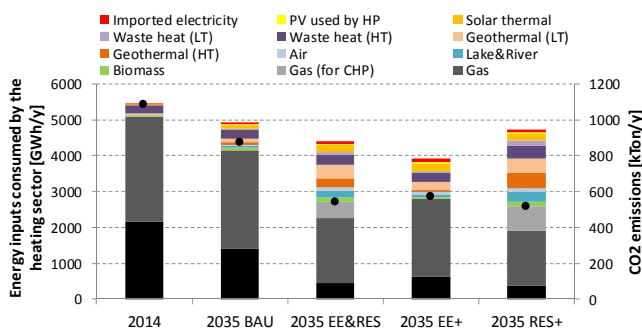


Figure 11: Energy inputs consumed by the heating sector and CO₂ emissions

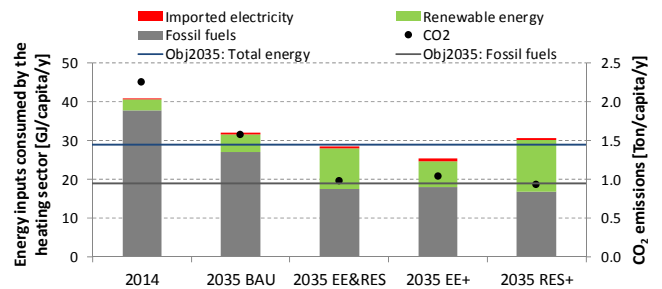


Figure 12: Energy inputs consumed by the heating sector and CO₂ emissions per capita (population: 482'000 in 2014 and 557'000 in 2035)

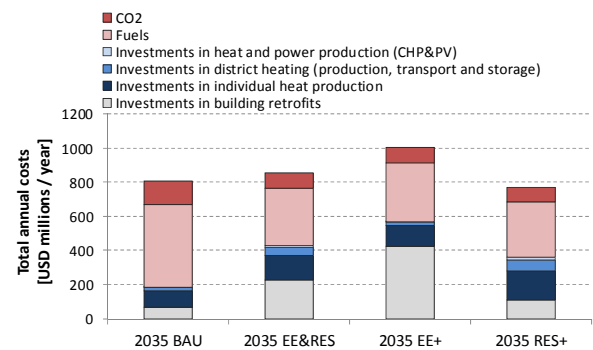


Figure 13: Total annual cost for the heating sector in 2035

Socio-economic costs

On the basis of the assumptions made regarding investment costs and energy prices, the results indicates that the EE+ scenario has higher annual costs than both RES+ and EE&RES scenarios (respectively +31% and +18%), while achieving about the same level of fossil fuels consumption and CO₂ emissions (figure 13). The three scenarios have relatively similar CO₂ and fuels costs, but the investment costs in the EE+ are more important due to the deep retrofitting of a significant share of the buildings stock.

The annual costs in the RES+ and EE&RES scenarios are quite similar to the BAU scenario. The main difference is the structure of the costs. As more district heating and renewable production units are developed in the RES+ and EE&RES scenarios, the heating system in these scenarios is more expensive. Moreover, additional investments are made in end-use energy savings. This increase in investments costs, however, is offset by the fuel and CO₂ cost reduction. Such a cost structure offers a double socio-economic benefit: reducing capital flight on the one hand, and local jobs creation on the other hand.

Of course, the annual cost difference between the BAU scenario and the other three is closely linked to the energy and CO₂ prices assumed.

DISCUSSION

The results show the importance of the CO₂ emission savings potential in the heating sector. By saving 1.2-1.3 tCO₂/cap (scenarios EE+, RES+ and EE&RES), the CO₂ emissions of the overall energy sector (4.2 tCO₂/capita) could be decreased by 30% in 2035 due to improvements in the heating sector. With improvements in the other sector (electricity and transport), higher savings should be reached. This reduction represents a first step toward the concept of 1 ton of emitted CO₂ per inhabitant by the end of the 21st century. (not including the airport)

Regarding the economic analysis, it should be noticed that the building retrofits costs are difficult to estimate. In this study, the costs only refer to measures that increase the energy buildings' efficiency. However, they involve some co-benefits that are difficult to quantify, such as additional comfort, increased building's value or indirect contribution to unavoidable building maintenance. Although these co-benefits are not taken into account, it should be mentioned that the costs used in this study are relatively low with respect to a benchmark performed on a sample of retrofitted buildings in Geneva [18].

Besides being more expensive, the EE+ scenario will probably be more difficult to implement. First, deep energy renovations require the building's owners to have high investment capacities. Secondly, from a technical point of view, some studies demonstrated that the actual energy savings are often significantly lower than the energy standards and the expected calculated values [18]. Last but not least, from a certain point, deep renovations may become a problem regarding the conservation of the architectural heritage [26]. This issue could also increase the buildings retrofitting costs.

In contrast, the RES+ and EE&RES scenarios, besides being cheaper than the EE+ scenario, seem easier to implement. In comparison with the EE+ scenario, which is very dependent on the implementation of significant heat savings, the RES+ and EE&RES scenarios offer more flexibility by leaving more choices to each particular situation.

In addition, the fact that renewable energy integration in the heating sector will partly be based on the development of heat pumps could involve an increase of the electricity consumption, especially in winter. In order to limit the electricity imports during this season, the development of CHP units seems necessary, especially since the Swiss parliament decided to ban nuclear energy. In this regard, it should be kept in mind that in Europe, the current marginal electricity production in winter is still essentially based on fossil fuels thermal plants. In this way, the need to develop

CHP is another reason that enhances the importance of DH extension.

On the other hand, DH allows to link CHP, HP (both technologies at the interface between electrical and DH networks) and storage facilities. This integration increase the flexibility of the overall energy system, which will be a key point for the massive integration of fluctuating renewable production such as wind power (not considered in this study because its regional potential is very low) [27].

Another important point in the scenarios developed is the fact that, even if its use will be lowered by 2035, natural gas will still play an important role in the heating system. However, whereas it is currently essentially used as fuel for individual boilers, it will be used in a more efficient and valuable way by supplying further both CHP and peak-load boilers.

Lastly, it should be noted that part of the waste heat at low temperature used by heat pumps (individual or centralized) in the different scenarios may come from district cooling systems. In this study, the energetic impacts on the cooling sector (reduction of the electricity consumption) have not been taken into account, as well as the cost related to district cooling networks.

CONCLUSION

The aim of this study was to assess different strategies regarding the future heating system and its integration into the overall energy system. The findings demonstrate the importance of district heating networks, which offer the possibility to use local heat sources that otherwise would be unused due to technical, spatial or economic constraints. Compared to a scenario essentially focused on very high energy savings in buildings, a more flexible scenario, combining district heating expansion and a smaller reduction in heat demand, enables to achieve the same reductions in fossil fuel consumption and CO₂ emissions, but with lower socio-economic costs.

Therefore the key messages are: (i) energy strategies should consider both demand and supply side of the energy system, (ii) district heating should be considered as an essential infrastructure for achieving sustainable cities.

REFERENCES

- [1] IPCC (Intergovernmental Panel on Climate Change), "Climate change 2007: Synthesis Report". Geneva, 2007. Available form: http://www.ipcc.ch/pdf/assessment-report/ar4/syr/ar4_syr_full_report.pdf
- [2] OFEV, "Ordonnance sur la réduction des émissions de CO₂, rapport explicatif." Berne, 2012. Available from :

- <http://www.bafu.admin.ch/klima/12006/14321/index.html?lang=fr>
- [3] OCSTAT (office cantonal de la statistique), statistiques de l'énergie, URL: <http://www.ge.ch/statistique/>, accessed 20th January 2015.
- [4] OFCL (office fédéral des constructions et de la logistique), Données des écobilans dans la construction, 2014.
- [5] Etat de Genève, Conception générale de l'énergie, 2013. Available from: <http://www.geneve.ch/grandconseil/data/texte/RD00986.pdf>
- [6] OCSTAT (office cantonal de la statistique), Projections démographiques pour le canton de Genève de 2010 à 2040, 2011. Available from: <http://www.ge.ch/statistique/tel/publications/2011/analyses/communications/an-cs-2011-39.pdf>
- [7] H. Lund, B. Möller, B.V. Mathiesen and A. Dyrelund, "The role of district heating in future renewable energy systems". Energy (2010), Vol.35, pp. 1381-1390.
- [8] D. Connolly et al., "Heat Road Map Europe: Combining district heating with heat savings to decarbonize the EU energy system". Energy policy (2014), Vol.65, pp. 475-489.
- [9] OFEN (Office fédéral de l'énergie), statistique de l'énergie. URL: <http://www.bfe.admin.ch/>, accessed 20th January 2015.
- [10] J. Faessler et al., "Projet REMUER : Réseaux thermiques multi-ressources, efficaces et renouvelables". University of Geneva, 2012. Available from: <http://archive-ouverte.unige.ch/unige:78921>
- [11] J. Faessler, "Valorisation intensive des énergies renouvelables dans l'agglomération franco-valdo-genevoise dans une perspective de société 2000W", University of Geneva, 2011. [PhD Thesis]. Available from: <http://archive-ouverte.unige.ch/unige:17272>
- [12] U. Persson and S. Werner, "Heat distribution and the future competitiveness of district heating". Applied Energy (2010), Vol.88, pp. 568-576.
- [13] H. Lund, EnergyPLAN: advanced energy systems analysis computer model. Aalborg University, 2008. Available from: <http://energy.plan.aau.dk/manual.php>
- [14] L. Quiquerez, J. Faessler and B. Lachal, "Réseaux thermiques multi-ressources, efficaces et renouvelables: Etude de cas de la connexion des réseaux thermiques Cadiom et Cadsig à Genève". Collection Terre&Environnement, Vol. 133, Genève, 2015. Available from: <http://archive-ouverte.unige.ch/unige:77547>
- [15] Office fédéral de la météorologie et de climatologie MétéoSuisse, Indicateurs de climat, 2015. Available from: <http://www.meteosuisse.admin.ch/home/climat/actuel/indicateurs-de-climat.html>
- [16] SITG, Système d'information du territoire à Genève. Geodata. URL: <http://ge.ch/sitg/>, accessed 15th October 2015
- [17] S. Schneider, J. Khoury, B. Lachal and P.Hollmuller, "Geo-dependent heat demand model of the swiss building stock". Sustainable built environment regional conference, Zurich, June 2016.
- [18] J. Khoury, "Rénovation énergétique des bâtiments résidentiels collectifs : Etat des lieux, retour d'expérience et potentiels du parc genevois", University of Geneva, 2014. [PhD Thesis]. Available from: <https://archive-ouverte.unige.ch/unige:48085>
- [19] CEREMA, Réseaux de chaleur et territoires. Relation entre linéaire de réseau de chaleur et linéaire de voirie. Website. URL: <http://reseaux-chaleur.cerema.fr/relation-entre-lineaire-de-reseau-de-chaleur-et-lineaire-de-voirie>. Accessed 28th January 2015.
- [20] P. Ineichen, "Solar radiation resource in Geneva, measurements, modeling, data quality control, format and accessibility". University of Geneva, 2013.
- [21] F. Mermoud, J. Khoury and B. Lachal, "Suivi énergétique du bâtiment 40-42 de l'avenue du Gros-Chêne à Onex (GE), rénové selon le standard MINERGIE". Collection Terre&Environnement, Vol. 109, Genève, 2012. Available from: <http://archive-ouverte.unige.ch/unige:23005>
- [22] L. Quiquerez et al., "GIS methodology and case study regarding the assessment of the solar potential at territorial level: PV or thermal?". International journal of sustainable energy planning and management (2015), Vol.6, pp 3-16. Available from: <https://journals.aau.dk/index.php/sepm/article/view/1043/1005>
- [23] G. Desthieux, P. Gallinelli and R. Camponovo, "Cadastre solaire du canton de Genève: analyse du potentiel de production énergétique par les panneaux solaires thermiques et PV". HEPIA, Geneva, 2014.
- [24] L. Quiquerez, B. Lachal, M. Monnard and J. Faessler, "Evaluation quantitative de scénarios de développement du marché de la chaleur à Genève à l'horizon 2035". University of Geneva and Industrial Services of Geneva, 2016.
- [25] S. Banfi, M. Farsi and M. Jakob, "An analysis of investment decisions for energy-efficient renovation of multi-family buildings". OFEN, 2012.
- [26] J. Tschopp, "Economies d'énergie et conservation du patrimoine, deux intérêts divergents ? Etude de cas de la cité du Lignon, Genève". University of Geneva, 2012. [Master Thesis].
- [27] H. Lund, "Large-scale integration of wind power into different energy systems". Energy (2004), Vol.30, pp. 2402-2412.

ASSESSMENT OF THE THERMAL ENERGY STORAGE IN FRIEDRICHSHAFEN DISTRICT ENERGY SYSTEMS

B. Rezaie¹, B.V. Reddy², M.A. Rosen²

¹ College of Engineering, University Of Idaho, Moscow, ID 83844-1011, USA

² Faculty of Engineering and Applied Science, University of Ontario Institute of Technology, Oshawa, Ontario, L1H 7K4, Canada

Keywords: *District Heating, Thermal Energy Storage, Exergy, Friedrichshafen District Energy, Solar Energy*

ABSTRACT

The thermal energy storage (TES) of an actual district energy (DE) system is analyzed thermodynamically, using energy and exergy approaches. With a case study, the results for the TES of the DE system are verified with previous studies. The actual case considered is the Friedrichshafen DE system in Germany. This system is solar assisted, uses natural gas as a backup, and is equipped with a TES. The TES stores the surplus solar energy until is needed by thermal energy users of the system. Using solar energy allows the DE system to use significantly less fossil fuel than would otherwise be the case. Seasonal TES, which normally requires significant thermal insulation to adequately reduce thermal losses, is used in the DE system. The use and role of thermal storage in a district energy system is assessed considering the Friedrichshafen DE system. The results show the significant influence of the return temperature of the circulating media (water) from the DE system thermal network. Furthermore, the financial impact of the TES is not limited to a reduction of the operational cost of the DE system but also to an increase in the initial costs for the DE system.

INTRODUCTION

TES is interpreted for district energy (DE) systems as a bridge to close the gap between the energy demand of a DE system and the energy supply to the DE system [1]. TES can be integrated with the DE system in the forms of sensible and latent heat storage. Applying sensible heat storage in the DE system is more commonly used than latent heat. However, some about latent heat storage in a DE system, such as that of Bo et al., discuss the capabilities of phase changing materials (PCMs) in cool storage integrated with DE systems [2]. For sensible heat storage, there has been more theoretical and practical research, such as that of Schmidt, which demonstrates the effect of TES on performance of a DE system and which focuses on low and high exergy systems for buildings and communities [3]. In that study, the quality of energy flow in buildings was examined by using exergy analysis. In a recent

study, the economic and environmental impact of using TES in a solar assisted DE system was inspected [4].

Research has been performed to examine a DE system coupled with TES. For instance, a DE system integrated with TES was assessed by an energy approach to find the optimum point where TES has the best effect on energy saving [5]. The method was applied to residential and commercial zones. In a similar study a DE system including TES was economically optimized [6]. Various studies have been reported, and several DE systems including TES have been built in different locations, mainly in Europe. Some well-known studies are noted here. TES is of assistance to energy suppliers in a DE system by allowing:

- The accumulation of thermal energy from off-peak periods for use when demands are high.
- The storage of excess thermal energy when it is available, for subsequent release to the DE distribution system when thermal demands increase (especially during periods when suppliers are not able to satisfy thermal energy demands with existing facilities). In this way, TES saves thermal energy that would otherwise be wasted.
- More effective utilization of renewable thermal energy sources such as solar than is otherwise possible due to the intermittent nature of the resource supply.

Regardless of the source of energy in a DE system, reducing energy losses is usually a main advantage of using TES in DE systems, which allows the reduction of thermal losses, resulting in energy savings and increased efficiency for the overall thermal system. Large seasonal TES systems have been built in conjunction with DE technology [7]. In addition, improved efficiency and economics, and environmental benefits are another reason for the expansion of TES technology in general and with DE.

Many beneficial applications of TES with DE exist or can be developed. Rosen et al. state that DE with hybrid systems can advantageously combine sources of energy such as natural gas, waste heat, wood wastes, and municipal solid waste [8]. TES can increase the benefits provided by such systems [8].

Similarly, Lund et al. point out that those “low energy” buildings can be operated with industrial waste heat, waste incineration, power plant waste heat and geothermal energy in conjunction with a DE network [9]. Incorporating TES can improve the design of such systems.

Tanaka et al. that state the use of TES, in conjunction with DE, decreases energy consumption compared to a reference system [5]. They also found that seasonal TES is more effective than short-term.

Andrepoint assessed the economic benefits of using TES technologies in DE systems [10]. He notes that cool TES is applied widely in heating, ventilation and air-conditioning systems by shifting the cooling load from peak periods during the day to off-peak periods at night. This time shift significantly reduces operating costs, benefit which is particularly noteworthy in large scale DE systems. Andrepoint lists the following additional advantages of using TES in DE systems:

- Preventing inefficient operation of chillers and auxiliary equipment during low-level operation;
- Enhancing system reliability and flexibility;
- Balancing electrical and thermal loads in combined heat and power (CHP) for better economy; and
- Lowering accident risks and insurance by enhancing fire protection (since the stored chilled water or other storage fluid in the TES is in the vicinity of the DE and may be utilized as a reserve firefighting fluid in the event of a fire).

The benefits of TES in facilitating the use of renewable energy, especially solar thermal energy for use in heating and cooling buildings, have been clarified [7]. Demand is growing for facilities that utilize TES, as they are more efficient and environmentally friendly, exhibiting reductions in

- Fossil fuel consumption;
- Emissions of CO₂ and other pollutants; and
- Chlorofluorocarbon (CFC) emissions.

Griffin reports that in many cases buildings with TES systems in DE applications consume more energy than buildings without TES, and that all systems are environmentally beneficial [11]. The U.S. Green Building Council (USGBC) did not discourage the use of TES in the first version of the Leadership in Energy and Environmental Design (LEED) criteria, but also did not deal with the use of TES in district heating systems. However, a building with TES is eligible to earn more points for its lower electrical power.

Building a TES requires initial capital for land, construction, insulation and other items. Determining the appropriate location, designing the proper structure and insulation, and executing the design are important

steps in installing a TES, which involve significant costs. The high initial cost is a disadvantage of TES.

The objective of this study is to assist in reducing substantially the cost of TES for DE systems. To do so, an existing TESs need to be analyzed in terms of technical and economic performance, but comprehensive reports of this type are sparse. This study quantifies the thermodynamic impact of the TES on the performance of the Friedrichshafen DE system, charging and discharging trends of the TES, and the impact of the return temperature on discharge energy by the TES. Analysing the role of the return temperature of the water (circulating and storing medium) from the DE system is important because that temperature is significant influence of the TES on the DE system. This study is performed with actual data from Friedrichshafen DE system. The outcomes of this study provide insights for designers in the field and enhance understanding of large scale TES performance. This is important not only from technical point of view but also to determine the economic impact of TES on a DE system.

METHODOLOGY

Various types of TES, including above-ground and underground systems, have found applications in different areas like DE. For a TES in the charging stage, a circulating media transport the heat of Q_{in} into the heat storage. Heat storage contains a medium with mass of M and specific heat capacity of c_p (if storage is constant pressure, c_v if it is constant volume). The initial temperature of the heat storage is T_i . It is also assumed TES is in the fully mixed condition. The ambient temperature surrounding the TES is T_0 . The temperature of the medium after absorbing Q_{in} and releasing heat loss of Q_{loss-c} is T_c which should be calculated based on the properties of the TES and inlet heat to the TES. Figure 1 illustrates energy flow in the TES in the charging stage.

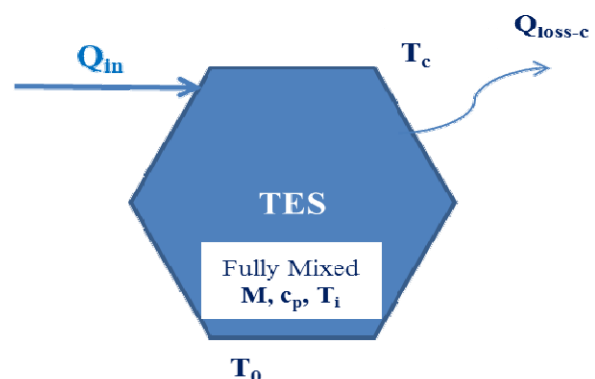


Figure 1: Single TES in the charging stage

The general energy balances for the charging stage is expressed as:

$$\text{Net energy input} - \text{Heat loss in charging} = \text{Energy accumulated in TES} \quad (1)$$

$$Q_{in} - Q_{loss,c} = Q_c \quad (2)$$

Here, $Q_{in, TES}$ denotes the net energy input to the TES and $Q_{loss,c}$ the TES energy loss when heat loss in the pipes is neglected. Moreover, Q_c denotes the energy accumulated in the TES during the charging, which can be also called as stored energy during the charging period and can be written as:

$$Q_c = M c_p (T_c - T_i) \quad (3)$$

where c_p denotes the specific heat of the storage medium, however it can be c_v , depends on the project situation (constant pressure or volume). Energy is transporting to/from the TES with a circulating medium. The mass of flowing media during the charging is calculated by:

$$m_c = Q_c / c_p (T_{in} - T_c) \quad (4)$$

Here m_c is the mass of circulating medium transporting energy to the TES in the charging stage, while T_{in} and T_c denote the TES inlet and the charging (outlet) temperatures respectively.

The exergy balance for the TES is as follows:

$$\text{Exergy input} - \text{Exergy destruction} - \text{Exergy loss} = \text{Exergy accumulation} \quad (5)$$

$$\begin{aligned} \text{Exergy input} &= Ex_{in} - Ex_c \\ &= m_c [h_{in} - h_c - T_0 (s_{in} - s_c)] \end{aligned} \quad (6)$$

where h_{in} and h_c denote the specific enthalpy of inlet and outlet water at charging for the TES respectively. Also, s_{in} and s_c denote the specific entropy of inlet and the charging (outlet) media for the TES respectively.

The exergy loss and accumulation during the charging stage are:

$$\text{Charging exergy loss} = Q_{loss,c} (1 - T_0 / T_c) \quad (7)$$

$$\text{Exergy accumulation} = Ex_c - Ex_i = M [u_c - u_i - T_0 (s_c - s_i)] \quad (8)$$

where u_c and u_i are the specific internal energy at the charging (final) and initial conditions of the TES respectively s_c and s_i show the final and initial specific entropy of the TES. The exergy destruction in the charging stage is given by:

$$\text{Exergy destruction} = m_c [h_{in} - h_c - T_0 (s_{in} - s_c)] - Q_{loss, TES} (1 - T_0 / T_m) - M [u_c - u_i - T_0 (s_c - s_i)] \quad (9)$$

The energy efficiency for the charging stage η_c can be written as:

$$\eta_c = \frac{\text{Energy accumulated in TES}}{\text{Energy input}} = \frac{Q_c}{Q_{in}} \quad (10)$$

This energy efficiency is purely for the TES in charging stage without considering the heat exchanger. The exergy efficiency for the charging stage ψ_c can be written as:

$$\psi_c = \frac{\text{Exergy accumulated in TES}}{\text{Exergy input}} = \frac{Ex_c}{Ex_{in}} \quad (11)$$

The discharging stage, in which the TES releases stored energy, is illustrated in Figure 2. In the charging stage the temperature of the storing TES reaches ultimately to the T_c , therefore T_c is the initial temperature for the TES in which starts releasing energy. During the discharge, heat loss of $Q_{loss,d}$ and Q_{out} are released by the TES. Q_{out} is the energy which is recovered by the TES. In this design Q_{out} is transferred to the next system through circulation medium. The temperature of the TES in discharging stage is T_d which is smaller than T_c . At this stage T_d and Q_{out} are unknown and are calculated based on the known properties of the TES.

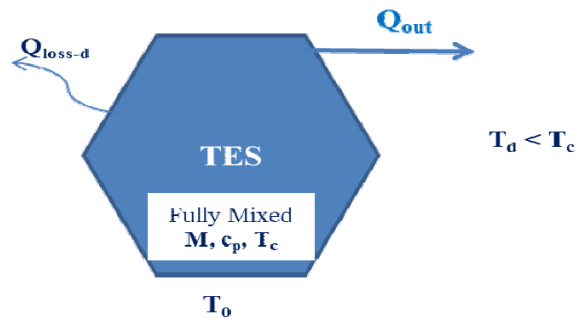


Figure 2: TES in discharging stage

An energy balance for this stage is expressed as follows:

$$(\text{Energy recovered} + \text{Heat loss}) = \text{Energy charged} \quad (12)$$

$$Q_c = (Q_{out} + Q_{loss,d}) \quad (13)$$

Here, Q_c denotes the charged energy from the TES, Q_{out} represents the energy recovered by the TES during the discharging, and $Q_{loss,d}$ is the heat loss of the TES. E_c and $Q_{loss, TES}$ are normally negative in value, and Q_{out} is given by:

$$Q_{out} = M c_p (T_c - T_d) \quad (14)$$

Here, T_d is discharge temperature and other parameters are introduced previously.

Energy is transported through the TES during the discharging via the circulating media. The mass of the outlet media from the TES in discharging stage m_d is evaluated as follows:

$$m_d = \frac{Q_{out}}{c_p (T_{out} - T_r)} \quad (15)$$

where T_r is the return temperature of the circulating medium from the system which supply recovered energy by the TES, and T_{out} denote the temperature of outlet flows of the TES.

The energy efficiency of the discharging stage for the TES η_d can be expressed as:

$$\eta_d = \frac{\text{Energy recovered by TES}}{\text{Energy released by TES}} = \frac{Q_{out}}{Q_{out} + Q_{loss-d}} \quad (16)$$

Equation (16) demonstrates that energy recovered from the TES divided by the total released energy from the TES results in energy efficiency of the TES in discharging stage.

An exergy balance for the discharging stage of the TES is evaluated as follows:

$$-(\text{Exergy recovered} + \text{Exergy loss}) - \text{Exergy destruction} = \text{Exergy accumulated} \quad (17)$$

where the exergy recovered Ex_{rec} is expressed as:

$$Ex_{rec} = Ex_{out} - Ex_r = m_d [h_{out} - h_r - T_0 (s_{out} - s_r)] \quad (18)$$

Here, h_{out} and h_r are the specific enthalpies of the TES outlet and the return medium respectively, and s_{out} and s_r are the specific entropies of the TES outlet and the return (inlet) medium. Moreover,

$$\text{Exergy loss} = Q_{loss,d} (1 - T_0 / T_d) \quad (19)$$

$$\text{Exergy accumulation} = Ex_f - Ex_r = M [u_f - u_r - T_0 (s_f - s_r)] \quad (20)$$

$$\text{Exergy destruction} = m_d [h_{out} - h_r - T_0 (s_{out} - s_r)] - Q_{loss,d} (1 - T_0 / T_d) - M [u_f - u_r - T_0 (s_f - s_r)] \quad (21)$$

where u_f and u_r are the final and initial internal energies respectively for the flow through the TES.

The discharging exergy efficiency for the TES Ψ_d is written as:

$$\Psi_d = \frac{\text{Exergy recovers by TES}}{\text{Exergy accumulate in TES}} = \frac{Ex_{rec}}{Ex_c} \quad (22)$$

$$\Psi_d = m_d [h_{out} - h_r - T_0 (s_{out} - s_r)] / M [u_f - u_r - T_0 (s_f - s_r)] \quad (23)$$

If there is any storing stage defined during the charging and discharging stages, there would be then another extra heat loss for the period of the storing which should be added to other heat loss.

The overall energy balance for the TES can be expressed as:

$$\text{Energy input} - (\text{Energy recovered} + \text{Heat loss}) = \text{Energy accumulation}$$

$$Q_{in} - (Q_{out} + Q_{loss}) = Q_c \quad (24)$$

The overall TES energy efficiency η_{TES} is determined as:

$$\begin{aligned} \eta_{TES} &= \frac{\text{Energy recovered from TES during discharging}}{\text{Energy input to TES during charging}} \\ &= \frac{Q_{out}}{Q_{in}} \end{aligned} \quad (25)$$

η_{TES} denotes energy efficiency of the TES and results from dividing recovered energy by the TES by the total energy input to the TES.

Similarly, an overall exergy balance for the TES is:

$$\begin{aligned} \text{Exergy input} - (\text{Exergy recovered} + \text{Exergy loss}) - \\ \text{Exergy Destroyed} = \text{Exergy accumulation} \\ Ex_{in} - (Ex_{rec} + Ex_{loss}) - Ex_{des} = Ex_c \end{aligned} \quad (26)$$

The overall exergy efficiency (ψ_{TES}) is calculated by:

$$\begin{aligned} \psi_{TES} &= \frac{\text{Energy recovered from TES during discharging}}{\text{Exergy input to TES during charging}} \\ &= \frac{Ex_{rec}}{Ex_{in}} \end{aligned} \quad (27)$$

Equation (27) means recovered exergy by the TES divided by input exergy to the TES results in exergy efficiency of the TES.

CASE STUDY

The Friedrichshafen DE system is considered as a case study. The first phase of the Friedrichshafen DE system included a hot water TES made of reinforced concrete with a volume of 12,000 m³ which served 280 apartments in multi-family houses and a daycare, and included flat plate solar collectors with an area of 2700 m² [12]. Solar heat provided 24% of the total heat demand for district heating. In the second phase, district heating was expanded to a second set of apartments comprising 110 units, and 1350 m² of the solar collector area was added to the system. Moreover, two gas condensing boilers were installed to cover the energy demand for district heating during periods when insufficient energy is available via the solar collectors and thermal storage.

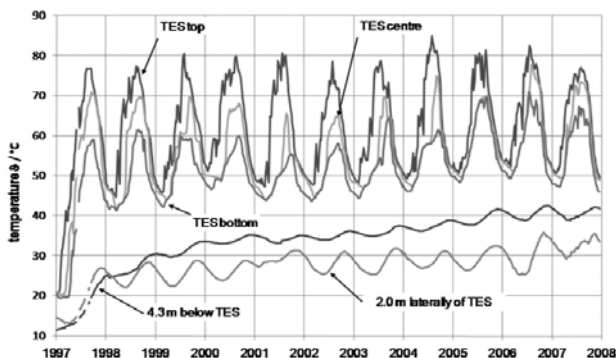


Figure 3: Historical variation of temperatures in and near the TES in the Friedrichshafen DE system [12], printed by permission

The Friedrichshafen DE system contains two natural gas boilers, solar thermal collectors mostly located on building roofs, a central solar heating plant with seasonal heat storage (CSHPSS), heat exchangers to transfer heat between the thermal network and solar collectors, and a thermal network which distributes heat to consumers, as well as pipes, pumps, and valves. Water is the heat storage media and the heat transfer media circulating in the Friedrichshafen system.

Historical temperature data for the Friedrichshafen DE system is presented in Figure 3. Data for a typical annual period is as follows:

- Return water (circulating media) from thermal network temperature: 55.4°C
- Measured TES heat loss: 421 MWh
- Storage efficiency: 60%
- Thermal energy yields of solar collectors: 1200 MWh
- Solar heat input to district heating network: 803 MWh
- Overall heat delivery to district heating network: 3017 MWh
- Heat delivered by gas boilers: 2310 MWh
- Solar fraction: 26%
- Maximum temperature in TES: 81°C (at top)

The temperature of the return water is reported as an annual average, although in reality the return temperature varies depending on the time of day and season. The temperature and mass flow rate of the water, the building profile, and weather conditions affect the return temperature. Nonetheless, the temperature of the return water is here considered constant to simplify the calculations in this preliminary study, thereby permitting the main objective of assessing the role of the TES to be more clearly illustrated.

It was reported that the design temperature of the thermal network on average is 70°C [13, 14].

Over the limited data available for the Friedrichshafen TES and for simplification, the following is assumed:

- When direct solar energy is not sufficient to cover energy demand, TES releases energy for the DE system.

- The priority is with solar energy, so it is assumed that the demand of the DE system is covered with solar energy; if solar is not sufficient then the TES/boiler is applied.
- When there is energy in the TES, the priority is to use stored energy rather than natural gas.

Heat losses in pipelines are neglected like a similar thermal system reported in China [15].

The year 2006 is considered as a typical year in the present analysis because this appears to be a typical year. Consequently, the TES temperature for each season is taken from Figure 3 for that year. Monthly temperatures during and near the TES for 2006 are listed in Table 1, along with the monthly environment temperature [16].

The total energy loss of the TES during 2006, reported as 421 MWh, needs to be broken down by month. The TES in the Friedrichshafen DE system is built in the ground, so heat loss takes place mostly between the TES and the surrounding soil. Data are available for soil temperature 4.3 m under the TES. Here, this temperature is assumed for TES heat losses in all directions. Because the volume of underground Friedrichshafen TES is high at 12,000 m³, most of the TES is deep in the ground. Since the ground temperature is almost constant at a depth of 10 m, the majority of the surrounding soil is thus at a constant temperature, so a single ground temperature is used in all directions here for simplicity. The temperature difference between the TES and the soil 4.3 m below the TES is calculated for each month. The soil temperature is read from Figure 3 and listed in Table 1, which also contains the breakdown of the estimated received solar energy by month and season [4].

Table 1: TES, soil and ambient temperatures during the year 2006

Season/ Solar generation	Month	TES temp. (top), °C	TES temp. (center), °C	TES temp. (bottom), °C	T _a , °C	Soil temp., °C	ΔT (T _{tes} - soil temp.), °C	Q _{loss, TES} , MWh
Spring / 376.07 MWh	Mar.	60	56	52	3.4	26	30	32.6
	Apr.	70	61	56	9.9	25	36	39.1
	May	80	69	60	13.7	25	44	47.7
Summer / 473.33 MWh	Jun.	83	74	63	19.8	26	48	52.1
	Jul.	82	76	67	19.7	28	48	52.1
	Aug.	87	74	66	16.1	31	43	46.7
Fall/ 233.42 MWh	Sept.	74	65	58	17.9	34	31	33.6
	Oct.	60	59	50	13.0	35	24	26.0
	Nov.	54	52	51	6.6	34	18	19.5
Winter / 116.76 MWh	Dec.	51	50	48	2.7	32	19	20.6
	Jan.	54	52	50	-2.6	30	22	23.9
	Feb.	55	54	51	0.3	29	25	27.1
Σ=388								Σ=421

Legend: ΔT is the temperature difference between the TES center temperature and soil temperature, Q_{loss, TES} is TES heat loss in each month (estimation is explained in the text). Sources: Solar energy breakdown [4, 12, 16]

Moreover, the sum of the monthly differences between the TES center temperature and the soil temperature for the year is 388°C; these values are used as weighting factors in determining the monthly breakdown of the TES annual heat loss. That is, the energy loss for each month is calculated by multiplying its temperature difference by the ratio 421 MWh/388°C. For example, the TES heat loss for March is determined as:

$$Q_{loss, TES} = 421(30/388) = 32.6 \text{ MWh (for March)}$$

CASE STUDY: ENERGY & EXERGY ANALYSIS

The main objective of this section is assessing the performance of an actual TES which is part of a solar assisted district energy system. The TES is analysed in charging and discharging stages with energy and exergy approaches.

Energy and exergy parameters for the TES, evaluated with equations (2) to (9) during the charging months, account for thermal stratification. The average temperature for the TES at any stage is assumed fixed at 72°C (for which c_p = 4.19 kJ/kg K). The energy and exergy efficiencies of the TES for the overall charging stage are determined using equations (10) and (11) as 54% and 24%, respectively. The TES in the Friedrichshafen DE system provides energy for the DE system when the top temperature of the TES is higher than 55.4°C; otherwise, the TES does not provide heating. From March to August, Q_c and Q_{in} for each month are increasing, which means the energy of the TES is increasing every month compared to the previous month. This pattern is repeated in the exergy section: from March to August, the exergy level is increasing relative to the previous month. Thus, from March to August is the charging stage of the TES.

From September, Q_{out} has a higher value, meaning the TES loses energy compared to the previous month as this discharges energy to the Friedrichshafen DE system. Energy and exergy parameters for the TES during the discharging months are evaluated using equations (14) to (21). For the overall discharging stage, energy and exergy efficiencies are evaluated with equations (22) and (23) for the TES in the Friedrichshafen DE system, as 85% and 41%, respectively.

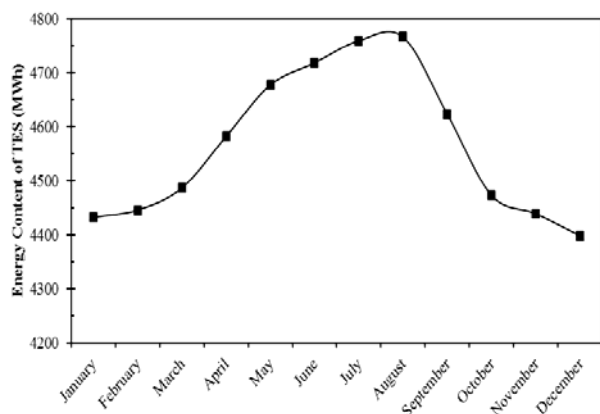


Figure 4: Energy content of the Friedrichshafen TES in 2006

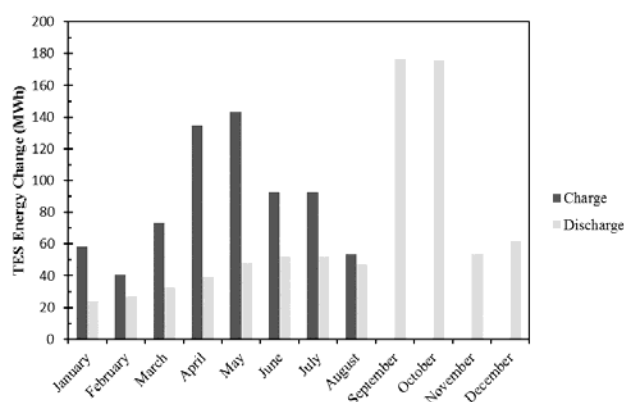


Figure 5: Friedrichshafen DE System TES monthly charging and discharging in 2006

Figure 4 is the result of the charging and discharging calculations of the TES in the Friedrichshafen DE system. This shows energy content of the TES in Friedrichshafen DE system. This can be observed from March to August energy level of the TES increases, in the charging stage, while in the Fall, energy levels drop, in the discharging stage.

Furthermore, results of the monthly calculations of the TES in Friedrichshafen are depicted in the form of the charging and discharging as Figure 5. This diagram demonstrates monthly performance of the TES in the form of the charging and discharging energy. This can be seen from the start of January charging of the TES because the day light starts increasing, ambient temperature is growing apparently heat demand decreases. From March, since the environment temperature and daylight rise and energy demand declines, therefore charging level is higher than discharging up to August. From that point, the ambient temperature and sunlight decline; so discharging occurs faster in the TES than charging.

Figure 5 is plotted based on the calculated data for year 2006, while actual performance of the Friedrichshafen DE system is influenced by some operational conditions which were not accessible. In this study, no operational condition is assumed over lack of operational information. Moreover, this was originally assumed that the priority is with TES discharging energy rather than using fossil fuel energy. This is the one reason to indicate why the major discharging happens in September and October. As mentioned previously, there must be some operational conditions that impact the prioritization of energy consumption.

For the TES, the overall energy efficiency η_{TES} is determined using equation (25) to be 60%. Similarly, the overall exergy efficiency Ψ_{TES} is calculated through equation (27) as 19%.

VALIDATION

To validate earlier estimations regarding the TES in the Friedrichshafen DE system, one source is the study in which the TES was analyzed by Raab et al. in 2002 [17]. The authors state that the TES generally charges from May to August and discharges in the fall months. It is understandable, that this depends on the operating return temperature. The environment temperature also impacts the amount of the charging and discharging energy.

Raab et al. present data for the early years' working of the Friedrichshafen TES [17]. Table 2 shows data for 2002 versus present study's calculation results for 2006. The bold numbers are calculated in the present study. Based on the bold numbers, efficiency of the TES is about 60% which is the same as results of other references [18-20]. Similarly, from 2002 data efficiency of the TES is 59% which is in good agreement with the present study findings, while heat data in 2002 are slightly different from 2006. Hence, up to this point it is clear that the assumption for the TES performance is reasonable, and the energy efficiency result are in good agreement with those of previous studies.

Table 2: Comparison of energy data (in MWh) in 2002 and 2006

Energy quantity	Year	
	2002	2006
Energy provided by gas boiler	1772	2310
Energy demand (buildings + loss)	2423	3017
Solar energy into DE	989	803
Charged energy in TES	823	591
Discharged energy by TES	485	353
Heat loss for TES	338	238

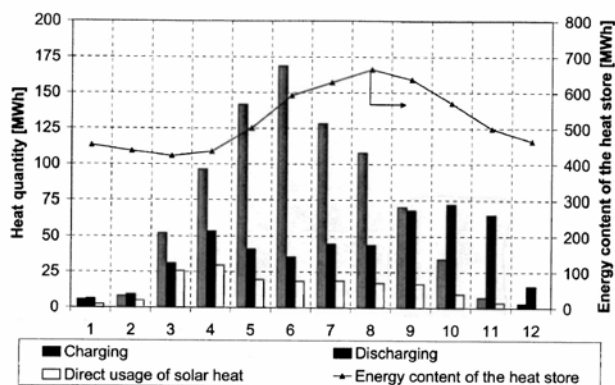


Figure 6: Charging and discharging heat store in 2002,
Source: [17]

The actual performance diagram of the TES in the Friedrichshafen DE system in 2002 is presented in Figure 6 by Raab et al. [17]. This diagram shows the energy content of the TES in that particular year (2002). In August the column is at its maximum, which means the TES is at its highest energy contents. The energy content of the TES increases between April and August, when it decreases through the fall. In addition, to the energy content of the Friedrichshafen, the bar charts in Figure 6 illustrate the charging and discharging of the TES in 2002, which occurs 11 months of the charging and 12 months of the discharging. This timing of the charging and discharging is in good agreement with the results of the present study.

In Figure 6, the trend of the energy content in the TES in the Friedrichshafen DE system in 2002 is similar to that presented in Figure 5 for 2006, which was the result of the present study. However, Raab et al. made Figure 4 based on actual data from the Friedrichshafen DE system [17]. Accordingly, it can be concluded that the initial assumptions in this research closely resemble actual performance.

Moreover, heat content of the TES depicted in Figure 6 for 2002 by Raab et al. is very similar to Figure 5 for 2006, which charts the results of the present study. However, there are some differences between the two graphs for the charging stage, especially for September and October. The difference is due to the following three reasons.

First, the returning water temperature in 2002 was 40 °C [17], while the returning water temperature in 2006 was reported as 55.4 °C. This difference is the key condition that defines the discharge stage period for the TES in the Friedrichshafen DE system. In other words, if the thermal conditions of 2002 were applied to

2006, there would be more discharge energy in November and possibly in December from the TES into the Friedrichshafen DE system.

Second, the wet condition of the TES insulation caused an increase of heat loss by the TES [17]. Faster use of restored energy in the TES is more efficient than use over a longer period. Thus, the bar charts for September and October 2006, show a higher discharge distribution compared in 2002. Furthermore, some valve malfunction and breakage in the TES in the Friedrichshafen DE system is not mentioned here because they were reported by [21].

Third, the environment temperature difference between 2002 and 2006 in Friedrichshafen has a minor impact on the discharging energy from the TES.

RESULTS and DISCUSSION

1. Impact of Return Water Temperature

To show the impact of return water temperature, the energy availability of the Friedrichshafen DE system TES is depicted with four different returning water temperatures at $T = 55.4$ °C, $T = 50$ °C, $T = 45$ °C, and $T = 40$ °C. The first temperature is the actual return water temperature in 2006 and the last three temperatures are only assumption value to show the impact of returning water temperature. Note that the system originally returned water at a temperature in 2002 of 40 °C [17]. Figure 5 demonstrates the energy availability of the TES with four various returning temperatures. As illustrated in Figure 7, the increasing return water causes a drop of energy availability of the TES in the performance period. Furthermore, the operating period of TES is also expanded by reducing the return water temperature.

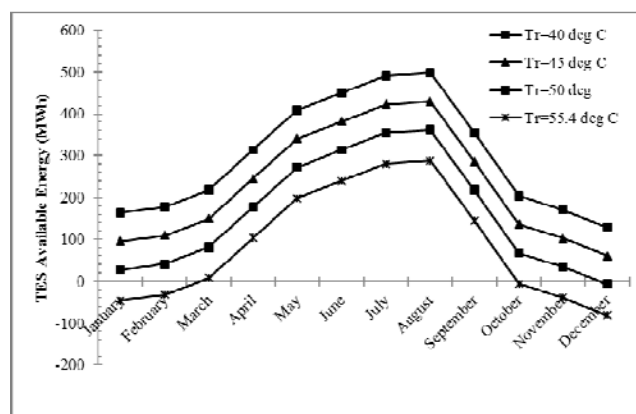


Figure 7: Energy availability of the TES in the Friedrichshafen DE system with return water temperature

2. Friedrichshafen Thermal Energy Storage: Actual and Design Variances

Raab et al. after years of observations explained that a moderate efficiency of 60% for the Friedrichshafen TES is due to heat loss [17]. The heat loss of the TES in the design stage was considered to be an annual maximum of 220 MWh. The actual heat loss is higher; in some years it was reported to be 360 MWh. The roots of higher heat loss follow:

- The main reason is the higher operational temperature of the Friedrichshafen DE system which causes the return temperature from the thermal network is greater than what originally designed; this makes the lower temperature difference between the TES and the returned water. Consequently, lower available energy by the TES for the Friedrichshafen DE system, as explained in the previous section.
- The lower third of the TES in the Friedrichshafen DE system is not thermally insulated. Since it was expected to have lower heat loss in the design stage.
- Part of the insulation of the TES is also wet due to drainage of ground water. Insulation issues are the origin of extra heat loss for the TES.
- Connection pipes as well as lengthy piping between heating plants and the TES, create noticeable heat loss and a drop in temperature from the TES outlet to the thermal network.

Nußbicker-Lux also expressed that the annual heat discharge is low because the network return temperature is high [21]. Nußbicker-Lux added that due to low temperature of the TES, it was previously charged with boilers and for the recent years TES has not been an active part of the DE system.

3. Economic Performance

The economic impact of the TES can be examined in two ways:

First, the cost of the TES(s) can be seen as added to the original cost of the DE system. The cost of the TES(s) is defined as initial and operating costs. The initial cost of the TES can be broken into installment payment of the loan. The operating cost of the TES(s) includes maintenance and insurance during the performance of the TES(s).

Second, the TES(s) assists the primary system to satisfy the heat demand of the consumers. Thus, through the presence of the TES(s) in the DE system, a smaller primary system can be applied, which means less capital can be allocated to the primary system. This reduces operating cost for maintenance and insurance. Furthermore, it results in a lower consumption of fuel for the primary system as well. Consequently, there is a saving on both the initial and operating costs of the primary system.

CONCLUSION

The TES in the Friedrichshafen DE system has been analysed. The input energy and exergy to the TES during the charging are energy and exergy which are harvested by solar collectors, mainly in the spring and summer, and the stored energy and exergy are subsequently discharged to the Friedrichshafen DE system. Energy and exergy analysis of the TES in the Friedrichshafen DE system is an application of some of these developed equations. Furthermore, the analysis provides a practical insight for actual TES as part of the DE system. The TES of the Friedrichshafen DE system was determined for the following parameters:

- The monthly charging and discharging energy of the TES in 2006;
- Energy and exergy level of the TES during the year 2006; and
- The overall energy and exergy efficiencies of the TES which are 60% and 19%, respectively.

The findings of the TES in the Friedrichshafen DE system show that by increasing the return media temperature, the exergy of the TES reduces.

Furthermore, by the comparing the performance of the Friedrichshafen DE system TES in 2002 and 2006, the following conclusions can be drawn:

- The pipe lengths from/to the TES, number and performance of valves, design and leakage risk factor of the TES insulations, and the return media temperature, are important factors that should be seriously studied prior to build the actual TES.
- Variances between original designed specifications of the above factors with the actual one in practice caused the moderate performance of the TES in the Friedrichshafen DE system.

ACKNOWLEDGEMENT

Financial support provided by the Natural Sciences and Engineering Research Council of Canada is gratefully acknowledged.

NOMENCLATURE

c_p	Specific heat capacity at constant pressure (kJ/kg K)
c_v	Specific heat capacity at constant volume (kJ/kg K)
Ex_c	Exergy of the TES in the charging stage (kJ)
Ex_{des}	Exergy destroyed (kJ)
Ex_i	Initial exergy in the TES (kJ)
Ex_{in}	Inlet exergy of the TES (kJ)
Ex_{out}	Outlet exergy of the TES (kJ)
Ex_{rec}	Exergy of recovered energy (kJ)
h_c	Specific enthalpy of the final charging (outlet) media for the TES (kJ/kg)
h_{in}	Inlet specific enthalpy (kJ/kg)
h_{out}	Outlet specific enthalpy (kJ/kg)
h_r	Specific enthalpy of the return media to the TES (kJ/kg)
M	Mass of storing medium (kg)
m_c	Mass of circulating media transporting energy to the TES in charging stage (kg)
m_d	Mass of the outlet media transporting energy from the TES in discharging stage (kg)
Q_c	Thermal energy accumulated in the TES during the charging stage (kJ)
$Q_{in, TES}$	Input thermal energy to the TES (kJ)
$Q_{loss, c}$	Heat loss the TES in charging stage (kJ)
$Q_{loss, d}$	Heat loss of the TES during the discharging stage (kJ)
Q_{out}	Output thermal energy to the TES (kJ)
s_{in}	Inlet specific entropy (kJ/kg K)
s_{out}	Outlet specific entropy (kJ/kg K)
s_r	Specific entropy of the return media to TES (kJ/kg K)
T_0	Ambient temperature (Reference temperature for exergy) (K)
T_c	Charging temperature (K)
T_d	Discharging temperature (K)
T_i	Initial temperature (K)
T_r	Temperature of the return flows to the TES (K)

GREEK LETTERS

η_c	Energy efficiency of the TES in charging stage (%)
η_d	Energy efficiency of the TES in discharging stage (%)
η_{TES}	Energy efficiency of the TES (%)

Ψ_c	Exergy efficiency of the TES in charging stage (%)
Ψ_d	Exergy efficiency of the TES in discharging stage (%)
Ψ_{TES}	Exergy efficiency of the TES (%)

ACRONYMS

CFC	Chlorofluorocarbon
CHP	Combined Heat Plant
CSHPSS	Central Solar Heating Plant with Seasonal heat Storage
DE	District Energy
LEED	Leadership in Energy and Environmental Design
PCM	Phase Changing Materials
TES	Thermal Energy Storage
USGBC	United States Green Building Council

REFERENCES

- [1] M. Kharseh and B. Nordell, "Sustainable heating and cooling systems for agriculture," *Int.J.Energy Res.*, vol. 35, pp. 415-422, 2011.
- [2] H. Bo, E.M. Gustafsson and F. Setterwall, "Tetradecane and hexadecane binary mixtures as phase change materials (PCMs) for cool storage in district cooling systems," *Energy*, vol. 24, pp. 1015-1028, 1999.
- [3] D. Schmidt, "Low exergy systems for high-performance buildings and communities," *Energy Build.*, vol. 41, pp. 331-336, 2009.
- [4] Rezaie, B., Reddy, B.V., Rosen, M.A., "Role of Thermal Energy Storage in District Energy Systems," in *Energy Storage*, M.A. Rosen, USA: NOVA Publisher, 2011.
- [5] H. Tanaka, T. Tomita and M. Okumiya, "Feasibility study of a district energy system with seasonal water thermal storage," *Solar Energy*, vol. 69, pp. 535-547, 2000.
- [6] J. Söderman, "Optimisation of structure and operation of district cooling networks in urban regions," *Appl.Therm.Eng.*, vol. 27, pp. 2665-2676, 2007.
- [7] I. Dincer and M.A. Rosen, *Thermal energy storage: systems and applications*, West Sussex, UK, Wiley, 2011.

- [8] M.A. Rosen, M.N. Le and I. Dincer, "Efficiency analysis of a cogeneration and district energy system," *Appl. Therm. Eng.*, vol. 25, pp. 147-159, 2005.
- [9] H. Lund, B. Möller, B.V. Mathiesen and A. Dyrelund, "The role of district heating in future renewable energy systems," *Energy*, vol. 35, pp. 1381-1390, 2010.
- [10] J.S. Andrepont, "Developments in thermal energy storage: Large applications, low temps, high efficiency, and capital savings," *Energy Engineering*, vol. 103, pp. 7-18, 2006.
- [11] T. Griffin, "LEED® District Energy The New Version 2.0 Guideline: It's here!" *District Energy*, vol. 96, pp. 55, 2010.
- [12] J. Nußbicker-Lux, D. Bauer, R. Marx, W. Heidemann and H. Müller-Steinhagen, "Monitoring Results from German Central Solar Heating Plants with Seasonal Thermal Energy Storage," in *EFFSTOCK 2009*, June 14-17, 2009.
- [13] N. Fisch and R. Kübler, "Solar assisted district heating-status of the projects in Germany," *Int J Sol Energy*, vol. 18, pp. 259-270, 1997.
- [14] V. Lottner and D. Mangold, "Status of seasonal thermal energy storage in Germany," in *Terrastock 2000, 8th International Conference on Thermal Energy Storage, August 28 - September 1, 2000*, 2000.
- [15] H. Zhai, Y. Dai, J. Wu and R. Wang, "Energy and exergy analyses on a novel hybrid solar heating, cooling and power generation system for remote areas," *Appl. Energy*, vol. 86, pp. 1395-1404, 2009.
- [16] Tutiempo network, "TuTiempo.net," vol. 2011, Accessed July 10, 2011, <http://www.tutiempo.net/en/Climate/FRIEDRICHSHAFEN/109340.htm>.
- [17] S., Raab, D., Mangold, W., Heidemann, H., Müller-Steinhagen, "Solar assisted district heating system with seasonal hot water store in Friedrichshafen (Germany)," in *EuroSun: The 5th ISUE Europe Solar Conference*, 2004.
- [18] T. Schmidt, J. Nussbicker and S. Raab, "Monitoring Results from German Central Solar Heating Plants with Seasonal Storage," *ISES 2005 Solar World Congress 2005*.
- [19] D. Bauer, R. Marx, J. Nußbicker-Lux, F. Ochs, W. Heidemann and H. Müller-Steinhagen, "German central solar heating plants with seasonal heat storage," *Solar Energy*, vol. 84, pp. 612-623, 2010.
- [20] *ASHRAE Handbook - Heating, Ventilating, and Air-Conditioning Applications*, American Society of Heating, Refrigerating and Air-Conditioning Engineers, Inc., 2007.
- [21] J. Nußbicker-Lux, "Performance of the TES in Friedrichshafen DE system" personal communication, 2012.

SIMULATION OF A DISTRICT HEATING NETWORK FOR A CASE STUDY IN THE CITY OF VIENNA CONSIDERING ENERGY AND EXERGY LOSSES

M. Potente¹, K. Ponweiser¹

¹ TU Wien, Institute for Energy Systems and Thermodynamics

Keywords: *District heating network, Urban energy systems, Energy losses, Exergy losses*

ABSTRACT

District heating networks are systems for the transport and distribution of thermal energy, responding efficiently to consumers' needs. They are an important part to take into account inside urban energy facilities.

A proper hydraulic simulation which calculates automatically mass and energy balances is the previous step before any design or project in this field. Likewise, calculating destroyed exergy gives advice to urban planners about the best option between different scenarios, like changes in operation conditions or installations, since the exergy measures the quality of thermal energy in a thermodynamic system.

A simulation of a district heating network was built, calibrated and started, with the aim of solving all pressure, mass, energy and exergy balances for a group of buildings situated in one of the districts of Vienna (Austria) under different scenarios, in order to understand the behaviour of the modelled network.

Additionally, other facilities like heat storage tanks were dimensioned and included in the model.

A research about exergy losses calculation adapted for a district heating system was considered, as well as synthetic heat demand profiles for both residential and special buildings, (for example hospitals, offices, churches...etc.) both for heating and hot water consumption.

INTRODUCTION

Since the first district heating network installation was created in Lockport (New York, USA) [1] at the end of XIX century, until the actual new possibilities based on low temperature systems [2], several studies have been carried out and now are focused on developing and evolve thermal networks combined with other technologies like renewables [3-4], thermal storages [5], heat pumps [6], or refurbishment [7].

Progressively, more and more cities have started to install and operate different kinds of district heating networks according to their needs, so that those systems are now the most popular way of thermal energy supply in the majority of cold climate countries, especially Scandinavia, central and eastern Europe.

The common issue which links all those projects is based on the necessity of tools which allow engineers, scientists and urban planners to predict how an urban thermal network will perform under the different situations. In addition, small simulations at district scale concerning low demands [8], have been revealed as the most realistic and appropriate options for the improvement of existing networks and their future extension and development.

BACKGROUND

The behaviour of the network is analyzed from two main variables:

- 1) Heat losses to the environment
- 2) Exergy losses or destroyed exergy

Exergy can be defined as the maximum theoretical work that could be obtained from the interaction between a thermodynamic system and the reference environment. If the state of a certain amount of matter differs from the state of the environment, the possibility of producing work will exist.

Just as the system evolves towards the equilibrium with the environment this possibility will be reduced.

Consequently, exergetic yield shows a measure of the quality of the energy for a thermodynamic system. In the other hand, the energetic yield deals with the total amount of utilized energy for the mentioned system.

The reference environment is defined as a portion of the atmosphere whose intensive properties do not change significantly as a result of any considered process. A simple huge compressible system will be assumed, considering constant and uniform values for temperature and pressure.

In this study, reference environment is the existing air inside the trench where the pipes are installed. It is considered as a constant value $T_{ref} = 281.15$ K.

For the calculation of energy and exergy balances applied to a district heating network, procedure of Çomaklı [9] was followed, which in turn comes from Kotas' findings related to the exergetic study of thermodynamic systems [10].

In this method the terms of global energy and exergy balances are calculated throughout the following expressions (all are energy and exergy flows, in kW):

$$\dot{Q}_i + \dot{W}_p = \dot{Q}_{losses} + \dot{Q}_c \quad (1)$$

- \dot{Q}_i = produced heat transferred to network's water, in this case it's considered as the heat exchanged in the substation.
- \dot{W}_p = electrical work introduced in the system.
- \dot{Q}_{losses} = total heat losses.
- \dot{Q}_c = heat which is finally supplied to the consumers

$$\eta_E = \frac{\dot{Q}_c}{\dot{Q}_i + \dot{W}_p} \quad (2)$$

- η_E = energetic yield.

$$Ex_i + Ex_w = Ex_{lossA} + Ex_{lossB} + Ex_{lossC} + Ex_c \quad (3)$$

- Ex_i = Exergy associated to the flow of hot water.
- Ex_w = Exergy associated to mechanical or electrical work introduced into the system.
- Ex_{lossA} = Destroyed exergy associated to heat losses in the system.
- Ex_{lossB} = Destroyed exergy associated to mechanical or electrical energy losses.
- Ex_{lossC} = Destroyed exergy associated to heat transfer in heat exchangers.
- Ex_c = exergy finally supplied to the consumers.

$$\psi = \frac{Ex_c}{Ex_i + Ex_w} \quad (4)$$

- ψ = exergetic yield of the system.

METHODS

In this article, a detailed analysis for a low heat demand residential urban area was carried out. A quasi-dynamic simulation which calculates hydraulic, exergy and energy balances is created and performed.

The studied case consists of one of the secondary district heating grids of the city of Vienna, which is heated from the primary network through the substation and covers a small neighbourhood of 21 buildings (20 residential and a special one which does not consume service hot water), as it is displayed in Fig. 1 below:

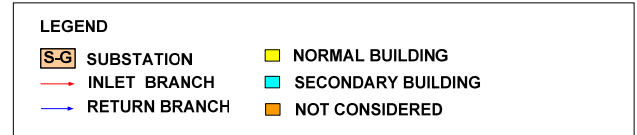


Figure 1. Map of the studied area, including buildings involved and probable outline of the district heating network

The model is based on heat demand profiles for buildings, distinguishing between heating and hot service water (potable water).

The entire simulation is structured in three parts:

- 1) Substation
- 2) Grid of pipes
- 3) Consumption points

Moreover, the program is prepared to calculate results before any changes made by the user, either from a structural point of view (addition, substitution or elimination of elements) or operational (changes in the values of the parameters or technical characteristics of the network, such as insulation, network temperature, heat exchanger's ΔT).

The main goal of the present study is show the performance of the network concerning heat and exergy losses.

The main method used was a simulation developed using the software environment Matlab-Simulink-Simscape.

A general schematic view explaining how the entire framework is structured can be seen in Fig. 2.

Table 1. Assumption for cases studied

Cases	Scenarios
Case A	actual situation
Case B	Inlet T reduced 20 °C
Case C	Inlet T reduced 40 °C (LTDHN*)

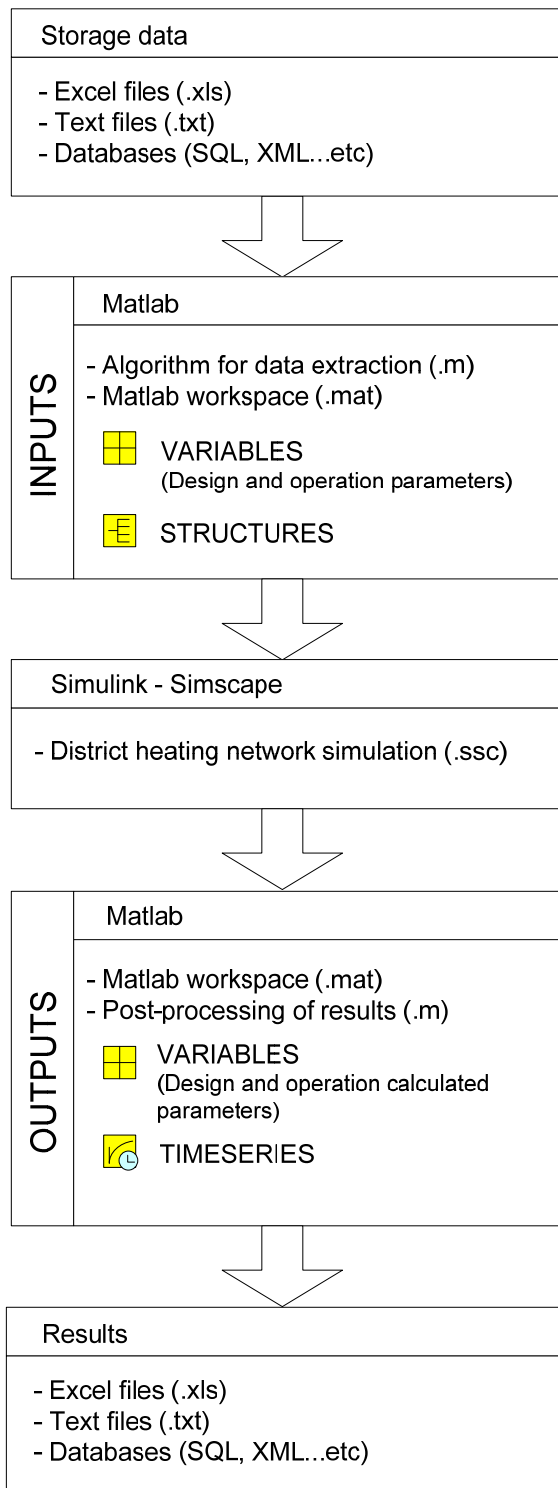


Figure 2. General diagram of the simulation

Most of the time the model was performed mainly for the actual situation, with no modifications and keeping the parameters always the same. But the simulation must be probed for different conditions as well, being the inlet temperature of the water flowing through the pipes one of the most important variables that could be changed. In Table 1 some scenarios are shown, with *LTDHN = Low Temperature District Heating Network, as a kind of network that requires buildings with high

energy efficiency [2], combining heat pumps with renewable energies. It's introduced now but will be considered again for further extensions of this work.

Mentioned network simulation is the .ssc file which sends and receives data from Matlab's workspace to other possible formats. Tables 2 and 3 below show the main inputs and outputs managed by the program.

(i) Specified value calculated for each building

The simulation is composed by blocks linked together representing the constitutive elements that make up a real district heating network, such as heat exchangers, storage tanks, insulated pipes, hydraulic pumps and the substation.

Each block is programmed to receive inputs, perform all necessary calculations and generate outputs which in turn will be inputs for the next block. These calculations are conditioned by those specific parameters such as for example: length, nominal diameter of the pipe...etc

As already mentioned, heat demand profiles are the main data input from which the circulating mass flow of the grid is calculated. In Fig. 3 a basic diagram is shown to indicate how the connections are installed inside each building, differentiating both services.

Table 2. Inputs of the simulation

Variable name	Abbr.	Unit
Heat demand for service hot water	HW	kW
Heat demand for heating	H	kW
Return pressure	Pr	Pa
Temperature of inlet service water	Tcr sw	K
External temperature	T ext	K
Reference temperature	T ref	K

Table 3. Outputs of the simulation (network)

Variable name	Abbr.	Unit
Pressures of the network	P	Pa
Temperature of the network	T	K
Temperature of radiators water	T rad	K
Return temperature radiators water (i)	Tr rad	K
Temperature hot service water	Tcs sw	K
mass flow district heating water	m flow	kg/s
mass flow consumed service water (i)	m flow sw	kg/s
mass flow radiators water (i)	m flow rad	kg/s

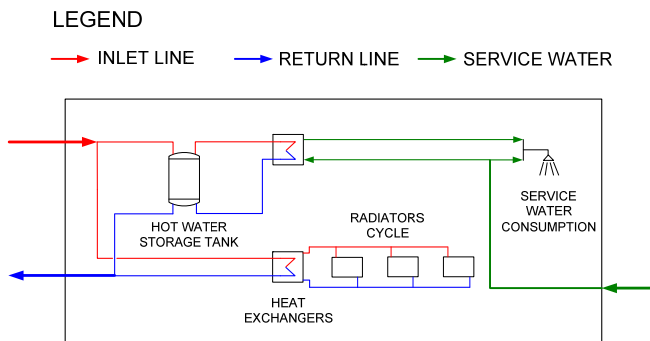


Figure 3. Basic schema about hot water and heating services inside the buildings

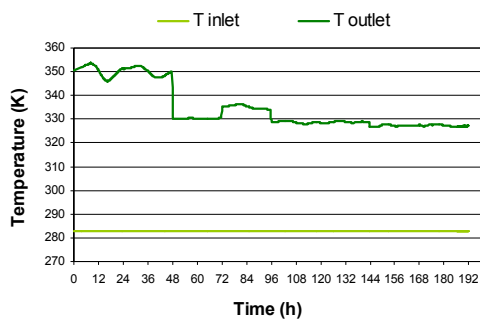


Figure 4. Service water temperatures for a random building.

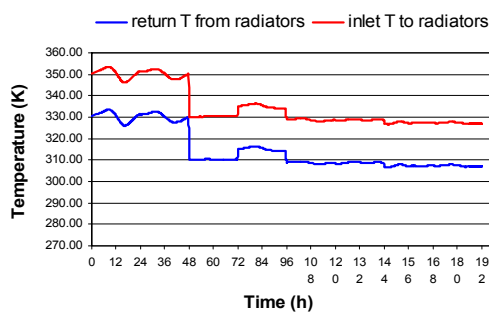


Figure 5. Radiators circuit temperatures for a random building

The other key input fed to the model through the substation block is the external temperature, according to which the temperatures of both primary and secondary networks are regulated. This regulation comes from the calibration lines, commonly referred to “heat lines” or “heat curves”.

The simulation has been programmed allowing the user to modify the temperature of the network, just indicating the desired supplied temperature recalibrates the parameters of the heat lines. In principle those parameters are tabulated depending on the temperatures generated by domestic radiators (between 75 and 85°C).

Both energy demand and external temperature profiles are based on 8 symbolic days (Extreme winter,

standard winter, midseason and summer), with the purpose of covering all possible weathers during the year. Time step considered (Δt) = 0.25 h (one value every 15 min.) Total profiles' length is 192 h.

RESULTS

Outputs produced by the simulation were classified as well into substation, network and buildings, in order to see the behaviour of the network and check if the results are realistic.

In the first place, all information related with one random building will be shown, starting with Fig. 4, which shows a clear dependence of hot water stream against supply temperature of the district heating network.

This close dependence appears also in Fig. 5, in which inlet and return temperature profiles for radiators circuit are displayed.

Minimum service water supply temperature is 330 K = 57°C, which is enough for the prevention of Legionella.

Table 4. Outputs of the simulation (balances)

Variable name	Abbr.	Unit
Total heat flow exchanged in the substation	Qi	kW
Total heat flow supplied to the consumers	Qc	kW
Total flow of heat losses	Q losses	kW
Total mechanical work supplied to the network	Wp	kW
Energetic yield of the system	E yield	-
Total exergy flow associated to a hot water stream	Ex_i	kW
Total exergy flow supplied to the consumers	Ex_c	kW
Exergy losses flow related to heat losses	Ex loss A	kW
Exergy losses flow related to hot water transportation	Ex loss B	kW
Exergy losses flow related to the heat exchange	Ex loss C	kW
Total flow of exergy losses	Ex loss	kW
Total mechanical work supplied to the network	Wp	kW
Exergetic yield of the system	E yield	-

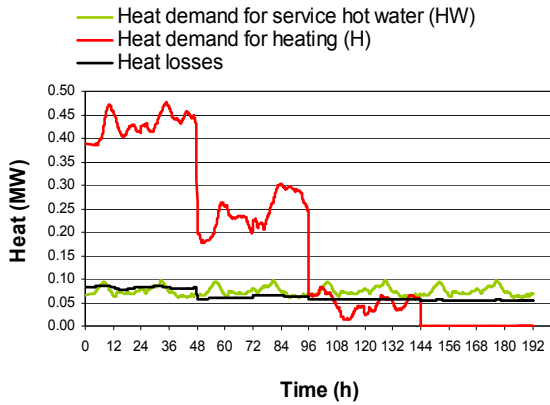


Figure 6. Energy balance of the random building

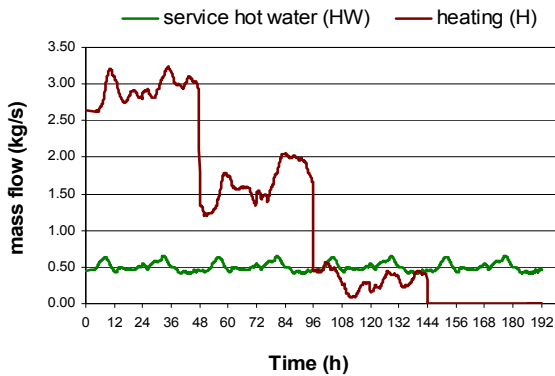


Figure 7. Mass flows consumption inside a random building

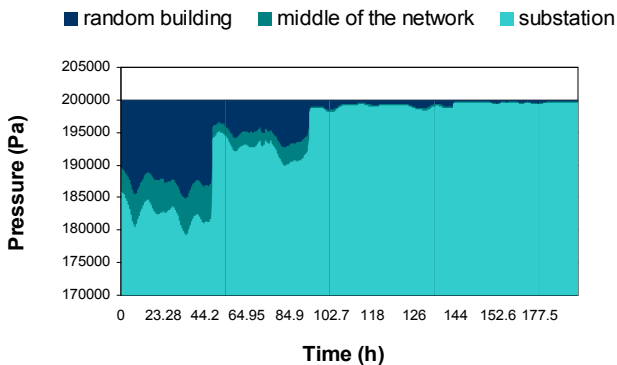


Figure 8. Evolution of pressure along the network (return branch)

In Fig. 5 both profiles are parallel because it has been stipulated the dependence between return water and supply water of the radiators cycle, with $\Delta T_{rad} = 20^{\circ}C$.

Fig. 6 defines the complete energy balance for the building, in which heating demand is more than four times higher than service hot water demand in the case of extreme winter (left side of the graph), and almost double for standard winter.

Heat demands for both profiles are quite similar. That was expected because the main heat losses of the buildings are supposed to be the storage tanks for hot service water.

Finally, Fig. 7 compares both mass flows consumed inside the building.

Next step is the analysis of the hydraulic and energetic performance of the network, without considering buildings and substation.

Pressure balances are also introduced inside all the pipe blocks included in the model, taking care of the elemental calculation of hydraulic grids which confirms that the farther building from the substation is defined as the last one, which defines the return pressure of the network. From here to the beginning of the structure all the other buildings and pipes will decrease progressively their pressures as obtained in Fig. 8. for the return branch and in Fig. 9 for the inlet branch.

The separation between lines in the left side of Figs. 8 and 9 corresponds to extreme winter period, in which the mass flow of district heating water is higher because demand is higher. This reasoning leads to higher volumetric flow and finally, greater fluid velocity, producing larger pressure losses

To understand the hydraulics of the network it's important to introduce here the concept of principal branch, which links the substation with the last building, defining the total pressure losses of the network, so that the other pressure drops from the rest of the branches are not considered.

As Figures. 8 and 9, graphs for figures 10 and 11 were obtained, showing supply and return temperature for three different distances in the network (substation, middle of the network and random building), which is one of the farthest consumption points of this area.

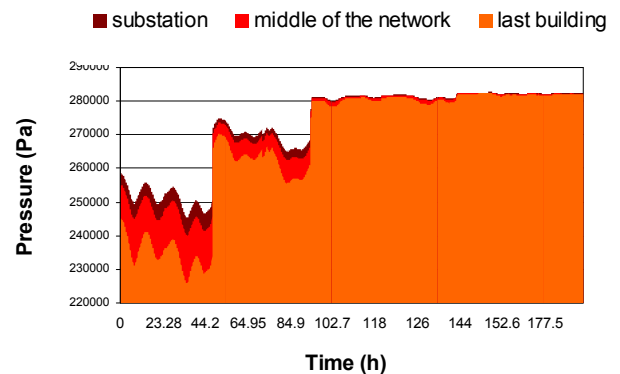


Figure 9. Evolution of pressure along the network (inlet branch)

Here it is possible to comment a significant phenomenon that portrays the physical behaviour of the network and results something interesting to be kept in mind. Observing Fig. 10 it is possible to appreciate for both extreme and normal winter days that all the curves are extremely close together. It means that for some periods of the year, distance is not a relevant factor which influences over the heat losses.

It is from midseason and clearly in summer when heat losses start decreasing strongly depending on the distance, and, since the temperature of the surrounding air of the pipes is accepted as constant, means that is the mass flow of hot water the relevant factor, which is commonly considered as the thermal inertia of the network, and defined as mass flow * calorific capacity. The higher the mass flow of hot water is, the smaller the heat losses will be.

In the case of return temperature (Fig. 11) no pattern or relationship with distance is observed. This is because this branch only receives return water at different temperatures from the buildings, each of them with its own and different return temperature.

During the summer nobody turns on the heating, so radiator circuits are not involved in the calculation. Therefore return temperature is assumed as a fixed value, because only heat for domestic water is involved in the energy balance.

Finally Fig. 12 must be shown, because describes the performance of the hydraulic pump, detailing pressure drop and consumed power W_p .

Power consumption keeps constant for warm days because only hot water supply is considered, whose mass flow keeps more or less constant for all the year

In third step, Fig. 13 owns illustrative values of the performance of the simulation.

The most remarkable issue here is analyzing the periods in which the external temperature reaches or exceeds a certain value, then both networks have constant temperatures, again calibration line is acting here.

Last group of results were calculated according to the considered scenarios in Table 1.

By comparison between the different results it can be deduced how the network behaves after changes, and where strengths and weaknesses are in order to understand how the system works and how can be improved.

Fig.14 gathers all total heat losses under different supply scenarios. Those results will be further used to calculate energetic yields, as shown in Fig. 15.

In the same way as Fig 14. is related with heat losses, Fig. 16 informs about the total destroyed exergy of the network under different supply temperatures.

Finally Fig. 17 was done summarizing the contribution of the different exergy losses in the system.

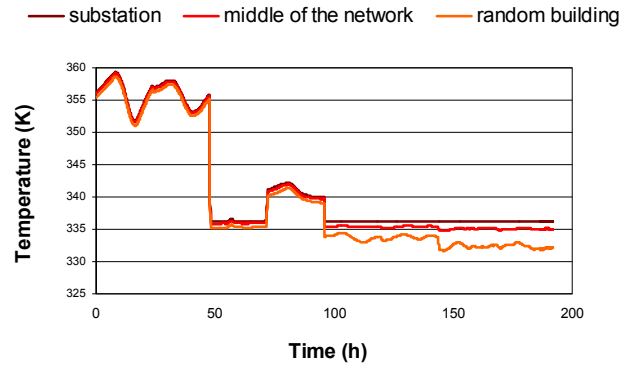


Figure 10. Evolution of temperature along the supply branch

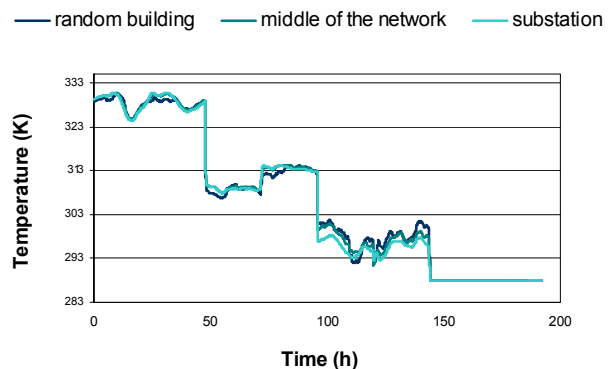


Figure 11. Evolution of temperature along the return branch

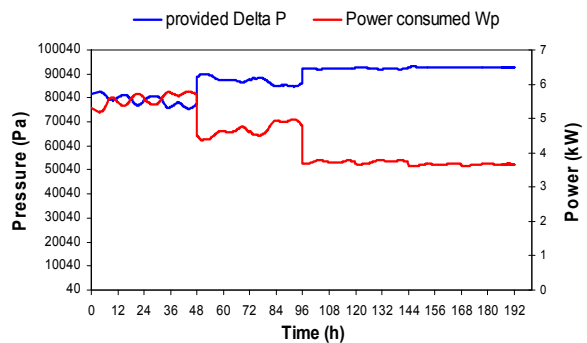


Figure 12. Operation values for the hydraulic pump

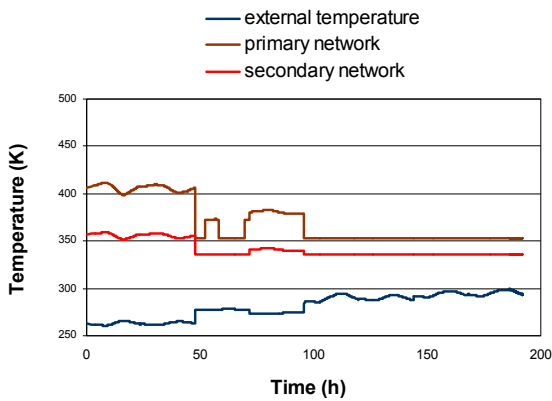


Figure 13. Comparison between the different temperatures of the system

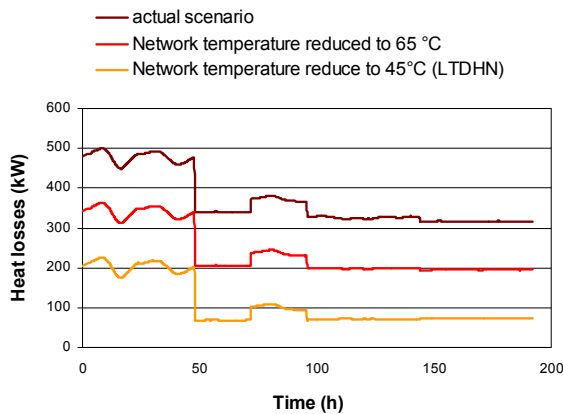


Figure 14. Comparison between the heat losses of the network for three different supply temperatures

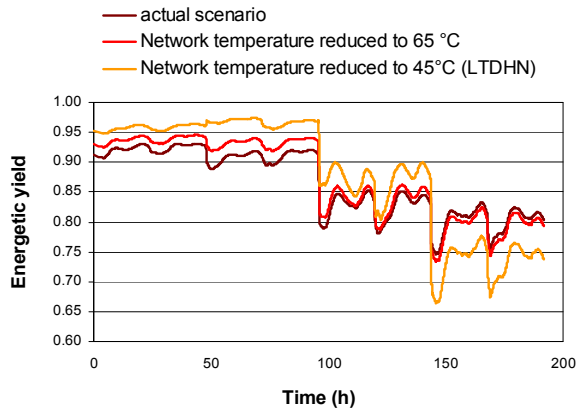


Figure 15. Comparison between the energetic yields of the network for three different supply temperatures

DISCUSSION

Both energy and exergy losses produced in the system are describing parallel profiles in their respective graphs (Figures 14 and 16), which means that those variables are strictly proportional to the supply temperature of the network. The lower the supply

temperature is, the lower the generated heat and exergy losses, and therefore the higher the energetic yield will be. This is logical because gradient of temperature is the driving force which generates heat transmission.

Even though, this relationship is not entirely followed by the energetic yield (see Fig. 15). Proportionality it is only valid for cold or midseason periods of the year. This proportion between the different results is also observed for exergy losses results (Fig. 16).

CONCLUSION

A simulation of an urban district heating network with low heat demand for heating and hot water was developed and started.

The simulation is able to calculate all energy, exergy and pressure balances according to the needs of consumption points. Other design and operation parameters like storage systems are also estimated.

Two kinds of buildings were represented, differentiating between heating and hot water consumers and only hot water consumers.

Obtained results can be used to predict the behavior of a thermal network at district level.

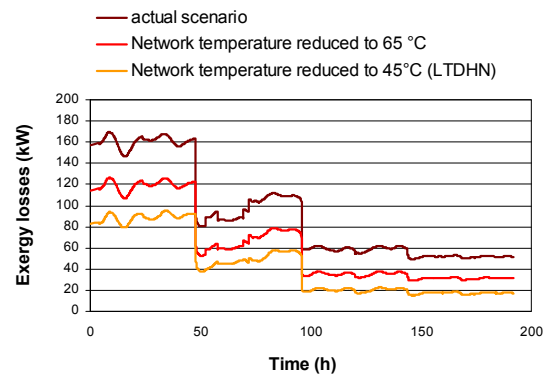


Figure 16. Comparison between the exergy losses of the network for three different supply temperatures

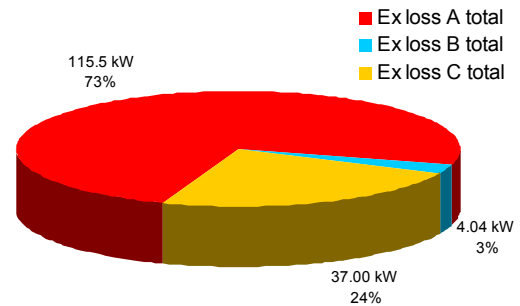


Figure 17. Distribution of exergy losses in the system

For LTDHN scenario, vulnerability in the system was revealed, pointing out an increment of the energetic yield for winter season followed by a drastic decrease for the summer period.

Therefore, reducing network inlet temperature reduces heat and exergy losses, increasing energetic efficiency of the system since exergy losses decreased. But this kind of low temperature networks cannot ensure the required comfort temperature for actual radiator systems in Vienna, but is the basis for a future study including heat pumps which will increase the temperature of inlet water to comfort temperature using other energy sources.

More capacities like thermal storages connected with renewable energies can also be implemented, completing the actual work.

The hot water storage tanks were included in the network in order to take their heat losses into account.

The used methodology allows the extension of the simulated network adding more buildings, without increasing significantly computation time.

ACKNOWLEDGEMENT

This paper is part of "CINERGY, Smart cities with sustainable energy systems" Marie Curie Initial Training Network (ITN) supported by the European Union.

REFERENCES

- [1] D. K. Baker, S. A. Sherif, "Heat transfer optimization of a district heating system using search methods", *Int. J. Energy Res.* 21 (1997) pp 233-252.
- [2] E. Zvingilaite, T. Ommen and B. Elmegaard and M.L. Franck, "Low temperature district heating consumer unit with micro heat pump for domestic hot water preparation, 2012, in Proc. The 13th

International Symposium on district heating and cooling, Copenhagen.

- [3] D. Lindenberger, T. Bruckner, H-M. Groscurth, R. Kummel, "Optimization of solar district heating systems: seasonal stage, heat pumps and cogeneration", *Energy* 25 (2000) pp 591-608.
- [4] R. Marx, D. Bauer, H. Drucek, "Energy efficiency integration of heat pumps into solar district heating system with seasonal thermal energy storage". *Energy Procedia* 57, Stuttgart (2014), pp 2706, 2715
- [5] B. Akkaya, D. Romanchenko, "Modeling and analysis of a district heating system containing thermal storage. Case study of the district heating system of Boras", Chalmers University of Technology, pp 9-51.
- [6] T. Ommen, W.B. Markussen and B. Elmegaard, "Heat pumps in combined heat and power systems", *Energy* 76 (2014) pp 989-1000.
- [7] D. Schmidt, "Low exergy systems for high performance buildings and communities", *Energy and Buildings* 41(2009) pp 331-336.
- [8] M. Rămă, J. Heikkinen, K. Klobut and A. Laitinen, "Network simulation of low heat demand residential area", 2014, in Proc. The 14th International Symposium on district heating and cooling, Stockholm, 4p.
- [9] K. Çomakli, B. Yuksel, and O. Çomakli, "Evaluation of energy and exergy losses in district heating network", *Applied Thermal Engineering*, pp 1009-1017.
- [10] T.J.Kotas, "The exergy method of thermal plant analysis", Krieger publishing company, Malabar (1995), pp 113-137, 197-204.

CHANCES FOR POLISH DISTRICT HEATING SYSTEMS

K. Wojdyga¹, M. Chorzelski¹

¹Warsaw University of Technology, Faculty of Building Services, Hydro and Environmental Engineering

Keywords: *district heating systems, district heating networks, leak detection in dh network.*

ABSTRACT

The most economical and rational means of heat supply for city inhabitants are district heating systems. Heat generated in power plants and large heat sources is cheaper than heat from individual sources. The reason for that is the amount of heat generated and the fuel used in district heating, a very important energy sub-sector for the Polish economy. Poland is one of the biggest users of district heating systems in Europe, and those district heating systems are mainly coal-fired.

What next with district heating systems, will they still be developing? In the perspective of a few dozen years, existing district heating systems in cities will be developing. In case when the investment in development of a district heating system is deemed unprofitable, densely built-up areas will develop local district heating networks powered from trigeneration sources, which will contribute to better comfort of living, as well as lower costs of heat supply. In the long term (50-100 years) in low-energy or passive buildings, the only source of energy will be electricity and the energy demand will be at a very low level.

The article will present some problems connected with district heating systems. Energy efficiency of district heating systems depends on many things: smart grid and hydraulic analysis, heat losses from pipelines, water leakages in district heating networks. Another chance for energy efficiency is cogeneration. Thanks to its developed and centralised heat supply system, Poland is ideal for cogeneration. At present, Polish district heating systems have an extensive infrastructure of pipelines and fully automated district heating substations. The advanced technical level of control equipment offers the possibility of rational heat supply for heat recipients. Polish district heating systems have a good chance to improve energy efficiency and decrease air pollution from power and heat sources. This article shows only some problems that can give opportunities for further development of the Polish district heating systems.

1. INTRODUCTION

The first water-based heating systems were created in the 19th century. In Poland, first such systems were constructed on the verge of the 19th and 20th century. These were modern systems (at the time) and their foundations are still correct. They were located in the

Infant Jesus Christ Hospital in Warsaw and on the Main Campus of Warsaw University of Technology. The systems consisted of a boiler house with coal-fired steam boilers, steam engines (piston engines) powering electricity generators and a system of engine waste heat recovery. The heat was used to heat buildings and electrical energy was used to light buildings and the area around them, as well as to provide electricity for other purposes (such as Warsaw University of Technology laboratories). The system at Warsaw University of Technology was commissioned in 1901 and the heating channels built at that time are still used until today.

After the Second World War, newly erected buildings were powered by local boiler houses located in residential areas. In 1953 in Warsaw, an old power plant was transformed into a heat and power plant. In 1954, the oldest, still working electrical power plant Żerań was commissioned (it provides circa 38% of heat for Warsaw). The largest Polish heat and power plant Siekierki (the second largest plant in Europe) was constructed in 1958-1961. Since the 1960s, in Poland larger and smaller power plants have been built based on LaMont boilers (water boilers, mechanical-stoker flow-through boilers, coal-powered boilers) of the 1.5-29 MW power. (Channel) water-based heating systems were also built, with the parameters 150/80oC and nominal pressures 6 and 16 bar. Internal installations were directly connected to the network with jet pumps (also often without them).

District heating substations created in the 1950s and 1960s did not have a system of usable hot water production due to the lack of appropriate controllers on the Polish market. Moreover, hydraulic regulation of the systems was very poor. Directly connected internal installations caused great network water losses and significant pollution of the water with corrosion products. In consequence, the existing networks suffered from very strong corrosion. Bad planning of city development resulted in significant oversizing of diameters of district heating networks built at the beginning of the 1990s.

Companies supplying heat to city inhabitants should provide reliability of supply in any conditions, along with low heat costs and limitation of combustion pollution emissions. In the last 20 years, there has been large progress in modernisation of both heat

generation systems and heat transmission and distribution systems. Efficiency of energy generation was improved, heat losses from transmission pipelines were limited. Modernisation of district heating substations and installation of weather control systems also contributed to better energy efficiency of the whole district heating system. Thermomodernisation processes of residential buildings conducted for circa 20 years significantly influenced the maintenance of district heating substations. The previously overloaded pipeline systems have turned out to be too large and oversized and so transmission efficiency has decreased. Further rationalisation of heat production and transmission is necessary and the benefits that can be achieved are significant.[1]

How can energy efficiency of district heating systems be improved? Actions should be versatile and aimed at:

- limiting heat losses from district heating pipelines,
- limiting heat losses connected with leakages from district heating system elements,
- conducting comprehensive hydraulic analyses for pipeline systems in various maintenance conditions,
- work of a few heat sources for a joint network in an open district heating system,
- introducing procedures of heat demand forecasting in the short and long term,
- building systems of heat and power cogeneration based on usable hot water demand,
- constructing heat reservoirs (especially in heat and power plants) to balance peak heat demand (they would also be reservoirs of additional water).

Introduction of such technical solutions will bring economic benefits and also contribute to limiting combustion pollution emissions.

Poland is the second (after Germany) biggest producer of district heat in the European Union. At present (2014), according to a report of the president of the Energy Regulatory Office, the installed power in Polish companies is 56.8 GW but the power ordered by recipients is only 33.6 GW, and the power used is 41.49 GW. Heat returned to the system was 250 PJ and heat supplied to recipients was 217 PJ [2]. More than 64% of heat from the sources was cogenerated but only 24% producers produce heat in cogeneration. Over 60% heat producers are small companies of the installed power less than 75 MW. They produce heat in (coal) boiler houses, without cogeneration. In future, this will give the possibility of heat cogeneration based on hot water demand. Poland depends on coal and

has great coal deposits. The fuel mix for heat generation is 75% for coal, 8% for gas, only circa 4% for oil and almost 8% for renewable energy sources. The average generation efficiency was 86% in 2014, and the average transmission efficiency 86.3% [2] (due to warm winter).

2. INFLUENCE OF EU DIRECTIVES ON THE POSSIBILITY OF DEVELOPMENT OF DISTRICT HEATING SYSTEMS

The Directive 2012/27/EU on energy efficiency and the resulting requirements on the thermal insulation of buildings will cause another significant decrease in heat demand in district heating systems. The heat transfer coefficient U [$W/(m^2K)$] for outer walls of buildings changed from 1.1 [$W/(m^2K)$] in buildings erected before 1975, through 0,25 [$W/(m^2K)$] present, to 0.2 [$W/(m^2K)$] from 2020 on. The Directive means a change in technical conditions for newly erected buildings in Poland. For example, for an apartment block, the index of annual primary energy demand for the purposes of heating, ventilation and usable hot water goes down from 105 [$kWh/(m^2*year)$] in January 2014 to 65 [$kWh/(m^2*year)$] in January 2021 (new buildings). A similar index for public buildings changes from 65 to 45 [$kWh/(m^2*year)$].

CO₂ emissions are regulated in Directive 2009/29/EU on the emissions trading system in the EU. The European Union has obliged itself to limit emissions of greenhouse gases in the sectors covered with the system EU ETS in 2020 by 21% in relation to the emissions level in 2005.

Poland has to reduce total CO₂ emissions (from all emission sources) from 406 mln Mg/a in 2013 to 383 mln Mg CO₂ in 2020 [2]. The Polish economy, also district heating, relies on coal as its own national resource. Therefore, CO₂ emissions limitations have a great impact on district heating. Higher price for CO₂ emissions, combined with a decreasing number of free emissions rights, results in a higher price of heat. This is a dangerous phenomenon, since it may lead to the situation in which the smallest recipients (single-family houses) will replace network heat with individual boilers, unfortunately powered with solid fuels (such as rubbish and coal), which in the end results in an uncontrolled increase of emissions of CO, CO₂, SO₂, dioxins, furans and particulate matter.

Directive of the European Parliament and of the Council 2010/75/EU on industrial emissions pertains to objects of fuel power greater than 50 MW (the object's total power). In Poland, this covers, for example, medium power plants, large heat and power plants and sources that work for the needs of the heat and power sector. Heating sources covered with the

directive are obliged to lower particulate matter emissions (installation of new dedusting systems), and then they will have to decrease emissions of SO₂ and NO_x by constructing relevant installations. The costs of building and maintenance of these systems entail a relatively small increase of heat prices in district heating systems, acceptable for the end recipient.

Medium Combustion Plant Directive no. 2015/2193 of the European Parliament and of the Council of 25 November 2015 is connected with limitation of emissions from medium combustion plants (fuel power from 1 to 50 MW). In Poland, there are a lot of objects (circa 4500) that fall into this category and the majority of them have the power under 5 MW. In district heating systems, there are about 676 boilers covered by the directive, of the total power of 5530 MW [2]. Appropriate combustion control of emissions of nitrogen oxides from existing furnaces with is possible without special installations. Harnessing SO₂ emissions, however, requires at least a desulphurisation installation based on the dry method of circa 70% efficiency (typically introduction of ground dolomite or limestone). This is due to the fact that on the market, coal of sulphur content lower than 0.2% is virtually impossible to obtain and only combustion of such coal would not require a desulphurisation installation. The dry desulphurisation method is the cheapest and the easiest one but it needs a good dedusting installation. Additionally, plaster stone that occurs during the desulphurisation may create low-fusible eutectics, which pollute the surface of heat exchange. This leads to the need to shut down the boiler and clean it from the sediment. Wet desulphurisation methods are not considered due to high investment and maintenance costs and for a simple reason – there is no place to locate them in small installations. A shift to gas sources is not always possible since gas is not available everywhere in Poland. It needs to be remembered that heat sources of this size are located outside big cities, where the typical income is below the national average. An increase in heat price may result in recipients leaving the network, which will lead to worse air quality (locally) instead of better quality (e.g. by connecting recipients to the district heating network). Boilers should also be equipped with high-efficiency dedusting installations (bag dust collectors), which is also the case for biomass boilers (apart from desulphurisation installations). Requirements may be higher in areas with locally increased air pollution. In future, district heating systems are expected to incorporate sources that combust municipal waste (or actually what is left from recycling), as well. Also cogeneration and trigeneration systems and building

heat accumulators will be developed to improve the efficiency of heat production systems. It will be also increased consumption of biomass as a fuel.

3. DISTRICT HEATING NETWORKS

The total length of Polish district heating systems (over 20,000 km), combined with their varied age and different manufacturing technologies, poses great challenges to district heating companies. Due to the Polish climate, heat supply must be constant. After 24-36 hours of a break in supply, the objects must be heated again, otherwise (at working parameters -20°C or -24°C) the buildings may freeze. On the other hand, network failure may lead to significant material losses (in case of a failure of a pipeline of a large diameter) and even severe burning (also lethal) when passers-by or employees are burnt. Therefore, the problem of network reliability and its failure rate are so important in the maintenance. An important role is played here by hydraulic calculations of the network. Hydraulic calculations for a district heating system should typically show the possibility of improving its work. Detailed studies are conducted for the existing condition in order to determine basic work parameters for pipeline sections and connections, such as:

- flow velocity,
- supply and return pressure,
- available pressure,
- temperature falls.

The obtained results allow to draw conclusions on improvements in the system, which cover:

- sections of pipelines where there are too high pressure losses that influence the operation of the whole network,
- sections of pipelines where pressure falls and flow velocity are too low, which means they are oversized. This influences the work of the whole network and also increases heat losses.

Other types of analyses are connected with simulation of the work of the district heating system in future. Various options of operation of the system are considered:

- the system works with lower power and flow due to thermomodernisation work done by heat recipients,
- cooperation of the district heating system with a new or modernised heat source of other working parameters than the previous source,
- with supply temperatures other than the previous ones,
- development of the district heating system and connection of new recipients.

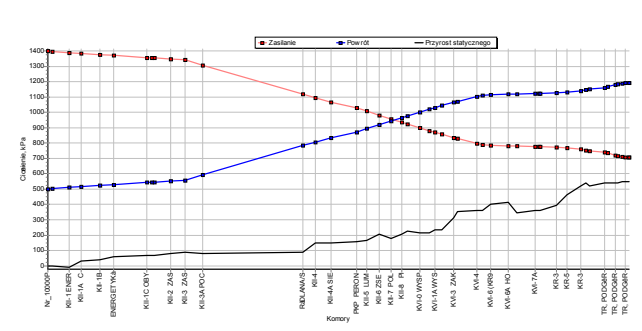


Fig. 1. Piezometric graph on the routes from the power plant to the heating chamber K1. From the chamber KII-7POL, there is negative available pressure [3]. The red line – supply pressure, the blue line – return pressure, the black line – topographic profile.

The results of hydraulic analysis for a district heating system where one of the heat sources is planned to be shut down shown on fig.1. An optimum solution of powering the whole system from one heat source is sought, because flow of network water in the power plant increased by 15%, which led to a shortage of available pressure at the end of the network, close to the shut down boiler house. Such great pressure losses make it impossible to supply the city with heat directly from the power plant. There is thus the need for significant modernisation of the network in that area, which has also been confirmed by field tests.

It is necessary to introduce technical changes in the existing system:

- make cuts of some rings in the system,
 - change control graphs of the heat source,
 - construct a network water pumping station,
 - replace parts of district heating pipelines.
- From the economic point of view, the recommended option would be the network water pumping station.

Virtually all large district heating systems (in big Polish cities) are powered from a few heat sources. An open district heating system means the work of the sources with optimum efficiency, which allows to obtain significant profits. Cogeneration systems have an advantage over separated systems due to better economic efficiency and the resulting less pollution of the natural environment. However, cogeneration systems do not always work according to optimum schemes. Sometimes, the share of water boiler power in the total power of the source is too big (or too small). Each source supplies heat only for a part of the district heating system and very often these sources work with powers significantly different from nominal powers (work for separate zones in the

network). The work of an open district heating network will allow optimum efficiency of the sources, which will bring significant profits and increase heat supply reliability for recipients.

Modernisation of district heat supply systems entails solving a number of problems connected with heat and electricity cogeneration in power plants and transmission of heat through district heating networks to recipients. Installed power reserves in heat sources (in relation to ordered power) allow to consider the possibility of a dynamic change of the location of the borders of supply zones depending on the current load of the system, independent of outdoor temperature. The freedom in determination of the borders of the zones is limited, for technical reasons:

- available powers of sources,
- transmission capacity of pipelines, and for economic reasons:
- higher costs of heat generation in sources if there is a significant shift from their optimum working condition,
- higher costs of heat transmission due to irrational changes in the structure of flow of the working fluid due to the changes of supply zones.

Work of a few sources for one network means completion of a number of technical conditions, which may require investment but may bring significant profits in the end. Costs of modernisation of the system will be borne in three groups:

- modernisation of district heating substations,
- modernisation and possible development of district heating networks,
- modernisation of pumping systems in heat sources.

Change of the supply area of each source may be done by changing the characteristics of the pumping systems (water flow and available pressure) with simultaneous change of the hydraulic resistance of the substations. Limiting heat losses in district heating systems may bring important profits for the distributor. Increasing the supply zone of one power plant will allow to decrease losses on the main pipelines powered from this source. Maintenance costs of the operator will be limited thanks to work of the network that allows to change the supply zones without the need for technical work by cutting off various parts of the network installations.

The total length of district heating networks in Poland is almost 20,255 km. This includes both networks of small heat losses and networks with virtually no

thermal insulation of very big losses. The average level of heat losses from district heating networks is systematically going down and at present stands at circa 11,8%. This is due to both the technology of construction of Polish district heating networks, and their age. According to 2014 data, circa 54% are networks in district heating channels and only 40% are preinsulated. There are also 6% of ground-based networks (on the ground and above the ground). The oldest Polish networks are over 40 years old (4%), there are circa 16% of networks that are 31-40 and 24% of networks of the age of 21-30. New networks (up to 10 years old) constitute circa 27% and at the age of 11-20 years – 29% [2].

Real annual heat losses in Polish district heating systems (both losses through heat transfer and losses connected with network water losses depending on production technology, technical condition and network size) may vary in the range of 10%-20% of the heat produced. In the summer season, when the district heating system works only for hot water purposes, relative heat losses sometimes exceed 50%. Comparing these with heat losses in foreign district heating systems, it can be assumed that there are real possibilities to significantly limit heat losses.

Determination of real heat and power losses in municipal district heating networks is a vital issue in both economic and technical terms. District heating systems where there are no steady states undergo constant changes of process parameters, which means the necessity to use complex analysis methods and physical studies connected with determination of the real values of transport losses. A precise method of determination of real transport heat losses must include numerical calculations verified with measurements of basic parameters of the district heating system. It may be stated that absolute heat losses are a complex function of a number of factors that include:

- length of pipeline sections,
- pipeline diameters,
- share of small pipeline diameters in the total network length,
- manufacturing technology of thermal insulation,
- age of district heating pipelines,
- structure of connections between pipelines,
- number and size of district heating chambers,
- methods of insulation of fittings in chambers,
- heat and hydraulic parameters of district heating systems, such as supply and return temperature and working water flows.

The simplest method of calculation of average heat losses from district heating pipelines is the balance method, which relies on comparing the amount of heat supplied from the district heating system with the amount of heat sold. A condition necessary to apply the method is the use of measuring devices of relevant class both by the recipients and the producer. The measurement must be conducted in longer balance periods, such as one month, or even a year. A disadvantage of the method is the need to make readings at the same time.

During modernisation of district heating systems and exchanging the pipelines to preinsulated ones, the possibility of decreasing the diameters of existing pipelines should always be analysed. Hydraulic calculations of pressure losses in district heating systems show that the majority of district heating systems are underburdened. The velocity of water flow in pipes in most parts of district heating networks does not exceed 0.8 m/s. Decreasing the diameters by one or even two orders of magnitude will bring a certain decrease of investment outlay and increase the profitability of the investment. Then, the possibility of connecting new recipients must always be taken into consideration.

Table 1. DH systems- data for selected countries [4]

Lp.	Country	Total district heating sales	Trench length of DH pipeline system	Load of DH network	Heat losses app./
		TJ/a	km	TJ/km	%
1	Czech Republic	89417	7738	11,56	13,8
3	Denmark	105563	29000	3,64	18,6
4	Finland	114160	13850	8,24	8,6
5	Germany	254839	20219	12,60	n.d.
6	Korea	172160	2037	84,52	n.d.
7	Poland	248693	20139	12,35	11,8
8	Slovakia	82726	4984	16,60	8,7
9	Sweden	175972	23667	7,44	8,9

/ Heat losses- uncertain.

The conducted economic analyses for an average Polish district heating system show that the most profitable is the replacement of pipelines of DN50-DN150 diameters. For these diameters, heat losses are relatively higher than for main pipelines, as well.

Leak tightness of the system is one of the main factors determining the quality of a district heating network and it is necessary for high quality of the work of all system components, such as heat sources, district heating networks and substations, and in particular heat exchangers, automatic control elements, circulating pumps etc. Moreover, system tightness, on the one hand, influences the quality of network water (with all the consequences of its lower quality) and on the other, it directly influences maintenance costs (and indirectly investment and repair costs). A decrease of district heating network tightness is the reason for a greater number of pipeline failures, greater costs of their repairs, and also more resulting damage.

A quality factor of a district heating network is the volume of network water losses, and this is measured with the number of network water replacements in the year. This is the ratio of the amount of water added and the total volume of the network. Good district heating systems in EU countries have the index in the range from 0.1 to 1.0.

In some Polish district heating networks at the beginning of the 1980s, the number of water replacements reached 25 to 60 over one year, which posed a threat to their reliable operation. The tightness of Polish district heating systems has improved a lot in recent years. The number of network water replacements decreased over four times. At present, the approximate average number of replacements, depending on the technical condition of the system, is estimated to be in the range of 3.0 to 12. Heat power losses due to losses of network water are between 1.5% in the heating season and 3.3% in the summer, for a district heating system of average technical condition.

Tightness tests conducted by a team from Warsaw University of Technology the authors participated in (unpublished results) in a district heating system of a large Polish city showed that losses due to leakages in heat sources, district heating substations and main pipelines and losses of working fluid during repairs (after failures and during planned renovations) do not exceed 6-7% of all losses. The conducted analyses showed that losses in these parts of district heating systems are respectively:

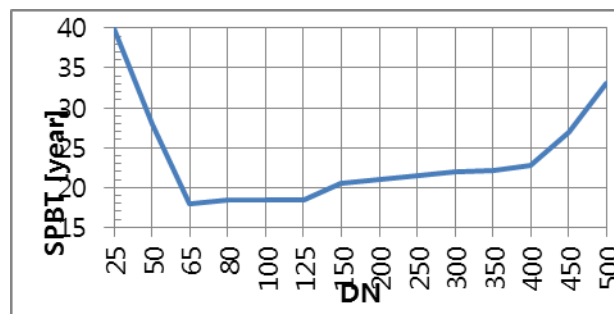


Fig. 2. Simplified relation of simple payback time of the return of investment outlay on district heating pipelines (according to the authors, approximated data) [5].

- heat sources - 1.5% on average
- district heating substations – 0.7% on average
- failures and renovations – 1.5% on average
- main pipelines - 4.5% on average

The results of the studies and conducted analyses clearly show that the main source of network water losses is micro-damage of district heating pipelines.

A perfectly tight installation simply does not exist. Whether it is considered tight or not depends on arbitrarily accepted requirements. Since greater tightness requirements are connected with higher costs of installation construction, its commissioning and operational control, designers and users try to balance a strive towards a perfectly tight installation and the cost of obtaining this tightness. In addition, there are the costs of the risk of leakages in the installation. In case of a cold water pipeline in agricultural areas or forests, possible losses connected with leakages will be low. There is small probability that even in the case of the pipeline bursting (maximum possible failure), an animal or person will die or be harmed. If a failure occurs in a district heating pipeline or network in a city, however, there is higher probability of significant losses due to bursting of the pipeline; even lethal burning of people is possible.

In order to minimise the risk of large failures (bursting) of pipelines, one should detect locations of potential failures as early as possible. There will be leaks which, due to corrosion and erosion, may lead to significant damage, including bursting of the pipeline if they are not detected and repaired. Even small leaks in the network, however, cause significant financial losses for district heating companies.

This is due to the fact that:

- a/ network water is treated water and its proper treatment is costly;
- b/ the cost of introducing it to the network has been borne;
- c/ water is heated (its temperature is higher than the surrounding temperature);
- d/ leakages generate water losses 24 hours a day.

In order to avoid losses due to leakages, they must be detected and repaired as soon as they occur. Analysis of failures in Polish district heating systems shows that the greatest number of failures occur in pipelines of the diameters DN40, DN50, DN65 and DN80. The percentage of failures in pipelines of these diameters clearly exceeds their percentage in the total length of these pipelines in the district heating system. At the same time, the majority of failures occur in pipelines of DN40 to DN200. There is also a dependence between the number of failures and the volume of network water losses.

According to the authors' studies, the most often used method is control of the volume of added water (almost all companies), along with visual inspection of the network [6].

The next most popular methods are: tests with a geophone and section tests of the network. Geophone tests are usually conducted by a company employee. Much more rarely are external specialist companies employed.

Colouring network water is used in few companies, usually those companies that have extensive networks since it helps to locate places where there are big leakages in the network.

Thermal imaging tests (usually with planes or rotorcraft) are used by very few companies that have extensive district heating networks.

According to information obtained from companies that do tests and district heating companies, tests with an acoustic correlator have too large errors and are therefore not used.

It is also possible to use robots with a camera for inspection of channels but according to information of the authors, other methods are not used in district heating companies active in Poland.

When improving tightness of district heating networks, it is important to introduce control water reservoirs which may also serve as heat reservoirs. This is due to the fact that when the temperature of network water rises with falling outdoor temperature, there is a greater volume of water in the network, which leads to

a pressure rise. In a leaking district heating system, the increase is levelled out by greater losses of network water. At the number of replacements under circa 5 per year, however, keeping the network tight means discharging the water (and then adding it) in order to prevent excessive pressure peaks or drops in the system. In case of a lack of control water reservoirs, the process is connected with a greater volume of treated network water lost and consequently, a greater cost of adding water to the network.

An important new issue connected with improving tightness of district heating systems (with fewer than 7-5 replacements per year) is the need to introduce water reservoirs which may also play the role of heat accumulators. Tightness of the system at this level leads to processes of letting out and adding water in sources (as a result of natural control changes of network water temperature, which is connected with changes in the volume of the liquid) in order to prevent excessive increases or decreases of static pressures in networks. Without control reservoirs, the process causes that more treated network water is lost and thus the costs of adding water to the system are higher.

There is no definition of a smart district heating system, but the following definition may be suggested:

A smart district heating grid is a system which can efficiently integrate the behaviour and actions of all users connected to it (generators, consumers and those that do both). It is equipped with measuring and control systems and integrated with tele-information systems which allow optimisation of its work in real time, minimise losses and ensure high quality of heat supply and security (certainty) of supply. Apart from its basic function (heat supply), the grid should also perform additional functions, such as:

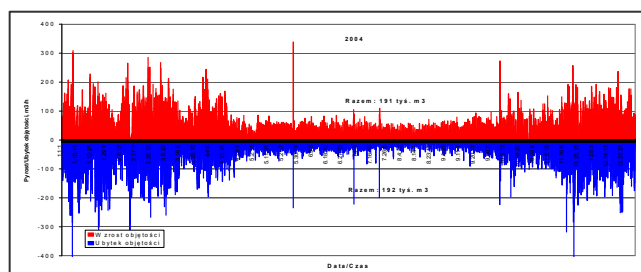


Fig. 3. Graph of the change in the volume of network water during natural changes of water temperature in a district heating system [6]. The red line – volume increase; the blue line – network volume loss [m³/h].

- relatively simple connection of new sources (e.g. from dispersed cogeneration or micro-generation)
- heat storage (e.g. heat storage in the network, so the so-called linear accumulator, accumulator in the source),
- forecasting changes in heat demand and adapting to this the work of sources and pumping stations,
- two-way communication with the consumer,
- smart metering,
- smart supervision and control systems.

At present, many Polish district heating systems have more or less developed smart grid elements. Work on “smart grid” has also been initiated by Veolia Warsaw. In Warsaw, there is a central system of network operation management and of ordering of water parameters in heat sources (in the CHP plants Siekierki and Żerań). It is planned to include in the system circa 2500 district heating substations, 3 pumping stations and 79 district heating chambers. Out of these, modernisation is needed in 2 pumping stations, 10 chambers (for remote control of their work), 26 chambers for telemetrics, and 1750 substations. The work is planned to be completed by mid-2017. It is planned to limit the emissions of like fortune-telling than forecasting of future needs and technology development.

The aim of carbon dioxide emissions limitation makes coal, gas and oil sources unwanted in the eyes of the law (emissions, CO₂ trade). The promoted sources are those fuelled with biomass. In many places, however, there is no biomass and its transport over long distances is pointless. The recommended biomass is from agriculture but its shortage on the market (already visible in Poland) and the resulting higher price may lead to the situation in which agricultural lands are taken over by energy crops, which leads to higher food prices, especially for poorer citizens. At the same time, biomass combustion is connected with a number of technical problems, such as increased chloride corrosion or sedimentation with biomass-related mineral compounds of low melting temperature (from 850°C) on inner surfaces of boilers. Combustion of municipal waste (after their segregation and recycling) will be a certain solution, since what is left from recycling is 40% biomass. This will, however, not solve the problem of heat supply for large agglomerations. One should remember about higher heat costs from these installations and technological problems connected with combustion plants, including emissions of dioxins, furans, particulate matter, heavy metals and the problem of solid waste (and its land filling). It seems that a certain solution is development of cogeneration. Nevertheless, in small and medium district heating

carbon dioxide by circa 14,500 Mg/a as a result of improvement of system control and higher speed of failure detection [1].

4. CONCLUSIONS

Polish district heating systems are facing many challenges. They are connected with their age and technical structure, as well as external circumstances. To face them, a vision for the next 30-50 years is needed (District Heating Companies), along with rational legal and economic regulations (the parliament, the government, EU). Similar challenges are posed to all district heating companies in the world. Differences in the starting point (e.g. technical condition of the devices or their age) do not make the task easier. Since these are local systems, each case must be analysed individually.

The strive towards the construction of “zero-energy” objects will lead to a significant fall in ordered power and the volume of heat sold. This will adversely influence the work of district heating pipelines. Aging of the technical infrastructure will require its modernisation, along with adaptation to present and future working conditions. On the other hand, forecasting changes in such a long timeframe is more

systems, there are many problems to solve, an example being the engine of the electricity generator. The simplest solution is here a gas-powered engine. But in many towns there is still no gas and the profitability of their gasification by building traditional networks is questionable. Construction of “island” gas systems is possible but this technology is only being developed by Polish gas companies. Powering the generator with a small steam turbine is expensive, though this technology is well known and developed. Another solution may be a traditional steam engine. However, the existing solutions still cause maintenance problems and need to be developed. It is possible to use ORC systems (Organic Rankine Cycle) with biomass-fuelled boilers but they are very expensive in terms of investment costs. A disadvantage of cogeneration-based solutions is the price of heat and electricity, which is higher than market prices of heat and electricity. Therefore, realisation of EU policy of promotion of biomass as a fuel for professional power engineering and district heating without a relevant support system is not possible. Of course, even people with the lowest income will buy electricity (low-power household boilers, fireplaces) by burning worst quality fuel. As a result, we will see greater local air pollution due to so-called low emissions. However, regardless of the type of fuel in the source, a cogeneration system should work along with a heat accumulator since it significantly increases system efficiency.

5. REFERENCES

- [1] K.Wojdyga „Prediction of Heat Demand for District Heating Systems”, Publishing House of the Warsaw University of Technology, Warsaw, 2007.
- [2] “Heat in Numbers” report 2014, President of Energy Regulation Office, Warsaw, Poland.
- [3] K.Wojdyga, M.Chorzelski , “The hydraulic analyses for district heating system in Zielona Góra, Warsaw 2003. Research Center for Power and Environmental Protection, Warsaw University of Technology.” Research report (in polish-unpublished).
- [4] District Heating and Cooling Country by Country Survey 2013, B-1040 Brussels, Published by Euroheat & Power
- [5] K.Wojdyga, M.Chorzelski, “The methodology of estimation of heat losses from district heating pipes in Wroclaw” , Warsaw, 2002. Research Center for Power and Environmental Protection, Warsaw University of Technology. Research report (in polish - unpublished).
- [6] K.Wojdyga, M.Chorzelski, “The methodology of leakages detection in district heating system in Warsaw” , Warsaw, 2007. Research Center for Power and Environmental Protection, Warsaw University of Technology. Research report (in polish - unpublished).

MAPPING ENERGY AND EXERGY FLOWS OF DISTRICT HEATING IN SWEDEN

Mei Gong¹, Sven Werner¹

¹School of Business, Engineering & Science, Halmstad University, PO Box 823, SE 30118 Halmstad, Sweden

Keywords: District heating, exergy, Sankey diagram, Sweden

ABSTRACT

District heating has been available in Sweden since the 1950s and used more than half of the total energy use in dwelling and non-residential premises in 2013. Energy and exergy efficient conversion and energy resources are key factors to reduce the environmental impact. It is important to understand energy and exergy flows from both the supply and demand sides. The exergy method is also a useful tool for exploring the goal of more efficient energy-resource use. Sankey diagrams together with energy and exergy analyses are presented to help policy/decision makers and others to better understand energy and exergy flows from primary energy resource to end use. The results show the most efficient heating method in current district heating systems, and the use of renewable energy resources in Sweden. It is exergy inefficient to use fossil fuels to generate low quality heat. However, renewable energies, such as geothermal and solar heating with relative low quality, make it more exergy efficient. Currently, about 90% of the energy sources in the Swedish district heating sector have an origin from non-fossil fuels. Combined heat and power is an efficient simultaneous generator of electricity and heat as well as heat pump with considering electricity production. Higher temperature distribution networks give more distribution losses, especially in exergy content. An outlook for future efficient district heating systems is also presented.

INTRODUCTION

District heating was introduced in 1948 and has been successfully expanded in Sweden since then. The district heating deliveries are mainly used to cover space heating and hot water demands in buildings, but have a low usage in the industrial processes. Currently, about 58% of total building heat demands for residential and service sector premises are covered by district heating [1].

Both the exergy concept and Sankey diagrams are used as tools for visualizing energy quality processes in this study. The exergy concept gains insights into its efficiency as well as the quantitative measure of quality, and the diagrams were used for mapping energy and exergy supplies, transformations and uses during 2014. Sankey diagrams together with energy and exergy analyses are presented to help policy/decision makers and others to better understand energy and exergy flows from primary energy resource

to end use. The combined methods have been applied for national levels in a country [2-5] and industrial heating processes [6], as well as in company levels in industry [7]. To our knowledge, there is currently no exergy flow analysis available for a national district heating sector. The purposes of this paper are to:

- map energy and exergy flows from primary energy sources to customer usages in the Swedish district heating systems
- show the most efficient heat supply methods in current Swedish district heating systems
- visualize the utilization of renewable energy resources in Sweden.
- give an outlook for more efficient district heating systems in Sweden

METHOD

Exergy analysis

Exergy is a measure of how far a certain system deviates from equilibrium with its environment, a given state of reference or equilibrium. In this analysis, the average outdoor temperature is used as reference temperature T_0 , and 100 kPa as reference pressure.

The exergy of material substances can be calculated as [8]:

$$E = \sum n_i (\mu_i^0 - \mu_{i0}^0) + RT_0 \sum n_i \ln \frac{c_i}{c_{i0}} \quad (1)$$

where n_i is the number of moles of different chemical materials i . μ_i^0 and c_i are the chemical potential and concentration of substance i in relation to its standard state. μ_{i0}^0 and c_{i0} are the chemical potential and concentration for the substance in the environment in relation to its standard state. R is the gas constant, $8.314 \text{ J mol}^{-1} \text{ K}^{-1}$.

The exergy factor is defined as the ratio of exergy to energy. The exergy factor of energy transferred as heat at a constant temperature T , i.e., a heat reservoir becomes [8]:

$$\frac{E}{Q} = \left| \frac{T_0 - T}{T} \right| \quad (2)$$

Heat used for space heating and domestic hot water was calculated by Equation 2. The exergy factor of district heat was calculated as [8]:

$$\frac{E}{Q} = 1 - \frac{T_0}{T_s - T_r} \ln \frac{T_s}{T_r} \quad (3)$$

where T_s is the temperature of the supplied heat, i.e., the temperature of the hot water used by the consumer for space heating. T_r is the temperature of the return water.

Table lists some energy forms used in this study. The exergy factors for fuel are based on lower heating values (LHV), which are the data available in Swedish energy statistics. It must be noted that some factors are only approximate due to unknown moisture and exact content. The exergy factor for current district heating grid is the average value for Swedish district heating system [9], and the outdoor temperature has a strong effect on the heat at room temperature, since the annual average temperature varies from -1°C in the north to 10°C in the south of Sweden.

Table 1 The exergy factor of some energy forms.

Energy form	Exergy factor
Oil, petroleum products [10]	1.06
Natural gas [10]	1.04
Electrical energy	1.0
Sunlight [8]	0.93
District heat (current generation) [9]	0.17
Heat at room temperature (20°C)	0.04-0.07

Both energy and exergy efficiencies are defined as the ratio between useful generation and used energy and exergy. The Coefficient of Performance (COP) of heat pump is the ratio of heat production to used electricity.

Sankey diagram

Schmidt [11] reviewed the importance in decision making and public policy. Sankey diagrams are the tools for indicating the flows in both energy and exergy from primary energy source to the end use. Left side of diagram shows incoming flows of primary energy, the middle part contains the conversion and transmission processes, the right side presents the end users, the energy losses go from up to down, while the exergy destructions disappear. The nodes indicated processes or distribution grids. The width of flow represented the amount of energy/exergy. Different colour represented different type of incoming and outgoing flows.

Data and assumptions

In this analysis the data are mainly from Statistics Sweden and the Swedish Energy Agency. In the Swedish statistics, the biomass energy flows are based on LHV, the value for exergy is not accurate since the

precise moisture contents are hardly to determine for biomass and municipal waste. In this study the exergy factor of biomass was assumed about 1.

When calculating exergy factors of space heating and domestic hot water usage, the temperatures of indoor and hot water are set as 20°C and 50°C , respectively. Two thirds for space heating and one third for hot water usage was assumed for heat usage for the household, but a higher share of space heating for service sector [12]. The characteristics of district heating for industry are uncertain, in this analysis the temperature used by industry was assumed to be 50°C . The temperature of incoming flue gases to flue gas condensation was assumed to be 150°C .

MAPPING FLOWS OF DISTRICT HEATING SYSTEM

Mapping district heating system in 2014

The energy and exergy flow diagrams for district heating in Sweden during 2014 are shown in **Figure** and **Figure 2**, respectively. The latter exergy diagram shows also the exergy usage for space heating and domestic hot water, while the rest was destroyed during heating process.

In the left side fossil fuels, peat, recovered gases, biomass and municipal waste produced 83% of total heat production though fuel boilers and combined heat and power (CHP) with flue gas condensation (FGC). The excess heat from industries and the large heat pumps contributed 8% and 9% of total heat production, respectively, and the electric boilers accounted for 0.5%. The supply sources besides industrial excess heat are high quality energy, there are not much difference in energy and exergy content. About 90% of primary energy or exergy supply came from renewable energy, excess heat, and waste.

The production of heat has large difference between energy and exergy since delivered heat have low temperature which means low energy quality. The average energy and exergy efficiency for CHP including FGC were 94% and 50%, respectively. The average conversion efficiency of fuel boilers were 91% in energy and 16% in exergy. Most of exergy content in fuel boilers and CHPs are mostly destroyed in the conversion processes. The average COP of heat pump was 3 and the average exergy efficiency was 50%.

Heat was delivered to the end users through the district heating grid. The distribution heat losses were 12% of heat production. The percentages of total heat demands were 89% in space heating and domestic hot water usage in the household and service sector, 10% in industrial sector, and less than 1% for ground heating.

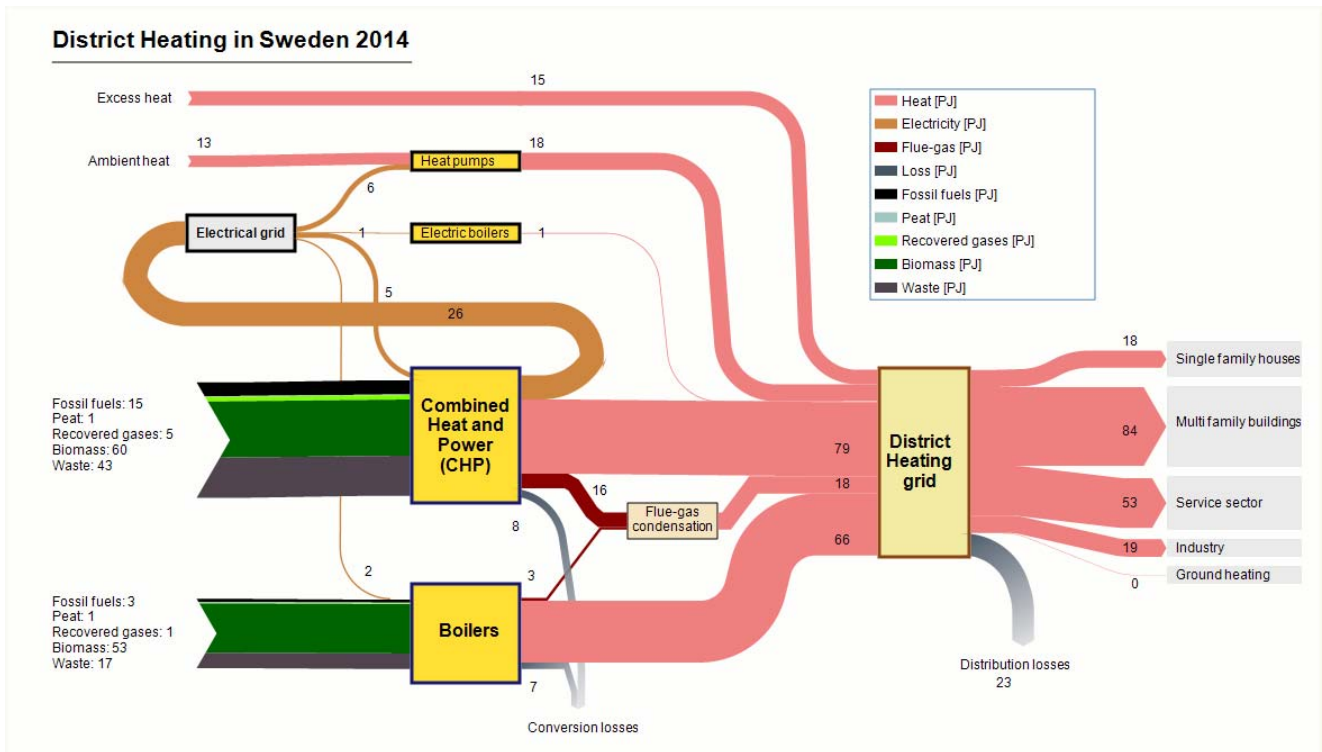


Figure 1 Sankey diagram of district heating, including corresponding part of electricity grid, in Sweden during 2014. Data source: [13].

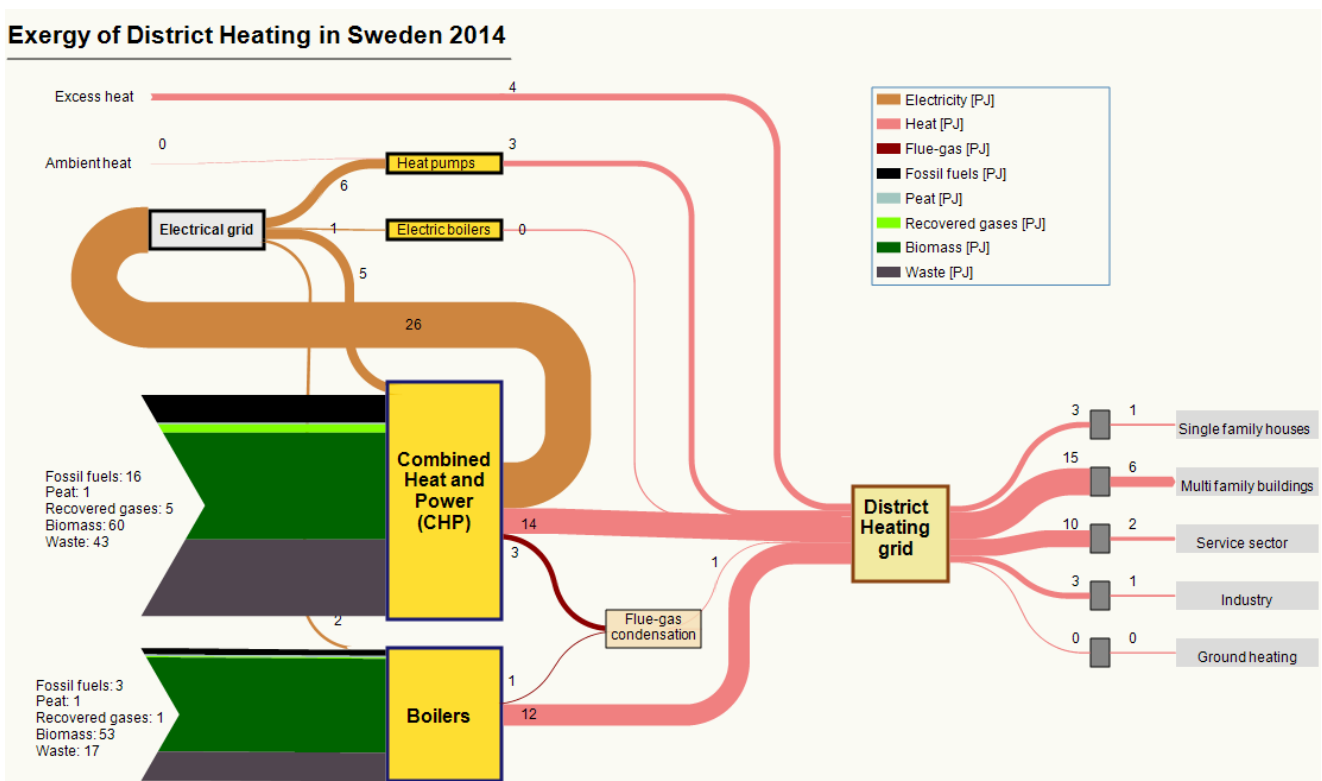


Figure 2 Sankey diagram of district heating, including corresponding part of electricity grid, based on exergy in Sweden during 2014. Data source:[13].

The right side of Sankey diagram based on exergy also showed exergy utilized in the end use. The left side of grey box was exergy from district heat grid to the end user, the right side of grey box was exergy finally used for space heating and hot water usage. Two thirds of incoming heat is destroyed by mixing hot water and cold water, and heat exchanger through substation and radiator.

The main differences between diagrams based on energy and exergy are the heat production and utilization, since the heat with lower temperature is low quality energy, this makes great exergy destruction in the district heating system.

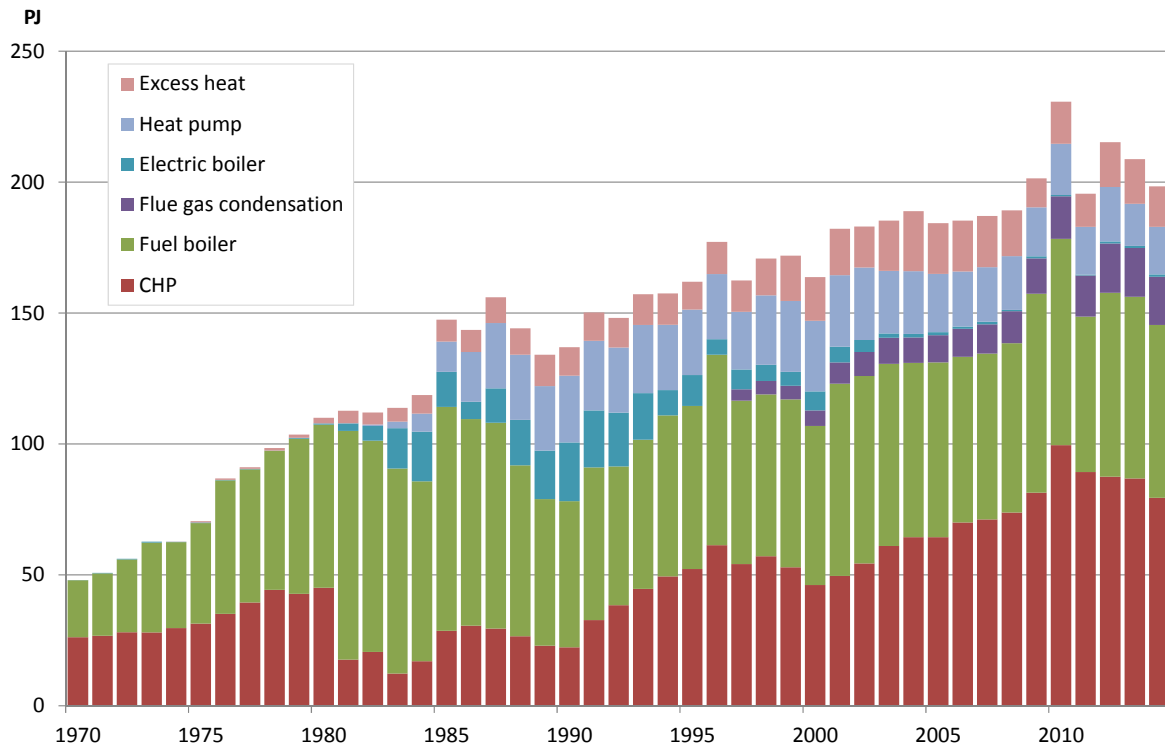


Figure 3 Heat produced per year by heat supply method during 1970-2014. Data source: Statistics Sweden and the Swedish Energy Agency.

Heat supplies

Figure 3 shows heat production from 1970 to 2014. The heat production was increased steadily with the average rate of 11% from 1970 to 1980 and 2% from 1980 to 2014. The peak of heat supplies appeared in 2010 due to a very cold winter.

CHP and fuel boilers dominate in heat supply. Almost all heat productions were from CHPs and fuel boilers during 1970s and early 1980s, and now one fourth came from large heat pump, electric boiler and industrial excess heat. The heat supply became more diversified.

In 1981, more than half of heat production from oil fuel CHP plant was reduced due to the second oil crisis and commissioning of new nuclear power stations. In the early 1990s, the biofuels started to play an important role in district heating. The primary energy input started to transfer from fossil fuels to biomass including waste. Investments of biofuel based CHP have good economic benefit since the green certificates for

renewable electricity were introduced in 2003, the production from CHP increased steadily until 2011, then the development is stagnating. Several cities produced heat from waste incineration plants as base loads, since the landfilling of combustible waste and organic waste were prohibited from 2002 and 2005, respectively.

Flue gas condensation is a method for increasing the efficiency of heat utilisation of a CHP or boiler plant by partially condensing flue gas vapour at low temperature to recover latent heat. In Sweden, Fagersta became the first to install FGC in 1980 to save energy and reduce emission. However, the national district heating statistics included FGC firstly from 1997. Today this technology is widely used in the Swedish biomass boilers and CHPs.

Several large-scale electric boilers and heat pumps were installed for district heating during the 1980s, since a national electricity surplus from new nuclear power stations became higher than the electricity

demand increase and need to be absorbed within the country [14].

Industrial excess heat is mainly available from energy intensive industries, such as pulp and paper industry, steel industry, and chemical industry. In this study, the temperature of industrial excess heat is assumed to be 100 °C for the exergy analysis.

Table 2 shows the average energy and exergy efficiencies since 1997 in Sweden. The efficiency of CHP includes electricity production and heat from FGC. The efficiency of boilers also included heat from FGC. The energy efficiencies are much higher than exergy efficiencies. Among them, the average energy efficiency is between 90% and 98%. The heat pumps have highest exergy efficiency, then CHPs. Both types of boilers have lowest exergy efficiency. However, the

electricity used in heat pump is secondary energy resource, the amount of the primary energy source will be degraded in order to produce electricity.

Table 2 The average energy and exergy efficiencies of CHPs, fuel and electric boilers and heat pumps in Sweden.

Supplier	Energy efficiency	Exergy efficiency
CHP	92%	34%
Fuel boiler	90%	15%
Electric boiler	98%	17%
Heat pump	3.3 (COP)	56%

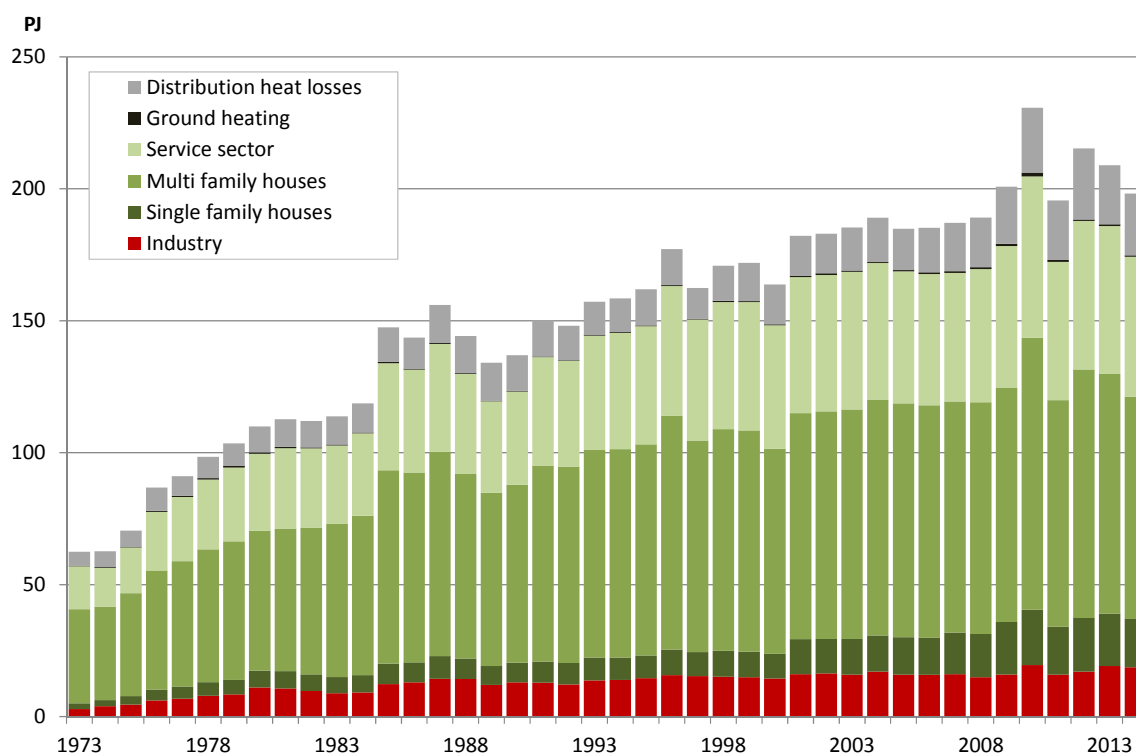


Figure 4 Heat demand by end user and distribution heat losses per year during 1973-2014. Data source: Swedish Statistics and Swedish energy Agency.

Distribution grid and Heat demands

The distribution heat losses were rising from 9% in 1970 to 12% in 2014 of total heat production with the increase of average linear heat density. The linear heat density is defined as the ratio between annual heat quantities utilised by customers to route length for the pair of pipes (normally half the pipe length) [12]. More and more single family houses were connected to the district heating grids, as shown in **Figure 4**, this caused the increase of the linear heat density.

In 2014, the exergy lost and destroyed in the district heating grid was 12% of total heat based on exergy supplied, the usage of space heating and hot water was about 30% of exergy of total heat delivered to building, the remaining exergy was destroyed.

About 10% of total heat usage was delivered to the industrial sector for space heating, hot water and low temperature processes with temperatures less than 100 °C. At present the district heating are more or less used for space heating and domestic hot water in Sweden.

DISCUSSION

Sweden aims to phase out fossil fuels in heating by 2020 and to have a sustainable and resource-efficient energy supply with zero net emissions of greenhouse gases by 2050. In order to achieve these goals, it should be to:

- use renewable energy and industrial excess heat with low quality energy source
- use biofuels including municipal waste
- improve technologies with more energy and exergy efficiency
- distribute heat with low temperature levels
- avoid mixing heat with high and lower temperature and use heat exchangers with long thermal lengths with less exergy destruction
- make policy in order to support these goals

Heat sources

At present the solar heating plants mainly contribute heat during summer. Large amounts of heat from industrial waste heat and waste incineration is enough to cover heat demand in many cities in Sweden, therefore, it is less attracted. However, several large-scale solar district heating systems with heat storage have been successfully operated in Denmark [15]. In southern part of Sweden, the annual solar radiator and condition is similar to Denmark, it would be possible to install such systems when the economic is feasible in the future.

Most part of Sweden lacks geological suitable conditions for deep geothermal exploitation. Only one deep geothermal plant in Sweden has existed since 1984 and is still in operation to support about 20% of the heat demand to district heating system in Lund [16]. The usage of geothermal energy in Sweden is currently dominated by ground source heat pumps for space heating and domestic hot water for single family buildings.

In 2014, the excess heat for district heating was 15 PJ. In Sweden the theoretical volume of excess heat from all today's industries have been estimated to between 22.3 PJ and 28.4 PJ, 70% of which come from energy-intensive industries, and low temperature excess heat from the premises are between 10.8 PJ and 18 PJ [17]. It is uncertain for supply and return temperatures in district heating, the estimated potential will be decreasing when the improvement of industrial process and increasing when transferring heat to the low temperature district heating systems. The estimated potential from excess heat can be covered about one fifth of today's total district heat production.

Technology

- Heat supply

The average energy efficiency for CHPs and boilers are more than 90%, but heat pumps and CHPs have higher average exergy efficiency than boilers. Heat only plants should be transferred to bio-fuel based CHP plants. The share of CHPs in district heating production should be raised from current 41% to at least 80% up to 2030 [18], new CHPs will be invested and old CHPs will be modernised or replaced. At same time, the efficiency of bio-fuel CHP should be increased by the introduction of new technology with economic benefit.

The hybrid technology of CHP and absorption heat pump, first initiated in China, will be possible applied in Swedish biofuel CHP plants in order to improve heat capacity and efficiency [19, 20].

Heat from heat pump together with renewable energy, such as solar and geothermal energy, should be widely applied for single family house with no district heating in future, when surplus electricity from renewable sources will be available in Sweden.

- Low temperature grid

The authors [9] concluded that the two thirds of the current exergy content is lost in the heat distribution chain from heat supplied into networks to heat demands in building, in the future with low temperature grid it is possible to reduce to one third. The aim maybe achieved by lowering distribution temperatures, avoiding mixing heat with high and lower temperature, and using heat exchanger with long thermal lengths with less exergy destruction.

In the future, current buildings will be refurbished with lower heat demand. However, the temperature difference between supply and return will be reduced with future low exergy district heating system, and thus the radiator in the house would be kept same size.

Energy Policy

With the support of energy and climate policy, the Swedish district heating systems have been transformed towards more sustainability, from fossil dependent system into biomass dominant system. The use of biomass in heat production was inspired the investment subsidies for construction of demonstration plants burning solid fuels from 1975 and 1980s, and further inspired through Solid Fuel Act with new boilers. The carbon tax was introduced in 1991. The local investment programme was funded during 1998 to 2002. A scheme for Tradable Renewable Electricity Certificate was introduced in 2003 in order to support electricity from renewable energy sources and peat, this lead fuel shifting in CHP plants from fossil fuels to biomass fuel.

Exergy is regarded as an essential tool in energy and environment policy making activates [21], and an exergy tax was introduced by Wall [22] in order to encourage the use of renewable resources and to improve the resource use. The differences between energy and exergy prices are small for almost all the energy sources except district heating. A good energy policy could speed up development towards efficient resource-saving and environmental friendly technology by ensuring exergy, rather than energy use.

CONCLUSION

In this paper, the flows based on both energy and exergy was mapped from primary energy source to customer usage with the aid of Sankey diagrams.

The diagrams viewed that more than half of exergy source was destroyed in CHP, even worse in boiler. In the current Swedish district heating system the most exergy efficiency methods is heat pump.

The utilization of renewable energy resource is high since biomass plays an important role in Sweden.

Future district heating systems with low distribution temperatures should use more low quality renewable energy and excess heat. It will be fossil fuel independent district heating system. CHPs and heat pumps in the aid of renewable energy will be possible dominant in future heat market.

REFERENCES

- [1] Swedish Energy Agency, *Energistatistik för småhus, flerbostadshus och lokaler 2014* (Summary of energy statistics for dwellings and non-residential premises for 2014), Eskilstuna, Sweden, 2015.
- [2] G. Wall, "Exergy use in the Swedish society 1994," in *International conference on thermodynamic analysis and improvement of energy systems*, Beijing, China, 1997.
- [3] G. Wall, E. Sciubba, and V. Naso, "Exergy use in the Italian society," *Energy*, vol. 19, no. 12, pp. 1267-1274, 12, 1994.
- [4] M. Gong, and G. Wall, "On exergy and sustainable development—Part 2: Indicators and methods," *Exergy, An International Journal*, vol. 1, no. 4, pp. 217-233, 2001.
- [5] B. Chen, G. Q. Chen, and Z. F. Yang, "Exergy-based resource accounting for China," *Ecological Modelling*, vol. 196, no. 3–4, pp. 313-328, 7/25/, 2006.
- [6] K. Soundararajan, H. K. Ho, and B. Su, "Sankey diagram framework for energy and exergy flows," *Applied Energy*, vol. 136, no. 0, pp. 1035-1042, 12/31, 2014.
- [7] M. Gong, "Exergy analysis of a pulp and paper mill," *International Journal of Energy Research*, vol. 29, no. 1, pp. 79-93, Jan, 2005.
- [8] G. Wall, and M. Gong, "On exergy and sustainable development—Part 1: Conditions and concepts," *Exergy, An International Journal*, vol. 1, no. 3, pp. 128-145, 2001.
- [9] M. Gong, and S. Werner, "Exergy analysis of network temperature levels in Swedish and Danish district heating systems," *Renewable Energy*, vol. 84, pp. 106-113, 12, 2015.
- [10] I. S. Ertesvåg, and M. Mielnik, "Exergy analysis of the Norwegian society," *Energy*, vol. 25, no. 10, pp. 957-973, 10, 2000.
- [11] M. Schmidt, "The Sankey Diagram in Energy and Material Flow Management," *Journal of Industrial Ecology*, vol. 12, pp. 82-94, 2008.
- [12] S. Frederiksen, and S. Werner, *District heating and cooling*, Lund, Sweden: Studentlitteratur AB, 2013.
- [13] Swedish Energy Agency, and Statistics Sweden, *El-, gas- och fjärrvärmeförsörjningen 2014* (Electricity supply, district heating and supply of natural gas 2014), SCB, Sweden, 2015.
- [14] A. Helge, P. Ingvarsson, U. Persson, and S. Werner, "On the use of surplus electricity in district heating systems," in *The 14th International Symposium on District Heating and Cooling*, Stockholm, Sweden, 2014.
- [15] S. Furbo, J. Fan, B. Perers, W. Kong, D. Trier, and N. From, "Testing, Development and Demonstration of Large Scale Solar District Heating Systems," *Energy Procedia*, vol. 70, pp. 568-573, 5, 2015.
- [16] S. Gehlin, O. Andersson, L. Bjelm, P.-G. Alm, and J.-E. Rosberg, "Country Update for Sweden," in *Proceedings World Geothermal Congress 2015*, Melbourne, Australia, 2015.
- [17] L.-Å. Cronholm, S. Grönkvist, and M. Saxe, *Spillvärme från industrier och värmeåtervinning från lokaler* (Waste heat from industries and heat recovery from the premises), Stockholm, Sweden: Svensk Fjärrvärme AB, Sweden, 2009.
- [18] CODE2, *D5.1 Cogeneration roadmap member state: Sweden*, 2014.
- [19] M. Gong, and S. Werner, *District heating research in China*, Svensk Fjärrvärme AB, Sweden: Svensk Fjärrvärme AB, 2014.
- [20] Y. Li, L. Fu, S. Zhang, Y. Jiang, and Z. Xiling, "A new type of district heating method with co-generation based on absorption heat exchange (co-ah cycle)," *Energy Conversion and Management*, vol. 52, no. 2, pp. 1200-1207, 2011.
- [21] I. Dincer, "The role of exergy in energy policy making," *Energy Policy*, vol. 30, no. 2, pp. 137-149, 1, 2002.
- [22] G. Wall, "Exergy, ecology and democracy - concepts of a vital society or a proposal for an exergy tax," in *International conference on energy systems and ecology*, Krakow, Poland, 1993, pp. 111-121.

BARRIERS AND ENABLERS FOR EXPANSION OF DISTRICT COOLING IN SWEDEN

J. Palm¹, S. Gustafsson²

¹ Linköping University, Department of Thematic Studies – Technology and social change, 581 83, Linköping, Sweden

² Linköping University, IEI/ Environmental Technology and Management, 581 83, Linköping, Sweden

Keywords: *District cooling, barrier, eco labelling, Sweden*

ABSTRACT

Even if Sweden is a northern country with fairly low outdoor temperatures most time of the year, the district cooling system in Sweden is expected to expand. The potential is at least the double according to some actors. The reason for this is that a demand for cooling increases with increased use of electronics such as computers, which results in higher indoor temperatures because of free heat. Although district cooling (DC) should have the potential to sell both on its convenience and its climate benefits, the trend is however surprisingly slow moving.

The aim with this paper is to discuss barriers and enablers for expansion of DC. We will present how energy companies, property owners and tenants of premises perceive barriers and enablers to install and use DC. How are these actors looking upon the need for cooling today and in the future? What would make DC more attractive according to these actors? These questions have been studied through surveys and in-depth interviews.

The results show that lack of information is the most important barrier today, a barrier that however has the potential to be turned to an enabler for DC. Earlier grid-based systems in Sweden have been established through public-private collaboration. When for example district heating was built, the municipalities played an important role, but that has not been the case for DC. Such a collaboration could benefit a continued expansion of DC. Another possible future enabler is eco-labelling of DC, that today plays a minor role in the Swedish system.

INTRODUCTION

Along with climate change and increasing temperatures, as well as intensification in the use of electrical equipment that causes excess heat, the need to cool indoor environments such as shops, offices, industries, hospitals will multiply in order to maintain comfortable indoor temperatures [1, 2]. This goes not only for the countries in warmer areas, but also for those in the northern hemisphere. Even though Sweden is a country that is situated in a geographic zone where, most of the year, the outdoor temperature is fairly low compared to many other countries, cooling

has become an issue [1]. There are different technologies for cooling premises, among which district cooling (DC) has been pointed out as effective for reaching the overall strategic energy goals [3]. This paper reflects on enablers and barriers for expansion for district cooling (DC), based on Swedish experiences.

The first known district cooling system was established in Rockefeller Centre in New York and U.S capital buildings in Washington in the 1930's. The expansion of DC in Sweden took off in the beginning of the 1990's [4] and today there are about 30 DC producing energy companies in the country. The delivery of DC in Sweden has increased with 63% between 2004 and 2015 and around 1 TWh was delivered in 2015 (which can be compared with that around 55 TWh district heating is delivered per year in Sweden) [5, 6]. According to the Swedish District Heating Association, Stockholm has the largest amount of customers and the most extensive DC grid world-wide [5]. DC can be produced in several different ways, e.g. through compression chillers, absorption chillers or through deep lake water cooling. In this paper, however, we do not analyse different technologies for DC, we rather look on the different aspects and preconditions for expansion of the use of DC as such. Few residential buildings have this type of cooling system in Sweden and cooling of premises seems to be the main market for DC in Sweden [4]. Therefore, this study will focus on premises.

The DC system in Sweden has potential to expand and a double of its capacity is often mentioned as realistic in a near future [5]. Different development paths are supporting an increase in demand for cooling. DC is mostly regarded as a sustainable system, especially when the system replaces electricity based cooling. Although DC should have the potential to sell both on its convenience and its climate benefits, the trend is surprisingly slow moving.

The overall aim with this paper is to discuss barriers and enablers for expansion of DC. The results are based on Swedish experiences, however, in the discussions we will put forward these issues in a wider context. In this paper, we will present how energy companies, property owners and tenants of premises

perceive barriers and enablers to install and use DC. How are these actors looking upon the need for cooling today and in the future? What would make DC more attractive according to these actors?

THEORY – LARGE TECHNICAL SYSTEM AND BARRIERS

In Sweden, state and municipal governments have traditionally been key actors in the building and operation of major public works systems such as water and sewage systems, electrical systems, and district heating (DH). One frequent argument for this has been the idea that the profits from such enterprises should not accrue to private interests, but rather benefit the Swedish citizenry, for example in the form of low tariffs. This is also one reason to why the majority of DH companies were run as municipal services up until the 1980s. Over the last 25 years, most of these services have been converted into municipal corporations. The majority of Swedish DH corporations are still under municipal ownership, even if there has been a trend toward increased privatization in the district heating industry.

DC has many similar characterizations with DH. DC is also centralized production and distribution of cooling energy. Chilled water is delivered in undergrounds pipelines to cool the indoor air in buildings within a district. Each building then have designed units that use the water to lower the temperature of air passing through the air conditioning system. In Sweden a big difference between the systems is that DH is an established and diffused system regulated by law, while DC is recently introduced and in an expansion phase. Furthermore, over the years there have been several governmental investment programs which, among other things, have had significant contribution to the pace and extent of the DH expansion in Sweden [7]. The municipalities in collaboration with the local energy companies played a key role in this. So far, there has been no similar initiatives to enhance for DC expansion. This makes DC interesting to study in the perspective of enablers and barriers for introducing new large technical systems in a country.

The development of infrastructural systems such as DC has often been analysed through the lens of the large technical system (LTS) framework. This framework, developed by Thomas B Hughes [8] has mainly been used to analyse establishment of systems in phases: the invention phase, the expansion phase, technological transfer phase, and finally the last phase momentum, when a system acquire autonomy from its environment and difficult to change. In this study the expansion phase is in focus.

Large technical systems can be viewed a natural monopoly. What characterize a natural monopoly is that an increase in terms of labour and capital does not generate more than a proportional increase in produced volume. What this means in practice is that it is more cost-effective for e.g. an existing DC company to expand its operations than it is for a new company to establish itself in the same area. The entrance of yet another company into the local market does not have the healthy regulatory effect associated with an optimal competitive situation [9]. The DC industry's character as a natural monopoly implies that there is room for only one company within a geographically delimited area. It is the distribution of water per se that is considered to constitute a natural monopoly. The production of chilled water could, in theory, be open to competition. Customers who choose DC are referred contractually, technically, and financially to a single seller, so that DC also exerts a certain "lock-in" effect. Changing cooling sources is an option, but the costs associated with such a switch makes it financially infeasible or, in any event, difficult to accomplish, which is why there is a lock-in effect.

DC can at the same time be viewed as a monopsony that is characterized by the fact that the market comprises only one customer, for whose business the sellers must compete [10]. One example in relation to DC is that e.g. a hospital can have such a dominant role that the seller's financial situation is dependent upon retaining the hospital as a purchaser of DC. The DC company's bargaining chip in this context is of course their power to shut off the supply of DC. [9]

From earlier research on grid based system (gas, DH, electricity, railway, broadband) we know that there are 5 key issues that need to be solved for establishing a new system:

- The technical uncertainties about e.g. risks with the technology and interference in environment, reliability and plant life.
- Inertia in the system, meaning that it takes time from the initiation to the system can be used. The pipes / distribution grid have a lifespan of up to 100 years. If there is doubt that the system can expand, that will be one of the major threats to the system.
- The economic conditions characterized by large initial investments in production and distribution facilities and the significant uncertainty of future profitability
- The organisational form of the business and primarily the question of the city itself should be

responsible for the construction and operation or transfer it to a private contractor.

- The legal relationship between supplier and customer. There is also a substantial uncertainty about subscriber behaviour and there are strong interdependencies between subscribers and their suppliers. Summerton [11] has shown the importance of having a big customer on board when initiating a grid system. Historically the municipal owned housing companies in Sweden have played a major role for assuring an initial market for district heating.

These five issues are more or less general for all grid based supply systems. From barrier theory it is possible to identify and specify further hindrance for DC to be established.

Barriers and enablers relevant for DC

Barriers are usually discussed in relation to energy efficiency and in this context a barrier is defined as a postulated mechanism that inhibits investments in technologies that are both energy-efficient and economically efficient [12-14]. Here we will look into some of the barriers that can be relevant also in relation to expansion of DC. Barriers that also be seen as potential enablers.

Imperfect information: A large body of research states that consumers are often poorly informed about market conditions, technology characteristics and their own energy use. The lack of adequate information about DC can lead to that DC is not even on the decision agenda. Information does not always receive as much attention as anticipated, since people are (often) not active information-seekers but rather selective about attending to and assimilating information. Research points out some characteristics in the way information is assimilated; some people, for example, are more likely to remember information if it is specific and presented in a vivid and personalized manner, and comes from a person who is similar to the receiver [15-17].

Insufficient information is one form of imperfect information. Another form of imperfect information is the cost of information, meaning that there are costs associated with searching and acquiring information about DC. Yet another form is the accuracy of information, meaning that the information provider may not always be transparent about the product being offered. Imperfect information is likely to be most serious when the product is purchased infrequently, performance characteristics are difficult to evaluate either before or soon after purchase, and the rate of technology change is rapid relative to the purchase intervals [12]. Issues related to imperfect information

may be countered with e.g. different forms of information campaigns and can if done right turn out to be an enabler for DC.

Another factor that may inhibit adoption is the receiver's perceived credibility of and trust in the information provider. Energy users cannot always easily gain accurate information about the ultimate comparative cost of different investment options; they will rely on the most credible available information [18].

Split incentives: A split incentive may occur when the potential adopter of an investment is not the party that pays the energy bill. If so, information about available cost-effective DC in the hands of the potential adopter may not be sufficient; adoption will only occur if e.g. a tenant can recover the investment from the real estate owner [19]. This is often referred to as the landlord-tenant relationship. This is a restriction to adopting energy-efficient technologies, in particular those with higher initial costs but lower life cycle costs than conventional technologies [20].

Hidden costs: Hidden costs is the high costs associated with information-seeking, meeting with sellers, writing contracts and other such activities [13].

Limited access to capital: Investing in DC can be more expensive than alternative technologies. Moreover low liquidity and limited access to capital may also be a problem. Sometimes such restrictions may be self-imposed [21].

Risk: Even though, for example, managers know what the capital cost is for an investment, there can be uncertainty about the long-term operating costs; this means the investment poses a risk. Such concerns have been found to be very important to decision-makers [20]. It can be hard to accurate estimates of the net costs of an investment which depend on future economic conditions in general, and on future energy prices. Energy prices have fluctuated as long as there has been a market for energy, leading to perceptions of uncertainty about future prices. Studies among small and medium-sized enterprises have found that some may not even be able to reduce uncertainty to a calculated risk due to a lack of time and money to calculate the required estimates [15].

Bounded rationality: Another explanation for why cost-effective energy efficiency measures are not undertaken is bounded rationality [22]. Organisations (just like individuals) to some extent do not act on the basis of complete information but rather make decisions by rule of thumb [23].

METHOD

This paper is based on an explorative study, and takes its point of departure in experiences from DC in Sweden. The study was carried out in 2015/2016 and it was performed in two steps. The purpose with the first step was to get insight into different actors' attitudes or approaches to DC. In order to get this insight, interviews were performed with representatives from energy companies, municipalities and with national real estate owner organisations. The main themes for these initial interviews were related to the (potential) market for DC the customer demands for DC and which technology they use.

The reflections from the first step fed into the second step, in which we developed and sent out an online based survey to around 900 members of a national real estate owner organisation. 176 responses were received, meaning a fairly low response (20%). One reason to the low response rate could be that many simply do not know enough about DC, which we also could see in our interviews (and we come back to that below). Lack of knowledge may have made them put the survey aside. We think however that the survey indicate some tendencies about perceived barriers and enablers for DC in Sweden. We have also triangulated the results with the interviews that we have conducted both before and after the survey, which increases the reliability of the results [24]. The topics covered in the survey include; what type of premises they have, assessment of their indoor comfort, their need for cooling, what type of cooling that they use, what they think of DC and why they use/do not use this type of cooling. The online survey was followed up by deep interviews with some of the online survey respondents. The same themes were addressed, however in the interviews, it was possible to get more in depth responses to the themes. In total we have conducted 33 interviews. We have interviewed representatives for 4 energy companies delivering DC, 5 umbrella organisations for real estate owners, 1 umbrella organisation for energy companies and 1 for business, 14 real estate owners and 6 companies that are tenants. We have anonymised the respondents and when quoting an interview we refer to them as:

- energy company: EC (1, 2 etc)
- umbrella organisations for real estate owners: UREO,
- umbrella organisation for energy companies: UEO,
- the umbrella organisation for business: UB,
- the real estate owners: REO, and
- the tenants: T.

The results from the interviews and the survey were compiled and categorized prior to analysis. The results were validated in workshops with practitioners (one

with energy companies that produce DC and one with real estate owners).

RESULTS AND DISCUSSION

In earlier research, 5 key issues were identified as important to deal with for a successful establishment of a grid-based system. The key issues concern everything from technical uncertainties, economic conditions and the legal relationship between suppliers and customers. Historically in Sweden, these key issues have been dealt with through collaboration between the government/the municipalities and public or private companies. This has however not been the case for the introduction of DC in Sweden. DC has mainly been an issue for the energy companies. When asking the representatives of the municipalities about their lack of engagement in DC their answers indicate that there is a lack of knowledge of DC in the municipal administration and that DC simply is not an issue on the local authorities' agenda (Interviews M1 and M2). One of the representatives did say however that DC might become of increased interest for the municipality in the near future. Many local responsibilities like elderly care already today need cooling systems and DC could play a much more important role in these buildings that it does today (Interview M1). When interviewing one of the real estate owners she meant that the expansion and development of DC grids should be the responsibility or interest of the municipality (REO6). The energy companies also pointed at the importance of expanding the grids so that they can connect larger amounts of buildings meaning that it would be easier to negotiate the costs etc (EC1, EC4). At present, one of the energy companies did not actively promote DC to new customers, but only negotiate with customers that make contact with them. In this case it would need an active involvement from e.g. the local authorities to expand the system further.

The four energy companies in our studied municipalities motivated their investment in DC in several ways. The energy companies have DH production which results in a heat excess summer time and then it is profitable to use the heat to produce cooling. In Sweden the DH market is under stagnation and the energy companies see the opportunity to offer their customers also DC as a way to also keep their DH customers. The energy companies did however experience that it was hard to find profitable solutions. The initial investment costs are large and DC is also more expensive to produce than DH, because of the resource costs that arises. One representative of an energy company mean that it takes at least 15 years before it is possible to reach some kind of profit (Interview EC1). It seems that all companies have used

the same strategy though, to start in a small-scale and let the expansion take time.

As discussed above, large technical systems are often natural monopolies and we discussed this with the interviewees in relation to DC. The energy companies did not perceive DC as a monopoly market in the same way as the DH market, because they needed to compete with existing individual cooling systems every time a new deal was discussed. DC is an immature market in Sweden and a consequence of that is that there are no fixed prices, but the price model is negotiated individually with the customer. The price is negotiated out from

"how much cooling the customer wants, what they need, what the alternative price is and what we can offer" (Interview EC1).

The lack of price lists also results in that a contract could take years to negotiate (Interview EC3). The customers had more easy to relate to DC as a monopoly and several mentioned lock-in effects as a reason to why they did not want to connect to the DC system.

As mentioned above it is possible that large technical systems develops to a monopsony, if there is one dominant customer that buy a large share of the supply. From our material it is clear that large customers that buy a lot of cooling are more satisfied than small customers. The large customers also feels that they have been able to influence the contract, something that the small customers did not have the possibilities to do. One major estate owner also stated that they have the ability to negotiate the contract with the local energy company, meaning that the price setting could be adjusted in favour for the real estate owner:

"I know that we pay much less than other customers, because we put an ultimatum to the provider" (REO2)

Still, in none of our studied cases, there was one single customer that was totally dominant in the market, but rather several larger customers that all could influence factors as price and service level.

Barriers to DC

The survey among real estate owners shows a widely spread result when it comes to the importance of cooling of their premises, about half of them thought cooling was important, while the other half considered cooling less important or unimportant. However, most of them (82%) cooled, at least some, of their premises. Compression chillers was the most common way of cooling, followed by free cooling. A little more than one

third of the respondents believed that the demand for cooling will increase in the future, while 20% of the respondents thought that the demand will remain at the same level as today. Only 2% believed in a decrease in the cooling demand.

Out of the 176 respondents in the survey, only 15 have installed DC. The main reasons for choosing DC were a need of cooling, along with an, as they experienced it, reasonable investment costs (see Table 1). Other reasons for using DC was that it was experienced as a maintenance free system (since other actors take care of the service etc.), and it provides a good indoor environment (silent system and good indoor climate).

Table 1. Survey responses on reasons for installation of district cooling (note that it was possible to give more than one answer to this question).

Reasons for installing district cooling	No. of answers
Need for cooling	8
Easy maintenance	7
Reasonable investment costs	5
Gives good indoor climate	4
Silent system	3
Value for money	2
Easy to install	2
Low operation costs	2
TOTAL NO OF ANSWERS	33

Table 2. Survey responses on why district cooling is not installed (note that it was possible to give more than one answer to this question).

Reasons for not installing district cooling	No of answers
There is no district cooling grid	40
Requires significant adjustments to the buildings	14
High investment costs	13
Lock-in effect	12
The flexible operation cost	11
Pricing is not competitive	10
The fixed operation costs	9
Maintenance is demanding	1
TOTAL NO OF ANSWERS	110

In the follow-up interviews to the survey, most of the respondents confirmed that their offering of DC is a consequence of tenants demand and most of them saw an increase in demand for cooling in general - especially in shops where the lighting causes excess heat and warmer indoor climate that needs to be cooled down to be comfortable. The interviewees all highlighted the environmental aspect of DC and its user-friendliness (no needs for system maintenance) as main arguments to DC.

Most of the respondents in the real estate owner survey said that they did not use DC in their premises. The reasons vary greatly, however the most common reason for not using/choosing DC is the lack of a grid (see Table 2).

The high costs for adjustments in existing buildings in order to install DC is the second most common reason for not choosing DC. Some of the respondents mention the lock-in effect as a reason for not installing DC since they do not want to be dependent on only one supplier. This was also discussed in the interview by a customer who needed a lot of cooling and was highly dependent on cooling for their business. Their local energy company could not guarantee to live up to the cooling demands of the company (with regards to amount and timeliness), which led to that one part of the company was cooled with DC while the other part (the most sensitive one) was cooled by a local cooling system. Hence, this company used both DC and a local system (Interview REO14).

Lack of knowledge was also mentioned as a reason not to invest in DC (Table 2). When it comes to *information* about DC in Sweden the information is technically oriented. Customers that have an energy managers or someone dedicated to work with DC could relate to the information and understand how it should be interpreted. Small customers without this special competence struggled to find information that make sense to them. These customers have a hard time to understand the technology, assess the environmental impact the system has and must therefore trust that the supplier gives them the right information. In Sweden it is difficult to find objective information, i.e. information diffused by someone not producing or distributing DC. We quite quickly noticed that it was difficult to even find informants for our study that were able to answer to our questions. Many simply answer that they did not know anything about DC or only had a vague idea of what it is. Even the question if they had access to DC was difficult:

"I don't know exactly but I think there is good availability of DC". (REO9)

Compared to DH, the knowledge of DC is much lower and less widely spread. Big umbrella organisations such as the Swedish Trade Federation had no one working with cooling (or energy), the Swedish Association of Public Housing Companies said that this was not an issue on their agenda and the Property Owner Association thought it was an interesting issue for the future, but that DC was not a current issue for them. During the interviews the real estate owners also said that they think that the energy companies could be better in informing and marketing the DC. One real estate owner pointed out that in order to attract more users of DC the energy companies needed:

"... take contact themselves to promote DC towards different actors and thus contribute to an increased demand for DC." (Interview REO11)

One of the representatives from the energy companies was also self-critical and said that DC was not marketed good enough so the customers simply did not know that DC existed (Interview EC4).

Split incentives as a barrier occur when an adopter of an investment is not the party that pays the bill. In our material this barrier becomes related to information. The real estate owners said that their tenants do not demand DC, but on the other hand no one inform the tenants that DC is an option. The tenants on the other hand were not always aware of whether they had DC or not in the premises:

"Is it district heating in [to the building] then it is district heating. Is it district cooling in, then it is district cooling we use ../ we must use what is installed" (T1)

Those who have invested in DC motivated that with that the investment cost for DC is reasonable. In contradiction to that, several of the respondents that do not have DC argue that the investment cost is a barrier and that the operation of DC is expensive, see table 2.

Both the factors *Split Incentives* and *Hidden costs* could be turned into enablers if business models were taken into account. Previous research on expansion of DH techniques shows that organisational aspects such as business models are an important issue for enabling expansion [25]. The knowledge of the importance of business models for developing the market of DC is so far limited, however it is reasonable to believe that similar aspects are important also for DC. This could also be indicated from the online survey and the interviews in this study. Therefore, to expand the use of DC it could be important to understand the underlying

economic mechanisms in order to be able to develop an attractive offer to potential customers. In this paper, we look upon business models as organisational and strategy-oriented tools (as discussed by [26]), where the business model could be seen as a strategic management tool and where the market competition is a driver to further the organisational performance.

The energy companies meant that low electricity prices are regarded as a barrier and in relation to that *bounded rationality* was mentioned as a problem. Furthermore, they thought that the customers did not really compare the different alternatives that exist on the market. The energy companies experienced that the customer has no knowledge about e.g. how much electricity their existing cooling equipment use, which makes it difficult for the suppliers to convince the customers that DC was a good deal. The customer only see how expensive the DC is, but have nothing to compare that with. (Interview EO1; E1). The customers that in the end chose DC are the ones that are capable of comparing the running cost, because they often experience that DC will be cheaper in the long run (Interview E3).

Hidden costs are not mentioned by the customers, but the energy companies told us that these costs are high. It takes time to come to a closure with a customer and as mentioned above it can take years to negotiate a contract.

Table 3. Survey responses on what would make district cooling more attractive (note that it was possible to give more than one answer to this question).

What would make district cooling more attractive	No of answers
Lower price	16
Access to grid	13
Develop working business model	5
Tenants' demand	7
More environmentally friendly	3
More competitive compared to its alternatives	2
Lower installation costs	2
If there was more information/knowledge of district cooling	2
Warmer summers	1
If it was easier to install	1

TOTAL NUMBER OF ANSWERS	52
--------------------------------	-----------

Limited access to capital is also a barrier mentioned rather by the energy companies than the customers. In Sweden DC is such a small part of an energy company's total business, so it is difficult to have DC prioritized by the company management.

When reflecting on what would make district cooling more attractive, the main reason given by the online survey respondents was related to economy and to increased access to DC grids (see Table 3). This, followed by tenants' demand and more knowledge of the environmental performance of DC and district cooling as such, seems to be enablers for real estate owners to install this technology in their premises.

Several interviewees mentioned the price issue and that DC would be more attractive if it was cheaper, both regarding installation costs and operation. Furthermore, several stressed the challenge in developing a reasonable pricing model and business model in which the costs are paid by those that use the DC. The pricing of DC is often individually set by the energy companies (different prices for different customers), which causes some doubts among customers. And also that they simply could not assess the value of DC:

"I have no idea about the economy, because I don't know the price on DC" (REO8)

Three of our studied energy companies were municipally owned energy companies and they emphasised that their local anchorage and the fact that they are locally known and trusted are important reasons when the customers choose DC. All companies otherwise highlighted values such as good comfort, reliability, simplicity and that the equipment doesn't need any space as important factors contributing to the choice of DC.

CONCLUSIONS

DC in Sweden is an emergent but still quite immature market. It is a market that has been developed solely by market actors, which stands in sharp contrast to how earlier grid based large technical systems have been developed in Sweden. Earlier systems have been developed in collaboration with public and private actors. The municipalities that we have talked to have no aversion to DC, but it is simply not an issue on their agenda. But when discussing it they meant that DC might have an important role to play in the future, not least to reach ambitious climate targets decided on in many of the Swedish municipalities. An increased collaboration between energy companies, real estate

owners and municipalities could be a future enabler for an expansion of the system. Furthermore, a more coordinated approach, as was seen in the Swedish DH expansion, where the national government issued grants and where municipalities and energy companies collaborated in a coordinated manner, would probably enhance the expansion of DC grids in Swedish municipalities.

The Swedish District Heating Association means that DC systems have potential to increase, at least to the double in a few years. There are however barriers that need to be overcome. Information is an obvious and perhaps the most important barrier for expansion of DC, but that also can be turned to an important enabler for expansion. If an expansion of DC is desirable it would most likely need to be preceded by a big promoting campaign, where general values with DC is highlighted, such as comfort and convenience. That is probably hard to manage by a single company but their umbrella organisation, the Swedish District Heating Association, or a campaign in collaboration with a number of energy companies and municipalities could be options.

The present DC market seems to be a market for large real estate owners who have many similarities with early adopters, i.e. they are rather interested in the technology as such and do not hesitate when discussing how the system is operated. The energy companies on their hand seem quite satisfied with targeting customers with deep knowledge about the technology and has not really adapted their information to a broader audience.

In our interviews we have also experienced that it is difficult to talk about DC because this is a technology that is unknown for many real estate owners and their tenants.

Noticeable is also that the arguments for and against DC are the same. The price is used to motivate both the investment in DC and the rejection of DC. But as mentioned above, it is not that easy to compare the prices, because many companies do not have fixed price lists but negotiate price with each customer.

Related to the pricing issue, there is a need to develop functional business models that could work as "market devices" (as defined by [27]) in order to make the DC attractive to real estate owners and tenants, as well as energy companies. This would enhance the innovation process through brokerage between different actors. From a sustainability perspective, this is important since new ways of competition and collaboration might be needed in order to market sustainability solutions. This would be an interesting field for future research.

Furthermore, it would also be interesting to dig deeper into the role for eco-labeling of DC and if this could be a way forward for DC in Sweden.

ACKNOWLEDGEMENT

This project is funded by the Swedish District Association and the Swedish Energy Agency.

REFERENCES

- [1] SOU (Swedish Governments Official Reports), Sverige inför klimatförändringarna : hot och möjligheter : slutbetänkande, Fritze, Stockholm, 2007.
- [2] E. Fahlén, L. Trygg, E.O. Ahlgren, Assessment of absorption cooling as a district heating system strategy - A case study, *Energy Conversion and Management* 60 (2012) 115-124.
- [3] EU Directive 2009/28/EC, on the promotion of the use of energy from renewable sources and amending and subsequently repealing Directives 2001/77/EC and 2003/30/EC.
- [4] K. Abrahamsson, J. Nilsson, Kartläggning av marknaden för fjärrkyla, Energimarknadsinspektionen, Eskilstuna, 2013.
- [5] Svensk fjärrvärme, Om fjärrkyla. 2016 (accessed 04/04/2016.2016).
- [6] Svensk fjärrvärme, Statistik fjärrkylaleveranser. 2015 (accessed 01/12/2015.2015).
- [7] K. Byman, Bättre miljö med utbyggd fjärr- och närvärme : en utvärdering av LIP-finansierade fjärr- och närvärmeprojekt, Naturvårdsverket, Stockholm, 2004.
- [8] T.P. Hughes, *Networks of power : electrification in Western society, 1880-1930*, Johns Hopkins Univ.Press, Baltimore, 1983.
- [9] J. Palm, District heating as a secure heat supply - A question of regulation, *Energy and Environment* 18(6) (2007) 747-760.
- [10] B. Jonsson, *Elements of the Asia Pacific gas market : market power and efficiency*, Luleå University, Luleå, 1999.
- [11] J. Summerton, *District heating comes to town : the social shaping of an energy system*, Department of Thematic Studies - Technology and Social Change, Linköping University, Linköping, 1992.
- [12] S. Sorrell, J. Schleich, S. Scott, E. O'malley, F. Trace, E. Boede, K. Ostertag, P. Radgen, *Reducing barriers to energy efficiency in public and private organizations*, SPRU Science and Technology Policy Research, Brighton, 2000.
- [13] P. Thollander, J. Palm, P. Rohdin, *Categorizing Barriers to Energy Efficiency-an Interdisciplinary Perspective*, in: J. Palm (Ed.), *Energy Efficiency*, INTECH Open Access Publisher, Croatia, 2010, pp. 49-62.
- [14] S. Sorrell, *The economics of energy efficiency : barriers to cost-effective investment*, Edward Elgar, Cheltenham, 2004.
- [15] E. Aronson, P.C. Stern, *Energy use : the human dimension*, W. H. Freeman and company, New York, 1984.

- [16] P. Gyberg, J. Palm, Influencing households' energy behaviour-how is this done and on what premises?, *Energy Policy* 37(7) (2009) 2807-2813.
- [17] J. Palm, The public-private divide in household behavior: How far into home can energy guidance reach?, *Energy Policy* 38(6) (2010) 2858-2864.
- [18] P. Thollander, J. Palm, Improving energy efficiency in industrial energy systems : an interdisciplinary perspective on barriers, energy audits, energy management, policies, and programs, Springer, London, 2013.
- [19] A.B. Jaffe, R.N. Stavins, The energy-efficiency gap What does it mean?, *Energy Policy* 22(10) (1994) 804-810.
- [20] E. Hirst, M. Brown, Closing the efficiency gap: barriers to the efficient use of energy, *Resources, Conservation and Recycling* 3(4) (1990) 267-281.
- [21] J. Palm, P. Thollander, An interdisciplinary perspective on industrial energy efficiency, *Applied Energy* 87(10) (2010) 3255-3261.
- [22] H.A. Simon, *Models of man : social and rational : mathematical essays on rational human behaviour in a social setting*, New York, 1957.
- [23] A.H. Sanstad, R.B. Howarth, 'Normal'markets, market imperfections and energy efficiency, *Energy policy* 22(10) (1994) 811-818.
- [24] R.K. Yin, *Case study research : design and methods*, SAGE, London, 2009.
- [25] S. Päivärinne, O. Hjelm, S. Gustafsson, Excess heat supply collaborations within the district heating sector: Drivers and barriers, *Journal of Renewable and Sustainable Energy* 7(3) (2015) 033117.
- [26] F. Boons, F. Lüdeke-Freund, Business models for sustainable innovation: state-of-the-art and steps towards a research agenda, *Journal of Cleaner Production* 45 (2013) 9-19.
- [27] L. Doganova, M. Eyquem-Renault, What do business models do?: Innovation devices in technology entrepreneurship, *Research Policy* 38(10) (2009) 1559-1570.

THE DEMAND FUNCTION FOR RESIDENTIAL HEAT THROUGH A DISTRICT HEATING SYSTEM AND ITS CONSUMPTION BENEFITS IN KOREA

S.-Y. Lim¹, S.-H. Yoo¹

¹ Department of Energy Policy, Graduate School of Energy & Environment, Seoul National University of Science & Technology, 232 Gongreung-Ro, Nowon-Gu, Seoul, 01811, Republic of Korea

Keywords: *Residential heat, District heating, Consumption benefit*

ABSTRACT

The demand for residential heat (RH) through a district heating system (DHS) has been and will be expanded in Korea due to its better performance in energy efficiency and the abatement of greenhouse gas emissions than decentralized boilers. The purposes of this paper are two-fold. The first is to obtain the demand function for DHS-based RH in Korea and investigate the price and income elasticities of the demand employing the quarterly data covering the period 1988–2013. The short-run price and income elasticities are estimated as -0.700 and 0.918, respectively. Moreover, the long-run elasticities are -1.253 and 1.642, respectively. The second purpose is to measure the consumption benefits of DHS-based-RH employing the economic theory that they are the sum of the actual payment and consumer surplus for the consumption. Considering that the average price and estimated consumer surplus of the DHS-based RH use in 2013 are computed to be KRW 87,870 (USD 84.1) and KRW 62,764 (USD 60.1) per Gcal, the consumption benefits of the DHS-based RH are calculated to be KRW 150,634 (USD 144.2) per Gcal. This information can be beneficially utilized to conduct an economic feasibility study for a new DHS project related to RH supply.

INTRODUCTION

The district heating system (DHS) is considered to be best for the supply of residential heat (RH), a vital part of a human being's life, in urban areas with high population density [1]. Plants for the DHS can give us better performance in energy efficiency than decentralized boilers and an abatement of air pollutant emissions [2]. Moreover, the DHS is a more effective measure for mitigating greenhouse gas emissions than the individual heating system, contributing greatly to the enhancement of public convenience and energy saving (e.g., [3-5]).

The Korean government established a public utility, the Korea District Heating Corporation (KDHC), in 1985 in order to expand the DHS nationwide, focusing on new satellite cities in the Metropolitan areas. Recently,

private DHS suppliers have emerged in the market. In 2013, 10,895,352 giga calorie (Gcal) was supplied to 1,248,846 households by the KDHC whose share in the DHS market was about 59%. The DHS has been provided for existing apartments, replacing individual heating systems, and newly planned cities are constructing new plants.

Korean residents prefer the DHS to individual heating systems according to three aspects. First, the rate of the former is lower than that of the latter. Second, the former does not demand an individual boiler. Finally, the overall price of houses in DHS areas is higher than that in individual heating system areas with other things being equal. Thus, the supply of RH through DHS will be expanded in Korea to meet residents' increasing demand for RH. For example, according to the mid- and long-term financial plan of the KDHC, the amount of RH supplied by the KDHC will be doubled in 2024 compared with that in 2010.

In order to complete the tasks, the KDHC is constructing and planning to construct several DHS facilities. Because the KDHC is a public utility, whether to build a new DHS facility should be decided in the context of an economic feasibility analysis, namely a cost-benefit analysis. To this end, uncovering the costs and benefits ensuing from the DHS construction is required. Information on the costs can be more easily obtained than that on the benefits. However, so far as the authors know, the consumption benefits of the RH have rarely been estimated in the literature, leading researchers to be asked to supply usable and quantitative information on them for policymakers.

Therefore, our study attempts to value the consumption benefits of the RH in Korea. The economic theory implies that the economic benefit of the RH consumed is the sum of consumer surplus (CS) and actual payment and for the consumption [6]. The computation of CS for RH consumption is quite a complicated work. This study will use an estimate of CS proposed by Alexander et al. (2000), which will be explained in detail in the next section [7]. In calculating the estimate, we need information on the price elasticity of RH demand that can be derived from the demand function for RH.

Thus, the purposes of the paper are two-fold. The first is to obtain the demand function for DHS-based RH in

Korea and find the price and income elasticities of the demand. The second purpose is to measure the consumption benefits of DHS-based-RH using the estimated price elasticity of the RH demand. The remainder of the paper is structured as follows. The methodology adopted here and the data used are explained in Section 2. The results and discussion are reported in Section 3. The paper is concluded in the final section.

METHODOLOGY AND DATA

Consumption Benefits of RH

A rational consumer maximizes his/her utility under income or budget constraints. The demand for a good or service is derived as a solution to the utility maximization problem when the market exists and the price is exogenously given. It is natural that if the price changes the demand should also change. Thus, we can define the demand function where the price is an independent variable and the demand is a dependent variable. The demand function is assumed to be smooth and continuous. Given that there exists the demand function and we can obtain it, microeconomic theory shows that we can utilize the demand function to assess the economic benefits of the RH consumption (e.g., [8-9]).

The inverse demand function or demand curve means the marginal benefit function or marginal willingness to pay (WTP) function [10]. The height of the demand curve indicates a consumer's benefit or WTP to get one unit of the goods in question. Thus, the area below the demand curve implies a consumer's total benefit from or WTP for the consumption of a specified quantity of goods. The CS is defined as the gap between a consumer's maximum WTP and the actual price, as shown in Figure 1. In other words, the economic benefits of the RH consumed are the sum of the CS and actual consumer expenditure.

When one unit of RH is consumed at a price, the economic benefit of RH use can be computed by dividing the sum of the CS and actual consumer expenditure by the amount of RH consumed. It is quite difficult to measure the CS for RH use, while the consumer expenditure is easily obtainable information. This is because the consumer's choke price, defined as the price at which demand is zero, should be computed to estimate the CS. However, this computation is almost impossible to implement in the real world because of the insufficiency of available data. Thus, usually, the choke price has been assumed using a proxy, which may significantly reduce the reliability of measured CS. Accordingly, an alternative to estimating the CS is needed.

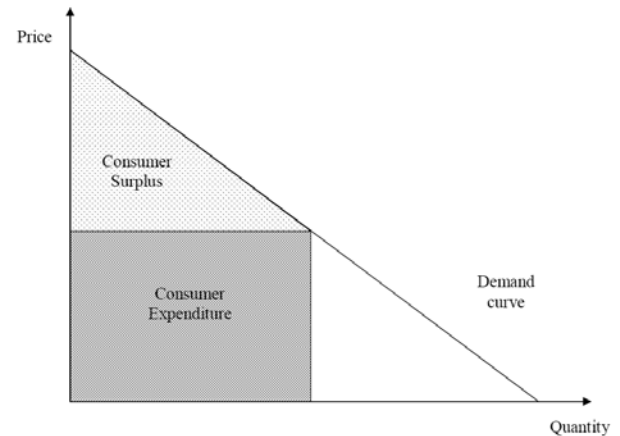


Figure 1. Demand curve and consumer surplus

Estimation of CS

Interestingly, Alexander et al. (2000) suggested a simple formula for CS that is based on only two values: the revenue from a commodity sale and the price elasticity of demand for the commodity [7]. Let P , X , and T be the price for RH, the demand for RH, and a vector of other variables that may affect the demand, respectively. A continuous and differentiable inverse demand function can be formulated as $P = P(X, T)$. If we assume that the levels of price and demand for RH are P_0 and X_0 , respectively, and omit T for brevity, then the first-order Taylor's expansion produces:

$$P(X) = P(X_0) + P'(X - X_0) + O(X) \quad (1)$$

Integration of this function from 0 to X_0 and subtraction of the consumer's actual payment, P_0X_0 , yields the CS (CS) as:

$$\begin{aligned} CS &= \int_0^{X_0} P(X) dX - P_0X_0 \\ &= -\frac{P_0X_0}{2\lambda} + \int_0^{X_0} O(X) dX \end{aligned} \quad (2)$$

where λ is the price elasticity of demand when the price is P_0 . When the second term in the last equality of (2) is sufficiently small, the first term in that is an approximation of the CS. For example, if the demand function has a linear form, the CS is exactly $-P_0X_0/2\lambda$. Thus, the approximation of consumption benefits can be derived as:

$$P_0X_0 + CS \approx P_0X_0 - \frac{P_0X_0}{2\lambda} = P_0X_0 \left[1 - \frac{1}{2\lambda} \right] \quad (3)$$

In applying Eq. (3) and assessing the consumption benefit, we require the information on λ , which can be obtainable from the demand function for RH. Thus, we need to estimate the demand function for RH.

Estimation of the Demand Function for RH

There are only a few studies that deal with the heat demand function. For example, Chramcov and Balátě (2008) applied the Box-Jenkins model to analyzing the heat demand function [11]. Wojdyga (2008) investigated how weather conditions make an effect on the demand for heat from DHS [12]. To the best of our knowledge, there is no work examining the demand function for RH and price and income elasticities of the demand. Thus, the message of our study is useful.

The Cobb-Douglas or double-logarithmic form is the most widely used in the literature to estimate the demand function [13-14]. The functional form is as follows:

$$\ln X_t = \beta_0 + \beta_1 \ln P_t + \beta_2 \ln Y_t + \beta_3 \ln N_t \quad (4)$$

where the subscript t indicates time; X_t is the demand for RH; P_t is the real price of RH; Y_t is the real income; N_t is the number of consumers; and β 's are the parameters to be estimated.

It is well-known that the demand for RH has a property of seasonality. In other words, the demand is high during winter and low during summer. Thus, the property should be reflected in formulating the form of the demand function. Let S_{1t} , S_{2t} , and S_{3t} be dummy variables for the first, second, and third quarters, respectively. Adding the quarterly dummy variables and a stochastic error term u_t to Eq. (4) produces the econometric specification:

$$\ln X_t = \beta_0 + \beta_1 \ln P_t + \beta_2 \ln Y_t + \beta_3 \ln N_t + \beta_4 \ln S_{1t} + \beta_5 \ln S_{2t} + \beta_6 \ln S_{3t} + u_t \quad (5)$$

The estimation results of Eq. (5) may suffer from the existence of a serial correlation. Our data is such a case, as will be explained below. In this case, we can apply a lagged dependent variable (LDV) model that contains LDV as an explanatory variable. The LDV model has an advantage of being able to investigate price and income elasticities in the long-run as well as in the short-run. Our LDV model is:

$$\ln X_t = \beta_0 + \beta_1 \ln P_t + \beta_2 \ln Y_t + \beta_3 \ln N_t + \beta_4 \ln S_{1t} + \beta_5 \ln S_{2t} + \beta_6 \ln S_{3t} + \beta_7 \ln X_{t-1} + u_t \quad (6)$$

where X_{t-1} is a lagged variable of X_t . In Eq. (6), the short-run price and income elasticities of the demand are β_1 and β_2 , respectively. Furthermore, the long-run price and income elasticities can be derived as $\beta_1 / (1 - \beta_7)$ and $\beta_2 / (1 - \beta_7)$, respectively.

Data

The quarterly data employed in this study covers the period 1988–2013. The supply of DHS-based RH in Korea was initiated in November 1987 by the KDHC. This made us choose the starting period for our

analysis as the 1st quarter of 1988. In Korea, the Bank of Korea (BOK) officially announces the estimated gross domestic product (GDP) [15]. Recently, the BOK changed the method of computing GDP. At the time of our analysis, the old series of GDP are available for the period 1970–2013, while the new series of GDP are available just for 2010–2015. That is, the GDP series over 1970–2013 are not comparable with those over 2014–2015. Thus, we use only the data during the period 1970–2013, excluding those of 2014–2015.

The RH demand is expressed in terms of Gcal and come from the KDHC. The prices of RH are obtained by dividing the RH sales by the RH demand and then converting nominal prices into real prices using the consumer price index published by Statistics Korea (2015) [16]. Thus, the prices of RH are interpreted as real average price measured in Korean won per Gcal. The nominal GDP series is converted to the real GDP series, which is assessed in billions of constant 2010 Korean won. The real income variables are calculated by dividing the real GDP by the number of households, which is obtained from Statistic Korea.

RESULTS AND DISCUSSION

Estimation Results of The RH Demand Function

As mentioned earlier, Eq. (5) does include seasonal quarterly dummy variables, but Eq. (4) does not. Table 1 contains the estimation results for Eqs. (4) and (5). The signs for all the coefficient estimates coincide with our prior expectations. For instance, the signs for the coefficient of price variable should be negative, while those of the income variable should be positive. We can perform a specification test of Eq. (4) versus Eq. (5). For this purpose, we apply the F -test for the null hypothesis of $\beta_4 = \beta_5 = \beta_6 = 0$; in other words, Eq. (4) is not mis-specified. The F -statistic follows the F -distribution with degrees of freedom 3 and 97 under the null hypothesis. The statistic is computed to be 325.35. Given that $F_{0.01}(3,97) = 2.70$, the null hypothesis can be rejected at the 1% level. Thus, our strategy of using quarterly dummy variables is appropriate for the analysis of the data.

However, considering that the Durbin-Watson statistic implies that there exists a first-order serial correlation in the model and Eq. (5) may be inappropriate for our data. Therefore, we try to apply a LDV model to overcoming the problem of the existence of the first-order serial correlation. It happens that when using the LDV model we can identify not only short-run elasticities but also long-run ones. Table 2 shows the estimation results of the LDV model for the RH demand function. All the coefficient estimates except for the constant term are statistically meaningful at the 1% level, while the coefficient estimate for the constant

term is so at the 5% level. Moreover, judging from the *F*-statistic, the null hypothesis that all the parameters are zero can be rejected at the 1% level. This means that the estimated RH demand function is statistically meaningful.

Once again, the existence of the first-order serial correlation in the model should be examined. The Durbin-Watson statistic is no longer valid for the LDV model, and Durbin's *h* statistic can be employed in such a case [17]. The *p*-value for the Durbin's *h* statistic is calculated to be 0.722 under the null hypothesis that there is no first-order serial correlation. Thus, the null hypothesis cannot be rejected, and the LDV model does not suffer from the existence of the first-order serial correlation. We can proceed to the computation of the elasticities using the estimation results of the LDV model.

Table 1. Estimation results of residential heat demand functions

Variables	Coefficient estimates for Eq. (4) ^a	Coefficient estimates for Eq. (5) ^a
Constant	2.822 (0.59)	1.524 (1.02)
Log of price	-3.412 (-10.95) [#]	-0.827 (-6.17) [#]
Log of income	4.548 (5.53) [#]	1.263 (4.46) [#]
Log of number of consumers	0.451 (3.03) [#]	0.774 (16.22) [#]
Dummy for 1st quarter		0.311 (5.93) [#]
Dummy for 2nd quarter		-0.806 (-15.10) [#]
Dummy for 3rd quarter		-1.640 (-23.76) [#]
Durbin-Watson statistic ^b	1.364 [#]	0.971 [#]
<i>F</i> -statistic ^c	135.39 [#]	889.07 [#]
Adjusted <i>R</i> -squared	0.797	0.981
Number of observations	104	104

Notes: ^a For the meaning of Eqs. (4) and (5), see the text. ^b The null hypothesis is that there is no first-order serial correlation. ^c The null hypothesis is that all the parameters are jointly zero. The dependent variable is the log of demand. The numbers in parentheses beside the coefficient estimates are *t*-values, computed from the analytic second derivatives of the log-likelihood. [#] indicates statistical significance at the 1% level.

Table 2. Estimation results of lagged dependent variable model for residential heat demand function

Variables	Coefficient estimates
Constant	2.524 (2.04)
Log of price	-0.700 (-5.91) [#]
Log of income	0.918 (3.74) [#]
Log of number of consumers	0.416 (6.41) [#]
Dummy for 1st quarter	-0.498 (-4.00) [#]
Dummy for 2nd quarter	-1.798 (-11.88) [#]
Dummy for 3rd quarter	-2.144 (-22.53) [#]
Log of lagged demand	0.441 (6.87) [#]
Durbin's <i>h</i> statistic ^a	-0.356
<i>F</i> -statistic ^b	1,121.54 [#]
<i>R</i> -squared	0.988
Number of observations	103

Notes: ^a The null hypothesis is that there is no first-order serial correlation. ^b The null hypothesis is that all the parameters are jointly zero. The dependent variable is the log of demand. The numbers in parentheses beside the coefficient estimates are *t*-values, computed from the analytic second derivatives of the log-likelihood. [#] indicates statistical significance at the 1% level.

Table 3 Estimation Results of Price and Income Elasticities

Classification	Short-run	Long-run
Price elasticities	-0.700 (-5.91) [#]	-1.253 (-5.44) [#]
Income elasticities	0.918 (3.74) [#]	1.642 (3.78) [#]

Notes: The numbers in parentheses beside the elasticity estimates are *t*-values. [#] indicates statistical significance at the 1% level.

Estimation Results of Price and Income Elasticities

Table 3 contains the results from estimating the elasticities of the RH demand. The *t*-values as well as the point estimates of short- and long-run elasticities are reported in the table. The *t*-values for short-run elasticities are calculated by the use of the analytic second derivatives of the log-likelihood, while those for long-run elasticities by the use of delta method. The estimates for four elasticities are all statistically significant at the 1% level.

The signs for price elasticities are negative, which implies that the law of demand applies for RH in Korea. The demand for RH is inelastic with respect to price change in the short-run. However, it is elastic with regard to price change in the long-run. This indicates

that a pricing policy for demand-side management may not be effective in the short-run. That is, RH has a property of being a necessity for humans' well-being. However, the pricing policy of raising the price to reduce the demand or lowering the price to expand the demand will be effective in the long-run.

The finding of income elasticity having a plus sign implies that the RH is normal goods. In other words, RH demand increases as income grows. Similar to price change, demand for RH is inelastic with respect to income change in the short-run and elastic with regard to income change in the long-run. The fuel used for production of RH, the supply of which is made in large cities with a high population density, is regulated to liquefied natural gas (LNG), a cleaner energy source. Most of the LNG consumed in Korea is imported from abroad, which makes a negative effect on the trade balance and imposes an economic burden on the national economy. Thus, it is necessary to encourage a more efficient use of RH to cope with the increasing demand for RH following economic growth.

Estimation Results of Consumption Benefits

Using Eq. (3) and a point estimate of short-run price elasticity presented in Table 3, we estimate the consumption benefits of RH in Korea for the period 2013. The results are shown in Table 4.

Table 4 Estimation Results of Consumer Surplus and Economic Benefit of Residential Heat (RH) Consumption in 2013

Sales of RH (Million KRW)	1,071,555 (USD 1,025 million)
Amount of RH sold (Gcal)	12,194,782
Average price of RH (KRW per Gcal)	87,870 (USD 84)
Price elasticity of RH	-0.700
Economic benefit of RH (Million KRW)	1,836,951 (USD 1758 million)
Unit economic benefit of RH (KRW per Gcal)	150,634 (USD 144)
Ratio of economic benefit to price	1.71

Note: At the time of late 2013, USD 1.0 was approximately equal to 1,045 Korean won.

As explained above, the CS corresponds to the actual payment subtracted from the value of the area below the demand curve. To compute the consumption benefits of RH, we need to add the estimated CS to the total expenditure for RH consumption. The CS for RH consumption in 2013 is computed to be KRW 765.4 billion (USD 732.4 million). This value corresponds to KRW 62,764 (USD 60.1) per Gcal. The total expenditure for RH consumption in 2013 was KRW 1,071.6 billion (USD 1,025.4 million). Thus, the consumption benefit for RH in 2013 is calculated to be KRW 1,837.0 billion (USD 1,757.8 million). This value amounts to KRW 150,634 (USD 144.1) per Gcal in 2013. This indicates that the consumption benefits of RH significantly outweigh the RH price.

Discussion

It appears that the measurement of RH consumption benefits has not been an important research topic in most countries because the price of RH fully reflects the cost involved in the production of RH as determined by the market. However, in Korea, the price of RH supplied by the KDHC is not led by market forces but rather is strongly regulated by the government to minimize the impact of change in it on the general price level of the national economy. The government can maintain low RH rates because the KDHC is a government-owned public utility. Consequently, uncovering the economic benefit of RH use is meaningful work in Korea.

The results show that the CS for RH consumption in 2013 is calculated to be KRW 62,764 (USD 60.1) per Gcal. Given that the average price of RH was KRW 87,870 (USD 84.1) per Gcal in 2013, the economic benefits that ensue from RH consumption are computed to be KRW 150,634 (USD 144.1) per Gcal. We can incorporate the value into the economic benefits of a DHS facility construction project and compare it with the economic costs of the project to decide whether the project is economically desirable. If we build a new DHS that can supply 1,000 Gcal of RH per day, we can easily compute the economic benefits as about KRW 150.6 million per day using the results. Thus, information on the consumption benefits of RH is essential for making investment decisions about whether to implement the project [18].

The information is also useful for non-structural policy options concerning RH management. If we have the information for each consumer sector, we can apply it to determine which sector should be preferentially supplied with RH during shortages. We can also consider the policy that limited RH is provided for sectors whose consumption benefits are relatively large.

CONCLUSION

The DHS is widely accepted as an excellent alternative for the supply of RH in urban areas with high population density, enhancing public convenience and energy saving. Moreover, the DHS is a more effective measure to mitigate greenhouse gases and air pollutant emissions than an individual heating system. The distribution of the DHS has been and will be rapidly expanded owing to the governmental policy to increase it, residents' preferences for it over individual heating systems, and active investments of the KDHC, a public enterprise in Korea. For example, the Korean government and the KDHC are planning to develop a new DHS project for gathering unused and/or discarded heat from thermal power plants and steel-making companies and distributing it to residents in the metropolitan areas that need RH. Therefore, policymakers demand information on the economic benefits of the DHS for decision-making about whether to implement the DHS project.

However, the consumption benefits of the RH have rarely been estimated in the literature, which asks researchers to supply usable and quantitative information on these benefits for policymakers to decide whether to build a new DHS for providing RH. Following the tenets of microeconomic theory, the economic benefit of RH use from the DHS is the sum of the actual expenditure for RH consumption and the CS for the use. In particular, as the Korean government has regulated the unit price of current RH from the DHS under the cost of production, the price does not reflect the resource cost involved in the supply of RH from the DHS. The benefit can be underestimated if the price is used to assess it. Therefore, in order to obtain information on the consumption benefits of RH from the DHS, one would need to measure the CS for RH use since its price is well-known information.

Our study estimated the demand function for RH using the LDV model and the quarterly data covering 1988–2013 to obtain information on the price and income elasticities of the RH demand. Furthermore, we assessed the consumption benefits of RH employing an estimate of CS computed from the estimated price elasticity. All the parameter estimates in the demand function secured statistical significance at the 5% level. The CS arising from DHS-based RH consumption in 2013 was calculated to be KRW 62,764 (USD 60.1) per Gcal. The price for RH from DHS per Gcal that can be interpreted as consumer expenditure is KRW 87,870 (USD 84.1) per Gcal in 2013. Therefore, the consumption benefits of RH from the DHS were calculated to be KRW 150,634 (USD 144.1) per Gcal.

This figure can be used to decide whether to invest in a new DHS to provide RH. Considering constrained public budgets, correct and valid estimates of the

economic benefits of the DHS for RH supply are required to make economically sound investment decisions. The estimates can be beneficially utilized to conduct an economic feasibility study for a new project related to the DHS. Economic evaluation is important because it helps ascertain whether the public favors a proposed DHS project for RH supply and estimates the degree to which the public is willing to pay for such a benefit.

For an illustrating example, we consider a new DHS project that has a three-year construction period and a 30-year operation period. Through the DHS project, 1,000 Gcal of RH is expected to be supplied and consumed per year. By using a social discount rate of 5.5%, the present value of total costs involved in the DHS project amounts to KRW 1.0 billion. The economic benefits that ensue from the DHS project are estimated to be KRW 150.6 million (= KRW 150,634 per Gcal × 1,000 Gcal). The present value of the consumption benefits is KRW 1.97 billion. The benefit and cost ratio is computed to be 1.97, which is greater than 1.0. Thus, we can conclude that the new DHS project is socially profitable and should be immediately implemented. If the ratio is smaller than 1.0, the project should not be conducted.

ACKNOWLEDGEMENT

This work was supported by the Korea Institute of Energy Technology Evaluation and Planning (KETEP) and the Ministry of Trade, Industry & Energy (MOTIE) of the Republic of Korea (No. 20164030201060). Moreover, we acknowledge that this research is financially supported by Korea District Heating Corporation (KDHC).

REFERENCES

- [1] Behnaz, R., Rosen M.A., 2012. District heating and cooling: review of technology and potential enhancements. *Applied Energy*, Vol. 93, pp. 2–10.
- [2] Gebremedhin, A., 2014. Optimal utilisation of heat demand in district heating system – A case study. *Renewable and Sustainable Energy Reviews*, Vol. 30, pp. 230–236.
- [3] Knutsson, D., Werner, S., Ahlgren, E.O., 2006. Combined heat and power in the Swedish district heating sector – impact of green certificates and CO₂ trading on new investments. *Energy Policy*, Vol. 34, pp. 3942–2952.
- [4] Ilic, D.D., Trygg, L., 2014. Economic and environmental benefits of converting industrial processes to district heating. *Energy Conversion and Management*, Vol. 87, pp. 305–314.
- [5] Euroheat & Power, 2015. District Heating and Cooling Country by Country 2015 Survey. Brussels.

- [6] Lee, J.-S., Yoo, S.-H., 2013. The economic value of residential natural gas consumption: the case of Korea. *Energy Sources Part B: Economics, Policy, and Planning*, Vol. 8, pp. 313–319.
- [7] Alexander, D.L., Kern, W., Neill, J., 2000. Valuing the consumption benefits from professional sports franchises. *Journal of Urban Economics*, Vol. 48, pp. 321–337.
- [8] Ku S.-J., Yoo, S.-H., 2012. Economic value of water in the Korean manufacturing industry. *Water Resources Management*, Vol. 26, pp. 81–88.
- [9] Park, S.-Y., Yoo, S.-H., 2013. The economic value of LNG in the Korean manufacturing industry. *Energy Policy*, Vol. 58, pp. 403–407.
- [10] Willig, R.D., 1976. Consumer's surplus without apology. *American Economic Review*, Vol. 66, pp. 589–597.
- [11] Chramcov, B., Balátě, J., 2008. Time series analysis of heat demand, *Proceedings*. In: *Proceedings 22nd European Conference on Modelling and Simulation*.
- [12] Woidyga, K., 2008. An influence of weather conditions on heat demand in district heating systems. *Energy and Buildings*, Vol. 40, pp. 2009–2014.
- [13] Yoo, S.-H., Lee, J.-S., Kwak, S.-J., 2007. Estimation of residential electricity demand function in Seoul by correction for sample selection bias. *Energy Policy*, Vol. 35, pp. 5702–5707.
- [14] Lim, K.-M., Lim, S.-Y., Yoo, S.-H., 2014. Short- and long-run elasticities of electricity demand in the service sector in Korea. *Energy Policy*, Vol. 67, pp. 517–521.
- [15] Bank of Korea. 2015. Available from: <http://bok.or.kr/> (accessed June 2015).
- [16] Statistics Korea. 2015. Available from: <http://kosis.kr> (accessed June 2015).
- [17] Greene, W.H., 2012, *Econometric Analysis*, pp.963–964. (7th ed.). Pearson.
- [18] Kaiser, M.J., Pulsipher, A.G., 2003. A generalized modeling framework for public benefit fund program valuation. *Energy*, Vol. 28, pp. 519–538.

PUBLIC PREFERENCES FOR POWER GENERATION SOURCE SWITCH FROM NUCLEAR POWER TO NATURAL GAS-BASED COMBINED HEAT AND POWER WITH A VIEW TO DECENTRALIZED GENERATION

H.-J. Kim¹, S.-Y. Lim¹, S.-H. Yoo¹

¹ Department of Energy Policy, Graduate School of Energy & Environment,
Seoul National University of Science & Technology, Seoul, Republic of Korea

Keywords: nuclear power, natural gas-based combined heat and power, power transmission facilities, decentralization, willingness to pay

ABSTRACT

This study attempts to analyze the public preference for natural gas (NG)-based combined heat and power (CHP) plants, which can be installed near electricity-consuming areas and do not require large-scale and long-distance power transmission facilities (PTFs), in the perspective of decentralized generation. More specifically, this paper assesses the public's additional willingness to pay (WTP) for substituting consumption of a unit of electricity generated from nuclear power plant, currently a dominant power generation source in Korea, with that produced from NG-based CHP plant in terms of decentralized generation using the contingent valuation (CV) method. To this end, a CV survey of 1,000 households was implemented. The results show that the mean additional WTP for substituting nuclear power plant by NG-based CHP plant is estimated to be KRW 55.3 (USD 0.047) per kWh of electricity, which is statistically significant at the 1% level. This value amounts to 44.2% of the average price for electricity, KRW 125.14 (USD 0.107) in 2014, which implies that the public are ready to shoulder a significant financial burden to avoid the social conflicts caused by PTFs construction. Moreover, the value can be interpreted as an external cost of nuclear power generation relative to NG-based CHP generation, or as an external benefit of NG-based CHP generation relative to nuclear power generation with a view to decentralized generation.

INTRODUCTION

Nuclear power has been widely accepted to have lower costs than other generation sources such as coal and natural gas (NG) in Korea and thus the government has expanded and will expand the construction of nuclear power plant. According to 'The 7th Basic Plan for Long-term Electricity Supply and Demand (2015-2029)' published by the Korean government in 2015 [1], an additional thirteen nuclear power plants are planned to be constructed. Nuclear power is presently a base-loaded and dominant power generation source in Korea. All the nuclear power plants in Korea are located around coastal areas in order to acquire sea water for cooling and are quite remote from the Metropolitan area for safety. Consequently, the nuclear

power plants inevitably require large-scale and long-distance power transmission facilities (PTFs) since they are located far from the consumers.

Some believe that there may be health hazards emitted from these facilities for those living close to them. Moreover, PTFs are a blot on the landscape. The rights-of-way for high voltage lines often run through high-value land and reduce the property values there [2]. In summary, the significant externalities of PTFs include electric and magnetic fields (EMFs), visual disamenity, and land use [3]. Whether or not the possible damage from PTFs is backed by scientific evidence, the construction of new high-voltage transmission lines is occasionally confronted by public opposition or political resistance. This usually causes a substantial amount of social costs.

The social costs caused by large-scale and long-distance PTFs are as follows. First, there is the construction cost; second, there are transmission losses due to the long-distance power transmission [4]; third, a transmission congestion cost from the transmission bottleneck effect is incurred as a result of the largest amount of electricity being consumed in the Metropolitan area [5]. Lastly, there is damage in the form of visual disamenity, depreciation of land prices and prohibition on land usage, and damage to the health of local citizens caused by large-scale and long-distance PTFs [3]. For example, Ju et al. [3] derived quantitative information on the cost of damage caused by overhead power transmission lines in Korea by applying a choice experiment technique that investigated public preferences for the above-mentioned damage. In addition, Navrud et al. [6], Giaccaria et al. [7], and McNair et al. [8] examined the external costs of PTFs by implementing various non-market valuation methods. Some related studies are also found in the literature [e.g., see 2, 9–13].

Recently, a number of social conflicts related to PTFs construction, which rarely arose in the past, have taken place in Korea. A representative conflict arose in Milyang, which is located between the Metropolitan area and Singori nuclear power plants. 765 kV power transmission lines and 69 transmission towers are scheduled to be constructed in Milyang to transmit

electricity generated at the Singori nuclear power plants to the Metropolitan area. The opposition has continued since the government first officially announced and approved the construction in 2008. One resident burned himself to death and another resident poisoned herself to death with the intention of objecting to the construction. Some Milyang residents took over the construction sites in protest. Unfortunately, these conflicts were not peacefully resolved. The government exercised its power to stop the opposition in 2014 through police action. Thus, externally, at least, the conflict seems to be resolved.

However, the anxiety of the Milyang residents is not yet healed and similar opposition is likely to arise in other areas. In the past, we suffered from an insufficient supply of power, as a result of insufficient power plants. The ceaseless public and private investment in power plant construction has successfully removed the problem of insufficient power supply. We are now confronted instead with the new and serious problem of social conflict related to the construction of large-scale and long-distance PTFs. As the social cost regarding PTFs has become a more significant issue, there has recently been more interest than previously in expanding decentralized generation which does not incur any social cost.

In order to deal with the problem, the Korean government planned to increase the proportion of decentralized generation from 9.6% in 2013 to 13.9% in 2029. In particular, decentralized generation sources such as NG-based combined heat and power (CHP) plant can be installed near to electricity-consuming areas and do not require large-scale and long-distance PTFs. Thus, the opposition can be eliminated by operating decentralized generation such as NG-based CHP generation. The government will increase the ratio of CHP generation from 3.1% in 2013 to 4.6% in 2029. This means augmenting the amount of electricity produced by CHP from 16,751 GWh in 2013 to 34,175 GWh in 2029 [1].

Obviously, the public preference for decentralized generation to avoid the damage caused by PTFs can be utilized as a proper and important reference for further discussion of the expansion of decentralized generation and decisions on the establishment of PTFs and power generation. The public preference can be investigated through their additional willingness to pay (WTP) for NG-based CHP over nuclear power. Moreover, the WTP can be taken as indicative of an external cost of nuclear power generation relative to NG-based CHP generation or an external benefit of NG-based CHP generation relative to nuclear power generation with a view to decentralized generation.

Therefore, this paper attempts to analyze the public preference for NG-based CHP plant over nuclear power in a perspective of decentralized generation using the CV approach. The message of this paper is all the more useful because, to the best of the authors' knowledge, this study is the first trial to address the issue quantitatively. The remainder of the paper comprises four sections. The methodology adopted in this study is explained in section 2. A model of WTP is described in Section 3. The results are reported and discussed in Section 4. The paper is concluded by the final section.

METHODOLOGY

Method for assessing the public preference for a power generation source switch

The CV technique has been very widely applied in the literature to obtain the WTP for non-market goods [14–15]. There are no restrictions on the objects that can be valued using the CV method. In particular, it is more useful than other methods because it can capture the non-use or existence value of goods, which cannot be measured through a market mechanism. Non-market goods include environmental goods or public goods such as a power generation source switch from nuclear power to NG-based CHP in the perspective of decentralized generation. Thus, as explained earlier, this study seeks to utilize the CV approach to assess the economic benefits that would follow from the switch. It asks a potential consumer a question concerning the WTP for conducting the switch using a well-structured survey of randomly chosen consumers [16].

Some people may doubt the practicality and usefulness of the CV method because it gathers information from a survey of respondents. In this regard, the blue-ribbon National Oceanic and Atmospheric Administration (NOAA) Panel came to the influential conclusion that the CV method can produce reliable quantitative information that can be utilized in decision-making both for public administrations and judicially, provided that several guidelines proposed by the NOAA Panel are observed [17]. Moreover, following the guidelines can secure the validity and accuracy of the CV method.

For example, the goods of concern should be familiar to the public, the CV survey should be administered through face-to-face interviews by professionally trained interviewers rather than through telephone or mail interviews, the number of respondents should be at least 1,000, a suitable payment vehicle should be adopted and presented to the respondents, and the substitutes for the goods should be explained to the respondents in the survey. The conditions are met in our study, as will be discussed in detail below.

The goods to be valued

The Korean government has a very clear long-term plan for decentralized generation. At present, there are national energy master plans for the expansion of NG-based CHP. The government declared its plans to expand the NG-based CHP plants as a representative decentralized generation source from 2013 to 2035. Accordingly, "The 8th Basic Plan for Long-term Electricity Supply and Demand", an official national plan expected to be published in 2017, seems to include the construction of additional NG-based CHPs.

The goods to be valued in this study is the power generation source switch from nuclear power to NG-based CHP in the perspective of decentralized generation in order to avoid damage caused by PTFs. NG-based CHP plant does not require PTFs, which are inevitably required in consuming the electricity generated from nuclear power. Therefore, any damage arising from PTFs can be eliminated by NG-based CHP plants since they are constructed near to electricity-consuming areas on a small scale. These points have been explicitly conveyed to the respondents in the CV survey.

In designing a CV survey, the current state (Q_0) and target state (Q_1) should be clearly defined. In our study, Q_0 and Q_1 mean the consumption of electricity generated from nuclear power and that from NG-based CHP, respectively. The CV survey elicits a response of WTP to achieve the change from Q_0 to Q_1 , the power generation source switch, from a respondent. In this regard, the WTP can be interpreted as a premium of NG-based CHP over nuclear power with a view to decentralized generation.

Survey design issues

We commissioned a professional survey firm to arrange the CV field survey. The firm drew a stratified random sample of 1,000 households from the national population to obtain information on the households' WTP and their socio-economic characteristics. A CV survey can be conducted using face-to-face in-person, telephone, or mail interviews. The response rate to a mail survey is usually quite low, and a telephone survey can present only a limited volume of information to respondents. We wished to convey a large amount of explanatory information on the power generation source switch from nuclear power to NG-based CHP in the perspective of decentralized generation, and to provide visual cards describing the situations with and without the switch, and the expected effects of the switch in the CV survey to the respondents [18–19]. This is why we used face-to-face interviews.

We gave the interviewers sufficient information about the purposes and background of the CV survey, and instructed them how to answer the questions that might be raised by the interviewees in the CV survey. Moreover, the supervisors affiliated with the survey company trained the interviewers to implement the CV survey as persuasively and effectively as possible. In order to derive the respondents' reliable and responsible decision-making, 20- to 65-year-old heads of households or homemakers were selected and interviewed in the CV survey. Judging from the interviewers' comments, the respondents gave their WTP responses without great difficulty. The final number of observations to be analyzed in our study is 1,000.

The survey instrument consists of three parts. The first is an introductory section, explaining general background information on NG-based CHP and nuclear power and then asking the respondents about their perceptions of it. The scenario in which the power generation source switch to be valued would be provided to the public should be clearly explained. The second part includes questions about WTP for the switch. These questions should be presented in a context that ensures that the WTP questions are plausible, understandable, and meaningful. The final part contains questions relating to the households' socio-economic variables.

Method of WTP elicitation

To elicit WTP responses, we employed a dichotomous choice (DC) question format reflecting the suggestion by Arrow et al. [17]. In a DC format, a respondent is asked to state whether he/she would pay a given bid to obtain a specified improvement in the quantity or quality of the goods to be valued. This DC format is usually called a single-bounded (SB) DC question format since it asks just one question. The double-bounded (DB) DC question format asks one more follow-up question to identify the WTP a higher amount when the first response is "yes" and a lower amount when "no".

While the DB question format results in higher efficiency, we do not use this format here because it increases the bias involved in WTP responses and thus Bateman et al. [20] and Carson and Groves [21] do not favor it. The findings from the focus group's interviews allowed us to derive a list of seven bids to be presented to respondents. The lists are KRW 10, 20, 30, 50, 70, 100 and 150 per kWh of electricity use through NG-based CHP rather than nuclear power in the context of decentralized generation. At the time of the survey, USD 1.0 was approximately equal to KRW 1170.40.

Payment vehicle

A respondent may be embarrassed when asked directly for his/her WTP. Introducing into the survey questionnaire a medium through which the amount would be paid helps the respondent to reveal his/her true WTP. We usually call the medium the payment vehicle. Payment vehicles found in the literature include taxes, funds, donations, and expenditure. The respondents should feel at home with the payment vehicle, and the goods to be valued should have a clear connection with it. For this reason, the electricity bill, which is familiar to most respondents and definitely related to actual expenditure, is appropriate for the payment vehicle [14, 22]. Thus, we employ electricity bills as the payment vehicle in this study.

The WTP question is “Is your household willing to pay a given amount for the power generation source switch from nuclear power to NG-based CHP in the perspective of decentralized generation through an increase in electricity bills for the next ten years, supposing that the switch will certainly be guaranteed?”

Moreover, some additional statements concerning payment are provided in the survey questionnaire. For example, the respondents are told: “If a majority of respondents refuse to pay the cost involved in the power generation switch, the switch cannot be implemented. However, if a majority of respondents accept the payment, the switch can be implemented. Please bear in mind that your household’s income is constrained and that there are various expenditures in your household”.

MODELING OF WTP RESPONSES

Model for dealing with zero WTP responses: spike model

Some people can have an interest in the goods to be valued, but others may be totally indifferent to or place no value on the goods. In this case, the proportion of zero WTP responses in the CV survey may be high. Researchers should pay close attention to how they deal with observations of WTP responses of zero. For this purpose, we apply a spike model suggested by Kriström [23] and Yoo and Kwak [24]. The following model is therefore theoretically based on Kriström’s [23] and Yoo and Kwak’s [24] spike model where the probability of zero WTP responses is modeled as a spike at zero in the distribution of WTP.

The spike model enables us to analyze both zero point and positive interval WTP data in a uni-variate setting. In the spike model, $F_X(B; \lambda)$ has the functional form:

$$F_X(B; \lambda) = \begin{cases} [1 + \exp(\alpha - \beta B)]^{-1} & \text{if } B > 0 \\ [1 + \exp(\alpha)]^{-1} & \text{if } B = 0 \\ 0 & \text{if } B < 0 \end{cases} \quad (1)$$

As explained earlier, the spike is defined as the probability of the respondent’s WTP being zero. Thus, the spike is computed as $[1 + \exp(\alpha)]^{-1}$. Some covariates such as the respondent’s household income can be incorporated into the spike model. A common method for doing this makes the covariates penetrate into α in Eq. (1). That is, α is simply changed into $\alpha + z' \delta$ where z is a vector of covariates and δ is a vector of the corresponding parameters to be estimated.

SB DC spike model

As explained above, an SB DC model yields greater consistency than a DB DC model. This is why we use an SB DC model in this study instead of a DB DC model. We have J observations to be analyzed. A bid, B_j , is given to the respondent j for $j = 1, \dots, J$. During the CV survey, bid B_j is presented to respondent j .

The respondents are provided with B_j as the bid. In this case, there are two outcomes, “yes” ($X > B_j$)

and “no” ($X < B_j$), and no further bid is required.

Therefore, for the two results we can introduce two binary variables, I_j^Y and I_j^N . That is, the value of each binary variable is one if the respondent’s response corresponds with its superscript and zero otherwise. For example, I_j^Y is one if the respondent j reports “yes” and zero otherwise.

One can combine the SB DC model and the spike model. In order to identify zero WTP observations, we asked the respondents who gave a “no” response when the presented bid was B_j an additional follow-up question that can distinguish true zero WTP from positive WTP. Thus, we can formulate one more binary variable, I_j^P whose value is one if the respondent j ’s WTP is positive and zero otherwise. The log-likelihood function of the SB DC spike model is:

$$\ln L = \sum_{j=1}^J \{ I_j^Y \ln [1 - F_X(B_j; \lambda)] + I_j^P \cdot I_j^N \ln F_X(B_j; \lambda) + (1 - I_j^P) \cdot I_j^N \ln F_X(0; \lambda) \} \quad (2)$$

Using Eq. (2), the mean of WTP can be computed as:

$$E(X) = \int_0^{\infty} [1 - F_X(B; \alpha, \beta)] dB - \int_{-\infty}^0 F_X(B; \alpha, \beta) dB \quad (3)$$

$$= \frac{1}{\beta} \ln[1 + \exp(\alpha)]^{-1}$$

RESULTS AND DISCUSSION

Data

The CV survey was administered to about 1,400 randomly chosen households from the whole population of Korea during June 2015. Some observations that did not contain important information or were judged by the interviewers to be of poor quality were deleted from the final dataset to be investigated. In this way, we obtained 1,000 useable observations. Table 1 describes the distribution of responses by bid amount. Each set of bids was allocated to a similar number of respondents, as is shown in the last column of Table 1.

Table 1 Distribution of responses by bid amount

Bid amount ^a	Number of responses (%) ^b			
	yes	no-yes	no-no	Totals
10	95 (66.4)	10 (7.0)	38 (26.6)	143 (100.0)
20	67 (46.9)	29 (20.3)	47 (32.9)	143 (100.0)
30	50 (35.0)	24 (16.8)	69 (48.3)	143 (100.0)
50	40 (28.0)	22 (15.4)	81 (56.6)	143 (100.0)
70	33 (23.1)	41 (28.7)	69 (48.3)	143 (100.0)
100	34 (23.9)	51 (35.9)	57 (40.1)	142 (100.0)
150	36 (25.2)	54 (37.8)	53 (37.1)	143 (100.0)
Totals	355 (35.5)	231 (23.1)	414 (41.4)	1,000 (100.0)

Notes: ^a The unit is Korean won. ^b The numbers in parentheses indicate the percentage of the sample size.

A “no-no” response indicates the zero WTP response. A total of 414 households (41.4%) revealed zero WTP for the power generation source switch. This implies that the use of a spike model to deal with zero WTP responses is a suitable approach in our study. Moreover, the zero WTP response is consistent with the microeconomic theory that non-consumption can be obtained as a corner solution to a utility

maximization problem under income constraint. Overall, the proportion of “yes” responses to a given bid declines as the magnitude of the bid increases. For instance, when a bid of KRW 10 per kWh was presented, 95 respondents (66.4%) accepted the additional payment, while just 36 respondents (35.3%) agreed to the additional payment of KRW 150 per kWh.

Estimation results of the SB DC spike model

The estimation results of the SB DC spike model with no covariates are reported in Table 2. The parameter estimates can be obtained by finding the parameter values maximizing Eq. (2), in other words, by applying the maximum likelihood estimation method. Each estimate for the two parameters, α and β , is statistically significant at the 1% level. Moreover, the null hypothesis that the parameter estimates are all zero can be rejected at the 1% level, in that the p -value for the Wald statistic calculated under the null hypothesis is less than 0.01. In particular, the estimate for the spike is 0.4246, which is similar to the sample proportion of the zero WTP responses provided in Table 1, 41.4%. This indicates that the spike model employed here fits our data well.

Table 2 Estimation results of the spike model

Variables	Estimates ^d
Constant	0.3040 (4.68) [#]
Bid ^a	-0.0155 (-18.43) [#]
Spike	0.4246 (26.78) [#]
Mean WTP per household per year	KRW 55.27 (USD 0.047)
t -value	18.03 [#]
95% confidence interval ^b	KRW 49.62 to 61.85 (USD 0.042 to 0.053)
99% confidence interval ^b	KRW 47.96 to 64.16 (USD 0.041 to 0.055)
Number of observations	1,000
Log-likelihood	-1049.45
Wald statistic (p -value) ^c	325.22 (0.000)

Notes: a The unit is 1,000 Korean won and USD 1.0 was approximately equal to KRW 1170.40 at the time of the survey. b The confidence intervals are calculated using the Monte Carlo simulation technique of Krinsky and Robb (1986) with 5,000 replications. c The null hypothesis is that all the parameters are jointly zero and the corresponding p -value is reported in parentheses beside the statistic. d The numbers in parentheses beside the coefficient estimates are t -values, computed from the analytic second derivatives of the log-likelihood. # indicates statistical significance at the 1% level.

Using Eq. (3) and the values presented in the upper panel of Table 2, we can obtain an estimate of the mean additional WTP, KRW 55.3 (USD 0.047) per kWh. Its *t*-value is 18.03 and thus the estimate is statistically meaningful at the 1% level. In order to handle the uncertainty related to the computation of the estimate, we try to report the confidence intervals for the point estimate. For this purpose, the parametric bootstrapping method proposed by Krinsky and Robb [25] is most widely employed in the literature. We use the method with 5,000 replications to get the 95% and 99% confidence intervals, which are contained in Table 2. The 95% confidence interval is tighter than the 99% confidence interval.

The mean additional WTP for the electricity generated from NG-based CHP over nuclear power in the perspective of decentralized generation, KRW 55.3 (USD 0.047) per kWh, amounts to 44.2% of the average cost of electricity, KRW 125.14 (USD 0.107) per kWh in 2014 in Korea. It is clear from the results that the public is willing to pay a significant additional amount to achieve the power generation switch to avoid the damage from large-scale and long-distance PTFs. In other words, an external cost of nuclear power generation relative to NG-based CHP generation or an external benefit of NG-based CHP generation relative to nuclear power generation with a view to decentralized generation is meaningful.

Estimation results of the SB DC spike model with covariates

We seek to estimate the spike model with covariates. Some variables used for the covariates are defined in Table 3. They are related to the characteristics of the respondent or the respondent's household.

Furthermore, the sample statistics of the covariates are also reported in Table 3. A total of six variables are contained in the model. The characteristics of the sample appear to reflect those of the population well, since we drew a random sample of Korean households with the help of the professional polling firm. The results of estimating the spike model, including the variables shown in Table 3, are described in Table 4.

In particular, the coefficient estimates for Gender, Age, Education, Income and Householder except for Family in the model are statistically significant at the 5% level. This implies that male respondents are less likely to report "yes" to a given bid than female respondents. The respondent's age has a positive relation to the likelihood of saying "yes" to a presented bid. More educated respondents are more likely to state "yes" to a specified bid than others. The respondents with a higher income have a tendency to report "yes" to a given bid. A respondent who is a householder has higher probability of replying "yes" to a bid than others.

Table 3 Definitions and sample statistics of the variables

Variables	Definitions	Mean	Standard deviation
Gender	The respondent's gender (0=female; 1=male)	0.49	0.5
Age	The respondent's age in years	46.48	10.36
Family	The size of the respondent's household (unit: persons)	3.34	1.02
Income	The household's monthly income before tax deduction (unit: million Korean won)	4.84	3.07
Education	The respondent's education level in years	13.79	2.34
Householder	Dummy for the respondent being a householder (0 = no; 1 = yes)	0.55	0.5

Table 4 Estimation results of the spike model with covariates

Variables	Estimates	<i>t</i> -values
Constant	-2.4165	-2.12*
Bid ^a	-0.0160	-16.96**
Gender	-0.4521	-2.17*
Age	0.1217	2.30*
Family	-0.0289	-0.43
Income	0.0601	2.39*
Education	0.9031	2.50*
Householder	0.4424	2.10*
Spike	0.4217	27.14**
Wald statistic (<i>p</i> -value) ^b	273.39 (0.000)	
Log-likelihood	-1033.19	
Number of observations	1,000	

Notes: The variables are defined in Table 3. a The unit is 1,000 Korean won and USD 1.0 was approximately equal to KRW 1170.40 at the time of the survey. b The null hypothesis is that all the parameters are jointly zero and the corresponding *p*-value is reported in parentheses beside the statistic. * and ** indicate statistical significance at the 5% and 1% levels, respectively.

Discussion of the results

It appears that the measurement of an external benefit of a power generation source switch from nuclear power to NG-based CHP in the perspective of decentralized generation has not been an important research topic in most countries. However, as explained above, the expansion of decentralized generation is widely and urgently required in Korea since large-scale and long-distance PTFs of nuclear power plants cause serious social conflict and regional economic damage. Therefore, valuing the external benefit of a power generation source switch from nuclear power to NG-based CHP in the perspective of decentralized generation is significant work in Korea.

For various reasons, a large expansion of other decentralized generation sources such as new and renewable sources is difficult to implement in Korea. For example, wind and photovoltaic power produce other environmental and disamenity problems [e.g., see 26–27]. Moreover, they are intermittent generation sources and thus demand sufficient capacity from back-up power plants to secure a stable supply of electricity. Currently, in Korea, fuel cell generation contributes more greenhouse gas emissions and costs than NG-based CHP generation since NG is required for making the hydrogen that is necessary for fuel cell generation.

Therefore, a realistic and effective method of electricity generation as a decentralized generation source is obviously NG-based CHP in the Metropolitan area of Korea. In this regard, our finding that the mean additional WTP for the electricity generated from NG-based CHP over nuclear power in the perspective of decentralized generation amounts to 44.2% of the average cost of electricity, supports the governmental plan to increase the amount of NG-based CHP generation from 16,751 GWh in 2013 to 34,175 GWh in 2029. Consequently, if the additional generation, 17,424 GWh, can be provided through NG-based CHP rather than nuclear power, its external benefit from the viewpoint of decentralized generation amounts to KRW 963.5 billion in 2029. This indicates that Korean households have a significant preference for NG-based CHP over nuclear power in terms of decentralized generation.

CONCLUSIONS

As base-loaded power generation, nuclear power plants, sited far from consumers, require large-scale and long-distance PTFs to transmit large amounts of electricity to where the demand is located. However, NG-based CHP, the most representative decentralized generation source in Korea, can be located close to electricity-consuming areas. Expansion of NG-based

CHP can be a fundamental solution to avoid the social conflict and regional damage arising from nuclear power plants. This damage includes EMFs, visual disamenity, depreciation of land prices, and prohibitions on land usage.

This study attempted to analyze the public preference for NG-based CHP plants, which can be installed near to electricity-consuming areas and do not require large-scale and long-distance power transmission facilities, in the perspective of decentralized generation. For this purpose, this study reported the results of a CV survey of 1000 randomly selected households. Based on the interviewers' comments, the value judgments the respondents were required to make were within their abilities. Moreover, all the parameter estimates from the model have high statistical significance. Thus, our estimated model possesses statistical meaning.

The mean additional WTP for substituting the nuclear power plant by NG-based CHP plant was estimated to be KRW 55.3 (USD 0.047) per kWh of electricity, which was statistically significant at the 1% level. This value amounts to 44.2% of the average price for electricity, KRW 125.14 (USD 0.107) in 2014, which implies that the public are ready to shoulder a significant financial burden to avoid the social conflict caused by PTF construction. Moreover, the value can be interpreted as an external cost of nuclear power generation relative to NG-based CHP generation or an external benefit of NG-based CHP generation relative to nuclear power generation from the perspective of decentralized generation.

The public preference for decentralized generation to avoid the conflict and damage caused by PTFs can be utilized as a proper and important reference for the further discussion of expansion of decentralized generation and decisions on the establishment of PTFs and power generation. Therefore, we can conclude that the Korean public supports the governmental plan to increase NG-based CHP generation from 16,751 GWh in 2013 to 34,175 GWh in 2029. If the plan is successfully implemented, the ensuing external benefits amount to KRW 963.5 billion as of 2029.

ACKNOWLEDGEMENT

This work was supported by the Korea Institute of Energy Technology Evaluation and Planning (KETEP) and the Ministry of Trade, Industry & Energy (MOTIE) of the Republic of Korea (No. 20164030201060).

Moreover, we acknowledge that this research is financially supported by Korea District Heating Corporation.

REFERENCES

- [1] Ministry of Trade, Industry, and Energy. The 7th Basic Plan for Long-term Electricity Supply and Demand (2015-2029). Sejong, Korea (2015).
- [2] Weimers L. "HVDC Light: A new technology for a better environment", in Proc. IEEE Power Engineering Review1998, Vol. 18, pp. 9–20.
- [3] Ju HC, Yoo SH. "The environmental cost of overhead power transmission lines: the case of Korea", in Proc. Journal of Environmental Planning and Management2014, Vol. 57, pp. 812–828.
- [4] Fitiwi DZ, Olmos L, Rivier M, de Cuadra F, Pérez-Arriaga IJ. "Finding a representative network losses model for large-scale transmission expansion planning with renewable energy sources", in Proc. Energy2016, Vol. 101, pp. 343–358.
- [5] Göransson L, Goop J, Unger T, Odenberger M, Johnsson F. "Linkages between demand-side management and congestion in the European electricity transmission system", in Proc. Energy2014, Vol. 69, pp. 860–872.
- [6] Navrud S, Ready RC, Magnussen K, Bergland O. "Valuing the social benefits of avoiding landscape degradation from overhead power transmission lines: Do underground cables pass the benefit-cost test?" in Proc. Landscape Research2008, Vol. 33, pp. 281–296.
- [7] Giaccaria S, Frontuto V, Dalmazzone S. "Who's afraid of power lines? Merging survey and GIS data to account for spatial heterogeneity" http://www.unito.it/unitoWAR/ShowBinary/FSRepo/D031/Allegati/WP2010Dip2_WP_Giaccaria_Frontuto_Dalmazzone.pdf/ 2010.
- [8] McNair BJ, Bennett J, Hensher DA, Rose JM. "Households' willingness to pay for overhead-to-underground conversion of electricity distribution networks", in Proc. Energy Policy2011, Vol. 39, pp. 2560–2567.
- [9] Furby L, Gregory R, Solvic P, Fischhoff B. "Electric power transmission lines, property values, and compensation", in Proc. Journal of Environmental Management1988, Vol. 27, pp. 69–83.
- [10] Ottinger RL, Wooley DR, Robinson NA, Hodas DR, Babb SE. Environmental costs of electricity. Oceana Publications, New York (1991).
- [11] Rowe RD, Lang CM, Latimer DA, Rae DA, Bernow SM, White DE. New York state environmental externalities cost, Study Oceana Publications, New York (1995).
- [12] Pasqualetti MJ. "Morality, space, and the power of wind-energy landscapes", in Proc. The Geographical Review2000, Vol. 90, pp. 381–394.
- [13] Zhu F, Zheng Y, Guo X, Wang S. "Environmental impacts and benefits of regional power grid interconnections for China", in Proc. Energy Policy2005, Vol. 33, pp. 1797–1805.
- [14] Lim KM, Lim SY, Yoo SH. "Estimating the economic value of residential electricity use in the Republic of Korea using contingent valuation", in Proc. Energy2014, Vol. 64, pp. 601–606.
- [15] Ladenburg J. "Dynamic properties of the preferences for renewable energy sources—A wind power experience-based approach", in Proc. Energy2014, Vol. 76, pp. 542–551.
- [16] Saz-Salazar S, Hernández-Sancho F, Sala-Garrido R. "The social benefits of restoring water quality in the context of the Water Framework Directive: A comparison of willingness to pay and willingness to accept", in Proc. Science of the Total Environment2009, Vol. 407, pp. 4574–4583.
- [17] Arrow K, Solow R, Portney PR, Leamer EE, Radner R, Schuman H. "Report of the NOAA panel on contingent valuation", in Proc. Federal Register1993, Vol. 58, pp. 4601–4614.
- [18] Yoo SH, Kwak SY. "Willingness to pay for green electricity in Korea", in Proc. Energy Policy2009, Vol. 37, pp. 5408–5416.
- [19] Ezebilo E. "Willingness to pay for improved residential waste management in a developing country" in Proc. International Journal of Environmental Science and Technology2013, Vol. 10, pp. 413–422.
- [20] Bateman IJ, Langford IH, Jones AP, Kerr G.N. "Bound and path effects in double and triple bounded dichotomous choice contingent valuation", in Proc. Resource and Energy Economics2001, Vol. 23, pp. 191–213.
- [21] Carson RT, Groves T. "Incentive and informational properties of preference questions", in Proc. Environmental and Resource Economics2007, Vol. 37, pp. 181–210.
- [22] Egan KJ, Corrigan JR, Dwyer DF. "Three reasons to use annual payments in contingent valuation surveys: Convergent validity, discount rates, and mental accounting", in Proc. Journal of Environmental Economics and Management2015, Vol. 72, pp. 123–136.
- [23] Kriström B. "Spike models in contingent valuation", in Proc. American Journal of Agricultural Economics1997, Vol. 79, pp. 1013–1023.
- [24] Yoo SH, Kwak SJ. "Using a spike model to deal with zero response data from double bounded dichotomous choice contingent valuation surveys", in Proc. Applied Economics Letters2002, Vol. 9, pp. 929–932.
- [25] Krinsky I, Robb AL. "On approximating the statistical properties of elasticities", in Proc. Review of Economics and Statistics1986, Vol. 68, pp. 715–719.
- [26] Brennan N, Van Rensburg TM. "Wind farm externalities and public preferences for community consultation in Ireland: A discrete choice experiments approach", in Proc. Energy Policy2016, Vol. 94, pp. 355–365.
- [27] Friedrich R, Voss A. "External costs of electricity generation", in Proc. Energy Policy1993, Vol. 21, pp. 114–122

SIMULATION BASED MULTI-CRITERIA EVALUATION OF DESIGN

SCENARIOS FOR AN INDUSTRIAL WASTE HEAT BASED MICRO DISTRICT HEATING NETWORK SUPPLYING STANDARD AND LOW-ENERGY BUILDINGS

C. Marguerite¹, R.R. Schmidt¹, N. Pardo-Garcia¹, R. Abdurafikov²

¹ AIT, Austrian Institute of Technology, Energy Department, Giefinggasse 2, 1210 Vienna, Austria

² VTT Technical Research Center of Finland Ltd, P.O. Box 1000 (Tekniikantie 4A, Espoo), FIN-02044 VTT, Finland

Keywords: *Micro-district heating, Waste heat, Heat storages, Design scenarios*

ABSTRACT

Urban waste heat released by industries, public transportation systems, data centers, sewage, etc. are available as distributed heat sources, but rarely used. These sources, as well as renewable heat sources could be exploited at less operating costs, into District Heating networks (DHN), while increasing the networks energetic and environmental performances. However, considering the difficulties implied by their varying local availability, low temperature level and production profile (not necessarily matching the demand), it may be more profitable to develop micro-DH networks combined with heat-pumps and heat storages. Considering these conditions, various designs and control strategies are possible for such micro-networks and the best energy-efficient or economical solution is not straightforward. This paper presents the results of a multi-criteria evaluation, considering environmental, energetic and economic indicators, of different design scenarios for the case of a micro-DH network in Vienna, Austria, which involves energy efficient buildings supplied by their own supply technologies (heat-pumps, solar thermal panels) and a standard building equipped with gas boilers. Four scenarios are simulated using APROS, a multifunctional dynamic simulation software and the results are evaluated based on energy, environmental and economic criteria. The aim is to assess the integration of industrial waste heat available on-site together with high and low-temperature storages, to balance the heat production and demand and a heat-pump booster, to supply the network with the required temperature level. Heat-pumps are operated at a minimum energy cost strategy. In two scenarios, an extension to the main DH of Vienna is investigated, to weigh back-up possibilities. The integration of different temperature levels and different profiles from both the production side and consumption side constitute the main challenges. Results show that the network design with only the high temperature storage instead of the combination of both storages is less polluting but more expensive. However the scenarios considering the DH-Vienna present the best performance indicators.

INTRODUCTION

The efficient waste heat recovery (excess heat from industrial processes, waste incineration and power stations) and use in district heating networks, together with other renewable energy (geothermal energy, large-scale solar thermal energy or large-scale heat pumps), is currently one of the main issues studied in order to make District Heating networks (DHN) more sustainable and to reduce their CO₂ emissions [1]-[3]. For instance the studies [4] and [5] show the potential of waste heat use in DHN, from a country perspective and from a system perspective. The conclusion is that industrial excess heat in district heating is beneficial in most cases and the incentives proposed by the European Commission to improve the efficiency of resource use should be taken to increase excess heat recovery, also reflected in national roadmaps, e.g. [6]. Concrete cases of waste heat utilization in DH networks are also being studied. For example in [7] a scheme is proposed to integrate the surplus heat of two steel plants into a large-scale district heating network. [8] presents a new system which recovers waste heat of exhausted steam from a steam turbine to power a CHP based DHN. In [9], a comparison between systems integrating both industrial waste heat and fossil-fuel heat shows that the heat sources are complementary. The base load of the DH system is provided by the industrial waste heat, while the fossil-fuel heat acts as the peak back-up solution.

Despite of its high potential, in our industrialized societies, waste heat is rarely used, because it presents several challenging characteristics [10]. Indeed, the availability profile as well as the temperature levels of the waste heat, can be predictable or completely random depending on the type of waste heat producer and doesn't always meet the heat demand requirements. These issues make it necessary to integrate other components together with the waste heat source into the DH system, such as heat storages, heat pump boosters, back-up solutions, in order to always satisfy the heat demand.

There are as many different ways to integrate components into a sustainable DH system as various corresponding control strategies and business models. Therefore the best solution is not always

straightforward, leading to the need of simulation tools to select the optimal design according to specific criteria. Indeed the integration of various sources is difficult to handle, since standard tools and operation strategies don't consider low-temperature and fluctuating sources with a significant share. These issues are tackled in the CITYOPT project [11] and illustrated in particular with the Vienna demonstration case, which consists of an industrial fed micro-DH network including existing and new buildings together with a high-temperature and low-temperature storages and renewable energy supply.

This paper is structured as follows. First, the CITYOPT project is briefly presented and the Vienna case study, one of the case studies addressed within that project, is described. The methodology used for the modelling of this case together with the scenarios simulated is described afterwards. Eventually, the results of the different simulated scenarios are presented and discussed.

BACKGROUND

Within the FP7 framework, the project CITYOPT, a collaborative European project, aims at developing a set of applications and guidelines to support the planning, the design (CITYOPT Planning tool) and the operation (CITYOPT Operational tool) of sustainable energy solutions in cities, based on social, energy, environmental and economic criteria. In particular, the CITYOPT Planning tool proposes a web-platform for simulation, optimization and analysis of urban energy systems. The simulations are performed by an external software coupled to the CITYOPT Planning tool, which is designed to be able to interact with any energy simulation engine and handle the simulation of a huge amount of scenarios. The simulation results are used further on within the tool in an optimization algorithm, in order to determine the best design configuration that optimizes the specific decision criteria. The structure of the CITYOPT tool is illustrated in the Figure 1.

Within the project timeframe, CITYOPT Planning tool was coupled with the APROS simulation software (a simulation energy software allows to model complex urban energy system in a flexible way [12]) and tested on two study cases in Helsinki (Finland) and in Vienna (Austria) using a holistic approach to integrate energy dynamics of local grids, buildings and consumption behavior and patterns, energy storages, and local energy production using renewables.

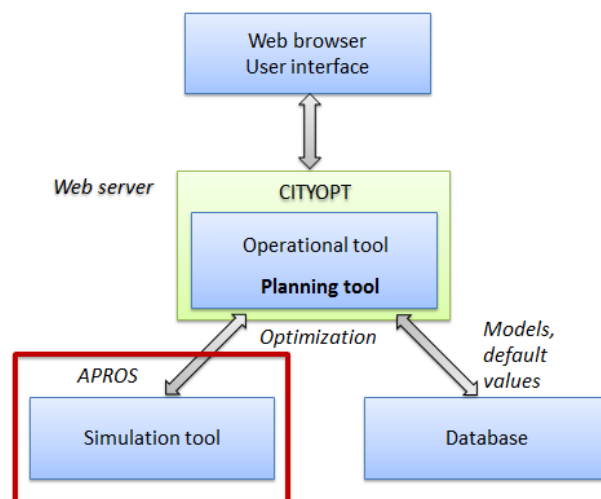


Figure 1. Structure of the CITYOPT tool.

The Vienna study case, also studied in [13], [14] is based on three office buildings, in the 21st district of Vienna: a standard building, TECHbase (Tb) and two energy efficient buildings, ENERGYbase (Eb) and FUTUREbase (Fb). Fb is under planning but not built yet, it will be similar to Eb. They are located very close to Rail Tec Arsenal GmbH (RTA), a facility using one of European largest climatic wind tunnels for testing various kinds of transportation systems and equipment. During these tests large amounts of heat are rejected from the chillers to the air via cooling towers, (3394MWh were rejected in 2014).

The current situation of the different buildings is summed up in Table . A gas boiler provides heat to Tb. Two ground source heat pumps and solar thermal panels provide heat to Eb. Fb, still in the planning phase, will be designed, as Eb for a maximal use of the internal gains from occupants and equipment in order to almost eliminate heating demand. In this study, Fb is considered to have the same heat demand as Eb.

Table 1. Characteristics of the main buildings of the Vienna study case.

	Fb	Eb	Tb
Own energy systems	-	Heat pumps Solar panels	gas boilers
Characteristics	10.83 kWh/m ² /a	10.83 kWh/m ² /a	71.93 kWh/m ² /a
Temperature levels	45-35°C	45-35°C	80-60°C
Yearly energy use	233 MWh	233 MWh	597MWh

The objective of test case is to take advantage of the waste heat available to provide heat to the three buildings considered in order to reduce their fossil fuels consumption as well as the CO₂ emissions associated. The idea is to connect all the components into a micro-DHN. As the heat rejected by RTA is only dependent on the experiments taking place in the facility, it is not really possible to forecast neither the amount of waste heat available nor its profile nor its temperature level. To deal with that characteristic of the waste heat source, two storages are included in the micro-DH. A water tank storage of 100m³ is used as a high-temperatures storage (HTS), for temperatures from 35°C to 100°C and another storage, made of 9 borehole heat exchangers, is used as a low-temperature storage (LTS) for temperatures from 20°C to 35°C, for a water equivalent capacity of 2000m³. A booster heat pump is coupled to the LTS to heat-up the outlet temperatures, to the required temperature level of the buildings. In addition to the waste heat source, the Eb and Tb buildings are prosumers, which means that they can take the heat from the grid, but they can also feed the grid with the heat they produce by their own energy systems.

OBJECTIVE

This case study of Vienna is particularly interesting, since it can bring a lot of knowledge and concepts for future developments of smart and micro district heating networks. Indeed, it addresses current and future challenges regarding DHN, such as how to integrate in a hydraulically connected system: renewable sources (heat pumps, solar collectors), industrial waste heat (fluctuating heat source, with different temperature levels), thermal storages (high and low-temperatures) in order to satisfy the heat demand of low energy buildings and standard prosumer buildings, with respect to environmental, energetic and economic objectives, such as reducing CO₂ emissions, primary energy use and costs of the heat supply. The optimum dimensioning and design of the system components (topology of the distribution network according to multi-temperature levels and pressure levels, hydraulics of the network and control strategy) require particular attention and the use specific tools.

Beside the network design, the control strategy is also of high importance in order to allow an optimum operation of the network, addressing at each time step issues such as, is it more profitable to store heat or to use the heat from the storages or to allow the prosumers to feed the network? How much heat and at which temperature level should be used? The energy supplied must of course consider the renewable and waste heat availability and temperatures profiles and the energy (electricity and gas) prices.

Additionally, the complexity of this system brings the need for the development of new business models which take into account local price regulations, customers' needs, the prosumers integration, network operators and industrial profitability [15].

Moreover, this micro-DH can be used as an example that could be scaled up or adjusted to many cases of networks that have to be refurbished or extended. These are some questions that arise with this specific study case that can help for similar case studies.

METHODOLOGY

Four scenarios (1A, 1B, 2A, 2B) and two status quo scenarios (1, 2) are selected for the Vienna study case. They are modelled and their operation is simulated through APROS, in order to determine the best scenario based on three evaluation criteria: the primary energy consumption, the CO₂ emissions and the operating costs.

The different scenarios are described in Table 2 and illustrated in Figure 2. All the scenarios are operated with a minimum cost-based strategy. The scenario 1 corresponds to the status quo of the scenarios 1A and 1B and the scenario 2 corresponds to the status quo of the scenarios 2A and 2B. For the status quo scenarios, the each building has its own heat source and Fb and Ab have a heat pump (in the other scenarios they do not have any heating system). As the Vienna study case is quite specific, the two last scenarios (2A and 2B) make it more general by adding a connection to the existing city-wide Vienna DH network and by adding another building (Ab), similar to the low-energy buildings Eb and Fb, to assess the performances of the network through a realistic scenario and evaluate the case of an extension of the main DH grid.

Table 2. Description of the scenarios assessed for the Vienna study case (Tb = Techbase, Eb = Energybase, Fb = Futurebase, RTA = industrial waste heat producer, HTS = High Temperature Storage, LTS = Low Temperature Storages, DH = Vienna main DHN).

	Tb	Eb Fb	Ab	RTA	HTS	LTS	DH
1	X	X					
1A	X	X		X	X		
1B	X	X		X	X	X	
2	X	X	X				
2A	X	X	X	X	X		X
2B	X	X	X	X	X	X	X

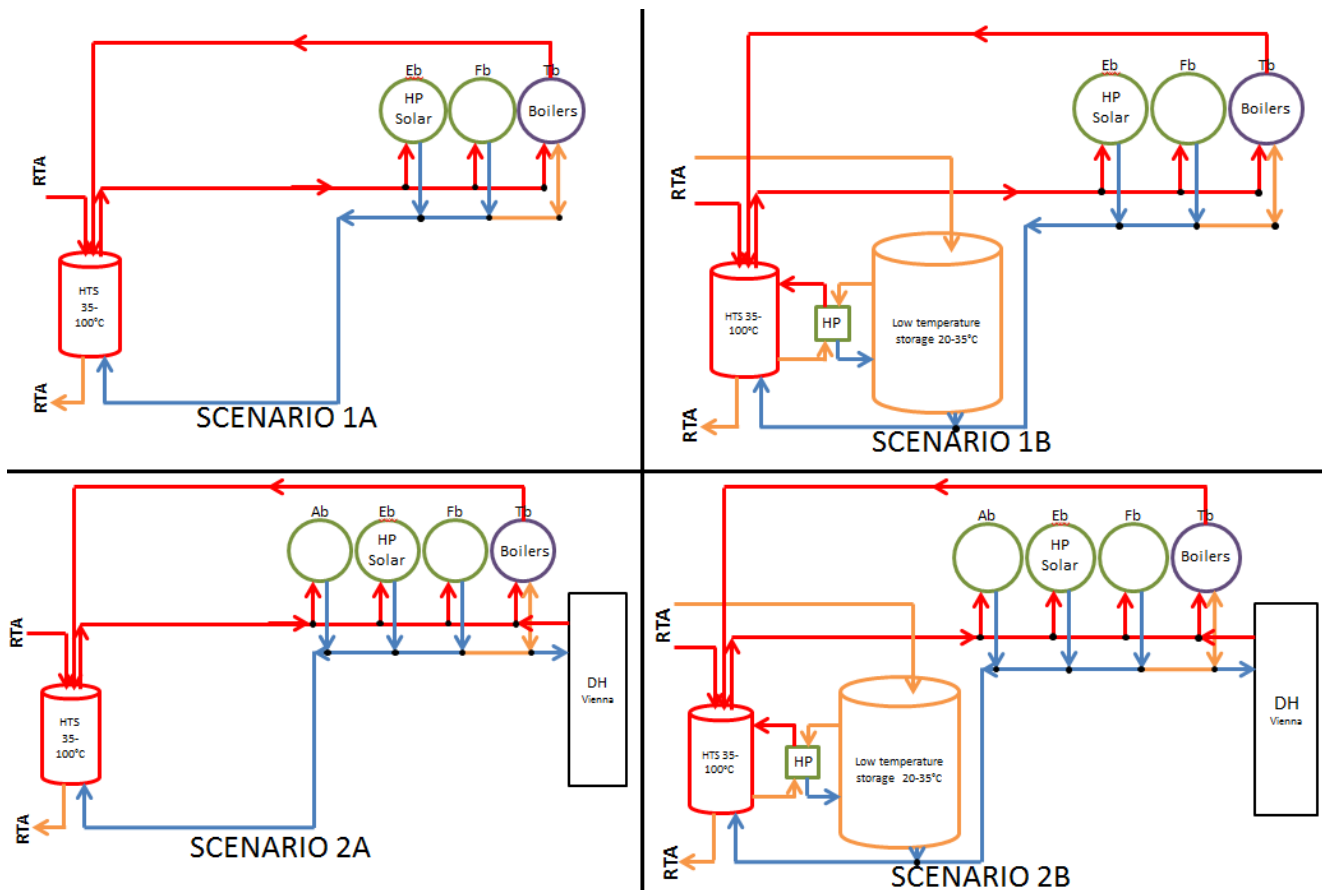


Figure 2. Diagrams of the scenarios 1A, 1B, 2A and 2B assessed for the Vienna study case.

APROS is a multifunctional software for modelling and dynamic simulation of processes and different power plants. It is used to model the different components considered in the Vienna case study and to run the scenarios.

For the Vienna study case, the buildings and the RTA waste heat sources are modelled as time series. The buildings consumption profiles are simulation results from TRNSYS [15], another energy tool, where monitoring data of the energy consumption are used to calibrate the simulation. The waste heat profile of RTA is based on monitored data of 2014.

The other components such as solar panels, heat pumps, gas boilers, low-temperatures heat storage are modelled and calibrated in APROS. To calibrate those models, either manufacturer information (solar panels, heat pumps, gas boilers) together with literature or monitoring data from 2014 (temperatures and fluctuations of the industrial waste heat source) are used. The LTS is validated and calibrated based on the results of energy software FEFLOW [16].

At each time step, the APROS model tries to satisfy the buildings heating needs using the cheapest heat supply option available. It is important to note that the waste heat goes to either to the HTS or to the LTS according to the temperatures rejected. However if the HTS is

fully loaded, the heat rejected from RTA at high temperatures, if any, goes also to the LTS. When both storages are full, the heat rejected from RTA cannot be recovered anymore and is released in the atmosphere.

RESULTS

The simulation results are analyzed via yearly energy balances, which represent the share of each heat source among the total heat production of the all system, presented in Figure 3. Some specific indicators are calculated and shown in Figure 4. The indicators were calculated for each scenario simulated, with the input parameters of Table 3. For these calculations, the MWh of demand do not include the heat losses.

Due to the particularity of the chosen scenarios (scenarios 2A and 2B involve an additional building and a connection to the main DH of Vienna), it is more relevant to compare the scenarios two by two: scenarios 1 to 1A at 1B at first, to evaluate the impact on the network performances of the LTS and then scenarios 2 to 2A and 2B to assess the influence of the connection to the DH of Vienna as well as the interest of the LTS in case of an increase of the heat demand.

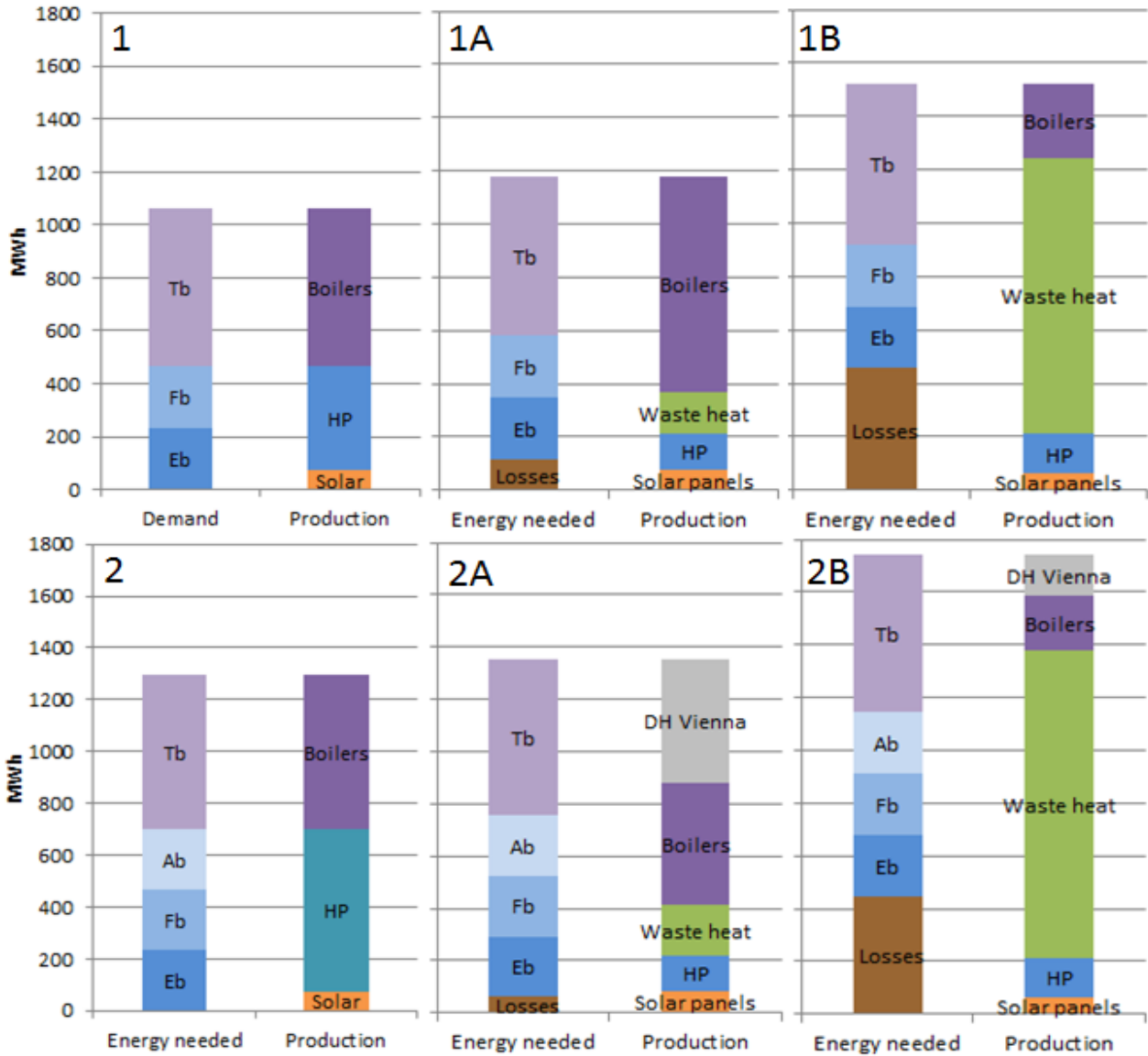


Figure 3. Diagram Energy balances corresponding to the scenarios simulated.

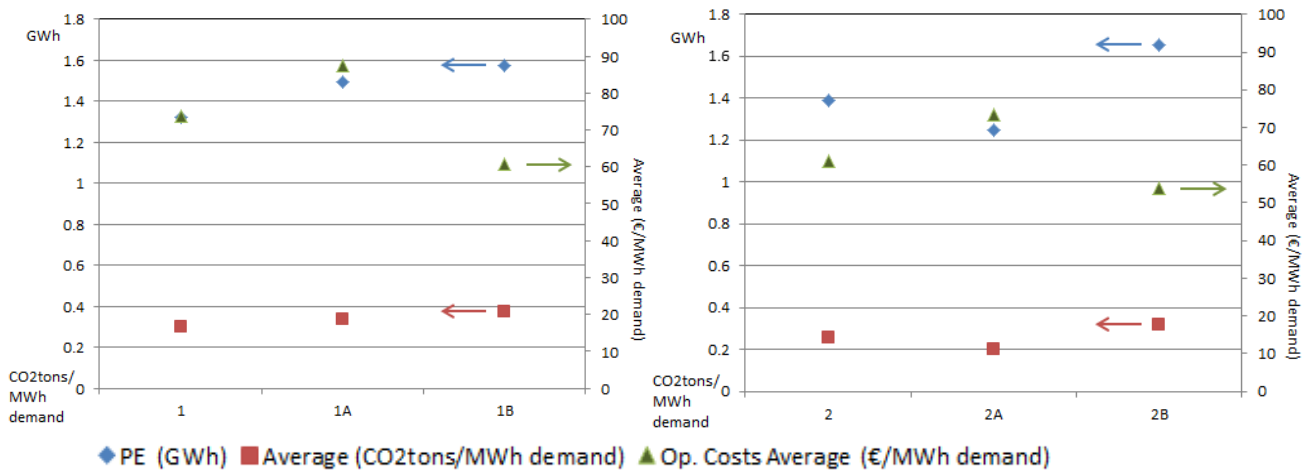


Figure 4. Indicators calculated for the scenarios and the corresponding status quo simulated: Primary Energy consumed, average CO₂ emissions and average operating costs.

Table 3: Input parameters used for the calculation of indicators [17].

	Primary Energy Factor	Fuel costs (€/kWh)	CO2 emission (tonsCO2/MWh)
Gas	1.17	0.075	0.236
Electricity	1.91	0.025	0.276
DH Vienna	0.33	0.06	0.02

An important thing to notice is that in all the scenarios simulated, the solar collectors and the heat pumps of Eb are responsible for almost the same amount of heat in the total production (5% to 7% for the solar and 11% to 13% for the heat pumps).

In the scenario 1A, the gas boilers of Tb contribute for more than half of the heat production (69%), while the solar panels produced 7% of the heat. The heat pumps together with the waste heat share equally the rest of the heat production (12%). In this scenario 1A, the waste heat is does not contribute to a major part because the heat with sufficient temperatures is not necessarily available when the buildings need it. In the scenario 1B, where only the LTS is added compared to the scenario 1A, the share of the heat production is rather different. The gas boilers of Tb produce less than 25% of the total heat produced, while the waste heat contributes for 58% of the production. The importance of the waste heat in this scenario can be explained by the availability profile of the different temperature levels of the heat rejected and the control strategy.

In the scenario 2A, where a connection to the main DH of Vienna is involved, both the gas boilers of Tb and the Vienna network contribute up to approximately 70% of the total heat produced. Moreover, as there is no LTS, the waste heat is used in the same way as in the scenario 1A. In the scenario 2B, where the LTS is considered, it is used like in the scenario 1B and produces also 58% of the total heat. However, due to the minimum cost-based strategy, (it is less expensive to use the LTS or the heat from the Vienna network than to run the gas boilers), the production of the gas boilers of Tb is reduced to 16% of the total heat production.

In the energy balances, three kinds of losses are accounted for: the losses of the HTS, the losses of the LTS and the other losses (distribution losses, losses happening at the heat exchanger and the valves for example). The lowest losses concern the HTS (around 1% of the total heat production) for all the scenarios simulated. The other losses represent between 2% (scenario 2A) and 7% (scenario 1A) of the total heat production, which is a common losses rate in DH

networks. The highest losses come obviously from the LTS, with 20% to 22% in the scenario 2B and scenario 1B, because of the storage intrinsic design (large exchange area of the borehole heat exchangers).

DISCUSSION

On the one hand, when the DH of Vienna is involved, the scenario 2A has the best indicator values concerning the primary energy consumption and CO2 emissions (indicators which are indirectly linked). This is due to the high share of heat fed into the network by the DH of Vienna, which is considered to be of rather good quality considering the high share of gas CHP and waste incineration. The scenario 2B presents the lowest price per MWh of demand. On the other hand, when the connection to the main DH of Vienna is not considered (scenario 1A and scenario 1B), the scenario 1A emits less CO2 and needs less primary energy than the scenario 1B because of the very high contribution of the LTS, which uses electricity to run a heat pump to heat up the low temperatures to the required supply level for the buildings. The scenario 1B has a better economic indicator than the scenario 1A, because the gas boilers of Tb are used 45% less. The scenario 1 (status quo scenario for scenarios 1A and 1B) has better indicators than the scenario 1A and less PE use and CO2 emissions than scenario 1B, due to a fewer share of the gas boilers in the heat production. In the same way, the scenario 2 (status quo scenario for scenarios 2A and 2B), needs less PE and emits less CO2 than the scenario 2B, again due to the gas boilers heat production, and is less expensive than scenario 1A, because of the contribution of the DH of Vienna which is in a yearly average cheaper than gas and electricity.

A simple economic analysis is carried out to roughly estimate the possible payback time of each scenario. Interest rates for the investment, subsidies, energy prices scenarios and cost benefits due to synergies for the construction of the LTS and the groundwork of Fb have not been considered, since this would require a detailed design of the system and as a consequence would go beyond the scope of work. A sensitivity analysis has been performed only for the most unsecure parameter: the investment cost of the LTS.

The payback time T of the investment for the additional equipment in scenarios 1A, 1B, 2A and 2B is calculated with Equation (1), where INV_X is the investment costs for the scenario X , $C_{statusquo1,2}$ and C_X are the operating costs for the status quo 1, 2 and the scenario X (X stands for 1A, 1B, 2A or 2B). $C_{statusquo1}$ and $C_{statusquo2}$ have respectively the values of 78k€ and 79k€.

$$T = INV_X / (C_{status quo 1} - C_X) \quad (1)$$

Table 4: Input parameters used for the economic evaluation, estimated from [18]- [20].

	Investment costs
HTS	500€/m ³
LTS	
low value	125€/m ³ water equivalent
high value	275€/m ³ water equivalent
Heat pump (160-250kW)	300€/kWth
Other costs (pipes, heat exchangers, pumps, planning etc.)	30% of the total investment costs for storages and heat pumps)
Connection pipes to DH of Vienna	300€/m

Since in the scenarios 1A, 1B, 2A and 2B, Fb and Ab are connected to the micro grid and don't have their own heating system (as it would be required in the scenarios 1 and 2), the investment costs for scenarios 1A, 1B, 2A and 2B are reduced by the investment costs for the individual heating system in order to have a fair comparison to the scenarios 1 and 2 respectively (it is assumed, that Fb and Ab would have 2 x 160 kW heat pump each if supplied individually). The distance between the current DH network of Vienna and the case study is estimated to 300 m. Further input parameters used for the calculations and the results are presented in Table 4 and Table 5

Table 5: Payback time for each scenario

	1A	1B	2A	2B
Operational costs (k€)	92.8	64.7	95.3	69.8
Low investment costs for LTS (k€)	65.0	295.5	246.6	477.0
Payback time (years)	x	20.9	x	46.8
High investment costs for LTS (k€)		685		867
Payback time T (years)		48.6		85.0

An important point to note from this economic analysis is that the scenarios 1A and 2A are never beneficiary compared to their status quo scenarios, these two scenarios will not pay off the investment costs. Indeed the operating costs of the status quo scenario 1 are lower than the operating costs of the scenarios 1A and 1B, due to the high share of the gas boiler in the heat production of these last ones. The scenarios 1B and

2B, which have wide range of possible investment costs (from 295k€ to 685k€ and from 477k€ to 867k€) have a long payback time. Scenario 1B, which includes three buildings and the two storages, will pay off after 21 to 49 years, whereas the scenario 2B, which includes the connection to the DH of Vienna (additionally to the scenario 1B), has a payback time period included between 47 and 85 years.

CONCLUSION AND FUTURE WORK

In this paper, a simulation based analyses of a building cluster including a possible micro district heating network integrating heat pumps, solar energy and waste heat from a nearby industrial facility has been described. Following conclusion can be drawn:

1. Applying a (low cost) heat storage only for utilizing available waste heat instead of installing individual heating systems is not economically feasible if its capacity is limited. Existing gas boilers in the micro network will be used for heating the buildings when the storage is empty, resulting in very high operation costs.
2. Adding a long term storage enables to use a high share of waste heat, although generating high heat losses. Since energy prices for the waste heat are assumed to be zero, the operational costs are lower than in the reference scenario.
3. One main difficulty for assessing the economic feasibility is the lack of reliable investment costs, especially for the ground storage. This uncertainty results in anticipated payback times between 21 to 49 years and 47 and 85 years respectively, where the lowest value is somewhat realistic for DH network operators.
4. In general, such micro networks are more likely to be economically feasible for new build areas or major retrofitting projects, where the heating and storage systems can be better adjusted, e.g. the higher investment costs for the storages can be (partly) balanced by reducing the need for individual heating systems. However, existing heating systems can be used as back-up and to boost temperature level.

Although the replicability of the case study in Vienna is limited due to its very individual characteristics, the above lessons learned are meaningful, since they embodies the main challenges of future DH systems, such as an energy supply with fluctuating characteristics, and/or low temperature levels and/or decentralised location as well as the integration of old and new buildings.

Future work will include the variation of the design of the ground storage and the application of the CITYOPT tool for overall optimizations.

ACKNOWLEDGEMENT

CITYOPT is a collaborative project supported by the European Commission through the Seventh Framework Programme (FP7).

REFERENCES

- [1] H. Lund, B. Moller, B.V. Mathiesen and A. Dyrelund, "The role of district heating in future renewable energy systems", *Energy*, 2010, Vol. 35, pp. 1381–1390.
- [2] H. Lund, S. Werner, R. Wiltshire, S. Svendsen, J.E. Thorsen, F. Hvelplund and B.V. Mathisen, "4th Generation District Heating (4GDH) Integrating smart thermal grids into future sustainable energy systems", *Energy*, 2014, Vol. 68, pp. 1-11.
- [3] R.R. Schmidt, O. Pol and J. Page, "Smart Cities: Challenges and Opportunities for Thermal Networks", in *Proc. 13th International Symposium on District Heating and Cooling 2012*.
- [4] S.J.G. Cooper, G.P. Hammond and J. B. Norman "Potential for use of heat rejected from industry in district heating networks, GB perspective", *Journal of the Energy Institute*, 2016, Vol. 89, Issue 1, pp 57-69.
- [5] J. Ivner and S. Broberg Viklund, "Effect of the use of industrial excess heat in district heating on greenhouse gas emissions: A systems perspective", *Resources, Conservation and Recycling*, 2015, Vol. 100, pp. 81-87.
- [6] R.R. Schmidt, R. Tichler, C. Amann, I. Schindler: „F&E-Fahrplan Fernwärme und Fernkälte, Innovationen aus Österreich“, Wien, Oktober 2015
- [7] Y. Li, J. Xia, H. Fang, Y. Su and Y. Jiang, "Case study on industrial surplus heat of steel plants for district heating in Northern China", *Energy*, 2016, Vol. 102, pp. 397-415.
- [8] F. Sun, L. Fu, J. Sun and S. Zhang, "A new waste heat district heating system with combined heat and power (CHP) based on ejector heat exchangers and absorption heat pumps", *Energy*, 2014, Vol. 69, pp. 516-524.
- [9] H. Fang, J. Xia and Y. Jiang, "Key issues and solutions in a district heating system using low-grade industrial waste heat", *Energy*, 2015, Vol. 86, pp. 589-602.
- [10] U. Persson, S. Werner: "District heating in sequential energy supply", *Applied Energy* 95 (2012) pp. 123–131
- [11] CITYOPT project website: <http://www.cityopt.eu>
- [12] APROS software website <http://www.apros.fi/en/>
- [13] C. Marguerite, R.R. Schmidt and N. Pardo-Garcia, "Concept development of an industrial waste heat based micro DH network", in *Proc. CISBAT 2015*, pp. 597-602.
- [14] N. Pardo, F. Nadler, C. Marguerite, B. Kelly, "CITYOPT – Holistic Simulation and Optimisation of Energy in Smart Cities – Vienna Study Case", in *Proc. ICERE 2015*.
- [15] TRNSYS software website <http://www.trnsys.com/>
- [16] FEFLOW software website www.mikepoweredbydhi.com/products/feflow
- [17] OIB Richtlinie 6, Energieeinsparung und Wärmeschutz März 2015, Online. http://www.oib.or.at/sites/default/files/richtlinie_6_2_6.03.15.pdf
- [18] M. Mangold, et al (2007). Solare Nahwärme und Langzeit-Wärmespeicher. Forschungsbericht zum BMU Vorhaben 0329607L.
- [19] Gössl, M. et al (2013). Beitrag von Fernwärme, Fernkälte und Erdgas zu energie- und umweltpolitischen Zielen. Umweltbundesamt 2013.
- [20] Bøhm et al., (2008), District heating distribution in areas with low heat demand density, IEA R&D Programme on "District Heating and Cooling, including the integration of CHP".

ECONOMIC OPTIMIZATION OF A COMBINED HEAT AND POWER PLANT: HEAT VS ELECTRICITY

F. Marty¹, S. Serra¹, S. Sochard¹, J.M. Reneaume¹

¹Laboratoire de Thermique Energétique et Procédés (LaTEP-UPPA), Rue Jules Ferry, Pau Cedex, 64075, France

Keywords: Economic Optimization, Cogeneration, MINLP, GAMS

ABSTRACT

This contribution presents the economical optimization of the parallel repartition between electric and heat production for geothermal application. The 350 m³/h flow of geothermal fluid, assimilated to liquid water at 185 °C, is then separated in two streams. Its reinjection temperature is fixed at 70 °C. An Organic Rankine Cycle (ORC) system is used to convert a part of geothermal energy into electricity. The refrigerant chosen is the R245fa. The different components of the ORC are sized in order to calculate the installation cost that depends on one characteristic dimension of each item (exchange surface for heat exchangers and power for the turbine and pumps). The operating cost is proportional to the installation cost. In this contribution, since we do not consider the detailed structural optimization of the District Heating Network (DHN), its investment cost is proportional to the supplied heat. The selling price of the electrical net power is a function of the recovered heat by the network. A Mixed Integer Non-Linear Programming (MINLP) optimization is performed using the GAMS[®] software. The problem is solved in order to determine the maximal profit of the global system. In this problem, the main optimization variables are the flow, temperature and pressure of refrigerant in ORC, the size and cost of equipment, the repartition between heat and electricity, and the structure of the DHN. Results show that it is preferable to produce electricity alone but this is dependent on the choice of the price of sale of heat by the owner. The sell price from which it is more profitable to produce and to sell the heat is determined for each case. The optimization for each case shows that it is not easy to predict the final results and it justifies the use of optimization.

1. INTRODUCTION

A consortium of ten partners, led by “FONROCHE Géothermie”, works on the FONGEOSEC project, an “Investissement d’Avenir” organized by the French Agency for Environment and Energy (ADEME). The aim of this project is to design and create an innovative demonstrator of a high-energy geothermal power plant. The geothermal energy will be used to produce electricity and heat. Among other tasks, this project aims to develop a support tool for the optimal design of a District Heating Network (DHN) and an Organic

Rankine Cycle (ORC) system, both supplied by the geothermal well.

Within the last ten years, many studies [1]–[3] have been dedicated to the choice of the organic fluid in the ORC. In the aim to protect the turbine, it is recommended to use a dry fluid (fluid with positive slope for the vapour saturation curve in *T-s* diagram). To help the research of the working fluid, S. Quoilin [4] proposes some options:

- Evaluate the cycle performance (efficiency, electrical production or economic analysis) for selected fluids in working conditions.
- Look the dangerousness of the fluid and its environmental impact.
- Verify that the fluid is easily available for purchase and inexpensive.

Z. Shengjun [2] observes that the best fluid is not necessarily the same according to the criterion chosen for the cycle performance. D. Wang [5] proposes some fluids usable per temperature range. The fluid chosen in this contribution is the R-245fa refrigerant.

For the optimization of the cycle, two approaches are confronted in literature: energetic [6], [7] or economic optimization. In case of comparison of the two approaches [8]–[11], the optimums obtained are different.

Studies for Combined Heat and Power (CHP) systems have been recently carried out for economic optimization and it permits to compare different algorithms [12]–[14]. H.R. Sadeghian [15] has also studied the environmental emissions and K. Sartor [16] has developed, in addition, the heat losses for the DHN.

In this contribution, only economic optimization is carried out. Heat for the DHN is recovered in parallel to the ORC system. The optimization of the MINLP (Mixed Integer NonLinear Programming) problem, described in the following section, is performed using GAMS[®] tool.

2. OPTIMIZATION MODEL

2.1. Description of the ORC system

In the ORC system, the fluid flow is split up in four steps. At outlet of the evaporator (high pressure),

temperature is the highest. The required heat for this evaporation is recovered from the geothermal source. Next, the turbine enables electricity production by lowering fluid pressure to its low level. The fluid is then condensed and passes through the pump that permits to transmit the fluid from low pressure zone to high pressure zone. At last, the fluid returns into the evaporator.

A sub-cooled fluid (respectively super-heated) enters the pump (respectively the turbine) to avoid the presence of vapour phase (respectively liquid phase) and preserve this component.

An ORC system is represented in **Figure 1**.

2.2. Parameters

Parameters values are represented in **Table 1**.

2.3. Variables

In this contribution, the main optimization variables are the flow, temperature and pressure of refrigerant in ORC, the size and cost of equipment and the repartition between heat and electricity. These variables are represented in **Figure 1**.

In addition, two binary variables are used. Ex_i stands for the connection to the network of the i th customer. If Ex_i is equal to 1, the customer is connected, and not if it is equal to 0.

Table 1: list of parameters

Parameters	Values
Geothermal source flow	350 m^3/h
Geothermal source temperature	185 $^{\circ}C$
Reinjection temperature	70 $^{\circ}C$
Minimal pinch temperature in evaporator	10 $^{\circ}C$
Minimal pinch temperature in condenser	5 $^{\circ}C$
Inlet cooling water temperature	20 $^{\circ}C$
Outlet cooling water temperature	30 $^{\circ}C$
Isentropic efficiency in turbine	83 %
Isentropic efficiency in pump	75 %
Electric generator efficiency	95.5 %
Super-heating of vapour	5 $^{\circ}C$
Sub-cooling of liquid	2 $^{\circ}C$
DHN temperature	65 - 95 $^{\circ}C$

$Ex_{path_{ij}}$ stands for the existence or not of the path between i and j . These two variables are used in **Figure 2** for an example with one producer and three customers.

These variables are involved in the different equations described below.

2.4. Equations and constraints

2.4.1. Model for the ORC system

The model for the ORC system described in section 2.1. is stated as follows in equations (1) to (11).

Figure 2. Schematic representation for the existence

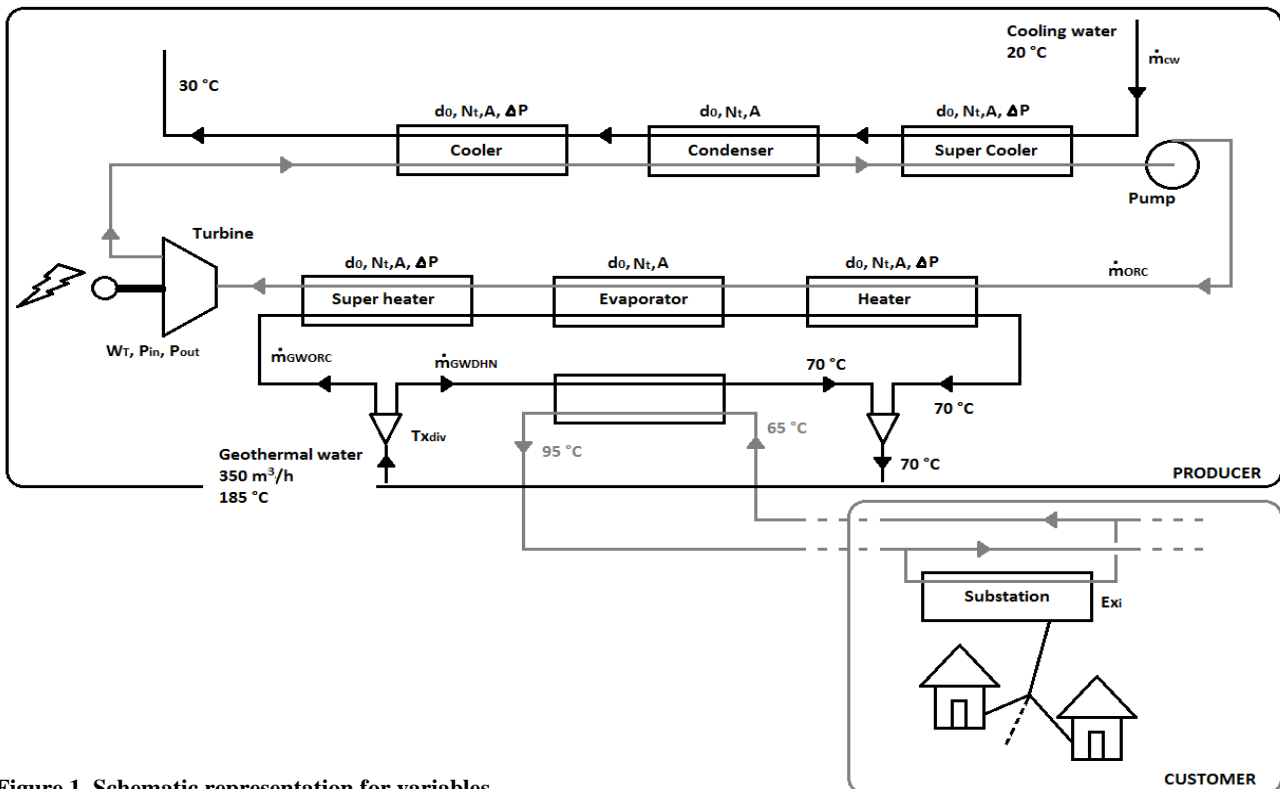
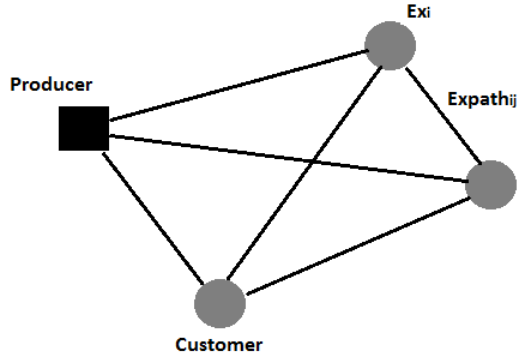


Figure 1. Schematic representation for variables.



of the path.

$$P_{out} = P_{in} - \Delta P \quad (1)$$

ΔP is the pressure drop of the working fluid.

For each component of the ORC system,

$$h_{in} = h(T_{in}, P_{in}) \quad (2)$$

$$h_{out} = h(T_{out}, P_{out}) \quad (3)$$

The change of state in the evaporator and the condenser are described by (4)-(6).

$$T_{out} = T_{in} - T \quad (4)$$

$$P_{out} = P_{in} = P \quad (5)$$

$$f^l(T, P) = f^v(T, P) \quad (6)$$

f^l and f^v are respectively the fugacity of the fluid in liquid phase and vapour phase.

The equation (5) leads to that pressure losses appearing in (1) are neglected in exchangers with change of state. An isentropic evolution is used for the turbine and pump modelling.

$$h_{out}^t = h(T_{out}^t, P_{out}^t) \quad (7)$$

$$s(T_{in}^t, P_{in}^t) = s(T_{out}^t, P_{out}^t) \quad (8)$$

The power lost by the fluid at the turbine and gained at the pump is calculated as follows.

$$W_T = \dot{m}_F \cdot (h_{out,T}^t - h_{in,T}^t) \cdot \eta_T^t \quad (9)$$

$$W_P = \dot{m}_F \cdot (h_{out,P}^t - h_{in,P}^t) / \eta_P^t \quad (10)$$

For exchangers, the exchanged heat is calculated by (11).

$$Q = \dot{m}_F \cdot (h_{out}^t - h_{in}^t) \quad (11)$$

In these equations, h , s and f are calculated using Peng-Robinson EOS (equation of state) [17]. Details of calculation are not represented here.

2.4.2. Exchanger calculation

In this study, Shell-and-tube design is chosen for the heat exchangers. The organic fluid circulates in shell side and water in tubes side.

Equations for heat transfer area calculation of exchangers are described as follows.

Heat transfer rate is calculated by (12).

$$Q = F \cdot U \cdot A \cdot \Delta T_{\ln} \quad (12)$$

Where U is the overall heat transfer coefficient. A is the heat transfer area. ΔT_{\ln} is the logarithmic mean temperature difference and F the correction factor.

Eq. (13)-(15) describe the usual calculation for ΔT_{\ln} . In order to avoid numerical problem, the Chen approximation [18] is used (15).

$$\Delta T_1 = T_{c,in} - T_{f,out} \quad (13)$$

$$\Delta T_2 = T_{c,out} - T_{f,in} \quad (14)$$

$$\Delta T_{\ln} = \left[\Delta T_1 \cdot \Delta T_2 \cdot \frac{\Delta T_1 + \Delta T_2}{2} \right]^{1/3} \quad (15)$$

ΔT_1 and ΔT_2 are the temperature difference on both sides of the counter-flow exchanger.

The heat transfer area is described by (16).

$$A = \pi \cdot d_o \cdot L \cdot N_t \cdot N_{\text{pass}} \quad (16)$$

Where d_o is the outer diameter of tube. In this study, d_o could be a value between $6.35e^{-3}$ and $6.35e^{-2}$ m. L is the tube length. N_t and N_{pass} are respectively the number of tubes and the number of passes in tube side. The number of tubes is computed by (17).

$$N_t = \frac{4 \cdot \dot{m}_W}{\pi \cdot d_o^2 \cdot \rho_W \cdot v} \quad (17)$$

Where \dot{m}_W is the water mass flow (water in tubes). ρ_W is the water density and v the velocity inside tube.

The F factor is calculated by (18) to (22) described by Bowman et al. [19].

$$R = \frac{T_{in}^s - T_{out}^s}{T_{out}^t - T_{in}^t} \quad (18)$$

$$P = \frac{T_{out}^t - T_{in}^t}{T_{in}^s - T_{in}^t} \quad (19)$$

$$\alpha = \left[\frac{1 - R \cdot P}{1 - P} \right]^{1/N_t} \quad (20)$$

$$S = \frac{\alpha - 1}{\alpha - R} \quad (21)$$

$$F = \frac{\sqrt{R^2 + 1}}{R - 1} \cdot \frac{\ln\left(\frac{1 - S}{1 - R \cdot S}\right)}{\ln\left[\frac{2 - S \cdot (R + 1 - \sqrt{R^2 + 1})}{2 - S \cdot (R + 1 + \sqrt{R^2 + 1})}\right]} \quad (22)$$

Where N_s is the number of passes in shell side. The overall heat transfer coefficient, relative to the outer surface, is defined by (23).

$$\frac{1}{U} = \frac{d_o}{h_i \cdot d_i} + \frac{d_o \cdot \ln(d_o/d_i)}{2 \cdot k} + \frac{1}{h_o} + \frac{R_i \cdot d_o}{d_i} + R_o \quad (23)$$

Where k is the thermal conductivity of stainless steel.

R_i and R_o are fouling resistances inside and outside tubes. The values of these data are specified in **Table 2**. d_i is function of d_o and it is calculated by (24).

$$d_i = d_o - 2 \cdot e \quad (24)$$

$$e = 0.047 \cdot d_o + 0.0007 \quad (25)$$

e is the thickness estimated by data presented in TEMA standards [20].

Table 2: data for exchangers

Parameters	Values
Thermal conductivity	16.3 W/m/h
Fouling resistance [20]	$1.76e^{-4} \text{ m}^2 \cdot K/W$

h_i and h_o stand for heat transfer coefficient inside and outside tubes. The Gnielinski correlation [21] is used to determine the heat transfer coefficient inside tubes.

$$h_i = \frac{Nu_i \cdot k_i}{d_i} \quad (26)$$

$$Nu_i = \frac{(f/8) \cdot (Re_i - 1000) \cdot Pr_i}{1 + 12.7 \cdot \sqrt{f/8} \cdot (Pr_i^{1/4} - 1)} \quad (27)$$

Where Nu_i , Re_i and Pr_i are respectively the Nusselt, Reynolds and Prandtl numbers. The friction factor f_i is predicted by the Petukhov correlation [21].

$$f_i = [0.79 \cdot \ln(Re_i) - 1.64]^{-2} \quad (28)$$

This method to predict the heat transfer coefficient is valid for $0.5 \leq Pr_i \leq 2000$ and $2300 \leq Re_i \leq 5 \cdot 10^5$

The total pressure drop inside tubes ΔP_i is calculated by (29) and should be inferior to 0.5 bar.

$$\Delta P_i = \left(f_i \cdot \frac{L}{d_i} + 4\right) \cdot \frac{\rho_m \cdot v^2}{2} \cdot N_{\text{tubes}} \quad (29)$$

For the outside tubes (shell side) coefficient, the McAdams correlation is used.

$$Nu_o = 0.36 \cdot Re_o^{0.22} \cdot Pr_o^{1/3} \cdot \left(\frac{\mu_{r,a}}{\mu_{r,p}}\right)^{0.14} \quad (30)$$

Where $\mu_{r,a}$ and $\mu_{r,p}$ stand for the refrigerant mean viscosity in the fluid and respectively at the wall. This is valid for no phase change.

The total pressure drop outside tubes ΔP_o is calculated by (31) and should be inferior to 0.5 bar.

$$\Delta P_o = \frac{f_o \cdot G_s^2 \cdot (N_b + 1) \cdot D_s}{2 \cdot \rho_m \cdot D_e \cdot \left(\frac{\mu_{r,a}}{\mu_{r,p}}\right)^{0.14}} \quad (31)$$

Where G_s is the mass velocity in the shell. N_b is the number of baffles. D_s and D_e are respectively the shell diameter and the equivalent diameter in shell-side. f_o is the friction factor for the shell estimated by (32).

$$f_o = e^{0.0005 \cdot \ln(Re_s)} \quad (32)$$

For condensation in shell side, the Nusselt model [22] is used and the condensation is considered to be a film condensation.

$$h_o = 0.729 \cdot \left[\frac{k_f^3 \cdot g \cdot \rho_l \cdot Lv'}{\mu_l \cdot N_{\text{tubes}} \cdot d_o \cdot (T_{\text{sat}} - T_p)} \right]^{1/4} \quad (33)$$

$$Lv' = Lv + 0.68 \cdot Cp_l \cdot (T_{\text{sat}} - T_p) \quad (34)$$

Where g is the gravitational acceleration. k_f , ρ_l , Cp_l and μ_l are thermal conductivity, density, heat capacity and viscosity of refrigerant in liquid phase at the saturation temperature T_{sat} . T_p is the wall temperature. Lv is the heat of vaporization. N_{tubes} is the number of layers of tubes and it is approximated by (35).

$$N_{\text{tubes}} = \sqrt{\frac{N_c \cdot N_{\text{tubes}}}{N_s}} \quad (35)$$

For evaporation in shell side, the superposition method is used and is described by Lallemand [23]. This method consists in taking into account the heat transfer coefficient for the liquid phase h_l and for the nucleate ebullition h_{en} .

$$h_o = E \cdot h_l + S \cdot h_{en} \quad (36)$$

Where E and S are coefficients determined as follows.

$$E = (\phi_f^*)^{\frac{0.692}{1 - \phi_f^*}} \quad (37)$$

$$\phi_f^* = 1 + \frac{20}{X} + \frac{1}{X^2} \quad (38)$$

$$x^{\frac{1}{m}} = \left(\frac{1-x}{x}\right)^{1-m} \cdot \frac{\rho_v}{\rho_l} \cdot \left(\frac{\mu_l}{\mu_v}\right)^{0.75} \quad (39)$$

Where x is the vaporization rate. ρ_v and μ_v are density and viscosity of refrigerant in vapour phase at the saturation temperature. m is the Blasius coefficient and is equal to 0.25.

The coefficient S is calculated by (40).

$$S = \frac{h_l}{0.041 \cdot \lambda \cdot E \cdot h_l} \left[1 - e^{-\frac{0.041 \cdot E \cdot h_l}{h_l}} \right] \quad (40)$$

$$\lambda = \sqrt{\frac{\sigma}{g \cdot (\rho_l - \rho_v)}} \quad (41)$$

σ is the surface tension of liquid. h_l is obtained by (42).

$$Nu = \frac{h_l \cdot d_p}{k_l} = 0.137 \cdot Re_l^{0.692} \cdot Pr_l^{0.324} \quad (42)$$

h_{sat} is determined by the next correlation.

$$h_{sat} = 0.00122 \cdot \frac{k_l^{0.78} \cdot cp_l^{0.43} \cdot \rho_l^{0.48}}{\sigma^{0.28} \cdot \mu_l^{0.28} \cdot Lv^{0.24} \cdot \rho_v^{0.24}} \cdot (T_p - T_{sat})^{0.24}$$

$$\Delta R_{sat} = \frac{Lv \cdot (T_p - T_{sat})}{T_{sat} \cdot \left(\frac{1}{\rho_v} - \frac{1}{\rho_l}\right)}$$

After the exchangers, the next step is to determine the dimension of the DHN.

2.4.3. District heating representation

In this study, the district heating is represented by one producer, one definite customer and three potential customers.

The producer is located near the geothermal well and represents the heat recuperation used to the DHN. Customers are represented by their demanded heat and their location.

In these conditions, the global balance for this system can be written as (45).

$$\sum_{i=1}^4 Ex_i \cdot Q_{customer,i} = 0.9 \cdot Q_{producer} = Q_{DHN}$$

Where the 0.9 coefficient permits to take into account heat losses. $Q_{producer}$ and $Q_{customer,i}$ are respectively the heat supplied by the producer and the heat demanded by the i th customer. Ex_i is a binary variable presented in section 2.3. The connection to the network of the producer ($i = 1$) and the definite customer ($i = 2$) leads to the following constraints.

$$Ex_1 = 1$$

$$Ex_2 = 1$$

To represent the path for the network (which customers are connected and in which order), the following equations are implemented.

Since, in this contribution, the return follows the same way than the outward path, this path is taken into account only once (48).

$$\forall i \text{ and } j: Ex_{path_{ij}} + Ex_{path_{ji}} \leq 1$$

$Ex_{path_{ij}}$ stands for the existence or not of the path between i and j .

Eq. (49) means that a customer has only one input if it exists. There are no entry for the producer (50).

$$\forall j \neq 1: \sum_i Ex_{path_{ij}} = Ex_j$$

$$\forall i: Ex_{path_{i1}} = 0$$

Each customers has only one output if it exists, except the last one that does not have output (51). The producer has necessarily a unique output (52).

$$\forall i \neq 1: \sum_j Ex_{path_{ij}} \leq Ex_i$$

$$i = 1: \sum_j Ex_{path_{1j}} = 1$$

The global length for the DHN can be calculated by (53).

$$dist_{tot} = \sum_i \sum_j (dist_{ij} \cdot Ex_{path_{ij}})$$

Where $dist_{ij}$ is the distance between i and j .

Using the dimension of the exchangers and DHN, it is then possible to describe the cost model and to define an objective function for the optimization problem.

2.5. Objective Function

Turton et al. [24] propose to calculate the total capital investment as a function of equipment cost. This takes into account other costs like the land cost, its preparation fees, unpredictable fees and the start-up cost.

In this contribution, these other costs are assumed to be equal to 60% of the sum of equipment costs. The total capital investment also includes the total cost for the start of geothermal well C_{well} (equal to 10 M€) and the DHN cost C_{DHN} (54).

$$C_{TOT} = 1.6 \cdot \sum (C_{ex}) + C_{well} + C_{DHN}$$

Where C_{BM} is the bare module cost expressed by (55).

$$C_{BM} = C_p^0 \cdot F_{BM}$$

F_{BM} is bare module factor. C_p^0 is the purchased equipment cost in base conditions : equipment made of the most common material and operating at ambient pressure. C_p^0 is calculated by (56).

$$\log_{10} C_p^0 = K_1 + K_2 \cdot \log_{10} A + K_3 \cdot [\log_{10} A]^2$$

Where A is the size parameter for the equipment. K_1 , K_2 and K_3 are constants given in table 3.

For heat exchangers and pump, the F_{BM} factor is calculated by (57) and (58).

$$F_{BM} = B_1 + B_2 \cdot F_M \cdot P$$

$$\log_{10} F_p = C_1 + C_2 \cdot \log_{10} P + C_3 \cdot [\log_{10} P]^2$$

The values of constants F_M , B_1 , B_2 , C_1 , C_2 and C_3 are given in Table 3. P is the relative pressure (unit: barg).

For electric generator, the purchase cost is calculated by (59) as proposed by Le et al. [11].

$$C_p^0 = 60 \cdot [W_{gen}]^{0.63}$$

Where W_{gen} is the electric power in kW delivered by the generator.

Table 3: Constants for calculation of bare module cost of equipment

Equipment	K_1	K_2	K_3	C_1	C_2	C_3	B_1	B_2	F_M	F_{BM}
Exchangers	4.3247	-0.303	0.1634	0.03881	-0.11272	0.08183	1.63	1.66	1.0	
Pump	3.3892	0.0536	0.1538	-0.3935	0.3957	-0.00226	1.89	1.35	1.6	
Turbine	2.2476	1.4965	-0.1618							6.1
Motor*	1.956	1.7142	-0.2282							1.5
Generator*										1.5

*Motor design the motor of the pump and Generator is the electric generator at the turbine and there are not directly included in the cost of pump or turbine.

The data presented in Turton's book [24] are expressed for a CEPCI (Chemical Engineering Plant Cost Index) of 397 and the unit of cost is the USD. In this contribution, the cost values are returned to 570 of CEPCI for the year 2015 and cost is given in € according to the change rate of 8 January 2016 (1 USD = 0.919 €).

The DHN cost is the sum of the costs of the substations and the installation of the canalisations (60).

$$C_{DHN} = C_{pipe} \cdot dist_{tot} + \sum_{i=1}^n C_{subst} \cdot EX_i \cdot Q_{customer,i}$$

Where C_{subst} is the cost in €/kW and depends on the size of the considered substation. This cost can be estimated by (61) according to data available in the report of the "Conseil général des Mines" [25].

$$C_{sub} = 1108.2 \cdot [Q_{customer}]^{-0.428}$$

$Q_{customer}$ is expressed in kW.

In this same report, the cost per linear meters of canalisation C_{pipe} for a city with a medium urban

density is considered to be equal to 500 €/m. This cost includes the cost of pipes, the cost of trenches and the cost of installation.

Similarly to the total capital investment, the annual working cost for the installation C_{TPC} is a function of costs previously described (62).

$$C_{TPC} = 0.15 \cdot [\sum (C_{DHN}) + C_{well} + C_{DMV}]$$

The sources of income for the CHP plant are the sale of electric power and heat produced during a year. These sales are represented by (63) and (64).

$$V_{elec} = W_{net} \cdot H_{fDHS}^{ELEC} \cdot C_{elec}$$

$$V_{heat} = Q_{DHN} \cdot H_{fDHS}^{DHN} \cdot C_{heat}$$

Where W_{net} is the net electricity produced (quantity produced by the generator minus quantity used by the motor of the pump). C_{elec} is the sell price of electricity to EDF (a French electricity distributor), defined by a decree of 23 July 2010 [26]. This sell price includes a fix tariff of 20 c€/kWh and a bonus up to 8 c€/kWh. The bonus depends on the valorisation of the heat towards

the network. The annual working time of the ORC system H_{FONC}^{ORC} is considered to be equal to 7900 h/an.

C_{heat} is the mean sell price of heat in France in 2012 for a DHN powered by a renewable energy source [27]. It corresponds on 60.5 €/MWh.

The objective of this optimisation is to maximise the profit defined by (65).

$$Profit = [1 - tax_{imp}] \cdot [V_{elec} + V_{heat} - C_{TRC} - C_{ann}]$$

Where tax_{imp} is the corporate tax rate in France and it is assumed to be equal to 33.33%. C_{ann} is the annuity calculated by (66).

$$C_{ann} = \frac{C_{TRC}}{n_{year}}$$

n_{year} is the number of year chosen to reimburse the credit, here 20 years.

3. RESULTS

As say in section 2.4.3., the district heating is represented by one producer and four customers. Their locations are represented by their GPS coordinates (not given here). The distance between each point can be calculated and are given in **Table 4**.

In this contribution, three cases are studied and compared. These cases are differentiated by the energy required by customers as presented in **Table 5**.

Table 4: distance in km between point i and j .

$i \setminus j$	1	2	3	4	5
1		4.461	2.441	3.560	2.924
2	4.461		2.428	1.465	1.726
3	2.441	2.428		1.174	1.722
4	3.560	1.465	1.174		1.744
5	2.924	1.726	1.722	1.744	

Table 5: energy required in GWh_{th} for each customers.

i	Case 1	Case 2	Case 3
2	28	28	28
3	6	6	1
4	1	3	3
5	3	1	6

As a reminder, i is equal to 1 for the producer and 2 for the definite customer.

For the three cases, the optimization gives the results presented in **Figure 3** for the connection to the network of the customers.

The best path is different in each cases and it corresponds to the path which permits to maximize the annual profit.

The results of the different costs are summarized in **Table 6**. The case 0 corresponds on the electricity production alone.

The results show that for the three cases, the cost of the ORC system is more important than three times the cost of the DHN. Even if the quantity of electricity sold is near the quantity of heat sold, the sale of electricity is more profitable than the sale of heat.

For cases 1 and 3, the same quantity of electricity and heat is produced. The case 3 permits the highest profit because the length of district heating is less important.

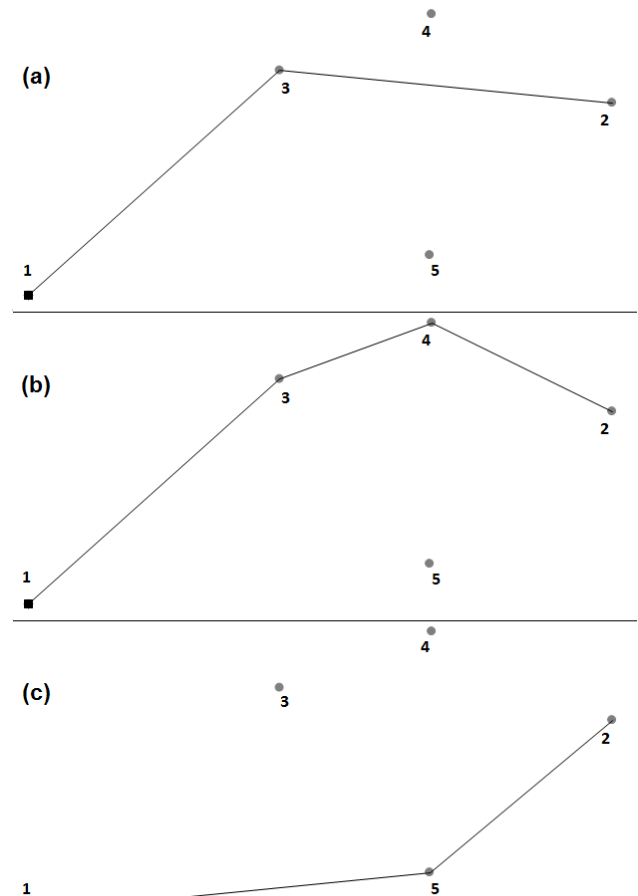


Figure 3. Best path given by the optimization for case 1 (a), case 2 (b) and case 3 (c).

Table 6: Summarized results

Case	0	1	2	3
T_{ratio} (%)	0	25.6	27.9	25.6
$E_{\text{net,elec}}$ (GWh _e /y)	43.9	32.7	31.7	32.7
$E_{\text{net,heat}}$ (GWh _{th} /y)	0	34	37	34
heater	515.1	414.6	405.6	414.6
evaporator	188.6	162	159.6	162
super heater	83.8	78.7	78.2	78.7
turbine	3166	2905	2877	2905
cooler	584.9	457.4	446.3	457.4
condenser	2049	1500	1453	1500
sub cooler	111.6	100.7	99.7	100.7
pump	184	145.5	142	145.5
motor	125	104.3	102.2	104.3
generator	314.4	237.6	230.7	237.6
C_{ORC} (k€)	11714	9769	9591	9769
C_{DHN} (k€)	0	2641	2790	2532
V_{elec} (k€/y)	8806	6796	6647	6796
V_{heat} (k€/y)	0	2057	2238	2057
$d_{\text{dist,heat}}$ (km)	0	4,87	5,08	4,65
Profit (k€/y)	3415	3280	3299	3295

Table 7: the low limit for the price of sale of heat in which it becomes more profitable to produce heat and power than electricity alone.

	Case 1	Case 2	Case 3
Sell price (€/MWh)	66.4	65.2	65.8

For the case 2, despite that the quantity of heat produced and the length of district heating is more important than for the case 1 or 3, the results show a higher profit. This is due to the bonus for valorisation in the price of sale of electricity.

The three cases in comparison to the case 0 show that electricity alone is better than couple electricity and heat in the domain of application. But it is evident that if the price of sale of heat increases, this will not be true anymore. **Table 7** shows this limit for the three cases.

4. CONCLUSION

Geothermal resource is used to provide heat to an ORC (electricity sale) or/and DHN (heat sale). We proposed an optimization problem formulation in order to determine the repartition of the resource between the ORC and the DHN, the design parameters of the ORC and the topology of the DHN. The optimization objective function is the annual profit of the whole

system. The DHN cost is estimated as a function of its length and quantity of heat used. The formulated problem is solved using the GAMS® environment. Three different cases are studied. Results show that it is preferable to produce electricity alone but this is dependent on the choice of the price of sale of heat by the owner. The sell price from which it becomes more profitable to produce and to sell the heat is determined for each case. Due to the combinatorial aspect of such problem, it is not that easy to predict the final results and it justifies the use of optimization approach.

ACKNOWLEDGEMENT

The authors thank the ADEME through the “Appel à Manifestation d’Intérêts (AMI)”. They also thank the Enertime society, for its expertise about the ORC systems, and the “FONROCHE Géothermie” society, coordinator of FONGEOSEC project.

REFERENCES

- [1] H. Chen, D. Y. Goswami, and E. K. Stefanakos, “A review of thermodynamic cycles and working fluids for the conversion of low-grade heat,” *Renew. Sustain. Energy Rev.*, vol. 14, no. 9, pp. 3059–3067, Dec. 2010.
- [2] Z. Shengjun, W. Huaixin, and G. Tao, “Performance comparison and parametric optimization of subcritical Organic Rankine Cycle (ORC) and transcritical power cycle system for low-temperature geothermal power generation,” *Appl. Energy*, vol. 88, no. 8, pp. 2740–2754, Aug. 2011.
- [3] B. Saleh, G. Koglbauer, M. Wendland, and J. Fischer, “Working fluids for low-temperature organic Rankine cycles,” *Energy*, vol. 32, no. 7, pp. 1210–1221, Jul. 2007.
- [4] S. Quoilin, M. Van Den Broek, S. Declaye, P. Dewallef, and V. Lemort, “Techno-economic survey of Organic Rankine Cycle (ORC) systems,” *Renew. Sustain. Energy Rev.*, vol. 22, pp. 168–186, Jun. 2013.
- [5] D. Wang, X. Ling, H. Peng, L. Liu, and L. Tao, “Efficiency and optimal performance evaluation of organic Rankine cycle for low grade waste heat power generation,” *Energy*, vol. 50, pp. 343–352, Feb. 2013.
- [6] J. P. Roy, M. K. Mishra, and A. Misra, “Parametric optimization and performance analysis of a waste heat recovery system using Organic Rankine

- Cycle,” *Energy*, vol. 35, no. 12, pp. 5049–5062, Dec. 2010.
- [7] J. Wang, Y. Dai, and L. Gao, “Exergy analyses and parametric optimizations for different cogeneration power plants in cement industry,” *Appl. Energy*, vol. 86, no. 6, pp. 941–948, Jun. 2009.
- [8] M. Astolfi, M. C. Romano, P. Bombarda, and E. Macchi, “Binary ORC (Organic Rankine Cycles) power plants for the exploitation of medium–low temperature geothermal sources – Part B: Techno-economic optimization,” *Energy*, vol. 66, pp. 435–446, Mar. 2014.
- [9] M. Astolfi, M. C. Romano, P. Bombarda, and E. Macchi, “Binary ORC (organic Rankine cycles) power plants for the exploitation of medium–low temperature geothermal sources – Part A: Thermodynamic optimization,” *Energy*, vol. 66, pp. 423–434, Mar. 2014.
- [10] S. Quoilin, S. Declaye, B. F. Tchanche, and V. Lemort, “Thermo-economic optimization of waste heat recovery Organic Rankine Cycles,” *Appl. Therm. Eng.*, vol. 31, no. 14–15, pp. 2885–2893, Oct. 2011.
- [11] V. L. Le, A. Kheiri, M. Feidt, and S. Pelloux-Prayer, “Thermodynamic and economic optimizations of a waste heat to power plant driven by a subcritical ORC (Organic Rankine Cycle) using pure or zeotropic working fluid,” *Energy*, vol. 78, pp. 622–638, Dec. 2014.
- [12] A. Haghrah, M. Nazari-Heris, and B. Mohammadi-ivatloo, “Solving combined heat and power economic dispatch problem using real coded genetic algorithm with improved mühlenbein mutation,” *Appl. Therm. Eng.*, vol. 99, pp. 465–475, Jan. 2016.
- [13] E. Abdollahi, H. Wang, and R. Lahdelma, “An optimization method for multi-area combined heat and power production with power transmission network,” *Appl. Energy*, vol. 168, pp. 248–256, Apr. 2016.
- [14] N. Ghorbani, “Combined heat and power economic dispatch using exchange market algorithm,” *Int. J. Electr. Power Energy Syst.*, vol. 82, pp. 58–66, Nov. 2016.
- [15] H. R. Sadeghian and M. M. Ardehali, “A novel approach for optimal economic dispatch scheduling of integrated combined heat and power systems for maximum economic profit and minimum environmental emissions based on Benders decomposition,” *Energy*, vol. 102, pp. 10–23, May 2016.
- [16] K. Sartor, S. Quoilin, and P. Dewallef, “Simulation and optimization of a CHP biomass plant and district heating network,” *Appl. Energy*, vol. 130, pp. 474–483, Oct. 2014.
- [17] D.-Y. Peng and D. B. Robinson, “A New Two-Constant Equation of State,” *Ind. Eng. Chem. Fundam.*, vol. 15, no. 1, pp. 59–64, 1976.
- [18] J. J. J. Chen, “Comments on improvements on a replacement for the logarithmic mean,” *Chem. Eng. Sci.*, vol. 42, no. 10, pp. 2488–2489, Jan. 1987.
- [19] R. A. Bowman, A. C. Mueller, and W. M. Nagle, “Mean temperature difference in design,” *Trans. Am. Soc. mech. Engrs.*, vol. 62, pp. 283–294, 1940.
- [20] TEMA, *Standards of the Tubular Exchangers Manufacturers Association*. 1999.
- [21] V. Gnielinski, “New equations for heat and mass transfer in the turbulent flow in pipes and channels,” *Int. Chem. Eng.*, vol. 16, pp. 359–368, 1976.
- [22] W. Nusselt, “The condensation of steam on cooled surfaces,” *Z.d. Ver. Deut. Ing.*, vol. 60, p. 541, 1916.
- [23] M. Lallemand, “Transferts en changement de phase - Ébullition libre,” *Tech. l’Ingénieur*, vol. 33, no. 0, pp. BE 8235–1 – BE 8235–22, 2012.
- [24] W. B. W. Richard Turton, Richard C. Baile, *Analysis, Synthesis, and Design of Chemical Processes*. 2009.
- [25] H. Prévot, “Les réseaux de chaleur,” 2006. [Online]. Available: <http://reseaux-chaleur.cerema.fr/les-reseaux-de-chaleur-conseil-general-des-mines-2006>. [Accessed: 28-Apr-2016].
- [26] “Obligation d’achat des énergies renouvelables.” [Online]. Available: <http://www.developpement-durable.gouv.fr/Les-tarifs-d-achat-de-l-12195.html>. [Accessed: 18-Jan-2016].
- [27] “Prix de vente de la chaleur en 2012.” [Online]. Available: <http://www.amorce.asso.fr/fr/espace-adherents/publications/rdc/prix-de-la-chaleur/rce-19-comparatif-des-modes-de-chauffage-et-prix-vente-de-la-chaleur-en-2012/>. [Accessed: 18-Jan-2016].

RISK OF INDUSTRIAL HEAT RECOVERY IN DISTRICT HEATING SYSTEMS

K. Lygnerud¹, S. Werner¹

¹School of Business, Engineering and Science, Halmstad University, PO BOX 823, Halmstad, 30118 Sweden

Keywords: Industrial heat recovery, risk assessment

ABSTRACT

Industrial heat recovery can be used in district heating systems. It is a possibility to make use of heat that is otherwise lost. Increased usage of industrial heat recovery reduces the need for fuel combustion lowering green-house gas (GHG) emissions, such as CO₂. Industrial companies can, however, move or close down industrial activities. This is apprehended as a risk and lowers the interest of district heating companies to invest in industrial heat recovery.

In Swedish district heating systems, industrial heat recoveries have been undertaken since 1974. Today, the heat recovery is active in about seventy systems. This leads to the question of how risky it is, for district heating companies, to engage in industrial heat recovery.

Over forty years of operation statistics have been collected and analyzed in order to estimate the risk of industrial heat recovery to district heating companies. Key results show that the risk is not linked to different industrial branches. Recommendations include suggestions to management on how to consider risk and consequence when assessing potential industrial heat recovery investments.

INTRODUCTION

There are ongoing initiatives in the European Union (EU) to save energy and to reduce greenhouse gas (GHG) emissions. By 2030 the goal is to save 27% of the primary energy used in the EU and to lower GHG emissions by 40% [1]. There are both environmental and economic gains to be made from industrial heat recovery [2] and there is a large potential for further industrial recovery [3]. In Sweden, residual heat is reused in district heating networks. Approximately 3TWh is reused per year whereas the available amounts of residual heat are in the range of 6,2-7,9 TWh per year [4]. The first EU level study on available residual heat considered three industrial branches; oil refining, chemicals and steel and dates to 1982 [5]. In it 2.4 million toe is identified as available resource. A more current study shows that only 1% of the available residual heat is being reused in the EU [6]. There is potential to use more residual heat. If the EU, Iceland, Norway and Switzerland resorted to residual heat in its district heating networks, to the same extent that Sweden does, it could lead to 300 TWh of heat per year [7].

Residual heat investments lead to lower costs of district heating production by putting energy that would otherwise be lost to alternative use. Also, since less fuel is incinerated the emission of GHG is lowered. There are, however, risks to residual waste investments. In Sweden, current legislation with landfill

ban and green certificates makes waste incineration and biofuelled combined heat and power plants (CHP) more competitive than utilization of industrial residual heat [8]. Other, known risks to residual heat investments are geography (where distance can hinder investments), different mindsets in industries compared to municipally owned district heating companies, a desire of industries to have own and independent heating solutions, volatile residual heat deliveries into district heating systems, the risk that industries go out of business, the notion that residual heat losses must be covered for by back-up facilities and an inability between parties to reach agreements that are mutually beneficial [ibid,2,4,9,10,11,12].

Swedish district heating companies and industries seem to have a greater ability to enter residual heat investments than corresponding parties in the EU. Why is that? Are Swedish district heating companies and industries better at managing investment risk than others or are residual heat investments in Sweden less risky than in other countries? Or are residual heat investments not as risky as they seem to be? In Swedish district heating systems, industrial heat recovery has been undertaken since 1974 and heat recovery is currently active in more than seventy systems. Analysis of Swedish data makes it possible to make a first estimation of the risk of residual heat investments. *The question of research in this study is if it is possible to assess risks of residual heat investments based on the Swedish experience.*

DATA COLLECTED

The first assessment of risk related to residual heat investments is performed in this pre-study by focusing on how long co-operations have existed in both current and terminated projects. Also, heat recoveries from various industrial branches have been analyzed. Later, complementary analysis will be performed focusing on why residual heat investments are undertaken and on how the risk of residual heat investments can be minimized.

Over forty years of operation statistics have been collected and analyzed in order to estimate the risk of industrial heat recovery to district heating companies. Main data resources have been the annual statistical surveys from the Swedish District Heating Association, the Swedish Energy Market Inspectorate, and Statistics Sweden.

Until 2014, 1570 years of residual heat deliveries have been identified in verified co-operations, as indicated in Table 1.

Table 1. Overview of data collected in verified co-operations

	Total number of localities	Total number of operation years	Average of operation years
Still in operation during 2014	69	1221	17.7
Terminated before 2014	28	349	12.5
Total	97	1570	16.2

Co-operations that are based on non-industrial processes (such as biomass boilers in sawmills for example) have been excluded from the report. Low temperature industrial sources as input to heat pumps have been included.

RESULTS

The data indicates that co-operations for recovering industrial heat to Swedish district heating systems are initiated with similar frequency across the time span of 1974 to 2014. In seven years no co-operations are initiated at all, seen from Figure 1.

As a result of the second, global oil crisis, a trend of including heat pumps in the heat recovery investments is discernable in the time span on 1983 to 1985. The trend ends in 1986 as a result of increasing electricity prices in Sweden in that year.

Considering the number of operation years the data shows that more than 85% of the co-operations have an operation lifetime of five years or more. This

indicates that industrial heat recovery co-operations tend to be long- rather than short-term.

On average, a co-operation that has been terminated lasted for 12.5 years. Co-operations that were still active in 2014 experienced an average 17.7 year life span. In Figure 2, the number of co-operations terminated before 2014 and the number of co-operations still in operation during 2014 are shown.

Analyses show that investments in industrial heat recoveries are undertaken in different industrial branches. The most long lived co-operations are found in the production of basic metals and in the extraction of metal ores, seen in Figure 3.

A peak of heat pump co-operations was identified for the time span of 1983-1985. Separate analysis of heat pump co-operations shows that this kind of co-operation is rare (one heat recovery investment out of five). Of the established co-operations approximately seven out of ten have gone out of business.

In Table 2, the number of heat pump investments that have been undertaken and that have gone out of business are compared to the total number of heat recovery investments undertaken (1974-2014).

Table 2. Co-operations with/without heat pump

	With heat pump	Without heat pump	Total
Still in operation 2014	6	63	69
Terminated before 2014	13	15	28
Total	19	78	97

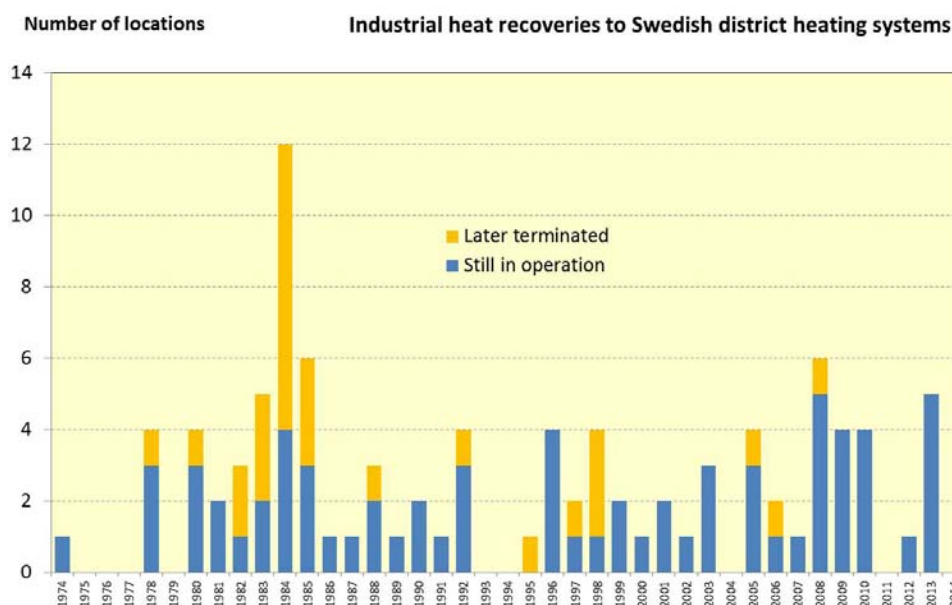


Figure 1. Initiated co-operations concerning industrial heat recoveries by commissioning year.

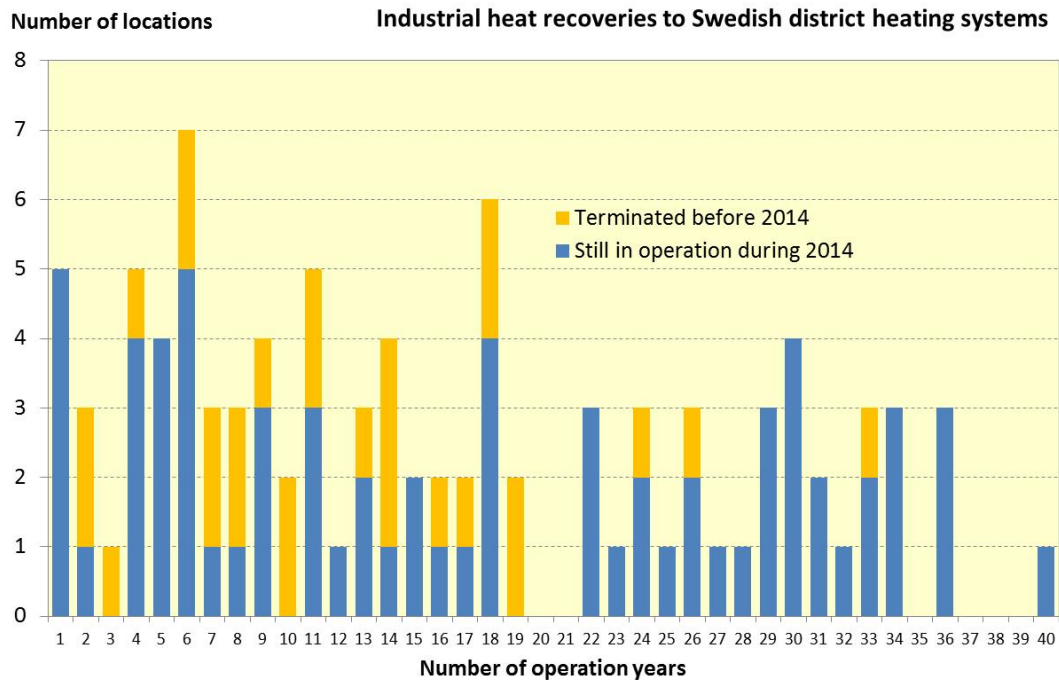


Figure 2. Number of operation years by terminated and ongoing co-operations concerning industrial heat recoveries.

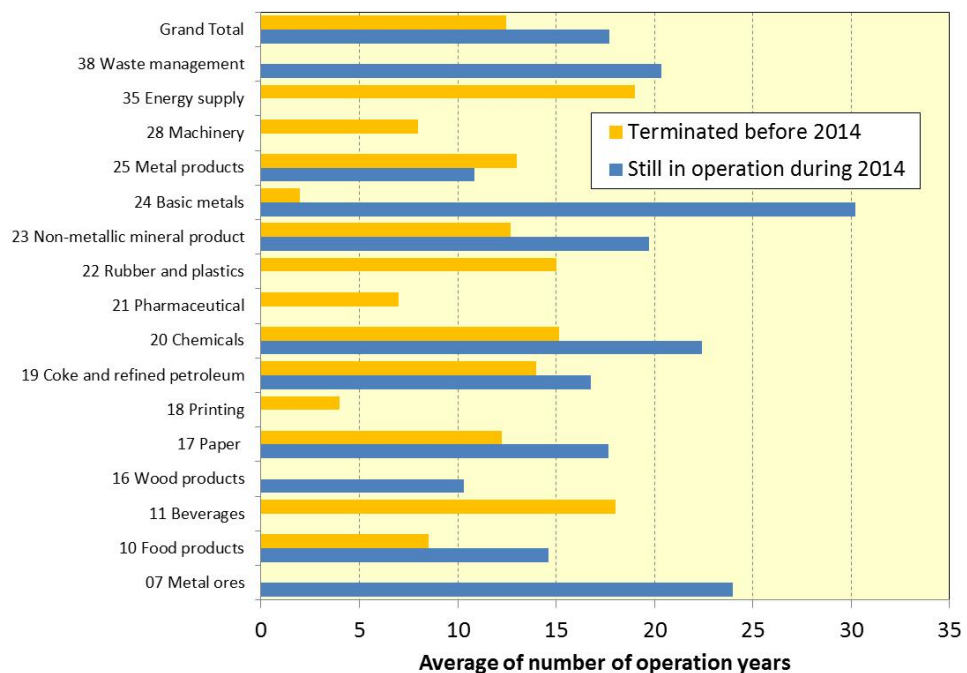


Figure 3. Average number of operation years for co-operations per industrial branch.

CONCLUSIONS

Industrial heat recovery investments are not a new phenomenon. Investments have been undertaken almost every year in different industrial branches.

A large majority of the identified co-operations have an operation life of 5 years or more. Such a time frame

should be enough for most industrial heat recovery investments to pay themselves back and to generate a return. It seems as if the investment risk of industrial heat recovery co-operations is rather limited.

Industrial heat recovery investments are undertaken in a variety of industrial branches. This diversity indicates that the idea to put the excess heat generated to use is spread and appeals to different kinds of industries. It

appears as if risks related to industrial heat recovery co-operations is not correlated to particular branches.

Heat pump investments are undertaken in one case out of five and seven investments undertaken go out of business. It appears as if heat recovery investments including heat pumps are more risky than investments excluding heat pumps. One probable reason is that heat pump residual heat investors rely on both cost for heat and electricity. Electricity has historically had a volatile price.

Returning to the question of research the conclusions drawn from this pre-study imply that it is possible to assess risks of residual heat investments based on the Swedish experience. However, more information is needed. Further statistical analyzes are going to be undertaken focusing on delivered residual heat volumes. Additionally, complementary interviews will be performed to discern why residual heat investments have been undertaken. Thereafter an analysis will be made on how the risk of residual heat investments can be minimized.

RECOMMENDATIONS

Decision makers considering if to enter an industrial heat recovery investment or not should note that heat pump co-operations create a dependency towards both heat- and electricity- price development.

The co-operations seem apt for different industrial branches and constitute an opportunity for energy savings that should be investigated when erecting new industries and/ or revisiting the energy system of existing facilities.

Industrial heat recovery investments are apt for long term investments. Investors with short investment horizons should opt for other energy solutions.

REFERENCES

- [1] European Council, Conclusions from the 23 and 24 October 2014 meeting, EUCO 169/14, 2014
- [2] Svensk Fjärrvärm, Spillvärme från industri till fjärrvärmenät, Svensk Fjärrvärme,2004, Report 2004:5
- [3] W. Moomaw, Industrial emissions of greenhouse gases, Energy Policy,1996, Vol. 24, pp- 951-968
- [4] Svensk Fjärrvärme, Spillvärme från industrier och lokaler, Svensk Fjärrvärme, 2009, Report 2009:12
- [5] European Commission, Waste heat from industry for district heating, 1982, Report EUR 8116
- [6] U. Persson, B. Möller, S. Werner, Heat Roadmap Europe: Identifying strategic heat synergy regions, Energy Policy, 2014, Vol. 74, pp. 663-681
- [7] Ecoheatcool, European heating and cooling market study (funded by the European Commission), European Commission, 2006
- [8] Swedish Energy Agency, Styrmedel för industriell spillvärme, 2008, Report ER:2008:15
- [9] Energistyrelsen, Skatteministeriets och energistyrelsens undersogelse af barrierer for udnyttelse afindustriell overskudsvarme, 2006
- [10] S. Viklund, Energy efficiency through excess industrial heat recovery- policy impacts, Energy Efficiency, 2015, Vol.8, pp. 19-35
- [11] A. Ajah, P. Herder, J. Greivink, Integrated conceptual design of a robust and reliable waste-heat district heating system,Applied Thermal Engineering, 2007, Vol. 27, No. 7, pp.1158-1164
- [12] S. Grönkvist and P. Sandberg, Driving forces and obstacles with regard to co-operation between municipal energy companies and process industries in Sweden, Energy Policy, 2006, Vol. 34, pp. 1508-1519

SOURCES FOR COLLECTED DATA

Svensk Fjärrvärme, Annual district heating statistics 1974-2014, 2015

Swedish Energy Market Inspectorate, Operation district heating information 2007-2014, 2015

Statistics Sweden, Municipal energy balances 2005-2014, 2015

DISTRICT COOLING – FUTURE DESIGN AND STANDARD

Jan H. Sällström¹

¹ SP Technical Research Institute of Sweden, PO Box 24036, Gothenburg, SE-400 22, Sweden

Keywords: *District cooling, pipes, insulation, soil temperatures, energy losses*

ABSTRACT

The measurements show that during a warm summer period the weekly mean soil temperature can reach 20°C at the depth 1.0 m below a sunlit asphalt surface in Sweden (northern Europe). Simulations of distribution systems buried at shallower than 1.0 m show that it is beneficiary in terms of energy losses to use insulated flow lines. The importance of using insulated return lines is a more open question, which also is related to the costs of production of cooling. An investment assessment of using uninsulated or insulated pipelines ought to be part of the planning of expansion of a cooling network.

INTRODUCTION

For cooling distribution systems, there is currently no unified industry practice how to design with regard to choice of materials and components. The result will be district cooling systems with non-optimal technical performance in terms of temperature losses and operation. Even a small increase of flow cooling water temperature caused by the inlet of heat, leads to a deterioration of delivered cooling capacity and less profit for the energy company.

The aim of this project is to compile current knowledge in the field of district cooling and to generate new knowledge concerning energy losses in distribution systems with uninsulated and insulated pipes in various soil conditions. Measurements of soil temperatures during the year below sunlit asphalt, paved and grass surfaces are carried out in Sweden. Models are developed and analyses are carried out for systems with different pipe types and soil conditions. A method for assessing if insulated district cooling network is economically beneficial, is presented.

LITERATURE STUDY

Euroheat & Power [1] has published recommendations for district cooling. In those there are a set of pipes listed that may be used: coated steel pipes, prefabricated district heating pipes, polyethylene pipes, cross-linked polyethylene, copper pipes, stainless steel pipes, and also steel pipes with steel casing pipes.

McCabe et al. [2] have written about large losses in a local cooling network at a university in north US with uninsulated piping. They measured soil temperatures below a grass and a road surface. During the measurement period the outdoor temperature reached 27°C. At

a depth of 300 mm below the road surface the maximum temperature was 23°C and the daily average 19°C. The temperatures below the grass surface was 2-3°C less. The results were much higher than they found in handbooks, which gave a daily average of 12°C.

Oppelt et al. [3] have studied transient heat flow for parallel district cooling pipes.

Sundberg [4] has treated heat transport in soil and rock. The transport can be divided into conduction radiation, convection and steam diffusion. The conduction is dominating and depends on the water content and the density. For wet sand the thermal conductivity lies in the span 1.5 to 2.6 W/mK. For dry sand the span is from 0.4 to 1.3 W/mK.

Prepar et al. [5] have developed method for determining thermal conductivity of soil. Energy losses of district heating pipes in service have been studied by measurements and calculations.

Analytical solutions for estimating heat losses have been presented by Persson and Claesson [6] & [7]. A case with a set of insulated pipes in the ground has been studied. The temperature field in the insulation of the pipes and the soil is given as sums containing complex valued poles.

FIELD MEASUREMENTS

Two field measurement sites have been installed in the south of Sweden in Göteborg (Almedal, network of Göteborg Energi) and in Stockholm (Kista, network of Fortum Värme). The purpose is to measure soil temperatures below sunlit surfaces and temperatures around district cooling and heating pipes. Sketches of measurement site in Göteborg are shown in Fig. . The measurement site is sunlit, but shadowed of an office building during late mornings. There is also a tree that shadow MP1-2 during late afternoons.

Cables to sensors are surrounded by stone dust of 0-8 mm close to sensors and remaining parts are placed in pipes going to an electricity cabinet. Beams of wood are used for fixing cables and sensors. At MP2 & 4, the temperature sensors are put into existing shaft wall. At MP2 top three sensors are sitting in existing gravel and bottom two in existing clay. Soil moisture sensor is set in stone dust. At MP4, temperature sensors are sitting in existing gravel.

The district cooling pipes are made of polyethylene, which can be used as water pipes. The flow pipe

Φ315 mm at MP1 is insulated by use of polyurethane and fitted with a polyethylene casing of Φ450 mm.

At MP3 the polyethylene service pipes are uninsulated. At MP5 standard pre-insulated district heating pipes are used. Temperatures of energy carriers are taken from measurements at nearby substations.

Sketches of the measurement site in Stockholm are shown in Fig. 2. Here, pre-insulated pipes with steel service pipe, polyurethane insulation and casing are used for the distribution system. The insulation is thin.

HEAT TRANSPORT

Stationary heat losses from a pair of district heating or cooling pipes, see Fig. 3, can be written

$$\begin{Bmatrix} q_a \\ q_b \end{Bmatrix} = \begin{bmatrix} U_{11} & U_{12} \\ U_{21} & U_{22} \end{bmatrix} \begin{Bmatrix} T_a - T_0 \\ T_b - T_0 \end{Bmatrix} \quad (1)$$

Parameters q_a and q_b denotes heat power per unit length [W/m] going from the pipes with temperatures T_a and T_b to the ground surface with temperature T_0 . The centres of the pipes lie in the complex plane at

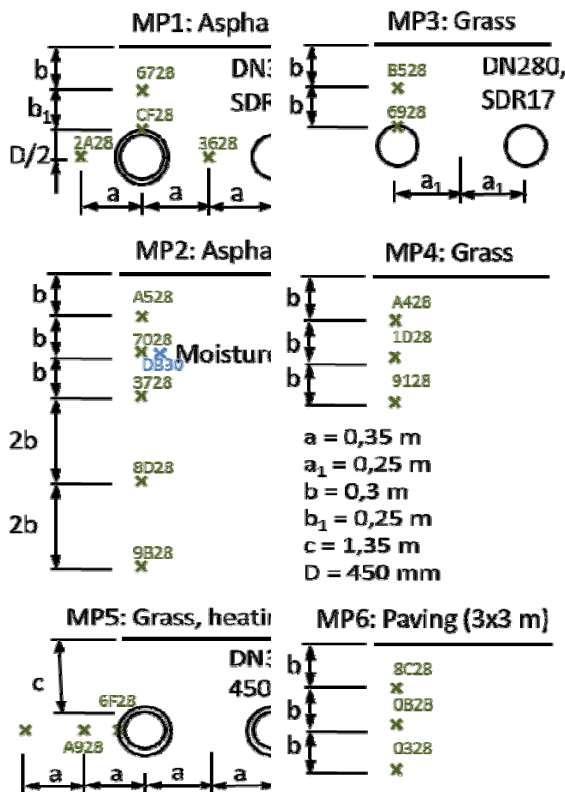


Fig. 1 Six measurement positions at field site in Göteborg. Temperature sensors are located in soil below asphalt surface in vicinity of pipes at MP1 and more than 3 m from pipes at MP2, where also soil moisture is measured. Temperature sensors located below grass surface in vicinity of pipes at MP3 and more than 3 m from pipes at MP4. At MP1 only flow line is insulated and at MP3 service pipes are uninsulated. Temperature sensors are placed near the heating pipes at MP5. At MP6 temperatures are measured below paved surface.

$$z_a = x_a + iy_a \quad (2a)$$

$$z_b = x_b + iy_b \quad (2b)$$

Heat transfer matrix is given as the inverse of the heat resistance matrix R

$$U = R^{-1} \quad (3)$$

Here, the solution given by Persson & Claesson [6] is used. The heat resistance matrix is given by the geometry, thermal conductivity of the pipe materials and the soil λ [W/m K]

$$R = \frac{1}{2\pi\lambda} \begin{bmatrix} \frac{\lambda}{\lambda_{ina}} \left(\ln \left(\frac{\alpha_a}{\alpha_a} \right) + \beta_a \right) + \ln \left(\frac{2r_a}{\alpha_a} \right) & \ln \left(\frac{|z_a - \bar{z}_b|}{|z_a - z_b|} \right) \\ \ln \left(\frac{|z_b - \bar{z}_a|}{|z_b - z_a|} \right) & \frac{\lambda}{\lambda_{inb}} \left(\ln \left(\frac{\beta_b}{\beta_b} \right) + \beta_b \right) + \ln \left(\frac{2r_b}{\beta_b} \right) \end{bmatrix} \quad (4)$$

where

$$\beta_a = \frac{\lambda_{ina}}{\alpha_a \alpha_a} + \frac{\lambda_{ina}}{\lambda_{sa}} \ln \left(\frac{\alpha_a}{\alpha_a} \right) + \frac{\lambda_{ina}}{\lambda_{ca}} \ln \left(\frac{\alpha_a}{\alpha_a} \right) \quad (5a)$$

$$\beta_b = \frac{\lambda_{inb}}{\alpha_b \alpha_b} + \frac{\lambda_{inb}}{\lambda_{sb}} \ln \left(\frac{\beta_b}{\beta_b} \right) + \frac{\lambda_{inb}}{\lambda_{cb}} \ln \left(\frac{\beta_b}{\beta_b} \right) \quad (5b)$$

Notations are

λ_{ina} [W/m K] thermal conductivity of insulation of line "a"

λ_{sa} [W/m K] thermal conductivity of service pipe of line "a"

λ_{ca} [W/m K] thermal conductivity of casing of line "a"

α_a [W/m² K] heat transfer coefficient of between fluid and service pipe for line "a".

Corresponding parameters for line "b" are denoted λ_{inb} , λ_{sb} , λ_{cb} and α_b . The heat transfer coefficient α_g between air and soil can be taken into account by increasing the laying depth by λ/α_g . A usual value used is $\alpha_g = 14.6$ W/m² K, see Reference [8].

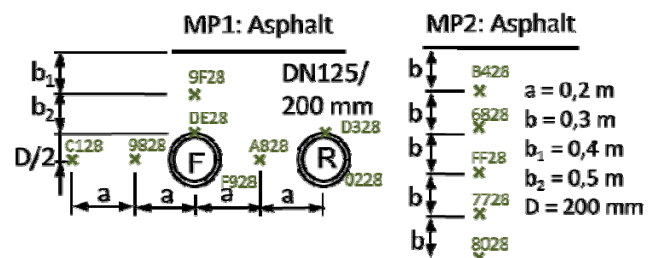


Fig. 2 Two measurement positions at field site in Stockholm below asphalt surface which is sunlit in clear weather. Temperature sensors are located in the vicinity of pipes at MP1 and more than 2 m from pipes at MP2. Carrier temperatures are measured by sensors in dive tubes in both pipes. Outdoor temperature and humidity are measured with shielded sensors.

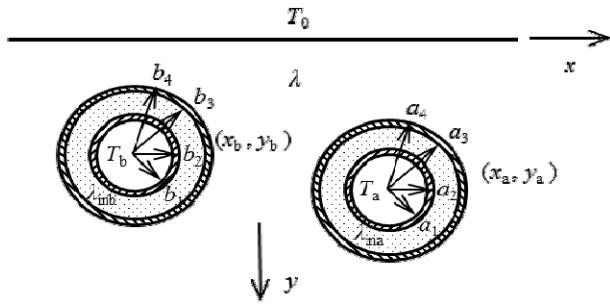


Fig. 3 Pair of insulated pipes with centres at (x_a, y_a) and (x_b, y_b) , respectively, buried in soil. Thermal conductivity λ , λ_{sa} , λ_{ina} , and λ_{ca} in soil, service pipe, insulation and casing, respectively.

MEASUREMENT RESULTS

The measurements have been carried out from July 2014 to December 2015 in Göteborg and from February to December 2015 in Stockholm. The soil acts as a low passage filter and the high frequency variations at the ground surface will not reach pipes buried at a depth of 1.0 m. It also takes time for the heat to reach the buried pipes. It is considered useful to dimension the cooling distribution system based on a longer period than one day. Here, one week is chosen as an appropriate period to base the temperature averages on.

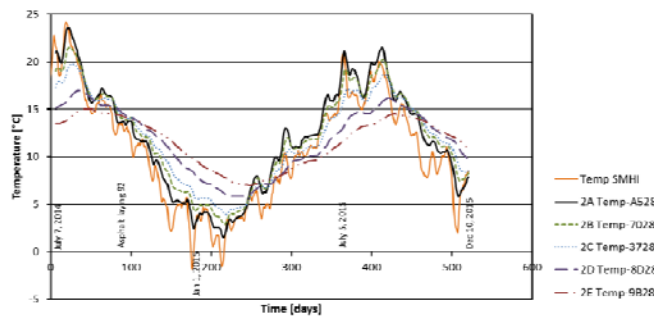


Fig. 4 Air temperature and soil temperatures at five levels below asphalt surface at MP2 in Göteborg. Weekly average values are plotted from July 7, 2014 to December 10, 2015.

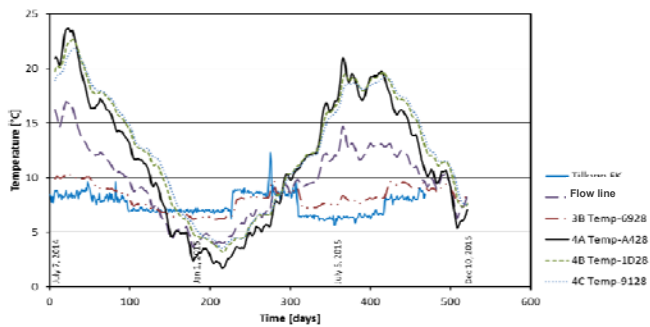


Fig. 5 Daily values of flow line temperatures. Soil temperatures at two positions close to flow line at MP3 and three levels at MP4 in Göteborg below grass surface. Weekly average soil temperatures are plotted from July 7, 2014 to December 10, 2015.

In Fig. 4 floating weekly averages of soil temperatures below a periodically sunlit asphalt surface are shown. The gauges are installed at depths 0.3 m to 2.1 m. The averages air temperature is also shown. The season variations are apparent. The weekly averages at the shallow soil levels are often higher than the average of the air temperature. During the summer the average of the soil temperature exceed 20 °C at normal laying depths. During the summer it is warmest at top levels, but in October this change and the temperature increase with depth instead. In March the order changes again.

In Fig. 5 the soil temperatures below a grass surface are shown. The temperature gauge at MP3 at depth 0.3 m is placed above the uninsulated district cooling line show considerably lower temperature than the gauge at the same level at MP4. A comparison of the soil temperatures at MP2 with asphalt and MP4 with grass gives a difference of 1-1.5 °C in the span from 400-415 days in August 2015. The grass has a cooling effect, but this effect might have been more significant if the asphalt surface at MP2 was not shadowed by a tree in the late afternoons.

A comparison of the soil temperatures at depth 0.6 m below asphalt, grass and paving is given in Fig. 6.

In Fig. 7 soil temperatures below an asphalt surface measured at MP2 in Stockholm are shown. The maximum weekly average at depth 0.6 m is about 23 °C during the summer 2015.

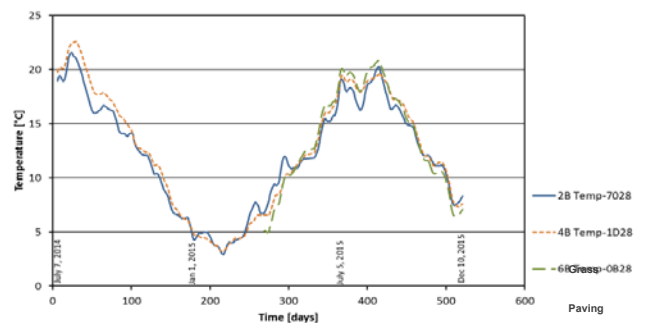


Fig. 6 Soil temperatures below asphalt, grass and paving at depth 0.6 m at MP2, 4 and 6. Weekly average values are plotted from July 7, 2014 to December 10, 2015.

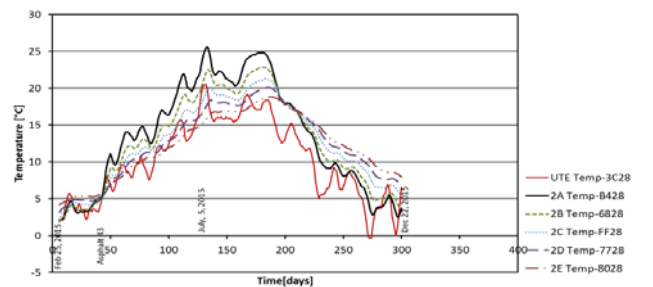


Fig. 7 Air temperature and soil temperatures at five levels below asphalt surface at MP2 in Stockholm. Weekly average values are plotted from February 25, 2015 to December 22, 2015.

ANALYSIS OF MEASUREMENT RESULTS

In order to dimension your district cooling network and calculate losses and flows of water, simplifications are needed. Many factors vary: the ambient temperature, temperatures in the flow and return pipe, the flows in the lines and the customer demands. Even though we have seen in the graphs that stationary ambient temperature never occurs, we have to assume that the ambient temperature is constant during the simulation of the network. Summary of measured weekly average temperatures are given in Table . Measured extreme values are given for the summer and the winter seasons. For the spring and the autumn, no extreme values can be given and representative values in the midterm seasons are given instead.

The summer conditions will be dimensioning, and therefore that case is studied more thoroughly. A stationary case similar to the conditions at MP3 in Göteborg on day 410 in August 2015, see Fig. 8. The ground surface temperature is set to 20 °C, and carrier temperature in flow and return lines are set to 6.5 °C and 16 °C. The measured temperature at gauge 3A-B528 is 13 °C on day 410 and the calculated, temperature becomes 16 °C, see also Fig. 5.

Table 1: Summary of measured extreme weekly average temperatures during winter and summer during 2014-15 at measurement sites in Göteborg and Stockholm, Sweden. Temperatures at two times during spring and autumn are also given.

Season	Depth [m]/Air	Temperature [°C]
Summer ¹	Air	22±2
	0.3	23±2.5
	0.6-0.9	21±2
	1.5-2.1	17±2
Autumn ² 15/10	Air	9±3
	0.3	11±2.5
	0.6-0.9	13±2
	1.5-2.1	14
Winter ³	Air	-2
	0.3	1.5
	0.6-0.9	3.5±0.5
	1.5-2.1	6.5±0.5
Spring ⁴ 15/4	Air	7
	0.3	9.5±1.5
	0.6-0.9	8±1.5
	1.5-2.1	7±0.5

¹Measurement data from Göteborg summers 2014-15, Stockholm summer 2015

²Measurement data from Göteborg autumns 2014-15, Stockholm autumn 2015

³Measurement data from Göteborg winter 2014/15

⁴Measurement data from Göteborg spring 2015, Stockholm spring 2015

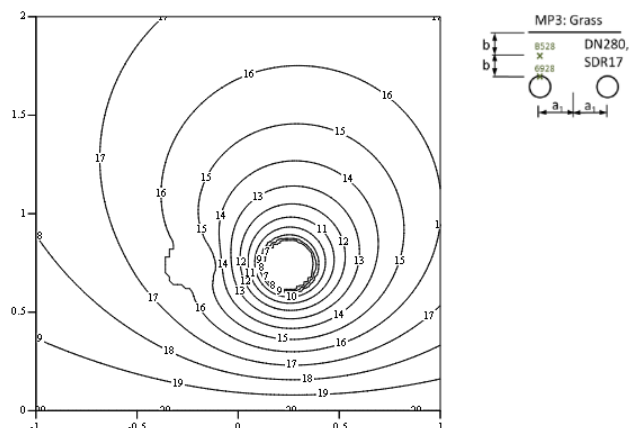


Fig. 8 Temperature of ground at stationary conditions at MP3 in Göteborg when carrier temperatures are 6.5 °C and 16 °C, respectively. Ground surface temperature 20 °C and thermal conductivity 1.5 W/m K in soil have been assumed. Thermal conductivity of polyethylene assumed to 0.4 W/m K. In diagram depth is upwards making supposed rotation of chart of 180° conformity with sketch to the right. Parameters $b=0.3$ m and $a_1=0.25$ m.

The stationary solution used here is given by Persson & Claesson [6] & [7].

SIMULATIONS

In order to better understand the result in terms of losses of insulating the district cooling service pipes, a pair of pipes buried in a shaft with a soil cover of 0.6 m is studied by use of Equations (1) to (5). The pair of pipes are studied for two soil surface temperatures 22 °C and 13 °C, see Table 2. For the first case, the losses are more than five times larger for bare service pipes as compared to a pair of insulated pipes. For the second case (13 °C), best alternative is to insulate only the flow line, since the soil will cool down the return line.

Table 2: Comparisons of losses of differently insulated pair of polyethylene pipes with diameter Ø180 mm. Soil cover is 0.6 m. Temperatures of flow and return are 6 °C and 16 °C, respectively. Thermal conductivity of polyurethane polyethylene are 0.020 W/m K and 0.4 W/m K, respectively. Soil conductivity is 1.5 W/m K. Losses are normalized to 1 when both lines are insulated. Comparisons within each column are only meaningful.

Pipe type	Insulation	Normed loss	Normed loss
Surface temperature		22 °C	13 °C
Ø180	None	5.6	5.6
Ø180/250	F&R	1.0	1.0
Ø180/250	F	2.5	-4.6

The district cooling network of E.ON Värme in Malmö, Sweden, has been studied. There are two production units AVP and KVP. The network consists of uninsulated pipes only. A simulation model built up in the software NetSim has been used, see Fig. 9. The software is initially developed for district heating networks. Heat losses are calculated as a heat transfer coefficient time a temperature difference between the pipe and the surroundings. There are no coupling between terms taking into account the heat transfer between flow and return as in Equation (1).

Two periods, one in August and one in October have been analysed. There are measured flow temperatures from the production and at the clients. The consumption of the clients and the return temperatures after the substations are also measured. The produced power and the return temperature at the production units are also recorded.

Two large clients far out in the network are at first considered. For the studied periods, the flow temperatures at these clients are calculated and compared to recorded values. Second, the return temperatures at the production units are calculated and compared to the recorded data. Input data to the simulations are the flow temperatures at the production units, consumption at the clients and the return temperatures from the clients. For the two periods, the flow carrier temperatures at the production and at the clients are similar.

After reasonably good agreement has been reached, the cases with two insulated lines and insulated flow line only have been simulated in the entire network. All details of the networks cannot be listed, but the chosen insulation goes from 30 mm to 55 mm for the small diameter pipes of Ø100 mm to large of Ø450 mm, respectively. Consumption and losses for one week in August and October are determined. Preliminary results are given in Table 3.

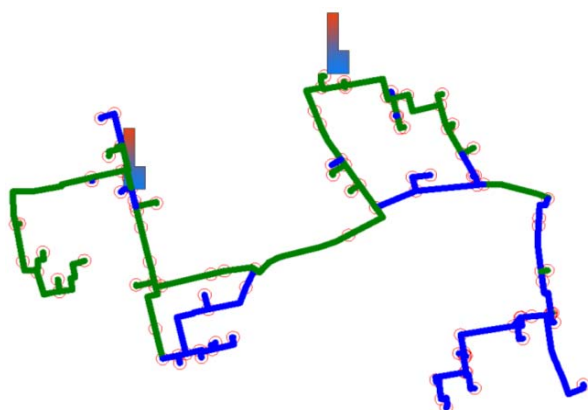


Fig. 9 Model of EON cooling network in Malmö. Blue lines represent polyethylene pipes and green steel pipes. Extension of the network is 1.5 km x 1 km. Production can take place at AVP and KVP. Pipe length (sum of flow and return) is 13 km, volume 670 m³, and design power 10 MW.

Table 3: Measured consumption and calculated losses per week in existing and modified networks in Malmö, Sweden. Ambient temperatures are 21 °C and 15 °C in August and October, respectively. Burial depth 1.0 m and thermal conductivity of soil 2.5 W/m K are used.

	Existing	Insulated lines	Insulated flow line
Consumption August [MWh/w]	498	498	498
Losses August [MWh/w]	55.8	9.3	25.1
Consumption October [MWh/w]	132	132	132
Losses October [MWh/w]	1.8	1.3	1.6

ANALYSIS OF SIMULATION RESULTS

It is essential that the district cooling system meets the technical demands and the consumers get the cooling they need. To ensure this, network simulations are needed for dimensioning cases including both comfort and process cooling. Furthermore, an investment evaluation of the insulated network as compared to the uninsulated one can be of interest before building it.

Let us look at the cooling network in Malmö again. Assume that we want to build the network from scratch and that we have to choose between to build the entire network with uninsulated lines, insulated flow and return lines, or insulated flow line only.

In Table 4 simplified estimations of yearly savings of cooling energy by insulation either both lines or flow line only are calculated by use of Table 3 as input data. In Table 5, the additional investment estimations that have to be done for insulating the lines with polyurethane and add a casing are given. Assumed production costs of cooling and discount rate are also given.

Table 4: Simplified estimation of yearly savings due to using insulated lines or insulated flow line only for network in Malmö.

	Uninsulated lines	Insulated lines	Insulated flow line
Losses Aug [MWh/week]	55.8	9.3	25.1
Savings Aug [MWh/week]		46.6	30.7
Representative weeks		16	16
Losses Oct [MWh/week]	1.8	1.3	1.6
Savings Oct [MWh/week]		0.5	0.2
Representative weeks		36	36
Yearly savings [MWh]		760	500

Table 5: Assumed input data for investment evaluation of insulation for network in Malmö.

	Input data	Insulated lines	Insulated flow line
Discount rate	5%		
Costs of cooling [EUR/kWh]	0.05		
Investment [kEUR]		600	300
Yearly savings [MWh]		760	500
Yearly savings [kEUR]		38	25

Table 6: Calculations of payback time for insulated lines in network in Malmö become profitable.

NPV(savings) - Investment [KEUR]	Number of years	Insulated lines	Insulated flow line
Profit after	0	-600	-300
Profit after	5	-436	-192
Profit after	10	-307	-107
Profit after	15	-206	-40
Profit after	16	-188	-29
Profit after	17	-172	-18
Profit after	18	-156	-8
Profit after	19	-141	2
Profit after	20	-126	12
Profit after	25	-64	52
Profit after	30	-16	84
Profit after	31	-8	90
Profit after	32	0.5	95

When the estimations of the investment and the yearly savings are done, the payback method can be used for calculating the period the cumulated cash flows becomes equal to the investment. The net present value of yearly savings B can be written

$$NPV = B \left[\frac{1}{1+K} + \frac{1}{(1+K)^2} + \frac{1}{(1+K)^3} + \dots + \frac{1}{(1+K)^n} \right] \quad (6)$$

In Table 6 the profit after different numbers of years are calculated. In the example, the payback time for insulating the flow line is 19 years.

CONCLUSION

The measurements data show that during a warm summer period the weekly mean soil temperature can reach 20°C at the depth 1.0 m in northern Europe. Simulations of district cooling systems buried at shallower than 1.0 m show that it is beneficiary, when it comes to energy losses, to use insulated flow lines. The importance of using insulated return lines is a more open question, which is related to the costs of production of cooling. Furthermore, an insulated flow line also has to be justified economically.

The effect of insulated lines as compared to uninsulated is not only that the losses to the surrounds decrease, but also the heat transfer between the flow line and the return.

It is essential that the district cooling system meets the technical demands and the consumers get the cooling they need. To ensure this, network simulations are needed for dimensioning cases including both comfort and process cooling. Insulation is not only of interest during the summers, since the cooling capacity needs to be maintained for process cooling, when the general consumption and the flows are less.

No detailed analysis concerning choices of materials in district cooling lines have been made. However, the usage of polyethylene pipes or traditional pre-insulated district cooling pipes with steel service pipe, polyurethane insulation and a casing of polyethylene are found attractive. The polyethylene pipes can be uninsulated, insulated in a similar way with polyurethane or insulated by use of blocks of expanded polystyrene.

The results of the project can provide a basis for future practice for design and standardization work of district cooling.

ACKNOWLEDGEMENTS

This work was carried out under the research programme Fjärrsyn administrated by Energiforsk and was financially supported by the Swedish Energy Agency and the Swedish District Heating Association. Our project partners were Vitec AB, Göteborg Energi AB and Telge Nät AB. Permissions to install a field measurement site in Fortum Värme's network in a building owned by Fastighets AB Balder were given. The financial support, the work of partners and the permissions are gratefully acknowledged.

REFERENCES

- [1] "District cooling pipes – Pipes and components in district cooling systems", Euroheat & Power, Technical recommendations, Brussels, BE, 2008.
- [2] R. E. McCabe, J. J. Bender, & K. R., Potter, "Sub-surface ground temperature: implications for a

- district cooling system”, ASHRAE Journal, 37 (12), pp 40-45, 1995.
- [3] T. Oppelt, T. Urbaneck, & B. Platzer, “District cooling networks: Comparison of moduls for calculating heat flow through walls of buried parallel pipes, Euroheat and Power (English Edition), 10(2), pp 26-31, 2013.
- [4] J. Sundberg, ”Thermal properties of soil and rock” (in Swedish), Statens geotekniska institut, Information 12, Linköping, SE, 1991.
- [5] M. Perpar, Z. Rek, S. Bajric & I. Zun, “Soil thermal conductivity prediction for district heating pre-insulated pipeline in operation”, Energy, 44 (1), pp 197-210, 2012.
- [6] C. Persson & J. Claesson, “Steady-state thermal problem of insulated pipes solved with the multipole method”, Report 2005:3, Division of Building Technology/ Building Physics, Department of Civil and Environmental Engineering, Chalmers, Göteborg, SE, 2005.
- [7] C. Persson & J. Claesson “Multipole Method to Compute Heat Losses from District Heating Pipes”, Proceedings of the 7th Nordic Symposium on Building Physics, Reykjavik, IS, June 13-15, 2005.
- [8] B. Kvisgaard & S. Hadvig, Varmetab fra fjernvarmeledninger (Heat loss from Pipelines in District Heating Systems), Teknisk Forlag, Copenhagen. ISBN 87-571-0635-5, 1980.

INTEGRATION OF SOLAR THERMAL SYSTEMS INTO EXISTING DISTRICT HEATING SYSTEMS

C. Winterscheid¹, S. Holler², J.-O. Dalenbäck¹

¹ Chalmers University of Technology

² HAWK University of Applied Science Göttingen

Keywords: *District Heating, Solar District Heating, Solar Thermal Systems*

ABSTRACT

Modern district heating (DH) networks are usually operated with a changing flow temperature to cover the heat load of the supply area, depending on the outside temperature. Due to the minimum temperature requirements of individual customers, DH networks also need to operate during the summer months. During this time, the load on the system is relatively low. This requires combustion facilities to operate on low load levels as well. These systems have a potential of improving the energy efficiency by utilizing other energy sources such as waste heat from industrial processes or solar thermal systems. The overall aim of the presented work is to provide a new methodology for the integration of solar heat into existing DH systems.

The feasibility of including solar thermal systems in existing DH networks will be analysed, based on the state of the art of solar DH. The main focus will be on large DH systems that are mainly supplied by fossil fuel powered combined heat and power (CHP) plants considering how such plants can be operated in the future. In this paper characteristic technical and ecological key performance indicators of a transformed DH system will be displayed.

The work was carried out based on real data of an example DH network in Germany. It was analysed how a sub-network of a system can be supplied during the summer season by a solar thermal system as far as possible independently from the main-network without using a back-up boiler system. The favoured solution in this article is to use a thermal storage that can be recharged once a day by a central CHP plant.

INTRODUCTION

The integration of solar thermal systems in DH systems is a more and more common practice in some countries; however few studies have been performed on methodologies and benefits of integrating solar thermal systems in DH systems that are mainly supplied by large scale CHP plants with low heat generation costs.

The general idea behind including solar collector fields in DH networks is to lower or even completely supply the low heat demand of a DH network during the summer months. Since the 1980s Denmark and Sweden have built many solar heating plants [1]. In

some of these cases a seasonal storage is used to provide a solar share even above 50 % of the total system demand. The high taxation of primary energy sources supported the ambitions in Denmark that lead to seasonal storages which are only feasible in a very large scale [2]. In comparison to the Danish and Swedish developments solar DH systems in Germany started to be built later, at the beginning of the 1990s.

The large DH systems in Germany are generally supplied by large CHP plants. These plants are often operating as base load power producers and can supply heat and electricity at a cost-efficient level during summer and winter due to funding through the CHP production law (KWKG) [3]. In addition to the availability of low-cost heat, high and very high system temperatures in the DH systems also prevented solar heat generating systems [4]. In the case of the DH system Chemnitz, only a large change in the system structure in one district made a change feasible. Possibilities of including solar collector systems in existing DH networks that are not about to change radically and are using large scale CHP plants as a main heat source were rarely analysed. Despite of the higher specific generation costs a solar collector field can also bring several advantages to systems of the mentioned kind.

This paper presents aspects where a solar collector field can be beneficial for a DH system based on a large scale CHP plant and how such a collector field can be included. The work was carried out by evaluating the load pattern of a part of an existing DH system in Germany. In the given case the system analyse was based on the following conditions:

- A fixed supply temperature in a connected sub-network that is not needed in the whole system
- A long connection pipeline between the main network plant and the connected sub-network
- A reduction of the primary energy factor (PEF)
- A reduction in CO₂ emissions

Taking into account the interests of the network owner different methodologies of including a solar collector field were developed. In the given case a solution without a local backup boiler is preferred; instead a daily reheat of a storage from the large CHP plant was suggested.

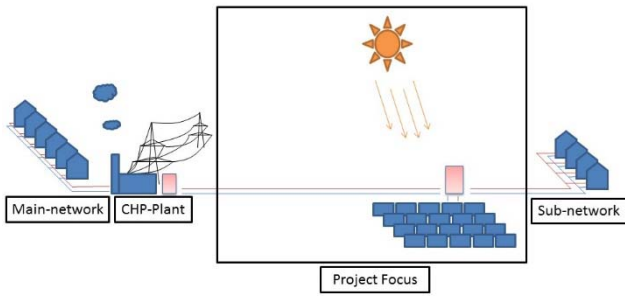


Figure 1. Project focus: The solar thermal field and the thermal storage are located between main-network and sub-network

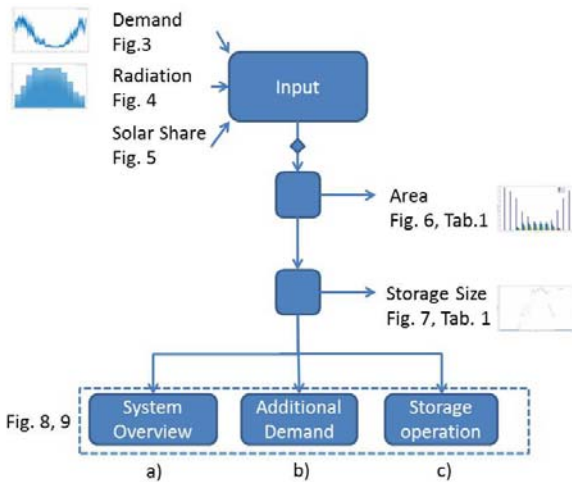


Figure 2. Methodology for the integration of solar heat into existing DH systems

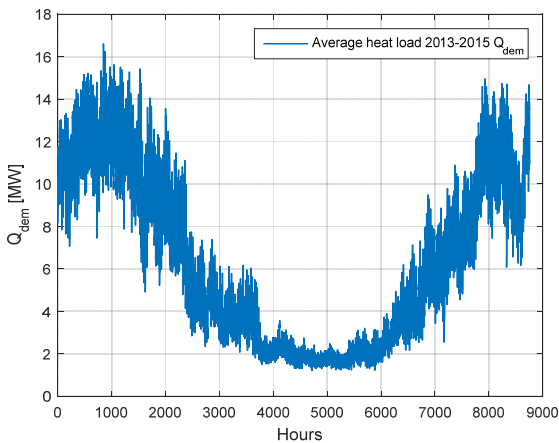


Figure 3. Example of annual the heat load curve in a sub-network

METHODOLOGY

The calculations for this project have been performed in MATLAB and are based on four years of measurements of heat consumption, volume flow and flow temperatures. Values in 15 min time steps for the solar radiation of an average day of each month were imported from PVGIS [5] for the specific location.

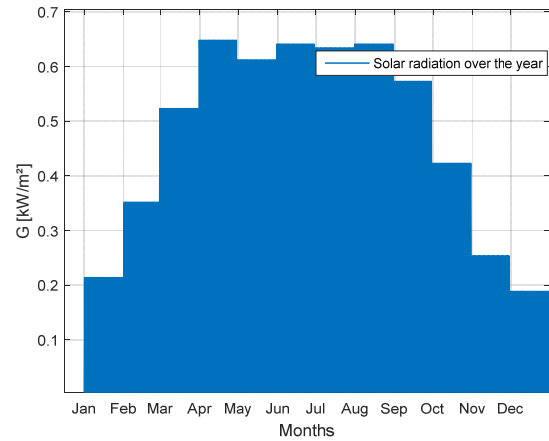


Figure 4. Example of maximum solar radiation on an average day on a south oriented 35° tilted surface in southern Germany

Additional weather evaluation has been performed using outdoor temperature data from 1974 to 2014 from Germany's National Meteorological Service (DWD) [6].

Figure 2 below visualizes the methodology in a flow-chart starting with the input over a decision in solar share, resulting in collector areas, storage sizes and finally an energy flow overview and a storage operation visualization.

Figure 3 shows the average heat load Q_{dem} of the given consumer, the sub-network of the years 2013-2015. The following figure 4 shows the solar radiation during a year on a surface tilted south with an angle of 35°.

Based on the smoothed outdoor temperature line of the average outdoor temperature from 1974 to 2014 given by DWD [6] and a graph displaying the required supply temperature to the sub-network, the time span from hour 3241 to hour 6337 of a year was calculated when the supply temperature is at its allowed minimum (Figure 5). In this time span the DH main-network could further decrease the supply temperature, if it could operate independently of the sub-network. The focus of this project was how the sub-network can be supplied by a solar heating system during this period.

The efficiency of solar collectors η_c was calculated according to the European Standard EN 12975 [7] as follows:

$$\eta_c(T) = \eta_0 - a_1 \frac{(T_m(T) - T_a(T))}{G(T)} - a_2 \frac{(T_m(T) - T_a(T))^2}{G(T)} \quad (1)$$

$$T_m(T) = \frac{T_{amb}(T) + T_{in}(T)}{2} \quad (2)$$

η_0 Collector zero-loss efficiency (-)

- α_1 First degree coefficients of the collector heat losses (W/Km²)
- α_2 Second degree coefficients of the collector heat losses (W/Km²)
- G Global radiation (W/m²)
- T_m Hourly medium temperature (K)
- T_a Hourly ambient temperature (°C)
- T_{out} Hourly collector outlet temperature (°C)
- T_{in} Hourly collector inlet temperature (°C)

- Q_{ch} Annual energy chosen to be supplied by solar (kWh)
- $Q_{sol,m}$ Specific net solar gain per month (kWh/m²)
- A Aperture area needed (m²)

Accordingly the net solar gain $Q_{sol}(t)$ is:

$$Q_{sol}(t) = \eta_c(t) \cdot G(t) \quad (3)$$

As the average global irradiance ins given in 15 minute steps the resolution was reduced to hourly steps in order to use the actual DH return temperature as collector inlet temperature T_{in} and the DH supply temperature as the collector outlet temperature T_{out} if it was above 80 °C, otherwise T_{out} was set to 80°C. The ambient temperature T_a was taken from PVGIS as well. The collector dependent values η_0 , α_1 and α_2 were taken from Solar Keymark Datasheets [8] of a representative flat plate collector (FPC) and a representative evacuated tube collector (ETC).

Area selection:

Field sizes were calculated depending on different annual solar shares of 5 %, 10 %, 15 % and 20 % of the total annual heat consumption. Additionally, one approach aims to supply the heat consumption of July completely, which corresponds to 13.2 % solar share, because this is the month with the lowest consumption throughout the year. The following calculation steps are used to receive the actual collector aperture area in m²:

$$Rel(t) = \frac{Q_{dem,m}(t)}{Q_{dem,an}} \quad (4)$$

$$Q_{sol,m}(t) = Q_{ch} \cdot Rel(t) \quad (5)$$

$$A = \max \left(\frac{Q_{sol,m}(t)}{\eta_{col,m}(T)} \right) \quad (6)$$

- Rel Relative monthly energy demand (-)
- $Q_{dem,m}$ Monthly energy demand by the sub-network (kWh)
- $Q_{dem,an}$ Annual energy demand by the sub-network (kWh)
- $Q_{sol,m}$ Monthly energy to be supplied by solar (kWh)

Figure 6 shows an overview of the different solar shares compared to the monthly energy demand. At an annual solar share of 13.2 % the solar heat energy fully covers the heat demand in the month of lowest demand (July). A higher annual solar share provides a surplus of solar heat during the summer that cannot be used.

Table 1 shows an overview of the calculated variations with the collector area, the relative storage dimension and the achieved CO₂ savings.

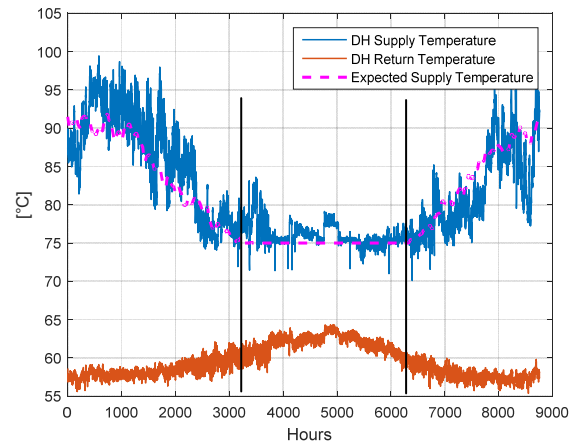


Figure 5. Average supply and return temperature and expected supply temperature of the sub-network

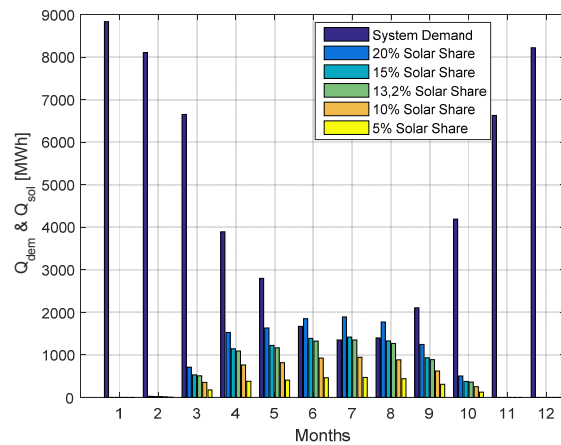


Figure 6. Net solar gain compared to demand for different solar share variations

Table 1. Calculation results for different annual solar share

Solar share	Collector area (m ²)	Specific storage volume (l/m ²)	Storage volume (m ³)	CO ₂ savings (t/a)
5 %	6467	7.3	47	480
10 %	12934	30.3	392	961
13.20 %	18481	39.5	730	1369
15 %	19401	40.5	785	1424
20 %	25854	46.2	1194	1725

Storage Dimensioning:

For this project it was required to store only the surplus solar heat that can be received within a single day and dimension the storage size accordingly. Figure 7 shows the solar surplus of each day that can be received when having an average load and a solar collector field size corresponding to the July demand (annual solar share of 13.2 %).

The conversion from MWh storage capacity to m³ water in storage capacity was performed according to the following formula:

$$V = \frac{Q_{st}}{\rho \cdot c \cdot (T_{max} - T_{min})} \quad (7)$$

- V Storage volume (m³)
- Q_{st} Storage energy capacity (MWh)
- ρ Density of water (kg/m³)
- c Heat capacity of water (Wh/(kg*K))
- T_{max} Maximum storage temperature (°C)
- T_{min} Minimum storage temperature (°C)

T_{min} is the maximum return temperature measured, 63 °C and T_{max} is the maximum allowed temperature in the storage 95 °C.

Storage operation:

To enable the sub-network to operate as independently as possible without having a backup boiler it is considered that the storage is reheated once per day. In this scenario the recharge from the main-network is set to be done every evening at 21.00 h with a supply temperature of 80 °C. This means that during summer time 3 different temperature zones will develop in the storage; one with the DH return temperature, one with 80 °C from the CHP plant and one with a maximum of 95 °C from the collector field.

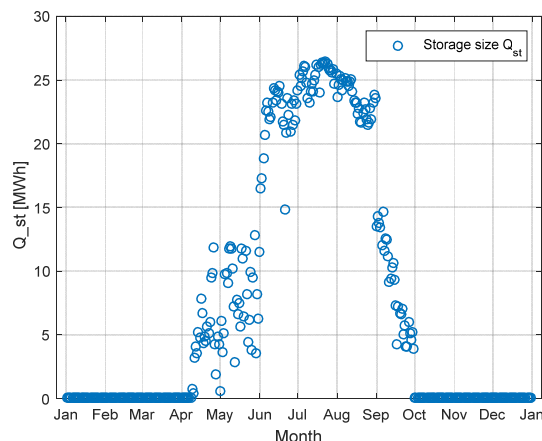


Figure 7. Needed storage capacity to store the solar surplus energy

RESULTS

The first thing to realize throughout the calculation was that the needed storage size to store a solar surplus was below 50 l/m² collector area. A relatively small dimensioned storage is also recommended by [2]. [2] also points out that a solar storage is normally not used for the largest part of the year. That the storage in this calculation is also only needed during the summer season can be seen in Figure 7.

Figure 8a shows the supply and demand curves for the summer season if a recharge every evening is done for a solar collector area of 18,481 m² which corresponds to 13.2 % solar share. Figure 8 b) shows the additional demand of the system, meaning the heat power that is needed at some hours to cover the demand of the sub-network if the storage is empty and not enough direct solar energy is available. Equation 8 below shows the relation between the different heat power terms:

$$\dot{Q}_{dem} = \dot{Q}_{sol,dtr} + \dot{Q}_{stb} + \dot{Q}_{add} \quad (8)$$

- \dot{Q}_{dem} Heat load of the sub-network (MW)
- $\dot{Q}_{sol,dtr}$ Directly used solar heat rate (MW)
- $\dot{Q}_{sol,stor}$ Stored solar heat rate (MW)
- \dot{Q}_{stb} Storage heat discharge rate (MW)
- \dot{Q}_{add} Additional heat supply rate (MW)
- Q_{re} Daily storage heat energy recharge (MWh)
- Q_{st} Level of storage charge (MWh)

Figure 8c and 9c display the storage charge and the energy the storage is charged with during the reheating process. In Figure 9a it can also be seen that when the storage is recharged, \dot{Q}_{dem} of the sub-network at that moment is covered by the main-network, too.

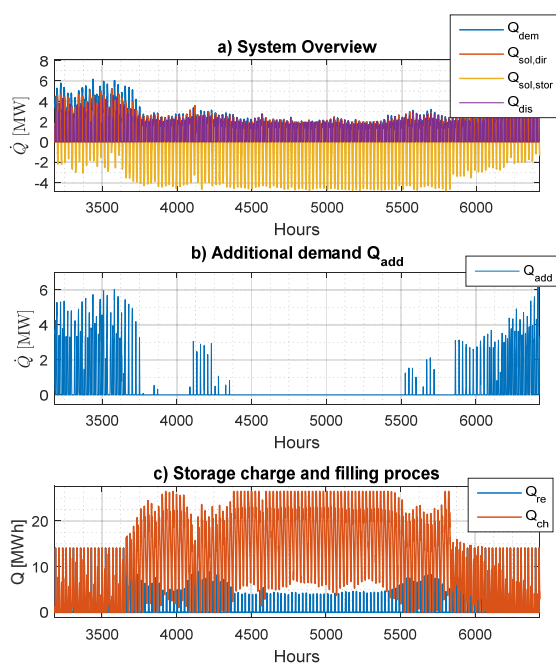


Figure 8. Supply and demand curves (a), additional heat power demand (b) and storage charging (c) during the summer season with 13.2 % solar share

While Figure 8 presents the complete summer season of a system with 13.2 % solar share, Figure 9 shows the supply and demand for the same system but this time only for 4 days. In Figure 9c, the excerpt of Figure 8c, it becomes visible that when the storage is empty, additional demand is needed from the main-network, visible in Figure 9b, at hours 4088, 4111 and 4135.

The optimal system choice is therefore an offset between a system that needs as little additional energy during the summer season as possible, with the aim to let the main-network operate as independent as possible and a system that has a collector area as little as possible to reduce the system costs as well as to reduce the losses during the summer due to storage limitations.

Figure 8 shows that a system of the given specification can supply the sub-network's demand during the summer season to a large extent independently of the main-network if an overnight charging of the storage to 80 °C is given. An increase from 13.2 % solar share to 20 % solar share will reduce the need for additional energy supply from the main network during the summer season but will also increase the losses of solar energy as the storage is not emptied for the largest part of the summer season. Furthermore, the difference in the collector area between 13.2 % and 20 % solar share is 7373 m² and will also have a large economic impact.

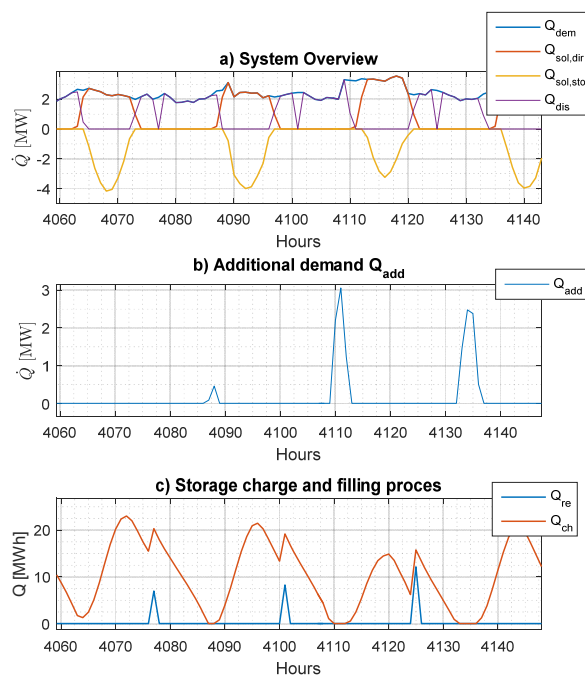


Figure 9. Zoomed in 4 days of supply and demand for the scenario with 13.2 % annual solar share

Q_{dem}	Heat load of the sub-network	(MW)
$Q_{sol,dir}$	Directly used solar heat rate	(MW)
$Q_{sol,stor}$	Stored solar heat rate	(MW)
Q_{dis}	Storage heat discharge rate	(MW)
Q_{add}	Additional heat supply rate	(MW)
Q_{re}	Daily storage heat energy recharge	(MWh)
Q_{ch}	Level of storage charge	(MWh)

Additionally, a decrease in CO₂ emissions, as visible in Table 1, is possible by up to 1725 t CO₂ per year in the case of 20 %.

DISCUSSION

The comparison of the presented results against results of a freeware calculation tool (SDH Online-Calculator [9]) with similar input data shows a generally good validity of the method. However, due to different methodological approaches the results cannot be compared to each other directly.

Firstly, the irradiation on the collector field was about 16% higher in this project. This is due to a different location that was chosen but most of all due to the different meteorological data source of both calculations.

Secondly, in case of higher collector outlet temperatures during summer, when the storage capacity is fully needed, the collector efficiency will decrease. This will reduce the net solar gains.

Thirdly, it has to be mentioned that losses in the piping system and the storage of about 5 to 10 % have to be added.

Fourthly, results in the CO₂ savings differ in this project compared to the SDH-Online tool as the CO₂-emission factor of 172 g/kWh for the given example DH system was used.

CONCLUSION

The integration of solar heat into existing DH systems brings benefits to a fossil CHP plant based system such as CO₂ reduction, primary energy factor improvement and operational flexibility. The possibility to supply a sub-network for certain periods of the year mainly by solar heat, allows an increasing efficiency of the CHP plant in the main network.

Furthermore it brings economic benefits due to the German CHP funding regulations. A solar thermal system enables the whole DH network to react better on future changes in the German electricity price market when it may be economically beneficial to decrease the energy production of the plant from an electricity production point of view.

The study shows that the accuracy of dimensioning a solar district heating system highly depends on the quality of the input data used. Calculations on the basis of annual data provide a rough idea on the necessary collector area and storage volume for a given heat demand. However, an exact dimensioning can only be done by using hourly-data of solar radiation and heat load for a whole year period.

The methodology for the integration of solar heat into DH systems that is presented in this paper leads to more detailed results and avoids over-dimensioning of solar fields and storage volume.

The example calculation shows that a solar thermal DH sub-network with an annual solar share of 13.2 % can be realised without auxiliary gas or biomass boiler, if a storage with recharging option is given. During the summer months the solar heat gains cover the total heat demand of the network whereas in other times of the year the main-network provides the additional heat. A short-term storage with a specific volume below 40 l/m² is sufficient.

OUTLOOK

The results of the presented calculations will be improved in the next phase of the project by optimising the storage recharging time and level as well as by

adding the piping system as a usable storage. In the example of a DN300 pipe without extractions an additional specific volume of 78 m³/km can be taken into account to store water at 80 °C for a short time once a day.

Furthermore an economic analysis will be undertaken in order to provide investment cost of the system as well as levelized costs of solar heat energy.

REFERENCES

- [1] M. . Fisch, M. Guigas, and J.-O. Dalenbäck, "A review of large-scale solar heating systems in Europe," *Sol. Energy*, vol. 63, no. 6, pp. 355–366, 1998.
- [2] R. Meißner, D. S. Abrecht, D. Beherrschen, D. Stagnation, F. E. E. Heizungsjournal-special, "Sinn und Unsinn von Solarspeichern," pp. 1–6, 2012.
- [3] Solites, "SOLAR-KWK Entwicklung multifunktionaler Systeme zur solar unterstützten Kraft-Wärme-Kopplung – solare Fernwärme und saisonale Wärmespeicher für die Energiewende," 2015.
- [4] T. Urbaneck, T. Oppelt, B. Platzer, H. Frey, U. Uhlig, T. Göschel, D. Zimmermann, and D. Rabe, "Solar District Heating in East Germany – Transformation in a Cogeneration Dominated City," *Energy Procedia*, vol. 70, pp. 587–594, 2015.
- [5] European_Commission, "PV GIS." [Online]. Available: <http://re.jrc.ec.europa.eu/pvgis/apps4/pvest.php#>. [Accessed: 10-May-2016].
- [6] Deutscher Wetterdienst, "DWD Deutscher Wetterdienst." [Online]. Available: <http://www.dwd.de/DE/leistungen/klimadatendeutschland/klimadatendeutschland.html>. [Accessed: 10-May-2016].
- [7] P. Kovacs, "A guide to the standart EN 12975," 2012.
- [8] "The Solar Keymark Database." [Online]. Available: <http://www.solarkeymark.dk/>. [Accessed: 10-May-2016].
- [9] Solites & AGFW, "SDH Online-Calculator." [Online]. Available: www.sdh-online.solites.de. [Accessed: 10-May-2016].

STATUS OF H2020 STORM-PROJECT

D. Vanhoudt¹, B. Claessens¹, J. Desmedt¹, C. Johansson²

¹EnergyVille/VITO, Thor Park 8310, Genk, 3600, Belgium

² NODA, Biblioteksgatan 4, Karlshamn, 374 35, Sweden

Keywords: *district heating and cooling networks, intelligent control, algorithm*

ABSTRACT

This paper describes the progress of the Horizon 2020 STORM-project, started in March 2015. The objective of this project is to develop and demonstrate a generic district heating and cooling network controller. Generic in this sense means that the controller is applicable to widely spread 3rd generation, but also very innovative 4th generation networks. Therefore, the controller will be tested in a traditional district heating scheme but also in an advanced low-temperature network.

The controller influences the demand of the network to achieve a certain objective. STORM focuses on three objectives: (i) a peak shaving objective used to minimize the use of often polluting peak boilers; (ii) a cell balancing objective striving to balance a cluster of consumers to producers of excess heat or/cold; and (iii) a market interaction objective, applicable for heat/cold producers with a connection to the electrical grid (heat pumps or CHPs), maximising the profit for the producer by switching these devices based on the electricity price.

To guarantee the generic applicability of the controller, self-learning control techniques are used. These techniques have the advantage that they 'learn' the behaviour of the network by themselves without the need to be extensively tuned at the installation (plug-and-play installation).

To date, the focus was on algorithms for a forecast module of the heat/cold consumption of the network. These algorithms are already implemented in the controller platform and were running in real-time in one of the demonstration sites. Also, a tracking module was already developed and is currently tested. This module which will try to match the actual network consumption to this optimal consumption profile by distributing the control signals to the right heat consumers. Next step is the implementation of a planning module, which determines the optimal consumption profile, taken into account the forecasts.

INTRODUCTION

Since heating represents 42% of the final energy consumption in the EU in 2011, compared to 21% for electricity, 28% for transport and 9% for non-energy use [1], the heating and cooling sector has the largest potential on greenhouse gas emission reductions. DHC

networks are very interesting technologies in this context, since investment in waste energy extraction for industry and in renewable energy sources is often too expensive for a single party. However, these sustainable energy sources have a large drawback. Opposite to traditional energy sources, they are often not controllable: thermal energy from the sun is only available when the sun shines, and since waste heat is per definition a waste product: companies are not willing to adjust their production to suited moments. Therefore, in combination with the addition of thermal storage capacity, demand side management in DHC networks - i.e. adjusting the demand of energy to the actual production - is an enabling technology. Demand side management can also make it possible to deliver more energy from a smaller sustainable energy source by applying a peak shaving control strategy limiting the demand of energy to the capacity of the source. Therefore, by applying demand side management DHC networks become 'smart', undergoing the same transition as the transition towards smart electricity grids.

The implementation of smart DHC networks has another large benefit: smart DHC networks can even support smart electrical grids, provided there is a connection between the two, as is the case for heat pumps or CHPs. As a result, smart DHC networks can not only reduce greenhouse gas emissions in the DHC network itself, but also at the production site of the electrical grid. Therefore, intelligent controlled DHC networks are indispensable systems in the transition towards zero carbon solutions.

Demand side management could therefore make existing networks more sustainable. However, to fully maximize the share of renewable energy and waste energy in DHC networks, a next step must be taken, a step towards a new generation of DHC networks: one speaks about the fourth generation [2]. This generation of networks is especially designed to deal with the fluctuation character of renewable energy sources and waste energy flows (Fig. 1). Evidently, also in these new networks, an intelligent control framework is essential. Ideally, this controller must control both the demand and production of heat and cold, taking into account the state of charge of the different storage capacities in the network.

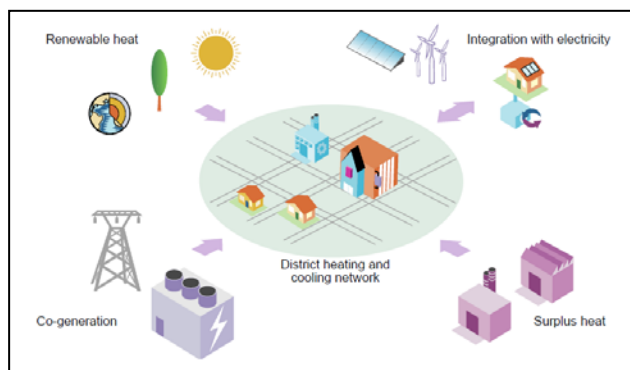


Fig. 1: The 4th generation DHC network. (Source: International Energy Agency)

It is in this field that STORM positions itself. Within the STORM project (approved in the H2020 EE13 2014-call, under ID number 649743), a controller is developed starting for state of the art control algorithms suited for both existing and new, 4th generation DHC networks. By harvesting the flexibility in this wide range of networks, the controller will contribute to a more sustainable energy mix of renewable energy and waste heat utilization.

OBJECTIVES OF STORM

In the project, 6 main objectives are identified:

1. **Development** of a generic controller for district heating and cooling (DHC) networks. The controller will be applicable to a wide range of DHC networks and will enable a significant increase of the use of waste heat, energy exchange and renewable energy sources in the DHC networks. The generic nature of the intelligent controller guarantees wide-range replicability.
2. To demonstrate this generic applicability, the controller will be **implemented and tested** in two existing DHC networks, i.e. a traditional medium temperature network in Rottne (Sweden) and a highly innovative low-temperature (28°C) 4th generation network in Heerlen (the Netherlands).
3. During the test cycles, the benefits of the developed generic control will be **quantified**. For this purpose, performance indicators will be closely monitored during two heating (and cooling) seasons and compared with reference data.
4. Development of **innovative business models** needed for the large-scale roll-out of the newly developed controller and to bring down energy costs. The new controller will create additional benefits, which should be distributed over the different market players.

5. **Increase awareness** of the need for smart control of DHC networks and quantify and demonstrate the benefits of smart control, through international dissemination and local dissemination platforms.
6. **Ensure market-uptake** of the new technology by investigating exploitation possibilities of the newly developed technology.

GENERIC FEATURES OF THE CONTROLLER

Wide-range replicability is the leading thread through the STORM project. This is realized by the following measures:

- **Add-on to existing controllers.** Today's DHC networks are controlled by different kind of controller, such as SCADA-systems (Supervisory Control and Data Acquisition), developed by different producers and often using specific communication protocols. To become generic, the STORM-controller will be an add-on to a large share of these existing controller systems.
- **Open-source protocols.** In order to ensure broad market compatibility, the control platform will use open-source protocols and standards. In this way, hardware manufacturers can develop compatible hardware components.
- **Self-learning algorithms.** A technical barrier for the large scale penetration of smart control of DHC networks is the complexity of developing and tuning the necessary models as it requires a significant amount of expensive expert knowledge. To help in mitigating these problems the control framework developed in STORM will focus on developing self-learning and self-adaptive control which is stooled upon combining recent developments in model-based multi-agent systems and model-free control (by means of reinforcement learning techniques).
- **Multiple control strategies.** Different networks ask for different optimization strategies (see further). Three strategies will be available in the controller, of which one or more can be enabled, dependent of the specific nature of the network.
- **Multiple thermal storage concepts.** Finally, the controller will have to able to deal with a number of thermal storage concepts. In most common district heating grids, a central storage tank is present next to the central heat production unit. Besides the short-term storage function, such tank is often used as a hydraulic separation between the

production unit and the DHC network. In more innovative grids, the storage capacities are often multi-levelled and decentralized, serving a small number of buildings or even a single building. In its most advanced way, the thermal mass of the building can even be used as a storage capacity. In next generations of thermal networks, also long-term thermal storage technologies like pit-storage or geothermal energy storage (e.g. the mine water storage in the demonstration site in Heerlen, the Netherlands) will be integrated. The control framework will be to take all these forms of storage into account.

MULTIPLE CONTROL STRATEGIES

A consequence of the generic character of the controller is that the controller must be able to deal with a number of control strategies since not every grid operator has the same objectives. The most obvious ambition could be balancing of the demand and production within a local cluster of producers and consumers of heat and/or cold. In this **'cell balancing'** control strategy the cluster will try to be as self-sufficient as possible. This means that energy exchange within the cluster is maximized, and only when an imbalance in the cluster persists, energy is exchanged with the higher transmission network. The motive for this control strategy is twofold. Firstly, since balancing is pursued within a cluster, the distance for energy exchange is minimized and as a result, also the thermal distribution losses. Secondly, since energy exchange with the higher transmission network is reduced, this transmission grid can supply more distribution grids. This leads to a more energy and cost efficient management of the energy system and associated benefits for energy suppliers, heat/cold producers and end users. Also, extensions of the thermal network are possible without additional costs to increase the capacity of district heating grids.

A second interesting objective is a **'peak shaving/valley filling'** control strategy. In a lot of smaller district heating grids supplied by a sustainable source (like e.g. CHP), the source is not dimensioned for peak load conditions. The reason is the investment costs for these sources are usually high and that peak load conditions only occur a number of hours per year. The high investment costs don't pay off for this limited number of running hours. Therefore, in these grids the sustainable source is assisted by cheaper fossil fuel fired sources, like gas boilers for example serving as peak production units. By applying peak shaving and valley filling control strategies, the number of running hours of these peak units can be minimized, and as a result the operation hours of the sustainable source will be maximized. In this way it is possible to increase the

share of renewable energy or waste energy in the thermal networks and to lower the energy production costs.

In the last control strategy the DHC network provides balancing services to the electrical grid, later called the **'market interaction'** control strategy. As explained above the clue in smart electrical grids lies in the creation and application of flexibility. When both grids are coupled, for example by means of a heat pump and/or a CHP, the intrinsic flexibility in the DHC network can be used to control these heat pumps or CHPs depending on prices on the day-ahead and intraday market, and therefore increase the production unit owner's profit. Another advantage is that this control strategy supports a production-mix with a high share of renewable energy at system level in this way.

When too much electricity is produced by wind turbines or solar photovoltaic panels for example, prices will be low, engaging heat pumps to switch on and CHPs to switch off. Contrary, because of high spot prices, heat pumps will be switched off and CHPs will get switched on when renewable sources are inactive.

A schematic overview of the STORM controller is presented in Fig. 2.

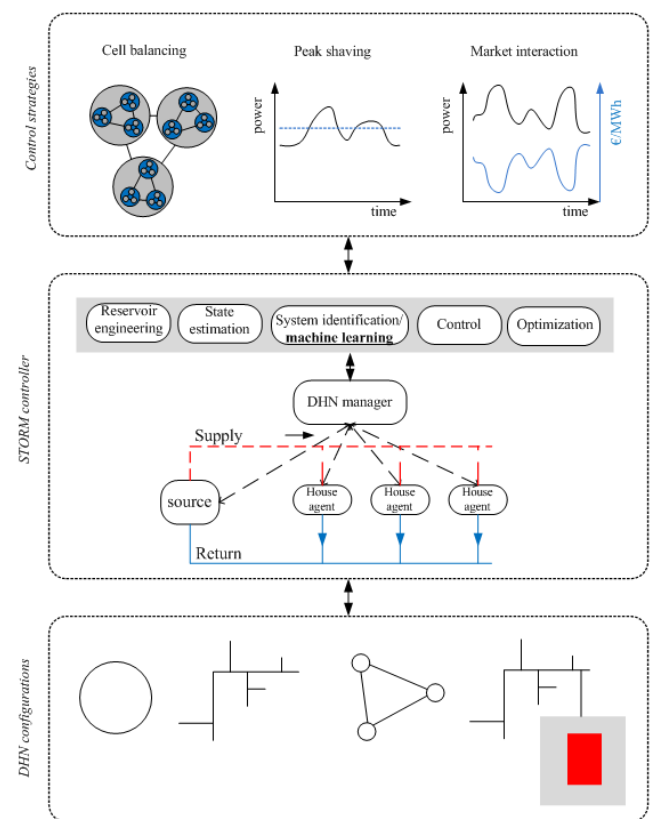


Fig. 2. Schematic representation of the STORM controller

CONTROLLER APPROACH

Smart DHC-network control

The controller developed in STORM builds partially on established research performed in the field of cluster control of thermostatically controlled loads (TCLs) in electrical grids. Examples of TCLs are water heaters, heat pumps, refrigerators, freezers, air conditioners or cooling machines. These are excellent candidates for demand side management due to their intrinsic flexibility provided through direct (e.g. hot-water storage) or indirect storage (e.g. thermal inertia of building). Control of these TCLs has received considerable attention in recent literature [3][6].

Translation to optimal control of DHC networks

When implementing a control concept at the level of a DHC network, be it centralized or distributed, one is confronted with (1) the non-linearities in the dynamics of a DHC network, and (2) the slow time scales compared to e.g. an electric network [7]. Taking these effects into account is essential for a good performance of the controller. To this end, several approaches using model-based optimization techniques have been identified in literature, explicitly incorporating the dynamics of the DHC network. For example in [8],[9] Model Predictive Control (MPC) solutions have been presented. Although model based solutions can have excellent performance, they require an accurate model of the DHC network and the consumers coupled to the DHC network. Tuning and shaping these models is considered an “expert task” making a generic roll-out of this technology challenging.

In contrast with a model-based approach, a scalable auction-based multi-agent control for integrated heat and electricity management has been presented in [10]. Here consumers and producers connected to the DHC network can interact through a multi-commodity bid-function, representing the cost for local consumption or production, both thermal and electric. Although this approach has an intrinsic scalability and practicality, the lack of dynamics (mainly delays) related to heat transport is expected to have a significant impact on the controller.

Beyond state-of-art: reinforcement learning as the breakthrough

In order to tackle the issue of scalability and modelling, STORM intends to build upon state of the art in market-based multi-agent systems in combination with the most recent advances in reinforcement learning, i.e. model free control approach. Combining these

techniques is expected to result in a scalable and performant self-learning control approach requiring limited expert knowledge, supporting a generic “roll-out” of STORM technology.

In recent work, VITO have been working with success on combining reinforcement learning at an aggregated level with an auction-based multi-agent system for the control of a large cluster of TCL's [11] and TCL's connected to a DHC network [12]. In this work excellent performance was obtained within a limited learning time of approximately 20-50 days.

BRIEF WORK PACKAGE DESCRIPTIONS

WP1: Definition of the features of the controller

In this preparatory work package, the boundary conditions of the project are determined. Three tasks were identified.

Firstly, a market analysis is performed on the DHC-networks in the EU, with the aim to determine the applicable control strategies of the networks. Therefore, the networks are categorised based on the main technical and operational characteristics of these networks. After this, for every type an analysis will be performed on which control strategy (e.g. peak shaving, cell balancing, and market interaction) is applicable.

Secondly, the two demonstration sites are analysed, to derive specific characteristics in the view of the testing and evaluation program. This ensures the compatibility with the existing control systems in the network.

Finally, decision parameters are defined for the controller with respect to the business models of DHC network operators. These parameters are needed to deal with sometimes contradictory objectives: on the one hand the optimizing process of the controller must serve these operators in the fulfilment of their day-to-day business, on the other hand the controller should meet maximal energy savings.

WP2: Simulation based controller and model development

In this work package the actual control algorithms are developed. Therefore, a simulation environment for the two demonstration sites is developed. This simulation environment is needed to test and to optimize the developed algorithms before transferring the algorithms to the actual STORM software.

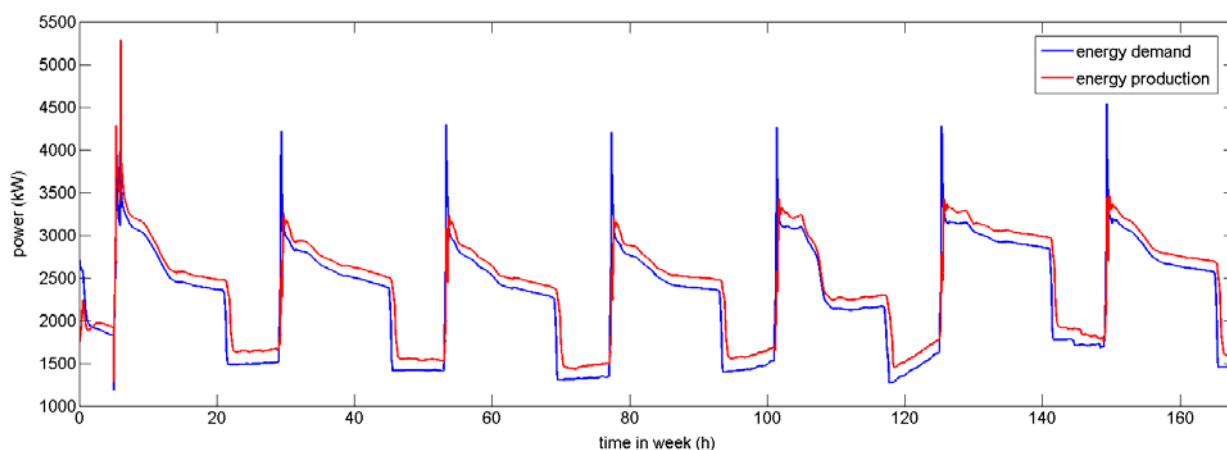


Fig. 3: Results from the Rottne simulator

Then, the self-adapting DHC network controller algorithms are developed built upon a multi-agent system, for the three main control strategies regarded in STORM. Attention is given to the field-tests so that the STORM algorithms do not have more information than is reasonably available at the demonstration sites. Also, the resilience of the controller developed will be evaluated for a range of disturbances such as missing or delayed communication, extension of the customer portfolio, user behaviour...

WP3: Development of controller framework prototype

In this work package, the algorithms developed in WP2 will be integrated in the software and hardware platform. This implementation will include software running on both the local hardware platform as well as on the server-side system, since the algorithms relate to both local and global optimization schemes.

Furthermore, a test-bed will be developed where the controller framework can be tested and evaluated on a small off-site scale before the full on-site implementation and evaluation in WP4 and WP5.

WP4: Implementation of controller framework prototype

This work package deals with the implementation of the controller platform in the two demonstration sites.

Firstly, for preparing the on-site implementation, a protocol for verifying the operational functionality of the system will be developed. A systematic failure analysis technique based on FMEA (Failure Mode and Effects Analysis) will be incorporated in the protocol.

Then, the controller developed and tested during WP3 will be transferred to the two demonstration sites, and will act there as an add-on to the existing DHC controller. A work plan will be used as a basis for the

installation work at both demonstration sites during the project. This work plan includes all required documentation for the system.

Next, the on-site verification is performed. This is done in order to ensure that the system conforms to the requirements specified in previous work packages.

WP5: Testing and evaluation of the performance

In this work package, the performance of the controller will be evaluated.

In order to compare the performance of the intelligent STORM-controller, first reference data should be generated. Therefore, during the first heating season of the project (M06-M14) measurements are undertaken in the demonstration sites with the existing controller. All important information is monitored.

In the next heating seasons, the actual performance of the controller will be tested. This testing period will cover two heating seasons. In this way, lessons learned from the first season can be assimilated and extra features can be added to the controller framework (e.g. weather forecasting) before the second heating season.

Finally, the data collected from the test period will be extensively analysed with regards to the performance of the develop controller framework. The outcome of the technical, business, sustainability and financial elements will be considered.

WP6: Replication and dissemination activities

In this work package, qualitative and quantitative business models for smart DHC networks will be developed.

Furthermore, in this work package, measures are taken to replicate the developed controller to other networks in other countries.

Communication and dissemination activities are also part of this work package. Besides the international dissemination, also two local dissemination platforms will be implemented around the demonstration sites, in order to target all local stakeholders (the energy company, users, local educational institutions, local politicians...).

Finally, educational packages are developed that will be implemented in the education in the University of applied science. They consist of a basic preparation package, a theoretical educational package and a practical educational package with real life learning cases. Moreover, training courses for professionals will be developed.

WP7: Project Management

This work package comprises all activities with respect to project coordination, project quality assurance and risk control and consortium management.

THE STORM CONSORTIUM PARTNERS AND THEIR ROLES

The Project Coordinator **VITO** has experience in multiple disciplines included in the STORM project targets and objectives (DHN control algorithm development, business model development...), ensuring the necessary cohesion between the different work packages. Within STORM VITO is responsible for the development of the controller algorithms.

NODA is an industrial SME active in DHC networks controllers for 10 years, and therefore has experience in developing and implementing innovative ICT solutions for DHC networks in real projects. Its presence in the consortium ensures that the developed algorithms are transformed into real products, in line with the current best practices and addressing today's market needs. NODA will therefore implement the control algorithms in their existing hard- and software platform.

The two demonstration sites are operated by **VEAB** (Rottne) and **Mijnwater** (Heerlen). They contribute to the project by their practical knowledge of the network to the tasks concerning business models, decision parameters, replication measures e.g. Furthermore, they play a large role during the demonstration phase of the project.

NEBER is a local university, located in the Netherlands. In this project, they will act as an independent party responsible for the quantification of the performance of the intelligent controller, by analysis and comparing the results of the test runs to the

reference data. Furthermore, NEBER is responsible the development of the educational packages and for the local dissemination platform in Heerlen.

Finally, communication and dissemination activities are coordinated by the partner **Sigma Orionis**, specialized in producing a comprehensive dissemination and awareness plan suitable of increasing the potential impact of the proposed initiative towards targeted communities throughout Europe and beyond.

STATUS OF THE PROJECT

The project started in March 2015. Therefore, by the submission of this paper (May 2016), the project is in month 15 of 42.

To date, the following results are achieved in the different work packages:

WP1: Definition of the features of the controller.

The classification of DHC-networks in operation was made, and will be made publically available on the STORM-website. This report gives an insight in the coverage and markets of DHC in Europe, the share of renewable in DH, future energy demands, barriers for DHC networks, potential greenhouse gas reductions, business cases, used control strategies, future trends in DHC and the needs for intelligent control of DHC networks.

Furthermore, technical audits were performed in the demonstration site to prepare the implementation of the controller.

Finally, a draft version of a report on the decision parameters of the controller was prepared. Based on the classification report as described above, in this report the technical requirements of the STORM controller are described. These parameters serve as an input for the algorithms that are developed in WP2.

WP2: Simulation based controller and model development.

To date, the simulation model for the Rottne network is finished, and the model for Heerlen is getting finalised.

The simulation models consist of a model for the connected buildings and a network model. The buildings are modelled as lumped capacitance models. These building models determine the power exchanged by the network, and the return temperature to the network, given a certain supply temperature.

The network model is an implementation of the node-model by Benonysson [13]. This network model

simulates the flow rates and temperature propagation through the network pipes.

A first result for the Rottne network is shown in **Fig.** It can already be seen that night set back in the network is problematic, since it causes power peaks in the morning. This is obviously the first issue to solve before the implementation of the controller.

Furthermore, in this WP, a technical ‘problem formulation’ for the controller was prepared. This describes the exact control problem and the optimization and control approach in a mathematic manner, and is the basis for the development of the algorithms. The controller will consist of three modules: a forecaster, a planner and a tracker. The forecaster will forecast the undisturbed heat and cold demand of the network. The planner will then determine the optimal heat demand profile for the next 24 hours, taking into account this forecast and also the objective that should be achieved in the network (i.e. peak shaving, cell balancing, market interaction, or a combination). Then the tracker module will try to make sure that the this optimal profile is actually achieved. Therefore it will make use of a dispatcher, which calculates individual control signals for all connected buildings, in combination with a feedback loop to eliminate deviations.

With respect to the development of the algorithms itself, the focus in this first phase of the project was on the development of a forecaster. Machine learning techniques were used to forecast the heat demand of a building or cluster of buildings for the coming 24 hours, taking into account the historical consumption of the building, the time and the forecast of the outdoor temperature for the next 24 hours. Also a first prototype of a tracker algorithm was developed so far.

WP3: Development of controller framework prototype.

Hardware adaptations for the existing controllers in the different networks were already prepared, and tested on some sites in Sweden. This is done to smoothen the implementation of the developed controller as much as possible.

Furthermore, the forecasting algorithms developed in WP2 were implemented in the controller platform and tested in the Rottne site. Without going into details in this paper, Mean Absolute Percentage Errors (MAPE) as low as 6-7% were achieved in the most optimal conditions. A lot more details on the forecast module and its performance in the real-life field tests can be found in a dedicated paper which is also presented during this symposium [14].

Finally, the prototype tracker algorithms were also implemented already in the controller platform and tested in the Rottne network. However to date no results of its performance can be reported yet.

WP4: Implementation of controller framework prototype.

This work package has not started yet.

WP5: Testing and evaluation of the performance.

This work package has not started yet.

WP6: Replication and dissemination activities

First steps are taken in the set-up of the exploitation plan.

A dissemination & communication plan (DCoP) was developed. This plan will be updated again in M18.

With respect to communication activities, a project website was set up (<http://www.storm-dhc.eu>) and joint social media accounts with 3 other EU projects were created: twitter @sustainplaces, LinkedIn group “Sustainable Places Community”. Also a first edition of the newsletter was released in M8.

Project logo, project posters, leaflets, presentation and document templates were prepared.

Regarding dissemination actions, in the coming weeks, two local dissemination workshops will be organised. One in Stockholm on May 18, and one in Heerlen on May 27. Also joint workshop with related initiatives and projects will be initiated.

ACKNOWLEDGMENT

The authors gratefully acknowledge the financial support of the funded project by the European Commission, granted in the Horizon 2020 EE13 2014-call on ‘Technology for District Heating and Cooling’, under no. 649743.

REFERENCES

- [1] A European Strategy for Sustainable, Competitive and Secure Energy, European Commission, Green paper, 2006.
- [2] Lund, H., Werner, S., Wiltshire R., et al., 4th Generation District Heating (4GDH): Integration smart thermal grids into future sustainable energy systems, 2014. Energy 68 (1): p. 1-11.
- [3] Koch, S., Mathieu, J. L. and Duncan S. Callaway. Modeling and control of aggregated heterogeneous

- thermostatically controlled loads for ancillary services, Proc. PSCC. 2011.
- [4] De Ridder, F., Claessens, B., Vanhoudt, D., et al. On the coordination of residential consumption in the interest of distribution system operators and balance responsible parties, submitted to ETEP.
- [5] Vanthournout, K., D'hulst, R., Geysen, D., et al., A Smart Domestic Hot Water Buffer, IEEE Transactions on Smart grid, 2012, vol.3 (4): p. 2121 – 2127.
- [6] Johansson, C., Towards Intelligent District Heating, Blekinge Institute of Technology Licentiate Dissertation Series No. 2010:06.
- [7] Vanhoudt, D., Koene, F., D3.2 Report on a combination of thermal storage techniques and components, 2013. FP7 E-hub project grant no. 260165.
- [8] Benonysson, A., Bøhm, B., Ravn, H.F., Operational optimization in a district heating system, 1995. Energy Conversion and Management 36 (5):p. 297-314.
- [9] Sandou G., Font S., Tebbani S., et al., Predictive Control of a Complex District Heating Network, 2005 Proceedings of the 44th IEEE Conference on Decision and Control, and the European Control Conference, Seville, Spain, December 12-15 2005, p. 7372-7377.
- [10] Booij, P., van Pruissen, O., Warmer, C., Multi-agent control for integrated heat and electricity management in residential districts, ATES 2013, Minnesota, USA, 6-7 May 2013.
- [11] Ruelens, F., Claessens, B., Vandael, S., et al., Demand response of a heterogeneous cluster of electric water heaters using batch reinforcement learning, Proceedings. PSCC. 2014.
- [12] Claessens B., Vanhoudt, D., Applying Batch Reinforcement Learning for the control of a District Heating Network, submitted for publication.
- [13] Benonysson A., Dynamic modeling and operational management of district heating systems, Technical University of Denmark (DTU) PhD dissertation, 1991.
- [14] Johansson, C., Bergkvist, M., De Somer O. et al. Operational demand forecasting in district heating systems using ensembles of online machine learning algorithms, 2016 Proceedings of the 15th International Symposium on District Heating and Cooling, Seoul, Korea, September 4-7 2016.

MEASURED LOAD PROFILES AND HEAT USE FOR "LOW ENERGY BUILDINGS" WITH HEAT SUPPLY FROM DISTRICT HEATING

Rolf Ulseth¹, Karen Byskov Lindberg², Laurent Georges², Maria Justo Alonso³, Åmund Utne⁴

¹ SINTEF Energy Research, Trondheim, Norway

² Norwegian University of Science and Technology (NTNU), Trondheim, Norway

³ SINTEF Building Research, Trondheim, Norway, ⁴ Statkraft Varme AS, Trondheim, Norway

Keywords: District heating, Load profiles, Heat use, Low energy buildings

ABSTRACT

In the development towards nearly zero energy buildings (nZEB) the load profiles for the heat demand and the heat use of the buildings are expected to be changed considerably compared to the situation today. This change will influence the design and the overall profitability of district heating (DH).

It is expected that the amount of heat for domestic hot water (DHW) in all types of "low energy buildings" (LEB) will remain relatively unchanged in the future even if the heat demand for space heating and may be also for heating of ventilation air will be reduced. This means that the heat use for DHW will be relatively more important for the economy of DH in the future.

From earlier heat use measurements we have already seen that the real heat use of LEB, for several reasons, quite often seems to be somewhat higher than the values from theoretical calculations.

This means that knowledge on measured values of the total heat load profiles and the heat use from all types of LEB will be important for evaluating the economy and the competitiveness of DH in the future.

The primary goal of the paper is to present measured load profiles and yearly heat use for three different blocks of flats connected to the DH-system in Trondheim, Norway. The official dimensioning outdoor temperature in Trondheim is -19°C.

The presented load profiles show statistical hourly mean specific maximum values for the three buildings. The paper also presents specific values for the yearly heat use and the outdoor temperature value when the heat demand goes down to zero. This temperature value is called the change point temperature (CPT).

Some considerations of the system efficiency of the DHW system in the buildings are also given. The presented information is assumed to be useful in the planning of DH-systems for the future.

INTRODUCTION AND BACKGROUND

As a reference to the two LEB in this study, one of the three buildings is built according to the technical

building code in Norway from 2010 (TEK10). The other two are built according to the actual Norwegian guidelines: *Norwegian standard, NS 3700:2010, Criteria for passive houses (PH) and low energy (LE) houses – Residential buildings* [1] where LE has two classes. One of the two LEB is built to meet the LE criteria (class 1), and the other one to meet the PH criteria in these guidelines.

In new built LEB connected to district heating in Norway, it is today quite common to install some sort of heat pumps in the buildings. One of the reasons for this is that according to the special requirements on the energy performance certificate for buildings in Norway, it is hard to get an A rated building when the heat supply to the building is district heat only.

Both the LE and the PH building in this study have a heat pump installation to supply base load heat. The LE building has a ground source heat pump (LE+hp), and the PH building gets heat from a condenser of a cooling system in a neighbouring shopping centre - (PH+hp).

All three buildings have so called "balanced, mechanical ventilation" with heat exchangers (HE). The requirement for the efficiency of the heat exchangers is $\geq 70\%$ for the LE buildings and $\geq 80\%$ for the TEK10 and the PH buildings. Detailed specifications of the three buildings are shown in Table 1.

Table1. Specifications of the three buildings

	TEK10	* LE+hp	PH+hp
Total heated area of the blocks (m ²)	~3750	~3400	~2380
Number of flats	49	39	26
Average heated area per flat (m ²)	~77	~87	~92
Ventilation air (m ³ /h•m ²) (Min. average values)	≥ 1.2	≥ 1.3	≥ 1.3

* The heating system in this building is providing some heat to a car shed and also to a smaller snow melting area.

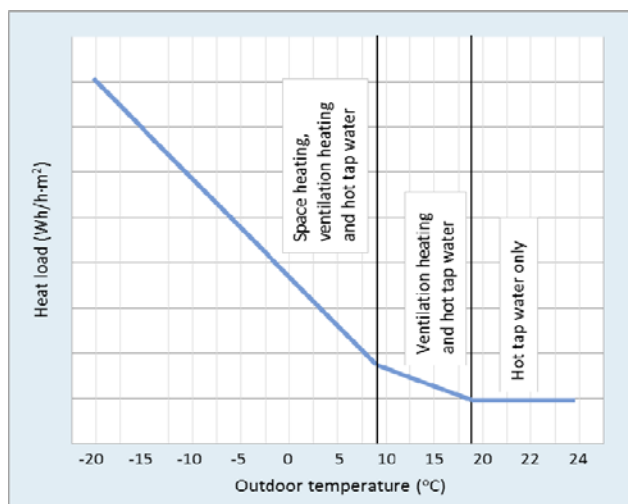


Figure 1. Generalised, theoretical HT-curve [4]

To get a reasonably good picture of the real heat use of a building often so called heat load-temperature, HT-curves, are used. Here the measured heat load values are correlated to the actual outdoor temperature.

Figure 1 shows a basic, theoretical curve of the heat load correlated to the outdoor temperature in a building that has heat demands for space heating, heating of ventilation air and hot tap water.

We see from figure 1 that the theoretical curve has two buckling points. The first one from the left shows the outdoor temperature where the space heating demand becomes zero. The second one shows the outdoor temperature from which it is only heat demand for DHW. In between these buckling points some heat is needed for heating the ventilation air. The slope of the curve in this area depends on the amount of ventilation air, the efficiency of the heat exchanger in the ventilation system, and the ratio between the heat demand for space heating and for ventilation air.

To decide the best estimate of the curve in figure 1 from measured data we need to perform a statistical regression analyse of the measured values. For several natural reasons the measured values may vary quite a lot for a certain outdoor temperature. The resolution on the heat load axis in such diagrams will normally be mean values for one hour, one day or one week. In the actual work the resolution is one hour.

In older days, where the buildings had no mechanical ventilation, the actual curve had only a buckling point where the heat for space heating and natural ventilation becomes zero. Even today it is common to make the statistical analysis for such curves only with one buckling point called the change point temperature (CPT). This point represents the outdoor temperature for which the heat demand for space heating and ventilation air

becomes zero. For the most common buildings this is assumed to give an acceptable picture of the heat use of the buildings. The statistical analyses in this work are done with only one CPT.

METHODS/METHODOLOGY

The load profiles are developed from measured hourly values of the delivered district heat to the blocks of flats. The DH-system is own by Statkraft Varme AS in Trondheim who has provided the measured data.

The measured hourly values are treated statistically mainly by the statistical tool STATA [2]. More detailed results from these statistical analyses will be presented in an ongoing PhD-work at NTNU in Trondheim, Norway [3]. Some results are also derived by a method developed through the work on a PhD theses [4] made at NTNU.

STATE OF THE ART

To make measurements of the heat demand of buildings have until the latest years been time consuming and rather expensive. There are therefore not shown too many results from such measurements in the literature. The ongoing effort to reduce the heat use in new buildings gives a running need to do measurements and document the actual improvements of the heat performance of new categories of LEB compared to theoretical calculations.

RESULTS

Figure 2 shows the actual measured values and the regression model values that make up the HT-curve for the PH+hp building for hour 10 on week days (WD). For week ends (WE) we get similar, but somewhat different, curves depending on changes in the activity in the building. Similar HT-curves are made for all 24-hours to get the complete picture of the variation of the heat load. We see that the lowest measured outdoor temperature in the actual measurement period is -11°C.

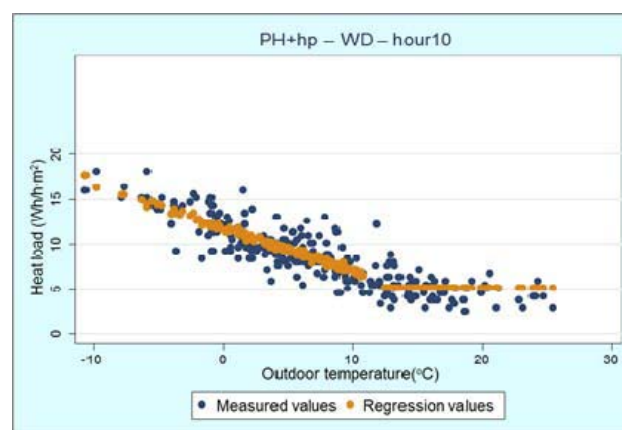


Figure 2. HT-curve for hour 10 on weekdays [3]

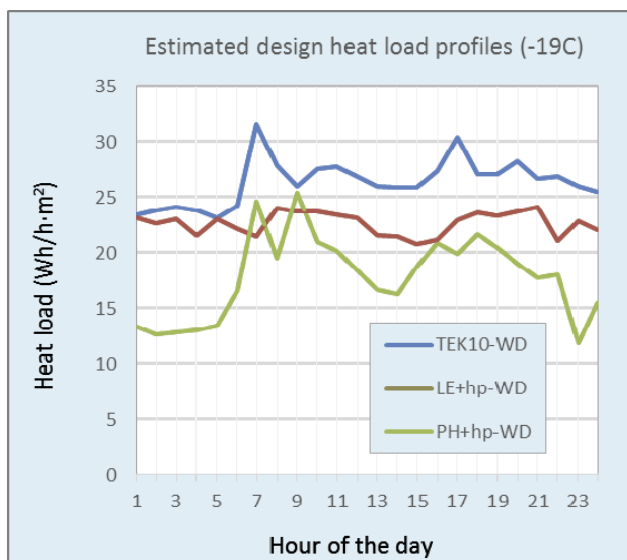


Figure 3. Design heat load profiles (WD) [3]

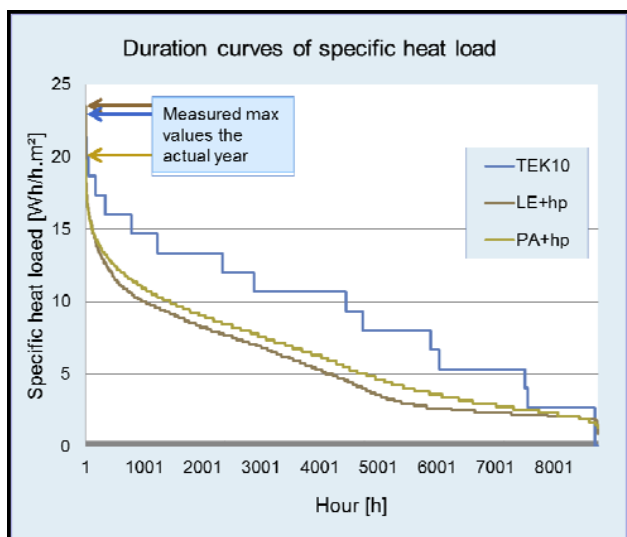


Figure 4. Calculated duration curves of measured specific heat load for the three buildings [4]

The measured district heat load values of a certain hour are depending on several other factors than the outdoor temperature in the actual hour. Depending on e.g. the thermal mass of the building we will have a time delay effects from the temperatures in earlier hours. By adding a third term to the linear equation you may get a better fit to the measured values.

From figure 2 we might-be able to see that the red-orange regression values do not make a complete straight line. This is due to the fact that in this paper a time delay term is added to the linear equation.

Normally it is considered satisfactorily to make a pure linear regression analyse to get sufficient accuracy for the actual purpose in such studies.

In figure 3 we see that the peak loads for the TEK10 and the PH+hp buildings occur in the morning hours. We may assume that this is normally due to an increased ventilation rate and the use of hot tap water for showers and hand washing.

The figure also indicates that an increased amount of hot tap water is used in the afternoon hours for these two buildings as shown by the peaks around the hours 17 and 18.

From the heat load profile for the LE+hp building we can correctly draw the conclusion that there are storage tanks installed in the local heating system. The reason for that is to get a steady heat collection from the heat pump. As we see, this will to a great extent even out the load profile.

In figure 4 we see duration curves for the measured specific load for the three buildings for the actual year (2014). We see that the measured maximum loads for the actual year are somewhat lower than the design heat loads in figure 3 and Table 2 which are estimated values by the regression lines down to the formal dimensioning outdoor temperature of -19°C.

We also see that the curves are stepped, depending on the resolution of the heat meters. For the TEK10 building the steps are rather big. This indicates that the heat meter for this building is oversized. One consequence of this oversizing is that most likely the shown maximum load for the TEK10 building is somewhat lower than it would have been with a correct dimensioned heat meter with an appropriate resolution.

From table 2 we see that the TEK10 building is just about to meet the criteria on heat use according to the actual building code.

Table 2. Specific yearly heat use, max heat load and equivalent duration time of maximum load

	TEK10	LE+hp	PH+hp
Yearly heat use from the DH system (kWh/m ²)	~82	~52	~52
Max heat load from the DH system (Wh/h·m ²)	~32	~24	~26
Equivalent duration time of max DH load (h)	~2562	~2167	~2000
Calculated requirements on max. yearly heat use according to TEK10 and NS 3700:2010 (kWh/m ²)	~85	60	45

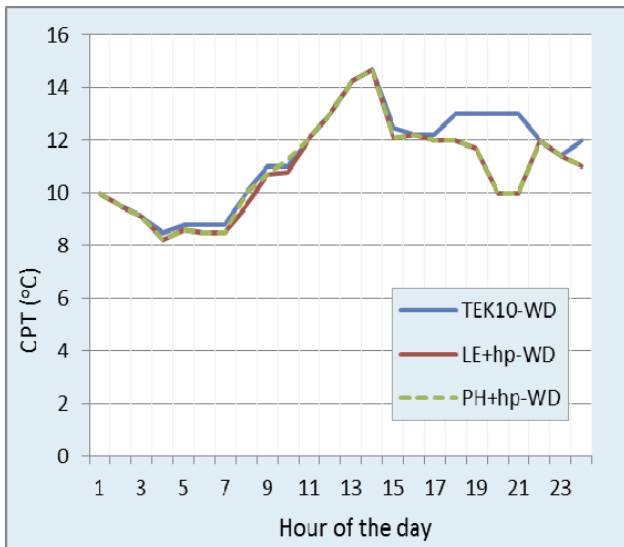


Figure 5. CPT for week days (WD) [3]

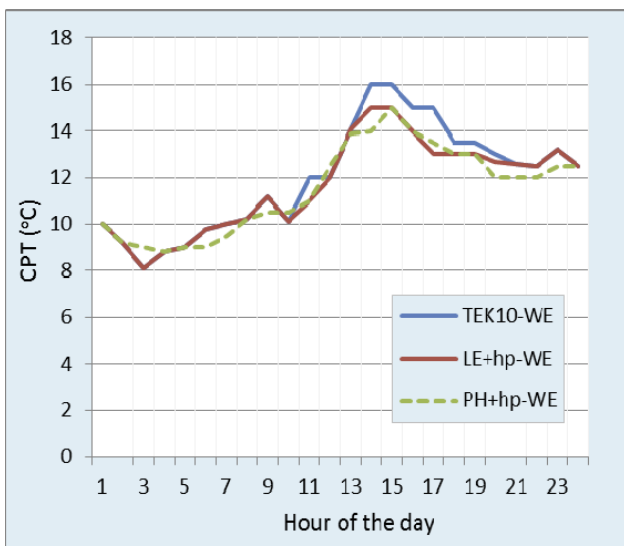


Figure 6. CPT for week end (WE) [3]

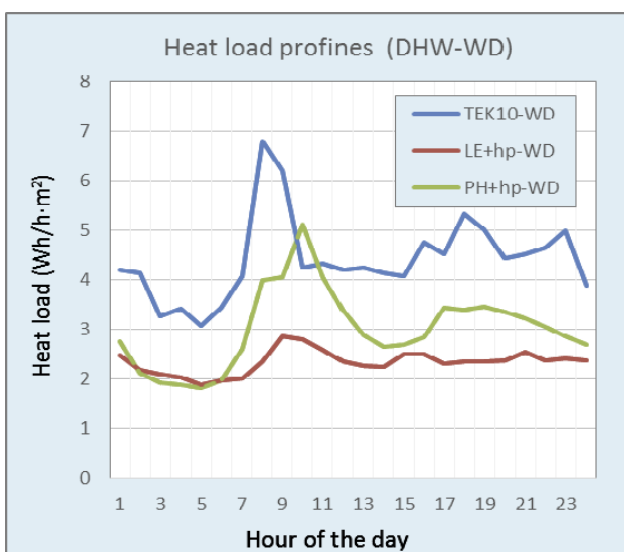


Figure 7. Heat load profiles for DHW for WD [3]

For the LE+hp building we see that the value for the heat use from DH is lower than the requirement according to NS 3700:2010. But, since this building gets additional heat from the heat pump we can't really decide from these figures if the building really meets all the criteria as a LE building. The overall picture for this building is also being confused by the fact that the heating system is providing some heat to a car shed and also to a smaller snow melting area.

For the PH+hp building we see that the value for yearly district heat supply is higher than the requirement according to NS 3700:2010 even if the building gets additional heat from the heat pump. This gives a clear indication that this building does not meet the criteria as a PH building.

In figure 5 we see the curves of the hourly values of CPT from the analyses of the actual buildings in this study on WD.

During night time we should theoretically expect that the CPT values for the TEK10 building would be somewhat higher than for the LE+hp building and that the values for the LE+hp building would be somewhat higher than for the PH+hp building.

We see from the figure that the CPT values are more or less the same for all three buildings except for the hours from 18-21 for the TEK10 building.

This could be explained by several reasons e.g. that the ventilation system is running with higher ventilation rate some more hours for the TEK10 building than the other two buildings. But all together the results give an indication that the thermal qualities of the three buildings are not very different due to the fact that CPT for the marginal heat supply from the DH system is more or less the same during the night hours 4-7.

In figure 6 we see the curves of the hourly values of CPT for WE. These curves show more or less the same tendency as for the WD. But here we see that the CPT values for the TEK10 building has a tendency to be higher than for the other buildings in the hours 14-21.

The difference in the CPT curves for WE are marginal, and may be explained by the fact that it could be within the margin of error of the analysing method.

From figure 5 and 6 we also see that the CPT for all three buildings is in the range of 8°C during night time where the amount of ventilation air is assumed to be at the minimum level according to the requirements.

In figure 7 we see the typical morning peaks for DHW for the TEK10 and the PH+hp buildings. We also see

that the morning peak for the PH+hp building is partly delayed a couple of hours. This indicates that quite a few of the residents in this building do not have to get up and go to work early in the morning.

This tendency may be explained by the fact that this new building is situated on the top of a shopping mall close to the centre of the city. We know that quite a few of the pensioners nowadays are selling their one family houses in the suburbs and move to flats in new built blocks in the city centres.

For the LE+hp building we see that the peaks of the DHW load profile is flattened out due to the heat storage system. The morning peak is also slightly delayed due to the storage system.

In figure 8 we see that we may assume that quite a few of the "working people" in the TEK10 building are getting out of bed several hours later on WE than on WD. The same tendency we also see for the LE+hp building. For the PH+hp building we see that most of the residents in the building, as we could expect, seem to be pretty much following the same routines on WE as on the WD.

EFFICIENCY OF THE DOMESTIC HOT WATER SYSTEM AND THE HEAT CONTRIBUTION FROM THE HEAT PUMP SYSTEM IN THE ACTUAL BUILDINGS

From figure 7 and 8 we see that the average heat use for DHW in the TEK10 building is in the range of 4.5 W/m². The lowest measured value in this house at night time is in the range of 3.1 W/m². If we assume that this represents the heat loss in the distribution system the efficiency of the DHW system is in the range of 30 %. Most likely this low value is due to the circulation loop.

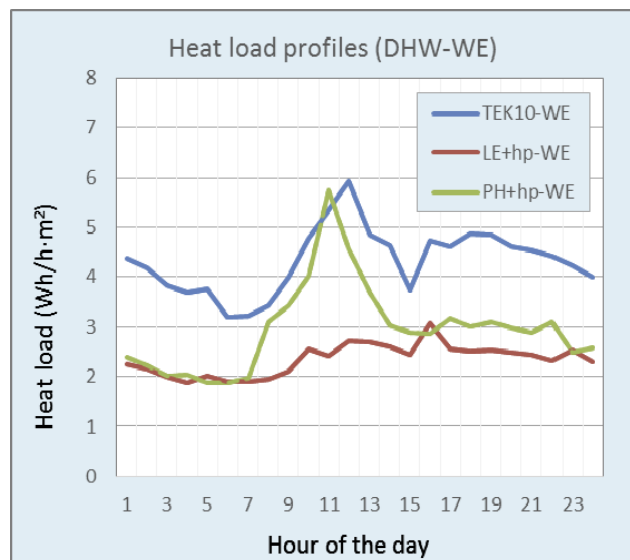


Figure 8. Heat load profiles for DHW for WE [3]

From figure 7 and 8 we also see that the average heat supply from the DH system for DHW for the LE+hp and PH+hp buildings is in the range of 2.9 and 2.5 W/m² respectively.

If we assume that the heat use for DHW is more or less at the same level for all the three buildings, the heat contribution from the heat pumps for the LE+hp and PH+hp buildings is in the range of 1.6 and 2.0 W/m² respectively in the summer season. These values correspond in total to a heat contribution from the heat pumps to each flat in the respective houses of about 3.3 and 4.4 kWh/day. In comparison, this study indicates that the heat use for DHW in the actual buildings is in the range of 10 kWh/day.

DISCUSSION

From the fairly low heat contribution from the heat pumps in the summer season it seems relevant to raise the question: Is the heat contribution from the heat pump in the LE+hp building high enough to justify the installations according to relevant economic criteria? From this study this question can not be answered properly without doing more measurements related to the heat pump and collecting a lot of detailed data and doing extensive economic calculations.

The use of the heat pump in the PA+hp building should anyway be justified by the fact that the motive here is to use heat that otherwise would have been lost.

We have noticed from figure 5 and 6 that the thermal qualities of the three buildings seem to be quite similar. Then it seems reasonable to raise the question if the heat pumps are installed for the purpose of meeting the demanded criteria on heat use according to NS3700:2010, or to achieve an A rated building according to the Norwegian requirement for the energy performance certificate for the building.

In Norway the ranking of the buildings for the energy performance certificate is based on delivered energy to the buildings without corrections for the primary energy factors (PEF) for the actual energy sources.

The European Union has passed the *REGULATION (EU) No 244/2012 "on the energy performance of buildings by establishing a comparative methodology framework for calculating cost-optimal levels of minimum energy performance requirements for buildings and building elements"*. This regulation presupposes that the actual countries shall perform cost calculations at macroeconomic level where also additional costs of greenhouse gas (GHG) emissions are included.

It seems relevant here to ask if installing heat pumps in houses heated by DH are cost-optimal in an optimal

GHG perspective if the heat pumps are not needed for cooling purposes.

OUTLOOK

In the effort to optimise GHG emission from a socio economic perspective, it seems to be a need for an extensive study on the cost-efficiency of installing heat pumps in buildings heated by DH when the heat pump is not needed for heating purposes.

We already know that in it may be profitable from a private viewpoint to install heat pumps in buildings with heat supply from DH due to tax rules and regulatory systems. In a GHG perspective the REGULATION (EU) No 244/2012 quite logically presupposes that the cost optimal calculations shall be performed without including possible tax and regulatory systems.

CONCLUSIONS

The following conclusion may be drawn from the results of this study:

- (1) The results from the study indicate that the thermal quality of the TEK10, LE+hp and PH+hp buildings are quite similar.
- (2) The TEK10 building seems to meet the requirement on heat use set in the actual Norwegian building code.
- (3) The LE+hp building seems not to meet the criteria on yearly heat use to be qualified as a LE building according to the Norwegian standard NS 3700:2010. But the fact that the heating system in this building is providing some heat to a smaller snow melting area is confusing the picture.
- (4) It seems clear that the PH+hp building does not meet the heat use criteria to be qualified as a PH building according to the standard NS 3700:2010.
- (5) The reduction in specific heat use from the DH-system for the LE+hp and the PH+hp buildings in this study is in the range of 35 % compared to the TEK10 building.
- (6) The ratio between yearly heat use from the DH-system and the maximum heat load is decreasing from the TEK10 building to the LE+hp building and further to the PH+hp building. This means that it is a development towards fewer kWh to charge the costs for the investments in heat load capacity in the DH system.
- (7) The derived values for the heat contribution from the heat pumps to the DHW system during the summer season for the LE+hp and the PH+hp buildings indicate that the contribution is rather low – about 3.3 and 4.4 kWh/day respectively for each flat.

- (8) Since the thermal qualities of the three buildings seem to be quite similar, it seems likely to assume that the installation of heat pumps in the LE+hp and the PH+hp buildings could partly be motivated by the aim to fulfil the heat use requirements set in NS 3700:2010, or to get an A rated building according to the Norwegian energy performance certificate system.
- (9) According to Regulation (EU) No 244/2012, the cost efficiency of installing heat pumps in DH supplied buildings where cooling is not needed should be evaluated through an exhaustive study on cost-efficiency at macroeconomic level according to socio-economic criteria.

ACKNOWLEDGEMENT

A special thank to Statkraft Varme AS for providing information and measured load values from the actual buildings. Thanks also to Norwegian Research Council and the private companies that have contributed with economic resources to make this project possible. And also thanks to the project group for a fruitful cooperation.

REFERENCES

- [1] Norwegian standard, NS 3700:2010; "Criteria for passive houses (PH) and low energy (LE) houses – Residential buildings".
- [2] A. Colin Cameron and Pravin K. Trivedi, "Micro-econometrics Using STATA", STATA press, ISBN-13:978-1-59718-073-3, Revised edition 2010
- [3] Karen Byskov Lindberg, "Regression analyses on measured hourly heat values from a district heating system for three residential blocks of flats in Trondheim". (Unpublished work report (by January 2016) for the PhD-theses at NTNU.
- [4] [4] Linda Pedersen, "Load Modelling of Buildings in Mixed Energy Distribution Systems", PhD-theses at Norwegian University of Science and Technology (NTNU), 2007:78.

OTHER RELVANT REFERENCES

- [5] Karen Byskov Lindberg, Gerard Doorman, "Hourly load modelling of non-residential building stock", Conference paper at; PowerTech 2013 IEEE Grenoble, Grenoble, France
- [6] Linda Pedersen, Rolf Ulseth, "Method for Load Modelling of Heat and Electricity Demand", The 10th International Symposium on District Heating and Cooling, Hanover, Germany, September 3-5, 2006.
- [7] Linda Pedersen, Jacob Stang and Rolf Ulseth, "Load prediction method for heat and electricity demand in buildings for the purpose of planning for mixed energy distribution systems", Energy and Buildings 40 (2008) 1124–1134.
- [8] Rolf Ulseth, Maria Justo Alonso and Linda Pedersen Haugerud, "Measured load profiles for domestic hot water in buildings", The 14th International Symposium on District Heating and Cooling, Stockholm, Sweden, September 7-9, 2014.

ENERGETIC AND EXERGETIC PERFORMANCE OF SHORT TERM THERMAL STORAGES IN URBAN DISTRICT HEATING NETWORKS

Georg K. Schuchardt(née Bestrzynski)¹, Stefan Holler²

¹ Fernwaerme-Forschungsinstitut, Max-von-Laue Straße 23, 30966 Hemmingen, Germany

² HAWK University of Applied Sciences and Arts Hildesheim/ Holzminden/ Goettingen, Büsgenweg 1a, 37077 Goettingen, Germany

ABSTRACT

Meeting the heat demand of all customers attached, is the main objective for the operation of district heating (DH) systems combined with combined heat and power (CHP) plants. On the other hand, the economic ratification for the operation of CHP plants strongly depends on highly volatile electricity prices on the market. This trend will be reinforced in future, due to the additional integration and exploitation of renewable energies. Within this techno-economic field of most different operational objectives, DH systems and CHP plants must find a way for a cost-covering and efficient operation in future.

Against this background, time shifts in producing and allocating heat supplied in parallel with electricity, are most attractive for DH system and CHP plant operators. Thus, margins on the electricity market could be maximized. On the other hand, heat amounts produced in parallel should be decoupled from the production of electricity as efficient as possible. Thus, thermal energy storages enter the limelight of interest for DH system operators. However, aspects concerning most different mechanisms for energetic and exergetic losses have to be considered for an optimized operation of these systems.

Within this paper, the energetic and exergetic performance of sensible thermal storages will be examined. Underlying loss mechanisms of typical urban thermal storages are described qualitatively and quantified energetically and exergetically. For this purpose, existing models from literature are combined with practically relevant operational parameters for simulations.

INTRODUCTION

CHP is a widespread and robust system for efficiently delivering electrical power and heat to customers. Thus, within urban areas of northern European countries, CHP is and will be a major partner for the energy turnaround [1]. Running these systems, the main focus of operation has been on meeting the heat demands occurring in the district heating (DH) network attached. On the other hand, revenues at the energy markets are mainly responsible for running these systems economically and profitable.

Against this background, measures for a more flexible and, in best case, a market-price-oriented operation of CHP, enter the limelight of interest for DH supply companies. Thus, the utilization of thermal storages (thermal accumulators) within urban areas is widely discussed for enhancing the economic performance and full-load hours of CHP, s. [2 to 7], whereas operational cost diminish due to raising efficiencies, s. [8].

However, knowing the energetic and exergetic contents utilizable within large scale thermal storages (hot water contents > 10,000m³) is the main prerequisite for an optimized, efficient and economic operation of these systems. As these contents are diminished by a multitude of thermodynamic processes, the contents of [9] are refined, improved and developed further. Therefore, the impact of different heat transfer and loss mechanisms on the energetic and exergetic contents utilizable as well as the thermal stratification within large scale thermal storages are described and quantified. Thus, potentials of CHP and thermal storages within the context of an overall DH system may be evaluated and analyzed.

Basing on relevant literature [2 to 16], typical operational parameters of sensible thermal storages within urban DH systems are defined. Regarding these studies, heat loss mechanisms of thermal storages are of major interest concerning operational efficiency and effect the energetic and exergetic contents of these systems, cf. [17 to 20]. However, the transferability of these results is not necessarily given for large scale applications. Against this background, approaches for approximating these mechanisms are refined and combined with operational parameters of large scale thermal storages. Regarding practically relevant operational parameters, energetic and exergetic losses are calculated and quantified for typical urban storage systems.

STATE-OF-THE-ART

Thermal storages will play a major role for an efficient and feasible operation of DH networks. Geometrical and operational parameters of these systems, mainly implemented as sensible, stratifying systems operating at atmospheric pressures, are closely connected to the operational parameters of the DH grid attached. Furthermore, technological key-performance indicators

(capacity, flexibility of operation, operational temperature, quality of thermal stratification, etc.), non-technological aspects (space required for installation, inherent operational safety, etc.), have to be considered **Table** summarizes the relevant literature and gives typical geometric, energetic and operational parameters of these systems [2 to 20].

Due to different internal and external thermo- and hydrodynamic processes, the efficiency as well as the stratification of these systems is diminished. Resulting, different heat and mass transfer mechanisms occur. Within this contribution, the following mechanisms are described qualitatively and quantitatively, cf. [9, 21 to 28]

- External Losses via the wall
- Thermal conduction within the storage media
- Thermal short-circuits via the wall
- Thermal absorptions due to thermal inertia
- Convective heat transfer due to free convection
- Turbulences induced by (dis-) charging

On the other hand, energetic losses due to radiant heat transfer, e.g. between the head and bottom of the storage, are not taken into consideration.

EXTERNAL LOSSES VIA THE WALL

Due to temperature differences between the storage media and the surrounding environment, thermal losses via the wall of thermal storages occur. These diminish the energetic and exergetic contents utilizable within the thermal storage. The storage media (generally at a higher temperature than the surrounding environment) loses heat. For storage periods $\varepsilon \rightarrow \infty$, heat losses \dot{Q}_{out} occurring result in a thermodynamic equilibrium with the environment. \dot{Q}_{out} (and Q_{out}) are lost for further technological utilization.

However, \dot{Q}_{out} is constrained by applying a thermal insulation (within the wall, roof and bottom). Low heat conductivities λ_{ins} and a thickness s_{ins} of these insulations limit the external losses. Thus, more than 95% of the temperature gradient between the environment and the storage media $\Delta T_{in,p}$ is degraded within the thermal insulation. $\Delta T_{in,p}$ might be approximated by applying the mean temperatures of the thermal storage media and the environment, s. [9, 23]. Additional layers within the wall of the thermal storage (bearing structures, diffusion barriers, etc.), as well as thermal boundary layers and steam cushions are negligible regarding \dot{Q}_{out} . Merely, the soil below the thermal storage influences the heat losses of thermal storages due to moderate heat conductivities $\lambda_{soil} = 1 \dots 5 \text{ W/mK}$ and a semi-infinite extension.

Nevertheless, the external losses are influenced insignificantly for typical $H_{Stor}/D_{Stor} > 0.5$ by the soil.

Thus, \dot{Q}_{out} may be approximated by

$$\dot{Q}_{out} = k A \Delta T_{in,p} \approx \lambda_{ins} / s_{ins} A \Delta T_{in,p} \quad (1)$$

Resulting, the heat losses via the wall $\dot{q}_{out} = \dot{Q}_{out}/A$ are typically below 10 W/m^2 . Regarding a 24h time-shift for a charging-discharging-cycle ε (s. Table 1), the relative losses Q_{out}/Q_{ch} are below 0.1%, s. **Table 2**.

Table 1: Typical geometric and operational parameters of large scale thermal storages [2 to 20]

Parameter	
Volume V_{St} [m ³]	10 ⁴ ...10 ⁵
Height H_{St} [m]	7...60
Diameter D_{St} [m]	10...50
Strength of wall ε_{Wt} [m]	0.03...0.05
Strength of Insulation s_I [m]	0.1...1.0
Heat Conductivity of Insulation λ_I [W/mK]	0.03...0.04
Max. Temperature T_{m} [°C]	95...98
Min. Temperature T_m [°C]	58...67
Ambient Temperature T_a [°C]	-15...30
Strength layer thermal stratification s_{Lk} [m]	2.3...4
Typ. Timescale for (dis-) charging [h]	5...10
Typ. Time-Shift charging-discharging [d]	1

Table 2: Approximation of external losses via the wall during 24h, assuming a relative height $H_{Stor}/D_{Stor} = 1$
 $\lambda_{ins} = 0,095 \text{ W/mK}$; $s_{ins} = 0,5 \text{ m}$;
 $T_a = 0^\circ\text{C}$; $T_{max} = 98^\circ\text{C}$; $T_{min} = 58^\circ\text{C}$

V_{St} [m ³]	10 ⁴	3*10 ⁴	5*10 ⁴	10 ⁵
Capacity Q [MWh]	467	1,400	2,333	4,667
Surface A [m ²]	2,570	5,345	7,513	11,927
\dot{Q}_o [kW]	18	37.4	52.6	83.5
Q_o [MWh]	0.43	0.90	1.26	2.00
Q_{out}/Q_{ch} [%]	0.09	0.06	0.05	0.04

CONDUCTION WITHIN THE STORAGE MEDIA

Thermal storages are mainly operating at atmospheric pressures, stratifying high- and low-temperature media due to temperature-dependent differences in density ρ . Thus, heat flows via the layer for thermal stratification occur, equalizing temperature differences. Neglecting external losses (adiabatic system) and assuming constant material properties for relevant temperatures and pressures, the thermal storage strives for an average temperature level \bar{T} ; $T_{max} > \bar{T} > T_{min}$. Internal heat flows occurring are mainly depending on the strength of the stratifying layer s_{Layer} and heat conductivity of the storage media λ_{med} .

Basing on an ideal initial strength of the stratifying layer ($s_{Layer}(t=0) = 0m$) the development of the temperature regime within the thermal storage, as well as the stratifying layer is calculated by a numerical model. Thus, time and height dependant temperatures $T = T(h, t, \lambda_{med})$, as well as the strength of the stratifying layer $s_{Layer}(t)$ is mapped. Basing on a discretization of the thermal storage into a defined number of layers n at different initial temperatures $T(t=0, n)$, heat flows between the layers $Q_{inter}(n \rightarrow n+1)$ are computed. Regarding the heat conductivity of the thermal media and the time step Δt , energetic and exergetic contents and temperatures (temperature shifts and drops) of each layer n are calculated for the following time step $t+1$. The temperature profiles $T = T(h, t, \lambda_{med})$ result, s. **Figure**. For further details on the numerical model as well as the algorithm utilized, s. [9]. Considering the results, the temperature profile within the stratifying layer, defined according to equation 2 is nearly linear, s. [24]

$$T_{max} - 0.1\Delta T_{sp} < T < T_{min} + 0.1\Delta T_{sp} \quad (2)$$

Furthermore, the energetic contents lost for utilization shall be approximated. For this purpose, a minimum temperature tolerable within the thermal storage/ layer for stratification $T_{minSupply}$, must be defined, e.g. for a direct feed into the supply flow without additional pre-heating. Clearly, $T_{minSupply}$ generally depends on economic and technological targets of operation and varies for different operational and market conditions, systems and in time, etc. In other words, the stratifying layer is partially utilizable for the DH-system applied.

Regarding **Figure**, the energetic contents utilizable is described by the area in between the temperature profile relevant and $T_{minSupply}$. Thus, the numerical

model may quantify the losses occurring in between two time steps t and $t+1$. However, prerequisite for this quantification is the definition of an initial (typical) temperature profile. This temperature profile defines the strength of the stratifying layer $s_{Layer}(t)$ at the beginning. Due to turbulences occurring while (dis-) charging the storage, $s_{Layer}(t)$ cannot be arbitrarily small, s. also below. The time dependant development of s_{Layer} within typical operational cycles \bar{E} is quantified for a typical urban thermal storage.

The vertical heat transfer within the thermal storage media leads to an expansion of the stratifying layer. Resulting, the energetic content directly utilizable decrease, depending on the operational boundary conditions of the DH system attached. On the other hand, the heat flow between high- and low-temperature media within the storage decreases as the strength of the thermal layer $s_{Layer}(t)$ increases. Thus, the insulating effect of the stratifying layer becomes more dominant over time.

Finally, the maximum reductions of the energetic contents within an urban thermal storage system are approximated by the numerical model. These losses Q_{losses} are approximately 0.4MWh/d for a 10,000m³ storage according to **Table** and **Table 2**. In relation to an initial energetic content of 213MWh, the relative losses are 0.2 % within 24h (thermal loading status of 50%), s. [6, 11, 17 to 22]. Thus, the strength of the stratifying layer ds_{Layer}/dt increases by 38mm/d., whereas ds_{Layer}/dt decreases with time. **Table 3** summarizes the results on the losses within the thermal storage media.

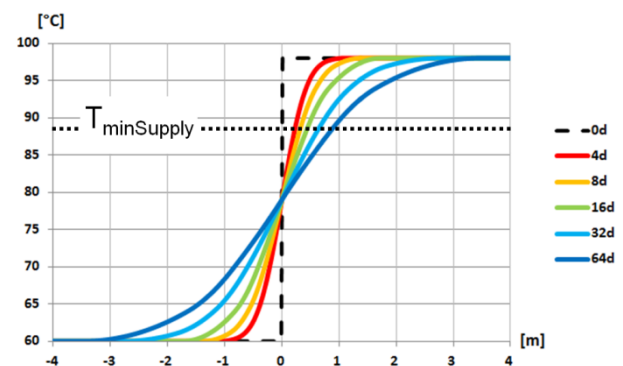


Figure 1: Development of the stratifying layer within a hot water storage (assuming an ideal stratification at $t = 0d$)

Table 3: Approximation of heat losses due to thermal conduction via the thermal storage media within 24h ($H/D = 1.0$, $\lambda_{H2O} = 0.70 \text{ W/mK}$, $s_{\text{lay}}(t) = 2.9 \text{ m}$, $T_{\text{max}} = 98^\circ\text{C}$, $T_{\text{maxsupply}} = 88^\circ\text{C}$, $T_{\text{min}} = 60^\circ\text{C}$, $s_{\text{lay}}(t) = 2.9 \text{ m}$)

$V_{\text{St}} [\text{m}^3]$	10^4	$3 \cdot 10^4$	$5 \cdot 10^4$	10^5
Energetic Content $Q_{\text{th}}(t, T > 88^\circ\text{C})$ [MWh]	213	654.3	1,102.1	2,231.4
Energetic Content $Q_{\text{th}}(t + 1, T > 88^\circ\text{C})$ [MWh]	212.6	653.4	1,100.9	2,229.4
Decrease of energetic content $Q_{\text{losswall}}(t \rightarrow t + 1)$ [MWh]	0.40	0.90	1.20	2.00
Q_{lossH2O}/Q [%]	0.19	0.15	0.11	0.09

THERMAL SHORT CIRCUITS WITHIN HIGHLY CONDUCTIVE PARTS

Due to the high conductivity λ_{St} within highly conductive parts of the thermal storage, the stratifying layer develops faster than within the thermal media itself. However, the development of the thermal layer within thermal short circuits may be approximated by the same numerical model as previously utilized for the thermal media. Resulting, additional heat transfer from high- to low-temperature parts of the storage occur, s. [6, 17].

Comparing the temperature profiles for the thermal storage media $T = T(r, t, \lambda_{\text{H2O}})$ and within the wall $T = T(r, t, \lambda_{\text{St}})$, s. [9] and **Figure 2**, additional heat flows occurring via thermal short circuits may be examined. Within this paper, additional heat flows occurring via the wall Q_{wall} (strength of wall s_{wall}), representing a major thermal short circuit, are calculated. Relating Q_{wall} to the heat flows occurring within the thermal media Q_{lossH2O} energetic losses might be approximated. For this purpose, the heat flows are assumed to be one-dimensional and vertically oriented.

$$\frac{Q_{\text{lossH2O}}}{Q_{\text{lossWall}}} = \frac{\left(\frac{\lambda_{\text{H2O}}}{s_{\text{lay}}}\right) \cdot \frac{\pi}{4} \cdot D_{\text{stor}}^2 \cdot \Delta T_{\text{H2O}}}{\left(\frac{\lambda_{\text{St}}}{s_{\text{wall}}}\right) \cdot \frac{\pi}{4} \cdot [(D_{\text{stor}} + s_{\text{wall}})^2 - D_{\text{stor}}^2] \cdot \Delta T_{\text{St}}} \quad (3a)$$

This equation may be simplified for $\Delta T_{\text{H2O}} \approx \Delta T_{\text{St}}$ (same temperature drop within the thermal storage media as

within the wall), $s_{\text{lay}} \approx s_{\text{wall}}$ (same distance between high- and low-temperature parts for the thermal storage media and the wall) and $s_{\text{wall}} \ll D_{\text{stor}} \rightarrow s_{\text{St}}^2 \approx 0$ (small relative strength $s_{\text{St}}/D_{\text{stor}}$ of the wall). Finally, for given thermal conductivities of the thermal storage media and the steel $\lambda_{\text{H2O}} \approx 0.70 \text{ W/mK}$ and $\lambda_{\text{St}} \approx 50 \text{ W/mK}$, the influence of thermal short circuits via the wall are approximated for a worst case, s. **Figure 3**.

$$\frac{Q_{\text{lossH2O}}}{Q_{\text{lossWall}}} = \frac{D_{\text{stor}}}{2s_{\text{wall}}} \cdot \left(\frac{\lambda_{\text{H2O}}}{\lambda_{\text{St}}}\right) = \frac{D_{\text{stor}}}{2s_{\text{wall}}} \cdot \left(\frac{0.7}{50}\right) \quad (3b)$$

The energetic losses within thermal storages according to **Table** and Table 2 are quantified for typical strengths of the wall $s_{\text{wall}} = 60 \text{ mm}$ and $H/D = 1$.

Additional losses occurring via the wall Q_{wall} are approximately 0.15 MWh/d, decreasing the energetic content of Q_{th} 213 MWh by 0.07% within

$$24 \cdot \frac{Q_{\text{lossH2O}}}{Q_{\text{lossWall}}} = \frac{23.25}{2 \cdot 0.06} \cdot \left(\frac{0.7}{50}\right) = 2.72 \quad (3c)$$

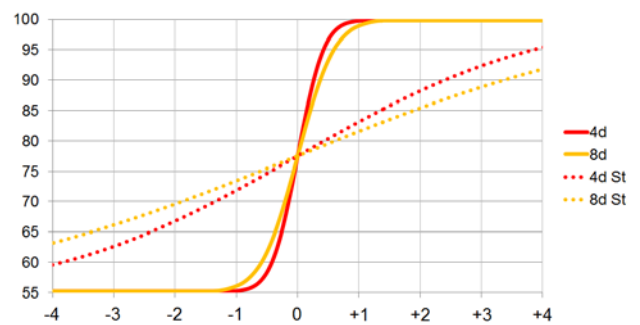


Figure 2: Development of the stratifying layer within the thermal media and the wall (assuming $\lambda_{\text{H2O}} = 50 \text{ W/mK}$)

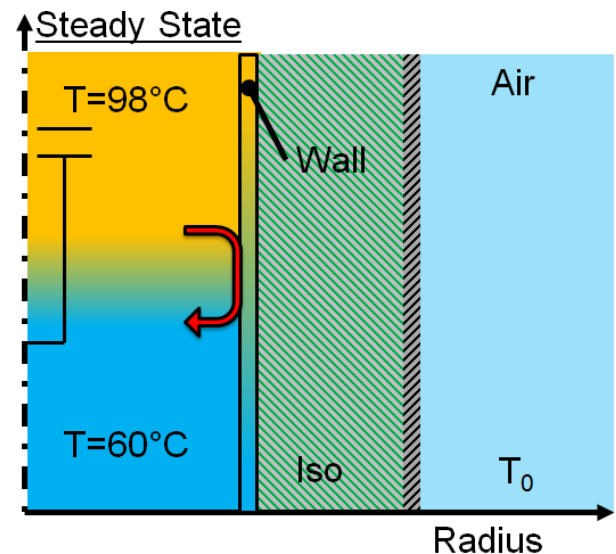


Figure 3: Heat transfer via thermal short-circuit, e.g. wall (scheme)

Table 4: Approximation of heat losses due to thermal short circuits via the wall within 24h ($H/D = 1.0$, $\lambda_{H2O} = 0.70\text{W/mK}$, $\lambda_{St} = 50\text{W/mK}$, $s_{Wall} = 60\text{mm}$)

$V_{St} [\text{m}^3]$	10^4	$3 \cdot 10^4$	$5 \cdot 10^4$	10^5
$Q_{lossWall}(t \rightarrow t+1)$ (cf. Table 3) [MWh]	0.40	0.90	1.20	2.00
s_{St}/D_{St}	1/390 ...	1/561 ...	1/665 ...	1/840 ...
$Q_{lossWall}/Q_{lossSt}$ (cf. eq. 3c)	2.72 ...	3.93 ...	4.66 ...	5.87 ...
$Q_{lossWall}$ [MWh/d]	0.07 ...	0.11 ...	0.13 ...	0.17 ...
$Q_{lossWall}/Q$ [%]	0.03 ...	0.02 ...	0.01 ...	0.01 ...

Generally, the influence of the wall on the losses decreases for increasing diameters of the thermal storage D_{Stor} , decreasing strengths of the wall s_{Wall} and decreasing conductivities λ_{St} (e.g. for stainless steel $\lambda_{Ststainless} \approx 15\text{W/mK}$). As a final remark, especially the simplification on the temperature gradients via the wall and via the stratifying layer ($\Delta T_{H2O} \approx \Delta T_{St}$) seems to be unsuitable for operational conditions in situ, as $\Delta T_{St} < \Delta T_{H2O}$. This again would lead to a diminished influence of thermal short circuits. Finally, **Table 4** summarizes the results for the additional heat losses occurring within the wall.

LOSSES DUE TO THERMAL INERTIA OF STORAGE INFRASTRUCTURE

During operation, the stratifying layer moves within the thermal storage due to operational needs. Thus, especially the wall of the thermal storage is cyclically in contact with high- and low-temperature fluid. (Assuming a steam cushion at the roof and a residual volume below the outlet, roof and bottom are steadily in touch with high- and low-temperature fluid.) Resulting from these movements of the stratifying layer, parts of the vertical wall absorb energetic contents $Q_{lossWall}$ of the storage media entering the storage while charging, s. **Figure 4**. Thus, the energetic content utilizable is diminished. On the other hand, while discharging the thermal storage, the thermal inertia of the wall causes an input of heat into the storage media. Unfortunately,

these energetic contents may not be utilized, as the temperature level of the heat flows are too low $T_{Mass} \approx T_{minSupply}$ and as the (dis-) charging infrastructure is located in the middle at the head and bottom of the thermal storage (and not next to the wall). Therefore, the energetic content is diminished due to $Q_{lossMass}$, whereas the stratification of the thermal storage is disturbed, s. [6].

Within this context, the energetic contents absorbed within the wall $Q_{lossMass} = Q_{Wall}$ shall be quantified, assuming that these contents are lost for further utilization. Resulting, the maximum losses occurring within thermal storages according to **Table 1** and **Table 2** are 2.1MWh/cycle, decreasing the energetic content Q_{th} of 467MWh by 0.5%.

$$\frac{Q_{lossMass}}{Q_{th}} = \frac{\frac{\pi}{4} \cdot [(D_{Sp} + s_{Wall})^2 - D_{Sp}^2] \cdot H \cdot \rho_{St} \cdot c_{pSt} \cdot \Delta T}{\frac{\pi}{4} \cdot D_{Sp}^2 \cdot H \cdot \rho_{H2O} \cdot c_{pH2O} \cdot \Delta T} = \frac{2.04}{467}$$

$$\frac{Q_{lossMass}}{Q_{th}} = 0.45\% \quad (4)$$

$$D_{Sp} (D_{Sp} = 10,000\text{m}^3) = H = 23.35\text{m}; \Delta T = 40\text{K};$$

$$\rho_{St} = 7,8970\text{kg/m}^3; c_{pSt} = 452\text{J/kgK}; s_{Wall} = 60\text{mm}$$

The relative losses $Q_{lossMass}/Q_{th}$ decreases for diminishing strengths of the wall s_{Wall} (or other thermal masses) and increasing volumes of the thermal storage V_{Stor} , s.

In addition to the thermal losses, the influence of thermal inertia on the quality of thermal stratification shall be approximated. Main parameter for these interactions is the relative heat storage capacity of the thermal storage media C_{H2O} in relation to the heat storage capacity of the overall system $\sum C_i$, s. [6]. For $C_{H2O}/\sum C_i \approx 1.0$, the response of the thermal inertia on changes in the temperature regime is quite dynamic, resulting in a minor impact on the thermal stratification. Considering the relevant literature, for thermal storages operating at 50...130°C and at a maximum internal temperature difference $\Delta T = T_{max} - T_{min} = 10 \dots 40\text{K}$, the influence of thermal inertia on the stratification might be neglected for, s. [6]:

$$0.95 < C_{H2O}/\sum C_i \quad (5)$$

Considering the wall of the thermal storages according to **Table 1** and **Table 2**, the minimum relative storage capacity equals 0.995. Thus, at least another 4,485 t of steel might be implemented within the thermal storage, e.g. as additional parts of the infrastructure, in order to violate the criterion (5).

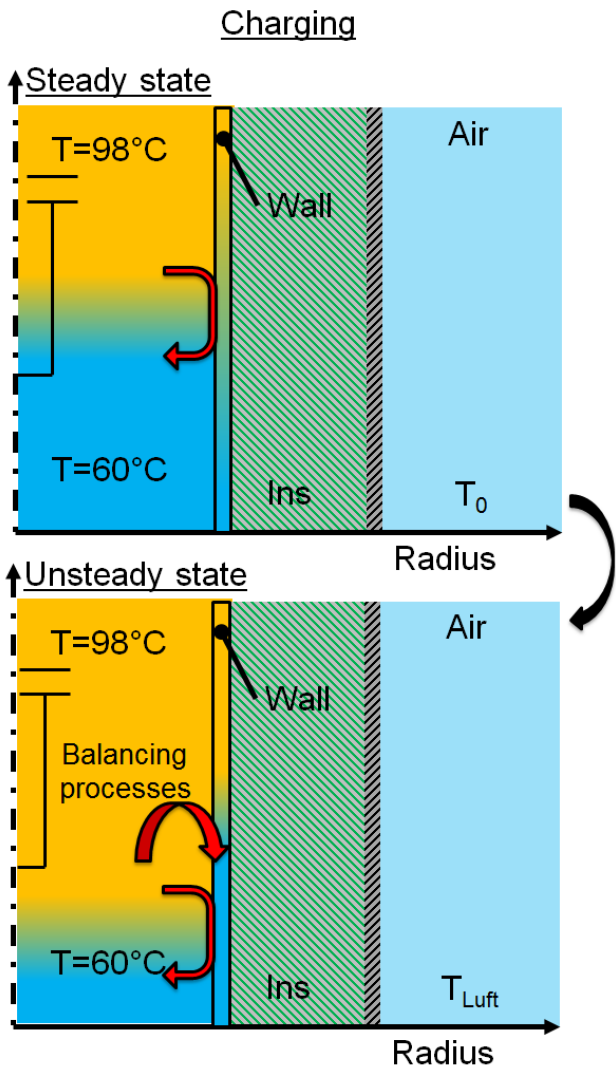


Figure 4: Balancing processes occurring due to thermal inertia of the wall during charging

Table 5: Approximation of heat losses due to thermal inertia of the wall for a full load-cycle 24h ($H/D = 1.0$; $\lambda_{H2O} = 0.70 \text{ W/mK}$; $\rho_{St} = 7.890 \text{ W/mK}$; $c_{p,St} = 452 \text{ J/kgK}$; $T_{min} = 58^\circ\text{C}$; $T_{max} = 98^\circ\text{C}$; $s_{Wall} = 30 \dots 60 \text{ mm}$)

$V_{St} [\text{m}^3]$	10^4	$3 \cdot 10^4$	$5 \cdot 10^4$	10^5
Q (cf. Table 2) [MWh]	467	1,440	2,333.3	4,666.7
$Q_{loss,wall} [\text{MWh/cycle}]$	1.02	2.12	2.98	4.73

$Q_{loss,wall}/Q [\%]$	0.22	0.15	0.13	0.10

	0.45	0.30	0.25	0.20

Table 6: Relative heat capacity of storage media and min. thermal masses required for a disturbing the thermal stratification $m_{St,min}$ acc. to equation (5) due to thermal inertia of the wall for a full load-cycle 24h ($H/D = 1.0$; $\lambda_{H2O} = 0.70 \text{ W/mK}$; $\rho_{St} = 7.890 \text{ W/mK}$; $c_{p,St} = 452 \text{ J/kgK}$; $T_{min} = 58^\circ\text{C}$; $T_{max} = 98^\circ\text{C}$; $s_{Wall} = 30 \dots 60 \text{ mm}$)

$V_{St} [\text{m}^3]$	10^4	$3 \cdot 10^4$	$5 \cdot 10^4$	10^5
$m_{St} [\text{10}^3 \text{ kg}]$	406	844	1,186	1,884
$C_{H2O}/(C_{H2O} + C_{Wall})$	0.996	0.997	0.998	0.998
$m_{St,min} [\text{10}^3 \text{ kg}]$	4,485	13,827	23,266	47,022
$V_{St,min} [\text{m}^3]$	568	1.753	2.949	5.960
Edge length cube [m]	8.28	12.06	14.34	18.13

Table 6 summarizes the relative capacities $C_{H2O}/(C_{H2O} + C_{Wall})$ considering the wall of the thermal storage. In addition, the thermal $m_{St,min}$ as well as the according volumes of steel $V_{St,min}$ are given. Furthermore, the edge lengths of according cubes are given for illustrative matters. This clearly illustrates that enormous quantities of steel/ thermal masses are required in order to violate criterion (5). Thus, a disturbance of the thermal stratification due to thermal inertia seems to be quite improbable.

Generally, the relative capacities $C_{H2O}/(C_{H2O} + C_{Wall})$ according to (5) increase for raising volumes of the thermal storage V_{St} . Finally, the edge lengths of according cubes are given for illustrative matters.

CONVECTIVE HEAT TRANSFER INDUCED BY FALLING FILMS

Within thermal storages, vertical falling films due to gradients in temperature and density occur, e.g. along the wall of the thermal storage. As soon as these falling films from the head of the thermal storage enter the thermal layer, the vertical flow velocity v_{Fall} changes as (temperature dependant) density gradients change. Frictional and inertial effects detach the vertical falling films from the wall, s. [25]. Thus, the falling films are integrated within the stratifying layer, s. **Figure 5**. Furthermore, within and below the stratifying layer, additional falling films are induced. These, attain lower vertical flow velocities v_{Fall} . Therefore, falling films occurring increase the strength of the stratifying layer.

The impact of these falling films on the strength of the stratifying layer s_{lay} is approximated by describing the flow boundary layer at the wall. Coupling the temperature and flow-field, the strength of the flow-boundary layer δ_{lay} is determined, s. [25 to 27]. Considering similarity of forces occurring within the falling films, the velocity field $v_{\text{fall}}(r)$ is described in a dimensionless form, s. [28] and **Figure 6**.

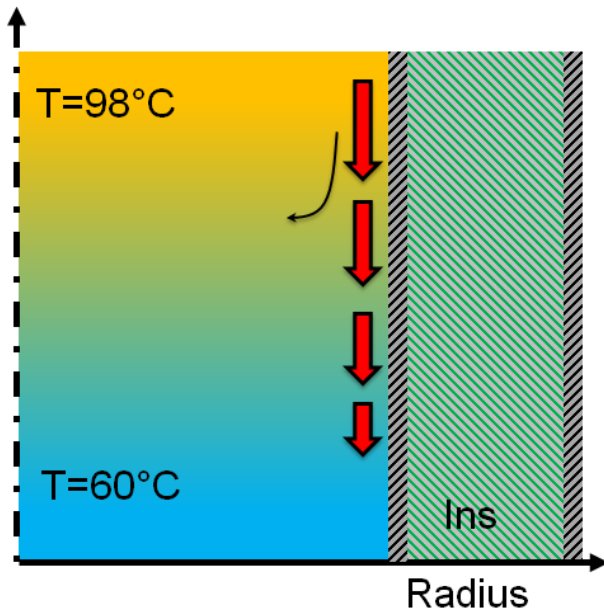


Figure 5: Implementation of falling films within the stratifying layer due to inertial and frictional effects

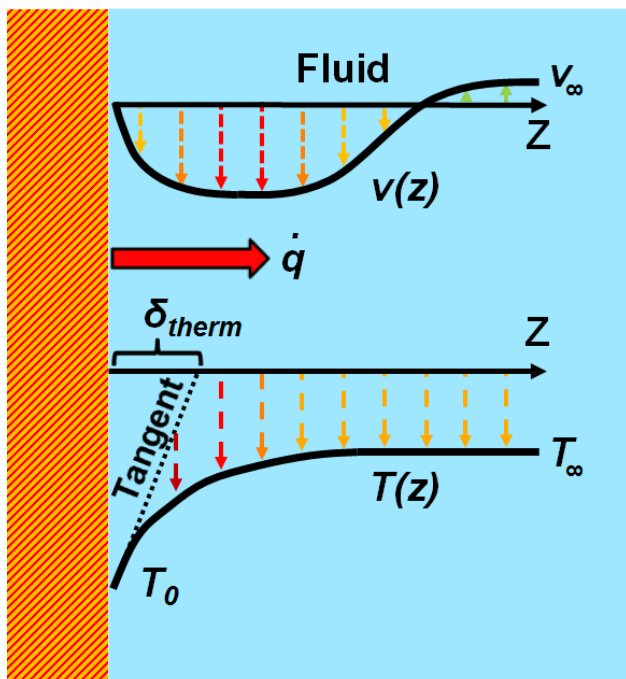


Figure 6: Field for temperatures and flow-velocities within the falling films occurring along the vertical wall

Main parameters influencing v_{fall} are the properties of the storage media, such as the density ρ_{med} , kinematic viscosity ν_{med} heat conductivity λ_{med} or Prandtl-number Pr_{med} (within and without the thermal boundary layer) as well as the free length for vertical flows l_{fall} , s. [25, 26].

$$v_{\text{Fall}} = 2\nu [Gr(\rho, \nu)]^{0.5} f'(\eta) / l_{\text{Fall}} \quad (6)$$

Within equation (6), $f'(\eta)$ is a function of the Grashof-number Gr_{med} , Prandtl-number Pr_{med} as well as the relative strength of the flow boundary layer $\delta_{\text{lay}}/l_{\text{fall}}$, s. [25]. Resulting from the relative strength of the flow boundary layer δ_{lay} and the falling film velocity v_{fall} , volumetric flows from high temperature parts of the thermal storage into the thermal boundary layer \dot{V}_{FallHT} as well as volumetric flows from the thermal boundary layer into the low temperature part of the thermal storage \dot{V}_{FallLT} may be derived. Thus, the growth of the thermal boundary layer due to falling films $ds_{\text{lay}}(t)/dt$ may be approximated.

Calculations for large scale thermal storages show an increase of the strength of the stratifying layer due to falling films. This reduces the energetic contents utilizable for DH purposes. Considering a thermal storage according to **Table 1** and **Table 2**, the growth ds_{lay}/dt is quantified assuming a free length for vertical flows $l_{\text{fall}} = H/2$, a minimum temperature utilizable $T_{\text{min}} = 58^\circ\text{C}$ and a maximum operational temperature $T_{\text{max}} = 98^\circ\text{C}$. According to these calculations, the stratifying layer increases within 24h by 7.5mm/d. Furthermore, a proportionality between heat flows induced and growth of the stratifying layer $ds_{\text{lay}}(t)/dt$ might be assumed. Thus, heat losses occurring due to falling films might be derived considering the ratio of the heat flows within the thermal storage media \dot{Q}_{lossMed} and falling film $\dot{Q}_{\text{lossFall}}$

$$\frac{\dot{Q}_{\text{lossMed}}}{\dot{Q}_{\text{lossFall}}} \approx \frac{88\text{mm/d}}{7.5\text{mm/d}} \quad (7)$$

For the given example, a convective heat flow due to falling films of 0.1MWh/d occurs, decreasing the energetic contents by a maximum of 0.05% within 24h. The impact of falling films on the energetic contents diminishes for bigger diameters D_{stor} . In addition, the free length for vertical flows l_{fall} strongly influences the falling film velocities and volume flows.

However, falling films might be reduced by adaptations of the internal wall structure of the storage, e.g. by implementing internal and circumferential obstacles for the falling film (rib-structure). Thus, the free length for vertical flows l_{fall} is reduced as these obstacles penetrate the flow boundary layer. **Table 7** summarizes the results for the additional growth of the stratifying layer induced by falling films within a thermal storage according to **Table 1** and **Table 2**.

TURBULENCES INDUCED BY CHARGING AND DISCHARGING

Finally, turbulence induced by operational cycles of the thermal storage shall be examined, as these may significantly diminish the energetic contents utilizable. Main parameters of this convective heat transfer mechanism diminishing the energetic contents are the distance between the in- and outlet for (dis-) charging and the stratifying layer, as well as the vertical components of the flows entering or leaving the thermal storage. However, the latter mainly depend on the geometry of the in- and outlet, s. [29]. Thus, radial in- and outlets (radial diffusers or deflector plates) seem to be optimal for stabilizing the stratifying layer and minimizing the energetic losses, s. **Figure 7** and [5, 16, 29, 30]. For this purpose, the shearing stresses τ between the fluid entering/ leaving (from/ into the DH network) and remaining within the thermal storage have to be minimized. This might be achieved by reducing the relative velocity c_{diff} , s. [31].

$$\tau \sim \frac{\rho}{2} c_{diff}^2 \quad (8a)$$

On the other hand, minimizing the shearing stresses τ (c_{diff}) consequently to a minimum, the flexibility of operation is diminished as the minimum time for a (dis-) charging cycle Θ shall be, s. **Table 1**.

$$\Theta = \frac{V_{stor}}{Q_{in,stor}(c_{diff})} \quad (9)$$

Against this background, the height of the diffuser s_{diff} and its diameter d_{diff} must be adjusted (geometry of the radial diffuser/ deflector plate), regarding the diameters of the in-/outlet pipe D_{pipe} and of the thermal storage D_{stor} , s. [6]. Resulting, within large scale storages, turbulent inlet flows occur ($Re_{diff} \gg 2,300$) at relative velocities $c_{diff} < 0.2 \text{ m/s}$. Thus, a direct dependence of the shear stresses τ and s_{diff} is given leading to a partially vertical momentum of the mass flows entering/ leaving the storage: $P_{vert} = (\rho \cdot \dot{V} = (\rho_{vert} \cdot \rho_{rad} \cdot \rho_{tan})^2)$. For $\Theta = const$ as well as

Table 7: Approximation of energetic losses induced by falling films within thermal storages without (top) and with (bottom) adaptations of the internal wall structure (thermal loading status $\Delta 50\%$; $H/D = 1.0$;

$$s_{lay}(\Theta) = 2.3 \text{ m}; T_{min} = 58^\circ\text{C}; T_{max} = 98^\circ\text{C}; l_{fall} = H/2; 10 \text{ m}$$

V_{st} [m ³]	10 ⁴	3*10 ⁴	5*10 ⁴	10 ⁵
l_{fc} [m]	11.68	16.84	19.96	25.15
High temperature partition (head of storage)				
c_{Fi} [mm/s]	1.02	1.23	1.34	1.51
δ_L [mm]	44.8	46.9	47.6	48.4
$V_{falling}$ [m ³ /d]	72.67	131.84	172.88	248.53
Stratifying layer (boundary layer)				
c_{Fi} [mm/s]	0.93	1.12	1.22	1.37
δ_L [mm]	44.8	46.9	47.6	48.4
$V_{falling}$ [m ³ /d]	66.24	120.18	157.58	226.54
Δ [m ³ /d]	6.43	11.67	15.30	22.00
$ds_{lay}(C)/s$ [mm / d]	7.5	6.5	6.1	5.5
Energetic analysis acc. to Table 3 & equation 7				
$Q_{loss,th}$ [MWh/d]	0.40	0.90	1.20	2.00
$Q_{loss,fc}$ [MWh/d]	0.08	0.15	0.19	0.29
$Q_{loss,fall}/Q$ [%]	0.04	0.03	0.02	0.01
V_{st} [m ³]	10 ⁴	3*10 ⁴	5*10 ⁴	10 ⁵
l_{fc} [m]	10			
High temperature partition (head of storage)				
c_{Fi} [mm/s]	0.95			
δ_L [mm]	43.7			
$V_{falling}$ [m ³ /d]	56.13			
Stratifying layer (boundary layer)				
c_{Fi} [mm/s]	0.51			
δ_L [mm]	43.7			
$V_{falling}$ [m ³ /d]	51.17			
Δ [m ³ /d]	4.97			
$ds_{lay}(C)/s$ [mm / d]	5.0	1.7	1.0	0.5
Energetic analysis acc. to Table 3 & equation 7				
$Q_{loss,th}$ [MWh/d]	0.40	0.90	1.20	2.00
$Q_{loss,fc}$ [MWh/d]	0.08	0.15	0.19	0.29
$Q_{loss,fall}/Q$ [%]	0.02	<0.01		

constant relative heights of the diffuser s_{diff}/D_{diff} the shear stresses are:

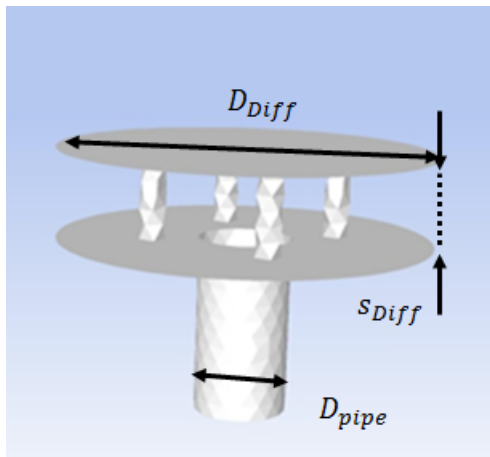


Figure 7: Scheme of a radial diffusor (deflector plate), s. [29]

$$v \sim \frac{v}{\rho} \cdot c_{D_{Diff}} \sim \frac{1}{s_{Diff}}, \text{ with } s_{Diff}/D_{Diff} = const \ \& \ \theta = const \ (8b)$$

Given that the thermal storage is fully charged (load status $A = 100\%$), the vertical component of the fluid elements discharged (containing a vertical momentum p_{vert}) induce an interaction with the stratifying layer. Likewise, an interaction of the fluid elements entering a thermal storage completely discharged (load status $A = 0\%$) is induced by the fluid elements entering the thermal storage (containing a vertical momentum p_{vert}). However, these interactions rapidly diminish for raising distances between the in-/ outlet and the stratifying layer.

Regarding these qualitative considerations, a minimum strength of the stratifying layer seems to be probable. This relation has been verified for a large scale thermal storage during a research project funded by the Federal Ministry of Economic Affairs and Energy Germany (BMW), s. [6, 18, 24, 29]. Thus, depending on the temperature drop within the thermal storage media $\Delta T_{top} = T_{Max} - \Delta T_{Min}$, the minimal (and typical) strength of the stratifying layer s_{Strat} is restored within 24h previous to unrepresentative load statuses of A .

s_{Strat} might be approximated by equation (10). However, during non-representative operational conditions, the thermal layer has been inserted into the supply or return flow of the DH system, reducing the strength of the thermal layer significantly. Nevertheless, the stratifying character of the thermal layer as well as the vertical temperature gradient dT/dh remains quite constant. Thus, considering constructive adjustments of the radial diffusor according to [6], the stratifying layer covers less than 15% of storage volume V_{Strat} for

all relative heights H/D relevant for large scale thermal storages.

$$s_{Strat} = 8 \dots 12 s_{Diff} \quad (10)$$

Considering the physical interactions between vertical momentum p_{vert} and flexibility of operation, a quantification of energetic losses occurring due to turbulent flows in and out of the thermal storage seems to be pointless. On the contrary, the stratifying layer must be comprehended as an unavoidable part within thermal storages, guaranteeing the applicability and economic utilization of these systems.

Against this background, the stratifying layer has to be considered during planning and projecting thermal storages. Technically, minimizing the strength of a stratifying layer is possible by a partial utilization within the DH system and reloading the thermal storage very carefully. As soon as the distance between the in or outlet meets the dimensions given in equation (10), the strength of the thermal layer remains small. However, enforced heat flows in the aftermath of this careful reload will enhance the growth of the stratifying layer significantly in comparison to the description given previously. Thus, the effect of this measure will diminish quite fast.

SUMMARY AND OUTLOOK/ PROSPECT

Thermal storages in urban DH networks, generally implemented as large scale applications ($V_{Strat} = 10,000 \dots 100,000 m^3$) will contribute to an optimized operation of CHP plants. In order to optimize the charging and discharging cycles of thermal storages, the energetic contents available and storable within the storage must be known for every operational state.

The major heat transfer mechanisms within atmospheric, sensible thermal storages utilizing a stratifying layer, have been analysed and evaluated according to their impact on the energetic contents. External heat transfers via the wall, conductive heat transfer within the thermal storage media itself and the wall of the thermal storage (representing thermal short circuits) and convective heat transfer mechanisms due to falling films have been examined. Within this context, heat transfer mechanisms resulting in heat flows out of the system (via the wall of the storage) as well as heat flows within the system itself (storage) have been considered.

Within this context, heat losses via the wall may be declared as "true" losses, whereas heat transfer mechanisms within the system itself cause no change of the energetic contents inside the thermal storage. However, these internal mechanisms cause a

temperature compensation between different layers within the thermal storage, generally characterized by the development of the stratifying layer. These losses are described by a numerical model for the time dependant development of the thermal layer, starting from an ideal stratification.

Approximating the energetic and exergetic losses of thermal storages, six major loss mechanisms have to be taken into account:

1. The external heat losses of a thermal storage mainly depend on the strength of the insulation. Within the insulation more than 95% of the temperature gradient between the environment and thermal storage media is bridged. Additional considerations of other parts of the wall structure (steel casing, etc.), the steam cushion, the soil below the storage or thermal boundary layers are of minor importance for a quantification of the external heat losses. The heat transfer mainly occurs due to conduction within the wall, whereas convective mechanisms at the interior/ exterior of the wall diminish these losses insignificantly. For typical large scale systems of thermal storages found in urban DH systems, external heat losses cause an energetic loss of less than 0.1% within 24h.

2. Besides exterior losses, internal temperature compensations via the stratifying layer diminish the energetic contents utilizable for DH systems within thermal storages. The heat flows from high- to low-temperature layers depend on the (growing) strength of the stratifying layer and diminish the energetic content utilizable. In order to quantify these internal losses, the minimum temperature directly integrable for DH purposes must be defined. Furthermore, operational conditions, especially the (dis-) charging of the thermal storage, as well as the typical strength of the stratifying layer influence these internal temperature compensations. Internal losses due to convective effects within the thermal storage media are approximately twice as relevant as external losses.

3. In addition to internal heat transfer mechanisms within the thermal storage media itself (having a comparatively low heat conductivity), thermal short-circuits having integrating high heat conductivities (e.g. steel) diminish the energetic contents utilizable. Within this context, the effect of the storage wall, representing the main thermal short circuit within thermal storages, is approximated. However, the impact of heat transfers via the wall on the energetic contents of a thermal storage is significantly smaller than the impact of heat transfers within the thermal storage media itself. This is directly connected to small relative strengths of the wall in comparison to the diameter of large scale storages.

4. Besides conductive effects within the infrastructure of thermal storages, its thermal inertia also diminishes the energetic contents utilizable and effects the

stratification within the thermal storage. Assuming a total loss of heat contents stored within thermal inertias, comparatively high energetic losses occur. However, the evaluation of these losses within the context of a DH system has to be done within the upcoming simulation of the overall DH system. Furthermore, the impact of the infrastructure on the thermal stratification may be neglected.

5. Falling films occurring at the interior of the wall additionally diminish the energetic contents utilizable for DH purposes. The growth of the stratifying layer is considered regarding the similarity of forces occurring within the flow boundary layer, as well as the interdependencies of temperatures and densities within the storage media. Thus, the impact of falling films on the strength of the stratifying layer may be quantified. However, the impact of falling films occurring is significantly smaller than the impact of heat flows occurring within the thermal storage media itself. Furthermore, constructive adjustments of the internal wall structure, such as circumferential obstacles (rib-structure), limit the free length for vertical flows. These obstacles must penetrate the flow boundary layer.

6. Turbulences induced by (dis-) charging are unavoidable within the context of a flexible operation of thermal storages. Therefore, a quantification of the losses occurring due to operational cycles seems to be inappropriate for a characterization of thermal storages. In fact, the strength of the stratifying layer occurring due to turbulences induced, guarantees a stable operation of these storages and a minor influence of internal heat flow mechanisms within the storage media as well as thermal short circuits. Against this background, the strength of the stratifying layer must be considered planning sensible thermal storage systems in large scale.

Summarizing, models existing and given in literature for the description of heat transfer mechanisms within stratifying heat storages, are appropriate for the description of thermal storages in large scale. Thus, energetic losses occurring may be described by adjusting these models according to the special boundary conditions of operation for large scale storages. Within this context, a numerical model for the time dependent development of the stratifying layer has been developed. Thus, an approximation and quantification of the energetic contents lost for utilization within DH purposes is possible.

The examinations and calculations done, certify the high efficiency of large scale thermal storages. Therefore, thermal storages are suitable for decoupling the generation and allocation of heat contents. Main characteristics of an efficient thermal storage system in large scale are:

1. low specific surfaces in relation to the volume of the thermal storage,
2. low vertical heat flows within the storage media, due to a stable stratifying layer,
3. low vertical heat flows within thermal short circuits, due to a small relative strength of the wall in comparison to the diameter of large scale storages, as well as a minimum of vertical and highly conductive parts of the storage infrastructure a
4. low ratio of thermal masses in comparison to the thermal mass of the storage media and
5. low radial gradients of temperatures and densities, due to thermal insulations.

Furthermore, a careful adjustment of the in and outlet (radial diffusors, deflector plates) considering hydrodynamic and operational parameters of the overall DH system attached to the thermal storage, supports these features. Against this background, a high relative share of heat losses occurring during the operation of large scale thermal storages are improbable, as long as common geometries and operational parameters are taken into account during the planning and dimensioning of storage systems.

Prospecting, the impact of thermal inertia and heat contents stored within thermal masses of the storage infrastructure have to be examined within the context of an overall DH system. Thus, especially vertical elements of the storage infrastructure, such as pipes within or the wall of the storage, may cause transient states of operation, resulting in additional energetic losses. Furthermore, turbulences induced during operational cycles (charging and discharging) must be in the limelight of future examinations. These are depending on the geometry of the in and outlet (radial diffusor, deflector plate), as well as technological and economical target parameters the overall DH system.

REFERENCES

- [1] AGFW | Der Energieeffizienzverband für Wärme, Kälte, KWK e. V. (Hrsg.): Die 70/70-Strategie Konzept und Ergebnisse. AGFW-Projektgesellschaft für Rationalisierung, Information und Standardisierung mbH, Frankfurt a. M.
- [2] Dubois, R.: Optimale Tageseinsatzplanung von Kraft-Wärme-Kopplungssystemen unter Berücksichtigung von Kurzzeitspeichern. Fortschrittsbericht VDI Reihe 6: Energieerzeugung Nr. 194, Düsseldorf: VDI-GmbH, 1986.
- [3] Gustafsson, S.-I., Karlsson, B.: Heat Accumulators in CHP networks. *Energy Conversion and Management* 33, pp. 1051-1061, 1992.
- [4] Ito, K., Yokohama, R., Shiba, T.: Optimal operation of a diesel engine cogeneration plant including a heat storage tank. *Journal of Engineering for Gas Turbines and Power*: 114, pp. 687-694, 1992. [5]
- [5] Pfeiffer, R., Verstege, J.: Committing and dispatching power units and storage devices in cogeneration systems with renewable energy sources. *Power System and Control Management*, pp. 21-25, 1996.
- [6] Huhn, R.: Beitrag zur thermodynamischen Analyse und Bewertung von Wasserwärmespeichern in Energiewandlungsketten. Dissertation, Stuttgart, 2006.
- [7] Verda, V., Colella, F.: Primary energy savings through thermal storage in district heating networks. *Energy* 36, pp. 4278-4286, 2011.
- [8] Dittmann, A., Nestke, C.: Wärmespeicherung erhöht die Effizienz der Kraft-Wärme-Kopplung, *EuroHeat & Power* 39, pp. 34-41, 2010.
- [9] Bestrzynski, G.K., Holler, S., Olbricht, M.: Energetic Performance of Short Term Thermal Storage in Urban District Heating Networks, 14th. Int. Symp on District Heating and Cooling (Stockholm), 2014.
- [10] Bode, W., Haziak, S., Leonhardt, K., Schurich, W.: Untersuchungen zum Ausnutzungsgrad und zur Ladeziffer von Heißwasserverdrängungsspeichern, *Energietechnik* 11, pp. 495-501, 1996.
- [11] Straub, J., Morlock, T., Rukes, B.: Wirkungsgrade großer Kurzzeitspeicher in Tankbauweise im Jahresmittel. *BWK* 39, pp. 123-126, 1987.
- [12] Prinz, W.: Konstruktive und wirtschaftliche Aspekte des Kurzzeit-Wärmespeichers in Flensburg. *Fernwärme International*: 4, pp. 249-257, 1982.
- [13] Schmidt, T. Danda, R.: Errichtung und Betrieb eines Fernwärmespeichers. *EuroHeat & Power* 6, pp. 366-367.
- [14] Roos, M. Kneiske, T., von Appen, J., Barth, H., Hidalgo, D., Hochloff, P., Braun, M., Schumacher, P., Fink, H.: Dezentrale Strom- und Wärmespeicherung im Smart Grid. FVEE Jahrestagung, Freiburg, 2013.
- [15] Neumann, W.: Dezentrale Kraft-Wärme-Kopplung mit Wärmespeichern Die Alternative zu Pumpspeicherwerken und Brücke zu erneuerbaren Energien. *Deutscher Naturschutztag* 31, Erfurt, 2012

- [16] Baur, F., Porzig, M., Noll, F.: Strom und Wärmespeicher als Bestandteil eines Dezentralen Energiemanagements. Solarzeitalter 4, IHRES 2010.
- [17] Nelson, J.E.B., Balakrishnan, A.R., Srinivasa Murthy, S.: Parametric studies on thermally stratified chilled water storage systems, Applied Thermal Engineering, 19, 1999, pp. 89 – 115.
- [18] Ismail, Kamal A. R., Leal, Janaina F. B., Zanadri, Mauricio A.: Models of liquid storage tanks. Energy 22, 1997, pp. 805 – 815.
- [19] Kumana, J. D., Kothari, S. P.: Predict storage-tank heat transfer precisely. Chemical engineering, 1982, pp. 127 – 132.
- [20] Jack, M. W., Wrobel, J.: Thermodynamic optimization of a stratified thermal storage device, Applied Thermal Engineering, 2009, pp. 2344 – 2349.
- [21] Petersen, M. K., Aagaard, J.: Heat accumulators. News from DBDH I, 2004.
- [22] Stads, V.: Wärmespeicherung – Technik und Wirtschaftlichkeit – Konventionelle Speicherung. Fernwärme International – FWI, Jg. 8, Heft 1, 1979, S. 20 - 23.
- [23] Bundesamt für Wirtschaft und Ausfuhrkontrolle, (Hrsg.): Leitfaden zum Nachweis der Speichereffizienz im Rahmen des Kraft-Wärme-Kopplungsgesetzes, Stand 2014.
- [24] Herwig, A, Rühling, K.: Fiber-Ptic Distributed Temperature sensing of Large Hot Water Storage Tanks, 14th. Int. Symp on District Heating and Cooling (Stockholm), 2014.
- [25] Incropera, F. P., DeWitt, D. P., Bergamnn, T. L., Lavine, A. S.: Heat and Mass Transfer. Wiley and Sons Inc., 6th Edition, 2007.
- [26] Baehr, H. D., Stephan, K.: Wärme- und Stoffübertragung (Heat and Mass Trasfer). Springer Press, 4th Edition, 2004.
- [27] Bejan, A., Kraus, A.: Heat Transfer Handbook. Wiley and Sons Inc., 2003.
- [28] Ostrach, S.: An Analysis of Laminar Free Convection Flow and Heat Transfer About a Flat Plate Parallel to the Direction of the Generating Body Force, National Advisory Committee for Aeronautics, Report 1111, 1953.
- [29] Huhn, R., Tödter, J.: Evaluierung der konstruktiven Gestaltung und Betriebsführung von Wärmespeichern nach einem einheitliche Kennziffersystem. Final report AiF-research project No. 12588 BG, Dresden, Hannover, 2002.
- [30] Bühl, R., „Planungsleitfaden zur geschichteten Be- und Entladung thermischer Speicher in solartechnischen Anlagen“, Chemnitz, 2009.
- [31] Schade, H., Kunz, E.: Strömungslehre, de Gruyter, 3. Auflage, 2007.

OPERATIONAL DEMAND FORECASTING IN DISTRICT HEATING SYSTEMS USING ENSEMBLES OF ONLINE MACHINE LEARNING ALGORITHMS

C. Johansson¹, M. Bergkvist¹, O. De Somer², D. Geysen², N. Lavesson³, D. Vanhoudt²

¹ NODA, Biblioteksgatan 4, 374 35 Karlshamn, Sweden

² EnergyVille/VITO, Thor Park 8310, Genk, 3600, Belgium

³ Blekinge Institute of Technology, 371 79 Karlskrona, Sweden

Keywords: *district heating and cooling networks, heat load forecast, algorithms*

ABSTRACT

Heat demand forecasting is in one form or another an integrated part of most optimisation solutions for district heating and cooling (DHC). Since DHC systems are demand driven, the ability to forecast this behaviour becomes an important part of most overall energy efficiency efforts.

This paper presents the current status and results from extensive work in the development, implementation and operational service of online machine learning algorithms for demand forecasting. Recent results and experiences are compared to results predicted by previous work done by the authors. The prior work, based mainly on certain decision tree based regression algorithms, is expanded to include other forms of decision tree solutions as well as neural network based approaches. These algorithms are analysed both individually and combined in an ensemble solution. Furthermore, the paper also describes the practical implementation and commissioning of the system in two different operational settings where the data streams are analysed online in real-time.

It is shown that the results are in line with expectations based on prior work, and that the demand predictions have a robust behaviour within acceptable error margins. Applications of such predictions in relation to intelligent network controllers for district heating are explored and the initial results of such systems are discussed.

INTRODUCTION

Operational data analytics where traditional engineering and modern data science solutions are merged is a driving force behind the development of innovative 4th generation district heating networks as well as the upgrading of current 3rd generation systems [1]. A key aspect of most such energy efficiency schemes is the ability to predict future behaviour within the network. Since district heating, by basic design, is demand driven, it follows that demand predictions are vital to the success of such endeavours. Heat demand is also an important support tool for traditional optimisation schemes due to the substantial time delays in heat delivery throughout a district heating

system. By using heat demand forecasting in such situations it is possible to increase the efficiency of heat generation in relation to the actual heat demand within the dispersed topology of the heating grid. Furthermore, the ability to control the demand is at the core of many operational optimisation solutions relating to smart grid technology such as demand side management and active load control, which further increases the value of heat demand forecasting [2].

Demand forecasting in district heating

The heat demand in a district heating system generally originates from space heating and tap water heating. While space heating is primarily weather dependant, the tap water usage is related to social behaviour [3]. This combination leads to a nonlinear, stochastic and non-stationary characteristic of the system that increases the complexity of any sufficiently good solution [4]. Furthermore, the development of modern real-time supervision systems increase the availability of real-time data, which although providing a valuable resource for extensive data analytics also increases the complexity of the situation.

Demand forecasting in district heating systems is not a new subject. Throughout the years a number of forecasting approaches have been proposed, including statistical models as well as machine learning solutions such as neural networks [5]. The statistical approach is normally focused on trying to separate the weather dependant heating demand from the tap water usage based on social behaviour. Such solutions can range from rather simple solutions, featuring linear functions, to more complex solutions combining physical knowledge of the system with statistical modelling [6, 7]. Using the physical knowledge of the network as a basis together with statistical models for identifying system parameters is also underpinning other similar approaches [8], in which the Box-Jenkins methodology is applied to an autoregressive moving average model (ARMA). The use of statistical models for demand forecasting also includes the application of seasonal autoregressive integrated moving average models (SARIMA) in which the forecasting values are derived using Kalman filtering [9].

The other major branch of demand forecasting is based on more machine learning related approaches such as neural networks or support vector machines [10, 11, 12]. This should in theory increase the ability of the solution to handle nonlinear and non-stationary behaviour in the data. These ideas have since been further explored, e.g. by introducing recurrent neural networks to improve the ability to handle non-stationary heat demands [13].

There are many influencing factors making up the total heat demand in a district heating system and it is in practice impossible to make an exact model of this behaviour. This is a contributing factor to the use of both statistical models and machine learning approaches in which exact physical models are not required. Furthermore, in addition to being dependant on the quality of historical data, the forecasting is also conditioned on the quality of the influencing factors during operational usage. For example, many demand forecasting models make use of an outdoor temperature forecast, which in itself can be of varying quality.

Machine Learning

Machine Learning is a methodology for finding and describing structural patterns in data [14]. Machine learning is a subfield of computer science and is usually regarded as a part of artificial intelligence research. The basic idea of machine learning is to construct algorithms, which in turn can generate models that can then make data-driven predictions or make decisions regarding classification of the data.

Normally a machine learning algorithm will use a set of training data to create a model. This model can then be used for subsequent predictions or classification tasks. A machine learning algorithm can consider static datasets as well as streaming data.

Ensemble learning

Ensemble learning is basically about taking the advice of several shareholders instead of only one, thereby arriving at a better conclusion. In the context of this paper, a forecasting model is a shareholder in the endeavour of generating sufficiently correct heat demand forecasts. Instead of only using one algorithm with one training set generating one single model to predict the future heat demand, several training sets and/or algorithms can be used to generate a set of models. This set can be combined in an intelligent way to obtain a better forecast. First results of applying this method are available, however in future research we will do an in-depth analysis of the different methods existing to define an optimal ensemble.

PROJECT OUTLINE

Previous work

Heat demand forecasting is an integrated part of our overall on-going endeavour to develop innovative smart grid technologies for district heating and cooling systems. The first part of this specific forecasting project was published at the 14th International Symposium on District Heating and Cooling in Stockholm, Sweden in 2014 [15]. In that paper we presented an online machine learning algorithm for heat demand forecasting. That the algorithm is online means that it automatically updates its model as new data becomes available. Due to the non-stationary nature of the heat demand such solutions represent an important step forward in domain specific data analytics.

The solution is based on a combination of decision tree machine learning algorithms and online functionality. The decision tree generation is based on ensemble bagging using the Fast Incremental Model Trees with Drift Detection (FIMT-DD) algorithm [16]. As the name implies FIMT-DD has the ability to detect concept drift in the data stream that helps it adapt to the non-stationary behaviour of an operational district heating system. The algorithm will grow sub-trees to replace those parts of the decision tree that becomes obsolete during the drift. Techniques for handling missing data and outliers were also added to the algorithm. All in all, this produces a solution that is efficient at processing streamed data while providing a robust forecasting ability.

As part of this previous work the performance of the algorithm was evaluated using operational data from the Karlshamn district heating system in the south of Sweden. Heat demand and outdoors temperature data was collected throughout a full heating season from residential buildings, commercial buildings and schools. This data was then analysed using the open source WEKA and MOA platforms [17, 18]. Two different approaches were studied in relation to the data. The first approach created one model for each building and then aggregated the predictions, while the second approach was to aggregate the building data and then create one single overall model.

The performance of the different approaches was evaluated using Mean Absolute Error (MAE) and Mean Absolute Percentage Error (MAPE) [19]. The results showed that the second approach (aggregate data before building a model) was slightly superior to the first approach (create individual models and then aggregate results). The mean absolute percentage error showed an error of 5,1 % (first approach) and 4.8 % (second approach) over the studied period.

It was concluded that the algorithm possessed a strong predictive ability during the experiment. The algorithm is memory efficient since it does not require the storage of large sets of data and each instance of data can be discarded after the algorithm updates the model. Furthermore, the algorithm is able to learn incrementally while processing large amounts of data in real time.

Current work for this paper

The primary purpose of this current study is to implement online machine learning forecasting algorithms in an industrial, fully operational real-time environment using actual weather forecasts as input for the system. Basically to run the system as it would have been used in an operational environment.

A selection of three algorithms was used to perform the tests, one of which is similar in construction to the algorithm presented in the previous work. Based on the results from the previous study only aggregated data was used to construct models (second approach). This also means that data such as meter data from production facilities can be used as input for the training. The first algorithm used is the Extra-Trees Regressor (ETR), which uses randomized decision trees in relation to sub-sets of the dataset in combination with averaging to increase predictive accuracy and to minimize over-fitting. The ETR algorithm is the one similar to algorithms used previous work. The second algorithm is Extreme Learning Machines (ELM) which is a feed-forward neural network used for regression analysis. An ELM uses a single layer of hidden nodes with randomized weights assigned to the input to the hidden layer. The third algorithm is an expansion of the ELM algorithm, in which a regularisation factor was added to prevent over-fitting of the training data. These algorithms were implemented according to the process described in the following section of the paper.

The main outcome of the work is to verify the accuracy of the forecasting schemes in an operational setting and to evaluate the influence of the added uncertainties due to the usage of actual weather forecasts.

EXPERIMENTAL SET-UP

The STORM project

STORM is a European Union Horizon 2020 project aimed at developing an innovative district heating and cooling network controller for enhanced district energy efficiency. The project started in 2015 will continue until 2018. The previous work was done outside of STORM, but since then the work has been merged with the overall effort of STORM.

The theoretical work in STORM is based on self-learning algorithms for efficient control of components within a thermal system, which is in line with the machine learning based efforts presented in this current work. The STORM controller is based on three generic modules relating to algorithms for forecasting, planning and tracking the operational behaviour with the thermal grid. The work presented in the paper is obviously related to the first of these three modules.

STORM will be implemented in two demonstration sites in Sweden and The Netherlands. The Swedish site is located in the city of Rottne in the south of Sweden. This district heating system is operated by Våxjö Energi and is a traditional 3rd generation system with two bio-fuel boilers, complemented with a peak load oil boiler. The IT-platform used in STORM is already operational in Rottne. This made it convenient to implement the forecasting algorithms described in this paper.

More information on the STORM project can be found in [1], a paper that will also be presented in this symposium.

Data management

Since the district heating system in Rottne is equipped with the STORM IT-platform, it is possible to access the operational data in real-time. This was used during the experiment for this study, in which historical heat demand and weather forecast data was used to train the forecasting models. Weather forecasts were used to train the models since such forecasts would later be used to evaluate the system. In addition to this, weather forecast data was continuously accessed on an hourly basis to make the actual predications for the coming days.

The forecasts were made every day based on weather forecast data available at 2:00pm. This time of day is used since it relates to the setting time of most spot price markets for electricity, which is relevant in relation to combined heat and power generation. This then generated hourly head demand forecasts for the coming day. The reason to use this set-up was that we wanted to evaluate the system in relation to combined heat and power generation, in which the day-ahead spot price market is relevant to optimize against. Since this market sets during the early parts of the afternoon the day before, it was relevant for us to follow those context boundaries. Also, in general it provides a more accurate prediction scenario since weather forecasts tend to become better and better the closer in time they get to the forecasted value. So using a deadline at around a day ahead for the weather forecast provides a better estimation of the actual operational ability of the system.

System implementation

The forecasting module is implemented on the STORM IT-platform, which in turn is based on the NODA Smart Heat Grid framework. This includes all required hardware and software, including communication infrastructure. The implementation of the operational module was a joint effort between VITO and NODA. Since they are located in different countries this required the sharing of data in a robust and secure manner.

Part of the NODA Smart Heat Grid framework is Linckii, which is a graphical user interface for managing data in graphs and other graphical schemes. For the forecasting module charts were created in Linkii by NODA. These charts were then accessed by VITO through HTTP GET requests on the chart data using the Python request package [20]. This data can be retrieved in either JavaScript Object Notation (JSON) or Comma-Separated Values (CSV) format. Both these formats are open standards for human-readable data exchange. This made it possible to exchange data between the NODA and VITO databases without affecting the overall function of the operational system. The forecasting module has been implemented with support for adding different database schemas through pluggable adapters set during configuration. Currently support for the NODA Linckii and VITO schemas are implemented. The database schemas supported are only limited by the dialects supported by SQLAlchemy, which at the time of writing includes Firebird, Microsoft SQL Server, MySQL, Oracle, PostgreSQL, SQLite and Sybase.

The development code for the project was separated on two different code repositories to retain proprietary information and data. Throughout the project GitLab was used as repository management and issue tracker [21]. Each new feature was tracked as an issue on GitLab, and all discussions regarding that feature was done in that specific issue. All development was done on feature branches. Then when a feature was considered complete a merge request was sent to another system developer for peer review. After a complete peer review of the code the feature branch was merged with the master development branch. The two different repositories were synchronised manually. This work process facilitated smooth integration and deployment throughout the prototype development effort.

Method

The forecasting module was evaluated during January, February and March of 2016 in the Rottne district heating system. The operational behaviour of each of the three algorithms was evaluated for each month separately as well as for the whole period. This

provided us with a diverse set of evaluation scenarios since the weather changed from winter to spring during that period of time. For the purpose of evaluation the algorithms were analysed using the common metrics of Mean Absolute Error (MAE) and Mean Absolute Percentage Error (MAPE). MAE and MAPE were also used during the previous work in the forecasting project, which makes it convenient to compare results.

In the context of this work the MAE shows the absolute difference between actual and predicted heat demand expressed in kW. The MAPE, however, is a relative metric, which means that it relates to the scale of the values being analysed. For example, consider two values of 50 and 100, both of which have an error of 10. Using MAE they would have the same error (i.e. 10), while having very different errors using MAPE (i.e. 10 is a larger percentage of 50 than of 100).

The forecasting module was part of the operational system, which basically means that it was run once a day at 2pm for the coming day using the weather forecast available at that point in time. This was repeated throughout the experimentation period.

RESULTS

Figure 1 shows the correlation between the outdoor temperature and the heat demand using forecasted as well as measured outdoor temperatures. During lower temperatures the weather forecast tends to consistently overestimate the outdoor temperature, which is why there are more low temperatures within the measured dataset.

Results are shown in relation to the evaluation metrics described in the previous section. Table 1 shows the evaluation metrics for the Extra-Trees Regressor (ETR) and the Extreme Learning Machines (ELM), for the whole experiment period as well as for each month individually. The results of the extended ELM are almost identical to the normal ELM, which is why they are not shown in Table 1.

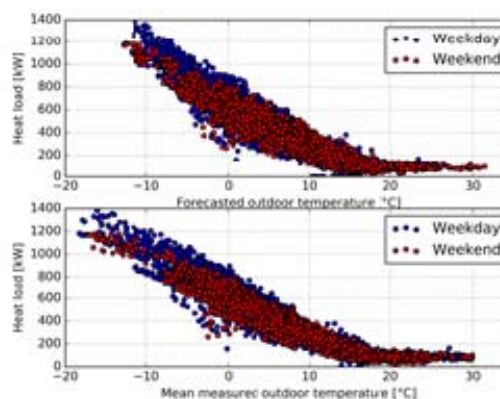


Figure 1: Correlation between outdoor temperature and heat demand

Table 1 Evaluation metrics

	ETR MAE	ETR MAPE	ELM MAE	ELM MAPE
Jan-Mar	73.24	11.7	91.72	14.31
Jan	89.84	10.2	145.25	17.62
Feb	48.05	7.59	43.13	6.84
Mar	76.28	16.56	75.26	16.86

results. This is especially true for ETR, which is not able to extrapolate predictions outside the span of the training data. Then in February the accuracy of the predictions is already significantly higher since the models are trained using the online data as this becomes available throughout the experiment period. There is also a decrease in accuracy during March due to systematic overestimation of the heat load in the second part of March. Reasons for this systematic overestimation cannot be found in the data as all algorithms lead to the same results in this time window.

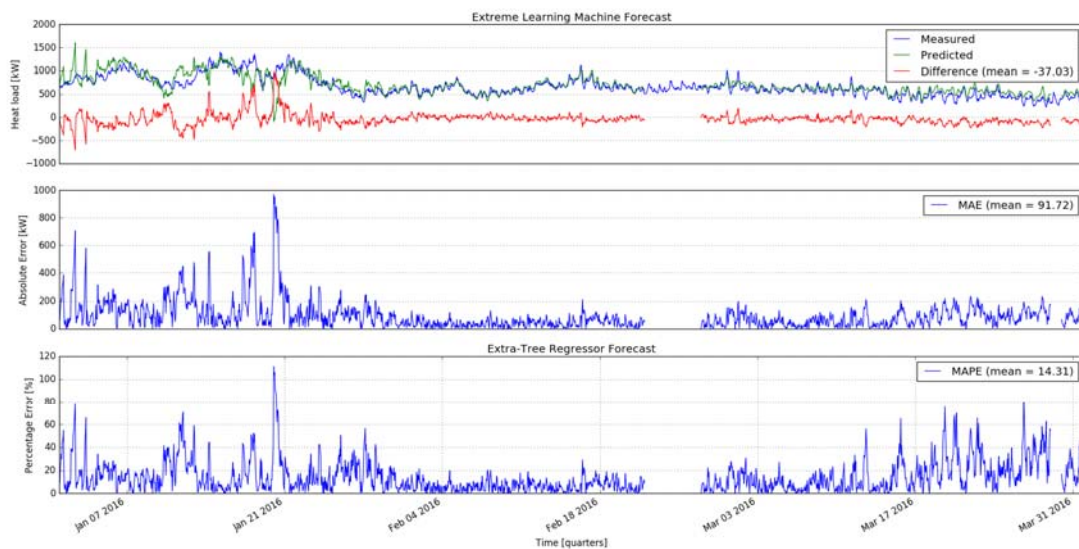


Figure 2: Operational behaviour of the ELM algorithm

Figure 2 shows a graph of the operational behaviour of the ELM algorithm during the period from January to March. There is a short period during late February with data missing due to communication error.

DISCUSSION

As shown in Figure 1 a strong correlation (-0.934) exists between the measured outdoor temperature and the heat load. A slightly less strong correlation (-0.909) holds between the forecasted outside temperature and the heat load. It follows that the temperature forecast is the most important feature for a heat load forecast. Due to the lower energy demand during the weekend it is also useful to add a feature representing the day of the week. A last feature representing the quarter of the day is also added because of the heat load being time dependent.

Table 1 shows that the accuracy of both forecasters is best in February. There are several reasons to explain this behaviour. In January there was a period with outdoor temperatures outside of the temperature span used to train the models, which leads to less accurate

In all probability this is due to a behaviour change in the system, which is not represented in the training set. Due to the origin of the errors being lacking training data, the models would be expected to improve their accuracy once this data is added into the training set.

Considering the above discussion February is the most appropriate metric to use since it most accurately resembles a long-term operational setting. Thus it can be concluded that ELM is superior to ETR.

It should be noted that the MAPE metric in March is high due to the lower total heat demand. This is due to the percentage centric approach by this evaluation metric. Considering the MAE metric it is clear that the accuracy is still acceptable given the context. This can be seen in Figure 2, as the forecast is following the measured data even though the head demand decreases.

There are multiple possibilities available to enhance the performance of the forecasters discussed in this paper. Preliminary analysis shows that adding a feature representing historical heat load information, more specific of the previous day, is important to improve the

accuracy. Next to this a feature representing the day of the year can be added to capture seasonal behaviour.

Furthermore, the ensemble concept can be improved by an optimal combination of the forecasting algorithms, for example by using intelligent weighting in more advanced machine learning methods.

CONCLUSION

It has shown that the forecasting algorithms work well during operational scenarios when relevant training data was available. The forecasting ability deteriorated when the models were confronted with scenarios not covered by their training data, which is especially apparent for ETR. However, it was also shown that through continuous re-training as new data becomes available, they were able to adapt which can be seen in the increased of accuracy in the transition between January and February. This shows that the algorithms become better over time and that they have the ability to improve using new datasets.

Several potential improvements have been identified during the practical experimentation phase, which can be implemented to increase the predictive ability of the system. The most significant of these is to add short term (24h) historical head demand data to the model. Also adding the day of year for seasonable purposes improves the accuracy. Adding the control signal corresponding to the historical heat demand only introduces slight improvements.

Artificial neural networks such as ELM provide the best forecasting ability of the studied algorithms, and they are able to handle data outside the training dataset.

ACKNOWLEDGEMENT

In this project EnergyVille/VITO, NODA and Växjö Energi are working within the context of the STORM project which is funded by the European Union's Horizon 2020 Programme under Grant Agreement no. 649743.

For Blekinge Institute of Technology this work is part of the research project "Scalable resource-efficient systems for big data analytics" funded by the Knowledge Foundation (grant: 20140032) in Sweden.

REFERENCES

- [1] D. Vanhoudt, B. Claessens, J. Desmedt and C. Johansson, "Status of the H2020 STORM", in proceedings of the 15th Symposium on District Heating and Cooling, Seoul, Korea, September 4-7 2016
- [2] C. Johansson, On Intelligent District Heating, Doctoral Thesis, Blekinge Institute of Technology, 2014
- [3] S. Fredriksen and S. Werner, District Heating and Cooling, Studentlitteratur AB, Lund, 2013
- [4] P. Bacher, H. Madsen, H. Aalborg and B. Perers, "Short-term Heat Load Forecasting for Single Family Houses", in Energy and Buildings, 2012, vol. 65, pp. 101-112
- [5] P. Giridhar (ed), Energy Management Systems, InTech, 2011
- [6] E. Dotzauer, "Simple Model for prediction of Loads in District Heating Systems", in Applied Energy, 2002, vol 73, pp. 277-284
- [7] H.A. Nielsen and H. Madsen, "Modelling the heat consumption in district heating systems using a grey-box approach" In Energy and Buildings, 2006, vol. 38, pp. 63-71
- [8] B. Chramcov, "Heat Demand Forecasting for Concrete District Heating Systems", in International Journal of Mathematical Models and Models in Applied Sciences, 2010, vol. 4, pp. 231-239
- [9] S. Grosswindhager, A. Voigt and M. Kozek, "Online Short-Term Forecast of System Heat Load in District Heating Networks". In proceedings of the 31st International Symposium on Forecasting, Prague, Czech Republic, 2011
- [10] M. Grzenda and B. Macukow, "Demand Prediction with Multi-Stage Neural Processing" in Advances in Natural Computation and Data Mining, 2006, pp. 131-141
- [11] K. Kato, M. Sakawa, K. Ishimaru, S. Ushiro and T. Shibano, "Heat Load Prediction Through Recurrent Neural Network in District Heating and Cooling Systems" in Systems, Man and Cybernetics, 2008, pp. 1401-1406
- [12] C.P. Tae, S.K. Ui, K. Lae-Hyun, W.J. Byung and K.Y. Yeong, "Heat Consumption Forecasting Using Partial Least Squares, Artificial Neural Network and Support Vector Regression Techniques in District Heating Systems" in Korean Journal of Chemical Engineering, 2010, vol 27, pp. 1063-1071
- [13] M. Sakawa, H. Katagiri, T. Matsui, K. Ishimaru and S. Ushiro, "Heat Load Prediction in District heating and Cooling Systems Through a Recurrent Neural Network with Data Characteristics", in Scientiae Mathematicae Japonicae Online, 2010, pp. 449-464
- [14] I.H. Witten, E. Frank and M.A. Hall, Data Mining – Practical Machine Learning Tools and Techniques 3rd ed. Elsevier Inc. 2010
- [15] S. Provatias, N. Lavesson and C. Johansson, "An Online Machine Learning Algorithm for Heat Load Forecasting in District Heating Systems", in proceedings of The 14th International Symposium

- on District Heating and Cooling, Stockholm, Sweden, 2014
- [16] E. Ikonovska, J. Gama and S. Dzeroski, "Learning Model Trees from Evolving Data Streams" in Data Mining and Knowledge Discovery, 2011, vol. 23, pp. 128-168
- [17] R.B. Remco, E. Frank, M. Hall, R. Kirkby, P. Reutemann, A. Seewald and D. Scuse, "WEKA Manual for Version 3-6-10", 2013
- [18] A. Bifet and R. Kirkby, "Data Stream Mining – A Practical Approach", 2009
- [19] U. Graham and I. Cook, A Dictionary of Statistics, 3rd ed. Oxford University Press, 2014
- [20] J. Danjou, The Hacker's Guide to Python – 3rd ed. Julien Danjou (Standard Copyright License), 2016
- [21] J.M. Hethey, GitLab Repository Management, Packt Publishing Limited, 2013

ESSENTIAL IMPROVEMENTS IN FUTURE DISTRICT HEATING SYSTEMS

H. Averfalk¹, S. Werner¹

¹ Halmstad University, PO BOX 823, Halmstad, SE 30118, Sweden

Keyword: *Low-temperature, system design, recirculation, thermal lengths, hydronic balancing*

ABSTRACT

The major common denominator for future efficient fourth generation district heating systems is lower temperature levels in the distribution networks. Higher efficiencies are then obtained in both heat supply and heat distribution. Heat supply becomes more efficient with respect to combined heat and power, flue gas condensation, heat pumps, geothermal extraction, low temperature excess heat, and heat storage. Heat distribution becomes more efficient from lower distribution losses, less pipe expansion, lower scalding risks, and plastic pipes. The lower temperature levels will be possible since future buildings will have lower temperature demands when requiring lower heat demands. This paper aims at providing eight essential recommendations concerning design and construction strategies for future fourth generation systems. The method used is based on a critical examination of the barriers for lower temperature levels and the origins of high return temperatures in contemporary third generation systems. The two main research questions applied are: Which parts of contemporary system design are undesirable? Which possible improvements are desirable? Key results and the corresponding recommendations include temperature levels for heat distribution, recirculation, metering, supervision, thermal lengths for heat exchangers and heat sinks, hydronic balancing, and legionella. The main conclusion is that it should be possible to construct new fourth generation district heating networks according to these eight essential recommendations presented in this paper.

INTRODUCTION

Policy

District heating systems are an important component in achieving future sustainable energy systems. The main idea is to utilise heat from sources otherwise unutilised [1, 2]. Effectively, this decrease energy demand and dependency of energy imports. Furthermore, implementation of district heating systems reduces the strain of scarce energy resources. Lower system costs and less anthropogenic climate change is a ripple effect of more district heating.

Due to the local nature of district heating systems, the technology has often been overlooked in international

policy assessments. This did, however, change in the Heat Roadmap Europe studies [3], wherein it was concluded that the European Union may reach its target of annual greenhouse gas emissions reduction to a lower cost with district heating compared to other proposed alternatives. Furthermore, the economic value of district heating was shown to be higher in a future scenario with a large degree of end-use energy efficiency measures [3] compared to a scenario with no end-use energy efficiency measures [4], when related to the reference alternative.

Some major recognition of district heating at a policy level can be observed in the United Nations Environment Programme report 'District Energy in Cities' [5] and by the European Union heating and cooling strategy [6, 7].

Technology change

In order to meet future conditions, the current district heating technology must be further developed. This technology has been referred to as third generation of district heating systems (3GDH) [2]. Hereby, the term for future development have been labelled as the fourth generation of district heating systems (4GDH), which has been defined in [2]. The basic idea is to maintain the best part of the current 3GDH technology while weak parts should be enhanced in 4GDH design.

Future conditions

Heat demands are expected to be lower in future buildings, as new buildings within the European Union are required to have a very high energy performance, referred to as nearly zero-energy buildings, from 2019 for public authorities and 2021 for others [8]. Furthermore, buildings which undergo major renovation should be upgraded to meet minimum energy performance requirements [8].

Lower heat demands entail opportunity, as adequate temperature requirement for space heating decrease as well, enabling lower temperature levels in distribution. In a long term structural perspective, levelling of adequate temperature requirements between supply, distribution, and end-use increase performance as there will be a better quality match between supply and demand and thus a better exergy utilisation rate [9].

Increased heat distribution costs are a consequence of future low heat demand energy systems. This relation

is of concern regarding feasibility of future district heating systems. However, the distribution cost component generally constitutes a smaller proportion of the total cost structure and thus have a moderate impact on feasibility [10].

Improved efficiencies in district heating systems are also centred on lower temperature levels in the distribution networks. In heat supply, low-temperature operation entail improved performance in combined heat and power, flue gas condensation, heat pumps, low temperature excess heat, geothermal extraction, solar thermal, and heat storage [11]. In heat distribution, low-temperature operation entails improvements by lower distribution losses, less demand for pipe expansion, lower risk for scalding, and potentially use of other piping materials, e.g. plastics [11].

Currently identified barriers to lower temperature levels in district heating systems consist of demand side limitations, legionella issue, substations faults, and bypass flows in networks [11]. From a technical system design perspective it is a challenge to overcome barriers which will allow low-temperature district heating operation. In current documentation of low-temperature systems, no annual average system return temperature below 30 °C has been recorded [11].

Implementation

Several possible options and alternative scenarios for transitions toward district heating systems with lower temperature levels in distribution networks are conceivable. The market is segmented into many different customer types with varying requirements of heat demands, for instance residential, commercial, and industrial. Four example areas of district heating expansion are described below, all of which may be classified in the spectrum of low or high heat density areas, i.e. single- or multifamily house areas, respectively:

- Development areas where prior district heating exist in surrounding urban area
- Development areas where no prior district heating system exist in surrounding urban area
- Urban areas where prior district heating system exist
- Urban areas where no prior district heating system exist

To maintain low-temperature level in new development areas wherein heat network operation already is established, concurrent operation are a feasible solution. Concurrent operation may be designed as:

- Parallel networks with different temperature levels

- Division into primary and secondary networks through hydraulic separation by central substations
- Supply-to-supply connections, cascading from customers with high temperature requirements to customers with lower temperature requirements
- Return-to-return connections, cascading from customers with medium temperature requirements to customers with lower temperature requirements

Aim

The aim of this paper is to provide a conceptual overview for desirable system design improvements in 4GDH for new distribution networks supplying heat to new buildings. The overarching goal is to elaborate the idea and initiate a discussion about proposed essential improvements regarding the issue of barriers, which obstruct transition to low-temperature operation. Thereby introducing, a potential path towards district heating systems with undisturbed annual average return temperatures lower than 30 °C.

This paper emphasise implementation of improved district heating design in residential development areas of high building density areas, i.e. multifamily house areas. The paper presumes a European harmonization perspective, availability of district heating supply, construction of buildings with very high energy performance, and expansion of district heating coordinated with simultaneous construction.

This paper is based on a qualitative approach. A critical examination perspective is applied, by searching for answers to the two main research questions:

- Which parts of contemporary 3GDH design is undesirable?
- Which potential improvements are desirable in future 4GDH design?

TEMPERATURE LEVELS

Undesirable 3GDH design

The temperature levels differ vastly between different networks, as may be observed [12]. Collected data on annual average supply and return temperatures display for Sweden 86-47 °C and for Denmark 78-43 °C, respectively. Similar national averages are not available for other countries, but corresponding system examples varies between 77 and 110 °C for supply temperatures and 41 and 76 °C for return temperatures.

The potential annual supply and return temperature levels achievable in contemporary system design are estimated to be 69 and 34 °C, respectively, according to simulations performed by [13].

Differences between actual and simulated network temperatures depend mainly on by-pass flows and temperature errors in substations and customer heating systems.

In a study which analysed many district heating substations, it was concluded that 74 % of the substations exhibited an erroneous function [14]. A brief overview of different cooling errors identified can be found in [1], these errors are based on 520 cooling errors found in 246 substations during 1992-2002.

The current higher temperature levels disable the use of low cost low temperature heat supply as these heat sources is only feasible at current supply temperature levels with the use of heat pumps.

Desirable 4GDH design

The lower boundaries for supply temperature in district heating systems are typically confined by the requirement to avoid legionella in domestic hot water preparation. As space heating demands typically may be fulfilled even at lower temperatures, particularly in buildings with very high energy performance.

There are of course other technical solutions which allows for lower temperature levels, such solutions does however require some form of auxiliary heating at the customer end of the system, commonly referred to as cold district heating systems. Whereas, the lower boundaries for return temperature in district heating systems typically are confined by the ambient indoor temperature. The envisioned temperature levels of future district heating systems are 50 and 20 °C for supply and return, respectively.

RECIRCULATION

Undesirable 3GDH design

Primary supply water is recirculated into the return pipe as a common contemporary system design in order to counteract supply temperature degradation.

Traditionally a summer problem, by-passes are built into the system to maintain sufficient primary temperature when network flow is low due to relative high heat losses at low space heating demands. The winter problem of freezing of non-used pipes is also managed with by-passes. These by-pass flows may be intentional, as described previously, but may also be unintentional, i.e. remnants or mistakes from older network expansion.

This traditional recirculation increases temperature levels in thermal networks, decrease efficiency, and increase costs [15].

By estimates, 10-20 % of total annual flows in district heating systems are by-passes. With regard to achieving an undisturbed return temperature, by-pass

flow in thermal networks is a major concern in heat distribution.

Desirable 4GDH design

Regardless of situation, by-passes are an undesirable component in future system design. Thus, future design should contain no by-passes between primary supply and return pipe. This should be achievable with the implementation of three-pipe systems. In which the smaller third pipe is used to recirculate supply temperature water when required, thus avoiding temperature degradation of supply flow and temperature contamination of return flow due to by-passes in the system.

METERING

Undesirable 3GDH design

At present, the dominating norm of district heat supply is collective metering in multi-apartment buildings, resulting in a low resolution of individual customer information.

The European energy efficiency directive [16] states that use of individual meters measuring use of heating in multi-apartment buildings supplied by district heating is beneficial only in buildings where radiators are equipped with thermostatic radiator valves thus enabling customers to have a means to control their own usage. This is not strictly true as there are additional benefits of individual metering, e.g. apartment metering enables the potential to isolate individual faulty substations which lead to increased return temperatures [14].

Furthermore, the energy efficiency directive [16] states that from 2017 multi-apartment building supplied by district heating shall install individual meters to measure use of heating, cooling, and domestic hot water for each apartment where technically feasible and cost-efficient. Hence, the current collective metering does not fulfil future legal requirements for individual metering.

Desirable 4GDH design

A transition to individual apartment substations will give a direct solution for providing individual metering according to the energy efficiency directive. The implications of a change from collective to individual metering will be:

- Heat transfer between apartments may occur if indoor temperature settings vary between apartments effectively allowing apartments with low temperature settings to be heated by other residents heating
- Residents may, if accessible, alter the ventilation systems in the interest of saving on heating expenses. For instance, by reducing or

eliminating ventilation air flow, less heat is required. In doing so residents endanger their own health and risk damages on the building itself [17]

- Heat losses associated with hot water circulation is allocated to the heat supplier with individual apartment substations

These implications must be considered when implementing individual apartment substations.

SUPERVISION

Undesirable 3GDH design

A deficit of individual customer information hinders heat suppliers to counteract temperature errors as there is no access to information to act upon.

Temperature errors can currently exist for months or years before discovered and eliminated, this situation is undesirable

Desirable 4GDH design

Use of continuous commissioning by increased implementation of information and communications technology (ICT) would alleviate the work to counteract temperature errors in substations and customer heating systems. Since, with increased capacities to retrieve, transmit, and analyse information electronically in a digital form a situation with affluence of individual substation information emerge.

THERMAL LENGTHS, HEAT EXCHANGERS

Undesirable 3GDH design

Current use of heat exchangers in substations creates an average difference in temperature levels of about 10-15 °C between the district heating network and the customer heating systems.

Sizing of heat exchangers have in Sweden typically been dependent on design requirements in industry standards. These industry standards use the performances indicator of thermal length, expressed as number of thermal units (NTU) for heat exchangers. These thermal lengths have increased from about two during mid-1960s to four today, regarding space heating. Development of heat exchangers for domestic hot water has seen similar improvements of required thermal lengths. Such design of thermal length in substation heat exchangers will be insufficient under future design conditions.

Desirable 4GDH design

An increase of thermal length is required to meet future design requirements of decreased temperature levels. By increasing thermal length in substation heat exchangers the mean logarithmic temperature gap between primary and secondary side is shortened. By

introduction of heat exchangers with a thermal length of 6-8, which is 1.5-2 times longer than contemporary design, the mean logarithmic temperature will be reduced to around 5-10 °C.

THERMAL LENGTHS, RADIATORS

Undesirable 3GDH design

By tradition high radiator temperatures have been used in order to reduce radiator sizes at high heat demands.

The secondary space heating system may also be assessed with the thermal length concept, since a radiator is a heat exchanger. Contemporary design temperature levels for radiator systems are in older buildings 80-60 °C and in newer buildings 60-40 °C, with a constant room temperature of 20 °C this yield thermal lengths of 0.4 and 0.7, respectively.

Desirable 4GDH design

To maintain a high temperature difference it is important to consideration radiator sizing. In future buildings with low heat demands, requirement of radiators sizing may be reduced. It is however desirable to have larger or at least to retain contemporary radiator sizing in order to facilitate the issue of high temperature difference in space heating system.

Envisioned temperature levels of future systems require change of design temperatures in radiator systems. Projected design parameters entail longer thermal lengths; a feasible setting for radiator supply and return temperatures are 45-25 °C, with a constant room temperature of 20 °C. The defined conditions for new developments result in a thermal length of 1.5, an increase by a factor two compared to contemporary system design.

Floor heating is an alternative to radiators for space heating, with an average supply temperature just a few degrees above room temperature [2]. A case study performed in [11], suggest a supply temperature for floor heating of about 30 °C, with approximately a 3 °C temperature drop to maintain an even temperature on the heated area. The advantage with floor heating is lower requirements of supply temperature levels, while the disadvantage is slightly higher return temperatures, compared to radiators.

HYDRONIC BALANCING

Undesirable 3GDH design

Unbalanced radiator systems inadvertently cause overflows in some parts of the system; these can be apprehended as by-passes creating higher return temperatures.

It is difficult to obtain a sustainable and reliable hydronic balancing in radiator systems as the

conventional way of managing hydronic flow regulation is through manual setting of balancing valves and radiator valves [18]. Manual hydronic balancing management is labour intensive as the whole system initially requires balancing. Readjustment may be necessary as misallocations may occur and even in a balanced system additional balancing may be required as time progress due to changes, intended or unintended, in existing hydraulic system.

Desirable 4GDH design

In order to avoid excessive amounts of endeavours to maintain a functional space heating system, perfect allocations are desirable. The issue of hydronic balancing become less extensive with the introduction of individual apartment substations. To maintain a high temperature difference between supply and return flow, automated hydronic balancing is although desirable.

Introduction of flow valve limiters at radiator outlets in customer space heating systems would ensure a certain return temperature, if flow is regulated with regard to outlet temperature. By limiting flow, heat emission to ambient heated space is ensured. Flow valve limiters can regulate radiators individually without impact of flow allocation of the overall system.

LEGIONELLA

Undesirable 3GDH design

Growth of the Legionella bacterium is a concern in domestic hot water preparation. The bacteria exhibit stagnation in growth at 46 °C and the concentration of bacteria decrease rapidly with higher temperatures, according to current knowledge [19].

Recent research suggest that the bacteria may grow in higher temperatures as well [20]. If such results become more apparent then it becomes even more significant to have efficient domestic hot water preparation.

The Legionella issue is related to slow domestic hot water preparation with long residence time in hot water circulation and storages.

Desirable 4GDH design

The key to this issue is low water volumes at secondary side and fast domestic hot water preparation, i.e. instantaneous discharge by heat exchanger, in order to obtain short residence times. District heating substations are able to provide this.

By implementation of individual apartment substations, large networks of hot water circulation, with volumes exceeding three litres, may be avoided in large buildings. Meanwhile, the requirement of domestic hot water circulation is avoided with individual apartment substations which further alleviate the issue of Legionella.

The German regulation for domestic hot water is commonly referred to in relation to low temperature district heating operation [21]. This regulation states that domestic hot water may occur without any specific safety measures against Legionella as long as total volume in the piping does not exceed three litres. In addition the regulation states that for small systems, i.e. on an individual household level, a recommended temperature of 60 °C is suggested, while it also states that temperatures below 50 °C should be avoided at all times.

Table 1 Summary of the overall and seven identified undesirable contemporary system design areas with corresponding desirable system design improvements

Location	Design area	3GDH traditions	4GDH requirements	4GDH Actions
System	Temperature levels	Sweden 86-47 °C Denmark 78-43 °C	Vision of 50-20 °C	No temperature errors, longer thermal lengths, and more efficient customer heating systems
Network	1. Recirculation	By-passes	No by-passes	Three-pipe systems
Substation	2. Metering	Collective	Individual	Apartment substations
Substation	3. Supervision	Many temperature errors	Continuous commissioning	ICT Supervision
Substation	4. Thermal lengths, heat exchangers	About 4	About 6-8	Longer thermal lengths
Customer	5. Thermal lengths, radiators	About 0.4-0.7	About 1.5	Longer thermal lengths
Customer	6. Hydronic balancing	Many misallocations	Perfect allocations	Automated hydronic balancing
Customer	7. Legionella	Hot water circulation and sometimes hot water storages	No hot water circulation and no hot water storages	Apartment substations

DISCUSSION

The main actions for enhancing the 4GDH system design are three-pipe systems for heat distribution and individual apartment substations for customer interfaces. Enhanced individual apartment substations, have several important synergy advantages as they

- fulfil future legal requirements from the European energy efficiency directive concerning individual metering
- increase resolution of which temperature errors may be identified by metering
- eliminate the demand for hot water circulation in buildings
- decrease volume of water in the secondary side, which implies less risk of legionella
- reduce the demand for complex manual hydronic balancing, as secondary system for space heating become limited to apartment level rather than building level
- will allow for large harmonized manufacturing volumes of universal components, such as heat exchangers, furthering the perspective of economy-of-scale

By ensuring coordination in early stages of project planning, agreements of new and improved technological solutions can be achieved. Also, coordination of pipeline construction with other building construction infer typically halve the construction cost compared do pipeline construction in pre-existing buildings areas [1].

CONCLUSION

In this paper, seven specific areas which imply barriers to achieve lower temperature levels are identified. Furthermore, commensurate technical system improvements to counteract the seven specific areas of barriers to achieve lower temperature levels in future district heating are suggested.

With respect to the first research question, the following undesirable design areas in contemporary 3GDH systems have been identified:

1. By-passes contaminate return flow and prevent an undisturbed return temperature in thermal networks.
2. Collective metering does not fulfil future legal requirements for individual metering.
3. Lack of systemic supervision of substations by district heating utilities, result in omission to rectify a large number of temperature errors.
4. Current thermal lengths in substation heat exchangers are to short hinder transition towards low temperature operation.

5. Short thermal lengths in customer radiator systems are remnants from a period of high heat demands.
6. Many misallocations occur in customer radiator systems due too high complexity of manual settings for hydronic balancing and radiator valves.
7. High residence time and large volumes of domestic hot water induce greater risk of legionella growth in customer systems.

With respect to the second research question, the following desirable actions in future 4GDH systems have been identified:

1. Three-pipe systems in order to supply water circulation without any pollution of the true return temperature.
2. Apartment substations in order to provide individual metering and supervision together with avoidance of Legionella growth and major hydronic balancing problems.
3. Longer thermal lengths in heat exchangers and radiator systems in order to reduce temperature differences at heat transfer.

By conducting this work we have identified seven important design areas to be considered for implementation of 4GDH systems. Only one design areas concern the distribution network, while three design areas are associated to the customer interface and three design areas are related to the customer heating systems.

Hereby, concluding that the essential key actions for transition towards 4GDH in new distribution networks for new buildings are located in substations and customer heating systems close to the final heat use.

ACKNOWLEDGEMENT

The present work was performed within the research project Future District Heating Technology financed by Fjärrsyn – the Swedish district heating research programme funded in collaboration by the Swedish Energy Agency and the Swedish District heating Association.

REFERENCES

- [1] Frederiksen S, Werner S. District Heating and Cooling. Lund: Studentlitteratur AB; 2013.
- [2] Lund H, Werner S, Wiltshire R, Svendsen S, Thorsen JE, Hvelplund F, et al. 4th Generation District Heating (4GDH): Integrating smart thermal grids into future sustainable energy systems. *Energy*. 2014;68:1-11.
- [3] Connolly D, Lund H, Mathiesen BV, Werner S, Möller B, Persson U, et al. Heat Roadmap

- Europe: Combining district heating with heat savings to decarbonise the EU energy system. *Energy Policy*. 2014;65:475-89.
- [4] Connolly D, Mathiesen BV, Alberg Østergaard P, Möller B, Nielsen S, Lund H, et al. Heat Roadmap Europe 2050 - First pre-study for the EU 27. Aalborg University and Halmstad University: 4DH; 2012.
- [5] United Nations Environment Programme. District Energy In Cities - Unlocking the Potential of Energy Efficiency and Renewable Energy. 2015.
- [6] European Commission. EU Strategy for Heating and Cooling (Part 1/2). (SWD(2016)24, 1622016; COM(2016) 51) 2016.
- [7] European Commission. EU Strategy for Heating and Cooling (Part 2/2). (SWD(2016)24, 1622016; COM(2016) 51) 2016.
- [8] Council Directive 2010/31/EU of 19 May 2010 on the energy performance of buildings. [2010] OJ L153/13.
- [9] Gong M, Werner S. Exergy analysis of network temperature levels in Swedish and Danish district heating systems. *Renewable Energy*. 2015;84:106-13.
- [10] Persson U, Werner S. Heat distribution and the future competitiveness of district heating. *Applied Energy*. 2011;88:568-76.
- [11] Rosa AD, Li H, Svendsen S, Werner S, Persson U, Ruehling K, et al. Annex X Final report | Toward 4th Generation District Heating: Experience and Potential of Low-Temperature District Heating. IEA DHC|CHP. 2014.
- [12] Gadd H, Werner S. Achieving low return temperatures from district heating substations. *Applied Energy*. 2014;136:59-67.
- [13] Gummérus P. Analys av konventionella abonnentcentraler i fjärrvärmesystem (Analysis of conventional substations in district heating systems). Göteborg: Chalmers Tekniska Högskola: Institutionen för Energiteknik; 1989.
- [14] Gadd H, Werner S. Fault detection in district heating substations. *Applied Energy*. 2015;157:51-9.
- [15] Herbert P. Rundgångars ekonomiska betydelse för fjärrvärmensäten investerings-, drift- och underhållskostnader (Economic consequences of extra by-passes in district heating networks investment-, running- and maintenance costs) ÅF-Energikonsult. Stockholm: Värmeforsk - Hetvattenteknik - nr. 525; 1995.
- [16] Council Directive 2012/27/EU of 25 October 2012 on energy efficiency amending Directives 2009/125/EC and 2010/30/EU and repealing Directives 2004/8/EC and 2006/32/EC. [2012] OJ L315/1.
- [17] Jagemar L, Bergsten B. Individuell värmemätning i flerbostadshus - Några energitekniska aspekter på mätning av tillförd värmeenergi respektive rumstemperatur (Individual heat metering in apartment buildings - Some energy technical aspects of the measurement of the thermal input and room temperature). *Effektiv*; 2003.
- [18] Petitjean R. Total hydronic balancing: A handbook for design and troubleshooting of hydronic HVAC systems. Ljung, Sweden: Tour & Andersson; 1994.
- [19] Brundrett GW. Legionella and Building Services: Butterworth-Heinemann; 1992.
- [20] Lesnik R, Brettar I, Hofle MG. Legionella species diversity and dynamics from surface reservoir to tap water: from cold adaptation to thermophily. *ISME J*. 2016;10:1064-80.
- [21] DVGW. Trinkwassererwärmungs- und Trinkwasserleitungsanlagen; Technische Maßnahmen zur Verminderung des Legionellenwachstums; Planung, Errichtung, Betrieb und Sanierung von Trinkwasser-Installation. Bonn: DVGW; 2004.

SPACE HEATING WITH ULTRA-LOW-TEMPERATURE DISTRICT HEATING – A CASE STUDY OF FOUR SINGLE-FAMILY HOUSES FROM THE 1980S

D. Østergaard¹, S. Svendsen¹

¹ Technical University of Denmark, Department of Civil Engineering, DK-2800 Kgs. Lyngby, Denmark

Keywords: *Ultra-low-temperature district heating, single-family house, radiator, IDA ICE, heating power, heat demand*

ABSTRACT

District heating is predicted to play a large role in the future fossil free energy system. Apart from providing energy savings by utilizing surplus heat, the district heating system also provides flexibility to fluctuating electricity generation by bridging the electricity and the heating sector. These benefits can be maximized if district heating temperatures are lowered as much as possible. In this paper we report on a project where 18 Danish single-family houses from the 1980s were supplied by ultra-low-temperature district heating with a supply temperature as low as 45 °C for the main part of the year. The houses were heated by the existing hydraulic radiator systems, while domestic hot water was prepared by use of district heating and electric boosting. This paper evaluated the heating system temperatures that were necessary in order to maintain thermal comfort in four of the houses. First the four houses were modelled in the building simulation tool IDA ICE. The simulation models included the actual radiator sizes and the models were used to simulate the expected thermal comfort in the houses and resulting district heating return temperatures. Secondly measurements of the actual district heating return temperatures in the houses were analysed for different times of the year. The study found that existing Danish single-family houses from the 1980s can be heated with supply temperatures as low as 45 °C for the main part of the year. Both simulation models and test measurements showed that there is a large potential to lower the district heating temperatures.

INTRODUCTION

District heating (DH) covers approximately 13% of the heat demand in the EU at the current state. This share is expected to increase in the future, as expansion of the DH networks has been found to be an economically beneficial tool in the transition to a low-CO₂ energy system [1]. The efficiency of the new DH systems can be increased significantly, if they are operated with low supply and return temperatures, according to the principles of 4th Generation District Heating [2]. A reduction of the DH temperature has two positive effects on the energy efficiency of the heat supply. Firstly, when the DH temperatures are reduced, the heat losses from the pipe networks are also reduced.

This can generate significant energy savings, as the reductions in heat loss can be estimated to 30 % when supply and return temperatures are reduced from 80 °C/40 °C to 60 °C/30 °C. Secondly the efficiency of the heat production is increased for heat sources such as geothermal heat, heat pumps or solar heating. The efficiency of the heat production is estimated to increase by approximately 10 % in solar thermal plants and 30 % in heat plants supplied by heat pumps, if supply and return temperatures are lowered from 80 °C/40 °C to 60 °C/30 °C. Additionally the heat production efficiency is increased when return temperatures are lowered in heat plants with flue gas condensation supplied by natural gas or wet biomass. Consequently a reduction in the DH temperatures can amount to significant total energy savings.

Danish DH is characterized by a large outspread, and relatively low supply and return temperatures. However recent research has shown that there is further potential to lower the DH temperatures. Currently, approximately 47 % of the total Danish heat demand is covered by DH [3]. Even low-density areas are at times supplied by DH, for example approximately 40 % of the Danish single family houses are heated by DH [4]. Current supply and return temperatures are as low as 70/40 on average [5]. Nevertheless a large effort is currently taking place to reduce the temperatures further. This is done by the DH companies, through installation of automatic temperature optimization software [6] or through research projects that investigate the opportunity to lower the DH supply temperatures to 55 °C or 60 °C in both new and existing buildings [7].

The temperature reductions in the DH networks are limited by the demands and technical requirements in the buildings. In houses or commercial buildings these limitations are generally set by either the domestic hot water (DHW) requirements or the design of the space heating installations. The supply temperature in current Danish DH networks is generally limited by the DHW systems, which are typically designed for preparation of hot water at a temperature above 60 °C. When DHW is stored at this temperature, the risk of Legionnaires' disease is reduced, as the Legionella bacteria mainly grow at lower temperatures. If DH temperatures go below 55 °C, the DHW must be prepared through for example an instantaneous heat exchanger, to avoid

Legionella growth in the DHW [8]. By use of the direct heat exchanger, or other solutions as described by Yang, Li & Svendsen in [9], the DH supply temperature can be lowered to around 50 °C, which is enough to deliver DHW at the required comfort temperature of 40-45 °C. This type of DH is commonly referred to as low-temperature district heating (LTDH).

The DH temperatures can be lowered further if the DHW is heated through a combination of DH and electricity. This is also referred to as ultra-low-temperature district heating (ULTDH). DH is used to heat the domestic hot water to a temperature of e.g. 35 °C and the temperature is then further raised to 40-45 °C by for example a micro heat pump [10] or an instantaneous electric heater. In this case the space heating systems are the limiting factor with regards to temperature reductions. For example it may not be possible to lower the supply temperature to 40 °C in old buildings where the heat loss is large and the heating elements are small. However recent research has shown that many existing buildings can be heated by low-temperature heating without problems. This is partly due to the fact that the supply temperature in a LTDH system can be increased in peak periods during cold winter times when the space heating requirements are higher. Ultimately the lower limit for the DH supply temperature could be as low as 30 °C in new buildings with floor heating. Fig. 1 summarizes the different types of DH based on the technical limitations and in correspondence with earlier definitions as described in [2,6,11].

Since the space heating system is the limiting factor in ULTDH-systems, it is crucial to investigate the design

of the space heating systems, when an existing building area is to be supplied by ULTDH. Most Danish houses are heated by hydraulic radiators that are designed for supply and return temperatures such as 90 °C/70 °C or 70 °C/40 °C. However even in these houses it is reasonable to expect that the typical space heating demands can be covered with low-temperature heating, since radiators are designed for extreme conditions with very cold outdoor temperatures. This was verified in our recent investigation of heating power and heating demands in typical Danish single-family houses from the 1900s [12]. Furthermore it is illustrated in several Danish pilot projects where the use of ULTDH in existing building areas has been successfully tested [6,10,11]. Nevertheless none of these projects investigated the limitations of the space heating systems in detail. This study therefore set out to perform a detailed analysis of the space heating systems in four Danish single-family houses heated by ULTDH.

Aim of study

This study aimed to investigate how far we can lower the heating system temperatures in existing Danish single-family houses without compromising thermal comfort. The study was carried out through measurements from a real test case where four houses were supplied by ULTDH. Since the actual heating system operation can be affected by technical malfunctions or occupant behaviour, the measurements were compared to results from dynamic simulation models, which were used to evaluate the ideal heating system temperatures and the thermal comfort in the houses.

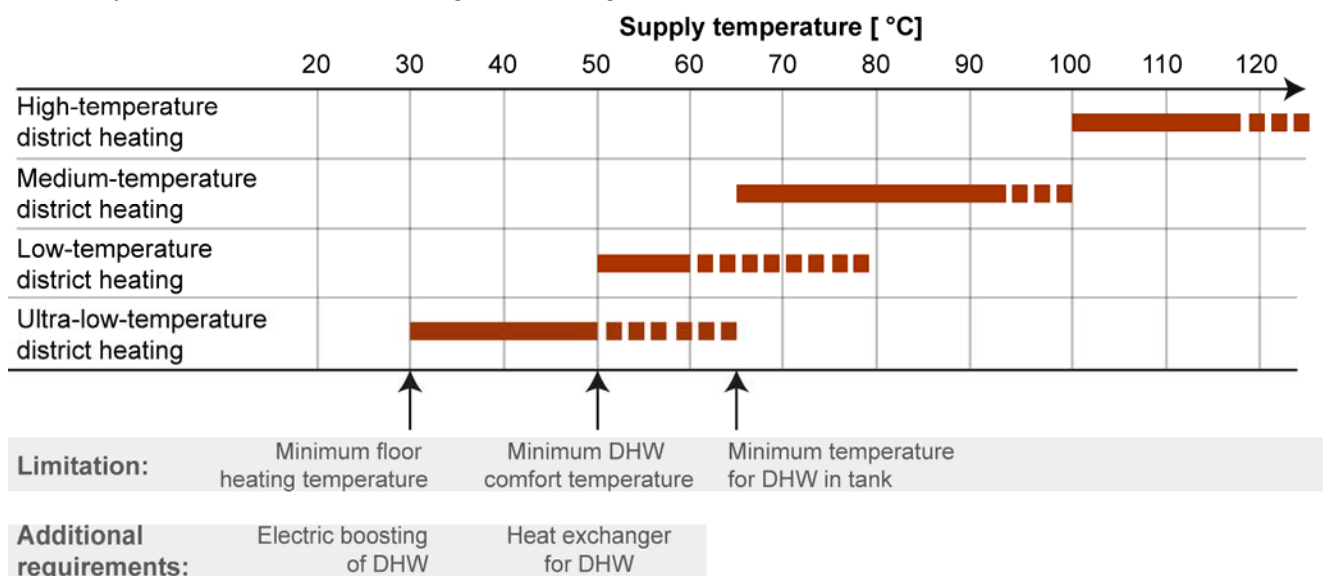


Fig. 1 Definition of four different types of district heating where temperatures are limited by the technical requirements of the buildings.

DESCRIPTION OF CASE HOUSES

The investigations were carried out as a case study of four single-family houses built around 1980. The houses are illustrated in Fig. 2. All of the houses have 2-3 occupants and a heated floor area of around 150 m². House 1 and 2 furthermore holds an unheated basement. All building elements in the houses were well insulated at the time of construction, and due to the young age, the only renovations carried out is replacement of windows in some houses. The constructions of the houses are described in Table 1, together with the estimated U-values of each construction element. Linear heat losses are based on internal measures and assumed to be 0.07 W/mK around windows, 0.15 W/mK at foundations and exterior wall joints, and 0.12 W/mK for connections between roof and exterior walls. Both constructions and U-values correspond to the standard for this type of houses as given by the Danish Building Research Institute [13] and the Danish Energy Agency [14].

All four single-family houses are supplied by DH and equipped with the original hydraulic radiator heating systems. DH is connected to the houses through a direct connection. The houses are equipped with different solutions for preparation of DHW by use of additional electric energy – these are described by Xiaochen in [15] and will not be described further here. The substation is not equipped with mixing valves or weather compensation control, as the overall DH supply temperature is controlled at plant level, according to outdoor temperature, as illustrated in Fig. 3. The radiators in the houses are standard Type 11 and Type 22 radiators, except from a few convector type radiators where windows begin at floor height. All radiators are equipped with individual thermostatic valves. The bathrooms in the houses are equipped with hydraulic floor heating systems, which are embedded in the concrete floors. The floor heating circuits are controlled by thermostatic valves. No central temperature control is installed in the houses.

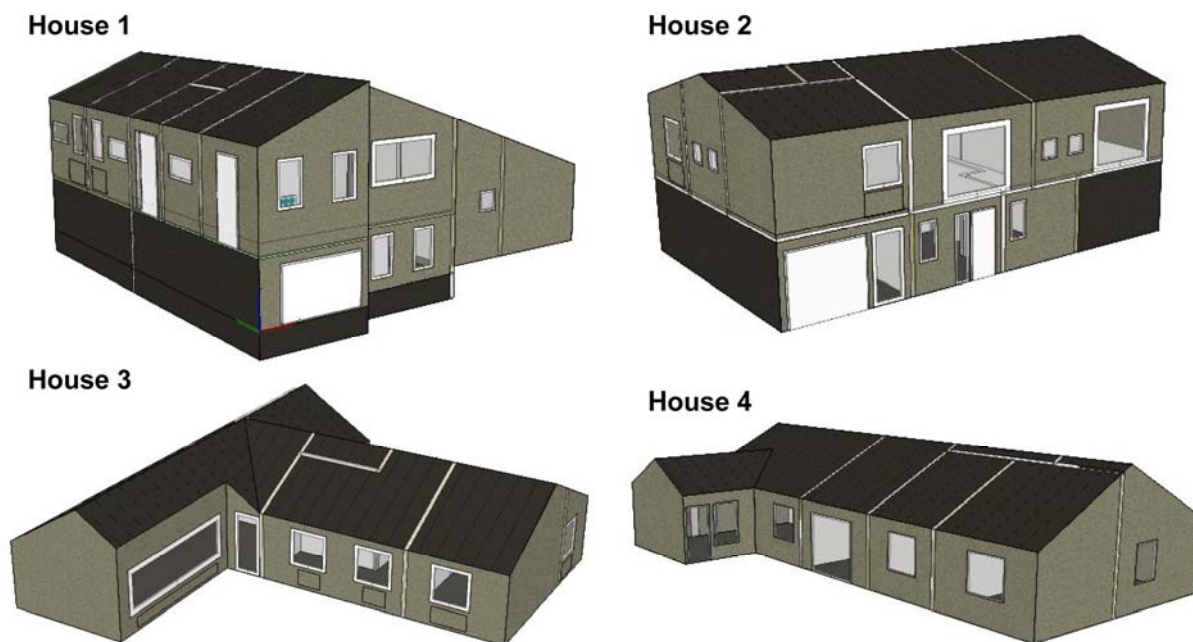


Fig. 2 Illustrations of the four case houses investigated in the study

Table 1 Estimated U-values and description of constructions of the four houses

	House 1	House 2	House 3	House 4
External walls – Brick, insulation, and light weight concrete	U=0.22 W/m ² K	U=0.32 W/m ² K	U=0.32 W/m ² K	U=0.32 W/m ² K
Basement floor – Concrete, insulation, and Leca insulation	U=0.26 W/m ² K	U=0.69 W/m ² K	U=0.28 W/m ² K	U=0.29 W/m ² K
Roof – 200mm insulation	U=0.2 W/m ² K			
Windows	U=1.86 W/m ² K	U=2.68 W/m ² K	U=1.86 W/m ² K	U=2.68 W/m ² K

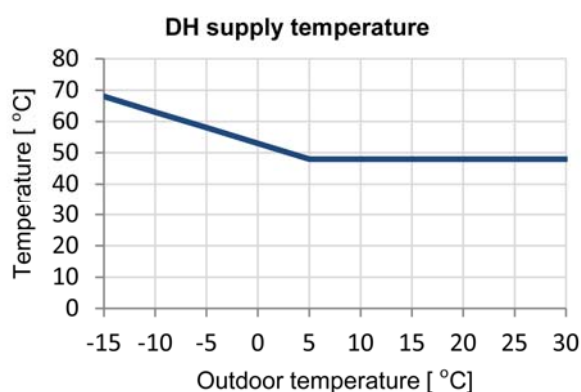


Fig. 3 Variation of supply temperature from the district heating plant according to outdoor temperature

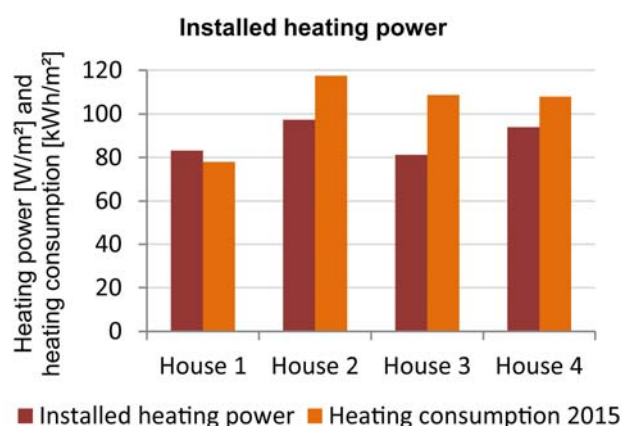


Fig. 4 Measured heating consumption in 2015 and installed heating power at the temperature set 70 °C/40 °C in the four case houses

METHOD

Dynamic building simulations

The houses were modelled in the dynamic building simulation tool IDA ICE in order to calculate the expected heating system return temperature, and evaluate the thermal comfort in the houses, when the DH supply temperature is lowered. IDA ICE is a commercially available node based multi-zone simulation tool. The tool has been validated in accordance with standard DS/EN 15265, which describes the accuracy of dynamic simulations of energy performance in buildings [16,17]. The program calculates the heat balance of the buildings for every hour of the year, and has a high level of detail, that includes amongst others thermal inertia of building materials, and air flow between building zones. The program does not take into account temperature gradients in the rooms, and therefore air is assumed to be perfectly mixed in all rooms. This is not assumed to be a problem as none of the rooms in the investigated houses are too high.

The input data required to perform a specified simulation in IDA ICE includes for example air change rates and occupant schedules. This information was

defined based on standard values for Danish single-family houses as given by [13,18]. All houses are naturally ventilated and it was assumed that the ventilation rate is 0.3 l/s per m² which is the standard minimum required air change rate in Danish single-family houses [19]. Internal heat gains from presence of occupants and use of equipment was modelled by weekly schedules that were constructed for each house according to the number of occupants. The total average internal heat gains in the houses according to the schedules were 4.11-5.08 W per m² living area, which corresponds well to the Danish standard value of 5 W/m² [18]. Energy consumption for domestic hot water was not included in the models and the simulation models were run with weather data for the Design Reference Year of Copenhagen 2001-2010. Measured heat consumption is therefore adjusted according to the number of degree days, before it is compared the calculated heat consumption.

The simulation models were used to calculate the average monthly heating system return temperatures. The program calculates the heating system temperatures based on the mass flows and return temperatures from the individual radiators in the houses. The radiator temperatures and mass flows are calculated for every hour of the year according to the indoor temperature set-point and heat loss in the given rooms. The radiators are therefore included in the models with the actual location, dimensions, and design heating power. Radiator types and dimensions were noted at a visit to the house, and used to find the design heating power of the radiators, by use of a tool that was acquired from the Danish Technological Institute through personal communication. The tool makes it possible to estimate the heating power of a given existing radiator based on empirical data. The average heating power installed in each house is summarized in Fig. 4. The figure also shows the total measured heat consumption in each of the houses during 2015. Each radiator is controlled by a P-control thermostatic radiator valve with a P-band of 2 °C that controls the water mass flow through the radiator and aims to maintain the indoor temperature set-point. The floor heating was assumed to be controlled by similar thermostatic valves, and according to a constant flow, and a maximum coil temperature difference of 5 °C. The heating pipes were assumed to be located at a depth of 0.04m in the concrete slab with tile flooring. The heating system supply temperature was defined according to the weather compensated DH supply temperature. Due to the heat losses in the DH pipes, the supply temperature reaching the houses was assumed to be 6 °C lower than the temperature illustrated in Fig. 3, which was found to correspond well to the measured temperatures.

The thermal comfort in the houses was evaluated through an analysis of the calculated indoor air temperatures in each room of the houses. This was done by counting the number of hours during the year, where the indoor air temperatures, according to the simulations, were below the temperature set-point. For this analysis the occupants were expected to maintain an indoor temperature of 20 °C in living areas and 18 °C in the basement. Even so, it should be kept in mind that actual indoor temperatures usually vary greatly due to differences in occupant preferences [20, 21].

Heating system measurements

The actual space heating temperatures in the houses were evaluated for the period from July 2015 to March 2016, where the houses were supplied by ULTDH. The measurements were conducted by use of energy meters that have an accuracy of approximately ±0.5 %, according to the manufacturer. The meters were used to measure temperatures, volume, and mass flow of the DH water for the overall district heating connections, and for the preparation of domestic hot water, as illustrated in Fig. 5.

The average monthly space heating temperatures were calculated based on the measurements as follows. First the volume of DH that was used for space heating purposes (V_{SH}) was calculated from the total volume of the DH water (V_{DH}) and the volume of DH used for DHW (V_{DHW}) as seen in Equation (1).

$$V_{SH} = V_{DH} - V_{DHW} \quad (1)$$

Afterwards the return temperature from the space heating ($T_{ret,SH}$) was calculated based on the volumes and the return temperature from the DHW ($T_{ret,DHW}$) and the DH in total ($T_{ret,DH}$). This was done according to Equation (2).

$$T_{ret,SH} = (V_{DH} \cdot T_{ret,DH} - V_{DHW} \cdot T_{ret,DHW}) / V_{SH} \quad (2)$$

The return temperatures were generally based on volume weighted averages. However for some months the DH return temperatures were calculated as an average of the daily volume weighted return temperature. This is not expected to cause significant inaccuracies, as there were rarely any large variations in the day to day measurements. Due to logger problems, it was not possible to calculate the space heating return temperature in house 4, until December. The space heating return temperature for this house, in the months before then, was therefore assumed to be equal to the DH return temperature. This was found to be reasonable, as the study generally found that the space heating return temperature and the DH return temperature were often merely the same.

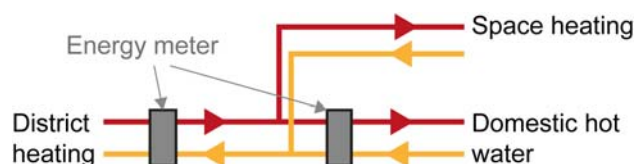


Fig. 5 Illustration of measurement setup

Table 2 Deviation between simulated and measured space heating consumption

House	Space heating consumption (July-March)		
	Calculated	Measured	Deviation
1	11.64 MWh	11.72 MWh	0.6 %
2	13.16 MWh	13.95 MWh	5.7 %
3	10.39 MWh	9.52 MWh	-9.1 %
4	10.82 MWh	12.53 MWh	13.6 %

RESULTS

Table 2 shows a comparison of the degree day adjusted space heating consumption that was measured in the houses and the heating consumption that was calculated by use of the simulation models. It can be seen from the table that the measured and calculated heating consumption differs by up to 13.6 %. The deviation could be partly explained by a difference between the indoor temperatures assumed in the simulation, and the actual indoor temperatures in the house. Some of the houses are additionally heated by a fire stove, which could furthermore cause a deviation between the measured and the calculated heating consumption. Alternatively, the numbers could indicate that the simulation model for House 3 tends to overestimate the heating demand, while the model for House 4 underestimates it.

Supply and return temperatures

The average monthly space heating temperatures in the houses, according to the simulations and the measurements, are compared for all of the four houses in Fig. 6. The figure also holds the average monthly outdoor temperatures for the measurement period and the DRY weather file. The average outdoor temperatures in the winter of 2015-2016 were found to be somewhat higher than the temperatures in the weather file.

The results show that the space heating in the houses was generally delivered by supply and return temperatures around 40 °C/30 °C or 45 °C/35 °C. The measured space heating return temperature was found to be below 30 °C in a few months of the year in

houses 1,3 and 4. Especially House 3 was seen to have a low space heating return temperature. As seen from Fig. 4 this does not seem to be explained by significantly lower heat consumption or higher installed heating power.

The simulated and measured space heating return temperatures were found to correspond well for most of the houses. This indicates that the technical potential to lower the heating system temperatures was met in most of the houses. The correlation between measured and simulated temperatures was striking especially in House 3, despite of the difference between the simulated and measured heating consumption. In House 2, on the other hand, it was found that there was a deviation between the simulated and measured return temperature of up to 10 °C. This could be due to the fact that the occupants in this house prefer higher indoor temperatures than the assumed 20 °C, which could be indicated by the high measured heat consumption seen in Fig. 4 and Table 2. Nevertheless, the simulation results could also indicate, that there is a potential to obtain significantly lower space heating

return temperatures in house 2, if the heating system control is optimized.

Thermal comfort

In most of the rooms in the single-family houses, it was found that the indoor air temperature never dropped below the set-points of 20 °C and 18 °C. However the simulation results indicated that it was difficult to maintain the thermal comfort temperature in the restrooms in Houses 2-4, where the indoor air temperature was found to be around 19 °C for a large part of the year. These rooms are heated solely by floor heating, which is generally operated with a low supply temperature, and therefore the thermal comfort in these rooms should not be affected by the changes in the DH temperatures. Rather the results may suggest that the installed floor heating is under-dimensioned or that the heating power of the floor was under-estimated, due to uncertainties on the construction and operation of the floor heating. Fig. 7 shows a visualization of the number of hours during the year, where the indoor air temperature drops below the indoor temperature set-point.

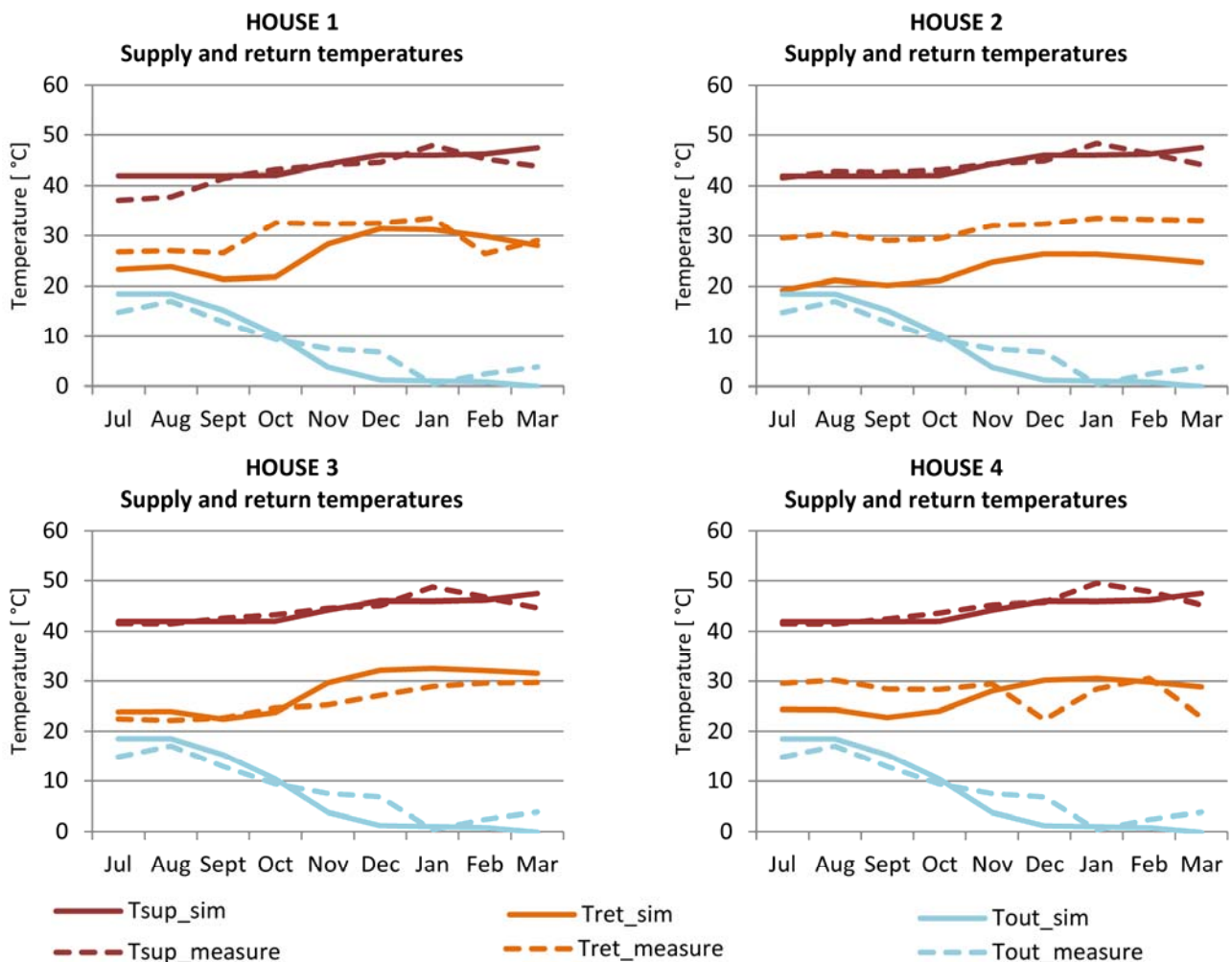


Fig. 6 Simulated and measured space heating temperatures in the four houses

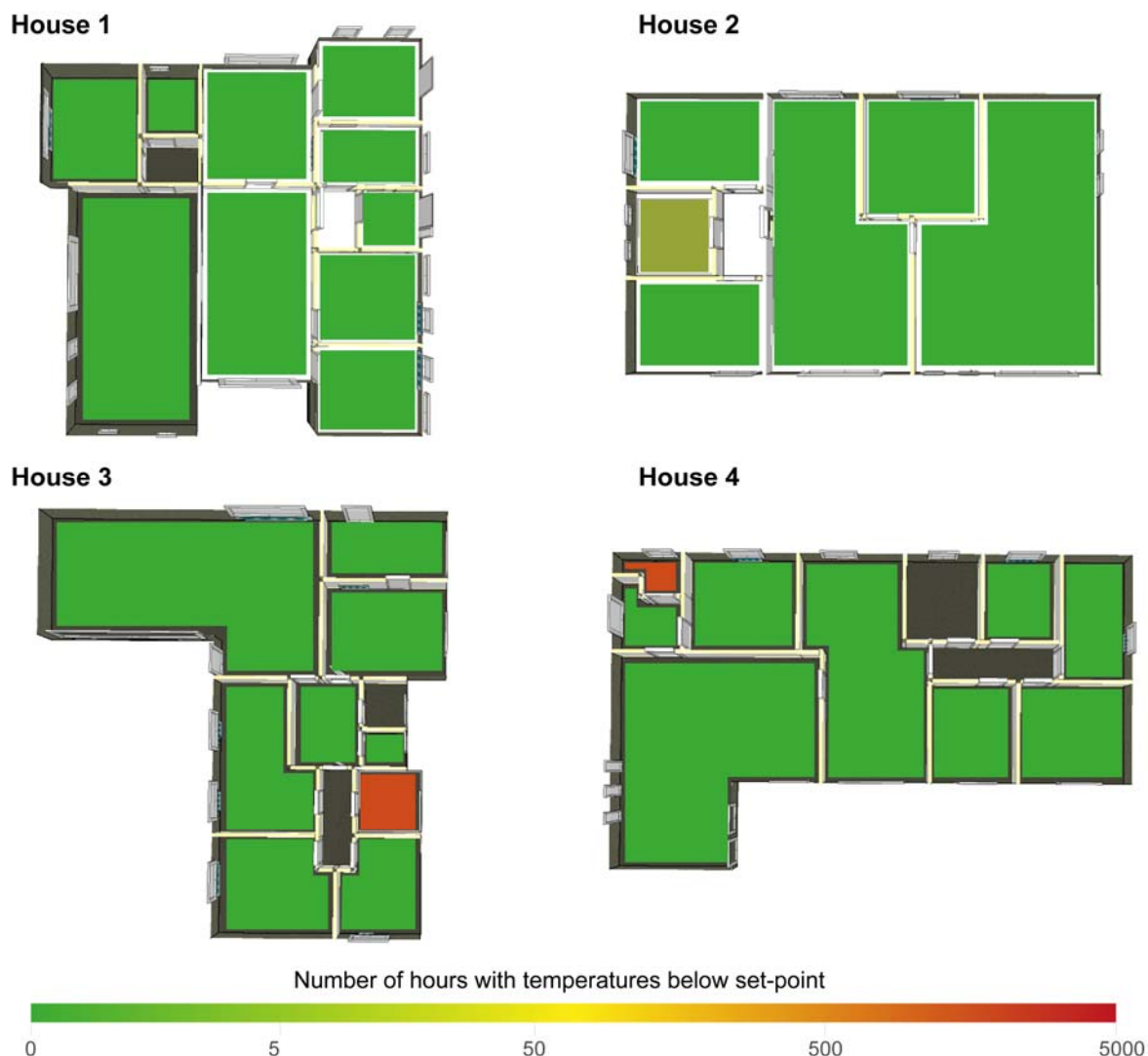


Fig. 7 Visualization of the simulated thermal comfort in the house

Uncertainties

There were found to be two main uncertainties in this study: the construction of the floor heating systems and the indoor temperature set-points. The impact of these uncertainties was evaluated through new simulations of the houses, where two changes were made in the models. Firstly, the floor heating was modelled as plain electric heating. Thereby the heating power of the floor was not affected by the floor construction, and the return temperature from the floor heating did not affect the overall space heating return temperature. Despite of the simplification of the floor heating in the restrooms, the test simulations showed, similar to the first simulations, that it can be difficult to meet the thermal comfort criteria in the bathrooms of House 3 and 4. This indicates that the floor heating systems in the bathrooms are under-dimensioned. On the other hand, the results of the test simulations showed, that indoor temperatures of approximately 21.5 °C could be maintained in all living areas of the houses. Even when

Secondly, the indoor temperature was set to approximately 21.5 °C in all living areas. According to a recent study of typical British homes, an indoor temperature of 20 °C or lower, could be a reasonable estimate of average living room temperature, but it is only an average temperature, and actual indoor temperature in many living rooms is higher [21]. Likewise our own studies have showed that indoor temperatures of 21-22 °C are not uncommon in living and dining rooms of Danish single-family houses [22].

the indoor temperature was increased, the return temperature from the radiators only increased slightly. In houses 1-3, the radiator return temperature was found to increase by 1-2 °C in the winter months, while in house 4 it was increased by approximately 4.5 °C. The increased return temperature in house 4 was mainly found to occur due to high return temperatures from the radiators in the entrance and the restroom, where indoor temperatures were also set at 21.5 °C.

The results of the test simulations suggest that the findings of the study are generally robust to uncertainties on occupant preferences and indoor temperature set-points. This conclusion is further underlined by the measurements and the fact that none of the customers' complained about problems with the indoor temperature during the test period with ULTDH.

CONCLUSIONS

The results of this study showed that there is a great potential to heat existing single-family houses with hydraulic radiator systems, with ultra-low-temperature district heating. Simulation results indicated that even when the heating system supply temperature was lowered to 45 °C for most of the year, this did not jeopardize the thermal comfort of the occupants living in the houses. This was further underlined by the fact that no consumers' complained about poor thermal comfort during a test with lowered return temperatures in a period from 2015-2016.

Both results from a simulation of the heating system operation in four single-family houses, and measurements from the test operation with ultra-low-temperature district heating, showed that there is a large potential to lower the district heating temperatures in existing single-family houses. Average supply and return temperatures for space heating in the houses were found to be 44 °C and 31 °C respectively.

ACKNOWLEDGEMENT

The work presented in this article was a result of the research activities of the Strategic Research Centre for 4th Generation District Heating (4DH), which received funding from the Innovation Fund Denmark. An extra thank you is due to Bjerringbro District Heating and Kamstrup for their great help and collaboration during the measurement process.

REFERENCES

- [1] Connolly, D., Mathiesen, B. V., Østergaard, P. A., Möller, B., Nielsen, S., Lund, H., ... Trier, D. (2013), Heat Roadmap Europe 2: Second Pre-Study for the EU27, Department of Development and Planning, Aalborg University.
- [2] Lund, H., Werner, S., Wiltshire, R., Svendsen, S., Thorsen, J. E., Hvelplund, F., & Mathiesen, B. vad. (2014). 4th Generation District Heating (4GDH). Energy, Energy the International Journal, 68, 1–11.
- [3] Dansk Fjernvarmes F&U konto, Varmeplan Danmark 2008 [Heating Plan Denmark 2008], 2008.
- [4] Statistics Denmark, Dansk Statistik, (2014). <http://www.dst.dk/da/> (accessed August 28, 2014).
- [5] Danish District Heating Association, Benchmarking Statistics 2015, Kolding (2016).
- [6] Dansk Fjernvarmes F&U konto, Etablering af lavtemperaturfjernvarme i eksisterende fjernvarmeforsyning [Establishment of low-temperature district heating in existing district heating systems], COWI, 2014.
- [7] Danish Energy Agency, EUDP 2008-II, CO₂-reductions in low energy buildings and communities by implementation of low-temperature district heating systems. Demonstration cases in EnergyFlexHouse and Boligforeningen Ringgården - Journalnr. 63011-0152, DTU BYG, 2011.
- [8] M. Brand, J.E. Thorsen, S. Svendsen, C.H. Christiansen, A direct heat exchanger unit used for domestic hot water supply in a single-family house supplied by low energy district heating, in: 12th Int. Symp. Dist. Heat. Cool., 2010.
- [9] Yang, X., Li, H., & Svendsen, S. Alternative solutions for inhibiting Legionella in domestic hot water systems based on low-temperature district heating. Building Services Engineering Research and Technology, (2015).
- [10] M. Markussen, B. Elmegaard, T.S. Ommen, M. Brand, J. Eric, J. Iversen, Heat Pumps for Domestic Hot Water Preparation in Connection with Low Temperature District Heating, 2013.
- [11] Danish Energy Agency, Demonstrations-projekter om varmepumper eller andre VE- baserede opvarmningsformer [Demonstration projects on heat pumps and other RE-based heating solutions], (2015) 1–50.
- [12] D.S. Østergaard, S. Svendsen, Theoretical overview of heating power and necessary heating supplytemperatures in typical Danish single-family houses from the 1900s, Energy Build. 126 (2016) 375–383.
- [13] K.B. Wittchen, J. Kragh, Danish building typologies - participation in the TABULA project, Danish Building Research Institute, 2012.
- [14] Danish Energy Agency, Håndbog for energikonsulenter. Enfamiliehuse. Beregnet forbrug - 2012 [Handbook for energy consultants. Single-family houses. Calculated consumption - 2012], 2012.
- [15] X. Yang and S. Svendsen, Achieving low return temperature for DHW preparation by ultra-low-temperature district heating, paper submitted to the 15th International Symposium on District Heating and Cooling, 2016.
- [16] Danish Standard, DS/EN 15265 - Energy performance of buildings - Calculation of energy needs for space heating and cooling using dynamic methods - General criteria and validation procedures, 2007.

- [17] Equa Simulation, Validation of IDA Indoor Climate and Energy 4.0 with respect to CEN Standards EN 15255-2007 and EN 15265-2007, 2010.
- [18] S. Aggerholm, K. Grau, Bygningers energibehov - PC-program og beregningsvejledning [Energy demand of buildings - PC-program and calculation guide] - SBi-anvisning 213, Danish Building Research Institute, 2005.
- [19] Danish Energy Agency, Bygningsreglementet [Danish Building Regulations], (2014). www.bygningsreglementet.dk
- [20] K. Gram-Hanssen, Residential heat comfort practices: understanding users, *Build. Res. Inf.* 38 (2010) 175–186.
- [21] Huebner, G. M., McMichael, M., & Shipworth, D. (2013). The reality of English living rooms – A comparison of internal temperatures against common model assumptions. *Energy and Buildings*, 66, 688.
- [22] D.S. Østergaard, S. Svendsen, Replacing critical radiators to increase the potential to use low-temperature district heating – A case study of 4 Danish single-family houses from the 1930s, *Energy*. (2016).

PERFORMANCE VERIFICATION OF DISTRICT COOLING SYSTEMS COMPARED WITH CONVENTIONAL COOLING SYSTEMS BASED ON MONITORED DATA

Wenjie Gang¹, Shengwei Wang¹, Fu Xiao¹

¹ Department of Building Services Engineering, The Hong Kong Polytechnic University

Keywords: District cooling systems, Individual cooling system, Efficiency, Energy saving

ABSTRACT

District cooling systems are widely used in many countries, especially where the density of buildings is high. Many studies have been done to investigate the performance of district cooling systems or to compare it with conventional cooling systems. However, most of these studies are based on simulations and hypothesis. The obtained results would be very ideal. The real situation can be very different and complex. It is therefore highly necessary to verify the efficiency of district cooling systems, especially when being compared with the conventional individual cooling systems (in-building systems). This study attempts to verify the energy saving potentials of district cooling systems using actual measurements of individual cooling systems. Operational data of cooling systems of several buildings in a university are collected. Based on the monitored cooling load and locations of each building, the district cooling systems can be designed. The energy consumption of both district cooling systems and conventional cooling systems in typical summer weeks and winter weeks is evaluated. The performance of district cooling systems under both indirect connection and direct connection is evaluated. By being compared with the individual cooling systems, the efficiency of district cooling systems can be verified. Results show that district cooling systems are not always energy efficient. The energy saving potential mainly happens when the cooling loads of individual cooling systems are low.

INTRODUCTION

Building energy systems with high efficiencies are needed due to increasing requirement on the green buildings or cities. Efficient cooling systems therefore play an important role in reducing the energy consumption of buildings in cooling dominated areas. District cooling systems (DCSs), which are regarded as efficient alternatives, are widely used in many countries such as Sweden, Japan [1], US, UAE, etc.[2]. In DCSs, cooling is generated centrally at the cooling plant and supplied to a group of buildings for cooling and dehumidification purposes. The advantages and applications of district heating and cooling systems are reviewed and summarized in [2, 3].

The performance of DCSs has been evaluated and compared with conventional individual cooling systems

(ICSs) in many studies [4-6]. A district cooling and heating system using sea water heat pumps was compared with a coal-fired heating system & a conventional air conditioning system [7]. Results show that the district cooling and heating system has a lower annual cost, together with significant energy saving and environmental benefits. Another district cooling and heating system using seawater in the north of China was compared with systems using centrifugal chillers & natural gas-fired boilers, steam-driven lithium bromide absorption chillers & hot water from a nearby power plant, and natural gas-fired lithium bromide absorption heat pump systems[8]. The energy consumption of a DCS for a new development area is evaluated by Chow et al. [5]. Authors of this paper [4] also conducted performance assessment of DCSs by comparing with ICSs and results show that DCSs are more energy efficient. From the above review and literatures, it can be found that DCSs are more efficient than the conventional ICSs.

In all the above studies, the conclusions and results are mainly based on hypothesis and simulation. The cooling loads are obtained using software such as Energyplus, TRNSYS, etc. [9]. The comparison or performance assessment of DCSs and ICSs is made before the buildings or systems are constructed [10]. Energy consumption of DCSs or ICSs are also based on simulation. Results based on simulation can be very ideal and the real situation can be very complicate. Studies on the actual performance of both systems are not found yet. Furthermore, the conclusion that DCSs are more energy efficient is still very controversial in China. It is therefore highly necessary to verify the performance of DCSs with actual measurements. The result will be very meaningful for both researchers and users. It will provide solid basis when the decision is made between the DCSs and ICSs. It will also help to improve the planning and design of cooling systems for a district/community. To fill these gaps, this study therefore attempts to verify the efficiency of DCSs with actual operational data of cooling systems collected from the Building management systems (BMS). Two objectives are achieved: 1) Based on actual measurements, the energy efficiency of DCSs will be verified when being compared with ICSs. 2) Conditions that are suitable for the application of DCSs will be investigated.

METHOD AND STEPS

The method to conduct the performance verification is shown in Figure 1. Detailed steps are introduced as follows:

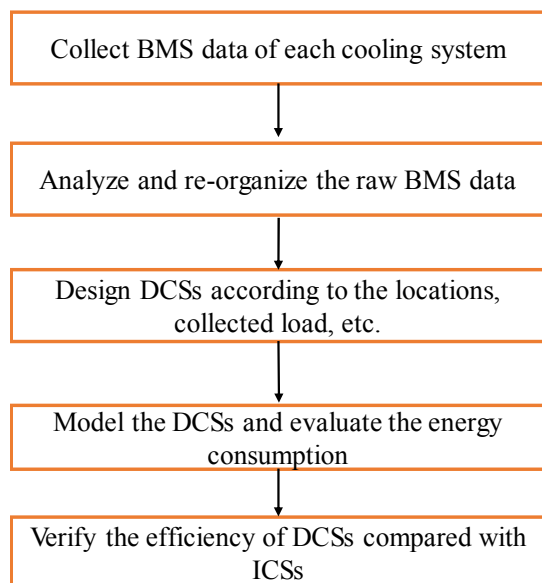


Figure 1. Method to conduct performance verification of DCSs

1) Operational data of the cooling systems are collected from the BMS, including the weather data, the cooling load, power consumption of subsystems, the operating numbers of chillers, pumps and cooling towers, the power or electricity consumption of the whole cooling plant etc.

2) The raw BMS data are analysed and re-organized. Data from different BMSs can be in different time steps or forms. All the data are consolidated to keep consistent. Not all the required variables are monitored. Even for the monitored variables, values during some periods may be missing or not right. It is necessary to re-organized these raw data after detailed analysis and calculations. Abnormal or fault data are to be excluded. Then the energy consumption of each ICS can be obtained. The coefficients of performance (COP) of the cooling systems can be calculated.

3) DCSs are designed according to the monitored cooling load. Chillers are selected from the product catalogues. The primary chilled water pumps, cooling water pumps and cooling towers can be selected based on the water flowrate of chillers. The chilled water systems can be designed based on the location of buildings and cooling loads of each building. The pressure drop can be evaluated and the size of chilled water pumps can be determined.

4) The energy consumption of DCSs can be evaluated. According to the actual cooling loads and the designed

DCSs, the energy consumption of DCSs can be obtained.

5) The efficiency of DCSs can be analysed and verified based on the comparison between the energy consumption of DCSs and monitored energy consumption of ICSs. The energy saving potentials can be obtained in different seasons or at different time of the day. Operation characteristics and conditions that benefit the DCSs are analysed.

SYSTEM DESCRIPTIONS

The performance of DCSs is verified through a case study, which is introduced in this section. Five cooling systems of buildings in the campus of the Hong Kong Polytechnic University (POLYU) are concerned. The campus map of POLYU is shown in Figure 2 and the buildings that served by the five cooling systems are marked. The buildings in the campus were constructed phase by phase. In this study, buildings named as 'Phase 1', 'Phase 2', 'Phase 7', 'Phase 8' and 'JCIT' are investigated. That is because currently the BMS data for these five cooling systems are available and the quality is acceptable. In some phase, more than one buildings are served by one central cooling system because these buildings are connected or very close to each other. In the selected five systems, Phase 1 includes Block CF, Block FJ, Block CD, Block DE, Block EF and Block EL. Phase 2 includes Block VA, Block VS, Block HJ, Block FG and Block GH. Phase 7 refers to Block Y. Phase 8 refers to Block Z. JCIT is a new and individual building. Each phase main contains labs, offices, classrooms, workshops, etc. Phase 2 has gyms and canteens.

Information about existing cooling systems of each phase is collected and summarized in Table 1. In the ICSs of Phase 1 and Phase 2, air-cooled chillers are used to supply cooling for users. The other three ICSs adopt water-cooled chillers and chillers with variable speed drives (VSD) are used in Phase 8. The cooling water systems of five systems are constant primary and variable secondary flowrate. Two typical summer weeks (Sep. 07 2015-Sep. 20 2015) and Two typical winter weeks (Nov. 30 2015-Dec. 13 2015) are selected to study the performance of DCSs and ICSs. BMS data of five ICSs in these four weeks are collected, consolidated and analysed. The hourly cooling loads in the summer weeks and winter weeks are shown in Figure 3 and Figure 4. It can be seen that all the buildings have cooling demand during both the daytime and night time in summer. In winter, the cooling loads are much lower and the cooling system for JCIT is shut down during night time in several days.

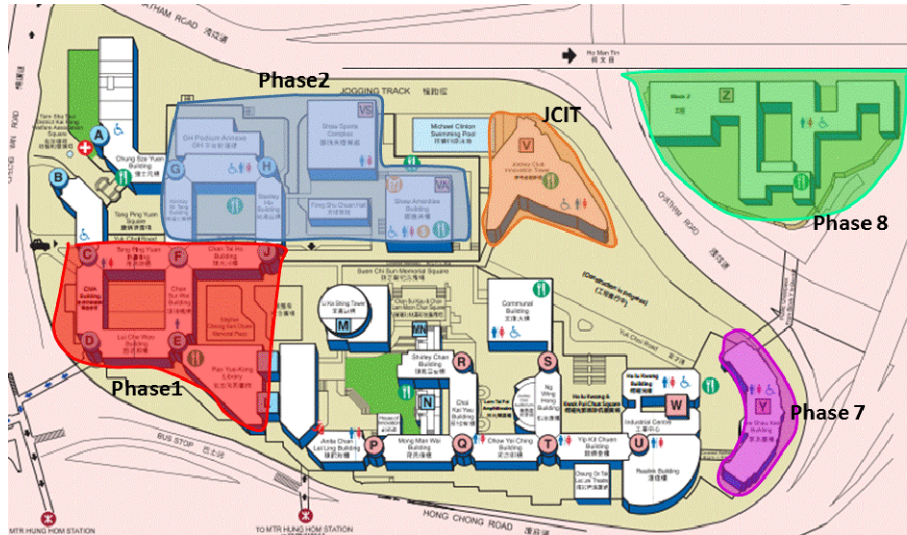


Figure 2. The campus map of POLYU and the five cooling systems concerned

Table 1 Design information of the cooling systems for each phase

		Phase 1	Phase 2	Phase 7		Phase 8		JCIT	
Type		Air-cooled	Air-cooled	Water-cooled		Water-cooled		Water-cooled	
Chiller	Number	5	5	4	1	4	1	3	1
	Capacity (ton)	313	313	430	200	800	300	550	150
	Primary chilled water pumps	Number	5	5	4	2	4	2	4
	Flowrate(L/s)	50	50	77	33.5	121.8	45.7	72	21
	Head(m)	20	20	13	15.1	15	15	15.5	13
	Motor (kW)	/	/	18.5	11	23.5	9	15	5.5
	Efficiency	0.85	0.85	0.85	0.7	0.8	0.76	0.81	0.75
Secondary chilled water pumps	Number	3	3	3	2	4	2	4	2
	Flowrate(L/s)	125	125	106	33.5	121.8	45.7	77	21
	Head(m)	43	43	35	35	30	30	25	25
	Motor (kW)	/	/	55	22	46.3	18.3	30	11
	Efficiency	0.85	0.85	0.82	0.68	0.8	0.75	0.83	0.75
Cooling water pumps	Number	/	/	4	2	4	2	4	2
	Flowrate(L/s)	/	/	87	41	167	62.8	116	32
	Head(m)	/	/	22	22	25	25	25	25
	Motor (kW)	/	/	30	15	55	18.3	45	15
	Efficiency	/	/	0.85	0.77	0.85	0.86	0.825	0.75
Cooling tower	Number	/	/	/	/	4	1	3	1
	Flowrate (L/s)	/	/	/	/	167.5	62.8	116	32
	Fan power (kW)	/	/	/	/	22	15	11*2	7.5

Table 2 Performance of each ICS

		Phase 1	Phase 2	Phase 7	Phase 8	JCIT
Summer Week	Load(kWh)	838882	709763	737056	893658	306034
	Energy consumption (kWh)	266962	227897	216113	164116	84493
	COP	3.14	3.11	3.41	5.45	3.62
Winter Week	Load(kWh)	302565	245753	228074	276585	79584
	Energy consumption (kWh)	99691	80971	78818	76122	27791
	COP	3.04	3.04	2.89	3.63	2.86

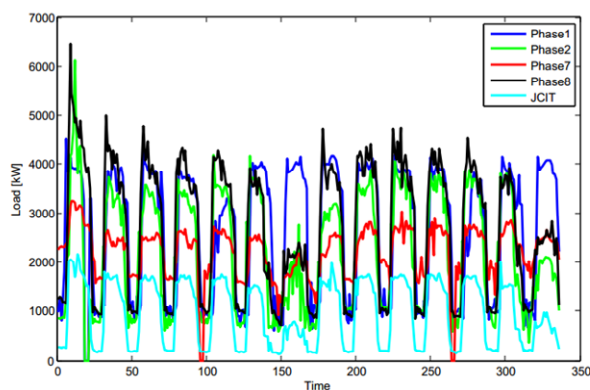


Figure 3. Cooling loads during summer weeks

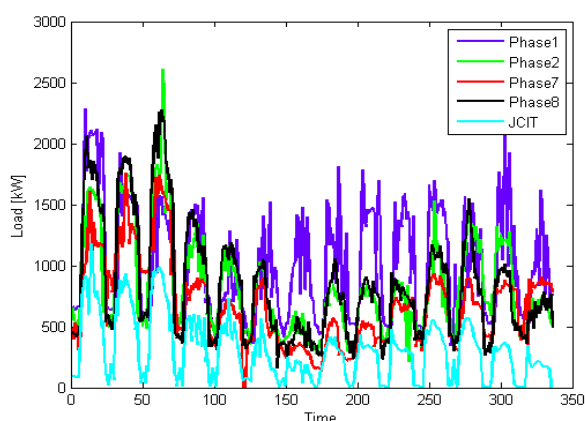


Figure 4. Cooling loads during winter weeks

Table 3 Design information of DCSs

System	Buildings	Peak load (kW)	Design capacity (kW)	Chiller			
				Large	Rated COP	Small	Rated COP
S1	Phase1->Phase2->JCIT->Phase7->Phase8	20138	21000	7*2800	5.8	1*1400	5.1
S2	Phase2->JCIT->Phase7->Phase8	16509	18200	6*2800	5.8	1*1400	5.1
S3	JCIT->Phase7->Phase8	11703	12600	4*2800	5.8	1*1400	5.1
S4	JCIT->Phase7	5584	7000	2*2800	5.8	1*1400	5.1

Table 4 Energy saving of DCSs when different buildings are involved under indirect connection

System	Buildings	Indirect connection	
		Summer	Winter
S1	Phase1->Phase2->JCIT->Phase7->Phase8	5%	11.50%
S2	Phase2->JCIT->Phase7->Phase8	0.40%	9.50%
S3	JCIT->Phase7->Phase8	-6.90%	4%
S4	JCIT->Phase7	5.70%	-1%

The performance of each ICS are summarized in Table 2. It can be seen that the performance of the ICS for Phase 8 is very high. The COP of the cooling plant can be up to 5.45. That's because the chillers with VSDs are used in the system. Table 2 also shows that the COP of each ICS in winter is lower than that in summer. That's because the cooling load is lower in winter and chillers work at a lower efficiency in ICSs.

According to the location of buildings and monitored annual peak cooling loads from the BMS, the DCS can be designed. To verify the performance of DCS under different conditions, DCSs with different users involved are designed. The design information for each DCSs under different combinations is shown in Table 3. For S1, all the buildings are connected and the arrows in Table 3 indicate the direction of chilled water supply pipelines. For S3, all the chillers of ICSs are water-cooled. The comparison between the DCS and ICS under such a case will be more general when chillers used belong to the same type. For S4, chillers in both the DCS and ICS are water-cooled with constant speed. By excluding the ICS of Phase 8 which uses VSD chillers, the comparison will be more proper for DCSs.

RESULTS

The central cooling plant of DCSs and users can be connected in two ways: direct connection and indirect connection. The performance of DCSs under both connection ways is evaluated and verified. Results are introduced respectively.

Indirect connection

The indirect connection indicates that plate heat exchangers should be used to isolate the central cooling plant of DCSs and users. Due to the heat exchange of chilled water at two sides of the plate heat exchangers, a lower supply temperature from the central plant of DCSs is required to ensure that the supply temperature to users is 7°C. The chilled water temperature leaving chillers is assumed to be 6°C. The actual COPs of chillers are about 5% lower than the rated ones. The configuration of chilled water systems of DCSs is assumed to constant primary and variable secondary pumping systems. The pressure drop across the remote plate heat exchanger is assumed to be 10m. The difference between the supply and return chilled water temperatures is assumed to be 5°C. The verification results of the DCSs under indirect connection are shown in Table 4.

From Table 4 it can be seen that the DCS cannot always achieve electricity saving under indirect connection. When all the buildings are connected (S1), the DCS consumes less energy in both summer and

winter. One reason is that chillers used in Phase 1 and Phase 2 are air-cooled, which are not as efficient as the water-cooled ones in the DCSs. This can also be proved by the energy saving of S2, where Phase 1 is not connected and the energy saving of the DCS is decreased. For S3, the DCS consumes around 7% more energy than the ICSs in summer weeks. That's because chillers in Phase 7, Phase 8 and JCIT are all water-cooled and they are very efficient, especially for Phase 8, where the VSD chillers are used. Therefore, the DCS using chillers without VSDs cannot be more efficient compared to ICSs. For S4, both the ICSs and the DCS adopt constant-speed chillers. It can be seen that around 6% energy can be saved during summer week. The energy saving of S1, S2 and S3 is higher in winter. It results from the lower cooling loads in winter and the efficiency of ICSs is lower. When the cooling is supplied centrally, chillers in DCSs can work at a higher efficiency. However, the energy saving is lower in winter than that in Summer for S4. That is because chillers in JCIT are shut down during night time in winter and the cooling system of Phase 7 works using the smaller chiller. The capacity of the smaller chiller (150 Ton) in the ICS of Phase 7 is much lower than that in the DCS (400 Ton). The efficiency of ICSs is therefore much higher than that of the DCS, which leads to a lower energy saving.

Energy savings of the DCS S1 (connecting all the buildings) in the summer weeks and winter weeks are shown in Figure 5 and Figure 6. It can be seen that the energy consumption of both ICSs and the DCS S1 is much higher during daytime than that during night time. However, the energy saving percentage is much higher during night time than that during daytime. In some hours of the day, the DCS cannot save any energy when the cooling load of ICSs is very high and the ICS can also be very efficient. In winter weeks, the DCS consumes much less energy compared with the ICSs. In the daytime of winter weeks, the DCS S1 is still hard to consume less energy than the ICSs.

Energy savings of the DCS S3 in the summer weeks and winter weeks are shown in Figure 7 and Figure 8. Figure 7 shows that S3 consumes much more energy than the ICSs during daytime in summer weeks. The percentage of excessive energy can be up to 30%. Even during the night time, it is hard for the DCS to be energy efficient compared with ICSs. That indicates that the ICS of each building is very efficient and the DCS have no advantages. Figure 8 shows that S3 can save some energy compared with ICSs in winter weeks and the energy saving mainly arise during the night time. During the daytime in winter weeks, no or ignorable energy can be saved.

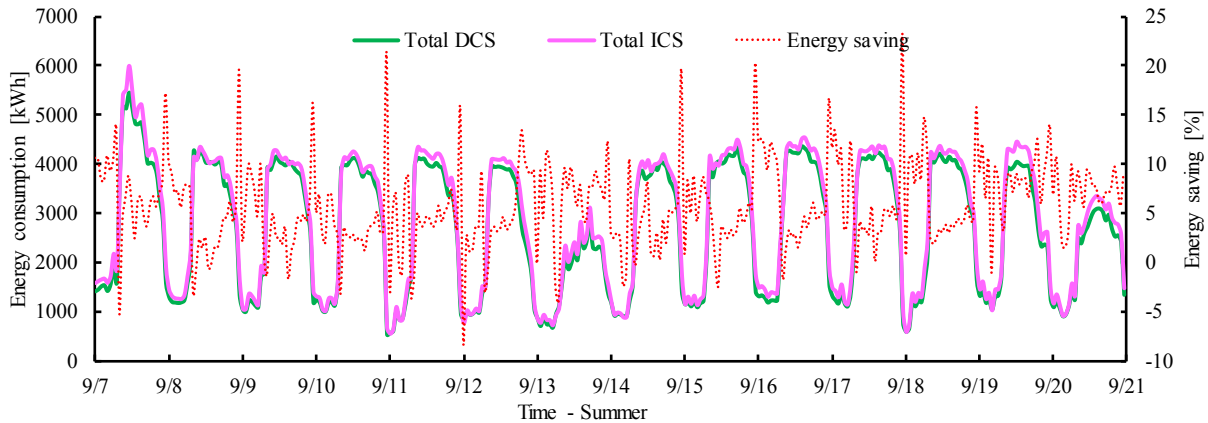


Figure 5. Energy consumption of the ICSs and the DCS S1 in summer weeks

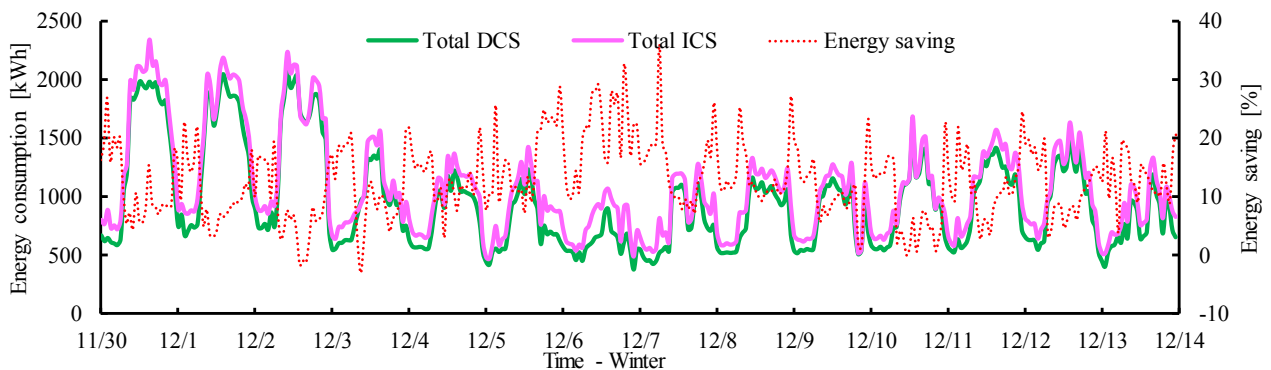


Figure 6. Energy consumption of the ICSs and the DCS S1 in winter weeks

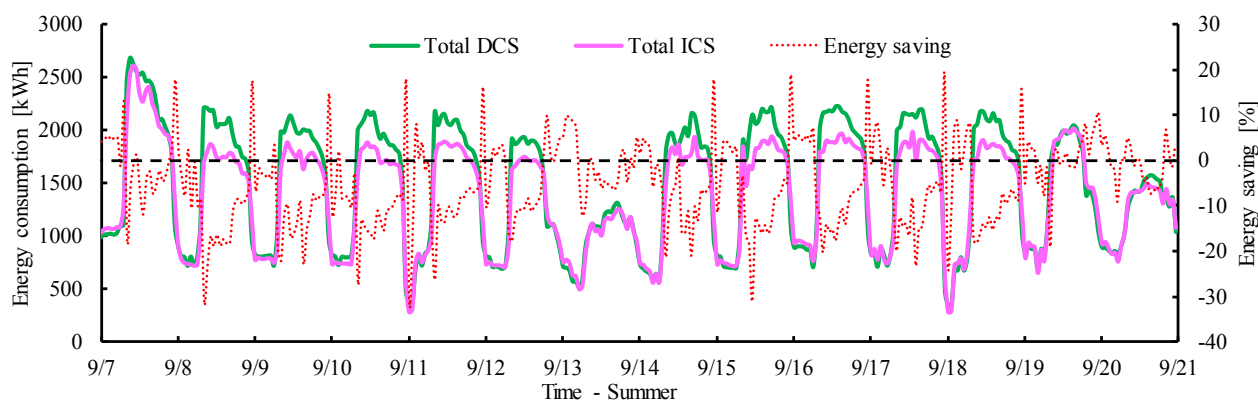


Figure 7. Energy consumption of the ICSs and the DCS S3 in summer weeks

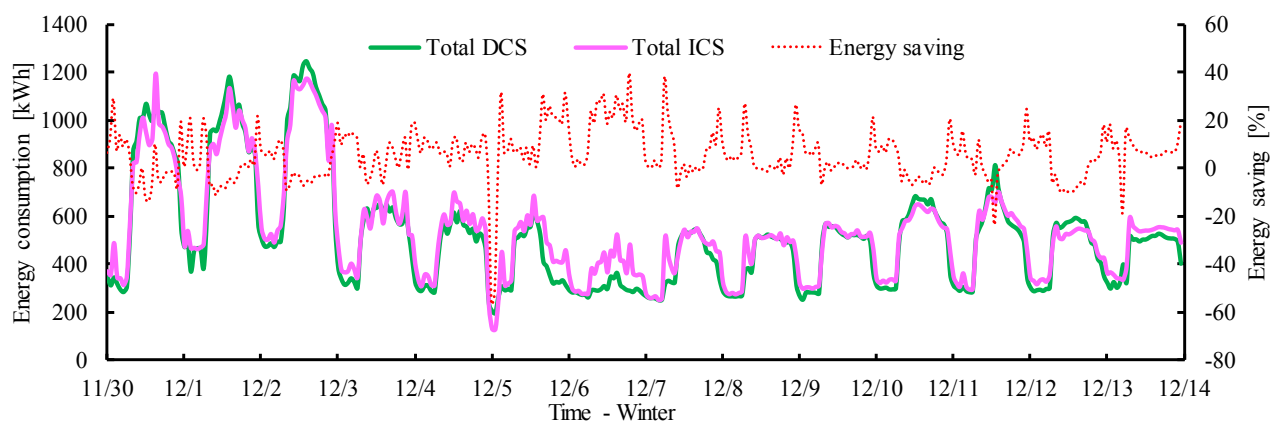


Figure 8. Energy consumption of the ICSs and the DCS S3 in winter weeks

Table 5 Energy saving of DCSs when different buildings are involved under the direct connection

System	Buildings	Direct connection	
		Summer	Winter
S1	Phase1->Phase2->JCIT->Phase7->Phase8	15%	23%
S2	Phase2->JCIT->Phase7->Phase8	11.40%	21.60%
S3	JCIT->Phase7->Phase8	5.10%	17.40%
S4	JCIT->Phase7	17.50%	12.50%

Direct connection

Without plate heat exchangers, the central plant of DCSs and users are connected directly. This connection way is very popular due to lower costs and high efficiency, especially when all the users connected to the DCS belong to the same owners. For DCSs serving the universities, direct connection is a very good option because all the buildings in the campus usually are managed by the same facility management office. The supply temperature of the chilled water from the chillers is assumed to be 7°C, which is consistent to that in ICSs. The primary-distributed chilled water system is selected in the DCSs, which is regarded as the most efficient configuration of chilled water pumps [11].

Results of the DCSs under direct connection are shown in Table 5. It can be seen that all the DCSs are more efficient compared with ICSs. The energy saving ranges from 5% to 23%. The DCSs have a higher energy saving potential during winter weeks due to low partial loads and load concentration effect, except for S4. Even when chillers with high efficiencies are used in ICSs for S3, DCSs still have energy saving potentials. From Table 5 and Table 6 it can be seen that DCSs under direct connection are much more energy efficient than that under indirect connection. The energy saving is increased by more than 10%. The direct connection therefore should be preferred for DCSs served users of the same owners.

Statistic results of the energy saving of the DCS S1 at different hours of the day are shown in Figure 9 and Figure 10. Figure 9 shows the mean energy saving. It shows that energy saving is high between 23:00 to 6:00, when the students and research staff leave the offices and the occupancy rate is low. The energy saving is much lower during the office hours. In Figure 10, the distribution of energy saving percentages at each hour is shown. On each box, the central mark is the median, the edges of the box are the 25th and 75th percentiles, the whiskers extend to the most extreme data-points and the red dots are the outliers. Figure 10

shows that the range of the energy saving is quite wide at each hour. Detailed values reply on the cooling loads at each hour. The relationship between the cooling loads and the energy saving of DCS S1 is shown in Fig. 11. It shows that higher energy savings mainly happen when the cooling loads is less than 5000 kW. The energy saving decreases gradually when the cooling loads increase and then stay stable around 15%. It indicates that the most suitable situation for DCSs is that when the cooling loads for ICSs are low. If a group of buildings have cooling demand during night time, the cooling is recommended to be supplied centrally to decrease the total energy consumption. It provides two directions for future application of cooling systems. One is that DCSs under direct connection should be preferred. The other is that even for the ICSs, two or several ICSs should be connected and share the cooling supply when the cooling loads for each ICS are very low.

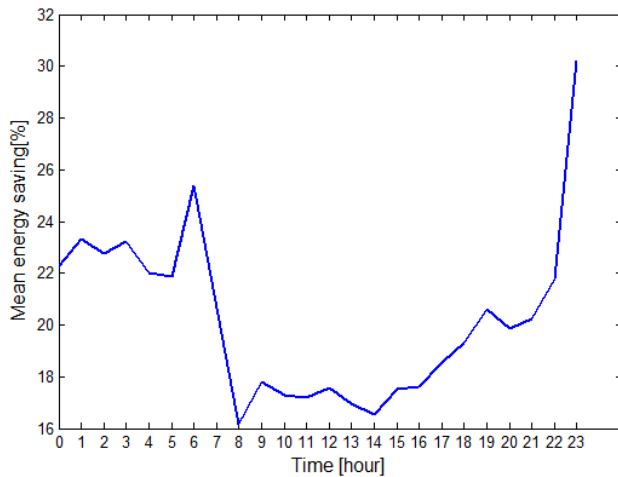


Figure 9. Mean energy saving of the DCS S1 at different hours of the day under direct connection

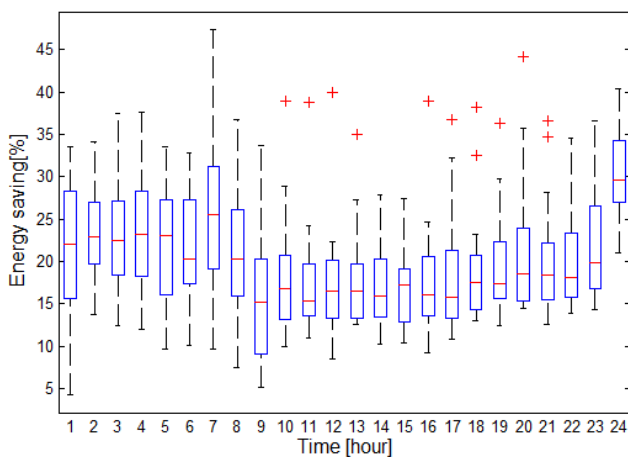


Figure 10. Distribution of energy saving percentages of the DCS S1 at different hours of the day under direct connection

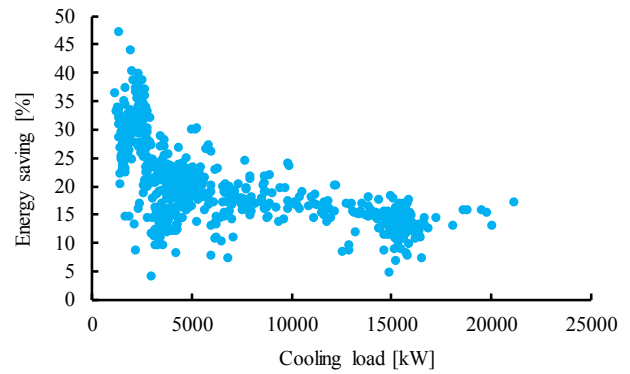


Figure 11. Distribution of energy saving VS. cooling loads

CONCLUSIONS

This paper conducts the performance verification of DCSs using actual operation data of ICSs in a university. The energy saving of DCSs under different connection ways and users is analysed. Performance of DCSs and ICSs in typical summer weeks and winter weeks is analysed. The following conclusions can be summarized:

- 1) DCSs under direct connection is much more energy efficient than that under indirect connection. The direct connection is highly recommended when all the involved users belong to the same owner or management teams.
- 2) DCSs cannot always save energy, especially when the ICS is very efficient (i.e. using VSD chillers).
- 3) DCSs mainly achieve energy saving when the cooling loads are low and the chillers in ICSs work at low efficiency. However, the lowest cooling loads do not correspond to the highest energy saving. It depends on that the low cooling loads are from one building or several buildings. If it is only from one building, the ICS is more energy efficient. Otherwise, DCSs can achieve higher energy efficiency.

ACKNOWLEDGEMENT

The research presented in this paper is financially supported by a research grant (Grant Number 152152/15E).

References

- [1] Yoshiyuki S., Tomoji N., Naoaki I., Minoru M. Verification of energy efficiency of district heating and cooling system by simulation considering design and operation parameters. *Build and Environ* 2008; 43(4): 569-577.
- [2] Gang W., Wang S., Xiao F., Gao D. C. District cooling systems: Technology integration, system optimization, challenges and opportunities for

- applications. *Renewable and Sustainable Energy Reviews* 2016; 53: 253-264.
- [3] Rezaie, B., Rosen M.A. District heating and cooling: Review of technology and potential enhancements. *Appl Energy* 2012; 93: 2-10.
- [4] Gang W., Wang S., Gao D., Xiao, F. Performance assessment of district cooling systems for a new development district at planning stage. *Applied Energy* 2015; 140: 33-43.
- [5] Chow, T. T., Au W. H., Yau R. Cheng V., Chan A., Fong K.F. Applying district-cooling technology in Hong Kong. *Appl Energy* 2004; 79(3): 275-289.
- [6] Chan A.L.S., Chow T.T., Fong S.K.F., Lin J.Z. Performance evaluation of district cooling plant with ice storage. *Energy* 2006; 31(14): 2750-2762.
- [7] Li Z., Duanmu L., Shu H.W., Shuang J., Zhu Y. X. District cooling and heating with seawater as heat source and sink in Dalian, China. *Renew Energy* 2007; 32(15): 2603-2616.
- [8] Shu H.W., Duanmu L., Zhang C.H., Zhu Y.X. Study on the decision-making of district cooling and heating systems by means of value engineering. *Renew Energy* 2010; 35(9): 1929-1939.
- [9] Gang W., Augenbroe G., Wang S., Fan C., Xiao F. An uncertainty-based design optimization method for district cooling systems. *Energy* 2016; 102: 516-527.
- [10] Sakawa M., Kato K., Ushiro S. and Inaoka M. Operation planning of district heating and cooling plants using genetic algorithms for mixed integer programming. *Appl Soft Comput* 2001; 1(2): 139-150.
- [11] ASHRAE. District cooling guide. Atlanta, GA. 2013.

A MINLP OPTIMIZATION OF THE CONFIGURATION AND THE DESIGN OF A DISTRICT HEATING NETWORK : STUDY CASE ON AN EXISTING SITE

T. Mertz^{1,2}, S. Serra¹, A. Henon², J.M. Reneaume¹

¹ LATEP-ENSGTI, Université Pau & Pays Adour, Pau, 64000, France,

² NOBATEK-INEF4, 33400, Talence, 33400, France,
tmertz@nobatek.com

Keywords: District Heating Network (DHN), centralized or decentralized heat supply, Mixed Integer Non-Linear Programming (MINLP) optimization

ABSTRACT

The aim of this work, included in the “THERMENERGY” project of the French energy transition institute INEF4, is to propose a tool to help the design of district heating networks (DHN) at the beginning of an urban project. The configuration (network layout, choice between the different production technologies, existence or not of such utilities) and the design (mass flow rate, temperature, heat capacity to install and area of the heat exchanger in sub-station) are optimized simultaneously. The tool works as well for energy supply systems to be created as for the expansion of existing sites.

The originalities of this work are to: 1 - avoid any constraint on pipe forcing them to be both supply and return, 2 - permit centralized - decentralized – or individual heat productions, 3 - permit cascade connections between consumers. Such a formulation enables to work on the 4th generation of DHN and also on branched or looped networks.

The formulation of the problem leads to a mixed integer non-linear programming (MINLP) problem. That means the optimization problem has a single nonlinear objective function (global cost) subjected to numerous linear constraints (e.g. mass flow rate balance) or nonlinear constraints (e.g. energy conservation) with both continuous (mass flow rate, temperature distribution, area of the heat exchanger, heat capacity to install...) and discrete variables (logical existence of the pipe or existence of the technology of production).

A study case based on an existing DHN is discussed. First some optimal design parameters (thermal generating capacity, temperature and network layout) are compared to the existing ones. Then, a potential expansion of the DHN to the neighbourhood and the introduction of renewable energy are studied.

INTRODUCTION

Energy savings in the building sector are needed. Although the high efficiency standard for new constructions and the current effort on refurbishment contribute to the European energy and climate policy,

further initiatives are needed to increase the savings. Indeed all the existing building stock cannot be refurbished simultaneously (technical and economic constraints) and in 2010 70 % of the city of the future 2050 are already built. Estimations evaluate that between 30 % and 40 % of buildings in 2050 would be built before 1975. Some reflexions about how to produce and distribute heat are complementary and relevant [1].

The isolated heat production (“individual” for one by dwelling or “collective” by building, illustration **Figure 2**) from renewable energy (geothermal, biomass, solar panels, heat pump, etc.) is an interesting solution for suburban residential area. But such individual solutions are quite difficult to implement in collective residential buildings (where 43 % of the population live) or the services sector, especially in high density areas, because those technologies need free surface on buildings or land (geothermal, solar, heat pump) or required large fuel volume (wood).

A District Heating Network (DHN) is a technical solution to supply heat at the urban scale. It enables to consider the heat demand at a larger scale and to exploit its diversity: each consumer does not need heat at the same time, especially if the building use is different (e.g. residential or office building). Moreover with such centralized heating system, costs are shared. And most of all, a DHN enables to exploit potential renewable sources and reuse wasted heat (excess heat from the industrial sector). This economy of scope, as underlined by FREDERIKSEN and WERNER [2], is the major asset of DHN. In return, the high initial investment cost has to be paid off through heat sales. The investment cost represents around 40 % up to 60 % of the total cost of the DHN (subsidies apart), they include the cost for the pipes (trench and materials), heat exchanger in substation and thermal generating power in power plant. Investors can secure their energy bills on the long term by varying the energy mix.

This work is part of the “THERMENERGY” project and receives financial support from the energy transition institute INEF4 R&D program. It aims at the creation of

a DHN design assistance tool (implemented in GAMS environment platform), to be applied in the context of new city planning - or refurbishment - projects. The core of this work is to optimize simultaneously in steady state the configuration (network layout and choice of the production technology), the design parameters (thermal generating capacity to install, exchange area of the heat exchanger, length and diameter of the pipes) and the state variables (temperatures, mass flow rates). one of the originalities of this work is to enable different network layout alternatives: consumer connection in parallel (classical design) or in cascade, the latter allowing the supply from a “hot temperature (HT) consumer” – such as an old building, a hospital, or an industrial utility – to a “low temperature (LT) consumer”. These connections between consumers, modelled by a heat exchanger, are depicted in (Figure).

This design helping tool helps also to choose between the following heat community supply alternatives (on the right **Figure 2** concerning DHN heat supply): one centralized heat production (like P1), numerous decentralized ones (like P2, a renewable source for instance), or a main network with isolated heat productions (like P3).

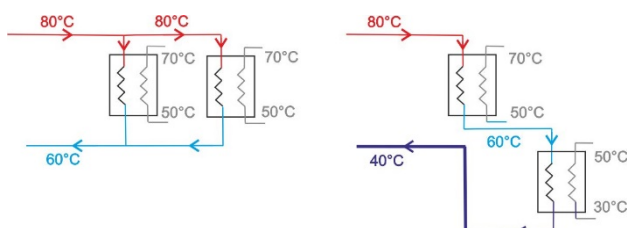


Figure 1 Consumer connection: in parallel – classical (left) and in cascade – innovation (right)

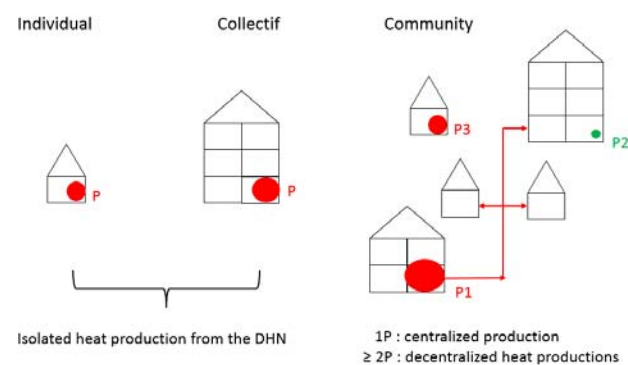


Figure 2 Comparison of different heat supply solution

OPTIMIZATION

Background

In this contribution, the word “optimization” refers to an algorithmic approach and not a heuristic (based on the experts experience) one. A mathematical formulation of the problem is stated: minimization of an objective function submitted to a set of constraints. Then an adapted method (algorithm) is selected in order to compute the optimal values of the optimization variables (both continuous and binary).

For a global overview of the different formulations of optimization problems (and their different ways to be solved), please refer to the retrospective on optimization from BIEGLER and GROSSMANN [3]. Briefly, an optimization problem is characterized thanks to the types of variables, the linearity or not of the equations (objective function and constraints), the number of objective function and the consideration of the time. Some studies applied to DHN:

- with continuous variables and non-linear (function and constraints), for instance [4]. In order to take into account nonlinearity such as pressure drop and thermal losses, the linear case is not suitable,
- in mixed variables (continuous and integer), most optimizations are linear [4] [5], a few are nonlinear [6],
- single objective function [4] [5] or multi-objective [6],
- single period [4], multi-period [5], [6] or even dynamic [7].

Each possibilities have pros and cons. The more complex the problem is, the more difficult the resolution is (because of the nonlinearity and the combinatory explosion). The issue of this present work is to optimize simultaneously the configuration (so mixed variables are needed) and the sizing (precisely, so nonlinear equations are included).

Problem formulation

A previous conference paper was more focused on the problem formulation [8]. Briefly the main aspects are explained below.

As the configuration is one of the expected results of this work, binary variables (Y letter variables) are introduced to rule the existence of the pipes and the existence of the technologies of production. They represent around 20% of the total amount of the variables. Because of these variables, lots of combinatory are introduced into the problem. And the continuous variables have to be defined only if the

utility exists, as for instance the pipe length is equal to the distance only when the binary variable is not null (1) and the mass flow rate existence is ruled thanks to equation (2) with M_{max} the maximum mass flow rate allowed and. If the pipe does not exist, the mass flow rate is equal to 0, otherwise if it exists, the mass flow rate value varies between 0 and M_{max} . In these examples, equations are written for the PC line (connection between one producer node to one consumer node). Similar equations are written for the return line and for connection between consumers (in cascade or in parallel).

$$L_{linePCij} = V_{linePCij} \cdot Dist_{linePCij} \quad (1)$$

$$\forall (i,j), 0 \leq M_{linePCij} \leq V_{linePCij} \cdot M_{max} \quad (2)$$

Concerning the sizing aspect, as the temperature, velocity and diameter are optimization variables, the energy balance equations are nonlinear, as for instance at the inlet of the consumer node. Moreover the thermal losses are calculated precisely, for example in the pipe PC equation (3). As well as the pressure drop is calculated thanks to equation (4), which helps estimating the pumping cost. More information about parameters (α , β , γ , C_p , T_{ext} and R_{tot}) in our previous paper [8].

$$T_{linePCij} = T_{ext} + (T_{linePCij} - T_{ext}) \cdot \exp\left(-\frac{\pi \cdot D_{outPCij} \cdot L_{linePCij}}{R_{totPCij} \cdot M_{linePCij} \cdot C_p}\right) \quad (3)$$

$$DP_{linePCij} \cdot L_{linePCij} = \gamma \cdot \frac{V_{linePCij}^5}{D_{linePCij}^5} \quad (4)$$

A MINLP (Mixed Integer Non Linear programming) problem has to be solved. As the problem is modeled with numerous constraints including continuous variables, a deterministic method is chosen for its accuracy and its rapidity, compared to a stochastic method. The problem is implemented in the GAMS environment, in which numerous available solvers can be called to solve the problem. The solver used in this study is DICOPT, which uses the OA/ER/PA resolution method.

The objective function to minimize is the total cost, equation (5), of a DHN over a 30 years' time horizon. It includes the initial investment (CAPEX) for the thermal generating capacity in power plant, the heat exchanger in the substation and the pipe and also the operative cost (OPEX) related to the pumping and fuel cost, each year, including the energy inflation price.

$$C_{tot} = (OPEX_{pump} + OPEX_{heat}) \cdot f_{opex} + (CAPEX_{pump} + CAPEX_{HX} + CAPEX_{pipe}) \cdot f_{capex} \quad (5)$$

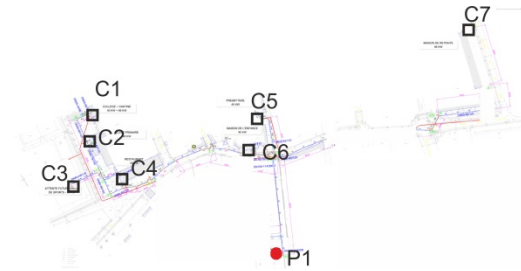


Figure 3 Localization of the input data of the existing network P1C7 (one producer and 7 consumers)

Table 1 Input data: location (abscissa and ordinate) and nominal heat power required for the nodes

	P1	C1	C2	C3	C4	C5	C6	C7
x (m)	280	91	91	69	146	267	245	465
z (m)	24	166	136	94	105	167	133	248
H _{req} (kW)	0	135	60	90	25	45	45	96

STUDY CASES DESCRIPTIONS

A previous conference paper was more focused on underling the cascade connection innovation [8].

Case 1: Comparison to the existing network

For this paper, the cases are based on an existing network in the south west France, near to Bordeaux. The seven consumers, shown in a plan (**Figure 3**), represents a total nominal heat demand of 496 kW. Each consumer heat demand is detailed in **Table 1**. To begin, only one producer is available, it requires no heat demand. The technology (k1) available in P1 is a gas boiler with a thermal generating capacity of 600 kW.

The actual existing network layout is similar to the optimized result shown in (**Figure 4**), when only one production node is available. The network total length (supply and return) is 1 224 m, so 612 m of trench (in this study, the line are both supply and return, which is not the case in [8]). In the case of the optimal configuration and design, the total cost reaches 11.13 M€ over 30 years. In (**Figure 5**) is represented the costs repartition. 42 % are operative costs (OPEX), which are in huge majority due to the fuels cost. More than the half of the total cost represents an investment cost (CAPEX), 41 % for the thermal capacity to install and also 15 % for the pipes (trench and materials). The pumping cost is very low thanks to the optimization that has chosen an appropriate sizing for the diameters, the velocities and the temperatures. In case of a bad network management or for very low temperature networks, the pumping cost share can represents around 10 % [9]. The balance between thermal losses

(17.4 W/m and thermal loss ratio less than 4 %) and pressure drop (1 kPa/m) is well optimized.

The optimal design (**Table 2**) proposes a higher supply temperature (97 °C) than the effective one (90 °C) and a lower return temperature (60 °C) than the effective one (70 °C). The optimal inner diameters are quite similar than the effective ones, around 100 mm exiting the production node and 50 mm at the end of the network. The optimal inner diameter for the return pipe is slightly bigger than for the supply pipe, which enables to reduce the pressure drops without increasing the heat losses (also possible because the return temperature is nearly 40 °C lower). The order of magnitudes are respected, even in the thermal generating capacity to install, the optimal one (574 kW) matches with the installed one (600 kW).

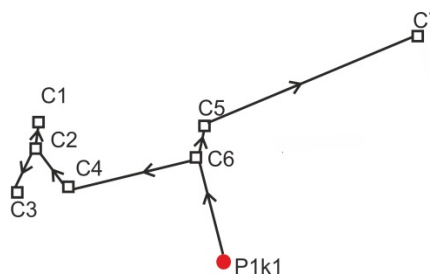


Figure 4 Optimal configuration L=1224 m and a centralized fossil fuel heat supply (when only P1k1 allowed)

Case 2 Isolated and renewable introduction

The consumer C7 is quite isolated from the rest of the district. We propose to test if an isolated heat production (P2, located at the same place as C7) would be economically profitable or not.

Moreover, a renewable energy (technology k2) in this P2 location is now allowed. This k2 technology has not price inflation. As it is not technically feasible to supply 100 % of the heat demand with only renewable energy (peak load heat consumption profile versus weather dependant renewable production), a peak-load technology (k3) based on gas is chosen to supply at least 10 %. This technology k3 has a higher investment cost (1200 €/kW) than k1 (800 €/kW), but the same fuels unit cost (8 ct€/kWh) and the same price inflation (4 %).

The problem formulation, with 2 potential producers, 3 technologies available and 7 consumers, admit nearly 3 500 variables.

To enhance this study case, let us consider a secondary potential producer node (P2), with a “small” renewable potential (the thermal capacity of P2k2 is limited to 90 % of the nominal heat power required by C7). In this case, the obtained optimal configuration (**Figure 6**) is one network with the previous fossil fuel technology (P1k1) and an isolated heat supply for the isolated consumer C7. The total cost is reduced to 10.30 M€ (-7.5 %) when the unit operational cost for k2 is 4 ct€/kWh instead of 8 ct€/kWh for k1 or k3.

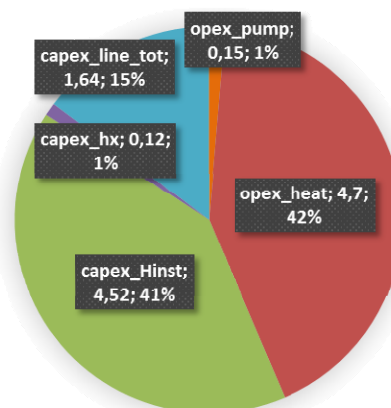


Figure 5 Cost repartition (in M€) for the optimal result (when only P1 allowed)

Table 2 Sizing results (when only P1 allowed) comparison for the line leaving the power plant (P1C6) and the line at the end of the network (C2C1)

	P1C6		C2C1	
	supply (real)	return (real)	supply (real)	return (real)
T _{in} (°C)	97.4 (90)	59.9 (70)	96.7	60.0
T _{out} (°C)	97.1	59.8	96.5	59.9
D _{int} (mm)	100 (100)	110 (100)	50 (60)	50 (60)
V (m/s)	0.41	0.35	0.46	0.46
M (kg/s)	3.28	3.28	0.88	0.88
DP (kPa/m)	0.23	0.13	0.52	0.44

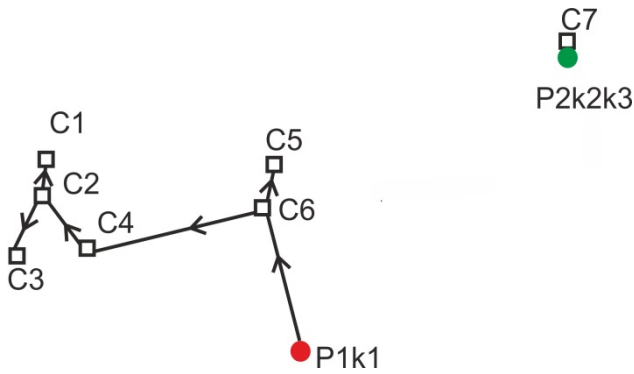


Figure 6 Optimal configuration L=796 m with a centralized fossil fuel supply (P1k1) and an isolated renewable energy heat supply (P2k2k3)

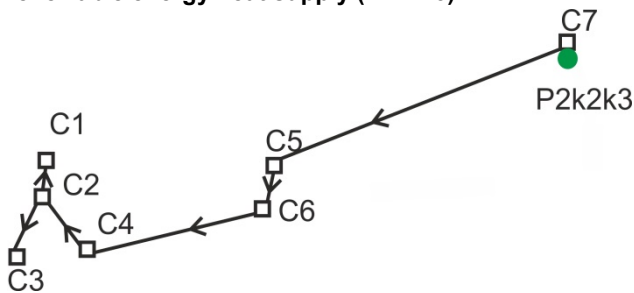


Figure 7 Optimal configuration L=995 m with a centralized renewable energy heat supply (P2k2k3)

If there is a “medium” potential to exploit renewable energy in P2 (the thermal capacity of P2k2 is limited to 90 % of the nominal heat power required by all the consumers), a third configuration is optimal (**Figure 7**). The total cost is now reduced up to 9.90 M€ when the unit operational cost for k2 is 4 ct€/kWh instead of 8 ct€/kWh for k1 or k3. This reduction is quite significant (-1.1 %) and underlines the importance to make more attractive renewable source, even if they are located further (than other classical locations, as P1) and their related investment costs are higher (1200 €/kW for k2 compared to 800 €/kW for k1).

To answer the question of uncertainty about price estimation, a **post optimal sensibility analysis** is proposed (**Figure 8**). 2 parameters about k2 cost are tested: its operative unit cost (6 values are tested, between nearly free, as in case of wasted heat reuse 1 ct€/kWh up to 6 ct€/kWh) and its investment cost (4 values tested, between 100 €/kW nearly zero investment, up to 1500 €/kW, nearly twice expensive than k1). The third parameter studied is the unit cost of the trench (3 typical values tested: 300 €/ml in the countryside, 800 €/ml the French average unit cost in city and 1500 €/ml in high density city).

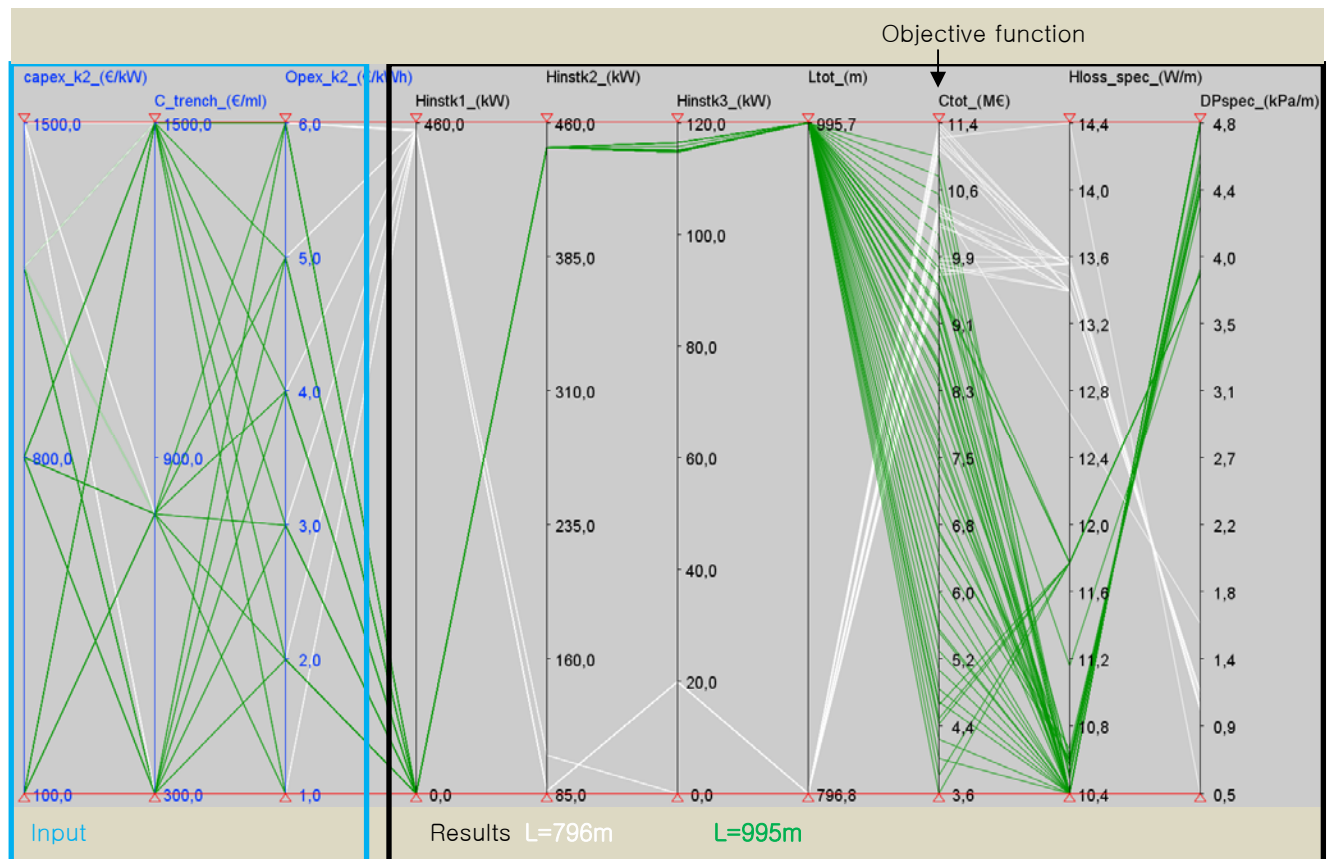


Figure 8 Post optimal sensibility analysis for case 2

To avoid locally minimum, 3 different initializations and 5 bounds are tested, only the best results are kept and represented. Which leads to solve 15 resolutions (3 different initializations times 5 different bounds) for each 3 input parameters tested (k2 capex, k2 opex and trench unit cost). As there are 72 cases in the sensitive analysis (6 k2 opex times 4 k2 capex times 3 trench cost), 1 080 resolutions are solved in this post optimal sensitive analysis.

Less than 1h20 calculation times are needed to solve these 1 080 resolutions. The results (Figure 8) reveal that if k2 capex=100 €/kW (nearly free of investment) or 800 €/kW (same investment price than the fossil fuel technology k1) then the configuration “centralized renewable heat production” (Figure 7) is always optimal, whatever are the k2 opex or the trench cost are. On the contrary, if k2 investment is really high (1500 €/kW), the centralized fossil fuel production with a renewable isolated heat production (Figure 6) is always optimal whatever the other costs are.

When the investment cost is 1200 €/kW, the two configurations could be optimal. The isolated renewable supply (Figure 6) is optimal when the trench cost is higher or equal to 800 €/ml and the k2 opex higher or equal to 5 ct€/kWh. Otherwise the renewable centralized heat supply (Figure 7) is optimal.

The centralized fossil fuel heat supply (Figure 4) is never optimal in this analysis. It is optimal, if and only if the renewable energy is really expensive (k2 capex higher than 2100 €/kW and k2 opex equal to 6 ct€/kWh). Thus in this case, the renewable energy introduction is promoted.

Case 3: Potential for expansion

Based on this existing district, a potential expansion study case is then proposed. In this residential area, it is assumed that the district construction are quite similar. So to build this case 2, the consumers C1-C6 are translated, horizontally (+500 m) for C8-C13 and vertically (+200 m) for C14-C19 (Figure 9). The heat demand are based on C1-C6 input (i.e. $H_{req_{C8}}=H_{req_{C14}}=H_{req_{C1}}$)

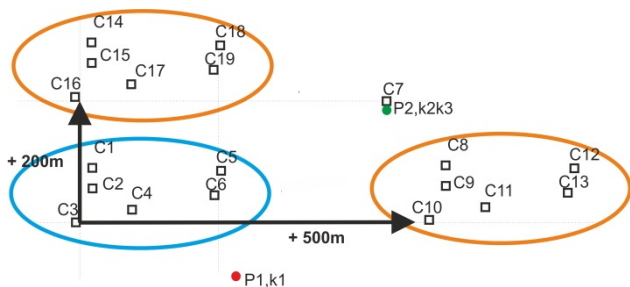


Figure 9 Construction of the input data for the case 2

As in the previous case, there is two potential production sites: in P1 location, a fossil fuel technology is allowed (k1), whereas in P2 location a renewable energy technology (k2) could potentially supply up to 90 % of the total district heat demand, with a peak load technology (k3) in addition.

As a renewable potential is identified (study case assumption), the core question to answer is not anymore only a potential P2k2 isolated heat supply, but why not considering to extend the network to the neighbourhood, supplied by this renewable source.

Now in this bigger case (19 consumers), there are more than 22 000 variables.

In comparison to (Figure 4) with only P1 allowed and 19 consumers, the optimal configuration is shown (Figure 10). As a consequence of the expansion, now the subnetwork C1C7 is different. In other words, C4 is not anymore supplied by C6 as before, but by C16. This centralized fossil fuel heat supply leads to a total cost of 29.53 M€ (with k1 opex of 8 ct€/kW).

As soon as a secondary potential production node is allowed, with the possibility to introduce renewable energy into the energy mix, this supply solution is optimal. In case of an “intermediate” renewable energy potential (thermal capacity of P2k2 limited to 90 % of the heat required by the consumers C7 to C13), two separated networks are optimal (Figure 11). The total cost is reduced to 26.76 M€ (-9.4 %).

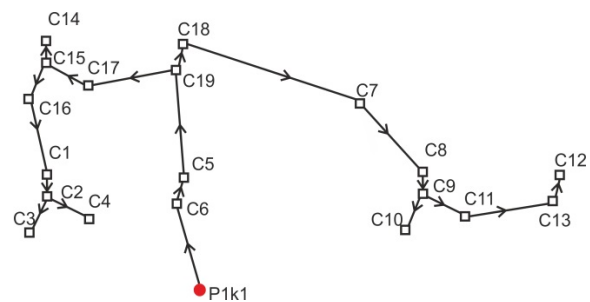


Figure 10 Optimal configuration L=2 635m, when only P1k1 is available

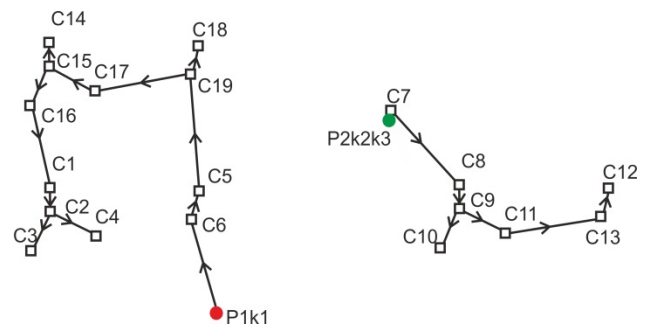


Figure 11 Optimal configuration L=2237 m, when P2k2 capacity is limited to 90 %

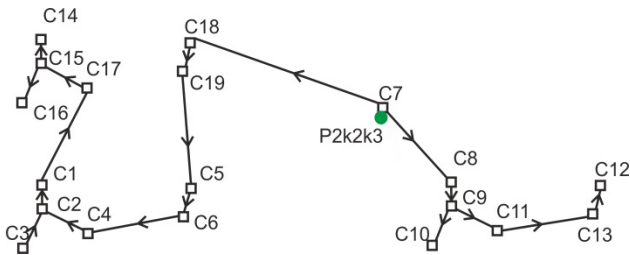


Figure 12 Optimal configuration L=2470m, one centralized network with renewable energy supply

In case of the highest renewable potential (but still a limitation of 90 % of the total heat demand due to technical reasons), the optimal configuration is shown (Figure 12). This centralized renewable energy heat production enables the highest total cost reduction up to 26.33 M€ (-10.8 %). And the potential cost reduction is even higher when k2 opex is lower than 4 ct€/kWh. For instance the total cost is only 24.61 M€ (-16.7 %) when k2 opex is equal to 1 ct€/kWh, that means nearly free of charge)

As before, a **post optimal sensibility analysis** is finally proposed (Figure 13). As before, 1080 resolutions have been done, among only the 72 best results are shown, which has required 3h20 calculation

time. Such a post optimal sensibility analysis is worth, because previously, with fixed unit cost, the renewable centralized heat production configuration was optimal. But what if this cost estimation is under uncertainty; will this configuration still be optimal?

The classic fossil fuel centralized heat production (Figure 10) is optimal, only if the k2 investment is the highest (1500 €/kW) and if the k2 opex is not so interesting (higher or equal 4 ct€/kWh). Otherwise the renewable introduction is optimal.

A medium renewable energy introduction, for only one separated network (Figure 11), is optimal if -1- k2 investment is the highest (1500 €/kW), the k2 opex is financially interesting (less or equal than 3 ct€/kWh) and if -2- k2 investment is high (1200 €/kW) and the k2 opex at its higher level (6 ct€/kWh).

Finally, when the renewable source has the highest potential, with investment cost lower or equal to 800 €/kW, whatever the operational cost, the centralized renewable heat production is optimal.

Thanks to this analysis (Figure 13), the trench cost has no influence, nor to the optimal configuration choice, neither to the sizing (same thermal capacity installed, heat losses and pressure drop). Logically, the higher the unit cost is, the higher is the DHN total cost.

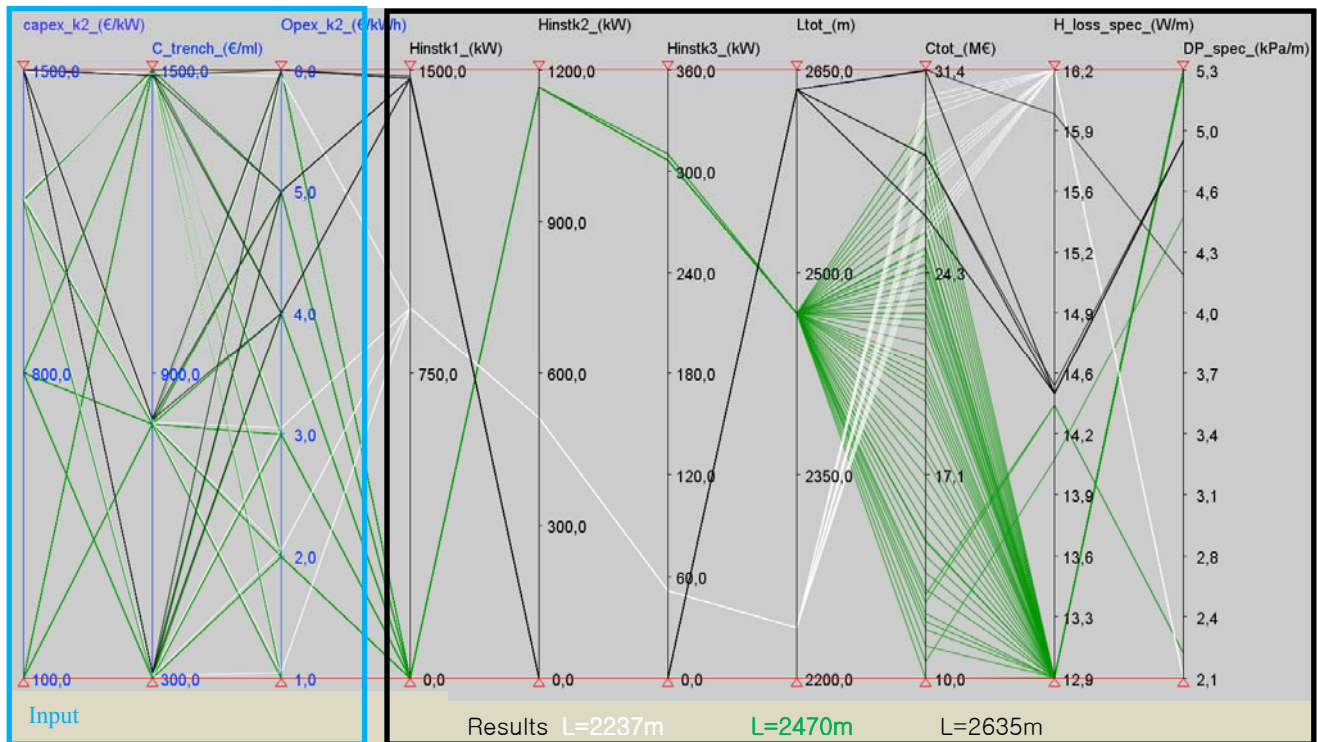


Figure 13 Results post-optimal sensibility analysis case 3

CONCLUSION

Thanks to this design helping tool, DHN configuration and sizing can be optimized simultaneously. A MINLP problem has to be solved within GAMS environment. The time calculation is less than 2 s to solve case 1 and 11 s for case 2, on an Intel i5 CPU 2.60 GHz and 4 Go RAM. So the post optimal sensitivity analysis (1 080 resolutions) required 1h20 calculation time in case 1 and 3h20 in case 2.

The first study case, based on an existing DHN, shows that when only one producer node were allowed, the DHN optimal configuration and design is closed to the existing network (thermal capacity installed and distribution temperature). An operative feedback is waited to confirm the order of magnitude founded, especially such a low pumping cost share.

But even on such a simple example of a district area, this optimization tool can help designing, as for instance in study case 2, when one other production location is available. In this secondary potential production location, a renewable energy source was proposed. The sensitive analysis reveals that this renewable source introduction was optimal, only if its investment cost were lower than fossil fuel investment (800 €/kW) and leads to a reduction up to 10 % of the DHN total cost.

The third study case highlights the strength of such an optimizing programming method on a bigger district area example. The previous location fossil fuel heat production is optimal only if the investment (>1500 €/kW) and the operational renewable cost (≥ 4 ct€/kWh) are expensive in comparison. Otherwise, like previous case, the introduction of renewable energy into the energy mix is economically profitable (more than 15 % total cost reduction).

In perspective, it would be interesting to solve a multi-period MINLP problem, so that thermal energy storage could be also studied, configuration (long term storage in heating plant and/or short term storage in sub-station) and sizing (volume, temperature and heat losses).

ACKNOWLEDGEMENT

This work is part of the project THERMENERGY and receives the financial support from the energetic transition institute INEF4 R&D program, a French institute for the energy transition focused on refurbishment and sustainable buildings.

NOMENCLATURE

Sets

C_j	consumer node
HX	heat exchanger

in	inlet
inst	installed
out	outlet
$P_{i,k}$	producer node (located in i technology k)
req	required
spec	specific value
tot	total

Roman letter

C_p	specific thermal capacity [J/(kg.K)]
C	cost [€]
D	diameter [m]
DP	pressure drop [W]
H	thermal capacity [W]
L	length between two nodes [m]
M	mass flow rate [kg/s]
R	surface thermal resistance [m ² .K/W]
T	temperature [°C]
V	velocity [m/s]
x	node (P or C) abscissa [m]
Y	existence binary variable [-]
z	node (P or C) ordinate [m]

REFERENCES

- [1] DHC+ technology platform. District heating and cooling - A vision towards 2020 - 2030 - 2050. [September 02, 2014]; Available from: http://www.dhcplus.eu/wp-content/uploads/2012/05/120529_Vision_DHC_final.pdf.
- [2] FREDERIKSEN S., WERNER S. District heating & cooling. first edition. ISBN:9789144085302. Lund: Studentlitteratur AB, Lund; 2013.
- [3] BIEGLER LT, GROSSMANN IE. Retrospective on optimization. Computers & Chemical Engineering 2004;28(8):1169–1192. doi:10.1016/j.compchemeng.2003.11.003.
- [4] BOHM B., HA S.-K., KIM W.-t., KIM B.-k., KOLJONEN T., LARSEN H. V. et al. Simple Models for Operational Optimisation: IEA District Heating and Cooling annexe XI, report S1. ISBN:90-5748-021-2; 2002.
- [5] SODERMAN J, PETERSSON F. Structural and operational optimisation of distributed energy systems. Applied Thermal Engineering 2006;26(13):1400–1408. doi:10.1016/j.applthermaleng.2005.05.034.
- [6] WEBER CI, MARECHAL F, FAVRAT D. Design and optimization of district heating systems. In: DHC10, The 10th International Symposium on the District Heating and Cooling; 2006.
- [7] SANDOU G, DESSANTE P, PETIT M, BORSENBERGER H. Technico-Economic Optimization of Energy Networks. In: ROBOAM X,

editor. *Integrated Design by Optimization of Electrical Energy Systems*. Hoboken, NJ, USA: John Wiley & Sons, Inc; 2012, p. 247–285.
doi:10.1002/9781118561812.ch6.

- [8] MERTZ T, SERRA S, HENON A, RENEAUME J. A MINLP optimization of the configuration and the design of a district heating network: academic study cases. In: *The 28th international conference on*

Efficiency, Cost, Optimization, Simulation and environmental Impact of Energy Systems; 2015.

- [9] GUELPA E, TORO C, SCIACOVELLI A, MELLI R, SCIUBBA E, VERDA V. Optimal operation of large district heating networks through fast fluid-dynamic simulation. *Energy* 2016;102:586–595.
doi:10.1016/j.energy.2016.02.058.

BOTTLENECKS IN DISTRICT HEATING SYSTEMS AND HOW TO ADDRESS THEM

L. Brange¹, J. Englund², K. Sernhed¹, M. Thern¹, P. Lauenburg¹

¹ Lund University, Faculty of Engineering, Energy Sciences Box 118, SE-221 00 Lund, Sweden

² E.ON Värme Sverige AB, Flintrännegatan 19, 211 24 Malmö, Sweden

Keywords: *District heating development, Bottlenecks, Optimization*

ABSTRACT

Problems with bottlenecks in district heating networks occur when the pipes have too small dimensions to sufficiently meet customer needs. This may result in insufficient differential pressure in DH areas attached to these pipes. Bottlenecks are especially common in expanding DH networks, as previously sufficient pipe diameters may become too small when more DH consumers are connected to the DH network. Historically, bottlenecks have often been addressed by increasing the supply temperature or by exchanging the pipe to a larger dimension. Other techniques are however available to solve bottleneck problems. Such techniques are for example installation of local heat supply on the other side of the bottleneck (LHS), demand side management (DSM), or installation of thermal energy storage (TES). The aim of this study was to identify different techniques for addressing bottlenecks and to see what solutions were used by the DH companies in Sweden. A literature study of the different techniques available was performed and a survey study with the DH distribution companies in Sweden that are members of the Swedish DH association was carried out. The survey was sent out to in total 131 companies, of which 89 answered. The results showed that the most used techniques in Sweden are a higher supply temperature and installation of a new pipe to increase the pipe area, whereas for example DSM and TES were more rarely used techniques. This work is an introduction to the different techniques used to address bottleneck problems and shows the bottleneck situation in Swedish DH networks. More research and tests are however necessary in order to more thoroughly evaluate which techniques that should be used in different situations.

INTRODUCTION

In district heating (DH) networks, pipes are dimensioned for a certain flow. If the flow increases, this leads to higher velocities in the piping system which in turn lead to bigger pressure loss. If the flow becomes too big, there may be problems to sufficiently deliver heat to the DH consumers in the affected areas, due to too high pressure loss. This could for example happen when the heat demand increases or if the supply temperature is lowered without correspondingly

lowered return temperature. DH networks undergoing expansion, densification or conversion to lower supply temperatures are thus at particular risk to experience this problem. Such heat supply problems due to too small pipe diameters compared to the flow are in this paper called bottleneck problems.

To overcome this problem either the initial temperature or the initial differential pressure (dp) could be raised, often resulting in higher costs and, in the increased temperature case, also bigger heat losses [1]. To avoid this, the measure often taken is to install an extra pipe or a new pipe of a bigger dimension, in order to increase the flow area and thus decrease the velocity in the pipe. There has however been a lot of development and progress in the DH research in recent years, which makes way for other solutions to bottleneck problems.

Two of the bottleneck elimination methods that will be discussed are the most conventional methods, i.e. increasing of the pipe area of the pipe that is used to distribute heat to the area in question and raising the supply temperature. An increased pipe area may be achieved by either a bigger pipe diameter or an extra pipe. The dp in the affected area could also be raised with extra pumps or increased initial dp. Another method is to install local heat supply (LHS) in the affected area. Installation of thermal energy storages (TES) could achieve the same objective. A reduction of the flow demand among consumers is another possible method to reduce the bottleneck impact. This could for example be accessed using different types of demand side management (DSM) or increased cooling in consumer substations.

Most research that concerns the different possible bottleneck measures in DH networks address the measures independently and does not include the bottleneck perspective. The purpose of this paper is therefore to do a review of the currently available techniques that address bottlenecks in DH networks, investigate the state-of-the-art of these techniques and also study how bottleneck problems occur and how DH companies presently address these issues. This is performed as it is important to know a problem before being able to solve it. The purpose will be achieved by literature studies and a survey to Swedish DH companies. Due to the lack of research of bottlenecks in the scientific DH community, the focus of the literature study will be on the research made of the

different techniques in other areas, to achieve a state-of-the-art knowledge of the techniques and measures.

METHODS

Different measures to handle bottlenecks in DH networks were identified through research and dialogue with the local district heating companies. Thereafter, a review of the recent research most relevant for the bottleneck problem was performed, to give a relevant picture of the different techniques available that could be used to solve bottleneck problems in DH networks. Information about the different methods was primarily collected among scientific papers. The different measures were divided into categories based on the way they solved the bottleneck problem. The three categories were 'increased distribution capacity', 'local supply' and 'consumer flow management'.

A survey was sent out to all the district heating distribution companies that are members of the Swedish District Heating Association (SDHA) to investigate how large problems with bottlenecks Swedish district heating companies consider themselves having and which measures are used to eliminate bottlenecks in Sweden. The member companies of SDHA distributes around 50 TWh heat annually, which also is the amount of heat distributed by DH totally in Sweden [2]. This survey was sent out to 131 DH companies and 89 answers were collected. Some companies in the study manage more than one DH network. From these companies we sometimes received different answers for the different networks. If more than one response was received from representatives for only one district heating network, the answers were analysed as one answer.

A quantitative survey was chosen because the purpose of the study was more sufficiently fulfilled by a quantitative rather than a qualitative method. The desired outcome was the general bottleneck state in Sweden, which a qualitative method would not be able to satisfy, as the sample would not be big enough.

BOTTLENECK ELIMINATION METHODS

Supply temperature (increased distribution capacity)

A lot of the recent DH research focus on the fourth generation of district heating and so called low temperature district heating (LTDH). The idea of LTDH is to decrease heat losses in the DH network [1], simplify the introduction of low grade heat sources [3], [4], and enable use of, for example, cheaper polymer pipes. Lower supply temperatures without correspondingly lowered return temperatures or lower heat demands will however result in a higher flow and thus a higher pumping power [5]. Tol and Svendsen similarly show that great savings in pipe diameter are achieved if the supply temperature in a low-energy DH

network is boosted during the peak load [6]. This means that by increasing the supply temperature, it is possible to avoid bottlenecks in DH networks. It also means that the trend towards lower supply temperatures in DH networks may induce more bottleneck problems, as the flow increases. This is especially a matter if lower supply temperatures are introduced without any other measures in already existing DH areas.

Bigger pipe area (increased distribution capacity)

The recent research of new pipes often address the idea of adapting the pipes to the 4th generation of district heating (4GDH), often defined as a smart thermal grid allowing low energy buildings to be supplied by low temperature heat from both centralised and decentralised heat sources in pipes with low heat losses [4]. Due to the focus on lower supply temperature and 4GDH, recent DH pipe research often focus on low heat losses and insulation of pipes, showing for example that a high insulation standard or vacuum insulation panels may decrease heat loss [7], [8]. Different sorts of pipes, for example twin pipes, double pipes and triple pipes are discussed as the pipe solutions in low temperature DH networks with highly efficient buildings [9]. Coupled to bottlenecks it is shown that larger pipe diameters may promote an avoidance of higher supply temperatures, as higher supply temperatures promotes lower pipe diameters [6]. A bigger pipe area is however also more expensive than a smaller one, even if the pressure losses are reduced with a bigger pipe area [10].

Pumps (increased distribution capacity)

Pumps are used for maintaining the pressure in DH networks and they may also be used to increase the pressure in bottleneck areas. With the assumptions and boundaries set in [11] it is suggested that decreasing the heat losses by a lower supply temperature and thus increasing the pumping power would improve the exergetic efficiency of the DH network. The optimal boundaries and assumptions are however different in each different DH system and case. Pumping power could also constitute a non-negligible part of the primary energy supplied to the district heating network, in Turin for example 2-8 %. With optimal pumping management, the pumping power needed may be decreased by around 20 %, which means that there could be noticeable energy savings in optimal operation of the pumps [12]. The use of distributed variable frequency speed pumps instead of one central circulation pump may also give substantial savings in pumping energy. In a Chinese case such a solution would for example give almost 50 % electrical energy savings compared to a conventional solution [13].

LHS (local heat supply)

Local heat supply (LHS) may also be a solution to bottleneck problems in DH networks. If a production unit is installed on the other side of the bottleneck, less heat will have to be transported through the bottleneck pipe and the flow and thus the pressure drop will decrease. Production units could for example consist of prosumers, heat pumps or peak heat boilers.

Prosumers are defined as DH consumers that also supply heat to the DH network. Prosumers heat production typically come from excess heat from cooling machines or solar collectors [5], [14]. If excess heat from cooling machines is used, the supply temperature often needs to be increased by for example a heat pump [14]. Distributed small-scale production units can both increase and decrease the local dp depending on how they are dimensioned and located in the network. A risk of decreased dp typically appears when the prosumer has a lower supply temperature than the rest of the DH network [15]. The reason for a prosumer to have a lower supply temperature is that both solar collectors and heat pump based prosumers are more efficient with lower supply temperatures. Therefore a DH system that allows lower temperatures might be necessary to be able to install prosumers [16]. The distributed heat supply from prosumers also results in lower pumping power needed in the central main pumps of the DH system, as less heat needs to be transported a long distance [5]. In some areas and DH networks prosumer heat may annually cover more than 100 % of the heat demand of the house or area [14] but that heat is often mostly available during the warm season. This means that thermal energy storages (TES) may be needed to utilise all the heat [17]. An important thing to keep in mind for heat pump based prosumers is that the environmental outcome is not always better than for the conventional DH, as this depends on the specific environmental characteristics of the electricity source and the DH source [14].

Another way to cope with bottlenecks is to use conventional peak heat boilers and small-scale decentralised combined heat and power plants (CHP:s). The peak heating units could for example consist of electric boilers, gas boilers or biomass boilers. When peak heat boilers are located in the periphery of the network, the overall energy efficiency of the DH network is improved, due to less electricity consumption needed for heat distribution [18]. This suggests that peak heat boilers advantageously may be placed in remote areas to address bottlenecks, as less flow than is needed to be transported long distances in the DH system.

Decentralised CHP:s is an interesting alternative to peak heat boilers, as they are more thermodynamically efficient than heat-only boilers [19] and they may lead

to a mitigation of CO₂ emissions and primary energy use [20]. There is a lot of research about micro CHP:s, discussing both regulation [21] and technology. A lot of work has been performed regarding optimisation of micro CHP:s, for example about heat dumping and thermal energy storage [22] and optimal sizing of residential CHP-systems regarding costs and operating time [23]. It is for example shown that an operation optimisation leads to cost reduction and is neither heat-led nor electricity-led [24]. As a method to eliminate the effects of bottlenecks, the CHP operation however needs to be heat-led. Alternative types of micro CHP:s are also investigated, such as fuel cell CHP:s [25] and biomass fuelled CHP:s [26]. Micro CHP:s are most common in countries like Germany and the UK with favorable regulatory framework for such installations [27].

Heat pumps is another heat source that may work as LHS. Large heat pumps for district heating are increasingly popular and are described as an important part of the next generation's district heating, to for example balance renewable electricity [4], [28]. Studies in both Denmark and the Netherlands have shown that there are a lot of low-grade heat sources available for heat pumps delivering heat to the DH network [29], [30]. Lund and Persson describe that 99 % of the district heating networks in Denmark have access to this type of heat sources [29]. Although there are a lot of low-grade energy available there are still some problems associated with the use of heat pumps in DH networks. The efficiency of the heat pumps is lower when higher temperature outputs are required [31]. This problem may be somewhat counteracted by using heat pumps in series [32] or by a heat pump system that has several compression stages [33].

TES (local supply/consumer flow management)

Instead of LHS, thermal energy storage (TES) could be used as a technique to avoid bottleneck problems. Accumulators could then be loaded when the DH demand is low and unloaded when the demand is high. This would lead to a more even external heat demand curve in the affected area and thus lower maximum flows and a better system performance [34]. TES is also an important component in enabling more renewable DH sources [35] and taking care of excess electricity from for example wind or solar power [36]. Another thing TES are used for is as a way to economically and environmentally optimise district heating networks supplied by heat from CHP:s [37]. By using TES, the heat demand and the heat production may also be partly decoupled, which will lead to a possibility to produce more electricity when it is economically viable and also to a displacement of more carbon intensive peak heat boilers [38].

DSM (consumer flow management)

Another way to address bottlenecks in DH networks is to use demand side management (DSM), in this paper defined as external control of DH consumers' heat use. During times with a large heat demand, such as mornings or evenings [39], the space heating in buildings in an area with bottleneck problems may be controlled and set to a lower level. This will not be much noticed by the inhabitants, especially not in heavy concrete buildings, as heat is stored in the building envelope [40]. The effect on the DH network is that the heat demand curve is levelled out and the peak heat load is reduced [41]. This may reduce or eliminate the bottleneck problem, as the maximum flow is decreased.

There is a Swedish company called NODA Intelligent Systems AB that helps DH companies perform DSM in their DH networks. Results from tests and investigations show that this system helps the consumers decrease their energy use and thus their energy costs. The DH companies on the other hand are given the possibility to handle flow and capacity problems in different parts of the DH network better, which among other advantages enables more expansion of the DH network. Up to 50 % of a building's DH demand can be reduced without impact on the indoor climate [42], [43].

Another way to achieve lower energy demand among consumers and thus decreased flow and pressure loss in pipes is improved energy efficiency. This may be achieved by for example building refurbishment measures, which is also needed among the buildings in Sweden in order to achieve the EU 2030 climate goals. Studies have shown a possible reduction of the DH demand by around 20-45 % [44], [45] and that a reduction of 12-17 % may be cost effective 2050 [45]. The level of cost effectiveness depends on the district heating system and how much the buildings are refurbished. Improved energy efficiency also makes way for lower temperatures in the DH network [46].

Fault elimination in substations (consumer flow management)

Bottlenecks might also be eliminated if all consumer substations worked perfectly. The substation and heat system performance at the consumers are very important parameters for the function of the DH network because the temperature difference in the substations affects the flow which affects the pressure drop in the pipes. A large part of the Swedish DH substations are not working optimally which means that there is a big potential in fixing faulty heating systems and substations. And as the most common problem is low average annual temperature difference, fixing faulty substations could have a positive effect on bottleneck problems [47]. With the fairly new ability to collect

hourly data from DH consumers, district heating companies also have a better tool to identify consumers with high return temperatures [48].

The best performing substation investigated in [47] had an annual temperature difference of 55 °C, which means that this is possible to perform with available technique. There are also examples of DH companies demanding that the return temperature from new buildings should be at highest 30 °C at all times, which means that this also should be possible to achieve [14]. An optimised DH network with low return temperatures and well-functioning substations is furthermore very important for the introduction of LTDH [49].

RESULTS

The results from the survey to the DH companies are based on the 89 DH network representatives that responded. 67 of those stated that they have or have had problems with bottlenecks in the DH network. This corresponds to 75 % of the answers. Swedish DH networks do not have very large bottleneck problems currently even if there are problems in many of them (see Figure 1). In the same figure, 1 means no bottleneck problems at all and 5 means very large bottleneck problems.

Figure 2 shows the most common causes for bottleneck problems in Swedish DH networks. It can be seen that expansion constitutes over 50 % of the total causes. Expansion means expansion of the DH network beyond the bottleneck pipe. Densification of the DH network, which means that more consumers are added to existing DH areas, is the second most common cause for bottleneck problems. Interconnection is the third most common cause and means that two or more DH networks were interconnected. Common causes among the non-specified other causes for bottleneck problems were changes in the production, exceptional events such as reparation of pipes and an under-dimensioned DH network from the beginning.

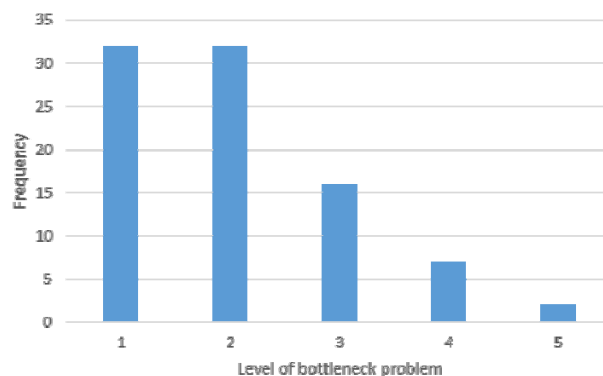


Figure 1. Perceived current problems in DH networks.

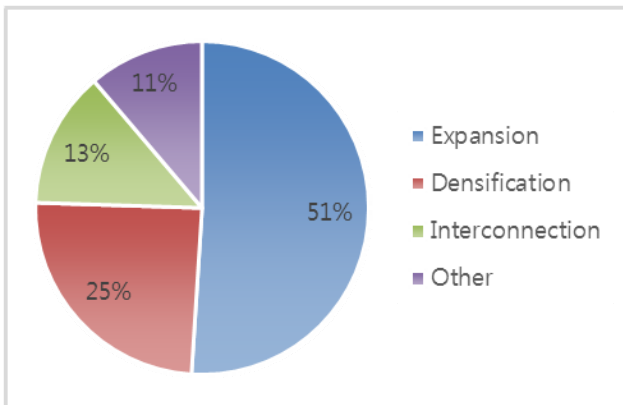


Figure 2. Reasons for bottleneck problems as percentage of total reasons in the survey answers.

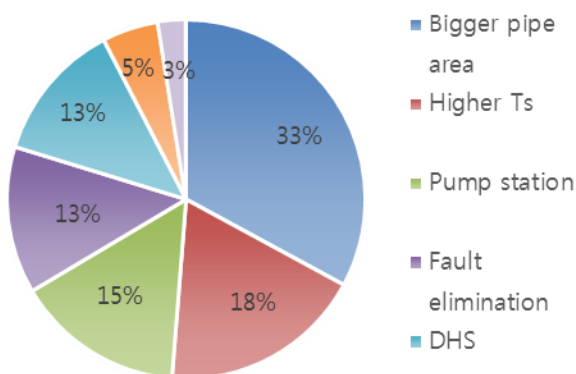


Figure 3. Methods for bottleneck elimination as percentage of total methods in the survey answers.

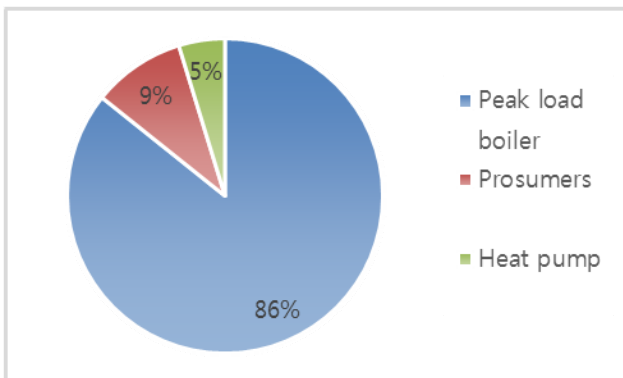


Figure 4. Percentages of type of LHS used to counteract bottlenecks.

Figure 3 shows which methods that are used for bottleneck elimination. It can be seen that the most usual method is to install a bigger pipe area, followed by a higher supply temperature. A new pump station, fault elimination and LHS are also used techniques, while DSM is a less used alternative and TES is not used at all. The category “other” comprises a change

of business models to one supporting lower return temperatures and building a ring structure in the network.

Figure 4 shows which kind of LHS that is used in the DH networks in which LHS has been used as a bottleneck elimination method. It can be seen that the most common method by far is the peak load boiler, with 86 %. Heat pumps have a share of 9 % and prosumers have a share of 5 %.

ANALYSIS

The result from the survey shows that there are different causes for bottlenecks. One conclusion that nevertheless may be drawn is that it is important to plan for potential expansions of and changes in the DH network early, to avoid future bottleneck problems.

The most popular method for bottleneck elimination is a bigger pipe area. This measure is conventional and works because it reduces the pipe velocity. New pipes and their installation may however be expensive. With the recent development towards the 4th generation of district heating with lower supply temperatures, the effect of bigger pipe areas could also be eliminated by the increased flow demand if the return temperatures are not lowered the same amount as the supply temperatures.

The desired lower temperatures of 4GDH are also directly contradictory to the second most used technique to eliminate bottlenecks – a higher supply temperature. A periodically raised supply temperature may however be advantageous to avoid higher costs of pipes, as shown in the literature study. But this could also prevent the possible use of cheaper polymer pipes.

More pumping is a frequently used, conventional bottleneck elimination method that also works, even if it might be more inefficient together with potential future higher flow demands due to a lower supply temperature. The inefficiency depends on the exponential relationship between the pressure losses in a pipe and the flow velocity. One solution to this could be to use more decentralised pumps to decrease the pumping electricity demand. Furthermore, the overall DH network exergetic efficiency may increase when heat losses are minimized and a higher flow is allowed, according to the literature study. Pumps are however expensive and need maintenance and service.

Elimination of faults and inefficiency among substations is something the whole DH network benefits from, even if this is not one of the most frequently used techniques. A better functioning DH network with lower return temperatures is also something that makes LTDH possible and more efficient. This measure is easier to perform with more and better data about the DH network available, which is something that is

becoming more available. This together with the possibility to simulate DH networks makes it easier to identify the most important consumers for the functioning of the DH network and address those first. This measure is thus probably something that will be more common in the future.

The use of LHS at the moment mostly consists of peak heat boilers, even if prosumers and heat pumps also are present. In the future, it should be possible to use more small scale CHP:s and heat pumps. This would be advantageous for the system due to their higher efficiency. Both these techniques are however often more expensive than peak heat boilers and also have some regulatory problems related to the coupling to the electricity market. For prosumers there are also probably some obstacles to overcome before they will be more common, for example their lower efficiency with higher supply temperatures and control issues.

DSM is a method that is not very common at the moment but with modern control, regulation techniques and products such as NODA, this method is a promising, cost effective method to solve bottleneck problems that probably will become more common in the future.

It is indicated when looking at the bottleneck elimination categories that bottleneck problems traditionally are seen as distribution problems, since 'increased distribution capacity', includes the three most used techniques. The techniques in the other categories, 'local supply' and 'consumer flow management', are however also used and are probably going to be more used in the future. This suggests that the view of bottleneck problems is changing to include the whole district heating system, including production, distribution and consumption.

DISCUSSION

The results in this study may be used by district heating planners and district heating companies, as it shows in which situations it is extra important to pay attention to potential upcoming bottleneck problems. It also shows the variety of methods available to solve bottleneck problems. A lot of the measures could also be used to solve other problems or accomplish other goals in DH networks. A lower return temperature may for example also create an overall better functioning DH network and DSM could decrease the need of peak heat production. Some methods are probably also more suitable in different situations. A bigger pipe could for example be better if the DH network is believed to or planned to expand even more beyond the bottleneck, as the bigger pipe area then allows for this, whereas a lower return temperature from the substations probably often is a good measure to take in most situations as the heat supplied from the production units then is more efficiently used.

The results may have been affected by the fact that not all asked DH companies answered the survey. For example, maybe only the companies with experience of and thus interest in bottleneck problems answered. This particular possibility would however not affect the picture of the measures actually used. And as 67 % of the asked DH companies answered the survey, the results hopefully reflects the reality relatively well.

Future studies may include more thorough studies of the individual measures, including real case studies showing the actual outcome of the measure in DH networks. Simulation studies could be a complement to show the theoretical results and economical evaluations could help evaluate the different measures in different situations.

CONCLUSION

Different ways to eliminate bottleneck problems in DH networks were studied. Bottleneck problems are defined as problems with too low dp due to pipes with too small diameters. A literature review of different measures was performed, as well as a survey about bottleneck problems among Swedish district heating companies. The researched measures were higher supply temperature, bigger pipe area, more pumping power, local heat supply, thermal energy storages, demand side management and fault elimination. Of the 131 asked companies, 89 responded and of those, 75 % perceived that they had or have had bottleneck problems. The most common causes for the problems were expansion or densification of the DH network. The most used methods to eliminate them were a bigger pipe area, a higher supply temperature and more pumping power. Local heat supply and fault elimination were also somewhat common techniques. Of the local heat supply, 86 % consisted of peak heat boilers. The main conclusion drawn from this is that it is important to plan for future settlements when developing the DH network to avoid bottleneck problems and that there are possible better and cheaper solutions to bottleneck problems beside the conventional ones that may become more used in the future, with more data and better technique available.

ACKNOWLEDGEMENT

The work presented in this paper was performed with support from E.ON Värme Sverige AB.

REFERENCES

- [1] H. Li och S. Svendsen, "Energy and exergy analysis of low temperature district heating network," *Energy*, vol. 45, nr 1, pp. 237-246, 2012.
- [2] Swedish energy agency, "Energy in Sweden - Facts and Figures 2016 available now," 18 02 2016. [Online]. Available: <http://www.energimyndigheten.se/en/news/2016/e>

- nergy-in-sweden---facts-and-figures-2016-available-now/. [Used 14 03 2016].
- [3] M. Köfinger, D. Basciotti, R. Schmidt, E. Meissner, C. Doczekal och A. Giovannini, "Low temperature district heating in Austria: Energetic, ecologic and economic comparison of four case studies," Energy, 2016.
- [4] H. Lund, S. Werner, R. Wiltshire, S. Svendsen, J. E. Thorsen, F. Hvelplund och B. Vad Mathiesen, "4th Generation District Heating (4GDH): Integrating smart thermal grids into future sustainable energy systems," Energy, vol. 68, pp. 1-11, 2014.
- [5] L. Brand, A. Calvén, J. Englund, H. Landersjön och P. Lauenburg, "Smart district heating networks – A simulation study of prosumers' impact on technical parameters in distribution networks," Applied Energy, vol. 129, pp. 69-48, 2014.
- [6] H. I. Tol och S. Svendsen, "Effects of boosting the supply temperature on pipe dimensions of low-energy district heating networks: A case study in Gladsaxe, Denmark," Energy and Buildings, vol. 88, pp. 324-334, 2015.
- [7] R. Lund och S. Mohammadi, "Choice of insulation standard for pipe networks in 4th generation district heating systems," Applied Thermal Engineering, vol. 98, p. 256–264, 2016.
- [8] Berge, C.-E. Hagentoft och B. Adl-Zarrabi, "Field measurements on a district heating pipe with vacuum insulation panels," Renewable Energy, vol. 87, nr 3, pp. 1130-1138, 2016.
- [9] Dalla Rosa, H. Li och S. Svendsen, "Method for optimal design of pipes for low-energy district heating, with focus on heat losses," Energy.
- [10] T. Nussbaumer och S. Thalmann, "Influence of system design on heat distribution costs in district heating," Energy, vol. 101, pp. 496-505, 2016.
- [11] Ljubenko, A. Poredoš, T. Morosuk och G. Tsatsaronis, "Performance Analysis of a District Heating System," Energies, vol. 6, pp. 1298-1313, 2013.
- [12] E. Guelpa, C. Toro, A. Sciacovelli, R. Melli, E. Sciubba och V. Verda, "Optimal operation of large district heating networks through fast fluid-dynamic simulation," Energy, vol. 102, p. 586–595, 2016.
- [13] X. Sheng och D. Lin, "Energy saving analyses on the reconstruction project in district heating system with distributed variable speed pumps," Applied Thermal Engineering, 2016.
- [14] L. Brange, J. Englund och P. Lauenburg, "Prosumers in district heating networks – A Swedish case study," Applied Energy, vol. 164, p. 492–500, 2016.
- [15] L. Brange, Technical and Environmental Analysis of Prosumers in District Heating Networks, Lund: Tryckeriet E-huset, 2015.
- [16] Paulus och P. Papillon, "Substations for decentralized solar district heating: design, performance and energy cost," Energy Procedia, vol. 48, p. 1076 – 1085, 2014.
- [17] D. Pietra, F. Zanghirella och G. Puglisi, "An evaluation of distributed solar thermal "net metering" in small-scale district heating systems," Energy Procedia, vol. 78, p. 1859 – 1864, 2015.
- [18] H. Wang, R. Lahdelma, X. Wang, W. Jiao, C. Zhu och P. Zou, "Analysis of the location for peak heating in CHP based combined district heating systems," Applied Thermal Engineering, vol. 87, p. 402–411, 2015.
- [19] N. Markides, "The role of pumped and waste heat technologies in a high-efficiency sustainable energy future for the UK," Applied Thermal Engineering, vol. 53, nr 2, p. 197–209, 2013.
- [20] Merkel, R. McKenna och W. Fichtner, "Optimisation of the capacity and the dispatch of decentralised micro-CHP systems: A case study for the UK," Applied Energy, vol. 140, p. 120–134, 2015.
- [21] N. Andersen och H. Lund, "New CHP partnerships offering balancing of fluctuating renewable electricity productions," Journal of Cleaner Production, vol. 15, nr 3, p. 288–293, 2007.
- [22] L. Mongibello, N. Bianco, M. Caliano och G. Graditi, "Influence of heat dumping on the operation of residential micro-CHP systems," Applied Energy, vol. 160, pp. 206-220, 2015.
- [23] H. Ren, W. Gao och Y. Ruan, "Optimal sizing for residential CHP system," Applied Thermal Engineering, vol. 28, p. 514–523, 2008.
- [24] Shaneb, P. Taylor och G. Coates, "Optimal online operation of residential CHP systems using linear programming," Energy and Buildings, vol. 44, pp. 17-25, 2012.
- [25] S. Pellegrino, A. Lanzini och P. Leone, "Techno-economic and policy requirements for the market-entry of the fuel cell micro-CHP system in the residential sector," Applied Energy, vol. 143, p. 370–382, 2015.

- [26] L. Dong, H. Liu och S. Riffat, "Development of small-scale and micro-scale biomass-fuelled CHP systems – A literature review," *Applied Thermal Engineering*, vol. 29, nr 11-12, p. 2119–2126, 2009.
- [27] González-Pino, E. Pérez-Iribarrena, A. Campos-Celador, J. Las-Heras-Casas och J. Sala, "Influence of the regulation framework on the feasibility of a Stirling engine-based residential micro-CHP installation," *Energy*, vol. 84, p. 575–588, 2015.
- [28] D. Lauka, J. Gusca och D. Blumberga, "Heat Pumps Integration Trends in District Heating Networks of the Baltic States," *Procedia Computer Science*, nr 52, p. 835 – 842, 2015.
- [29] R. Lund och U. Persson, "Mapping of potential heat sources for heat pumps for district heating in Denmark," *Energy*, 2016.
- [30] Ajah, A. Mesbah, J. Grievink, P. Herder, P. Falcao och S. Wennekes, "On the robustness, effectiveness and reliability of chemical and mechanical heat pumps for low-temperature heat source district heating: A comparative simulation-based analysis and evaluation," *Energy*, vol. 33, pp. 908-929, 2008.
- [31] L. Brand, P. Lauenburg och J. Englund, "District heating combined with decentralised heat supply in Hyllie, Malmö," i *The 14th International Symposium on DH and Cooling*, Stockholm, 2014.
- [32] Y.-J. Baik, M. Kim, K.-C. Chang, Y.-S. Lee och H.-S. Ra, "Potential to enhance performance of seawater-source heat pump by series operation," *Renewable Energy*, vol. 65, pp. 236-244, 201.
- [33] Kwon, D. Cha och C. Park, "Performance evaluation of a two-stage compression heat pump system for district heating using waste energy," *Energy*, vol. 57, p. 375–381, 2013.
- [34] L. F. Cabeza och E. Oró, "7 – Thermal energy storage for renewable heating and cooling systems," i *Renewable Heating and Cooling*, Lleida, 2016, p. 139–179.
- [35] D. Čulig-Tokić, G. Krajačić, B. Doračić, B. Vad Mathiesen, R. Krklec och J. Møller Larsen, "Comparative analysis of the district heating systems of two towns in Croatia and Denmark," *Energy*, vol. 92, nr 3, p. 435–443, 2015.
- [36] Bachmaier, S. Narmsara, J.-B. Eggers och S. Herkel, "Spatial Distribution of Thermal Energy Storage Systems in Urban Areas Connected to District Heating for Grid Balancing," *Energy Procedia*, vol. 73, pp. 3-11, 2015.
- [37] Bachmaier, S. Narmsara, J.-B. Eggers och S. Herkel, "Spatial Distribution of Thermal Energy Storage Systems in Urban Areas Connected to District Heating for Grid Balancing," *Energy Procedia*, vol. 73, pp. 3-11, 2015.
- [38] Christidis, C. Koch, L. Pottel och G. Tsatsaronis, "The contribution of heat storage to the profitable operation of combined heat and power plants in liberalized electricity markets," *Energy*, vol. 41, nr 1, pp. 75-82, 2012.
- [39] H. Gadd och S. Werner, "Heat load patterns in district heating substations," *Applied Energy*.
- [40] Kensby, A. Trüschel och J.-O. Dalenbäck, "Potential of residential buildings as thermal energy storage in district heating systems – Results from a pilot test," *Applied Energy*, vol. 137, pp. 773-781, 2015.
- [41] H. Li och S. Jia Wang, "Load Management in District Heating Operation," *Energy Procedia*, vol. 75, pp. 1202-1207, 2015.
- [42] Wernstedt, P. Davidsson och C. Johansson, "Demand Side Management in District Heating Systems," i *The 6th International Conference on Autonomous Agents and Multiagent Systems*, Honolulu, Hawaii, 2007.
- [43] Jönsson, "Special Report: It's time to release the energy," *Horizon 2020 Projects*, Brussels, 2016.
- [44] T. Lidberg, T. Olofsson och L. Trygg, "System impact of energy efficient building refurbishment within a district heated region," *Energy*, vol. 106, pp. 45-53, 2016.
- [45] E. Zvingilaite och O. Balyk, "Heat savings in buildings in a 100% renewable heat and power system in Denmark with different shares of district heating," *Energy and Buildings*, vol. 82, p. 173–186, 2014.
- [46] M. Brand och S. Svendsen, "Renewable-based low-temperature district heating for existing buildings in various stages of refurbishment," *Energy*, vol. 62, p. 311–319, 2013.
- [47] Gadd och S. Werner, "Fault detection in district heating substations," *Applied Energy*, vol. 157, pp. 51-59, 2015.
- [48] Gadd och S. Werner, "Heat load patterns in district heating substations," *Applied Energy*, vol. 108, pp. 176-183, 2013.
- [49] X. Yang, H. Li och S. Svendsen, "Decentralized substations for low-temperature district heating with no Legionella risk, and low return temperatures," *Energy*, 2016.

ECONOMICALLY OPTIMAL HEAT SUPPLY TO LOW ENERGY BUILDING AREAS

Akram Fakhri Sandvall¹, Erik O Ahlgren¹, Tomas Ekvall²

¹ Energy Systems Technology, Division of Energy Technology, Department of Energy and Environment, Chalmers University of Technology, SE-412 96 Gothenburg, Sweden

² Swedish Environmental Research Institute (IVL), SE- 400 14 Gothenburg, Sweden

Keywords: *Low temperature district heating, energy system modelling, TIMES, passive houses*

ABSTRACT

European Directives and Swedish national goals aim at increasing buildings' energy efficiency. The construction of low energy building (LEB) areas in Sweden has increasingly attracted attention due to national support. Compared to conventional buildings, LEBs require little space heating during the cold seasons. Still, there are various options for supply of the required heating. Thus, this study aims at comparing the long-term system cost of three heat supply options to a hypothetical LEB area assumed to be located close to an urban area: an "individual" (i.e. separate heat supply), an "on-site" (i.e. local district heating (DH) system) and a "large heat network" (i.e. heat production in a nearby DH system and transmission to the LEB area). A dynamic approach is applied allowing the heat supply system to develop with time, and an energy system model being able to account for the interactions between the building, heat and power sectors, is utilised for the calculations. Two climate policy scenarios are applied to address the uncertainty in future energy prices etc. A systematic sensitivity analysis is designed to investigate the threshold for cost-effectiveness of the large heat network option compared to the other two options. The sensitivity analysis takes into account different combinations of three key parameters: plot ratio of the LEB areas, specification of nearby DH, and distance between LEB area and nearby DH system. The results show, for most of the tested combinations and under both scenarios, that heat supply from the nearby DH system has the lowest system cost if the distance to this system is no more than 2 km, because of the low-cost sources of heat available in the large DH system. A local DH system is more cost-effective than individual heating of buildings even in a LEB area, if it is densely built.

INTRODUCTION

The building sector accounts for 40 % of the total energy consumption and 36 % of carbon dioxide (CO₂) emissions in the European Union [1]. The European Commission has passed two Directives - the 2010 Energy Performance of Buildings Directive and the 2012 Energy Efficiency Directive - aiming at reducing buildings energy consumption. In Sweden, the residential and service sector accounted for 38 % of

the total final energy use, 144 TWh, in 2011. About 60% of this was used for space heating and to provide hot tap water [2]. The national goal is to reduce the total energy use per unit of area in residential and commercial buildings by 20 % to 2020 and by 50 % to 2050 compared to the 1995 level [3]. The development of buildings with very low energy use (i.e., at least 50 % lower than the present requirements; see [4]) is supported by the Swedish Energy Agency, which aims at promoting energy efficient new construction and renovation [3]. Consequently, the buildings in some of the new residential areas are built based on low energy buildings (LEB) standards. These buildings require little space heating even during the cold seasons.

There are generally three options to supply heat to new LEB areas within or near urban areas: an "individual", an "on-site" and a "large heat network" option, assuming that there is a district heating (DH) system in the urban area. The "individual" option means that each building is provided with a separate heat production technology to meet its heat demand. The "on-site" option implies heat supply by a small local district heating (DH) system within the LEB area, including a centralized heat production unit and a distribution network for heat distribution to each building. Similar to the "on-site" option, the "large heat network" option also includes a distribution network within the LEB area while the heat is produced in the DH system of the urban area and transmitted to the LEB area by a transmission pipeline.

In Sweden, DH has developed substantially since the 1960's and today accounts for over 60% of the heat market in the residential and service sectors [5]. Due to ongoing urbanisation, LEB areas are often built within or in the vicinity of a city or town, and thus there is the possibility of DH heat supply to the LEB areas. However, this option seems often not to be preferred implying that opportunities associated with large DH systems might be missed: the greater efficiency of energy conversion in large-scale heat production plants, co-generation of heat and electricity, and the use of excess heat from industrial processes, waste incineration or thermal power plants. Four parameters that could discourage investments in the large heat network include: low heat demand of LEB areas leading to large heat losses [5], high investment cost of construction of DH transmission and distribution

pipelines [6, 7], business strategy disagreements between building and energy companies [8] and fossil fuel use in the DH production.

The impacts of different heat supply options to LEBs have been assessed by studying a single building [9, 10]. Since such assessments do not include the full systems effects of simultaneously implementing heat supply options at a greater scale, sub-optimization could occur if the conclusions from such studies are implemented in areas with many LEBs.

Studies at the national level (e.g., [11-13]) represented the existing building stock in Sweden and applied various energy efficiency measures to the buildings to assess energy system impacts of different heat supply options with a long-term perspective. They also investigated trade-offs between heat supply options and energy efficiency measures by minimizing the total system cost. In these studies the local conditions, of great importance for optimal heat supply, were partially ignored since the buildings were represented in an aggregate way.

The environmental and economic impacts of heat supply options in LEB areas have also been assessed at the local level. The connection of 20,000 new energy efficient apartments to an existing DH system led only to a small increase of DH demand while it contributed to levelling of the annual DH demand profile [14]. The study excluded changes in the DH system (e.g. forward temperature reduction in the DH network) that could occur due to low heat demand of the apartments. An even more recent study compared energy system impacts of on-site and individual heat supply options in a new building area in which half of the buildings are built as LEB. The area, located in mid-Sweden, would be occupied by 10,000 inhabitants by 2025 [8]. The study excluded an assessment of a heat connection between the new building area and its close-by town.

Decisions on economically optimal heat supply to LEB areas require comprehensive knowledge. Due to the different heat supply options and the dynamics of the systems and fuel costs, a long-term system approach taking into account the dynamics and the interactions between the heat, electricity and buildings energy systems is needed to acquire the necessary knowledge.

The aim of this study is to find the threshold of the techno-economic optimal heat supply to the presented LEB area in a systematic way. The approach is based on widened system boundaries including not only the LEB area but also the assumed nearby city DH system in the assessment. This allows for a comparison of the three heat supply options. A dynamic approach is applied, implying that the heat and electricity systems are allowed to develop with time during the studied time period.

METHOD

The study is carried out based on a hypothetical case study, scenario analysis, and dynamic energy system modelling. The case study is inspired by a real LEB area and its nearby town DH system. Two scenarios are designed corresponding to long-term carbon emissions charges. A dynamic energy system model, including the heat sector and part of the electricity and building sector, is built and used for calculations.

Assuming heat demand inelasticity, the objective function of the model is the cost minimization of one of the following four modes over the entire model time horizon, 2014 – 2052, when revenues for selling electricity at exogenously assumed prices are also taken into account:

- Individual heat supply in the LEB area (i.e. individual)
- DH supply to the LEB area (i.e. on-site)
- DH supply to the town
- DH supply to the town and LEB area

For each of these modes and each scenario, the model generates future energy system developments and calculates the associated system costs discounted to the year 2014 with an annual discount rate of 5%. While the system cost of the individual and on-site options is directly calculated by the model, the system cost of the large heat network option is obtained by inserting the model results in equation (1):

$$\text{System cost}_{(\text{Large heat network})} = \text{system cost}_{(\text{DH supplied to town and LEB area})} - \text{system cost}_{(\text{DH supplied to town})} \quad (1)$$

In order to be able to draw a general conclusion of the results of the study, a systematic sensitivity analysis is used to illustrate the scale effects on the assumptions of the case study. The systematic sensitivity analysis also allows for the investigation of the threshold for cost-effectiveness of the large heat network option compared to the other two options. In the sensitivity analysis three key parameters: the plot ratio (i.e. the ratio between the heated area and the associated land area [15]) of the LEB area, the distance between the LEB area and its nearby city/town, and the scale and characteristics of the nearby city DH system, are one at a time varied to represent a wide range of LEB areas.

Case study

Since the heat demand profile, the linear heat density and the plot ratio of residential areas differs and also the characteristics of DH systems varies depending on local conditions in terms of fuel use and heat production technology, the assessment is carried out in the form of a hypothetical case study. The choice of a hypothetical case allows us, while using real information, to investigate different heat supply options without limiting our assessment to the characteristics of an existing heat supply in the area.

The hypothetical case study is inspired by a real LEB area, hereafter Area, which is located in the suburb of a small town, hereafter Town, in the Halland County in west Sweden. Area consists of 26 single family houses, four small apartment buildings, six terraced houses, a nursing home for elderly people with 64 apartments and commercial buildings [17], corresponding to the total heated area of 15,300 m², the heat density (i.e. the ratio between the heat demand and the associated land area [15]) of 27.2 MJ/m² and the plot ratio of 0.15 [18]. In our study Area is selected as a starting point since all the buildings were designed and built based on LEB requirements (< 45 kWh/m²/year [17]). The total annual heat demand in Area, including space heating and hot tap water demand, accounts for approx. 756 MWh (2720 GJ) [18, 19]. The annual heat demand is unevenly distributed over the year. For the 26 single family houses, while the peak load lasts one month, the base load lasts six months. In addition, the corresponding demand in the peak load is 35% higher than the subsequent month.

An existing local DH system in Town annually supplies 105 GWh of heat. The heat demand is annually increasing by approximately 4 GWh due to the Town DH network expansion. The DH system is today based on a biomass combined heat and power (CHP) plant, biomass heat only boilers (HOB), oil HOBs and a heat pump [20]. Given an assumption of a linear development, a heat demand of 165 GWh is expected by 2050. In our study, as a starting point, the distance between Area and the Town DH network is assumed to be zero.

The systematic sensitivity analysis includes various combinations of the following parameters:

- The plot ratio of Area is increased by about 5 times (PT-5A) and 9 times (PT-9A). The plot ratios have been chosen based on the common range of plot ratios (i.e. 0.05- 2) [21] in Sweden.
- The small Town DH system is replaced by one medium and one large DH system which each owns specific characteristics in terms of DH technologies and fuel use.
- The distance between Area and Town DH system is varied from zero to 1 km, 2 km and 3 km.

The LEB area, PT-5A (plot-ratio of 0.73), is inspired by a real LEB area located within the Falkenberg town in the Halland County in Sweden. The area consists of four multi-family buildings with the total heated area and specific heat demand of 10208 m² and 36.7 kWh/m²/year, respectively [15]. In order to make the PT-5A area comparable to Area in terms of the total annual heat demand (i.e. about twice as the one in Area), the number of buildings in PT-5A is increased by three times while the plot ratio is kept constant. Thus,

in this study the total annual heat demand in PT- 5A is equal to 4041 GJ.

The low energy building area, PT-9A (plot-ratio of 1.3), is inspired by a real LEB area located within the Munich City in Germany. The area consists of 13 multi-family buildings with the total heated area of and specific heat demand of 28550 m² and 62 kWh/m²/year, respectively. The measured annual heat demand in PT-9A is equal to 6267 GJ [15] (i.e. about three time as the one in Area).

The medium DH system is based on a biomass HOB, an oil HOB, an electric boiler, a coal CHP, Oil CHPs, municipal solid waste (MSW) CHPs and a biomass CHP with a total heat demand of 1312 GWh [22]. The large DH system is based on biomass HOBs, oil HOBs, natural gas (NG) HOBs, industrial excess heat, heat pumps, electric boiler, NG CHPs, a biomass CHP and MSW CHP with a total heat demand of 3177 GWh [23].

Policy scenarios

Two policy scenarios represent possible future development of energy markets and climate policies; 450PPM and BAU, corresponding to the 450 ppm and New Policies scenarios of International Energy Agency (IEA) World Energy Outlook (WEO) [24]. The 450PPM scenario represents ambitious climate policies in line with the Paris Agreement aiming at limiting global warming to below 2°C [25]. However, the less ambitious scenario, BAU, represents broad policy commitments and plans that had been announced by countries before the Paris agreement, including national pledges to reduce greenhouse gas emissions and plans to phase out fossil fuel subsidies. In each of the policy scenarios, fossil fuel prices and CO₂ charges are consistent and correspond to the 450 ppm and New Policies scenario, respectively, of IEA WEO (Table 1).

In addition to the CO₂ charge, both scenarios include a subsidy supporting renewable electricity generation until 2030. The subsidy level is constant, at 20 €/MWh_{electricity} until 2020, in line with historical values of tradable green certificates in Sweden. Subsequently, it is assumed that the high CO₂ charge provide sufficient support for renewable electricity. Thus the subsidy level linearly declines and reaches to zero in 2030 (**Table 1**).

In the 450PPM scenario, wood chips prices correspond to the regional/local marginal prices of forest residues until 2030. After that, it is assumed that with increasing CO₂ charges competition for biomass between different energy sectors creates an international biomass market leading to higher biomass prices. However, in the BAU scenario with lower climate ambitions, wood chips prices are assumed to equal production costs and are thus remain constant (**Table 1**).

Electricity prices are calculated based on the assumptions that the variable cost of the marginal technology (i.e. sum of fuel cost, CO₂ charge and variable operation and maintenance cost) determines the electricity price. They are scenario dependent since the price setting technology depends on the CO₂ charge. The calculations are based on a selection of various coal and natural gas thermal power plants. The variable cost of marginal technology is assumed to set the electricity price for each time period and time slice. The carbon capture and storage (CCS) technology is assumed to be available after 2040. The cost of CCS increases the electricity price by 1.5 and 1.4 times in coal and natural gas technologies, respectively [26]. **Table 1** presents the results of the electricity price calculations.

Model

For the purpose of this study a local TIMES (The Integrated MARKAL [27] -EFOM [28] System) model, TIMES_UH (Urban Heating), was developed and applied. A TIMES model [6, 29, 30] is a partial equilibrium optimization model which can be used to optimize energy systems over a short to long-term horizon. The TIMES modelling framework was developed by IEA Implementing Agreement Energy Technology System Analysis Program (ETSAP). The TIMES model is driven by demand and based on a perfect-foresight, linear programming bottom-up approach, where the objective function minimizes the total system cost. The studied energy system is represented, in the model, by different technologies that are connected by flows of commodities. Each technology is described by its input and output commodities, efficiency, availability, costs and environmental impacts, whereas each commodity is described by which technologies it can be produced or consumed, and its availability, extraction or import cost and demand.

The TIMES_UH model covers the time between 2014 and 2052 divided into 10 time periods with shorter lengths in the beginning (two one year; 2014 and 2015 and one two years; 2016-2017) and longer lengths from 2018 (5 years). Each year has been divided into eight time slices, representing day and night in four different seasons. The seasons are: summer (6 months), spring/ fall (3 months), winter (2 months) and cold winter (1 month). Days last 8 hours, 8 hours, 12 hours and 16 hours during winter, cold winter, intermediate and summer, respectively. The model includes two regions; Area and Town. In Area, the duration curve of the DH demand and the individual heat demand for each building type are defined for the each time slice.

Table 1. Summary of input data for the 450PPM and BAU scenarios.

	Unit	450PPM	BAU
		2014/2020/ 2030/2040/ 2050	2014/2020/ 2030/2040/ 2050
Policy tools			
CO₂ charge	€/tonne	16.9/25.2/6 8.4/110/15 3	16.9/14.4/2 3.8/33.5/43
Renewable electricity subsidy	€/MWh	20/20/0/0/0	20/20/0/0/0
Energy prices/costs			
Natural gas	€/MWh	28.7/28.3/25 .1/22/18.5	28.7/29.2/30 .2/32/33
Fuel oil, light	€/MWh	64.2/64.7/61 .8/58/54.9	64.2/66.2/70 /75/80
Fuel oil, heavy	€/MWh	41.6/42/39.8 /37.2/34.6	41.6/43.1/46 /50/53.5
Coal	€/MWh	8.8/8.9/7.6/6 /4	8.8/9.4/9.7/9 .7/9.7
Bio-oil	€/MWh	42/44.5/53.9 /62.5/71.5	42/42.6/47.7 /53.9/59.5
Wood chips	€/MWh	20/20/20/40. 5/55	20
Bio pellets	€/MWh	35/44/50/59 /78	35/41/45/50 /53
Excess heat	€/MWh	0.56	0.56
MSW	€/MWh	-14.5	-14.5
Electricity			
Winter cold (1 month)	€/MWh	55.2/62.9/98 /122.2/74.4	55.2/54.6/63 .8/72.5/80.9
Winter (2 months)	€/MWh	54.3/61.4/93 .2/122.2/74. 4	54.3/53.7/62 .1/70/77.6
Spring and fall (3 months)	€/MWh	51.3/57.9/73 .1/80/74.4	51.3/50.8/57 /60.8/67.5
Summer (6 months)	€/MWh	51.3/64.2/73 .1/80/74.4	51.3/50.8/63 .2/61.4/67.8

The existing DH production in Town is represented in detail, including technologies, fuels input, capacities, efficiencies, lifetimes, availabilities, heat to electricity ratios (only for combined heat and power (CHP) plants), and operation and maintenance costs. The DH distribution network in Town is in the model represented with its seasonal efficiency.

Table 2. Main model input assumptions regarding DH technologies in the LEB areas, Town and the medium and large DH systems, based on [31-32].

Technology (Heat capacity)	Parameter	Unit	Value
Combined heat and power plants (Electricity capacity)			
Biomass CHP (0.6 MW-100 MW)	Efficiency Electricity (Total)	-	0.25 - 0.46 (1.03 - 1.05)
	Specific investment cost	[k€/kW _{Electricity}]	1.37 - 7.0
	Total O&M cost	[% of inv. cost/year]	0.7 - 3
[€/MWh _{electricity}]		3.2 (only belongs to 70 MW - 100MW)	
MSW CHP (20.5 MW-28.5 MW)	Efficiency Electricity (Total)	-	0.26 (0.97)
	Total O&M cost	[k€/kW _{Electricity}]	0.08
NGCC CHP (10 MW - 400 MW)	Efficiency Electricity (Total)	-	0.48 - 0.58 (0.9 - 1.0)
	Specific investment cost	[k€/kW _{Electricity}]	0.82 - 1.5
	Total O&M cost	[€/MWh _{electricity}]	2.5
NGGTCHP (5 MW - 125 MW)	Efficiency Electricity (Total)	-	0.42-0.5 (0.82-0.92)
	Specific investment cost	[k€/kW _{Electricity}]	0.46-1.2
	Total O&M cost	[€/MWh _{electricity}]	3.4-7

From 2015 investment options for DH supply technologies in Area and Town (**Table 2 and Table 3**), DH transmission pipeline between Area and Town (**Table 4**) and DH distribution network (**Table 5**) and individual heat production technologies (**Table 6**) in Area are included in the model. All investment options for DH technologies and individual heat production technologies in Area and Town can only made at discrete capacity levels. Thus, these investment options change the linear model into an integer programming model (IP).

Table 3. Main model input assumptions regarding DH technologies in the LEB areas, Town and the medium and large DH systems, based on [26, 31, 32].

Technology (Heat capacity)	Parameter	Unit	Value
Heat plants (Heat capacity)			
Biomass HOB (0.5 MW-50 MW)	Total efficiency	-	1.08
	Specific investment cost	[k€/kW _{heat}]	0.17-1.3
	Total O&M cost	[% of inv. cost/year]	6.7 (only belongs to 50MW)
[€/MWh _{heat}]		5.4	
Oil, Natural gas and Bio-oil HOB (0.5 MW-20 MW)	Total efficiency	-	0.97
	Specific investment cost	[k€/kW _{heat}]	0.061-0.13
	Total O&M cost	[% of inv. cost/year]	0.05-2.0
Heat pump (0.5 MW-10 MW)	Coefficient of performance (COP)	-	3.7
	Specific investment cost	[k€/kW _{heat}]	0.49-1.1
	Total O&M cost	[% of inv. cost/year]	0.7
Solar collector (0.5 MWh/m²/yr)	Specific investment cost	[k€/m ²]	0.23/0.17
	Variable O&M cost	[€/MWh _{heat}]	0.57

Table 4. Assumptions for the LTDH transmission pipelines (55/25 °C) to Area, PT-5A and PT-9A.

	Transmission efficiency ^[33] , [35]	Specific investment cost ^[34]	Fixed O&M cost
	Summer/ Spring& fall / Winter/ Cold winter	[€/kW/km]	[% of inv. cost/year]
Area	0.65-0.68/	1073	0.7
PT-5A	0.87-0.92/	600	0.5
PT-9A	0.93-0.97/ 0.97-0.99	180	0.6

Table 5. Characteristics and costs of LTDH network (55/25 °C) in Area, PT-5A and PT-9A.

	Distribution efficiency ^[15] , [33]	Spec. inv. Cost ^[34] *	Fixed O&M cost	Variable O&M cost
	Summer/ Spring& fall/ Winter/Cold winter	[€/kW]	[% of inv. cost/ yr]	[€/MWh _{heat}]
Area	0.63/0.85/0.9/ 0.915	2830	1.2	3.57
PT-5A	0.68/0.92/0.97/ 0.99	870	2.6	-
PT-9A	0.68/0.92/0.97/ 0.99	431	3	-

* The investment cost includes both the cost of DH network and substations. A lifetime of 50 years is assumed for the investments in the DH networks. The linear heat density is equal to 1.29 GJ/m/yr, 3.9 GJ/m/yr and 5 GJ/m/yr in Area, PT-5A and PT-9A, respectively.

RESULTS

The model results of the main case together with the systematic sensitivity analysis for each combination of LEB and DH system together with the LEB area – DH system distance specifies the thresholds for the most cost-effective heat supply option during the entire studied time period.

Figure 1 illustrates that the large heat network with zero transmission distance has the lowest system cost in both scenarios independent of the plot ratio of the LEB area or the DH system scale.

For the main case, i.e. zero distance between Area and Town, the on-site option has a much higher system cost. While the cost of the DH distribution network is equal in the on-site and the large heat network with zero distance, the cost of DH supply in the large heat network option is smaller than the on-site option. The reason is that in the large heat network option the existing and newly-invested DH supply technologies in Town just slightly increase their production to supply heat to Area, whereas in the on-site option new investments are needed to produce any DH (**Figure 1**).

In the individual option the model only invests in pellet boilers for the all types of buildings, except for the small apartment buildings, in both scenarios. For the apartment buildings in the 450PPM, the model invests in pellet boilers in 2015 and in electric boilers in 2050 whereas in the BAU scenario it only invests in electric boilers. The specific heat supply cost for the individual option in the 450PPM (BAU) scenario is equal to 15.2 (14.3) €/GJ.

Table 6. Main model input assumptions regarding individual heat supply options in Area, PT-5A and PT-9A from single family houses to large multi-family buildings, based on [36].

Technology	Parameter	Unit	Value	
Heat capacity				
	Bio pellet boiler (6 kW - 1000 kW)	Efficiency	-	0.8-0.85
		Specific investment cost	[k€/kW _{heat}]	0.2 - 0.63
		Fixed O&M cost	[% of inv. cost/year]	0.2 - 3
Variable O&M cost		[€/MWh _{heat}]	36	
Heat Pump - brine to water (5 kW – 300 kW)	Coefficient of performance (COP)	-	3.3	
	Specific investment cost	[k€/kW _{heat}]	1.77-4	
	Fixed O&M cost	[% of inv. cost/year]	2 - 22.6	
Electric boiler (5 kW- 400 kW)	Efficiency	-	1	
	Specific investment cost	[k€/kW _{heat}]	0.7-0.8	
	Fixed O&M cost	[% of inv. cost/year]	1.6 - 15	

The sensitivity analysis shows that, compared to our starting point where the Area is within Town in the 450 PPM (BAU) scenario, the system cost of the large heat network option decreases by 6 (9) % and 21 (23) % when Area is located within medium DH and large DH systems, respectively (Figure 1). One reason for the lower cost is the availability of low cost heat sources in these DH systems, i.e. MSW CHP in the medium DH system, and MSW CHP and industrial excess heat in the large DH system. The other reason for the lower cost is the possibility of investments in larger heat production plants with lower specific investment cost in these DH systems. Consequently, the low-cost heat supply in these DH systems allows for increased distances between the LEB urban areas, i.e. extending the length of the DH transmission pipeline, up to 1 km and 2 km in the BAU and 450PPM scenarios, respectively, while still supplying heat to Area with lower system cost compared to the individual option.

The model results also show that the cost-efficient DH transmission pipeline length is scenario dependent. In the 450PPM scenario, with higher CO₂ charges, the cost-efficient pipeline distance is extended compared to the BAU scenario.

In similarity to Area, the large heat network option represents the lowest system cost in PT-5A under the 450PPM (BAU) scenario. The system cost of the large heat network is 44 (40) % and 50 (45) % less than the on-site and individual options, respectively, when PT-5A is located within Town.

Likewise, in PT-9A in the 450PPM (BAU) scenario the large heat network option represents the lowest system cost among the three heat supply options. The system cost of the large heat network is 36 (34) % and 58 (55) % less than the on-site and individual options, respectively, when PT-9A is located within Town.

The individual option has the highest system cost among the three heat supply options for PT-9A. The specific heat supply cost for the individual option in the 450PPM (BAU) scenario is equal to 16.4 (15.5) €/GJ.

DISCUSSION

In this study the DH systems were assumed to be LTDH in the LEB areas. The reason is that the concept of LTDH has been recently developed and was successfully tested to overcome the shortcomings of current DH systems, i.e. high heat losses, in areas with low plot ratio and low linear heat density. If instead of LTDH, the current DH system were used, the on-site and large network options would be more costly, especially in LEB areas with plot ratio equal to or less than 0.15.

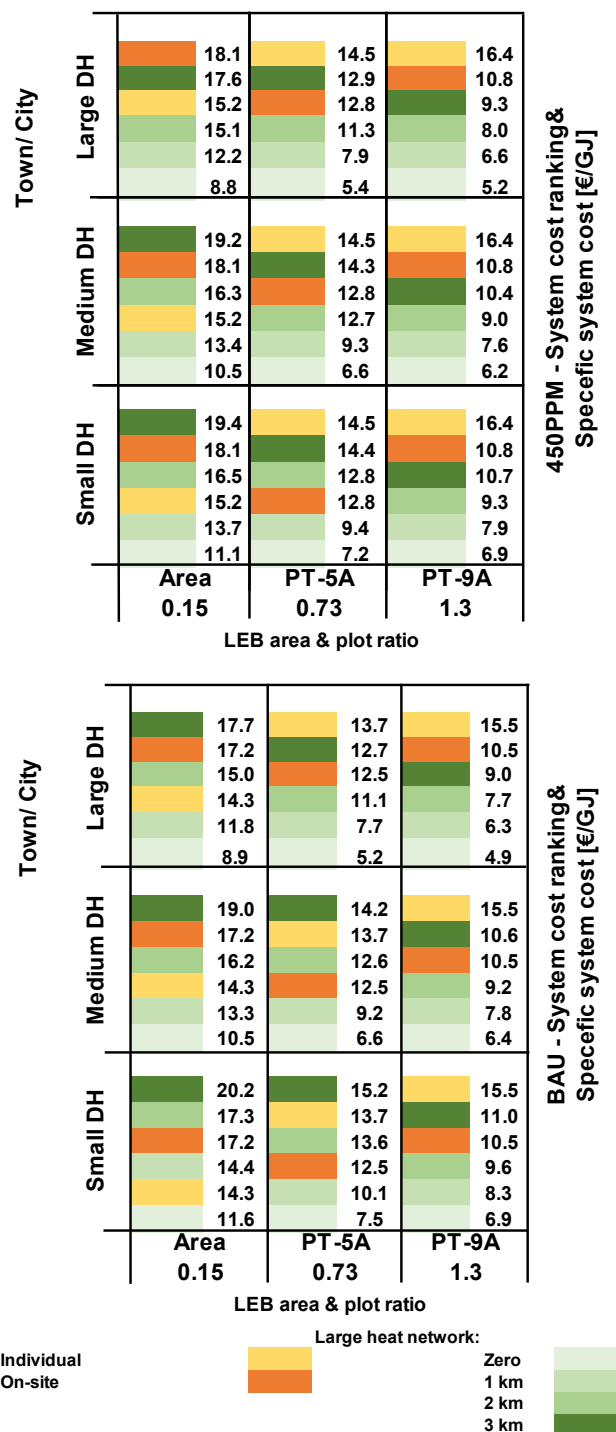


Figure 1. Comparison of different heat supply options to LEB areas and the threshold for the cost-effectiveness of large heat networks.

In PT-5A the specific heat supply cost for the individual option in the 450PPM (BAU) scenario is equal to 14.5 (13.7) €/GJ.

In this study real life data on total heat demand, heat demand of each building and relative location of buildings were used to represent the LEB areas. This was done both due to lack of reported values and since the use of real life data allowed for achieving higher

precision in the design of the LEB area heat supply options and, thus, in better estimation of the DH distribution network cost. This also included DH distribution costs based on LTDH distribution specifications. The results illustrate, due to the importance of the DH distribution network costs, that good cost estimates of these are critical for the cost-efficiency assessment.

CONCLUSIONS

From the model results, in the long-term the economically optimal heat supply to LEB areas within or near urban areas in Sweden seems to be the large heat network option, i.e. heat production in the DH system of the urban area and transmission to the LEB area by a pipeline. However, in order to keep the large heat network an economically optimal option, these LEB areas cannot be built far from the urban area. Under strict climate policies, corresponding to high CO₂ charges, for the LEB areas with a plot ratio less than one and a linear heat density less than 4 GJ/m/yr the large heat network is the economically optimal option if the area is within a couple of km from a large DH system or within one km from a small or medium DH system. However, for the LEB area with a plot ratio above one and a linear heat density above 4 GJ/m/yr the large heat network is the optimal option even if the area is built up to 3 km away from the urban area.

Since a large share of the system cost of the large heat network option is due to the DH distribution and transmission costs, these results are rather robust with respect to climate policies. Under less ambitious climate policies, i.e. low level of CO₂ charges, in some cases the distance between the LEB area and the urban area need to be one km shorter compared to the ones with the high CO₂ charges.

The model results show that with increasing scale of the urban DH system the large heat network is still the economically optimal option at increasing transmission distances. A major characteristic of large DH systems in Sweden is the existence of low cost DH production technologies, e.g. MSW CHP and industrial excess heat in these systems. As the heat supply cost in the large heat network option decreases, the large heat network option can be economically competitive despite the higher DH transmission cost associated with longer transmission distances.

From the model results, for areas with a plot ratio above 0.73, the individual option is the least economically viable one, independent of the future climate policy scenarios. This indicates that a small local DH system is more economically efficient than individual heating solutions even in LEB areas, if they are sufficiently densely built.

ACKNOWLEDGEMENT

The study was financed by the Swedish Energy Agency and the multi-partner 4DH project, led by Aalborg University. The authors also would like to acknowledge Professor Sven Werner for valuable discussions and Eksta Bostads AB for supporting the project with real life data.

REFERENCES

- [1] EC, Eurostat Database, European commission (EC): Brussels, Belgium (2015).
- [2] SEA, Energy in Sweden 2013. Swedish Energy Agency: Eskilstuna, Sweden (2014).
- [3] SEA, Energy Efficiency Policies and Measures in Sweden. Swedish Energy Agency: Eskilstuna, Sweden (2012).
- [4] Valik, J. and A. Petersson, Boverket's mandatory provisions on the amendment to the Board's building regulations (2011:6) –mandatory provisions and general recommendations (Boverkets föreskrifter om ändring i verkets byggregler (2011:6) - föreskrifter och allmänna råd), in Boverkets författningssamling. Boverket (2015).
- [5] Frederiksen, S. and S. Werner, District Heating and Cooling. 1st ed., Studentlitteratur AB, Lund (2013).
- [6] Karlsson, K.B., S. Petrovic, and R. Næraa, Heat supply planning for the ecological housing community Munksøgård, Proceedings of the 10th Conference on Sustainable Development of Energy, Water and Environment Systems (SDEWES 2015).
- [7] Reidhav, C. and S. Werner, Profitability of sparse district heating. Applied Energy, 2008. 85(9): p. 867-877.
- [8] Sahlström, C., O. Crondahl, and S. Hesse, The heating system of Nydal, An individual or a common solution? Teknisk- naturvetenskaplig fakultet, UTH-enheten. Uppsala University: Uppsala, Sweden (2015).
- [9] Marszal, A.J., et al., On-site or off-site renewable energy supply options? Life cycle cost analysis of a Net Zero Energy Building in Denmark. Renewable Energy, 2012. 44(0): p. 154-165.
- [10] Milan, C., C. Bojesen, and M.P. Nielsen, A cost optimization model for 100% renewable residential energy supply systems. Energy, 2012. 48(1): p. 118-127.
- [11] Mata, T., A. Sasic Kalagasidis, and F. Johnsson, Energy usage and technical potential for energy saving measures in the Swedish residential building stock. Energy Policy, 2013. 55: p. 404-414.

- [12] Mata, É., A. Sasic Kalagasidis, and F. Johnsson, Cost-effective retrofitting of Swedish residential buildings: effects of energy price developments and discount rates. *Energy Efficiency*, 2014.
- [13] Nässén, J. and J. Holmberg, On the potential trade-offs between energy supply and end-use technologies for residential heating. *Energy Policy*, 2013. 59: p. 470-480.
- [14] Åberg, M., System Effects of Improved Energy Efficiency in Swedish District-Heating Buildings, in *Engineering Sciences*. Uppsala University: Uppsala 2014.
- [15] Dalla Rosa, A., H. Li, S. Svendsen and S. Werner, et al., Toward 4th Generation District Heating: Experience and Potential of Low-Temperature District Heating, in Annex X Final report. IEA DHC/CHP (2014).
- [16] Nielsen, C.K., M. Haegermark, and J.O. Dalenbäck. Analysis of a novel solar district heating. in *EuroSUN 2014*. Aix-les-Bains (France): International Solar Energy Society (2014).
- [17] Christensson, N. Eksta Bostads AB, Kungsbacka, Sweden (2015).
- [18] Jimmefors, H. and J. Östberg, Energy performance and indoor climate investigations in the passive house residential area Vallda Heberg, in Department of Civil and Environmental Engineering. Chalmers University of Technology: Gothenburg (2014).
- [19] Fahlén, E., et al., Vallda Heberg- The largest passive house area in Sweden with renewable energy (Vallda Heberg – Sveriges största passivhusområde med förnybar energi), in LÅGAN Report, Gothenburg, Sweden (2014).
- [20] Statkraft. Kungsbacka District Heating. Available from: <http://www.statkraft.com/energy-sources/Power-plants/Sweden/Kungsbacka/> (accessed 2015-05-20).
- [21] Werner, S. Energy Technology, Halmstad University, Personal communication: Halmstad (2016)
- [22] Difs, K., et al., Biomass gasification opportunities in a district heating system. *Biomass and Bioenergy*, 2010. 34(5): p. 637-651.
- [23] GöteborgEnergi. Environmental reports [Miljörapporter]. 2014; Available from: <http://www.goteborgenergi.se/Privat/Kundservice/Informationsmaterial/Miljorapporter> (accessed 2015-11-02).
- [24] World Energy Outlook 2013. IEA (International Energy Agency): Paris (2013).
- [25] EC. Climate Action, Paris agreement 2015; Available from: http://ec.europa.eu/clima/policies/international/negotiations/future/index_en.htm (accessed 2016-01-12).
- [26] Ingrid Nohlgren, et al., Electricity from new and future plants [El från nya och framtida anläggningar] 14:40, Editor. 2014, Elforsk AB, Swedish Energy Research Centre [Svenska Elföretagens Forsknings- och Utvecklings]: Stockholm (2014).
- [27] Fishbone, L.G. and H. Abilock, MARKAL, A Linear Programming Model for Energy Systems Analysis: Technical Description of the BNL Version. *International Journal of Energy Research*, 1981. 5: p. 353-375.
- [28] Voort, E.v.d., et al., Energy Supply Modelling Package EFOM-12C Mark I, Mathematical description, in EUR-8896. Commission of the European Communities: Louvain-la-Neuve, Cabay (1984)
- [29] ETSAP, Energy Technology Systems Analysis Program. <http://www.etsap.org/index.asp>.
- [30] Gargiulo, M., Getting started with TIMES-VEDA, Version 2.7., Energy Technology Systems Analysis Program (ETSAP) (2009).
- [31] Technology Data for Energy Plants- Generation of Electricity and District Heating, Energy Storage and Energy Carrier Generation and Conversion. Danish Energy Agency and Energinet.dk: Denmark (2012).
- [32] Technology Data for Energy Plants. Danish Energy Agency and Energinet.dk: Copenhagen (2010).
- [33] Li, H. and S. Svendsen, Energy and exergy analysis of low temperature district heating network. *Energy*, 2012. 45(1): p. 237-246.
- [34] Olsen, P.K., et al., A new-low-temperature district heating system for low-energy buildings, in 11th international symposium on district heating and cooling. Reykjavik (2008).
- [35] Li, H. and S. Svendsen, District Heating Network Design and Configuration Optimization with Genetic Algorithm. *Journal of Sustainable Development of Energy, Water and Environment Systems*, 2013. 1(4): p. 291-303.
- [36] Danish Energy Agency and Energinet.dk, Individual Heating Plants and Energy Transport, Technology Data for Energy Plants, Danish Energy Agency and Energinet.dk: Copenhagen (2012).

TECHNO-ECONOMIC ASSESSMENT OF THE IMPACT OF LOW-TEMPERATURE DISTRICT HEATING SUBNETS IN A DISTRICT HEATING NETWORK

J. Castro Flores^{1,2}, J. NW. Chiu¹, B. Lacarrière², V. Martin¹

¹ Royal Institute of Technology, Department of Energy Technology, Stockholm, Sweden

² École des Mines de Nantes, Department of Energy Systems and Environmental Engineering, Nantes, France

Keywords: *District Heating, Low-Temperature, Subnet, Energy Savings, Techno-economic Assessment*

ABSTRACT

The 4th generation Low Temperature District Heating (LTDH) is envisioned as a more efficient and environmentally friendly solution to provide heating services to the building stock. LTDH substations at the distribution level are key components that can be implemented as interfaces between the current and new generation DH grids. Although buildings supplied by LTDH have lower heat demands due to their higher energy efficiency, LTDH also brings potential savings compared to conventional DH technology. This work explores the advantages of connecting LT loads via LTDH substations to a DH network supplied by a Combined Heat and Power (CHP) plant. A techno-economic analysis is performed, through modelling and simulation, in order to evaluate the savings in DH operating costs achieved by LTDH, due to the reduction in return temperature and flows. The savings estimated are related to: (1) the reduction in distribution losses in the return pipe; and (2) lower pumping power needs. Additional earnings are assessed from: (3) improved Power-to-Heat ratio for electricity production; and (4) enhanced heat recovery through Flue Gas Condensation (FGC). The savings per kWh of delivered heat are estimated on the network level as a function of the penetration percentage of the LT load over the conventional DH network. Key outcomes show the trade-offs between the potential savings in operating costs and the reduction in heat demand due to building renovation: relative losses in this scenario are maintained at 13.1% compared to an expected 15.3% with conventional DH; also relative pumping power demand decreases. In other words, the costs of supplying heat are lower, even though the total heat supplied is lower. Thus, this study represents a step forward in the understanding of the next generation DH technologies that will shape the future smart energy system.

INTRODUCTION

The district heating technology of today is facing new conditions that challenge the profitability of the DH industry in the future. The existing DH production and distribution networks have been appropriately designed technically and economically for the current level of heat demands. However, due to factors such as new

energy efficiency policies in place, the heat demands in urban areas are expected to gradually decrease in the future [1],[2]. New directives on the construction and refurbishment of buildings define higher requirements of building energy performance for buildings, so the existing DH system may not be as technically and economically effective to cope with a decrease on heat demand and heat density. Thus, the system requires an enhancement to effectively adapt to the new conditions so as to maximize their benefits [3].

The heat demand and linear heat density are two related parameters that determine the profitability of a DH system. However, heat density in the future will decrease due to multiple factors [4],[5], including building renovation and global warming. Consequently relative heat losses are higher, and so, from the supply and distribution perspectives, investment and operating costs increase relative to total heat sales. Since the return of investment in DH systems is based on heat sales which depend on the heat demand over periods of several years, the profitability of new DH networks and/or expansions and refurbishment of the existing ones should be carefully planned and analysed.

The DH industry is thus facing the challenges of lower linear heat density in the existing DH areas on top of servicing newly built energy efficient buildings, whose connection might not be either effective or profitable if the conventional DH technology is used. In light of these issues, the 4th generation Low Temperature District Heating (LTDH) is projected as a solution able to cope with the coming challenges to provide heating services to the building stock in the future. LTDH is characterised by network operating temperatures below 65°C for the forward flow and aiming for 25°C in the return. In [6] the authors have presented a high-level description of LTDH technologies as well as their advantages and challenges.

Due to the lower operating temperatures, LTDH has the potential, among others, to reduce the network distribution heat loss. Lower heat losses then lead to lower temperature drops along the network, thus a lower flow rate is required, and so the pressure drop is also reduced at a given heat demand. This also results in less pumping energy demand [5]. LTDH represents an advantage for DH utilities by keeping relative losses

at margin, and potentially making the connection of low heat density areas economically feasible. Moreover, the DH network coverage could be expanded by servicing more customers with minimum investments.

It is expected that the DH sector will experience a transition period of several decades during which both the conventional DH networks and the LTDH will be operating simultaneously, complementing each other to meet the thermal energy demand of the building stock. Particularly, in countries with a large share of well-established DH systems, LT networks can be integrated to the existing systems as secondary (cascade) networks operating at lower temperatures and pressures. In the longer term, a total penetration of the 4th generation DH technology is the target [1],[6].

Operating temperatures and distribution costs

Nominal and operating network temperatures (supply/return) influence investment and operating costs of the system components. Since production and distribution costs are closely related by these temperatures, they are key factors in the overall system techno-economic design and operation, as well as its optimisation [7].

Regarding heat generation costs, the influence of the supply temperature depends basically on the type of heat generation technology in place. On the other hand, the influence of the return temperature on these costs is usually larger, and it benefits renewable energy systems such as solar and geothermal, heat pumps operation, as well as heat recovery from industrial processes and exhaust gases. Likewise, a lower return temperature enables a higher production capacity of electricity at CHP plants. Concerning heat distribution costs, lower operating temperatures in both, supply and return flows, lead to reduced heat losses. Moreover, a decrease of return temperature (or increase of supply temperature) increases the delivery capacity or heat transport per unit mass of flowing water, thus reducing the flow rate in the distribution network and hence the pressure drop. Assuming the same amount of heat shall be supplied, increasing the temperature difference between the supply and return flows lead to lower pumping costs.

In terms of distribution heat losses and pumping energy, there are until now, limited studies on the impact of end-use energy savings on the existing DH systems. In one study [8] the authors compare the optimisation of a conventional DH scenario to a LTDH so as to minimize losses and pumping energy. Then, on a secondary analysis they considered a heat demand reduction of 20% due to end-user energy savings. In another contribution, a methodology to estimate cost savings and additional production resulting from of lower return temperatures was

described in [9] and summarized in [7]. However, this methodology is applied on existing DH systems with conventional operation without referencing LTDH technology.

The purpose of this paper is to present an approach of a techno-economic assessment of the impact of LTDH subnets in the conventional DH system. This study considers both the impact of the reduction of the return temperature, as well as the demand reduction as a result of the end-user savings due to renovation and LTDH. Furthermore, besides the thermodynamic analysis of the temperatures, distribution heat losses, and pumping power, an economic evaluation of the savings and potential earnings is performed for the scenario of a small network mainly supplied by a CHP plant.

METHODOLOGY

Scenario Description

In this study, we assess the impact of introducing LTDH loads into a conventional DH network from a techno-economic perspective. The studied scenario is developed based on a small Swedish DH network studied in [10] supplied mainly by a CHP plant (two-stage extraction) introducing some simplifications and assumptions on the inputs for practical reasons. The total heat supplied is estimated at 82 GWh in one year, from which 10.6 GWh are distribution losses (13%). The load duration curve in **Fig. 1** depicts the heat production units, their power and operating hours. The heat input to the DH network is driven by a bio-fueled CHP station such that the heat demand drives the electricity production. The LDC shows that the year could be divided in four periods as far as heat production is concerned:

- During the period of low heat demand or no space heating load (3100 hrs/yr), all heat is produced by a heat-only boiler.
- The largest part of the year (4980 hrs/yr) the supply comes from a CHP unit delivering heat to the network at part load, also producing electricity. The FGC unit does not run during this period in order to generate the maximum electricity possible in the CHP unit.
- When CHP reaches full load, the flue gas condensation unit (FGC) starts operation (330 hrs/yr), adding a maximum of 14% heat.
- During the periods of highest load (350 hrs/yr), when both the CHP and the FGC unit are at maximum capacity, an auxiliary oil boiler enters operation.

Assuming a moderate building renovation that allows the use of LTDH, it is assumed that the space heating load is 20% lower, leading to a 15% reduction in total annual heat demand when all buildings in the network have been refurbished.

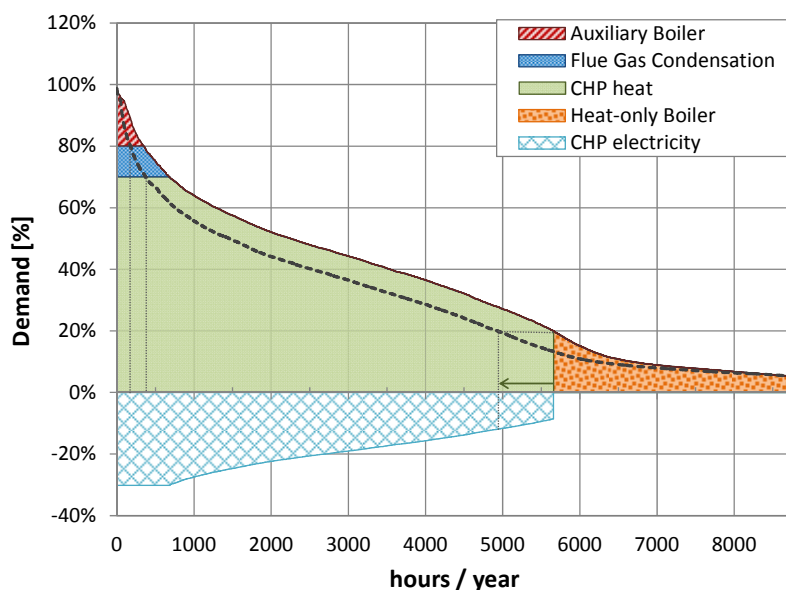


Figure 1. Load duration curve (LDC) and heat production units for the DH network: The LDC shows the DH network is supplied mainly by the CHP plant, with additional heat recovery through flue gas condensation (FGC) and supported by heat only boilers. The dotted line represents the shifted heat load profile occurring when all the network customers have sustained a moderate renovation based on LTDH.

Likewise, necessary to estimate savings and earning are the electricity tariff paid for the pumping work and the electricity market spot price at which the CHP electricity is sold. All prices vary throughout the year, so average values are used for these periods. **Table 1** shows the corresponding costs and prices of the heat production units and electricity.

When several heat production units are operating simultaneously, the marginal cost of heat generation is established by the unit with the highest cost, corresponding to the last produced MWh (the most expensive).

Network & Scenario Modelling

In order to study the temperature profile in an accurate and simplified manner, a representative network branch is modelled. The loads on this single branch

are assumed to be of the same magnitude and regularly distributed along the length of the branch so as to define a constant baseline. Each load represents a subnet coupled by a substation, all with similar load and temperature patterns. The temperature drop along the pipes due to distribution heat losses is neglected.

The supply flow temperature is defined by the heat production unit. The supply mass flow rate is calculated with **Equation (1)** as the addition of the flow rates demanded by the individual substations according to the corresponding loads, plus the make-up water flow required to compensate for heat losses.

$$\dot{m}_{tot} = \sum_1^n \dot{m}_n + \dot{m}_{q_loss} = \sum_1^n \frac{\dot{q}_n}{(h_s - h_{sr})} + \frac{\dot{q}_{loss}}{(h_s - h_r)} \quad (1)$$

Where \dot{m} is the mass flow rate, n the number of

Table 1. Heat Production Units Capacity and Costs

	Maximum Capacity	Marginal Cost of Heat (average)	Electricity Market Spot Price (CHP)	Electricity Tariff (avg.) (Pumping)	Heat Production (baseline scenario)
	MW_{th}	EUR/MWh	EUR/MWh	EUR/MWh	GWh_{th}/yr
Heat-only boiler	5	69	-	59	9.1
CHP (partial load)	17.5	62	22	55	56.8
CHP (full load) + FGC	17.5 + 2.5	62, 10	30	51	7.2 + 0.3
CHP + FGC + Aux. Boiler	17.5 + 2.5 + 5	62, 10, 84	30	51	7.1 + 0.9 + 0.8
Network Total	25	Ref. [11]	Ref. [12]	Ref. [13]	82.1

Table 1.: The characteristics of the heat generation units in place for the standard case are shown. The marginal cost of heat generation depends on each production unit, being the highest for the auxiliary oil boiler. Electricity prices and tariffs vary slightly from summer to winter, so average values are used for each period.

substations, \dot{q} the load per substation, and h the enthalpy of the flowing water. The subscripts are s for supply, r for return, and sr for the substation return.

The return mass flow rate is equal to the supply, but the temperature profile varies depending on the individual substations return temperature and flow. In order to calculate the local temperatures of the return flow a mixing flow equation is used. The temperature is then calculated from the local enthalpy values as in **Equation (2)**:

$$\dot{m}_{tot} h_{tot} = \sum_1^n \dot{m}_n h_n \quad (2)$$

Distribution heat losses

In DH networks, the magnitude of distribution heat losses commonly have a rather uniform distribution throughout the year, particularly for the return pipe whose temperature has comparatively less variation than the supply pipe [14]. For the latter, losses are slightly lower in summer compared to winter due to the lower supply temperature set by the utility during the non-heating season. Therefore, as absolute losses are rather uniform, relative losses are the highest during summertime when loads are the lowest.

Typically, for a piping type of two buried pipes (or conduits), the ratio of losses from the supply pipe to the return hold a relation of at least 2:1, i.e. for every kW of heat lost in the return pipe, 2 kW or more are lost in the supply pipe. Hence, the heat losses in the return pipe count up, in average, to a maximum of one third of the total heat loss.

In this study, the distribution losses are calculated for steady-state conditions, and the total heat loss in the network is calculated as the sum of the individual heat losses in each pipe section assuming regularly distributed loads. The heat losses per pipe can be calculated as:

$$q_s = (t_s - t_g) \lambda_{eq_s} \quad (3)$$

$$q_r = (t_r - t_g) \lambda_{eq_r} \quad (4)$$

Where q represents the heat flow from each pipe in W/m, t_s and t_r are the supply and return temperature of the pipes respectively, t_g the undisturbed ground temperature and λ_{eq} the equivalent thermal coefficient in W/m_K. The undisturbed ground temperature is approximated [15] as the average annual air temperature.

In this analysis, the steady-state loss is estimated with a constant average value for thermal resistance; this approach commonly employed yields acceptable results from the engineering point of view. In this case, two values are used: one for the supply pipe and another for the return, in order to account for the dependence on the average supply/return

temperatures: $\lambda_{eq_s} = 0.520$ and $\lambda_{eq_r} = 0.505$, which are within the typical value range of DH piping in northern Europe.

Heat losses are also proportional to the pipe diameters, which are larger near the supply unit or backbone distribution loops, and smaller at the end of branches. In this case, the lambda coefficients used assume an equal average pipe diameter [16]. The total distribution heat losses are calculated using an average representative network branch of 20.5 km length.

Pumping Effort

Pumping work is necessary to circulate the flow from the heat production unit to the customers. Thus, the pumps have to be able to overcome the pressure drop due to friction and keep the differential pressure between the supply and return pipes of the critical customer above the minimum. For a given load, a reduction in the return temperature increases the temperature difference between the supply and return, and so the delivery capacity of the network. Thus, the total energy input required for pumping and its related costs are lower.

In this analysis, the pumping power is calculated using the characteristic curve of an existing pump and determining the power for the different operating points depending on the volumetric flow and head [17]. As variations in pressure drop are neglected, and with a constant pressure difference required at the critical customer, the pressure head is assumed constant.

Additional heat and power generation

Lower return temperatures have a positive effect on cogeneration plants and increase the possible heat recovery from exhaust gases. It also benefits renewable energy systems such as solar and geothermal, as well as heat pumps allowing higher operating efficiencies.

The FGC recovers latent heat of the water vapour content of the exhaust gases from the combustion process. This technology is used to preheat the district heating water before entering the boiler (heat exchanger) resulting in an improvement of the plant efficiency. A lower return temperature increases the cooling capacity of the condenser, so more moisture is condensed and thus more latent heat is recovered from the flue gases.

FGC increases the total heat recovery in a range from 10% to 35% depending on the technology and the fuel characteristics. In this analysis, a maximum value of 14% is used typical for gaseous fuels. Also, in terms of the return temperature, the heat recovery at the FGC unit is assumed to increase 1% over the total heat production per every 5 degree reduction of the return temperature [7].

The economic advantage of the FGC lays on the fact that fuels are priced according to their dry energy content –Low Heating Value (LHV). Therefore, the heat recovered through this technology is virtually ‘free’. For this reason, the marginal cost of heat production of a FGC is very low around 5-10 EUR/MWh compared to the driving CHP plant.

Regarding electricity generation, the return temperature has also an important effect on 2-stage CHP plants where electricity generation is driven by the heat production. The Power-to-Heat ratio, also referred as the *alpha value*, expresses how many MW of electricity are produced per every MW of heat (**Equation 5**). Only heat recovered in the condensers is considered (excluding heat recovery from FGC), and is influenced by various operating parameters, the return temperature being one of them. As the return temperature decreases, the alpha value increases making it possible to generate more electricity from every MW of total heat produced.

$$\alpha = \frac{P_{el}}{P_{th}} \quad (5)$$

Although the alpha value varies slightly throughout the year, a constant average value of 0.43 is selected as baseline and the increase of electricity production is assumed to be 5 kW_{el}/MW_{th} for every 10 degree reduction of the return temperature [7]. Although this amount may not seem significant enough from the energy perspective, from the economic point of view it is valuable due to the electricity sales in a yearly basis.

Description of the DH substations

The DH loads or customers are assumed to be connected to the primary network via individual DH substations. The substations allow hydraulic separation from the main network as well as the operation at different temperature levels. In this analysis, each substation is assumed to operate with conventional DH

temperature programs, and they are gradually replaced by LTDH substations. This replacement occurs at the subnet level assuming large buildings are renovated or secondary networks with a group of customers are refurbished. The various load and temperature dynamics inside the subnets are aggregated in the substation patterns. It is assumed that all substations present similar patterns and only hourly steady-state conditions are simulated.

In order to compare the impact of the LTDH subnets on the primary network, one LTDH substation arrangement is simulated and compared to a conventional substation selected as a reference. The reference substation is based on commercially available equipment [18], suitable for this type of application (a multi-dwelling building with c.a. 50 multi-family households). **Figure 2** shows the schematic of the configurations. In the case of the conventional substation (**Fig. 2a**), the primary DH supply flow goes through the heat exchanger sized for the standard temperature program. The flow leaving the substation on the primary return side is then channelled to join the primary DH return pipe. In the other substation arrangement (**Fig. 2b**), the main DH return and supply flows are mixed in a 3-pipe shunt arrangement that also regulates the flow rate ratio. The mixed stream then enters the primary side of the heat exchanger sized for a temperature program suitable for the LTDH subnet. The substation return flow is then also discharged into the main return pipe, where it is mixed with the return flow at higher temperature.

This substation requires a larger heat exchanger due to the heavier thermal duty, which is in line with the conclusions drawn in [19] for LTDH substations supplying small dwellings. Although the cost of this substation would be higher, it allows a further cooling of the main DH return flow, and the recovery of some of the energy already present in this flow, thus increasing

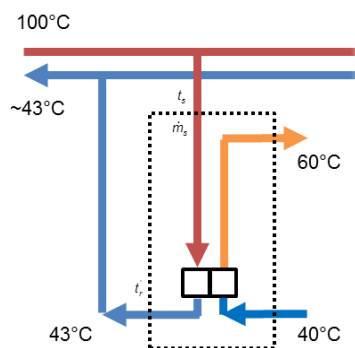


Figure 2a, Conventional DH

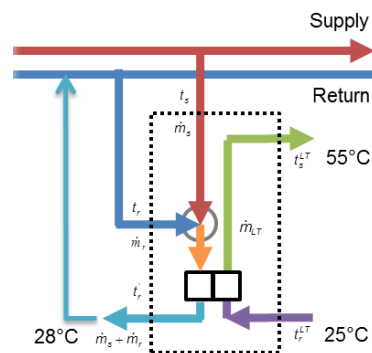


Figure 2b, Mixed-Flow

Figure 2. Schematic of substation arrangements: The flow diagrams and operating temperatures for nominal operation are shown for (a) the conventional substation, the (b) Low-Flow, and (c) Mixed-Flow substation types.

the system efficiency.

To study and compare the performance of the substations described above, a thermodynamic simulation model of each system was developed. A particular toolbox [20] was employed based on Matlab/Simulink, and the numerical models are then solved by the software internal optimization algorithm.

Each substation is designed for a nominal load of 250 kW_{th} that is assumed to occur when the outdoor ambient temperature reaches -20°C. For this study, the outdoor ambient temperature distribution data used correspond to a Typical Meteorological Year (TMY) which is a statistically representative year at the selected location, in this case Stockholm, Sweden. The data are obtained from the uniform meteorological data base Meteonorm [21].

Estimation of savings and additional earnings

The thermodynamic assessment of the network yields as main outputs: the total mass flow rate of the network, the temperature profile of the return pipe of the branch, and the return temperature at the heating plant. The savings and additional earnings are calculated based on the baseline scenario without LTDH. The savings are in terms of heat losses and pumping energy, while the earnings are the additional electricity generation from the CHP and additional heat recovery from the FGC. The total is calculated using the prices from **Table 1**, and **Equation (6)**:

$$S = Q_{los sav} \cdot C_{mch} + E_{pum p sav} \cdot C_{el tariff} - 0.75 \cdot E_{pum p sav} \cdot C_{mch} + E_{CHP} \cdot C_{el spot} + Q_{FGC} \cdot C_{mch} \quad (6)$$

Where Q represents heat saved or produced, E_{pump} the energy saved in the pumps, E_{CHP} the additional electrical energy produced by the CHP; C_{mch} is the

marginal cost of heat production; $C_{el tariff}$, the electricity tariff and $C_{el spot}$, the electricity market spot price. Note that it is assumed that on average 75% of the pumping work is converted into heat, thus the equivalent saved pumping energy has to be produced as heat at the corresponding marginal cost.

RESULTS & DISCUSSION

Heat recovery from the primary return line

The mixed-flow substation (Fig. 2b.) allows heat recovery from the primary return to be used in the LT subnet. In this case, once the substation recovers this energy, the substation return flow is then mixed with the primary return flow.

Initially, an overall analysis at the nominal operating point of the network and substations is performed. **Figure 3a** shows the total energy recovered from the primary return as percentage of the total energy supplied at nominal operation. The maximum achievable for the network is near 5%, and it occurs when the percentage of LTDH is near 58%. After this point, the decrease the primary return temperature is such that adding more LTDH substations don't increase the total heat recovered from this flow.

The previous result is explained as follows: when having several substations one after the other, because of the reduction in the primary return temperature due to the mixed flow, not all substations can recover the same amount of heat (see **Fig. 3b**). Moreover, as the percentage of LTDH substations approaches 100%, the return temperature becomes closer to that of the LT subnets level and thus the possible heat recovery from the primary return is minimal.

However, the potential of energy recovery is also dependent on the original primary return temperature

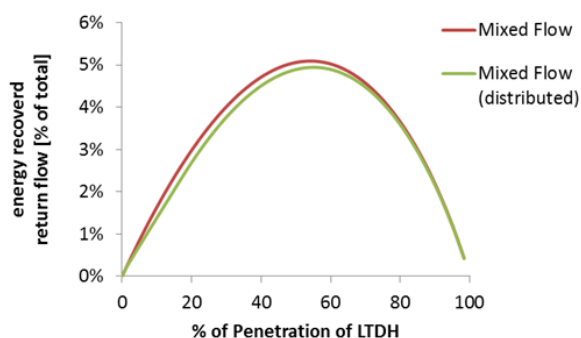


Figure 3a

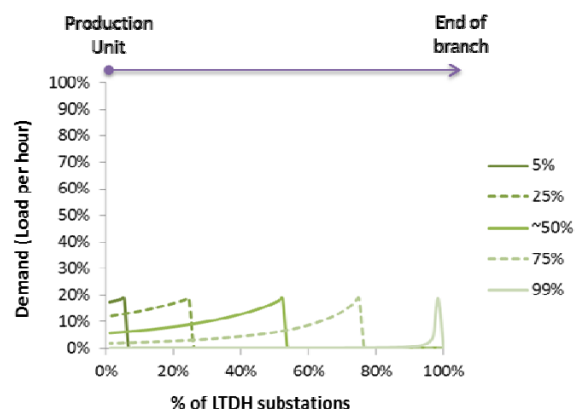


Figure 3b

Figure 3. Energy recovered from the primary return flow: The total energy recovered from the return flow in respect of the total demand as a function of the percentage of LTDH mixed-flow substations. The figure on the left (a) shows the maximum at 58% of LTDH penetration rate. In (b) the areas under the curves represent the recovered energy considering the substations location. The LTDH substations closer to the end of the branch recover more energy due to the higher temperature of the primary return at this point.

Table 2. Heat Production Units and Operating Conditions

	Operating hours	(with 15% demand reduction)	T _{out} (avg)	T _s (avg)	T _r (avg)	L _{Ts} (avg)	L _{Tr} (avg)	Relative Losses
	hr/yr	hr/yr	°C	°C	°C	°C	°C	%
Heat-only boiler	3100	3830	14,9	74,2	49,7	54,8	32,8	34,22
CHP (partial load)	4980	4560	2,2	83,9	44,7	55,7	29,0	11,39
CHP (full load) + FGC	330	195	-7,5	92,6	44,5	56,5	27,4	7,62
CHP + FGC + Aux. Boiler	350	175	-11,3	96,5	46,9	56,3	27,0	6,56
Network (annual)	8760	8760	5,3	81,7	46,3	55,2	30,1	13,05

Table 2.: The operating conditions of the heat production units and the primary and secondary networks are detailed. Relative losses are considerably higher during the periods of low heat demand. The difference in operating hours of the units with higher capacity is due to the building renovation and so the shift in the load duration curve.

and the low return temperature of the subnet. Considering the same low return temperature at the subnet, if the original primary return temperature of the network would be 10 degrees higher (Tr=53°C) it would be possible to recover 10.5% from the primary return, and with 10 degrees more (Tr=63°C) it would be 18%. In all cases, these maximum is reached at 58% of LTDH penetration.

Network Annual Scenario

The influence of the LTDH subnets on the network operation is also assessed in an annual scenario. The mixed-flow substation type that yields lower return temperatures at the heating plant is considered to gradually replace the conventional DH types, so as to benefit the CHP plant operation.

For this evaluation, the input operating parameters in terms of the average values of each corresponding

period are described in **Table 2**. The reduction on the heat demand due to LTDH building renovation modifies the operating hours of each heat production unit (see **Table 2**, and in **Fig. 1** the dotted line).

Distribution heat losses and pumping effort

The first section of these results comprises the impact of the LTDH penetration on the two operating parameters related to distribution costs: heat losses and pumping energy. It is estimated that if this demand reduction would occur at the conventional DH temperature levels, the relative losses would increase from 13% to 15.3%. **Figure 4** compares the relative heat losses as a function of the percentage of LTDH load. We found that, despite the lowered heat demand, the reduction on the operating return temperature keeps the relative heat losses at a similar level instead of increasing, and so the same occurs with their cost

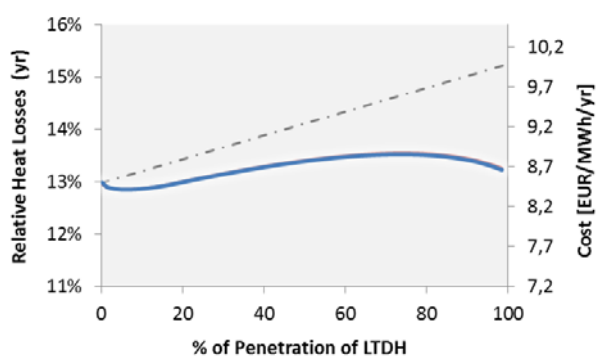


Figure 4. Relative losses as a function of LTDH load percentage: the two curves refer to both axes, the relative losses shown on the left, and the equivalent annual cost on the right. Due to the renovation with LTDH, relative heat losses are kept in a similar level in spite of the total 15% demand reduction. The dotted line represents the increase in relative heat losses assuming the demand reduction occurs with conventional DH temperature levels.

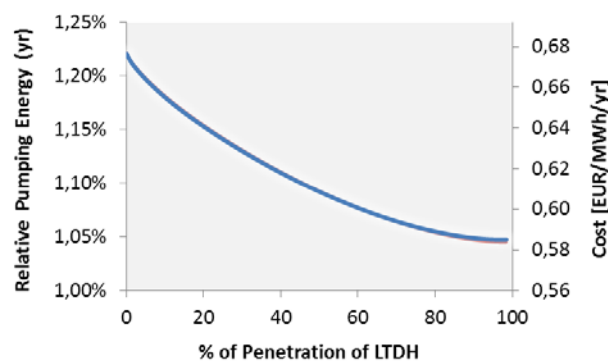


Figure 5. Pumping energy relative to the annual heat demand as a function of LTDH load percentage: the relative pumping energy (left axis) and the corresponding related costs (right axis) decrease due to the LTDH return temperature levels; if the demand reduction due to renovation would occur with the conventional DH temperature levels this figure would yield 1.31% at the total penetration rate; instead with LTDH, it decreases to 1.05%.

per MWh of heat delivered.

This result is similar to that of a previous study [8] where the authors compare the relative heat losses, assuming a 20% annual heat demand reduction, in a conventional DH network compared to a LTDH network. In that study, the authors estimated that the relative losses in conventional DH would increase from 10.9% to 13.1%. Conversely, with the LTDH operation they found that it is possible to maintain the relative heat losses at 11.2% maximum on a yearly basis.

With respect to the pumping effort, we analyse the ratio of energy required for pumping throughout the year to the total heat delivered. The results show that the ratio decreases in spite of the reduction in annual heat demand; and this is due to the increase in delta T caused by the lower return temperature, as well as the decrease in distribution losses. If this demand reduction would occur holding the same temperature levels, the relative pumping power would increase to 1.31% (see Fig. 5).

In absolute terms of savings in distribution heat losses and pumping energy, it is estimated that for a 10 degree drop in the return temperature, there is a reduction of 6.7% in total distribution heat losses and 23% in total pumping energy. This occurs when LTDH penetration would reach 75%. According to previous studies [7], for a 10 degree drop in the return temperature the heat loss reduction expected would be 6%, and the pumping energy would be reduced by 40% approximately. The difference in the latter figure is partly due to the fact that this study considers a constant differential pressure at the heating plant assuming constant pressure drop along the network. Yet, this difference is also partly attributed to the fact that in this study we are considering the variation in the pumps efficiency and curves of already existing equipment: the operating pump efficiency decreases as

the pumped flow is less.

Annual Savings and Additional Earnings

The total savings and additional earnings are calculated using the results from the previous analysis, and taking into consideration the total annual heat delivered. As seen from Fig. 6a, the combined potential earnings and savings increase as the percentage of LTDH also increases. It is possible to conclude that although the annual heat demand decreases due to the renovation, the costs for supplying each MWh of heat also decrease. For percentages below 20% of LTDH there is a steeper slope that is driven by the savings in heat losses as seen from Fig 6b.

It is possible then to consider different points of the curve shown in Fig. 6a. For instance, at 10% penetration of LTDH the total cost reduction would be 19.5 k€/yr distributed as: 68% heat losses, 14% pumping costs, 8% CHP electricity, and 10% FGC heat. This represents 2.8% of the total costs of heat losses of the baseline scenario, achieving a reduction of ~1.5 degrees in the return temperature at the heating plant. Moreover in Sweden, with the green certificate system in place, additional earnings are generated, due to the extra 54.7 MWh_{el}/yr which can be produced by the CHP plant. In a second example: a return temperature drop by 10 degrees (occurring at 75% penetration of LTDH) leads to a total cost reduction of 65.6 k€/yr distributed as: 57% heat losses, 18% pumping costs, 12% CHP electricity, and 13% FGC heat. This represents 9.7% of the total costs of heat losses of the baseline scenario. In this case, 297 MWh_{el}/yr extra are produced by the CHP plant that would become additional earnings from the green certificate system.

With regard to the heat recovery from the primary return flow, the results indicate that a maximum of 4.8% of the total annual heat demand of the whole

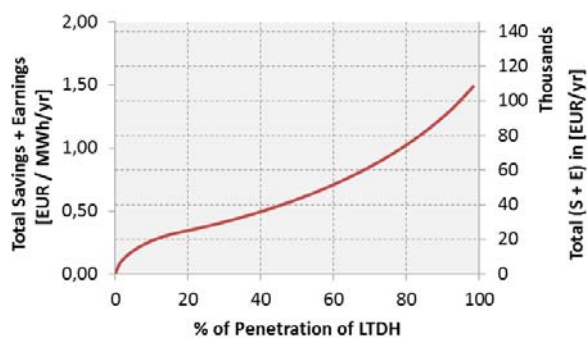


Figure 6a Total Savings & Earnings

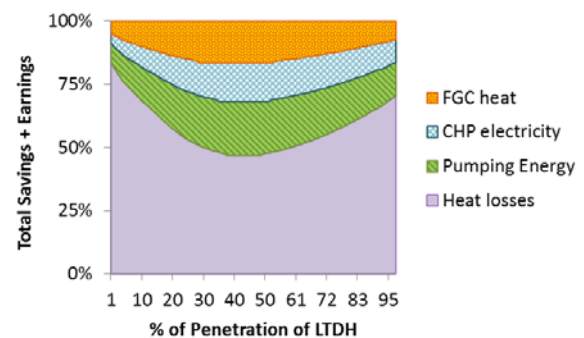


Figure 6b Savings & Earnings Share

Figure 6. Total savings plus earnings as a function of LTDH load percentage: The curve (a) shows a positive relation between savings and the increase of LTDH load. Moreover, the proportion of the contribution of savings and earnings varies depending on the LTDH load percentage (b). It is also noted that more than half of the total amount is given by the savings in heat losses.

network can be reached, when the LTDH load reaches

58% of the total, similar to the case of nominal operation.

Overall Discussion & Outlook

With respect to the decrease in operating hours of the heat production units caused by the future heat demand reduction due to renovation, there are both advantages and drawbacks: on the one hand, it reduces the amount of heat produced by the top oil boiler (with higher marginal cost and more GHG emissions) which is beneficial; on the other hand, it also reduces the operating hours of both the FGC which produces heat at a very low marginal cost, and the CHP, such that less valuable electricity is generated during the year. Nonetheless, in a long term perspective it also means that additional LTDH customers can be connected to the network without causing bottlenecks or increasing peak demands, and thus additional investments can be postponed or avoided.

The substitution of conventional DH loads by LTDH is a process that will take place gradually spanning several decades. Therefore, the utilities will have to adapt to the different conditions and plan their investments carefully. We note that using the mixed-flow substation type can yield interesting advantages for low percentage of LTDH loads. Yet, it would be only recommended for a maximum of 20-50% penetration since it is a more expensive substation type and the benefit of heat recovery from the return flow gradually disappears after reaching the maximum. Thus, after a certain point the same advantages can be achieved by using a low-flow substation type.

A possible alternative in order to use the mixed-flow substation for all loads would be the addition of a third pipe to separate the primary return from the low-temperature return. Nevertheless, due to the higher investment costs the returns might not balance the investment.

The impact of changes in the network operating temperatures can be conflictive for costs reduction. Therefore, a careful evaluation is needed with respect to each specific DH system. The potential savings of the combined measures should be then compared with the respective investment costs or depreciation, such that the most economical alternative can be chosen. Still, in most cases, lowering the network operating temperatures leads to reduced operating costs, and if the investment necessary for achieving these lower temperatures based on LTDH are balanced, an improved economic performance is achieved.

CONCLUSIONS

This study presented a techno-economic assessment of the impact of LTDH subnets in a conventional DH

network considering both reductions in return temperatures and demand. The outcome comprises, besides the technical assessment, an economic estimation of the savings and potential earnings in the defined scenario. The key takeaways of these results are:

- With the lower return temperature, due to the LTDH loads, relative distribution heat losses are maintained at a similar level even though the heat demand is lower.
- Relative pumping power decreases due to the combination of lower return temperatures and lower heat demand.
- For a 10 degree drop in the return temperature, there is a reduction of 6.7% in total distribution heat losses and 23% in total pumping energy.
- With the combination of savings and earnings, despite the demand reduction, the costs for heat supply relative to the total demand still decrease.
- With a 'cascade' use of the primary return flow, a maximum of 5% of the annual heat demand can be recovered from this flow, when LTDH percentage is near 58%.

These results represent a step forward in understanding the advantages and drawbacks of the next generation DH technologies that will shape the future smart energy system.

ACKNOWLEDGEMENTS

The research presented is performed within the framework of the Erasmus Mundus Joint Doctorate SELECT+ 'Environomical Pathways for Sustainable Energy Services' and funded with support from the Education, Audiovisual, and Culture Executive Agency (EACEA) of the European Commission. This publication reflects the views only of the author(s), and the Commission cannot be held responsible for any use which may be made of the information contained therein. The lead author would also like to express his gratitude to the National Council on Science and Technology (CONACYT) of Mexico for providing supplementary funding.

REFERENCES

- [1] DHC+ Technology Platform (2012) DHC Strategic Research Agenda, Euroheat and Power, Brussels, Belgium, March 2012
- [2] A. Hepbasli, (2012) Low exergy (LowEx) heating and cooling systems for sustainable buildings and societies, in *Renewable and Sustainable Energy Reviews*, Volume 16, Issue 1, January 2012, Pages 73-104
- [3] B. Rezaie, M.A. Rosen, (2012) District heating and cooling: Review of technology and potential

- enhancements, in *Applied Energy*, Volume 93, May 2012, Pages 2-10
- [4] I. Andrić, N. Gomes, et. al. (2016) Modeling the long-term effect of climate change on building heat demand: case study on a district level, in *Energy and Buildings*, doi:10.1016/j.enbuild.2016.04.082
- [5] A. Dalla Rosa, J.E. Christensen (2011) Low-energy district heating in energy-efficient building areas, in *Energy*, Volume 36, Issue 12, December 2011, Pages 6890-6899
- [6] H. Lund, S. Werner, et. al. (2014), 4th Generation District Heating (4GDH): Integrating smart thermal grids into future sustainable energy systems. *Energy* 2014;68:1-11
- [7] H. Zinko, (2005) IEA ANNEX VII: Improvement of operational temperature differences in district heating systems, *Senternovem*, Netherlands, March 2005 | 2005:8DHC-05.03
- [8] Y. Xing, A. Bagdanavicius, et. Al. (2012), Low temperature district heating network planning with focus on distribution energy losses. In: *ICAE 2012: Proceedings of the International Conference on Applied Energy*; 2012 July 5-8; Suzhou, China. ICAE2012-A10103
- [9] H. Walleton, (2002) Description of Lava calculus for calculation of district heating network temperature economy, ZW working document, Nyköping, Sweden 2002
- [10] Johansson, P.-O., Jonshagen, K., Genrup, M. (2009), Influence of district heating temperature level on a CHP station. In: *ECOS 2009: Proceedings of the 22nd International Conference on Efficiency, Cost, Optimization, Simulation and Environmental Impact of Energy Systems*; 2009 Aug 31- Sep 3; Foz do Iguaçu, Brazil.
- [11] Swedish Energy Market Inspectorate, "The accounts of district heating companies" [datasheet] – Available at: < <http://ei.se/sv/Fjarrvarme/inrapporterad-data/> > [accessed 04.04.2016].
- [12] NordPool "Elspot prices SE" [datasheet] – Available at: < <http://www.nordpoolspot.com/Market-data1/Elspot/Area-Prices/SE/Monthly/?view=table> > [accessed 04.04.2016].
- [13] Statistics Sweden "Priser på el för industrikunder 2007–" [datasheet] – Available at: < http://www.scb.se/sv_/Hitta-statistik/Statistik-efter-amne/Energi/Prisutvecklingen-inom-energiomradet/Energipriser-pa-naturgas-och-el/24719/24726/Genomsnittspriser-per-halvar-2007/212961/ > [accessed 04.04.2016].
- [14] B. Bøhm (2001) Experimental Determination of Heat Losses from Buried District Heating Pipes in Normal Operation, in *Heat Transfer Engineering*, 22:3, 41-51
- [15] American Society of Heating, Refrigerating and Air-Conditioning Engineers. (2009) ASHRAE Handbook—HVAC Systems and Equipment :: District Heating and Cooling. Atlanta, GA: American Society of Heating, Refrigeration and Air-Conditioning Engineers.
- [16] Vesterlund, J. Sandberg, et. Al. (2013), Evaluation of losses in district heating system, a case study. In: *ECOS 2013: Proceedings of International Conference on Efficiency, Cost, Optimization, Simulation and Environmental Impact of Energy Systems*; 2013 July 16-19; Guilin, China.
- [17] Grundfos, 5TUF13B -2-UL-1/9-P-M-MA-R - 98907334 [datasheet] – Available at: <<http://product-selection.grundfos.com/product-detail.product-detail.html?custid=GMA&productnumber=98907334&qcid=110578220>> [accessed 10.04.2016]
- [18] Alfa Laval, Midi Compact (Swedish market) [datasheet] – Available at: <<http://www.alfalaval.com/solution-finder/products/district-heating-systems/pages/documentation.aspx>> [accessed 08.09.2014].
- [19] J.E. Thorsen, O. Gudmundsson and M. Brand (2014), Performance Specifications for heat exchangers of district heating substations of the future. In: *DHC14: Proceedings of The 14th International Symposium on District Heating and Cooling*; 2014 Sep 7-9; Stockholm, Sweden. Swedish District Heating Association: ISBN 978-91-85775-24-8
- [20] Thermolib [software toolbox], Modeling of thermodynamic systems in Matlab/Simulink – Available at: <<http://www.thermolib.de/>> [accessed 15.04.2016]
- [21] Meteonorm [computer software], Global Meteorological Database – Available at: <<http://meteonorm.com/products/meteonorm-dataset/>> [accessed 12.04.2015]
- [22] S. Frederiksen and S. Werner (2013) District Heating and Cooling, Studentlitteratur AB, Lund, 2013, pp. 586,

TOPIC B:

Resource Efficiency and Environmental Performance



LOW-CARBON AND RESILIENT URBAN DISTRICT IMPLEMENTING A SMART ENERGY NETWORK IN THE TAMACHI STATION NORTH-EAST URBAN RENNAISSANCE PROJECT IN TOKYO

Osamu Kunitomo¹, Masashi Bansai¹, Akinari Takeda², Tomomi Yamamoto², Kenichi Sasajima³

¹ Tokyo Gas Engineering Solutions Co., Ltd.

² Tokyo Gas Co., Ltd.

³ Nihon Sekkei Co., Ltd.

Keywords: Smart Energy Network, Low-Carbon Society, District Energy, Resilient District, Demand Side Management

ABSTRACT

In November 2014, Japan's first "Smart Energy Network", an integrated district energy system featured by both demand-side and supply-side control, was implemented in Tamachi, a district in Minato Ward, metropolitan area in Tokyo.

Several low-carbon technologies contribute to remarkable CO₂ reduction and to maintain a high level of energy resilience including supply to a disaster relief facility of Minato Ward, which has become increasingly important since the Great East Japan Earthquake (March 2013).

The Tamachi Smart Energy Network designed to utilize renewable energy reduce CO₂ emission from the area by use of district thermal, electrical and information network. The latest technologies are adopted in order to achieve ambitious goals. We use not only highly efficient natural gas cogeneration units (fuel cells and gas engines) and the waste heat absorption chillers for air conditioning, but also renewable energy sources such as photovoltaic and unused thermal energy generated from water in underground tunnels. An innovative approach based on ICT is also introduced which controls equipment in energy supply plants and further responsible for the optimal control of equipment on the consuming end.

The target of CO₂ emission reduction is shared among the stakeholders, from the district to be 45% of CO₂ emission of the BAU of 1990 level.

This report describes the outline, the performance evaluation of energy saving/CO₂ deduction items of the Smart Energy Network in Tamachi Station North-east District, and confirm that the Smart Energy Network was constructed and a low-carbon and disaster-resistant city.

1. INTRODUCTION

It is demanded in future city planning to enhance the resilience of the energy infrastructure and to establish a flexible energy demand and supply structure in which the energy demand side and the energy supply side are incorporated as one body, in addition to lowering

carbon emissions through introduction of cogeneration systems (hereinafter referred to as CGS), renewable energies, and so forth, and effective use of energy.

Under these circumstances, the Tokyo Gas Group constructed the Smart Energy Network in Tamachi Station North-east District as one of the ways to supply energy that covers the smart city, and started operation in November 2014.

The Smart Energy Network is a self-supporting and decentralized energy system in which a gas CGS is introduced, the utmost use is made of renewable energies such as sunlight occurring in the region and unused energies such as waste heat from a waste incineration plant, and the generated heat and electric power energies are used on an area-wide basis and optimally through the energy network and information communication technology (ICT) among buildings and regions.

This report describes the outline, the performance evaluation of energy saving/CO₂ deduction items of the Smart Energy Network in Tamachi Station North-east District.

2. OUTLINE

Tamachi Station North-east District is located in the center of Tokyo in Japan. This district is broadly divided into two zones, that is, the "Living base zone (Block I)" in the east-side block, which is mainly being developed by Minato Ward, and the "New urban base zone (Block II)" in the west-side block, which is planned to be developed mainly by Tokyo Gas, and step-by-step development has been carried out. (Figure 1)

In Block I, which was developed in advance, the Smart Energy Network was constructed, which connects, via thermal, electrical and information networks, the central Smart Energy Center serving as the regional energy supply base and the facilities such as "Ward Public Facilities", which is a disaster prevention base in Minato Ward, "Aiiku Hospital", and "Ward Nursery School", and the operation of a "low-carbon and disaster resilient city" was started in cooperation with the government and the private sector, with the target

set at CO₂ reduction in the whole area by 45% (compared to the 1990 level in Minato Ward).

The construction of the Smart Energy Network in new city planning as described above is the first such project in Japan.

The Smart Energy Network in this area aims at optimally controlling the supply and demand and continuously reducing CO₂ in the whole region through construction of thermal, electrical and information networks centered on the Smart Energy Center (hereinafter referred to as the SEC), which is operated by Tokyo Gas Engineering Solutions Corporation, introduction of renewable and unused energies occurring in this region for full-scale use, and connection of the demand side (building side) and the supply side (SEC) via the network. In order to realize such the Smart Energy Network, it is difficult to efficiently operate the network only by improvement of infrastructure in terms of hardware such as "introduction of renewable and unused energy" or "introduction of ICT for connection of the demand and supply sides," and improvement of infrastructure in terms of both hardware and software including "humans" as shown in Figure 2 is important.

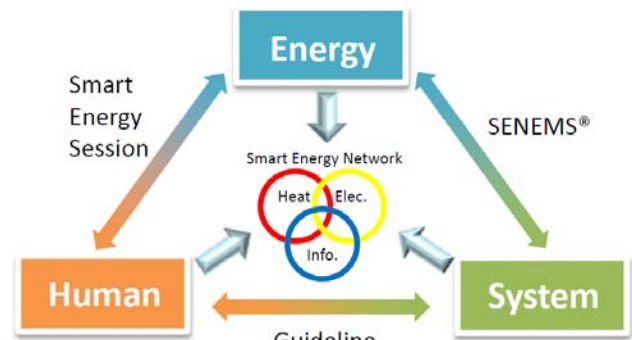


Figure 2. Improvement of Infrastructure of Smart Energy Network [2]

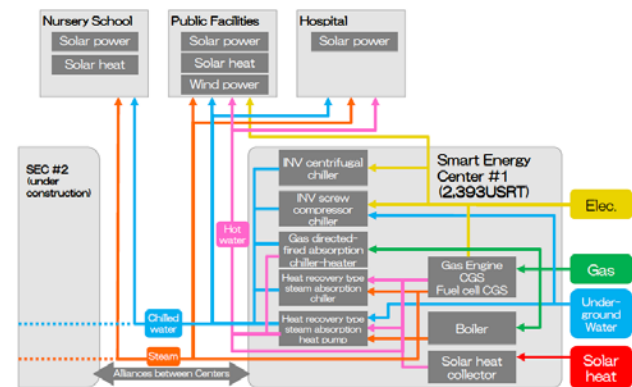


Figure 3. System Flow [1]

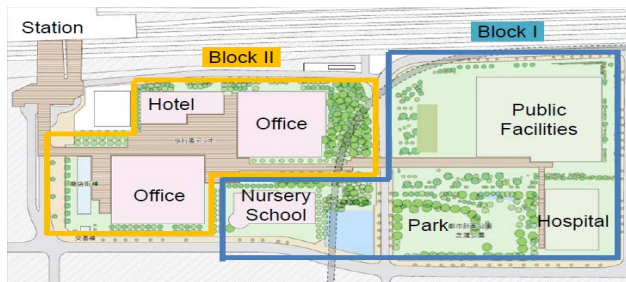


Figure 2. Area Planning Map [3]

3. THE SMART ENERGY NETWORK FACILITIES

At the SEC, the Smart Energy Network is constructed with the aim of making the most of renewable and unused energies occurring in this area. To respond to the customer demand, the heating and cooling source is configured to realize a 6-pipe supply with cold water of 7°C for cooling load, hot water of 47°C for heating load and steam of 782 kPa for hot water supply/humidification load. The system flow is shown in Figure 3.

In the construction of the SEC, the top-runner machines having the highest efficiency at this point in time such as heat source machines and CGS were adopted. In order to realize diversified selection and a stable supply of energy, the best mix heat source is provided, in which not only gas heat source machines but also electric-powered heat source machines such as inverter centrifugal chiller is adopted.

On the other hand, in order to increase the electric power load covered by CGS, Public Facilities and the SEC collectively receive power. The CGS capacity is selected so that the amount of waste heat used by the SEC is maximized.

4. FEATURES OF THE SMART ENERGY NETWORK

Six features of the Tamachi Smart Energy Network are as described below.

4.1. Effective use of renewable energy

Making use of the locational condition that Public Facilities faces a park on its southern side, a large-scale vacuum tube-type solar heat collector was set up on the roof of the deck for pedestrians for the first time as a District Heating and Cooling system in Japan. The vacuum tube-type solar heat collector can produce high temperature water (about 90°C), which is used, together with the waste heat of CGS, in input of the heat source machine for air conditioning throughout the year. (Figure 4)

This solar heat collector is also designed to visualize use of solar heat with the roof of the deck for pedestrians being partially glazed, helping to build environmental awareness in visitors.

In addition, solar power panels and wind power generators are set up on the roof of each building, and renewable energies are positively used in the whole area.

4.2. Effective use of unused energy

The underground tunnel water, which springs out of the tunnel of the subway and is kept at an almost constant temperature of around 20°C throughout the year, is used as cooling water for the screw compressor chiller in summer and as heat source water for the Heat recovery type steam absorption heat pump in winter. As a result, a substantial improvement of the Coefficient Of Performance (COP) of the heat source machines is exhibited throughout the year as the COP of the cold heat source machine has been increased from 5.5 to 8.1 in summer and the COP of the hot heat source machine has been increased from 0.8 to 2.3 in winter. The use of the underground tunnel water in this way is also the first attempt as a District Heating and Cooling system in Japan. (Figure 5)

4.3. Increase of resilience performance

This area includes important facilities, such as Public Facilities and Hospital, which serve as disaster prevention bases in the event of a disaster. Therefore, it is necessary to increase the resilience performance and enhance the self-sustaining degree of energy in the whole region.

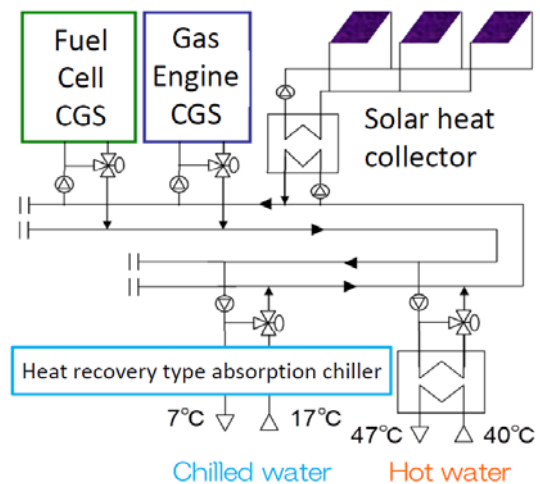


Figure 4. System Flow Using Solar Heat [1]

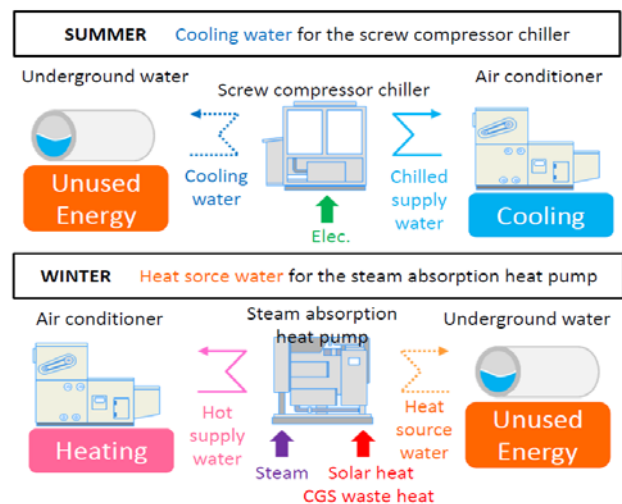


Figure 5. Method of Using Unused Energy [1]

To that end, we have studied with the parties concerned in the region about optimum distribution of energy during an emergency. Specifically, concerning heat, it has been estimated that the SEC can supply heat for the maximum cooling and heating load of Hospital continuously for 72 hours. The electric power is to be continuously supplied from the CGS using medium-pressure gas, which is set up at the SEC, and the emergency power generators owned by the buildings to Public Facilities serving as the disaster prevention base. Therefore, it has been planned so that electric power can be supplied to important loads for a longer period even in the event of a disaster such as a blackout.

4.4. Connection of buildings and Smart Energy Center

In this area, the buildings and the SEC are connected through ICT, and the SENEMS[®] (Smart Energy

Network and Energy Management System) is used to keep track of the outside air temperature, the status of energy used by air conditioners, and so forth, and the operational status of the heat source machines. The collected data is analyzed in real time, and not only the heat source machines (on the supply side) but also the air conditioners (on the demand side) are controlled, realizing low-carbonization in the whole area. In addition, the collected data is used to effectively visualize use of smart energy for promotion.

Such an optimum control of supply and demand in which the supply side moves into the demand side is also the first attempt as a District Heating and Cooling system in Japan. (Figure 6)

In addition, the following efforts are also conducted in relation to interaction between supply and demand in this area: in order to minimize the supply pressure of chilled and hot supply water to be fed to the customers, actual terminal pressure control is introduced, where the terminal pressure of the heat exchanger for each customer is measured and the supply water pressure is optimized based on the measured value, and in order to positively save energy and reduce CO₂ emissions through reduction of conveying power, the temperature difference of chilled and hot water is secured.

Here, the SENEMS[®] implemented in this area is specifically introduced.

In the SENEMS[®], demand is predicted from the past heat load records, air conditioner operation schedule, and weather forecast, an optimum simulation of heat source machines and air conditioners is conducted based on the predicted load, and an optimum operation plan for the next day of heat source machines and air conditioners is devised. On the day, the weather data and customers' event data, as external information, the setting and operation status data for air conditioners, and so forth, from the building BEMS, and the setting data for heat source machines or CGS from the central monitoring system of the SEC are collected, and based on the data, the optimum operation plan devised on the previous day is revised. After that, in order to make the operation status of air conditioners and heat source machines more ideal, the control commands for temperature setting and change of schedule for air conditioners and heat source machines are transmitted to each piece of equipment by the SENEMS[®], thereby optimally controlling supply and demand. In this way, the important concept is that the supply side does not always meet the amount of heat requirement from the demand side. Instead, customers' thermal comfort is kept with less amount of heat supply through the control of heat demand from the supply side. It contributes further energy saving/CO₂ reduction in the area.

In addition, the optimum supply temperature of chilled water is determined from the customer's loading status and the amount of energy used in the region, and command is issued to the heat source machines.

Through effective use of the collected data, visualization toward promotion of user's energy saving activities is implemented, and verification of the effect and study of improvement of energy saving measures and long-term equipment planning are conducted.

4.5. Establishment and operation of the Smart Energy Management Committee

For construction of the Smart Energy Network and to obtain the maximum effect, the important points are not only an optimum design of the energy system but also its appropriate operation after completion. It is also necessary to make not only improvements in terms of hardware but also improvements of infrastructure in terms of both hardware and software including "humans".

To that end, in this area, on the planning stage, the SEC and the building-side concerned parties started up the "Smart Energy Management Committee," which functions as something similar to a neighbourhood association for energy, toward efficient and effective energy use, and it has come into operation. (Figure 7)

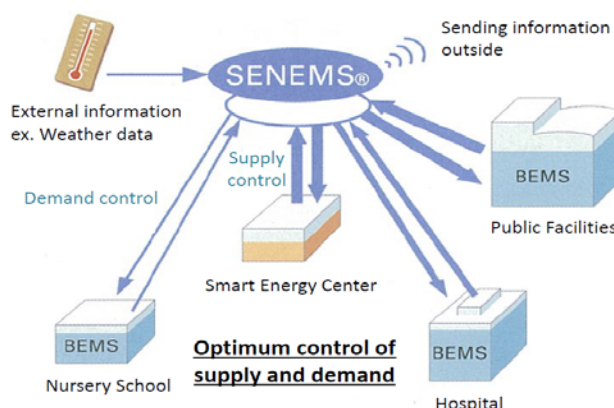


Figure 6. Image of SENEMS[®] [5]

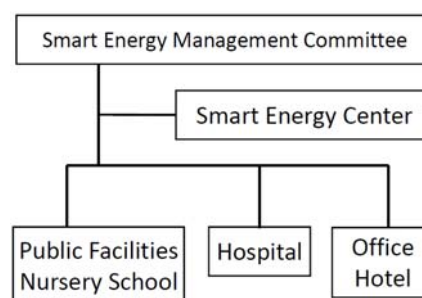


Figure 7. Organization of the Smart Energy Management Committee [2]

Table 2 List of energy saving/CO₂ reduction Major items [3]

System		Item
Smart Energy Center		Solar heat
		Underground tunnel water
		Increase in the efficiency of heat source machines, etc.
SENEMS [®] Connection of Building and SEC		Supply water pressure control
		Large temperature difference control
		Chilled water supply temperature control
		Heat load peak shift control
		Air conditioner temperature control
		Start prevention control of the heat source machines
Cust- omer	Construction	High air tightness/high thermal insulation/shielding
		Super-low carbon atrium
	Air conditioning	Outdoor air cooling
		CO ₂ /CO control
		Heat recovery
		Air conditioning in areas occupied
		Natural ventilation
		VAV/VWV
		Low- friction-loss duct
	Electricity	LED lighting
		High-efficiency OA equipment
	Sanitation	Use of rain water
	Renewable energy	Solar power

In this Smart Energy Management Committee, all concerned parties in this area participate and conduct preparations and check for "setting a CO₂ reduction target in the whole area," "improvement of the guideline

toward connection of the SEC and the buildings," "adjustment of execution of work for realizing cooperation," "verification of effect after operation," "study about visualization," and so forth.

4.6. Efforts for visualization

In this area, the efforts for visualization to understand how energy is produced and used in the whole city and to check whether energy saving or CO₂ reduction is properly conducted are positively made. Specifically, a website was created to make the efforts in this area known to the public, the CO₂ reduction state in the whole area is visualized, and a special site is available so that the customers can check the position of each building's energy saving efforts. In addition, digital signage has been set up in Public Facilities and Hospital to visualize the real-time energy supply and demand data, thereby trying to build environmental awareness in visitors.

5. ENERGY SAVING AND CO₂ REDUCTION ITEMS THAT FORM THE SMART ENERGY NETWORK

In completed Block I of the Tamachi Smart Energy Network, the CO₂ reduction target is a 45% reduction of CO₂ emissions in the whole area as compared with those in 1990 (when CO₂ reduction measures were not taken).

To evaluate the achievement of the target by CO₂ reduction measures, it is necessary to verify the effects of the CO₂ reduction measures planned for the buildings/SEC. So, the evaluation for the whole of area I and each energy saving item is conducted by the SENEMS[®]. Table 1 shows the list of major item of 37 items.

Optimum control by the SENEMS[®] covers not only control of the the SEC side but control of the building side. In verification of the effects, since some methods that are effective in energy saving on the SEC side may increase energy consumption on the building side, an integrated evaluation is conducted and measures are taken so that energy consumption in the area is minimized.

In this paper, 3 items of energy saving is described. 3 items are "Solar heat", "Use of underground tunnel water" and "Supply water pressure and large temperature difference control". These evaluations are based on results data from April, 2015 to March, 2016.

6. PERFORMANCE EVALUATION OF USE OF RENEWABLE ENERGY AND UNUSED ENERGY

6.1. Performance evaluation of solar heat (renewable energy)

The solar heat collecting amount by the solar heat collector and the solar heat utilization amount are shown in Figure 8.

In the year, the collecting amount is 439GJ/year, but the utilization amount is 328GJ/year. Because the operating time for heat source machines using solar heat was short in May, June, September and October. It is considered because chilled water load according to the time has a bigger change than expectation, and other machines are operated for the optimum operation plan inspection. So the rate of solar heat utilizing can be improved by adjustment of SENEMS[®] (optimum operation plan and control).

6.2. Performance evaluation of underground tunnel water (unused energy)

The amount of underground tunnel water used and the underground tunnel water temperature are shown in Figure 9, and the monthly average COP of these machines using underground tunnel water is shown in Figure 10 and 11. By the plan, the underground tunnel water is used in the steam absorption heat pump from November through April and used in the screw compressor chiller from June through September.

For a plan, the amount of underground tunnel water is small in Term A (from June to September) and Term B (from November to February). In Term A, it is considered 2 reasons. Because the underground tunnel water temperature is over 22°C, the screw compressor chiller used a highly efficient cooling tower without using the underground tunnel water. And other machines are operated for the optimum operation plan inspection which was confirmed various mode except unused energy priority mode. In Term B, in addition to a reason same as Term A, it is considered because the steam absorption heat pump was not able to operate by a request of the underground tunnel water manager and the maintenance. So the operating time of these machines can be improved by adjustment of SENEMS[®] (optimum operation plan and control) and proper operation.

The monthly average COP of these machines includes partial load. So COP of the steam absorption heat pump is smaller than rated value. COP of the screw compressor chiller is larger than rated value. In conclusion, we confirmed that these machines showed performance as planned.

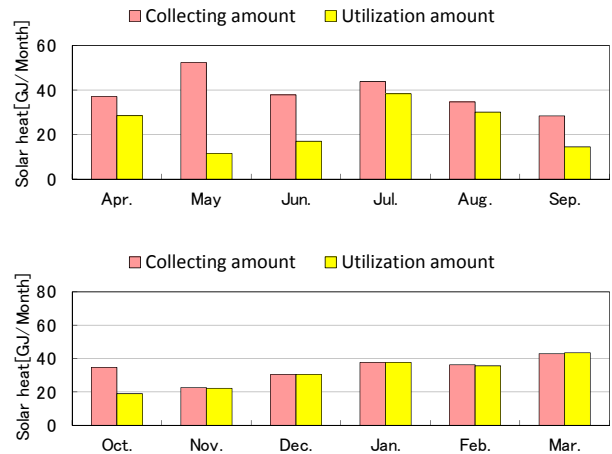


Figure 8. Performance of use of solar heat

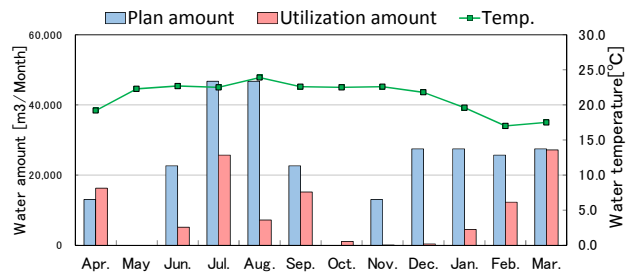


Figure 9. Performance of use of underground tunnel water

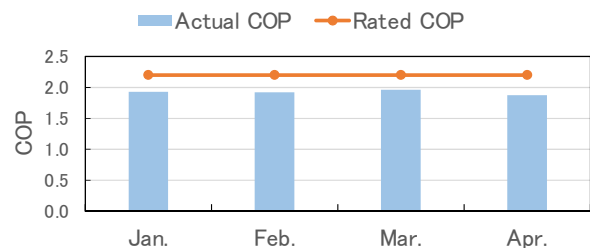


Figure 10. Actual efficiency of the steam absorption heat pump (COP = heat out put ÷ input steam)

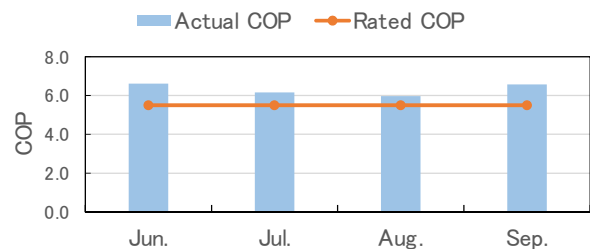


Figure 11. Actual efficiency of the screw compressor chiller (COP = heat out put ÷ input electricity)

7. THE ENERGY SAVING OF SUPPLY WATER PUESSURE AND LARGE TEMPERATURE DIFFERENCE CONTROL

7.1. Configuration of chilled/hot water systems

In the SEC, the supply water pressure and large difference temperature control is applied in the chilled water system and the hot water system. The customers indirectly use the heat from the SEC for chilled water and hot water separately and via a plurality of heat exchangers. The heat source machines are a primary pump type that means it supplies chilled and hot water to consumers only with a pump connecting to the machines.

The configuration of the primary pump is shown in Table 2. The flow control range is 50 to 100% according to the specification of the heat source machines. For the steam/hot water heat exchanger, there is no restriction by the specification of the heat source machines and the flow control range is 25 to 100%.

7.2. Design concept

In control of the heat exchanger of the heat receiving equipment in the customer's building, generally, the flow regulating two-way valve on the heat supplying side (primary side) of the heat exchanger is controlled so that the flow according to the heat load of the customer side (secondary side) is provided by each heat exchanger. Therefore, in a heat exchanger with a small differential pressure, wasteful conveying power is generated in order to secure the flow on the primary side that adapts to a large differential pressure caused by throttling the flow regulating two-way valve more than necessary.

Table 2 Configuration of the primary pump [4]

System	Name of machine	Specification of pump
Chilled	Steam absorption chiller	151.2m ³ /h × 45kW
Chilled	Steam absorption heat pump	74.1m ³ /h × 37kW
Hot		83.0m ³ /h × 30kW
Hot	Steam/hot water heat exchanger	197m ³ /h × 45kW × 2
Chilled	Gas absorption chiller- heater	151.2m ³ /h × 45kW × 2
Hot		
Chilled	Centrifugal chiller	151.2m ³ /h × 45kW
Chilled	Screw compressor chiller	45.4m ³ /h × 18.5kW

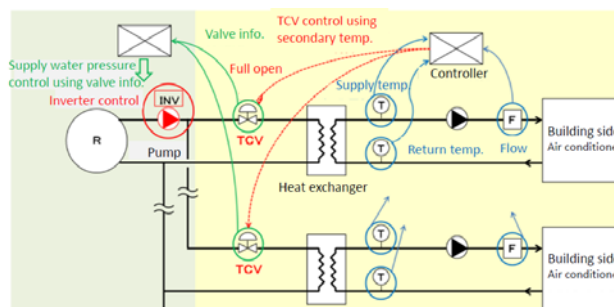


Figure 12. Supply water pressure control using valve information [4]

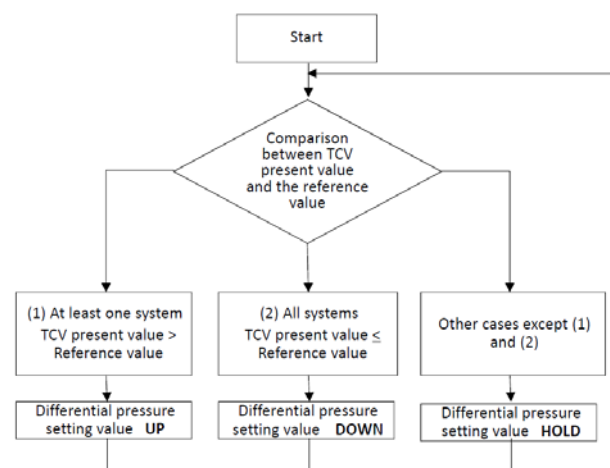


Figure 13. Flow of control [4]

In order to minimize the conveying power associated with circulation of heat medium, a control method by which the primary side TCV is fully opened was considered, and the "variable differential pressure water supply control according to the information of TCV opening degree on the primary side of the heat exchanger" was implemented. (Figure 12)

7.3. Outline of the control

Step 1: Operation of the TCV

The primary side TCV is controlled so that the supply temperature of the secondary side (building side) becomes the setting temperature.

Step2: Supply water pressure control

The opening degree of the TCV and the opening degree of the reference valve (= target value on control) are compared, and according to the result, the setting value for differential pressure is changed. The setting value for the supply differential pressure is reduced till at least one of the primary side TCVs of the heat exchangers of all consumers becomes fully opened. (See Figure 13) As a result, the conveying power is reduced by inverter control of the pump.

By a combination of supply water pressure control and large difference temperature control, realize reduction of the conveyance power of both supply and demand. In large difference temperature control, both control the SEC side and building side is important.

7.4. Performance evaluation

The supply water pressure control and the constant flow control are shown in Figure 14 and 15. “The supply water pressure control” is result values from April 2015 to March 2016, and large difference temperature control is considered. “The constant flow control” is the calculated value that supply differential pressure is constant using non-inverter pump, and large difference temperature control isn’t considered.

The quantity of annual energy saving (reduction rate) was 307MWh (93.8%) for chilled water system and 226MWh (87.4%) for hot water system. Through the year, a big effect was provided. When both the supply water pressure control and the large difference temperature control function, the big effect can be realized. Generally, in Japan, it is difficult to functionalize both control with winter chilled water, summer hot water, but can realize it in this area. It is considered that Not only this is the system which installed both control, but also it adjusted this control in both the SEC and building through the Smart Energy Management Committee. So it is confirmed that both control is effective.

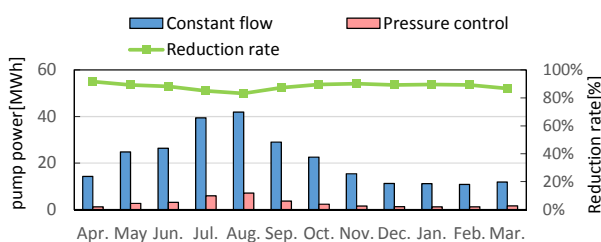


Figure 14. Performance of both control (Chilled water)

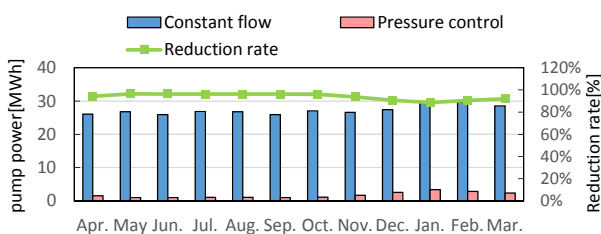


Figure 15. Performance of both control (Hot water)

8. PERFORMACE EVALUATION OF THE CO₂ EMISSION REDUCITON

In March 2016 from April 2015, the quantity of CO₂ reduction is 3,603ton-CO₂/year in the whole area, and 1,577ton-CO₂/year in the SEC in that. A CO₂ reduction rate is near to a target (= reducing 45% compared to 1990) in the whole area. The effect of solar heat, underground tunnel water and supply water pressure/ large difference temperature control is 314ton-CO₂/year (20% of the SEC). It is a big effect.

Further energy /CO₂ reduction target would be achieved by more effective use of solar heat and underground tunnel water through adjustment of SENEMS[®] and proper operation.

9. CONCLUSION

In the construction of the Smart Energy Network, it is necessary that the concerned parties, including not only the building owners but also the designers, and the Smart Energy Network operator closely cooperate, study the utilization methods for renewable or unused energies occurring in the region, and conduct technological studies about integrated operation of the buildings and the Smart Energy Center and establishment of a BCP function for incorporation into the design.

In city planning in harmony with the environment and toward advancement of urban functions, it is indispensable to put ICT technologies such as SENEMS[®] introduced here to full use to optimally control the energy supply and demand in the area and unitarily manage the collected data.

Specifically, some major items of performance regarding energy saving/CO₂ reduction have been evaluated at the Tamachi Smart Energy Network. A big effect is supply water pressure control and large difference temperature control. Solar heat and under ground tunnel water, it is considered that a further effect is expected by adjusting SENEMS[®] and proper operation. So we can expect the achievement of the target of CO₂ reduction (= reducing 45% compared to 1990).

As described above, in Tamachi Station North-east District, the Smart Energy Network was constructed and a low-carbon and disaster-resistant city.

In the future, the Smart Energy Network will be expanded step-by-step according to the progress of city planning, including connection with the Second SEC, which is in the planning stage, along with the development of Block II, continuously realizing a low-carbon and disaster-resistant city.

REFERENCES

- [1] Kenichi Sasajima, Osamu Kunitomo and etc, CO₂ – Reduction City Planning by Smart Energy Network, Collected papers of meeting of the Society of Heating, Air Conditioning and Sanitary Engineers of Japan 2011, Vol. 1, pp. 1227-1230
- [2] Kenichi Sasajima, Osamu Kunitomo and etc, CO₂ – Reduction City Planning by Smart Energy Network Part3. The Guideline of Control and Management System between SEC and Buildings, Collected papers of meeting of the Society of Heating, Air Conditioning and Sanitary Engineers of Japan 2013, Vol. 2, pp. 61-64
- [3] Osamu Kunitomo, Masashi Bansai and etc, CO₂ – Reduction City Planning by Smart Energy Network Part5. The System Outline and The Performance of Renewable (Unused) Energy, Collected papers of meeting of the Society of Heating, Air Conditioning and Sanitary Engineers of Japan 2015, Vol. 2, pp. 257-260
- [4] Kenichi Sasajima, Osamu Kunitomo and etc, CO₂ – Reduction City Planning by Smart Energy Network Part6. The Performance of the Optimum Pipe Water Pressure Control, Collected papers of meeting of the Society of Heating, Air Conditioning and Sanitary Engineers of Japan 2015, Vol. 2, pp. 261-264
- [5] Tomomi Yamamoto, Japanese Association of Building Mechanical and Electrical Engineers, Building mechanical and electrical engineers (2016), pp. 23-27

ANALYSIS OF THE INFLUENCE ON GREENHOUSE GAS EMISSION REDUCTION POTENTIAL BY DISTRICT ENERGY SUPPLY IN KOREA

Kyoung-A Shin¹, Jaesung Kang², Yonghoon Im³, Dahye Kim¹

¹ Korea District Heating Corp., 368 Bundang-ro, Gyeonggi-do, South Korea

² Korea Energy Economics Institute, 405-11 Jongraro, Jung-gu Ulsan, South Korea

² Korea Institute of Energy Research, 152 gajeong-ro, Yuseon-gu, Daejeon, South Korea

Keywords: climate change, greenhouse gas, energy efficiency, Environmental benefit

ABSTRACT

South Korea submits 2030 target of reducing greenhouse gas (GHG) emissions by 37 percent from business-as-usual levels to UNFCCC and encourages industry to cut its GHG emissions. As district energy sector emits 2.81% of total national GHG emissions in South Korea [1], we studied the contribution of district energy business mainly based on including Combined Heat and Power (CHP) plants as a means of securing reduction GHG emissions and saving energy efficiently. Firstly this paper examines that the actual carbon intensity by electricity production of conventional power plants and district energy which are mainly based on CHP plants. To allocate the GHG from CHP plants, two of different methods, Alternative Method and Power Bonus Method, are investigated. The carbon intensity for electricity production of district energy plants (0.43 tonCO₂e/MWh) is relatively lower than conventional gas-fired power plants (0.57 tonCO₂e/MWh). Secondly we analysed the cost effectiveness in reduction GHG emission of CHP based district energy sector compared to the other means using TIMES model method. We find that GHG marginal abatement cost of CHP plants (-\$134/tonCO₂) is even below than renewable energy sources such as photovoltaic power generation (\$87/tonCO₂). Finally the GHG emission reduction potential is reviewed on the projected GHG emission emitted when same amount of energy produced in combination of conventional power plants and individual boilers as substitution of district energy. It showed there were 10.1~41.8% of GHG emission reduction potential in district energy compared to the combination of conventional power plants and individual boilers.

BACKGROUND

As results of previous researches, there have been conclusion of energy efficiency of district energy system based on CHP. Since many countries have set its ambitious greenhouse gas reduction targets to strongly deal with global warming, studies related to CHP or district energy become more focusing on effects of greenhouse gas reduction by supplying

district energy and show CHP plants have potential in energy efficiency and greenhouse gas emission. [2] In 2014, 15.1% of all houses were supplied by district heating in South Korea. Along with that the government is planning to expand district energy continuously for its economic and environmental benefit. To assess feasible effect of expanding district energy in South Korea, we surveyed the actual greenhouse gas emission, energy consumption and plant efficiency of 23 major district energy providers and analysed their emission reduction potential.

RESULTS

1. District Energy Operation in South Korea

District energy that includes heating, cooling, power generation distributed from a central source can be divided into residential/commercial and industrial use by its consumers and main fuel. There were differences clearly between the two types of district energy businesses in South Korea and the table below describes district energy operation in 2014 in South Korea. Power to heat ratio means electricity generation per heat production.

Table 1. District energy operation in South Korea (2014) [3]

Type of district energy	Number of district energy provider	Heat produced, Tcal	Electricity generated, GWh	Average power to heat ratio
For residential and commercial use	31	20,736	16,063	1.34
For industrial use	29	56,135	11,941	0.14
Total	60	76,871	28,004	-

1-1. Fuel Sources in district energy

District energy for residential and commercial use must be placed near the village where home and commercial buildings are and supply heat and power. Those district energy plants has the main characteristic that usually burning natural gas emits relatively lower air pollutant as the air around the village should be cleaner by more strict air pollution control act. As a result of actual research, the sources of district energy for residential and commercial use in South Korea in 2014 were natural gas (92.6%), heavy oil (5.9%), landfill gas (0.8%), wood chip (0.6%) and kerosene (0.1%) in 13 major providers. On the other hand, District energy plants for industrial use produce hot and high pressure steam for factories in the industrial park. As its purpose is different to the plants above, most of these district energy plants prefer cheaper fuel price due to the competitive productivity of those factories. The sources of district energy for industrial use in South Korea in 2014 were bituminous coal (81.7%), heavy oil (8.8%), natural gas (3.5%), petroleum coke (2.2%), and fuel gas (2.05%) in 10 major providers.

2. Influence on GHG emission reduction by district energy supply

In 2013, emissions of greenhouse gases (CO₂, CH₄, N₂O, HFCs, PFCs, SF₆) by the electricity & district energy sector in South Korea were 267,859 kilotons which contributes about 38% of national emissions of greenhouse gases. The separate emissions of greenhouse gases of district energy sector were 19,286 kilotons, or about 2.8% of national emissions of greenhouse gases. However 19,286 kilotons were emit by only 23 major district energy providers not all of 60 providers because it was only obligatory whom emit the greenhouse gases over 50,000 metric tons a year to assess and report on their emission in South Korea. As the emissions of rest of those district energy providers were negligible, we only covered 23 major district energy providers for this study. The emission was reported in accordance with Korea Greenhouse Gas & Energy Target Management Scheme which applies IPCC emission factor and national emission factor depends on the size of emission from an installation.

Although the energy consumption of district energy for residential and commercial use is higher than industrial use, the greenhouse gas emission is lower as its main source is natural gas which emit less greenhouse gases than coal.

Table 2. GHG emission in power & district energy sector in South Korea

(Unit : kiloton(kt) of greenhouse gas)

Sector		2011	2012	2013
District Energy (A)	For residential and commercial use	7,491	8,382	8,442
	For industrial use	10,596	10,489	10,844
	Total	18,087	18,871	19,286
Power (B)		233,406	239,534	248,573
Power & District Energy (A+B)		251,493	258,405	267,859

2-1. Carbon intensity

To compare the carbon intensity with a various type of conventional power plants, we calculated carbon intensity of district energy plants for electricity generation which is the common product of a various type of CHP plants. To calculate the carbon intensity, we collected annual data such as GHG emission, electricity generation and heat production of 23 major district energy providers from 2011 to 2014. Both of allocation method, Power Bonus Method and Alternative Generation Method were applied for the allocation of greenhouse gas emission. The allocation method shows how emissions are shared between heat production and electricity generation in CHP plants. Alternative Production Method allocates emissions to the heat and power production in proportion to the energy needed to produce the same amount of heat and power in separate plants as in (1).[4] The efficiencies for heat and power production of alternative plants directly affect to the proportion of allocated emission. Heat production efficiency value was 85% that assumed as an individual boiler for residential use fired by natural gas. We estimated 41.9% of power generation efficiency value by calculating weighted average of efficiencies from the amount of power generation of each power sources in South Korea. [5] After determining the fraction of emissions for heat and power, we calculated carbon intensity by dividing allocated emissions into electricity generation.

$$f_h = \frac{\frac{H}{\eta_{alt\ heat}}}{\left(\frac{H}{\eta_{alt\ heat}} + \frac{P}{\eta_{alt\ power}} \right)} \quad (1)$$

$$f_p = \frac{\frac{H}{\eta_{alt\ power}}}{\left(\frac{H}{\eta_{alt\ heat}} + \frac{P}{\eta_{alt\ power}}\right)}$$

f_h : Allocation factor for heat, f_p : Allocation factor for power

$\eta_{alt\ heat}$: Heat production efficiencies of producing thermal energy via an alternative plant

$\eta_{alt\ power}$: Power generation efficiencies of producing power energy via an alternative plant

H : Heat production, P : Power generation

With the power bonus method the primary energy allocated to the electricity produced in the CHP-plant will be equal to the primary energy that would have been used to produce the electricity in an alternative production, usually the electricity that will be replaced by the electricity produced in the CHP-plant. [6] Primary energy factor of district heating is calculated according to (2).

$$f_{P,DH} = \frac{\sum_i Q_{F,i} \cdot f_{P,F,i} - W_{chp} \cdot f_{P,alt}}{\sum_j Q_{c,j}} \quad (2)$$

$f_{P,DH}$: Primary energy factor for the district heating system

$f_{P,F,i}$: Primary energy factor of the i-th fuel or final energy input

$f_{P,alt}$: Primary energy factor of replaced electrical power

$Q_{c,j}$: Sum of the heat energy consumption

W_{chp} : Power generation of CHP plants

$Q_{F,i}$: Fuel input to the heating plants and to the CHP plant of the i-th fuel

$$A_{heat} = \frac{f_{P,DH} \cdot Q_{c,j}}{Q_{1(tot)}} \quad (3)$$

$$A_{power} = 1 - A_{heat}$$

Primary energy factor of district heating is calculated according to equation (2) then allocation proportion for heating can be calculated as in equation (3).

The average carbon intensity by electricity generation in district energy plants was 0.44 tonCO₂e/MWh (tons of carbon dioxide equivalent per MWh) in case of Power Bonus Method. When we applied Alternative Method it was lower than Power Bonus Method, 0.43 tonCO₂e/MWh. Especially in the case of the district energy for residential and commercial use, their carbon intensity were 0.35~0.40 tonCO₂e/MWh which is a little higher or similar to gas fired combined cycle power

plant. Besides of district energy, the carbon intensity by other energy sources was previously researched. [7]

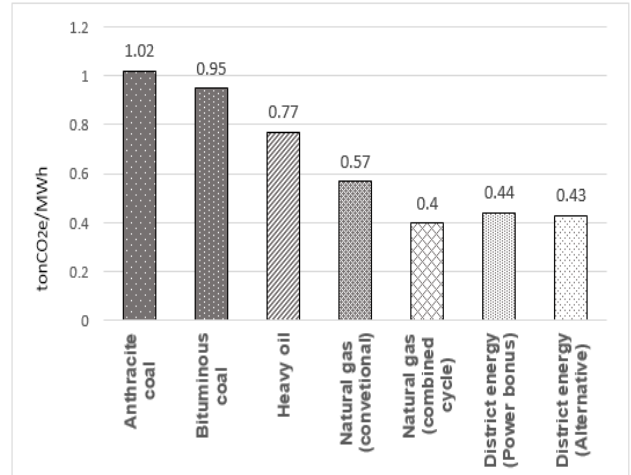


Figure 3. Carbon intensity by energy sources of power plants and district energy

Table 3. Scenario assumption by GHG emission reduction technologies in Power & District Energy sector

Technologies	Scenario assumption
USC generation	Introduce USC generation as 1% of total coal (bituminous)-fired power plant capacity in 2020. Extra construction of USC generation plants in addition to base scenario which assumes all of newly constructed coal (bituminous)-fired power plant.
CCS	Introduce CCS as 2.9% of total coal (bituminous)-fired power plant capacity in 2020. It was assumed 2,200 kilotons of greenhouse gas would be captured in the power sector.
Expansion of renewable energy power generation	Introduce extra photovoltaic power and windmill power generation 10% of base scenario in 2020. As the renewable energy power generation has been increasing rapidly, additional construction was assumed.
Expansion of CHP plants	Expand power generation by CHP plants additionally in 2020. It was assumed switched 1% of electricity generation from conventional power plants to CHP plants.
Reduction of heat loss during distribution	The heat loss during hot water distribution in district heating is 10% now. It was assumed that the heat loss would be reduced by 5% in 2020.

Table 4. Cost assumption by GHG emission reduction technologies in Power & District Energy sector

Technologies	Cost assumption
USC generation	Investment costs of USC generation are 38% more expensive than coal (bituminous) fired power plant
CCS	Investment costs are 3 times more expensive than coal (bituminous) fired power plant and fixed costs are 60%
Expansion of renewable energy power generation	Photovoltaic power generation: Compare to coal (bituminous) fired power plant, Investment costs are 490% and fixed costs are -50%. Windmill power: Compare to coal (bituminous) fired power plant, Investment costs are 82% and fixed costs are -54%. We assumed operation costs of both of power generation were none.
Expansion of CHP plants	Compare to coal (bituminous) fired power plant, Investment costs are 21% and fixed costs are -83%.
Reduction of heat loss during distribution	We assumed the cost for reduction of heat loss in distribution pipe as 0.1% of (\$75 per Gcal) heat price for residential use.

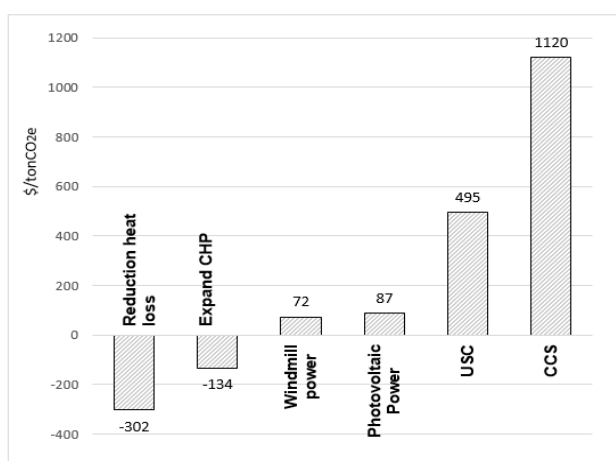


Figure 2. GHG marginal abatement costs by emission reduction technologies

2-2. GHG marginal abatement cost

The TIMES modelling tool was developed as part of the IEA-ETSAP (Energy Technology Systems Analysis Program) and we applied TIMES modelling tool to calculate the GHG marginal abatement cost of several technologies related to district energy. Since there haven't been very specific prospect related to emission

reduction technologies in the power & district energy sector, we set scenario bring in emission reduction technologies. The emission reduction technologies are Ultra-Supercritical (USC) generation, Carbon Capture and Storage (CCS), expansion of renewable energy power generation, expansion of CHP plants and reduction of heat loss during distribution.

Cost assumption for modelling is assessed by greenhouse gas emission reduction technologies in Power & District Energy sector as the table below.

We compared the cost and greenhouse gas emission of the expansion of CHP plants scenario to base scenario. Base scenario were based on the demand applied the second energy supply basic plan of South Korea government as well as the portion of each source of electricity generation. The greenhouse gas marginal abatement costs are calculated as a gap between costs of two scenarios per a gap between greenhouse gas emission (\$/tonCO₂e). As the quantity of each greenhouse gas emission reduction is based on the assumption not a specific plan, the quantity would be depends on the scenario. Therefore the quantity of emission reduction was not considered on this study.

2-3. GHG reduction potential in district energy

To access the integrated GHG reduction potential in district energy, we assumed that the same amount of heat and power from district energy plant were produced in individual heating and conventional power plant and compared the GHG emission. As two different type of district energy providers have dissimilar characteristics such as fuel and purpose of heating, we separately assumed and calculated for each district energy provider.

2-3-1. GHG reduction potential in district energy for residential and commercial use

Heat loss (10%) and power loss (1.6%) during its distribution were considered on this calculation. The amount of heat was calculated as {(Amount of heat sold by district energy * (1-heat loss)) / efficiency of individual heating} and electricity was calculated as {(Amount of electricity sold by district energy * (1-power loss)) / efficiency of individual heating} to apply to individual boilers and conventional power plants.

2-3-2. GHG reduction potential in district energy for industrial use

Heat loss during distribution would be zero for these providers as their customer mainly factories were placed very close to central energy source. We assumed 1.6% of Power loss. Also we compared to

coal fired power plant for electricity generation because their main fuel was coal. Calculation of amount of heat and power was same as above.

The GHG reduction potential of these district energy was 10.1% that lower than the GHG reduction potential for residential and commercial use (12.1%~41.8%) but it shows still there are reduction of the GHG emission.

Table 5. Assumption criteria by type of installation

Type of installation	Efficiency of installation	Fuel
District Energy	Actual GHG emission data	
Power generation (Fuel mixed)	43.1%	Coal (67%) Heavy oil (4%) Natural gas (29%)
Power generation (Gas fired)	49.1%	Natural gas (100%)
Individual boiler for residential use	85%	Natural gas (100%)

Table 6. GHG reduction potential in district energy for residential and commercial use by each scenario

Type of installation	GHG reduction potential
Power generation (Fuel mixed) & Individual heating for residential use	41.8%
Power generation (Gas fired) & Individual heating for residential use	12.1%

Table 7. Assumption criteria by type of installation

Type of installation	Efficiency of installation	Fuel
District Energy	Actual GHG emission data	
Power generation (Fuel mixed)	38.9%	Coal (100%)
Individual boiler for industrial use[3]	76.0%	Coal (83%) Heavy oil (8%) Natural Gas (10%)

Table 7. GHG reduction potential in district energy for industrial use

Type of installation	GHG reduction potential
Power generation(Fuel mixed) & Individual heating for industrial use	10.1%

CONCLUSION

Summarizing the study, Our result that TIMES modelling was applied indicates that CHP for district energy supply is more efficient and cost effective way in the emission mitigation as the GHG marginal abatement cost is minus (-). Also we assessed the comparison between the emission in district energy and the emission in conventional power plants & individual boilers. The emission reduction rate in district energy is found to be 10.1~41.8%. To deal with global action driven by post-2020 climate change agreement, district energy could be profitable and effective energy source in mitigation of emission.

REFERENCES

- [1] Korea Ministry of Environment, National GHG emission statics (2015)
- [2] J. Korhonen, "A material and energy flow model for co-production of heat and power," 6, J. of Cleaner Production (2002)
- [3] Korea energy agency, District energy statics (2015)
- [4] Magnhild Kallhovd, "Analysis on Methods and the Influence of Different System Data When Calculating Primary Energy Factors for Heat from District Heating Systems", Norwegian University of Science and Technology, pp. 58-59 (2011)
- [5] Korea Electro-technology Research Institute, Energy census (2014)
- [6] SP Technical Research Institute of Sweden, Korea District Heating Technology Research Institute, SINTEF Energy Research, Norway, "The potential for increased primary energy efficiency and reduced CO2 emissions by district heating and cooling", IEA-DHC, pp. 29(2011)
- [7] Byoung-Oke Cho, Shin-Jong Kim and Jum-Su Kim, "An analysis on contribution to the GHG emission reduction and the economic effect of Korean nuclear power plants", Journal of Energy Engineering, Vol.19, No. 4, pp. 203-214

CONSIDERING INVESTMENT RESOURCES WHEN ASSESSING POTENTIAL CO₂ REDUCTIONS OF CHP – A CASE STUDY

L. Nordenstam^{1,2}, M. Bennstam^{1,2}, L. Trygg¹

¹ Division of Energy Systems, Department of Management and Engineering, Linköping University, SE-581 83 Linköping, SWEDEN

² Tekniska verken i Linköping AB (publ), Box 1500, SE-581 15 Linköping, SWEDEN

Keywords: CHP, district heating, CO₂ emissions, GHG, reduction potential, investment resource

ABSTRACT

Combined heat and power (CHP) can increase electricity production efficiency and decrease global CO₂ emissions. Studies have shown large unrealised economic CHP investment potentials. An assessment of profitable CO₂ reduction based solely on net present value (NPV) implicitly assumes unlimited investment resources. This study analysed the impact of the assumption of unlimited/limited investment resources on the assessment of profitable reduction potential of global CO₂ emissions due to CHP investment. The correlation between changes in direct and global fossil CO₂ emissions was also analysed. This was done by evaluating alternative CHP and heat-only boiler investments in a district heating system. When investment resources were unlimited, NPV was used to determine whether an investment was profitable and to rank the profitability of the investment. When investment resources were limited, equivalent annual annuity ratio (EAAR) was used to rank the investment's profitability and determine whether its level of profitability was acceptable.

The results showed that the profitability ranking of an investment can change depending on whether investment resources are considered unlimited or limited. Moreover, an investment with positive NPV may be regarded as insufficiently profitable when investment resources are limited. This could have an important impact on profitable CO₂ reduction potential. Furthermore, when CHP investments are considered, local views on CO₂ emissions may be counterproductive for global CO₂ emission reductions.

INTRODUCTION

Combined heat and power (CHP) is advocated by the EU as a technique for increasing energy efficiency and thereby reducing fossil CO₂ emissions [1], [2]. Stankeviciute and Riekkola [3] found that the electricity output of profitable European CHP is potentially around 43 % greater than with existing CHP. Danestig *et al.* [4] found potential in Stockholm for profitable bio-fuelled CHP that was more than 100 % higher than the CHP production at that time. The existence of unrealised

profitable energy-efficiency measures is often referred to as the energy-efficiency gap or paradox. As in the work of Stankeviciute and Riekkola [3] and Danestig *et al.* [4], studies on the assessment of profitable energy-efficiency potential are often based on the standard net present value (NPV) rule [5]. NPV is the net present value of the initial investment and all future changes in costs and revenues that are affected by the investment [6]. According to the standard NPV rule, all independent investments with positive NPV should be accepted in order to maximise a company's value [6]. Assessments of profitable energy-efficiency investments based solely on NPV implicitly assume that investment resources are unlimited, but in reality this is not always the case [7]. If investment resources are limited, the productivity of these limited investment resources should be maximised. Some discounting methods have been developed indicating how net cash flow relates to the investment cost, which can be used with NPV when investment resources are limited [7]. One method is to rank investments according to NPVR, which is the ratio of NPV to the initial investment (I_0) [6]-[8]. The alternative with the highest ratio is then considered the most beneficial investment. Swedish literature also includes the annuity of NPVR, here called the equivalent annual annuity ratio (EAAR) [7], [9]. EAAR measures the annual increase in value or the annual "interest" gained in addition to the cost of capital. The investment alternative with the highest value is considered to be the most beneficial. EAAR is suitable for repeatable projects [7].

The aim of this study was to analyse the way in which the assumption of unlimited or limited investment resources affects the assessment of profitable reduction potential of global fossil CO₂ emissions due to bio-fuelled CHP or heat-only boiler (HOB) investment in CHP-based district heating systems (DHS). The correlation between changes in direct and global fossil CO₂ emissions for investments in CHP or HOB in a CHP-based DHS was also analysed. This was done by evaluating alternative investments in a real investment decision case at a local energy utility, using two cash flow-based investment measures: NPV and EAAR.

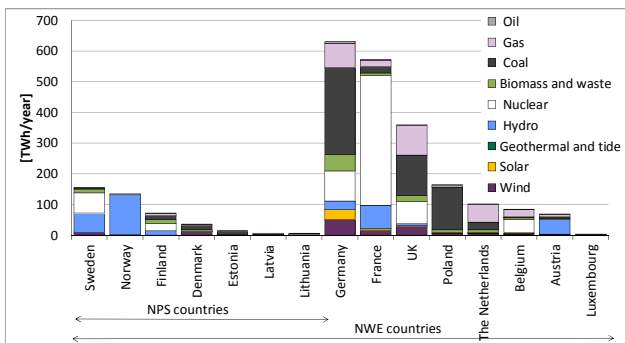


Figure 1. Electricity production in NPS countries and NWE countries in 2013 [18, 19]

Related work

Academics have offered different explanations for the energy-efficiency gap, such as asymmetric information, organisational barriers, split incentives and market failures [10]-[12]. Jaffe and Stavins define the energy-efficiency gap as the difference between actual and optimal use of energy [10]. They found that the economists' economic potential is reached when "market failures in the market for energy-efficiency technologies" are removed, while the technologists' economic potential requires high discount rates due to irreversible investments and uncertainty to be eliminated, inertia around the dispersion of new technologies to be overcome and any heterogeneity to be ignored [10].

A number of studies concerning energy-related investment decisions are based on the real options theory, which assumes that the irreversibility of an investment and the uncertainty of future prices of fuel or electricity, for example, can increase the value of postponing an investment [13]. Using ex-post data, Löfgren *et al.* [5] studied the impact of uncertainty in the future price of polluting fuel. They found that the price of the polluting fuel would need to be 2.7-3.6 times greater in order to trigger the realised investments according to the standard NPV rule [5]. Sundberg and Sjödin [14] conclude that companies applying different rates of interest when calculating the profitability of investment may prioritise differently between CHP and HOB. Wickart and Madlener [15] developed an economic model for handling "the decision-making problem under uncertainty", taking volatile energy prices into account. They found that the standard NPV rule can be misleading when choosing between an investment in CHP or HOB since it does not consider uncertainties in policy measures or volatile energy prices. Investments often involve some kind of risk taking. Studies show that risk management can include the adjustment of discount rates or the adjustment of cash flow, for example [16], [17]. Another method of risk management that is sometimes used in

practice is to apply safety margins, for example to EAAR [7]. The main contribution of the present study to this body of work is an analysis of the impact of the assumption of unlimited or limited investment resources on the assessment of profitable reduction potential of global fossil CO₂ emissions due to CHP investment in DHS. To the authors' knowledge, this is an area that has not previously been studied.

BACKGROUND

The northern European electricity market

NordPool Spot AS (NPS) operates the common day-ahead electricity spot market in the Nordic and Baltic region, including Sweden. NPS and three other power exchanges use a single price-coupling algorithm to calculate day-ahead electricity prices and optimise the interconnectors within and between the countries of north-western Europe (NWE) (Fig. 1).

Shared data are used to calculate hourly bidding area prices, other reference prices and transmission flows between the bidding areas [20]. Electricity is traded for delivery each hour the next day. When producers and buyers have submitted their orders, hourly prices are calculated on the equilibrium point between the aggregated supply and demand curves [20]. The price at the equilibrium point reflects both the most expensive production source needed to balance the system and the highest price that buyers are willing to pay to meet their demand [21].

Bidding area prices are used to price electricity traded on the day-ahead electricity spot market. An hourly system price (SP), used as a reference price for financial contracts, is calculated for the NPS area, disregarding any transmission limitations (Fig. 2). The city of Linköping, where this case study takes place, is located in the Swedish bidding area Stockholm (SE3). The single price-coupling algorithm causes competition between electricity production within Sweden and electricity production in the other participating countries taking limitations in transmission capacity into consideration, resulting in import/export of electricity [22]. The extent to which the price at the equilibrium point for SE3 correlates with the short-term variable costs for coal condensing and gas-fuelled power plants is shown in Figure 2.

The European emissions trading system

The European emissions trading system (EU ETS) is an EU tool for meeting its commitments on GHG emissions reductions under the Kyoto Protocol. Companies are required to hand in EU allowances (EUA) equivalent to their emissions of fossil CO₂. Fossil fuels such as oil, coal and rubber waste require EUAs [26], [27].

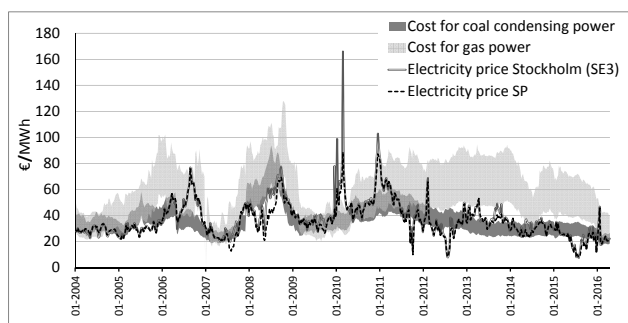


Figure 2. Weekly average electricity spot prices SE3 and SP and short-term variable costs for coal-fuelled (efficiency 35-46 %) and natural gas-fuelled (efficiency 32-58 %) electricity [23]- [25]

Table 1. Technical data for the existing production units in Linköping-Mjölby DHS at the time of the TvAB project [30]

<i>Production units</i>	Total boiler capacity [MW _{steam}]	Boiler efficiency	Power-to-heat ratio	FGC [MW _h]
CHP plant Gärstadverket				
Waste-fuelled 1-3	69	0.9	0.16	10
Waste-fuelled 4	65	0.9	0.3	15
CHP plant Kraftvärmeverket				
Bio-fuelled	53.5	0.8	0.3	12
Coal/rubber-fuelled	56	0.8	0.3	0
Oil-fuelled	130	0.9	0.3	0
Others				
Bio HOBs	26	0.85	0	8
Oil HOBs	240	0.85	0	0

The electricity certificate system

The Swedish/Norwegian electricity certificate (EC) system is a market-based support system aimed at increasing the production of electricity from renewable sources, e.g. bio, wind and hydropower plants. Over a 15-year period, producers are assigned one EC per MWh electricity produced from renewable sources. Through a statutory quota obligation, electricity suppliers are obliged to purchase ECs in proportion to their electricity sales, creating a demand for ECs [28], [29].

CASE STUDY

The city of Linköping is located 200 km southwest of Stockholm and has about 150,000 inhabitants. The local energy utility Tekniska verken i Linköping AB (TvAB) owns and runs the DHS in Linköping. In 2008-2010 TvAB analysed multiple investment alternatives for Linköping DHS in order to reduce the company's dependence on oil and cut costs. Costs for

reinvestment and maintenance of the Kraftvärmeverket CHP plant were debated and consideration given to increasing the reserve capacity for heat production. The present study used the bio-fuel based investment scenarios from the TvAB project, including cost and price assumptions and capital budgeting measures used by TvAB.

Annual district heating (DH) production in Linköping is about 1600 GWh and electricity generation in the CHP plants is about 350 GWh. The maximum heat demand is about 500 MW. The base for production of Linköping DH is energy recovery from household and industry waste at the Gärstadverket CHP plant, which at the time of this study had four boilers and two steam turbines (Table 1). During the TvAB project, the mid-merit production of heat took place at Kraftvärmeverket, an older CHP plant comprising three boilers jointly connected to three steam turbines (Table 1). In addition to the CHP plants, there are a number of oil-fuelled HOBs for peak and reserve purposes. The production strategy is that heat demand is always met, whereas electricity is produced when profitable. Electricity is sold on the NPS spot market. Electricity production is principally limited by the heat demand, but some production of condensing power is possible. Boilers fuelled by waste or biofuel are equipped with heat recovery by flue gas condensation (FGC) [30]. TvAB's DHS is connected to that of Mjölby-Svartådalen Energi AB (MSE) in Mjölby by a 30-km-long transit main. TvAB and MSE co-optimize their production on a daily basis and share the savings in production costs. At the time of the TvAB project, MSE's base production of DH consisted of three bio-fuelled HOBs (Table 1), and it bought about 40 % of its total heat demand of just over 200 GWh/year from TvAB [30].

METHOD

Economic optimisation of DHS

Linköping DHS is optimised using an optimisation framework called MODEST [31]-[33], which is designed to model and optimise operations and investments in local and national energy systems. It can include many components and energy flows, from sources through conversion to demand. Linear programming is used to find the solution with the lowest present value of future system costs (FSC). FSC includes costs and revenues of operation for meeting a certain energy demand, by means of existing and new optional components, such as HOB or CHP. FSC also include capital costs for investments in new components. A flexible time division can be used to reflect yearly, seasonal, weekly and diurnal variations in input data, such as energy demand, capacities and prices. MODEST has been tested and applied to over 50 local Swedish energy systems in studies on, for example, CHP potential [4],

the impact of energy conservation measures [34] and the integration of ethanol production into a DHS [35].

In this study, MODEST was used to minimise the present value of FSC for a pre-determined heat demand at Linköping DHS. Essential input data were costs for investments, operations and maintenance, costs and income for economic policy instruments and prices of fuels and electricity, including annual real increases where relevant. Time was subdivided into 88 periods per year, reflecting variations in heat demand, electricity prices and boiler maintenance periods. Optimisations were made for a 20-year period. For the reference scenario, the DHS was modelled with existing plants only, resulting in optimal production of heat and electricity representing business as usual. For each investment scenario, the DHS was modelled with existing plants and one optional investment, resulting in an optimal size of investment and an optimal production plan for the DHS. The four investment scenarios included the following mutually exclusive optional investments:

- S1: Replacement of the existing coal- (and rubber-) fuelled boiler and a turbine at the Kraftvärmeverket CHP plant with a bio-fuelled boiler and a new turbine
- S2: Replacement of the existing oil-fuelled boiler and a turbine at the Kraftvärmeverket CHP plant with a bio-fuelled boiler and a new turbine
- S3: Construction of a new bio-fuelled CHP plant
- S4: Construction of a new bio-fuelled HOB plant.

The results obtained in this study were thoroughly checked against other calculations and real data for the DHS.

Capital budgeting measures

The financial solidity required by TvAB's owner limited the total size of the company's loans, thereby limiting available investment resources [30]. In addition to NPV, TvAB therefore also used relative investment measures such as EAAR to rank competing investments. Investments due to regulatory requirements and necessary replacement needs were prioritised first. Thereafter, investments due to profitability generally needed EAAR of 4-5 % in order to be accepted at the time of the TvAB project. However, low-risk investments with EAAR of 2-3 % could be accepted, while investments with high risk, e.g. uncertain contribution margin and long implementation time, needed EAAR of at least 6-8 % [30]. In this study, NPV was used to determine whether an investment was profitable and to rank the attractiveness of an

investment when investment resources were unlimited. When investment resources were considered limited, EAAR was used to rank the attractiveness of the investment and to determine whether the profitability of the investment was acceptable, *i.e.* sufficiently high.

$$NPV = I_0 + \sum_{t=1}^n \frac{CF_t}{(1+r)^t} \quad (1)$$

$$EAAR = \frac{NPV}{I_0} * \frac{r}{1 - (1+r)^{-n}} \quad (2)$$

where I_0 is the initial investment in period zero, CF_t is the expected net cash flow in period t , r is the cost of capital (interest) and n is the lifetime of the investment.

MODEST presents an optimal (minimised) present value of FSC, before corporate taxes, for the reference scenario and each investment scenario. NPV is the decrease in the present value of the FSC that is achieved in the investment scenario compared with the reference scenario. Costs and revenues stated in MODEST results are used as input data when calculating NPV and EAAR, all after Swedish corporate taxes.

Calculation of the net effect on global fossil CO₂ emissions

The net effect of DHS changes on global fossil CO₂ emissions was estimated here using a general systems approach, as used by [4], [34], [36] for example. The net effect on global GHG emissions is defined as:

$$\Delta GHG_{global} = \Delta GHG_{direct} - \Delta GHG_{avoided} \quad (3)$$

where the direct net effect on local GHG emissions (ΔGHG_{direct}) and the indirect net effect on GHG emissions avoided elsewhere ($\Delta GHG_{avoided}$) are defined as:

$$\Delta GHG_{direct} = \sum_{k=1}^n \Delta F_k * f_k \quad (4)$$

$$\Delta GHG_{avoided} = (\Delta E_{CHP} - \Delta E_{use}) * f_E \quad (5)$$

where ΔF_k is the change in use of a specific fuel k for production of heat and electricity at the local DHS, f_k is the emissions factor for that specific fuel, ΔE_{use} is the change in electricity use, ΔE_{CHP} is the change in electricity production in the CHP plants in the local DHS and f_E represents the emissions factors of the replaced electricity production in the electricity system. In the present study only GHG fossil CO₂ was considered.

Assumptions and limitations

There are different opinions on how the use and production of electricity affect global warming [37]. It was assumed that the future electricity market in northern Europe will work as it does today, with marginal electricity production consisting of the most expensive electricity production needed to balance the system. This was an important assumption in the present study.

Here, the cap on the EU ETS [26], [27] was not considered to be rigid in the long term due to the risk of carbon leakage and future political decisions [37], [38]. It was therefore assumed that reductions within the EU ETS would contribute to the reduction of global GHG emissions.

Biomass is a limited resource. However, CHP with FGC is a very efficient method of utilising biomass. In this study, it was assumed that CHP is the best energy use for biomass.

Table 2. Assumed costs for challenged boilers and the optional investment of each scenario [25], [30]

	Investment costs	Operation and maintenance	
	[k€/MW _{steam}]	[€/MW _{steam}]	[€/MWh _{steam}] and year]
Coal-fuelled boiler		-	16.2
Oil-fuelled boiler		-	11.7
S1	650	26.5	1.9
S2	650	26.5	1.9
S3	950	20.9	1.9
S4	40	29.9	2.2

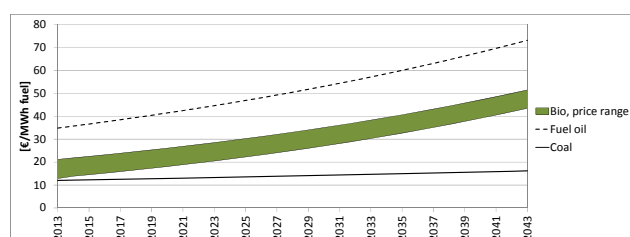


Figure 3. Estimated fuel costs (€/MWh fuel) [30]

Table 3. Assumed prices for EUAs, ECs and fuel taxes [30], [39], [40]. Annual real increases are shown in brackets

	Prices
EUAs for all fossil fuels	€ 33 / EUA (2.5 %)
Fuel tax on coal for CHP heat	€17.6 / tonne fuel (0 %)
Fuel tax on oil for CHP heat	€ 20.2 / m ³ fuel (0 %)
ECs	€ 30 / EC (0 %)

Input data

All input data were retrieved from the TvAB project. All costs and prices given in this study are 2010 values using an exchange rate of € 0.1 / 1 SEK.

By using much of the existing infrastructure in the old plant, lower initial investments costs were assumed for S1 and S2 compared to S3 (Table 2).

Furthermore, it was assumed that all bio-fuelled boilers are equipped with FGC and, due to a lack of space, the maximum capacity of replacement boilers for the old CHP plant (S1 and S2) was limited to 100 MW_{steam}. The power-to-heat ratio was assumed to be 0.5 for S3 and 0.4 for S1 and S2. The investment cost for oil-fuelled HOBs, a value needed to make the scenarios equivalent regarding available heat production capacity for peak and reserve purposes, was assumed to be € 1*10⁵ / MW_{heat}. The lifetime of all optional investments was assumed to be 20 years and a nominal bank interest rate of 6 % was used for optimisations. Assumed prices of fuels and financial control mechanisms are shown in Figure 3 and Table 3 [30].

Emission factors used for fuels in this study were 0 kg CO₂/MWh for bio, 327 kg CO₂/MWh for coal, 274 kg CO₂/MWh for oil and 204 kg CO₂/MWh for natural gas [41]. In a sensitivity analysis of replaced electricity production, two alternative technologies of future marginal electricity production were assumed: coal-fuelled or natural gas-fuelled plants, with efficiency of 46 % and 58 % respectively, which is representative of plants being built now [25]. This results in emission factors of 711 and 352 kg/MWh electricity respectively for these plants. Figure 4 shows the assumed electricity prices for all days, except five winter days per year when prices are assumed to peak at € 89/MWh for ten hours each day and € 169/MWh for one hour each day [30].

RESULTS AND DISCUSSION

Studies using NPV only when assessing profitable CO₂ reduction potential through CHP investments implicitly assume unlimited investment resources. In reality, however, investment resources are not always regarded as unlimited. This study analysed how the assumption of unlimited or limited investment resources affected the assessment of profitable reduction of CO₂ emissions by evaluating CHP and HOB investments in a DHS at a local utility using two cash flow techniques.

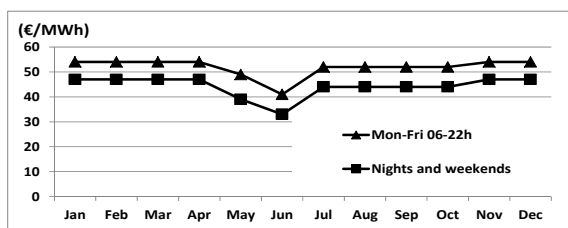


Figure 4. Assumed prices of electricity, except for peak days. Annual real increase assumed to be 1.5 % [30]

Table 4. Initial investment (I_0) and capacity of new boiler for each scenario

	Initial investment* [M€]	Optimal capacity of bio-fuelled boiler [MW _{steam}]	Capacity of replaced boiler [MW _{steam}]	Capacity of additional HOB [MW _{steam}]
S1	69.4 (64.5)	100	56	49
S2	74.4 (64.5)	100	130	99
S3	93.8 (93.8)	99	0	0
S4	17.1 (9.6)	24	0	75

*Investment costs in brackets do not include the costs of additional oil-fuelled HOBs

The optimal investment for each scenario, the investment that gives the lowest present value of FSC for the DHS, is presented in Table 4. Based on the assumptions made, similar boiler capacities were reached for all three CHP scenarios (S1-S3). However, the boiler capacities for replacing boilers (S1 and S2) were limited to 100 MW due to a lack of space and would otherwise have been higher. The replacement scenarios (S1 and S2) had lower initial investments than the new bio-fuelled CHP (S3) since the existing building and much of the auxiliary equipment could be reused in the replacement scenarios. This was not outweighed by the costs for additional oil-fuelled HOBs with which the replacement scenarios were burdened in order to make the scenarios equivalent with regard to available heat production capacity for peak and reserve purposes. When the optional investment was a bio-fuelled HOB (S4), the optimal bio-fuelled boiler capacity was comparatively low. The owner of this DHS deemed that it was impractical to handle such a small HOB given the size of the changes in heat demand [30].

The base production of heat with waste-fuelled CHP was the same in all scenarios (Fig. 5). For the CHP scenarios (S1-3) the mid-merit production was similar, although the replacement scenarios (S1 and S2) had a slightly higher heat production capacity from the replacing bio-fuelled CHP due to the lower power-to-

heat ratio compared to S3. However, the peak production of the CHP scenarios differed since S1 and S2 comprised the replacement of the coal-fuelled and oil-fuelled CHPs respectively. In addition, the order of priority for MSE bio HOBs was affected in all CHP scenarios due to limitations in the capacity of the transit main. The production of S4 with the new bio-fuelled HOB was similar to the reference scenario. However, the new bio-fuelled HOB increased the total capacity of bio-fuelled HOBs, decreasing the operation time of the oil-fuelled CHP and oil-fuelled HOBs.

The change in electricity production for each scenario (Fig. 6) compared to the reference scenario (325.5 GWh/year) was used when estimating avoided CO₂ emissions. All CHP scenarios (S1-S3) increased total electricity production by the DHS. The new bio-fuelled CHP (S3) generated the greatest increase in electricity production due to a higher power-to-heat ratio and because no existing CHP capacity was replaced. In contrast, a new bio-fuelled HOB (S4) replaced some of the heat production of existing CHPs, thereby decreasing total electricity production by the DHS.

When investment resources were considered to be unlimited, NPV was used to determine whether an investment was profitable and to rank the investments. The replacement of the existing oil-fuelled CHP (S2) was the preferred investment since it had the highest NPV, although it was just 1.6 % higher than the new bio-fuelled CHP (S3) (Fig. 7). The negative NPV for the new bio HOB (S4) is noteworthy. Although this bio-fuelled HOB had a lower present value of FSC before corporate taxes than the reference scenario, NPV dropped below zero when Swedish corporate taxes were considered.

When coal-fuelled electricity was replaced, the greatest total global reduction in CO₂ came from the new bio-fuelled CHP (S3) (Fig. 7), correlating with the greatest increase in electricity production in the DHS (Fig. 6). The same applied when natural gas-fuelled electricity was replaced, but less clearly.

However, based on the EAAR measure used to complement the NPV result when investment resources were limited, the most profitable investments were the two replacement scenarios (S1 and S2) (Fig. 8). EAAR of these investments was almost 30 % higher than EAAR for investing in a new bio-fuelled CHP (S3). EAAR of the bio-fuelled HOB was negative since it had a negative NPV.

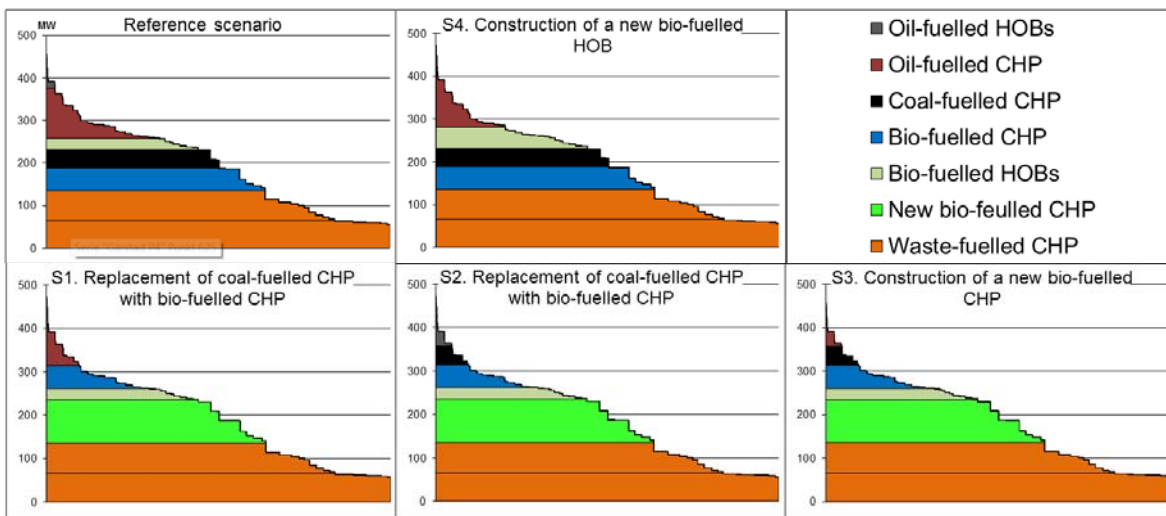


Figure 5. Duration diagrams (somewhat simplified) showing optimised heat production in each scenario

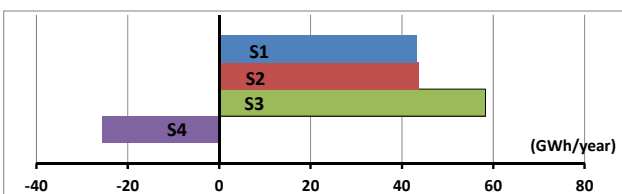


Figure 6. Change in electricity production by Linköping DHS

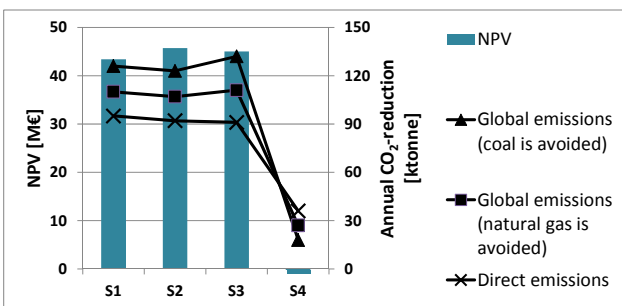


Figure 7. Total measures: NPV and total emission reductions

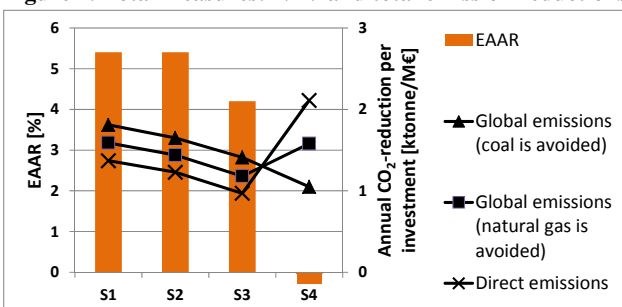


Figure 8. Relative measures: EAAR and relative emission reductions

Emissions reduction per euro invested is of interest when investment resources are considered limited. Here, both replacement scenarios (S1 and S2) gave a higher reduction per euro invested than the new bio CHP (S3) (Fig. 8) due to the high initial investment of the new bio-fuelled CHP (S3). The replacement of the coal-fuelled CHP (S1) had the highest global reduction effectiveness when replacing coal-fuelled electricity production. When natural gas-fuelled electricity production, which has a lower emissions factor than coal-fuelled electricity production, was replaced, the replacement of the coal-fuelled CHP (S1) and the HOB alternative (S4) were approximately equal in terms of global reduction per euro invested. Finally, when only direct reduction was considered (which is equivalent to assuming that electricity production with zero CO₂ emissions is replaced), then the new bio-fuelled HOB (S4) produced the greatest emissions reduction per euro invested (Fig. 8).

Thus if investment resources are unlimited, in this case study the replacement of the oil-fuelled CHP (S2) was the preferred investment. The new bio-fuelled CHP was a good runner-up and would also result in a greater reduction in global CO₂ emissions. On the other hand, if investment resources are limited, both replacement alternatives (S1 and S2) would clearly be preferred over the new bio-fuelled CHP (S3), both from a profitability perspective and when considering global reduction effectiveness. The replacement of the coal-fuelled CHP (S1) had the highest global reduction effectiveness.

However, an investment with positive NPV may not necessarily be considered sufficiently profitable to be implemented when investment resources are limited. Uncertain price forecasts and long implementation times entail greater risk for the investments included in this study, whereby EAAR of at least 6-8 % would be required by the owner of the DHS. With EAAR of 4.2-5.4 %, it is less likely that any of these CHP alternatives would be accepted as an investment and therefore less likely that the associated CO₂ emissions reductions would be achieved.

The correlation between changes in direct and global fossil CO₂ emissions was also analysed. One important assumption of this study was that the electricity market in northern Europe would work as it does today, with marginal electricity production consisting of the most expensive production needed to balance the system. Two alternative technologies of future marginal electricity production were assumed: coal-fuelled and natural gas-fuelled plants. Changes in direct emissions from the DHS system and the investment's effect on global CO₂ emissions were calculated. Based on the assumptions made, the results showed that investment in a bio-fuelled CHP (S1-3) in a CHP-based DHS could reduce global CO₂ emissions more than direct emissions when electricity from coal-fuelled or natural gas-fuelled electricity production was replaced. Between 15 and 41 ktonne of CO₂ reduction per year could take place outside Sweden. They also showed that investment in a bio-fuelled HOB, when introduced to a CHP-based DHS, could reduce global CO₂ emissions less than direct emissions would be reduced. When investments in CHP or in measures that affect production in existing CHP-based DHS are considered, changes in direct CO₂ emissions are therefore not necessarily representative of changes in global emissions.

CONCLUSIONS

Based on the assumptions made, the results showed that the profitability ranking of investment alternatives can differ depending on whether investment resources are considered to be unlimited or limited. Furthermore, the results indicated that this difference in ranking could bring about a smaller reduction in global CO₂ emissions when investment resources were considered to be limited than when they were considered to be unlimited. Investments that are profitable according to the NPV rule may, however, not be implemented at all since they are not necessarily considered to be sufficiently profitable when investment resources are regarded as limited. Consequently, whether investment resources are assumed to be unlimited or limited can have a significant impact on the assessment of profitable global CO₂ reduction potential.

Information about whether investment resources are assumed to be unlimited or limited, as raised by Stankeviciute *et al.* [3], is therefore of interest when presenting an assessment of profitable CO₂ reductions, since this can affect the conclusions drawn. If assessments are based on the assumption of unlimited investment resources, relevant information regarding prospective investments could be provided if, for example, a method indicating how net cash flow relates to investment costs for the prospective investments were included. Alternatively, basic information on assumptions about cost of capital (interest), lifetime and estimated NPV and investment costs, for example, is vital.

The analysis of the correlation between the abatement of direct and global emissions showed that when investments in CHP or in measures that affect production in existing CHP are considered, a local view on CO₂ emissions could be counterproductive to the reduction in global CO₂ emissions. This could be an important factor to take into consideration, for example when developing climate goals for municipalities, nations or other geographical areas.

ACKNOWLEDGEMENTS

The authors wish to thank Tekniska verken i Linköping AB for financial support. We would also like to thank all the participants in the work groups at Tekniska verken i Linköping AB who contributed important input data. The usual disclaimer applies.

REFERENCES

- [1] European Parliament. Directive 2012/27/EU of the European Parliament and of the Council of 25 October 2012 on energy efficiency, amending Directives 2009/125/EC and 2010/30/EU and repealing Directives 2004/8/EC and 2006/32/EC, (2012).
- [2] European Commission. Energy 2020 A strategy for competitive, sustainable and secure energy. (2010)
- [3] L. Stankeviciute, AK. Riekkola. "Assessing the development of combined heat and power generation in the EU". *Int. J. Energy sector Management*, Vol. 8, (2014) pp.76-99.
- [4] M. Danestig, A. Gebremehdin, B. Karlsson. "Stockholm CHP potential – An opportunity for CO₂ reductions?" *Energy Policy*, Vol. 35, (2007) pp. 4560-4660.
- [5] Å. Löfgren, K. Millock, C. Nauges. "The effect of uncertainty on pollution abatement investments: Measuring hurdle rates for Swedish industry". *Resource and Energy Economics*, Vol 30, (2008) pp. 475-491.

- [6] JH. Lorie, LJ. Savage. "Three problems in rationing capital". *The Journal of Business*, Vol. 4, (1955) pp. 229-239.
- [7] P. Bergknut, J. Elmgren-Warberg, M. Hentzel. 4th ed. *Investering i teori och praktik (Investment in theory and practice. In Swedish)*. Studentlitteratur. (1981).
- [8] A. Skorek-Osikowska, T. Bartela, J. Kotowicz, A. Sobolewski, T. Iluk, L. Remiorz. "The influence of the size of the CHP (combined heat and power) system integrated with a biomass fuelled gas generator and piston engine on the thermodynamic and economic effectiveness of electricity and heat generation". *Energy*, Vol. 67, (2014) pp. 328-340.
- [9] S-Å. Nilsson, I. Persson. *Investeringsbedömning (Investment appraisal. In Swedish)*. Liber Ekonomi, Malmö (1998).
- [10] AB. Jaffe, RN. Stavins. "The energy-efficiency gap: what does it mean?" *Energy Policy*, Vol 22, (1994) pp. 804-810.
- [11] L. Weber. "Some reflections on Barriers to the efficient use of energy". *Energy Policy*, Vol. 25, (1997) pp. 833-835.
- [12] F. Venmans. "Triggers and barriers to energy efficient measures in the ceramic, cement and lime sectors". *J. Cleaner Production*, Vol. 69, (2014) pp. 133-142.
- [13] AK. Dixit, RS. Pindyck. *Investment under uncertainty*. Princeton university press. Princeton. (1994).
- [14] G. Sundberg, J. Sjödin. "Project financing consequences on cogeneration: industrial plant and municipal utility co-operation in Sweden". *Energy Policy*, Vol. 31, (2003) pp. 491-503.
- [15] M. Wickart, R. Madlener. "Optimal technology choice and investment timing: A stochastic model of industrial cogeneration vs. heat-only production". *Energy Economics* Vol. 29, (2007) pp. 934-952.
- [16] T. Brunzell, E. Liljebloom, M. Vaihekoski. "Determinants of capital budgeting methods and hurdle rates in Nordic firms". *Accounting and finance*, Vol. 53, (2013) pp. 85-110
- [17] JR. Graham, CR. Harvey. "The theory and practice of corporate finance: evidence from the field". *J. Financial Economics*, Vol. 60, (2001) pp. 187-243.
- [18] *EU Energy in figures Statistical pocketbook 2015* (2015).
- [19] <http://www.ssb.no/energi-og-industri/statistikker/elektrisitetaar/aar/2015-03-25> [accessed 01.05.16]
- [20] <http://www.nordpoolspot.com/How-does-it-work/> [accessed 09.12.14]
- [21] http://www.energimarknadsinspektionen.se/Documents/Publikationer/fakta_och_informationsmaterial/Sa_satts_ditt_elpris.pdf [accessed 14.12.14]
- [22] <http://www.svk.se/Drift-och-marknad/Statistik/Elstatistik-for-hela-Sverige/> [accessed 26.03.15]
- [23] syspower.skm.no [accessed 22.04.15]
- [24] IPCC. *Climate Change 2007: Mitigation of climate change. Working Group III: Mitigation of climate change. 4.4.3.1 Plant efficiency and fuel switching* (2007).
https://www.ipcc.ch/publications_and_data/ar4/wg3/en/ch4s4-4-3-1.html [accessed 04-09-2014]
- [25] I. Nohlgren, S. Herstad Svärd, M. Jansson, J. Rodin. *El från nya och framtida anläggningar 2014, Elforsk rapport 14:40 (Electricity from new and future plants 2014 Elforsk Report 14:40. In Swedish.)* Elforsk. (2014).
- [26] European Parliament. *Directive 2003/87/EC of the European Parliament and of the Council of 13 October 2003 establishing a scheme for greenhouse gas emission allowance trading within the Community and amending Council Directive 96/61/EC* (2003).
- [27] European Parliament. *Directive 2009/29/EC of the European Parliament and of the Council of 23 April 2009 amending Directive 2003/87/EC as to improve and extend the greenhouse gas emission allowances trading scheme of the Community*, (2009).
- [28] *Lag om elcertifikat (Electricity Certificate Act. In Swedish)*. SFS 2011:1200. Swedish Parliament. (2011).
- [29] *The Electricity Certificate System 2012. Report no. ET2012:31*. Swedish Energy Agency. (2012).
- [30] *Tekniska verken i Linköping AB* (publ)
- [31] D. Henning. "Cost minimization for local utility through CHP, heat storage and load management". *Int. J. Energy Research*, Vol. 22, (1998) pp. 691-713.
- [32] D. Henning. *Optimization of local and national energy systems; Development and use of the MODEST model (Dissertation No. 559)*. Linköping University (1999).
- [33] A. Gebremedhin. *Regional and industrial co-operation in district heating systems. Dissertation No. 849, 2003*. Linköping University. (2003).
- [34] K. Difs, M. Bennstam, L. Trygg, L. Nordenstam. "Energy conservation measures in buildings heated by district heating – A local energy system perspective". *Energy*, Vol. 35, (2010) pp. 3194-3203.

- [35] D. Djuric Illic, E. Dotzauer, L. Trygg. "District heating and ethanol production through polygeneration in Stockholm". *Applied Energy*, Vol. 91, (2012) pp. 214-221.
- [36] D. Knutsson, S. Werner, EO. Ahlgren. "Combined heat and power in the Swedish district heating sector - impact of green certificates and CO2 trading on new investments". *Energy Policy*, Vol. 34, (2006) pp. 3942-3952.
- [37] E. Dotzauer. "Greenhouse gas emissions from power generation and consumption in a Nordic perspective". *Energy Policy*, Vol. 38, (2009) pp. 701-704.
- [38] J. Gode, K. Byman, A. Persson, L. Trygg. Miljövärdering av el ur systemperspektiv (Environmental assessment of electricity from a system perspective. In Swedish). IVL Swedish Environmental Research Institute. (2009).
- [39] The Council of the European Union. Council directive 2003/96/EC restructuring the Community framework for the taxation of energy products and electricity. (2003).
- [40] Lag om skatt på energi (Law on energy tax. In Swedish). SFS 1994:1776. Swedish parliament. (2010).
- [41] Swedish Environmental Protection Agency. Emissionsfaktorer, växthusgaser och luftföroreningar från förbränning (Emission factors, GHG and air pollutants from combustion. In Swedish). <http://www.naturvardsverket.se/Stod-i-miljoarbetet/Vagledning/Luft-och-klimat/Beraknatslapp-av-vaxthusgaser-och-luftfororeninga/> [accessed 26.03.15]

HEAT COLLABORATION FOR INCREASED RESOURCE EFFICIENCY: A CASE STUDY BETWEEN A REGIONAL DISTRICT HEATING SYSTEM AND A MINE

Louise Trygg¹, Curt Björk², Peter Karlsson², Mats Rönnelid³, Danica Djuric Ilic¹

¹Linköping University, SE-581 83 Linköping, Sweden

²IndLast, SE-590 34 Tjällmo, Sweden

³Dalarna University, SE-791 88 Falun, Sweden

Keywords: *District heating, mine, collaboration, system perspective*

ABSTRACT

To rapidly develop sustainable energy systems is crucial for the whole society's transition towards sustainability. System efficiency and reduced climate impact are important parts of this. Swedish district heating systems are fairly well developed and mainly based on non-fossil fuels. Increased use of district heating is therefore considered as a way to phase out fossil energy for heating purposes. Furthermore, the increased use of district heating provides a basis for further combined heat and power production. Considering that coal condensing is the marginal production of electricity in Europe, enhanced use of district heating leads to even greater reductions of global carbon dioxide emissions when considering an energy system with combined heat and power production.

The aim of this paper is to study system impact of increased demand of district heating by analyzing a collaboration on heat supply between the local energy supplier of Ludvika in Sweden and a nearby mine. The heating demand of the mine is analyzed and the consequences of connecting the heat demand of the mine with the municipal district heating system is analyzed using the cost optimization model MODEST. The results show that when the heating demand of the mine is integrated with the local district heating production in the city of

Ludvika, the overall energy system cost of the combined system of the energy utility and the mine is reduced with about 120 000 euro per year. The integration of the district heating system and the mine also leads to reduced emissions of global carbon dioxide.

INTRODUCTION

Energy systems of today significantly contribute to society's unsustainable situation [1], [2]. In Europe electricity use has a distinct connection to high CO₂ emissions [3]. Energy efficiency measures (EEMs) to lower the use of electricity are therefore particularly interesting. The potential of reducing electricity use is

especially high within industry [4]. In Sweden, per-capita use of electricity is among the highest in the world and a large part is used for processes that are not electricity specific, such as heating and drying. A likely explanation for such a high use is the historically low price of electricity [5]. Thus, both from a climate point of view and a more short-term economic point of view, there are good reasons for Swedish industries to make their use of electricity more efficient and, in some cases, to also convert from electricity to other types of energy carriers. There are also wider sustainability potentials from a systems perspective. Electricity-related EEMs in industry can free up electricity for vehicles, allowing for reductions of fossil fuels in the transportation sector. And most importantly, EEMs can pave the way for more renewable energy. With a more efficient use of energy, the total volume of renewables needed to replace current energy sources will be smaller and therefore easier to accomplish within sustainability constraints. Furthermore, the economic savings resulting from EEMs can be invested in development of renewables. Identification and implementation of EEMs should consequently be of great importance for Swedish industry in order to maintain its competitiveness as well as for society to promote sustainability in general. In the view of the high use of electricity in Swedish industries, energy audits have been performed in, e.g., industrial Small- and Medium-Sized Enterprises (SMEs). Generally, these studies show that there is a great potential for improved energy efficiency and that many of the identified measures would in fact be profitable (e.g. [6], [3], [7], [8]). For example, to study if and how Swedish industries can reduce their use of electricity and thereby change the relation between electricity and fuel, over 50 industrial SMEs in the Swedish municipalities of Oskarshamn, Örnsköldsvik, Ulricehamn, Borås and Vingåker were analysed. In the municipality of Oskarshamn, ten industrial energy audits were carried out in 2001 [6]. The municipalities of Örnsköldsvik, Ulricehamn, Borås and Vingåker were part of a pilot project of the programme "Sustainable Municipality", financed by the Swedish Energy Agency. The energy audits were carried out during 2003-2004

in about ten industrial SMEs in each of these municipalities [9], [10], [11]. The result of the study showed an average possibility to reduce the use of electricity within the range from 20% to 58%.

In the same way, previous studies have shown how cooperation on heat between an industry and a local district heating utility will lead to reduced system cost for the combined energy system [6].

The aim of this paper is to study system impact of increased demand of district heating by analyzing a collaboration on heat supply between the local energy supplier of Ludvika in Sweden and a nearby mine.

METHOD

The method used in this study consists of 2 different scenario calculations using the linear optimization program MODEST.

MODEST is an abbreviation of "Model for Dynamic Optimization of energy systems Time-dependent components and boundary conditions". MODEST is used to optimize the production of electricity, steam, heat and cold. The model calculates how the demand of energy should be met at the lowest cost taking into account variations in the short and long term when considering for example electricity prices and heating use. Other measures that can be modelled and studied with the MODEST model are consequences of more efficient use of electricity and conversion between electricity and heat.

The figure below shows schematically how MODEST is constructed by input, optimization and performance.

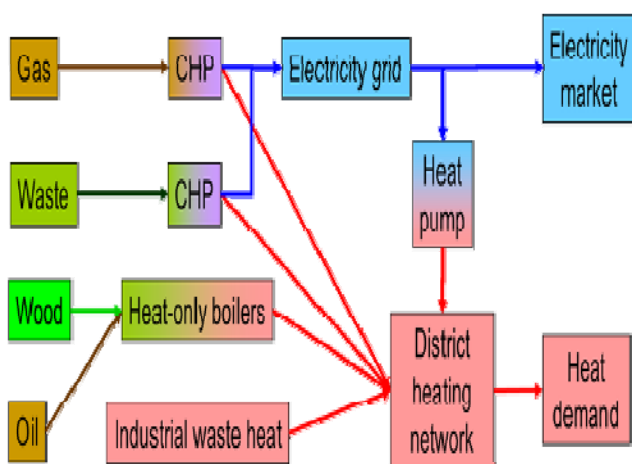


Figure 1 Schematic picture of the MODEST model [12]

The optimisations aim to minimise the total system cost of supplying the demand for heat and steam by finding the most optimal types and sizes of new investments and the best operation of existing and future plants. The total system cost is calculated as the present value of all capital costs of new installations, operation and maintenance costs, fuel costs, taxes and fees. In this study the system is optimised over a period of 10 years and the capital costs are based on a discount rate of 6%. Each year in the optimisation model is divided into seasons, which are then divided into daily periods to give a total of 28 different periods during one year [12].

The method assumes perfect conditions where the capacity of the plants is available and the demand for district heating and electricity is known. It is vital to stress that MODEST is not primarily a tool for operational optimisation, even if such an optimisation can be done in an approximate manner. MODEST has also no other aim than total minimisation of cost such It is also vital to stress that the MODEST model has its limitations as for example:

- Hourly and daily operations are not the aim of the model, although every hour of the year could be reflected. Even faster or continuous fluctuations can, however, not be treated at all.
- Binary variable and mixed-integer linear programming included in the model. This means that start-up costs cannot be represented and minimum operation capacity consequently must be modelled manually.
- Investment costs are stated per output unit (SEK/MW). This is important to point out since smaller installations are characterized by higher cost per capacity than larger installations.

Further limitations within the MODEST model are described in [12]

CASE STUDY

In this paper the energy utility in Ludvika are studied together with a nearby situated mine, Blötberget. The energy utility in Ludvik, VB Energi (Västerberglagens Energi AB), is owned by Vattenfall together with the municipalities of Ludvika and Fagersta in Sweden.

Table 1 below presents the production units for heta supply situated in Ludvika. The total production of heat is about 100 GWh annually

Tabel 1 Ludvika energy system

Boiler 1, pellets	10 MW
Boiler 2, pellets	10 MW
Flue gas condensor	5 MW
Accumulator	2 000 m ³

Tabel 2 Scenarios

Scenario BAU	Existing system where the heat demand of the mine is supplied by a local biofueled boiler, and thus are not connected with Ludvika district heating system.
Scenario COOP	Collaboration on heat demand which means that the mine and the district heating system of Ludvika is connected through a pipeline. The heat demand of the mine is thus supplied by heat from Ludvika's district heating network.

The heat demand of the mine Blötberget has been estimated to 6,4 GWh [13].

To study a collaboration on heat supply between the local energy supplier of Ludvika and the nearby mine Blötberget a model of the analysed energy system was designed using MODEST. Two different scenarios were analysed; (1) scenario BAU describing the existing energy system where the energy system of the municipality of Ludvika is not connected with the mine, and (2) scenario COOP which analyses the consequences of cooperation on heat supply between the mine and Ludvika district heating system.

RESULT

Analyzing the result from the two modeled scenarios gives possibilities to compare the system cost for the existing system and the combined system. Analyses show that when the two systems are not connected (scenario BAU) the total system cost for satisfying the heat demand of the mine and of the municipality of Ludvika is about 26 MEUR for the studied period of ten years.

When modelling a cooperation on heat. i.e when there is a pipeline connecting the district heating system of Ludvika with the mine (scenario COOP) the

corresponding system cost is about 25 MEUR for the studied period of ten years. This indicates that building a pipeline that connects the two energy system will lead to a more resource efficient use of energy and thus lower the joint system cost with about 120 000 EUR per year.

Connecting the two system will also lead to lower emissions of carbon dioxide. When connecting the heat system of the mine with the local district heating system the heat demand for the mine will be supplied by heat from Ludvika district heating system. This will lead to a more resource efficient energy system compare to when the mine has its own production of heat from local placed boilers.

CONLUCDING DISCUSSIONS

In a future sustainable energy system with high percentage of renewable energy source and in the same time low and volatile electricity price it will be of even greater importance to find measures that will support a full balanced energy system. More efficient use of electricity and conversion between electricity and district heating will play an important role. Increased use of district heating in combined heat and power (CHP) system will consequently lead to higher possibilities to increase the production of electricity. This gives CHP and district heating a prominent role in the design of a secure and fully balanced energy system.

In this study the effects of collaboration o heat demand between a municipal energy system and a nearby mine are analysed. Combining the two energy system will increase the heat load for the municipal district heating system. The result show that when these two separated energy system of the mine and of the municipality are connected in a way that there is a collaboration on heat, the total system cost will be reduced which indicates that it is more resource efficient to concentrate the production units on one geographic place compared to two having to different production sites.

The increased use of district heating will also open up possibilities to invest in a combined heat and power plant for the municipal energy system. This concludes that the suggested cooperation on heat will not only reduce the total energy system cost but also give possibility to produce electricity.

To further study the consequences of similar cooperation on heat different energy market scenario with variations regarding for example policy instruments and fuel prices needs to be analysed. In the same way it is recommend for further study how alternative solutions for the heating demand of the mine will effect a future cooperation on heat.

ACKNOWLEDGEMENT

The authors would like to thank Vinnova for financing this work. The authors also would like to thank Kathrine Abrahamsen and Lars Lindblom at High Voltage Valley for valuable support.

REFERENCES

- [1] Steffen, W., A. Sanderson, J. Jäger, P. D. Tyson, B. Moore III, P. A. Matson, K. Richardson, F. Oldfield, H.-J. Schellnhuber, B. L. Turner II, and R. J. Wasson, eds. (2004). *Global Change and the Earth System: A Planet Under Pressure*, IGBP Book Series. Heidelberg, Germany: Springer-Verlag.
- [2] IPCC. (2014.) "Climate Change 2014: Impacts, Adaptation, and Vulnerability. Part A: Global and Sectoral Aspects. Contribution of Working Group II to the Fifth Assessment Report of the Intergovernmental Panel on Climate Change", Cambridge University Press, Cambridge, United Kingdom and New York, NY, USA, 1132 pp.
- [3] Trygg, L., Karlsson, B. (2005). "Industrial DSM in a European electricity market - a case study of 11 industries in Sweden" *Energy Policy*, 33:1445-1459 Elsevier.
- [4] EC. (2005) *Green Paper on Energy Efficiency or Doing More With Less*. COM(2005) 265 final
- [5] [5] Stenqvist, C., (2014). *Industrial energy efficiency improvement – the role of policy and evaluation*. Dissertation. Lund University. Download at: <http://lup.lub.lu.se/record/4220512>
- [6] Trygg, L. (2004). "Generalized method for analysing industrial DSM towards sustainability in a deregulated European electricity market - method verification by applying it in 22 Swedish industries." *Proceeding of the 2nd International Conference on Critical Infrastructures*, Ed. J-C Sabonnadiere, s10-a2, Grenoble, France.
- [7] Thollander, P., Rohdin, P., Danestig, M. (2007). "Energy policies for increased industrial energy efficiency: Evaluation of a local energy programme for manufacturing SMEs", *Energy Policy*; 35(11): 5774-83.
- [8] Backlund, S., Thollander, P., (2015). *Impact after three years of the Swedish energy audit program*. Accepted for publication in *Energy*.
- [9] Henning D, Hrelja R, Trygg L. (2004). "Energianalys Örnköldsvik". (Energy analysis of Örnköldsvik, in Swedish) ER 15:2004, Swedish Energy Agency, Eskilstuna, Sweden.
- [10] Bohlin H, Henning D, Trygg L. (2004). "Energianalys Ulricehamn" (Energy analysis of Ulricehamn, in Swedish) ER 17:2004, Swedish Energy Agency, Eskilstuna, Sweden.
- [11] Gebremedhin A, Palm J. (2005). "Energianalys Borås" (Energy analysis of Borås, in Swedish, ER 28:2005, Swedish Energy Agency, Eskilstuna, Sweden.
- [12] Henning D. 'Optimisation of Local and National Energy Systems: Development and Use of the MODEST Model'1999, Dissertations No. 559, Linköping university, SE-581 83 Linköping, Sweden.
- [13] Björk C, Karlsson P, Jonson M (2015) 'Testbed efficient energy supply mines' report Vinnova

ENERGY PERFORMANCE OF DECENTRALIZED SOLAR THERMAL FEED-IN TO DISTRICT HEATING NETWORKS

Pilar Monsalvete Álvarez de Urbarrí^{1,2}, Ursula Eicker¹, Darren Robinson²

¹University of Applied Sciences, Schellingstrasse 24, Stuttgart, 70174, Germany

²University of Nottingham, University Park, Nottingham, NG7 2RD, United Kingdom

Keywords: District heating, distributed solar generation, solar thermal, prosumer, excess heat

ABSTRACT

Many papers have been written over the last years addressing the potential of decentralized solar thermal systems in District Heating Networks (DHN), assuming that the network can be used as a virtual storage so that prosumers can release excess solar energy into the network and use it later when it is needed.

When looking at the district heating systems in detail, many questions still remain unanswered. Is it possible to feed in all the surplus solar energy into the net? How does the solar input affect the network and the other prosumers? Is it sensible from the energy balance perspective? We have studied an existing DHN in an attempt to answer these questions.

A simulation model of the DHN in the Southern German city quarter Ludwigsburg-Sonnenberg was developed and extended to include decentralized feed-in of heat from solar thermal collectors to evaluate their potential contribution to network demands. It could be shown that prosumers supply during summer period significantly more heat than they demand, so that the thermal network could operate as an autonomous micro-grid.

By comparing the amount of electrical pumping energy that is needed to feed heat to the DHN with usable solar thermal energy, the benefit ratio of feeding heat into the DHN can be quantified.



Figure 1. Urban structure planning Grünbühl/Sonnenberg with a city extension to the South West (Source: City of Ludwigsburg)

INTRODUCTION

The present paper forms part of a larger research project investigating the intelligent management of an existing heating network.

The main objective of this project is the simulation of the integration of distributed renewable heat sources in the existing district heating network of Ludwigsburg-Sonnenberg and its extensions.

Among other possibilities contemplated within the project, this paper studies the integration of distributed solar heat generation and local storage in the new branch of the DHN, which will be built to feed a planned extension of the district (shaded area in Figure 1).

The new buildings to be constructed will become prosumers as they will be able to “consume” energy from the net as well as “produce” renewable energy for self-consumption or feeding into the net thanks to a solar thermal system.

The term “prosumer” is already used in the power sector [1],[12], and in recent years, starts to be also used in the thermal energy sector [2],[3],[9],[10],[11],[16], although we do acknowledge that this terminology is incompatible with the first law of thermodynamics.

BACKGROUND

Some papers have been written over the last years addressing the potential of decentralized energy systems in DHN as well as some of the possible technical problems that this connection could provoke.

Excess energy has first been discussed for the industrial sector in terms of the thermal energy contribution to DHN [13],[17].

More recently the concept has been extended to the residential sector.

An interesting overview of the state of the art includes distributed solar energy in DHN in combination with seasonal storage or using heat pumps [9]. The influence of excess heat production with seasonal storage has also been analysed [14].

Others investigate the benefits of local thermal storage for direct utilisation of heat from solar collectors in a dwelling connected to a DHN, but with no injection into

the net [7]; or connected and using the net as a virtual storage system [2].

The impacts of feed-in to the net have also been studied, in particular how the temperatures, pressure or flow rates and velocities can be affected by the introduction of small scale prosumers into the DHN [9].

But these past studies tend to treat the network as an ideal storage facility without constraints on capacity or dynamics, so that prosumers can release excess solar energy into the network and use it later when it is needed [2],[3],[7],[14]. This idealisation may lead to optimistic results especially for the warm seasons.

Thus, this study takes into account the possible thermal saturation of the net by simulating it together with the prosumers.

The simulation software INSEL8.2 [8] has been used to dynamically model the net thermodynamics [4], as well as the thermal (but not hydraulic) behaviour of the prosumers. The weather and the heat demand of the prosumers are considered as inputs to the model.

CASE STUDY AND MODEL DESCRIPTION

Geographical area and heat demand

Ludwigsburg is a city located in Baden-Wurttemberg in the South-west of Germany. Annually, this temperate region receives around 1.2 MWh/m² solar irradiation (Figure 2).

The city quarter Ludwigsburg-Sonnenberg, where the new residential area extension will be built, is mainly composed of dwellings that are connected to a 1.1 km long DHN that operates between 40°C and 70°C, supplied by a cogeneration engine (235 kW thermal) and a heat pump (200 kW thermal) with vertical geothermal heat exchangers.

An existing heating network branch in Sonnenberg, close to the new area has been selected to be modelled so that the obtained solar thermal potential can be extrapolated to the new area.

The selected branch has two different kinds of dwellings, five single-family and two multi-family houses (SFH and MFH respectively). Most are constructed according to the current energy saving standards, here denominated class 100 of the German financing institution KfW, but SFH1 is a passive house and SFH4 is class 55. This means that these buildings have a lower heating demand, around 20% and 55% of the upper permissible limit.

The dwellings have been numbered in the same order as they are connected to the DHN, first the five SFH and last the two MFH. Upstream of the SFH1 can be found the central heat source SFH1 can be found, which can deliver heat to the other nodes.

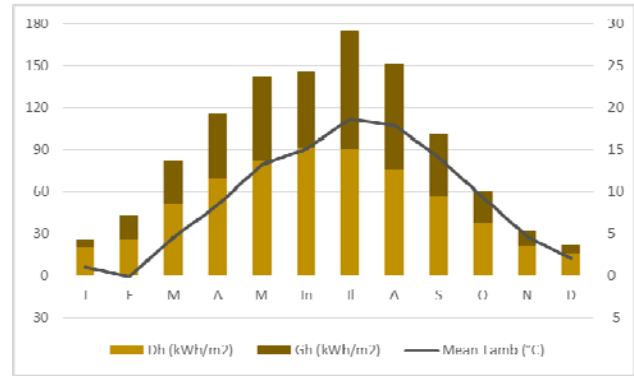


Figure 2. Monthly meteorological data extracted from the TRY of Ludwigsburg

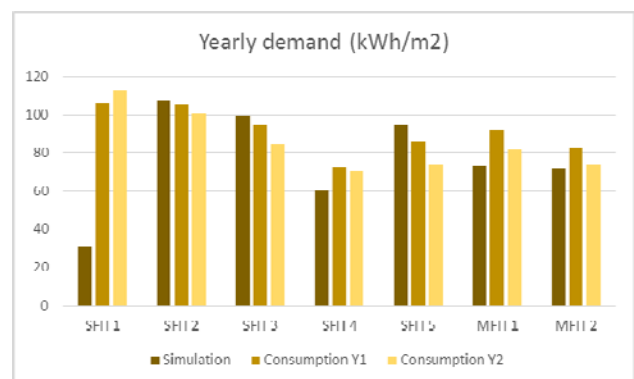


Figure 3. Simulated vs. observed heating demand for two different years

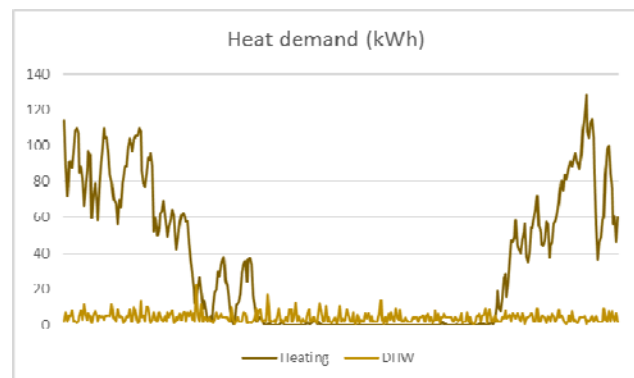


Figure 4. Simulated heat demand of MFH2

The space heating demands of the dwellings has been simulated using EnergyPlus [6] and the DHW demand with DHWcalc [15] using local Test Reference Year [5] weather data. Both demands together have been compared with the annual consumption during two different years measured and provided by the energy supply company of Ludwigsburg, from which a good match has been confirmed (Figure 3).

The only exception is SFH1. Taking into account that in passive houses the inhabitants' behaviour plays a much bigger role, the mismatching may be induced by

this fact. Nevertheless, this paper does not go deep into the demand simulation, so the obtained results have been considered good enough for the study especially when considering that in absolute terms the demand of SFH1 is only about 3% of the total demand.

These demands, together with the weather file are the main inputs of the model.

Figure 4 shows the daily resolved annual demand for both DHW of 22 kWh/m² annual and space heating of a multi-family house (MFH).

During the winter, the space heating demand dominates, while in summer there is only DHW demand.

The solar systems

In these buildings a solar thermal system was simulated with two different configurations, one for SFH and another for MFH (Figure 5 and Figure 6 respectively).

The main difference between them lies in the presence of a second storage tank with an intermediate heat exchanger in the case of MFH.

The same components of the system were selected for all dwellings. Table 1 and Table 2 show the simulation parameters of the collectors and tanks.

The primary storage tank volumes depend on the case, but the secondary tank ones are always 0.5 m³.

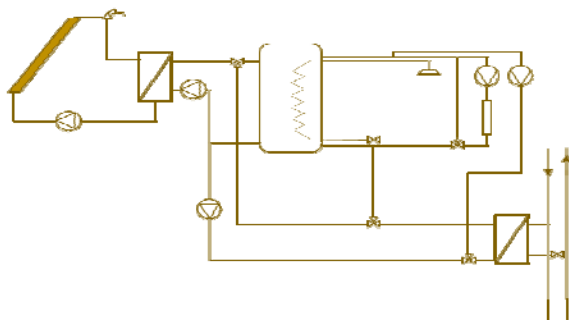


Figure 5. Solar thermal system for SFH

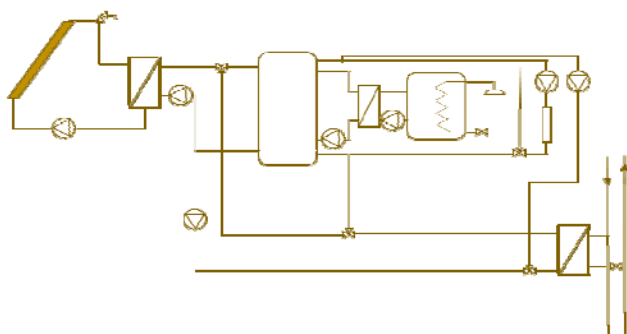


Figure 6. Solar thermal system for MFH

Table 1. Solar thermal collector data

Latitude (UTM)	Degree	48.77
Inclination of solar collector	Degree	30
a0 at normal incidence	-	0.644
Linear heat loss coefficient	W/(m ² K)	2.247
Quadratic heat loss coefficient	W/(m ² K ²)	0.015
IAM	-	0.9

Table 2. Storage tank data

Fluid	-	water
Overall eat loss coefficient	W/(m ² K)	0.5
Ambient temp. around tank	°C	8

The heat exchangers used in the solar systems as well as those connecting to the network are counterflow, with an overall heat transfer coefficient of 3 kW/K.

Those connected to the network have a pressure loss of 200kPa on the primary side.

Finally, a control system for pumps and valves with the following strategy has been included:

- Whenever the radiation is high enough, the solar collector pumps start working to feed the tank.
- If the tank is full (of energy), its energy is supplied to the net.
- If the tank is empty and the solar input is insufficient, the deficit is supplied from the net.
- The pumps or valves on the demand side work whenever there is a corresponding demand.

The scenarios

Our modelling scenarios are based on the characteristics presented in Table 3. Apart from the reduction factor (R_f), which indicates the energy standard as a percentage of the legal requirements (KfW value or the passive house standard), two other criteria have been defined: the reference heated area ratio (RAR) and the maximum solar area.

System dimension are similar for all dwellings of the same type, but take into account the reference heated area ratio as well as the construction type. So, the solar area for each dwelling i is calculated as in (1):

$$A_{coll}^i = A_{coll}^{ref} \cdot \frac{R_f}{100} \cdot RAR \quad (1)$$

Moreover, we assume that no more than half of the roof area is available for installation of solar collectors.

Table 3. Dwelling characteristics

	Heated area	R _f	Roof area	RAR	Max solar area
	(m ²)	(%)	(m ²)	(-)	(m ²)
SFH1	115.2	100	72	1	30
SFH2	130.4	100	85	1	30
SFH3	147.6	100	76.9	1	30
SFH4	127.7	20	79.8	1	30
SFH5	205.7	55	115.1	1.4	42
MFH1	2077.6	100	506.2	2	250
MFH2	1070.1	100	288	1	125

Table 4. Scenarios

Simulation case	Dwelling type	Reference solar area (m ²)	Tank volume (m ³ /m ²)
Case 1	SFH	10	0.05
	MFH	100	0.05
Case 2	SFH	30	0.05
	MFH	125	0.05
Case 3	SFH	10	0.2
	MFH	100	0.2
Case 4	SFH	10	0.05
	MFH	100	0.02
Case 5	SFH	Max solar area in all buildings	0.05
	MFH	Max solar area in all buildings	0.02
Case 6	SFH	Max solar area in all buildings	0.05
	MFH	Max solar area in all buildings	0.02
Case 7	SFH	Max solar area in all buildings	0.05
	MFH	Max solar area in all buildings	0.05

In all cases we considered a solar volume flow rate of 54 l/(hm²), and the following control constraints:

- Maximum solar collector temperature: 100 °C
- Maximum tank temperature: 97 °C
- Temperature to feed the net: 83 °C
- Minimum irradiance for starting solar pumps: 150 W/m²

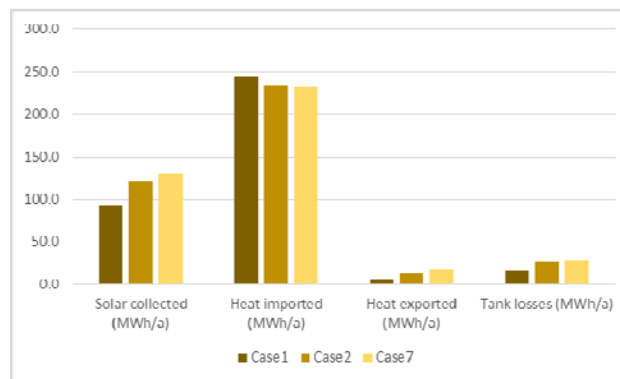


Figure 7. Effect of increasing collector area

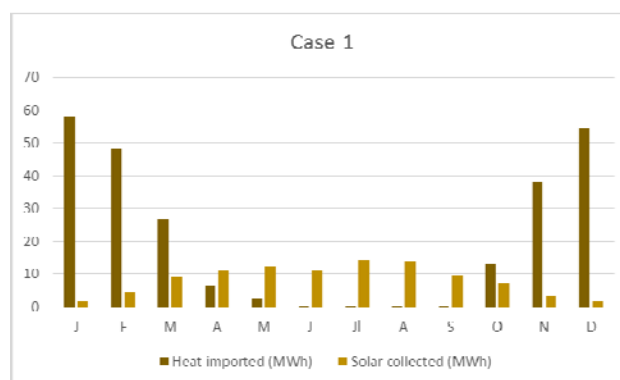


Figure 8. Monthly mismatch

Different scenarios have been proposed to study the impact of the solar systems as shown in Table 4.

Case 1 is considered the base case, to which several modifications have been tested.

The effect of increasing the solar collector area is shown comparing cases 1, 2 and 7. Comparing cases 3 and 4 with case 1, the effect of modifying the storage tank volume is studied.

Cases 5 and 6 show the importance of modelling the district heating net together with the prosumers, so the effect of the saturation of the network can be taken into account. Case 5, is normally connected to the network and case 6 is connected to a network with infinite virtual storage.

The saturation of the network is one of the main issues found in the literature, where in most cases the network behaves as an infinite virtual thermal storage system. This idealisation normally leads to optimistic results.

RESULTS

The first interesting output from the study is that, even though the solar energy collected increases with the solar area and also with the tank volume this does not necessary lead to bigger savings.

Figure 7 compares cases 1, 2 and 7, increasing the collector area but conserving the volume ratio.

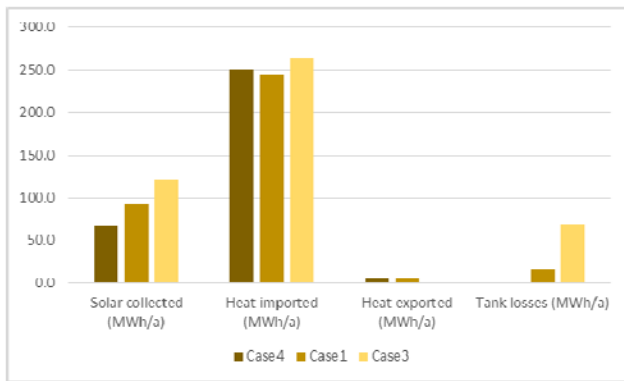


Figure 9. Effect of modifying tank volume

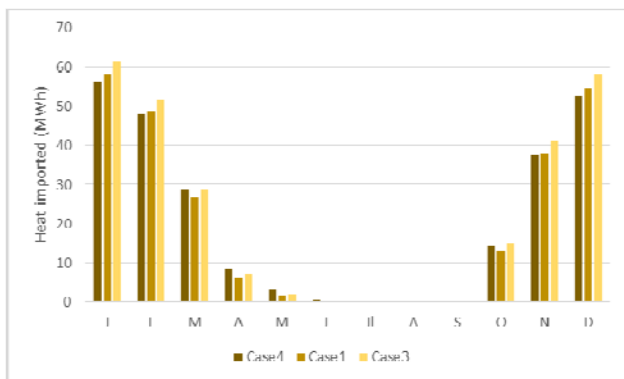


Figure 10. Monthly disaggregation

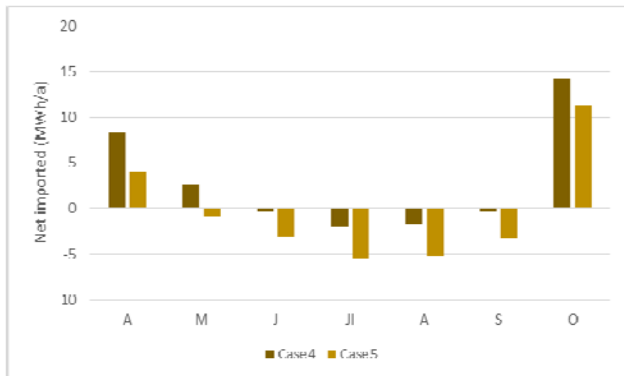


Figure 11. Net energy imported from network during warm period

It can be seen how the collected solar energy increases with the collector area, but from case 2 to 7 there isn't substantial reduction in the imported energy. This is due to asynchronicity in periods with higher demand and higher solar energy conversion. (Figure 8).

A similar situation occurs when increasing the tank volume. Up to a certain point increasing the volume leads to an increase in the solar energy collected and a reduction of the imported energy. But if the volume is too big, the extra solar energy collected is mainly used to reach the operation temperatures. Also a higher volume means higher tank losses (Figure 9).

Furthermore, a bigger tank implies bigger losses and, therefore, more imported energy during winter time (Figure 10.).

Figure 11 shows the difference between imported and exported energy to the network, called here "net imported".

As expected, this net imported energy is negative during the summer season, the magnitude depending upon the solar system capacity (the figure shows the results for the smaller and bigger systems considered in this study). The negative values mean that during those months the dwellings export more energy that they import from the net. This energy, as there is no storage considered in the network branch, is transformed into net losses or exported out of the branch to the main network. Nevertheless, this suggests that isolation of the branch is feasible.

Looking more closely, it can be observed that a storage facility in the branch is needed to actually carry out this disconnection. That is true especially at the extremes of the period (Case 4 in Figure 12) and not that pronounced for intermediate months (Figure 13). An increase of the total storage volume of the prosumers is another option but can increase demand for imported energy during winter as discussed before. Furthermore, seasonal storage in the branch could extend the period of disconnection.

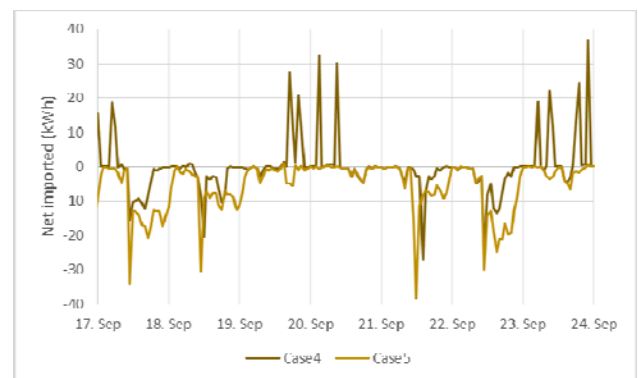


Figure 12. Hourly net exported energy in a week in September

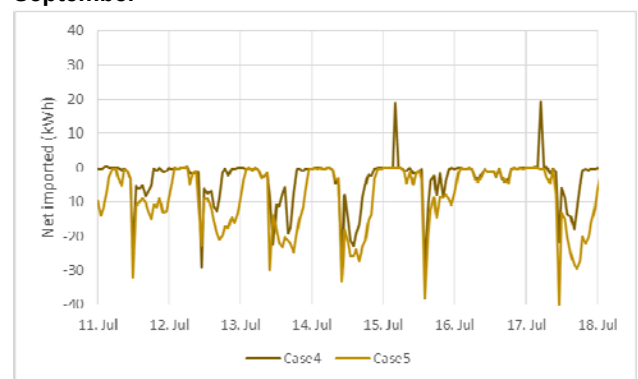


Figure 13. Hourly net exported energy in a week in July

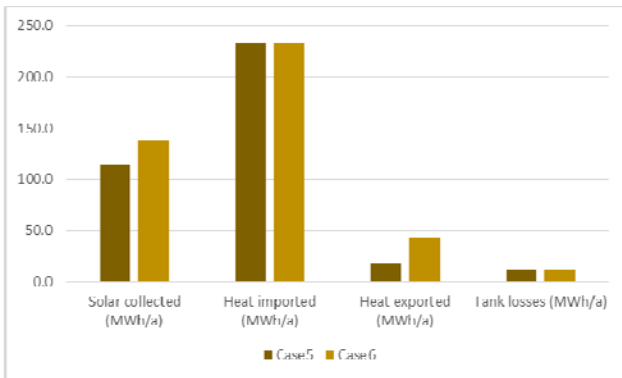


Figure 14. Comparison between ideal and not ideal network

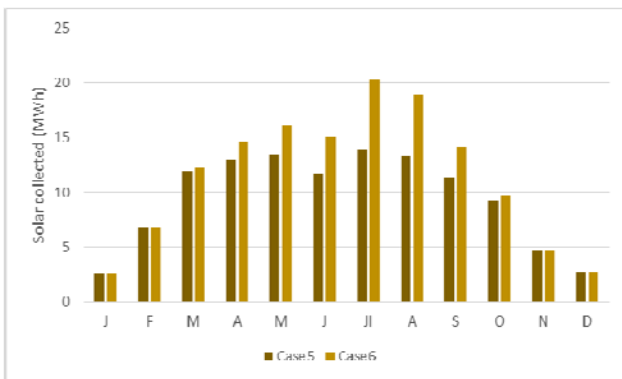


Figure 15. Solar energy collected for cases 5 and 6

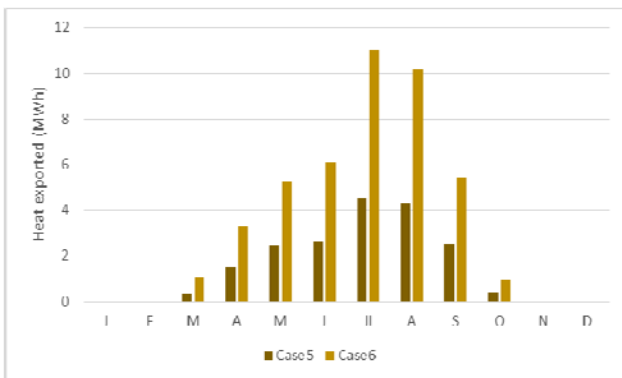


Figure 16. Heat exported for cases 5 and 60

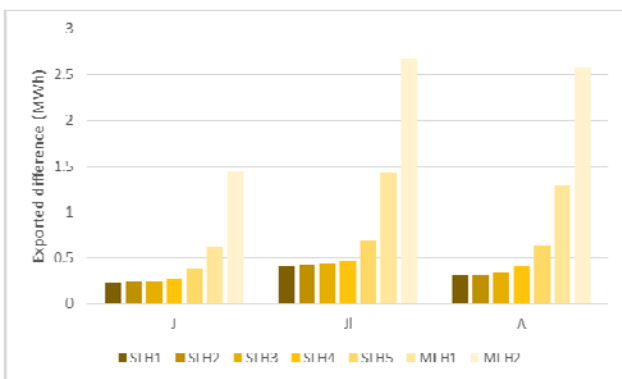


Figure 17. Impact of saturation in downstream neighbours

Finally, Figure 17 how saturation of the net impacts on downstream neighbours. The more remote the dwelling from the starting point of the branch, the difference between the ideal exported energy of case 6 and the exported in case 5 grows. A bigger difference means the more difficult it is to export the energy into the net. This is due to the rise of the temperature of the return line. Every subsequent dwelling experiences a reduced temperature drop; reducing the capacity to export heat.

Table 5 and Table 6 summarise the main results from this study. The annual demand for all the cases is 311.1 MWh.

Figures 14 to 17 show the behaviour of the system with or without the idealisation of the network.

Figure 14 shows how including the thermodynamics of the net in the simulation (Case 5) results in a decrease of heat exported compared to the ideal case (Case 6). This leads to a reduction of the total solar energy that the system is able to collect, which is more prominent during the summer season (Figure 15 and Figure 16).

The energy consumed by the pumps has been calculated assuming that the pumps operate with a constant efficiency always, as the dynamics of the prosumer are not simulated. A correlation of the power of the pumps as a function of the mass flow has been extracted from a water pumps catalogue.

$$E_p = \sum_i P_i \cdot h_i \quad (2)$$

Where h_i are the hours of operation of each pump and P_i its power calculated with the correlation as in (3).

$$P_i(W) = 7.897 + 35.104 \cdot \dot{m}_i(kg/s) \quad (3)$$

The first column in Table 6 presents the energy savings that are calculated as the total demand minus the imported energy (it is assumed that the reference case is a consumer dwelling which has no internal system and takes all the needed energy from the net). Between 20 and 25% of the total demand can be saved by the solar thermal systems. As discussed before, the larger energy savings result from the larger solar area but with an adequate storage volume ratio. For example, case 3 has smaller savings because the volume ratio is too big.

The second column compares the specific solar energy collected. The values are in general rather low, but they could be increased if the network had a storage facility to store the exported energy (compare cases 5 and 6).

Finally, two ratios are calculated and presented in the table. The first one is the specific energy used by pumps which gives an idea of how much electrical energy is needed for every kWh saved. The ratios are

very low, which is very positive from an energy saving perspective.

The potential contribution of the solar systems is between 20% and 25% of the total demand, with specific auxiliary energy requirements lower than 7%.

Table 5. Results summary 1

Case	Collector area	Tank volume	Solar collected	Heat imported	Heat exported	Net imported	Pump for exporting heat	All pumps consump.
	(m ²)	(m ³)	(MWh/a)	(MWh/a)	(MWh/a)	(MWh/a)	(MWh/a)	(MWh/a)
1	341.5	18.1	92.6	244.5	5.6	238.9	0.183	2.9
2	499.5	26.0	121.7	233.9	14.0	219.9	0.292	3.7
3	341.5	69.3	121.7	262.5	1.0	261.5	0.017	2.8
4	341.5	9.1	67.7	250.0	5.5	244.5	0.131	2.8
5	537.0	16.6	114.5	233.1	18.7	214.4	0.292	3.7
6 (ideal)	537.0	16.6	137.9	233.1	43.3	189.8	0.077	3.6
7	537.0	27.9	129.7	232.6	7.9	224.7	0.321	3.8

Table 6. Results summary 2

Case	Energy savings	Specific solar energy	FE _p / FE _s	FE _p / FE _e
	(MWh/a)	(kWh/m ² a)	%	%
1	66.6	271.1	3.8	8.3
2	77.2	243.7	6.1	5.3
3	48.7	356.2	5.0	4.5
4	61.1	198.4	4.0	6.1
5	78.0	213.1	6.6	4.0
6 (ideal)	78.1	256.8	6.3	0.5
7	78.6	241.5	6.6	4.6

The second ratio is the specific energy used only for the pump used to export the heat into the net. This ratio can be useful for the energy supply company of Ludwigsburg, which operates the network and has to calculate the costs for selling or buying energy from the prosumers.

Cases 2 and 5 are the most promising of those studied, in terms of both savings and exported heat. The choice between these two may however lie in other considerations, such as available room for storage tanks or the difference in price between solar collectors and storage tanks (Case 5 involves a larger collector area and case 2 a larger storage volume); factors that are not taken into direct account in this study.

CONCLUSION

An existing heating network branch in Sonnenberg has been modelled and used in this paper to evaluate the questions exposed in the abstract.

During the summer season, this contribution is high enough to enable the branch to be isolated for about three months (depending on the size of the solar thermal system). The period can be increased if a seasonal storage facility is added to the branch.

Furthermore, the study indicates that bigger solar systems do not necessarily imply higher savings, mostly because of the asynchronicity in periods with higher demand and higher solar energy conversion. Again, seasonal storage in the net could help to increase the total savings for bigger systems.

Finally, the thermodynamics of the network must to be taken into account. When the network is not idealised, the influence of the first prosumers to the others is considered, as well as the total thermal capacity of the net, resulting in lower but more realistic values of exported energy.

ACKNOWLEDGEMENT

The authors gratefully acknowledge the European Commission for providing financial support during conduct of research under FP7-PEOPLE-2013 Marie Curie Initial Training Network "CI-ENERGY" project with Grant Agreement Number 606851.

The authors would also like to thank the leaders of the project "Simulationsbasierte Optimierung energieeffizienter Wärmenetze mit Umsetzung in EnEff:Stadt Ludwigsburg", included in the EnEff:Stadt research initiatives promoted by the Federal Ministry of Economics and Energy in Germany for providing data for this study.

And finally, Ruben Pesch and Ilyes Ben Hassine for their suggestions and discussions during the work.

REFERENCES

- [1] A. Di Giorgio and F. Liberati, "Near real time load shifting control for residential electricity prosumers under designed and market indexed pricing models", *Applied Energy*, Volume 128, 1 September 2014, Pages 119-132.
- [2] B. Di Pietra, F. Zanghirella and G. Puglisi, "An Evaluation of Distributed Solar Thermal "Net Metering" in Small-scale District Heating Systems", *Energy Procedia*, Volume 78, November 2015, Pages 1859-1864.
- [3] E. Vesaoja, H. Nikula, S. Sierla, T. Karhela, P. Fliikkema and C-W. Yang, "Hybrid modeling and co-simulation of district heating systems with distributed energy resources", In *Workshop on Modeling and Simulation of Cyber-Physical Energy Systems (MSCPES)*, (April, 2014), pp. 1-6.
- [4] I.B. Hassine and U. Eicker, "Control Aspects of Decentralized Solar Thermal Integration into District Heating Networks", *Energy Procedia*, Volume 48, 2014, Pages 1055-1064
- [5] I.J. Hall, R.R. Prairie, H.E. Anderson and E. Boes, 1978. "Generation of Typical Reference Years for 26 SOLMET stations". Sandia Laboratories Report SAND 78-1601, Albuquerque, NM, USA.
- [6] J. Feng., Y. Ding and H.W. Wu, *EnergyPlus energy simulation software [Software]*, (2012). Website: <https://energyplus.net/>
- [7] J. Heikkinen, M. Rämä, K. Klobut and A. Laitinen, "Solar Thermal Integration Into A District Heated Small House", Submitted to the 14th International Symposium on District Heating and Cooling, 2014 Stockholm.
- [8] J. Luther and J. Schumacher-Gröhn, *INSEL- A Simulation System for Renewable Energy Supply Systems [Software]*. Version 8.2. Website: <http://www.insel.eu/>
- [9] L. Brand, A. Calvén, J. Englund, H. Landersjö and P. Lauenburg, "Smart district heating networks – A simulation study of prosumers' impact on technical parameters in distribution networks", *Applied Energy*, Volume 129, 15 September 2014, Pages 39-48.
- [10] L. Brand, P. Lauenburg and J. Englund, "District Heating Combined With Decentralised Heat Supply In Hyllie, Malmö", Submitted to the 14th International Symposium on District Heating and Cooling, 2014 Stockholm.
- [11] L. Brange, J. Englund and P. Lauenburg, "Prosumers in district heating networks – A Swedish case study", *Applied Energy*, Volume 164, 15 February 2016, Pages 492-500.
- [12] R. Schleicher-Tappeser, "How renewables will change electricity markets in the next five years", *Energy Policy*, Volume 48, September 2012, Pages 64-75.
- [13] S. Broberg, S. Backlund, M. Karlsson and P. Thollander, "Industrial excess heat deliveries to Swedish district heating networks: Drop it like it's hot", *Energy Policy*, Volume 51, December 2012, Pages 332-339.
- [14] S. Nielsen and B. Möller, "Excess heat production of future net zero energy buildings within district heating areas in Denmark", *Energy*, Volume 48, Issue 1, December 2012, Pages 23-31.
- [15] U. Jordan and K. Vajen, 2000. *DHW-calc. [Software] Version 1.10: Universitat Kassel*.
- [16] U. Ottosson, "Next generation district heating – Findings and lessons from the project", Submitted to the 14th International Symposium on District Heating and Cooling, 2014 Stockholm.
- [17] U. Persson, B. Möller and S. Werner, "Heat Roadmap Europe: Identifying strategic heat synergy regions", *Energy Policy*, Volume 74, November 2014, Pages 663-681.

EXERGY ANALYSES ON THE USER-SIDE THERMAL FACILITIES OF KOREAN DISTRICT HEATING SYSTEM

B.Y. Jang¹, C. Lee¹, H.W. Park², H. Kim², J. Y. Yi², J.S. Eom³, S. Y. Im³

¹Dept. of Mech. Eng., Univ. of Suwon, Hwaseong, Republic of Korea

²Yujin Energy Consulting Co., Anyang, Republic of Korea

³Korea District Heating Corp., Seoul, Republic of Korea

Keywords: Exergy Analysis, User-side Thermal Facility, District Heating System

ABSTRACT

The present study conducts energy and exergy analyses on four different user-side thermal facilities of Korean district heating systems with different thermal configurations and operation conditions. Exergy analysis method is developed and applied to the field test results of the user-side facilities to calculate their exergy destructions and efficiencies. From the present exergy analysis results, the overall exergy efficiencies of Korean user-side thermal facilities are ranging within 50~70%, and the main exergy destructions are observed in the heat exchangers for residential heating and hot water supply.

INTRODUCTION

In Korea, district heating system are supplying thermal energy to 1.36 million households in many urban areas, and it is composed of cogeneration power plants producing thermal energy, thermal pipe networks transporting the thermal energy and user-side thermal facilities supplying end-users the thermal energy. Therefore, the thermal efficiency of the Korean district heating system can be improved by reducing energy losses of the three subsystems. The cogeneration plant and the thermal pipe networks have been being efficiently operated by the Korean District Heating Corp.(KDHC) as public-sector supplier. However, for past 30 years, the most of Korean user-side thermal facilities have not shown any significant technological advances in energy saving because they have been owned and operated by private-sector users. For this reason, there are growing R&D demands and concerns on high efficiency user-side thermal facility.

Exergy is known as very useful concept for analyzing available energy in thermal system and its analysis methods were applied to various thermal systems and showed remarkable energy saving effects[1,2,3]. Therefore, in order to reduce energy loss and improve thermal efficiency of Korean user-side thermal facility, exergy analysis method can be applied to investigate the locations and the

magnitudes of energy losses of facility and used to find the methods for energy loss reductions.

In the present study, the exergy analysis method is developed and applied to investigate the operation and energy utilization status of four different user-side thermal facilities of Korea. Prior to exergy analyses on the Korean user-side thermal facilities, on-site measurements are made on the operation conditions of each facility component such as temperature, pressure and mass flow rate, and then exergy analysis method is applied to the measured results. From the present exergy analysis results, the locations and the magnitudes of exergy destruction/loss are determined and then component and overall facility exergy efficiencies are calculated.

CONFIGURATION OF KOREAN USER-SIDE THERMAL FACILITY

As shown in Fig.1, Korean user-side thermal facility is composed of two heat exchanger units where the thermal energy of heat source water supplied from the distribution network of KDHC is utilized for the residential heating and the hot water supply of households. The heat source water stream from the KDHC is distributed to two streams for residential heating(HX1) and hot water supply(HX2 & HX3) heat exchangers to heat up water streams recirculated through households. As can be seen in Fig.1, in residential heating heat exchanger(HX1), some part of supplied water(DHS) is bypassed and then mixed with returned water(DHR). Hot water supply heat exchangers(HX2 & HX3) are installed to reheat the temperature of returned water(HWR) upto the supplied water(HWS) and to preheat make-up water. It is noted that all the heat exchangers used in the Korean facilities are plate-types, and linked at three mixing points(MP1, MP2 and MP3). In addition to the above-mentioned heat exchangers, there are auxiliary components such as pumps, valves and flow meter equipped on water pipelines in the user-side facility.

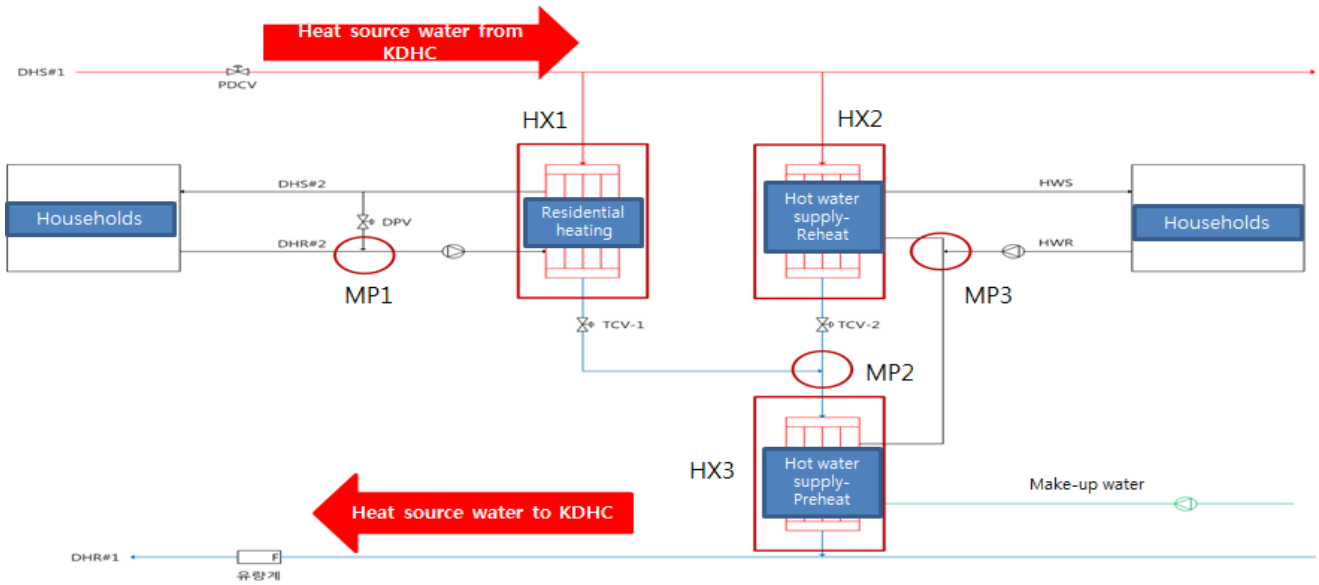


Figure 1. Process Flow Diagram of Korean User-side Thermal Facility

EXERGY ANALYSIS METHOD

According to the theoretical formulation by Wu et al.[3], the specific flow exergy(e_x) of open system is defined as

$$e_x = h - h_{\infty} - T_{\infty}(s - s_{\infty}) \quad (1)$$

where h , s and T are specific enthalpy, entropy and temperature of water liquid, and subscript ∞ stands for surrounding condition.

Applying and integrating the equation (1) from inlet to outlet of heat exchanger, total exergy variation(ΔEx) of water fluid for heat exchanger as open system can be determined as

$$\Delta Ex = m C_p (T_o - T_i - T_{\infty} \ln \frac{T_o}{T_i}) - m v \Delta p \quad (2)$$

where m , C_p , v and T represent mass flow rate, specific heat and specific volume of water, and subscripts o and i mean outlet and inlet of heat exchanger.

Referring to Fig. 2, the energy effectiveness(ϵ) and the exergy effectiveness(ϵ_e) as heat exchanger performance indices[4] are defined as follows:

$$\epsilon = \frac{T_{hi} - T_{ho}}{T_{hi} - T_{ci}} = \frac{\epsilon(A-R)NTU - 1}{\epsilon(A-R)NTU - R} \quad (3)$$

$$R = \frac{(\dot{m} C_p)_{\min}}{(\dot{m} C_p)_{\max}} \quad (4)$$

$$\epsilon_e = \frac{\text{actual exergy transfer rate}}{\text{max. possible exergy transfer rate}} = \frac{\epsilon(1-\epsilon) - \epsilon_e \ln(1+\epsilon) + \epsilon(1-\epsilon)/\epsilon_i - \frac{\epsilon^2}{\epsilon_{pa} \epsilon_{to}} \Delta p}{1 - \epsilon + \epsilon_e \ln \epsilon} \quad (5)$$

$$U = \frac{\dot{Ex}}{\dot{F}_{hi}}, \quad U_D = \frac{\dot{Ex}}{\dot{F}_{hi}} \quad (6)$$

where Δp and NTU represent pressure drop and the number of transfer unit of heat exchanger, and subscripts c , h represent cold, hot streams of heat exchanger.

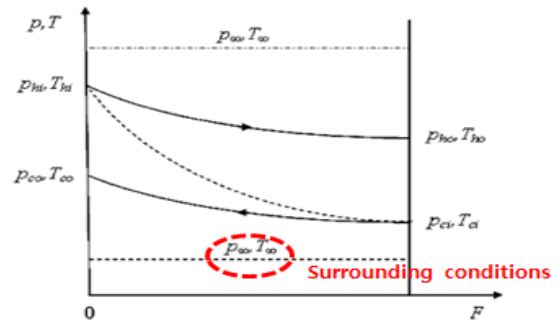


Figure 2. Typical heat transfer profile in a heat exchanger.

Exergy efficiencies for component and system are defined as the ratio of net exergy product to net exergy fuel[1], so the overall exergy efficiency of user-side thermal facility can be expressed as

$$\epsilon_e = \frac{\text{energy gains through heat exchangers}}{\text{net energy input from KDHC to facility}} \quad (7)$$

EXERGY ANALYSIS RESULTS

The present study considers four Korean user-side thermal facility models(A, B, C and D) with different configurations and operation conditions. Referring to Fig.1, the models of A, B and D have no HX3, while the model C has HX3. Prior to the exergy analyses on four different Korean user-side thermal facilities, on-site measurements were conducted on the operation parameters of water streams in the facilities, temperature, pressure and mass flow rate. The present measurements were made at the outside conditions of

1 atm and -15°C, 0°C, 5°C or 3°C for model A, B, C or D.

Based on the on-site measurement results, the present study conducts energy/exergy analysis on each flow element such as heat exchanger, valve or mixing point. After the energy/exergy calculation of each flow element, system exergy analysis is carried out to determine to overall facility exergy destruction/loss and efficiency. In calculating entropy and exergy of water from the measured data, the present study uses the IAPWS(The International Association for the Properties of Water and Steam) formulation[5].

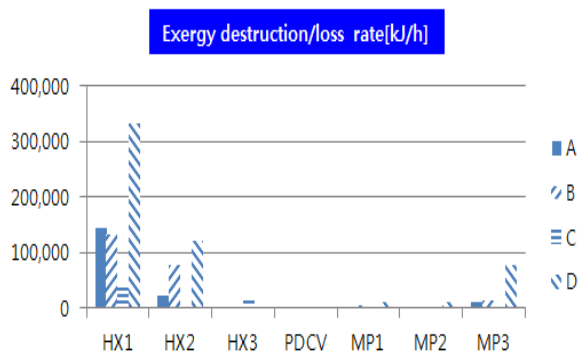


Figure 3. Exergy destruction/loss rates in facilities

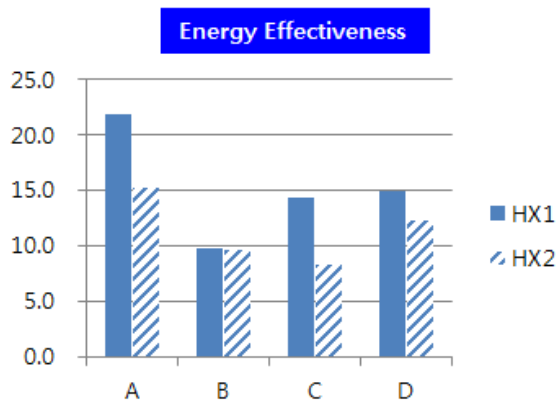


Figure 4. Energy effectiveness of heat exchanger

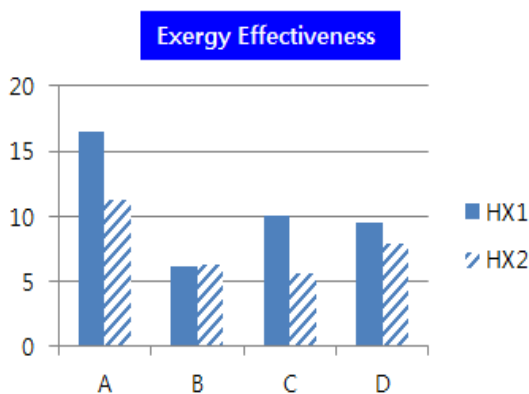


Figure 5. Exergy effectiveness of heat exchanger

Fig. 3 shows the magnitudes and the locations of exergy destructions/losses in the four facilities. Comparing the magnitude of exergy destruction/loss of each location in a facility, regardless of facility model, the exergy destruction in HX1 is much bigger than those in other locations. This means that the thermal efficiency reduction of facility would be influenced mainly by the inefficient operation of residential heating heat exchanger(HX1). As also shown in Figs. 4 and 5, HX1 is operated with very low energy or exergy effectiveness of 10~20% or 10~15%.

Table 1 Comparisons on the operation parameters of heat exchangers

Description	Energy Effectiveness(%)		NTU		Exergy Effectiveness(%)		Supply-return Temp. Difference[C]		Bypass Ratio(%)	
	A	B	A	B	A	B	A	B	A	B
HX1	21.9	9.8	0.2560	0.1041	16.5	6.14	14	6	0.3	25.0
HX2	15.3	9.7	0.1677	0.1027	11.3	6.26	9	6	-	-

Description	Energy Effectiveness(%)		NTU		Exergy Effectiveness(%)		Supply-return Temp. Difference[C]		Bypass Ratio(%)	
	C	D	C	D	C	D	C	D	C	D
HX1	14.3	15	0.1559	0.1653	10.0	9.52	7	9	22.2	18.2
HX2	8.3	12.3	0.0873	0.1320	5.6	7.85	4	7	-	-
HX3	67.2	-	1.4201	-	52.7	-	24	-	-	-

Table 1 summarizes the operation conditions of three heat exchangers in the four facilities. From the results of Table 1, it can be known that all the heat exchangers are operated at relatively low supply-return temperature differences, 6~24 °C, compared with the heat source water temperature difference, 46~56 °C. Table 1 also shows the most of residential heating heat exchangers(HX1) are operated with high by-pass ratio within 18~25%. These operation modes of the heat exchangers with low supply-return temperature difference and high by-pass ratio cause very low energy, exergy effectiveness or NTU.\

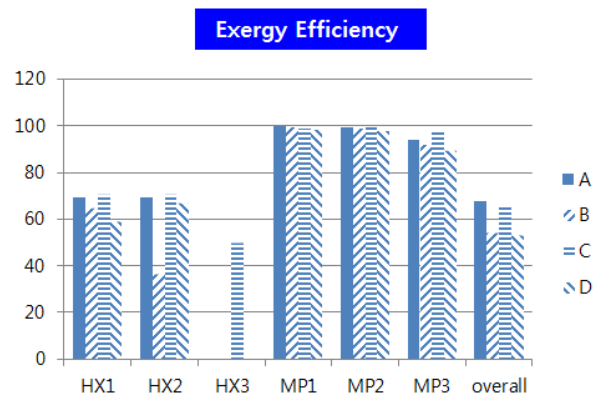


Figure 6. Exergy efficiencies of component and system

Fig.6 shows the comparisons on the component and the overall facility exergy efficiencies of the four thermal facilities. The exergy efficiencies of heat exchangers(HX1, HX2 and HX3) are within 36~70%, while all the mixing elements(MP1, MP2 and MP3) are operated with the high exergy efficiencies of 90~99%. The overall facility exergy efficiencies are within 53~67%. These comparison results also show that the overall facility exergy efficiencies are reduced mainly due to the inefficient operations of heat exchangers and the mixing elements have minor effects on overall facility efficiency.

CONCLUSION

Exergy analyses are made on four Korean user-side thermal facilities, and their analysis results are investigated to determine the magnitudes and the locations of exergy destructions/losses in the facilities. The present analysis results show that the main exergy destructions occur at the heat at heat exchanger units and overall facility exergy efficiencies are within 53~67%. The overall facility exergy efficiency can be improved by increasing the supply-return temperature

difference and/or decreasing the by-pass ratio of heat exchanger.

ACKNOWLEDGEMENT

The authors wish to thank the research grant from Korea District Heating Corp.(KDHC).

REFERENCES

- [1] A. A. Bejan, G. Tsatsaronis and M. Moran, "Thermal Design & Optimization," John Wiley & Sons, Inc., 1996, ch3, pp.113-166.
- [2] I. Baldwinsson and T. Nakata, "A comparative exergy and exergoeconomic analysis of a residential heat supply system paradigm of Japan and local source based district heating system using SPECOC(specific exergy cost) method," *Energy*, vol. 74, pp.537-554, 2014.
- [3] S. Y. Wu, X. Yuan, Y. Li and L. Xiao, "Exergy transfer effectiveness on heat exchanger for finite pressure drop," *Energy*, vol. 32, pp.2110-2120, 2007.
- [4] G. F. Hewitt, G. L. Shires and T.R. Bott, *Process Heat Transfer*. Begellhouse; 1994.
- [5] Revised Release on the IAPWS Industrial Formulation 1997, IAPWS, 2007.

PREDICTIVE SUPPLY TEMPERATURE OPTIMIZATION OF DISTRICT HEATING NETWORKS USING DELAY DISTRIBUTIONS

L. Laakkonen¹, T. Korpela², J. Kaivosoja¹, M. Vilkkö², Y. Majanne², M. Nurmoranta¹

¹Valmet Automation Ltd, Lentokentäkatu 11, 33900, Tampere, Finland

²Tampere University of Technology, Dept. of Automation Sci. and Eng., Korkeakoulunkatu 3, 33720 Tampere, Finland

Keywords: *District Heating, Flexibility, Supply Temperature, Optimization*

ABSTRACT

Fluctuating power production in combined heat and power (CHP) plants may cause unwanted disturbances in district heating (DH) systems, which leads to the situation that the best efficiency in CHP production is not achieved. DH -systems are often automated, however, supply temperature is still primarily chosen manually by the operator. This is because of the uncertain heat demand in near future and uncertain behaviour of delay from heat supplier to consumers, which make the temperature scheduling problematic.

In this work, future heat demand and return water temperature are predicted based on outdoor temperature forecast and process data history using neural network estimators. Consumers in network are presumed to be similar, but their distances from production site vary thus creating a distribution function of range. Delay is modelled as a distribution function based on the distances between heat consumers and the suppliers, which weights the supply temperatures from last few hours calculating the average supply temperature received by the consumers. The derived function models how the temperatures develop along the network, finally covering the entire network.

A brute force optimizer was developed to minimize both pumping costs and heat losses as well as to smooth temperature gradient originated thermal stresses. System delays are fixed during an optimization cycle, and after each cycle the delays are updated according to new system flowing rates and the optimization is recalculated. The resulting supply temperature curve is a discrete curve that cuts the heat load peaks by charging and discharging the energy content of the District heating network (DHN). Optimization keeps the supply water temperature and flow rates in control and stabilizes the network smoothly and efficiently after disturbances. Optimization is demonstrated by using case data of one year from a district heating system in Finland.

INTRODUCTION

Control of district heating systems (DHS) consists of pressure controls and temperature controls. Pressure

controls regulate the pump stations to produce desired mass flow and pressure difference for DH customers. Dynamics of pressure transients are relatively rapid enabling the utilization of basic control methods. Transient dynamics of temperature behaviour along the network is related with the flow rate of DH water typically resulting to delays of several hours. Varying transport delay behaviour, estimation of heat consumption, and definition of optimal supply temperature are issues that have contributed for the current situation of low level of automation in temperature controls. For those reasons the supply temperature is usually set manually by operator according to the time of the day and the outdoor temperature.

With functional supply temperature controls the heat losses and pumping costs can be balanced to provide minimum running costs of the system. It also enables the utilization of DH network energy storage capacity to avoid temporary starts of supporting heat stations with significantly higher running costs. According to [1]...[5] the supply temperature is usually set too high if it is ran manually.

There are not many DHS applying advanced control methods to control supply temperature even though the subject has been studied a lot. Production optimization has been studied already in 1980s and [6] studied supply temperature optimization in early 90s. Temperature optimization is usually connected with the solution of the unit commitment and economic dispatch problems [5]. Other optimization methods are presented in [7]...[9]. Supply temperature can also be controlled by model based control methods [2], [10], [3] and [11]. However, most of the methods do not consider pressure dynamics but assume that mass flows can be produced within certain boundaries. Including pressure dynamics to the system model improves the results slightly, but complicates the calculations significantly.

The result of optimization can be at its best as good as the forecast used for heat consumption and customer return temperature estimation. Consumption and return temperature can be determined by stochastic black box

and grey box models as ARX [2], neural network [12], and soft computing [13].

District heating network (DHN) can be modelled from one generalized customer to all real customers. There is a significant potential to create exact models of pipe networks as there usually exist a lot of measured data from the network. The challenge is the decision of the level of generalization. Whole DHN of Uppsala in Sweden was modelled in [3] by TERMIS, but the simulation was too slow to be used for control purposes. Hereby the model should be simple. However, the heat delivery distribution can be modelled as a distribution function based on real DHN dimensions, which is presented in this paper.

HEAT LOAD MODEL

The heat consumption depends on customer behaviour affected by weather and daily routines. Process model, such as neural network model can be trained to model that behaviour. In this work, the heat load and return water temperature are both modelled by a neural network. Inputs to neural network presented in Figure 1 are heat loads from 24, 48, 72 hours and 7 days ago. Also the average heat load from last 24h, outdoor temperature forecast and day of the week as a binary variable are used as model inputs. There are 10 neurons in the hidden layer that are trained using Levenberg-Marquardt algorithm.

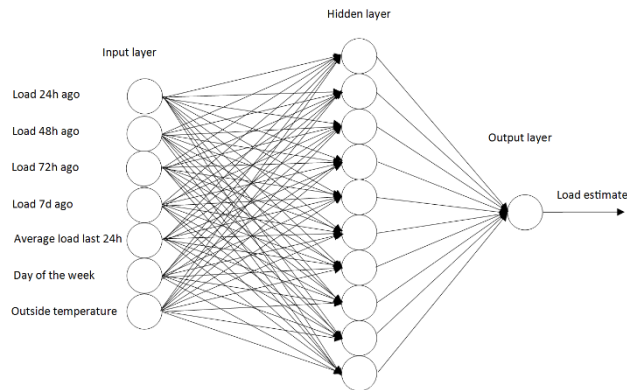


Figure 1. Neural network model for heat load predictor

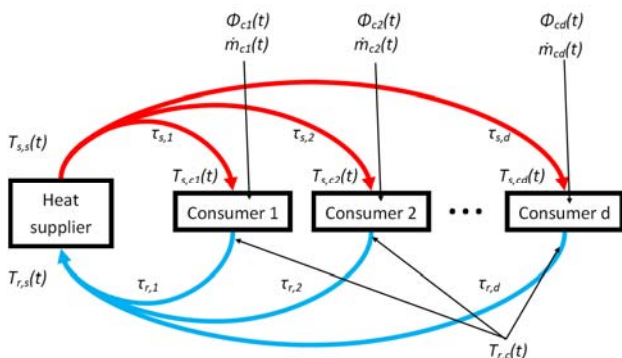


Figure 2. Delay distribution model

It is assumed that all heat consumers behave similarly according to the average consumption. When the whole DHN is reduced into one consumer, the consumption can be presented as [14]

$$\phi_c = \dot{m}_c c_p (T_{s,c} - T_{r,c}), \quad (1)$$

where customer heat load ϕ_c is calculated from mass flow \dot{m}_c at the customer, supply water temperature $T_{s,c}$, return water temperature $T_{r,c}$ and heat capacity c_p of water. Heat consumption can be determined by data collected from consumer substations. However, online data from customer substations is not usually available and so the heat consumption has to be calculated from production plant data as [2]

$$\phi_c(t) \approx \dot{m}_c(t) c_p (T_{s,s}(t - \tau_s) - T_{r,s}(t + \tau_r)),$$

where $T_{s,s}$ is the supply water temperature and $T_{r,s}$ the return water temperature at heat supplier. τ_s is the delay from supplier to customer and τ_r the delay from customer back to supplier.

Return water temperature model

Return water temperature depends on weather and similar to heat load follows a daily pattern. Therefore it is modelled according to the same principle except the heat loads are replaced with return water temperature measurements.

DELAY DISTRIBUTION MODEL

Delay distribution is a function to model the different transport delays to customer around the DHN. According to Figure 2, there are d customers that have similar delays. Each consumer is fixed such that 1st consumer has delay of 1 time step, 2nd consumer delay of 2 time steps etc. The current heat load is distributed to the consumers based on mass flow rate such that during high flow rate the heat load is weighted on consumers with short delays.

In the example case, the distribution function is based on the real distances from production plant to customer along with DH delivery pipes. It is assumed that the water flows to the customers along the shortest route.

All the real individual customers have reference consumptions $\phi_{c,i}$ and certain distance from presumed production plant that is dependent on current production plan. With the exact network data, it is possible to calculate how much consumption exists within certain range from suppliers.

$$\phi_p = \sum_{i=1}^d \phi_{c,i}, \quad (3)$$

where $p \in \mathbb{Z}$ is the range interval between suppliers and customers, r is the distance of customer to presumed supplier and ϕ_p is the total heat load within certain range. Histogram of heat load is formed using (3) and placed into

$$f_{range} = \frac{1}{\sum_{p=1}^n \phi_p} \begin{bmatrix} \phi_1 \\ \phi_2 \\ \vdots \\ \phi_n \end{bmatrix}, \quad (4)$$

where unscaled probability vector f_{range} is based on predetermined heat load distribution on range axis. The distribution is scaled according to reference mass flow of the network \dot{m}_j to fit into time scale $j = 32$ time steps. The probability function is scaled into time axis by scaling function f with following inputs. The discrete moment of time $k \in \mathbb{Z}$ and the discrete time step of optimization Δt is a constant, such that $\Delta t \in \mathbb{R}, \Delta t > 0$.

$$f_{time}(k\Delta t) = f(f_{range}, \dot{m}_j(k\Delta t)). \quad (5)$$

Function f scales f_{range} according to scaling parameter \dot{m}_j such that low value spreads the function in time scale. Finally f fits the scaled probability function into vector of j time steps. Theoretical customer temperature $T_{s,c,h}$ without disturbances is

$$T_{s,c,h}(k\Delta t) = [T_{s,s}(k\Delta t) T_{s,s}((k-1)\Delta t) \dots T_{s,s}((k-f)\Delta t)] f_{time}(k\Delta t). \quad (6)$$

Delay distribution model also considers heat losses and pumping energy, which are considered with network-specific parameters in equation

$$T_{s,c}(k\Delta t) = T_{s,c,h}(k\Delta t) - K_1 \bar{\tau}(k\Delta t) (T_{s,c,h}(k\Delta t) - T_g(k\Delta t)) + K_2 \dot{m}_c(k\Delta t)^x, \quad (7)$$

where K_1 is heat loss factor, $\bar{\tau}$ the average delay, K_2 pumping energy factor, T_g temperature of ground surrounding the pipes and x the parameter to determine the relation between pressure difference and mass flow.

BRUTE FORCE OPTIMIZER

Because of the process nonlinearity with varying distributed delay, derivation of a linearized process model is a complex task. Instead, brute force search will calculate all the possible trajectories of supply water temperature within prediction horizon. There might be restrictions in gradients, upper and lower boundaries, fixed initial and final values, which must be included in the calculation. The optimizer calculates the mass flow presented in Eq. (1), according to supply temperature $T_{s,c}$ by Eq. (7), estimated return temperature and heat demand.

Trajectories are formed within certain constraints to exclude the unreasonable ones before the calculation.

- Optimization is discrete with time step $\Delta t = 0.5$ hour. The dynamics of DHN is slow and rapid fluctuations in temperatures stress the network. Therefore shorter time step would not give any advantage.
- Trajectories have 7 possible gradients. $0 \text{ } ^\circ\text{C}/\Delta t$, $\pm 1 \text{ } ^\circ\text{C}/\Delta t$ for minor changes, $\pm 2 \text{ } ^\circ\text{C}/\Delta t$ for moderate changes and $\pm 5 \text{ } ^\circ\text{C}/\Delta t$ for extreme changes
- Only the first 6 time steps are optimized, while next 18 steps are fixed during optimization of one time step. Fixed time steps ensure that the final accumulation level of the network is same in all of the trajectories.

Thus the optimization of 24 hours horizon is formed by 48 stepwise optimizations. The cost function of optimizer is based on total production and delivery costs and penalty cost for rapid control changes

$$J(k\Delta t) = C_{pump}(k\Delta t) + C_{heatloss}(k\Delta t) + C_{penalty}(k\Delta t), \quad (8)$$

which consists of simplified cost functions

$$C_{pump}(k\Delta t) = a_1 E_{ei}(k\Delta t) \Delta p(k\Delta t) \dot{m}_c(k\Delta t), \quad (9)$$

$$C_{heatloss}(k\Delta t) = a_2 E_{fuel}(k\Delta t) \frac{[T_{s,s}(k\Delta t) - T_g(k\Delta t)]}{\dot{m}(k\Delta t)}, \quad (10)$$

$$C_{penalty}(k\Delta t) = a_3 [T_{s,c}(k\Delta t) - T_{s,c}((k-1)\Delta t)]^2, \quad (11)$$

where a_1 and a_2 and are constant parameters depending on system dimensions, a_3 is adapted according to other parameters, Δp is the reference

pressure difference over the pumps, T_g the ground temperature around the DH pipes. E_{fuel} is the average price of fuels used hourly and E_{el} the total price of electricity based on hourly spot price.

CASE STUDY

Optimization was applied in a municipal case study using DHN of Kuopio located in Eastern Finland. The DHN is operated by Kuopio Energia Oy, which has 5778 customers with total annual consumption of 865 GWh. There are two CHP plants at the same location near the city centre that produce 97 % (2015) of the annual heat demand. The plants use peat and biomass as main fuels and one of them is equipped with a flue gas condenser. Rest of the heat is produced by a small biogas CHP engine and eight oil-fired heat-only stations. The electricity production is maximized in CHP plants, because the electricity price is most of the time high enough to make it profitable. Hereby DHN should support electricity production by being operated with as low DH supply water temperature level and high flow rate of DH water as possible. Low return water temperature is also targeted as it increases the efficiency of flue gas condenser. Currently the supply water temperature is controlled manually in order to accumulate network before peak loads. The baseline is good, but without predictive controls the future events are difficult to calculate. [15]

RESULTS

Results are based on consumption data from customer substations and production data from automation system of power plants and DHN.

Heat load and return water temperature predictors

Neural network prediction error to target value depends on the quality of input data. Heat consumption and customer return water temperature predictions can be calculated from production data, but not accurately.

Table 1. Standard deviations (SD) and variances (VAR) of neural network predictors' errors

	Substation data as input	Production data as input
SD (MW)	5.69	7.00
SD (%)	7.82	9.71
VAR (MW ²)	56.5	82.9
T_g SD (°C)	0.59	0.83
T_g VAR (°C ²)	0.67	1.30

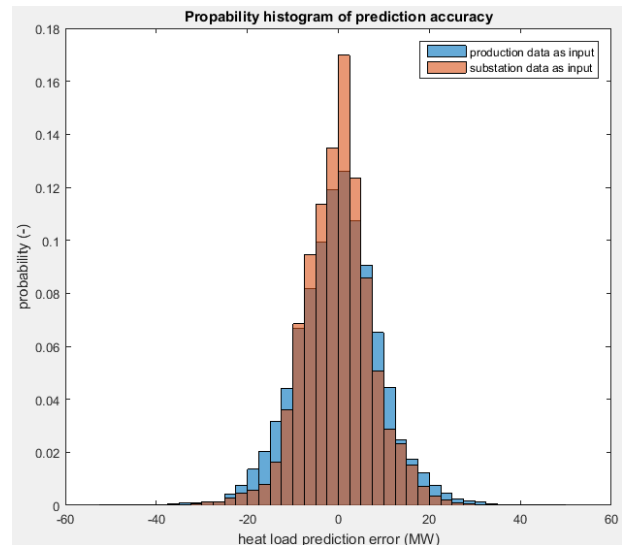


Figure 3. Heat load prediction accuracy

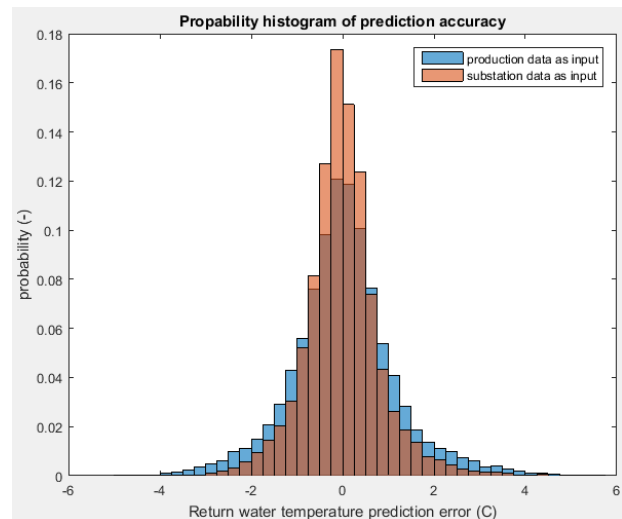


Figure 4. Return temperature prediction accuracy

The challenge may be that consumer substation data cannot be gathered online. In that case the consumption has to be estimated by using Eq. (2) Standard deviations (SD) and variances (VAR) of prediction errors are presented in Table 1. Histogram of the heat load predictor accuracy is presented in Figure 3.

Accuracy of return temperature predictor can be seen in Figure 4.

It can be seen that real substation consumption data provides better prediction results than the production data. However, in this optimization case the production data is used as input data as the substation measurements are not available for distributed control system.

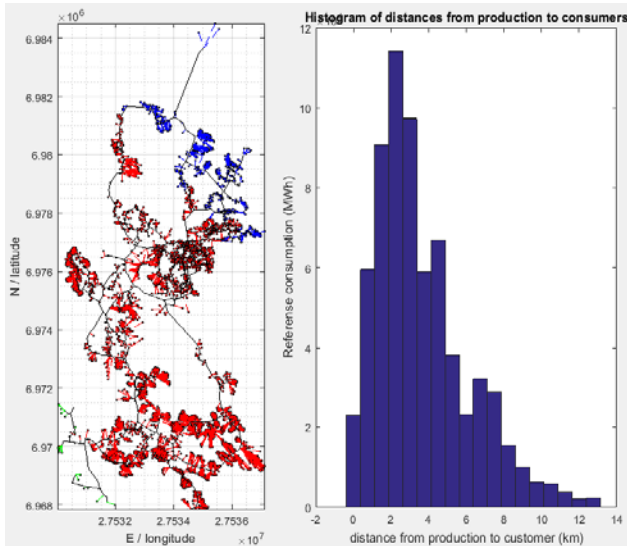


Figure 5. Case example of supply areas at specific heat load and combined delay distribution from distances along the distribution lines. Left graph is in coordinates of ETRS-TM35FIN projection.

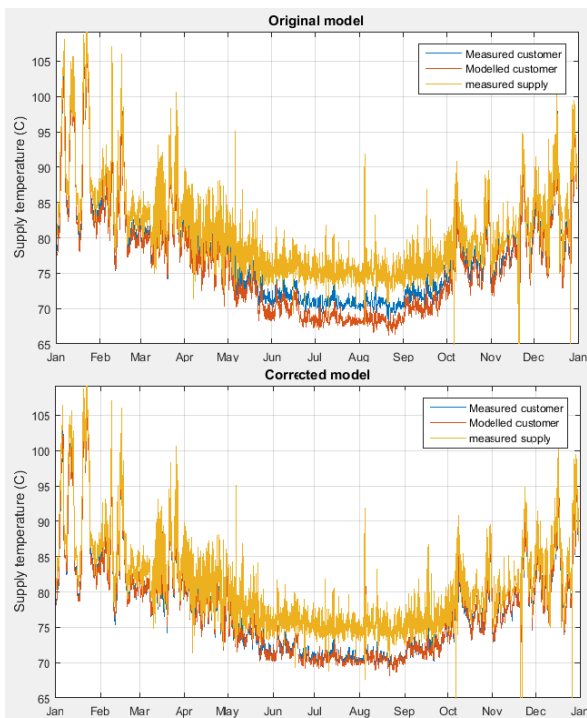


Figure 6. The first graph shows the customer supply temperature model response according to Eq. (7). Second graph is fitted to match measurements by the correction factor.

Customer supply water temperature modelling

To model customer supply water temperature, customers' distances from heat producers at certain heat loads are noteworthy. In Figure 5, heat production is distributed into three generation plants, Haapaniemi CHP plant (red, 258 MW), Bio heat station (green, 2 MW) and Saarijärvi Heat station (blue, 40 MW). On the

right there is a histogram of distances from the supplier to consumers. The shape of heat distribution function is the same as the histogram.

During a medium or high load, the delay responses are almost linear to mass flow, but on low demand the delay is shorter than modelled. This phenomenon was corrected by weighting more the temperature difference.

There were problems on modelling the summer temperature as can be seen in first graph of Figure 6. By multiplying the heat loss term in (7) with correction

factor $\left(\frac{T_{s,s}(t) - T_{s,c}(t)}{T_{s,s}(t) - T_{s,c}(t)}\right)^{0.8}$, the model was able to match the real customer temperature accurately enough. The correction factor parameters were solved by data fitting to match the measured and modelled supply water temperatures. With the correction term the $T_{s,c}$ could be modelled more accurately with SD=0.35 °C. Modelled and measured customer supply temperatures with correction term are presented in lower graph of Figure 6.

Optimization

The optimized supply temperature is compared with the measured supply temperature (Meas) during observed period. Figure 7 introduces an instructional control curve proposed by Energiategollisuus ry (ET, Finnish Energy Association) to Finnish district heating operators to operate their networks as a function of outdoor temperature [16]. This curve is used as the second baseline in the simulations.

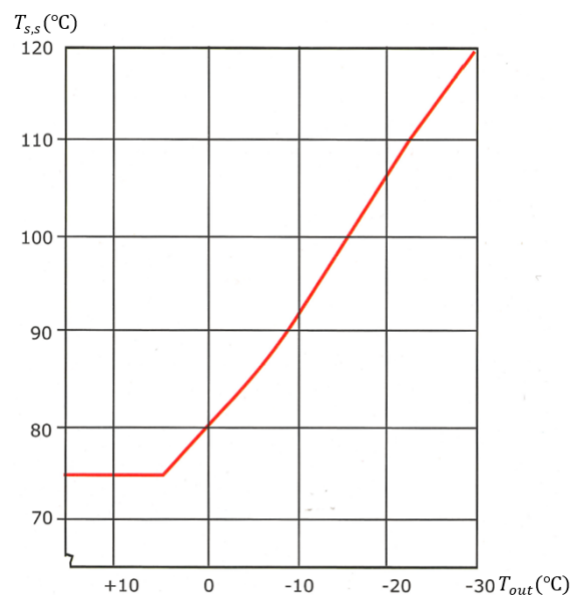


Figure 7. Supply temperature control curve by Energiategollisuus [16].

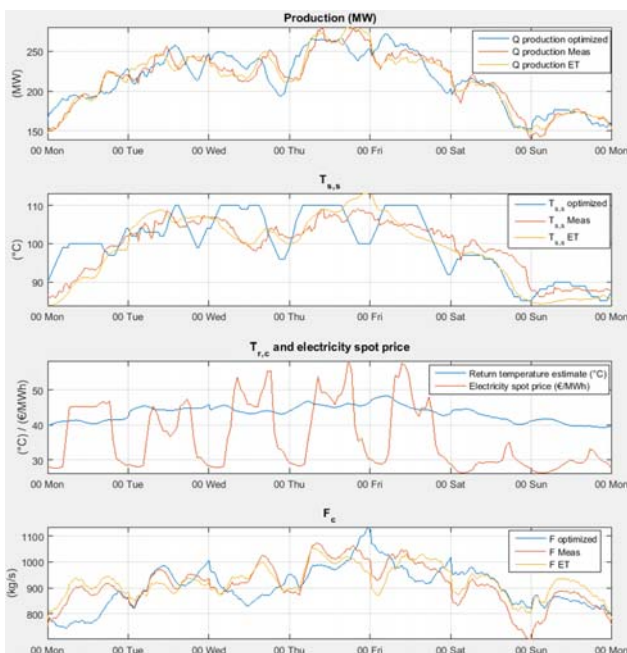


Figure 8. Comparison of three control methods during high heat load at 19.1.-25.1.2015. Blue is Opt3, red is measured and yellow is 'ET' curve. There is time and week day on x-axis (00 =midnight).

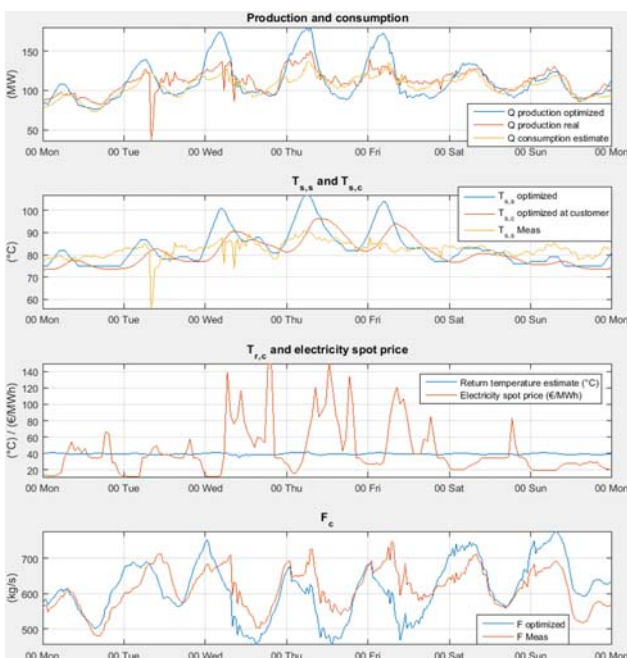


Figure 9. Opt3 at medium heat load at 5.10. - 11.10.2015. There is time and day on x-axis.

Time period 2.1. – 30.12.2015 was optimized using predicted heat load and return water temperature. Delay distribution was used to determine supply temperature at customer $T_{s,c}$ and return temperature at the plant $T_{r,s}$.

The actual electricity consumption of DH pumps was not available in the measurement data. Therefore exact balance between pumping cost and heat loss cost was not able to be determined. However, there is a tuning parameter for that and the optimization was performed with three different values giving three optimization results (Opt1, Opt2 & Opt3). The effect of parameter links straight to mean supply temperature by raising the cost of pumping. For optimizations the parameters were chosen such that the mean supply temperature is around the mean value of ET -curve. Opt3 was chosen for inspection in Figures 8...10, because the daily variations can best be compared with measured values, as the mean supply water temperature of Opt3 is highest of the optimizations and closest to the measured.

There is a comparison between three $T_{s,s}$ -control methods in Figure 8. Measured supply temperature 'Meas' is quite noisy, whereas outdoor temperature and instruction curve based 'ET' is smooth because of the smooth behaviour of the outdoor temperature. The optimized supply temperature curve is quite conservative because of the penalty for unnecessary fluctuations and steep gradients. The upper limit of the supply water temperature in DHN is 110 °C, which was reached in some conditions. Additionally, Figure 8 shows the three different strategies and their impact on flow rate and heat production.

Figure 9 shows optimized supply temperature at the supplier $T_{s,s}$ and the modelled supply temperature at customer $T_{s,c}$ in another case example. Also the predicted consumption and production are shown on top of the figure in addition to measured values as comparison. There are extremely high electricity price peaks during Wed – Fri.

According to Figure 9, the peaks in heat consumption and electricity price lead to a raise of the supply temperature. Therefore, optimization works very well minimizing pumping during high electricity price and maximizing during low price.

Supply temperatures of the three methods (Meas, ET and Opt3) are plotted into same graph as a function of outdoor temperature in Figure 10. Even though the mean temperature of optimization is only 0.88 °C higher than ET, it diverges from the ET more than Meas on cold temperatures. This is partly based on anticipation of delay in optimization and partly because of the electricity price variation.

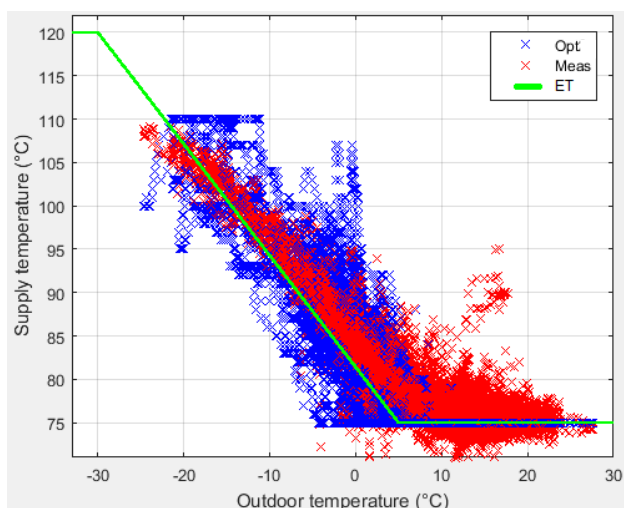


Figure 10. Meas (red), ET (green) and Opt3 (blue) in function of outdoor temperature 2.1.-30.12.2015.

Table 2. Optimization results compared to measured supply temperature. Values are differences between optimization and baseline (Opt - Meas).

	Opt1	Opt2	Opt3
Total cost (%)	-1.52	-1.33	-1.18
Heat production (GWh)	-14.00	-9.22	-5.72
Heat production (%)	-1.63	-1.07	-0.66
Return temperature (°C)	-0.32	-0.22	-0.15
Supply temperature (°C)	-2.75	-1.82	-1.13
Pumping energy (%)	+11.17	+6.88	+3.92
Pumping cost (%)	+9.12	+4.52	+1.42

Table 3. Optimization results compared to supply temperature by ET -curve. Values are differences between optimization and baseline (Opt - ET).

	Opt1	Opt2	Opt3
Total cost (%)	-0.53	-0.53	-0.63
Heat production (GWh)	-4.20	+0.58	+4.08
Heat production (%)	-0.49	+0.07	+0.48
Return temperature (°C)	-0.07	+0.03	+0.10
Supply temperature (°C)	-0.74	+0.19	+0.88
Pumping energy (%)	+3.76	-0.24	-3.00
Pumping cost (%)	+1.69	-2.59	-5.48

To compare the benefits of the three optimizations, they are compared to two baselines: measured T_s (Meas) and ET -curve (ET). Optimization period is 2.1. – 30.12.2015. Results are presented in Table 2 and 3, such that (-) is for decrease and (+) increase because

of optimization. The differences between the optimizations are based on the different level of supply water temperature caused by a different pumping cost term.

According to Table 2 and 3, the mean supply temperature of Opt1 is below Meas and ET such that heat loss is smallest and pumping costs highest of all. The supply temperatures of Opt2 and Opt3 are between ET and Meas. Heat production is clearly proportional to supply water temperature as heat losses increase along with increased supply water temperature. Respectively pumping power reduces along with increased supply temperature. However, pumping costs are dominating in optimizations compared to pumping power as optimizer increases pumping during low electricity price and vice versa. Pumping power measurements should be done to determine which of the three optimizations fit best for the real set-up.

Impact of prediction error on flow rate and heat production

Prediction error in heat load and return water temperature predictions may lead to false optimization. Error in the supply temperature will result an error in flow rate if the real consumption and return temperature do not match with the estimates. Error in flow rate is directly reflected into current heat production. Table 4 presents error mean (EM) and error standard deviation (SD) of error caused by neural network prediction error. As the prediction error SD of heat load is 9.71 %, and return temperature is 0.83 °C, the 11 % of SD in heat production is only a little bit higher.

Table 4. Prediction errors' reflection to flow rate and heat production.

	Meas	ET	Opt1	Opt2	Opt3
Φ_{PR} EM (MW)	0.010	0.019	0.026	0.029	0.030
Φ_{PR} SD (MW)	5.37	5.36	5.36	5.36	5.36
Φ_{PR} SD (%)	10.9	11.0	11.0	11.0	10.9
EM (kg/s)	1.20	1.11	0.80	0.76	0.73
SD (kg/s)	36.2	37.9	38.6	37.7	37.0
SD (%)	6.56	6.55	6.52	6.52	6.52

DISCUSSION

The role of the CHP production together with DHNs exploited as an energy storage will increase significantly in the future. This is because the more alternating renewable power generation will be connected in the power systems, the more flexible generation will be needed to balance the systems. The total thermal efficiency of CHP-generation is about twice as good as that of the conventional condensing power generation. For this reason it is reasonable to utilize CHP-generation as much as possible.

The storage capacity of DHN can be utilized to decouple the power generation in a CHP plant from temporary heat load. However, utilization of the storage capacity of the DHN requires that the dynamic behaviour of the DHN can be monitored/estimated reliably. The primary function of the CHP-generation is to produce the required heat load to customers together with the production units in the DH network during every moment of the year. Thus, the utilization of the heat storage capacity of the DHN is constrained by the customers' heat demand. Another important issue in using the DHN as an energy storage is thermal stresses caused by temperature gradients in the system. Charging and discharging rates of the stored energy in the system must be constrained according to the maximum temperature change rates determined for the DHN structures. Hot water accumulators connected with the DHN will increase the degree of freedom when planning the operation of the system.

The level of optimization in the operation of DHNs has been traditionally pretty low. The reasons for that come from the complex dynamics of the DHN and the lack of measurement information from geographically extensive systems. Thus, the operation strategy of these systems is mostly based on empirical result and the results may be far from optimal regarding to fuel consumption and other operation costs, e.g. pumping costs. However, progress in computation capacity and IT-technology has made it possible to apply more sophisticated control methods also to DH-systems, which is a fundamental requirement to be able to utilize the flexibility potential of CHP and DH-systems.

The neural network predictors act as they are trained. They are tools that process the input data providing some result. It is good tool for this application, if the data has some repetitive cyclic behaviour and strong connections to target data. The success of prediction is dependent on choosing and processing the input data and choosing the time scale such that the DHS functions similarly whole time period.

As neural network predictor, also the optimizer is a tool that provides a solution according to defined cost functions and delay distribution model. In this study, the

cost functions were created to serve DHS, such that power production was excluded. Optimization minimizes the flow rate during high electricity price to avoid expensive pumping. However, to maximize the production of CHP the condensing heat load of steam turbine should be as high as possible to enhance the power output of turbine and boiler. Thus the flow rate should be high to provide a maximum cooling load. Pumping costs and condensing load are partly in contradiction. Therefore, condensing load should be in cost function to provide an optimization that fully satisfies the requirements of CHP suppliers.

CONCLUSIONS

This research was carried out because of the low level of supply water temperature controls in district heating systems (DHS). The aim was to find some solution to control the supply temperature such that there would be more flexibility and predictability in perspective of heat and power co-generation. Also, improved cost and energy efficiencies were objectives. Heat load demand and return water temperature of district heating (DH) customers were predicted by neural network predictors. The dynamic response of supply temperature was modelled through delay distribution model. The supply water temperature was optimized by brute force optimizer that minimizes the total costs of heat loss and pumping. The research was carried out by modelling the DHN of Kuopio by scaling and validating the models with the system data and measurements.

The optimization was performed for period of one year with three different values of cost tuning parameters. Optimizations were compared with measured supply temperature and instructional supply temperature curve. Compared with measured values, supply water temperature reduced in range 1.1 – 2.8 °C, reducing the total operating costs 1.2 – 1.5 %. Cumulative error caused by prediction error was rather small as the standard deviation of heat production was only 11 %. However, better accuracy would be achieved if neural network predictor was trained for each season separately.

The results of optimization are good and in accordance with the definitions. The most remarkable factor determining the supply water temperature, was the rapidly fluctuating electricity price that sets the pumping costs. The results did not give remarkably high savings in total operating costs as the supply temperature could not be lowered that much, as measured supply water temperature was fitted near to the instructional green line presented in Figure 9. However, the results can be tuned with other weight factors in cost function case specifically.

In the future the optimization should be extended to CHP-production, such that DHN could support electricity production by supply temperature control.

Additionally, to improve the optimization algorithm, linear parameter varying (LPV) state-space model could enhance the speed and accuracy of the optimization. The varying delay is challenging for basic state-space models. LPV model of DHS would be similar to marine cooling systems, which is modelled in [17]. LPV model is also formulated for DHS, but was failed to implement due to numerical difficulties [18].

ACKNOWLEDGEMENT

This work has been carried out in research program Flexible Energy Systems (FLEXe) and supported Tekes - Finnish Funding Agency of Innovation. This work aims to increase flexibility of controlling district heating networks in cogeneration power plants. District heating system time series for the research was provided by Kuopion Energia Oy, who is gratefully acknowledged.

REFERENCES

- [1] M. Falkvall and V. Nilsson, "Optimerad framledningstemperatur i Lunds fjärrvärmenät," Lund University, Lund (2013).
- [2] L. Saarinen, "Modelling and control of a district heating system," Uppsala University, Uppsala (2008).
- [3] L. Saarinen and K. Boman, "Optimized district heating supply temperature for large networks," Stockholm (2012).
- [4] T. Viander, "Optimization of district heating network usage," Lappeenranta University of Technology, Lappeenranta (2014).
- [5] S. Velut, P. Larsson, J. Windahl, K. Boman, and L. Saarinen, "Non-linear and Dynamic Optimization for Short-term Production Planning," Stockholm (2013).
- [6] A. Benonysson, B. Bøhm, and H. F. Ravn, "Operational optimization in a district heating system," *Energy Convers. Manag.*, vol. 36, no. 5, (1995), pp. 297–314.
- [7] P. Jie, N. Zhu, and D. Li, "Operation optimization of existing district heating systems," *Appl. Therm. Eng.*, vol. 78, (2015), pp. 278–288.
- [8] L. Giraud, R. Bavière, C. Paulus, M. Vallée, and J. Robin, "Dynamic Modelling, Experimental Validation and Simulation of a Virtual District Heating Network," no. JUNE, (2015).
- [9] M. Vesterlund and J. Dahl, "A method for the simulation and optimization of district heating systems with meshed networks," *Energy Convers. Manag.*, vol. 89, pp. 555–567, (2014).
- [10] L. Saarinen, "Model-based control of district heating supply temperature," Stockholm (2010).
- [11] S. Grosswindhager, A. Voigt and M. Kozek, "Predictive Control of District Heating Network using Fuzzy DMC," (2012).
- [12] N. Eriksson, "Predicting demand in district heating systems - A neural network approach," Uppsala University, (2012).
- [13] M. Protić, S. Shamshirband, M. H. Anisi, D. Petković, D. Mitić, M. Raos, M. Arif, and K. A. Alam, "Appraisal of soft computing methods for short term consumers' heat load prediction in district heating systems," *Energy*, vol. 82, no. 0, (2015), pp. 697–704.
- [14] S. Frederiksen and S. Werner, *District Heating and Cooling*, 1st ed. Lund (2013).
- [15] Finnish Energy Association Energiategollisuus, *Statistical yearbook 2014, District Heating in Finland*, (2015).
- [16] Finnish Energy Association Energiategollisuus, *Kaukolämmön käsikirja (Handbook of district heating)*, (2006).
- [17] M. Hansen, J. Stoustrup, and J. D. Bendtsen, "An LPV Model for a Marine Cooling System with Transport Delays," *Proc. 14th Int. Conf. Harb. Marit. Multimodal Logist. Model. Simul.*, no. c, (2011), pp. 119–124.
- [18] A. Jochumsen, "Modeling and control of a District Heating System," Aalborg University, (2010).

UTILIZATION OF DISTRICT HEATING NETWORKS TO PROVIDE FLEXIBILITY IN CHP PRODUCTION

T. Korpela^{1*}, J. Kaivosoja², Y. Majanne¹, L. Laakkonen², M. Nurmoranta², M. Vilkkö¹

¹Tampere University of Technology, Department of Automation Science and Engineering, Korkeakoulunkatu 3, 33720 Tampere, Finland, * Corresponding author: timo.korpela@tut.fi

²Valmet Automation Ltd., Lentokentänkatu 11, 33900 Tampere, Finland

Keywords: District heating, flexibility, CHP production, electricity, frequency control

ABSTRACT

Increasing penetration of intermittent renewable energy production in power systems will remarkably increase the need of flexible and controllable power generation. Subsidised renewable generation has revolutionized energy markets and brought down electricity prices leading to lack of investments to new controllable generation plants. As numerous existing thermal power generation units have been closed down, there is no doubt that all the possible flexibility available in power systems should be harnessed to stabilize the power systems. Combined heat and power (CHP) generation is widely used in district heating (DH) systems. As total heat production into the DH network needs to be balanced with the total heat consumption, this sets significant limitations to the long term power production. However, the coupling between the heat load and electric production can be decoupled temporarily by using the heat storage capacity of DH network consisting of network volume and optional heat accumulators. This paper presents the results of research work dealing with the analysis of dynamic operability of interconnected CHP plants and district heating networks. The flexibility of generation capacity was compared with the requirements set to power producers to be able to participate the Automatic Frequency Restoration Reserve (FRR-A) market. For that, two case studies were presented that include FRR-A tests in two municipal CHP plants that utilize a heat only boiler and a DH accumulator to balance the heat production variations that are caused by changes in power production. The results indicate that both cases fulfil the requirements and that the DH network operation is affected only slightly. However, the rapid power level change is a disturbance to CHP boilers and DH networks that the process components and automation systems must adapt to. Therefore these aspects must be considered carefully when applying such new operation practises in existing CHP plants.

INTRODUCTION

As a global trend, the capacity of intermittent renewable power production, i.e. wind and solar power, has increased rapidly and the drive to carbon neutrality ensures the upward trend also in the future. As the life

cycles of energy system components are traditionally very long, it is cost and resource efficient that the existing systems can be modified compatible to new operation environments with accelerated dynamics and flexibility. The special need is for the momentary change and especially the increase of the power production so that the other production and consumption units shall have time to adapt to a new state, e.g. additional boilers to start-up or running plants to increase their power output, or some consumers to reduce their consumption in a well-organized manner. A review of energy system flexibility measures that are applicable in existing technologies to enable variable renewable electricity is presented in [1].

District heating (DH) is a system for distributing heat that is generated in centralized units. DH has a high coverage especially in North, Central and Eastern Europe and it is primarily based on combined heat and power (CHP) production supported by heat only boilers. In CHP production, back-pressure turbo generators that produce electricity and heat at fixed ratio are very common. As total heat production into the DH network needs to be balanced with the total heat consumption, this sets significant limitations to the power production. This issue is important, as CHP production and DH are seen as a future prospect to lower CO₂ emissions [2].

The momentary power increase in CHP production can be conducted in two ways, when the steam turbine is not yet running at its full capacity. The first option to increase the power production is to disconnect the fixed ratio of heat and power production in the unit, e.g. by controlling the bypassing reduction valves of turbines (by-pass), by reducing internal steam consumption (condensate stop) or other respective actions. The second option to momentarily increase the power production is to maintain the fixed ratio but increase the boiler power output, and to store or waste the excess heat that is produced along with electricity. The storing can be conducted by utilizing heat accumulators [3-7] and district heating networks as heat buffers [8-10]. In practise, the solution can be a combination of these both methods, depending on the required power change rate and capacity requirements. The second approach is studied in this article.

The most effective exploitation of the flexibility potential of CHP plants take place when the plant owners are able to take part in some market where the flexibility in electricity production can be tendered. One of such market is Automatic Frequency Restoration Reserve (FRR-A) in the Nord Pool power market in Nordic countries. The market structure defines the change rate and capacity requirements to enter the market. The attainment of the requirements depends on the CHP plant and DH network structures and their momentary operation regions. Therefore, it is useful to analyse the potential of different flexibility sources, to assess the possibility to take part in different markets and to analyse how the plant operates during momentary change of power level driven by external control signal. However, the flexibility markets are still developing, and as a part of the process the FRR-A is not currently active in Nordic countries. However, it provides indication of possible requirements and prospects in the future market structures.

In FRR-A type of operation, an external signal activates the power set point change without a prior notice, which can be considered as an external disturbance that will affect the operation of the boiler and the DH network and its nearby components such as heat accumulators and heat only boilers. When considering the effect of a sudden power level increase in a typical CHP boiler, the steam flow through the turbine increases. As the result, the steam pressure starts to drop, which the steam pressure controller starts to compensate by increasing the fuel power set point. The pressure control is typically assisted by feedforward connection from live steam flow to fuel feed. The pressure drop is modest if the fuel feeding system components, especially the coal mills, are fast enough to compensate the fuel power drop. On the other hand, the power increase will contribute also to increased heat power to DH network with fixed heat to power ratio. If the DH network is in balance before the disturbance, the supply water temperature will increase, which will again affect the operation of nearby DH accumulators and heat only boilers. Therefore, the sudden power set point change will affect widely the operation of the whole system and can be considered as external disturbance that the processes and automation systems must tackle. However, this kind of operation principle with fast dynamics is unfamiliar to existing and especially to municipal CHP plants, as the components, automation systems including controller tunings are not designed for that kind of operations and disturbances. Therefore, in addition to analysing the capability of CHP plants to fulfil the requirements of FRR-A, the operation of other system components and automation system should also be analysed carefully, to discover the possible operational bottle necks that

might actually limit the utilization of rapid power change rate and volume in practise.

This paper studies technical flexibility potential of CHP production in DH network by analysing measured data to estimate the transient capability of CHP production and DH in relation to FRR-A requirements. For that, analyses of two case studies are made from two municipal CHP plants and DH networks. Although FRR-A requirements are of special concern of this article, the principles are somewhat the same in different flexibility market mechanisms but with different change rate and volume requirements, and hence the study is applicable to other markets as well.

The structure of this article is such that first the general control principles in DH network are described. After the introduction of principles and requirements of the FRR-A market, two case studies are presented that include FRR-A tests in CHP plants that utilize a heat only boiler and a DH accumulator to balance the heat production variations that are caused by changes in power production. Finally, the results are discussed and concluded.

DYNAMICS AND CONTROL OF DH NETWORKS

Control of DH systems consists of pressure controls and temperature controls. Pressure controls regulate the pump stations to produce desired DH mass flow and pressure difference for the DH customers. Dynamics of pressure transients are relatively rapid enabling the utilization of standard control methods. Instead, dynamics of temperature behaviour in DH network is related with the flow rate of DH water typically resulting to delays of several hours that vary depending on load and production characteristics and the structure of the network. Due to varying time delay, the uncertainty in estimation of heat consumptions and definition of optimal supply temperatures at different times are issues that have contributed for the current situation of low level of automation in temperature controls. For those reasons the supply temperature is usually adjusted manually by the system operators according to the time of the day and outdoor temperature, and empirical knowledge about the system characteristics. However, with functional supply temperature controls the heat losses and pumping costs can be balanced to provide minimum running costs of the system. As the pumping costs are significantly lower than the heat losses, it is desirable that the supply temperatures in DH networks are kept as low as possible still to meet the load requirements [11].

The option to increase momentarily the supply temperature and flow in DH network enables the utilization of DH network as an energy storage capacity to avoid temporary start-ups of supporting heat stations

with significantly higher running costs, and especially in the future to utilize the DH network to accumulate heat in case that CHP plants increase their power output according to power grid requirements. However, there is a limit for temperature gradients (ΔT), in order to keep the thermal stresses of network structures at permissible levels. For this reason some rule of thumbs are provided for ΔT_{supply} in literature: maximum of 1–2°C in 6 minutes that is generally applied in Finland. In practise, some of the DH operators have much more conservative change rates, which is understandable when the increase of ΔT is not really required, e.g. due to objective to minimise thermal stress. However, the opposite goals are also presented [12]. In addition to the change rate, there is a limit that supply water temperature from a CHP plant should not differ more than 10 °C from that of other units on operation in the same DH network to avoid excess thermal stresses in boundaries where the supply waters mix [13]. As a conclusion, the ΔT_{supply} should be constrained when utilizing the DH network accumulation capacity in varying process conditions.

ELECTRICITY MARKET IN NORD POOL

Nord Pool is a power market that offers trading, clearing and settlement in day-ahead and intraday markets across nine European countries: day-ahead market in the Nordic, Baltic and UK and intraday market in the Nordic, Baltic, Germany and UK. Additionally, balancing power and reserve markets exist in the countries that contribute to joint transmission system grid operation. [www.fingrid.fi] Finland is a Nordic country, and the Finnish market is of special concern in this article, although the markets in other Nordic countries are similar.

The reserve market products available in Finland are divided in respect to activation timeframes (seconds to hours) and procedures (manual and automatic), which are illustrated in Figure 1. Frequency Containment Reserves (FCR) are used for the constant frequency control in second-minute time scale. Frequency Restoration Reserves (FRR) are used for returning the frequency to its normal range and to release activated FRC back into use up to fifteen minutes. Replacement Reserves (RR) release the activated FRR's back to back-up, but this market is not currently active in Nordic power system. [www.fingrid.fi]

An applicable reserve market product for CHP plants is Automatic Frequency Restoration Reserve (FRR-A¹),

¹ Application of FRR-A was interrupted for the present in December 2015 due to delays in development of capacity and energy markets in Nordic countries [Nord Pool]

which enables that the frequency backup (upward and downward) capacity can be tendered in hourly market but are only activated in special cases when the frequency in Nordic transmission grid is significantly deviated from the reference 50 Hz. If the bid is accepted in the market, the operator receives a separate energy compensation based on regulation carried out in addition to the capacity payment. In those cases, the FRR-A operation is activated based on external activation signal by the local transmission system operator (TSO), which is Fingrid in Finland. There are two types of activation signals depending on the plant performance to change the power level. For the slower processes, e.g. for CHP plants, the reaction time requirement to activation signal is presented in Figure 2, which illustrates that at least 90 % of the power change must be achieved in less than seven minutes. The dashed line corresponds to transfer function $f(t) = 1/(1+sT)^4$, where 's' is Laplace variable and the time constant T is 35 seconds. [14]

When joining the FRR-A market, a contract is signed between a resource owner and the local TSO, in order to provide at least 5 MW_{el} in the defined time frame. The reserve unit can consist of one or several production units, which enable company level contributions. Before joining the market, activation test that include step changes up and down in a predetermined matter must be approved. [14] An indication of the test runs are presented in next section.

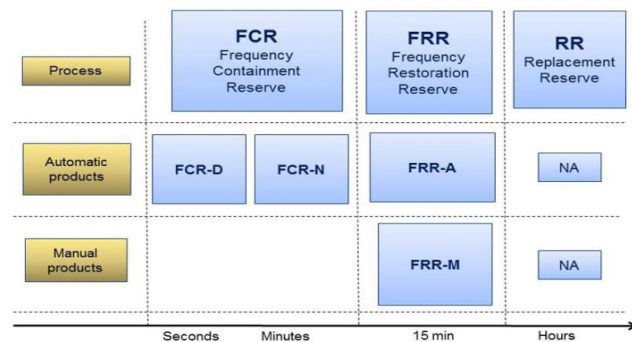


Figure 1. Reserve products in Finland. [Fingrid]

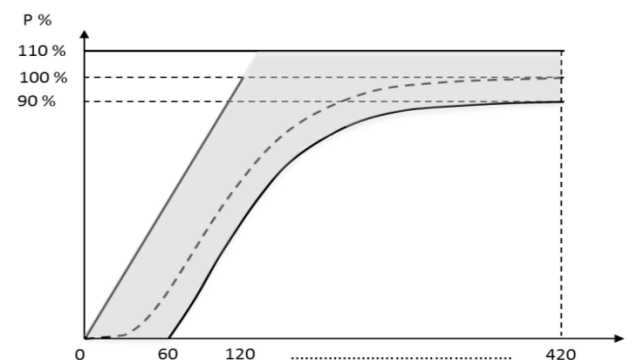


Figure 2. Step response requirement for the power change (s) from the arrival of activation signal in FRR-A. [Fingrid]

FRR-A TEST CASE STUDIES

For the study, step response tests were made in two municipal coal fired CHP plants. The plants are located in Finland and they produce electric power to the Finnish power grid and district heat to their local municipal DH networks. The CHP units in both cases consist of pulverized coal fired boilers connected to single-stage back-pressure turbines. The first CHP plant is roughly half of the capacity compared to the second one. In the first plant, there is a heat only boiler in parallel with the CHP unit. It is used as a base load capacity, which can be used to compensate heat production variations in the CHP plant. In the second plant, there is a DH accumulator in parallel with the CHP unit which is used as buffer and back-up capacity to stabilize the misbalance between DH consumption and production. Other balance methods, e.g. turbine by-pass, additional condensing LP-turbine, or condensate stop for feed water preheating, were not applied during the tests.

Next the test results are presented and discussed. In both cases, first the operation of the boilers is studied followed by the responses to the DH networks.

Case 1

In the first case study, the validation test of FRR-A was conducted with the fixed power to heat ratio. Before the test, the CHP plant was operated at ca. 80 % of its nominal load. The electric power production was manipulated based on FRR-A type of control signal, which is presented in scaled form along with the response in Figure 3 (up). It can be seen that the measured power production followed the set point excellently. After the set point changes, the power levels started to change within 15 seconds and the desired power levels were reached in less than 3 minutes, which satisfy the FRR-A requirement clearly. Next in Figure 3, the set point signal for fuel power from the live steam pressure controller (middle) and relative steam pressure and its set point (low) are presented. The boiler automation system is able to control the fuel power accurately and fast enough that the variations in the steam pressure remain low.

Figure 4 (up) presents the supply water temperature of the CHP unit (measurement and set point) in addition to the supply water temperature of total (CHP + heat only boiler) flow to the DH network. It can be seen that the manipulation of fuel and hence the heat power of the CHP unit to the DH network affects the supply water temperature to a minor extent. The middle and lower figures at Figure 4 present the relative DH flows and powers from the CHP unit, heat only boiler and their total effects. It can be seen that the effects of power production variations are compensated by the heat only boiler, and hence the DH network is not affected.

As a conclusion for Case 1, the disturbance affected by the FRR-A test to the DH network is negligible. The boiler and its components were fast enough to compensate the effect of the disturbances smoothly without significant fluctuations. Therefore, the CHP plant is ready for FRR-A operation as such.

Case 2

In the second case, the similar validation test of FRR-A was conducted with the fixed power to heat ratio, but at this time the disturbed heat production was compensated by manipulating heat power output of the DH accumulator. In the current control structure, the district heating pumps control the DH supply temperature of the CHP plant, and the DH accumulator is used to control the pressure in the DH network. In the test the output temperature of the DH accumulator was constant 87 °C, and the return water temperature from the DH network was constant 41.8 °C.

During the test, the electric power production was altered based on FRR-A type of control signal, shown in scaled form along with the response in Figure 5 (up). As the capacity of the CHP plant is roughly the double compared with the plant presented in Case 1 and the magnitude of power level changes were also double, the relative power set point changes were roughly same in both CHP units. It can be seen in Figure 5 that the measured power production followed the set point fairly well, despite at time period ca. 800-1600 seconds. The reason for the overshoot was a human error in operation when conducting the test. Additionally, the turbine inlet pressure controller limiting the load change rate conducted by turbine controller was undesirably active at period 0–5000 seconds. Despite that, the power levels started to respond within 30–40 seconds after the set point changes and the desired power levels were reached within 2–3.5 minutes, which satisfy the FRR-A requirement. Additionally, Figure 5 presents the set point signal for fuel power from live steam pressure controller (middle), and the relative live steam pressure and its set point (low). Despite the operation of the inlet pressure controller, there were significant fluctuations in live steam pressure that were caused by the rather slow dynamics of the coal boiler. The plausible explanation for the slow response is the sluggish response of coal mills, which might have time delays of several minutes without the excessive overloading of mill air feeds. Therefore, the fuel set point was not reached in fast transients and hence the steam pressure fluctuated. Despite that, the desired FRR-A requirements were fulfilled, and the results were adequate for the boiler that is not designed for such the fast transients.

Figure 6 presents similar figures presented in Figure 4 in Case 2.

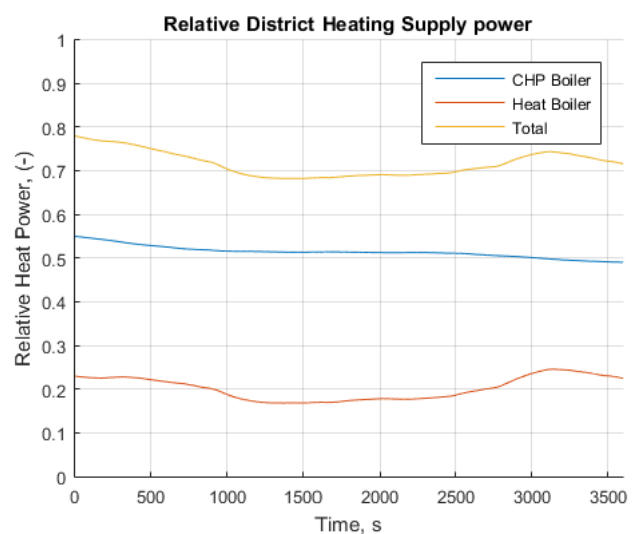
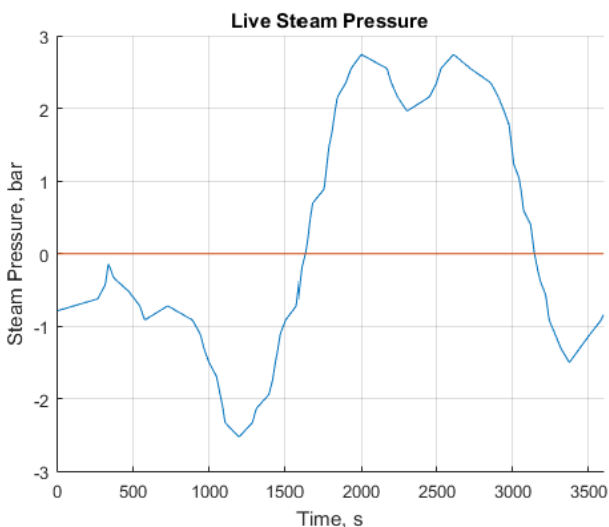
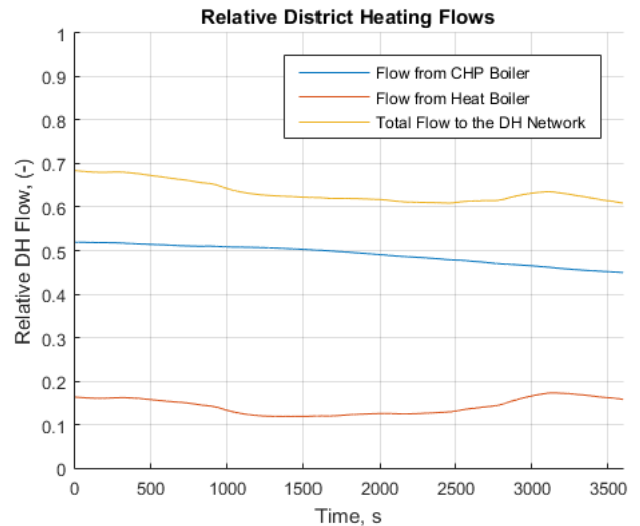
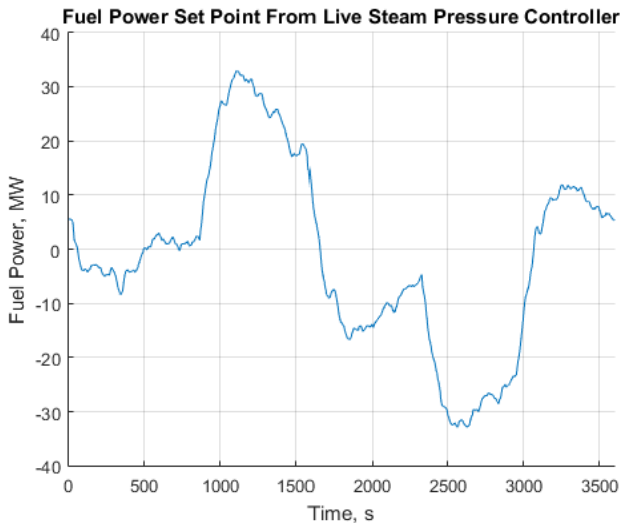
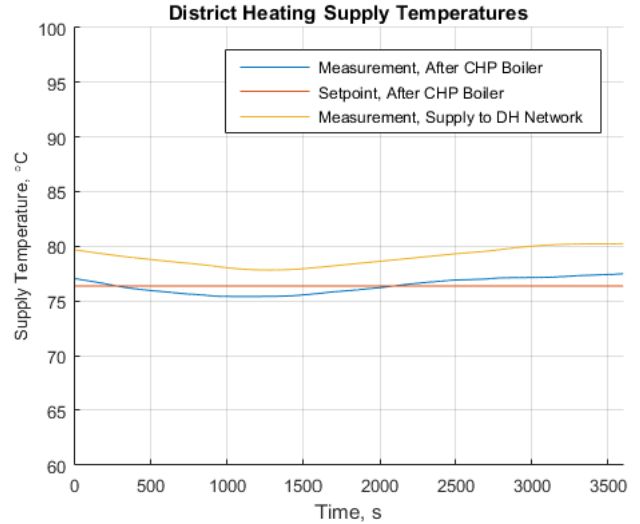
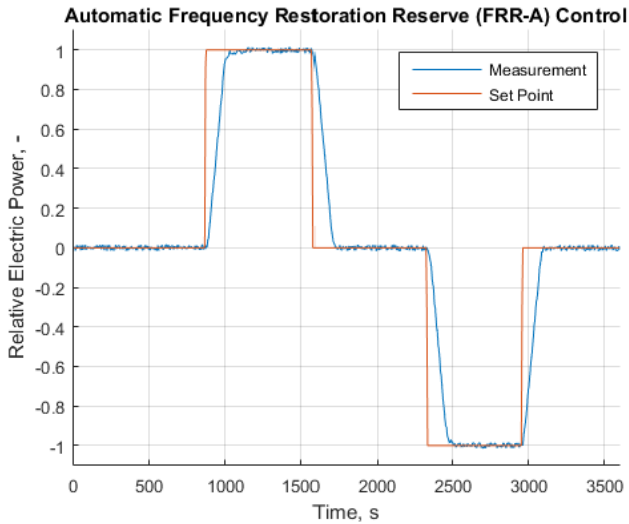


Figure 3. Case 1: Relative FRR-A control signal and generated power (up), set point signal for fuel power from live steam pressure controller (middle), and live steam pressure and its set point (low).

Figure 4. Case 1: Supply water temperature of the CHP plant (measurement and set point) and total (CHP + heat boiler) flow to the DH network (up), relative DH flows (middle) and relative DH supply powers (low).

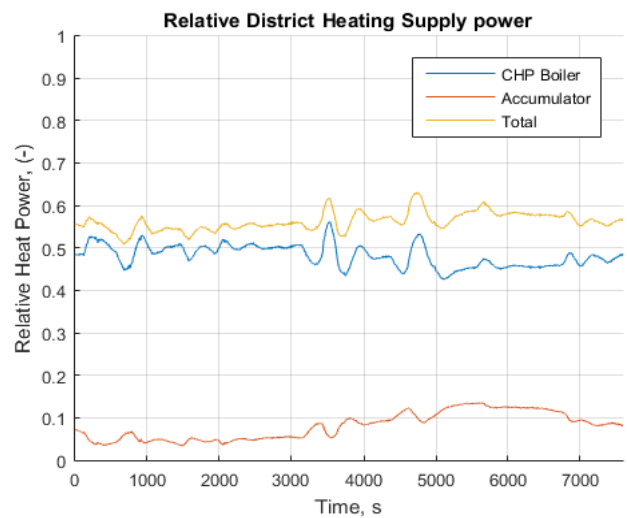
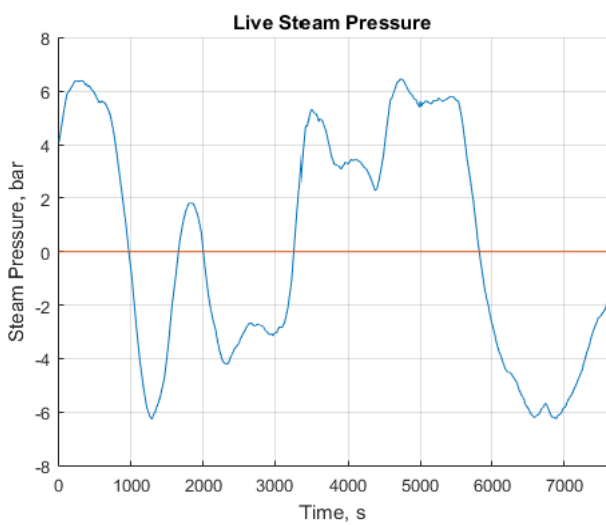
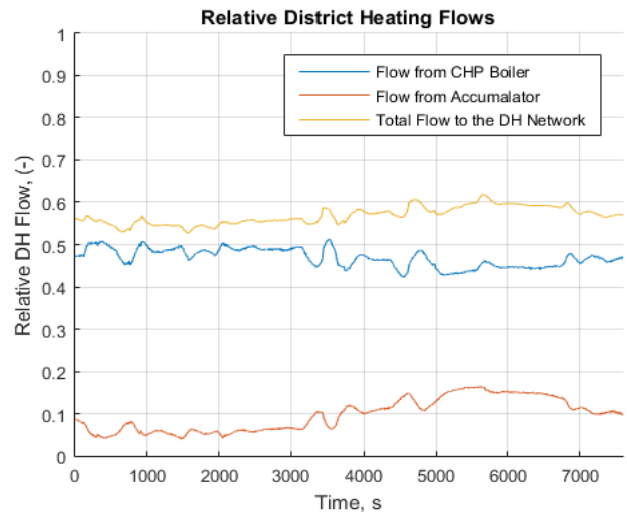
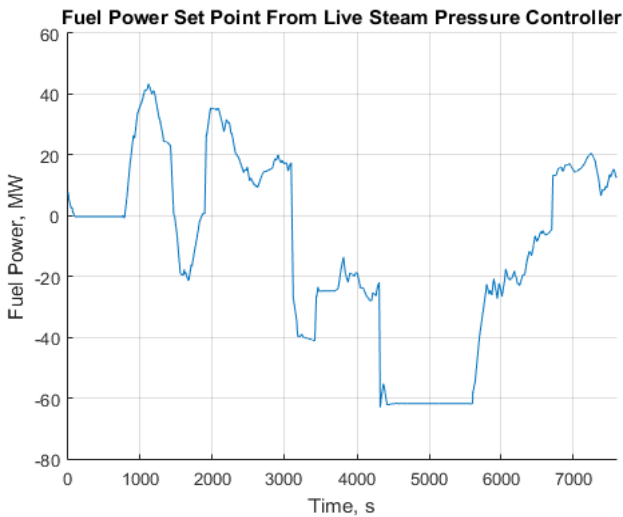
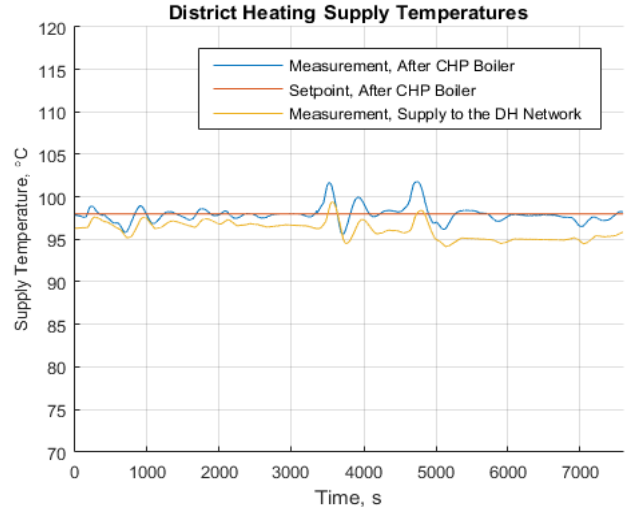
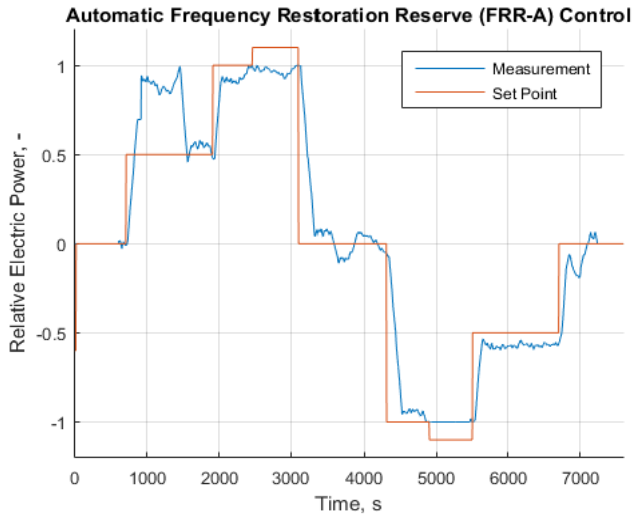


Figure 5. Case 2: Relative FRR-A control signal and generated power (up), set point signal for fuel power from live steam pressure controller (middle), and live steam pressure and its set point (low).

Figure 6. Case 2: Supply water temperatures from accumulator and from heat exchanger (CHP) (up), relative district heating flows (middle) and relative DH supply powers (low).

Figure 6 (up) presents the supply water temperature of the CHP plant (measurement and set point) and the total supply water temperature (CHP + heat accumulator) supplied to the DH network. Moreover Figure 6 indicates the relative district heating flows (middle) and relative DH supply powers (low). It can be seen that the manipulation of fuel power of the CHP unit affects the supply water temperature to some extent in smaller power changes, but the largest power level changes start the DH supply water temperature and flow to oscillate due to overcompensation. The excessive DH flow compensation can be seen in supply water temperature variation and after a delay in the discharge of accumulator that compensates the power fluctuations. Therefore, it seems that the control loops interfere with each other in large transients, so retuning of control loops is likely to improve the performance significantly.

As a conclusion, the slow response of coal mills and hence the slow dynamics of the boiler load change limited the dynamic change rate of the CHP plant. Additionally, the heat power fluctuations caused fluctuations in the DH network which can to significant extent be compensated by improved controller tunings that also consider the cases of fast and sudden disturbances caused by momentary power level changes. Despite of these facts, the dynamic transient requirements of FRR-A were clearly fulfilled, which is a good result from a CHP system that was not originally designed for such operation.

DISCUSSION

CHP production can contribute to balancing the power grid and increase power production flexibility in two ways that are either relatively small amounts of power that can be obtained fast or relatively significant amount of power that can be obtained slowly. The first category was considered in this article. In the presented case studies, the first CHP plant is able to satisfy the FRR-A requirement without causing any disturbances to boiler pressure stability or to DH network. The second CHP plant is also able to meet the FRR-A requirement, but the slow dynamic responses of coal mills cause more fluctuations to the steam pressure. Additionally, the DH network was affected. The significance and value of all these flexibility actions depend on the amount of uncontrollable renewable power production compared to controllable power production, in addition to development of power consumption, storage technologies and other flexibility measures. However, cost correlation should be maintained in the new energy system, and therefore the primary and secondary effects of the flexible operation in existing CHP systems should be considered carefully e.g. in maintenance costs and emission control. In the short

term the increased amount of renewables contribute to changes in operation practices of existing CHP systems and in long term to changes in dimensioning of the plants and their components, e.g. in coal mills, boiler energy capacity, turbine, materials etc. In all these cases the bottle necks must be identified and carefully considered, in order to provide safe and sound operation of the plants also in the future.

As was discussed, the reserve unit taking part in FRR-A can consist of one or several production units, which enable company level contributions. Therefore, all the existing system components can contribute to flexibility if they do not pass the test individually or the secondary effects of rapid power level changes are not acceptable for some reason, which is very advantageous in order to exploit all the flexibility there reasonably exists.

CONCLUSION

In this paper, utilization of district heating network to provide flexibility in CHP production was studied. In special interest were the properties of the grid balancing market (FRR-A) that sets requirements for change rate and volume in power production. For that, two case studies were presented that include FRR-A tests in two municipal CHP plants that utilize a heat only boiler and a DH accumulator to balance the heat production variations. The sudden and rapid power level changes are disturbances to CHP units and the DH networks, which the automation systems must take care of. Therefore, the operation of the whole system must be considered, not just the power change properties. Despite of some operational aspects, the dynamic transient requirements of FRR-A were clearly fulfilled with both CHP plants, which is a good result from CHP systems that are not designed for such operation.

In order to provide dynamic flexibility to power production and when considering the CHP production, the dynamic bottle neck can be in the dynamics of boiler or in the DH network. For relative small power variations, e.g. provided in FRR-A market, the DH network operation is not affected that much, but this depends on the properties of the CHP unit, the DH network and the prevailing conditions. In cases where the variations in power output of CHP unit to the DH network can be compensated by the operation of DH accumulator or heat only boiler, the dynamics of the boiler might be the limiting factor. An indication of this was observed in Case 2 where the limiting factor for fast power changes were the properties of the coal mills. However, the operation of control systems should be carefully studied when new operation principles are put into operation.

In the future, the effect of flexibility to boiler and component structures should be studied thoroughly in

order to operate the existing systems safely in operation environments that they are not designed for. Also the other dynamic balancing methods, e.g. turbine by-pass, additional condensing low pressure turbine, or condensate stop for feed water preheating should be studied. Additionally, district cooling should be included in the flexibility studies, since the application of district cooling has started to increase rapidly and it provides possibilities to improved overall energy efficiency. Additionally, the effect of power level to dynamic flexibility in CHP systems should be studied in the future.

ACKNOWLEDGEMENT

This work was carried out in Task 2.3 of research program Flexible Energy Systems (FLEXe) and supported by Tekes - Finnish Funding Agency of Innovation. The aim of FLEXe was to create novel technological and business concepts enhancing the radical transition from the current energy systems towards sustainable systems. FLEXe consortium, coordinated by CLIC Innovation Ltd, consisted of 17 industrial partners and 10 research organisations.

The authors of the article gratefully acknowledge the financiers and project partners.

REFERENCES

- [1] P. D. Lund, J. Lindgren, J. Mikkola and J. Salpakari, "Review of energy system flexibility measures to enable high levels of variable renewable electricity," *Renewable Sustainable Energy Rev*, vol. 45, pp. 785-807, 2015.
- [2] D. Connolly, H. Lund, B. V. Mathiesen, S. Werner, B. Möller, U. Persson, T. Boermans, D. Trier, P. A. Østergaard and S. Nielsen, "Heat roadmap Europe: Combining district heating with heat savings to decarbonise the EU energy system," *Energy Policy*, vol. 65, pp. 475-489, 2014.
- [3] S. Rinne and S. Syri, "The possibilities of combined heat and power production balancing large amounts of wind power in Finland," *Energy*, vol. 82, pp. 1034-1046, 2015.
- [4] H. Wang, W. Yin, E. Abdollahi, R. Lahdelma and W. Jiao, "Modelling and optimization of CHP based district heating system with renewable energy production and energy storage," *Appl. Energy*, vol. 159, pp. 401-421, 2015.
- [5] T. Nuytten, B. Claessens, K. Paredis, J. Van Bael and D. Six, "Flexibility of a combined heat and power system with thermal energy storage for district heating," *Appl. Energy*, vol. 104, pp. 583-591, 2013.
- [6] T. Fang and R. Lahdelma, "Optimization of combined heat and power production with heat storage based on sliding time window method," *Appl. Energy*, vol. 162, pp. 723-732, 2016.
- [7] M. Noussan, G. Cerino Abidin, A. Poggio and R. Roberto, "Biomass-fired CHP and heat storage system simulations in existing district heating systems," *Appl. Therm. Eng.*, vol. 71, pp. 729-735, 10/22, 2014.
- [8] Z. Li, W. Wu, M. Shahidehpour, J. Wang and B. Zhang, "Combined heat and power dispatch considering pipeline energy storage of district heating network," *IEEE Trans. Sustainable Energy*, vol. 7, pp. 12-22, 2016.
- [9] A. Pini Prato, F. Strobino, M. Broccardo and L. Parodi Giusino, "Integrated management of cogeneration plants and district heating networks," *Appl. Energy*, vol. 97, pp. 590-600, 2012.
- [10] K. Sartor, S. Quoilin and P. Dewallef, "Simulation and optimization of a CHP biomass plant and district heating network," *Appl. Energy*, vol. 130, pp. 474-483, 2014.
- [11] S. Frederiksen and S. Werner, *District Heating and Cooling*. Lund: Studentlitteratur Ab, 2013.
- [12] V. D. Stevanovic, B. Zivkovic, S. Prica, B. Maslovaric, V. Karamarkovic and V. Trkulja, "Prediction of thermal transients in district heating systems," *Energy Convers. Manage.*, vol. 50, pp. 2167-2173, 2009.
- [13] L. Koskelainen, R. Saarela and K. Sipilä, *Kaukolämmön Käsikirja*. Helsinki: Energiateollisuus, 2006.
- [14] Fingrid, "LIITE 1: Automaattisen taajuudenhallinta-reservin sovellusohje (8.1.2014)." 2014.

TOPIC C:

Key Elements in District Heating and Cooling Systems



DETERMINATION OF ESSENTIAL PARAMETERS INFLUENCING SERVICE LIFE TIME OF POLYURETHANE INSULATION IN DISTRICT HEATING PIPES

Nazdaneh Yarahmadi¹, Alberto Vega^{1}, Ignacy Jakubowicz²*

¹ SP Technical Research Institute of Sweden, Gibraltargatan 35, Gothenburg, SE40022, Sweden

^{1*} SP Technical Research Institute of Sweden, Gibraltargatan 35, Gothenburg, SE40022, Sweden, Presenting author

² SP Technical Research Institute of Sweden, Brinellgatan 4C, Borås, SE50115, Sweden

Keywords: Polyurethane insulation, District heating pipe, PUR degradation, Accelerated ageing, Life time prediction

ABSTRACT

Pre-insulated district heating pipes (DHP) have been in use during the last forty years. Many improvements and development have been done in the system. However, life-time prediction is still an uncertain issue. This paper is a part of a bigger project with the objective to determine mechanisms related to the deterioration of the mechanical and insulation properties of pre-insulated heating pipes as a result of ageing. The focus in this project is on degradation mechanisms of the PUR material at high temperatures. In this paper some results of the two types of exposure are presented. The first type comprises a condition where the new pipes are subjected to accelerated ageing at three different temperatures. The second type comprises condition, when the PUR material itself is aged in different atmospheres in order to identify different degradation mechanisms. The chosen ageing temperatures in the first condition were 130 °C, (close to the supply temperature), 150 °C and 170 °C, (accelerated ageing temperature in EN 253). Changes in thermal insulation and the adhesion force between the PUR and the steel pipe were evaluated using the transient plane source (TPS) technique and the SP plug method respectively. The results of ageing show that the degradation of PUR is a multi-stage process composed of a rapid change in properties followed by a plateau phase which changes later to a gradual deterioration of the properties. The results of the PUR material exposure at 150 °C in air and in nitrogen showed significant differences in the degradation characteristics between the two environments as were revealed by DSC and FTIR methods.

INTRODUCTION

Thermal energy makes up about 50 % of the worldwide energy use and all over the world goals are made to reach lower and lower energy consumption. For example under the EU Energy Performance of Buildings Directive (2002/91/EC, EPBD), EU member states are required to achieve near zero energy status for all new constructions by 2020. All these goals demand development of more sustainable district

heating systems (DHS).

Pre-insulated district heating pipes (DHP) have been in use during the last forty years in different countries. A pre-insulated pipe contains a steel pipe as media pipe, polyurethane (PUR) foam as insulation and a high density polyethylene (HDPE) pipe as mantel. Until now, many improvements in manufacturing methods have been introduced and some developments of the pipe component materials have been performed [2]. The most important was the phase-out of the chlorofluorocarbons (CFC) in the 1990s and the use of high-density polyethylene for the casing pipe in order to improve the pipe's long-term property. Changing uni-modal HDPE to bi-modal and foam gas from CFC to cyclopentane has improved some functionality and technical performance, however, life time prediction is still an uncertain issue. Improvement of thermal insulation and mechanical properties of the PUR foam has a great relevance to minimize energy losses from the DHPs. The importance of studying thermal degradation, understanding the processes occurring during thermal stress as well as the parameters affecting the thermal stability of PUR insulating material are essential in order to effectively design the pipe and in particular polyurethanes properties suitable for a certain environment. Furthermore, the foam is expected to restrain axial movement due to thermal changes of the pipeline. Most of the studies related to the parameters that can have impact on ageing are focused on the analyses of gas diffusion through PE jacket or diffusion process and associated change in the cell gas composition in the PUR insulation [3], [4]. These works have focused on the relation of the diffusion of oxygen and replacement of the cell gases to the decrease of the foam strength.

As district heating networks operate with high service temperatures up to 120 °C, a good long-term heat resistance is necessary to maintain the most important properties e.g. good adhesion of the foam to the pipe and good insulation efficiency. The minimum properties the foam must fulfil are outlined in the European quality norm for pre-insulated bonded pipe systems for buried hot water networks, EN 253. This standard, prescribes the life time prediction of pipes by testing and

evaluation of the adhesion strength between PUR and steel pipe after accelerated ageing at an elevated temperature of 170 °C. The expected life time for PUR insulation is calculated using Arrhenius relationship.

To understand how the thermal and mechanical properties of PUR foam are related to each other and how they are changed with time at high service temperatures further studies are needed.

This paper reflects a part of a Ph.D. research project. The main aim is to study and determine the different degradation mechanisms in PUR foam over time. Furthermore, another objective is to improve the model used to calculate the expected service life of a DHP.

EXPERIMENTAL

Results from the previous projects have shown that a better understanding of the degradation mechanisms of PUR when it is aged at high temperatures is needed [5]. In this project, three DHP DN50/160 of length 4 m with a 3 mm thick PE casing were placed in a chamber with a controlled ambient temperature. The DHPs were manufactured by Power Pipe in Gothenburg using the traditional discontinuous, pour-in-place method filling the pipe from the middle, which gives some variations in the overall density of the PUR.

The chosen ageing temperatures were 130 °C, which is very close to the highest working temperature of DHS, 150 °C and 170 °C, which is used as accelerated ageing temperature in EN 253. The steel pipes of the DHP were connected to a controlled electric source. Before blowing of the polyurethane mantel, some temperature sensors were placed in the DHP to follow the internal temperature at the contact surface between the PUR and the steel serve pipe during the experiments. These sensors were placed along the steel service pipe; one of the sensors was placed in the middle of the DHP and the other two sensors in the ends.

In the same way, two special thermal sensors made by Hot Disc AB were placed in the PUR insulation of the DHP at two distances from the steel pipe viz. 5 mm and 30 mm. The sensors are both heat source and temperature sensor, which means, they are able to measure the thermal transport property and the real temperature in the PUR during the tests. This measurement is based on the transient plane source (TPS) technique, which is a faster method in comparison with steady-state techniques and can be used in place without taking out large sample pieces.

To evaluate the degradation of DHP after specified ageing intervals, mechanical and thermal properties were followed. The thermal conductivity of the three

pipes were measured first at the corresponding ageing temperatures and then the DHPs were allowed to cool down to room temperature, and the measurements were carried out again. At this temperature, the DHPs were also subjected to mechanical stress test to measure the loss of adhesion between the PUR and steel service pipe. The method used was the SP plug method as described in [5]. A torque was applied manually and recorded by a static torque transducer. The maximum torque needed to separate the test sample (PUR) from the steel service pipe was registered.

Basic research has established that degradation of PUR is a complex heterogeneous process that consists of several partial degradation reactions. In order to better understand the material performance as well as to obtain characteristic thermal decomposition data for further studies we exposed PUR foam only, to high temperatures in air and in nitrogen atmosphere. The exposed materials were characterised using mechanical, physical and analytical test methods.

The mechanical and thermal tests were complemented with analytical laboratory tests for characterization of the materials including physical, thermos-analytical and spectroscopic methods such as Differential Scanning Calorimetry (DSC) and Fourier Transform Infra-Red (FTIR).

SUMMARY OF THE RESULTS

Few literatures can be found on the degradation path and mechanism of the PUR material itself when it is exposed to moderate temperatures. In Fig. 1, the results of ageing at 170 °C are demonstrated. It is quite obvious that the degradation of PUR is a multi-stage process composed of a first stage expressed as a rapid change in properties followed by a plateau phase which changes after about 2000h to a gradual deterioration of the properties.

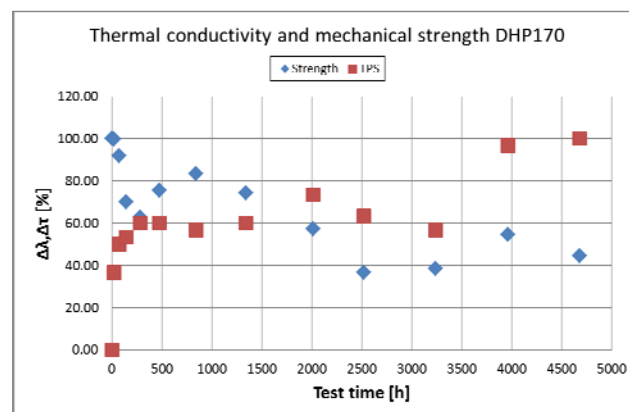


Figure 1. Change in thermal conductivity and adhesion strength as a function of ageing time at 170 °C.

The results of the PUR material exposure to 150 °C in air and in nitrogen showed significant differences in the degradation characteristics between the two environments as was revealed by DSC and FTIR methods. However, the mechanical properties changed in a very similar way. First, the adhesion strength decreased rapidly followed by a plateau part.

ACKNOWLEDGEMENT

The authors are grateful to the Swedish District Heat Association and Swedish Energy Agency for financial support. Powerpipe Systems AB, Mr. Göran Johansson and Mr. Roger Hwartz, BASF Polyurethanes GmbH Mr. Carsten Ellersiek are gratefully acknowledged for manufacturing and supplying of the pipe and useful and stimulating comments. I would like to thank Hot Disk AB Mr. Daniel Cederkrantz for kind cooperation, help and assistance with thermal sensors.

REFERENCES

- [1] Svend Fredriksen and Sven Werner, District Heating and Cooling, Svensk Fjärrvärme (2013).
- [2] Camilla Persson, Prediction the long-term insulation performance of district heating pipes, Chalmers University of Technology (2015)
- [3] Christian Ting Larsen, Peter Togeskov and Andreas Leuteritz Analyses of Diffusion rates through PE and impact on ageing, Euro Heat & Power English Edition .vol 6. (11/2009)
- [4] Nazdaneh Yarahmadi and J.H Sällström, Improved maintenance strategies for district heating pipelines. The 14th International Symposium on District Heating and Cooling, Stockholm (2014)

STRATIFICATION IN HOT WATER PIPE-FLOWS

Denis F. Hinz¹, Simon Graner¹, Christian Breitsamter²

¹ Kamstrup A/S, Industrivej 28, Stilling, 8660 Skanderborg, Denmark, dfh@kamstrup.com

² Technische Universität München, Institute of Aerodynamics and Fluid Mechanics, Boltzmannstrasse 15, 85748 Garching, Germany

Keywords: *Thermally stratified pipe-flow, Laser-Doppler velocimetry, buoyancy effects*

ABSTRACT

In district heating and cooling networks, hot or cold fluid is transported in pipe systems over long distances. Heat loss (or gain) from the fluid-carrying pipes to the surrounding is a primary driving mechanism that can lead to various thermal dynamics effects in the fluid. Here, we investigate the thermal dynamics of low-Reynolds number hot water flow in horizontal pipes. In such flows, density differences between hot and cold water generate buoyancy effects. Further, the coupling between heat transfer and momentum transfer along with the temperature-dependent viscosity of water can result in stratified asymmetric flow profiles where fluid is transported with high velocities in the top region of the pipe cross-section and can be almost stagnant in the bottom region. In the flow laboratory at Kamstrup A/S, we carried out experiments to analyze thermally stratified flow profiles with laser-Doppler velocimetry. In this article, we present results for the downstream development of stratified flow profiles for different flow parameters including temperature, pipe diameter, and flow rate (or dimensionless Reynolds number and Rayleigh number, respectively.) Further, we discuss the impact of thermally stratified flow profiles on metering applications in district heating and cooling networks.

INTRODUCTION

Single-phase thermally stratified flow may appear in horizontal pipes in which two layers of the same liquid with high temperature and density differences flow at low velocities [1]. This stratification is driven through heat transfer between the water, the pipe wall, and the surrounding air. The colder and therefore heavier fluid accumulates at the bottom part of the pipe, while the hotter and lighter fluid occupies the upper part [1]. This phenomenon is driven by buoyancy forces, emerging through a top to bottom temperature gradient in the pipe [2]. Stratification is expected to emerge when the forced-flow has a small Re and the buoyancy forces are relatively high. For large buoyancy forces, which are characterized through high Grashof numbers Gr, effects of forced convection are negligible but for lower Gr forced convection needs to be taken into account. In

most practical situations, both phenomena have to be taken into account [3]. In this article, we study experiments to quantify the influence of different water temperatures and pipe diameters on the emergence of stratified flow profiles.

MATERIALS AND METHODS

We use a commercial Nd:YAG laser-Doppler velocimetry (LDV) probe from ILA/Optolution with a window chamber that enables full three-dimensional optical access. The probe is mounted on a traversing system for automated displacement in a Cartesian coordinate system (Figure 1 (a) and (b)). We perform all experiments on a verification and calibration test bench in the flow laboratory of Kamstrup A/S using brass pipes of inner diameter $D = 15.0$ mm (DN15) and $D = 25.0$ mm (DN25). The pipes are not insulated to provide an experimental setup with maximized heat exchange between the fluid, the pipe, and the environment. The volumetric flow rate Q , the water temperature T , and the pressure p are actively controlled and adjusted within a PID feedback loop.

We perform experiments at various flow rates and temperatures corresponding to different Reynolds numbers Re and Rayleigh numbers Ra. The Reynolds number is defined as

$$\text{Re} = \frac{w_{\text{vol}} D}{\nu}, \quad (1)$$

where $w_{\text{vol}} = Q/A$ is the volumetric velocity and ν is the kinematic viscosity based on the mean temperature

$$T_{\text{mean}} = \frac{T_i + T_o}{2} \quad (2)$$

in the test section with T_i the inlet temperature and T_o the outlet temperature. To assess the downstream development, we perform measurements at cross sections located at $z_{\text{ST}} = 12D, 30D, 60D$, and $110D$ downstream from the inlet (Figure 1 (c)).

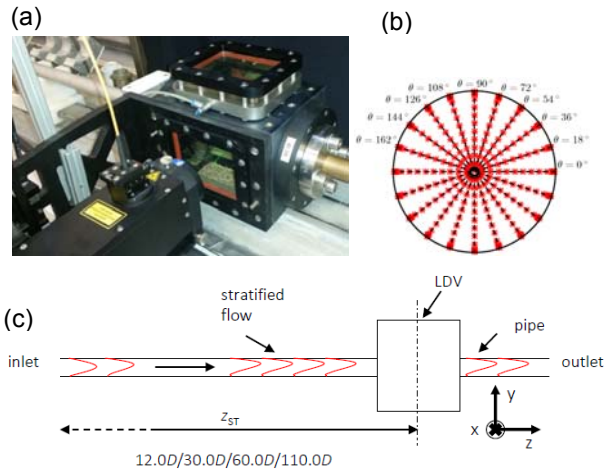


Figure 1. Setup of the stratification experiment. (a) LDV window chamber. (b) LDV measurement grid. (c) The LDV window chamber is placed at different downstream locations.

RESULTS

First, we show results for $Re = 1.0 \cdot 10^3$ which corresponds to $Q = 0.0392 \text{ m}^3/\text{h}$ with the DN25 pipe and $Q = 0.0235 \text{ m}^3/\text{h}$ with the DN15 pipe. Figure 2 shows 2D contour plots of stratified velocity profiles in two different pipe diameters at various distances downstream from the inlet. For the DN15 velocity profiles (Figure 2 (a)–(d)), the stratification increases with increasing downstream distance, as indicated through the red color zone with $w/w_{vol} \approx 2$. Hence, the asymmetry is highest for $z_{ST} = 110D$ whereas all profiles are symmetric along the x -axes. A visual comparison of the DN15 contour plots with the DN25 contour plots shows that the flow is already strongly stratified at $30D$ for DN25. Further downstream at $60D$ and $110D$, only slight differences in the profiles are visible. This indicates that a fully developed stratified flow emerges at around $30D$ for $T = 60^\circ\text{C}$ with a DN25 pipe. In practice, profiles with the shapes shown in Figure 2 arise in district heating systems where hot water is transported between production and consumption points. This means that flow meters are likely to be confronted with similar profiles in the field although insulation may weaken thermal dynamics effects. In the remainder of this article, we will analyze the velocity profiles in more detail.

Stratified profiles in DN25 pipe

Figure 3 shows a comparison of stratified flow profiles at locations $12D$, $30D$, $60D$, and $110D$ downstream and for $T = 40^\circ\text{C}$, $T = 50^\circ\text{C}$, and $T = 60^\circ\text{C}$. The downstream development on the profiles depends on the water temperature (Figure 3). At the closest distance from the inlet, the stratification is already present but appears to become more prominent further downstream. For water

temperature $T = 50^\circ\text{C}$, the developing stratification is also visible at $30D$, whereas the stratification is fully developed at $60D$, since the profiles at $60D$ and $110D$ coincide (Figure 3 (b)). For $T = 60^\circ\text{C}$ the stratified profile is fully developed at $30D$ downstream, since the profiles at $30D$, $60D$, and $110D$ coincide (Figure 3 (c)).

The velocity profiles at different distances downstream from the inlet for various temperatures are shown in Figure 4 (a)–(d). The flow profiles at $12D$ are similar for the three temperatures $T = 40^\circ\text{C}$, $T = 50^\circ\text{C}$, and $T = 60^\circ\text{C}$ and exhibit a flat center region without pronounced peak (Figure 4 (a)). For $T = 40^\circ\text{C}$ and $30D$ downstream, the development of the stratification is less pronounced (Figure 4 (b)). This difference illustrates the dynamics of stratification depending on the temperature difference ΔT between the pipe-flow and the environment. For lower temperatures the flux from the pipe-flow to the environment is smaller. In consequence, it takes longer to get a similar velocity distribution (Figure 4 (a)).

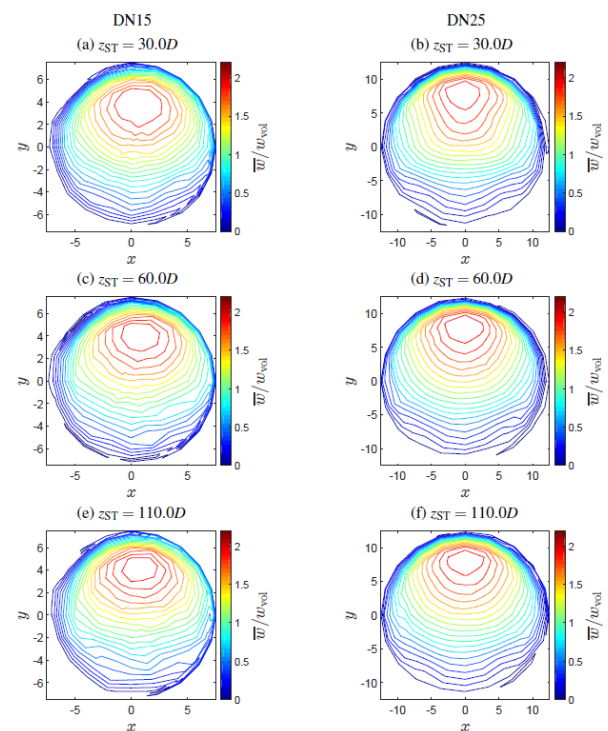


Figure 2. 2D velocity contours for a stratified flow at $30D$, $60D$ and $110D$ and $T = 60^\circ\text{C}$ in a DN15 and DN25 pipe with $Re = 1.0 \cdot 10^3$.

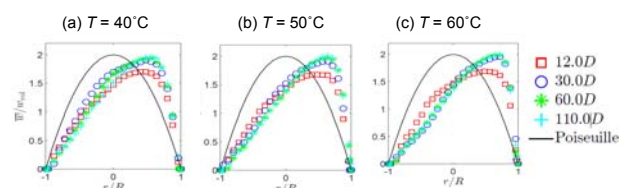


Figure 3. Flow profiles at $12D$, $30D$, $60D$ and $110D$ for $T = 40^\circ\text{C}$, $T = 50^\circ\text{C}$ and $T = 60^\circ\text{C}$ at $\theta = 90^\circ$ in a DN25 pipe.

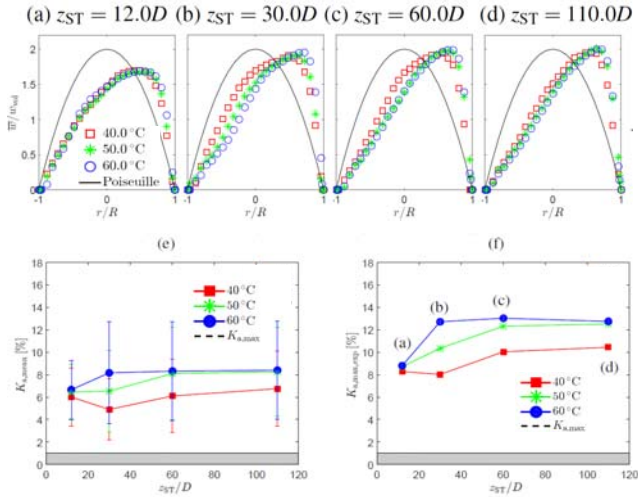


Figure 4. Mean asymmetry factor $K_{a,mean}$ for all profile angles θ (e) and maximum asymmetry factor $K_{a,max,exp}$ for $\theta = 90^\circ$ (f) at different temperatures along with velocity profiles at different distances in a DN25 pipe (a)–(d).

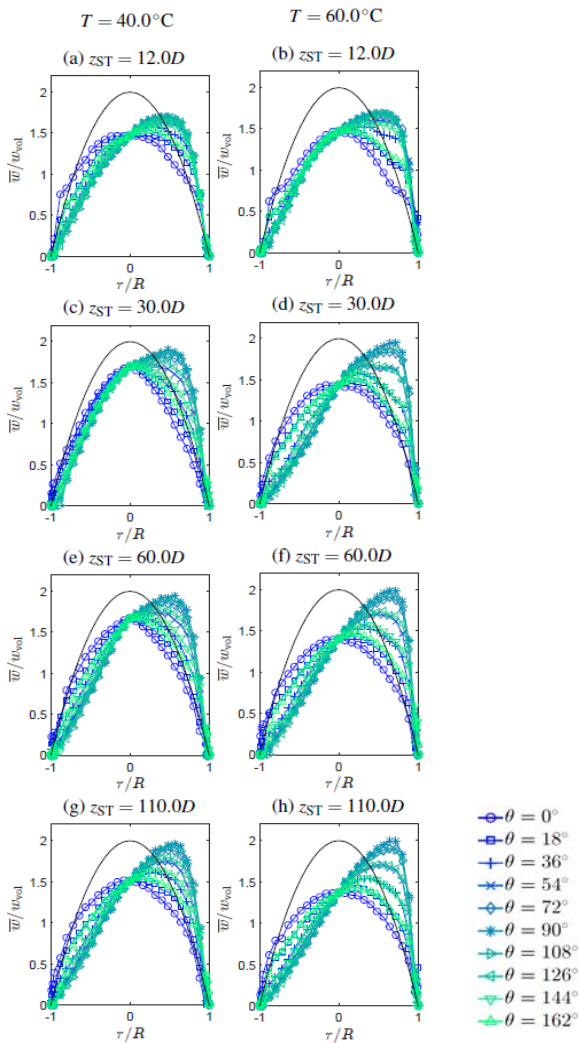


Figure 5. Comparison of stratified profiles at 12D, 30D, 60D, and 110D for $T = 40^\circ\text{C}$ and $T = 60^\circ\text{C}$ in a DN25 pipe.

Further downstream at 60D, the flow profiles for $T = 50^\circ\text{C}$ show only a slight difference to the velocity profiles for $T = 60^\circ\text{C}$. This indicates a fully developed stratification at 60D downstream from the inlet for $T = 50^\circ\text{C}$. At 110D both, the $T = 50^\circ\text{C}$ and the $T = 60^\circ\text{C}$ profiles coincide, whereas the profiles for $T = 40^\circ\text{C}$ are still stratified. Consequently, the pipe-flow at $T = 40^\circ\text{C}$ needs a longer downstream distance to saturate towards a fully developed stratification due to the weaker heat transfer. For $T = 60^\circ\text{C}$, the velocity profiles are similar at all measurement cross sections downstream from the inlet, which indicates a fast build-up of the stratification effect.

Figure 5 shows the velocity profiles for all measurement paths (different θ according to the measurement grid in Figure 1 (b)) at $T = 40^\circ\text{C}$ and $T = 60^\circ\text{C}$. For $T = 40^\circ\text{C}$, the velocity profile at 30D already shows a strong deviation from the Poiseuille reference profile (Figure 5 (a)). At 60D the profile at $\theta = 0^\circ$ reaches a maximum of approximately $w/w_{vol} = 0.85$ (Figure 5 (c)). With increasing distance from the inlet, the displacement between the peak of the Poiseuille reference profile and the peak of the stratified profiles becomes more prominent (Figure 5 (c) and (e)). This behavior is even stronger for $T = 60^\circ\text{C}$ (Figure 5 (b), (d), (f), and (h)) in which the velocity at $\theta = 0^\circ$ reaches roughly 70% of the fully developed velocity profile. Furthermore, the velocity profile for $T = 40^\circ\text{C}$ at 110D (Figure 5 (g)) is similar to the profiles for $T = 60^\circ\text{C}$, which confirms that the stratification effect develops faster for higher temperatures using a DN25 pipe.

Quantification with performance indicators

Performance indicators are integral metrics to measure the shape of flow profiles and to quantify the deviation of flow profiles from reference profiles such as the Poiseuille profile for laminar flow. The so-called asymmetry factor K_a is suitable for quantifying the shape of stratified profiles [4]. The mean $K_{a,mean}$ and maximum $K_{a,max,exp}$ of the asymmetry factor for different temperatures $T = 40^\circ\text{C}$, $T = 50^\circ\text{C}$, and $T = 60^\circ\text{C}$ and downstream distances 12D, 30D, 60D, and 110D is shown in Figure 4 (e) and (f). At 12D the asymmetry factors coincide for all temperatures. This suggests that the profiles at the inlet are dominated by disturbance effects due to the bend installed approximately 0.5 m before the inlet. This means that at the inlet region for $z_{ST} \leq 12D$ the disturbances through the bend have more influence on the velocity profile than the temperature effects.

In contrast, the temperature has a significant impact on the downstream development with increasing distance from the inlet. At 30D, differences in $K_{a,mean}$ for different temperatures emerge (Figure 4 (e)). In general, the

stratification increases with increasing temperature at all downstream distances. At 60D and 110D for $T = 50^\circ\text{C}$ and $T = 60^\circ\text{C}$ the highest in $K_{a,mean}$ and $K_{a,max,exp}$ are found. This suggests that the profiles saturate towards a stratified equilibrium profile that does not change anymore with increasing temperature beyond 60°C . However, the profile for $T = 60^\circ\text{C}$ saturates faster, since the maximal $K_{a,mean}$ and $K_{a,max,exp}$ are attained at 30D already. Hence, for $T = 60^\circ\text{C}$ the stratification develops very fast and is nearly constant after 30D. In contrast, for $T = 40^\circ\text{C}$ the stratification increases continuously over the test section, indicating that this stratification does not saturate within the considered downstream distances. An extrapolation of the results for 30D, 60D, and 110D with $T = 40^\circ\text{C}$ suggests that a value of about 7% is likely to be reached at a distance of approximately 200D. Thus, the maximum of $\approx 8\%$ attained by the 50°C and 60°C flows is unlikely to be exceeded with 40°C water temperature. The maximal values $K_{a,max,exp}$ show an analogous development as the mean asymmetry factor $K_{a,mean}$ (Figure 4 (f)).

Table 5: Summary of three different temperature pairings to test for Rayleigh similarity.

Ra	$T_{w,15}$	$T_{w,25}$
$2.27 \cdot 10^6$	40°C	27°C
$5.67 \cdot 10^6$	50°C	32°C
$9.92 \cdot 10^6$	60°C	37°C

REYNOLDS AND RAYLEIGH SIMILARITY

To test for Re and Ra similarity, we design experiments in different pipe diameters DN15 and DN25 and adjust flow rate and water temperature to achieve matching Re and Ra numbers. The objective is to determine to what extent Re and Ra similarity hold and to determine if secondary effects cause deviations in the similarity.

The material properties of water change with temperature and similarity properties are captured by dimensionless parameters (see, for example, [32, 111]). The Grashof number

$$\text{Gr} = \frac{g\alpha(T_w - T_\infty)L^3}{\nu^2} \quad (3)$$

is the characteristic ratio of buoyancy to viscous forces acting on a fluid, where g is the gravitational acceleration, α is the thermal expansion coefficient, T_w is the wall temperature, T_∞ is the ambient temperature, and $L = D$ is the characteristic length for flow in a pipe with circular cross-section. The Prandtl number

$$\text{Pr} = \frac{\nu}{a} \quad (4)$$

defines the characteristic ratio of momentum diffusivity and thermal diffusivity. A combination of (3) and (4) yields the Rayleigh number

$$\text{Ra} = \text{Gr} \text{Pr} . \quad (5)$$

The thermal expansion coefficient α , the kinematic viscosity ν , and the thermal diffusivity a are temperature dependent.

The conditions $\text{Ra}_{15} = \text{Ra}_{25}$ yields

$$\frac{\text{Ra}_{15}}{gD_{25}^3} = \frac{\alpha_{25}(T_{w,25} - T_\infty)}{\nu_{25}a_{25}} , \quad (6)$$

where the subscript 15 denotes values associated with the DN15 pipe and the subscript 25 denotes values associated with the DN25 pipe. Substituting $D_{25}^3 = 4.6296 D_{15}^3$ in (6) yields

$$\frac{\text{Ra}_{15}}{4.6296gD_{15}^3} = \frac{\alpha_{25}(T_{w,25} - T_\infty)}{\nu_{25}a_{25}} . \quad (7)$$

From (7), the temperature $T_{w,25}$ can be computed. For temperatures within the range $0^\circ\text{C} < T < 60^\circ\text{C}$ the thermal diffusivity α is estimated through [7]

$$\alpha = (1.35 + 0.002T_w)10^{-7} . \quad (8)$$

The dynamic viscosity μ for water is estimated through [8, 9]

$$\mu = \mu_0(\bar{T})\mu_1(\bar{\rho}, \bar{T}) , \quad (9)$$

where,

$$\mu_0(\bar{T}) = \frac{(\mu^* \sqrt{\bar{T}})}{(\sum_{k=0}^3 a_k \bar{T}^{-k})} \quad (10)$$

with $\mu^* = 1.0 \cdot 10^{-6}$ Pa·s and coefficients a_k . $T = T/T^*$ is the dimensionless temperature with $T^* = 647.27$ K and

$$\mu_1(\bar{\rho}, \bar{T}) = \exp \left[\bar{\rho} \sum_{i=0}^5 \sum_{j=0}^4 b_{ij} \left(\frac{1}{\bar{T}} - 1 \right)^i (\bar{\rho} - 1)^j \right] \quad (11)$$

is a function with the coefficients b_{ij} and the dimensionless density $= \rho/\rho^*$ with $\rho^* = 317.763$ kg/m³. Expression (6) holds for temperatures within the range by $0^\circ\text{C} \leq T \leq 800^\circ\text{C}$ and pressures within the range 0 MPa $\leq p \leq 100$ MPa. Using the results for the dynamic viscosity μ , the kinematic viscosity ν is estimated through the corresponding densities ρ [10]. The thermal expansion coefficient α for various temperatures is given by Eisenberg and Kauzmann [11]. The calculations show that the water temperature $T_{w,25}$ required to achieve Ra similarity is lower than $T_{w,15}$, as summarized in Table 5.

Figure 6 shows velocity profiles at $\theta = 90$ for flow in DN15 and DN25 subject to Re and Ra similarity. The associated mean and maximum asymmetry factors are summarized in Figure 6 (j) and (k). Rayleigh similarities are assessed for three different temperature pairings to find out under which conditions the Rayleigh similarity is best captured.

For the lowest temperature pairing with $T = 40^\circ\text{C}$ for DN15 and $T = 27^\circ\text{C}$ for DN25, the velocity distribution as well as the location of the peaks are different for the three distances (Figure 6 (a)–(c)). The flow profiles in the DN15 pipe appear to have a more shallow slope in the bottom part of the pipe until the maximum value at around $r/R = 0.5$. In the DN25 pipes the stratification is less developed and characterized through a steeper slope and a peak of $w/w_{vol} \approx 1.9$ at $r/R = 0.2$.

The slopes of the flow profiles agrees well at $30D$ and $60D$ downstream for the intermediate temperature pairing with $T = 50^\circ\text{C}$ for DN15 and $T = 32^\circ\text{C}$ for DN25 (Figure 6 (d) and (e)). However, at $110D$ the flow profile is more stratified in the DN15 (Figure 6 (f)). Similarly as for the lower temperature pairing, the velocity profiles in the DN25 pipe do not reach the peak of $w/w_{vol} = 2$ as it is the case for DN15.

The asymmetry factors $K_{a,mean}$ and $K_{a,max,exp}$ exhibit a large spread in values because of the disagreement in the shape of the profiles (Figure 6 (j) and (k)). This indicates that Rayleigh similarity does not hold for the low and intermediate temperatures. Consequently, a small temperature difference may lead to secondary effects in a temperature range where the Rayleigh similarity does not hold anymore.

For the highest temperature pairing with $T = 60^\circ\text{C}$ for DN15 and $T = 37^\circ\text{C}$ with DN25, the flow profiles converge to each other with increasing distance downstream from the inlet. Additionally, the velocity peak is of similar magnitude at $110D$, which leads to a reasonable Rayleigh similarity confirmed by the agreement in asymmetry factors (Figure 6 (j) and (k)).

Thus, only at a high enough temperature pairings the necessary heat transfer conditions are given and the flow profiles are self-similar for $z_{ST} \geq 60D$. Consequently, Rayleigh similarity is achieved when the temperature and therefore the heat exchange as well as the downstream distance are chosen appropriately.

DISCUSSION AND CONCLUSIONS

We have studied the influence of temperature effects on the flow profile. Velocity profiles of DN15 and DN25 pipes were discussed through an approximate Re and Ra similarity. We found that stratification develops slower in DN15 pipes where a fully stratified flow is found at around $100D$ downstream. In contrast, in

DN25 pipes and for high enough temperatures, a fully stratified flow is found at $30D$ downstream already.

Tests of the Rayleigh similarity suggest that the flow profiles are self-similar at high temperature pairings, whereas self-similarity does not hold for smaller temperature pairings resulting in weaker heat exchange between the fluid and the surrounding. The breakdown of similarity for lower temperature pairings suggest that secondary effects have a larger influence. Secondary effects may depend on the temperature of fluid, pipe, and environment, the uniformity of the heat flux and other factors. Therefore, additional measurements with different parameter ranges may yield further conclusions regarding the self-similarity of stratified flow profiles.

For flow laboratories, the Rayleigh similarity has important practical implications. For example, experiments on large diameters can be scaled down to smaller diameters using Reynolds and Rayleigh similarity. Since it is usually cheaper, faster and more convenient to test on smaller pipe diameters, such scaled experiments have potential to save costs and test time on larger test equipment.

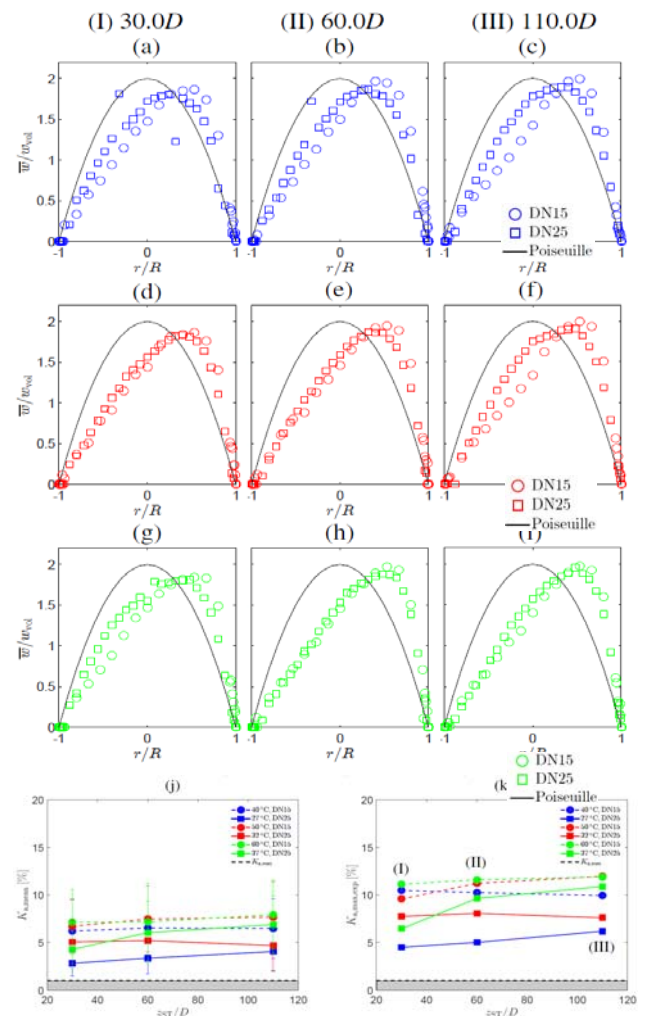


Figure 6. Assessment of Rayleigh similarity for profiles at $\theta = 90^\circ$ ((a)-(i)) and along with mean (j) and maximal (k) asymmetry factors for distances 30D, 60D and 110D in DN15 and DN25 pipes.

ACKNOWLEDGEMENT

DFH acknowledges the support of Viola Koch in preparing this manuscript.

REFERENCES

- [1] H. C. Rezende, M. A. Navarro, E. Jordao, A. Augusto, and C. dos Santos, "Experiments on onephase thermally stratified flows in nuclear reactor pipe lines", International Nuclear Atlantic Conference - INAC, 27. September – 2. October, Rio de Janeiro, 2009.
- [2] J. H. Kim, R. M. Roidt, and A. F. Deardorff, "Thermal stratification and reactor piping integrity", Nuclear Engineering and Design, 139(1):83–95, 1993.
- [3] A. Kupper, E. G. Hauptmann, and M. Iqbal, "Combined free and forced convection in a horizontal tube under uniform heat flux", Solar Energy, 12:439–446, 1969.
- [4] "U. Müller, Richtlinie zur strömungstechnischen Validierung von Kalibrier-Prüfständen im Rahmen der EN 1434" 2009.
- [5] K. Gersten and H. Herwig, "Strömungsmechanik: Grundlagen der Impuls-, Wärme- und Stoffübertragung aus asymptotischer Sicht. Grundlagen und Fortschritte der Ingenieurwissenschaften", Vieweg & Teubner, Wiesbaden, 1992.
- [6] J. Spurk and N. Aksel, "Strömungslehre: Einführung in die Theorie der Strömungen", Springer, 2010.
- [7] D. W. James, "The thermal diffusivity of ice and water between -40 and + 60 degrees", Journal of Materials Science, 3:540–543, 1968.
- [8] A. A. Aleksandrov, A. I. Ivanov, and A. B. Matveev, "Teploenergetika", Thermal Engineering, 22(4):77, 1975.
- [9] G. Smithberg and F. Landis, "Friction and forced convection heat transfer characteristics tubes with twisted tape swirl generators", Journal of Heat Transfer, 86:39–49, 1964.
- [10] D. Eisenberg and W. Kauzmann, "The structure and properties of water", Oxford Classic Texts in the Physical Sciences, 1969.
- [11] K. Gasljevic, G. Aguilar, and E. F. Matthys, "Buoyancy effects on heat transfer and temperature profiles in horizontal pipe flow of drag-reducing fluids", International Journal of Heat and Mass Transfer, 43(23):4267–4274, 2000.

LONG TERM PERFORMANCE OF VACUUM INSULATION PANELS IN HYBRID INSULATION DISTRICT HEATING PIPES

A. Berge¹, B. Adl-Zarrabi¹

¹ Chalmers University of Technology, Sven Hultins gata 8, Göteborg, SE- 412 96, Sweden

Keywords: vacuum insulation panels, VIP, district heating, heat losses, long term performance

ABSTRACT

A new concept for high performance district heating pipe insulation have been under development, where a vacuum insulation panel replace the innermost layers of polyurethane around the service pipe. During the last years, the concept has been tested through a series of measurements, showing that a 10 mm vacuum insulation panel can reduce the heat losses by around 30% when used in pipes of dimension DN 100/225. When the panel is placed around the supply pipe of a twin pipe simulations indicated that the losses from the supply water could be reduced by up to 50%. One of the main challenges with the vacuum insulation panels are their long term performance. Over time, air will enter the panels and the insulation performance will be reduced. To evaluate the long term performance of hybrid insulation district heating pipes, measurements have been ongoing during the last four years. Prototypes of hybrid pipes have been tested both in field as pipe segments connected to a municipal district heating grid and in laboratory with a constant temperature in the pipe. The temperature have been logged at various positions on and around the panels. Variations in the temperatures can be used to evaluate the thermal performance of the pipes. The results indicate that the panels are intact after four years in field. In the laboratory, the pipes have been exposed to a constant temperature of 115°C for over three years without damage to the panels. Thus, the panels have been shown to withstand a higher temperature within a polyurethane embedding than panels heated in open air. Also there are indications that the panel, if it collapses, will be filled with the pore gas of the polyurethane instead of air, reducing the impact of the damage compared to other applications of the vacuum insulation panels.

INTRODUCTION

Statistics Sweden show that 10% of the energy input to the district heating network is lost as heat losses from the district heating pipes [1]. Reidhav and Werner show that the proportion of the losses might be even higher for areas with a less dense energy outtake [2].

IEA-DHC Annex VIII [3] suggests some different methods to reduce the losses by either changing the

symmetry of the district heating pipes or arranging more pipes in the same casing pipe.

Dalla Rosa et al show that placing the supply pipe closer to the center of a twin pipe could reduce the losses by up to 3.2%. Further, Bøhm and Kristjansson [4] show that making the casing egg-shaped decrease the heat losses even more, by up to 7% compared to a circular twin pipe of the same size.

IEA-DHC Annex VIII [3] also suggests using high performance insulation close around the supply pipe. In a cylindrical geometry the effect of the insulation is larger, closer to the center of the cylinder. This is investigated in this paper.

Vacuum insulation panels (VIP)

Polyurethane foam (PUR), blown with carbon dioxide and some pentane isomers, is commonly used as insulation in district heating pipes. PUR district heating pipes are commercialized with a thermal conductivity in the range of 24-28 mW/(m·K) at 50°C [5]–[7]. This is in a similar range as that of researchers [8]–[10]. These values can be compared to vacuum insulation panels (VIPs), a new type of insulation for the district heating sector. With a fumed silica core the thermal conductivity at the center of the panels are as low as 4-5 mW/(m·K) as long as they are kept evacuated [11].

A VIP consists of a core material, commonly made of a porous silica structure, evacuated and encapsulated in a highly diffusion tight envelope, as shown in **Figure 1**. The envelope commonly consists of a laminate, alternating polymer layers and aluminium layers. The metal in the envelope creates thermal bridges along the edges of the panels which in turn creates an optimization problem. More aluminium in the envelope creates larger heat losses through the edges but

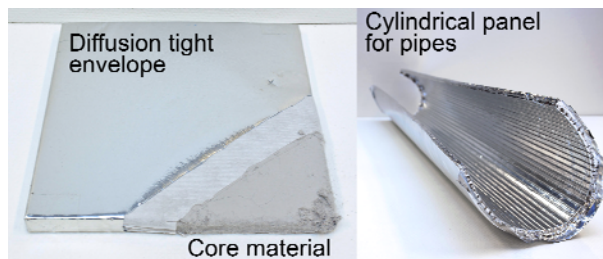


Figure 1. An opened VIP to the left and a cylindrical VIP to the right.

reduce the diffusion of gas into the panels and thus prolongs the life span.

The long term performance of VIPs have been investigated for building insulation by Simmler and Brunner [12] but in district heating the temperatures are much higher. Both Simmler and Brunner [12] and Schwab et al [13] show an exponential relation between temperature and rate of diffusion into the panels. Apart from the diffusion, the high temperatures of the district heating pipes might melt or damage the polymer in the envelope, leading to a fast deterioration.

Hybrid insulation

In a cylindrical geometry, the influence of the insulation is higher the closer it is to the center. This can be seen in the equation for heat flow through a cylindrical material layer, presented in Equation (1):

$$Q = \Delta T \cdot \frac{2\pi\lambda}{\ln(\Delta r/r_0 + 1)} \quad (1)$$

where Q [W/m] is the heat loss from the pipe, ΔT [°C] is the temperature difference over a material layer, λ [W/(m·K)] is the thermal conductivity, Δr [m] is the layer thickness and r_0 [m] is the inner radius of the layer.

If the inner radius, r_0 , increases the heat flow increases for the same layer thickness. Also, the needed amount of material will increase with the square of the radius. This means that at a certain insulation thickness it will be cheaper to pay extra for a high performance insulation close to the center rather than to increase the thickness.

A concept for hybrid insulation district heating pipes have been under development through a series of research projects, where VIPs have replaced the innermost part of the insulation in a PUR pipe. The concept is presented in **Figure 2**.

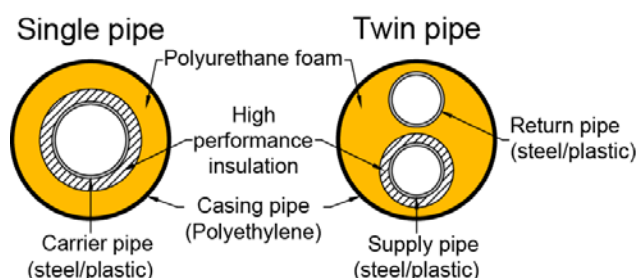


Figure 2 concept for hybrid insulation district heating pipes.

The heat losses have been measured through guarded hot pipe by Berge and Adl-Zarrabi for both single pipes [14], [15] and twin pipes [16]. The measurements on single pipes showed a reduction of almost 30% when a 10 mm VIP was added to a DN 100/225 pipe. The measurements also showed that a destroyed panel still

had a thermal conductivity as good as that of PUR. For the twin pipes, a 10 mm VIP around the supply pipe reduced the total heat losses from a DN 2*80/315 by 12-18% depending on the overlap length of the panel. The losses from the supply water pipe was reduced even further by up to almost 40%.

The hybrid insulation district heating pipes have also been investigated through field measurements by Berge et al [17]. The paper presents a method to evaluate the long term performance of the vacuum panels through temperature measurements in field. The measurements showed that the panels are intact after three years of measurements. A slow diffusion might be present, but it can so far not be detected through the measurements.

This paper aim to summarize the measurements on the long term performance of hybrid insulation district heating pipes with vacuum insulation panels. The paper presents continuation of the field measurements by Berge et al [17], which have been active for another year. The field measurements are complimented by a new field measurements station and also by laboratory measurements of the long time performance.

FIELD MEASUREMENTS

Three pipe prototypes have been installed into field, connected to active district heating networks. The performance of the pipes have been monitored by continuous measurements of the temperatures throughout a cross-section of the pipes. The temperature have been measured with the use of type-T thermocouples mounted before the PUR was added.

Two of the pipes were installed 2012 and connected to the district heating network in the city Varberg, a coastal city in south-western Sweden. Both were twin pipes with the dimensions DN 2*80/250 and DN 2*25/140. The measurement positions for the two pipes are shown in **Figure 3**. The temperature in every position was measured at least at two places along the pipe on two separate VIPs.

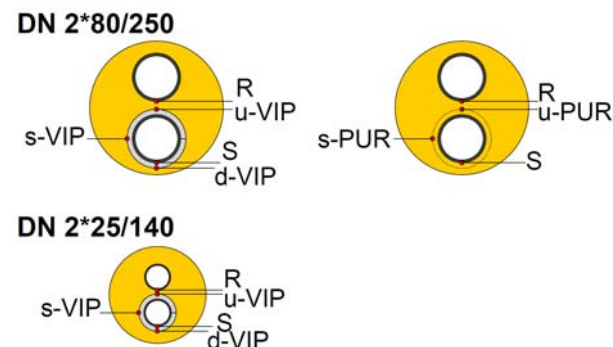


Figure 3. The measurement position for the temperature measurements on the two twin pipes in Varberg.

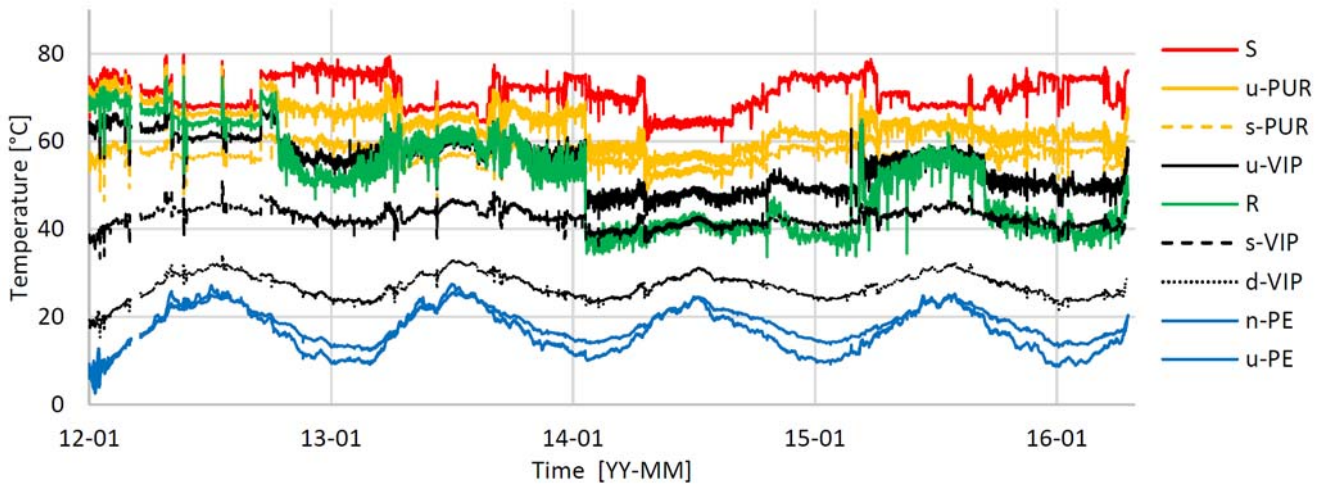


Figure 5. Resulting averages for the positions of the pipe DN 2*80/250 in Varberg.

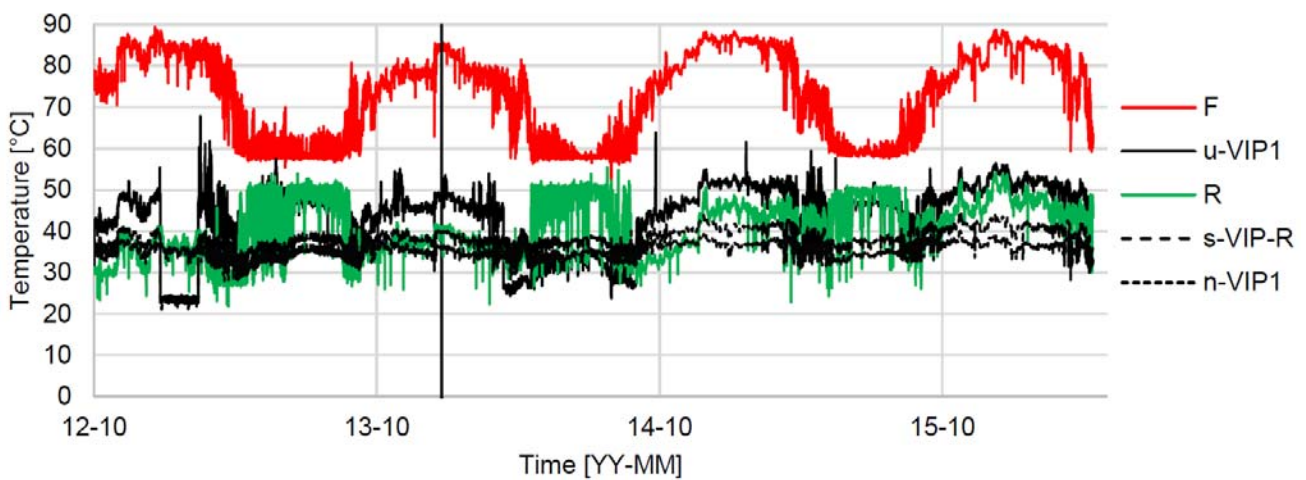


Figure 4. Resulting averages for positions of the pipe DN 2*25/160 in Varberg.

The results from the field measurements in Varberg are presented in Figure 5 for DN 2*80/250 and Figure 4 for DN 2*25/260. The measurements show that there is typically low temperatures in the system, up to a max below 90°C. The results for both pipes are continuous with an apparent cyclic behaviour over the years. The temperature in the supply and return pipes seems to be at similar levels with the exception of the return temperature in Figure 5 which have decreased some over time.

In DN 2*80/250 the temperatures were measured in a reference part of the pipe without VIP. The measurements were made at corresponding positions to the measurements on the backside of the vacuum panels, in the middle of the polyurethane. In Figure 5 it can be seen that the reference points have considerably higher temperatures which is a sign that the heat flow from that point and out is larger in the reference. The VIPs show a direct result, lowering the temperature in the pipe.

The measurement results have been investigated by the error method by Berge et al [17]. The results are

shown Figure 6 for DN 2*80/250. The result show a continuing slow change but still no alarming deterioration rate.

The third field measurement pipe is placed in the city Göteborg, also on the coast of south-western Sweden but a bit further north. The pipe was installed in the summer 2015 and the temperature was put on later during the fall. The pipe had the dimensions DN 150/280 and temperatures were measured on the backside of the VIP, on the service pipe and on the casing of the pipe.

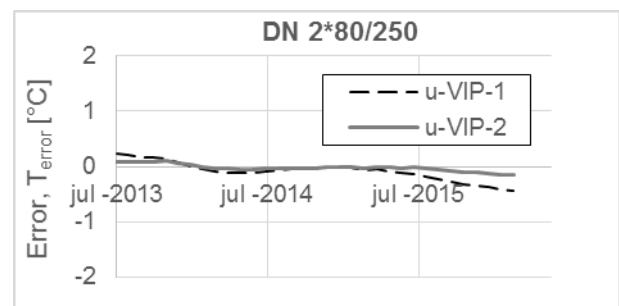


Figure 6. Results for DN2*80/250 from the error model according to [17].

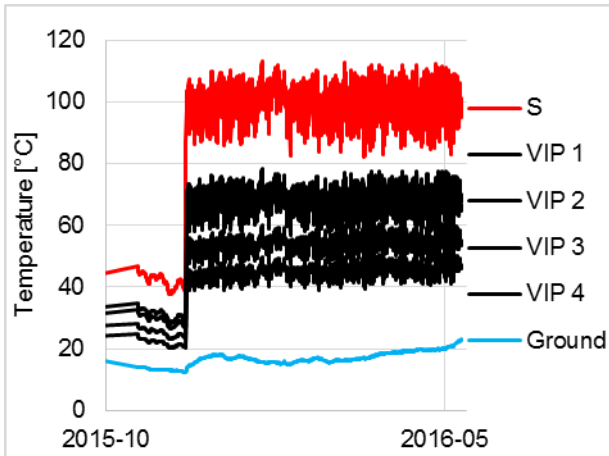


Figure 7. Resulting Temperatures in the pipe DN 150/280 in Göteborg.

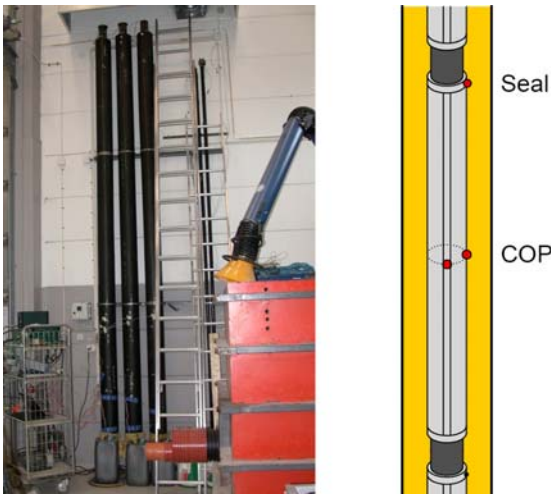


Figure 8. Rig for high temperature measurements of hybrid insulation district heating pipes.

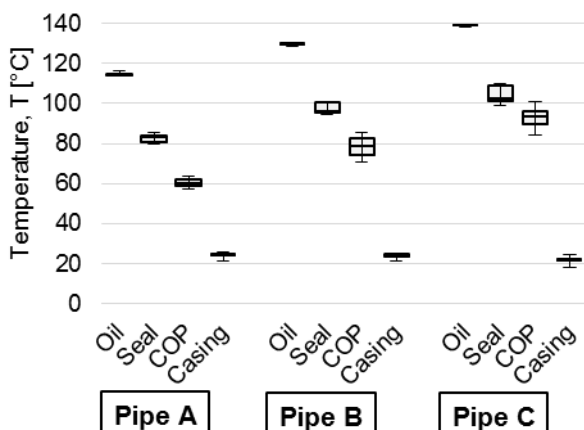


Figure 9. Temperature measurements for the last 15 days for the three high temperature test pipes.

The results from the measurements are shown in **Figure 7**. The single pipe in Göteborg contained four VIPs but when the pipe was installed, two of the VIPs

were found to be broken (VIP 1 and VIP 2 in **Figure 7**), probably due to some mistake during production. This indicates another challenge with using vacuum insulation panels: how to handle them in production so that they are protected from injuries.

The measurements are just recently initiated so the long term performance of the vacuum panels can so far not be analysed.

LABORATORY MEASUREMENTS

Single pipe prototypes have been investigated through long time measurements in the laboratory. Three hybrid insulation pipes were put in a rig with heated oil circulated through the service pipe. The temperature of the circulating oil was held constant and the temperature on the backside of the VIPs (center of panel, COP) and the temperatures at the envelope seals were monitored, together with the oil temperature and the casing pipe temperature. The rig is shown in **Figure 8** together with a description of the temperature measurements.

Each pipe contained three 10 mm thick VIPs. The temperature in the pipe A, B and C was set to 115°C, 125°C and 135°C respectively. The measurements indicated that the VIPs were destroyed after 4 days at 125°C and instantly at 135°C. The measurements on pipe C was continued for 16 days and the measurements on pipe B was continued for 60 days. The measurements on pipe A is still ongoing after 3.5 years. The temperature levels for the last 15 days of measurement can be seen in **Figure 9**.

The seal temperature is investigated since it is assumed that the seals are a weak point in the envelope. During the production of VIPs, the seals are commonly closed by melting the two sides of the envelope together. A high temperature could thus open the seals again. Therefore, the seals were folded to the backside of the panels where the temperature is lower. The results are shown clearly in **Figure 9** where the temperatures in the seals are more than 30°C lower than the steel pipe temperature.

Already in **Figure 9** the temperature on the center of the panel (COP) in pipe A is proportionally closer to the casing temperature compared to pipe B and pipe C. This is a clear indication that the performance of the VIPs are better in pipe A compared to the polyurethane.

The performance VIPs can be investigated by how the temperature on the COP is proportional to the temperature on the casing and in the oil. The pipe can be seen as two cylindrical material layers one with VIP and one with PUR. By assuming a one dimensional, axisymmetric steady state heat flow out through the pipes, the temperatures can then be used to calculate

the quotient between the thermal conductivity of the two layers, as in Equation (2):

$$\frac{\lambda_{PUR}}{\lambda_{VIP}} = \frac{\Delta T_{VIP}}{\Delta T_{PUR}} \cdot \frac{\ln(\Delta r_{PUR}/r_{0,PUR} + 1)}{\ln(\Delta r_{VIP}/r_{0,VIP} + 1)} \quad (2)$$

where λ [W/(m·K)] is the thermal conductivity, ΔT [°C] is the temperature difference over a material layer, Δr [m] is the layer thickness and r_0 [m] is the inner radius of the layers of PUR and VIP.

The results from the calculations of the quotients can be seen in **Figure 10**, **Figure 11** and **Figure 12** for pipe A, B and C respectively.

At the beginning of the measurements, the thermal conductivity is around 3-5 times that of the VIPs. Seen both for pipe A and B in **Figure 10** and **Figure 11**. Panel E in pipe B, **Figure 11**, stands out with a start quotient of 5. The large variation can otherwise be explained by the amplified effect of a shift in the temperature on the backside of the VIP. If the temperature is measured slightly wrong or there are inhomogeneities in the area around the thermocouple on COP, both the temperature differences in Equation (2) would change in opposite direction. Thereby, the change in the quotient get amplified. There could for example be a large air bubble outside of panel E in pipe B, making the thermal conductivity of the PUR locally lower, forcing up the quotient.

Pipe B in **Figure 11** also show a clear deterioration of the VIPs where the quotient decrease with time at various pace for different panels. While VIP C and E show instant very fast collapses, VIP A slowly gets gas filled over a month.

For Pipe A, in **Figure 10**, there is no detectable change in the thermal conductivity quotient after more than three years of measurement.

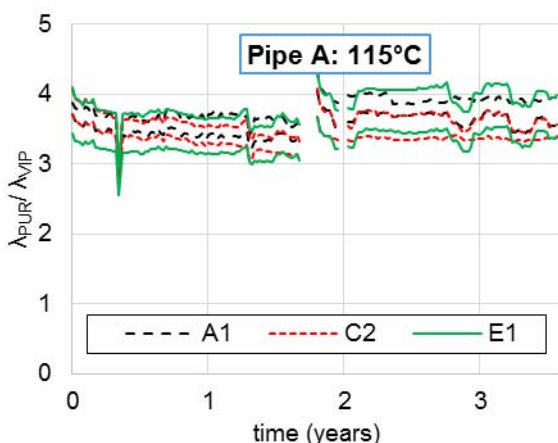


Figure 10. Thermal conductivity quotient ($\lambda_{PUR}/\lambda_{VIP}$) for Pipe A (time scale in years).

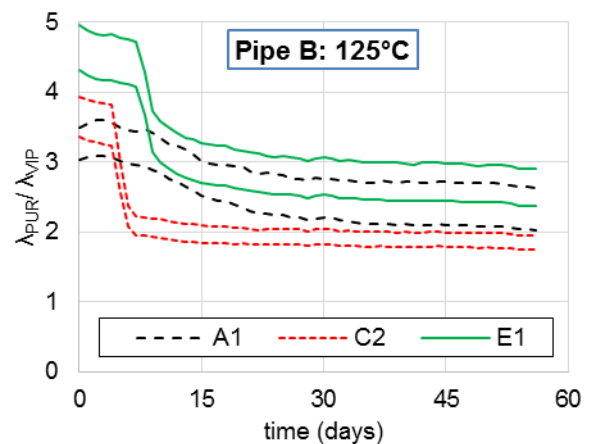


Figure 11. Thermal conductivity quotient ($\lambda_{PUR}/\lambda_{VIP}$) for Pipe B (time scale in days).

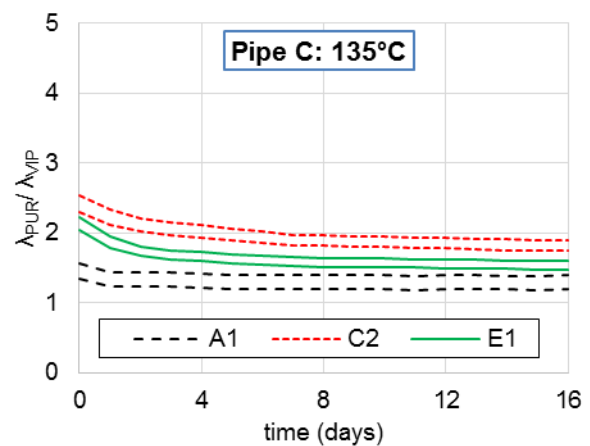


Figure 12. Thermal conductivity quotient ($\lambda_{PUR}/\lambda_{VIP}$) for Pipe C (time scale in days).

A quotient of three could be interpreted as a quite small difference since the presented properties of the PUR and VIPs are 26 mW/(m·K) and 5 mW/(m·K) respectively. On the other hand. The average temperature of the insulation will be influenced. The average temperatures of each material layer is presented in Table 1, showing a considerably higher temperature in the VIP than in the PUR which commonly give higher thermal conductivities for thermal insulations.

Table 1 average temperature in the layers with VIP and PUR.

	$T_{avg} \text{ VIP [}^\circ\text{C]}$	$T_{avg} \text{ PUR [}^\circ\text{C]}$
Pipe A	88	43
Pipe B	104	51
Pipe C	116	57

It is important to note that the quotient is over 1 and for some cases almost three, even when the panel is considered destroyed. In 20°C air, fumed silica have a thermal conductivity around 21 mW/(m·K) [11]. But this could be lowered if the surrounding gas consists of carbon dioxide and pentane isomers.

CONCLUSION

The measurements presented in this paper show promise for hybrid insulation district heating pipes with VIPs. After four years in field the vacuum in the VIPs are still intact. The error model show some possible degradation of the thermal performance, but it is small and not possible to separate distinctly from the effect of a decreasing return water temperature.

He same goes for the vacuum panel which have been continuously exposed to 115°C for more than 3 years. There is still no sign of deterioration. But, when the temperature reaches above 125°C the VIP starts to deteriorate fast and the VIP seems to be gas filled in a couple of days. When the temperature reached over 135°C, the damage was instant.

The measurements are made on vacuum panels optimized for lower temperatures than these in district heating. A change of polymers in the diffusion barrier might improve the heat resistance considerably.

In the applications the VIPs showed a thermal conductivity 1/5 to 1/3 of that of the PUR. But the average temperature in the VIPs are high. Since the VIP has a lower thermal conductivity than the PUR it will actually lower the temperature in the PUR and thus improve its thermal conductivity.

The thermal performance of the VIPs have been investigated by the quotient between thermal conductivity of the VIP and the PUR calculated from the temperature gradients through the pipes. This method is sensitive to small variation in position or temperature of the thermocouples.

The damaged VIPs still showed a considerably better thermal conductivity than the PUR which could be a consequence of the low conductive pore gas of PUR.

ACKNOWLEDGEMENT

The work in this paper have been financed by the Swedish district heating association (Svensk fjärrvärme) through the research project *Livslängd och statusbedömning av fjärrvärmenät*.

All prototype pipes have been produced by *Powerpipe systems AB*. The field measurement stations are connected to the district heating grids of *Varberg energi* and *Göteborg energi*.

REFERENCES

- [1] Statistics Sweden, "El-, gas- och fjärrvärmeförsörjningen 2013. Slutlig statistik," SM1401, 2013.
- [2] C. Reidhav and S. Werner, "Profitability of sparse district heating," *Appl. Energy*, vol. 85, no. 9, pp. 867–877, Sep. 2008.
- [3] H. Zinko, B. Bohm, U. Ottosson, M. Rämä, and K. Sipilä, "District heating in areas with low heat demand density," IEA-DHC, 8DHC-08-03, 2008.
- [4] B. Bøhm and H. Kristjansson, "Single, twin and triple buried heating pipes: on potential savings in heat losses and costs," *Int. J. Energy Res.*, vol. 29, no. 14, pp. 1301–1312, Nov. 2005.
- [5] Isoplus, 2016. [Online]. Available: www.en.isoplus.dk. [Accessed: 10-May-2016].
- [6] Logstor, 2016. [Online]. Available: www.logstor.com. [Accessed: 10-May-2016].
- [7] Powerpipe, 2016. [Online]. Available: <http://www.powerpipe.se/>. [Accessed: 10-May-2016].
- [8] J. Kuhn, H. Ebert, M. Arduini-Schuster, D. Büttner, and J. Fricke, "Thermal transport in polystyrene and polyurethane foam insulations," *Int. J. Heat Mass Transf.*, vol. 35, no. 7, pp. 1795–1801, 1992.
- [9] M. Kutz, *Handbook of measurements in science and engineering.*, vol. 2013. Web: John Wiley & Sons, 2013.
- [10] U. Jarfelt and O. Ramnäs, "Thermal conductivity of polyurethane foam. Best performance," in *Proceedings of 10th International Symposium on District Heating and Cooling*, Germany, 2006.
- [11] R. Caps and J. Fricke, "Thermal conductivity of opacified powder filler materials for vacuum Insulations1," *Int. J. Thermophys.*, vol. 21, no. 2, pp. 445–452, 2000.
- [12] H. Simmler and S. Brunner, "Vacuum insulation panels for building application," *Energy Build.*, vol. 37, no. 11, pp. 1122–1131, Nov. 2005.
- [13] H. Schwab, U. Heinemann, A. Beck, H.-P. Ebert, and J. Fricke, "Permeation of Different Gases Through Foils used as Envelopes for Vacuum Insulation Panels," *J. Build. Phys.*, vol. 28, no. 4, pp. 293–317, Apr. 2005.
- [14] A. Berge and B. Adl-Zarrabi, "Using high performance insulation in district heating pipes," in *13th international symposium on district heating*

and cooling, Kobenhaven, Denmark, 2012, pp. 156–162.

[15] A. Berge and B. Adl-Zarrabi, “Evaluation of vacuum insulation panels used in hybrid insulation district heating pipes,” in *14th international symposium on district heating and cooling*, Stockholm, Sweden, 2014, pp. 454–461.

[16] A. Berge, B. Adl-Zarrabi, and C.-E. Hagentoft, “Assessing the Thermal Performance of District

Heating Twin Pipes with Vacuum Insulation Panels,” *Energy Procedia*, vol. 78, pp. 382–387, Nov. 2015.

[17] A. Berge, C.-E. Hagentoft, and B. Adl-Zarrabi, “Field measurements on a district heating pipe with vacuum insulation panels,” *Renew. Energy*, vol. 87, pp. 1130–1138, Mar. 2016.

CORROSION BEHAVIOR OF PIPELINE STEEL UNDER DIFFERENT IRON OXIDE DEPOSIT IN THE DISTRICT HEATING SYSTEM

Y.-S. Kim¹, J.-G. Kim¹, W.-C. Kim²

¹ School of Advanced Materials Engineering, Sungkyunkwan University, 300 Chunchun-Dong, Jangan-Gu, Suwon, 16419, South Korea

² R&D institute, Korea District Heating Coporation, Yangjaedaero 781, Gangnam-gu, Seoul, 06340, South Korea

Keywords: *under deposit corrosion, polarization, Mott-Schottky analysis, XRD, carbon steel*

ABSTRACT

The corrosion behavior of iron oxides (α -FeOOH, Fe₃O₄, Fe₂O₃) deposits on pipeline steel was investigated in simulated district heating water by electrochemical methods and surface analysis. From the potentiodynamic polarization tests, polarization behavior was different according to the iron oxides deposits. The pitting corrosion was observed on the α -FeOOH-covered specimen. Also, the acceleration of corrosion at boundary between the covered and uncovered deposit was observed on α -FeOOH, Fe₃O₄ deposit-covered specimens. To analyze the surface condition under iron oxides deposit, the Mott-Schottky and X-ray diffraction tests were conducted. The chemical reactions by iron oxides deposit and the reason for localized corrosion under α -FeOOH deposit was explained by crevice corrosion mechanism under rust layer.

INTRODUCTION

With the increase of satellite and planned city near the megalopolis, the DH system application is also increased. In this process, the DH system has the resting long period during the construction of numerous urban, housing facilities and infrastructure. Also, maintenance and improvement work have been actively developed. During this period, the pipeline in distribution part of DH system was exposed to the low temperature, about 40 °C, heating water and stagnant or little flow condition. The long stagnant condition has some problems in corrosion aspect such as deposits from solid particle (sand, debris and iron oxides), ion conductivity, ferrous ion and dissolved oxygen effect [1]-[3]. Especially, the deposits on internal surface of a pipeline cause serious localized corrosion (such as pitting corrosion and crevice corrosion), which is called under deposit corrosion (UDC) [4],[5].

Under-deposit corrosion is dissimilar to other corrosion forms since the condition, like pH, concentration of aggressive species, under deposit is different from the condition in the regions without deposit covered. Then,

there will be galvanic corrosion between the areas under deposit and the areas without deposit [6],[7] Because of these properties, UDC is serious problem in pipeline system due to the unexpected failure from localized damage. Thus, in order to prevent the pipeline failure from UDC, it is important to investigate the mechanism of UDC. Jeannin et al. found that the corrosion process of carbon steel was different according to the kind of deposited minerals (silica, kaolinite, chlorite and montmorillonite) [8]. Zhang et al. revealed the galvanic corrosion between the covered mixed deposit on the carbon steel and bare carbon steel (uncovered mixed deposit) in gas filled environment [9]. However, the deposit is composed of not only minerals (clay and sand) but also the corrosion products (iron oxide and carbonate etc.) because the corrosion products floated in fluid combined each other and deposited at the stagnant condition. Therefore, the investigation of corrosion process under different corrosion product deposits is important.

The corrosion products can inhibit further corrosion by shielding the metal from environments. However, there are cases where corrosion products accelerate corrosion [8]. The corrosion process can be dependent on the oxide film because the oxide is directly formed in close connection with the crystal of the metal, while the deposit is just stacked on the metal [10]. Thus, the corrosion reaction in oxide film and deposit cases was significantly different. In this work, corrosion behavior of carbon steel under different iron oxides (goethite; α -FeOOH, magnetite; Fe₃O₄, hematite; Fe₂O₃) was evaluated by electrochemical measurements and surface characterization. These iron oxides are usually produced on the pipeline surface in DH system. Furthermore, the corrosion mechanism under different iron oxides was investigated for the prevention of unexpected corrosion and failure in DH system by the UDC. Thus, the aim and purpose of this study are to demonstrate of the corrosion risk of DH pipeline system caused by iron oxides deposits and to remind the importance of iron oxide removal in DH water.

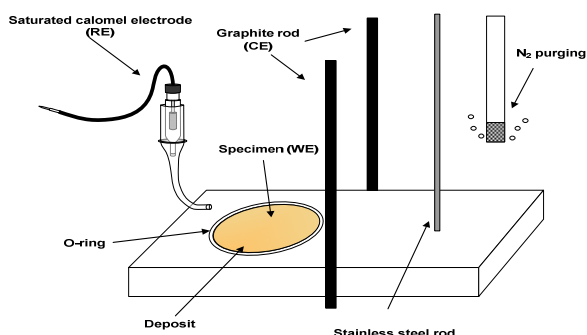


Figure 1. Three-electrode electrochemical cell used in this study.

Table 1. Chemical composition of test solution (mg/L).

pH	Fe ³⁺	Cl ⁻	NO ²⁻	NO ³⁻	SO ₄ ²⁻	NH ₄ ⁺
9.8	5.6	46	5	0.5	14.3	5

EXPERIMENTAL PROCEDURES

The material used in this work was SPPS 38 (Korean Standards; KS D 3562) pipeline carbon steel (C: 0.25 wt%, Si: 0.35 wt%, P: 0.04 wt%, S: 0.04 wt%, Fe: Bal.). Specimens were machined into square shape with the area of 1 cm² and sealed with epoxy resin. A copper rod was connected to each electrode to ensure electrical-connection for electrochemical tests. Before deposition process, the specimens were abraded with silicon carbide paper starting from 100 to 600 grit size, and then rinsed with deionized water, cleaned with ethanol.

Table 1 gives the chemical composition of the tests solution which is based on the heating water in 10 years stagnant condition. To adjust the chemical composition of the test solution, FeCl₃, NaNO₂, NaNO₃, NaCl, H₂SO₄ and NH₄OH were used and pH was controlled by 0.1 M NaOH solution. Although the heating water is usually soft and pure water, detection of the ferric ion (Fe³⁺) and chloride ion (Cl⁻) is due to the long period stagnant condition. Prior to the testing, the solution was deaerated by purging N₂ (99.999%) for 2 h, because the DH system is block with the outside, i.e., the closed system, so that the dissolved oxygen is very low. The temperature is maintained at 40 °C by using the constant-temperature water bath.

The three iron oxides (α -FeOOH, Fe₃O₄, Fe₂O₃) used in this study were purchased from SAMCHUN chemical cooperation. Because the powder state iron oxides are difficult to deposit on the specimen and to avoid corrosion of the steel specimen during the deposition process, ethanol was mixed with the iron oxides. The specimen was covered with a rubber 'O' shaped ring (diameter: 3 cm, height: 3 mm) filled with iron oxide deposit mixed with ethanol state, which have the same

thickness to rubber ring about 3 mm, to simulate the under deposit corrosion environment. Before the immersion in the test solution for electrochemical tests, the deposit-covered specimen was dried under the air condition for 30 minute to vaporize the ethanol in the deposit. To evaluate the corrosion behavior and properties of iron oxide deposits, electrochemical tests were conducted. A three-electrode electrochemical cell was constructed with the SPPS 38 carbon steel electrode uncovered and covered with iron oxide deposits as the working electrode (WE), two pure graphite rods as counter electrodes (CE) and a saturated calomel electrode (SCE) as the reference electrode (RE). The schematic of the three-electrode electrochemical cell used in this experiment is shown in Figure 1. Before potentiodynamic tests, the working electrode was immersed in the test solution for 6 h until steady state, and the open-circuit potential (OCP) was attained. Potentiodynamic polarization curves were measured by scanning potential from -250 mV vs. OCP to 400 mV_{SCE} at a sweep rate of 0.166 mV/s. For the acceleration of corrosion process, potentiostatic tests were carried out at an applied potential of -0.65 mV_{SCE}, slightly higher than the corrosion potential (E_{corr}) of each specimens for 20 h. Also, to investigate the difference of corrosion behavior under covered and uncovered deposits, the deposit was only covered half of the specimen. After potentiostatic tests, the iron oxide deposits and corrosion products on the carbon steel surface were removed and cleaned for 10 min in the cleaning solution containing 500 ml HCl, 3.5 g hexamethylenetetramine (C₆H₁₂N₄) and distilled water to make 1000 ml. The specimens were then rinsed in distilled water and dried by nitrogen gas.

In addition, to analyse the surface properties of uncovered and covered deposit specimens, the Mott-Schottky measurements were carried out with the PARSTAT 2263. Before Mott-Schottky measurements, each specimen was immersed in test solution for 340 h. The Mott-Schottky plots were obtained by sweeping in the positive direction at a frequency of 1 kHz with an amplitude signal of 10 mV, the potential range from -0.7 V_{SCE} to 0.1 V_{SCE} and the potential step of 25 mV.

After the potentiostatic tests, the morphology of the corroded specimens was observed by optical microscope (OM). Also, to investigate the surface condition under the oxide deposits, the specimens were analysed by X-ray diffraction (XRD, Burker D8 Advanced) using Cu-K α radiation operated at 18 kW and the scanning speed was 2 °/min after 340 h immersion. Before the XRD analysis, the deposit on the specimens was removed by distilled water and dried by air compressor. The XRD patterns were analyzed by ICDD database.

RESULTS

• Potentiodynamic Polarization Tests

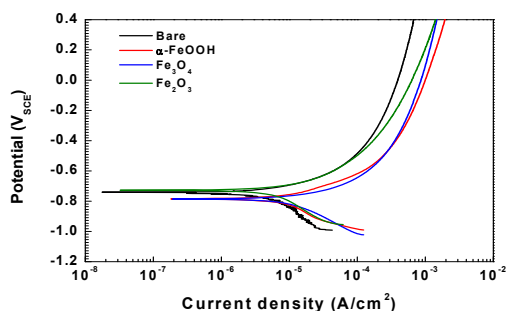


Figure 2. Polarization curves of the specimens covered with different iron oxides (α -FeOOH, Fe_3O_4 , Fe_2O_3) and uncovered after 6 h immersion in test solution at 40°C.

Figure 2 shows the polarization curves of bare specimen and different iron oxides (α -FeOOH, Fe_3O_4 , Fe_2O_3)-covered specimens after 6 h immersion in the test solution at 40°C. All the polarization curves showed active corrosion behavior. However, the cathodic and anodic reactions were changed on the iron oxides-covered deposits and the changing tendency was also different according to the kind of iron oxides. In cases of Fe_3O_4 and α -FeOOH, both cathodic and anodic current densities were increased in comparison with bare specimen, which result in negative shift in corrosion potential. It indicated that the Fe_3O_4 and α -FeOOH deposits increased the cathodic and anodic reactions. In addition, the negative shift of corrosion potential can cause the galvanic corrosion at the boundary of the bare and deposit-covered region. On the other hand, in case of Fe_2O_3 , only cathodic current density was increased and the corrosion potential was not shifted.

Table 2. Electrochemical Parameters of the Polarization Curves of Bare Specimen and Iron Oxides (α -FeOOH, Fe_3O_4 , Fe_2O_3) Covered Specimens in the Test Solution at 40 °C

	β_a (mV/decade)	$-\beta_c$ (mV/decade)	$-E_{\text{corr}}$ (mV _{SCE})	i_{corr} ($\mu\text{A}/\text{cm}^2$)
Bare	102 ± 3	246 ± 1 2	741 ± 9	3.8 ± 0.05
α -FeOOH	122 ± 6	215 ± 5	775 ± 6	9.1 ± 0.03
Fe_3O_4	99 ± 12	202 ± 9	786 ± 9	8.6 ± 0.12
Fe_2O_3	105 ± 5	265 ± 8	735 ± 7	5.3 ± 0.09

• Potentiostatic Tests

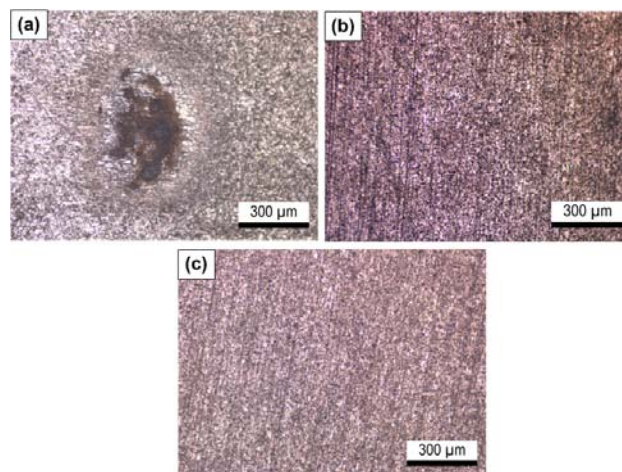


Figure 3. Optical microscope images of the specimens covered iron oxides deposit, (a) α -FeOOH, (b) Fe_3O_4 , (c) Fe_2O_3 , after potentiostatic tests under -650 mV_{SCE} for 20 h in the test solution at 40 °C.

The corresponding kinetic parameters in polarization curves such as corrosion potential (E_{corr}), corrosion current density (i_{corr}), and anodic and cathodic Tafel slopes (β_a , β_c), are listed in Table 2. As shown in polarization curves, the i_{corr} and E_{corr} were changed on iron oxides-covered specimens. The i_{corr} related to corrosion rate was increased in all oxide-covered specimens, indicating the deposit state of iron oxides increases the corrosion of steel substrate. In short, the anodic reactions were affected by Fe_3O_4 and α -FeOOH deposits and the iron oxides deposits (α -FeOOH, Fe_3O_4 , Fe_2O_3) activates the cathodic reactions [11]-[13].

To investigate the corrosion behavior of the iron oxide-covered specimens, the potentiostatic tests were conducted. Also, to identify the galvanic corrosion between covered and uncovered specimens, half of the specimen is covered with deposit. Figure 3 shows the specimen covered iron oxides after the potentiostatic tests under -650 mV_{SCE} for 20 h in the test solution at 40 °C. As shown in Figure 3(a), the numerous pitting was observed on the α -FeOOH-covered specimen and the pitting size was in the range 150 μm to 300 μm . However, as shown in Figures 3(b) and (c), pitting was not observed on the Fe_3O_4 and Fe_2O_3 -covered specimens. It is indicated that the corrosion behavior is different in α -FeOOH and Fe_3O_4 , Fe_2O_3 cases.

Figure 4 shows the boundary of the specimens with covered (left side) and uncovered (right side) deposit after the potentiostatic tests under -650 mV_{SCE} for 20 h in the test solution at 40 °C. In Figures 4(a) and (b), the corrosion was accelerated at the boundary of the α -FeOOH and Fe_3O_4 -covered specimens, which showed

more negative corrosion potential than bare specimen, moreover the localized corrosion at the boundary was more severe in α -FeOOH case. On the other hand, the boundary between the Fe_2O_3 -covered and uncovered did not show the accelerating corrosion behavior shown in Figure 4(c), which could be due to the absence of corrosion potential difference [14]-[16]. These results indicate that the α -FeOOH and Fe_3O_4 deposits can cause the galvanic corrosion under stagnant condition, while Fe_2O_3 deposit did not cause galvanic effect.

• Mott-Schottky Tests

It is well known that there are relationships between the surface film properties, which related to semi-conducting behavior of surface film, and the corrosion behavior of materials [17]. These properties and behavior can be investigated by analyzing the curves of Mott-Schottky plot. Thus, from this aspect, the surface film properties of steel substrate under iron oxide deposits (α -FeOOH, Fe_3O_4 , Fe_2O_3) were investigated by Mott-Schottky plot based on measurements of the electrode capacitance as a function of electrode potential (E). It is assumed that the capacitance of the space-charge was much less than that of the Helmholtz layer, and thus the electrode capacitance was equal to C.

According to Mott-Schottky theory, the space-charge capacitance and n-type and p-type semi-conductors are given by equations (1) and (2), respectively:

$$\frac{1}{C^2} = \frac{2}{\varepsilon\varepsilon_0eN_D} \left(E - E_{FB} - \frac{kT}{e} \right) \quad (1)$$

$$\frac{1}{C^2} = -\frac{2}{\varepsilon\varepsilon_0eN_A} \left(E - E_{FB} - \frac{kT}{e} \right) \quad (2)$$

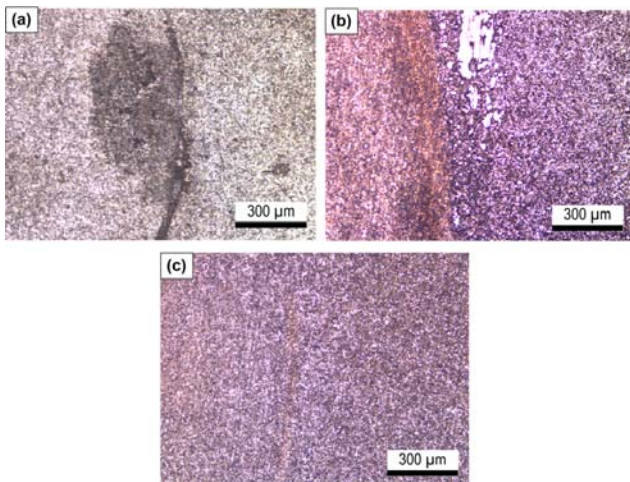


Figure 4. Optical microscope images of boundary covered (left side) and uncovered (right side) iron oxides deposit, (a) α -FeOOH, (b) Fe_3O_4 , (c) Fe_2O_3 , after potentiostatic tests under $-650 \text{ mV}_{\text{SCE}}$ for 20 h in the test solution at $40 \text{ }^\circ\text{C}$.

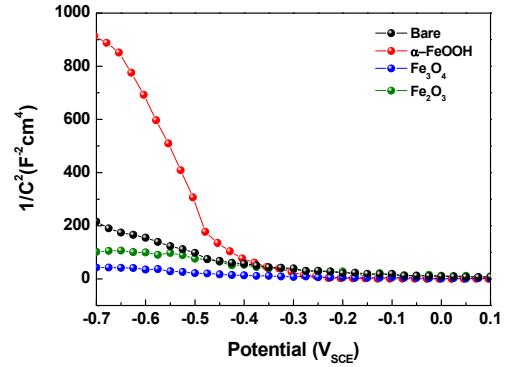


Figure 5. Mott-Schottky plots for iron oxides-covered and uncovered specimens immersed in the test solution for 340 h at $40 \text{ }^\circ\text{C}$.

where ε denotes the relative dielectric constant of layer, ε_0 is the permittivity vacuum ($8.8542 \times 10^{-14} \text{ F/cm}$), e is the absolute value of the electron charge ($1.6029 \times 10^{-19} \text{ C}$), k is the Boltzmann constant ($1.389 \times 10^{-23} \text{ J/K}$), T is the absolute temperature, E_{FB} is the flat band potential which can be obtained from the extrapolation of $1/C^2$ to 0 V_{SCE} , N_D and N_A are the donor and acceptor densities that can be determined from the slope of the experimental $1/C^2$ versus applied potential [18].

Figure 5 shows the Mott-Schottky plots for iron oxides-covered and uncovered specimens immersed in the test solution for 340 h at $40 \text{ }^\circ\text{C}$. These measurements were obtained by sweeping the potential in the positive direction around E_{corr} at a frequency of 1 kHz. Note that Mott-Schottky measurements were performed at various frequencies between 1 and 10 kHz and identical results were obtained whatever the frequency [19]. The frequency of 1 kHz was then chosen as appropriate frequency. The slope of the Mott-Schottky diagram is negative, indicating a p-type semiconducting behavior of the surface films in all conditions. According to equation (3), acceptor density N_A can be determined from the slope of the experimental C^2 versus E plots. Thus, the decrease of N_A was observed according to the following order: α -FeOOH, bare, Fe_2O_3 and Fe_3O_4 , indicating that the surface film of p-type semiconducting property is actively produced according to the above order.

In addition, the thickness (W) of the space-charge layer which is the surface film at a film formation potential can be calculated by [20]:

$$W = \left(\frac{2\varepsilon\varepsilon_0}{eN_A} \right)^{\frac{1}{2}} \left(E_f - E_{FB} - \frac{kT}{e} \right)^{\frac{1}{2}} \quad (3)$$

In this equation, E_f is the film formation potential, and the other parameters have the same physical

meanings as those in equation (3). The film thickness (W) is proportional to the $1/C^2$ value so that the W is increased according to the following order: α -FeOOH, bare, Fe_2O_3 and Fe_3O_4 . It indicated the two things, first is that the iron oxide deposits were not considered as a surface film. Second is that the formation of surface film of p-type semiconducting property was increased according to the following order: α -FeOOH, bare, Fe_2O_3 and Fe_3O_4 .

• Surface Characterization

Figure 6 showed the XRD results for the iron oxides-covered and uncovered specimens immersed in the test solution for 340 h at 40 °C. In the Fe_3O_4 -covered specimen, Fe and few Fe_3O_4 peaks were observed. Likewise, in case of the Fe_2O_3 -covered specimen, the Fe, Fe_2O_3 and few Fe_3O_4 peaks were shown. It is indicated that the Fe_3O_4 and Fe_2O_3 deposits did not influence on the formation of surface film on the steel substrate. Even though the Fe_3O_4 peaks were observed in Fe_2O_3 case, the Fe_3O_4 peaks were overlapped with Fe_2O_3 -peaks and the amount of intensity was insignificant. Thus, the Fe_3O_4 was formed under the Fe_2O_3 -covered state but the formation and reaction activities were too small. However, in cases of α -FeOOH-covered and bare specimens, the Fe_3O_4 diffraction peaks were mainly observed. These results indicate that the Fe_3O_4 is main surface film in the test environment at the bare state and the α -FeOOH has an influence on the formation of Fe_3O_4 surface film on the steel substrate compared to the Fe_2O_3 and Fe_3O_4 cases.

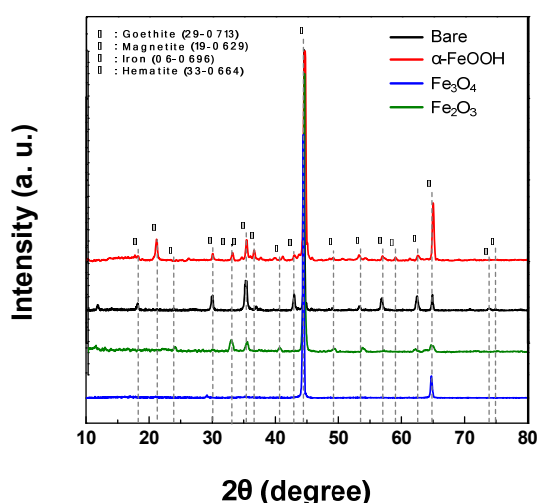


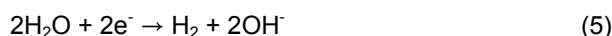
Figure 6. XRD spectra for the specimens covered with iron oxides and uncovered, which immersed in the test solution for 340 h at 40 °C.

DISCUSSION

• Surface Reaction under the Iron Oxide Deposits

Potentiodynamic polarization curves indicated the negative direction shift of the corrosion potential and different increases of the cathodic and anodic reactions on the iron oxides-covered specimens. The negative shift of corrosion potential in α -FeOOH and Fe_3O_4 -covered specimens means that the increase of the anodic reaction area is due to the surface reaction from the Fe_3O_4 and α -FeOOH. Also, the cathodic and anodic reactions were increased in α -FeOOH and Fe_3O_4 covered specimens. It means that the oxide deposit does not act as a surface barrier of the substrate, which is due to the porous properties of iron oxide particles [21].

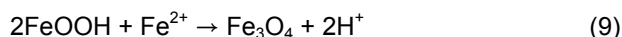
The following anodic and cathodic reactions are happened on the steel substrate under the test solution conditions (deaeration and pH 10). The reaction (4) is the anodic dissolution and (5) is the cathodic reaction in alkaline solution under the deaeration condition [14]:



Also, the Fe_3O_4 formation reactions were occurred as shown in the XRD results by the following reactions [22], [23]:

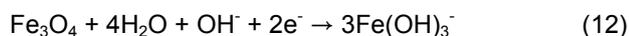
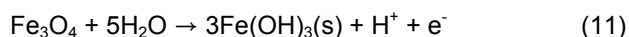


However, these surface film formation reactions are affected by the iron oxide deposits (α -FeOOH, Fe_2O_3 , Fe_3O_4) on the substrate. Under the α -FeOOH and Fe_3O_4 -covered specimens, the following cathodic and anodic reactions can be occurred. Under the α -FeOOH deposit, the following reactions are occurred on the steel substrate [24]:



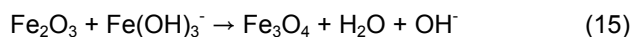
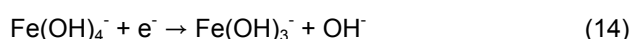
Due to these reduction reactions, the cathodic reaction was increased in polarization curve. In addition, with the increase of α -FeOOH reduction reactions, the more Fe^{2+} ions are needed to satisfy the equilibrium of reactions (9) and (10) so that the anodic dissolution reaction (4) is increased simultaneously shown in polarization curve as the increase of anodic reaction. Consequentially, from these reactions, the formation of Fe_3O_4 can be activated under the α -FeOOH deposit.

Under the Fe₃O₄ deposit, the following reaction can be happened on the substrate [22], [25]:



Reactions (11) and (12) indicate the oxidation and reduction of Fe₃O₄ with water and hydroxide ion in alkaline solution like the test solution, respectively. These oxidation and reduction reactions of Fe₃O₄ are indicated by the increase of anodic and cathodic reactions in the polarization curve. Also, the Fe₃O₄ formation reaction on the substrate is obstructed because the Fe₃O₄ deposit is existed on the substrate, which restricts the Fe₃O₄ formation reaction as a surface film on the substrate.

Lastly, under the Fe₂O₃ deposit, the following reaction is developed on the substrate [26]:



The hematite, Fe₂O₃, is the last oxidation product among the iron oxides. Thus, the additional oxidation is different so that the hydration reaction (13) and reduction reaction (14) can be occurred, which increase the only cathodic reaction of the Fe₂O₃-covered specimen as indicated in polarization curve. The formation of Fe₃O₄ under the Fe₂O₃ deposit can be induced by reaction (15) but the reaction can be limited due to the multiple reaction steps of Fe(OH)₃⁻. Thus, the formation of Fe₃O₄ under the Fe₂O₃ deposit is difficult.

The above reaction results are confirmed by the Mott-Schottky and XRD analysis. In the Mott-schottky results, the p-type semiconducting property and film thickness were increased in the following order of α-FeOOH, bare, Fe₂O₃ and Fe₃O₄. Among the iron oxides, the Fe₃O₄ indicated the p-type semiconducting properties [27]. Consequently, it indicated that the formation of Fe₃O₄ increased in the following order: α-FeOOH, bare, Fe₂O₃ and Fe₃O₄. In addition, although the iron oxides deposit actually has the semiconducting property like α-FeOOH and Fe₂O₃ (n-type), Fe₃O₄ (p-type) [28]. However, the iron oxides deposit properties were not shown in the Mott-Schottky results. It means that the iron oxides as a deposit on the surface do not have the surface film or barrier properties like oxide film. Therefore, the iron oxides deposit did not act as surface film or barrier which obstructs the electrochemical reaction but a reaction product like catalyst on the steel substrate.

• Mechanism of Different Corrosion Behavior under the Iron Oxides Deposit

In the potentiostatic tests, the uniform corrosion behavior was indicated in all conditions, except α-FeOOH-covered specimen. The pitting corrosion only occurred under the α-FeOOH-covered specimen. The uniform corrosion under iron oxides deposit takes place due to the diffusion of the external parameters such as water and anion in the test solution by porous properties of iron oxides which revealed from the Mott-Schottky tests [29]. However, under the α-FeOOH, the pitting corrosion was observed, which means the cathode and anode areas are separated on the substrate.

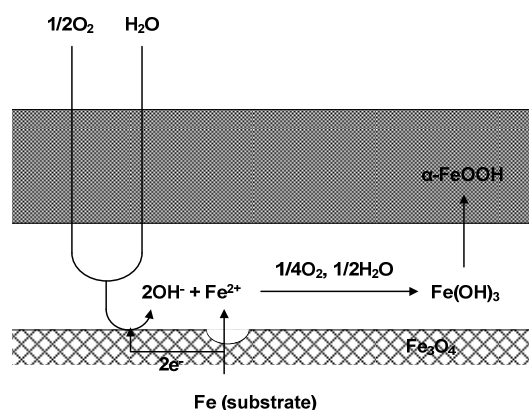


Figure 7. of rust film formed on the steel at the initial stage of corrosion [10].

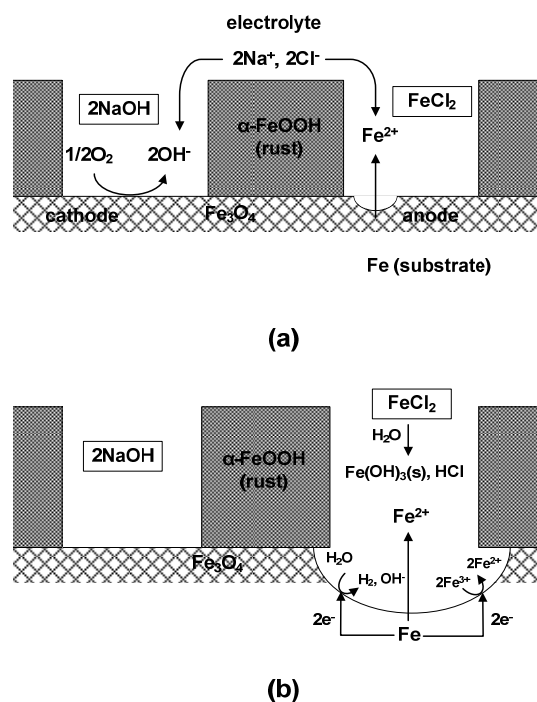


Figure 8. Mechanism of (a) crevice corrosion and (b) acidify corrosion under the α-FeOOH rust.

H. Tamura proposed the localized corrosion mechanism due to the rust on the steel substrate [10]. The rust on the steel and iron at the initial stage of corrosion is generally composed of outer $\text{Fe}(\text{OH})_3$, $\alpha\text{-FeOOH}$ and Fe_3O_4 from the each other transformation. It is visualized schematically in Figure 7. With the aging proceed, the $\text{Fe}(\text{OH})_3$ is transformed to the $\alpha\text{-FeOOH}$. And then, $\alpha\text{-FeOOH}$ is transformed to Fe_3O_4 by reactions (9) and (10). From these reactions, the porous defect such as crack and void are developed in the rust layer, and the outside environments reach the metal. The corrosion in these defects initiates, but the Fe^{2+} and OH^- ions cannot have reaction directly because the remaining $\alpha\text{-FeOOH}$ rust obstructs their direct reaction. Due to these separated reactions, the FeCl_2 and NaOH are formed in anode and cathode regions, respectively. And then, acidification is taken place due to the FeCl_2 in the anode region, the anode dissolution is accelerated. This corrosion under thick rust layer can be considered as crevice corrosion. Figure 8 shows the crevice corrosion process under $\alpha\text{-FeOOH}$ rust layer. Thus, the localized corrosion is occurred under the $\alpha\text{-FeOOH}$ -covered specimen, even though the passive behavior was not observed on the polarization curve.

CONCLUSION

- I. In the potentiodynamic polarization results, i_{corr} was increased in all deposit-covered specimens, which means that the corrosion reaction is increased due to the deposit. The $\alpha\text{-FeOOH}$ and Fe_3O_4 -covered specimens present the negative shift of corrosion potential and increase of anodic and cathodic reactions, and the Fe_2O_3 -covered specimen only presents the increase of cathodic reaction.
- II. The pitting corrosion was only shown on the $\alpha\text{-FeOOH}$ -covered specimen, while the uniform corrosion was observed in the others. The reason of these results can be a crevice corrosion phenomenon which is the localized corrosion under $\alpha\text{-FeOOH}$ rust layer on the steel substrate. Also, the corrosion at the boundary between deposit-covered and uncovered was observed on the $\alpha\text{-FeOOH}$ and Fe_3O_4 due to the galvanic effect.
- III. Mott-Schottky and XRD analyses revealed that surface reactions are different according to kind of iron oxide deposits, which influence the formation of surface film and reaction rate of anode and cathode sites.
- IV. From this study, it is seen that iron oxide covered as a deposit on the steel substrate has a negative

effect on the corrosion in district heating water. Especially, the $\alpha\text{-FeOOH}$ can lead to the localized corrosion-caused failure in early stage. Thus, prevention of stagnant condition and filtering of floating mater are important tasks for maintenance of pipeline.

REFERENCES

- [1] M.R. Schock, Water Quality and Treatment: A Handbook of Community Water Supplies, 5th ed., McGraw Hill, New York (1999), pp. 958-962.
- [2] J.R. Rossum, Dead ends, red water and scrap piles, J. Am. Water Works Ass. 1987, Vol. 79, pp. 113-115.
- [3] T. Kuppan, Heat Exchanger Design Handbook, 2nd ed., CRC Press, New York (2000), pp. 168-175.
- [4] M.A. Winters, P.S.N. Stokes, P.O. Zuniga, D.J. Schlottenmier, Real-time performance monitoring of fouling and under-deposit corrosion in cooling water system, Corros. Sci. 1993, Vol. 35, pp. 1667-1675.
- [5] 13. Y.J.Tan, Y. Fwu, K. Bhardwaj, Electrochemical evaluation of under-deposit corrosion and its inhibition using the wire beam electrode method, Corros. Sci. 2011, Vol. 53, pp. 1254-1261.
- [6] Z.H. Dong, W. Shi, H.M. Ruan, G.A. Zhang, Heterogeneous corrosion of mild steel under SRB-biofilm characterized by electrochemical mapping technique, Corros. Sci. 2011, Vol. 53, pp. 2978-2987.
- [7] A. Turnbull, D. Coleman, A.J. Griffiths, P.E. Francis, L. Orkney, Effectiveness of corrosion inhibitor in retarding the rate of propagation of localized corrosion, Corrosion 2003, Vol. 59, pp. 250-257.
- [8] M. Jeannin, D. Calonnec, R. Sabot, Ph. Refait, Role of clay sediment deposit on the corrosion of carbon steel in 0.5 mol L^{-1} NaCl solutions, Corros. Sci. 2010, Vol. 52, pp. 2026-2034.
- [9] G.A. Zhang, N. Yu, L.Y. Yang, X.P. Guo, Galvanic corrosion behavior of deposit-covered and uncovered, Corros. Sci. 2014, Vol. 86, pp. 202-212.
- [10] H. Tamura, The role of rusts in corrosion and corrosion protection of iron and steel, Corros. Sci. 2008, Vol. 50, pp. 1872-1883.
- [11] M. Stern, A.L. Geary, Electrochemical polarization: I. A theoretical analysis of the shape of polarization curves, J. Electrochem. Soc. 1957, Vol. 104, pp. 56-63.

- [12] D. Tromans, J.C. Silva, Behavior of copper in acidic sulfate solution: Comparison with acidic chloride, *Corrosion* 1997, Vol. 53, pp. 171-178.
- [13] H. Huang, W.J.D. Shaw, Electrochemical aspects of cold work effect on corrosion of mild steel in sour gas environments, *Corrosion* 1992, Vol. 48, pp. 931-939.
- [14] D.A. Jones, Principles and Prevention of Corrosion, 2nd ed., Prentice Hall, New Jersey (1996), pp. 168-177.
- [15] S.M. Wilhelm, Galvanic corrosion in oil and gas production: Part 1-Laboratory studies, *Corrosion* 1992, Vol. 48, pp. 691-703.
- [16] G. Gao, Effect of salt deposition and temperature on polarization resistance of steel and the galvanic current of steel-aluminum couples during exposure to cyclic humidity, *Corrosion* 1999, Vol. 55, pp. 432-437.
- [17] Z. Feng, X. Cheng, C. Dong, L. Xu, X. Li, Passivity of 316L stainless steel in borate solution studied by Mott-Schottky analysis, atomic adsorption spectrometry and X-ray photoelectron spectroscopy, *Corros. Sci.* 2010, Vol. 52, pp. 3646-3653.
- [18] M.F. Montemor, M.G.S. Ferreira, N.E. Hakiki, M.D.C. Belo, Chemical composition and electronic structure of the oxide films formed on 316L stainless steel and nickel based alloys in high temperature aqueous environments, *Corros. Sci.* 2000, Vol. 42, pp. 1635-1650.
- [19] M. BenSalah, R. Sabot, E. Triki, L. Dhouibi, Ph. Refait, M. Jeanin, Passivity of Sanicro28 (UNS N-08028) stainless steel in polluted phosphoric acid at different temperatures studied by electrochemical impedance spectroscopy and Mott-Schottky analysis, *Corros. Sci.* 2014, Vol. 86, pp. 61-70.
- [20] T. Dan, T. Shoji, Z. Lu, K. Sakaguchi, J. Wnag, E.-H. Han, W. Ke, Effects of hydrogen on the anodic behavior of Alloy 690 at 60 °C, *Corros. Sci.* 2010, Vol. 52, pp. 1228-1236.
- [21] R.M. Cornell, U. Schwertmann, The Iron Oxides : Structure, Properties, Reactions, Occurrences and Uses, 2nd ed., WILEY-VCH, Weinheim (2003), pp. 95-109.
- [22] L. Cabrera, S. Gutierrez, N. Menedez, M.P. Morales, P. Herrasti, Magnetite nanoparticles: Electrochemical synthesis and characterization, *Electrochim. Acta* 2008, Vol. 53, pp. 3436-3441.
- [23] T. Otake, D.J. Wesolowski, L.M. Anovitz, L.F. Allard, H. Ohmoto, Mechanism of iron oxide transformations in hydrothermal systems, *Geochim. Cosmochim. Acta* 2010, Vol. 74, pp. 6141-6156.
- [24] U.R. Evans, Mechanism of rusting, *Corros. Sci.* 1969, Vol. 9, pp. 813-821.
- [25] F. Fajaroh, H. Setyawan, W. Widiyastuti, S. Winaradi, Synthesis of magnetite nanoparticles by surfactant-free electrochemical method in an aqueous system, *Adv. Powder Technol.* 2012, Vol. 23, pp. 328-333/
- [26] A. Allanore, H. Lavelaine, G. Valentin, J.P. Birat, P. Delcroix, F. Lapique, Observation and modeling of the reduction of hematite particles to metal in alkaline solution by electrolysis, *Electrochim. Acta* 2010, Vol. 55, pp. 4007-4013.
- [27] K. Azumi, T. Ohtsuka, N. Sato, Mott-Schottky plot of the passive film formed on iron in neutral borate and phosphate solutions, *J. Electrochem. Soc.* 1987, Vol. 134, pp. 1352-1357.
- [28] N.E. Hakiki, S.Boudin, B. Rondot, M. Da Cunha Belo, The electronic structure of passive films formed on stainless steels, *Corros. Sci.* 1995., Vol. 37, pp. 1809-1822.
- [29] J.L. Crolet, Mechanism of uniform corrosion under corrosion deposits, *J. Mater. Sci.* 1993, Vol. 28, pp. 2589-2606.

DEVELOPMENT OF A REINFORCED BEND WITH SHEAR CONTROL RING FOR DISTRICT HEATING

Jooyong Kim¹, Chongdu Cho²

¹ Korea District Heating Corp.(KDHC), Yangjae-daero 781, Gangnam-gu, Seoul 06340, Korea, jykim43@kdhc.co.kr

² Inha University, Inha-ro 100, Nam-gu, Incheon 22212, Korea, cdcho@inha.ac.kr

Keywords: District heating pipe, Reinforced bend, Shear control ring, Shear stress

ABSTRACT

As a fitting to changing the direction of district heating pipes, bends are subjected to a transverse loading by the soil reaction. Generally the foam cushion are buried together to absorb the expansions. However foam cushions are often squeezed by the repetitive thermal axial forces and the soil reactions, it loses its function to secure the expansion space of pipes. It can be a cause of pipe fracture and decreasing the lifetime.

In this study, the new reinforced bend was developed without foam cushion but satisfying the structural safety level of current bends with foam cushion. Shear control ring (SCR) was suggested and determined to deconcentrate the shear stresses in the polyurethane insulation based on the finite element analysis [1]. The Taguchi method which is one of design of experiment (DOE) method was introduced to optimize the specification of the SCR [2].

In situ test was also performed to validate the performance of SCR bend without foam cushion by comparing to current bend with foam cushion. Shear stresses of two bends were measured and analysed under the same burying and operating conditions. As a result, it was confirmed that the SCR band without foam cushion has a similar safety level itself with the current bend with foam cushion.

INTRODUCTION

District heating pipe is an important facility on district heating system to supply the hot water from production part, such as combined heat and power (CHP), heat-only boiler, waste incineration, etc., to consumer installation. There are many different types of district heating pipe but recently, the pre-insulated bonded pipes are used mainly. Pre-insulated bonded pipes have a sandwich structure comprising a steel carrier pipe, polyurethane insulation foam and casing pipe with high density polyethylene as shown in figure 1.

Through the pipes inside, hot water with maximum temperature of 120°C and maximum pressure of 16bar is supplied.

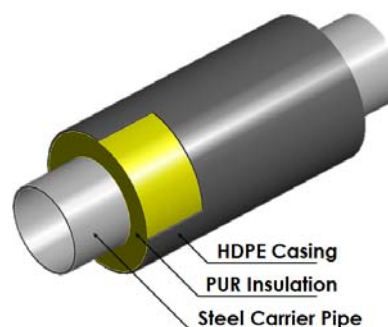


Figure 2. Structure of a pre-insulated bonded pipe

After the district heating system has been started from the early 1980s due to the spreading of high-density residence, such as an apartment and the district heating technology in Korea has undergone a remarkable growth in a short time. Meanwhile, Korea is a country with four distinctive seasons, many problems due to the preference of intermittent heating and the high temperature range have acquired.

Especially, in the case of the fittings such as bends are structurally fragile. The force and displacement could be concentrated due to the thermal expansions. Therefore, there is a high possibility that damage will occur. Generally the foam cushion has been installed around the bends in order to absorb the large lateral displacement. However, as time passed, the foam cushion gradually lost its design function due to the deterioration by compression. It may also be the reason of reducing the lifetime of the piping, structural instability, etc.

To overcome this kind of problems due to compression of the foam cushion, the developments of a reinforced bends are needed and SCR bend could be one of solution.

DESIGN OPTIMIZATION OF SHEAR CONTROL RING USING TAGUCHI METHOD

As shown in figure 2, in the case of the bend of underground embedded, the highest shear stress at the adhesion section of the steel pipe and PUR insulation was distributed in a narrow line along the curved direction of the bend.

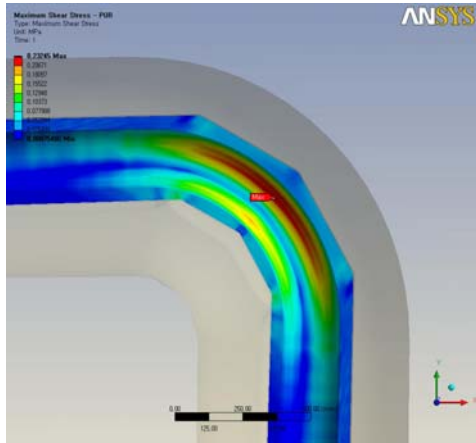


Figure 2. Example of shear stress distribution of PUR insulation

The SCR was suggested with the expectation that the effect of scattering the concentration of shear stress at the PUR insulation inside can be obtained if the structure of the ring shape (see figure 3) was added to the external wall of steel pipe.

Shape and number of the SCR shall be decided in such a way that the maximum shear stress generated in accordance with the application of the SCR will be lowered as much as possible. The SCR for each of the corresponded pipe diameters was optimized by introducing the Taguchi method which is a kind of design of experiment (DOE).

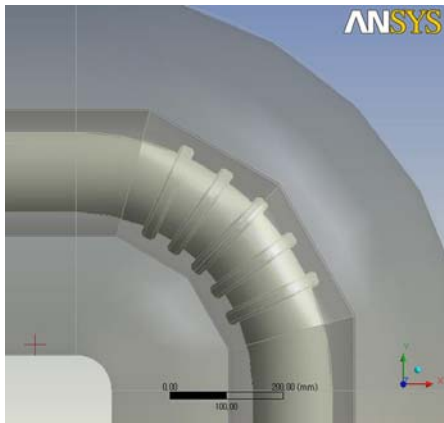


Figure 3. 3D model for SCR bend

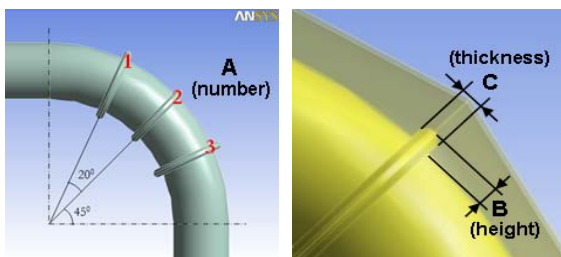
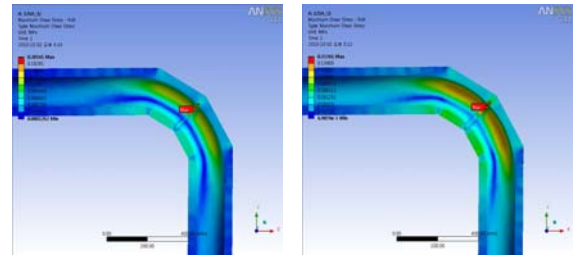
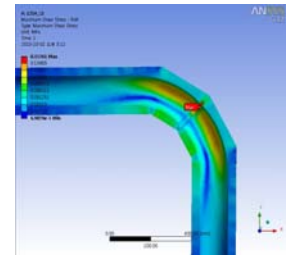


Figure 4. Definition of design factor

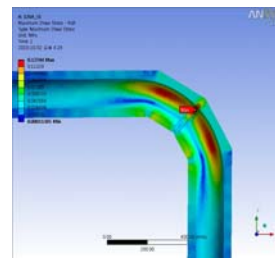
For the optimization of the SCR, the number A, height B, and thickness C of the SCR were selected as the design factors, and three levels as shown in the table 1 were defined and analyzed for each design factor.



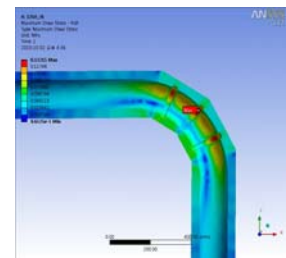
(a) A1B1C1



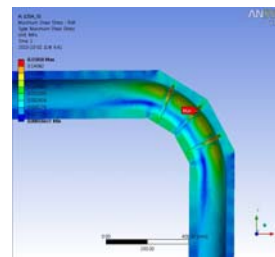
(b) A1B2C2



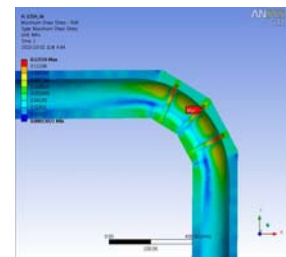
(c) A1B3C3



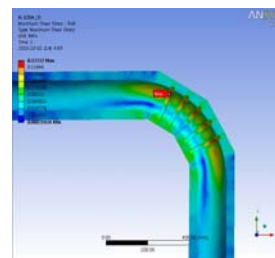
(d) A2B1C3



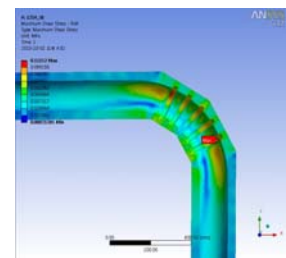
(e) A2B2C1



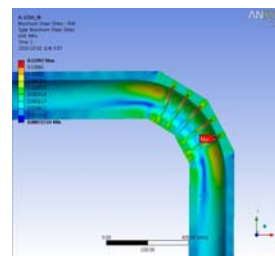
(f) A2B3C2



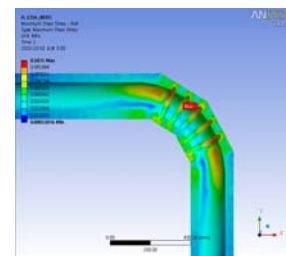
(g) A3B1C2



(h) A3B2C3



(i) A3B3C1



(j) A3B3C3

Figure 5. Optimization of the SCR shape

Table 2 Design factor and level of SCR

ND	Number (A)			Height (B)			Thickness (C)		
	1	2	3	1	2	3	1	2	3
900A	1	3	5	25	30	35	50	60	70
850A	1	3	5	25	30	35	50	60	70
800A	1	3	5	20	25	30	50	60	70
750A	1	3	5	20	25	30	45	55	65
700A	1	3	5	20	25	30	40	50	60
650A	1	3	5	20	25	30	40	50	60
600A	1	3	5	20	25	30	35	45	55
550A	1	3	5	20	25	30	35	45	55
500A	1	3	5	20	25	30	30	40	50
450A	1	3	5	20	25	30	30	40	50
400A	1	3	5	20	25	30	25	30	35
350A	1	3	5	20	25	30	25	30	35
300A	1	3	5	15	20	25	20	25	30
250A	1	3	5	13.5	18	22.5	15	20	25
200A	1	3	5	12	15.5	19	15	20	25
150A	1	3	5	11	15	18	15	20	25
125A	1	3	5	10.5	14	17.5	15	20	25
100A	1	2	3	9	12	15	12	16	20
80A	1	2	3	6.8	9	11.3	9	12	15
65A	1	2	3	6	8	10	8	10.5	13
50A	1	2	3	4.5	6	7.5	6.5	8.5	10.5
40A	1	2	3	4	5	6	5.5	7	8.5
32A	1	2	3	3	4	5	4	6	7
25A	1	2	3	2	3	4	3	4	5
20A	1	2	3	2	3	4	3	4	5

Figure 4 illustrates the definition of the design factors. Three design factors have three levels respectively. Therefore, the possible number of combination is 27. In this case, considering the limit of the rectangular coordinates which can be used by Taguchi method, $L_9(3^4)$ orthogonal table with which up to four factors can be arranged was selected, and after arranging each of the factors, A, B, and C the remaining factor was disposed as e (empty). The prepared orthogonal table is shown in table 2.

Table 2 $L_9(3^4)$ orthogonal table of SCR

Name	A	B	e	C	Experiment Condition
	1	2	3	4	
1	1	1	1	1	A1B1C1
2	1	2	2	2	A1B2C2
3	1	3	3	3	A1B3C3
4	2	1	2	3	A2B1C3
5	2	2	3	1	A2B2C1
6	2	3	1	2	A2B3C2
7	3	1	3	2	A3B1C2
8	3	2	1	3	A3B2C3
9	3	3	2	1	A3B3C1

FINITE ELEMENT ANALYSIS OF THE SUGGESTED SCR BENDS

Figure 5 illustrates the example of the 125A for the shear stress distribution of PUR insulation of the SCR specification which was obtained from the performance of the finite element analysis (FEA) in accordance with the prepared DOE. The items of (a) to (i) are the FEA results in accordance with the experiment condition, and the last item (j) is the analysis result obtained by acquiring the SN (signal to noise) ratio which is calculated from the previous nine analysis results and performing the dispersion analysis (ANOVA) [3]-[4].

IN SITU TEST

In situ test was performed in new piping site of Korea District Heating Corp. (KDHC). Figure 6 shows the outline of the test site and pipelines. 45m long straight pipe was installed with 2 bends in each end of the pipeline. To validate the performance of shear control ring, SCR bend without foam cushion was installed in position ①, and normal bend with foam cushion was installed in position ②. Nominal diameter of pipelines is 250A.

The SCR bend made from same material with steel carrier pipe and welded on the outside of the carrier pipe. Strain gauge was used to obtain the stress data, and thermocouple was also installed on the outer surface of steel pipe to get the temperature data. Figure 7 shows the steel pipe which installed SCR and figure 8 shows the test specimen which equipped the sensors.

Figure 9 shows the axial stress and inner temperature of each bend when the hot water starts to supply. Some thermal impact was concerned on the pipe because of rapidly temperature changing. However the measured maximum axial stress was 95.7MPa which was lower than allowable value 154MPa.

Figure 10 shows the equivalent Von Mises stress in accordance with the temperature changing. The maximum equivalent stress of the SCR bend was higher than the current bend. It was caused by excluding the foam cushion. However the level of maximum stress 206MPa was still quite lower than allowable stress range 841MPa. Then the structural stability of the SCR bend without foam cushion was confirmed.

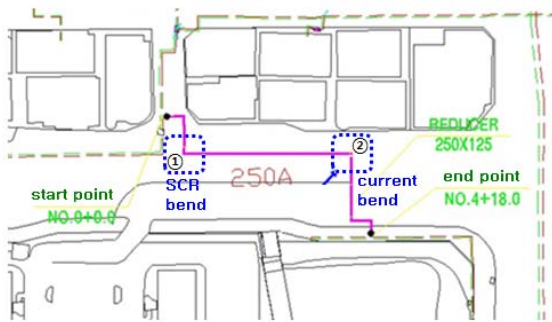


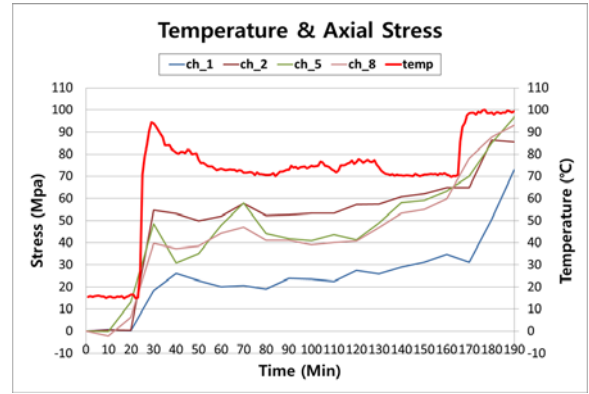
Figure 6. Outline of the test site and pipelines



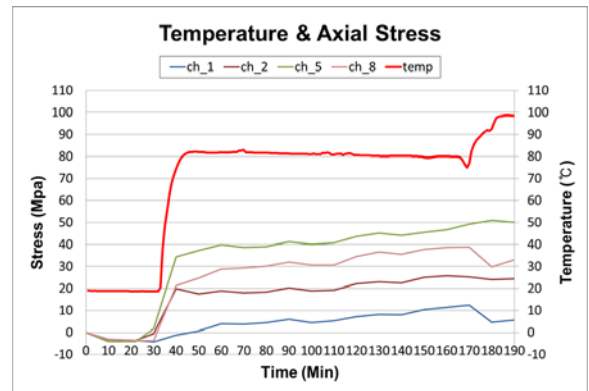
Figure 7. Shear control rings



Figure 8. Test specimen

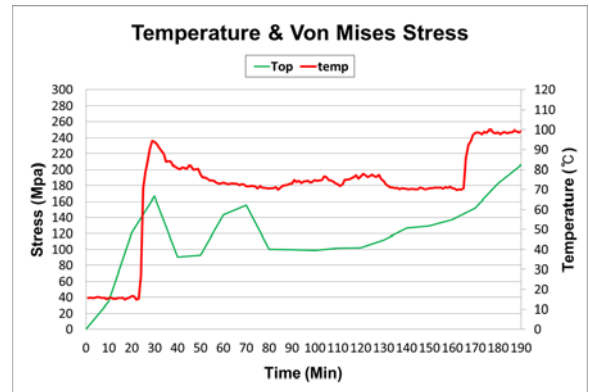


(a) SCR bend without foam cushion

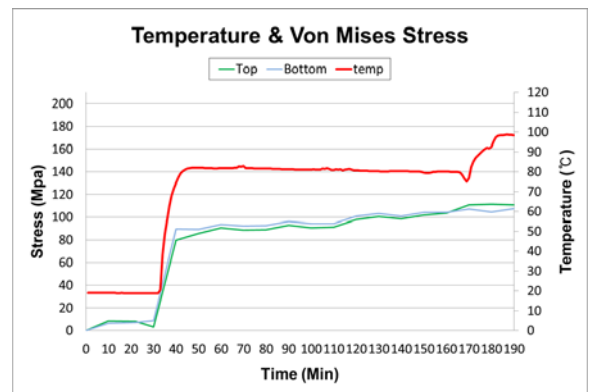


(b) Current bend with foam cushion

Figure 9. Axial stress and temperature



(a) SCR bend without foam cushion



(b) Current bend with foam cushion

Figure 10. Von Mises stress and temperature

Table 3 shows the shear stress of PUR insulation. The average shear stress of the SCR bend was 23.5kPa and of the current bend was 42.7kPa. Although the SCR bend had no foam cushion, the shear stress decreased under the effect of the SCR.

Table 3 Shear stress of PUR insulation

Type	Average Shear Stress [kPa]
SCR bend without foam cushion	23.5
Current bend With foam cushion	42.7

CONCLUSION

In this study, the new reinforced bend was developed and test validation was performed.

The design specification of Shear Control Ring (SCR) was decided by Taguchi method with various design factors such as number, height, and thickness of SCR. For 25 nominal diameters, from 25A to 900A, the optimized dimension of SCR bend was suggested.

By the in situ test, the performance of the SCR bend was confirmed. The axial and equivalent stresses of the SCR bend increased compared to the stressed of the current bend, but the values is in the allowable level even though the foam cushion did not used.

Especially, as an effect of shear control ring, the shear stress was dramatically decreased in the SCR bend.

REFERENCES

- [1] Jooyong Kim, Hobum Kim, Hyun Il Ko, Yong Mo An and Chongdu Cho, 2009, "Design Validation and Improvement of District Heating Pipe Using FE Simulation," Trans. of the KSME(A), Vol. 33, No. 4, pp. 337~345.
- [2] Moondeok Choi, Jooyong Kim, Hyun Il Ko and Chongdu Cho, 2010, "Shape Design of Bends in District Heating Pipe System by Taguchi Method" Trans. Korean Soc. Mech. Eng. A, Vol. 34, No. 3, pp. 307~313..
- [3] Sangbok Lee, 2003, "The Taguchi Technique from the Field to Apply," Sangjosa, pp. 15~268.
- [4] Sangbok Lee, 2006, "Taguchi Techniques for Use with Minitab," Eretec inc., pp. 18~70.

ON THE INFLUENCE OF THERMALLY INDUCED RADIAL PIPE EXTENSION ON THE AXIAL FRICTION RESISTANCE

T. Gerlach¹, M. Achmus¹

¹ Leibniz University of Hannover, Institute for Geotechnical Engineering (IGtH), Appelstr. 9A,
30167 Hannover, Germany, gerlach@igth.uni-hannover.de and achmus@igth.uni-hannover.de

Keywords: *Soil-structure interaction, numerical modeling, buried pipelines, radial extension*

ABSTRACT

Within the design process of district heating networks, the maximum friction forces between the pipeline and the surrounding soil are calculated from the radial stress state and the coefficient of contact friction. For the estimation of the radial stresses, the soil unit weight, geometric properties such as the pipe's diameter and the depth of embedment, as well as the groundwater level are taken into account. For the coefficient of contact friction, different values are proposed, dependent on the thermal loading condition of the pipeline. Although this is an assumption of practical use, physically the coefficient of friction is a material constant.

To revise the interaction behavior of the soil-pipeline system with respect to thermally induced radial pipe extension, a two-dimensional finite element model has been developed. Here, the frictional contact was established using Coulomb's friction law. For the embedment, sand at different states of relative density was considered. This noncohesive, granular material was described by the constitutive model HSsmall, which is able to predict the complex non-linear soil behavior in a realistic manner by stress-dependency of stiffness as well as isotropic frictional and volumetric hardening. In addition to the basic Hardening Soil model, the HSsmall model accounts for an increased stiffness in small strain regions, which is crucial for the presented investigation.

After a model validation, a parametric study was carried out wherein a radial pipe displacement was applied due to thermal changes of the transported medium. Different combinations of geometry and soil property were studied. We conclude by presenting a corrective term that enables for an incorporation of thermal expansion effects into the prediction of the maximum friction force.

INTRODUCTION

In operation, a district heating pipeline is subjected to loads resulting from changes of the medium temperature. Beside the temperature rise of the transported medium, usually water, the inner pressure also varies. The stress state around the pipeline is affected by the resulting loading condition, leading to a

higher maximum friction resistance under axial pipeline displacement. In common design practice in Germany [1], the maximum friction resistance is estimated from:

$$F_{\max} = \mu * (F_N' + F_G'). \quad (1)$$

Herein F_{\max} denotes the maximum resistance force per meter length, μ is the coefficient of contact friction and F_N' and F_G' are the integrated normal stresses around the pipes circumference and the sum weight force of the filled pipeline, respectively. To incorporate the effects resulting from changes of operating temperature, the coefficient of contact friction is taken to $\mu = 0.4$ for increasing temperature conditions. During unloading (decrease of temperature), a value of $\mu = 0.2$ shall be applied [1]. However, the coefficient of contact friction is a material specific constant. Although, this misappropriation as a correction factor might be practical, for a safe design of district heating networks a more sophisticated approach is needed.

Therefore, the presented research focuses on the derivation of a new corrective term that is able to describe the influences of a temperature rise on the maximum friction resistance. Analytical and numerical methods are used within these investigations. For practical purposes, it is important to keep the derivation of the needed input parameters simple. Therefore, well-funded correlations and appropriate simplifications may be used.

STATE OF THE ART

In general, the estimation of the maximum resistance force is based on Coulomb's friction law [2]. Following Coulomb, the maximum shear stress that can be mobilized between the pipe's mantle and the surrounding soil is proportional to the current normal stress. The constant of proportionality is the coefficient of contact friction μ . Neglecting the shear stresses in circumferential direction, the maximum resistance force that soil can exert on the pipeline due to axial relative displacement can be calculated from equation 1, wherein

$$F_N' = \sigma_0 * \pi * D_a * \frac{1 + k_0}{2}. \quad (2)$$

Herein D_o denotes the outer diameter of the pipeline and k_0 is the coefficient of earth pressure at rest. Assuming the groundwater level to be beneath the bottom of the pipeline, the overburden stress at the centre of the pipeline is considered as the average normal stress σ_0 :

$$\sigma_0 = \gamma * H. \quad (3)$$

The second term in brackets (equation 1) denotes the sum weight force of the pipeline:

$$F_G' = 2 * \pi * r_m * s * \gamma_s + \pi * r_i^2 * \gamma_w, \quad (4)$$

where r_m and r_i are the mean and the inner radius of the medium pipe, respectively. The wall thickness is denoted with s and γ_s and γ_w are the steel and water unit weights. This calculation procedure was proposed by *Rumpel* [3]. He assumes the angle of contact friction φ'_c to be solely dependent on the angle of internal friction φ' :

$$\varphi'_c = 0.8 * \varphi'. \quad (5)$$

For the coefficient of earth pressure at rest he uses *Jaky's* formula [4]:

$$k_0 = 1 - \sin(\varphi'). \quad (6)$$

Gramm [5] recommended an increased coefficient of earth pressure, resulting from the densification process during the installation of the pipeline. Values between $0.5 < k_0 < 0.85$ are proposed, dependent on the intensity of densification.

The dependency of the maximum friction resistance on the medium temperature was investigated in full scale field tests by *HEW* (1987) [6]. Two DN700 pipelines of 19.65m length were installed and tested under different thermal conditions. Overburden heights of 0.8m and 1.15m were realized. Within 57 tests a dependency on medium temperature as well as on ambient temperature was observed. The maximum friction force at $T=136^\circ\text{C}$ medium temperature was about four times greater compared to $T=18^\circ\text{C}$. For comparable ambient temperatures (in the range of $8.5\text{-}10.0^\circ\text{C}$) a correlation between medium temperature and radial pipeline extension was found, as depicted in Figure 1:

Further experimental investigations were made by *Gietzelt et al.* (1991) [7]. Pipelines of different diameter were tested in a 25m long trench with concrete walls. For an increase of temperature of $\Delta T=100\text{K}$ a two times greater resistance force was measured. However, due to the testing conditions, e.g. rigid walls and very high compaction, the practical relevance of their results seems questionable [8].

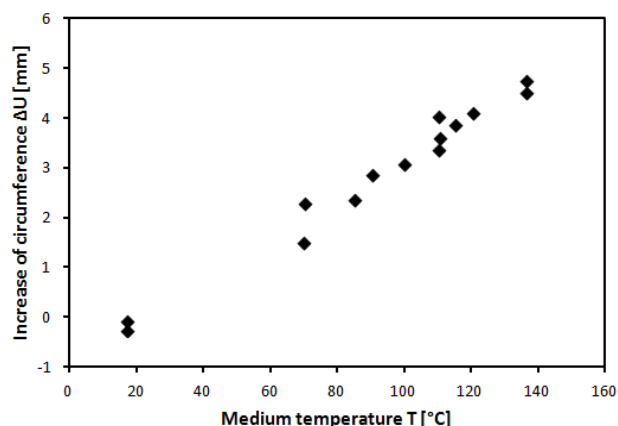


Figure 1. Dependency of pipeline circumference on medium temperature for DN700 [8]

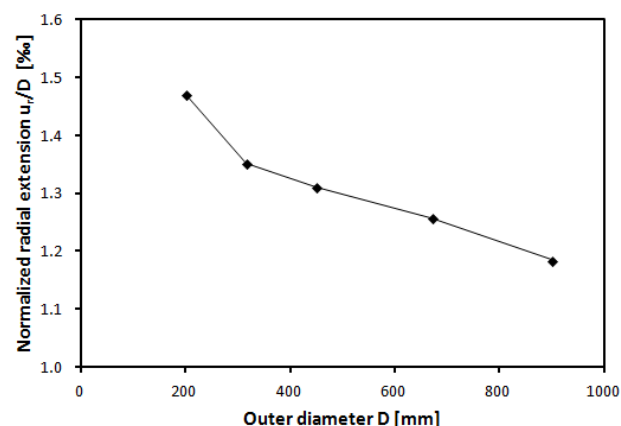


Figure 2. Normalized radial extension dependent on diameter for $\Delta T=120\text{K}$ [8]

Huber and Wijewickreme (2014) [9] presented results from experimental tests using a pipeline with an outer diameter of $D=520\text{mm}$. Inside a chamber $3.8\text{m} * 2.5\text{m} * 2.5\text{m}$, pipelines with different medium temperatures were axially displaced until failure. For $\Delta T=50\text{K}$ an increase of maximum resistance force could be observed. An about 10% higher value was measured, which is only a small increase compared to the aforementioned investigations.

Using analytical and numerical methods, *Achmus* (1995) [8] made investigations in the field of soil-pipeline interaction covering a wide range of topics. Within his investigations on radial pipeline extension, first the ratio between changes of media temperature to mantle temperature was evaluated. Assuming rotational symmetry of heat flux, the mantle temperature was calculated using the method of fictive heat sources and sinks. A thermal conductivity of $\Lambda_s=2.5\text{W/mK}$ for the surrounding soil was found to be in a good agreement with the test results of [6] and [7].

The applied values for the elastic constants E and ν ,

the thermal expansion coefficient α_t and the thermal conductivity Λ can be found in [8] for the three components of the pipeline. The resulting ratio between changes of media temperature and mantle temperature was found to be between 0.05 and 0.1. In a next step, the radial displacement was evaluated. For the steel pipe and the mantle the theory of thin-walled shells and for the insulation the shell theory in plain strain conditions was considered. The same methodology was also used by *Beilke* (1993) [10].

For an increase of medium temperature $\Delta T=120K$, the radial displacements normalized on diameter are depicted in Figure 2 for different pipeline diameters. Due to the high stiffness of the steel pipe compared to the other materials involved, changes of inner pressure and initial soil stress state were found to have only minor influence on the radial expansion.

Finally a finite element model was established, using the nonlinear elastic Duncan and Chang model [11, 12] to describe the soil behavior. An increase factor κ was introduced, quantifying the increase of maximum resistance force for a medium temperature increase of $\Delta T=100K$. For other thermal conditions, linear inter- and extrapolation is recommended. Within a parametric study was pointed out, that the main influences on κ are the overburden depth h and the deposit density D_r , while the outer diameter has only a minor impact. A functional relation for the increase factor was introduced:

$$\kappa = 1.18 - 0.1h[m] + 1.22D_r[1]. \quad (7)$$

NUMERICAL MODEL

General

In order to investigate the impact of a temperature increase on the average radial stress, two-dimensional numerical models were developed using the PLAXIS finite element program [13]. With regard to the symmetry of geometry and loading, only one half of the system was modeled in order to reduce computational effort. Prior to the main analyses, investigations on mesh fineness and model dimensions were made to ensure accurate results. Model dimensions of 18 times the pipeline diameter in horizontal direction and 16 times the diameter in vertical direction, both measured from the pipeline centre, were found to be sufficient. For the developed model, elements with quadratic shape functions were chosen. In contrast to elements with first-order (linear) interpolation, these second-order elements are capable of representing all possible linear strain fields. Additionally the shape approximation of curved structures is much better.

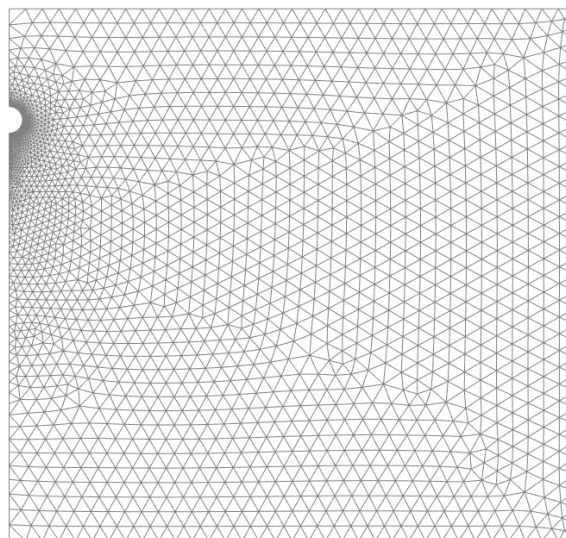


Figure 3. Exemplary finite element mesh

Thus, a more accurate solution may be obtained with fewer elements in contrast to first-order elements. The region near the pipe was discretized finer than the far field, where the mesh density can usually be reduced because of lower stress gradients. Figure 3 shows an exemplary finite element mesh.

Contact model

A relative displacement between the pipe and the surrounding soil occurs under radial or axial pipe displacement. To enable the possibility of relative slipping within the finite element model, a contact condition was defined. The frictional contact was established using the simple friction law according to Coulomb. The classical Coulomb's friction law considers the stick-slip phenomenon, which describes the transition between stick and slip states, depending on the magnitude of applied contact pressure.

An important parameter for the determination of friction forces is the coefficient of friction. In the terminology of soil mechanics the coefficient of friction is written as:

$$\mu = \tan(\varphi'_c), \quad (8)$$

wherein φ'_c is the angle of contact friction. According to *Rumpel* [3], it is solely dependent on the angle of internal friction (compare equation 5). This equation has not been confirmed by theoretical or experimental investigations. *O'Rourke et al.* [55] carried out 450 laboratory tests, from which an influence of the shore hardness H_D on the angle of contact friction was inferred:

$$\varphi'_c = (-0.0088H_D + 1.15) * \varphi'. \quad (9)$$

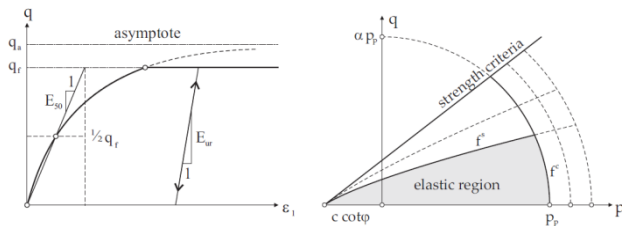


Figure 4. Hyperbolic stress-strain relation (left) and yield surfaces of the HS-Model (right) [21]

The value of H_D for the commonly used HD-Polyethylene material is in the range of 58 to 62 [14]. With increasing shore hardness, the amount of penetration of the soil particles into the HDPE material decreases, leading to a deterioration of interlocking effects and thus to a decrease in the angle of contact friction. Generally, the proposed values according to this approach are smaller than the ones given by *Rumpel*. Another influence on the angle of contact friction is the relative density D_r . From experiments, *Achmus* [8] determined the following dependency:

$$\varphi'_c = 8.0D_r + 20.0. \quad (10)$$

Experiments by *Weidlich* (2008) [14] confirmed the dependence on relative density, resulting in the relation:

$$\varphi'_c = 3.0D_r + 22.3. \quad (11)$$

Weidlich chose medium sand with a rounded grain shape, which is representative for commonly used fill material. Therefore, in the following, equation 11 is considered for the determination of the coefficient of contact friction.

Constitutive model

For the prediction of material behavior using the finite element method, mathematical equations are needed. These so called constitutive equations should describe the stress-strain relationships for any possible problem. However, in contrast to balance equations, which describe physical laws exactly, constitutive equations can only approximate the mechanical behavior. Even if only noncohesive soil is taken into account, numerous constitutive models of different complexity exist. Since complexity is usually associated with many input parameters, which are in practice hard to evaluate, choice has been made for the *Hardening Soil model*.

The *Hardening Soil model* (HS-Model) is an advanced material model for sand. On the basis of *Vermeer* [15], it was developed by *Schanz* [16, 17]. It is formulated in the framework of the classical theory of elastoplasticity. Here, it is assumed that the strain tensor can be decomposed in elastic and plastic components. A yield criterion, stated with the use of a yield function, defines

the limit state between purely elastic behavior and the appearance of plasticity. The elastic law describes the stress-strain-relation in the elastic region of the material. Additionally, a plastic flow rule, defining the evolution of the plastic strain, and, if any kind of hardening is taken into account, a hardening law characterizing the evolution of the yield limit has to be formulated. The HS-Model uses a Mohr-Coulomb failure criterion, which involves the cohesion c' and the angle of internal friction φ' . Using the hyperbolic relationship postulated by *Duncan and Chang* [11] the axial strain ϵ_1 is related to the differential stress q , controlled by the secant modulus E_{s0} (figure 4 left):

Stiffness parameters are defined for primary loading as well as for un- and reloading. The moduli E_{s0} and E_{wr} can be derived from triaxial testing. They are both determined to be stress dependent, which is also true for the oedometric stiffness E_{os0} . To take the stress dependency into account, the power laws of *Janbu* [18] and *Ohde* [19] are used. Another feature of the *Hardening Soil model* is the incorporation of hardening. Hardening is characterized by a dependence of yield stress level on the history of plastic straining [20]. As a result, the yield surfaces are not fixed in principal stress space and, thus, can expand from the initial state (Figure 4 right). In the HS-Model two types of hardening are distinguished: shear and compression hardening, resulting from deviatoric primary loading and isotropic primary loading, respectively. Both types of hardening consider the occurrence of irreversible strains. In this form, the HS-Model needs eight input parameters. All of them can easily be derived from standard laboratory tests.

An extension of the model, termed *HSsmall model*, was developed by *Benz* [21] and is able to account for strain dependency of soil stiffness. An increased stiffness in small strain regions is already known from dynamic analyses. However, this stiffness is mainly dependent on the magnitude of applied strain, not on strain rate [21]. To take this phenomenon into account, the soil stiffness for small shear strains ($\gamma < 10^{-6}$), is defined by the small-strain shear modulus G_0 . To describe the stiffness degradation with shear strain, a relationship formulated by *Santos & Correia* [25] is implemented in the *HSsmall model*:

$$G/G_0 = (1 + 0.385 * |\gamma / \gamma_{0.7}|)^{-1}. \quad (12)$$

The parameter $\gamma_{0.7}$ denotes the shear strain at which the shear modulus G is reduced to 72.2% of its initial value G_0 . A value of $\gamma_{0.7} = 10^{-4}$ is common practice [13]. Together with these two additional parameters, the *HSsmall model* requires a total number of ten

parameters. Because usually, during the design process of district heating networks, only limited field data are available, a simplified determination process comes into use. In PLAXIS, all four stiffness moduli have to be defined for a reference stress p_{ref} .

$$\begin{aligned} E_{oed} &= E_{oed,ref} * (\sigma_1 / p_{ref})^m \\ E_{50} &= E_{50,ref} * (\sigma_3 / p_{ref})^m \\ E_{ur} &= E_{ur,ref} * (\sigma_3 / p_{ref})^m \\ G_0 &= G_{0,ref} * (\sigma_3 / p_{ref})^m \end{aligned} \quad (13)$$

In all calculations the pipe centre level is used as reference and therefore the vertical stress in this depth is assigned as reference stress p_{ref} . To determine the oedometric stiffness modulus at reference stress $E_{oed,ref}$, the empirical power law of *Ohde* [19] comes into use, which is well-funded and often used in engineering practice:

$$E_S = \kappa * 100kPa * (\sigma_m / 100kPa)^\lambda. \quad (14)$$

σ_m denotes the mean principal stress. Note that the inherited reference stress of 100kPa is defined within *Ohde's* power law and should not be mistaken with p_{ref} from the *HSsmall* model. A bandwidth for the parameters κ and λ , dependent on soil type and relative density, can be found in [1]. It is obvious that the stiffness exponents λ and m have the same meaning and can therefore be used analogous. Because $\sigma_1 = p_{ref}$ at reference depth, no further conversion is necessary and it follows:

$$E_{oed,ref} = E_S. \quad (15)$$

Within experimental investigations on different sand types, *Schanz and Vermeer* [22] observed a correlation of the normalized oedometric stiffness modulus $E_{oed,n}$ and the normalized secant stiffness modulus in drained triaxial tests $E_{50,n}$:

$$E_{oed,n} = E_{50,n}. \quad (16)$$

Note that in [22], the normalization for the oedometric stiffness modulus was done with respect to the major principal stress σ_1 , while the secant stiffness modulus was normalized on σ_3 . Since we used σ_3 as reference stress p_{ref} , a simple conversion must be done:

$$E_{50,ref} = E_{oed,ref} * \left(\frac{\sigma_3}{\sigma_1} \right)^\lambda. \quad (17)$$

In initial configuration the major and minor principal stresses are related by the coefficient of earth pressure at rest ($\sigma_3 = \sigma_1 * k_0$). Substitution of σ_3 leads to:

$$E_{50,ref} = E_{oed,ref} * k_0^\lambda. \quad (19)$$

For completeness, the reference stiffness for un- and reloading $E_{ur,ref}$ must be assigned. *Schanz and Vermeer* [22] suggest a value of five, while *Plaxis* [13] recommends a value of three times the reference secant stiffness modulus. Because this parameter is of minor interest for the given problem, the following ratio seems appropriate:

$$E_{ur,ref} = 4 * E_{50,ref}. \quad (19)$$

For the small-strain shear modulus $G_{0,ref}$, a relation given by *Hardin & Black* [23] is considered:

$$G_{0,ref} = 33 * \frac{(2.97 - e)^2}{1 + e} [MPa]. \quad (20)$$

This equation is valid for a reference stress of 100kPa and has therefore to be adopted using equation 13. The parameter e denotes the void ratio. Assuming a particle density of 2.65kg/dm³, the void ratio can be determined from the soil unit weight γ .

Beside the stiffness parameters, shear parameters have to be assigned. For the angle of internal friction φ' , the recommendations from the *AGFW* guideline [1] can be used. Thereby, consistency with the soil unit weight γ and the stiffness coefficients κ and λ is ensured. According to *Schanz* [24], the angle of dilatancy ψ' can be correlated with the angle of internal friction:

$$\psi' = \varphi' - 30^\circ. \quad (21)$$

The parameter sets used in this investigation are summarized in Table 1. To obtain the input parameters for the *HSsmall* model, the described simplified procedure comes into use. This set is completed by the poisson's ratio of $\nu = 0.25$, as it is common practice for sand, and a cohesion yield stress of $c' = 0.1kN/m^2$ for the sake of numerical robustness.

Calculation steps

Each calculation was divided in three steps. In the first step the geostatic stress state was calculated, followed by the installation step, where the pipeline was added to the model. The pipeline was modeled *wished-in-place*, so that effects from the installation process were only approximately considered by the increased value of k_0 . The pipeline was fixed in vertical direction and also its self weight was neglected. So, in comparison with equation 1, only the evolution of the term F_Y' was

investigated within the final step. Herein, a radial displacement was incrementally applied until the diameter dependent final value according to Achmus [8] (Figure 2) was reached. These values represent a temperature increase of $\Delta T=120K$. For the evaluation of the average radial stress σ_r , the contact stresses of the soil-pipeline interface were considered.

Table 3: Soil parameters used in num. investigations

Description			dense	medium dense	loose
Unit weight	γ	[kN/m ³]	19	18	17
Friction angle	φ'	[°]	35	32.5	30
Stiffness parameter	κ	[-]	700	475	250
Stiffness parameter	λ	[-]	0.55	0.65	0.75
Coefficient of earth pressure	k_0	[-]	0.75	0.65	0.55

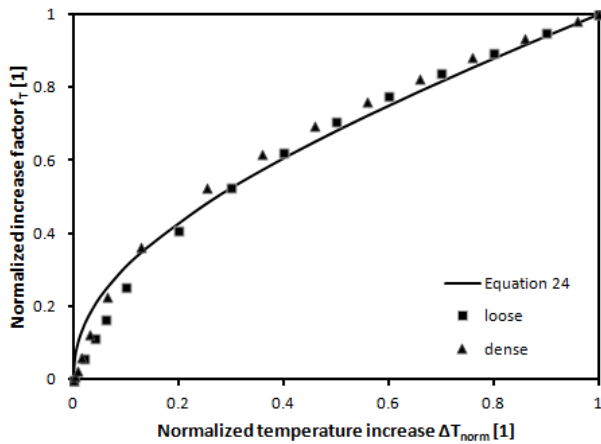


Figure 5. Normalized description of temperature dependency (DN200, h=3m)

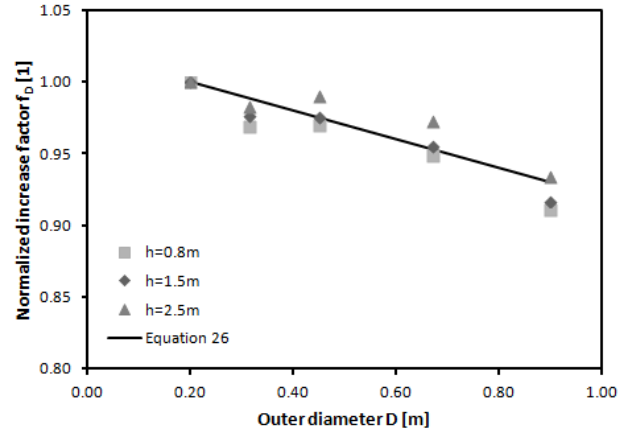


Figure 6. Normalized description of diameter dependency for medium dense sand

PARAMETRIC STUDY

Within the parametric study, a total number of 45 calculations were performed. In this section, the results are presented, showing impacts of geometric properties, relative density and magnitude of temperature increase.

Influence of medium temperature

To investigate the impact of a temperature rise on the average radial stress, a normalized description is introduced. Therefore the normalized temperature increase ΔT_{norm} :

$$\Delta T_{norm} = \frac{\Delta T [K]}{120 K}, \quad (22)$$

and the normalized increase factor of average radial stress due to medium temperature f_T :

$$f_T = \frac{f_I}{f_{I,(\Delta T=120K)}}, \quad (23)$$

were defined. The factor f_I denotes the ratio of actual average radial stress to its value at initial state. In Figure 5, the results of a reference system are depicted. They are representative for the whole parametric study. For small temperature

risers, the higher soil stiffness, resulting from the small-strain extension of the HS-model becomes obvious. In consequence, a nonlinear approximation, using a hyperbolic sine function, was chosen:

$$f_T = \frac{\sinh(\Delta T_{norm}^{0.45})}{\sinh(1)}. \quad (24)$$

A value of 0.45 for the exponent was found to give the best agreement with regard to all investigated models.

Influence of diameter

As a first geometric property, the pipelines diameter was varied in the range of $D=0.2\text{m}$ (DN100) and $D=0.9\text{m}$ (DN700). Since medium dense is the relative

density with the highest practical relevance, these results are shown in figure 6. The factor f_D is again a normalized value:

$$f_D = \frac{f_I}{f_D(D = 0.2\text{m})}. \quad (25)$$

All results belong to the final increase of temperature $\Delta T=120\text{K}$. Despite small deviations, a linear regression seems appropriate to approximate the effect of diameter:

$$f_D = 1.02 - 0.1 * D[m]. \quad (26)$$

Influence of overburden height

The second geometric parameter under investigation is the overburden height h . For the sake of clarity, and to evaluate the reference increase factor $f_D(D = 0.2\text{m})$, results of different overburden height were written in their corrected form with respect to the outer diameter:

$$f_D(D = 0.2\text{m}) = \frac{f_I}{f_D}. \quad (27)$$

Herein, f_D was calculated according to equation 26. As can be seen from Figure 7, the reference increase factor decreases almost linear with overburden height. Thereby, a good agreement can be achieved with the following relation:

$$f_D(D = 0.2\text{m}) = 2.7 - 0.135 * h[m]. \quad (28)$$

So, concerning the impacts of geometry, we can conclude that both, influence of diameter and overburden height, can adequately be described by the presented equations.

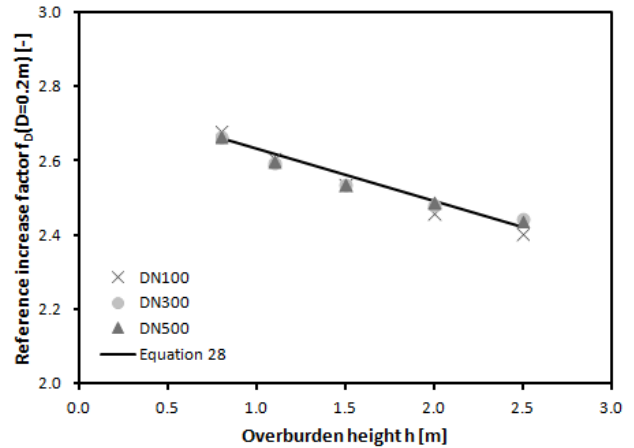


Figure 7. Reference increase factor for different overburden heights

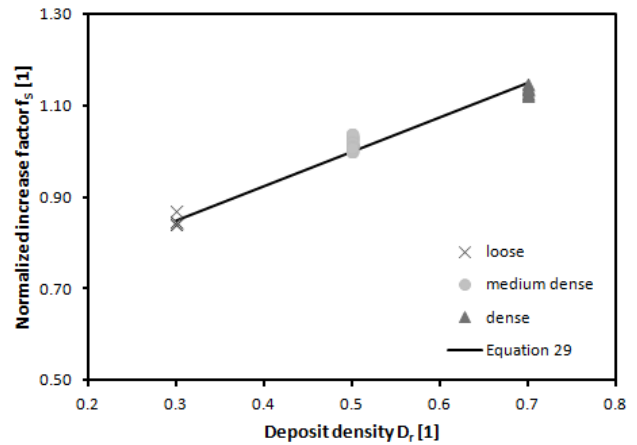


Figure 8. Influence of relative density of sand

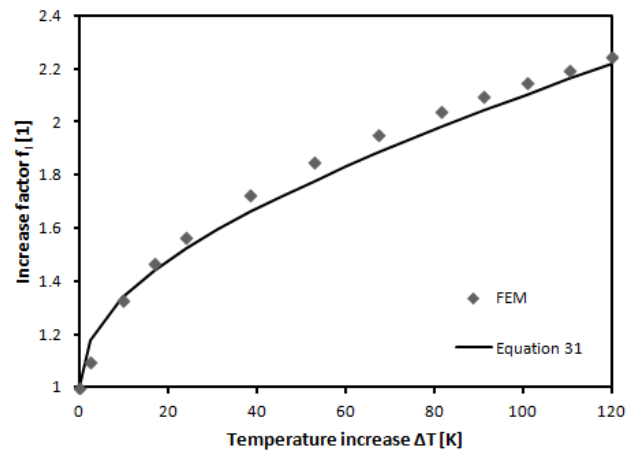


Figure 9. Comparison between FEM und proposed procedure (DN700, $h=2.5\text{m}$, medium dense sand)

Influence of relative density

Although medium dense sand is commonly used as backfill material within the trench, the relative density was varied in a wide range to define upper and lower limits. The results are depicted in Figure 8. Herein,

overburden heights of $h=0.8\text{m}$, 1.5m and 2.5m as well as the nominal diameters DN100, DN300 and DN500 are inherited. Therefore, the geometrically corrected increase factor f_s was plotted over deposit density (cf. Figure 8). The following equation takes different relative densities into account:

$$f_s \equiv \frac{f_I}{f_D * f_D(D=0.2\text{m})} = 0.625 + 0.75 * D_r \quad (29)$$

Thereby, the main influences within the scope of work were considered.

Derivation of a corrective term

In this section, explanation is made how the derived correction terms can be used to determine the increase factor for different boundary conditions. If, e.g. for pipeline design, only the maximum increase of average radial stress is of interest, the increase factor can be calculated in the following way: The overburden height dependent reference value according to equation 28 has to be evaluated and multiplied with the factor for diameter correction (eq. 26) and, if other than medium dense sand is considered, with the correction term for deposit density (eq. 29):

$$f_T(\Delta T = 120\text{K}) = f_D(D = 0.2\text{m}) * f_D * f_s \quad (30)$$

If, in addition, the evolution of the increased radial stress due to an arbitrary temperature rise should be evaluated, equation 24 must be incorporated:

$$f_I(\Delta T) = f_T(\Delta T = 120\text{K}) * f_T - f_T + 1 \quad (31)$$

To verify the accordance of the proposed procedure compared to the results gained from the finite element model, a DN700 pipeline embedded in medium dense sand was investigated (Figure 9). A very good accordance between the finite element solution and the proposed derivation approach can be stated.

CONCLUSIONS

Within the paper at hand, the influence of medium temperature increase on the average radial stress was investigated. Therefore, after a brief introduction, the state of knowledge concerning this topic was summarized. It can be concluded that, beside few experimental investigations with a limited bandwidth of investigated parameters, solely *Achmus* [8] made comprehensive studies on radial pipeline extension. Based on this work, numerous finite element models were developed using the sophisticated *HSsmall model*. Since this model needs numerous input parameters, a simplified derivation procedure was presented. By the use of well-funded correlations, all parameters can be calculated based on empirical values that can be found in the AGFW design code [1].

Within the parametric study, variations of temperature increase, pipeline diameter, overburden height and relative density of sand were carried out. For the dependency on medium temperature, a nonlinear approximation, resulting from the higher stiffness in small strain regions was proposed. The normalization on geometric properties and deposit density could be achieved by the use of linear dependent relations. In agreement with *Achmus* [8], the overburden height and the deposit were identified to have the strongest influences on the increase factor f_I . The increase factor reaches the highest value for small diameters and overburden heights. As expected, it increases with relative density of sand. A minor impact of the outer diameter was found and therefore considered within the derivation of a corrective term. Qualitatively, the results were similar to *Achmus*. However, the calculated increase factors within this investigation were slightly higher. For medium dense sand, the increase factor was in the range of 1.9-2.3 for a temperature rise of $\Delta T=100\text{K}$. As a consequence, significantly higher axial friction resistances must be expected during the operation of district heating networks.

Finally, the use of the developed correction factors was shown for an exemplary model. The agreement between the results gained from the finite element method and the proposed relations were satisfactorily. For the estimation of the maximum friction resistance dependent on medium temperature, the following relation may be used:

$$F_N'(\Delta T) = f_I(\Delta T) * F_N'(\Delta T = 0) \quad (32)$$

Nevertheless, some simplifications were made and therefore, further research is needed. First, the installation process of the pipeline was only considered roughly. This might be of major impact on the initial state of the surrounding soil. Additionally, a homogenous half space with just one pipeline was modeled, what differs from the field conditions. Another open question is the interdependency with a lateral pipeline displacement, possibly near arch sections or joints. The latter mentioned is currently under the author's investigation. Incorporating the findings of these investigations, a more reliable design of district heating pipelines should be possible in the near future.

ACKNOWLEDGEMENT

The presented research work was funded by the German Federal Ministry of Economic Affairs and Energy. The support is gratefully acknowledged.

REFERENCES

- [1] AGFW e.V.: FW401-10: "Verlegung und Statik von Kunststoffmantelrohren (KMR) für Fernwärmenetze", Frankfurt (2007) (in German)
- [2] Coulomb, C. A.: *Essai sur une application des regles des maximis et minimis a quelques problems de statique relatifs, a la architecture*. In: *Mem. Acad. Roy. Div. Sav.* 7 (1776), p. 343–387 (in French)
- [3] Rumpel, G.: *Erdverlegte Verbundrohre für Fernwärme*. In: *Rohrleitungstechnik* (1976), p. 420–434 (in German)
- [4] Jaky J.: *Pressure in silos*. 2nd ICSMFE, London (1948), Vol. 1, pp 103-107.
- [5] Gramm, G.: *Statik und Festigkeit des Kunststoffmantelrohres*. In: *3R International* Jg. 22, Nr.7/8 (1983), p. 355–357 (in German)
- [6] HEW, *Fernwärmehtransportleitung Karoline-Wedel Kunststoffmantelrohr DN 700*, final report (1987), unpublished
- [7] Gietzelt, M.; Engelhardt, H.; Mantley, W.; Grage, T.: *Ermittlung der Reibungskräfte an erdverlegten wärmeleitenden Leitungen zur Sicherstellung wirtschaftlicher Konstruktionen*, final report (1991) (in German)
- [8] Achmus, M.: *Zur Berechnung der Beanspruchungen und Verschiebungen erdverlegter Fernwärmeleitungen*, PhD thesis (1995), Universität Hannover (in German)
- [9] Huber, M.; Wijewickreme, D.: *Thermal Influence on Axial Pullout Resistance of Buried District Heating Pipes*, 14th International Symposium on District Heating and Cooling (2014), Stockholm, Sweden
- [10] Beilke, O.: *Interaktionsverhalten des Bauwerks "Fernwärmeleitung-Bettungsmaterial"*, PhD thesis (1993), Universität Hannover (in German)
- [11] Duncan, James M., and Chin-Yung Chang. "Nonlinear analysis of stress and strain in soils." *Journal of the soil mechanics and foundations division* 96.5 (1970): 1629-1653.
- [12] Duncan, James M. "Hyperbolic stress-strain relationships." *Application of Plasticity and Generalized Stress-Strain in Geotechnical Engineering*. ASCE, 1980.
- [13] Brinkgreve, R.B.J.; Engin, E.; Swolfs, W.M.: *PLAXIS 2D 2013 Manual*.
- [14] Weidlich, I.: *Untersuchung zur Reibung an zyklisch axial verschobenen erdverlegten Rohren*, PhD thesis (2008), Universität Hannover (in German)
- [15] Vermeer, PA: *A double hardening model for sand*. In: *Geotechnique* 28 (1978), Nr. 4, S. 413–433
- [16] Schanz, T; Vermeer, PA; Bonnier, PG: *The hardening soil model: formulation and verification*. In: *Beyond 2000 in computational geotechnics* (1999), S. 281–296
- [17] Schanz, T: *Zur Modellierung des mechanischen Verhaltens von Reibungsmaterialien*, PhD thesis (1998), Universität Stuttgart (in German)
- [18] Janbu, Nilmar: *Soil compressibility as determined*

- by oedometer and triaxial tests. In: European Conference on Soil Mechanics and Foundation Engineering Bd. 1 (1963), S.19–25
- [19] Ohde, Johannes: *Zur Theorie der Druckverteilung im Baugrund*. (1939) (in German)
- [20] Souza Neto, Eduardo A. ; Peric, Djordje ; Owen, David Roger J.: *Computational methods for plasticity: theory and applications*. John Wiley & Sons (2011)
- [21] Benz, Thomas: *Small-strain stiffness of soils and its numerical consequences*, PhD thesis (2007), Universität Stuttgart
- [22] Schanz, T. and P. A. Vermeer: *On the stiffness of sands*, Géotechnique 48 (1998): 383-387.
- [23] Hardin, Bobby O., and William L. Black. "Closure on vibration modulus of normally consolidated clay." *Journal of Soil Mechanics & Foundations Div* (1969).
- [24] Schanz, T, and Vermeer, P.A.: *Angles of friction and dilatancy of sand*, Géotechnique 46 (1996): 145-151.
- [25] Dos Santos, J. A., and A. G. Correia: *Reference threshold shear strain of soil. Its application to obtain an unique strain-dependent shear modulus curve for soil*. Proceedings of the Fifteenth International Conference on Soil Mechanics and Geotechnical Engineering, Istanbul, Turkey, 27-31 August 2001. Volumes 1-3. (2001)

SENSITIVITY ANALYSIS ON THE AXIAL SOIL REACTION DUE TO TEMPERATURE INDUCED PIPE MOVEMENTS

Ingo Weidlich¹

¹ FFI, Fernwärme-Forschungsinstitut in Hannover e.V., Max-von-Laue-Str. 23, 30966 Hemmingen

Keywords: buried pipe design, pipe soil interaction, friction force

ABSTRACT

Buried District Heating pipes are subjected to thermal loads. Thermal strain and the resulting interaction with the surrounding soil have to be considered for safe operation. A sensitivity analysis was carried out to estimate the significance of relevant parameters and existing calculation approaches for axial soil reaction. This paper identifies the most significant parameters and suggests parameter sets for lowest and highest axial soil reaction.

INTRODUCTION

Seen from an international perspective pipe laying according to state of the art in heat distribution is primarily based on preinsulated bonded pipe systems. These pipe systems are usually buried in sand. The interaction of soil and pipe hinders thermal strains, making economic solutions for bow- and T-sections possible. Regarding the static design, pipe-soil interactions must be known as accurate as possible. However, several parameters are influencing the quantity of the expected soil reaction [1]. Main influencing factors are the bedding material utilized and its parameters (e.g. average effective unit weight, compactness or coefficient of lateral earth pressure) and the geometry of the pipe and trench (e.g. depth of the pipe (crown) below the surface or external pipeline diameter). Furthermore, current research results evidently showed the influence of additional phenomena, such as hardening effects and stress redistribution during operation [2]. A new calculation approach for the axial soil reaction was developed in 2015 basing on existing test results and numerical simulations [3].

Soil reactions relevant for the design of district heating pipelines are divided into two groups: Axial soil reaction and lateral soil reaction. Since the magnitude of the expected lateral soil reaction is a current research topic [4] the axial soil reaction, which is the skin friction among the perimeter of the pipe, was suggested to be described sufficiently by standard calculation approaches in the last decades. However, major deviations between calculated reactions and measurement of the bearing behaviour of district heating pipes in situ have been reported by engineers quite frequently. Against this background, a new

approach for calculating the skin friction was developed taking into account contemporary research results.

STATE OF THE ART

The European state of the art for the calculation of pipe skin friction of district heating pipes is defined in EN13941 [5]. According to this approach, the skin friction F_R is assumed to be proportional to the radial contact pressure around the pipe and may be calculated using equation (1).

$$F_R = \mu \left(\frac{1 + k_0}{2} * \sigma_v * \pi * D_a + G - \gamma_B * \pi * \left(\frac{D_a}{2} \right)^2 \right) \quad (1)$$

Where:

k_0 =earth pressure coefficient at rest = $1 - \sin \varphi'$
 G =effective weight of the pipe filled with water
 σ_v =effective soil stress at pipe axis
 for granular soils:
 $\sigma_v = \gamma_B * H_w + \gamma_{BW} * (Z - H_w)$ for $H_w < Z$
 $\sigma_v = \gamma_s * Z$ for $H_w \geq Z$
 Z =depth of the pipe axis
 H_w =depth of ground water table
 γ_B =unit weight of the soil
 γ_{BW} =buoyant weight of the soil
 γ_s =weight of the saturated soil

The term in brackets describes the resulting earth pressure acting on the pipe. However, several other methodologies are available for the calculation of the resulting earth pressure on pipes (e.g. Marston [6], Spangler [7], Leonhardt [8]). μ is the coefficient of friction according to COULOMB, generally ranging between $\mu=0.3$ to 0.4 for normal conditions, cf. according to EN 13941 [5]. Alternatively, equation 2 may be used for the calculation of μ .

$$\mu = \tan \delta = \tan \left(\frac{2 * \varphi'}{3} \right) \quad (2)$$

Where:

μ =coefficient of friction
 δ =contact friction angle [°]
 φ' = internal soil friction angle [°]

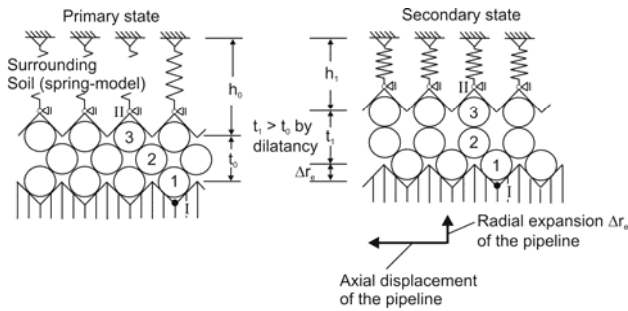


Fig. 1, Two major effects during initial operation

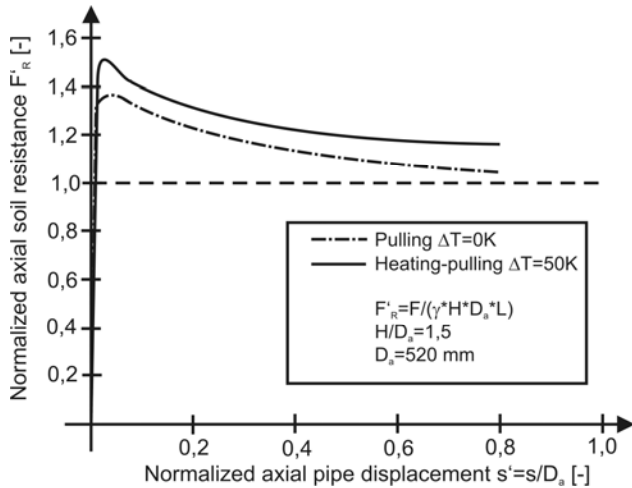


Fig. 2 Results from HUBER et al. [2]

Since the internal friction angle ranges between $\varphi' = 32^\circ$ to 40° for sands, equation (2) leads to $\mu = 0.39 \dots 0.5$. Considering fast movements, $\mu = 0.6$ is given in [5], which is 1.5-times higher than the value occurring due to normal movement.

INITIAL STRESS CONDITION

Regarding constant geometric boundaries, the initial stress condition after installation depends on the properties of the bedding material. In order to avoid settlements of the surface, a high degree of compactness is usually wanted for the trench backfill. The compactness achieved within the trench influences the unit weight of the soil and the earth pressure coefficient [1]. Thus, an increased coefficient of earth pressure probably occurs and has to be taken into account when calculating the maximum friction force in the sense of a worst case scenario.

STRESS CONDITION DURING OPERATION

During initial operation of the pipeline, two main effects have to be taken into account for the description of axial soil reaction: 1. Due to temperature dependent radial expansion Δr_e the normal soil stress increases among the perimeter of the pipe and 2. Temperature driven axial expansion leads to axial pipe movements

resulting in a hardening effect due to dilatant soil reaction. Both effects are illustrated in Figure 1.

The radial pipe-soil interaction was investigated in a two-dimensional numerical model by ACHMUS in 1995 [9]. Axial hardening effects due to dilatancy are known from buried structural components such as piles and anchors and were transferred to district heating pipelines by the author in 2007 [10].

Achmus calculated 1995 typical parameter combinations for sand with different relative densities. As a measure of temperature dependence, the factor κ_l , was defined:

$$\kappa_l = \frac{\sigma_{r,avg}(\Delta T = 100K)}{\sigma_{r,avg}^{(0)}} = \frac{F_{r,u}(\Delta T = 100K)}{F_{r,u}^{(0)}} \quad (3)$$

Where:

κ_l = factor for the relationship between initial stress state and subsequent stress state

$\sigma_{r,avg}$ = average contact pressure on the pipe perimeter

$F_{r,u}$ = ultimate friction force,

ΔT = temperature increment

The results indicated that this factor is significantly depending on the relative density of the sand, as well as the overburden height h . Achmus derived equation (4) for the calculation of κ_l from the results (valid for $\Delta T = 100K$). For lower ΔT , κ_l may be interpolated.

$$\kappa_l = 1.18 - 0.1 * H[m] + 1.22 * D_r \quad (4)$$

Where:

κ_l = factor for the relationship between initial stress state and secondary stress state

H = depth of overburden to the top of the pipe

D_r = relative density of soil bedding.

Systematic fundamental investigations on the interacting effects of radial expansion and hardening due to dilatancy are missing. However, few isolated single results exist, but an overall evaluation was not carried out yet. An example for current results is the investigation of HUBER et al. from 2014 [2], which are shown in extracts in Figure 2.

HUBER et al. observed an increased friction force, represented by $\kappa_{l,Huber} = 1.5$ for a temperature increment of $\Delta T = 50K$. Medium dense boundary conditions of the bedding were reported, which is related to $D_r \approx 0.5$. After interpolation, equation (4) delivers $\kappa_{l,Achmus} = 1.36$ for $\Delta T = 50K$. Thus, experimental 3d-results approximately showed values 10% above the results of the 2d-approach. Values of this magnitude for axial hardening were observed before without temperature load in [11].

Merging the two-dimensional numerical investigations of ACHMUS with the axial hardening effect due to dilatancy, a more realistic approach for the calculation of friction force during initial loading is assumed, s. equation (5).

$$\kappa_{L,mod} = \frac{F_{R,\Delta T=100K}}{F_{R,0}} = \kappa_{L,Achmus} * 1,1 = 1,30 - 0,11 * H[m] + 1,34 * D_r \quad (5)$$

Considering repeated thermal loading, the soil contact pressure will decrease due to stress redistribution in the surrounding soil. In present practice, the initial friction force is assumed to drop by 50% simulating the residual state upon cyclic loading according to EN13941 [5]. The actual phenomena of friction degradation were investigated by the author, whereas additional equations describing stresses occurring during operation are given e.g. in [10].

SENSITIVITY ANALYSIS

A sensitivity analysis was carried out considering two boundary parameter sets resulting in low and high friction, s. Table 1. A high temperature increment ΔT was used for operation temperatures up to 120°C according to EN13941 [5].

Furthermore, equation (1) was used according to EN13941 representing the lower boundary. In addition, $\kappa_{L,mod}$ was applied for describing the upper boundary. A common single beam static model was used for the sensitivity analysis, which is shown in Figure 3.

Table 1 – Parameter set

Parameter	Low friction	High friction
Overburden height	H=0.8 m	H=0.8 m
Nominal Diameter/Outer Diameter	DN100/200	DN100/200
Temperature Increment	$\Delta T=100K$	$\Delta T=100K$
Unit weight of soil	$\gamma=16kN/m^3$	$\gamma=20kN/m^3$
Earth pressure coefficient	$K=0.5$ $=1-\sin(\varphi'=30^\circ)$	$K=1.0$
Coefficient of friction	$\mu=0.36$ $=\tan(2^*(\varphi'=30)/3)$	$\mu=0.54$ $=\tan(2^*(\varphi'=43)/3)$
Relative density	Loose	Dense, $D_r=0.7$
Equations	(1)	(1) and (5)

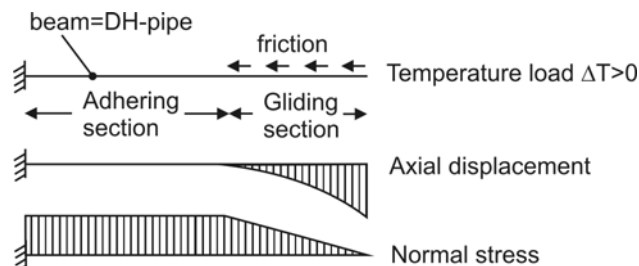


Fig. 3, Single beam model for DH-pipe

According to equations (6) and (7), the length of the gliding section l_0 and the maximum displacement u_{max} may be derived for this model.

$$l_0 = \frac{\alpha_T * \Delta T * A_s * E}{F_R} \quad (6)$$

$$u_{max} = \frac{F_R * l_0^2}{2 * E * A_s} \quad (7)$$

Where:

α_T = thermal expansion coefficient

ΔT = temperature increment

A_s = area of steel medium pipe

E = Young's Modulus

F_R = ultimate friction force

l_0 = length of the gliding section

The results of the calculations are given in table 2. The ratio of high and low friction is 5.41. This difference demonstrates the importance of choosing accurate parameters for the bedding conditions in the field in order to calculate the friction forces occurring correctly.

Basing on the examinations on a future development of the supply flow temperatures for district heating conducted by LUND et al. in 2014 [12], the sensitivity analysis was enhanced for a future scenario according to the temperature development shown in Fig. 4.

Table 2 – Results

Results	Low friction	High friction	Ratio High vs. Low
Skin friction F_R	2.33 kN/m	12.6 kN/m	5.41
Gliding length l_0	137.26 m	25,35 m	0.18
Maximum displacement u_{max}	84.6 mm	15.6 mm	0.18

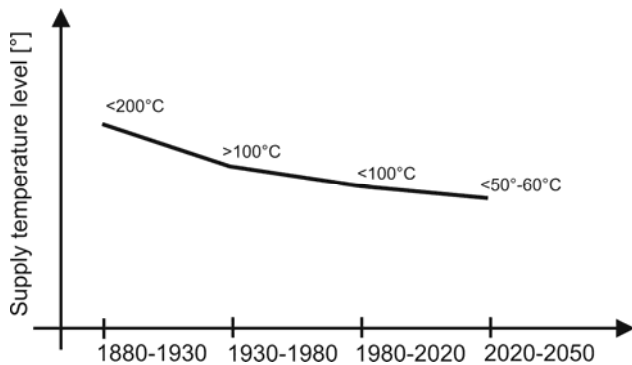


Fig. 4. Future supply temperature according to [12]

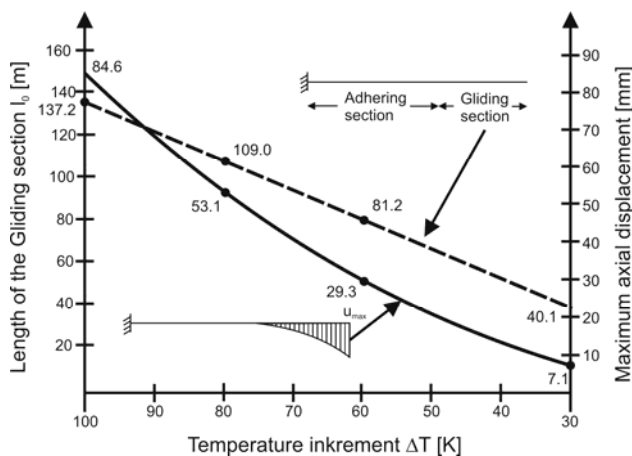


Fig. 5. Significance of decreasing temperature

For a fictitious average ambient temperature $T_a=20^\circ\text{C}$, the relevant temperature increment ranges here between $\Delta T_{1880}=180\text{K}$ and $\Delta T_{2050}=30\text{K}$. The results for u_{\max} and l_0 under low friction condition according to Table 1 are given for decreasing ΔT in Fig. 5.

This simple parametric study for the single beam system shows a significant reduction of maximum displacement and gliding length as well as the related strains and stresses. For a future temperature increment of $\Delta T=30\text{K}$ only a displacement of 7.1 mm remains which is less than 10% of the displacement for $\Delta T=100\text{K}$.

CONCLUSIONS

After a review of scientific results from numerical and experimental investigations, higher values for the friction force during initial temperature loading are expected for dense bedding conditions. Since two soil-mechanical phenomena have been examined independently in the past, a new empirical calculation approach is suggested. A sensitivity analysis is done, applying two boundary parameter sets, showed major discrepancies in friction forces assessing the magnitude of the characteristic designs. However, the presented merged calculation approach for initial skin friction is based only on limited data. Before practical

implementation the approach shall be evaluated by field measurements and additional experimental investigations.

Finally it must be noted for the predicted future scenario with decreasing supply temperatures in district heating grids, static engineering and soil-pipe interaction issues may play a minor role in the future.

REFERENCES

- [1] I. Weidlich, D. Wijewickreme, „Factors influencing soil friction forces on buried pipes used for district heating“ 13th International Symposium on district heating and cooling, Copenhagen September 2012, Symposium
- [2] M. Huber, D. Wijewickreme, “Thermal Influence on axial pullout resistance of buried district heating pipes”, The 14th International Symposium on District Heating and Cooling, Stockholm, 2014
- [3] I. Weidlich, „Zur Reibungskraft bei Inbetriebnahme einer Fernwärmeleitung“, (*On the friction force during taking into operation a district heating pipeline*), EuroHeat&Power, 44.Jg., Heft 12, Verlag: EW Medien und Kongresse GmbH, Frankfurt am Main, Seiten: 32-36, 2015
- [4] M. Achmus, M. Grehl, “Cyclic lateral soil resistance on district heating pipes”, The 14th International Symposium on District Heating and Cooling, Stockholm, 2014
- [5] EN 13941:2010, and installation of preinsulated bonded pipe systems for district heating, DIN, Deutsches Institut für Normung e.V. Normenausschuss Heiz- und Raumlufttechnik (NHRS), Beuth Verlag, Berlin, (2010)
- [6] M. Spangler, Stresses in pressure pipe-lines and protective casting pipes. Journal of Structural Engineering (82), (1956), pp. 1-33.
- [7] M.G. Spangler and R.L. Handy, „Soil Engineering“. Harper and Row, Publishers, New York, (1982)
- [8] G. Leonhardt, „Belastung von starren Rohrleitungen unter Dämmen“ Promotionschrift, Mitteilungsheft 4, Institut für Grundbau, Bodenmechanik und Energiewasserbau, Universität Hannover, (1973)
- [9] M. Achmus, Zur Berechnung der Beanspruchungen und Verschiebungen erdverlegter, Fernwärmeleitungen. (*On the calculation of loads and displacements of buried district heating pipelines*) Promotionschrift, Mitteilungsheft 41, Institut für Grundbau, Bodenmechanik und Energiewasserbau, Universität Hannover, (1995)
- [10] I. Weidlich, Untersuchung zur Reibung an zyklisch axial verschobenen erdverlegten Rohren.

(Investigation on the interface friction of cyclic axial displaced buried pipelines) Promotionsschrift 64, Institut für Grundbau, Bodenmechanik und Energiewasserbau, Leibniz Universität Hannover (2008)

[11] D. Wijewickreme, H., Karimian and D. Honegger,, "Response of Buried Steel Pipelines Subject to Relative Axial Soil Movement", Canadian

Geotechnical Journal, Vol. 46, No. 7, (2009), pp. 735-752.

[12] Lund H., Werner S., Wilthire R., Svendsen S., Thorsen J.E., Hvelplund F., Mathiesen B.V., "4th Generation District Heating (4GDH) Integrating smart thermal grids into future sustainable energy systems", Energy 68, 1-11, Elsevier. (2014)

NON-DESTRUCTIVE METHODS FOR ASSESSMENT OF DISTRICT HEATING PIPES: A PRE STUDY FOR SELECTION OF PROPER METHOD

P.Lidén¹, B. Adl-Zarrabi^{1,*}

¹Chalmers University of Technology, Sven Hultins gata 8, Göteborg, SE- 412 96, Sweden

Keywords: District heating pipes, lifetime status, non-destructive methods, degradation, PUR, Cooling methods, TCR-method

ABSTRACT

Many energy companies are facing renewal of their district heating and cooling (DHC) network. However, there are no methods to determine the performance of existing pre-insulated district heating and cooling pipe during its operation. The insulation performance of the pipes decreases gradually during time due to degradation of polyurethane (PUR) foam. The aim of our project is to find /develop non-destructive methods for assessing the lifetime and the status of both existing pipes and new pipes. All present methods demand some kind of excavation and interference in the system in order to assess the status of the pipes, the methods determine the status of the excavated part i.e. pointwise assessment and not the status of the system. In existing pipes, it is common to have copper wires which are used for detection of moisture/water intrusion into the insulation part of the pipes. The copper wires may possibly be used to assess thermal properties of the pipes by using other measuring methods or evaluation techniques. For new pipes there are much more possibilities e.g. attach sensors inside the pipes, in order to easily monitor the thermal status in the future, simplicity and price are though very important. A pre-study has been performed in order to scan the field of possible non-destructive methods for district heating use. The pre-study has led to a selection of a couple of methods that will be further evaluated and tested in field and in laboratory with old and new pipes. The selected methods are cooling methods and evaluations of the temperature coefficient of resistance (TCR) for copper wires versus thermal conductivity (λ). Another method that is of interest could be a modification of an electrical reflectometry method such as time domain reflectometry (TDR).

INTRODUCTION

DHC-systems may consist of hundreds of kilometres of pipes which most likely are of different quality concerning carrier pipe, insulation, single and twin pipe. A system normally grows gradually and thereby the age and type of pipes consequently vary with time. DH-networks have been used for decades and they expanded a lot in the 1960s in the US and Europe, the pipe types that have been used varies [1]. Pipes with for example PUR insulation have been used for decades, especially in Sweden. Many energy

companies need to renew their district heating (DH) networks. The Energy companies can measure what they produce in heat energy and what they deliver, so the heat losses for the whole network can be calculated. In Sweden, around 10% of the energy supplied to the district heating networks are lost through heat losses from the distribution pipes [2]. There is tough no method to assess the status of the different parts of the piping network, in terms of local heat losses. Consequently, the desire to detect and monitor the location of potential hot spots (poor insulation) in DH networks are significantly favourable issues for energy companies. It is favourable for many energy companies to estimate the remaining service life of pre insulated district heating pipes. The length of the pipe stretch that might need to be changed has to be long enough in order to make the excavation and change beneficial. Beneficial lengths for change depend on the thermal quality but also other factors like for example accessibility of the existing pipes, reasonable lengths is predicted to be in the kilometre scale. Today the TDR-method is used for detection of moisture/water intrusion into the insulation part of the pipes. This method is well functioning for the purpose of finding suspected water leaks but not for thermal status identification of longer stretches. The European Standard EN 253:2009 states that pre insulated pipes should survive at least 30 years at a constant operating temperature of 120°C and new pipes should have a thermal conductivity coefficient at 50 °C (λ_{50}) $\leq 0,029$ W/mK [3].

Single pipe with PUR insulation

A common type of pipe in Swedish DH-systems consist of an inner media pipe of steel and an outer casing of Polyethylene (PE). Between the media pipe and outer casing there is a PUR-insulation together with two thin 1.5 mm² copper wires, a typical pipe product that has been used during decades, different component of a pipe is illustrated in Figure 1. The copper wires are used for moisture detection by using TDR-methods. Aging and degradation of the PUR insulation take place due to high temperatures in the steel pipe (carrier pipe) and intrusion of gasses through the PE-casing pipe. Thermal properties of pre insulated pipes, which normally are filled with polyurethane (PUR), deteriorate during the real operation conditions. The degradation of PUR occurs due to diffusion of gas molecules between

the foam and surrounding air. In this process oxygen and nitrogen molecules penetrate from air to the foam bubbles and replace the blowing agent gases, which are mainly cyclopentane and carbon dioxide [4].

Aging of the pipe insulation leads to higher heat losses. Temperature is the most significant factor that accelerates the aging process of insulation [5]. Therefore; when the PUR insulation is exposed to high temperature, thermal conductivity coefficient, λ , of insulation increases subsequently and greater heat flow (losses) is expected based on Fourier's law (1).

$$q = -\lambda \cdot \nabla T = -\left(\lambda \cdot \frac{\partial T}{\partial x}, \lambda \cdot \frac{\partial T}{\partial y}, \lambda \cdot \frac{\partial T}{\partial z}\right) \quad [W \cdot m^{-2}] \quad (1)$$

Where:

q = Heat flow [$W \cdot m^{-2}$]

λ = Thermal conductivity [$W \cdot m^{-1} \cdot K^{-1}$]

∇T = Temperature difference [K]

Pre study

As a consequence of the need of finding methods for assessing the status of DH networks a pre study was conducted [6]. Several reports and scientific articles was scanned in order to find possible methods for remote detection of chemical, electrical and thermal properties of PUR after natural thermal degradation. The studied methods was limited to be only non-destructive. The methods that have been evaluated for this purpose were ultrasonic methods, chemical analysis, electromagnetic methods, reflectometry methods, voltage response, Tan-Delta, ground penetrating radar and infrared thermography test. The suitability for applying these methods on the DH pipes was evaluated by ranking them against each other through weighting from a number of criteria, for example portability, level of consistency, inspection time, level of non-destructiveness etc.

A modified TDR-method has been highlighted as a potential method for evaluation. A development of this type of method is on the other hand assessed to be hard and time consuming.

NON-DESTRUCTIVE METHODS

As was concluded in the pre study, an important criteria in order to find a well-functioning method is its non-destructiveness. The two methods that have been interesting to proceed with are the TCR-method, cooling method and TDR-method. A modified TDR-method will be evaluated depending on the outcome from the two fore-mentioned methods.

TCR-method

One of the tested methods, here called the TCR-method, are going to be conducted in laboratory with new and artificially aged pipes. Aging will be done by circulating heated oil within the pipe according to SS-EN 253:2009. The temperatures will be around 190°C compared to the stated 170 °C but with a proportional decrease in heating hours, approximately 200h compared to 1450h. The pipes will be placed for aging as in Figure 2.

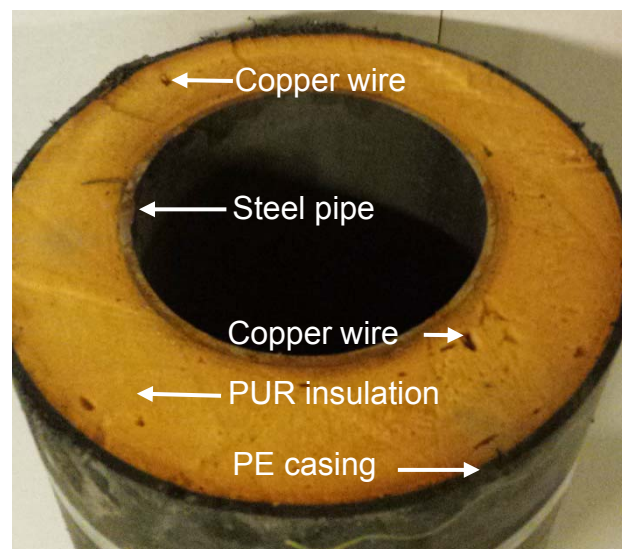


Figure 1 An old and naturally aged district heating pipe with a carrier pipe of steel, PUR foam insulation, copper wires and casing of PE.



Figure 2. Illustration of experimental set up for electrical resistance measurements before, during and after aging. Pipes are artificially aged by heated oil inside the steel pipe.

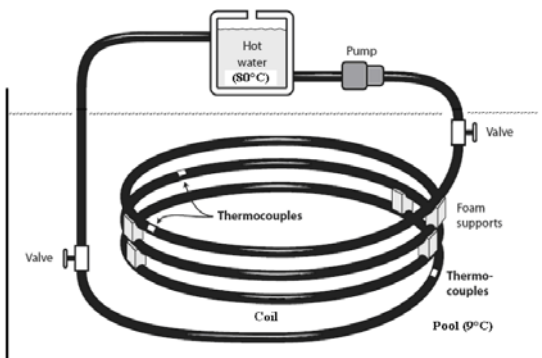


Figure 3 Experimental set-up. The coil and pool temperatures are measured by thermocouples at three positions along the pipe [8].

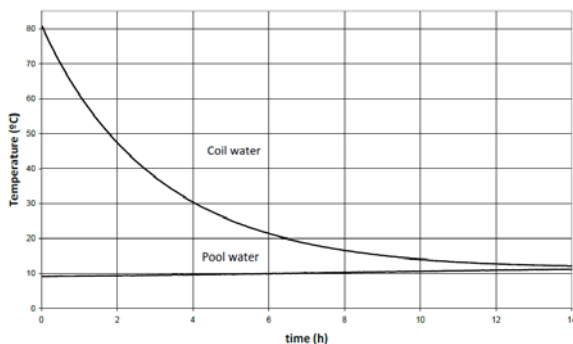


Figure 4 Measured coil water temperature and pool water temperature for a single pipe [8].

The method is aiming to find a relation between the electrical resistance of the copper wires inside the PUR foam and the thermal conductivity for a specific pipe dimension. There is a difference in thermal conductivity for new and old pipes and the method is striving to see whether this change can be detected by measuring the electrical resistance in the copper wires.

For many materials, the resistivity changes with temperature, so also for copper. If the temperature interval is not too large, the resistivity is a linear function of the temperature, T , and can be expressed as in (2) [7].

$$R(T) = R(T_0) \cdot (1 + \alpha(T - T_0)) \quad (2)$$

Where:

- T_0 = reference temperature [K]
- T = temperature of interest [K]
- $R(T_0)$ = resistivity at reference temperature [ohm]
- $R(T)$ = resistivity at temperature of interest [ohm]
- α = temperature coefficient of resistivity [1/K]
- $\alpha_{\text{copper}} = 3.9 \cdot 10^{-3}$ [1/K]

The thermal conductivity of virgin and aged pipes will be measured by using guarded hot pipe method according to the standard SS EN 253:2009. The standard is for homogenous pipes with polyurethane insulation and the output is a mean thermal conductivity of the insulating material. The aim is to assess thermal degradation by measuring and logging electrical resistance during a temperature drop. The electrical resistance drop (curve) in the copper wire during a certain temperature drop in service pipe will differ between a virgin pipe and an aged pipe. It will take longer time for a virgin pipe to reach stationary conditions in resistance and temperature compared to an aged pipe. Finally the thermal conductivity and the electrical resistance can be correlated by using the measured change of electrical resistance ΔR and the measured change in thermal conductivity $\Delta \lambda$ for virgin and aged pipes (3), it is also possible to determine the temperature at the position of copper wire (4).

$$\Delta \lambda \approx \Delta R \quad (3)$$

$$T = T_0 + \frac{R(T) - R(T_0)}{\alpha \cdot R(T_0)} \quad (4)$$

Cooling method

If an operating DH network would be shut down for a couple of hours there may be possibilities of analyzing the cooling time and temperature in order to assess the thermal conductivity of the pipes. A similar method is created by [8] and can assess the thermal conductivity of flexible twin pipes. The flexible pipe is placed in a pool with water, warm water (80 °C) is circulated in the flexible pipe and the surrounding water is colder (for example 9 °C), see Figure 3.

The circulated water is then stopped through valves and the cooling time and temperature is analyzed, see Figure 4. Coil water temperatures and pool temperatures are measured. The temperature decline of hot stagnant water in the pipe, immersed in cool water, depends on the thermal conductivity of the pipe. The thermal conductivity can be calculated by transient inverse calculation of the partial differential equations of heat transfer. The ideas from this method may be possible to modify and apply in field on an operating DH network for old pipes that may need to be replaced. If temperature sensors can be attached on the pipes without greater effort and in a reliable way the method is worth proceeding with.



Figure 5 measurement of electrical resistivity in a copper wire during heating of the surrounding water.

Time domain reflectometry (TDR)

Time domain reflectometry is an accurate non-destructive method for identifying and measuring dielectric properties of transmission and distribution lines. Within the field of district heating and cooling the method is used to detect and locate water leakage in the insulation between steel pipe and casing. In this method a pulse generator generates incident electrical direct current (DC) signal over a conductor such as the copper wire and the steel pipe in district heating

system. The measurement probe registers the reflected voltage if impedance mismatches are detected on the conductor. Impedance mismatches will cause all or some of the transmitted signal to be sent back towards the oscilloscope. The oscilloscope monitors the pulses that are generated from TDR. The distance of discontinuity can also be determined by measuring the reflection time between reflected impulse and pulse generator [9].

RESULTS OF INITIAL EXPERIMENTS

TCR-method

Laboratory experiments of the TCR-method is ongoing and results are expected within short.

In an orientating lab test a measurement has been done for a copper wire [1.5mm²] in a tempered bath, see Figure 5.

The results indicates that the method is worth proceeding with since relatively large change in ohm compared to temperature can be observed, see Table . The experiment is made in a rough environment, meaning no stable climate. With stable climate (as in district heating pipes) and with equipment with higher resolution, every change in degree Celsius can be observed as a change in electrical resistance.

Table 1 Electrical resistance in a 6 meter copper wire 1.5mm² during heating of the surrounding water

Temperature [°C]	Ohm [Ω]	Time after start [min]
8.0	0.060	0
16.0	0.063	9
25.0	0.065	16
35.0	0.067	24
43.0	0.070	32
50.0	0.072	41
25.0	0.065	47
23.0	0.064	55

The results indicates that the resistance interval stretches from 60-72 mΩ during a temperature raise of 42°C. This means that for every degree Celsius the electrical resistance change with 48 μΩ/m, for this specific 6 meter copper cable.

Cooling method

Field test of the cooling method for an operating DH-network is under investigation and preparation. Results are expected to be presented as possibilities and limitations for further development of this method.

- [4] Persson C. Predicting the Long-Term Insulation Performance of District Heating Pipes

CONCLUSION

A pre study has been conducted from which it can be concluded that there are no existing methods that can fulfil the need regarding a tool for assessing heat losses at different parts and stretches of a DH network, the lifetime and status of a DH network can thereby not be evaluated. The pre study shows that the most suitable existing technique that could be used if it is further developed is the TDR-method. Two other non-destructive methods are of more interest since they appears to be easier to test, a cooling method and a TCR-method. The main advantages of these methods are that they are non-destructive. Both methods are also relatively simple to perform. The limitations differ for the two methods. All networks are built up in different ways and the accessibility for temperature measurements and possibilities for temporary shutting down parts of the network differ, therein lies the challenge for the cooling method. For the TCR-method the limitation that seems to be the most critical, is the difference in copper wire distance in relation to the tempered steel pipe, small deviations results in large temperature change. This may be solved by evaluating longer stretches and finding a mean value for the copper wire distance, a statistical approach would be suitable. This method is on the other hand assessed to be most appropriate for new pipes since all measurements will be relative to the start value when the pipe was new, the problem with the copper wire distance can then be neglected. The cooling method is assessed to be suitable for both old and new pipes. If these methods can be further evaluated and developed energy companies may have tools for making an efficient cost-benefit analysis for renewing parts of their networks

REFERENCES

- [1] Fredriksen S, Werner S. District Heating and Cooling. First edition ed: Studentlitteratur AB; 2013.
- [2] Berge A, Adl-Zarrabi B, Hagentoft C-E. Assessing the Thermal Performance of District Heating Twin Pipes with Vacuum Insulation Panels. Energy Procedia. 2015;78:382-7.
- [3] SS-EN253:2009. District heating pipes – Pre insulated bonded pipe systems for directly buried hot water networks - Pipe assembly of steel service pipe, polyurethane thermal insulation and outer casing of polyethylene. Swedish standards institute.

[Dissertation]: Chalmers University of Technology;
2015.

- [5] Kręcielewska E, Menard D. Thermal conductivity coefficient of PUR insulation material from pre-insulated pipes after real operation on district heating networks and after artificial ageing process in heat chamber. The 14th International Symposium on District Heating and Cooling, September 7th to September 9th, 2014; Stockholm, Sweden,2014.
- [6] Adl-Zarrabi B, Kakavand A. Introduction of possible inspection methods for evaluating thermal aging status of existing pre-insulated district heating systems. Chalmers University of Technology: 2015 Report 2016-0.
- [7] Cutnell JD, Johnson KW. Physics. 6th edition ed: Wiley; 2003.
- [8] Reidhav C. Sparse district heating and flexible district heating pipes [Dissertation]: Chalmers University of Technology; 2010.
- [9] Ariffin AM, Kuan TM, Sulaiman S, Illias HA, editors. Application of time domain reflectometry technique in detecting water tree degradation within polymeric-insulated cable. Condition Monitoring and Diagnosis (CMD), 2012 International Conference on; 2012 23-27 Sept. 2012

ADVANCED MONITORING TECHNOLOGY FOR DISTRICT HEATING PIPELINES USING FIBER OPTIC CABLE

Sukyong Song¹, Jooyong Kim²

¹ AP Technologies Inc, 1213, 21, Yangpyeong-ro 22-gil, Yeoungdeungpo-gu, 150-105, Seoul, Korea

² KDHC, 781, Yangjae-daero, Gamgnam-gu, Seoul 135-220, Korea

Keywords: Monitoring system, District heating, Fiber optic cable, Leakage Detection, Code correlation technology

ABSTRACT

District heating is an efficient system that transports hot water produced from heat sources such as heat plants, waste incinerators, etc. The heated water can then be used for heating and hot water needs in apartments or large buildings. A district heating pipe is a sandwich construction consisting of a steel carrier pipe, a polyurethane insulation, and a high-density polyethylene casing to protect from the condition of installation and operation also to prevent heat loss.

Heat pipes should be monitored for leakages; in case they are damaged or become old. District heating pipes are designed to use a leakage detection system inside the insulation. However, most detection systems cannot adequately identify the exact location or the extent of damage of a leak, which can lead to expensive repairs.

In this study, a fiber-optic based monitoring system is used to monitor the status of the buried district heating pipelines, with the results verified by evaluation tests and field applications.

An optical fiber acts as a temperature sensor. A low-powered semiconductor laser sends pulses along the fiber. By using code correlation technology, the back-scattered light is measured, If a leakage occurs the change in temperature can be located to within 1 meter in real time.

This study confirms that the fiber optic sensing performance in a variety of locations and conditions can quickly and accurately identify leakages. As a result, the fiber optic monitoring system was confirmed to accurately detect the temperature near the ground in accordance with the pipe above.

By locating leakages quickly and accurately, the correct safety and repair measures can be taken quickly, keeping damages and repair costs low.

INTRODUCTION

Heat transfer pipe buried underground can have degradation due to its heat shock and pressure occurred over long period of time. Degradation also

can come from external geological changes and vibrational stress. It is visually challenged to examine the level of degradation underground. Thus, importance of separate sensor installation is increasingly recognized to prevent the incidents. In general, degradation becomes an issue at connection areas. When the HDPE connection is damaged, exposed internal insulation (Polyurethane foam) begins to be melted with penetration of external fluid. If it were exposed to degradation for long, it would accelerate the aging speed, ultimately causing damage to steel pipe. If steel pipe (primary pipe) were deteriorated, high heat and pressure from it would be exposed to over ground, leading to significance consequences. their actual cases have been reported. To prevent such cases, it intends to make the database to expect the possible damaged area for repair.

BACKGROUND

The monitoring technology for this research is based on DTS (Distributed Temperature Sensing) instrument which is optimized and certified for measuring temperature over distance. This system utilizes Raman-effect which was discovered 90 years ago by C.V. Raman, Indian physicist. [1] This phenomenon is that the light is reflected changes in wavelength. [2]

$$\frac{I_{as}}{I_s} \propto \exp\left(-\frac{hc\nu}{kT}\right) \quad (1)$$

I_{as}: intensity of Anti - Stokes light

I_s: intensity of Stokes light

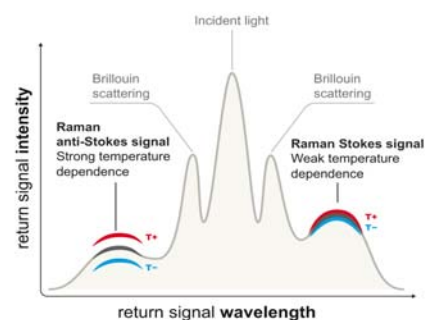


Figure 1. Distribution of laser reflection scattered light

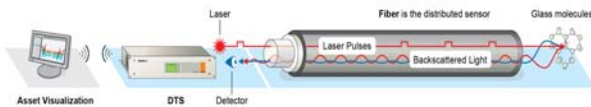


Figure 2. Conceptual diagram of DTS temperature and distance measurement

³ 300A: HDPE O/D-450, Insulation-434.4, Steel-318.5/ (mm)

⁴ 150A: HDPE O/D-250, Insulation-242, Steel-165.2 / (mm)

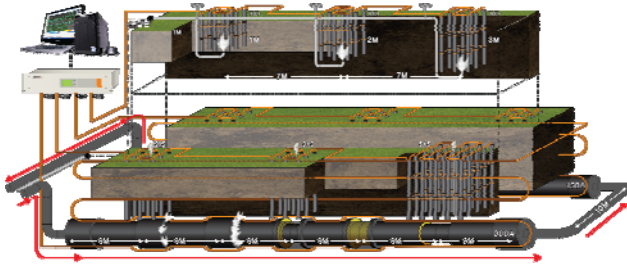


Figure 3. Test setup diagram

The backscattered light is across a range of wavelengths. Some of these wavelengths (Stokes and anti-Stokes scattering) [2] are affected by temperature changes while others are immune. Their ratio depends on the temperature (which can practically be exploited for the measurement of temperature).

By very accurately measuring the difference in the signal intensity of the backscattered light an accurate temperature measurement can be made. [3]

$$x = c \times \frac{t}{2} \quad (2)$$

c: Speed of light in an optical fiber (2×10^8 m/sec)

[5]

SYSTEM DESIGN AND STRUCTURE

Feature of heat transfer is to find thermal equilibrium. And the process of heat transfer involves conduction and convection. For heat transfer occurred underground, it largely depends on conduction, which take long time to transfer heat, as there is almost no convection. Heat generated from damaged heat transfer pipe is conducted via soil media as described in the following equation.

$$q = kA \frac{T_1 - T_2}{L} \quad (3)$$

It is possible to install the optical sensor cable for heat transfer line underground directly for two to fifty kilometers. It is possible to measure the thermal change and indicate the temperature by length. Thus, it is ideal to use a DTS system to monitor distinct pipes. In particular, DTS systems and the passive optical fiber

have very long lifespans and are basically maintenance-free.

OUTLINE OF TEST

We bury two heat transfer pipes 1.5 m under the ground while diameter of one pipe is of 300A³ and the other 150A⁴ just same as the typical structure. To measure the heat source release by damage type, we did similar damage to the connection areas of pipes. Optical sensor cables which were coiled over perforated drainpipe with helical shape of 0.1m installed over the top of the heat transfer pipes vertically to measure and analyze the vertical heat transfer. In order to test detection performance during heat sources release of heat transfer pipe, sensor cable was also installed in depth with 0.5m, 1m, and 1.5m from the surface along the burial route.

The above test described that it is performed to verify the efficiency of new heat transfer pipe installation and validity of optical sensor cable installed over the existing heat transfer pipe.

TEST EQUIPMENT

1. DTS (Distributed Temperature Sensing)

Manufacture: AP Sensing

Model: Linear Power Series N4385B 4Km 4Ch

Spatial Resolution: 0.5m

Sampling Interval: 0.25m

Measurement time: 60sec per channel

2. Fiber Optic Cable Sensor

50/125 μ m /Multi-mode Fiber and special designed cable (Single-end configuration)

TEST CONDITION

◆ Heat source supply condition

1. Heat source temp: water at 95 °C
2. Supply pressure: 5.81gf/cm²
3. Return pressure: 5.18kgf/cm²

◆ Damage conditions of heat transfer pipe

To differentiate the heat quantity of source, it sets 3 different sizes for damages and two for insulation damages.

Table 1. Failure scenarios of heat transfer pipe

Part / Damage	①	②	③	④	⑤
Insulation material	100%	50%	100%	100%	50%
Connection damage	PE 100%	PE upper	PE upper	Sleeve gap	Sleeve gap

*Damage on upper area: 280(W) x 110mm(L) cutting

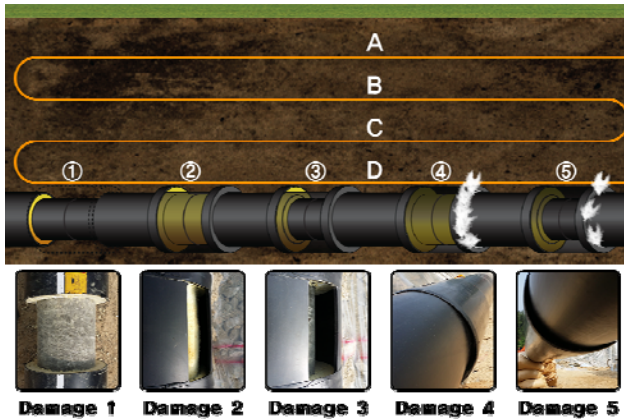


Figure 4. Image and picture of regular damage of heat transfer pipe

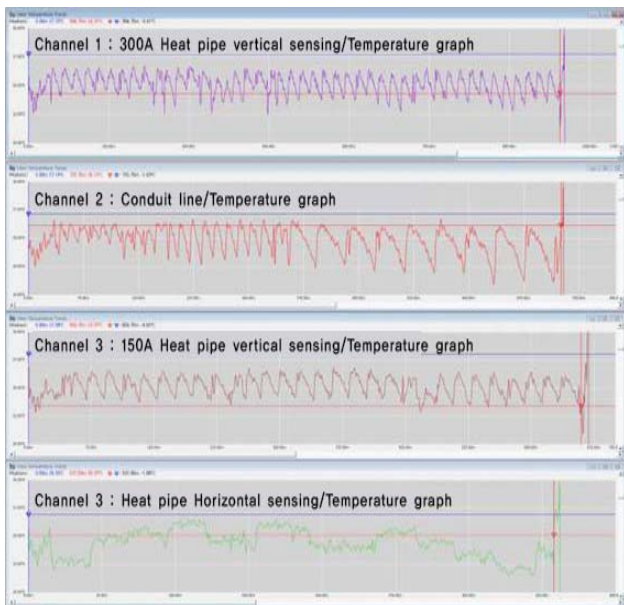


Figure 5. Raw data screen of whole area after installation

As indicated in the feature above, the test result shows that the performance of optical cable sensor is good regardless of horizontal or vertical, and size of heat transfer pipe. The reason why upper 3 graph patterns are different from lower 1 pattern is from installation

method. (Upper 3 are installed at 0.1m in perforated pipes in helical shape to do monitoring in triangular wave while lower 1 is installed on tope of heat transfer pipe in a lineal way to do monitoring in horizontal wave.)

Time consumed to transfer heat depends on the quantity of heat source and distance. It is expected the heat would disperse further as time goes by. However, within less than one day, the significant temperature changes are recorded for each failure mode during the test.

Table 2. Test result of temperature

	PIPE SIZE	Jan/27th	Feb/3rd					
			*[4]	①	②	③	④	⑤
A ⁵	150A		2.3	4.9	3.1	3.5	3.4	3.3
	300A		2.3	5.4	3.6	5.7	3.7	4.5
B ⁶	150A	6.1	4.8	8.4	6.9	7.9	6.8	6.3
	300A	6.1	4.8	9.8	7.3	11	9	7.4
C ⁷	150A	7.8	7.6	15	10	15	11.4	9.6
	300A	7.8	7.6	19.3	11	21.1	13.8	11.2
D ⁸	150A	9.3	9.4	42	18.5	42.7	36.1	19.5
	300A	9.3	9.4	53.3	18.4	56.5	36.7	20

[4] Normal underground temp. (outer temperature measures by Meteorological administration: 0.6°C)

⁵ A: underground 0.1m (above heating pipe 1.4m)

⁶ B: underground 0.5m (above heating pipe 1m)

⁷ C: underground 1m (above heating pipe 0.5m)

⁸ D: underground 1.5m (above heating pipe 0m)

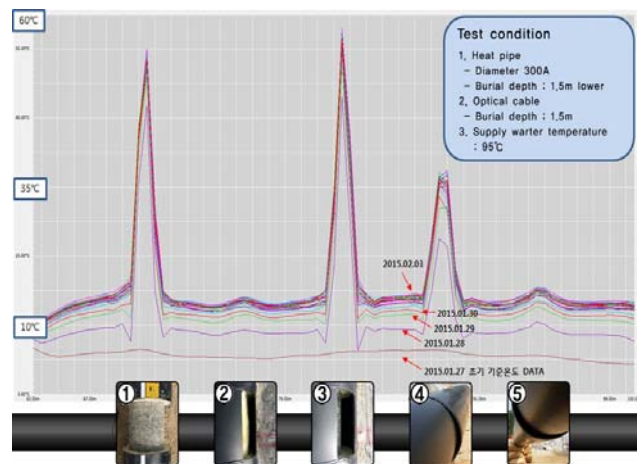


Figure 6. Setting of pipe damage_ temperature trend in time (1 week)

Table 3. Temperature trend over time (1.5m depth)

Date Temp	①	②	③	④	⑤
1/27	9.3°C	9.3°C	9.3°C	9.3°C	9.3°C
1/28	50.1°C	15.5°C	51°C	30.1°C	16.7°C
1/29	51.4°C	16.3°C	52.9°C	31.9°C	17.5°C
1/30	51.6°C	17.1°C	54°C	33°C	18.3°C
1/31	52.1°C	17.4°C	54.3°C	33.8	18.7°C
2/1	52.2°C	17.9°C	55.9°C	35.5	19.4°C
2/2	53.2°C	18.4°C	56.7°C	36.2°C	19.9°C
2/3	53.3°C	18.4°C	57°C	37°C	20°C

In other words, heat is estimated transferred by conduction not by convection.

For the purpose of this test, we created the condition of heat source as doing vertical and horizontal installation at the interval of 0.5m, 1.0m, and 1.5m on the top of heat transfer pipes (150A, 300A). And the test result is summarized in the table above.

As optical cable is wired close to heat transfer pipe, it is possible to get a relatively accurate temperature values. The bigger the outer diameter of pipe is, the higher the temperature goes. (In other words, compared to 150A, pipe of 300A is having proportionally larger insulation damage of pipe, so heat source turns out to be bigger.)

It means that the degree of insulation damage is more detrimental than the degree of external PE damage to heat source release.

It is expected that insulation damage without PE damage would release huge heat source. When both insulation and PE are damaged at the same time, it would pose a risk to not only heat source release but to safety related accidents.

CONCLUSION

To tell and identify the degree of degradation of heat transfer pipe, we verified regular damage heat transfer under 5 different conditions and analyse the temperature measured by optical sensor cable, which is installed on top of transfer pipe. By doing so, it is possible to determine correctly the degree of damage and its location of heat transfer pipe without visual check of heat transfer pipe.

Throughout the whole life span of heat transfer pipe from the initial burial, it is possible to monitor the heat transfer condition effectively through DTS using optical sensor cable. And it allows us to have optimal

maintenance. In addition, DTS helps us to secure and collect enough data for analysis. If collected and analyzed data through DTS develops into life span expectation program, it would dedicate to enhance the overall safety management system and the efficiency of heat transfer, and the prevention of huge safety accident.

Advantage

- It detects the complicate damaged parts and fast due to consistent temperature sensor throughout the whole span of heat transfer pipe as well.

- It is very efficient for maintenance as well as construction plans as detecting the damaged types in advance.

- It can save initial cost for data collecting and transferring.

- This optical fiber can apply for designing Optical Network for data communication and sensor with no limit lifetime and length.

ACKNOWLEDGEMENT

It develops a program to control risky areas through seasonal DB and alarm setting since installation. It also studies screen composition to control temperature boundaries and effective installation method.

In addition, it verifies heat source leakage test via measuring tube and on-site verification test (Bundang, Seoul) to proof the efficiency of supervising function of heat transfer pipe via optical sensor cable.

Medium of soil consist of aggregate, sand, fine sand, and clay. We couldn't test them under diverse conditions. It was impossible to analyze the degradation development with long term (longer than 1 year) environmental experimental data.

REFERENCES

- [13] C.V Raman, Wikipedia, www.wikipedia.org, accessed October, 2015
- [14] Raman Scattering, Wikipedia, www.wikipedia.org, accessed October, 2015
- [15] AP Sensing GmbH, N4385B Linear Power Series User Guide, Edition 10, March 2011
- [4] S.O.Kim, "The Status of Soil Temperature Observations and Their Climatology in Korea", Unpublished master's dissertation, Kongju National University, Korea(2004),pp.28-32.
- [5] C.K.Lee, Y.S.Kim, M.M.Gu,B.G.Kim," Real Time Temperature Monitoring System Using Optic Fiber Sensor", published dissertation, Korea Society of Computer & Information, Korea(2010),pp.209-212.

RISK MANAGEMENT FOR MAINTENANCE OF DISTRICT HEATING NETWORKS

K. Sernhed¹, M. Jönsson²

¹ Lund University, Department of Energy Sciences, Lund, Sweden

² Sweco Energuide AB, Malmö, Sweden

Keywords: *Risk management, maintenance, district heating pipes, renewal plan*

ABSTRACT

Underground infrastructure such as buried district heating pipes are difficult to inspect. The methods available to assess the status of the district heating pipes are often both expensive and do not provide enough evidence to determine the condition of the pipelines. This paper discusses how utilities systematically can work with risk assessments and risk classification to plan the maintenance and renewal of district heating networks. The results were based on interviews with a selection of Swedish district heating companies that were already using risk and vulnerability analysis as a tool for maintenance and renewal of their networks, as well as on a literature study of methods for risk and vulnerability analysis. The study showed that a rather limited number of methods were used by the selected utilities, mainly those based on risk matrices. Risk classification of pipes were carried out based on age, type and dimensions of pipes, identification of pipes to customers with greater need for security of supply, history of damages on the pipes and statistics over probability of damage for different kind of pipes, working environment and safety. Personnel involved in the management and maintenance planning of reinvestment in the district heating network emphasized that strategic work with risk management really can aid the foreseeing of coming needs for reinvestments and planning of maintenance. The study rendered in advices and a checklist for how district heating companies can start working with the area of risk management.

INTRODUCTION

Underground infrastructure such as buried district heating pipes are difficult to inspect. However, the example of 23.000 kilometres of district heating pipes, with an estimated value of 12 billion euros in Sweden alone, shows that such infrastructure constitutes substantial values.

Fixed assets in the form of a distribution networks for district heating could be even more valued in the future, in networks where the network owner allows other operators to deliver thermal heat to the district heating network through a so-called third-party access (TPA).

With such a procedure supply security will be even more important and thus the network condition.

The methods available to assess the status of the district heating pipes are often both expensive and do not provide enough evidence to determine the condition of the pipelines. Financial considerations speaks for keeping the pipes as long as possible, but without compromising reliability of supply, the working environment and safety for the general public and

without risking damage on property. In newer pipes, moist alarm are inbuilt, which gives better possibilities to monitor the grid. For older types of pipes, however, the technique for moist alarm was not yet developed when the pipes were placed in the ground.

This paper aims at illustrating how district heating companies can plan renewal without the full knowledge of the status of the underground pipes and how the district heating industry tackle this problem by the use of risk rating and risk and vulnerability analysis.

METHODS IN STUDY

To provide a background for risk and vulnerability assessments from a broad perspective, a literature review was conducted. The literature study focused on describing definitions of key terms and concepts, and describing different methods used for risk and vulnerability assessments in general.

Personnel from the three largest district heating utilities in Sweden (Vattenfall, E.ON and Fortum) were interviewed about their methods of using risk management for the planning of renewal and maintenance of the grid. The selection of companies to interview was done on the basis that these three had probably made the most progress in their work on risk management in the Swedish district heating industry. Interviews were made with personnel on different levels within the utilities, including persons with technical expertise of maintenance as well as persons with financial responsibilities for planning the maintenance of the district heating network.

PLANNING OF RENOVATION

Normally district heating pipes are exchanged only when there has been detection of leakage. The common procedure is that the leak is repaired urgently, and then more permanent measures are planned and

budgeted. The choice of whether the whole pipeline should be replaced or not is based on a consideration of the pipe condition, the replacement cost and the impact of an additional injury [1]. Although it is a rather reactive strategy with some risks involved to only exchange pipes when leaks or other injuries have been detected, there are no economic benefits to exchange well-functioning district heating pipes prematurely. Although older district heating pipes typically have a lower degree of insulation, the reduced heat losses from replacement do not constitute a large enough financial incentive to replace lines prematurely [2].

With the current reinvestment rate in the Swedish district heating networks (as has been explored in this and other studies, see for example Sernhed et al, 2012 [3], parts of the district heating networks would reach an age of 300-800 years before exchanged. It goes without saying that the pipes do not last that long, but it is not until injury rate begins to increase that the reinvestment rate also will be increased. An explanation for the low reinvestment rate is that the district heating networks in Sweden are relatively young. The first networks were set up in the 1940s, but the greatest expansion of district heating took place in the 70s and 80s, which means that the pipes built in this period most likely has not reached its service life yet [3]. This means that most of the Swedish district heating pipes are located at the horizontal part of the bathtub curve showed in Figure 1 and hence have a low failure rate.

The bathtub curve does not depict the failure rate of a single item, but describes the relative failure rate of an entire population of products over time. The bathtub curve is used as a visual model to illustrate the three key periods of product.

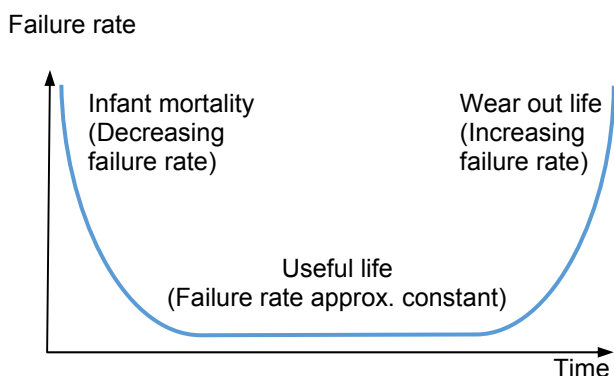


Figure 1: The bathtub curve illustrating hypothetical failure rate versus time and the three key periods of a product's life.

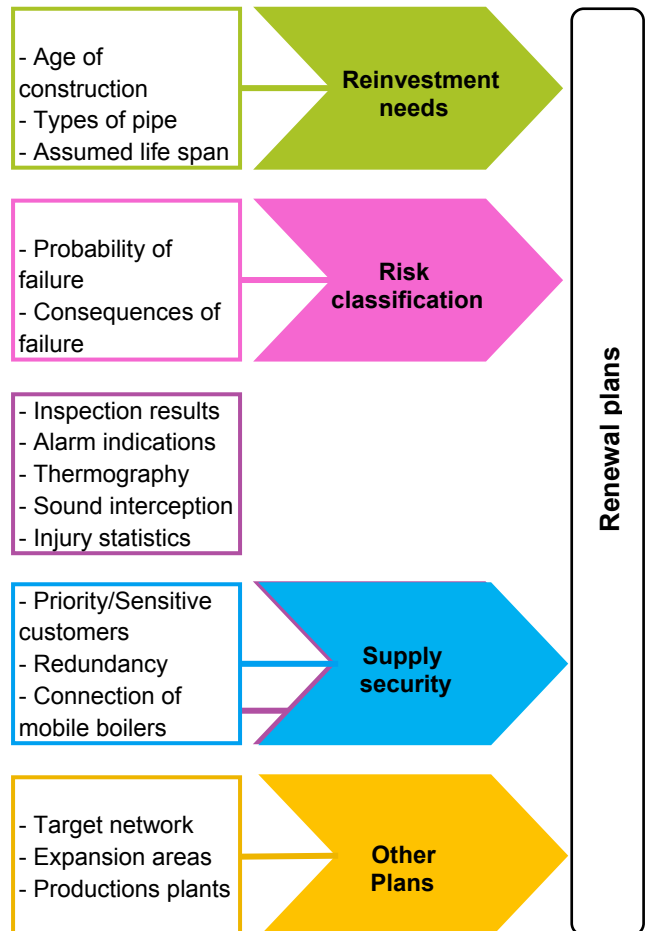


Figure 2: Overview of how Fortum works with renewal plans for their district heating networks. Source: Fortum.

The risks involved with this reactive strategy include heat supply deficiencies, but also major failures that can cause accidents where people are injured or even die or where property is damaged. Another risk is that the utilities do not anticipate a large hump of reinvestment needs that may arise for example if a large part of the network was built at the same period. If such a hump occurs, one has to be prepared both financially and organizationally in order to meet the increased rate of reinvestment needed.

To work strategically and systematically with the reinvestment needs and security of supply, renewal plans should be developed. One of the interviewed district heating companies, had made a good overview of the different parts needed to develop renewal plans, see Figure 2.

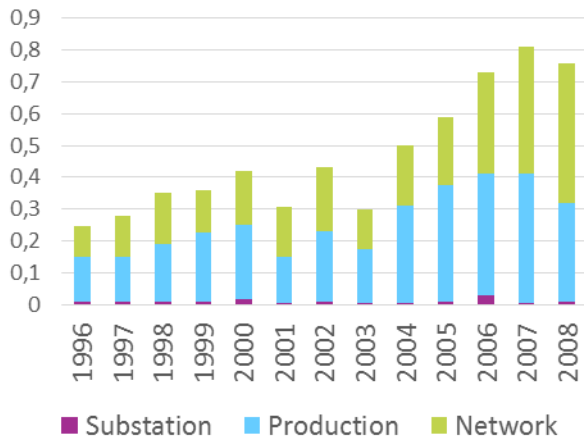


Figure 3: Investments in the Swedish district heating sector, 1996-2008, billion EURO, reported in the 2008 price level. Source: Swedish District Heating Association [4].

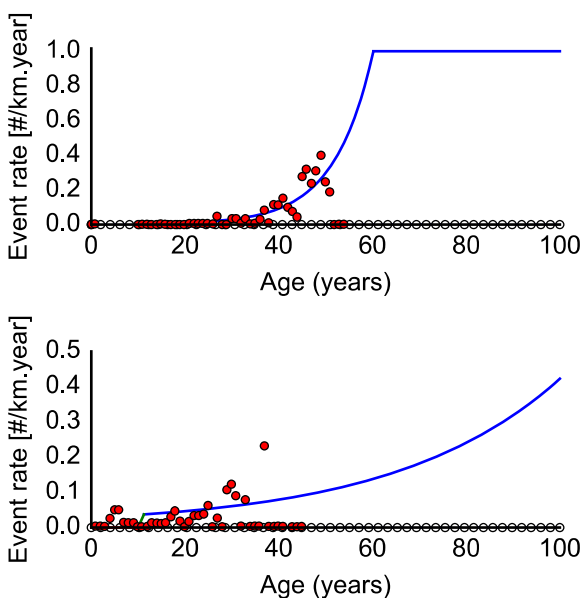


Figure 4: Estimated future need for replacement of two different types of district heating pipes in Vattenfall's grid in Uppsala. The top diagram shows concrete culverts and the lowermost modern plastic sheathed pipes.

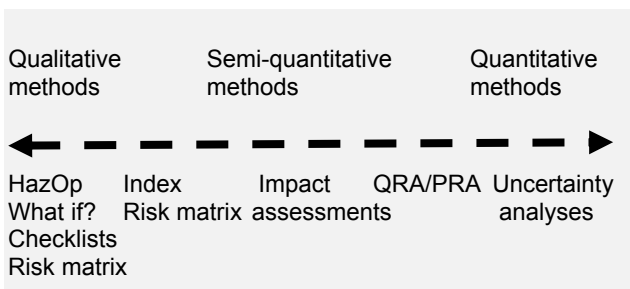


Figure 5: Range of different risk analysis methods with regard to the degree of quantitative and qualitative elements [5].

REINVESTMENT NEEDS

In recent decades, one can see that the district heating business in Sweden have increased their investment costs in terms of both production and distribution networks. It can also be seen that the investment costs for distribution proportionately has increased more than the investment costs for production, see Figure 3.

In order to calculate the needs for renovation in the district heating network, the interviewed district heating utilities used the parameters of age and assumed life span for different types of district heating pipes.

Figure 4 shows estimated future need for replacement of concrete culvert pipes and modern plastic sheltered pipes in the utility's grid in the city of Uppsala (a grid owned by Vattenfall AB). Vattenfall uses a software named IKOS, originally designed for the water and sewerage industry. In this GIS-based maintenance system, life span curves are continuously improved based on injury statistics and other experiences gathered by the company about the specific pipe types. The graphs show the proportion of a given pipe type expected to remain after a specific number of years.

As can be seen in Figure 4, the expected life span for a steel pipe in a concrete culvert is much shorter than the expected life span of modern pre-insulated steel pipe with plastic casing. After 60 years, no concrete culvert pipes are expected to last in the Uppsala grid, while there will still remain some share of plastic sheltered pipes after 100 years according to the estimations. As the estimations are (mostly) based on actual injury statistics, the results are affected by the fact that there are no statistics for plastic pipes older than 45 years which might make the estimations less reliable.

Risk Classification

The conducted literature study gave a theoretical overview of available methodologies for risk and vulnerability analysis that included qualitative, semi-quantitative and quantitative approaches, see Figure 5.

The intention of showing Figure 5 here is not to describe all of the methods under the dotted line, but merely to show that there is a range of different methods available and to be able to place the methods used by the utilities on the line in the figure. The interviews showed that the methods used by the utilities were either qualitative or semi-quantitative methods usually based on risk matrices. The use of quantitative risk analysis methods, such as for example fault-tree analysis, did not appear to have come to an extensive practical use in the utilities at all.

Risk matrices can be used to report the results from, for example, a preliminary result of a process hazard analysis (PHA). Probability is usually shown on the vertical axis and consequence on the horizontal axis as illustrated in the example in Table 1. The acceptance

criteria may be expressed by different colours. Basically, risks in the lower left corner are considered acceptable while risks in the upper right corner are considered unacceptable. The area in between is usually called ALARP range (as low as reasonably practicable) in which risks should be reduced as far as is reasonable. This means that when the ratio between costs and benefits is disproportionate it is not necessarily reasonable to take action.

Probabilities and consequences from the risk matrix approach can be an important tool when prioritising different proposed projects. Some projects may have to be implemented immediately for various reasons, but a risk analysis can sometimes provide argument for when a project can wait or not.

The risk matrix in Table 1 shows acceptable risks in green and unacceptable risks in red. In addition, it shows two yellow areas. The vertical yellow area to the right illustrates pipes and components identified to provide major consequences on for example delivery interruptions. But as the probability is relatively low, extended supervision might be sufficient.

On the other hand, the horizontal, upper yellow area illustrates pipes and components that have been identified as having a high probability of malfunctioning, but with limited foreseen consequences. For these risks, the way forward should be cost-benefit analysis of the possible mitigation actions.

The ways to determine the probabilities and consequences for various events and components vary from manual to automated methods.

PARAMETERS

According to the interviews, and a workshop with personnel from ten different district heating utilities, the following parameters were considered important for the rating of probability of failure and impact from a breakdown in a district heating network:

Table 1: Risk matrix with measures.

Probability		Risk Matrix			
Very high	4	Cost-benefit!		Resolve!	
Probable	3				Keep track!
Possible	2				
Improbable	1				
Consequence		1	2	3	4
		Small	Considerable	Serious	Disastrous

- **Age.** Materials degenerate with age. This parameter has the advantage of being easy to automate in a computer system, but it is generally not a particularly reliable indicator for the actual condition of a pipe or a component.
- **Type of pipe.** Different types of pipes have different failure tendencies and weak points, which may have implications for the expected life. Also this parameter has the advantage of being easy to automate in a computer system.
- **Pipe dimension.** The dimension of the pipe may indicate the expected impact of a failure. Also, pipes with smaller dimensions usually have a higher rate in the damage statistics.
- **Identification of sensitive customers.** Customers, with activities that will be particularly impacted from failures in the supply, should be identified as sensitive customers. This can for example be hospitals, nursing homes, retirement homes and kinder gardens.
- **Damage and damage statistics.** Information on damage could be used for decision on where immediate action is required as well as for life estimations and for long-term renewal planning.
- **Specific pipelines or components.** Pipelines and components located where the probability of failure is high or the impact of a failure is severe, should be identified.
- **Working environment and safety.** Negative impact on the working environment or safety should always be given high priority and be considered in the renewal plans or be subject of intensified maintenance measures.

Age of Pipes and Components

The parameter of age could provide information regarding the probability of problems. The general opinion among the interviewees was, however, that the age of a pipeline in itself gives very little information on the actual status. This opinion is consistent with results of previous studies, such Sernhed et al [3]. The reason for the limited importance of the pipeline age is that the life depends on a variety of external factors such as [5]:

- Planning, project management, construction
- Material
- Installation
- Operating Conditions
- Maintenance operations
- Ambient and internal environment
- External influences and impacts

Further evidence on the impact of the ambient conditions is given by Sund [6] in a report from 2002 stating that the rate of external corrosion of district heating pipes can be as high as 0.5 mm per year at the combination of high surface temperature and ingress of water with high corrosiveness.

The studied utilities emphasized that pipes were never replaced solely on the parameter of age. However, Vattenfall said that if an old pipe started to show problems, this could lead to the decision that a longer distance of the pipe would be replaced compared to if the pipe had been younger. For automatic risk classification in a GIS system or a maintenance system, however, the age parameter can be advantageous to use as it is objective, accessible and thus easy variable to collect and use.

Pipe type

The parameter pipe type combined with the age of the pipe could provide information regarding the probability of failure. As showed in Figure 4, different types of pipes seems to have different length of life. Among the three interviewed companies fewest problems were experienced with modern plastic sheltered pipes. In Fortum's network about half of the discovered leaks occurred in pipes other than plastic sheltered pipes. It was anticipated in the three utilities that all types of pipe except plastic sheltered pipes would be replaced within ten to fifteen years. E.ON also stated that they had seen an increase in harmful tendency of fibre cement culvert, first generation of pipes "Aqua Warm" and the first generation of the plastic sheltered pipes (especially sleeves and shrink discs, and the outer sheathing of PE prior to PEH).

Pipe dimension

The parameter pipe dimension can be used both to assess the probability of failure and the consequence of failure. Large dimensions means that a lot of customers will suffer from a pipe failure. E.ON experienced branches on large pipes to be of high risk for failure. As a parameter used to assess impact of failure, Vattenfall used a network calculation program to identify important hydraulic pipes (which often coincided with the major main pipes).

Sensitive customers

All three district heating companies answered that they marked sensitive customers in their GIS systems. Examples of sensitive customers were health care facilities, pre-schools, industrial processes and sporting facilities. Certain consideration was given to these customers at risk of disruption or other events. This may involve informing about disruptions in extra good time, to customize planned interruptions to customer needs, or to arrange temporary heat supply during supply interruptions.

Injury and injury statistics

All three companies reported injuries on pipes into the GIS system, sometimes with photos taken on the damaged pipe. Vattenfall used the information of injury

to heat pipe as one of three parameters used for probability estimation in the IKOS software, along with age and pipe type. E.ON used their leakage and injury statistics as an important input to the assessments in the manual risk evaluation systems that they used.

Pipes or components that needs specific requirements

Some individual pipes do require special consideration. For example, Vattenfall stated that in the city of Uppsala they use a special coverage on pipes for-laid under the river Fyrisån and under bridges, etc. Fortum used the parameter "placement" to deal with risk classification of pipes that needed special attention. The parameter of placement was used both to classify risk level for consequence and for probability. Placement together with pipe dimension was used for assessing consequences of failure. The consequence of failure of a given pipe dimension was judged to be greatest when placed indoors or in a tunnel, and lowest when placed in the ground or in a lake. Probability of failure due to placement was judged to be lower in indoor pipes and in tunnels. E.ON stated that intersecting pipes placed in the ceilings of the great tunnel "the City Tunnel", would provide particularly serious consequences in case of failure.

Working environment and safety

All three companies stressed that pipes that can pose risks to the working environment or risk of injury to the public was always given high priority. Issues related to the working environment have, according to the interviews, been given increased focus during the last years. A main concern for the three companies was about heating chambers and concrete culverts, where the lid, gully covering, inside environment, ladders etc. could pose a danger of personal injury. There were explicit strategies in all of the companies to try to diminish the number of chambers in the district heating grid as much as possible.

THE RISK CLASSIFICATION SYSTEM OF FORTUM

The risk classification system of Fortum may be of special interest, because they automated their system and connected it with their GIS-system. Fortum had chosen to build its risk classification system on variables that were relatively easy to measure or categorize. For assessment of the probability of failure, they used the parameters of age, type of pipe and placement. For assessment of the consequences of failure parameters of pipe dimension and placement were used. Table 2 shows the weights that Fortum has given to the parameters used for risk assessment of the consequences of a breakdown.

Table 2: Impact assessment based on pipe size and placement.

Dimension	Placement: ground, lake	Placement: tunnel, air	Placement: Indoor
0-40	Insignificant (1)	Insignificant (1)	Small (2)
42-65	Insignificant (1)	Small (2)	Average (3)
80-100	Small (2)	Small (2)	Average (3)
125-175	Small (2)	Average (3)	Severe (4)
150-200	Small (2)	Average (3)	Severe (4)
250-350	Average (3)	Average (3)	Severe (4)
400-500	Average (3)	Severe (4)	Disastrous (5)
600-700	Severe (4)	Severe (4)	Disastrous (5)
>700	Severe (4)	Disastrous (5)	Disastrous (5)

In Table 3, the weighting of the parameters that are used to determine the probability of failure is shown. Regarding probability, Fortum focuses primarily on pipe type, installation, and if there is an alarm installed or not, to produce a 'risk pipe type' (which form the risk pipe type classes of low, average or high) that combined with age of the pipe will give the specific risk value for the actual pipe, see Table 3. Higher values were given to higher pipe diameters, as well as to pipes placed indoor.

The probability of failure in Table 3 is estimated to rise with the age of the pipes, although new pipes are set to have a slightly higher probability of failure than somewhat older pipes (this is consistent with the Weibull distribution in the bathtub curve showed in Figure 1). Table 4 shows the evaluation that Fortum made from combining the probability of failure with consequences of failure.

Because of the simplicity in the choice of variables, Fortum has been able to automate the risk rating system, so that the system will update itself as the pipes are getting older. There is also the option to upgrade a pipes risk class manually in the system, for example, based on results of the status assessments or discoveries on patrol. Different risk classes are then illustrated in the GIS-system through different colors, see Figure 4.

BENEFITS OF IMPLEMENTING RISK CLASSIFICATION

To work with risk rating systems and risk analyses can provide several benefits when planning the maintenance and renovation of district heating networks. This involves being able to obtain an overview of the renovation needs, and also to work out a structure that systematically helps the network owner to prioritize between different needs and projects. Furthermore, it is also about working methodically with documentation. Also, risk analyses are important for analysing health and safety issues. Certain legal requirements within the health and safety legislation in Sweden and elsewhere could be met by working with risk analyses.

Table 3: Probability Assessment based on type of pipes and age of pipe.

Age (years)	Low	Average	High
0-10	Small (2)	Average (3)	Highly plausible (5)
11-15	Improbable (1)	Average (3)	Highly plausible (5)
16-20	Improbable (1)	Average (3)	Highly plausible (5)
21-25	Small (2)	Average (3)	Highly plausible (5)
26-30	Small (2)	Average (3)	Highly plausible (5)
31-35	Small (2)	Average (3)	Highly plausible (5)
36-40	Average (3)	Plausible (4)	Highly plausible (5)
41-45	Average (3)	Plausible (4)	Highly plausible (5)
46-50	Average (3)	Plausible (4)	Highly plausible (5)
51-55	Plausible (4)	Highly plausible (5)	Highly plausible (5)
56-60	Plausible (4)	Highly plausible (5)	Highly plausible (5)
61-65	Plausible (4)	Highly plausible (5)	Highly plausible (5)
66-70	Plausible (4)	Highly plausible (5)	Highly plausible (5)
>70	Highly plausible (5)	Highly plausible (5)	Highly plausible (5)

Table 4: Risk matrix used by Fortum after weighing the probability and consequences of different parameters.

Probability	Consequence				
	Insignificant (1)	Low (2)	Average (3)	Severe (4)	Devastating (5)
Highly plausible (5)	Average (3)	High (4)	Extreme (5)	Extreme (5)	Extreme (5)
Plausible (4)	Low(2)	Average (3)	High (4)	Extreme (5)	Extreme (5)
Average (3)	Improbable (1)	Low (2)	Average (3)	High (4)	Extreme (5)
Low(2)	Improbable (1)	Improbable (1)	Low (2)	Average (3)	High (4)
Implausible (1)	Improbable (1)	Improbable (1)	Improbable (1)	Low (2)	Average (3)

and placement, long-term planning can be facilitated. Life curves can be developed and an estimated remaining life can be calculated for the pipes in the network. This gives a clear indication of how great the need for renovation is expected to be over time, which in turn enables the dissemination of reinvestments over time and reduces the risk of suffering a sudden, unexpected and large reinvestment need. Investments may have to be accrued if the estimated remaining life coincides to a large part of the network.

CHECKLIST

The examples given above are from large district heating companies that may have greater capacity to take on the development of the maintenance of the district heating network than smaller district heating companies. So how should the ordinary small or middle-sized district heating utility start their process towards a systematic approach based on risk analysis for their maintenance and renewal planning? Once the utility has decided that they have a need for the risk analysis approach, Table 5 provides a simple checklist of relevant issues for discussions when settling the initial status. The checklist is a revised version of a checklist made in the Swedish Water and Sewage Manual from 2012 [8].

CONCLUSION

The district heating networks installed underground is a type of infrastructure, which represents substantial financial values and where malfunctioning components could cause serious problems for societal functions. Basing the maintenance and renewal planning on direct inspection of the installations is typically not possible, but various indirect methods with different precision do exist. At the same time, the industry is interested in transferring more of their resources from emergency repair to planned maintenance and renewal. In the long term, this is expected to reduce costs and increase the security of supply.

Larger district heating utilities have developed and are continuously improving various maintenance and renewal planning tools based on risk and vulnerability analysis, GIS databases and computerised analysis tools, while many smaller utilities rather work on ad hoc basis.

With more and more network parts reaching considerable age (50 years and above), the requirements on improved maintenance and renewal planning aiming at the correct allocation of financial, technical and human resources will increase.

By drawing upon experiences from leading district heating and other utilities as well as basic risk management theory, this paper outlines a way forward



Figure 4: Screenshot of how different risk classes are illustrated by different colours on the pipes in Fortum's GIS-system.

The documentation generated from the systematic risk analysis approach does also have a value by itself. It has the potential of becoming an important basis for discussion of the maintenance and renewal needs with the management and the board of the utility. Backing up the budget proposal with relevant and objective documentation increases the likelihood of a well-educated decision process.

By collecting data on age and year of construction of the pipes in the network, connected to the pipe type

for small and medium-sized utilities in their development of systematic approach to maintenance and renewal planning.

Table 5: Suggested checklist to get started with risk analysis for renovation and planning (revised version of the checklist in the Swedish Water and Sewage Manual from 2012).

	Yes	Partly	No
Data about grid			
Is GIS system used and updated for grid documentation?			
Is the following information included in a database or GIS-system?			
- Asset data with dimensions, type, age			
- Patrolling remarks, leakages, third party inspections			
- Important information from key personnel and other personnel			
- Information about sensitive and important clients, special agreements			
Operational Statistics			
Is the following information included in a database or GIS-system?			
- Operational disruptions			
- Customer complaints			
Safety			
Are risk analyses to find vulnerable points of the grids carried out?			
Are disruptions handled in such a way that it is possible to study the events in retrospect?			
Renewal Planning			
Is an action plan with concrete measures compiled?			
Is there a reasoned opinion on the renovation demand for the next 10 years or more, including costs?			

Follow-Up			
Is it possible to follow up on annual costs and cost changes of the operation and maintenance of the district heating network?			
Is it possible to follow up on annual costs and cost changes of renovation?			
Is it possible to follow on annual costs and cost changes of emergency measures?			
Are key data and information on the network status compiled? Are they analysed and compared over time?			
Are data collected and sent to the national damage statistics database?			
Are the grid's status compared with the status of the grids in other district heating companies (benchmarking)?			
Are there any sharing of experiences with other district heating companies about procedures and methods?			
Personnel			
Are there staff who can take care of and document malfunctions and complaints?			
Are there staff who can manage the GIS system and databases?			
Are there staff who can take care of financial monitoring?			
Are there staff who can analyse the malfunction and devote at least 1-2 days per year for long-term planning?			
Are there personnel for at least biannual updates of the risk analysis?			
Are there resources (internal or external) to implement the measures in the renewal plan?			
Communication			
Are there any documentation developed that help to provide decision makers with an understanding of renewal needs?			

ACKNOWLEDGEMENT

The study, which this article is based upon, was financed by the research programme Fjärrsyn, which was developed by the Swedish District Heating Association and The Swedish Energy Agency.

REFERENCES

- [1] Swedish District Heating Association, "Fjärrvärmenäten - en tillgång som måste underhållas"(In English: District heating grids – a fixed asset that needs maintenance), Newsletter 2015-01-26
- [2] Å. Åkerström, Reinvesteringsmodell för befintligt fjärrvärmenät (in English: Reinvestment Model of an existing district heating network). Master thesis at Lund University, 2004
- [3] K. Sernhed, E. Ekdahl and P. Skoglund, Statusbedömning av betongkulvertar (In English: Status assessments of concrete culverts). Fjärrsyn report 2012:9, 2012
- [4] Swedish District Heating Association, Turnover and employment, Webb source: <http://www.svenskfjarrvarme.se/Statistik--Pris/Fjarrvarme/Ekonomi--Anstallda/>, downloaded Jan 2016
- [5] J. Nilsson, Introduktion till riskanalysmetoder (In English: Introduction to risk analysis methods), Lund University Report 3124, 2003
- [6] Swedish District Heating Association, Underhållshandboken för fjärrvärmedistribution (In English: Maintenance Manual for district heating distribution), 2015
- [7] G. Sund, Utvändigt korrosion på fjärrvärmerör (In English: External corrosion of heating pipes), Fjärrvärmeföreningen, FOU 2002:80, 2002
- [8] A. Malm, A. Hosrtmark, E. Jansson, G. Larsson, A. Meyer and J. Uusijärvi, Handbok I förnyelseplanering av VA-ledningar (In English: Handbook for renovation planning of sewerage), Report 2011-12, Svenskt Vatten Utveckling, 2011

INTEGRATION OF SOLAR THERMAL SYSTEMS INTO DISTRICT HEATING – DH SYSTEM SIMULATION

M. Heymann¹, K. Rühling¹, C. Felsmann¹

¹Institute of Power Engineering, Professorship of Building Energy Systems and Heat Supply
Technische Universität Dresden, 01062 Dresden, Germany

Keywords: *DH simulation, solar thermal energy, distributed generation, optimal control*

ABSTRACT

This paper presents latest results and outcomes of a research project about the decentralized feed-in of solar thermal energy into district heating networks. While solar heat exemplarily stands for any other heat source (as waste heat) the focus is on smaller distributed solar thermal heating plants rather than large central systems. The idea is to use the district-heating system as thermal source and sink to ensure the supply of the local heat consumers as well as the transmission of solar heat to other customers. This approach is supposed to minimize investment costs and increase the solar share, thus substituting fossil fuels.

Analyses and investigations were done based on computational DH system simulations. A special version of the TRNSYS-simulation program was applied to calculate transient operation of a 3rd generation DH network (following IEA-DHC Annex X classification, see [Ros+14]). Several feed-in substations have been integrated into the model. Heat consumption and load profiles of the consumers have been estimated using the Typical-Day Method. This approach allows to adapt any measured data (daily load profiles) to a specific weather data set and to scale heat load profiles of the same type according to a given peak load or daily heat consumption. The simulation offers the opportunity to have a look to any internal state of the system as local pressure, fluid temperature or mass flow. With this information component stress can be analyzed very well.

The paper presents findings of the recently finished project “Dezentrale Einspeisung in Nah- und Fernwärmesysteme unter besonderer Berücksichtigung der Solarthermie”¹ and the ongoing research project “Kostenreduktionspotential beim Ausbau der Solarisierung von Fernwärmenetzen durch Standardisierung”². It is based on the German publications [HR15] and [Rüh+15].

¹ Founded by Federal Ministry for Economic Affairs and Energy FKZ 03ET1039B.

² Founded by Federal Ministry for Economic Affairs and Energy FKZ 0325553A.

BACKGROUND

A multi-functional use of district heating systems can provide significant contributions to the realization of a low-carbon heat supply. Especially the decentralized feed-in of solar heat into district heating networks offers many advantages. The presence of the network as continuously available system for the heat transport is expected to realize low average temperatures with high solar utilization levels. Stagnation times can be minimized or avoided and the summery global irradiance can be used as long as there are no negative effects on the network and the fossil fired central heat generator.

The current paper presents the results of a number of DH system simulations varying the location, the size, and the number of distributed feed-in substations within a district heating network. All computational results have been analysed using a consistent procedure. Main emphases are:

- Statistical evaluation of all-year network simulations (case study)
- Thermo-hydraulic impacts of decentralized solarthermal input on district heating networks

The heat flow rates of the solar-thermal systems, the central heat generator, the consumers and to the ambient have been estimated and the annual quantity of the produced heat have been calculated using the results of the full year network simulations (case study). The detailed results allow the identification of crucial operating states and evidences about the frequency of occurrence of these states. Flow conditions (local mass flow rates, progression of pressure and temperature) vary a lot with increasing fraction of locally produced and fed in heat. It is examined if both, the pressure and temperature of the heating water along the pipe system, stay in the allowed operation range of the district heating network.

The district heating network is stressed periodically depending on daytime and weather based fluctuations of the global solar irradiation not correlating with heat demand. Extreme values of pressure, temperature and load gradients as well as the fatigue-stress on the pipe system during the simulated year have been analysed. The goal is to derive general recommendations how to increase solar share in district heating networks, all the

while maintaining reliable supply and stable system operation.

ASSUMPTIONS/CONSTRAINTS

DH Network Simulation

The thermal-hydraulic simulation of the district heating system is based on TRNSYS-TUD. It is an inhouse development on base of TRNSYS, which has been proceeded since 1995. TRNSYS-TUD has its own hydraulic solver for heating networks as well as comprehensive models for building and equipment simulation. The hydraulic solver was adopted for the usage with district heating networks in [Fel+11] and [Rob13] and developed further in the current research projects.

A real secondary network with 2:2MW design heat load, 2:65km trench length and 51 heat consumers was considered (see Figure 2). The pipeline route, the available pipe and operation parameters were mainly provided by the network operator. The assumptions and constraints made for the network simulation are:

- Real secondary network, 3rd generation
- Simulation time is 1year
- Time step is fixed at 3min
- Weather data is a modified German test reference year 2011 (see [DWD11])
- Central heat generator
 - Supply water temperature is provided following a weather compensation control $v_{SL} = f(v_a)$
 - Main circulation pump is controlled with constant pressure difference of 1;2bar
 - Pressure maintenance is connected at the return line of the central generator
 - Overflow from the supply to the return line at the central generator is allowed (bypass)

No central heat storage tank was considered. The simulation model allows conditions, where the solar gains exceed the heat load of the consumers and the heat losses of the pipe system. For the current study this excess heat is stored in the piping system, which is achieved by allowing the overflow of the central heat generator via an intended bypass (compare Figure 1). Hot heating water runs from the supply line to the return line of the network. So the net return line is used as a short-term heat storage.

The district heating network shown in Figure 2 is regarded as reference DH network. It supplies the buildings of a serial house neighborhood via the three network segments 01 to 03. The corresponding ends of the segments are called E01 to E03. The central heat

generator is labeled with G. There are two main diversions D1 and D2.

Modeling of heat consumers

Individual load profiles are needed for all of the 51 heat consumers to avoid problems of overestimated simultaneity. They are created using an adopted Typical-Day Method following VDI 4655 (2008). This approach allows to adapt measured data (daily load profiles) to a specific weather data set and to scale heat load profiles of the same type according to a given peak load or daily heat consumption. It is described in detail in [Hey+14a] and [Hey+14b].

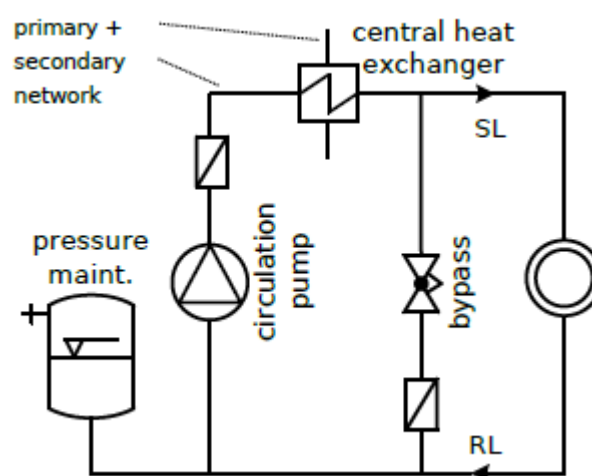


Figure 1: Equivalent network of the central heat transfer station including a bypass

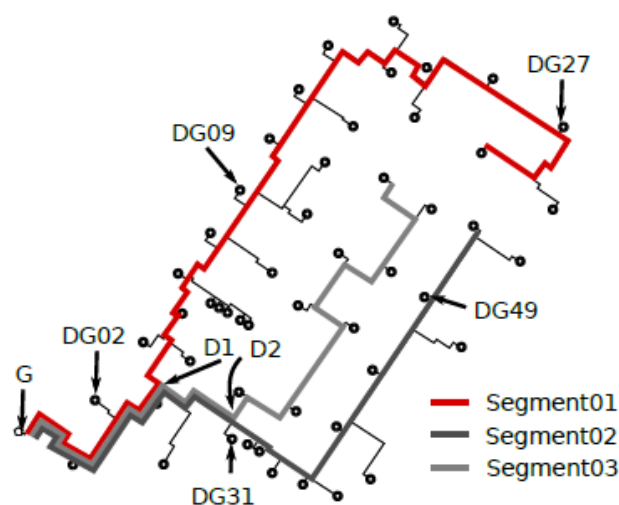


Figure 2: 3rd generation network, 2:2MW design heat load, 2:65km trench length, 51 heat consumers

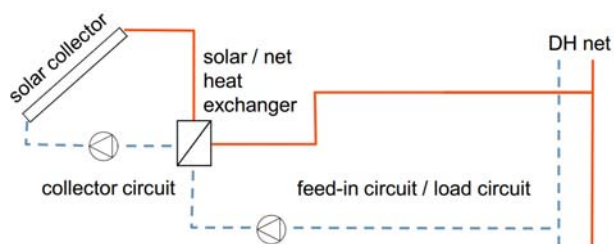


Figure 3: Solar-thermal system and feed-in substation (source: [SM15])

Table 1: Glossary of the presented simulations

Name	Comment
0NFS	no decentralized feed-in
1NFS_DG02	DG02
1NFS_DG27	DG27
2NFS	DG02, DG27
3NFS	DG02, DG27, DG49
4NFS	DG02, DG27, DG49, DG09
5NFS	DG02, DG27, DG49, DG09, DG31
5NFS-S	DG02, DG27, DG49, DG09, DG31 with small storage tanks

Each of the district heating substations supply the directly connected space heating and domestic hot water system, which is built as storage-charge system. The load profiles for the heating and the domestic hot water systems are regarded aggregately. An accurate representation of the supply and return line temperatures at the consumers is necessary to correctly model the hydraulic conditions in the network. The supply water temperature along the pipeline results from the heating set-point reset curve of the district heating network and the heat losses in the supply line. The temperature along the return line results from the load and return line temperature at each heat consumer and the heat losses in the return line. The the consumer return line temperature is calculated using a correlation. It depends on the heating load ratio $\phi_{C,j}$ and the supply line temperature $v_{SL,C,j}$ at the connection point of the consumer.

Modeling of decentralized feed-in substations

The solar-thermal system and the feed-in substations (Figure 3) are modeled in separate simulations (see [SM15]). For that matter the course of the thermal output for one year $\dot{Q}_{DGi;SolarSim}(t)$ is calculated for every considered feed-in substation using a detailed model of the solar-thermal system. Input values are the weather data of the location as well as the net temperatures calculated in the network simulation for the connection point of the substation. Further parameters of the

solarthermal reference system (decentralized generator - DG) are:

- Usage of feed-in only substations (from return line to supply line), without a storage (NFS) and with a 1:5m³ storage tank (NFS-S)
- High temperature flat plate collector with 100m² aperture area
- Orientation to south-east or south-west as the orientation of the roof
- Supply line or target temperature is reproduced via set-point reset curve as $f(v_w)$ and additional offsets due to the heat exchanger
- Stagnation is allowed if the heat can not be dissipated on target temperature level

The decentralized feed-in substations are integrated in the network simulation by transferring the calculated feed-in mass flow $m_{DGi;SolarSim}$ and the corresponding supply line temperature $v_{SL,DGi;SolarSim}$ to the TRNSYS-TUD network simulation. The simulations of the solarthermal system and of the network have to be repeated in turn until they are aligned because the decentralized feed-in affects the net temperatures. The both separate simulations are claimed to be aligned, if the calculated difference of the fed-in heat flows $\dot{Q}_{DGi;TRNSYS} - \dot{Q}_{DGi;SolarSim}$ as well as the resulting aberration of the net temperatures meet a stop criterion.

Case study

In the case study, the effects of different integration points of the decentralized network feed-in substations (NFS) as well as increasing amounts of solar-thermal generated heat are to be examined. A network simulation without solar-thermal feed-in (0NFS) is used as reference case. A single solar system (solar-thermal reference system) was integrated next to the central generator (DG02) or next to the end of Segment 01 (DG27) (compare Figure 2). The amount of solar heat fed into the DH network was increased in further simulations by installing up to five decentralized feed-in substations. The collector fields of the feed-in substations DG02, DG09 and DG49 have south-eastern orientation with an azimuth angle of $\beta = -57^\circ$ and the substations DG27 and DG31 have a south-western orientation with $\beta = 33^\circ$ depending on the orientation of the respective buildings.

The case studies done are summarized in Table 1. The name of the simulations is based on the name or of the number of the active decentralized feed-in substations.

RESULTS

Some representative results of the realized simulations are presented below. This is done on the one hand via statistical processing of all-year network simulations (case study) by comparing the annual energy balances. On the other hand the effects of decentralized solar-thermal input to district heating networks are discussed exemplary for the case 3NFS using a detailed graphical representation of the flow conditions. Alternating thermal stress is analyzed for the simulation case with the highest solar-thermal output (5NFS).

Annual Balances

Equation 1 shows the heat flow balance of the heating network, with $dU_{net}/d\tau$ for the change of the internal energy (heat capacity of the network), \dot{Q}_G for the heat flow of the central generator, $\sum \dot{Q}_{DGi}$ for the solar-thermal gains of the substations, $\sum \dot{Q}_{Cj}$ for the current heat demands of the consumers and \dot{Q}_{Loss} for the current heat losses of the piping system. The heat balance can be derived through integration over time (different amount of internal energy between start and end time is neglected).

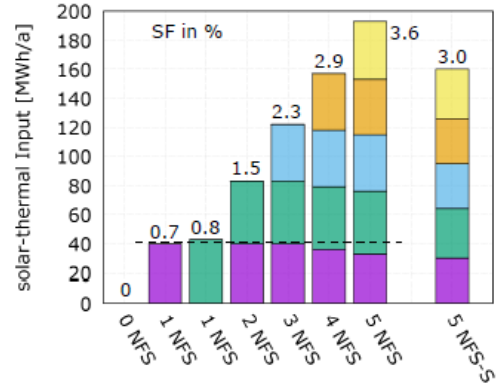
$$\frac{dU_{net}}{d\tau} = \dot{Q}_G + \sum \dot{Q}_{DGi} - \sum \dot{Q}_{Cj} - \dot{Q}_{Loss} \quad (1)$$

$$0 = \dot{Q}_G + \sum \dot{Q}_{DGi} - \sum \dot{Q}_{Cj} - \dot{Q}_{Loss} \quad (2)$$

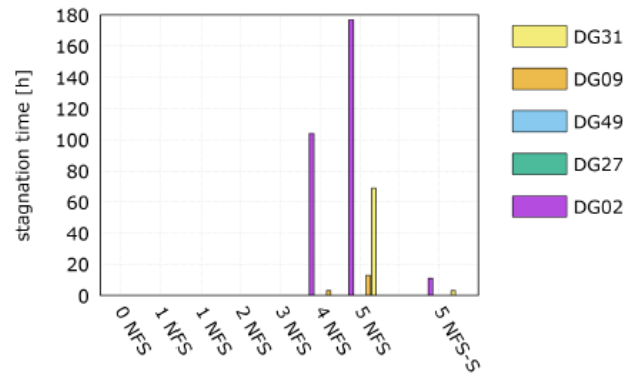
Furthermore the solar net fraction SF based on [Qua11] is defined as the ratio of the solar heat fed into the network and the sum of the consumer heat demands inclusive heat losses of the network.

$$SF = \frac{\sum \dot{Q}_{DGi}}{\sum \dot{Q}_{Ci} + \dot{Q}_{Loss}} \quad (3)$$

For the reference case 0NFS the heat provided by the central generator \dot{Q}_G is 5500MWh=a, the heat demand of the consumers $\sum \dot{Q}_{Ci}$ is 5290MWh=a and the heat loss of the piping is 210MWh=a. According to the simulations the annual heat losses of the pipeline system amount to about 4% and are about 12% for a summer week. The heat losses of the network are not affected noticeably due to the decentralized feed-in. For the substations without storage tanks the feed-in hours are about 1200h, for the stations with the heat storage about 750h. The annual amount of heat transferred to the DH network is shown in Figure 4a for all considered cases. The stagnation time of the solarthermal system in one simulated year can be seen in Figure 4b.



(a)



(b)

Figure 4: Solar-thermal input, solar fraction and stagnation time

It can be concluded:

- An increasing ratio of solar produced heat leads to decreasing heat quantity over the central generator as expected. A solar fraction of up to 3:6% for the total year can be achieved (500m² installed collecto area, compare 5NFS). In the summer week this fraction goes up to 35%.
- The solar-thermal input decreases for cases with four or more decentralized feed-in substations. This mainly affects the substations next to the central generator (DG02, but also DG09 and DG31). Reason for that is the occurrence of stagnation in these systems. In DG02 stagnation occurs for up to 180h.
- The annual solar gains in the 5NFS-S case are well below the 5NFS. This results from a more complex system and heat losses in the storage tank due to delayed discharge. The solar-thermal outputs in the summer week are almost equal, due to reduced stagnation time for the NFS-S.

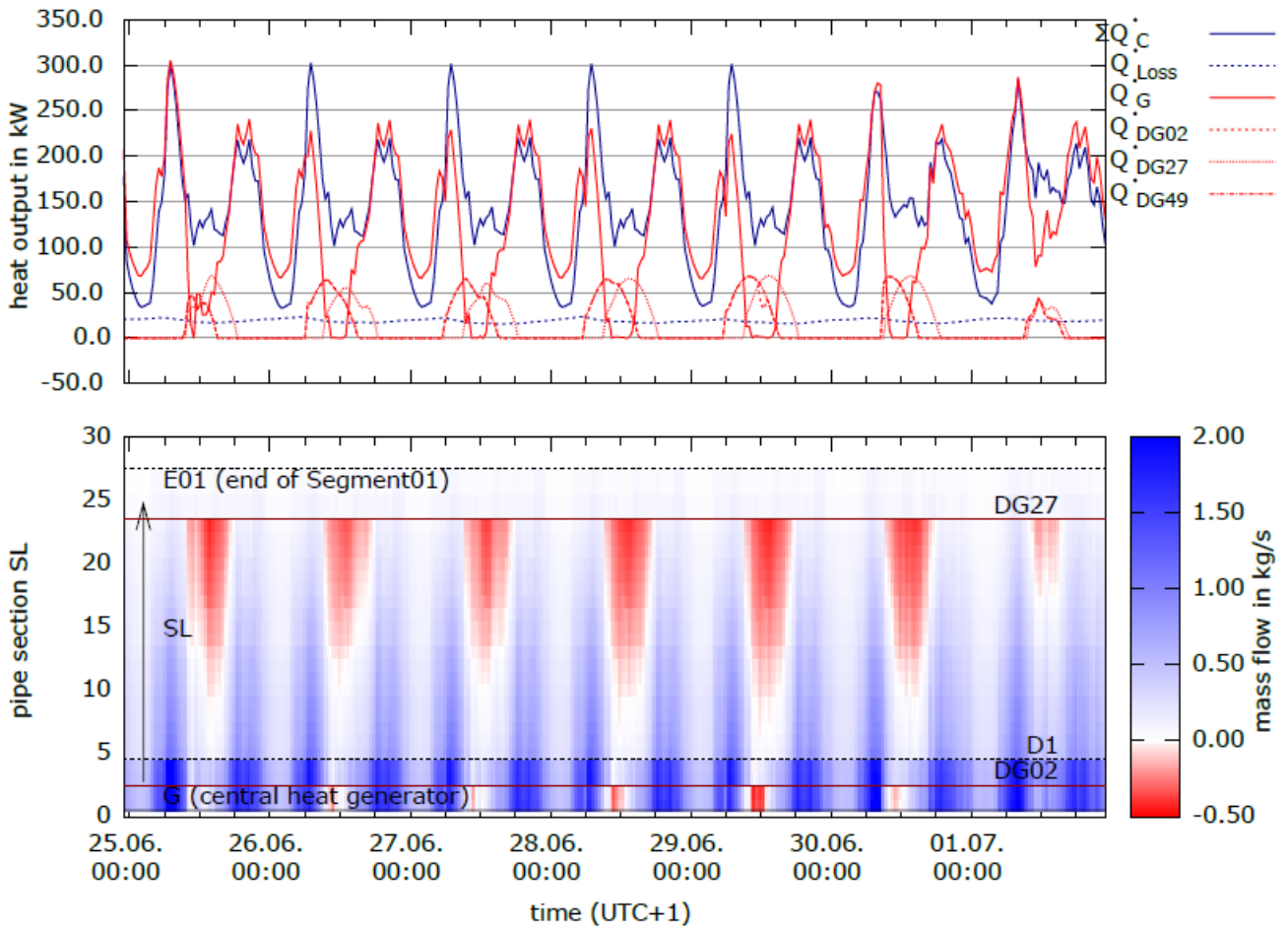


Figure 5: top: heat flow profiles; bottom: mass flow distribution, Segment01; case 3NFS, summer week

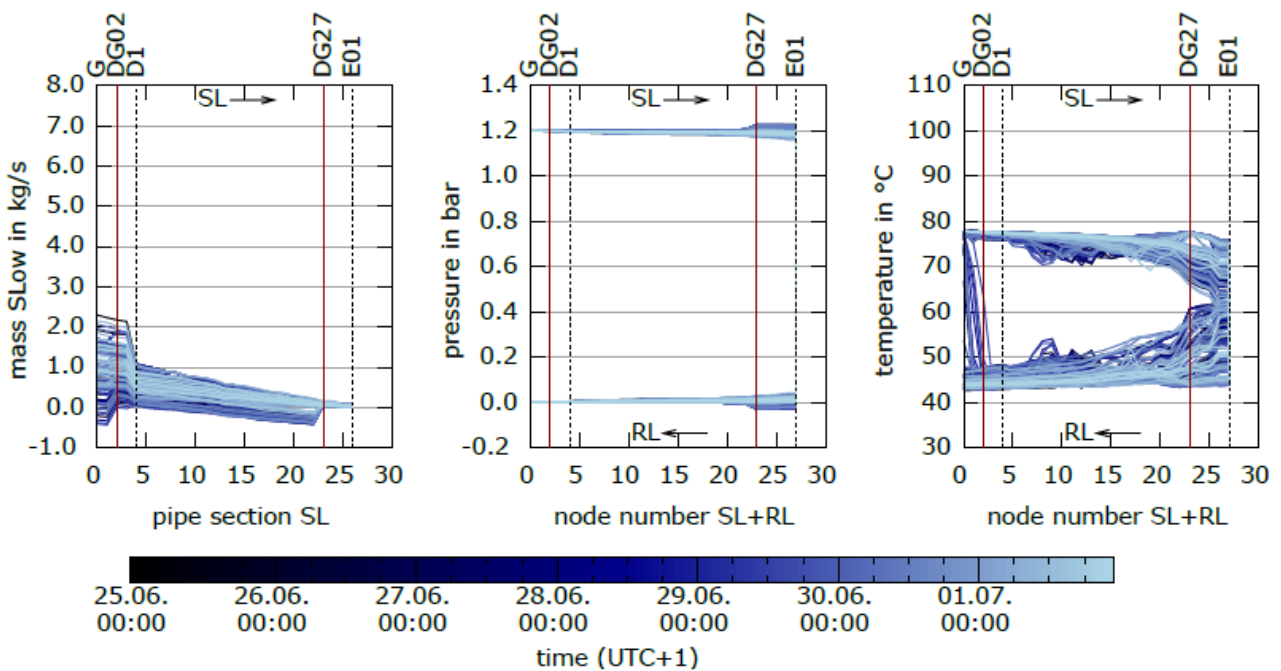


Figure 6: Distribution diagrams of mass flow, pressure, temperature; case 3NFS, summer week, Segment01

A collector area, which covers about 25% of the heat demand of a summer week, can be easily integrated without the usage of centralized or decentralized storage. This corresponds to a maximum solar-thermal output³ of 1/10 of the total heat load to be provided by the central heat generator.

Flow Conditions

In the following, the flow conditions are investigated exemplarily for a summer week and case 3NFS. Three display forms illustrate the complex conditions in the network:

1. *Line Charts* show time sequences of a quantity at specific locations in the network (x-axis: time, y-axis: considered quantity, compare Figure 5 top).
2. *Distribution Diagrams* display the local progress of a quantity alongside one network segment using instantaneous values. Several colored charts represent several points in time. This display form is used to show the spread of possible operating states. (x-axis: location along network segment, y-axis: considered quantity, color scale: time, compare Figure 6)
3. *Carpet Plots* can show the time sequence of a quantity for a whole network segment by color. In that manner transient effects can be visualized. (x-axis: time, y-axis: location along network segment, color scale: considered quantity, compare Figure 5 bottom)

This paper presents the flow conditions in Segment01 (compare red segment in Figure 2) and discusses the occurring effects. Node or pipe section numbers are used as location identifier. It has to be taken into account that the different pipe sections have differing length and the nodes and sections use a slightly different grid. Local gradients are not drawn to scale in the charts. Distinctive points along the network trace are labeled in the diagrams.

Figure 5 (top) shows the progression of the heat flows as a line chart. The sum of consumer demands $\sum Q_{Cj}$, generated using the Typical-Day method, fluctuates during the day with clear load peak in the morning and evening hours. The course is similar for the first five days, because the same typical-day was used due to similar weather conditions. A weekend profile for a clear and a cloudy day is applied for the 6th and 7th day. The heat loss of the pipe system \dot{Q}_{Loss} is only changing slightly during the day. The heat flows of the decentralized feed-in substations show a typical course with a clear offset between south-western and south-

eastern orientated systems (DG02, DG27). A considerable amount can be covered by solar-thermal.

Fluctuations of the mass flow in Figure 5 (bottom) are represented by different shades of blue. A leap in the color gradient occurs due to the dividing mass flow in the diversion D1. The output of feed-in substation DG27, which is located near the end of the segment, exceeds the heat demand of the consumers connected downstream. Therefore a reversal of the flow direction appears in large parts of the considered pipeline. This can be seen in terms of the red area starting at label DG27 of the carpet plot in Figure 5. The feed-in substation DG27 supplies all consumers connected to this areas. The supply frontier originating between the central heat generator and the decentralized substations can be identified via the white areas with a mass flow near zero. Heating water grants to a halt in this region of the pipeline and will cool down slowly.

At noon of day two to six the solar-thermal output \dot{Q}_G is at least as high as the heat demand. The central heat generator switches off completely in this time period (compare Figure 5 top). At this time, the first pipeline section (central generator) is colored white or red in the lower chart. This means, that the central district heating station is overflowed via the intended bypass (compare Figure 1). The heat produced by substation DG02 is not needed by the heat consumers during this period. Hot supply line water streams into the return line using it as short term storage.

Meanwhile, the decentralized feeder DG49 supplies consumers alongside the network segments 02 and 03. The effects can not directly be seen in the presented diagram. All of the output of DG49 can be used by the consumers of the segments 02 and 03, because no negative mass flow occurs between DG02 and diversion D1 at any time.

Figure 6 presents the distribution diagrams of the mass flow (left), the pressure (middle) and the temperature (right) alongside of Segment01. States of the network for discrete instants of time (time step 1h) are colorcoded. This allows to show the spread of possible operating states. The comparatively low maximum mass flow at the central heat generator, resulting from the summertime part-load operation, stands out in the left hand plot. A leap of the mass flow can be seen at diversion D1. Negative flow rates occurs directly at the central generator as well as in the zone between diversion D1 and the end of section Segment01. The point of intersection with the x-axis marks the supply frontier moving according to the load situation.

³ Estimated with a peak load of $0.7 \cdot A \cdot 1000W = m^2$.

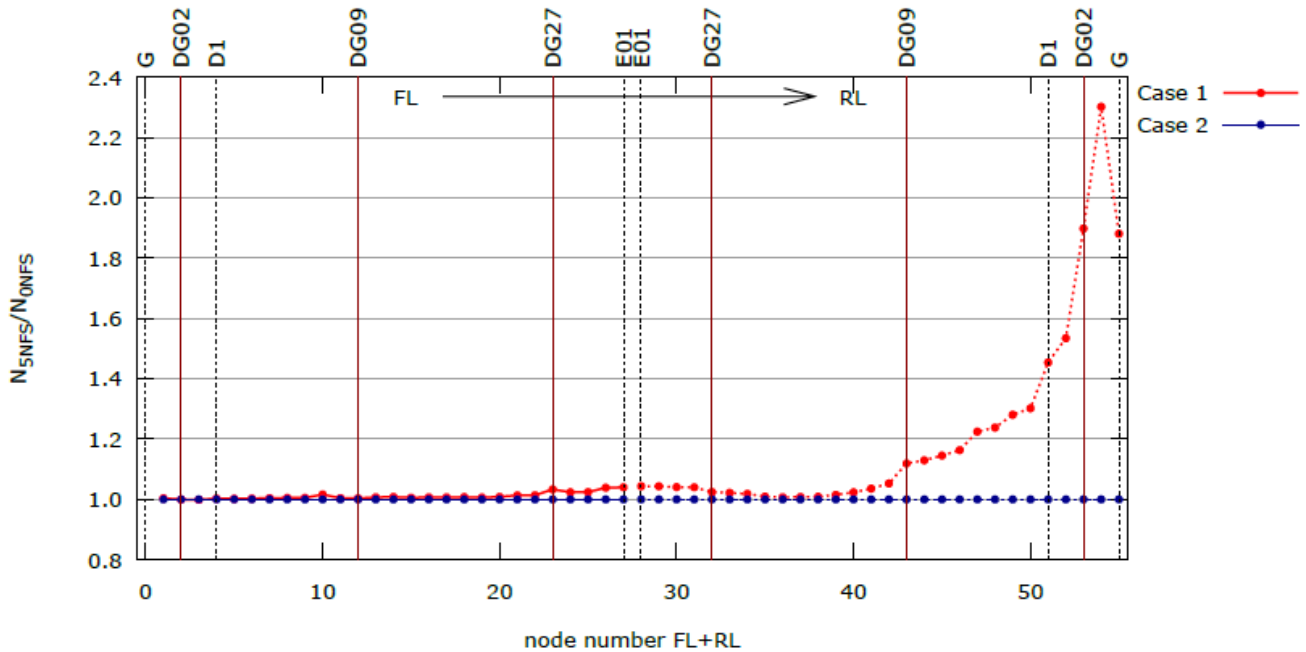


Figure 7: Ratio of the number of load changes for case 5NFS to the reference case
solid line: supply line; dashed line: return line

The pressure curves in the middle diagram of Figure 6 illustrate the minimal pressure losses due to the summertime part-load operation of the district heating network. The largest proportion of the pressure drop occurs in the consumer connection stations. The minimal valid consumer pressure difference is 0,53bar. It would have been possible to maintain this with a strongly lower pressure difference at the central heat generator, which could have reduced the consumption of auxiliary energy of the main circulation pump and of the feed-in pumps of the decentralized substations. Those have to overpower the flow pressure losses in addition to the pressure drop of the central circulation pump (see pressure gradients next to substation DG27). This results in an unfavorable operating point of the feed-in pump. Advanced control concepts are necessary to provide a better matching of network operation and decentralized feed-in.

Figure 6 (right) shows the distribution of the temperature alongside the supply and return line. Partly a high temperature difference between central heat generator and the end of Segment01 are apparent. This results from the low consumer heat demand so that fluid elements remain in the forward line for a long time period. This temperature differences in the network can be reduced on account of the feed-in substation DG27 which applies a supply line temperature identical to the supply line temperature of the network. In return, a minimum in the forward line temperature occurs at the actual location of the supply frontier. In some cases a temperature gap can be seen in the return line in the zone of the central heat

producer. This follows from the temporal overflow of the central generator.

Alternating Thermal Stress

The thermohydraulic conditions in the pipeline system vary due to the decentralized feed-in. The reversal of the flow direction in parts of the network and the resulting supply frontier with cooled down heating water can increase the stress on pipes. Two cases of damage were investigated:

- Case 1 Fatigue fracture of the steel tube, e. g. breakaway of a welded orthogonal diversion due to the longitudinal motion of the main pipe,
- Case 2 Disbandment of the composite material pipe due to shearing force longitudinal to the pipe.

The evaluated quantity is the number of full-load changes N according to AGFW FW 401 – Part 10 [AGFW401] or rather the ratio to the reference case. Exemplary the results for Segment01 and simulation case 5NFS can be seen in Figure 7.

$$\frac{N}{N_{\text{reference}}} = \frac{N_{5\text{NFS}}}{N_{0\text{NFS}}} \quad (4)$$

For Case 1 the full-load changes in the supply line are slightly higher (< 5%) then for the reference case. This mainly effects the pipes at the end of Segment01 after the feed-in point of DG27. A similar pattern can be seen for the return line nearby the end of Segment01. A increase on up to 2.3 times occurs for the return line next to the central heat generator. This results from using the return line as short-term heat storage with the overflow of hot supply line water to the return line. This concept increases the risk for the DH pipes significantly, from which can not be inferred the absolute damage risk. The risk for disbandment of the composite material pipe (Case 2) is not increased in the whole piping system.

CONCLUSIONS/PROSPECTS

The realized simulation studies deliver detailed insight into the operating conditions and the component stress of district heating networks with decentralized solar heat supply. The distributed feed-in of heat may lead to the inversion of the flow direction in parts of the net branch (negative mass flow) and to moving points with stagnating heating water. The heating water will cool down in this points. At some time steps the distributed solarthermal heat generators can supply the demand of the whole DH-network. This results in mass flow rates of nearly zero at the central heat generator or if provided even in negative flows.

The installation of total collector area with a maximum thermal output of about 1/10 of the connected load of the district heating network is possible without central or decentralized storage tanks and with very short stagnation periods, in case the pipe system is used as a short-term storage. It has to be taken into account, that this concept increases the alternating thermal stress to the affected district heating pipes.

Questions, which central or decentralized storage capacity is necessary for more installed collector area as well as which adapted control concepts are required, are only briefly touched. Further research to this has been done in the current project "DELFIN"⁴.

NOMENCLATURE

Symbols

N	number of load changes according to AGFW FW 401 – Part 10	
Q	heat	MWh
\dot{Q}	heat flow	W
SF	solar fraction	-

β	azimuth angle	°
φ	heating load ratio, $\varphi = \dot{Q} = \dot{Q}_N$	-
τ	time	s
u	celsius temperature	°C

Abbreviations/Indices

C	Consumer
D	diversion
DG	decentralized heat generator
SL	supply line
G	central heat generator
i, j	index
N	nominal
NFS	network feed-in substation
NFS-S	network feed-in substation, with storage
RL	return line

REFERENCES

- [1] [AGFW401] AGFW FW 401 Part 10 - Verlegung und Statik von KMR in Fernwärmenetzen Statische Auslegung; Grundlagen der Spannungsermittlung. AGFW. Frankfurt a. M.: AGFW e.V., Dezember 2007.
- [2] [DWD11] Aktualisierte und erweiterte Testreferenzjahre von Deutschland für mittlere, extreme und zukünftige Witterungsverhältnisse. Projektbericht. Bundesamtes für Bauwesen und Raumordnung (BBR) in Zusammenarbeit mit der Climate & Environment Consulting Potsdam GmbH und dem Deutschen Wetterdienst (DWD), July 2011.
- [3] [Fel+11] C. Felsmann et al. Zusammenfassung LowEx Fernwärme: Multilevel District Heating. FKZ:0327400B. TU Dresden, 2011.
- [4] [Hey+14a] M. Heymann, T. Kretzschmar, T. Rosemann, and K. Rühling. "Integration of Solar Thermal Systems into District Heating". In: 2nd International Solar District Heating Conference. Hamburg, June 2014.
- [5] [Hey+14b] M. Heymann, T. Kretzschmar, K. Rühling, and C. Felsmann. "Modellierung dezentraler Einspeisung solarer Erträge in Nah- oder Fernwärmenetze". In: 24. Symposium Thermische Solarenergie. Staffelstein: OTTI e.V., Mai 2014. ISBN: 978-3-943891-35-5.
- [6] [HR15] M. Heymann and K. Rühling. "Integration of Solar Thermal Systems into District Heating – Results of a Case Study Done in the R&D Project "DECENTRAL"". In: 3rd International Solar District Heating Conference. Toulouse, June 2015.

⁴ Founded by Federal Ministry for Economic Affairs and Energy FKZ 03ET1358B.

- [7] [Qua11] Volker Quaschnig. Regenerative Energiesysteme: Technologie-Berechnung-Simulation. Carl Hanser Verlag GmbH Co KG, 2011.
- [8] [Rob13] S. Robbi. "LowEx-Fernwärme – Vergleichende Bewertung von Maßnahmen für eine effiziente, multifunktionale Fernwärmeversorgung". PhD thesis. TU Dresden, Mai 2013.
- [9] [Ros+14] A. D. Rosa et al. Annex X Final Report: Toward 4th Generation District Heating. Tech. rep. IEA DHC|CHP, 2014.
- [10] [Rüh+15] K. Rühling et al. Dezentrale Einspeisung in Nah- und Fernwärmesysteme unter besonderer Berücksichtigung der Solarthermie. FKZ:03ET1039B. TU Dresden, 2015.
- [11] [SM15] K. Schäfer and D. Mangold. "Integration of Solar Thermal Systems into District Heating – Results of a Case Study Done in the R&D Project "DECENTRAL"". In: 3rd International Solar District Heating Conference. Solites. Toulouse, June 2015.
- [12] [VDI4655] VDI 4655 - Reference load profiles of single-family and multi-family houses for the use of CHP systems. VDI. Verein Deutscher Ingenieure e.V, May 2008.

COMPARATIVE ANALYSIS BETWEEN DISTRICT AND GEOTHERMAL HEAT PUMP SYSTEM

J-S. Lee¹, H-C. Kim¹, S-Y. Im¹

¹Korea District Heating Corp., 781, Yangjae-daero, Gangnam-gu, Seoul, 06340, Korea

Keywords: *District heating, Geothermal, Heat pump, Greenhouse gas reduction*

ABSTRACT

In Seoul, most of the new private buildings were mandated renewable energy installations more than 12% of total energy use in 2015. There are solar power, solar heat, geothermal, sunlight collecting, fuel cell, and small cogeneration systems in applicable renewable energy. Accordingly, some reconstruction apartments want to apply geothermal heat pump systems as heating and cooling. This has resulted in reducing the demand for district heating since district heating had been supplied in these areas. From the point of view of district heating suppliers, new competitor such as heating by geothermal heat pump system seems to appear in district heating market. District heating system is considered preferentially to apply in heating area abroad due to its high efficiency. However, district heating isn't recognized properly as a renewable energy in domestic situation. Therefore, in this study, we analysed primary energy use and greenhouse gas reductions of district heating and geothermal heat pump system. As a result, primary energy use and greenhouse gas reduction of district heating system are bigger than them of geothermal heat pump system.

INTRODUCTION

Aside from of environmental impact assessment of the government, Seoul city established its own standards for management systems complement of the high-density urban development in Korea. For the introduction of its own environmental impact assessment, Seoul city enacted and performed an Environment, Traffic and Disaster Impact Assessment Ordinance in 2002. Other municipalities also expected to introduce the same level of future environmental impact assessment.

Most of the new private buildings should implement more than 12% renewable energy installation obligation of the total energy usage in 2015. Public buildings is expected to expand step by step up to 30% renewable energy rate in 2020. Applicable renewable energy is photovoltaic, solar heat, geothermal, sun-light collecting, fuel cell and cogeneration (more than 10% recognition rate only) energy.

All new apartment of land area 90,000 ~ 300,000 m² (about 1,500 ~ 6,000 generations) is subject to Seoul environmental impact assessment. From the point of district heating system's view, new competitors appeared. Renewable facilities corresponding to 12% of total energy use, especially geothermal heat pumps, can supply heating and cooling autonomously. The introduction of geothermal heat pumps are increasing because of their technology development and low variable cost. In addition, the introduction of fuel cell is also increasing. The government abolished geothermal heating and cooling progressive electricity rates in 2009.

However, district heating systems are unappreciated renewable facilities properly. Thus, in this research, we analysed primary energy use and greenhouse gas reductions of district heating and geothermal heat pump system.

BACKGROUND

Geothermal heat pumps have been supplying heating and cooling to 180 generations of S apartment(located in Incheon, Korea) in 2012. Thus, using the operating data of S apartment in 2014, we calculated primary energy use and greenhouse gas reductions of district heating and geothermal heat pump system. Heating consumption of S apartment in 2014 was 989 Gcal/year and electricity consumption was 527 MWh/year.

However, geothermal heat pump system produces only heat, but district heating system produces heat and electricity simultaneously. Thus, we assumed, in geothermal heat pump system, common power plants produced electricity production amount of district heating system.

Primary energy use was calculated based on electricity production amount of each power source and greenhouse gas emission factor of 0.4428 tCO₂e/MWh (Korea power exchange 2011 year data) was used.

RESULTS

We calculated primary energy use and greenhouse gas emission based on 2014 year operating data in Korea District Heating Corporation. If district heating system in Korea District Heating Corporation produces the heat

of 989 Gcal/year, it produces the electricity of 689 MWh/year proportionally. Thus, in geothermal heat pump system and common power plants, we assumed

Division	District heating		Geothermal heat pump + Common power generation	
	Primary energy use (Gcal)	Greenhouse gas emissions (tCO ₂ e)	Primary energy use (Gcal)	Greenhouse gas emissions (tCO ₂ e)
Heat	1,090	254	1,088	234
Electricity	797	174	1,422	305
Sum	1,887	428	2,510	539
Comparison			33% ↑	26% ↑

common power plants produced the electricity of 689 MWh/year.

Table 1 shows primary energy use and greenhouse gas emission of geothermal heat pump and common power generation system, and them of district heating system when COP of geothermal heat pump system is 2.2.

As a result, primary energy use and greenhouse gas emission of geothermal heat pump and common power generation system are each 33% and 26% bigger than them of district heating system.

Therefore, we can say district heating system reduces fossil fuel consumption and greenhouse gas more than geothermal heat pump system.

DISCUSSION

However, COP of geothermal heat pump system is commonly very low. Thus, we assumed COP of geothermal heat pump system was 4.0.

Table 2 shows primary energy use and greenhouse gas emission of geothermal heat pump and common power generation system, and them of district heating system when COP of geothermal heat pump system is 4.0.

As a result, primary energy use and greenhouse gas emission of geothermal heat pump and common power generation system are also each 2.4% and 0.9% bigger than them of district heating system.

Therefore, we can also say district heating system reduces fossil fuel consumption and greenhouse gas more than geothermal heat pump system.

Table 1 Comparison of primary energy use and greenhouse gas emissions between district heating and geothermal heat pump system (COP=2.2)

Table 2 Comparison of primary energy use and greenhouse gas emissions between district heating and geothermal heat pump system (COP=4.0)

Division	District heating		Geothermal heat pump + Common power generation	
	Primary energy use (Gcal)	Greenhouse gas emissions (tCO ₂ e)	Primary energy use (Gcal)	Greenhouse gas emissions (tCO ₂ e)
Heat	1,090	254	510	127
Electricity	797	174	1,422	305
Sum	1,887	428	1,932	432
Comparison			2.4% ↑	0.9% ↑

CONCLUSION

In this study, we compared primary energy use and greenhouse gas emission of district heating and geothermal heat pump system. This study is based on some assumptions which are made by KDHC and Korea electric power corporation's operating data.

Consequently, primary energy use and greenhouse gas emission of geothermal heat pump and common power generation system are each 33% and 26% bigger than them of district heating system.

Even though COP of geothermal heat pump system increases, primary energy use and greenhouse gas emission of geothermal heat pump and common power generation system are slightly bigger than them of district heating system.

Therefore, district heating system is required to be reflected properly in government policy as renewable facilities since district heating system reduces fossil fuel consumption and greenhouse gas more than geothermal heat pump system.

REFERENCES

- [1] Korea electric power corporation, "Statistics of electric power in Korea", 2015, pp. 19–58.
- [2] Korea power exchange, "Power sector greenhouse gas emission factor", <http://www.kpx.or.kr>, 2012.
- [3] ASHRAE Handbook HVAC Applications, "Geothermal Energy", Chapter 32, 2007.

TREND ANALYSIS TO AUTOMATICALLY IDENTIFY HEAT PROGRAM CHANGES

S. Abghari¹, E. G. Martin¹, C. Johansson², N. Lavesson¹, H. Grahn¹

¹ Blekinge Institute of Technology, SE-371 79, Karlskrona, Sweden

² NODA Intelligent Systems AB, Biblioteksgatan 4, SE-374 35, Karlshamn, Sweden

Keywords: District heating, Trend analysis, Change detection, Smart automated system

ABSTRACT

The aim of this study is to improve the monitoring and controlling of heating systems located at customer buildings through the use of a decision support system. To achieve this, the proposed system applies a two-step classifier to detect manual changes of the temperature of the heating system. We apply data from the Swedish company NODA, active in energy optimization and services for energy efficiency, to train and test the suggested system. The decision support system is evaluated through an experiment and the results are validated by experts at NODA. The results show that the decision support system can detect changes within three days after their occurrence and only by considering daily average measurements.

INTRODUCTION

In the district heating (DH) domain, operators address several conflicting goals, such as satisfying customer demand while minimizing production and distribution costs. To achieve this, one solution is to equip each customer building with a smart system. Such a system should continuously monitor heat usage, predict future demand, exchange information with operators, and perform demand-side management. Moreover, the system needs to automatically learn the energy usage of the building and adopt its behavior accordingly.

NODA Intelligent Systems AB⁶, an active company in the DH domain, is developing and providing retrofit smart systems to maximize energy efficiency in buildings. These systems consist of controlling hardware together with a range of sensors, which are added on top of the existing control system.

Self-learning and adaptation are two important features of any smart system. However, these two features make the system sensitive to manual changes in the heating system, forcing the system to re-learn its characteristics. Most commonly this relates to applying changes in the temperature program of the controller e.g. by the owner's building. These changes can lead to use more energy and to add extra charges in the case of increasing the temperature of the system.

Although retrofit solutions such as NODA's smart system can decrease the cost of replacement of the

existing control system, their functionality can be affected by the limitation of these existing controllers. Due to this reason, NODA's smart system is unable to detect manual changes online. Hence, NODA's operators need to spend significant efforts to detect the manual changes by analyzing the received information from each building controller. To make this process more efficient, a decision support (DS) system can be used to assist operators. DS systems are computer-based information systems, which aim to facilitate and support the decision making processes [1]. The major components of DS systems are: 1) the user-interface, 2) the models and main logic, 3) the database, and 4) the DS functionalities and architecture. DS systems are categorized based on their functionalities into: data-driven, knowledge-driven, model-driven, document-driven and communication-driven DS systems [1]. Among these different types, data-driven systems can provide an online support for decision making through applying machine learning (ML) and statistical techniques to analyze large collections of data.

Machine learning is a branch of artificial intelligence, which includes the study of algorithms that can learn and improve their knowledge by building models from input data to perform specific tasks. Most common tasks in ML, such as classification and regression modeling, are solved with supervised learning methods. Supervised learning uses labeled data to train models [2]. Suppose we are given data in the form of $(\vec{x}_1, y_1), (\vec{x}_2, y_2), \dots, (\vec{x}_n, y_n)$. In each pair or instance \vec{x}_i (input) denotes a vector, which consists of feature values such as indoor and outdoor temperature, and y_i (output) indicates a label or outcome of the target attribute. The aim is to train a model to predict the label of the target attribute (y_i) of each new instance, e.g. predicting the secondary supply temperature based on the indoor and outdoor temperature. The target attribute in regression modeling is numeric and in classification modeling it is categorical.

In this paper, we propose a data-driven decision support system that uses ML techniques to detect manual changes by predicting the secondary supply temperature based on the outdoor temperature and analyzing the energy consumption of each building. The aim of such a system is to provide complementary

⁶ www.noda.se/en/main

decision support for NODA's operators to detect manual changes easily and efficiently. The proposed DS system uses a two-step classifier, a combination of k-means and support vector regression (SVR), to detect manual changes within three days after their occurrence by considering daily average measurements.

BACKGROUND AND RELATED WORK

A district heating system (DHS) is a centralized system with the aim of producing space heating and hot tap water for consumers based on their demand at a limited geographic area. A DH system consists of three main parts: production units, distribution network, and consumers. The heated water supplied in a production unit circulates through the distribution network and will be available to consumers.

The main aim of a DHS is to minimize the cost and pollution by considering consumers' demand and producing just the necessary amount of heat. Hence, being able to predict the heat demand can assist production units to plan better. However, modeling the heat demand forecasting is a challenging task, since water does not move fast. In some situations, the distribution of heated water can take several hours. Moreover, there are a number of factors that affect the forecast accuracy and need to be considered before any plan for production units can be constructed. Some of these factors include [3], [4]:

- Weather condition, mainly the outdoor temperature
- Social behavior of the consumers
- Irregular days such as holidays
- Periodic changes in conditions of heat demand such as seasonal, weekly and day-night

Fumo [5] pointed out in his review two commonly used techniques for energy demand estimation, namely; forward (classical) and data-driven (inverse) techniques. The first approach describes the behavior of systems by applying mathematical equations and known inputs to predict the outputs. In contrast, data-driven techniques use ML methods to learn the system's behavior by building a model with training data in order to make predictions.

Dotzauer [4] introduced a very simple model for forecasting heat demand based on outdoor temperature and social behavior. He showed that the predictions of his simple model were comparable with complicated models such as autoregressive moving average model (ARMA). The author concluded that better predictions can be achieved by improving the weather forecasts instead of developing complicated heat demand forecasting models.

In general, different ML methods and techniques have been used to predict the heat demand. Some of the most popular prediction models are autoregressive moving average (ARMA) [6], support vector regression (SVR) [7], [8], multiple linear regression (MLR) [9] and artificial neural network (ANN) [10], [11]. In [8] the authors compared four supervised ML methods for building short-term forecasting models. The models are used to predict heat demand for multi-family apartment buildings with different horizon values between 1 to 24 hours ahead. The authors concluded that SVR achieves the best performance followed by MLR in comparison to feed forwards neural network (FFNN), and regression trees methods. Recently, Provatas et al.[12], proposed the usage of on-line ML algorithms in combination with decision tree-based ML algorithms for heat load forecasting in a DH system. The authors investigated the impact of two different approaches for heat load aggregation. The results of the study showed that the proposed algorithm has a good prediction result. In another study [13], the authors showed the application of a context vector (CV) based approach for forecasting energy consumption of single family houses. The proposed method is compared with linear regression, K-nearest neighbors (KNN) and SVR methods. The results of the experiment showed that CV performed better in most cases followed by KNN and SVR. The authors concluded the proposed solution can help DH companies to improve their schedule and reduce operational costs.

There are a number of studies that focused on the application of DS systems in domains such as DH and mainly related to advanced energy management [14], [15], [16], [17], [18], [19]. In these studies, the main focus is on forecasting and optimization methods that facilitate and support the decision making processes to increase the energy management quality and bring considerable savings. Furthermore, there are some other works that focused on DH network design [20], [21]. Bordin et al. [20] presented a mathematical model to support DH system network planning by selecting an optimal set of new users to be connected to a thermal network that maximizes revenues and minimizes infrastructure and operational costs.

In summary, the main focus of the studies that have been done in the context of heat demand forecasting in the DH domain was related to using weather forecast data and mainly the outdoor temperature. In contrast, the aim of the proposed solution in this study is twofold: 1) to provide decision support for operators to detect manual changes efficiently, and 2) to decrease the energy consumption cost and control heat demand by identifying these changes and resolving them at each building.

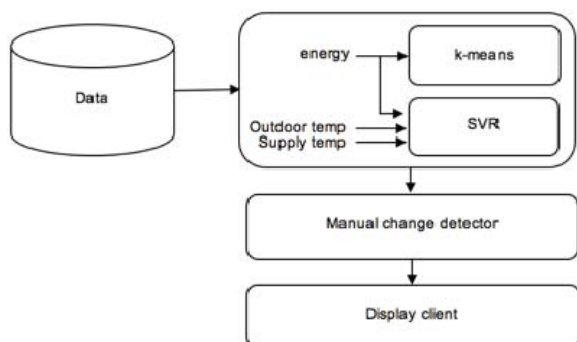


Figure 1. The process of automatically identifying the manual changes for each building by the DS system

DETECTION OF CHANGES IN TRENDS BY USING REGRESSION METHODS

In DH, operators try to address several conflicting goals, such as satisfying customer demand while minimizing production and distribution costs. One way to solve this is to use demand side management and data analytics in the customer substations. This can be achieved by a system that continuously predicts the future heat demand, exchanges information with the operator and performs demand side management when the need arises. Such systems can be implemented both in the existing heating controllers as well as in retrofit solutions. One such retrofit system is developed by NODA and it has been used within this study. To make the system efficient, its behavior has to be as automated and self-learning as possible. However, this also makes the system sensitive to manual changes (i.e. changing the temperature) in the heating system, since such changes forces the system to re-learn the characteristics of the heating system.

In order to assist operators to detect these manual changes more efficiently a DS system is implanted to provide decision support for operators. The proposed DS system uses a two-step classifier, k-means and SVR, to detect manual changes. To achieve this goal and to avoid generating false alarms in confront with noisy data, changes should be monitored for some days. Hence, in this study only those deviations that last for at least 3 consecutive days would be marked as manual changes. k-means, which is the most well-known algorithm for classification task, is used to identify the operational status of the heating system (on or off) by partitioning the consumed energy at each building.

The main reason to perform this task is to decrease the effect of outliers when the heating system is not operating. SVR has been used for both electricity and heat demand forecasting and has been found to be very efficient and accurate [8], [22]. Therefore, SVR is

chosen to predict secondary supply temperature based on outdoor temperature and consumed energy for each building. By considering the status of the system and the predicted value of the secondary supply temperature, the DS system can identify manual changes as follows:

IF the absolute difference (actual – predicted) is greater than the threshold **FOR** 3 consecutive days **THEN** changes have occurred during these days.

The warning *threshold* determines the sensitivity of the system to change. This threshold, set to 4.6°C, was determined empirically after performing some preliminary tests and checking the results with the subject matter experts. Figure 1 summarizes the process of automatically identifying the manual changes for each building by the proposed DS system.

Algorithms

The k-means algorithm belongs to the group of distance-based clustering methods. It is the best known greedy algorithm for partitioning data into k clusters. This popularity is mainly related to k-means' simplicity, efficiency, and applied success in partitioning and pattern recognition tasks [2], [23]. It works by reducing the total sum of the squared error over all k clusters. k-means iterates by generating partitions and assigning data to the closest cluster and computing the centroid from a partition until no further improvement can be achieved [23].

The support vector machine (SVM) algorithm is based on statistical learning theory. SVM is a state-of-the-art algorithm, which belongs to a group of supervised learning methods that can solve different ML tasks such as classification, pattern recognition and regression [24]. An extended version of SVM for regression tasks is called support vector regression. SVR uses the training data to find the regression line that best fits the data. Using an epsilon-intensive loss function, SVR produces a decision boundary, a subset of training data which is called support vectors (SVs), in order to determine a tube with radius ϵ fitted to the data. In other words, epsilon defines how well the regression line fits the data by ignoring errors as long as they are less than ϵ .

RESEARCH METHOD

Data collection

The data used in this study consists of daily average measurements from 9 buildings equipped with the NODA controller. The buildings are located in Karlshamn in south Sweden. The collected data was obtained on the period between April 2014 and March 2016. This yields 730 instances per building (one instance per day). However, since data collection

instruments, such as sensors, might be faulty, or since data transmission errors can occur [25], some of the measurements were incomplete. Therefore, after performing the data cleaning process the number of instances decreased to approximately 630 per building. Table 1 summarizes the information and the way the data is split to train and test set for each building.

Figure 2 shows the daily average of the secondary supply temperature of building D with respect to the outdoor temperature for the year 2015 (365 instances). The plot shows that the secondary supply temperature has a strong correlation with the outdoor temperature.

We used R and RWeka package to conduct the experiment. R is a language and a free software environment for statistical computing with data [26]. R is widely used for visualization and statistical tasks such as linear and non-linear modelling, regression analysis, and statistical tests. RWeka is an R interface to WEKA (Waikato environment for knowledge analysis) [27]. WEKA [28] is a well-known machine learning and data mining workbench written in Java. It contains a wide range of algorithms for different ML tasks such as classification, regression, and clustering. We used RWeka's k-means and SVR implementation with their default parameters.

Experimental design

To detect manual changes in the heating system for each building, the implemented DS system uses a two-step classifier. 10-fold cross validation is used on data from April 2014 to March 2015 to build the model for each building. m-fold cross validation is a standard procedure for a model evaluation in ML. The main idea is to randomly split the dataset into m equal subsets.

Table 1. Summary of the data collection for each building

Building ID	Data (no. instances)		
	Train set (Apr 14 - Mar 15)	Test set (Apr 15 - Mar 16)	Total
A	251	249	500
B	349	365	714
C	357	365	722
D	357	365	722
E	347	347	694
F	270	365	635
G	251	249	500
H	357	332	689

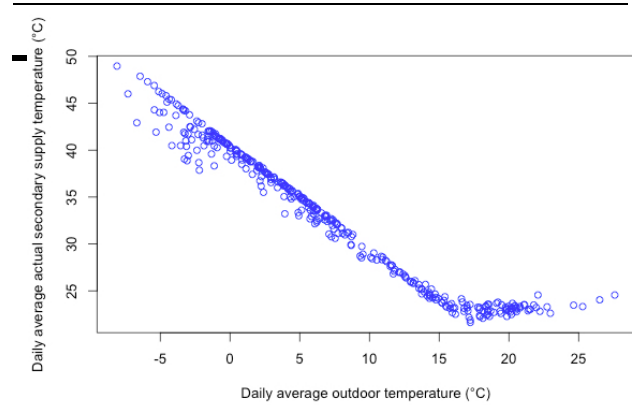


Figure 2. Daily average secondary supply temperature of building D with respect to the daily average outdoor temperature for the year 2015 (365 instances).

The model is trained and tested m times. Each time one of the m subsets is used as a test set and the other m-1 subsets are form the training set. The overall performance of the model is computed as the average error across all m runs [29]. The train set is preprocessed and cleaned to make sure that the DS system only learns the normal behavior of the heating system.

Additionally, the quality of the model is tested with the data from April 2015 to March 2016.

The performance of the system is evaluated in two ways:

- 1) using mean absolute error (MAE) as a performance measure to evaluate the accuracy of SVR in terms of predicting the secondary supply temperature.

$$MAE = \frac{1}{n} \sum_{i=1}^n |\text{actual} - \text{predicted}| \quad (1)$$

In equation (1), the actual refers to the measured secondary supply temperature by the controller system, predicted refers to the estimated secondary supply temperature by the proposed DS system, and n is the total number of predicted instances.

- 2) validating the detected changes by subject matter experts at NODA. In this case the accuracy of the system is calculated based on the number of true positive (TP), true negative (TN), false positive (FP) and false negative (FN) alarms in equation (2). The TPs and TNs are correct classifications. A false positive happens when the result is classified incorrectly as a detected change while it is actually not a change. A false negative occurs when an actual change in the system is not detected [25].

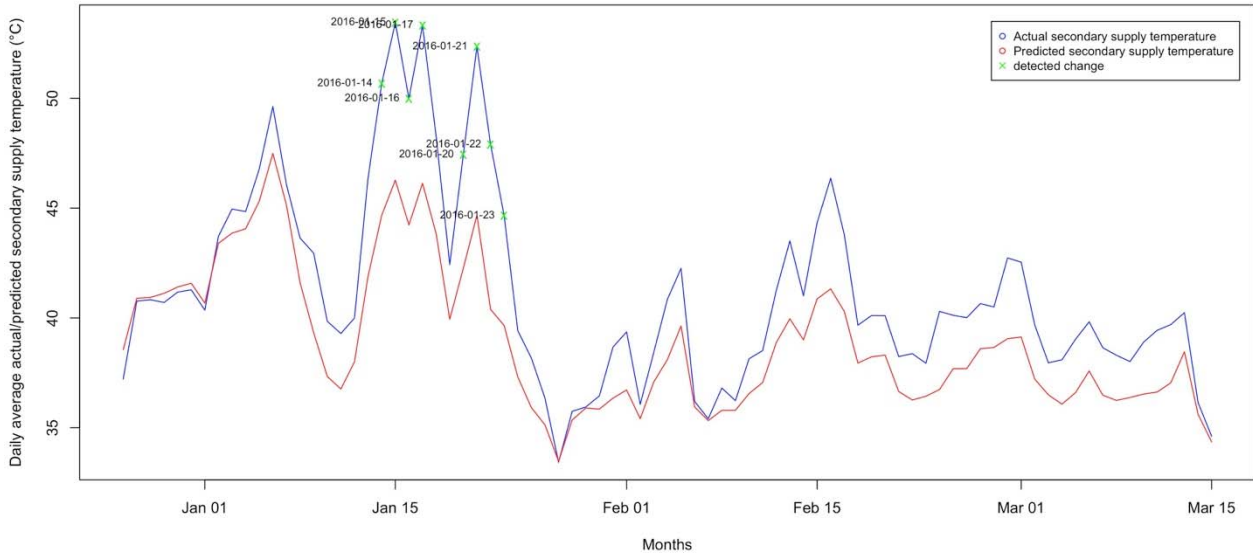


Figure 3. Identified manual changes during January 2016 at the C building. The actual secondary supply temperature is showed in blue against the predicted secondary supply temperature in red. The green crosses identify the detected manual changes by the DS system.

$$Accuracy = \frac{TP + TN}{TP + TN + FP + FN} \quad (2)$$

RESULTS

The performance of the proposed DS system is evaluated by using the test data (April 2015 – March 2016) and 10-fold cross validation for each building. Furthermore, the identified changes at each building is validated with NODA’s experts. Table 2 summarizes the performance of the SVR together with the number of manual detected changes at each building. The results show that the DS system detected, in total 60 changes correctly in 3 out of 9 buildings buildings.

These changes either related to manual changes or hardware failures. This value represents the number of TP alarms. The majority of the results belonged to the TN category with the value of 2,888. The false positive alarms occurred in 2 buildings and in total contain 34 changes. The main reason for these detected changes are related to a sudden drop in the outdoor temperature, and the fact that the system was not trained for such a situation. No false negative is detected during the experiment. By considering these values and using the equation (2) the accuracy of the system can be computed as follow: $(60+2,888)/(60+2,888+34) = 0.98$.

Figures 3 and 4 depict the outcome of the system for

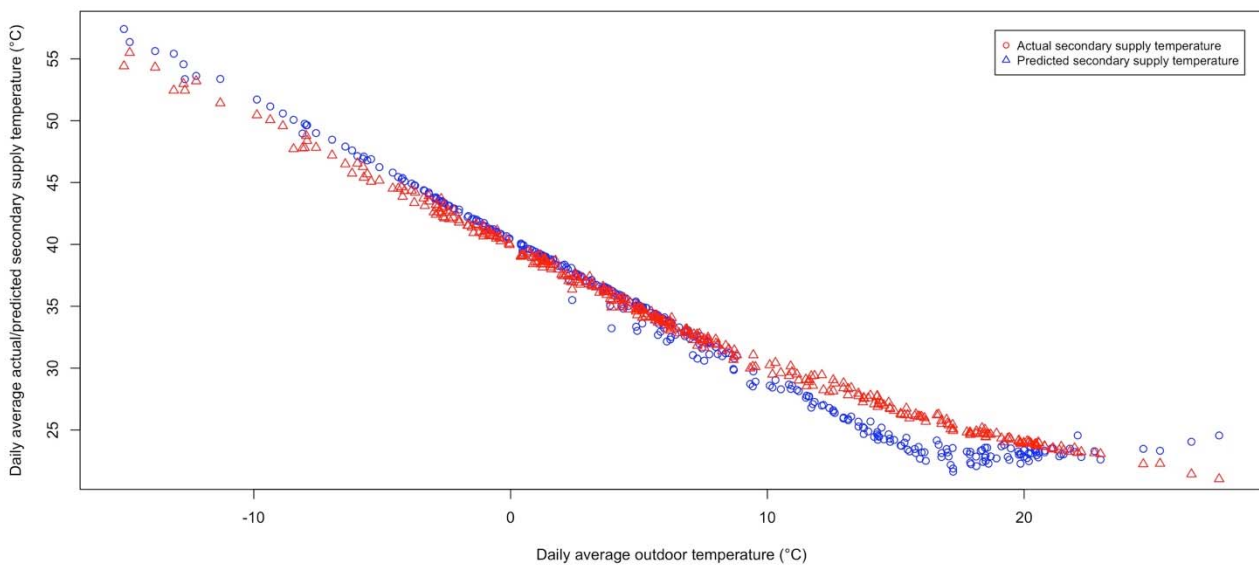


Figure 4. The actual and predicted secondary supply temperature related to building D. This building has no changes during April 2015 – March 2016.

two different buildings. Figure 3 shows the detected manual changes occurred during 14th until 23rd of January 2016 at the C building. These manual changes are related to the modification of the temperature of the heating system. Figure 4 is related to the D building. This building has no changes, which can be seen since the actual and predicted secondary supply temperature are closely following each other's.

DISCUSSION

The experimental results show that the proposed DS system with a two-step classifier is able to detect manual changes within three days after their occurrence. The accuracy of the system is evaluated by the experts from NODA. The results of the evaluation show that the system has a solid detection ability with an accuracy of 98%. In general, the important aspect of such system is its ability to detect changes correctly and does not miss any changes. To decrease the false alarms (both FP and FN) in the detection task, the main solution is to train the system with the data that represents the normal behavior of the heating system. Moreover, only those deviations that last at least three days are classified as manual changes. In addition, considering an adjustable threshold instead of a fix one can decrease the number of false alarms. Though the false positive alarms can be quickly determined and dismissed by experts, considerable number of false alarms can be disturbing.

The proposed DS system is generalizable to similar applications such as detection of change in energy demand or detection of faulty equipment based on abnormal behavior of the heating system.

Table 2. Mean absolute error and standard deviation for SVR and detected changes for each individual buildings

Building ID	MAE	Detected changes			
		TP	TN	FP	FN
A	1.64 (±0.016)	26	223	-	-
B	1.70 (±0.008)	-	358	7	-
C	2.40 (±0.006)	8	357	-	-
D	0.72 (±0.002)	-	365	-	-
E	1.07 (±0.003)	-	320	27	-
F	0.73 (±0.004)	-	365	-	-
G	1.64 (±0.016)	26	223	-	-
H	0.49 (±0.002)	-	332	-	-
I	1.02 (±0.004)	-	345	-	-
<i>Total</i>	-	60	2,888	34	0

Note. MAE = mean absolute error, Standard deviation appears within the parentheses.

CONCLUSION

We propose a decision support system for operators in the district heating domain. Currently, the proposed system is applied to detect manual changes in the heating system at the building level. The decision support system uses a two-step classifier, k-means and support vector regression, to identify manual changes within three days after their occurrence and by considering daily average measurements. The performance of the system is evaluated with the real data related to 9 buildings in Sweden. The validity of the results was investigated by the experts at the NODA Intelligent Systems AB. The validation of the results showed that the majority detected changes by the system were true alarms.

Since each building has special characteristics, e.g. its geographical location, used construction materials, and the social behavior of its tenants, having a fixed threshold for all buildings is impractical. Hence, in the future, it is important to investigate how to automatically set the threshold value for each building. Moreover, it is more convenient that operators can have interaction with the DS system by providing feedbacks. Thus, the performance of the system can improve through time.

ACKNOWLEDGEMENT

This work is part of the research project "Scalable resource-efficient systems for big data analytics" funded by the Knowledge Foundation (grant: 20140032) in Sweden.

REFERENCES

- [1] D. Power, *Decision Support Systems: Concepts and Resources for Managers*. Greenwood Publishing Group, 2002.
- [2] P. Flach, *Machine Learning: The Art and Science of Algorithms that Make Sense of Data*. Cambridge University Press, 2012.
- [3] N. Eriksson, "Predicting demand in district heating systems A neural network approach," *Uppsala University*, 2012. .
- [4] E. Dotzauer, "Simple model for prediction of loads in district-heating systems," *Appl. Energy*, vol. 73, no. 3–4, pp. 277–284, Nov. 2002.
- [5] N. Fumo, "A review on the basics of building energy estimation," *Renew. Sustain. Energy Rev.*, vol. 31, pp. 53–60, Mar. 2014.
- [6] H. Wiklund, "Short term forecasting on the heat load in a DH-system," *Dist. Heat. Int.*, vol. 20, no. 5–6, pp. 286–294, 1991.
- [7] L. Wu, G. Kaiser, D. Solomon, R. Winter, A. Boulanger, and R. Anderson, "Improving

- efficiency and reliability of building systems using machine learning and automated online evaluation,” in *IEEE Long Island on Systems, Applications and Technology Conference (LISAT)*, 2012, pp. 1–6.
- [8] S. Idowu, S. Saguna, C. Ahlund, and O. Schelen, “Forecasting heat load for smart district heating systems: A machine learning approach,” in *IEEE International Conference on Smart Grid Communications (SmartGridComm)*, 2014, pp. 554–559.
- [9] T. Catalina, V. Iordache, and B. Caracaleanu, “Multiple regression model for fast prediction of the heating energy demand,” *Energy Build.*, vol. 57, pp. 302–312, Feb. 2013.
- [10] K. Kato, M. Sakawa, and S. Ushiro, “Heat load prediction through recurrent neural network in district heating and cooling systems,” in *IEEE International Conference on Systems, Man, and Cybernetics (SMC)*, 2008, pp. 1401–1406.
- [11] M. Sakawa, S. Ushiro, K. Kato, and K. Ohtsuka, “Cooling load prediction in a district heating and cooling system through simplified robust filter and multi-layered neural network,” in *IEEE International Conference on Systems, Man, and Cybernetics (SMC)*, 1999, vol. 3, pp. 995–1000.
- [12] S. Provatias, N. Lavesson, and C. Johansson, “An online machine learning algorithm for heat load forecasting in district heating systems,” in *The 14th International Symposium on District Heating and Cooling*, 2014.
- [13] S. Rongali, A. R. Choudhury, V. Chandan, and V. Arya, “A context vector regression based approach for demand forecasting in district heating networks,” in *IEEE Innovative on Smart Grid Technologies - Asia (ISGT ASIA)*, 2015, pp. 1–6.
- [14] K. Marik, Z. Schindler, and P. Stluka, “Decision support tools for advanced energy management,” *Energy*, vol. 33, no. 6, pp. 858–873, Jun. 2008.
- [15] D. Chinese and A. Meneghetti, “Optimisation models for decision support in the development of biomass-based industrial district-heating networks in Italy,” *Appl. Energy*, vol. 82, no. 3, pp. 228–254, Nov. 2005.
- [16] P. Bardouille and J. Koubsky, “Incorporating sustainable development considerations into energy sector decision-making: Malmö Flintränen district heating facility case study,” *Energy Policy*, vol. 28, no. 10, pp. 689–711, Aug. 2000.
- [17] S. N. Petrovic and K. B. Karlsson, “Danish heat atlas as a support tool for energy system models,” *Energy Convers. Manag.*, vol. 87, pp. 1063–1076, Nov. 2014.
- [18] A. Meneghetti and G. Nardin, “Enabling industrial symbiosis by a facilities management optimization approach,” *J. Clean. Prod.*, vol. 35, pp. 263–273, Nov. 2012.
- [19] E. Brembilla and A. Sciomachen, “Design and verification of a large size district heating network by a DSS,” *Methods of Operations Research*, vol. v 64. .
- [20] C. Bordin, A. Gordini, and D. Vigo, “An optimization approach for district heating strategic network design,” *Eur. J. Oper. Res.*, vol. 252, no. 1, pp. 296–307, Jan. 2016.
- [21] A. Sciomachen and R. Sozzi, “The algorithmic structure of a decision support system for a design of a district heating network,” *Comput. Oper. Res.*, vol. 17, no. 2, pp. 221–230, Jan. 1990.
- [22] B.-J. Chen, M.-W. Chang, and C.-J. Lin, “Load Forecasting Using Support Vector Machines: A Study on EUNITE Competition 2001,” *IEEE Trans. Power Syst.*, vol. 19, no. 4, pp. 1821–1830, Nov. 2004.
- [23] A. K. Jain, “Data clustering: 50 years beyond K-means,” *Pattern Recognit. Lett.*, vol. 31, no. 8, pp. 651–666, Jun. 2010.
- [24] V. N. Vapnik, *Statistical Learning Theory*. Wiley, 1998.
- [25] I. H. Witten, E. Frank, and M. A. Hall, *Data Mining: Practical Machine Learning Tools and Techniques: Practical Machine Learning Tools and Techniques*. Elsevier, 2011.
- [26] R. Development Core Team, “R: A language and environment for statistical computing,” *Vienna, Austria R Found. Stat. Comput.*, 2008.
- [27] K. Hornik, C. Buchta, and A. Zeileis, “Open-source machine learning: R meets Weka,” *Comput. Stat.*, vol. 24, no. 2, pp. 225–232, May 2008.
- [28] M. Hall, E. Frank, G. Holmes, B. Pfahringer, P. Reutemann, and I. H. Witten, “The WEKA data mining software: an update,” *ACM SIGKDD Explor. Newsl.*, vol. 11, no. 1, p. 10, Nov. 2009.
- [29] R. Kohavi, “A study of cross-validation and bootstrap for accuracy estimation and model selection,” *Int. Jt. Conf. Artif. Intell.*, 1995.

A METHOD FOR TAKING INTO ACCOUNT SEASONAL STORAGE IN A DISTRICT ENERGY SYSTEM OPTIMISATION PROBLEM

J. Robineau¹, J. Page^{1,2}, F. Maréchal¹

1. EPFL Valais-Wallis, Rue de l'Industrie 17, Sion, CH-1951, Switzerland

2. HES-SO Valais-Wallis, Route du Rawyl 47, Sion, CH-1950, Switzerland

Keywords: *Seasonal storage, Micro-district heating network, Multi-objective optimisation*

ABSTRACT

In this work, a method for taking into account seasonal storage in an energy optimisation problem is developed. A master-slave optimisation procedure is applied, in which the master optimisation is an evolutionary algorithm, while the slave optimisation is a Mixed Integer Linear Programming (MILP) problem. The results of this optimisation can provide insight on the choice of technologies during the study of potential new district heating networks, and especially evaluate if a seasonal storage is worthwhile.

The method developed is applied to a case study. The goal is to optimise the design of a micro-district heating system consisting of 3 buildings and a neighbouring source of industrial waste heat. The technologies considered are heat pumps, solar thermal collectors, a hot water storage tank, geothermal borehole seasonal storage, a gas boiler and industrial waste heat.

The results show that, with the given assumptions, the use of combined seasonal and daily thermal storage can significantly reduce operating costs (by 65 %), fossil fuel consumption and CO₂ emissions, with a payback time of 4.5 years compared to a reference solution with no storage.

INTRODUCTION

The European building sector accounts for 40% of total energy use and 36% of CO₂ emissions [1]. A major part of this energy is used to heat buildings. Renewable sources of heat, such as geothermal and solar, can be harnessed using district heating networks, thus allowing a decrease in CO₂ emission. Moreover, district heating can take advantage of waste heat recovery of energy intensive industries which would otherwise throw it away into the environment.

One of the drawbacks of many renewable or recovery energy sources is that they are intermittent, and are often not synchronised with demand. However, the use of thermal storage systems can greatly increase their share. As the fluctuations can be both daily and seasonal (example of solar), specific storage systems for each of these time scales can be combined. Nevertheless energy storage comes at a cost, typically decreasing with size. The appropriate choice in terms of size and combination of storage types should therefore be the results of a cost optimisation.

Optimisation methods can be applied to support the choice of design and operating strategy of an energy system, including district heating systems. In this work, a master-slave optimisation method was applied to a micro district heating network case study, in order to identify a set of optimal design options for the system. A methodology was developed to integrate seasonal storage in the optimisation, and it was combined with an existing daily thermal storage model.

After a brief literature review of previous work on integration of storage in energy optimisation, the article presents the methodology developed by the authors with a focus on the method to integrate seasonal storage. Then, the case study and main assumptions are presented. Finally, the results of the optimisation are shown and discussed.

STATE OF THE ART

A review of seasonal thermal storage technologies is given in [2]. One of these technologies consists in using the soil as a storage medium. In this concept, vertical boreholes are drilled in the ground to insert tubes in which a heat transport fluid circulates in a closed loop in order to inject (resp. extract) heat in (resp. from) the ground material. One of the advantages of such a system is its lower price compared to other seasonal storage systems, as was observed in [3]. However, these costs do not include the heat pumps which are required to bring the temperature to a useable level.

A review of simulation models used to model seasonal storage is given in [2] that, however, does not consider optimisation. There are numerous examples in the literature of energy supply optimisation models which consider thermal storage. However, they have often been designed for short term thermal storage (e.g. daily) rather than long term storage (seasonal), although some of the principles can be applied to both short and long term storage. An optimisation model including daily thermal storage was implemented in [4], which is also the model that was used for daily storage in this paper. The daily thermal storage is divided into a number of virtual storage tanks with ordered temperature levels. At a given time, a mass of fluid can be transferred from one temperature level to another, exchanging heat with the rest of the system as it does.

The formulation of the model can be used for both optimisation of design and operation. A thermal storage model was also developed in [5], but the 2nd principle of thermodynamics was not considered (the system was divided into high and low temperature). As for long term storage, such a model was implemented for example in [6], but the model is non-linear due to the CHP operation being modelled using 3rd degree polynomials.

Combination of long term and short term storage is rare in the literature. Nevertheless, this was done by Rager in his thesis [7]. In his model, there is a daily storage in a multi-time problem, similar to the one developed by Fazlollahi et al. in [4]. The multi-time problem is embedded in a multi-period problem (i.e. each period is composed of several “times”), and a similar model is implemented at the level of the periods, corresponding to the seasonal storage.

METHODOLOGY

The methodology that was used in the present study consists in the following main steps:

1. Typical days are generated from the available data
2. A specific Mixed Integer Linear Programming (MILP) model is created for each typical day
3. A two stage master/slave multi-objective optimisation is carried out

Generation of typical days

Typical days are used as a means to reduce the complexity of the MILP problem by limiting the number of periods, and hence the number of variables. The generation of typical days was done by applying the k-means centroid clustering algorithm developed by Fazlollahi et al. in [8]. The k-means algorithm minimises the Euclidian distance between each observation (i.e. a real day) and the centre of the cluster (i.e. the typical day) to which it belongs, the distance being calculated over all measurements (i.e. 24 hourly values in a day) of selected attributes (i.e. heating demand, solar irradiance).

The number of clusters was chosen based on the assessment of 3 statistical measures. Additionally, for each attribute, five quality indicators detailed in [8] were calculated in order to compare the typical days obtained with the original data. Once the typical days have been generated, an extreme day is added in order to take into account the highest demand during the year for the sizing of the equipment. Moreover, all of the 365 days of the year are associated to a typical day, and the number of occurrences of each typical day is calculated.

A nearby industry provides a source of waste heat during certain periods of the year. Due to the nature of the industry, the availability of the source is both

intermittent and unpredictable (it can be activated at varying time intervals and for varying durations). To integrate the use of this industrial waste heat, the thermal power and temperature levels have to be defined for each period (i.e. each hour of each typical day). To achieve this, a procedure was developed taking into account the stochastic nature of the industrial waste heat source. The following steps were carried out:

1. The industry’s daily activation profile was created using 3 years of operating data. A boolean variable was associated to each real day if the source was available (i.e. with a heat output >0).
2. As each real day $i \in \{1, \dots, 365 \times 3\}$ over the 3 years of operating data has a corresponding typical day $d \in TD = \{1, \dots, N_d\}$, the probability p_d of activation of the industry was calculated using:

$$p_d = \frac{\text{card}(A_i = 1 \mid d_i = d)}{\text{card}(d_i = d)} \quad \forall d \quad (1)$$

where A_i is the boolean variable corresponding to the activation of the industry during day i and $d_i \in TD$ the typical day which is used to represent that day.

3. Two typical days are derived from each original typical day. In one of the derived typical days, the industry is activated, and in the other it is not. All other data (heating demands, etc.) are identical to the original typical day.
4. The number of occurrences of each derived typical day is calculated using the probability of activation obtained in the previous step and the number of occurrences of the original typical day.
5. The average waste heat load available is calculated for each typical day that the industry is activated. This is done by calculating, for each hour, the average over the 3 years of data represented by the typical day.
6. A similar procedure is applied to calculate the average temperatures of the industrial waste heat source for each typical day, except that the average is only calculated on non-zero values.

It is to be noted that the typical days generated using this method are not sequential, meaning that a given typical day can represent real days scattered across the year.

Mixed Integer Linear Programming model

Each typical day was represented by a specific MILP model. The MILP problem consists in minimising the

operating cost of a set of energy conversion technologies which produce heat, either to fulfil the demand of given buildings, or to store it in daily or seasonal thermal storage units so that it can be used at a later period. The heat cascade constraint is applied to make sure the thermodynamic principles are respected. The problem is multi-period and consists of 24 periods corresponding to the hours of the day. The objective function is expressed as:

$$\min_{y,f} \left[\sum_{p=1}^{N_p} \sum_{u=1}^{N_u} (OC1_u \times y_{u,p} + OC2_u \times f_{u,p}) \times \Delta p \right] \quad (2)$$

where $f_{u,p}$ (resp. $y_{u,p}$) is the continuous (resp. binary) decision variable accounting for the usage level (resp. activation) of unit $u \in U$ during period $p \in \{1, \dots, 24\}$. The set of units U is composed of all the energy conversion technologies, building demands to satisfy, energy sources and storage technologies. $OC1_u$ and $OC2_u$ are the fixed and variable operating costs, respectively, associated to unit u . No investment cost is considered in the MILP model.

It is subject to the following constraints:

- The usage of unit u during period p is governed by:

$$F_u^{\min} \times y_{u,p} \leq f_{u,p} \leq F_u^{\max} \times y_{u,p} \quad \forall u, p \quad (3)$$

where F_u^{\min} and F_u^{\max} are the minimum and maximum capacity of unit u respectively. Their values can be fixed by the master optimisation. The usage level of building demands is fixed and equal to 1.

- For each temperature interval $k \in K = \{1, \dots, N_k\}$, the heat cascade constraint is defined as follows:

$$\sum_{u=1}^{N_u} \left[f_{u,p} \times \left(\sum_{u_h=1}^{N_{u_h}} \dot{Q}_{u_h,k,p} - \sum_{u_c=1}^{N_{u_c}} \dot{Q}_{u_c,k,p} \right) \right] + \dot{R}_{k+1,p} - \dot{R}_{k,p} = 0 \quad \forall k, p \quad (4)$$

$$\dot{R}_{k,p} \geq 0 \quad \forall k, p, \quad \dot{R}_{1,p} = 0, \quad \dot{R}_{N_k,p} = 0 \quad \forall p \quad (5)$$

where $\dot{Q}_{u_h,k,p}$ (resp. $\dot{Q}_{u_c,k,p}$) represents the reference heat requirement of the hot stream u_h (resp. cold stream u_c) associated to unit u , in temperature interval k and period p . $\dot{R}_{k,p}$ is a

continuous variable for the residual heat from the temperature interval k , which cascades down to the lower temperature interval $k - 1$.

There are two types of thermal storage units included in the model: daily storage and seasonal storage. For the daily storage, the model from Fazlollahi et al. in [4] was used. The storage is discretised into 3 temperature levels: 25, 50 and 75°C. The heat can be charged into the storage either at low temperature, corresponding to a cold stream going from 25 to 50 °C (discharge via a hot stream: 50 to 25°C), or high temperature, corresponding to a cold stream going from 50 to 75 °C (discharge via a hot stream: 75 to 50°C). The generic set of equations describing the daily storage can be found in [4]. The total daily storage volume (high temperature + low temperature) is fixed in the MILP problem, but can be a decision variable of the master optimisation.

Multi-objective optimisation

A master-slave optimisation procedure was applied and is illustrated in Figure .

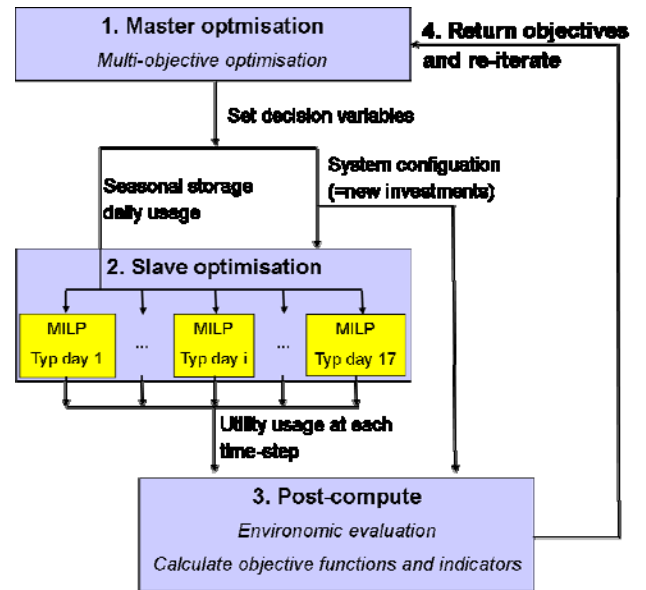


Figure 1. Master slave optimisation procedure

The following steps are carried out at each iteration, for a given number of iterations:

1. The multi-objective master optimisation generates a set of continuous and binary decision variables. These decision variables control both i) the existence, sizing and overall operation of the seasonal storage, and ii) the selection and sizing of the daily storage units and energy conversion technologies. The algorithm used here is the evolutionary algorithm developed by Leyland in his PhD thesis [9].

2. The decision variables of the master optimisation are passed on to the slave optimisation, which is in fact a set of independent MILP optimisation sub-problems (one for each typical day).
3. The results of all the slave optimisations as well as the decision variables of the master optimisation are passed on to a post compute function which calculates the objective functions of the master optimisation, as well as any other indicator.
4. The objectives are returned, evaluated and ranked by the master optimisation, which can then generate a new set of decision variables and re-iterate the whole process.

Seasonal storage model

In the MILP sub-problem, the seasonal storage is represented as two units: one unit associated to a cold stream representing the charging (the cold stream is taking heat from the system), one unit associated to a hot stream representing the discharging of the storage (the hot stream is providing heat to the system).

The temperatures of the hot and cold streams are rough assumptions based on the study carried out in [10] and are defined as follows:

- In charging mode: the temperature of the fluid injected into the seasonal storage was set to 40°C. This means that any source of heat at a higher temperature can be charged into the seasonal storage. The output temperature (which also has to be fixed to define the cold stream) was set to 20 °C. This requires the soil to be at a lower temperature.
- In discharging mode: the temperature of the fluid extracted from the storage was set to 25°C, which means that a heat pump would need to be installed to increase the temperature to a level compatible with the demand. Similarly, this requires the soil to be at a higher temperature. This is only valid under the assumption that enough heat has been stored in the soil. The input temperature was set to 5°C (i.e. evaporator of a heat pump).

The total amount of heat Q_{ss}^{in} (resp. Q_{ss}^{out}) that can be charged (resp. discharged) into (resp. from) the seasonal storage over a day is fixed for a given typical day. This leads to the following equations:

$$\sum_{p=1}^{24} f_{ss,p}^{in} \times \dot{Q}_{ss,p}^{in} = Q_{ss}^{in} \quad (6)$$

$$\sum_{p=1}^{24} f_{ss,p}^{out} \times \dot{Q}_{ss,p}^{out} = Q_{ss}^{out} \quad (7)$$

where $\dot{Q}_{ss,p}^{in}$ (resp. $\dot{Q}_{ss,p}^{out}$) is the reference heat requirement of the seasonal storage charging (resp. discharging) unit at period p , and $f_{ss,p}^{in}$ (resp. $f_{ss,p}^{out}$) is the usage level decision variable of the same unit.

The decision variables of the master optimisation dealing with the seasonal storage are:

- The existence of the seasonal storage Y_{ss} (binary variable)
- The total amount of heat $Q_{ss,d}$ (continuous variable) that can be charged or discharged each typical day d except one which is left out in order to balance the storage over the year. $Q_{ss,d}$ takes a positive value if it is charged, and a negative value if it is discharged.

Those decision variables are used to define the seasonal storage constraints of the MILP sub-problems through the following equations:

$$Q_{ss}^{in} = \begin{cases} Y_{ss} \times Q_{ss,d} & \text{if } Q_{ss,d} \geq 0 \\ 0 & \text{otherwise} \end{cases} \quad \forall d \quad (8)$$

$$Q_{ss}^{out} = \begin{cases} 0 & \text{if } Q_{ss,d} \geq 0 \\ -Y_{ss} \times Q_{ss,d} & \text{otherwise} \end{cases} \quad \forall d \quad (9)$$

This means that for a given day, the seasonal storage can either be in charging or discharging mode (not both on the same day).

In order to close the energy balance of the seasonal storage over the year, the energy charged into the storage for one of the typical days $d' \in TD$ is calculated (instead of being a free decision variable) using:

$$Q_{ss,d'} = \frac{1}{n_{d'}} \times \left(\sum_{\substack{d \in TD \\ d \neq d'}} Q_{ss,d} \times n_d \right) \quad (10)$$

where n_d is the number of occurrences of typical day d during the year.

The choice of the “balancing” typical day corresponds to the one with the highest number of occurrences. A higher number of occurrences $n_{d'}$ makes $Q_{ss,d'}$ less sensitive to variations in the decision variables $Q_{ss,d}$ and therefore reduces the risk of having unrealistic values.

The size of the borehole storage l_b (i.e. total length) is calculated in such a way that the maximum daily

charge or discharge can be exactly fulfilled if it is operated at the maximum power throughout the whole day (linear thermal power of 40 W/m was taken from [10]):

$$l_b [\text{m}] = \frac{\max_{d \in TD} |Q_{ss,d}|}{40 \left[\frac{\text{W}}{\text{m}} \right] \times 24 [\text{h}]} \quad (11)$$

The maximum charging/discharging rate is also fixed in the MILP sub-problem based on these values:

$$f_{ss,p}^{in/out} \times \dot{Q}_{ss,p}^{in/out} \leq 40 \times l_b \quad \forall p \quad (12)$$

To choose the range of decision variables $Q_{ss,d}$, the assumption was made that if the daily demand of all the buildings was lower than the average daily demand during the year, then the seasonal storage should only be able to discharge heat ($Q_{ss,d} \leq 0$). On the contrary, it should only be able to charge ($Q_{ss,d} \geq 0$). Moreover, the maximum energy that can be charged into or discharged out of the seasonal storage on any given day corresponds roughly to the maximum daily solar heat produced.

CASE STUDY

The methodology described above was applied to a case study. The goal was to optimise the heat supply system of a micro-district consisting of 3 office buildings, where only space heating was considered. Out of the 3 buildings, 2 already exist (TB and EB) and they both have an existing independent heat supply infrastructure (the two buildings are currently not connected via a district heating network). Building TB is equipped with a gas boiler of 1000 kW, while EB has 285 m² of solar thermal collectors and two ground source heat pumps of 52 kW_{el} each. The third building (FB) is currently being planning and its heat supply system has yet to be decided.

The idea is to connect the three buildings via a micro-district heating network (μ -DHN) in order to share the infrastructure and maximise the use of fossil-free energy sources. The μ -DHN is also connected to a nearby industry providing an intermittent source of waste heat. The μ -DHN/building interface is bi-directional, meaning that buildings can either provide or take heat. The other technologies that were considered as investment options in the optimisation were: geothermal borehole (seasonal storage), a hot water tank (daily storage) and a high temperature heat pump.

RESULTS

The attributes used for the generation of the typical days were the simulated hourly heating demand profiles of the two existing buildings TB and EB and the hourly solar irradiance profile for a reference year. For the heating demand of building FB, a scaling factor of 256/190 was applied to the demand profile of EB. The extreme day was chosen based on the peak demand of TB.

Applying the methodology described above, 9 typical days (including the extreme day), each consisting of 24 hourly values, were generated to represent the yearly profiles.

As described in the methodology, those typical days were then duplicated to take into account the availability of the industrial waste heat source. This then led to 17 typical days, for which the data on availability, heat load and temperatures of the waste heat were also known. The extreme day was not duplicated as there was only one (the waste heat source was activated during that day).

The multi-objective optimisation procedure described above was applied to the case study, whereby the two objective functions were:

- Investment cost: only the investment cost of new equipment was considered, including the investment cost of the μ -DHN which was chosen by default.
- Operating cost: only fuel and electricity costs were considered (e.g. no maintenance).

The decision variables of the master optimisation were the existence of the technologies considered as investment options, the size of the technologies and the daily usage of the seasonal storage for each typical day except one. The size of the latter (number and depth of boreholes) results from the decision variables chosen for the daily usage. The range of values that the decision variables could take is given in **Table 1**.

Table 1. List and range of values of master decision variables

Decision variable	Range
Seas. storage (on/off)	{0;1}
Seas. storage (daily usage in kWh)	[-1000;0] or [0;1000] (depending on typ. day)
Daily storage (on/off)	{0;1}
Daily storage (size in m ³)	[10;353]
HP (on/off)	{0;1}
HP (size in kW _{el})	[30;300]

In the slave optimisation, where the operation of the system is optimised for each typical day, heat can only be supplied from a higher temperature heat source (hot stream) to a lower temperature heat sink (cold stream). This constraint is respected thanks to the heat cascade described in equation (4). The temperature levels of all the hot and cold streams are given in **Table 2**. The input and output temperatures of the cold streams representing the buildings' heating demand are a function of the outdoor temperature, as are the heating requirements. The heat pumps have a constant hot stream and cold stream temperature for the condenser and evaporator respectively. The condenser temperature can be optimised in order to adapt to the building requirements while maximising the coefficient of performance. This is achieved by representing the heat pump as several units, each associated to a different condenser hot stream, and adding a constraint that prevents more than one of these units to be activated at a given period (in order to prevent duplication of the heat pump). Excess heat which is not stored in one of the storage units is dissipated in a "free" cooling tower.

Table 2. Input/output temperatures of all hot and cold streams in the case study

Name	T _{in} / T _{out} (°C)
TB demand	Function of outdoor temp. (max: 60 / 80)
EB/FB demand	Function of outdoor temp. (max: 35 / 45)
Gas boiler	210 / 190
Solar thermal	85 / 50
Low-temp. HP	Evap: 6 Cond: 30 - 55
High temp. HP	Evap: 10 - 20 Cond: 40 - 80
Industrial waste heat	60 / 25
Ground water source	10 / 13
Low-temp. daily storage	25 / 50 (charging mode)
High-temp. daily storage	50 / 75 (charging mode)
Seasonal storage	Charging mode: 20 / 40 Discharging mode : 25 / 5

The results of the multi-objective optimisation are represented on **Figure 2**. On this graph, each point represents a solution of the multi-objective optimisation (corresponding to a given set of master decision variables). The value of one objective (operating cost) is plotted against the other (investment cost) for each solution. The results shown here took around 2 days to obtain using Matlab 2014b running on a computer with the following characteristics: Intel Core i7-4600U CPU @ 2.1 GHz, 8 Gb RAM, Windows 7 64 bits.

The colours used in **Figure 2** show the superstructure of each solution, that is to say the technology choices regardless of their size (i.e. the combination of binary decision variables). For a given superstructure, different solutions are obtained due to the variation of the continuous decision variables. As the reference solution corresponds to the case where no new equipment is chosen (all binary decision variables set to 0), the system configuration cannot vary, leading to a unique solution. The investment cost of the reference solution corresponds to the μ -DHN, which is always present.

The first observation which can be made is that the demand of the future building FB can entirely be fulfilled with the existing heat supply systems providing that a heating network is installed to connect the buildings together and with the industry. This solution corresponds to the lowest investment, but also has the highest operating cost among Pareto solutions.

On the other end of the spectrum, the solution giving the lowest operating cost uses all the investment options available. Compared to the reference, it requires an additional investment of 142 k€, but allows 32 k€ of savings per year, leading to a theoretical payback time of 4 years and 6 months with the economic assumptions that were taken.

Table 3. Investment choices for selected Pareto solutions

	Seas. stor. ⁷ (m)	Daily stor. (m ³)	HP (kW _{ei})
1	943	43	84
2	996	11	49
3	798	0	78
4	0	10	120
5	0	0	67
6	0	10	0

⁷ For sizing of the seasonal storage, the total borehole length in metres is considered here. This total length then needs to be divided into a number of boreholes which each have a limited depth.

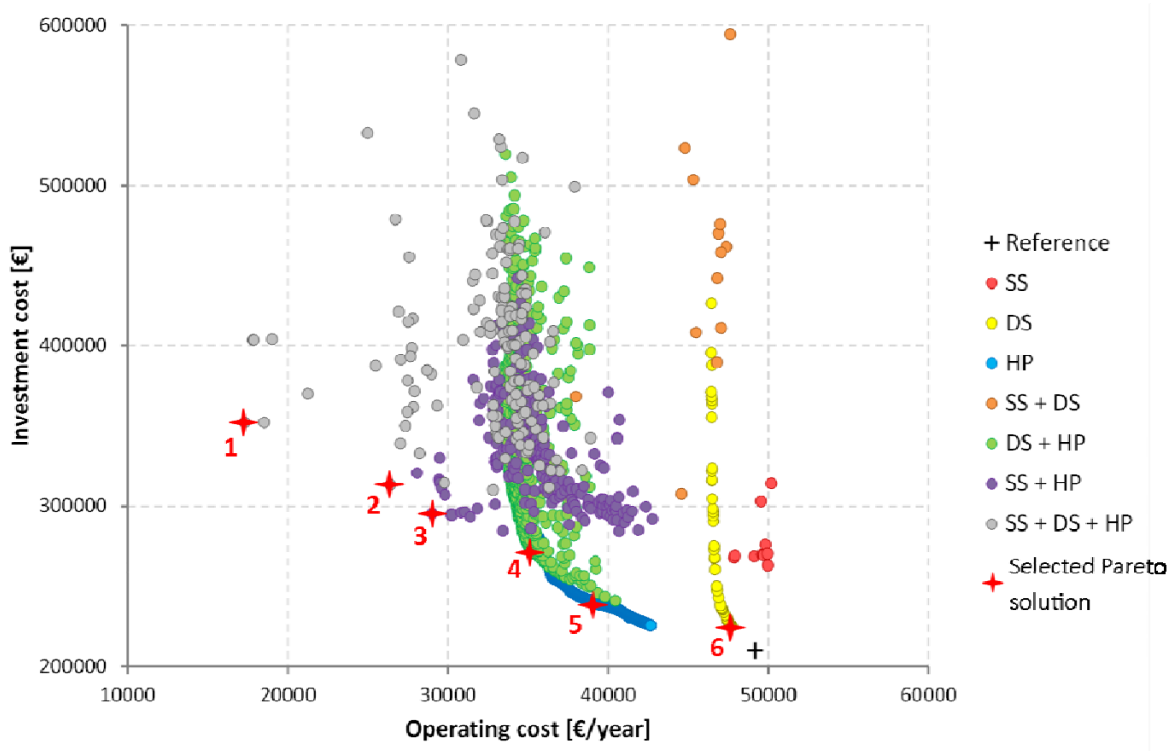


Figure 2. Superstructure of the 5012 solutions of the multi-objective optimisation (SS: seasonal storage; DS: daily storage; HP: heat pump)

The solutions of the Pareto front can be broken down into different “clusters”, which are mostly differentiated by their superstructure. **Table 3** zooms on 6 Pareto optimal solutions which are shown on **Figure 2**, and which are each representative of a cluster of solutions.

DISCUSSION

A closer analysis of the results show that the seasonal storage is only interesting when combined with a new high temperature heat pump (points in grey and purple in **Figure 2**). Indeed, the heat available from the seasonal storage is too low to be used anywhere, and the existing heat pumps are already used at full capacity to supply heat to the low temperature buildings. As a result, it would be a good idea to force the selection of the heat pump to be chosen if the seasonal storage is chosen. This would result in reduced search space and therefore faster convergence towards optimality.

Depending on the solution, 5 to 19 % of the heat demand transits in the seasonal storage, if it exists. This corresponds to between 62 and 226 % of the solar heat produced, meaning that most of the heat stored in the seasonal storage must come from the industrial waste heat. In fact, a lot of the heat stored in the seasonal storage is dissipated in the cooling tower. This happens because the daily amount of heat going

into/out of the seasonal storage is fixed in the master, leading to constraints in the MILP problems which have to be fulfilled no matter what. To prevent this, restricted matches should be applied between the seasonal storage and the cooling tower. Also, the range of values for the decision variables of the seasonal storage should be chosen more wisely. Finally, a cost factor should be applied to the cooling tower to reduce its use.

A very different behaviour is observed between solutions with and without seasonal storage. The latter tend to converge nicely towards a well-defined Pareto front for each superstructure, which clearly marks the boundary between feasible and non-feasible solutions. On the other hand, solutions with seasonal storage are very scattered and no clear Pareto front can be identified. This can be explained by the fact that the size and operating strategy of the seasonal storage is defined by the combination of 16 decision variables in the master optimisation, leading to a complex interaction between those decision variables and the objective functions, whereas it is only defined by one decision variable for the other equipment. As a consequence, the best solutions obtained with seasonal storage are most likely not the optimal ones, and perhaps better solutions could be obtained should more iterations be carried out.

A major limitation in the current model should be pointed out here, and improved in the future. This concerns the temperature level of the storage. According to the temperature levels that were chosen for the hot and cold streams, the soil should be below 20°C in charging mode, and above 25°C in discharging mode. In reality, this corresponds to a case where the soil has been heated up prior to the cycle, as the average temperature of the soil is usually lower than that. Moreover, the temperature of the soil depends on the charge state, and the hot/cold stream temperature should be adapted accordingly. For example, at the beginning of summer, the temperature of the soil will be lower than at the end of summer, and it is easier to charge the storage at that period. However, the optimisation cannot know the charge state because the typical days are not sequential (each typical day corresponds to as many charge states as its number of occurrences). Obtaining a reasonable number of sequential typical days is very tricky because of the stochastic nature of the activation of the waste heat source. Finally, heat losses should also be accounted for, but this would also require the typical days to be sequential.

CONCLUSION

In this work, a methodology for integrating seasonal storage in a district energy system optimisation has been developed. A master-slave optimisation procedure was used, in which the master is a multi-objective evolutionary algorithm and the slave a set of independent MILP problems. The master decision variables are the investment choices, but also the daily amount of heat charged or discharged into/out of the seasonal storage.

The methodology was applied to a case study where the goal was to optimise the design of the heat supply system of a micro-district heating network consisting of 3 buildings and a neighbouring source of industrial waste heat. The technologies considered were heat pumps, solar thermal collectors, a hot water storage tank, geothermal borehole seasonal storage, a gas boiler and industrial waste heat.

The results showed that the use of combined seasonal and daily thermal storage can significantly reduce operating costs (by 65 %), with a payback time of 4.5 years compared to a reference solution with no storage. However, these results are most likely sub-optimal due to the large search space which was not fully explored and complex interaction between decision variables and objective values.

Although the case study presented in this work is simple, the methodology developed for the seasonal storage can be used in case studies including more

technologies. The results can provide insight on the choice of technologies during the study of a new DHN.

OUTLOOK

Several perspectives of improvement to the seasonal storage model have been identified and need to be addressed:

- systematic coupling of seasonal storage and heat pump
- improving the range of values for the seasonal storage decision variables
- taking into account heat losses and variation of soil temperature

The last point requires having sequential typical days, which is challenging when there is a stochastic heat source independent of the time of year. An option could be to consider longer typical operating periods (e.g. typical weeks). Another option would be to produce a dynamical simulation of a handful of optimisation results, with either actual waste heat production data or Monte Carlo time series based on the actual data, as a validation of their feasibility.

ACKNOWLEDGEMENTS

The authors gratefully acknowledge the European Commission for providing financial support during the conduct of research under the FP7-PEOPLE-2013 Marie Curie Initial Training Network "CI-ENERGY" project with Grant Agreement Number 606851.

This method was applied in the Austria research project called 'RecoverHeat' funded by the Austrian 'Klima- und Energiefonds' within the programme "Energy Mission Austria" and the 1st Call of "e!MISSION" 2012, FFG project number 838769.

We thank our research partners for their valuable collaboration in particular the team from the Austrian Institute of Technology (AIT), especially Tim Selke and Renate Teppner, as well as Edith Haslinger and Olivier Pol (ATP), without whose inputs an important part of this work would not have been possible.

REFERENCES

- [1] J. O. Lewis, S. N. Hógáin, and A. Borghi, 'Cities of Tomorrow – Action Today. URBACT II Capitalisation. Building energy efficiency in European cities', May 2013.
- [2] P. Pinel, C. A. Cruickshank, I. Beausoleil-Morrison, and A. Wills, 'A review of available methods for seasonal storage of solar thermal energy in residential applications', *Renew. Sustain. Energy Rev.*, vol. 15, no. 7, pp. 3341–3359, Sep. 2011.

- [3] T. Schmidt, D. Mangold, and H. Hüller-Steinhagen, 'Seasonal thermal energy storage in Germany', presented at the ISES Solar World Congress, Göteborg, Sweden, 2003.
- [4] S. Fazlollahi, G. Becker, and F. Maréchal, 'Multi-objectives, multi-period optimization of district energy systems: II—Daily thermal storage', *Comput. Chem. Eng.*, vol. 71, pp. 648–662, Dec. 2014.
- [5] D. Steen, M. Stadler, G. Cardoso, M. Groissböck, N. DeForest, and C. Marnay, 'Modeling of thermal storage systems in MILP distributed energy resource models', *Appl. Energy*, vol. 137, pp. 782–792, Jan. 2015.
- [6] T.-M. Tveit, T. Savola, A. Gebremedhin, and C.-J. Fogelholm, 'Multi-period MINLP model for optimising operation and structural changes to CHP plants in district heating networks with long-term thermal storage', *Energy Convers. Manag.*, vol. 50, no. 3, pp. 639–647, Mar. 2009.
- [7] J. M. F. Rager, 'Urban Energy System Design from the Heat Perspective using mathematical Programming including thermal Storage', EPFL, Lausanne.
- [8] S. Fazlollahi, S. L. Bungener, P. Mandel, G. Becker, and F. Maréchal, 'Multi-objectives, multi-period optimization of district energy systems: I. Selection of typical operating periods', *Comput. Chem. Eng.*, vol. 65, pp. 54–66, Jun. 2014.
- [9] G. B. Leyland, 'Multi-objective optimisation applied to industrial energy problems', EPFL, Lausanne, 2002.
- [10] E. Haslinger, M. Fuchsluger, and R. Niederbrucker, 'RecoverHeat Deliverable D2.1: Subjects report Geothermal use of the subsurface at the site XXX', Austrian Institute of Technology, 838769, May 2014.

HYDRAULIC BALANCING OF DISTRICT HEATING SYSTEMS OPERATED ACCORDING TO A PUSH PRINCIPLE

O. Gudmundsson¹, J.E. Thorsen¹, C. Thybo¹

¹ Danfoss A/S, Heating Segment, Application and Technology, Nordborgvej 81, Nordborg, 6430, Denmark
og@danfoss.com

Keywords: *Fixed billing, Fair distribution, Hydraulic balance, Push philosophy*

ABSTRACT

There is a fundamental difference in the operating principles between Chinese and Western district heating (DH) systems. Unlike Western DH systems, which are consumer driven, the Chinese DH systems operate according to the principles of planned economy. The planned economy approach in the Chinese systems results in heat generated is decided at the plant level fulfilling the basic heat demand of the connected consumers, which is to achieve 18°C indoor air temperature. Further, the consumers pay fixed fee based on square meters for the heat, unlike in Western systems which are billed according to the heat consumption. These differences result in that Chinese systems are typically operated as PUSH systems, where heat is delivered independent if the consumer needs it or not, while Western systems are operated as PULL systems, where the consumer is in control of how much heat is received. Modern district heating control equipment has been developed with focus on fulfilling the requirements of PULL systems, leading to a gap between the available control equipment and what the PUSH systems need to ensure good hydraulic balance and fair distribution of the heat supply. In PUSH systems the time delay from the time a change at the heat source is carried out until it reaches the buildings becomes an issue, once the change reaches the building the supply is out of phase with the demand, leading to the tendency to generally oversupply. To ensure energy efficient operation of PUSH systems Danfoss has developed a new control solution that operates according to the PUSH principles by adjusting the heat supply at the area substation with respect to the change at the heat source. This effectively takes out the transportation delays and minimizes the oversupply at the same time. Using this new control solution significant energy savings and consumer comfort increase can be achieved.

INTRODUCTION

In 1953 the urban percentage of the total Chinese population was about 13.3%, since then there has been a very rapid urbanization and currently the urban percentage is about 56.1%. At the same time the population of China has grown from about 583 million to 1,376 million people. This rapid growth and urbanization has required rapid built up of the

infrastructure, there among the district heating in the northern part of China. Today the Chinese heating market is the second biggest one in the world, with 3,2 PJ DH sales in 2013 [1] and is expected to grow due to ongoing urbanization and higher comfort demands.

The initial introduction of district heating to China was through the Soviet Union and was then further developed in accordance to the initial mind set. In short the Chinese philosophy in regards to district heating has been that it is the role of the local government to supply the urban population with a minimum heat supply to achieve 18°C indoor air temperature and the consumer only pays a fixed price according to the number of connected heated square meters. In this approach all consumers should be treated equally and the flow should be split fairly among them, although taking into account the different building conditions. To achieve this, the traditional approach has been to run the main pumps, located at the heat plant, at a constant head and apply manual balancing valves in the distribution network and buildings, see Figure . In a report from the Chinese Ministry of Housing it is stated that room temperature regulation and control functions are applied in only 16% of the total heating area in China [2]. Due to a lack of automatic controls the heat supply is then adjusted at the heat plant according to the outdoor air temperature. As the aim is only to deliver enough heat to achieve 18°C indoor air temperature the general assumption has been that there is no need for automatic controls. This has however resulted in very inefficient systems. According to a World Bank report in 2012 the heat consumption per square meter in China is almost twice that in developed countries, which have comfort heating, at the same latitude [3]. The high heat consumption is due to low insulation levels and inefficient controls. In the 2011 Annual Report on China Building Energy Efficiency [4] it is stated that at least 15%-30% of the total heat is being lost due to excessive heat supply, i.e. overheating of apartments. The oversupply could even be underestimated.

In comparison, the western district heating systems are running under a different philosophy. In the western heating system the aim is to provide the consumer service, the consumer is given the freedom to choose his own indoor air temperature and then pays according to his measured heat consumption. This has

resulted in the general requirement of automatic controls at all levels in the systems.

This paper will underline the differences between the Chinese and western district heating systems, give explanation on why control of Chinese district heating systems is problematic and propose a new solution to control the system.

COMPARISON OF CHINESE AND WESTERN DISTRICT HEATING SYSTEM PHILOSOPHIES

The basic philosophy of district heating systems can be described as:

- Achieve maximum energy utilization of input fuels
- Distribute the heat from a central heat source via pipe network to its connected users
- Minimize losses in the distribution system
- Utilize the most economic and environmental friendly heat source at any given time
- Provide stable, secure and uninterrupted heat supply
- Fulfill the heating demand of the connected users

Those basic points are applied in both Chinese and Western district heating systems, but in a slightly different way.

In the western district heating the aim is to provide comfort, that is, the heat user can decide how much heat he is drawing off the system and then he pays for

the heat according to a heat meter. The system is comfort driven in the way that the user will apply individual controls to adjust his heat consumption, typically this would be thermostatic radiator valves. This kind of a system is generally referred to as a PULL system, the user will pull the heat from the network when he needs it.

In the Chinese district heating systems the aim is to provide basic heat service, which is decided to be 18°C by the government. Here the approach is that the heat output from the heat plant is decided according to the outdoor air temperature and is then distributed fairly around the system with a constant flow principle, that is, the main pump will operate at a constant head. The heat distribution is then in theory achieved by adjusting manual valves in the beginning of the heating season so that each consumer gets his fair share of the heat supply and then the valves are kept at fixed opening to the end of the heating season. As 18°C indoor temperature is considered to be a basic service the consumers only pay according to the connected square meters, independent on their actual heat consumption. This kind of a system is generally referred to as a PUSH system, the heat is pushed to the user independently if he wants it or not.

PROBLEMS WITH PUSH SYSTEMS

Difficulties with balancing of PUSH systems

The general control equipment in PUSH systems is manual balancing valves. Carrying out commissioning in a manual controlled system can be quite difficult and

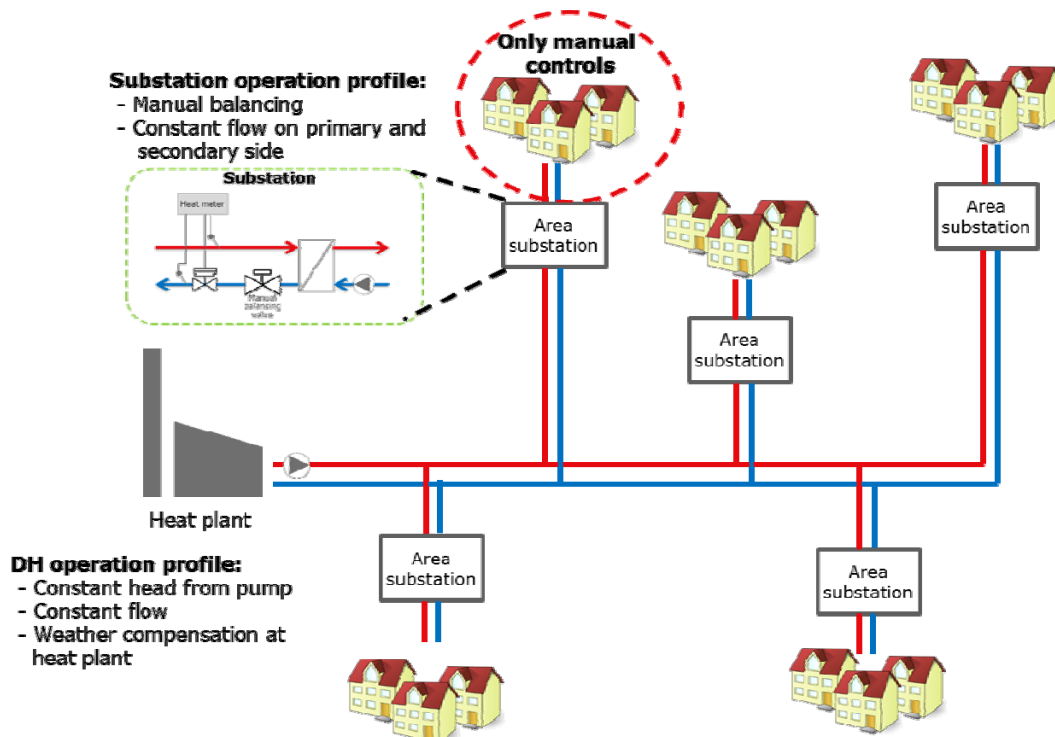


Figure 1. Example of a typical Chinese district heating system.

time consuming, especially if the system covers a large area and has many connections that need to be adjusted. The experience in China indicates that it can take the first 3-4 weeks in each heating season to make initial and to some extent acceptable adjustments of the manual valves. Even after the initial adjustments the experience shows that constant adjustments are needed to adapt the flow to the actual situation in the system. This can easily lead to control issues as any valves changes in the network will change the system characteristics and consequently influence consumers downstream. This can be shown by using a simple static model of 5 substation, see Figure 2.

In the model both pipes and valves are modelled through a k_v value, which indicates the flow rate through the pipe section or valve under standard conditions, typically 1 bar pressure drop across the unit. Given the available head and k_v values the flow through each of the pipe sections and valves can be estimated with Eq. 1.

$$Q = k_v \sqrt{\Delta P} \quad (1)$$

The difficulties of keeping a balance in a manual balancing system can be shown by keeping the pump head constant, as is the general case in China, and vary the k_v value at one of the substations. In Figure 3 the impact a change in one substation has on the rest of the system is shown. From the figure it can clearly be seen that a change in one substation will impact the rest of the substation, although the main impact will be downstream, while upstream substations will experience limited impact.

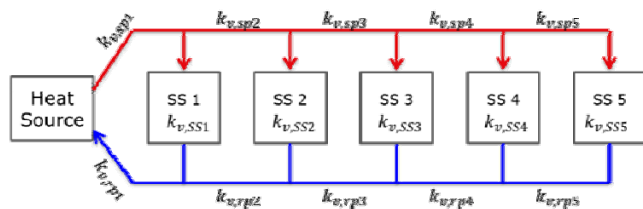


Figure 2. Example of a simple district heating model where pipes and substations are represented with a k_v value.

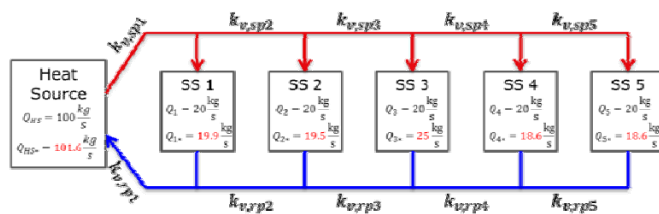


Figure 3. Example of how a change in one substation affects the hydraulic balance of the whole system. $Q_{\#}$ marks the original flow and $Q_{\#*}$ the flow rate after the change in substation 3.

Table 1 shows the impact on the substations given the case considered.

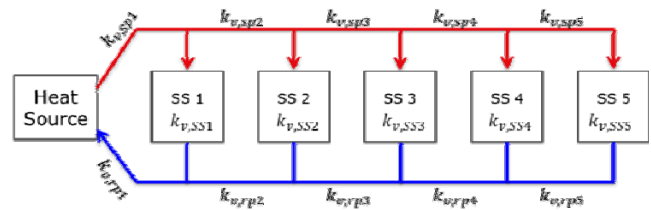


Figure 2. Example of a simple district heating model where pipes and substations are represented with a k_v value.

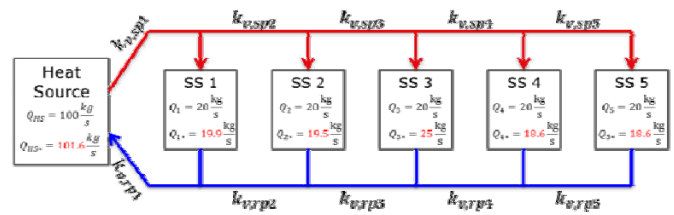


Figure 3. Example of how a change in one substation affects the hydraulic balance of the whole system. $Q_{\#}$ marks the original flow and $Q_{\#*}$ the flow rate after the change in substation 3.

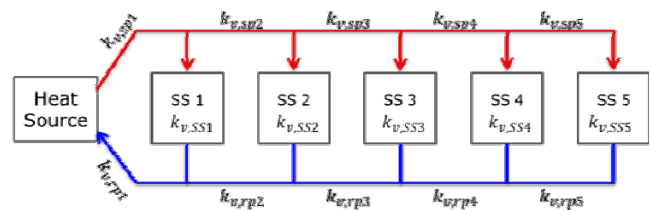


Figure 2. Example of a simple district heating model where pipes and substations are represented with a k_v value.

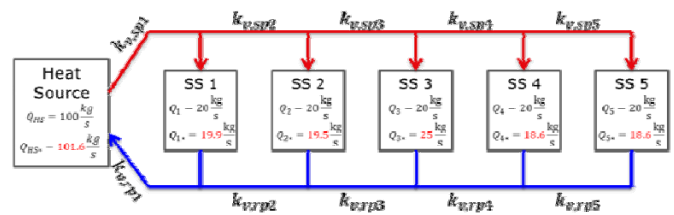


Figure 3. Example of how a change in one substation affects the hydraulic balance of the whole system. $Q_{\#}$ marks the original flow and $Q_{\#*}$ the flow rate after the change in substation 3.

Table 1. Flow changes along the network as the flow in substation 3 is increased.

Substation	Flow change	Relative change in %
SS 1	20 → 19.9	-0.5%
SS 2	20 → 19.5	-2.5%
SS 3	20 → 25	25%
SS 4	20 → 18.6	-7%

SS 5	20 → 18.6	-7%
Total	100 → 101.6	+1.6%

The simple explanation for this behaviour is that since the pump head is constant the total flow will depend on the total k_{v} value, $k_{v, total}$, of the system. If the $k_{v, total}$ increases the total flow rate through the system increases. This increase in the total flow rate will result in higher pressure drop in the pipe network, which will then result in decrease in available pressure head across the substations. The impact on the flow through the valve will then depend on the relative change in the available pressure across the valve. In the first substations the impact will be small as the relative change of the available pressure head across the valve is small, in the last substations the relative change in the available pressure head will be large and therefore cause large changes in the flow rates through the substations. The same issues will rise in case there is a need to reduce the flow rate in one of the substation, except in that case the flow will be redistributed to the rest of the consumers, with the biggest impact on downstream substations.

Due to this inherent nature of manual balancing the actual operation of large networks becomes very tricky and will generally lead to overall oversupply to avoid customer complaints. The district heating company has limited, in reality no possibility, to redistribute the flow in a simple and controlled manner after the system has been put in operation.

Matching supply to the demand

Space heating is by nature a dynamic process which depends among others on:

- Outdoor air temperature
- Solar radiation
- Wind
- Humidity
- Number of people in the room/flat
- People behaviour and preferences
- Usage of electric appliances

When applying district heating there is an additional factor that needs to be considered, the system time delay. The system time delay is the time it takes a supply temperature change at the heat source to reach the heat user. Although the system time delay is generally not a concern in PULL systems as the automatic controls will adjust the flow according to the demand it becomes a significant issue in the PUSH systems. The system time delay results in that the heat supply becomes out of phase with the actual heat

demand. This can be explained with an example of a system where it takes the water 6 hours to travel from the heat plant to the farthest connected user, see Figure 4.

From a heat demand point of view it would be ideal if the building supply temperature in the constant flow system would be changed to reflect the outdoor air temperature, this case is shown by solid red line in Figure 5. However as the system are in general manually controlled the only location the supply temperature can be adjusted is at the heat plant, this will lead to a mismatch between what is demanded and what is delivered, the broken red line in Figure 5 shows the delivered supply temperature in furthest substation.

Assuming that the approach taken in Figure 5 would be applied in a perfectly balanced PUSH system, given design condition, throughout the heating season the following results would be achieved. Further, it is assumed that the given district heating system is experiencing the same weather conditions and typical building heat demand as in Tianjin, China, see Table 2.

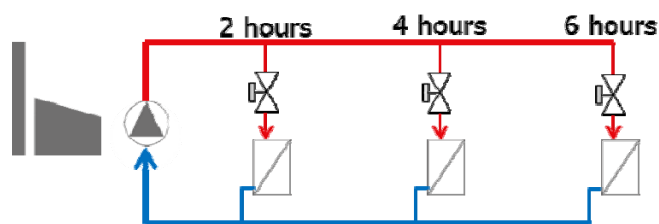


Figure 4. Example of a network with 6 hours of time delay.

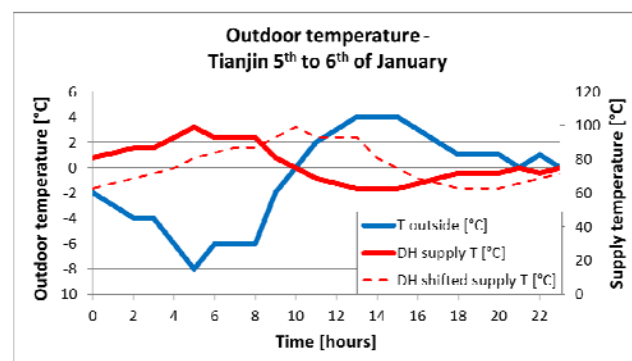


Figure 5. Example of an outdoor temperature change within one day and how it would reflect the network supply temperature at the heat plant and at the last substation in the given example.

Table 2. Fraction of the time the heat supply is within +/- 10% of heat demand.

Substation #	Supply within +/-10%
Substation 1	63.8%
Substation 2	44.1%

Substation 3	27%
Average	44.9%

Rest of the time there will be either an under- or an oversupply situation. During oversupply periods heat will be lost due to “open window regulating”. During undersupply periods tenants will complain to the district heating utility. To avoid complaints the plant operator will generally increase the supply temperature as going around the system to adjust valves can be a very complicated process in large district heating schemes, as described above. The fact is that all additional heat supply will be a loss to the DH company. In an effort to quantify an upper limit on the possible loss the supply temperature was increased until the following condition were met: At least 80% of the heat demand was met 90% of the time. That is in only 20% of the heating period it was allowed that the heat supply deviated more than 20% from the actual heat demand. This could be considered a rather loose condition. Under these assumptions the supply temperature would need to be increased by 6.7°C and the heat supplied would go from 88.7 kWh/(m year) to 108.2 kWh/(m year). This is about 22% oversupply that could be avoided.

The out of phase between the actual supply and actual demand explained above cannot be avoided in manual balanced system. It can therefore be concluded that by applying manual balancing principles there will be no possibility to adapt the supply to the actual demand of the connected buildings.

DANFOSS SOLUTION

Danfoss has developed a new patent pending solution to simplify and automate the system balancing process in Chinese district heating systems, at the same time as it takes into account the Chinese district heating philosophy of a fair split of the heat supply.

The solution requires that in each substation there is a control valve, supply and return temperature sensors and a way to estimate the flow rate, see Figure 6.

The flow rate could be measured by a flow meter as shown in the figure or by estimating the flow through the valve, depending on the required accuracy of the flow estimation.

In a network perspective the solution would look like is shown in **Figure 7**.

The solution is designed to operate in different modes:

- a) Fair split of the flow capacity.
- b) Fair split of the heat capacity.
- c) Weather compensation at the substation level.

In a) the approach is to automate the currently applied practice and give simple and a controlled way of

redistributing the flow once the system has been put in operation. The initial adjustment of the control valves in the beginning of the heating season is then made at the control room through the control box. The network operator will define the allowable flow rate in a simple table for each substation. Once the network operator has defined the set points the control system will communicate the set points to the control valves which will start adjusting their position until the set flow has been reached.

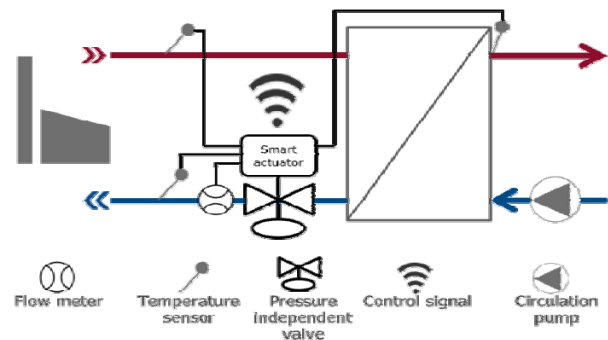


Figure 6. Simplified view of the required components for the new Danfoss control solution for Chinese district heating systems.

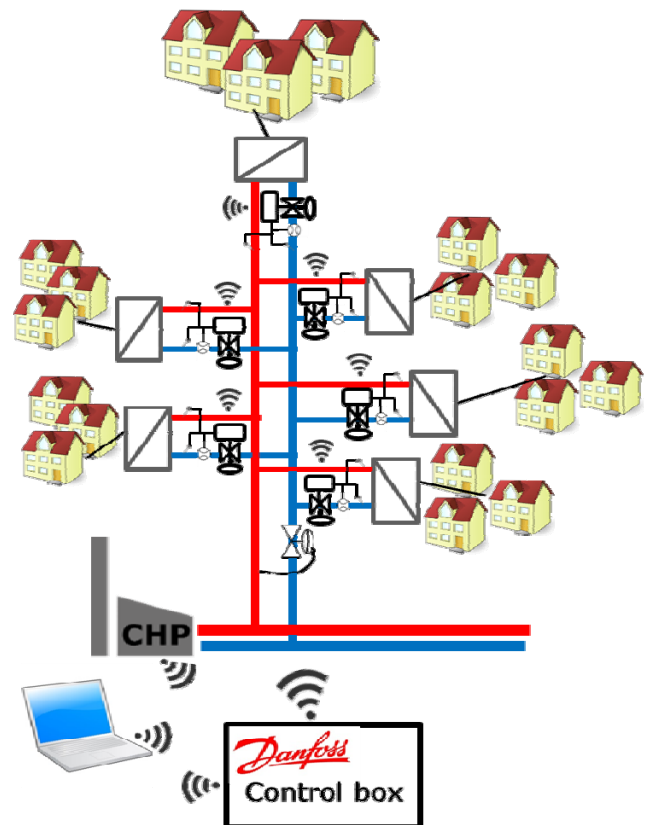


Figure 7. The new solution applied at one branch in the primary side of a Chinese district heating system.

solve the out of phase between heat supply and demand mentioned above.

Future adjustments can then be made using the same interface with the benefit that the operator can define

which substations will be receiving higher flow rates and which substations will give away part of their flow rates. An example of the interface can be seen in **Figure 8** where the network operator has locked changes in substations 1 and 10 and proposed flow changes in substation 3, 4 and 6 and asked the control system to distribute the impact from the proposed flow changes on substations 5, 7, 8 and 9.

With a) the flow adjustments can be achieved in a simple and controlled manner. However it does not

In b) the approach is that the network operator can define how large share of the heat plant heat output each substation is allowed to take. In this case the added complication is that the control system will need to get a read out of the heat output from the heat plant. Once the heat output is known the control system will communicate the allowable heat draw off to the smart actuator. The smart actuator will then adjust the valve position so that the allowable heat draw off is reached. For b) the same principle applies when the operator needs to redistribute the flow shares during operation, he can than choose which substation will get more/less and which substations will be affected by the changes.

Check all	<input type="checkbox"/>			
Substation	Affected?	Current flow	Change	New flow
1	<input checked="" type="checkbox"/>	200		200
2	<input type="checkbox"/>	300		300
3	<input type="checkbox"/>	200	+100	300
4	<input type="checkbox"/>	500	+100	600
5	<input checked="" type="checkbox"/>	400	-25	375
6	<input type="checkbox"/>	800	-100	700
7	<input checked="" type="checkbox"/>	600	-25	575
8	<input checked="" type="checkbox"/>	400	-25	375
9	<input checked="" type="checkbox"/>	300	-25	275
10	<input checked="" type="checkbox"/>	600		600
		$\Sigma=4300$	$\Sigma=0$	$\Sigma=4300$

Figure 8. Example of a consumer interface.

In c) the idea is that the network operator can define a supply temperature index curve for each substation, see **Figure 9**, the control system will communicate the heating index curve to the smart actuator which will then adjust the heat delivery according to the outdoor temperature. At later stages the network operator can adjust the supply temperature index curve up or down to fit the requirements of the buildings. Unlike the other modes this will effectively transform the primary side system from a PUSH system to a PULL system.

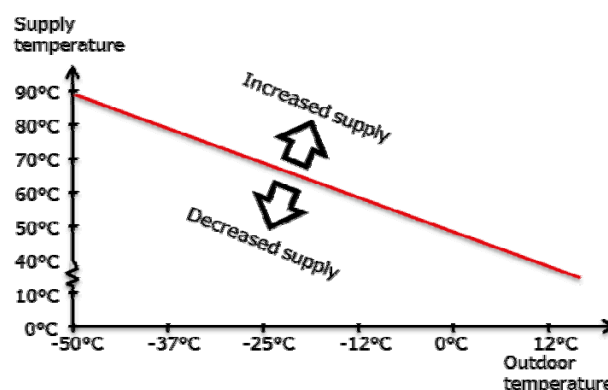


Figure 9. Supply temperature index curve in relation to outdoor temperature.

In all cases the secondary side of the network can be operated the same way as it is done today, that is with a constant flow, PUSH principle.

CONCLUSIONS AND DISCUSSIONS

The first operation mode of the new solution can save significant amount of man hours that are currently used for visiting each of the connected area substations for commissioning of the system and unavoidable adjustments during the heating season. Further the adjustments will be much more precise than what is experienced today as influences from other substations will be avoided.

The second operation mode can limit the existing oversupply to a large extent by preventing the issue with the water transportation time. After applying the second operation mode only the time lag in the secondary network will remain, which is generally much smaller than in the primary network.

The third operation mode will bring the primary side operation to a demand driven operation, as is the norm in western district heating system. It will bring out even further energy savings than the second operation mode and make it simple to adjust the heat supply to the heat demand in each of connected area.

The proposed control solution has the potential to revolutionize the Chinese district heating industry and move it from the PUSH approach to the PULL approach applied in the rest of the world. By changing the Chinese district heating systems to the PULL philosophy significant energy savings can be achieved as it will open up for the possibility to adapt the supply to the actual demand of the building, this is not possible with today manual balancing approach. The potential savings can be at least 15-30%, probably even higher. The energy savings would have positive impact on the pollution level, which is a very big issue in China and is the leading cause of 17% of all deaths in China [5].

Although the proposed control solution is still under development it is expected that it will be tested in a real system in the 2016-2017 heating season in China.

REFERENCES

- [1] EURO HEAT & POWER, "Euroheat & power - Statistics," 2013. [Online]. Available: <http://www.euroheat.org/Statistics-69.aspx>. [Accessed: 01-May-2015].
- [2] Ministry of Housing and Urban-Rural Development, "Ministry of Housing and Urban-Rural Development." [Online]. Available: <http://www.mohurd.gov.cn/>.
- [3] A. Baeumler, E. Ijjasz-vasquez, and S. Mehndiratta, "Sustainable Low-Carbon City Development in China", World Bank, 2012.
- [4] Tsinghua University Building Energy Research Center, 2011 Annual Report on China Building Energy Efficiency. 2011.
- [5] R.A. Rohde, R.A. Muller, "Air Pollution in China: Mapping of Concentrations and Sources". PLoS ONE 10(8): e0135749, 2015.

METHOD FOR ACHIEVING HYDRAULIC BALANCE AND OPTIMIZING INDOOR TEMPERATURE CONTROL IN CHINESE BUILDINGS' HEATING SYSTEMS

Lipeng Zhang¹, Jianjun Xia², Oddgeir Gudmundsson³, Jan Eric Thorsen³, Hongwei Li⁴, Svend Svendsen⁴

¹ Danfoss Automatic Controls Management (Shanghai) Co., Ltd. F20, Building A, No.2A Gong Ti Bei Lu, Chaoyang District, Beijing, 100027, China

² Tsinghua University, Building Energy Research Center, School of Architecture, Beijing, 100084 China

³ Danfoss A/S, Heating segment, Application Center, Nordborgvej 81, Nordborg, 6430 Denmark

⁴ Technical University of Denmark, Civil Engineering Department, Brogvej Building 118, Kgs. Lyngby, 2800 Denmark

Keywords: *district heating, hydraulic balance, thermostatic radiator valves, differential pressure control*

ABSTRACT

A common problem with Chinese district heating systems is that they supply more heat than the actual heat demand of the connected buildings. The reason for this excessive heat supply is the general failure to use control devices to adjust the temperature and flow in the district heating systems in accordance with the actual heat demand. This results in 15–30% of the total supplied heat being lost. This paper proposes an integrated approach that aims to achieve hydraulic balance and control room temperatures by introducing thermostatic radiator valves with automatic balancing valves. Pre-setting thermostatic radiator valves combined with automatic balancing valves establishes hydraulic balance, and activating thermostats stabilize indoor temperatures. By moving the system from centrally planned heat delivery to demand-driven heat delivery, excess heat loss can be significantly reduced. Results show that once the hydraulic balance is achieved with pre-setting thermostatic radiator valves and automatic balancing valves, and room temperatures are controlled at standard valve 18°C, 17% heat savings and 42.8% pump electricity savings can be achieved. The energy savings will also have a positive environmental effect since coal is the dominant district heating fuel in China.

INTRODUCTION

Upon the backdrop of rapid urbanization and industrialization, China has become one of the largest district heating (DH) markets in the world in the past 20 years. Statistics show that total DH sales in 2013 amounted to 3,197,032 TJ [1]. This number is still increasing along with the process of rapid urbanization, expansion of total building area and enhancement of building services. One of the main issues influencing the efficiency of Chinese DH systems is the energy wasted due to hydraulic imbalances and the lack of room temperature control. In China, multi-storey and

high rise buildings are typical, see Figure . The heat, generating in the heat source, mostly indirectly transfers to the building heat system via the area-substation. In the secondary side of the area-substation, hot water goes into a number of building heating systems through their own heat entrance. The heat entrance is the interface connecting the DH network to the building heating systems. It is usually equipped with shut-off valves and measurement devices like thermometers, pressure gauges and heat meters[2]. In terms of heat sources, 2013 data shows the main heating production facilities are coal-fired boilers, which account for 48%; and Combined Heat and Power (CHP) plants, which account for 42%[3]. Due to the failure to install control devices to enable pressure and flow control in the building heating systems, nearly 30% of the total heat supply is being wasted. Subsequently, the building heating systems are under hydraulic imbalance and the apartment rooms are overheated [4][5]. Moreover, from the perspective of temperature control, room temperature regulation and control functions are not available in approx. 84% of the total heating area in China [6]. Furthermore, due to fixed heating charges based on heating area, not actual heat consumption, consumers have no incentive to consciously reduce the TRV (Thermostatic Radiator Valves) settings in an oversupply situation – instead, they open windows, thus the energy is wasted. Consequently, the efficiency of DH systems is compromised.

The development of DH in high-population and cold regions has become an environmentally friendly and energy-efficient strategy to provide energy supply security and air pollution abatement, which are the two most important challenges facing China today [7][8][9]. Modernizing the DH systems by applying appropriate control devices to improve the efficiency of DH systems is particularly critical.



Figure 1. Typical high-rise building (left) and multi-storey building (right) in China

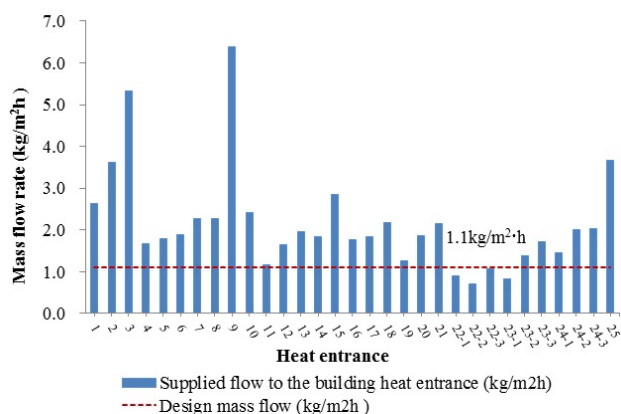


Figure 2. Mass flow of the 31 heat entrances of CASE-A

Hydraulic situation in a real case

To understand the actual hydraulic situation in Chinese multi-storey building heating systems, data from a real heating system in China (CASE-A) was measured and presented. This heating system supplies heat to 25 multi-storey/high-rise residential buildings, totalling nearly 278,000 m² of heat area. As the heat-carrying medium, water is heated at central gas-fired boilers, and transported to those 25 buildings via 31 heat entrances. Certain buildings, like #22, #23 and #24, those buildings have three building units. The building units have their own heat entrances. In this case, manual balancing valves were installed at the heat entrances to manage the water flow into the connected buildings. After initial commissioning is finalized, the setting values of these manual balancing valves are kept for the complete heating season, except for minor adjustments.

We measured the mass flow for all 31 heat entrances by using an ultrasonic flow meter. By dividing the measured mass flow by the corresponding heat area, the mass flow per square meter of the individual heat entrance was obtained, and it is shown in Figure 2.

These data reflect the water flow through the 31 heat entrances and into the 25 connected buildings via the horizontal pipelines. Since all the buildings were featured as having the same exterior envelope insulation properties, and the heating system operates by following constant flow principles, theoretically, the unit mass flow should be numerically equal to the design mass flow, 1.1 kg/h·m². This flow rate m (kg/h) is obtained because the heat load, Q (W) under design outdoor temperature -9 °C, is 32 W/m² according to Eq. (1). the design supply and return temperatures, T_s (°C) and T_r (°C) are 75/50 °C, where C stands for the heat capacity of hot water and is equal 4,187 J/kg·°C.

$$m = \frac{Q}{C \cdot (T_s - T_r)} \cdot 3600 \quad (1)$$

When compared with the design unit mass flow, 27 of 31 heat entrances are in a state of overflow; additionally, the unit mass flow through 31 heat entrances is uneven. Those data show the hydraulic imbalance exists among the horizontal distribution network.

In addition, to investigating the vertical flow distribution, one of the high-rise buildings with 21 stories was selected for measurement of the mass flows along the internal vertical riser, see Figure (left). Figure 3 illustrates the mass flow per square meter along the riser at the 1st, 6th, 13th, 14th, 18th and 21st floors. The water-flow direction was from the bottom to the top, and the mass flow rate per square meter gradually dropped along the water supply direction; the top floor received the lowest flow rate, even though the top floor could be expected to have a greater heat demand than the others due to its greater exterior surface. The data indicated that the flow supply per square meter to each floor was unequal, and all the flows are higher than 1.1 kg/m²·h.

CASE-A showed that the heating system was in hydraulic imbalance, both in the horizontal distribution network and in the internal vertical riser of the building. CASE-A typically reflects the real hydraulic situation of Chinese heating systems. Hydraulic imbalance occurs mostly due to the failure of the appropriate control devices in the heating system; therefore, the flow distribution is distorted. Initially, since overflow inevitably causes the underflow, the critical rooms, which are far away the pumps, cannot obtain the design room temperature of 18°C according to the building code [10]. In order to guarantee the design indoor temperature in the critical rooms, DH Company usually increases the total flow rate so that sufficient flow can be distributed to the critical end user. The overflow condition is further aggravated. Consequently,

the supply temperatures cannot be cooled down effectively, and the system is operating with large flow and small temperature differences. All of these imply higher fuel consumption and pump electricity consumption, and the efficiency of the heating system will be decreased.

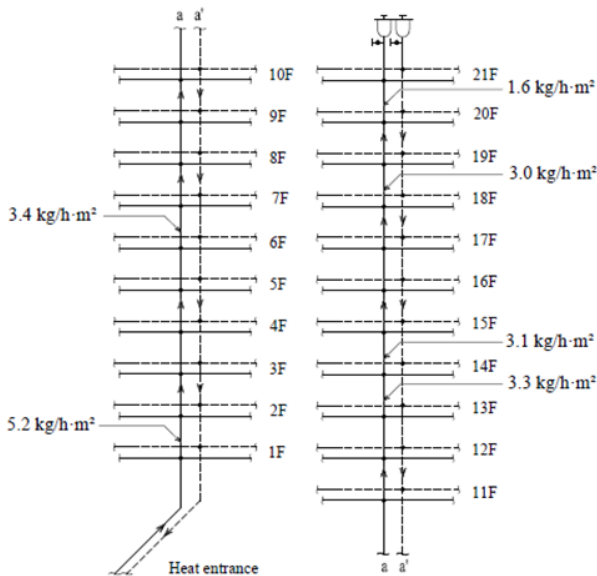


Figure 3. Building #3 appearance and mass flow along one of the vertical riser supplies

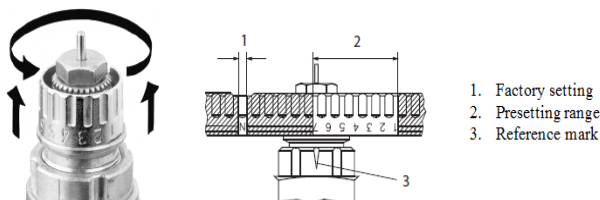


Figure 4. Pre-setting scales of radiator valve [11]

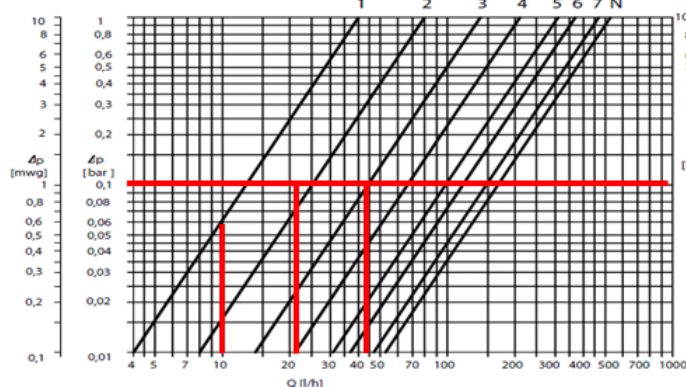


Figure 5. Selection of the pre-set scale of radiator valve for the radiators

METHODOLOGY

In view of the problems mentioned above, the integrated approach is proposed to establish hydraulic balance and control the room temperature based on the building heating systems. Thermostatic radiator valves and automatic balancing valves as two key devices are applied in this approach. The hydraulic balance is achieved by applying the pre-set radiator valve [11] combining with automatic balancing valves [12]. The radiator valve can limit the flow through the valves by utilizing the integrated pre-setting function. The pre-set scale is from 1 to 7, N means the valve is fully open, see Figure 4. The automatic balancing valve can keep constant the differential pressure across the valve, thus the good control performance of the radiator valve can be ensured. After the heating system achieves hydraulic balance under design conditions, the thermostats are activated to investigate the heat performance of the heating system in a dynamic situation.

The main purpose of this study was to clarify that the proposed technical approach can manage the pressure and flow in multi-story building heating systems, achieving hydraulic balance and reducing energy consumption. The central hypothesis of this study rests on the philosophy that the design flow must pass through each radiator in design conditions to build hydraulic balance, and the maximum flows through the radiators are limited, and the overflow or the underflow can be effectively avoided in all the terminal units. Thus, the flow distribution at all the branches is even, the hydraulic balancing is achieved under either peak load or partial load conditions. According to the design flow of the radiators, and the pressure drop across the radiator valve, the pre-setting value of the valve can be determined, and radiator valves are pre-set, see Figure 5. Based on the precondition of hydraulic balancing, room temperature control is applied to simulate the heat performance of the heating system.

To carry out this study, an eight-storey residential building was developed using IDA-ICE 4.2.6 [13]. A 1990s typical residential buildings in Harbin City is the model's prototype – for example, in terms of the building layout and building exterior envelope properties (see Figure 5, right). The building envelope properties and the thermal characteristics were as specified in China's energy conservation design standard JGJ26-95 [14]. One of the apartments was modelled as a multi-zone model. Each room in the apartment was a separate zone. This multi-zone model contained five heated zone areas: Bedroom N (north), Bathroom, Bedroom S (south), Kitchen, and Living Room, as well as three non-heated balconies and a non-heated staircase/hall (see Figure 6). The outdoor heating design temperature was -26 °C for Harbin and

the indoor design room temperature was 18 °C. Based on the information, we ran the multi-zone model equipped with ideal radiators, and obtained the peak heat load of each zone.

We dimensioned the radiators in accordance with Chinese standard [2]. In each zone, an M132-type radiator [15] was modelled as the room heating unit. The design parameters of the space heating (SH) system were 80/60/18 °C (supply/return/indoor air temperatures). Correction factors were derived to correct for the actual output of each radiator. Accordingly, the maximum power of each radiator was determined, and the design flow limitation through the radiators and the design heat load for the SH system were defined. The flow rates were inputted into the IDA-ICE to simulate the heat performance.

To reflect real conditions, an internal heat gain of 5.0 W/m² was considered [14]. Real weather data in Harbin in 2014 was used to estimate the energy consumption. The source of the weather data is from [16]. Two scenarios were considered: 1) without TRVs fitted to the radiators, which is the most common situation in Chinese SH systems; and 2) with TRVs fitted to the radiators to adjust the indoor temperature by setting the thermostat of the TRVs. The room temperature of each zone, the energy consumption including heat consumption, and the electricity consumption of the pumps as well as the volume flow of the heating system were all compared based on the simulation results.

RESULT

Firstly, the room temperatures were compared under different two scenarios. Generally, the results showed that without TRVs the room temperatures in all the zones were much higher than 18 °C except for a few hours at the beginning of the heating period. The average room temperatures in all five zones over the entire heating period were around 22 °C. With TRV control, the room temperatures in all the zones were constant at around 18 °C. Since 0.5 °C proportional band (P-band) is set, some minor deviations between the set temperature and the simulated room temperature existed. Because TRVs are proportional temperature controllers, they respond to any deviation from the set temperature by increasing or decreasing the flow into the radiators until the required room temperature is achieved. Figure 7 shows the simulation results for two typical rooms in the multi-zone model: the northern room 'Bedroom N' and the largest room, the 'Living Room', which reflects these small variations particularly clearly. The indoor air temperature can also be seen to have lagged a few days behind outdoor temperature changes because of the thermal inertia of the building envelope materials.

Secondly, the heat consumption and pump electricity consumption were compared for the two scenarios, and the results in Figure 8

Figure 8 show that design flow rates are set for the radiators. Meanwhile, because the thermostats were activated, heat energy consumption was reduced by 17% and pump electricity consumption by 42.8% for this particular apartment. Here it should be noted that the pump energy consumption is very small compared to the heating energy consumption, only 0.1% of the heat energy delivered.

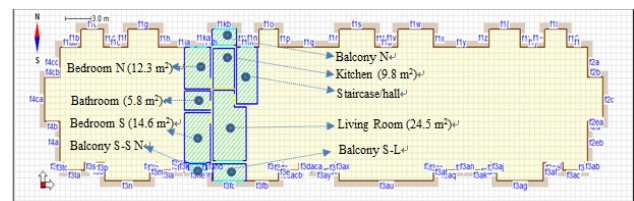


Figure 6. Multi-zone model

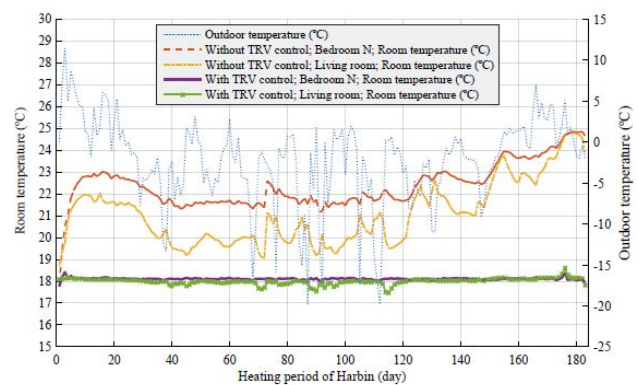


Figure 7. Zone room temperature of Bedroom N and the Living Room during the heating period

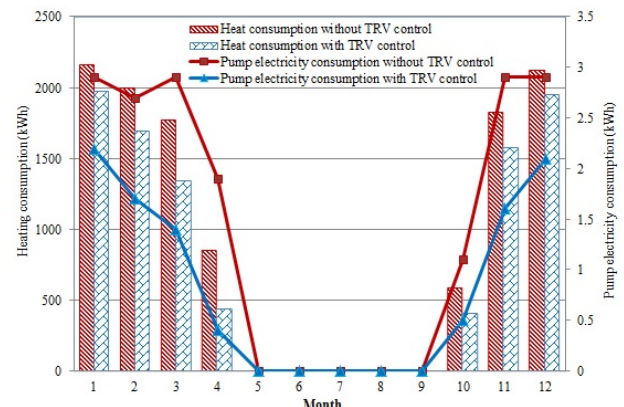


Figure 8. Heat consumption comparison between the scenarios with and without TRV control

Thirdly, with regard to the system's operation, it is important to note that applying TRVs changes the SH system from constant flow to variable flow. The circulation pump will operate at variable speed, which can save a lot of pump electrical energy.

Coal is the dominant DH fuel, and the dominant fuel for Chinese power plants. Burning coal is one of the main causes of air pollution in China [17]. Hydraulic balance and room temperature control can achieve 17% heat savings and 42.8% pump electricity savings. This will result in positive environmental impacts. Burning 1 ton of Chinese standard coal (29.3GJ/tce) releases about 2,600 kg CO₂, 24 kg SO₂, 7kg NO_x [18]. By applying the proposed controls in Chinese DH systems, energy consumption would be reduced, which would consequently have positive environmental impacts.

CONCLUSION

Without pressure and flow controls, increases in the flow rate to ensure sufficient room temperatures to distal or critical rooms result in considerable hydraulic imbalance, large flow rates, and high pump electricity consumption. In contrast, combining DP controllers at the apartment level with pre-set radiator valves achieves a fair flow distribution, and activating thermostats can control room temperatures at the desired level. Consequently, 17% heat savings, 42.8% pump electricity savings were achieved, and the heating system transformed from constant flow to variable flow.

Traditional Chinese DH systems seldom have control at the end users. By moving the control close to the end users, it is possible to bring the heating supply into line with the heating demand. A well-balanced SH system can improve consumer thermal comfort and at the same time save significant pumping power, also allowing heat users to pay less if the heating is charged on the basis of real consumption. The heat users will be satisfied with the improved room temperature control. At the same time, it would also be cost-effective for DH utilities, which could increase their profits, because well-controlled space heating systems bring out the good operation of the entire DH system.

The developed integrated approach would help decision makers and stakeholders to plan new or renovated district heating projects so they are more energy efficient and cost effective. It would make a considerable contribution to energy supply security and air pollution abatement in Chinese society by raising the energy efficiency of heating systems to a new level.

REFERENCES

[1] EURO HEAT & POWER, "Euroheat & power - Statistics," 2013. [Online]. Available:

<http://www.euroheat.org/Statistics-69.aspx>. [Accessed: 26-Oct-2015].

- [2] Y. Lu, *Practical Handbook of heating and air conditioning design*. Beijing, China: China Building Industry Press, 2008.
- [3] Building Energy Research Center of Tsinghua University, *Annual Report on China Building Energy Efficiency in 2015*. Beijing, China: China Architecture & Building Press, 2015.
- [4] Building Energy Research Center of Tsinghua University, *Annual Report on China Building Energy Efficiency in 2011*. Beijing, China: China Architecture & Building Press, 2011.
- [5] D. Yan, T. Zhe, W. Yong, and Z. Neng, "Achievements and suggestions of heat metering and energy efficiency retrofit for existing residential buildings in northern heating regions of China," *Energy Policy*, vol. 39, pp. 4675–4682, Sep. 2011.
- [6] Ministry of Housing and Urban-Rural Development, "Ministry of Housing and Urban-Rural Development." [Online]. Available: <http://www.mohurd.gov.cn/>.
- [7] National Development and Reform Commission of China, "The 12th Five-Year Guideline for National Economic and Social Development of China," 2011.
- [8] B. Lin and H. Liu, "China's building energy efficiency and urbanization," *Energy Build.*, vol. 86, pp. 356–365, 2015.
- [9] X. Chen, L. Wang, L. Tong, S. Sun, X. Yue, S. Yin, and L. Zheng, "Energy saving and emission reduction of China's urban district heating," *Energy Policy*, vol. 55, pp. 677–682, Apr. 2013.
- [10] Ministry of Housing and Urban-Rural Development of China, "Industry standard JGJ 26-2010: Design standard for energy efficiency of residential buildings in severe cold and cold zones." China Building Industry Press, Beijing, China, CHINA, 2010.
- [11] Danfoss, "RA-N Valves with Pre-Setting," 2014. [Online]. Available: <http://products.danfoss.com/productrange/list/heating-solutions/radiator-thermostats/radiator-valves/pre-setting-valves/>. [Accessed: 21-Jan-2015].
- [12] Danfoss, "ASV Automatic Balancing Valves." [Online]. Available: <http://products.danfoss.com/productrange/heating-solutions/balancing-control-valves/automatic-balancing-valves/asv-automatic-balancing-valves/>. [Accessed: 21-Jan-2015].

- [13] EQUA, "IDA-ICE 4.2.6." [Online]. Available: <http://www.equa.se/index.php/en/ida-ice>.
- [14] Ministry of Housing and Urban-Rural Development of China, *JGJ26-95:Design standard for energy efficiency of residential buildings in severe cold and cold zones*. CHINA, 1995.
- [15] P. He, G. Sun, F. Wang, and H. X. Wu, *Heating Engineering(4th edition)*. Beijing, China: China Building Industry Press.
- [16] EnergyPlus, "CHN_Heilongjiang.Harbin.509530_CSWD." [Online]. Available: http://apps1.eere.energy.gov/buildings/energyplus/weatherdata_about.cfm.
- [17] H. Zhang, B. Zhang, and J. Bi, "More efforts, more benefits: Air pollutant control of coal-fired power plants in China," *Energy*, vol. 80, pp. 1–9, Feb. 2015.
- [18] Nation Planning and Energy Commission, "Energy basic data compilation." 1999.

A SYSTEM PERSPECTIVE ON ALTERED DISTRICT HEATING DEMAND IN MULTIFAMILY BUILDINGS

Stefan Blomqvist¹, Louise Trygg¹

¹ Division of Energy Systems, Linköping University, Sweden

Keywords: District heating, system perspective, collaboration, multifamily buildings

ABSTRACT

District heating (DH) in Sweden is mainly based on non-fossil fuel and since increased use of DH also increases the possibilities to further production of electricity in a combined heat and power plant (CHP) system, increased use of DH in Sweden will lead to lower global emission of CO₂ when assuming coal condensing as the marginal production of electricity in a European electricity market.

In this study, we analyze how large-scale renovation of buildings connected to a DH system will affect the local and global emissions by using simulations, optimization and workshops. The study has been performed in close collaboration with energy utilities and housing companies.

INTRODUCTION

Our current use of energy is a major part of the sustainability problem that we are facing today. Increased system efficiency and reduced climate impact are important parts in the transition towards a more sustainable society. With high percentage of renewable energy sources and varying electricity prices efficiency measures, conversion and control of energy use will have an important role. In the same way, CHP and DH will play a more prominent role towards a secure and fully balanced energy system. However, the demand of heating is decreasing and there is an intense competition in today's energy market, i.e. between DH and heat pumps of various types. Swedish

heating demand per building area will probably decrease which will lead to an altered DH demand for regional DH companies in Sweden

Based on the above argumentation the aim of this study is to analyze how an altered heating demand will affect a regional DH system in Sweden

BACKGROUND

Today, we are facing in many respects quite revolutionary situation in which renewable energy sources on economic conditions out-compete not only nuclear power but also coal power. We also meet lower and more variable electricity prices than we have seen in a long time in Sweden. At the same time, we know that the ongoing climate change is one of the biggest threats we are facing. With high percentage of renewable energy sources and varying electricity prices efficiency measures, conversion and control of energy use will have an even more important role. In the same way, CHP and district heating can get a more prominent role towards a secure and fully balanced energy system. However, the demand of heating is decreasing and the DH faces intense competition in today's market, i.e. heat pumps of various types.

CASE STUDY

The system in this case study is illustrated **Figure 1**. The study is based on two existing multifamily residential buildings located in central Linköping. Both buildings were constructed in 1961 and has since then not undergone extensive renovation until 2014 and

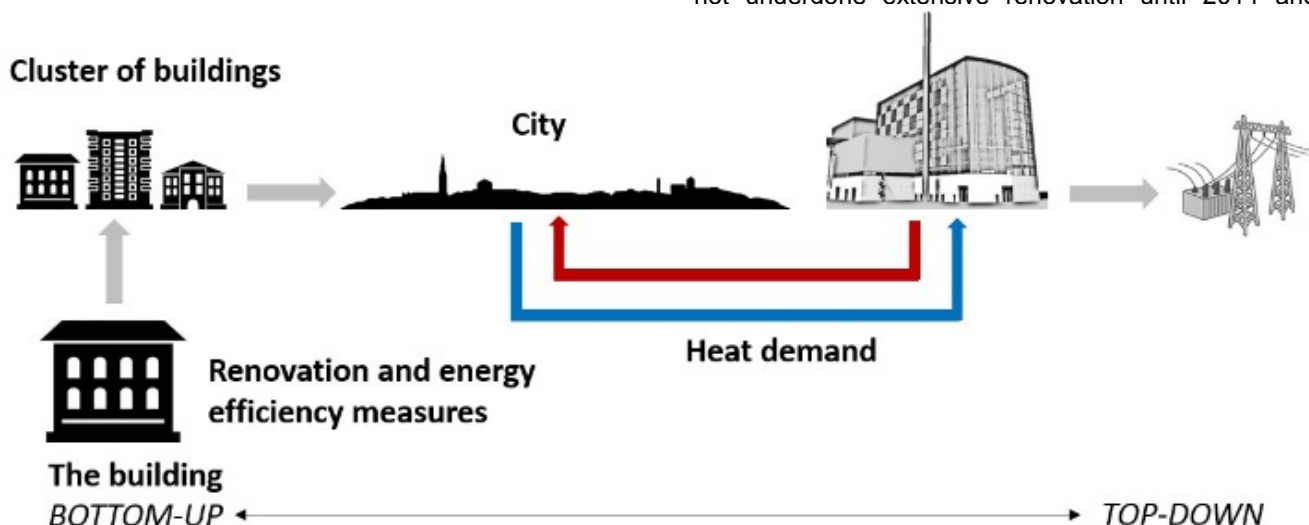


Figure 1 The system of study

Table 1 Energy efficiency measures in the case study

	BUILDING ENVELOPE	TYPE OF VENTILATION	HEAT SOURCE	RADIATOR TEMPERATURE [°C]	HOT WATER DEMAND
CASE 1 (REFERENCE)	Non renovated	Exhaust air	District heating	80/60	25 kWh/m ² , year
CASE 2	Renovated	Exhaust air	District heating	50/35	25 kWh/m ² , year
CASE 3	Renovated	FTX-system (75%)	District heating	50/35	25 kWh/m ² , year
CASE 4	Non renovated	Exhaust air	Geothermal heat pump	80/60	25 kWh/m ² , year
CASE 5	Renovated	Exhaust air	Geothermal heat pump	50/35	25 kWh/m ² , year
CASE 6	Renovated	FTX-system (75%)	Geothermal heat pump	50/35	25 kWh/m ² , year

The DH system in this case study uses waste, wood chips, coal and oil as fuel for their CHP plants. The baseload consists of waste, wood chips and coal, while oil is used as fuel for peak demand.

This project involves several companies which in close collaboration contributed to this case study. Through workshops, interviews and various inputs, information were collected for this study. The project's companies consists of two energy companies and five housing companies.

METHOD

A framework is used based on detailed results from a simulation of energy efficiency measures applied on a multifamily building in Linköping, Sweden. Six simulations are done, each with different energy efficiency measure as seen in **Table 1**. The results from the building simulation program IDA ICE are then scaled up to correspond to a larger housing area. To analyze how this altered district heating demand would affect the regional DH system a model was built in the linear optimization program MODEST

The building was modeled in IDA Indoor Climate and Energy (IDA ICE) version 4.6.2. IDA ICE provides a dynamic simulation of the energy use in an entire building for one year or part of the year. The level of detail is high and the software has undergone several validations to test cell measurements and other simulation software with good results [1].

The model was created based on existing geometry has undergone validation against measured data to ensure that the physics of the model is correct [2].

The results at the building level has been scaled up to city level through a selection of similar types of buildings in the municipal housing stock. The stock is equivalent to approximately 273 500 m² out of Linköping 3 000 000 m² residential area of multi-family

buildings. Variations in specific energy is always in stock, and therefore are all the buildings in the stock assumed to have the same energy use per m² as in the reference case (Case 1). This gives a total annual heating use in the selected stock of 35.6 GWh, representing approximately 3% of the total Linköping district heating demand.

MODEST is an optimization program for regional energy systems. The acronym MODEST is short for long "Model for Dynamic Optimization of Energy Systems with Time dependent components and boundary conditions". MODEST may be used to analyze many different energy systems and components. Inputs are for example cost, technical specifications and efficiency. MODEST has a flexible time division, meaning that power peaks and other variation in energy use during day/night or summer/winter may be reflected. The models objective is to analyze the lowest possible cost to supply a demand [3]. In **Figure 2** a coarse description of the case study can be seen. The heat demand (entitled "Heat demand (Case study)") is altered and the system then optimized to see how the system supplies the demand.

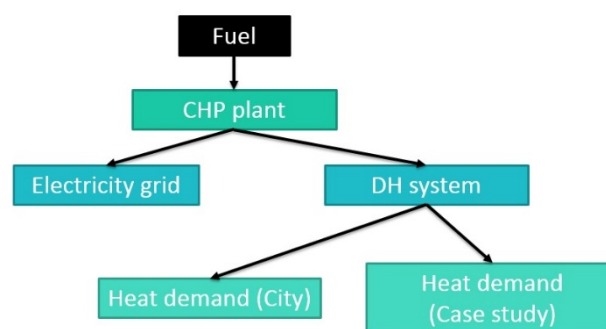


Figure 2 Coarse description of the optimization model in MODEST

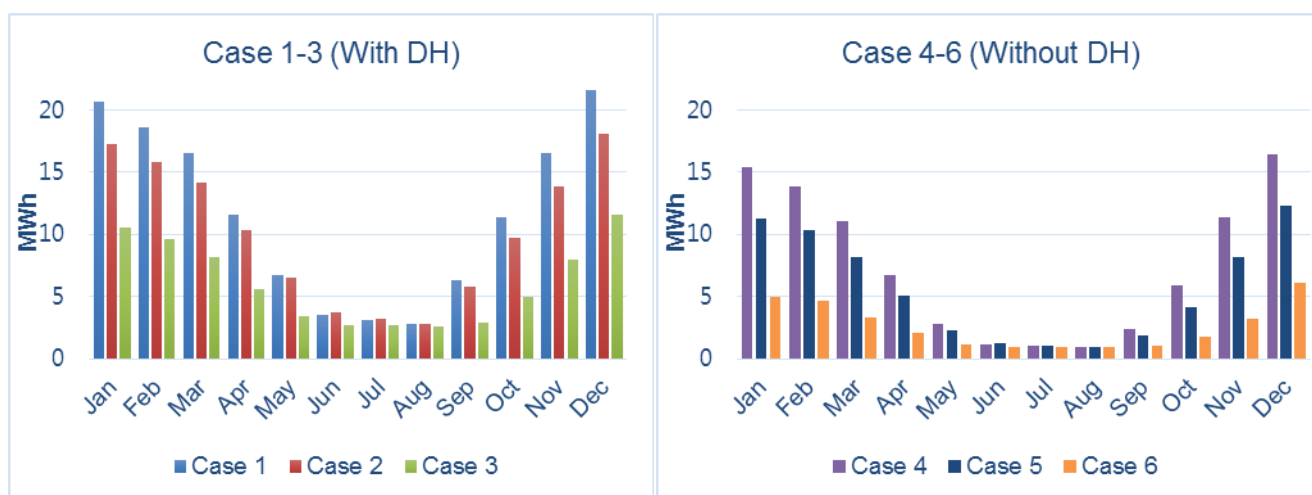


Figure 3 Diagrams of energy use from IDA ICE per calendar month

RESULTS

The results from IDA ICE can be seen in **Figure 3** and **Table 2**, showing monthly use of energy and total numbers annually respectively. It is worth noting that all cases are better than the reference case (Case 1) for the building's energy use. The largest difference from the reference case is found in case 6 with a 78% reduction of heat demand per year. In its non-renovated condition, the building has an annual energy demand for heating and domestic hot water at 140 MWh_{DH}, equivalent to 130 kWh_{el}/m². If the heating system is switched to a geothermal-based system the energy use is reduced to 121 MWh_{el}, equivalent to 113 kWh_{el}/m², see **Table 2**. Alone, the building envelope measures only provide a small energy savings. When both the building envelope measures and ventilation measures is the potential to achieve nearly a halving of the energy use. However, these ventilation measures is increasing the need for electricity to supply fan, which means that the total electricity for ventilation increases from 3.8 MWh_{el} to 9.0 MWh_{el} annually.

In **Figure 3** Sweden's seasons becomes visible with high energy use during winters and a low use of heat during summers. Since the need of domestic hot water are evenly distributed over the year, there is a heating demand during the summer, see **Figure 3**. In case 6 domestic hot water use constitutes a significant portion of the energy.

Figure 4 illustrates the results from MODEST, that is after upscaling of the results from IDA ICE. The altered heat demand for the DH system is in the range of 0-35.6 GWh annually between the cases. Zero change being the reference case and a decrease of 35.6 GWh of DH demand annually for case 4-6 when using geothermal heat pump instead. The graph illustrates the reduction of fuel usage for the various fuels in the DH system. Also, reduced electricity sales due to decreased production of DH is reported in the graph. For the same reason, the local emissions are reduced.

Figure 5 demonstrates a comparison between local and global emissions. The local emissions are reduced but depending on how the loss of electricity production in the DH system is replaced it leads to different level

Table 2 Summary of results from IDA ICE

	ANNUAL HEAT DEMAND [MWH]	HEAT DEMAND [KWH/M ²] ¹	REDUCTION FROM CASE 1 (CASE 4)	ELEC. FOR DOMESTIC AND BUILDING SERVICE [MWH] ²	ELECTRICITY FOR VENTILATION [MWH]
CASE 1 (REFERENCE)	139.1 (DH)	130.1 (DH)	-	34.0	3.8
CASE 2	121.3 (DH)	113.1 (DH)	13%	34.0	3.8
CASE 3	72.8 (DH)	67.8 (DH)	48%	34.0	9.0
CASE 4	83.2 (Electricity)	77.6 (Electricity)	36%	34.0	3.8
CASE 5	66.9 (Electricity)	62.4 (Electricity)	52% (25%)	34.0	3.8
CASE 6	31.1 (Electricity)	29.0 (Electricity)	78% (65%)	34.0	9.0

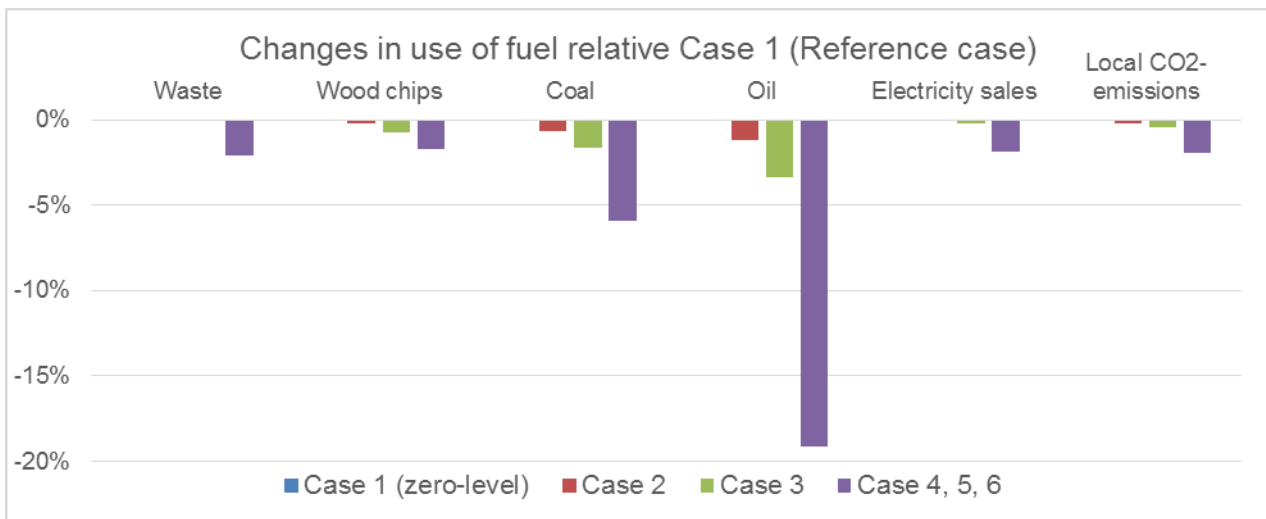


Figure 4 Results from optimization of the DH system in MODEST

of increased global emissions. In all cases the increase of global emissions is greater than the decrease of local emissions.

CONCLUDING DISCUSSIONS

In close collaboration with the projects companies the results were communicated and discussed. This group of representatives from the companies consists among others of a CEO, regional managers, property managers, HVAC technologies and energy technologies. Thus, there is a broad base of knowledge in this group and overall a very good set up for a forum of discussions.

The large reduction in oil use in **Figure 4** can be explained by an initially low use of oil and mainly usage during power peaks. In connection with the renovation of buildings, the reduction of energy use occurs mainly during seasons with power peaks (as seen in **Figure 3**) which makes the peak power to decrease and therefore also the use of the peak fuel.

As seen in the results large scale renovations of a multifamily building with these energy efficiency measures results in lower heat demand which consequently reduces the electricity production in the CHP plants. In Sweden, DH is mainly based on non-fossil fuel which in turn lead to lower global emissions if a high use of DH is reached. These two statements contradict each other, meaning that these two different actors (energy and housing companies) have problems when their actions affect each other and their system boundaries are different.

It should be noted that energy efficiency measures are important steps towards a more efficient use of energy and sustainable future. But formerly, the system development were driven by the energy company. By time and progress of new technologies, the development have shifted to be driven, though unknowingly, by the user/client. However, the responsibility of the system and to i.e. provide power during peak loads remains in the hands of the energy company.

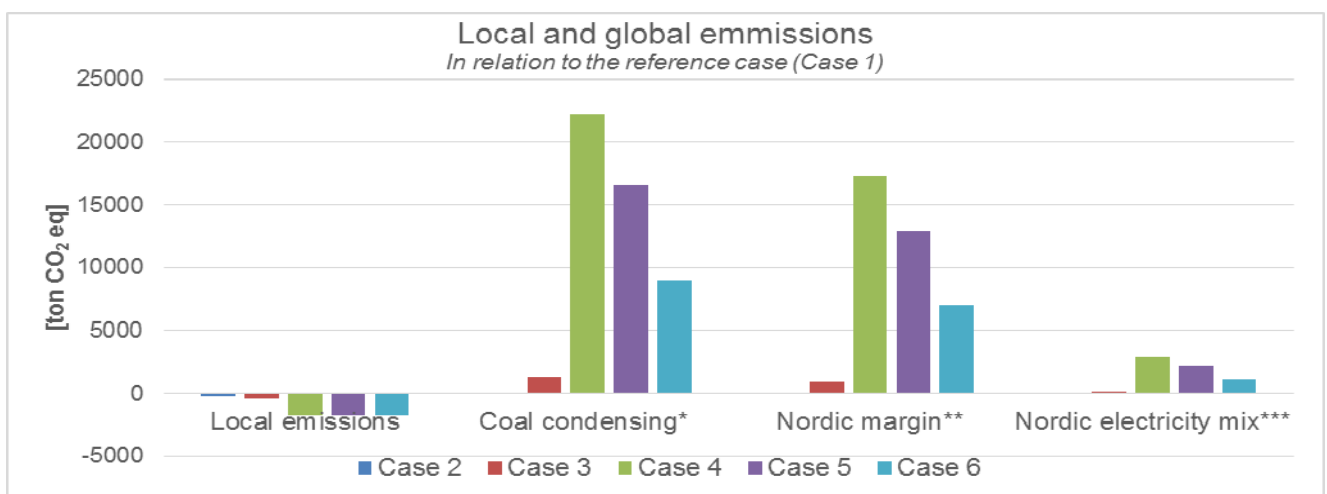


Figure 5 Results from MODEST of decreased local emissions and increased global emissions

* 974 kgCO₂eq/MWh [6]

** 759 kgCO₂eq/MWh [4]

*** 125.5 kgCO₂eq/MWh [5]

This study indicates that energy efficiency measures that are most cost-efficient from a system perspective with the building in focus, are not as good from a global perspective. By this, the study suggests that the DH companies faces challenges to in the future increase the system efficiency, whilst housing companies keep renovating their property portfolio resulting in a lower heat demand per area. This indicates that a closer collaboration is needed to stay on the path to a sustainable future.

ACKNOWLEDGEMENT

Many thanks to my PhD-fellows Lina La Fluer, Tommy Rosén at Linköping University for all your valuable contributions. A warm thanks to the companies involved in this project for valuable inputs, discussions and funding.

REFERENCES

[1] Bring, P. Sahlin and M. Vuolle, "Models for Building Indoor Climate and Energy Simulation," 1999.

- [2] L. La Fleur, B. Moshfegh and P. Rohdin, "Using whole buildings energy simulation to study the effect from renovation of a multi-family building in Sweden," *Energy and Buildings*, 2016.
- [3] D. Henning, "MODEST- An energy-system optimisation model applicable to local utilities and countries," *Energy*, vol. 22, no. 12, pp. 1135-1150, 1997.
- [4] J. Gode, F. Martinsson, L. Hagberg and D. Palm, Miljöfaktaboken 2011 Uppskattade emissionsfaktorer för bränslen, el, värme och transporter, 2011.
- [5] F. Martinsson, J. Gode and J. Höglund, "Emissionsfaktor för nordisk elproduktionsmix," IVL, 2012.
- [6] Wolf and M. Karlsson, "Can industrial symbiosis be evaluated?," in *13th Annual International Sustainable Development Research Conference*, Linköping, 2007.

A NEW DH CONTROL ALGORITHM FOR A COMBINED SUPPLY AND FEED-IN SUBSTATION AND TESTING THROUGH HARDWARE-IN-THE-LOOP

T. Rosemann¹, J. Löser¹, K. Rühling¹

¹Institute of Power Engineering, Professorship of Building Energy Systems and Heat Supply,
Technische Universität Dresden, 01062 Dresden, Germany

toni.rosemann@tu-dresden.de

Keywords: Feed-in substation, Prosumer, Solar thermal, Control, hardware-in-the-loop

ABSTRACT

The integration of decentralized feed-in of solar heat into district heating networks results in a high volatility regarding daily and seasonal pressure and temperature characteristics. Therefore new control and automation devices and algorithms are required to handle the complexity of the system. Furthermore the presented combined supply and feed-in substation – a so-called prosumer substation – needs a state machine (automation of switching between the several operation modes) in order to optimise the distribution of solar heat gains: feed-in into the district heating network and/or partly to local consumption. This paper presents results regarding the developed controller system, the test rig for emulation of the solar thermal system and a building as well as measurement data of a complex part of chosen daily load curves. The latter is the synthesis of the emulation test rig, the functional model of the combined supply and feed-in substation and the control system. The presented results are gained as parts of the R&D projects “Dezentrale Einspeisung in Nah- und Fernwärmesysteme unter besonderer Berücksichtigung der Solarthermie” and “Kostenreduktionspotential beim Ausbau der Solarisierung von Fernwärmenetzen durch Standardisierung” (see [1] and [2],[3]).

INTRODUCTION

Substation Concepts

The classic district heating network consists of one or more centralized heat generators and multiple consumers. The consumer is connected to the network via a supply substation, which is used for control, heat transfer and often hydraulic separation (see Figure 1). Decentralized heat generators need a feed-in substation in order to transfer small fractions of the design heat load of the network into it. Their position within the network is more arbitrary than the placement of centralized heat generators and one main task is to deal with the dynamic pressure difference of the network while transferring the maximum heat at the given temperature setpoint. A new plant concept of a combined supply and feed-in substation hereinafter referred to as COMBINED SUBSTATION is presented in this paper.

In comparison to the combination of a standalone feed-in and a supply substation the COMBINED SUBSTATION has the following advantages:

- higher collector efficiency due to
 - lower temperature setpoint of the solar thermal system during local supply,
 - lower return temperatures of the solar thermal system (STS) during simultaneous feed-in and local supply
- less components due to shared hydraulic circuits.

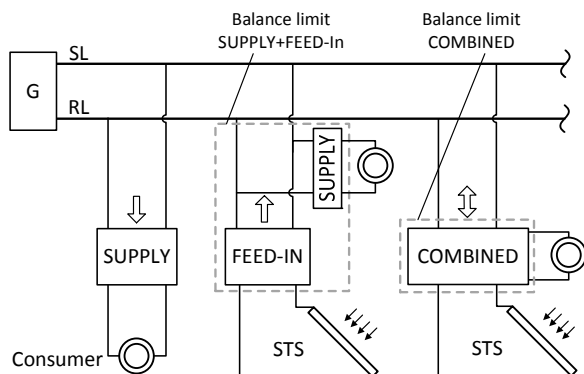


Figure 1 General types of substations (G.. centralized generator)

Combined Substation

The paper presents first measurement results of a COMBINED SUBSTATION. The paper is a further development of the publication [3]. The main objects are:

- The demonstration of the developed control strategy for the feed-in pump.
- The discussion of an exemplary part of the COMBINED SUBSTATION operation during a day.
- The introduction of the Emulation Test Rig.

The planned field of application of the COMBINED SUBSTATION is urban areas with existing district heating networks but lack of space for large central solar thermal plants.

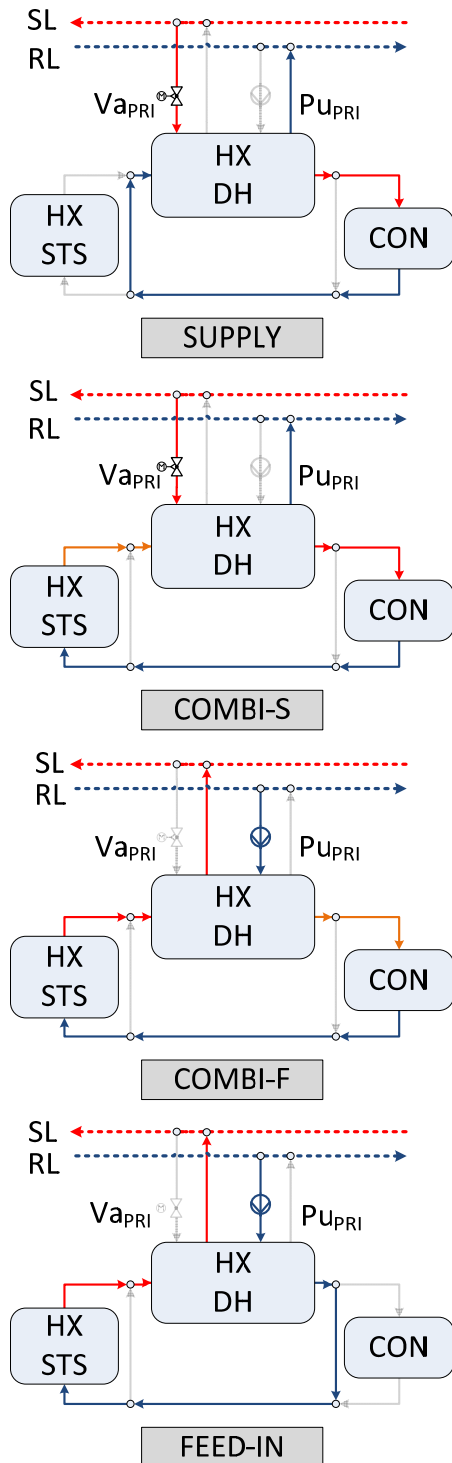


Figure 2: Simplified schematics of the operation modes of the COMBINED SUBSTATION

Therefore buildings like multiple dwellings with local heat requirement and space for average sized solar thermal systems are well suited for this concept.

The basic functioning of the COMBINED SUBSTATION can be explained using the four operation modes showed in Figure 2. Each operation mode is characterised by the constellation of radiation respectively solar gains and the consumers heat demand:

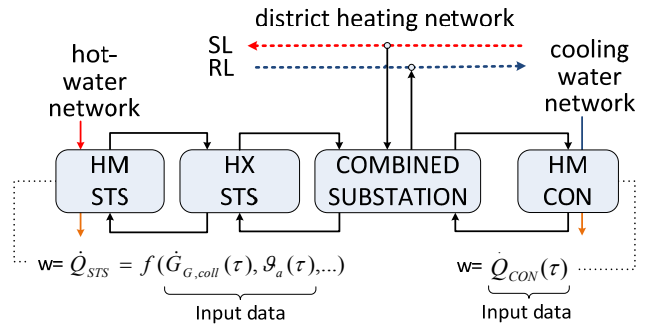


Figure 3 Structure of the Emulation Test Rig

- SUPPLY: the demand of the consumer is covered completely by the district heating network
- COMBI-S: the demand of the consumer is covered by the solar thermal system and the district heating network
- COMBI-F: the demand of the consumer is covered by the solar thermal system while excess energy is fed into the district heating network
- FEED-IN: there is no demand of the consumer thus solar thermal gains are fed into the district heating network.

Further background information on the COMBINED SUBSTATION concept can be found in [3].

EMULATION TEST RIG, CONTROL STRATEGY AND CONSTRAINTS

Emulation Test rig

The Emulation Test Rig as shown in Figure 3 consists of the functional model of the COMBINED SUBSTATION and so called hydraulic modules (HM) for the emulation of the solar thermal system (HM solar plant) and the consumer (HM consumer). They can provide or use heat at specified temperatures and in a time-controlled way in order to behave like a realistic solar plant or consumer. The district heating network is a small secondary network with one additional supply station.

Control Strategy

The functional model of the COMBINED SUBSTATION is shown in Figure 4. The components which are connected directly to the district heating network are on the primary side (PRI). These are the control valve V_{aPRI} for the supply of district heat and the RL-SL feed-in pump P_{uPRI} . The other three valves $V_{aPRI,1}..V_{aPRI,3}$ are used to switch between supply and feed-in. The secondary solar pump $P_{uSEC,STS}$ is located on the secondary side (SEC) and moves the fluid between the heat exchanger (HX) of the solar system and the heat exchanger of the district heating network. The secondary valve V_{aSEC} is a distribution valve which fulfils two different functions depending on the

operation mode. During the operation mode SUPPLY it's in the position AB-B in order to bypass the pump $P_{U_{SEC,STS}}$ preventing it from generating operation. During all other operation modes it's in the position AB-A acting as a hydraulic separator between the points C-D (see Figure 4) in order to decouple the pumps $P_{U_{SEC,STS}}$ and $P_{U_{CON}}$ hydraulically. The latter is the consumer pump $P_{U_{CON}}$ which is located on the side of the consumer (CON) for moving the fluid through the domestic hot water system and/or heating circuits. The solar thermal system is used in matched-flow operation in order to adapt the solar thermal supply temperature to the district heating network or consumer.

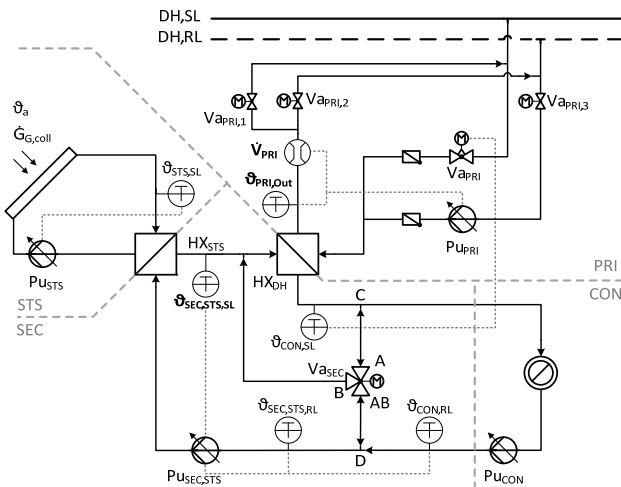


Figure 4 Schematic of the functional model of the COMBINED SUBSTATION

Table 1 Actuators with corresponding control variable and the operation modes their closed loop is active in (● – active, ○ – inactive)

actuator	control variable	active in			
		SUPPLY	COMBI-S	COMBI-F	FEED-IN
V_{aPRI}	θ_{CON}	●	●	○	○
$P_{U_{PRI}}$	$\theta_{PRI,OUT}$	○	○	●	●
$P_{U_{SEC,STS}}$	$\theta_{SEC,STS,SL} - \theta_{CON}$	○	●	○	○
$P_{U_{SEC,STS}}$	$\theta_{SEC,STS}$	○	○	●	●
$P_{U_{CON}}$	$\Delta p_{P_{U_{CON}}} = const$	●	●	●	○
$P_{U_{STS}}$	θ_{STS}	○	●	●	●

The active actuators and their control variable for each operation mode are shown in Table 1. The used closed-loop controllers are discrete PID controllers with conditional integration as anti-windup method and a sample time of $\Delta T = 3 s$.

The parameterization is done with the *MATLAB pidtune* function with a model gained through experimental process identification as well as estimation and trial.

The control of the feed-in pump has two differing tasks:

1. exceeding the pressure difference of the district heating network in order to generate a volume flow V_{PRI}
2. controlling the feed-in supply temperature by adapting the volume flow V_{PRI} .

Therefore the cascaded closed-loop controller showed in Figure 5 is used in combination with the control algorithm showed in Figure 6. Only the inner controller alias volume flow controller is used for task 1 getting into the district heating network. Since the inner controller is parameterized for continuous feed-in – task 2 – the setpoint $W_{V_{PRI}}$ has to be relative high resulting in a high control deviation and respectively in a fast growing control signal for the feed-in pump $P_{U_{PRI}}$. During task 2 the outer controller sets the setpoint of the inner controller for achieving the setpoint $W_{\theta_{PRI,OUT}}$ of the feed-in supply temperature. This setpoint equals the operation curve $\theta_{DH,SL} = f(\theta_a)$ of the district heating network.

CONDITIONS

The conditions used for the calculations in the emulation test rig are:

- weather data is a modified German test reference year 2011 (see [4])
- consumer
 - the consumer heat load profile $Q_{CON}(t)$ is calculated by an adapted tydial-day method following VDI 4655 which is presented in [1]

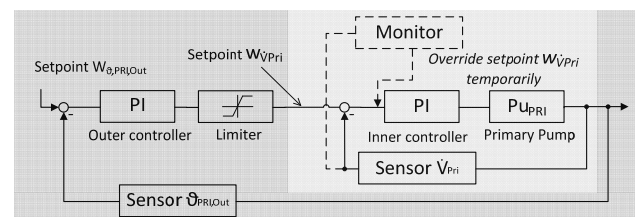


Figure 5 cascaded closed-loop control of the feed-in pump $P_{U_{PRI}}$ (bright grey – task 1, dark grey – task 2)

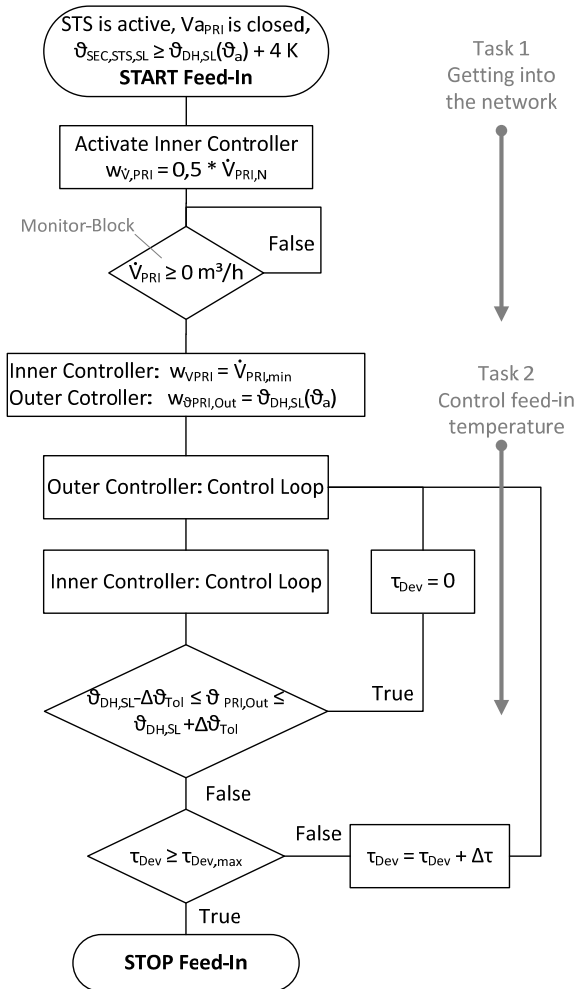


Figure 6 Flowchart of the control algorithm of the feed-in pump Pu_{PRI}

- a fixed return line temperature at the building side
 $\vartheta_{CON,RL} = 30\text{ }^{\circ}\text{C}$ is assumed
- a common algorithm is used for switching between domestic hot water heating and space heating (see [1])
- district heating network
 - Supply temperature $\vartheta_{DH,SL} = f(\vartheta_a)$ with a linear range between $\vartheta_a = -6.8\text{ }^{\circ}\text{C}$ and appropriate supply temperatures in range of $\vartheta_{DH,SL} = 110.75\text{ }^{\circ}\text{C}$
 - constant return temperature
 $\vartheta_{DH,RL} = 30\text{ }^{\circ}\text{C}$
- collector efficiency model for solar thermal system emulation

- collector parameters of a double glazed flat plate collector with selective absorber $\eta_0 = 0.8$,
 $c_1 = 3.757\frac{\text{W}}{\text{m}^2\cdot\text{K}}$, $c_2 = 0.0147\frac{\text{W}}{\text{m}^2\cdot\text{K}^2}$
- aperture area $A_{AP} = 100\text{ m}^2$

Using this conditions the input data shown in Figure 7 is generated for a day during the transition period with a highly volatile course of radiation.

RESULTS

Measurement in the emulation test rig

The measurement results of the presented typical day are shown in Figure 8. In the initial situation at [A] the operation mode is COMBI-F. With decreasing solar radiation $G_{G, coll}$ the thermal power of the solar thermal system is not sufficient to keep the secondary solar supply temperature $\vartheta_{SEC,STS,SL} \geq 4\text{ K} + \vartheta_{DH,SL}(\vartheta_a)$ which is seen at [B]. When the solar supply line temperature falls below the desired feed-in temperature $\vartheta_{SEC,STS,SL} < \vartheta_{DH,SL}(\vartheta_a)$ the feed-in is stopped at [C] and the operation mode switches to COMBI-S. Since the solar gains cover the consumer heat demand completely there is no supply by the district heating network. This changes at [D] because of the solar thermal deficiency indicated through low consumer supply temperatures $\vartheta_{CON,SL} < \vartheta_{CON,SL} + 5\text{ K}$ additional heat out of the network \dot{Q}_{CONDH} is obtained.

The solar radiation $G_{G, coll}$ reaches it's minimum at [E]. Approximately 70 % of the consumer thermal power demand are covered by the solar thermal system while the other 30 % are covered by the supply of the district heating network. The high return temperatures of the district heating network $\vartheta_{PRI,OUT} \approx 57\text{ }^{\circ}\text{C}$ are a drawback of the chosen series connection of the heat exchanger HX_{STS} and HX_{PRI} . The regulations of the district heating operator determine the admissibility of the operation mode COMBI-S in those cases. Full solar thermal coverage is reached again at [F] and with further rising secondary solar supply temperatures $\vartheta_{SEC,STS,SL}$ the transition to the operation mode COMBI-F happens at [G] due to the criterion $\vartheta_{SEC,STS,SL} \geq 4\text{ K} + \vartheta_{DH,SL}(\vartheta_a)$. A short and random failure of the secondary solar pump $Pu_{SEC,STS}$ at [H] causes the drop in the feed-in power \dot{Q}_{STTDH} .

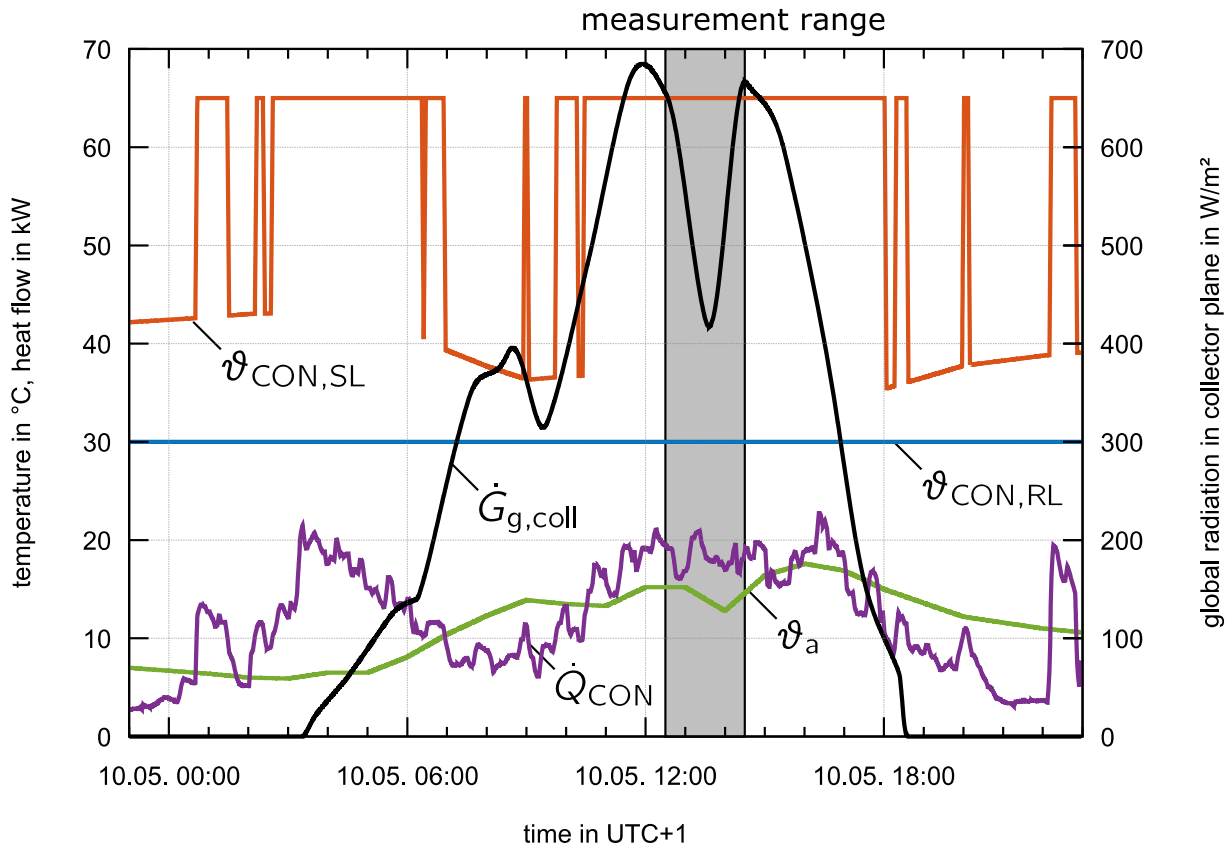


Figure 7 Input data for the emulation test rig for the typical day 10.05. of the reference year 2011

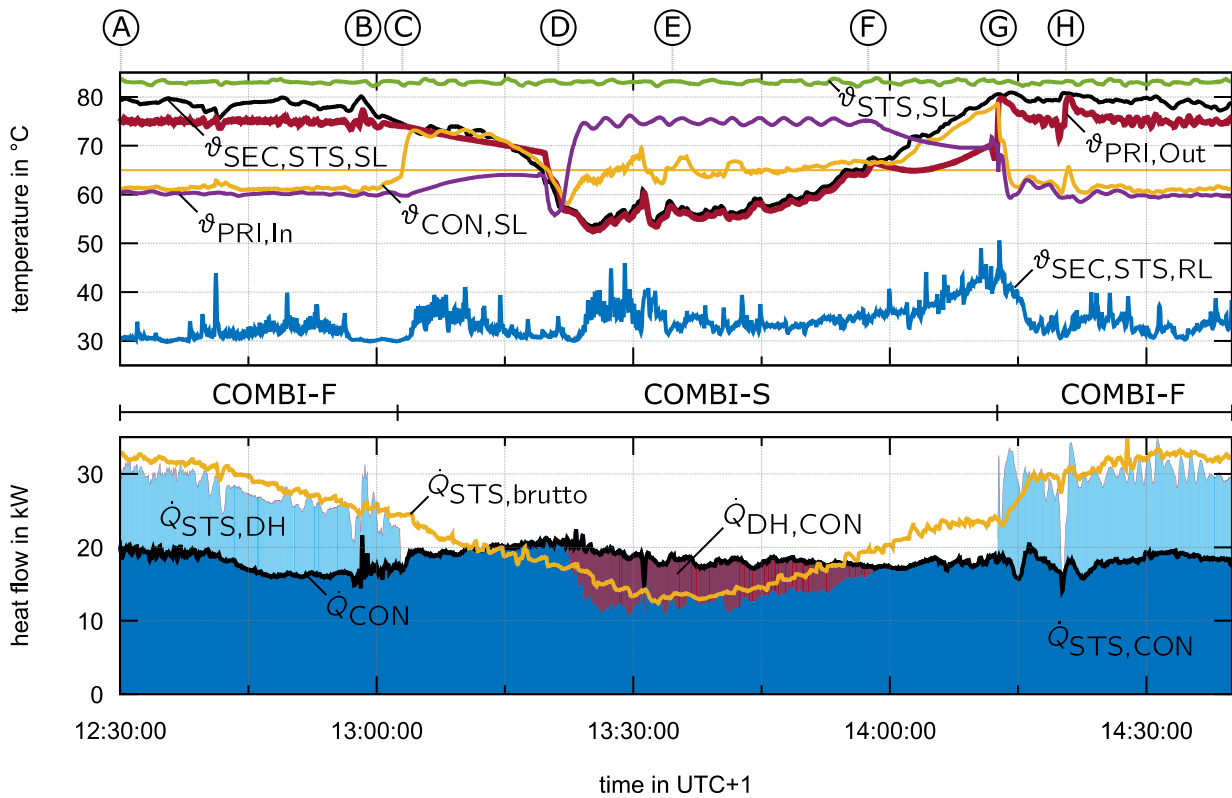


Figure 8 measurement results of highlighted range shown in Figure 8 for the typical day 10.05. in the transition period

Improvement of the combined substation

The following improvements will be considered for further development based on the experience gained of the operation in the emulation test rig.

The installation of a control valve as a bypass to the feed-in pump Pu_{PRI} and the primary heat exchanger HX_{PRI} (see Figure 9) would improve the system behaviour during the startup phase of the feed-in and the part-load performance during phases of low radiation. This affects especially the operation mode FEED-IN and is therefore object of investigation of the R&D project "Kostenreduktionspotential beim Ausbau der Solarisierung von Fernwärmenetzen durch Standardisierung" (see [2]).

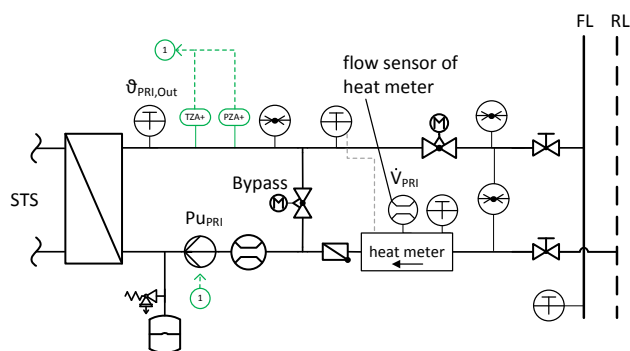


Figure 9 Schematic of the primary side of a feed-in substation with bypass

Furthermore it is necessary to consider an additional design criteria for the solar pump Pu_{STS} and the secondary solar pump $Pu_{SEC,STS}$. This design criteria is to ensure low volume flows \dot{V}_{STS} and $\dot{V}_{SEC,STS}$ during phases of low radiation or low consumer heat demand. An additional control valve connected in series to these pumps can be used if no sufficient pump is found.

CONCLUSIONS/PROSPECTS

The shown measurement results are a proof of concept for the two unique operation modes of the presented COMBINED STATION concept. The designed and successfully applied control algorithm of the feed-in pump is presented. The exemplary measurement also shows the behaviour of the plant during reduced radiation and the transition into the feed-in mode and the necessity of improvement. The gained experience about the operation behaviour leads to improvements which will be tested in a pilot plant in Berlin whose operation starts in autumn 2016.

NOMENCLATURE

Symbols

A	area	m^2
c	collector parameter	-
	radiation	W/m^2
	heat	kW
	heat flow	kW
	volume flow	m^3/s
w	setpoint	-
η	optical degree of efficiency	-
	Celsius temperature	$^{\circ}\text{C}$
	time	s

Abbreviations/Indices

AP	aperture
coll	in collector plane
COMBINED SUBSTATION	combined supply and feed-in substation
CON	consumer
Dev	Deviation
DH	District heating
FEED-IN	operation mode (like a feed-in substation)
G	global
HX	heat exchanger
In	entrance heat exchanger
Out	outlet heat exchanger
Pu	pump
PRI	primary
RL	return line
SEC	secondary
SL	supply line
STS	solar thermal system
SUPPLY	operation mode (like a district heating substation)
Tol	tolerance
Va	valve

REFERENCES

- [1] K. Rühling and S. Gnüchtel and C. Felsmann and M. Heymann and T. Rosemann, Dezentrale Einspeisung in Nah- und Fernwärmesysteme unter besonderer Berücksichtigung der Solarthermie, Final Report, 2015, Project founded by Federal Ministry for Economic Affairs and Energy
FKZ 03ET1039B
- [2] Ongoing project „Kostenreduktionspotential beim Ausbau der Solarisierung von Fernwärmenetzen durch Standardisierung“ founded by Federal Ministry for Economic Affairs and Energy FKZ 0325553A
- [3] K. Rühling and M. Heymann and T. Rosemann and B. Hafner “Technische Aspekte der Dezentralen Einbindung von Wärme in bestehende Fernwärmenetze” in Proc. OTTI-Fachforum Dezentrale Einbindung von Wärme in Nah- und Fernwärmenetze 2016
- [4] T. Rosemann and J. Löser and K. Rühling "Controller Development for a Combined Supply and Feed-In Substation and Testing Through Emulation" in Proc. 3rd International Solar District Heating Conference.
- [5] Bundesamtes Für Bauwesen und Raumordnung (Bbr) and Climate & Environment Consulting Potsdam Gmbh and Deutscher Wetterdienst (Dwd): Aktualisierte und erweiterte Testreferenzjahre von Deutschland für mittlere, extreme und zukünftige Witterungsverhältnisse, 2014

ACHIEVING LOW RETURN TEMPERATURE FOR DOMESTIC HOT WATER PREPARATION BY ULTRA-LOW-TEMPERATURE DISTRICT HEATING

XC. YANG¹, S. Svendsen²

^{1,2} Civil Engineering Department, Technical University of Denmark, Denmark

Building 118, Brovej

DK-2800 Kgs. Lyngby, Denmark

Keywords: *Ultra-low temperature district heating, domestic hot water, micro tank, electric heater, return temperature, heat loss*

ABSTRACT

District heating (DH) is a cost-effective method of heat supply, especially to area with high heat density. Ultra-low-temperature district heating (ULTDH) is defined with supply temperature at 35-45 °C. It aims at making utmost use of the available low-temperature energy sources. In order to achieve high efficiency of the ULTDH system, the return temperature should be as low as possible. For the energy-efficient buildings in the future, it is feasible to use ULTDH to cover the space heating demand. However, considering the comfort and hygiene requirements of domestic hot water (DHW) preparation, supplementary heating devices should be combined, which can affect the return temperature in different extents. This study analysed the return temperatures of different types of substations for DHW preparation with ULTDH, and developed improvements in the substation for better energy efficiency. Both the instantaneous and storage-type electric heating methods were Long-term measured as supplementary heating for ULTDH in the case substations in Denmark. We analysed the seasonal impacts of the return temperature from the DHW loop on the overall return temperature of district heating. To achieve lower return temperature and higher efficiency for DHW supply, an innovative substation was devised, which replaced the bypass with an instantaneous heat exchanger and a micro electric storage tank. The energy performance of the proposed substation and the resulting benefits for the DH system by the lower return temperature were investigated.

INTRODUCTION

District heating is a cost-effective way of utilizing renewable and recycle energy as heating sources for covering the heat demand of the high-heat-density areas. The temperature levels of district heating systems is of great importance for better efficiency. Low supply temperature can increase the efficiency of recovering heat from industrial excess heat and geothermal heat, and can also improve the coefficient of performance (COP) of a heat pump for heat production[1]. Low return temperature can improve the

efficiency of flue gas condensation in the heat plant. In addition, the distribution heat loss will be reduced if the distribution heat loss is lowered. Therefore, to implement low-temperature district heating (LTDH) plays an important role in improve the whole district heating system.

However, the comfort and hygiene requirements for heat supply should be taken into account when reducing the DH supply/return temperatures. In Nordic countries, such as Denmark and Sweden, DH supply covers both the space heating (SH) demand and domestic hot water (DHW) demand. For space heating, a comfort room temperature (20-22 °C) can be reached with a supply temperature at 40 °C if efficient heating equipment and operation methods are applied [2]. Regarding to DHW supply, the DHW should be able to be produced at 60 °C and circulated at 50 °C to avoid Legionella [3], and the water temperature at the faucet is required to reach 45 °C for the comfort reasons [4].

This study is based on an ultra-low-temperature district heating project in Denmark, where the heat demand of the test houses are covered by a DH system with supply temperature at 46 °C most of the year. To guarantee comfort and hygiene heat supply for DHW, different types of supplementary heating devices were installed in the house substations. However, the return temperatures of the DHW circuits are various according to the different substation layouts. This study investigated the return temperatures and energy performances resulted by different substations. In addition, a new DHW preparation method with ULTDH was devised, which aims at improving the overall system efficiency and reducing the return temperature to DH.

BACKGROUND OF THE ULTDH CASE STUDY

The case project is located in Denmark. The heat source is the industrial excess heat from a local pump factory. A heat pump is used to recover the waste heat and deliver the heat to the heat consumers at 46 °C most of the year. The supply temperature is able to be increased to compensate the extreme cold climate during the winter.

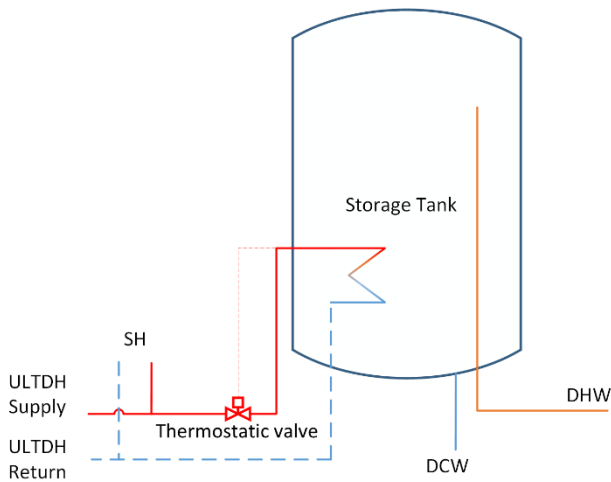


Figure 1. Schematic of the DHW configuration in house #1 with storage tank

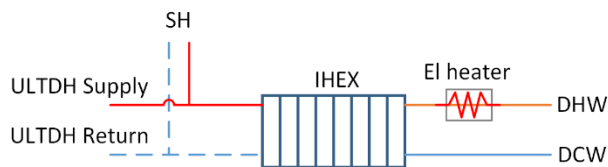


Figure 2. Schematic of the DHW configuration in house #2 with IHEX and electric heater

COMPARISON OF RETURN TEMPERATURES FROM DIFFERENT DHW CONFIGURATIONS

The DHW preparation configurations play an important role in the average return temperature of the DHW circuits to DH. Two single-family houses in the area were selected for the analyses of this study. Both of the houses have the in-house substation. House #1 uses a storage tank for DHW preparation, while house #2 uses an instantaneous heat exchanger (IHEX) and a direct electric heater. House #1 and house #2 were built in similar time, and both of the houses have two occupants.

The schematics of the substations of the two case houses are shown in Figs. 1 and 2.

In house #1, a 160L storage tank with 3 kW immersion heater is installed. The domestic cold water (DCW) is preheated by the district heating, and is further heated by the immersion heater in the tank to the set-point temperature (50 °C). Since DHW is stored in the tank, the tank should have sufficient capacity to heat the water to 60 °C.

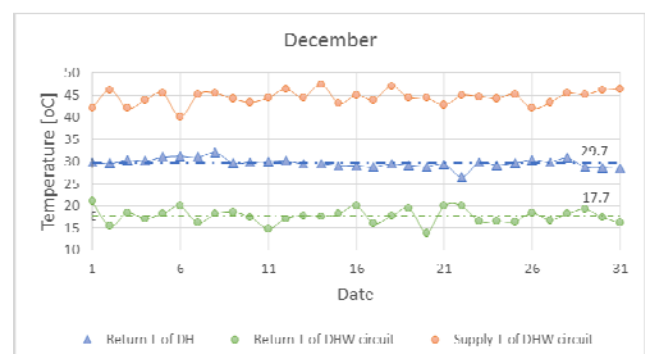
In house #2, an instantaneous heat exchanger with bypass function is installed. The DCW is preheated by the ULTDH through the heat exchanger, and is further

heated by the direct electric heater after then heat exchanger. Since the total volume of the DHW in the distribution pipes inside the house is very small, the risk of Legionella is eliminated. The set point temperature of the electric heater was made at 45 °C to meet the comfort requirement. In Denmark, the waiting time for DHW at comfort temperature should be no longer than 10s [4]. Considering the transmission time in the pipes, normally bypass is operated for the IHEX. The bypass set-point temperature in the case house was made to 40 °C.

Long-term measurements were performed for the test houses. energy meters were located on both the DH main pipe (including both SH and DHW) and the DHW preparation circuit. The meters can measure the overall supply and return temperatures, flowrates and supply heat of ULTDH, as well as the values of the DHW preparation loop. The measurements of August 2015 and January 2016 were selected to represent for the summer season and winter season. The impact of the return temperature from the DHW circuit on the overall return temperature to DH was also investigated.



(a) House #1



(b) House #2

Figure 3. Temperature measurements of return temperature in December in house #1 and #2

Table 2. Average return temperature of the DHW circuit , average return temperature of DH and the temperature difference with standard variation of December

	House #1		House #2	
	Average	Standard variation	Average	Standard variation
Return T of DH [°C]	32.0	2.2	29.7	1
Return T of DHW circuit	25.5	1.7	17.7	1.7
Supply T of DHW circuit	44	1.4	44.5	1.6
ΔT	18.5	1.6	26.8	2.7

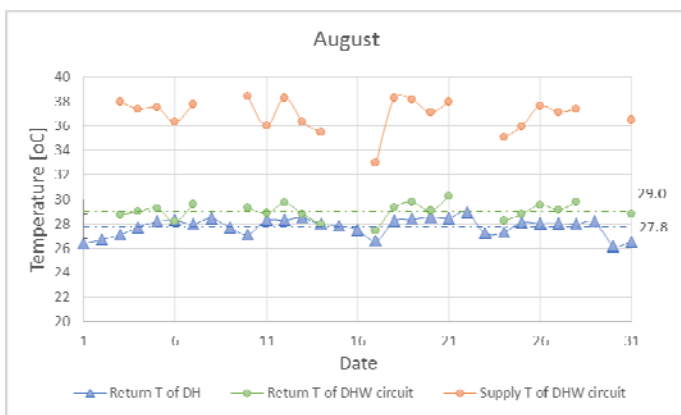
Results of the return temperatures from different DHW configurations

The results of the temperature measurements in the summer season and winter season in the two houses are shown in the following diagrams:

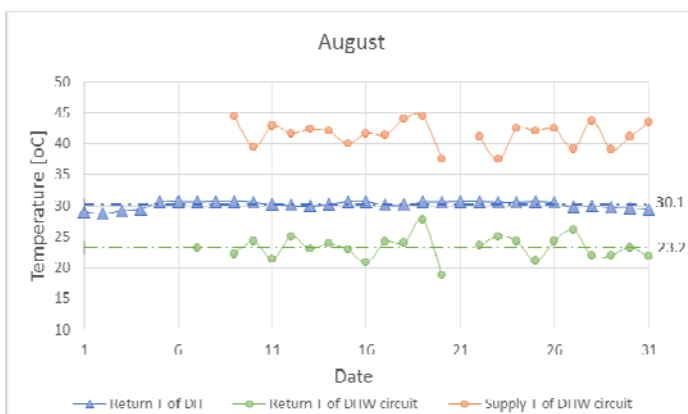
The blue curves represent the overall return temperature of district heating, which integrates the return temperatures of both the space heating circuit and domestic hot water circuit. From the diagrams, the supply temperatures of the ULTDH system were both around 45 °C when they reach the substations in house #1 and house #2. However, house #2 with IHEX and electric heater had much lower return temperature for DHW preparation compared with house #1 with a storage tank.

The average return temperature to DH and the return temperature of the DHW circuit on monthly basis as well as the temperature difference are shown in table 1:

From Table 2, the average return temperature of house #2 with IHEX and electric heater is 7.8 °C lower than house #1 with a storage tank. With similar supply temperature, the temperature difference for DHW preparation with IHEX and electric heater is 8.3 °C larger compared with the substation with storage tank. That indicates that the instantaneous preparation of DHW with IHEX and electric heater has better energy and exergy efficiency than the storage type. The difference of the overall return temperature to DH is insignificant between house #1 and house #2. The overall return temperature of house #2 is only 2.3 °C lower than that of house #1. However, the overall return temperature of DH also includes the space heating flow. During the winter time, the space heating flow dominates the overall DH flow, which can have a more significant impact on the overall return temperature. The higher overall return temperature also indicated that the return temperature of the space heating circuit is higher.



(a) House #1



(b) House #2

Figure 4. Temperature measurements of return temperature in August in house #1 and #2

Figure 4 shows the temperature measurements during the summer period. The periods without any data points means the occupants were leaving for a vacation.

The DH supply temperature was lowered during the summer time. The results in house #1 shows different trend compared with the winter time. As shown in Figure 4 (a), the return temperature of DHW circuit in house #1 is slightly higher than the overall DH return temperature.

In terms of house #2, the average return temperature of the DHW circuit is higher in summer, but still lower than the overall return temperature of DH, which

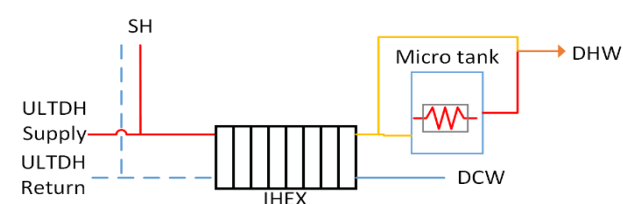
indicates the space heating loads in the house during the summer.

The average temperatures of August with standard variation and the actual temperature difference for DHW production are calculated, the results are shown in table 2.

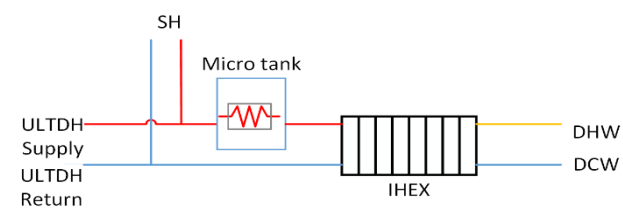
In August, the return temperature from instantaneous DHW production is 5.8 °C lower compared with the storage type. However, compared to the winter period, the return temperature of the DHW circuit in both houses increased. This might be caused by the lower efficiency of the heat exchanging process due to the lower DH supply temperature. As a result, the actual temperature difference for DHW production in summer season reduced by 10.6 °C for house #1 and 8.5 °C for house #2. According to the temperature difference for DHW production, the instantaneous DHW production still performed better than the storage type.

Table 1. Average return temperature of the DHW circuit , average return temperature of DH and the temperature difference with standard variation of August

	House #1		House #2	
	Average	Standard variation	Average	Standard variation
Return T of DH [°C]	27.8	0.7	30.1	0.6
Return T of DHW circuit [°C]	29.0	0.7	23.2	2.0
Supply T for DHW circuit [°C]	36.9	1.3	41.5	2.0
ΔT [°C]	7.9	0.8	18.3	2.7



(a) Micro tank installed on the consumer side



(b) Micro tank installed on the primary side

Figure 5. Schematics of the DHW configuration with micro tank

Comparing the return temperatures of DHW circuit in winter and summer, house #2 has more significant temperature increase in the summer period. One reason can be the operation of bypass, which is used to keep the service pipe warm between the DHW draw offs, so that the consumers can get DHW at comfort temperature within acceptable waiting time. However, since the bypass flow has to be operated at high temperature and does not exchange heat with DHW, the operation of bypass will result in extra heat losses and higher return temperature due to direct mixing into the return flow. Therefore, improvements of the DHW configurations are expected by avoiding the bypass.

NEW DHW CONFIGURATION TO ACHIEVE LOWER RETURN TEMPERATURE

According to the Danish standard, the peak load of DHW is 32.3 kW. If no bypass is operated, the power of the electric heater should be as large as 32.3 kW during the beginning of the tapping, so that DHW can be heated to comfort temperature immediately. However, the capacity of the power supply then has to be increased substantially compared to the normal supply. Therefore, an electric heater with small storage volume is devised to replace the bypass function and to avoid the too large starting power for DHW production.

The schematics of the new DHW configurations are shown in Figure 5.

As shown in the diagrams, the micro tank with small storage volume of hot water is used to buffer the peak load of the starting power. As a result, a normal electrical heater can be used without enlarging the capacity of the power transmission.

The system configuration and the dimension of the micro tank can vary according to the supply temperature of LTDH as well as the location of the micro tank. The operation of the micro tank is also different consequently.

As shown in Figure 5 (a), DCW is preheated by DH through the heat exchanger. Afterward, the preheated water is further heated by the micro tank and is stored in it. To avoid Legionella, the water in the tank is heated to 60 °C [3]. When DHW draw off occurs, the hot water from the tank will mix with the hot water preheated from DH to achieve the comfort temperature (45 °C for kitchen use and 40 °C for other uses).

The other type of the configuration is to install the micro tank on the primary side, as Figure 5 (b) shows. The micro tank is used to heat and store the DH water. Therefore, the DHW circuit has no storage or circulation, which allows the set-point temperature of the micro tank to be lower than 60 °C.

Table 2. Parameters for micro tank dimension

	Micro tank on consumer side	Micro tank on primary side
Demand for kitchen use	45 °C with 15 L water consumption	
Demand for shower	40 °C with 42 L water consumption	
Interval time between tappings	20 min	
Electric heater power	2 kW	
DCW temperature	10 °C	
Set point temperature of then tank	60 °C	50 °C

Micro tank systems with different ULTDH supply temperature levels

The supply temperature of ULTDH were assumed to 30 °C, 40 °C, and 45 °C as three scenarios for comparison. The electric heater in the tank was assumed to be a normal product with the power of 2 kW for all scenarios. In accordance with the Danish standard [4], the peak load of the DHW supply is 32.3 kW, which assumes one shower and one kitchen tapping occur simultaneously. The shortest interval between two tappings of the same type is 20 minutes. Therefore, the volume of the micro tank can be decided.

The parameters for dimension the micro tank are shown in table 3.

The IHX are assumed to be the same one used in the case study, which is specialized for LTDH substations and can reach the return temperature of 18.8 °C with effective cooling [5]. The temperature difference of the heat exchanging process through the heat exchanger was assumed to 5 °C. It was assumed that the micro tank should contain enough hot water to cover one peak load of DHW at least. The electric heater is switched on as soon as the draw off finished, and should be able to prepare sufficient hot water for the next draw off with peak load.

For the micro tank installed on the consumer side, to cover one peak DHW load, the required water flow at 60 °C can be calculated as:

$$V_{\alpha}^k = \frac{(t_k - t_{pre}) / (t_{tank} - t_{pre}) * V_k + (t_{sh} - t_{pre}) / (t_{tank} - t_{pre}) * V_{sh}}{(t_{tank} - t_{pre}) * V_{sh}} \quad (1)$$

where

t_k, t_{sh} are the DHW temperature for kitchen use and shower [°C],

t_{pre} is the temperature of DHW preheated by ULTDH [°C],

t_{tank} is the set-point temperature of micro tank, here is 60 [°C],

V_k, V_{sh} are the flow for one kitchen tapping and one shower according to the standard [L].

If the assumed 2 kW electric heater is insufficient for preparing DHW at peak load within 20 min interval, extra volume should be added to V_{α} for the tank dimension. Otherwise, the micro tank was dimensioned as V_{α} . The peak load of the electricity can be calculated as:

$$P_{max}^k = \frac{(c * m_k * (t_k - t_{pre}) + c * m_{sh} * (t_{sh} - t_{pre}))}{\tau_{inter}} \quad (2)$$

where

c is the specific heat of water [kJ/kg·°C],

m_k, m_{sh} are the mass flow of kitchen tapping and shower [kg],

τ_{inter} is the interval time [s].

For the micro tank on the primary side, the DH water flowing out of the tank is 50 °C for all three scenarios with different ULTDH supply temperature. The required water flow was calculated as:

$$V_{\alpha}^p = \frac{((t_k - t_{dmv}) * V_k + (t_{sh} - t_{dmv}) * V_{sh}) / (t_{tank} - t_{dmv})}{(t_{tank} - t_{dmv})} \quad (3)$$

where

t_{dmv} is the temperature of DCW [°C],

t_{dmr} is the return temperature from the heat exchanger [°C].

For the micro tank on the primary side, the peak load of the electric heater was calculated differently compared to the tank on the consumer side, since the water from the tank is unnecessary to mix with other flows but to heat the DCW directly.

$$P_{max}^p = \frac{(c * m_k * (t_k - t_{dmv}) + c * m_{sh} * (t_{sh} - t_{dmv})) * (t_{tank} - t_{dmv}) / (t_{tank} - t_{dmr})}{\tau_{inter}} \quad (4)$$

where

t_{dmv} is the supply temperature of ULTDH [°C].

Comparison with direct electric heater with bypass function

Comparisons were made between the storage type electric heater system and direct electric heater system with bypass function. All the systems were assumed to supply the equivalent DHW demand, which is 250 L/ m² annually. The service pipe was assumed to have the length of 6m with heat loss coefficient of 0.2 W/m K. The ambient air temperature was assumed to 15 °C. The ground temperature was assumed to 10 °C.

The heat loss of different systems in different scenarios were investigated. For the system with micro tank, the heat loss mainly refers to the heat loss of the tank. The heat loss coefficient of the tank was referenced from the Danish standard [6], which should be no larger than 0.35 W/ m² K. For the direct electric heater system with bypass function, the heat loss mainly includes the heat loss generated by bypass. The set-point temperature of the bypass was assumed to be 5 °C lower than the supply temperature of ULTDH.

The heat loss of the micro tank therefore can be calculated as

$$Q_{\text{tank}} = q_{\text{tank}} * s * (t_{\text{tank}} - t_{\text{amb}}) \quad (5)$$

where

q is the heat loss coefficient of the tank [W/ m² K],

s is the surface area of the tank [m²].

The heat loss of the service pipe caused by bypass function can be calculated as

$$Q_{\text{pipe}} = q_{\text{pipe}} * (t_{\text{pipe}} - t_{\text{ground}}) \quad (6)$$

where

q_{pipe} is the heat loss coefficient of the service pipe [W/ m K],

t_{pipe} is the average pipe temperature when bypass is operated [°C],

t_{ground} is the ground temperature [°C].

One thing should be pointed out is that the heat loss of the micro tank is covered by both heat and electricity. Considering the different primary energy factor, the proportion of different energy used for heat loss covering is equivalent to the proportion for water heating.

As an important parameter, the return temperature to DH was also investigated for the three configurations. For the micro tank system, since no bypass was operated, the average return temperature is the return temperature for water heating. While for the direct electric heater system, it was calculated as the volume-

based average return temperature, which integrated the water heating flow and bypass flow.

The volume-averaged return temperature can be calculated as

$$t_{\text{ret}} = (t_{\text{wr}} * v_{\text{w}} + t_{\text{br}} * v_{\text{b}}) \quad (7)$$

where

t_{wr} is the return temperature for water heating [°C],

v_{w} is the flow for water heating [L/day],

t_{br} is the average temperature of the service pipe when bypass is operated [°C],

v_{b} is the flow for bypass [L/day].

RESULTS

Dimension of the micro tank for different scenarios

The dimensions of the micro tank on the primary side with different ULTDH supply temperature are shown in **Table 3**.

As shown in the table, the scenario with supply temperature at 35 °C is the only scenario that required power of the electric heater larger than 2 kW. As a result, it is the only scenario requires extra volume for the tank.

In terms of the micro tank on the primary side, the results are shown in Table 5.

Table 3. Dimension of the micro tank on the consumer side with supply temperature at 35 °C, 40°C, and 45 °C.

		Supply temperature of ULTDH		
		35 °C	40 °C	45 °C
V_{a}	[L]	21.5	14.4	3.8
P_{max}	[kW]	2.3	1.3	0.3
V_{extra}	[L]	2.5	0	0
Tank size	[L]	25	15	5

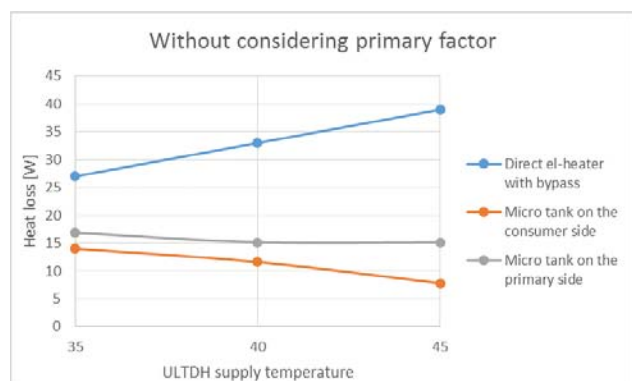
Table 4 Dimension of the micro tank on the primary side with supply temperature at 35 °C, 40°C, and 45 °C.

		Supply temperature of ULTDH		
		35 °C	40 °C	45 °C
V_{a}	[L]	57.2		
P_{max}	[kW]	3.0	2.0	1.0
V_{extra}	[L]	76.3	0	0

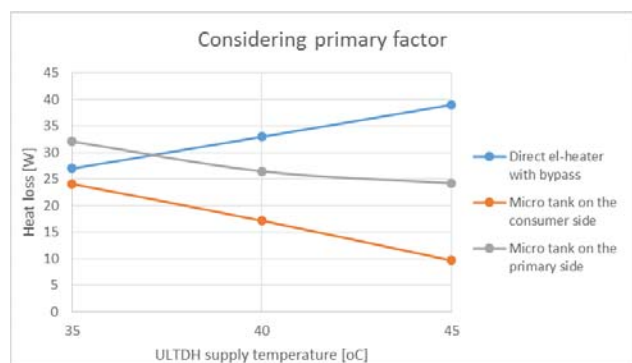
Tank size [L]	80	60	60
---------------	----	----	----

All the tank sizes were made to approach the closest existing product.

Comparing the results from **Table 3** and **Table 4**, the micro tank on the primary side requires much larger dimension with the same ULTDH supply temperature, which can increase the investment cost.



(a) Without considering the primary energy factor



(b) Considering the primary energy factor of 2.5 for electricity

Figure 6. Heat losses for three DHW configurations with different ULTDH supply temperatures

Table 5. Average return temperature of the electric heater system with bypass

	Supply temperature of ULTDH		
	35 °C	40 °C	45 °C
Set-point temperature of bypass [°C]	30	35	40
Water-heating flow [L/day]	127.2	121.5	117.9
Bypass flow [L/day]	111.1	135.8	160.5
Average return	24.0	27.4	31.0

temperature [°C]

Comparisons of three configurations

The heat losses of the three configurations are calculated. The results of considering / without considering the primary energy factor (2.5 for electricity) are shown in Figure 6.

From Figure 6 (a), without considering the primary energy factor, the heat losses of the micro tanks systems are much less than the direct electric heater system with bypass. However, the trends along the temperature increase are different. The heat loss caused by bypass increases if the ULTDH supply temperature is higher. While for the micro tank system, the tank size is smaller if the supply temperature is higher. Moreover, the proportion of the electricity consumption in covering the heat losses also decreases with higher supply temperature.

If taking the 2.5 primary energy factor for electricity into account, the system with a micro tank on the primary side has the largest heat loss when the supply temperature of ULTDH is lower than 37 °C. After that, the heat loss of the direct electric heater system with bypass becomes the largest. The system with a micro tank on the consumer side always has the lowest heat loss.

The results of the average return temperature of the direct electric heater system with bypass are shown in Table 5.

From the results, by mixing the bypass flow, the average return temperatures of the direct electric heater system increase significantly. Compared to the micro tank system, the average return temperature increases by 5.2 °C, 8.6 °C, and 12.2 °C with the supply temperature at 35 °C, 40 °C, and 45 °C.

DISCUSSION

The return temperature plays an important role in improving the energy efficiency of the DH system. The influence of the DHW configuration was discussed in this study, however, to obtain full knowledge about it, the analyses for the space heating loop should be taken into account. Further information regarding to the impact by the space heating loop can be found in [7]. In addition, the room temperature of the substation also plays a role in the heat loss from the distribution pipes inside the building, which can influence the average return temperature of DH system. In this study, the room temperature of the substation was assumed to 15 °C all the year. However, in reality this temperature can

be varied, the impact of which should be taken into account for the analysis of DH return temperature in the future.

As shown in the results, the operation of bypass can increase the average return temperature substantially, which makes conflict for improving the overall efficiency of the ULTDH system. In Denmark, if the average return temperature to district heating is below 42.9 °C, for every 1 °C reduction further, the overall cost for heat supply can reduce by 1%. According to the results of this study, it means the total cost for heat supply can save up to 12.2% if replacing the bypass by applying the micro tank solution. However, the actual savings should be analysed according to specific cases, since the results can be affected by many practical factors. Moreover, to target the appropriate DHW configuration, the economy of each system, the installation difficulty and etc. should also be taken into account in the future.

CONCLUSION

In this study, long-term measurements were performed in two Danish houses with ULTDH supply. The performances of the DHW configurations were investigated accordingly. The house with direct electric heater had lower return temperature compared with the house with storage tank. The difference of the return temperatures was 7.8 °C in winter and 5.8 °C in summer.

To improve the electric heater system, system with a micro tank with immersion heater was devised to eliminate the bypass function. Depending on the location of the tank, two types of micro tank systems were invented. The heat losses of the micro tank systems were compare to the direct electric heater system with bypass under standard condition. Considering the primary energy factor of 2.5 for electricity, the heat loss of the direct electric heater system was larger than the micro tank systems when the ULTDH supply temperature is higher. The system with a micro tank on the consumer side had the lowest heat loss. Moreover, the micro tank system also achieved significant reduction on the average return temperature by avoiding the bypass.

ACKNOWLEDGEMENT

The work presented in this paper is a result of the research activities of the Strategic Research Centre for 4th Generation District Heating (4DH), which has received funding from the Innovation Fund Denmark.

REFERENCES

- [1] H. Gadd, S. Werner. "Achieving low return temperatures from district heating substations", *Applied Energy*. 2014, Vol.136, pp. 59-67.
- [2] H. Lund, S. Werner, R. Wiltshire, S. Svendsen, and et al. "4th Generation District Heating (4GDH) Integrating smart thermal grids into future sustainable energy systems", *Energy*, 2014, Vol. 68, pp. 1-11.
- [3] DS/CEN/TR16355. Recommendations for prevention of Legionella growth in installations inside buildings conveying water for human consumption. Danish Standards; 2012.
- [4] DS 439:2009. Norm for vandinstallationer [Code of practice for domestic water supply installations] (in Danish). Danish Standards; 2009.
- [5] Danfoss Redan A/S. Akva LES II VXi - Fully insulated district heating unit for future district heating. 2015.
- [6] DS 452:2013. Termisk isolering af tekniske installationer [Thermal insulation of technical service and supply systems] (in Danish). Danish Standards; 2013.
- [7] D. Østergaard, S. Svendsen. "SPACE HEATING WITH ULTRA-LOW-TEMPERATURE DISTRICT HEATING – A CASE STUDY OF FOUR SINGLE-FAMILY HOUSES FROM THE 1980S", in submission to the 15th international symposium on district heating and cooling.

REDUCTION OF RETURN TEMPERATURES IN URBAN DISTRICT HEATING SYSTEMS BY THE IMPLEMENTATION OF ENERGY-CASCADES

M. Köfinger¹, D. Basciotti¹, R.R. Schmidt¹

¹ AIT Austrian Institute of Technology, Energy Department, Giefinggasse 2, 1210 Vienna, Austria

Keywords: district heating, energy-cascade, return temperature reduction, heat transport capacity

ABSTRACT

High return temperatures in district heating networks are a significant barrier for the transformation into 4th generation systems. In order to transport high amount of heat in winter times, there is the need of increased supply temperatures (>120 °C) or mass flow rates due to high return temperatures. This leads to an inefficient operation of the system. High heat losses, decreased efficiency of heat production units, reduced potential of alternative heat sources and increased pumping costs are the consequences. Further is the connection of new customers often linked with high investment costs due to limited transport capacities in an existing system.

The aim of this paper is to analyse potentials and to develop concepts to reduce return temperatures by implementing thermal energy cascades between different building types in order to improve the performance of the system. This is related to the use of the return flow of high-temperature consumers (e.g. buildings with high-temperature heating systems) for supplying low-temperature consumers (e.g. buildings with floor heating and direct domestic hot water preparation). Based on available data from existing buildings, energy suppliers and network structures, potentials for energy-cascades for representative case studies have been evaluated. To enable energy cascaded interconnections, the temperature and heat load profiles of the investigated buildings in characteristic districts were analysed and different connection scenarios were developed and evaluated. Special attention was given to the hygienic preparation of domestic hot water in the low-temperature consumers and the security of the heat supply.

As a result, the temperature level of the local return line could be reduced (up to >10 K) and transport capacities in the districts were increased (up to 16 %). By implementing this approach in several districts of an urban network, the overall system efficiency can be increased.

INTRODUCTION

In recent years, the profitability of many traditional district heating networks has significantly been reduced. The reasons for this are the uncertain price development of fossil fuels, combined with the close

link to the electricity market (especially for cogeneration plants falling electricity prices are problematic). The integration of alternative heat sources such as solar thermal, geothermal or ambient heat and industrial waste heat into district heating networks is in many cases difficult due to low temperature (LT) levels and fluctuating availability. A significant reduction of temperatures in heating networks, both in the supply and in return line is a key action to a transition to the next, the so called 4th generation of district heating, see also [1]. Substantial benefits of reduced system temperatures are:

1. A significant increase of the potential to integrate renewable heat sources
2. In extraction condensing turbines the efficiency increases, in extraction-back-pressure thermal power plants the share of generated electricity increases.
3. With a constant power input, the mass flow decreases in the network and this reduces the pumping costs. At the same mass flow, the network capacity can be increased (enabling the connection of new consumers). Thus the transport lines can have smaller dimensions, resulting in lower investment costs.
4. Reduced heat losses due to the lower temperature difference to the surrounding soil.

Studies on the effect of decreased return temperatures (e.g. [2]) show a reduction in operating costs in the entire heating network of approximately 0,15 € / (K * MWh).

The temperatures in a district heating network are determined by the connected consumers. So the return temperatures resulting mainly from the cooling of the heat carrier in the buildings heating system respectively the properties of the substations. However, the return temperatures show a slight upward trend with increasing heat demand, resulting from the mass flow control in the buildings and any existing bypasses between the supply and return line in the grid.

The supply temperatures are determined on the one hand by domestic hot water (DHW) preparation requirements (especially in summer) and the design of heating systems, on the other hand by the amount of transferred heat (especially in winter). As the difference

between supply and return temperature (ΔT) in case of an increasing heat demand is adjusted linearly, the supply is directly dependent from the return temperatures (at most times in the year). Accordingly, a reduction of the consumer side return temperatures is an essential measure to also reduce the supply temperatures. The increased potential of renewable heat sources is simplified shown in Figure .

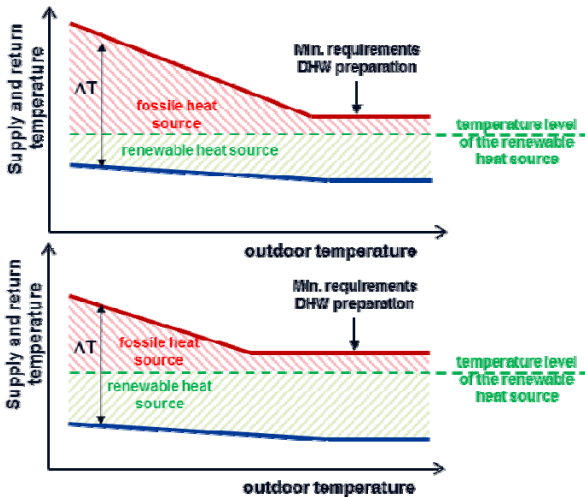


Figure 1: simplified representation of the influence of decreasing return temperatures on the potential of renewable heat sources with a low temperature level, above: the initial state with high return temperatures, below: possibility to reduce the temperatures

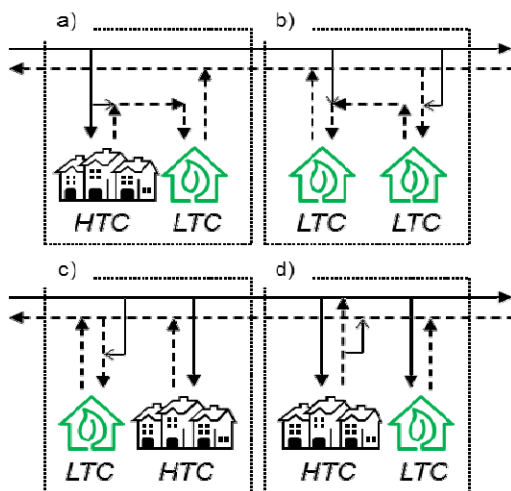


Figure 2: Option for direct or indirect cascading connection of high- and low-temperature consumers, a) direct use of HT-return, b) double cascade: indirect use of HT-consumer and direct use with an admixture, c) indirect use of HT return via the return line of the network d) indirect use via the supply line of the network, e.g. analysed in [11]

OBJECTIVE

The aim of this contribution is to develop and evaluate concepts for the reduction of local return temperatures in urban district heating systems by implementing energy-cascades between buildings, e.g. using the return flow of high-temperature consumers (HTC) as supply flow for low-temperature consumers (LTC). Therefore optimization potentials are identified in characteristic building clusters, considering the influence of these measures on the momentary and the average return temperatures and mass flow rates. All investigations and assumptions are based on Austrian case studies and regulations (e.g. DHW preparation, typical heating systems, etc.)

STATE OF THE ART

Heat cascades

To be able to connect buildings, building cluster or neighbourhoods in a heat cascade with each other, different options are possible. Using the return of HTC as supply for LTC can be done either indirectly through the return line of the network or directly through an interconnection of the buildings. In Figure 2 options of direct or indirect cascading connection of high- and low-temperature consumers are presented. Some of these options are already realised (e.g. in Klagenfurt [4] or Berlin [13]), but a general investigation on a scientific and systematic level as it is done in this project was not carried out before.

Building stock

Due to investment costs, property developers in Austria often implemented standard heating systems (in most cases radiators) in their buildings, regardless of the type and year of construction. As a consequence, the required temperature levels are often similar in different building types and ages. Therefore it is usually not possible to interconnect buildings as described in Figure 2 without further action. For existing buildings, to reduce the temperature levels, different measures like thermal retrofitting, exchange of radiators and hydraulic balancing can be implemented, see e.g. [4]. By optimising/reducing the required temperatures in individual buildings through these measures, this problem could be solved and heat cascades are possible. Another option is to integrate new low-temperature consumers in areas where high-temperature costumers are existing and where the above mentioned measures could not be implemented. However, a big challenge for lowering temperatures is the hygienic preparation of domestic hot water. Therefore different standard solutions can be used (e.g. fresh water modules). More advanced options can be found in [3].

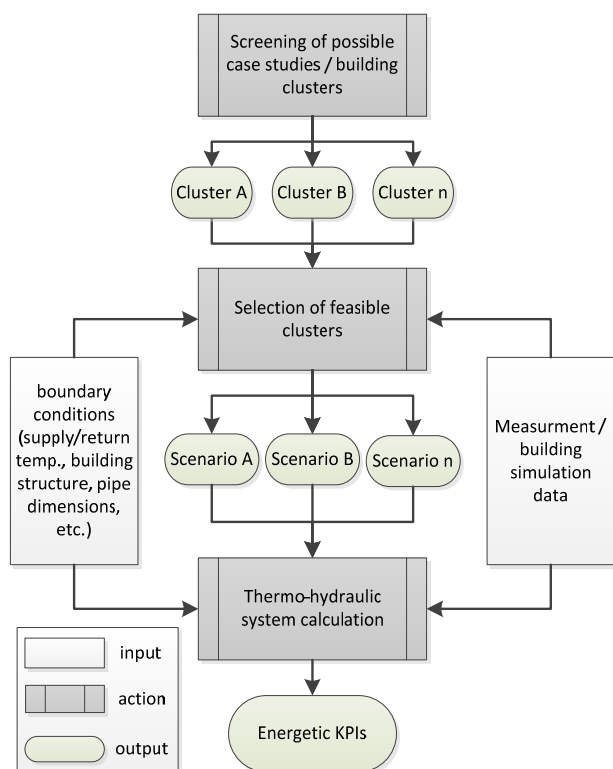


Figure 3: Methodology for analysing cascaded interconnections

In this paper only results concerning the indirect connection of new LT-consumers (with standard DHW-systems) to the return line were considered.

METHODOLOGY

To be able to connect buildings, building cluster or neighbourhoods in a heat cascade with each other, the respective buildings must be analysed according to their heat consumption profiles, their temperature profiles and their location. The used methodology for analysing cascaded interconnection in building clusters is shown in Figure 3.

The first step was to detect potential building clusters. Therefore, a GIS based screening of potential network sections was carried out. Depending on the location and the building stock in the respective section different possible clusters were detected. On the basis of local boundary conditions (e.g. pipe dimensions, street topology, available areas for new buildings etc.) and measured data in the detected sections (e.g. temperature levels, mass flow rates etc.) a representative case study / building cluster was chosen. Data of the building stock which were not available so far, were collected either by own measurements or taken from experiences of other regions. The following values of the building stock have been collected and analysed:

- Supply temperature [°C]
- Return temperature [°C]
- Volume flow [m³/h]
- Heat demand [kWh]

With these data it was possible to evaluate the chosen cluster and the buildings contained therein, if they are suitable for an energy cascade. The next step was to develop different scenarios for the cascaded energy use. The scenarios described in the section “Scenario description and Results” differ in the connection principles but also in terms of domestic hot water production in the new LTC. As far as there were no measured data available for the new LTC, the buildings have been modelled and the thermo-physical behaviour was simulated in Dymola/Modelica ([5], [6]) based on models of the Modelica Fluid library [7] and on the DisHeatLib [8] developed at the Austrian Institute of Technology. Therefore a simplified building model developed in Modelica has been used (based on the “one node model” described in VDI 6020 [9]). The simulation results (heat demand profiles and temperatures) were validated with monitoring data from similar buildings in other sections. For the thermo-hydraulic system calculations, the simulated data were used together with measured data from the building stock in the investigated cluster. The output were energetic KPIs, especially the new return temperature, new volume flow rates and new heat demand from the supply line.

CASE STUDIES DESCRIPTION

The investigated section of the district heating network is located in the city of Vienna. The closely meshed ring network is divided into a primary network to which all supply unit systems (heat and power plants) are connected, and in numerous secondary networks.

The primary network has a pipeline length of about 560 km. The flow temperature is controlled according to the outside temperature between 95 °C and 160 °C. The secondary networks (around 630 km) are supplied by the primary network and operated between 63 °C and 95 °C.

The considered grid section (a secondary network) in Vienna consists of 5 apartment block consumers. Currently all buildings are connected via a “standard” connection to the supply line of the secondary network. The area is connected in the west to the primary heating network via a transformer station (GUFO). There is no ring closure and as a consequence, the flow direction in the secondary network is unique (west to east for the supply line). Thus, the use of the return is in principle possible without the risk of flow reversal and short circuits. Considering the fact that in the west side there is a large empty field, there is the possibility

in the future that new buildings at this point could be built. In Figure 4 the topology of the network section is shown.

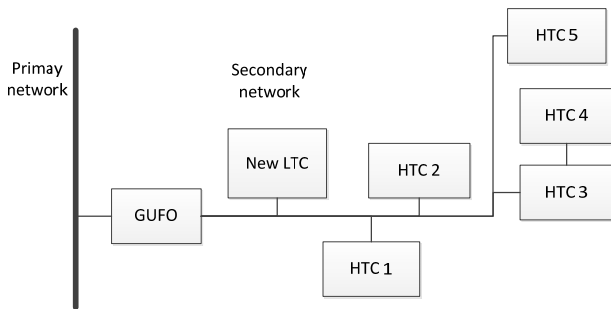


Figure 4: network section and consumer locations

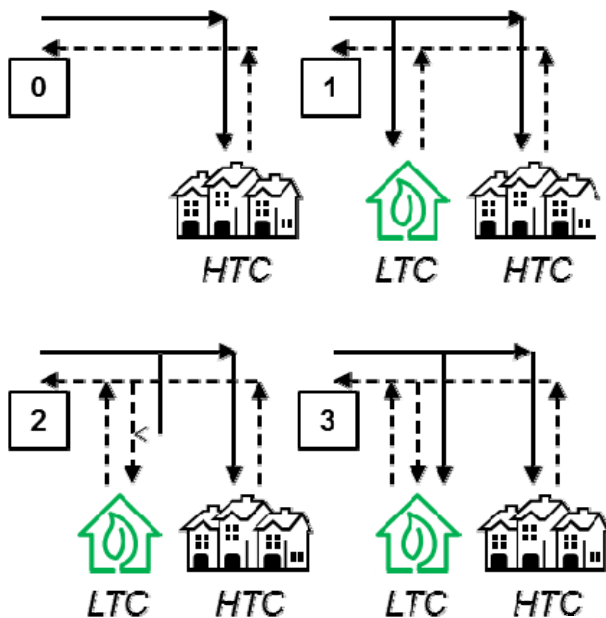


Figure 5: connection schemes; up left: Reference scenario 0; up right: Scenario 1; down left: Scenario 2; down right: Scenario 3

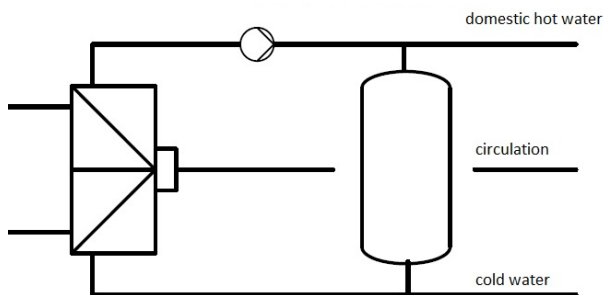


Figure 6: Scheme of the centralized DHW preparation with heat exchanger and storage system including a circulation line (simplified hydraulic scheme)

It was examined if a possible new LTC could be supplied at this point from the return line, and the effect on the secondary network, in particular on the return temperature. The heated gross floor area of the possible new LTC is assumed to 8.500 m². This corresponds to 100 residential apartment units which should be supplied with heat via floor heating systems in order to scope with the lower supply temperatures. The design heat load is $\approx 33,2 \text{ W/m}^2$ without DHW preparation and $45,4 \text{ W/m}^2$ incl. DHW preparation. The annual heat demand is $\approx 640 \text{ MWh}$. The return temperature is calculated as a mixed temperature from space heating return and DHW preparation return. The return temperature of floor heating is considered at the district heating side of $35 \text{ }^\circ\text{C}$. The return temperature and tap profiles were simulated and validated by measurement data. To investigate the effects of a return line connection of a new LTC, 3 scenarios were considered according to Figure 2 c) which are each compared with the current status. In Figure 5 the schemes of the connections are shown.

SCENARIO DESCRIPTION AND RESULTS

Reference scenario - Status quo (as comparison scenario)

In order to compare the scenarios developed, the status quo was analysed for the selected building cluster. The HTC are connected to the grid (standard supply connection) and no LTC is connected (see Figure 5 up left). From the measurement data the heat demand of the already existing HTC is approximately 2.400 MWh. The maximum peak load reaches values of around 830 kW. The supply temperature in the observed section is depending on ambient temperature and is controlled between $63 \text{ }^\circ\text{C}$ and $90 \text{ }^\circ\text{C}$. Throughout the year, the average supply temperature is $\approx 65,7 \text{ }^\circ\text{C}$ and the average return temperature at the beginning (west end) of the section is $\approx 53,5 \text{ }^\circ\text{C}$. The average flow rate is about $18,4 \text{ m}^3/\text{h}$. The maximum flow rate is $34,1 \text{ m}^3/\text{h}$. The values of the reference scenario are used later for comparison with the other scenarios.

Scenario 1 – Standard connection of the LT-consumer to the supply line

In this scenario, the new LTC is linked via a standard connection to the supply line of the district heating network (see Figure 5 up right). The DHW preparation is done in the same way as in the HTC (standard storage systems, see Figure 6).

By supplying the additional consumers the heat demand of the section increases to around 3.030 MWh. The maximum peak load reaches values of around 1.000 kW. The annual profiles of the network section are shown in Figure 7 (the values shown are daily

average values, so the peaks are actually lower than the real peaks).

The supply temperature in the section is not changed and has an average of around 65,7 °C. Since the new LTC is standard connected to the supply line, there is no cascading heat utilization. The average return temperature at the beginning of the section (at the GUFO) is reduced by the new consumer in this scenario due to the LT heating system (floor heating) to around 52,8 °C. The maximum reduction of the return temperature is $\approx 6,9$ K. The average flow rate in the line increases by around 18 % to $\approx 21,7$ m³/h. The maximum flow in the line is increases to $\approx 49,5$ m³/h.

Scenario 2a: Connection of the LT-consumer to the return line; DHW preparation with standard storage system

The new LTC is connected in this scenario to the return line of the network. The domestic hot water of the new consumer is prepared in the same manner as the existing consumers (storage system, see **Figure 6**). For this purpose, supply temperatures of minimum 63 °C must be provided throughout the year (according to Austrian regulations [10] 60 °C are needed to store DHW; additionally a temperature difference of 3 K at the heat exchanger has to be considered). This value is guaranteed by using a 3-way mixing valve which mixes the return line with the supply line of the existing network. In scenario 1 and 2a it is considered the same LTC with floor heating and storage system for DHW preparation, therefore, both scenarios also have the same heat demand or power characteristic (**Figure 7**). The supply temperature of the new consumer is constant as described above and controlled to a value of 63 °C. Since the new consumer is connected to the return line, there is partial cascading heat utilization due to the mixing of return with supply line. The return temperature at the beginning of the section is reduced by the cascade in this scenario, to $\approx 52,8$ °C. The maximum reduction of the return temperature is $\approx 7,8$ K. The average flow rate in the line increases by around 18 % on $\approx 21,6$ m³/h. The maximum flow in the line is increases to $\approx 50,6$ m³/h.

Scenario 2b - Connection of the LT-consumer to the return line; DHW preparation with decentralized fresh water module

The LTC is connected in this scenario to the return line of the DH network. In contrast to Scenario 2a it is now assumed that the DHW of the new consumer is prepared decentralized with fresh water modules. Furthermore, a buffer storage is integrated to smooth heat load peaks, see **Figure 8**. Even in this scenario sufficiently high supply temperatures must be provided. In this case, considering that no drinking water is stored, temperatures of 55 °C are sufficient. Since the

buffer is separated hydraulically with a heat exchanger from the network supply and due to the temperature difference of the heat exchanger, ≈ 60 °C is required as supply temperature. This temperature is achieved as in scenario 2a by mixing the return with the supply line of the existing network. The return temperature of the DHW preparation is assumed in operation to be 35 °C (district heating side). At time when there is no consumption, the pipes in the building will be kept warm by a bypass to quickly provide the desired temperatures. This results in a return temperature of ≈ 45 °C outside operating hours.

Since the new consumer is connected to the return line of the secondary network mixed with supply line, it comes here to partial cascading heat utilization. In this scenario, the return temperature at the beginning of the section (GUFO) is reduced to $\approx 51,7$ °C. Due to the decentralized DHW preparation the reduction is higher in the summer period by $\approx 9,6$ K. The average volume flow rate in the line increases by only about 8 % to $\approx 19,9$ m³/h. The maximum volume flow in the line in comparison to the reference scenario increases to $\approx 40,6$ m³/h.

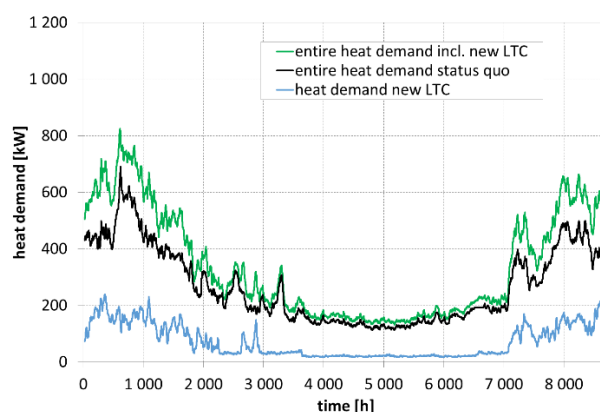


Figure 7: Yearly heat load profiles in the network section (daily average values)

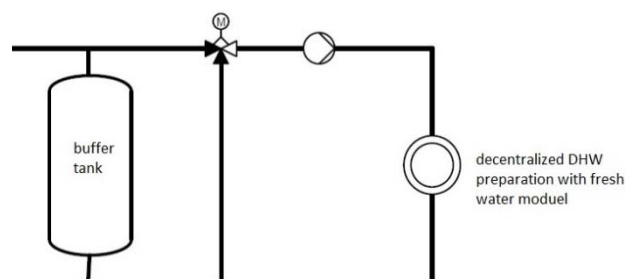


Figure 8: Scheme of a DHW preparation with decentralized fresh water module and a buffer tank (temperature and hydraulic connection are simplified)

In the presented study, the new LTC is connected with a heat exchanger. In some cases it is also possible to connect consumers directly to the secondary network (without separating exchanger). In these cases, the temperatures can be lowered even further, as there would be no temperature difference of the heat exchanger, thus allow to go to lower return temperatures.

Scenario 3 – Connection of the LT-consumer with a 3-pipe-system

In this scenario, the LTC is connected to the secondary network with a 3-pipe-system. One pipe supplies the building from the return line of the secondary network. This pipe is used for space heating. A second pipe is connected to the supply line of the secondary network and is used for DHW preparation, which is prepared by means of storage systems, see **Figure 6**. The third pipe is the return line of the LTC.

The return temperature at the beginning of the section (GUFO) is reduced to approximately 52,1 °C through the cascade (for space heating) in this scenario. The maximum reduction of the return temperature is ≈11,6 K. The average volume flow rate in the line increases by around 13% to ≈20,5 m³/h. The maximum volume flow in the line increases to ≈46,3 m³/h.

DISCUSSION

As mentioned above the average return temperatures can be reduced in the investigated section in all scenarios 1-3 compared to the reference scenario 0. The temperatures of the return line of the network section of the different scenarios over the whole year are shown in Figure 9. Especially during the heating season the possible reduction reaches the highest values due to the investigated heat cascades.

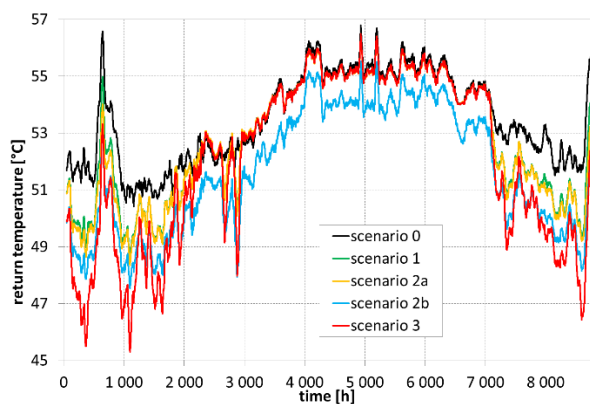


Figure 9: return temperature profiles in the investigated network section over one year (2-day average values)

The yearly average reduction of the return temperature and the maximum reduction is shown in Figure 10. The results show, that scenario 2b has the highest average reduction over one year, due to the DHW preparation with fresh water modules. Scenario 3 has the highest maximum reduction. This appears in times when only the heating system of the LTC is operating and therefore a full cascaded usage of the heat is realised, due to the 3-pipe-system where the space heating is supplied only via the return line of the network.

In Figure 11 a more detailed view over one week in winter shows the temperature reduction. It can be seen that Scenario 3 including a 3 pipe system leads to the highest temperature reduction in winter times, whereas the temperature reductions in Scenarios 1, 2a/b are similar.

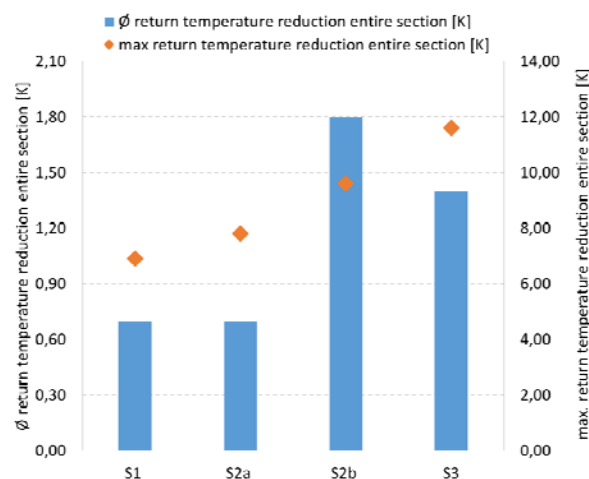


Figure 10: average and maximum return temperature reduction compared to scenario 0 (status quo)

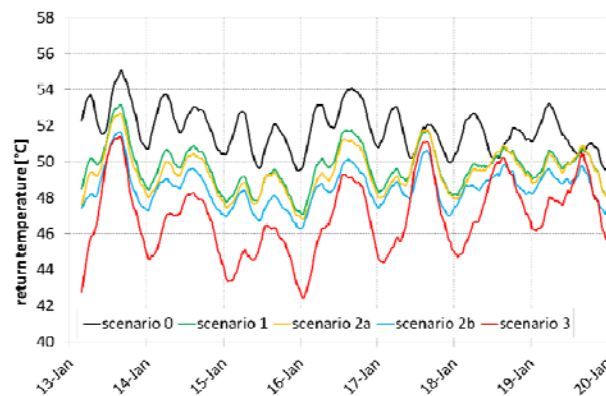


Figure 11: return temperature profiles in the investigated network section during 1 week in winter (4-hour average values)

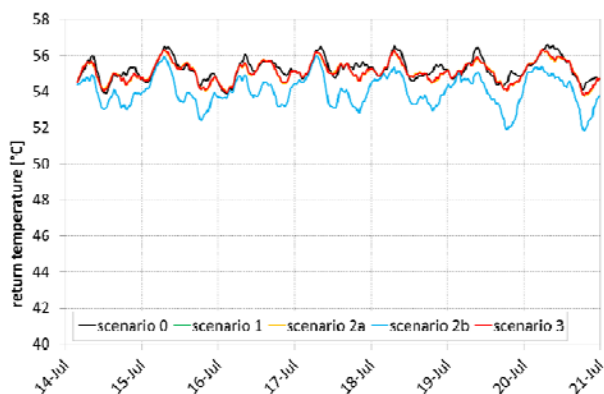


Figure 12: return temperature profiles in the investigated network section during 1 week in summer (4-hour average values)

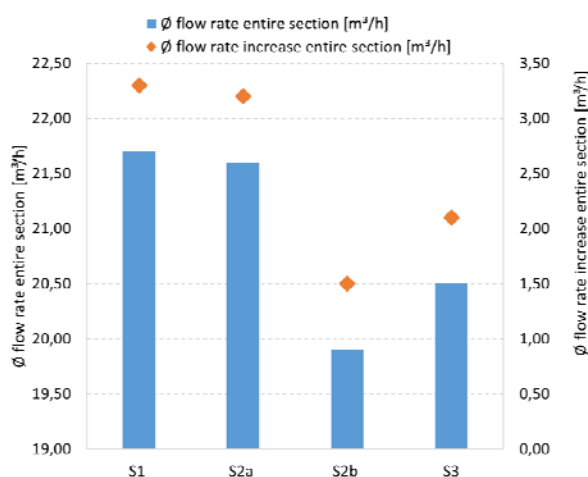


Figure 13: average flow rate and flow rate increase compared to scenario 0 (status quo)

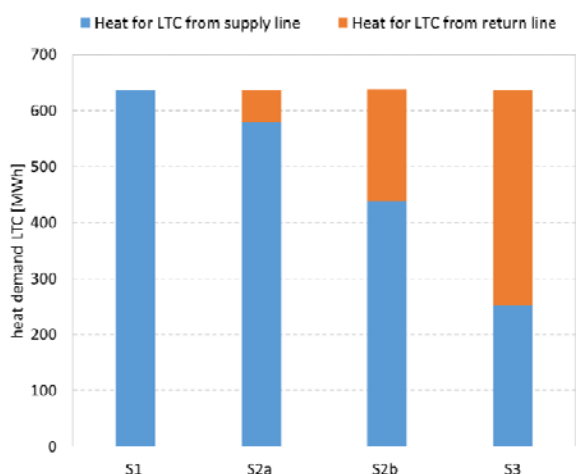


Figure 14: distribution of heat for LTC from supply and return line

During summer times the reduction of the return temperature is less than in winter times. Due to the absence of space heating only domestic hot water preparation needs heat from the network. Therefore there is almost no difference in scenario 1, 2a and 3 compared to the return temperature of the reference scenario. Only in scenario 2b a reduction is apparent, see Figure 12. This temperature reduction is due to the decentralized DHW preparation including fresh water modules. As described above, the fresh water modules lead to reduced return temperatures in the DHW preparation, and so reductions can be achieved also in summer times.

Concerning the flow rates Figure 13 shows, that scenario 2b has the lowest increase of flow rate. This is due to the fresh water modules and the high reduction of the (average) return temperature. Therefore only a smaller amount of flow rate is needed to transfer the same amount of heat.

The comparison of the heat flows show, that scenario 3 has the highest amount of return usage compared to the other scenarios, due to the 3-pipe-system and the complete supply of the space heating through the return line, see Figure 14.

In Table the results are summarized. It turns out that through the involvement of the LTC, the return temperatures can be reduced. By cascading heat use (return line use), as well as implementation of fresh water modules for the DHW preparation and alternative interconnections (3 lines pipes), this effect of reducing return temperatures can be further strengthened. It also enables new consumers to be supplied with district heating by only a small increase in volume flow in the pipeline.

The average return temperature reduction in the investigated case study is especially in the summer period low to moderate. Looking on an overall network perspective, the measures have a negligible effect unless implemented to the greatest possible extent. Similar results have been seen in [12]. Nevertheless, also a local return temperature reduction can have benefits as it is explained in the sections before.

For the investigated kind of cascading, following tariff system has been applied already in single cases in some Austrian cities: The standard tariff has two parts: the base price in €/kW and the energy price in €/MWh. If a customer is connected to the return line, for the heat extracted from the return line only the energy price is charged to the customer. For any additional energy that is extracted from the supply line (e.g. via mixing into the local return connection), the base price is added equivalently according to the extracted amount. However, following problem can occur using this tariff system: If the return temperature in the network or in the relevant branch is reduced, the amount of

additional heat energy extracted from the supply line increases. As a consequence, the customer needs to pay more without the customer's own fault – and this is not allowed according to Austrian law.

CONCLUSION AND OUTLOOK

In this paper, the indirect cascading of heat between buildings using the return line of a high temperature customer (HTC) via a DH network as a supply for a low temperature customer (LTC) has been investigated using a case study. From the results, following conclusions can be drawn:

- Following technical conditions are required for realising the heat cascading: A sufficient and unidirectional mass flow, the balancing of the demand and temperature profiles between the LTC and HTC as well as measures for guaranteeing supply security such as mixing with the supply line and storages (especially for domestic hot water generation). Also measures for reducing the return temperatures such as retrofitting and hydraulic balancing of the HTC have to be considered.
- One of the main benefits of the investigated heat cascading is the possibility to connect new customers (with low supply temperature demand) to the network, that couldn't be connected using standard connections due to mass flow restrictions in the branch.
- In suitable network sections with high return temperature reduction potential, the local supply of low temperature sources can be very efficient. By matching the return temperature reduction potentials with potential locations for renewables and industrial waste heat, decisions for investing in local resources and return temperature reduction measures can be supported.
- The effective implementation of heat cascading requires new business models and tariff systems for the customers and also for possible suppliers to the return line. Here, the overall network developments need to be taken into account, e.g. reduction of the temperature regimes, changes in the flow directions etc.

Table 1: overview of results; Reductions and increases always refer to scenario 0 (status quo).

	S1 supply line	S2a RL + storage system	S2b RL + Fresh water module	S3 3-pipe + storage- system
Ø Supply temp. LTC [°C]	65,7	63,0	60,0	SL for DHW, RL for SH
Ø Return temp. LTC [°C]	49,6	49,9	36,5	48,8
Ø Return line entire section [°C]	52,8	52,8	51,7	52,1
Ø return temp. reduction entire section [K]	0,7	0,7	1,8	1,4
Max. return temp. reduction entire section [K]	6,9	7,8	9,6	11,6
Heat for the LTC from supply line [MWh]	637	580	438	252
Heat for the LTC from return line [MWh]	-	57	200	385
Ø Flow rate entire section [m ³ /h]	21,7	21,6	19,9	20,5
Ø Flow rate increase entire section [m ³ /h]	3,3	3,2	1,5	2,1

ACKNOWLEDGEMENT

This paper is a result of projects which are supported with funds from the Austrian Climate and Energy Fund.



REFERENCES

- [1] H. Lund, S. Werner, R. Wiltshire, S. Svendsen, J. E. Thorsen, F. Hvelplund und B. V. Mathiesen, „4th Generation District Heating (4GDH): Integrating smart thermal grids into future sustainable energy systems,“ *Energy*, Bd. 68, pp. 1-11, 2014.
- [2] S. Frederiksen und S. Werner, *District Heating and Colling*, Lund: Studentlitteratur, 2013.
- [3] D. Basciotti, R.-R. Schmidt, M. Köfingger und C. Doczekal, „Simulation based analysis and evaluation of domestic hot water preparation principles for low temperature district heating networks,“ *The 14th International Symposium on District Heating and Cooling*, Stockholm, 2014.
- [4] M. Köfingger, R.-R. Schmidt, D. Basciotti, K. Eder, W. Bogner, H. Koch und H. Ondra, „URBANcascade - Optimierung der Energie-Kaskaden in städtischen Energiesystemen zur

- Maximierung der Gesamtsystemeffizienz und des Anteils erneuerbarer Energieträger und Abwärme,“ Wien, 2016.
- [5] Modelica, „<http://www.modelica.org>,“ [Online]. [Zugriff am 2013].
- [6] D. Dynasim, „Dynamic Modeling Laboratory User Manual,“ Dynasim AB, Lund, 2011.
- [7] F. Casella, M. Otter, K. Proelss, C. Richter und H. Tummescheit, „The modelica fluid and media library for modeling of incompressible and compressible thermo-fluid pipe networks,“ in *Proceedings of the Modelica Conference*, 2006.
- [8] D. Basciotti und O. Pol, „A theoretical study of the impact of using small scale thermo chemical storage units in district heating networks,“ in *Proceedings of the International Sustainable Energy Conference*, Belfast, 2011.
- [9] VDI, „VDI 6020: Requirements on methods of calculation to thermal and energy simulation of buildings and plants - Buildings,“ Beuth Verlag GmbH, 2001.
- [10] Austrian Standard Institute, „ÖNORM B5019 - Hygienerrelevante Planung, Ausführung, Betrieb, Wartung, Überwachung und Sanierung von zentralen Trinkwasser-Erwärmungsanlagen,“ Wien, 2011.
- [11] M. Köfinger, D. Basciotti, R.R. Schmidt, E. Meissner, C. Doczekal, A. Giovannini: “*Low temperature district heating in Austria: Energetic, ecologic and economic comparison of four case studies*“, *Energy - The International Journal*, January 2016
- [12] D. Basciotti, M. Köfinger, C. Marguerite, O. Terreros, Agugiaro G.; R.-R. Schmidt: Methodology for the Assessment of Temperature Reduction Potentials in District Heating Networks by Demand Side Measures and Cascading Solutions, CLIMA 2016: 12TH REHVA WORLD CONGRESS, 22-25 May 2016, Aalborg, Denmark
- [13] D. Bublitz: Ausbau der Fernwärmeversorgung in Berlin, Elektrizitätswirtschaft Jg.86 (1987) booklet 12 S.487-492

INDIVIDUAL APARTMENT SUBSTATION TESTING – DEVELOPMENT OF A TEST AND INITIAL RESULTS

Martin Crane CEng¹

¹ Carbon Alternatives Ltd

Keywords: *district heating, substation, low return temperature, performance testing*

ABSTRACT

To address poor performance of new DH networks in the UK a substation test procedure for individual dwelling substations was developed from the Swedish District Heating Association Technical Regulation F103-7e test. The test aims to 1) determine the performance of individual substations, 2) to demonstrate the impact of other DH design variables on substation performance and 3) to highlight issues arising from poor commissioning. The test uses volume weighted average return temperature (VWART) as the main performance metric and calculates this for DHW generation, space heating and standby, under conditions representative of typical operation. Other analysis has developed average DHW and space heating demand patterns for a typical UK city centre apartment, which allow an annual substation specific VWART to be calculated. The calculated VWART should represent substation operation in use in a typical new build flat.

This paper discusses the generic issues and observations arising from the substation testing and does not comment on individual manufacture performance.

The results show a wide range of substation performance, with significant variation in DWH, space heat and standby performance between substations. The space heating heat exchangers were oversized, for the small UK required heat outputs, in most the substations causing high return temperatures. The performance variation was greatest for the standby functions with substations having very different standby flow, return temperatures and substation heat losses.

The test results have generated significant discussion within the UK DH community and are being used by suppliers to publicise their products. It is hoped this raising of awareness of substation performance will lead to improved substation and DH specification, installation and performance. It is planned for the test standard to be adopted by an independent body and further developed by a committee of DH operators.

INTRODUCTION

Currently District Heating (DH) in the UK supplies less than 1.5% of properties in the UK [1]. Due to building code requirements new DH is being developed at all

large developments in London and this has been the case for nearly 10 years now. DH is being developed in other parts of the UK for both new build and retrofit. Much of this DH has been designed and built by engineers and contractors with insufficient knowledge of DH. As a result, many of the new schemes are oversized and have high heat losses. The growing number of poorly performing DH schemes is gaining the notice of consumer protection organisations, despite the relatively small numbers of customers served. These organisations are reporting, 'Poor design or a lack of insulation can lead to system heat loss, causing unnecessarily high costs and poor thermal comfort for customers' [2]. The 'poor thermal comfort' noted refers to corridors that are uncomfortably hot due to heat losses from DH pipework. The new market opportunity for DH products has led to a large number of substations being offered into the UK market. The problem is that the limited DH knowledge is hampering good substation selection, efficient system design and commissioning to get the best performance from the substation.

The UK Government Department of Energy and Climate Change (DECC) is promoting DH as a route to reduce CO₂ emissions and lower heating costs. DECC has responded to the issues of poor DH performance by offering funds for research into improving DH systems. Using this DECC funding, as part of a larger DH research project, a substation test procedure was developed and 6 of the more popular UK substation substations were tested.

The most common DH setup for new DH schemes in the UK is for individual substations in each residence, the substation having a heat exchanger for instantaneous supply of Domestic Hot Water (DHW) and an indirect connection for the space heating radiators. It is this configuration of substation that the test procedure evaluates.

TEST DEVELOPMENT

There were four aims of the testing:

- 1) To establish the performance of individual substations
- 2) To demonstrate the impact of different design decisions e.g. DH flow temperatures and domestic hot water (DHW) temperatures

- 3) To highlight impacts of other factors that affect overall DH system performance e.g. poorly set up radiators and the scope for some substations to manage this poor setup better
- 4) Provision of substation performance data for the wider research project.

Points 2 and 3 were included to help develop a wider understanding of the impacts of issues such as choice of DHW flow temperature and the impacts on the overall system efficiency of the operation of substation standby / keep warm functions.

The individual house substation tests from the Svensk Fjärrvärme (Swedish District Heating Association) Technical Regulation F103-7e [3] was used as the basis for the test standard. The Swedish test was adapted to more typical UK DH operating conditions and extra tests added to explore and demonstrate issues less well understood in the UK. The main changes being the use of fixed DH flow temperatures, lower space heating loads, higher DHW output and removal of most of the pass/fail criteria – the new test explores substation performance and does not certify the substation in any way. Additional test were included to demonstrate the impacts of poor radiator set up, higher DHW temperatures and scope for the substation to deliver more than rated DHW output.

Quantifying substation performance

The key performance criteria are: safe operation, sufficiently fast DHW delivery and low return temperatures back to the network.

1) Safety – the main requirement used, as in the F103-7, was that DHW temperatures should not exceed 65°C for more than 10 seconds.

2) DHW delivery – the substation needs to deliver DHW in a reasonable time and at a reasonably stable temperature. It is difficult to determine what is 'reasonable' for either of these parameters. The DHW response time is affected by DH system upstream of the substation and the time to tap affected by DHW pipework volume – both of these being different for every substation installation. Very few mixer taps are set for the full 55°C DHW temperature so the stability of the DHW the user experiences is affected by both the substation and the thermostatic mixer valve.

3) Low return temperatures – the importance of low return temperatures is not universally understood in the UK, hence this objective has a dual purpose of both raising awareness of the importance of reducing return temperatures and providing a metric for individual substation performance. The annual volume weighted average return temperature (VWART) was chosen as it best represents the temperature of most of

the return pipework (and therefore heat losses) and the temperature that returns to the heat source (and therefore impacts upon plant efficiency and capacity of thermal storage).

In the UK, substations for individual domestic connections are commonly referred to as 'HIUs' - Hydraulic or Heating Interface Units. The UK test standard uses the term HIU throughout the document.

This paper refers to version 1 of the test procedure, a simpler version 2 is to be published in June 2016 which removes some of the tests which were included to inform general DH design discussions. The aim of the test now is to provide a measure of substation performance at lowest test cost.

VWART CALCULATION.

The Volume Weighted Average Return Temperature (VWART) is defined as follows:

$$VWART = \frac{\sum(t_{1,2,t} \times q_{1,t})}{\sum q_{1,t}} \quad (1)$$

where t represents each read during the test period (the substation test rig at SP in Sweden records the test data. every second), $t_{1,2}$ is the primary return temperature and q_1 is the primary flow rate.

The VWART seeks to simulate the return temperature from a typical year of substation operation, for a typical London flat (typical average size of 60 m² [4]). The space heating loads assumed for the VWART analysis are 1450 kWh/yr and the DHW load is 1470 kWh/yr. These heat loads are based on Standard Assessment Procedure (SAP) demand estimates. SAP is the UK Government's assessment methodology through which domestic building demonstrate compliance with energy efficiency regulations. Analysis of DH customer heat meter data [4] for new flats in London from shows space heat and DHW typical space heat demands of 1900 kWh/yr and DHW demands of 1030 kWh/yr. The heat meter data demonstrating a similar annual heat demand but a different split between the DHW and space heating. The VWART calculation methodology could be followed for different space and DHW heat loads to give a more representative indication of substation performance where heat loads are known to be different from the VWART calculation base assumptions.

Representative demand pattern were then needed for the DHW and space heating use. The Energy Savings Trust [5] had a database of 120 UK properties where the DHW use was monitored on a one minute basis for

a year. From this data a typical pattern of operation could be assessed, and a substation test designed to deliver representative DHW demand conditions. The key issues arising in the DHW demands was the prevalence of short, low flow rate demands. The test rig restricted the number of DHW flow rates to 3 so this imposed an additional constraint. The DHW component of VWARD is based on the usage pattern as in **Table 1**.

Table 1 Composition of DHW demands and durations used for VWARD calculation

Flow Rate (litres/min)	Estimated Annual Demand (kWh)	Number of events per year	Average Duration (seconds)
6	729	10,000	30
10	297	660	75
13	444	300	145

The substation test and VWARD calculation includes data for the 60 seconds after the DHW draw off ceases as this then incorporates into the data the impacts of any delayed shutting of the DHW control valve.

The distribution of 1 kW, 2 kW and 4 kW space heating loads are based on analysis of Guru Systems [6] collected consumer heat meter data for a typical modern high-rise residential block in London as in Table 2

Table 2 Composition of space heating demands used for VWARD calculation

Space Heating Load (kW)	Estimated Annual Demand (kWh/year)
1	98
2	787
4	565

During those times of the year when no space heating is required, or at times when no domestic hot water is being drawn off, it is common on UK substations that various types of temperature-holding functions come into operation. These functions ensure that domestic hot water will be quickly available and provide a background flow rate on the DH network to keep the network warm. The VWARD calculation assumes that for all periods that DHW is not being drawn or the space heating is operating the substation is in standby / keep warm.

The VWARD calculations are based on a DH flow temperature of 75°C, DHW at 55°C and the space heating operating at 70°C flow and 40°C return. 70/40°C are the currently recommended maximum operating temperatures for space heating in the UK [7].

The substation test procedure and VWARD calculation methodology documents are available at www.fairheat.com via a link from www.carbonalternatives.com

THE TESTS.

The following tests were undertaken. Unless otherwise stated all tests were at 75°C DH flow temperature, space heating secondary at 70°C flow and 40°C return, DHW supply temperature at 55°C and dP across the substation of 0.5 bar.

- Space heating performance at 1, 2, and 4 kW used in VWARD calculation
- DHW at flow rates for VWARD calculation and at peak 40 kW output
- Standby – the standby test measured the DH temperatures and flowrates for an eight hour standby period
- DHW Response time – how quickly was DHW generated by the substation after the eight hour standby period
- DHW at 50°C and 60°C delivery temperatures
- Performance of DHW and space heating at 65°C DH flow temperatures and secondary system at 60/35°C
- Performance of substation using 2 kW of radiators not commissioned to deliver 40°C return temperatures - a common occurrence in the UK
- Scope for substation to rectify poor radiator setup
- Maximum DHW output, what kW output of DHW can be delivered if DHW temperature is allowed to drop below setpoint
- Low DHW flow – to ensure the substation can control DHW temperatures at low flow rates and not exceed safe DHW delivery temperature
- Combined DHW and space heating demands and the combined demands at higher primary differential pressure.

Not all of the tests undertaken are commented on in this paper.

Table 3 Overall VWARD results

	Overall VWARD (°C)
Substation A	47
Substation B	44
Substation C	45
Substation D	35
Substation E	23

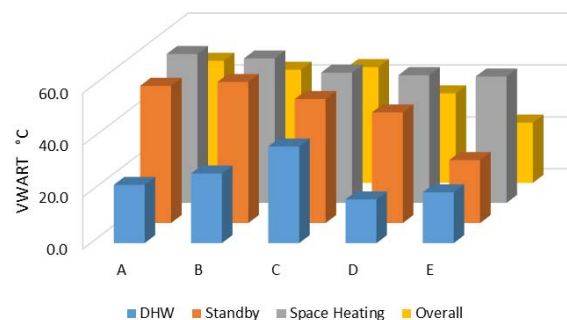


Figure 1 Components of VWARD and overall VWARD

VWARD RESULTS

The results are presented as substations A-E, without the manufacturers being named. The intention of this paper is to discuss the generic issues and observations arising from the substation testing and not comment on individual manufacture performance. The tests are for one particular substation model supplied by each supplier/manufacturer and so are not necessarily representative of all substations from that supplier. The test reports which detail the manufacturer and model of each substation tested are available at www.fairheat.com or via a link from www.carbonalternatives.com

The overall calculated VWARDS for the substations tested are shown in **Table 3** and varied between 23°C and 47°C.

To understand the substation VWARD it helps to break the VWARD down into the DHW, standby and space heat component VWARDS and associated annual volumes. These are shown in Figure 1 and Figure 2.

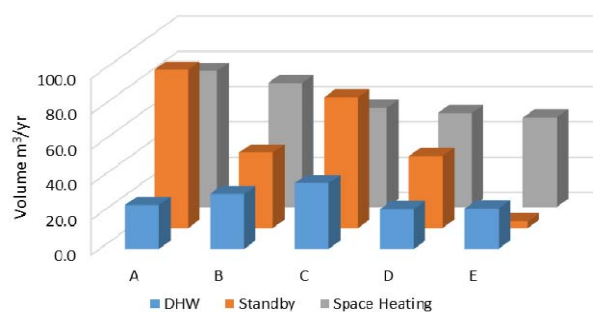


Figure 2 Annual component volumes for an individual substations

DISCUSSION

Standby

To those less experienced with this type of substation the magnitude of the impacts of the standby operation is a surprise. In the author's experience it is rare for a UK substation procurement specification to detail substation performance during standby. It follows that the designers are unlikely to be considering the DH system performance during periods when the substations on standby are the predominant system load. The standby performance is also the component that varies most between substations, with a wide variation in the volume weighted return temperatures (24 to 52°C), the annual volume of primary flow (4 to 90 m³/yr) and the heat loss as shown in **Table 4**. It is hoped the substation testing will raise the designers' and specifiers' awareness of the importance of substation standby operation.

Table 4 Standby performance

Substation standby	Average DH return (°C)	Flow rate (l/hr)	Heat loss (Watts)	Average DH flow (°C)
Substation A	54	11.5	79	58
Substation B	49	7.3	25	51
Substation C	48	10.1	96	58
Substation D	42	6.2	53	53
Substation E	25	3.9	33	39

The keep warm operation varied between the substations with two of the substations tested pulsing the DH flow to keep the substation hot with cycle time ranging from 30 minutes to 3 hours. The other substations settled down to a constant steady trickle DH flow.

The standby/keep warm performance should be considered along with the DHW response times as reported in **Table 5**. The response time is the number of seconds the substation takes to deliver DHW to the substation DHW outlet after the substation has been standing by / idling for 8 hours.

It could be expected that warmer standby temperatures would increase the speed of delivery of the DHW, but increase heat losses from DH network and substation.

Table 5 DHW response time test DHW at 55°C set point

Time to DHW flow temperature	Seconds to 42°C	Seconds to 50°C	Seconds to 55°C
Substation A	22	30	48
Substation B	41	76	85
Substation C	11	17	28
Substation D	3	23	91
Substation E	22	27	29

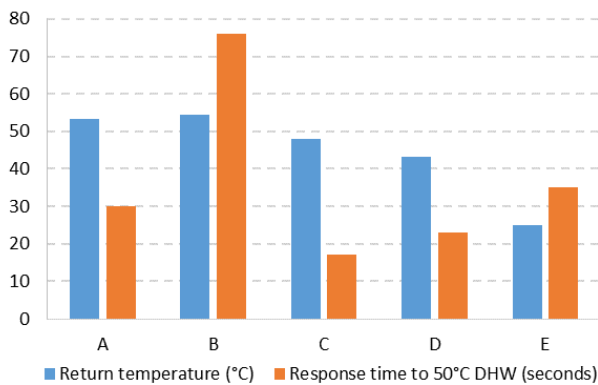


Figure 3 Comparison of average return temperatures and DHW response time



Figure 4 Non airtight 'insulating' substation cover, top in upper photo, underside in lower photo

The test results in **Figure 3** show this is not necessarily the case. The DHW response time, the return temperature and the standby flow rate all need to be considered to optimise the standby design and DHW delivery speed. There are clearly substations with better standby configurations. There also is a range in the DHW delivery times and this also varies for different target DHW temperatures, so it is important to consider what DHW temperature it is best to use in any response time performance assessment – e.g. Substation D is the fastest to deliver 42°C but the slowest to 55°C.

The testing shows a wide variation in the substation heat losses. Clearly the lower the substation standby heat losses are the better as this will reduce unwanted heat gains and reduce the customers' bills – the heat meters in the substation will be recording a significant proportion of these losses. The heat losses are a function of the temperature of the DH water in the substation and the effectiveness of the substation insulation. To be effective the insulation needs to totally surround the hot components, this is where the pipe insulation approach fails as all the joints, elbows, valves, strainers etc are not insulated – only the relatively short elements of pipe in between all the fittings tend to get insulated. For this reason some manufacturers have moved to insulating the substation outer casing, so the air inside the substation warms up and then the heat losses from the components is minimised, but for this to work the case needs to be air tight – which is not the case for some of the substations as shown in **Figure 4**. Additionally on this substation the back half was an uninsulated steel box which also supported the incoming pipework with no thermal break incorporated between hot pipework and case. These details will also increase the heat losses from the substation.

SPACE HEATING

Figure 1 and **Figure 2** show the space heating VWARTs to be higher than expected based on a 40°C secondary return temperature with the primary return ranging from 49 to 57°C.

Figure 5 shows the data from the 1, 2 and 4 kW space heating load tests which are used in the VWART calculation. For this test the DH flow temperature was 75°C, the secondary flow temperature 70°C and secondary return 40°C. The space heating performance of the substations was poor as many of the substations showed large temperature differences between the secondary and primary return temperatures. Analysis of the heat exchangers sizes using manufacturers' heat exchanger performance software shows the heat exchangers to be over sized for the low flow rates of these low heat demands and

30°C temperature differences. The author suggests three issues are driving this oversizing – overestimation of peak space heat loads, insufficient awareness of the poor performance of significantly oversized heat exchangers and the lack of rigorous monitoring of the performance of installed substations.

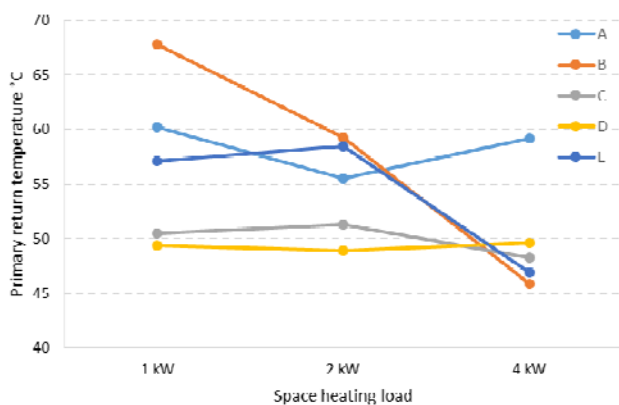


Figure 5 Substation space heat performance based on 40°C secondary return temperature

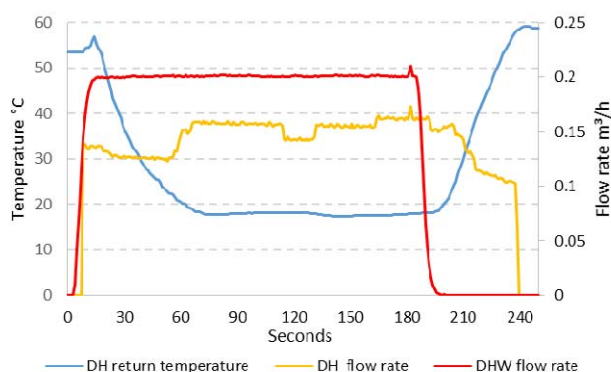


Figure 6 Substation B DHW production

Table 6 Primary return temperatures from DHW generation

40kW DHW at 55°C	Primary return temperatures (°C)	DH dT (°C)
Substation A	27	48
Substation B	26	49
Substation C	32	43
Substation D	19	56
Substation E	27	48

DHW TESTS

VWART results

There are a range of VWARTs arising from DHW production too. In particular Substation C stands out in **Figure 5**, the control of the DHW heating in this substation is primarily based on the DHW flow rate – but the valve design is optimised for a specific DH flow temperature and DHW temperature, not the 75°C DH flow and 55°C DHW temperatures of the test. Under the test conditions the DHW was overheated and then reduced in temperature by a thermostatic mixing valve in the substation. Substation C generated lower return temperatures during DHW production at lower DH flow temperatures – which is counter to heat exchanger theory, because the lower DH temperatures were closer to those the valve control was designed for. Another observation from Substation B is shown in **Figure 6**, which is part of the dynamic test that is used to provide the VWART calculation. The substation performance during DHW generation is good, delivering a sub 20°C return temperature, but when the DHW demand stops at 200 seconds the control valve takes 40 seconds to close and during this period the return temperatures rises, as the primary continues to flow lifting the overall DHW VWART to 27°C

Peak Load DHW test

The DHW tests done at the peak load of 40kW, detailed in **Table 6**, showed a range in return temperatures and resultant primary delta T (dT). At 55°C DHW temperature and a cold water supply temperature of 10°C, the best substation has a primary dT of over 55°C the worst 43°C, so the flowrate is 32% higher at the lower dT. Typically reducing a pipe by one size reduces capacity by 36%, so in many cases the best performing substation could potentially be supplied with a service pipe one size smaller than the worst performing substation (the peak DHW load is the dominating pipe sizing factor for the pipework close to the substation). Typically a pipe one size smaller at the same temperature loses 10% less heat [8].

Maximum DHW output

In the UK a DH specification commonly requires over 50 kW of DHW from the substation. This is excessive, there are millions of UK homes with instantaneous gas water heaters [9] which have a DHW output of under 35kW and it is common in countries where DH is widespread for the required DHW to be below 35 kW. For example the Swedish F103-7 certification and the standard for Arhus in Denmark is for the substation to deliver 32.5 kW DHW [10]. The 40 kW test point was a conscious decision to try to reduce the size of the peak DHW output mainly to allow reduced service pipe size.

The physics of heat exchangers will allow higher heat transfer if the return temperature is allowed to rise, so a

test was included to explore how much DHW could be drawn from the substation by increasing the differential pressure across the substation, allowing the DHW temperature to drop and the return temperature to rise. Analysis of heat meter data shows very few demands over 40kW [6]. This should give confidence to specifiers to lower the peak DHW requirements for substations, safe in the knowledge that if the DHW demands did exceed 40kW they would be supplied with little impact on the customer.

The test aim was to increase the DHW flow rate until the DHW supplied dropped to 10°C below the DHW set point of 55°C. The logic behind this is that most DHW outlets are thermostatically limited to lower than 50°C or the mixer tap is set to lower than the maximum DHW temperature so the end users would be unaware that the DHW temperature had dropped. The results are shown in **Table 7**. Unfortunately despite increasing the cold water supply pressure the pressure drop on the test rig was too high to enable sufficient flow to get the DHW temperatures to drop by 10°C. But the results still demonstrate that all of the substations can significantly over deliver on the DHW output with very limited reduction in DHW temperature – indicating that actually a far higher flowrate could be delivered at a 45°C DHW temperature.

CONCLUSIONS

The testing clearly shows performance differences between substations. The simplicity of the VVART as a benchmark of substation performance is having an impact – with manufacturers starting to publicise the VVART figure for their substations. Most of the manufacturers have made or brought forward planned substation improvements as a result of the testing. The hope is that the VVART may become part of the specification of substations, but time will tell if this occurs.

The testing is bring into focus the requirement for and design of standby / keep warm systems.

Table 7 Maximum DHW output from substations

Max DHW output	Output kW	DHW temperature °C	Increase in return temperature °C
Substation A	68	54	3.8
Substation B	65	54	4.4
Substation C	52	49	-9.8
Substation D	71	51	1.7
Substation E	51	55	2.4

Substations A, B and E had electronic controls and substations C and D were purely mechanical. The tests undertaken shows that both approaches can perform well.

It is planned that the management of the test procedure will move to a suitable independent organisation within the UK and then be further reviewed and developed by a representative body of DH system operators.

ACKNOWLEDGEMENTS

Guru Systems and FairHeat who the author worked for developing the test procedure. UK Government Department of Energy and Climate Change for funding the research, Swedish District Heating Association for the test standard F103-7 (and publishing a version in English), SP for the testing of the substations. The substation UK suppliers and manufacturers, for supplying substations for testing: Altecnic (Caleffi), Evinox; Pegler (Meibes), SAV (Danfoss), Thermal Integration (HSF). UK DH operators Eon, Engie and SSE and others for commenting on the test procedure developed.

REFERENCES

- [1] Ricardo Energy & Environment, National Comprehensive Assessment of the Potential for Combined Heat and Power and District Heating and Cooling in the UK, Ricardo Energy & Environment for DECC, London (2015). Page7 :
- [2] Which, Turning up the heat: Getting a fair deal for District Heating users, Which, (2015), Page 25 .
- [3] Svensk Fjärrvärme AB, Certification of district heating substations Technical Regulations F103-7e, Svensk Fjärrvärme AB, Stockholm (2009).
- [4] Burzynski, Robert, M. Crane, R Yao, V. M. Becerra “Space heating and hot water demand analysis of dwellings connected to district heating scheme in UK.” Journal of Central South University of Technology, 2012, Vol. 19, pp 1629-1638
- [5] Energy Savings Trust, Measurement of Domestic Hot Water Consumption in Dwellings, EST / DEFRA, London (2008).
- [6] Guru Systems Ltd. Open data. Guru Pinpoint. [Online] 16 05 2016. https://pinpoint.gurusystems.com/open_data/.
- [7] Woods, P, Heat Networks Code of Practice, . : CIBSE, London (2015) Page 37.
- [8] Crane, M. “Energy efficient district heating in practice – the importance of achieving low return temperatures”. CIBSE Technical Symposium Edinburgh 2016, p. 10.
- [9] The Department for Communities and Local Government.. English Housing Survey Energy Efficiency of English Housing, DCLG London (2012).
- [10] AffaldVarme Aarhus. Requirements for recommended substations. via Google Translate, : www.carbonalternatives.com, Jan 2014.

AN ON-OFF CONTROL STRATEGY TO REDUCE RETURN WATER TEMPERATURE

Yemao Li¹, Jianjun Xia¹

¹Department of Building Science, Tsinghua University

Keywords: District heating, Heat control, On-off control, Low return water temperature

ABSTRACT

Heat control can reduce the return water temperature, playing an essential role in efficient heating system. On-off valve with simple action and low resistance is more reliable and durable than the common thermostatic valves, especially in Chinese network whose circulating water is in bad quality. In this article, we explore the relation between the on-off time and return water temperature, which is further used to raise a new control strategy. The strategy can prevent the hot water flowing into the return pipe so that keep the return water at low temperature. Some corresponding devices have been applied in several apartments and their performance achieves the expectation to reduce the return water temperature. Furthermore, some other methods that can even reduce the temperature are proposed based on this control strategy, which show the good prospects for development.

INTRODUCTION

Heat control plays an essential role in efficient heating system. It saves energy via three methods: preventing over-heating, reducing circulating flow, and decreasing the return water temperature. Firstly, many researches have illustrated the energy saving potential in preventing over-heating by improving the heat control performance. Through some surveys on the district heating systems of China, it is indicated that 10%~15% of the heat consumption is unnecessary because of the over-heating [1]. In some case studies, energy consumption has more than 10% reduction potential by using thermostatic radiator valves [2], [3]. Secondly, heat control can eliminate the hydraulic unbalance between users, which can decrease the water flow and thus save the electricity consumption of water pumps. Thirdly, low return water temperature can also be achieved by heat controlling. The low return water temperature contributes to increasing the efficiency of heat sources, especially the renewable energy or waste energy such as the geothermal heat and industrial waste heat, because they usually stay in low-grade [4], [5]. However, the effect on reducing return water temperature by heat control methods is not well explained, but as more and more low-grade energy become the heat sources of heating system, it will attract more and more attention.

Nowadays, heat control devices are not commonly used in Chinese urban heating systems. One reason is the charging mechanism. In most district heating

systems of northern China, heating is still charged by floor area. Users has no enthusiasm to save heating energy, but on the contrary, prefer to open the windows since it can adopt more fresh air. The other reason is the bad water quality in secondary network. The water mingled with soil and corrosion not only hinders the operation of the heat control devices but also shorten their life. Most thermostatic valves that are installed in new apartments are found being jam-up in one or two years and they will be finally removed as useless resistance components. Both of the above two problems should be solved for advancing energy saving in heating systems, especially the latter, which also is the basis for applying new charging mechanisms.

Some researchers proposed to use on-off control because of its reliable and durable performance even in bad-quality water. According to several pilot application case study, the on-off control can keep the indoor temperature around the target temperature and few meets failures during the long-time track testing [6], [7].

The reliability and the heat control ability of the on-off control have been investigated in former researches. However, the effect on reducing the return water temperature is still not clear. In this paper, we explore the relation between the on-off control strategy and return water temperature. We propose a new strategy for the on-off control which will be applied in several apartments. Through an experiment, the performance of the new control strategy is revealed.

THEORY

Different from the flow control valves, on-off control valves have two work status. When the valve is "off", the water stays in the terminal and gradually cools as the heat is emitted. And when it is "on", the cool water will firstly drain out and then followed by the hot water. The return water is a mixture of cold water and hot water. Its temperature is decided by the volumes and the temperatures of the two flows. In general, the temperature of the hot water is higher than that of the cold water, since it flows faster through the terminal and has shorter time for heat transfer. Therefore, the mixed return water temperature will be between the temperatures of the hot water and the cold water. Furthermore, the more the hot water is mixed, the higher the return water temperature will be.

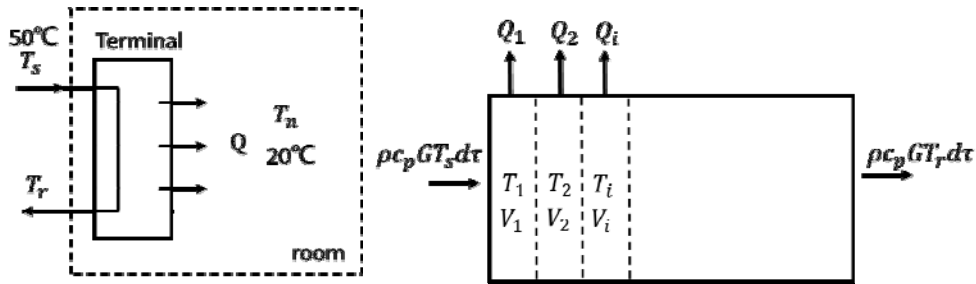


Figure.1. Model of the on-off control process (left: room model; right: terminal model)

The main factor that decides how much hot water flow out is the “on” time. The longer the “on” time is, the more the hot water flows out, resulting in higher return water temperature. For explaining relation between the “on” time and the return water temperature, we built a model to simulate the control process. As it is shown in Figure.1 (left), a terminal is assumed to be installed in a room. The indoor temperature is set at 20°C and the supply water temperature is at 50°C. The terminal model is dispersed into several part along the water flow. In each part, the inside water temperature will change according to the energy input and output. The energy balance equation can be described as (1) and (2).

$$\rho c_p V_i (T_{i,t} - T_{i,t-\Delta t}) = \rho c_p G_i \Delta t (T_{i-1,t-\Delta t} - T_{i,t-\Delta t}) - Q_{i,t-\Delta t} \quad (1)$$

$$Q_{i,t-\Delta t} = KF_i (T_{i,t-\Delta t} - T_r)$$

(2)

where ρ and c_p are separately the density and specific heat of the water, V_i , T_i , K , F_i and Q_i are separately the volume, temperature, heat transfer coefficient, heat transfer area and emitted heat of the part terminal i , t means the time of the process, G is the water flow.

In this model, the on-off control can be simulated by changing the water flow (G) as the time changes (t). When the valve is on, the water flow is set at 83cm³ per sec, which needs around 4 min to fulfil the 20L terminal, while the valve is off, the water flow is 0. The K and F of the terminal are separately 6.7W/(m²K) and 3m² according to steel column radiator.

The heat demand of the room is set at 0.51W. When the “on” time changes, the on-off cycle period will change as well so that keep the heat supplied stably. The relations between the “on” time and on-off cycle period as well as the return water temperature are shown in figure.2. It can be seen that the return water temperature reduces as the “on” time shortens. The lowest return water temperature is achieved when the “on” time is 4 minutes. 4 minutes is the time that the

cool water needs for flowing out from the terminal according to the model setting. When the “on” time is longer than 4 min, there are more or less hot water flowing into the return water pipe and mixing with the cold water.

The “on” time will affect the return water temperature because the hot water will mix with the cold water and then rise the return water temperature, but has less impact on the heat control performance because the quantity of the supplied heat can be adjusted by changing the on-off cycle period. Therefore, even though the existing strategy can well control the heat supplied, the strategy still needs to be modified for reducing the return water temperature.

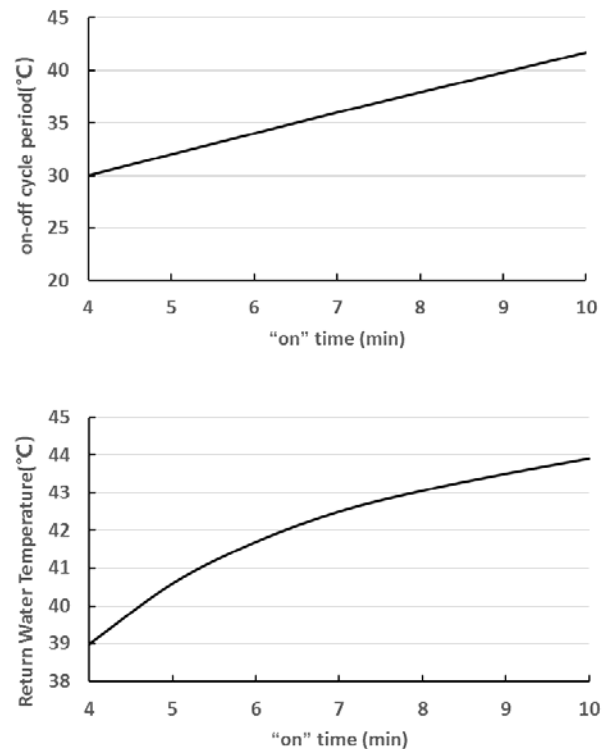


Figure.2. The effect of changing the “on” time

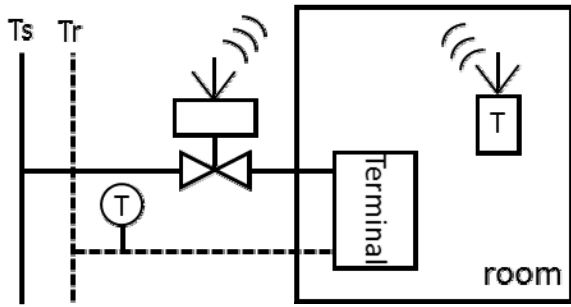


Figure 3. schematic diagram of the control device

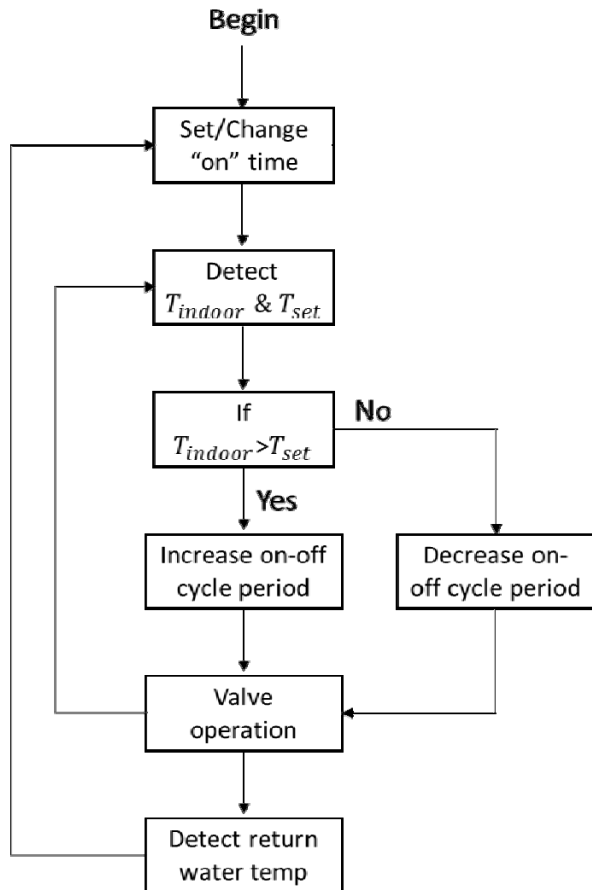


Figure 4. Control logic

ON-OFF CONTROL STRATEGY

The modified strategy can control the “on” time. As shown in figure.3, three devices are designed for implementing the new strategy: a temperature controller, a temperature sensor, and an automatic control on-off valve. The temperature controller will be placed in the room to detect the indoor temperature and accept the set temperature. The temperature sensor will be placed on the return water pipe to detect the return water temperature. The on-off valve will be installed on the pipe before or after the terminal, which can control the water flowing according to the information from the temperature controller and the return water temperature sensor.

The new control logic is explained in figure.4. It can be divided into two processes. One is to control the indoor temperature by adjusting the on-off cycle period. When the indoor temperature is higher than the set temperature, the period will increase, otherwise it will decrease. The other process is to reduce the return water temperature by shortening the “on” time. However, the “on” time should not shorten unrestricted. We set a minimum on-off cycle period to limit it. When the on-off cycle period decreases lower than the minimum, the “on” time will increase. In fact, too short cycle period leads to frequent operation of valve which should be prevented.

EXPERIMENT

The experiment about the new strategy is in a seven floor residential building. As shown in figure.5, two apartments locate in one floor. They have the similar layout, since the indoor heating systems are built by the developers. There is a water separator (collector) in each apartment, separating (collecting) the water into (from) seven loops of floor-heating terminals who take charge of the heating of different rooms.

The on-off control valves are installed in the piping shaft before the water separators, which can control the water flowing in/out one apartment. The temperature controller is placed in the living room and the set temperature can be changed by user. Two temperature sensors are separately placed on the supply water pipe and return water pipe. They measure and record the temperature during the testing period.

The “on” time is calculated by the testing data. During the on-off valve operating, the temperature change that is measured from the supply and return water pipes are shown in figure.6. Even the “on” time is set at 7 minutes, but the actual “on” time is around 5 minutes. This is because of the delay of the valve operation. The valve used in this experiment is thermo-motive. There is a component that will deform when heated with electricity or cooled without electricity, driving the valve to change the on-off status. After the “on” or “off” instruction is sent out, the valve status will change a few minutes later. Therefore, the “on” time is not between the on instruction and off instruction, but from the supply water temperature rise to decline.

The experiment lasts from 10th April to 16th. The change of the outdoor temperature is shown as figure.7. From 11th afternoon to 14th afternoon, the outdoor temperature stays around 15°C, so it can be assumed that the heating demand of the apartments has no significant change. Thus the testing data during these three days are picked out for analysis. Besides, apartments of 4th floor west and 5th floor west are chosen as typical samples.

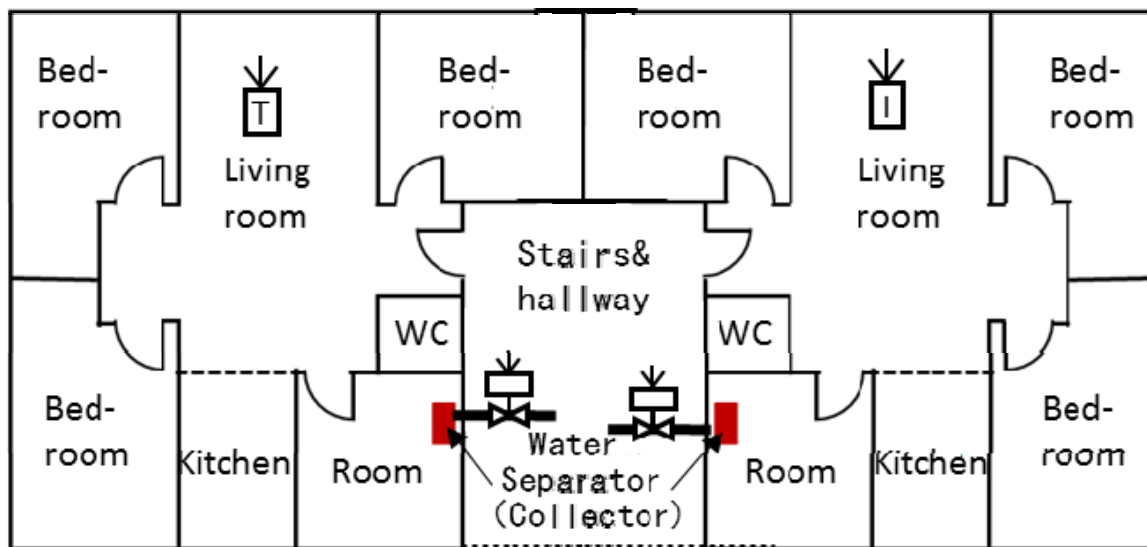


Figure.5. Layout of the experimental systems

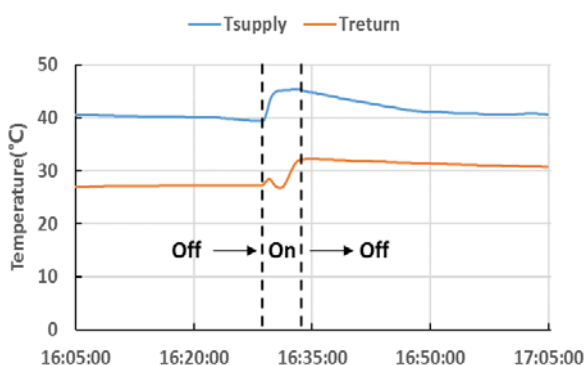


Figure.6. Temp change during valve operating

Both the measured temperature and set temperature of indoor air are recorded. The set indoor temperatures of the 4th floor west and the 5th floor west are separately 25°C and 26°C. Under the new heat control strategy, whenever the “on” time changes, the indoor temperatures can always be kept around the set temperatures, which proves the new strategy has good performance in heat control and the changing of “on” time will not influence the heat control performance.

When comparing the return water temperature as the “on” time changes, the conclusion from the theoretical analysis is proved. As it is seen from the 5th floor west apartment, the “on” time increases from approximately 3min 20sec to 7min in 12th afternoon and then decreases to around 4min 30sec in 13th afternoon. The return water temperature rises from 27°C to 28.5°C and then decrease to 27.6°C. It must be mentioned that the return water temperature is calculated by the average

of the measured temperature during the “on” time. The testing data proves that the longer the “on” time is, the higher the return water temperature will be. In addition to the two samples, the data of many other apartments shows the same relation.

In addition to the “on” time, some other factors that will affect the return water temperature can also be found. One of the factors is the hydraulic unbalance inside the apartment. Different loops of floor heating pipes have different length, so the time for draining out the cool water is not the same among different loops. As it is shown in figure.9, when the seven loops inside an apartment is controlled by one valves, the return water temperatures do not change synchronously. When the left water still remains, the fresh water has flown out from some loops. In the experiment, the loops of 5th floor west have been balanced by manual adjusting, while those of 4th floor west have not. As shown in figure.8, the return water temperature of 5th floor west is lower than that of 4th floor west, implying that the hydraulic balance inside the apartment has effect on reducing return water temperature.

The other factor is the indoor temperature. The 2nd floor west apartment is a sample without heat control device. During the testing period, its indoor temperature has reach to 29°C and its return water temperature is higher than 40°C (Figure.10). Both the indoor temperature and return water temperature is much higher than the apartments with heat control devices. Implementing heat control devices and encouraging users to decrease the set temperature is also necessary in reducing the return water temperature.

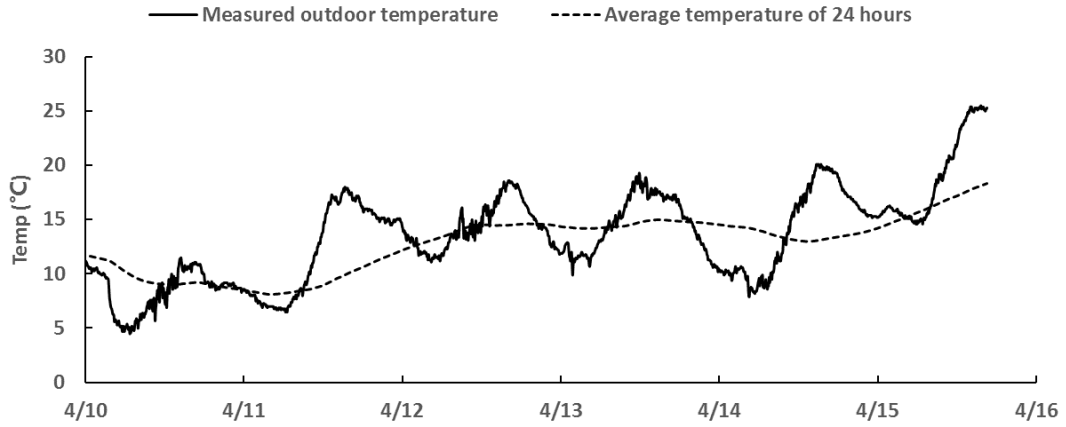


Figure.7. Outdoor temperature during the testing period

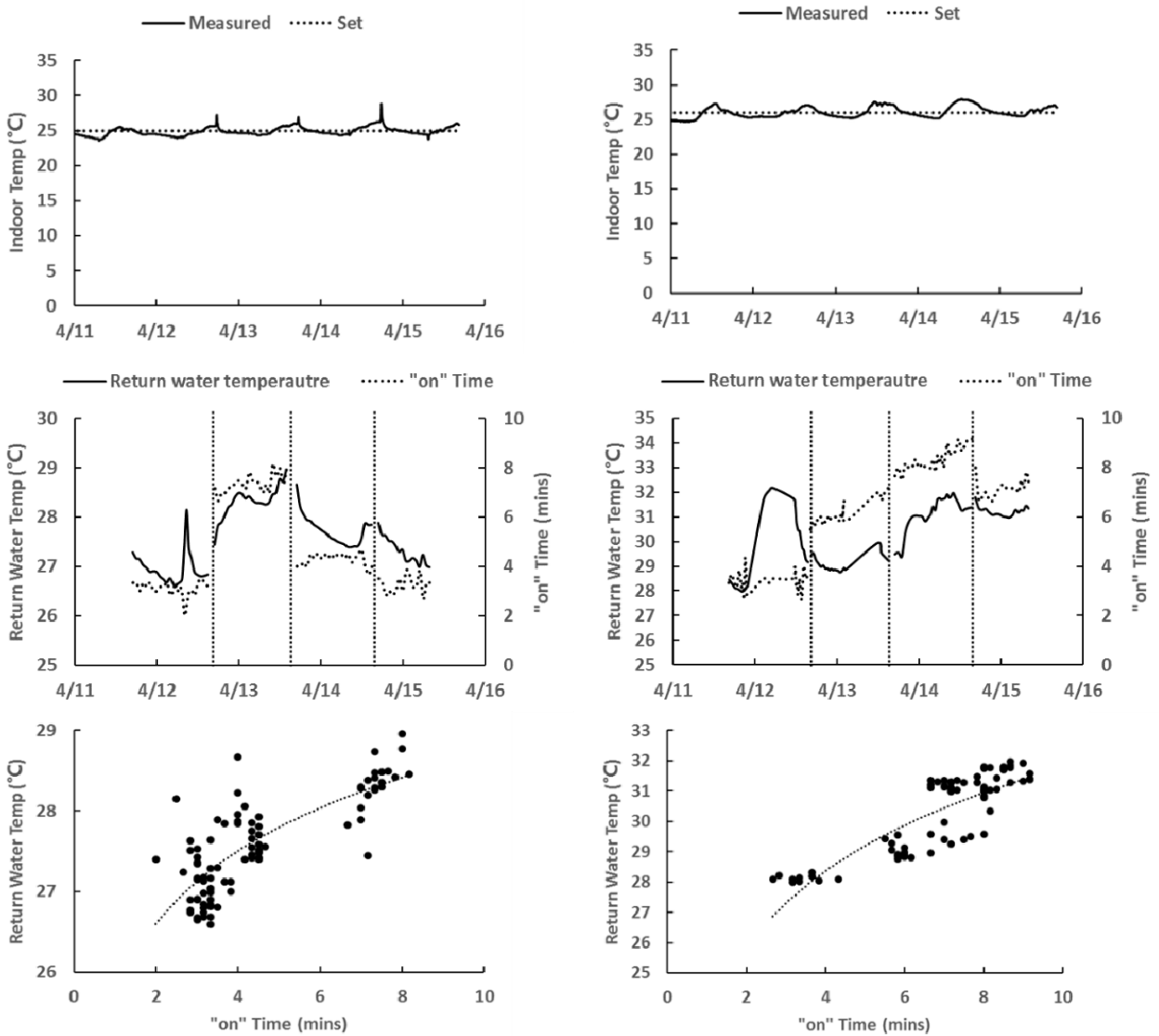


Figure.8. Testing data of two apartments (left: 5th floor west; right: 4th floor west)

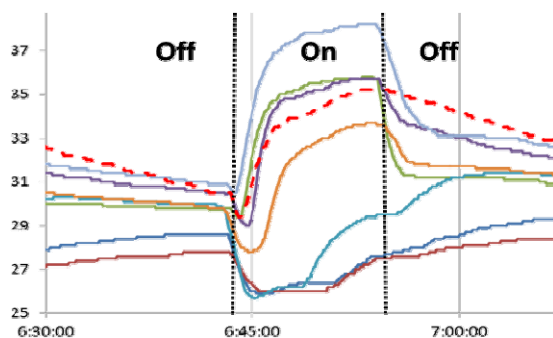


Figure.9. Hydraulic Unbalance in apartment

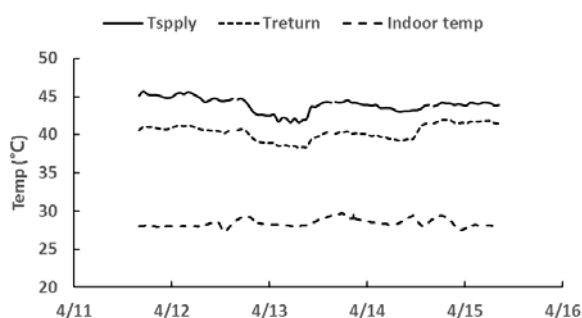


Figure.10. Data of the 2nd floor west apartment

CONCLUSION

On-off valves are more reliable and durable than the other thermostatic valves when working in bad quality water. This paper explores the strategy on controlling the on-off valve in order to reduce the return water temperature.

The relation between the “on” time and return water temperature is revealed in theory. A model is built for simulating the operating state under different heat control strategies. The result shows that the more the “on” time is, the higher the return water temperature will be, because more hot water flows into return water pipe and mixes with the cool water as the “on” time rises. For reducing the return water temperature, the “on” time should be shortened for preventing the hot water flowing into the return water pipes.

A new heat control strategy is proposed for reducing the return water temperature. The “on” time is adjusted at the time that the cool water needs for flowing out of terminal. The hot water will be kept in the terminal until the next “on” time arrives. The on-off cycle period can change for regulating the heat supplied so that control the indoor air temperature.

This new strategy has been applied in new device. An experiment is conducted in some apartments of a residential building. The return water is kept at lower temperature after the devices installed. The testing data also shows that as the “on” time increases, the

return water temperature rises. It proves effect of the heat control strategy.

Furthermore, it can be found in the experiment that the heat control strategy is not the only factor that affects the return water temperature. Some other factors such as the hydraulic unbalance and indoor temperature should be concerned. How to keep the return water at lower temperature still needs further research.

REFERENCE

- [1] Tsinghua University Building Energy Research Center, 2011 Annual Report on China Building Energy Efficiency, China Architecture & Building Press, Beijing, 2011, (in Chinese).
- [2] Monetti V, Fabrizio E, Filippi M. Impact of low investment strategies for space heating control: application of thermostatic radiators valves to an old residential building[J]. Energy & Buildings, 2015, 95:202-210.
- [3] Xu B, Fu L, Di H. Dynamic simulation of space heating systems with radiators controlled by TRVs in buildings[J]. Energy & Buildings, 2008, 40(9):1755-1764.
- [4] Fang H, Xia J, Jiang Y. Key issues and solutions in a district heating system using low-grade industrial waste heat[J]. Energy, 2015, 86.
- [5] Brand M, Svendsen S. Renewable-based low-temperature district heating for existing buildings in various stages of refurbishment[J]. Energy, 2013, 62(6):311-319.
- [6] Liu L, Fu L, Jiang Y. A new “wireless on-off control” technique for adjusting and metering household heat in district heating system[J]. Applied Thermal Engineering, 2009, 36(36):202-209.
- [7] Liu L, Fu L, Jiang Y, et al. Maintaining uniform hydraulic conditions with intelligent on-off regulation[J]. Building & Environment, 2010, 45(12):2817-2822.

TOPIC D:

Customer Relations and Market Issues



ASSESSING THE FEASIBILITY OF USING THE HEAT DEMAND-OUTDOOR TEMPERATURE FUNCTION FOR A LONG-TERM DISTRICT HEAT DEMAND FORECAST

I. Andric^{1,2,3}, A. Pina¹, P. Ferrão¹, J. Fournier², B. Lacarrière³, O. Le Corre³

¹ IN+ Center for Innovation, Technology and Policy Research, Instituto Superior Técnico

² Veolia Recherche & Innovation

³ Département Systèmes Énergétiques et Environnement, Ecole des Mines de Nantes

Keywords: Heat demand, forecast, climate change

ABSTRACT

District heating networks are commonly addressed in the literature as one of the most effective solutions for decreasing the greenhouse gas emissions from the building sector. These systems require high investments which are returned through the heat sales. Due to the changed climate conditions and building renovation policies, heat demand in the future could decrease, prolonging the investment return period.

The main scope of this paper is to assess the feasibility of using the heat demand – outdoor temperature function for heat demand forecast. The district of Alvalade, located in Lisbon (Portugal), was used as a case study. The district is consisted of 665 buildings that vary in both construction period and typology. Three weather scenarios (low, medium, high) and three district renovation scenarios were developed (shallow, intermediate, deep). To estimate the error, obtained heat demand values were compared with results from a dynamic heat demand model, previously developed and validated by the authors.

The results showed that when only weather change is considered, the margin of error could be acceptable for some applications (the error in annual demand was lower than 20% for all weather scenarios considered). However, after introducing renovation scenarios, the error value increased up to 59.5% (depending on the weather and renovation scenarios combination considered). The value of slope coefficient increased on average within the range of 3.8% up to 8% per decade, that corresponds to the decrease in the number of heating hours of 22-139h during the heating season (depending on the combination of weather and renovation scenarios considered). On the other hand, function intercept increased for 7.8-12.7% per decade (depending on the coupled scenarios). The values suggested could be used to modify the function parameters for the scenarios considered, and improve the accuracy of heat demand estimations.

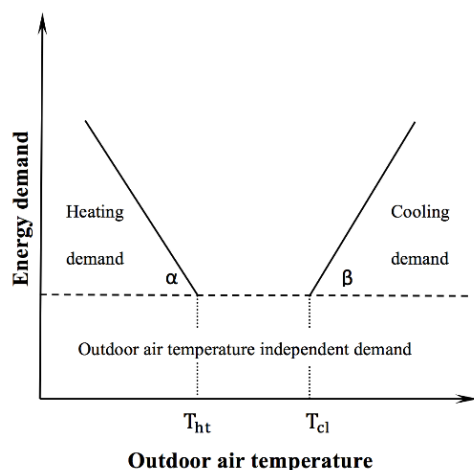
INTRODUCTION

District heating networks are commonly proposed in the literature as an environmentally friendly solution for providing heating services for urban environment.

Centralized heat production located outside municipalities, utilization of renewable heat sources (biomass, solar, geothermal etc.) and comfort for the consumers are usually stated as the main benefits of such systems. The subject has been widely researched in several scientific reports [1-4]. The conclusions were that the district heating should be considered as an essential cost effective technology for the EU energy system decarbonisation. The construction of such infrastructure requires significant investments costs, which are returned through the heat sales. However, due to the changed weather variables caused by the climate change, the amount of heat required to maintain comfort indoor conditions could decrease in the future. Additionally, new governmental policies that tackle the refurbishment of the existing building stock (such as EPBD - Energy Performance of Buildings Directive, or the Directive 2010/31/EU), along with the implementation of advanced construction and insulation for new buildings, could decrease the heat loss through the building envelope. Consequently, heat demand could decrease even further. Thus, modelling the future heat demand evolution in the decades to come could be the crucial aspect for assessing the district heating networks construction/expansion project feasibility.

The impact of climate change on building heat demand was already addressed within the existing bibliography. Based on the study scale and weather scenarios considered, these studies can commonly be categorised into three major groups:

- **Building scale, one location** – one representative building was selected for the location studied, with weather scenarios developed based on the local climate [5-6];
- **Building scale, multiple locations** - one representative building from the national building stock was selected, with weather scenarios developed for all major climate types found within that particular country [7-10];
- **Large scale (district/city/country level)** – methodologies developed were applied on a large building sample (that vary in both type and construction period), with single or multiple weather scenarios considered [11,12];



• **Figure 1. Energy demand – outdoor temperature function**

Within these studies, to calculate the heat demand, the authors either used detailed simulation software such as Energy Plus and TRNSYS (for the case studies on a building scale), or estimations based on the statistical data (for large-scale case studies). However, urban environment is usually consisted of various building types originating from different construction periods that can differ significantly in both size and geometry. Thus, up-scaling the heat demand calculated for a representative building or downscaling the demand calculated on a statistical basis could provide misleading results. Consequently, this motivated the authors of the present study to develop a dynamic model that is capable of calculating heat demand for a large number of buildings without significant calculation time or computing power required, and that is yet able to take into account all significant building properties (geometry, thermal properties, occupancy profiles etc.). The dynamic aspect is particularly important from the district heating network operator point of view (for the production units and storage optimisation). Model description, validation and possible limitations were described in detail within the previous publications by the authors [13, 14].

However, the model requires multiple input data for each building within the district. For the previous case study [13], input data was obtained by using different tools (such as Geographical Information System (GIS), Light Detection and Ranging (LiDAR)), bibliography, as well as local municipality database. Since the source and data availability can vary from one location to another, the margin of error for using a less complex approach (that requires less detailed inputs) for estimating the heat demand in the future is considered within this study.

Heat demand - outdoor temperature function (Fig.1) is commonly used to represent the dependency of energy

consumed in buildings on the outdoor temperature. The main assumption in this approach is that the energy demand for heating use the same set-point temperature over the year, and that the change in energy demand corresponds to a change in the outdoor temperature (i.e., sensible heat exchange through the building envelope has significantly higher impact on energy demand compared to other heat losses/gains such as heat gain from the occupants/lighting/appliances and infiltration loss). In the study of Hekkenberg et al. [15], the authors suggested that the function angles could prove to be suitable for expressing the change in heat demand caused by the climate change in the future. This V-shaped linear symmetric relationship between the building energy demand and outdoor temperature was also addressed in the paper of Brown et al. [16]. The authors addressed both linear symmetric and non-linear asymmetric relationships between temperature and energy use in buildings, as well as semi-parametric and non-parametric models. However, the authors focused on the electricity demand for meeting the cooling demand (due to a higher non-linearity in electricity consumption-outdoor temperature correlation compared to heating). Additionally, building renovation was not considered.

The main scope of this study is to assess the feasibility of using the heat demand-outdoor function for heat demand forecast on a district scale, taking into account climate and building renovation scenarios for the future.

METHODOLOGY

Primarily, heat demand was calculated on an hourly basis for each building within the district (for the reference district state and weather scenarios) by using RC (resistance-capacitance) model based on the thermo-electrical analogy. With the reference district heat demand calculated, the heat demand – outdoor temperature function for each building was expressed as:

$$Q_{h,i} = \alpha_i \cdot t_{o,j} + \theta_i \quad (1)$$

where $Q_{h,i}$ [W] is the hourly heat demand of the i -th building for the regarded j -th hour, α [W/°C] and θ [W] are the function slope and intercept (respectively) for the corresponding i -th building, and $t_{o,j}$ [°C] is the outdoor air temperature for the regarded j -th hour.

Three future weather scenarios were created by using the CCWeather Generator tool (developed at the University of Southampton) for morphing reference .epw weather files. The software uses the .epw files as a primary input. Other required inputs are the output

climate scenario files (for A2 family of IPCC scenarios) from the HadCM3 (Hadley Centre Coupled Model, version 3) - coupled Atmosphere-Ocean General Circulation Model (AOGCM) developed at the Hadley Centre located in the United Kingdom. As an output, CCWorldWeatherGen produces morphed weather data for three years: 2020, 2050 and 2080. However, within this study, obtained results were used to develop three weather scenarios: low scenario (weather data calculated for the year 2020 is used as the weather data for the year 2050), medium scenario - weather data calculated for year 2050 is used as the weather data for the year 2050) and high scenario (weather data calculated for year 2080 is used as the weather data for the year 2050). For all three scenarios, weather data for the years 2020, 2030 and 2040 was linearly interpolated between the values for a reference year (2010) and the values for the year 2050. We found that our low, medium and high scenarios correspond to RCP2.6, RCP6.0 and RCP8.5 IPCC (Intergovernmental Panel on Climate Change) scenario (respectively), within the range of uncertainty defined within the IPCC report [17].

Additionally, three district renovation paths for the future were developed to account different depths of district renovation (i.e. the amount of building renovated) and levels of building renovation (different levels of building envelope improvements). Three main criteria were considered for renovation scenarios:

- **Building selection criteria** – defining which buildings are renovated;
- **Renovation depth** – defining the amount of buildings renovated out of the total buildings selected by the first criteria;
- **Renovation level** - level of improvement in the building envelope that defines new thermal properties;

Finally, for each year considered in scenarios (2020, 2030, 2040 and 2050), hourly demand of each building within the district was calculated by using two approaches:

- **RC model simulation** – for each year of the scenarios, hourly heat demand for each building within the district was calculated by using the detailed input data from weather scenarios (outdoor air temperature, solar radiation) and renovation scenarios (new building envelope thermal properties, improved after the renovation);
- **Heat demand-outdoor air temperature function estimation** – primarily, function parameters (slope and intercept) for each building were calculated based on the RC model heat demand results for a reference year (2010, reference weather and district state). Then, for each year of the regarded

scenarios, hourly district heat demand for each building within the district was estimated by using these function parameters (see eq.(1)) and forecasted outdoor air temperatures.

To estimate the difference between the results obtained from these methods, two parameters were used: annual heat demand percentage error (Δ [%], eq.(2)) and standard deviation between the hourly demand values (σ [SD], eq. (3)):

$$\Delta = \frac{(\sum_{j=1}^n Q_{RC,j} - \sum_{j=1}^n Q_{func,j})}{\sum_{j=1}^n Q_{RC,j}} \cdot 100 \quad (2)$$

$$\sigma = \sqrt{\frac{\sum_{j=1}^n (Q_{RC,j} - Q_{func,j})^2}{n}} \quad (3)$$

where the $Q_{RC,j}$ [W] and $Q_{func,j}$ [W] are the hourly district heat demands (sum of hourly heat demands of all buildings within the district for the regarded j -th hour of total n hours during the heating season) estimated by the heat demand-outdoor temperature function and calculated by the RC model, respectively.

CASE STUDY

The district of Alvalade, located in Lisbon (Portugal), was used as a case study. The district is consisted of 665 buildings that vary in both construction period and typology (single-family houses, multi-apartment buildings, offices, educational buildings and hotels). Reference building database (building geometry, position, shading etc.) was created by using ArcGIS and remote sensing (LiDAR), as well as already existing database from the local municipality. Thermal properties for the reference buildings state were obtained from the BPIE (Building Performance Institute Europe) online database [18] and a specific case study for Portugal [19], based on the construction period and type considered. For the reference weather data, .epw weather file for Lisbon from Energy Plus weather database [20] was used. Weather scenarios were developed by using the the CCWeather Generator tool. For the building renovation scenarios, building selection criteria (i.e. the definition of which buildings will be selected for renovations) was based on the administrative division of the district, while the values for the amounts of buildings renovated each year within the sections were obtained from the BPIE report [21]. Thermal properties for the improved envelope elements after renovation measures were estimated based on the available bibliography [22]. In this case study, first renovation step would be to refurbish the existing building stock to the current commercial level (the U-values for the buildings built around 2010, as given in [22]) before upgrading it to higher levels of insulation. Thus, for each building type (and for its elements),

upgrade to 2010 values is considered as a minor renovation, while for the nearly-zero energy buildings level the values from the previously mentioned study ([12]) were assigned. Accordingly, the values for the moderate and deep renovations are derived through the linear interpolation between these values. For more detailed description of the district data collection and creation of weather and renovation scenarios, please refer to a previous study by the authors [13].

RESULTS AND DISCUSSION

Primarily, the results for a reference year (2010) are compared to verify the suitability of the heat demand – outdoor temperature function to estimate building heat demand based only on the calculated function parameters for the reference year and outdoor temperature. The precision was quite high, with the annual error of $\Delta=0.25\%$ in estimated heat demand and standard deviation between the hourly demand of $\sigma=0.06$ (as it can be seen on Fig.2). To further estimate the ability of the function to represent the dependency between the heat-demand and outdoor temperature, Pearson's product-moment correlation coefficient was used (commonly used in the bibliography as a measure of linear correlation between two variables). The coefficient is defined as the covariance of the two variables divided by the product of their standard deviations. The value of the coefficient was $r=-0.91$, which proves high linearity (on scale from 0 to -1 for total negative correlation (negative due to the fact that the heat demand decreases with a temperature increase)). The results proved that, in our context, the major factor in heat demand are clearly sensible heat losses through the envelope (due to the high linearity).

However, in the case of heat demand forecast with developed weather scenarios accounted (without any renovations considered), the error and deviation increased (Fig. 2). The average error increase is within the range of 0.4 - 2.5% per decade (depending on the weather scenarios considered), while the standard deviation slightly increases within the range of 0.061 - 0.064. Considering that within the bibliography it is stated that for the simplified building models, acceptable margin of error is 20% [23], and taking into account that in this case the highest margin of error is less than 20% (11.9%, high weather scenario, year 2050), this approach could be suitable for simplified estimations of heat demand in the future. However, since the acceptable margin of error further depends on the scope of the study (stage and the value of the project in development etc.), in some instances the error of 12% could be considered as quite high. Thus, depending on the margin of error expected by the

decision-makers, dynamic models (such as mentioned RC model) could be necessary.

As presented in the paper by the authors for the previous International Symposium on District Heating and Cooling [23], the number of heating hours has the crucial effect on the function perimeter values. As a result of shifted temperature values for the future weather conditions, the number of heating hours (n_{hh}) is decreased, and the hour dataset that is consisted of these values and used for the heat demand calculations is consequently not the same. The effect of decreased number of hours that require heating on district heat demand function parameters (calculated for the demand of the whole district) can be observed on Fig.3 and Fig.4

The number of hours with heat demand during the heating season decreases for an approximately 14h, 46h and 108h per decade (for low, medium and high weather scenario, respectively). The values of the slope coefficient α increase for 0.01 to 0.08MW/°C per decade, while the values of the intercept θ decrease for 0.18 to 1.92MW per decade (depending on the weather scenario considered). Thus, it can be concluded that for the decrease in number of heating hours of 4% per decade (that correspond to an average of all weather scenarios increase in outdoor temperature of 0.4°C per decade), the value of the slope increase for 0.04MW/°C, while the intercept values decrease for 0.74MW.

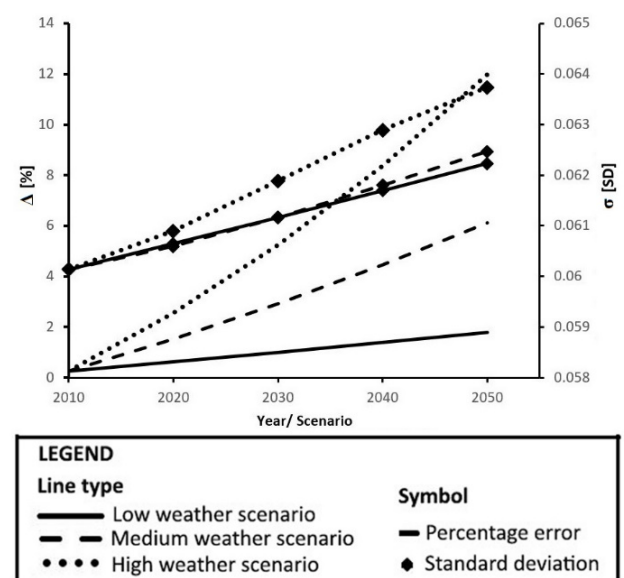


Figure 2. Percentage error and standard deviation between the two approaches considered (only weather scenarios)

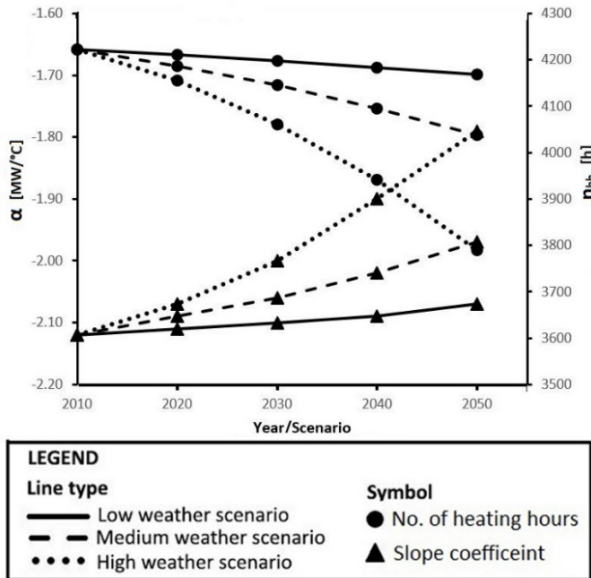


Figure 3. The impact of decrease in heating hours on the district heat demand function slope coefficient (only weather scenarios)

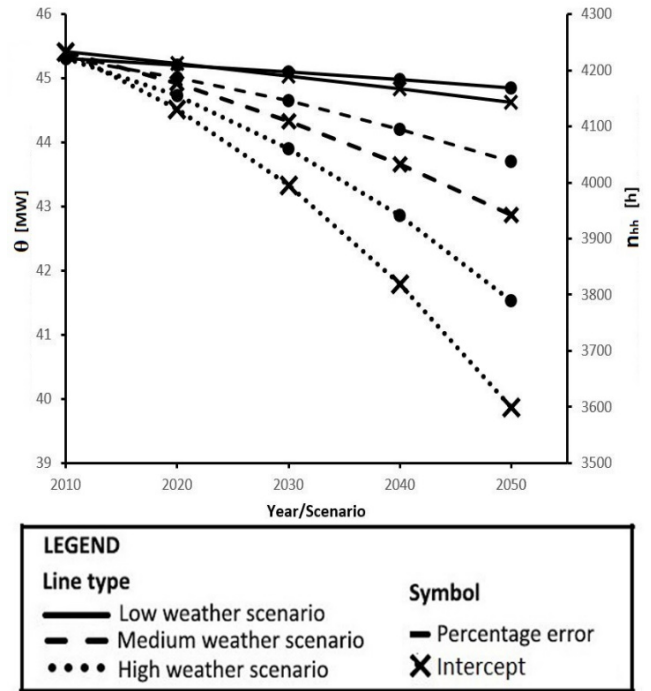


Figure 4. The impact of decrease in heating hours on the district heat demand function intercept (only weather scenarios)

However, due to the new building renovation policies, the probability of envelope retrofitting over the district in the future is relatively high, and thus, the effect of renovation scenarios should be also considered. Consequently, we have recalculated the error in results between the two models, taking into account both weather and renovation scenarios. The percentage error increased significantly, and for all combinations of weather and renovation scenarios, the margin of error was higher than 20% in year 2030. For the year 2050, for the lowest heat demand reduction scenario combination (low weather scenario and shallow renovation path), the margin of error is 27.6%, while for the highest demand reduction scenario (high weather scenario and deep renovation path) the margin of error is 59.5%. Thus, the margin of error increases significantly when renovation scenarios are considered, due to the inability of the function to account for the changes in the thermal performance of building envelope elements (please see eq.(1)). Consequently, it can be concluded that the use of solely reference function parameters and future weather conditions is not suitable for heat demand forecast. Hence, the impacts of coupled weather and renovation scenarios on the reference function parameter values (calculated for the whole district demand) are explored.

The impact of coupled scenarios on the number of heating hours (and consequently demand function slope and intercept) are illustrated on Fig 5 and Fig.6. The values of the function slope coefficient increase on average within the range of 3.8% up to 8% per decade, that correspond to the decrease in the number of heating hours of 22-139h during the heating season (depending on the combination of weather and renovation scenarios considered). On the other hand, function intercept increases for 7.8-12.7% per decade (depending on the coupled scenarios). Comparing the results from Fig. 3/Fig.4 and Fig.5/Fig.6, it is clear that the renovation of buildings within the district has a higher impact on the function parameters, and consequently on the number of heating hours and errors in heat demand estimations by using the reference values of slope and intercept. Thus, the values of the slope and intercept coefficients (α, θ) would have to be corrected in order to decrease the margin of error and make the heat demand-outdoor temperature function feasible for a long-term district heat demand forecast.

CONCLUSION

The main scope of this paper was to explore the feasibility of using a simplified numerical approach based on the heat demand – outdoor temperature function to estimate the heat demand in the future on a district scale. The impact of climate change was considered through the developed weather (low, medium, high) and renovation (shallow, renovation, deep) scenarios. The results were compared with an output from a dynamic heat demand model, previously developed and validated by the authors. Proposed methodology was applied on the district of Alvalade, located in Lisbon (Portugal), that is consisted of 665

buildings that vary in both typology and construction period. Three weather scenarios were considered (low, medium and high), along with three building renovation scenarios (shallow, intermediate, deep renovation path).

The results indicated that for the reference year (reference weather and district state), the precision of estimated demand values through the proposed function was satisfactory. After taking into consideration weather scenarios, the margin of error was still below 20% on all occasions, and the approach could be considered accurate enough for some applications, if no district renovation measures are planned. However, after introducing the renovation scenarios, the error value increased up to 59.5%

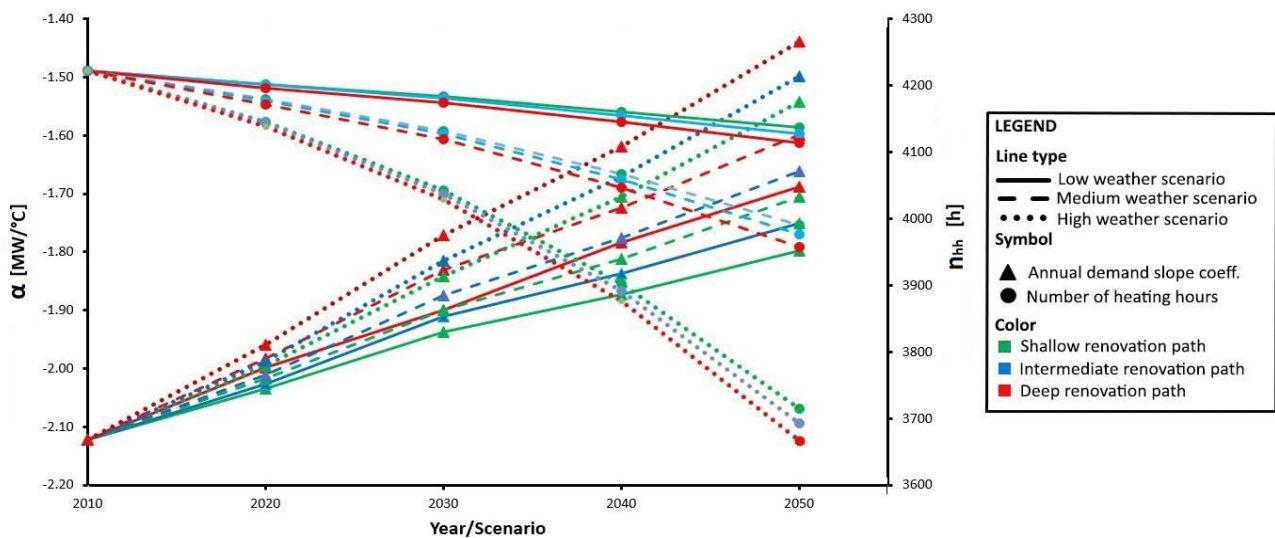


Figure 5. The impact of decrease in heating hours on the district heat demand function slope coefficient (both weather and renovation scenarios considered)

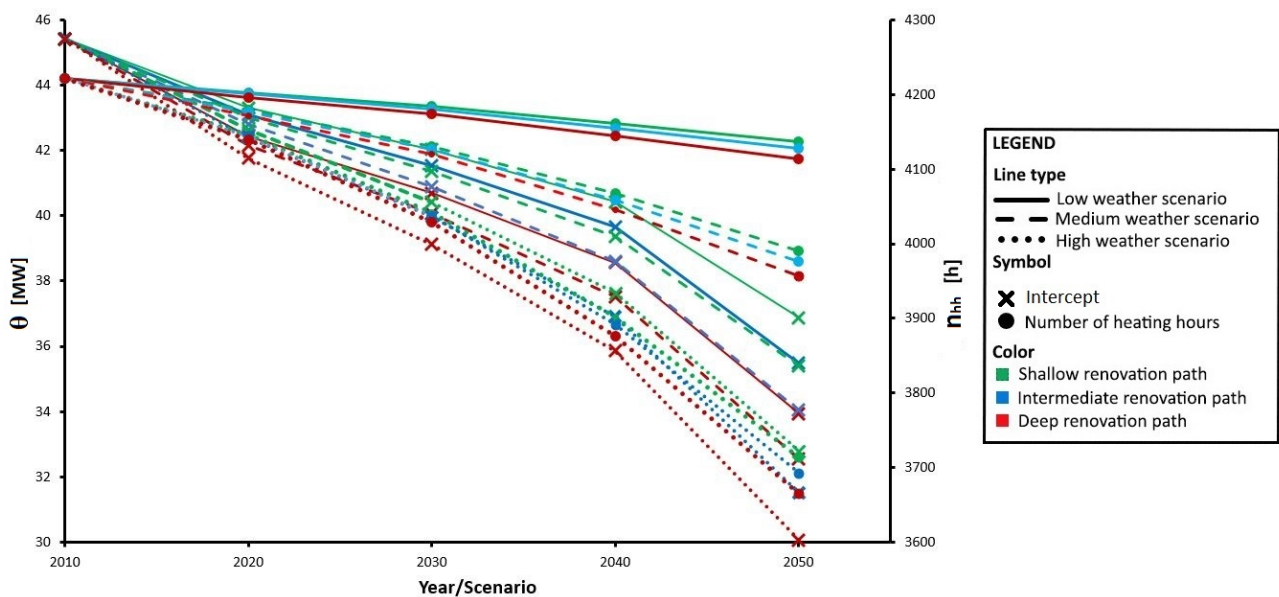


Figure 6. The impact of decrease in heating hours on the district heat demand function intercept (both weather and renovation scenarios considered)

(depending on the weather and renovation scenarios combination considered). Considering the values of function parameters, slope coefficient increased on average within the range of 3.8% up to 8% per decade, that correspond to the decrease in the number of heating hours of 22-139h during the heating season (depending on the combination of weather and renovation scenarios considered). On the other hand, function intercept increased for 7.8-12.7% per decade (depending on the coupled scenarios).

The values suggested could be used to modify the function parameters for the scenarios considered, and improve the accuracy of heat demand estimations (by correcting the function parameter values for the regarded year and considered weather and/or renovation scenarios). However, the coefficient correction values presented are based on the findings for a particular case study addressed in this paper and renovation scenarios considered. The impact of changed weather variables could be different for locations in different climate and building stocks, as well as renovation parameters. Furthermore, behind the renovation scenarios, three aspects are considered (building selection, renovation depth and renovation level). Instead of connecting the function parameters to renovation scenarios, a deeper insight on the impact of envelope element U-values improvements and element surface on the function parameters, combined with weather variables change, could be useful for future estimations. However, these complex relationships between multiple parameters should be presented in a clear and simplified manner, which is a challenging task itself.

ACKNOWLEDGEMENT

The research presented is performed within the framework of the Erasmus Mundus Joint Doctorate SELECT+ program 'Environomical Pathways for Sustainable Energy Services and funded with support from the Education, Audio-visual, and Culture Executive Agency (EACEA) (Nr 2012-0034) of the European Commission. This publication reflects the views only of the author(s), and the Commission cannot be held responsible for any use, which may be made of the information contained therein. The authors would like also to acknowledge Fundação para a Ciência e Tecnologia for the Post-Doctoral financial support, (SFRH/BPD/96459/2013).

REFERENCES

- [1] D. Connolly, B. Mathiesen, V.P.A: Østergaard, "Heat Roadmap Europe 2050", Euroheat & Power (2012), pp. 99;
- [2] M. Dolman, M. Abu-Ebid, J. Stambaugh, "Decarbonising heat in buildings 2030 - 2050.

Summary report for The Committee on Climate Change", (2012), pp. 2030–2050;

- [3] Scottish Government, "Towards Decarbonising Heat : Maximising the Opportunities for Scotland Draft Heat Generation," (2014), Available at: <http://www.gov.scot/resource/0044/00445639.pdf>. [Accessed January 27, 2014];
- [4] H. Lund, H., B. Möller, B.V. Mathiesen, A. Dyrelund, "The role of district heating in future renewable energy systems," (2010), Energy, vol. 35, no. 3, pp. 1381–1390;
- [5] T. Frank., "Climate change impacts on building heating and cooling energy demand in Switzerland.", Energy and Buildings, 37(11), (2005), pp. 1175–1185;
- [6] T. Berger, C. Amann, H. Formayer, A. Korjenic, B. Pospischal, C. Neururer, R. Smutny, "Impacts of climate change upon cooling and heating energy demand of office buildings in Vienna, Austria". 580 Energy and Buildings, 80, (2014), pp. 517–530.
- [7] M. Dolinar, B. Vidrih, L.K. Bogataj, S. Medved, "Predicted changes in energy demands for heating and cooling due to climate change", Physics and Chemistry of the Earth, (2010), Parts A/B/C, 35(1-2), pp. 100–610 106;
- [8] M. Christenson, H. Manz, D. Gyalistras, « Climate warming impact on degree-days and building energy demand in Switzerland", Energy Conversion and Management, 47(6), (2006), pp. 671–686;
- [9] P. Xu, Y:J: Huang, N. Miller, Schlegel, P. Shen,"Impacts of climate change on building heating and cooling energy patterns in California", Energy, 44(1), (2012), pp. 792–804;
- [8] X. Wang, D. Chen, Z. Ren, "Assessment of climate change impact on residential building heating and cooling energy requirement in Australia", Building and Environment, 45(7), (2010), pp. 1663–1682;
- [10] V. M. Nik ,A. Sasic Kalagasidis, "Impact study of the climate change on the energy performance of the 718 building stock in Stockholm considering four climate uncertainties", Building and Environment, 60, 719 (2013) pp. 291–304;
- [11] M. Olonscheck, A. Holsten, J.P. Kropp, "Heating and cooling energy demand and related emissions of the German residential building stock under climate change", Energy Policy, 39(9), (2011), pp. 4795–4806;
- [12] I. Andrić, I., N. Gomes, A. Pina, P. Ferrão, J. Fournier, B. Lacarrière, O. Le Corre, "Modeling the long-term effect of climate change on building heat demand: case study on a district level", Energy and Buildings, (2016), in print;
- [13] I. Andrić, I., C. Silva, A. Pina, P. Ferrão, J. Fournier, B. Lacarrière, O. Le Corre, "The impact of climate change and building renovation on heating related CO₂ emissions on a neighborhood level", in proc.

- CISBAT International Conference. Lausanne, 9th-11th of September, (2015), pp 621-626;
- [14] M. Hekkenberg, H.C. Moll, J.M. Uiterkamp, J.M.S., "Dynamic temperature dependence patterns in 657 future energy demand models in the context of climate change". *Energy*, 34(11), (2009) pp. 1797–1806;
- [15] M.A. Brown, M. Cox, B. Staver, P. Baer, "Modelling climate-driven changes in U.S. building energy demand", *Climatic Change* 134, (2016), pp 29-34;
- [16] IPCC (Intergovernmental Panel on Climate Change), "Climate Change 2014: Synthesis Report Summary for policy makers". IPCC, Geneva, Switzerland, (2014) Available at: https://www.ipcc.ch/pdf/assessment-report/ar5/syr/AR5_SYR_FINAL_SPM.pdf [Accessed July 27, 2015];
- [17] BPIE (Building Performance Institute Europe), "Data hub for the energy performance of buildings, country factsheets: Portugal". Available at: <http://www.buildingsdata.eu>. [Accessed January 27, 2015];
- [18] J. Sousa, L. Braganca, M. Almeida, P. Silva, "Research on the Portuguese Building Stock and its Impacts on Energy Consumption – An Average U-Value Approach", *Archives of Civil Engineering*, 59(4), (2013);
- [19] U.S. Department of Energy, Energy Plus energy simulation software, Weather data. Available at: <https://energyplus.net/weather> [Accessed January 27, 2015];
- [20] BPIE (Building Performance Institute Europe), "Europe's buildings under the microscope", (2012), Tech. report. Available at: <http://bpie.eu/publication/europes-buildings-under-the-microscope/> [Accessed January 27, 2014];
- [21] A. Pappas, Reilly, C., "Streamlining energy simulation to identify building retrofits. *ASHRAE Journal*, (2011) Available at: http://bookstore.ashrae.biz/journal/download.php?file=ASHRAE-D-728_AJ11Nov02-20111101.pdf [last accessed: February, 2016];
- [22] I, Andric, I., Darakdjian, Q., Ferrao, P., Le Corre, O., Lacarriere, "The impact of global warming on district heating demand: the case of St Félix", in proc. The 14th International Symposium on District Heating and Cooling, Stockholm, September 6th-10th, (2014);

HEAT SOURCE SHIFTING IN BUILDINGS SUPPLIED BY DISTRICT HEATING AND EXHAUST AIR HEAT PUMP

J. Kensby¹, A. Trüschel¹, J.O. Dalenbäck¹

¹ Division of Building Services Engineering, Department of Civil and Environmental Engineering, Chalmers University of Technology, SE-412 96, Gothenburg, Sweden

Keywords: *Heat source shifting, Exhaust air heat pump, District heating, Hourly pricing*

ABSTRACT

The heat supply for Swedish multi-family residential buildings is becoming more complex, and today it is fairly common to combine district heating with a second heat source e.g. a heat pump. There is a lost potential in cost and CO₂ savings when one heat source is given full load priority, since marginal production costs and CO₂ emissions constantly vary in both the electrical grid and the district heating system. The aim of this study is to evaluate how buildings with several heat sources should be operated using hourly energy prices. Hourly heat and electricity prices for Gothenburg have been established for two years based on the marginal costs of heat and electricity generation. These prices have been used to evaluate the most common combinations of heat sources that is found in a survey of Energy Performance Certificates for residential properties. Results show that the most common heat source to combine with district heating in Sweden is an exhaust air heat pump. On average, the exhaust air heat pump covers 31% of the yearly heat load and is given full load priority. Equipping such heating system with a control system that allows heat source shifting and gives load priority to the heat source with the lowest cost each hour can reduce the heating cost by 3.2%. The potential for heat source shifting is highly dependent on a number of factors where the energy prices is of great importance but also the temperature levels in the heating system.

INTRODUCTION

The total energy usage in Sweden for the year 2012 was divided among buildings (38%), industry (36%), transportation (24%), and other (2%) [1]. This makes buildings the largest energy-using sector in Sweden, which is also true for the world as a whole. Energy in buildings is primarily used for heating, ventilation, and air-conditioning (HVAC) and secondarily for electrical appliances [2]. The main heat sources for HVAC purposes vary greatly between different countries. In Sweden, district heating (DH) has a market share of 60% [3], and every town with more than 10,000 inhabitants has a DH system [4].

The marginal cost of heat generation (the extra cost per MW associated with increasing the generation) can

vary significantly within a single day, and a factor of 2–3 in cost difference is not uncommon in DH systems. All Swedish DH providers have a heat tariff where the price of heat is constant during all hours in one month [5]. Some companies have a tariff that is constant for the whole year, while some provide seasonal pricing. The most common pricing model for electricity in Sweden today is also to have fixed prices over one month or longer periods of time. Customer prices are set by the electricity traders based on their estimates of the average price for electricity on NORDPOOL, the deregulated electricity spot market for northern Europe. How long the prices are fixed is up to the customer, but the longer the prices are fixed, the larger the risk is for the trader that charges a premium on top of its price for taking the risk. What is true for both DH systems and the electrical system is that having constant prices and large variations in generation costs can lead to suboptimal solutions, since the customer has no incentive to regard his or her heat usage from a system perspective.

Since the need for space heating in buildings can be fulfilled by either DH or electrical heating, primarily with a heat pump (HP), it is also of interest to consider optimizing the two together from a system perspective. Buildings with DH and HP today most often have fixed prices for heat and electricity and utilize the HP for base load and DH for peak load. This is a suboptimal solution, since the marginal production cost of the two systems varies during each day; hence, the system that is best for providing the base load also shifts.

Today it is possible for any customer of the Swedish electrical grid to receive a tariff with hourly prices based on the NORDPOOL day-ahead electricity spot market. This opportunity is seldom seized except by large industries and a few enthusiasts. Hourly prices make it possible for electricity customers to optimize their local systems within a larger system perspective. Load can be shifted to low-price hours to save money, and such actions help to balance the electrical grid. It has been shown in previous studies that shifting heat loads over time is possible by utilizing buildings for thermal energy storage [6-8]. Even greater possibilities can emerge if customers with DH and HP make the choice to switch to hourly electricity pricing and are also provided with hourly heat pricing. This makes it beneficial not only to

shift heat loads over time but also to shift loads between DH and the electrical grid. It is these possibilities that are studied in this paper. Adding flexibility in heat sources on the consumer side might increase the interaction between the DH system and the electrical grid, enhancing the possibility of the two systems balancing each other. This can be very beneficial if there is no strong correlation between the marginal cost of heat and electrical generation.

The aim of this project is to study the effects of implementing a heat tariff with hourly pricing for buildings with both DH and HP for space heating. The correlation between NORDPOL day-ahead spot prices and the marginal costs of heat generation in Gothenburg is studied for the years 2013 and 2014. A case study is carried out for a building with both DH and HP and hourly energy prices for both. To decide what type of HP should be used in the case study, a survey of a national building database is carried out. The case study shows how economically beneficial it is to shift load between the two systems and whether they can supplement each other. It is assumed here that the customer pays heat and electricity prices based on the marginal production costs for each; hence, the economic benefit is allocated to the customer. However, the reduced cost for the customer should reflect the reduced cost of heat and electricity generation for the energy suppliers. It should be possible to implement the same control of the heating system with another business model without hourly prices.

DH systems can have very different mixes of heat sources. This study is limited to the DH system in Gothenburg, Sweden, which has a very wide mix of heat sources. A total of 28 heat sources can be grouped into these categories:

- Industrial excess heat
- Garbage incineration combined heat and power (CHP)
- Biofuel CHP
- Natural gas CHP
- Heat pumps
- Bio fueled heat only boilers (HOBs)
- Natural gas HOBs
- Oil HOBs
- Import/export to neighbor DH systems

For the case study, a multi-family residential building is chosen, because it is the most common customer in the DH system, accounting for more than 50% of the heat load. For other building types, the heat load profile might be different.

It should also be stressed that this study is not a comparison of which is the more economical alternative between HP and DH. Such a study would need to take

into account investment costs, maintenance, etc. This is a study of existing buildings where the investments are already made, and the study focuses on optimizing the control of the combined space heating system from a system perspective.

METHODOLOGY

This study can be divided into three steps:

- Survey of residential buildings with several heat sources
- Establishing hourly heat and electricity prices
- Simulation and optimization

The first step in the study (Survey of residential buildings with several heat sources) is to find what heat sources are most often combined with DH and thus what combination of heat sources to further focus on. For this purpose, a database covering Energy Performance Certificates for Swedish properties was used. The database covers the vast majority of multi-family residential properties in Sweden and is further described in [9, 10].

The second step is to find the marginal cost of electricity and heat generation for every hour during the simulation period. The hourly electricity used in this study is based on the NORDPOOL electricity spot market [11]. The electricity trading is split on a day-ahead market, an intraday market, and a balancing power market, with the vast majority of the electricity traded on the day-ahead market. The function of the intraday market is to correct the mismatch in supply and demand that occurs due to imperfect predictions. As a customer, if you want hourly electricity prices, they are based on the day-ahead market; therefore, this data is what is used in this study. Due to transfer capacity limitations in the national and international electricity grid, NORDPOOL is divided into 16 geographical areas. These areas will share the same prices when the transfer capacity in the grid is not limiting, and the prices will differ when the transfer capacity is limiting. Since the building simulated in this project is located in Gothenburg, Sweden, the prices from the associated area SE3 are used. The price a customer with hourly electricity prices pays consists of five components:

- NORDPOOL ELSLOT SE3 day-ahead price
- Electricity tax (294 SEK/MWh)
- Electricity certificate (varies ~35 SEK/MWh for the studied time period)
- Premium to the provider
- Value added tax (VAT) (25%)

The premium to the provider is excluded for both electricity and DH in this study, since the target is to minimize the system cost. VAT is also excluded, so the modelled hourly electricity price consists of the

NORDPOL ELSLOT SE3 day-ahead price, electricity tax, and electricity certificate. This should be an electricity price with a zero contribution margin for the trader.

The hourly DH price is based on the marginal costs of heat generation in the DH system. This data is provided by the operational management group at Göteborg Energi AB (the DH provider in Gothenburg, Sweden). The marginal costs are primarily based on the variable costs for the most expensive heat generation plant that was running each hour, with a few exceptions. One exception is if the plant with the highest variable cost is running on a minimum load and therefore can't be turned off; then the plant with the second highest variable cost is the one operating on the margin. Another exception is when a plant is in operation because there are tests or pollution measurements at the site. The idea is that the marginal cost in the model should be the extra cost associated with generating, for example, 1 MW extra heat in the DH system. Like the established electricity prices, this should be the heat price with a zero contribution margin. Marginal costs are provided for the years 2013–2014; hence, these are the years simulated in this study. In all graphs, prices are presented as relative values with 1 = non-weighted average.

The third and last part of the study involves analyzing and optimizing a heating supply system in a building with the most common heat source combination found in the study. Based on parameters found in the first part of the study, an average building is established to be used in the simulation. Parameters such as building size, yearly heat use, and year of construction can be found this way. To simulate the building with an hourly resolution also requires having a heat load profile. This profile is based on measurements from a residential building typical for the same time period as the buildings found in the first part of the study.

It is also important to have a model configured with the heating system that represents systems that are actually installed in the buildings. Some of the parameters can be extracted from the building database used in the first part of the study. Yearly electrical input to the heat pumps, yearly bought heat from the DH system, and the division of heat use between space heating and domestic hot water are examples of parameters that can be found this way. However, there are other parameters more difficult to find representative data for. One is the system configuration. Here, practices can vary among different companies, cities, and countries. The system configuration used in this study is based on the regulations from the DH provider in Gothenburg and on experiences of consultants working with such solutions

in the city. Two main things stand out that could be different in other cities due to local conditions:

- The heat pump is only used for space heating (no domestic hot water). The reason is that there is a large share of low-cost industrial excess heat in the Gothenburg DH system, and customers pay a seasonal price that is very low in the summer. It is therefore not economically viable to have the HP produce domestic hot water, and the consultants design it this way.
- The heat pump is assumed to be connected in parallel with the district heating substation. This is a part of the customers' contract with the DH provider; if they are to install a second heat source, it should be connected in parallel, so it does not increase the return temperatures to the DH network. The heat pump can still supply heat to the same radiator system as the DH network, and the flow will be split between the two heat sources.

With these constraints, a model for the heat pump is established. Other parameters are kept fairly simple but accurate enough for the purpose of this study. The hot side of the HP is assumed to include the supply temperature of the radiator heating system plus a Δt of 3 °C at maximum load on both the warm and cold sides (decreasing linearly with decreasing load). The supply temperature of the radiator heating system is set to 60 °C at the design outdoor temperature (DOT) of -16 °C, and it decreases at higher outdoor temperatures, following Kärkkinen's equation [12]. According to consultants who were asked, a common design for an exhaust air HP is to allow cooling of the exhaust air down to 5 °C to avoid the need for defrosting, so this condition is used in this study. The amount of exhaust air is set to 0.35 L/m²s [13].

The parameter with the largest impact on the results is the coefficient of performance (COP) of the HP. Since this value has such a large impact, it is included in a sensitivity analysis. In the base case, it is set to 35% of Carnot COP, which, in the simulations, gives a seasonal COP of around 3.0, in line with surveys of performance of existing systems [14, 15]. These values may seem a bit low, but the existing installations are often decades old and thus not top of the line.

The major part of the study involves the statistical analysis, which is carried out in Excel. The tools provided by Excel are enough to study correlations between electricity and heat prices and also for designing a heating system for a building that switches heat sources depending on which source is the cheapest at the present hour.

RESULTS AND ANALYSIS

This chapter is divided into three sections covering the three steps in the study, as presented in the

Methodology section. The first sections study which combinations of heating sources are most common in multi-family residential properties. It also studies how the heat load is shared between the heat sources in these properties. This provides input data for the simulations in the third section.

The second section establishes hourly heat and electricity prices that reflect the cost of heat and electricity production for every hour. The variations in the established prices and their correlation are also studied.

The third section studies the heat load of a residential area and calculates the heating cost based on the established price models. The most common configuration of heating sources found in the first section is used as a simulation case together with a reference case with only DH and a sensitivity analysis where key parameters are altered.

Survey of residential buildings with several heat sources

During the year 2013, there were 20,056 properties that were customers of the DH system in Gothenburg. Out of these properties, 4,457 were multi-family residential properties, although they represent >50% of the heat use. This only includes properties with the main application area as “residential” and which also house at least three families. Villas, semidetached houses, and properties where only a minor part of the area is used for residential purposes are thereby excluded. One property can include several buildings, which is fairly common; usually, buildings that share the same yard belong to the same property. Of the 4,457 multi-family residential properties, 170 also have at least one other heat source. These are presented in Table 1.

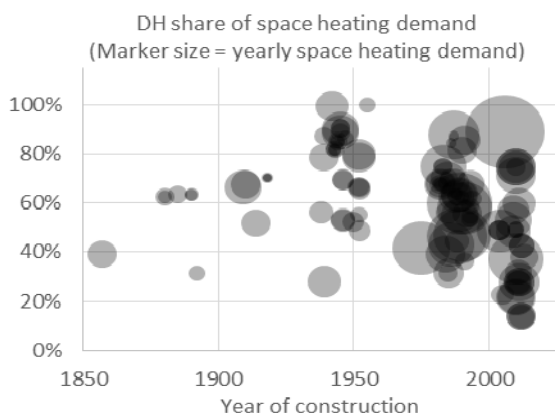


Figure 1. DH share of space heating demand in buildings with DH and exhaust air HP, assuming all domestic hot water is provided by DH and HP with SPF=3. Markers are transparent, darker color indicates higher concentration of properties.

From Table 1, it is clear that by far the most common combination of a second heat source in DH-connected buildings is with exhaust air HP. This heating combination is present in 2.7% of the multi-family residential properties in Gothenburg. This can be compared to Sweden as a whole, where this combination is present in 2.2% of multi-family residential properties with DH. It might seem surprising that the DH share of the heat load is on average 87% in these properties, but that is because property owners only report the input electricity to the HP (not the output heat).

Assuming seasonal performance factor (SPF) = 3.0 for this category, the average coverage of DH instead becomes 69% of the yearly heat load. Furthermore, in these 119 properties, 21% of the total heat output is used for domestic hot water. Assuming that only DH is used for domestic hot water, on average 61% of the yearly heat use for space heating is covered by DH for the buildings in Gothenburg. For Sweden as a whole, this value is 56%. However, the share of DH is unevenly distributed among the 119 properties in Gothenburg, as shown in Figure 1. It is therefore of interest to study several system configurations in a sensitivity analysis.

Establishing hourly heat and electricity prices

Hourly heat prices for 2013 and 2014 have been established based on the marginal cost for heat generation in Gothenburg. They are presented in Figure 2 with the actual prices customers pay today as a reference.

Figure 2 shows that the modelled hourly price, reflecting the marginal cost for heat generation, has a large variation, not only seasonally but also within short periods of time. It is not uncommon that there is a factor of 2–3 in price difference within the same day. It is also shown that the actual consumer price does not reflect the cost in an accurate way. There are many hours where every extra MWh of heat sold is a loss for the DH provider, since the marginal production cost is greater than the actual customer price. It can also be noted that during some hours, the marginal heat production is zero. This is when industrial excess heat is on the margin or when there is an excess of heat in the DH system that needs to be cooled in a river.

Hourly electricity prices for 2013 and 2014 have been established based on the NORDPOOL ELSPT SE3 day-ahead price, electricity tax, and electricity certificate. They are presented in Figure 3 together with the modelled hourly heat price for comparison.

Table 1. Multi-family residential properties in Gothenburg supplied by DH and at least one other heat source. The DH share is the share of DH of the total energy for heating purposes delivery to the building. The average heat load is converted to an average year using the degree day method.

Extra heat source (all properties also have DH)	Number of properties	Average heat load [MWh/year]	DH share [%] (of bought energy for heating)	Average year of construction
<i>Combination of 2 heat sources</i>				
HP (exhaust air)	119	591	87%	1956
EI (air distributed)	16	910	91%	1967
HP (air/water)	7	429	78%	1965
HP (ground source)	6	260	34%	1962
HP (air/air)	4	418	95%	1935
EI (water distributed)	2	2940	97%	1973
Natural gas	1	292	81%	1924
<i>Combination of 3 heat sources</i>				
EI (direct) & HP (exhaust air)	8	617	79%	2010
Firewood & EI (direct)	3	241	99,7%	1934
Natural gas & EI (water distributed)	2	211	89%	1933
Pellet & EI (water distributed)	1	45	44%	1902
EI (water distributed) & HP (air/air)	1	432	83%	1916

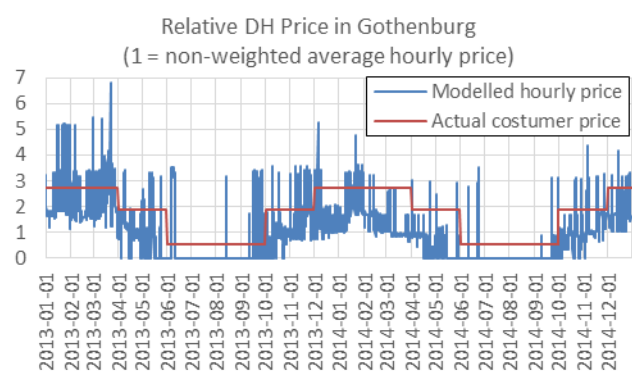


Figure 2. Modelled hourly heat price and actual consumer heat price in Gothenburg 2013–2014, excluding VAT.

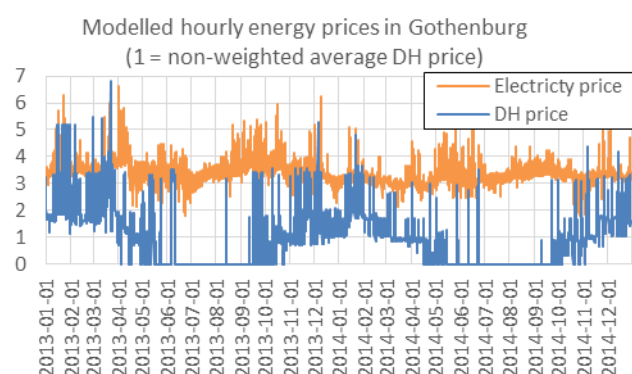


Figure 3. Modelled electricity and heat price in Gothenburg 2013–2014, excluding VAT.

It is clear from Figure 3 that the variation in heat price is greater than the variation in the electrical price. The heat price has a strong seasonal variation that is not present in the electrical price. There are a few hours when the heat price is higher than the electrical price.

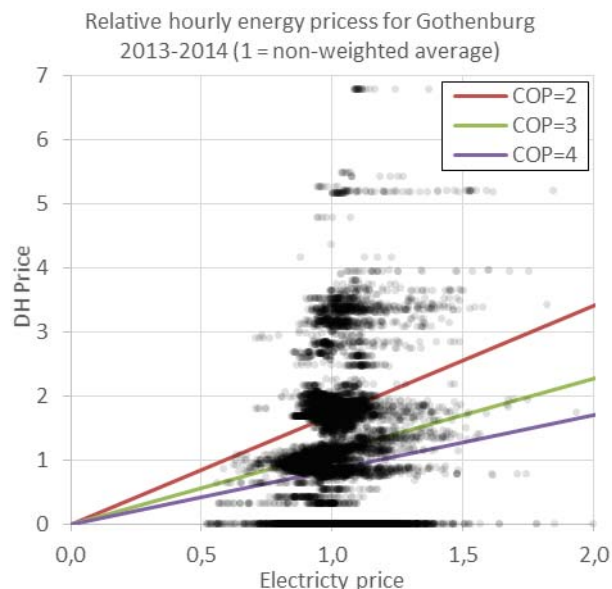


Figure 4. Scatter plot for modelled electricity and heat price in Gothenburg 2013–2014, excluding VAT. The lines represent the break-even point between heating a building with DH and HP with specified COP.

During these hours, it would even be beneficial to produce heat with electrical heaters in the DH network. These hours are very few today, but in a future with much intermittent renewable electricity generation, they may become more common. It should also be noted that electricity prices were at a historically low level during 2013–2014 (and were even lower during 2015), due to a number of circumstances on the Swedish electricity market such as e.g. increased efficiency on the consumption side and a recent expansion of wind power. Forecasts of future electricity prices are highly dependent on the rate of decommissioning of nuclear power.

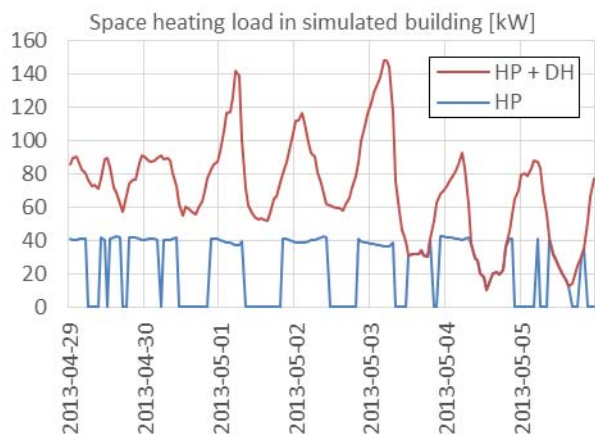


Figure 5. Operation of the base case heating system with shifting load priority during one spring week (warm days and cold nights).

To make a fair comparison of energy prices for a building with HP and DH, the electrical price would have to be divided by the COP of the HP. It is also of great interest to study the price variations in the short term to see whether daily price peaks occur at the same time for heat and electricity or whether there is little correlation. For these purposes, a scatter plot of all data points from 2013 and 2014 was established. The result is shown in Figure 4.

Figure 4 shows that there is very little correlation between electricity and heat prices. Further, 61% of the points in Figure 4 is below the COP=3 line. This means that the cost for DH is lower than the cost for heat from an HP with COP=3 during 61% of the hours in 2013–2014. For an HP with COP=2 and COP=4, DH is cheaper than the heat from the HP for 76% and 46% of those hours, respectively. Many of the points are quite far away from COP lines, indicating that during these hours, one of the heat sources is significantly cheaper than the other. This result shows that having double heating systems in a building can be very beneficial for the building owner and that both the electricity system and the DH system would benefit from more interaction. However, COP values are constantly shifting depending on the temperatures in the system, and the points are not equally valuable, since the heat load is shifting in the buildings. Therefore, a more detailed analysis is required and is covered in the next section.

Simulation and optimization

In this section, the hourly prices established earlier are applied to a building with both DH and exhaust air HP for space heating. The heat cost for the building is analyzed for several cases. It should be stressed that this is not an economic comparison between DH and HP as heating alternatives, since neither installation

costs nor maintenance costs or other economic factors are taken into account.

The space heating demand in the simulated building is based on measurements from 2013–2014 in a residential building in Västra Gårdsten, Gothenburg. The building is typical for the time period when a large part of the buildings with DH and exhaust air HP are from. It is a three-story building with a structural core of concrete and only tenancy apartments.

The simulations are run in two modes: HP prioritized and shifting priority. HP prioritized should represent how the systems installed today operate, where the HP always delivers as much heat as it is capable of, and DH fills the remaining demand when the heat output if the HP does not meet the total demand. Shifting priority means that the cheapest heat source has load priority each hour. When the DH price is lower than the electricity price divided by COP for the present hour, DH is prioritized, and the HP is turned off. The size of the HP is chosen so that when it is prioritized, it covers 39% of the yearly space heating demand like the average building in the survey of residential buildings with several heat sources. This corresponds to an HP that can cover 9.9% of the heat load that occurs at the design outdoor temperature (DOT) of -16 °C. Results from the simulation are presented in Table 2.

From Table 2, we can see that the change from prioritizing HP to having a shifting priority in heat sources has a big impact on how the system operates. The share of DH increases from 61% to 75%, and the average DH price drops by 14%. This is a consequence of turning the HP off during the summer and in daytime in spring/autumn when the DH price is very low. However, the total savings are only 3.2%; this may seem small, but it should be noted that there is no material investment necessary—only a change in the control logic. It can also be noted that the savings for installing an HP at all when provided with hourly prices is only 6.5% (9.5% with shifting priority), which is associated with a significant investment. These investments are probably more beneficial for building owners that pay the actual consumer prices for DH today, since they do not benefit from the periodically very low hourly DH prices. How the system operates during a typical spring week is shown in Figure 5.

From Figure 5, we can see that the HP is often turned on during the nights and off during the days. This is a consequence of the DH price usually being high when the load in the DH system is high (cold nights) and low when the load in the DH system is low (warm days). The decrease in SPF from 3.2 to 3.0 occurs because the HP is turned off for many of the hours when the COP is high. It is still economical to do so, since these hours often coincide with very low (or even zero) DH prices. This correlation is further shown in Figure 6.

Table 2. Results from the base simulation case and a reference case with only DH and no HP in the building.

Case	Prioritized heat source	HP share at DOT -16 °C	DH yearly share	SPF	DH price average [SEK/MWh]	El. price average [SEK/MWh]	Total heating cost [kSEK]
Only DH (ref)	-	-	-	-	328	-	400
Base	HP	9.9%	61.0%	3.2	375	642	374
	Shifting		75.0%	3.0	324 (-14.0%)	642 (±0.0%)	362 (-3.2%)

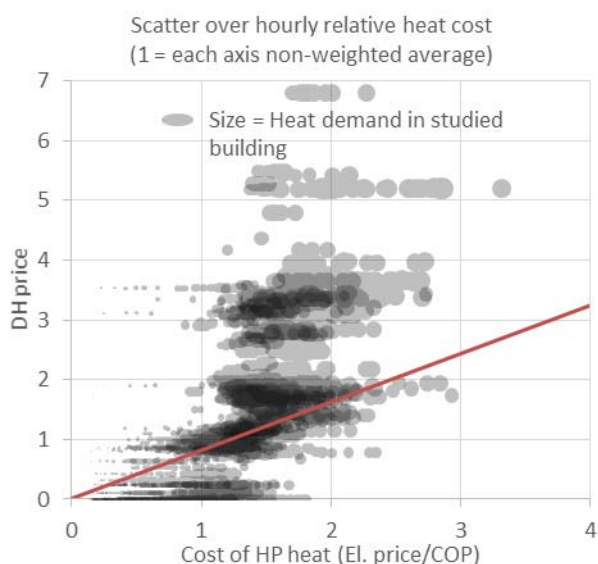


Figure 6. Comparison of heat cost from the two heat sources where the COP of the HP is considered every hour, 2013–2014. Points below the line indicate that heat from DH is cheaper than heat from the HP.

If we compare Figure 4 to Figure 6, we can see that the data is “tilted clockwise” in Figure 6. This indicates that there is a correlation between COP and the DH price. This pushes many of the points closer to the line of equal cost, reducing the incentives for load shifting.

The incentives for heat source shifting could be much more prominent in markets with a more volatile and/or higher electrical price and in systems with less variation in COP (e.g., ground-coupled HP).

Since there are a number of uncertain parameters and parameters that can have a high impact, a sensitivity analysis is carried out. The results of the analysis are shown in Table 3. It is, not very surprising, shown that a lower ventilation flow rate increases the total energy cost in the system but also reduces the incentive for load shifting (from 3.2% savings to 2.5% savings). This is because there is less load to be shifted, since the HP covers a smaller share of the total load when it is prioritized. However, having a newer HP with a higher COP decreases the total energy cost and also reduces the incentive for heat source shifting (from 3.2% savings to 2.1% savings), even though there is more load available to be shifted. This is because the cost of the heat from the HP is further reduced during the hours when the DH price is very low. The temperatures of the radiator system also have an impact on the incentive for heat source shifting. Higher radiator temperatures (70 °C at DOT) increase the savings for heat source shifting to 3.6%, and lower radiator temperatures (50 °C at DOT) decrease the savings for heat source shifting to 2.9%. However, all cases significantly reduce the average DH price (between 9.0% and 14.6%) when shifting load priority is applied.

Table 3. Results from the sensitivity analysis.

Case	Prioritized heat source	HP share at DOT -16 °C	DH yearly share	SPF	DH price average [SEK/MWh]	El. price average [SEK/MWh]	Total heating cost [kSEK]
Base	HP	9.9%	61.0%	3.2	375	642	374
	Shifting		75.0%	3.0	324 (-13.6%)	642 (+0.1%)	362 (-3.2%)
Vent. flow 0.20 L/m2s	HP	9.1%	73.2%	3.0	353	645	385
	Shifting		84.1%	2.8	321 (-9.0%)	648 (+0.5%)	375 (-2.5%)
COP=45% of Carnot COP	HP	11.9%	60.2%	3.9	371	644	352
	Shifting		68.0%	3.7	333 (-10.2%)	644 (±0%)	344 (-2.1%)
Rad. temp. 70°C at DOT	HP	8.8%	62.4%	3.1	375	642	381
	Shifting		79.3%	2.8	320 (-14.6%)	646 (+0.7%)	368 (-3.6%)
Rad. temp. 50°C at DOT	HP	11.3%	59.8%	3.4	375	642	366
	Shifting		70.9%	3.2	328 (-12.4%)	641 (-0.2%)	355 (-2.9%)

CONCLUSION

About 4% of all multi-family residential properties in the DH network in Gothenburg have at least one other heat source. By far the most common combination (present in 2.6% of the properties in Gothenburg and 2.2% of the properties in Sweden) is DH combined with exhaust air HP. On average, HP covers 39% of the yearly heat load for space heating and is not used for domestic hot water.

If heat and electricity prices were hourly and were based on the marginal cost of heat/electricity generation, the heat price would have a much greater variation than the electricity price. This is especially true for the seasonal variation but also for the daily variation. There is very little correlation between the established hourly heat and hourly electricity prices.

An average multi-family residential building with the most common size of exhaust air HP and DH would save 3.2% of the heating cost by utilizing the cheapest heat source each hour compared to always using the HP for base load. This would increase the share of DH for space heating in the building from 61% to 75% and reduce the average DH price by 13.6%. These savings can be achieved if the building is provided with hourly heat and electricity prices (or is controlled as if it were). The investment needed to achieve these savings is to update the control system with simple logic criteria.

What limits the savings from heat source shifting is that the costs of the output heat from both systems are often low at the same time. This occurs even though there is low correlation between the DH price and the electricity price, since there is a stronger correlation between DH price and HP COP.

Suggestions for future work include studying other types of installations and building types such as ground source HP and commercial buildings. Future scenarios for heat and electricity prices are also of interest, especially since electricity prices were historically low during this study. Practical tests are also planned.

ACKNOWLEDGEMENTS

This work was financially supported by Göteborg Energi AB (Gothenburg Energy). Thanks to Tim Johansson and Mikael Mangold for providing data from the database covering Energy Performance Certificates for Swedish residential properties.

REFERENCES

- [1] IEA. Energy Balance Sweden 2012. (2012) Available from: <http://www.iea.org/Sankey>
- [2] F. Oldewurtel et al., "Use of model predictive control and weather forecasts for energy efficient building climate control," *Energy and Buildings* (2012), Vol. 45, pp. 15–27.

- [3] S. Frederiksen and S. Werner, *District Heating and Cooling* (2013). Lund, Sweden: Studentlitteratur AB.
- [4] C. Johansson, F. Wernstedt and P. Davidson, "Deployment of Agent Based Load Control in District Heating Systems," in *First Agent Technology for Energy Systems Workshop, Ninth International Conference on Autonomous Agents and Multiagent Systems*. 2010: Toronto, Canada.
- [5] B. Rydén et al., "Fjärrvärmens affärsmodeller" (Business models of district heating), in *Fjärrsyn, Svensk Fjärrvärme AB* (2013).
- [6] J. Kensby, A. Trüschel and J.O. Dalenbäck, "Potential of residential buildings as thermal energy storage in district heating systems - Results from a pilot test," *Applied Energy* (2015), Vol. 137, pp. 773–781.
- [7] J. Kensby, A. Trüschel and J.O. Dalenbäck, "Utilizing Buildings as Short-Term Thermal Energy Storage," in *14th Int. Symp. District Heating and Cooling* (2014), Stockholm, Sweden.
- [8] J. Kensby, "Buildings as thermal energy storage – Pilot test and large-scale implementation for district heating systems," in *Department of Civil and Environmental Engineering. Chalmers University of Technology: Gothenburg*.
- [9] M. Mangold, M. Österbring and H. Wallbaum, "Handling data uncertainties when using Swedish energy performance certificate data to describe energy usage in the building stock," *Energy and Buildings* (2015), Vol. 102, pp. 328–336.
- [10] T. Johansson et al., "Energy performance certificates and 3-dimensional city models as a means to reach national targets – A case study of the city of Kiruna," *Energy Conversion and Management* (2016), Vol. 116, pp. 42–57.
- [11] NORDPOOL (2016) Available from: <http://www.nordpoolspot.com>
- [12] A. Kärkkäinen, Gasfri påfyllning av värme- och kylsystem samt injustering av radiatorsystem, in *Fakulteten för ingenjörsvetenskap och arkitektur* (2010), Aalto University: Espoo.
- [13] Boverket, Teknisk status i den svenska bebyggelsen – resultat från projektet BETSI (2010).
- [14] M. Maivel and J. Kurnitski, "Heating system return temperature effect on heat pump performance," *Energy and Buildings* (2015), Vol. 94, pp. 71–79.
- [15] O. Ottoson et al., Nästa generations fjärrvärme (Next generation district heating), in *Fjärrsyn, Svensk Fjärrvärme AB* (2013).

PRACTICAL AND ACCURATE MEASUREMENT OF COGENERATED POWER

A. Verbruggen¹

¹ University of Antwerp

Keywords: extraction-condensing steam turbine, quantify cogenerated electricity, power-to-heat ratio, production possibility set, incentive regulation

ABSTRACT

The performance of CHP activity is measured by the amount of cogenerated electricity (E_{CHP}) during a considered period. It is the proper yardstick because it combines attributes of quality (power-to-heat ratio σ) with those of quantity (recovered heat Q_{CHP}), given that $E_{CHP} = \sigma \times Q_{CHP}$ is a commonly accepted identity. In practical applications of the formula, problems arise in finding the appropriate numerical values of power-to-heat ratios. The EU Commission, expert groups, and published literature expose circular logics, concealed by flawed approximations. The enigma is most relevant for extraction-condensing steam turbines, which mix cold condensing with one or more cogeneration activities, making the power flow E_{CHP} not directly observable.

This paper presents a generic and neat solution to the E_{CHP} measurement problem. It starts with a clear problem statement. Then, the components of the solution are exposed. First, in a Mollier diagram the unit mass flow expansion path of a Rankine steam cycle with backpressure heat extraction(s) ahead of the cold condenser is noted. Second, the characteristic points on the expansion path provide the contours of the (Electricity E – Heat Q) production possibility set of the steam power plant. Third, the real capacities of the steam flows of the power plant are mapped on the possibility set expressed in electricity and heat capacity (Watt). It shows how limits on extracted steam flows truncate a significant part of the theoretical possibility set in an extraction-condensing turbine. By merging the extraction capacities with design characteristics of a plant, the accurate measurement of cogenerated power becomes self-evident. The method is documented with numerical cases.

Applying the presented, transparent and accurate, method is prerequisite for regulations being effective in promoting optimal CHP plant investments and operations. Promotional support may imply subsidies for energy efficiency, priority ranking of generated power in merit orderings of integrated power systems, among others.

INTRODUCTION

Combined Heat & Power (CHP) plants are one of the major heat sources in District Heating (DH) systems. In 2014, 61.1% of Danish thermal electricity production was produced simultaneously with heating, and 68.9%

of district heating was produced with electricity [1]. Large-scale DH networks often source the major share of the distributed heat from large steam power plants, designed as extraction-condensing Rankine cycles. This type of plants likely delivers the major part of globally cogenerated electricity. The word 'likely' in the preceding sentence is necessary because there is no agreement about a standard method for measuring the quantity of cogenerated electricity in plants where cogeneration and condensing activities occur simultaneously. At the plant's alternator but one current is sent out and metered by the plant operator. The metered quantity is the sum of two electricity flow components: cogenerated plus condensing power. Splitting the metered flow requires a computational method. The purpose of this paper is to illustrate a generic, proper and accurate splitting method [2]. The method is rooted in basic engineering thermodynamics [3], and the description is documented with a numerical example to emphasize the accuracy and the practicality of the approach.

In common language we speak about CHP plants when they deliver power and heat for end-uses. However, it is more accurate to specify that CHP is an activity occurring in a thermal power generation plant [4]. The activity may be added on (with no power output loss) or embedded in (with some loss of power output) the thermal power generation process. The plant may be equipped with one, or with more than one, opportunity to perform CHP activity. The CHP activities recover all or part of the point-source heat exhausts of the thermal conversion process. In this way, CHP also mitigates local thermal pollution, in addition to improving the overall efficiency in converting primary energy. Such advantages are the basis for public authorities eventually supporting CHP. Support systems function best when they apply effective and fair regulations, providing incentives to CHP actors to optimize performance and results [5-6].

The novelty of this paper is the combination of straightforward technical know-how (thermodynamic cycles) with concepts of economic analysis (production possibility sets), to develop a generic and accurate method solving the long-standing issue of splitting electricity flows metered in CHP plants. The method is applicable for all cogeneration technologies, and is fully transparent and manageable by regulators. It dissolves the present confusion forthcoming from differing

practices adopted in various regions. For example, the European Union has formulated an approach in a Directive of 2004 [7], reconfirmed in 2012 [8].

BACKGROUND

The central indicator of performance of a CHP activity is the amount of cogenerated electricity (E_{CHP}) during a considered period. The amount of cogenerated electricity is linked to the amount of recovered heat (Q_{CHP}) from the thermal conversion process, by the equation $E_{CHP} = \sigma \times Q_{CHP}$, where σ is called the “power-to-heat ratio”. Because Q_{CHP} is readily measured, for obtaining E_{CHP} , the crucial unknown is σ , representing also the quality of the particular CHP activity recovering the measured Q_{CHP} .

Although the basic merit of CHP is its ability to recover otherwise rejected and wasted heat, one should avoid measuring the performance of a CHP activity by the sole variable of recovered heat Q_{CHP} . Maximizing only Q_{CHP} entails perverse effects because efforts to raise the power-to-heat ratio, i.e. the thermodynamic quality of the process, are not stimulated. There is a broad consensus that CHP activity should be gauged by the quantity of cogenerated electricity E_{CHP} [9, 10]. This yardstick combines performance in quality (power-to-heat ratio) with performance in quantity (recovered heat).

The task to fulfil is straightforward: find the quantity E_{CHP} for a considered period (for example, one year). In practice, fulfilling the task is simple in some cases, but intricate and confusing in other cases. The simple cases are cogeneration plants without facilities to reject heat to the ambient environment, such as backpressure steam turbines not owning a cold condenser, or a gas turbine with flue gas heat exhaust coupled to a heat recovery boiler without a bypass to directly reject part of the flue gases to the ambient environment. In this case all electricity from the plant is cogenerated electricity. It is not necessary to know the power to heat ratio σ ; on the contrary, the value of σ may be derived by dividing the quantity of electricity generated in the plant by the quantity of heat recovered during the same period.

The real challenge is to assess E_{CHP} when cogeneration and condensing power generation occurs simultaneously in a thermal power plant. As exemplary case an extraction-condensing steam cycle is selected. For clarity the following assumptions are made:

- 1000 MJ/s (MW) maximum fuel input, with 8% non-recoverable losses (stack flue gas, diverse heat radiation, etc.)
- Full load cold condensing generates 442 MW electricity, with 478 MW rejected condenser heat

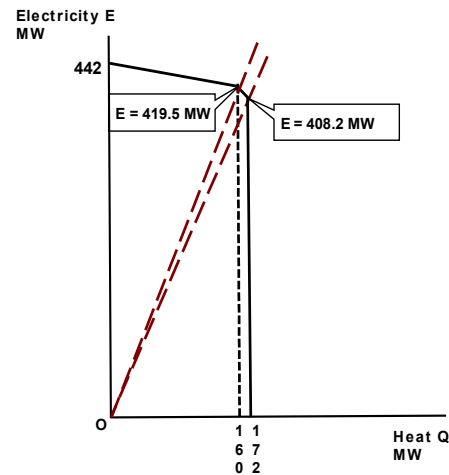


Figure 1. Electricity-Heat Production Possibilities of Extraction-Condensing Steam Cycle with two hot condensers ahead of the cold condenser

- Large heat extraction is feasible at two points in the low-pressure turbine: 160 MJ/s at 100°C or 172 MJ/s at 200°C, reducing the electricity supplies to respectively 419.5 MW and 408.2 MW at full load plant operation

All the above numbers belong to the standard metered variables at a managed power plant. They help in drawing the electricity-heat (E-Q) production possibilities set of the plant, shown in figure 1.

In an (E-Q) quadrant the electricity and heat capacities at full load make up the efficiency frontier(s) of the production possibilities set(s). The ordinate point at 442 MW shows the cold condensing electricity output, without any heat recovery. Heat can be recovered up to the maximum flow at the hot condensers. When the heat capacity flow is entirely extracted at 100°C it delivers 160 MW heat and 419.5 MW electricity, respectively at 200°C useful heat increases to 172 MW and electricity decreases to 408.2 MW. The numbers of the metered electric output are the sum of E_{CHP} plus E_{Cond} , not discernable without a division rule like $E_{CHP} = \sigma \times Q_{CHP}$. Figure 1 contains the relevant Q_{CHP} values, but not the relevant power to heat ratios. Obviously wrong is the use of the slopes of the rays through point O shown in figure 1 as values for the unknown σ . It is necessary to develop an appropriate computational method to find the right σ values.

In the professional and academic literature [9, 11-13] no consistent method has been provided. The flaws have been highlighted in [10] and [2], with the latter publication also offering the arguments and theoretical development of an appropriate computational method, although only explained for the extraction-condensing cycle.

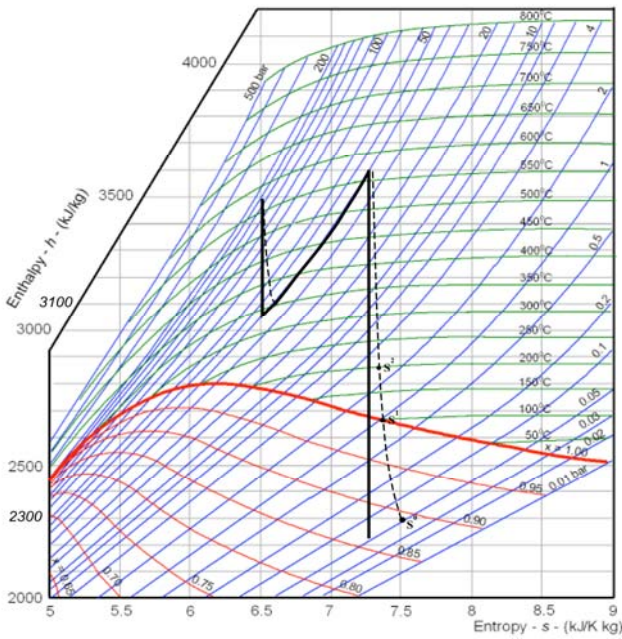


Figure 2. Rankine extraction-condensing steam cycle. Isentropic and actual steam expansion with reheat, hot condensers (S^1 , S^2) and cold condenser S^0

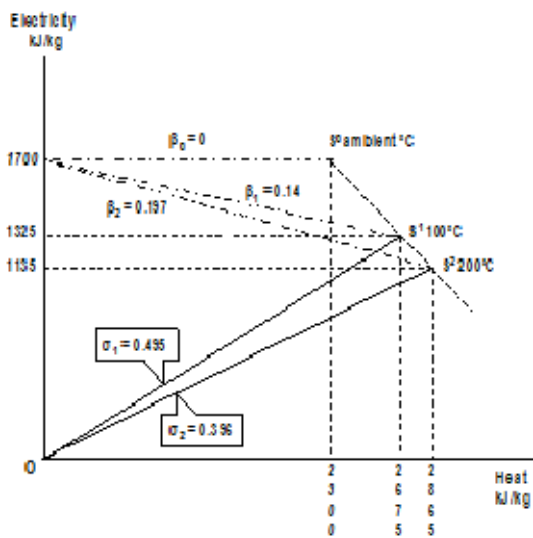


Figure 3. Electricity-Heat Production Possibilities of a Unit Mass for the Steam Expansion with three Major Exhaust Points as shown in figure 2

The focus of this publication is on highlighting the practicability of the method. It also shows the generic validity of the method by illustrating its extension to gas turbines with CHP activity (internal combustion engines or fuel cells are not discussed here, but generalizing the assessment method is feasible by collecting information about the equipment and by applying the constituent calculations).

RESULTS

When CHP activity is embedded in a Rankine cycle, one or two (more is feasible but unusual) hot condensers are installed in the low-pressure part of the steam expansion path. Isentropic (vertical line segments) and actual (dashed bending-off curves) expansion path segments are shown in figure 2: the left segments refer to the high-pressure turbine, followed by a reheating at constant 40-bar pressure, and then the expansion in the low-pressure turbine to a near-vacuum pressure of 0.06 bar (point S^0).

Two hot water condensers are installed to extract steam at respectively S^1 and S^2 . The enthalpy values of the start and of the end points of the actual expansion segments characterize the power cycle and the CHP activities embedded in it.

The steam expansion enthalpy data of figure 2 allow to picture the paths followed by a unit mass. The (E-Q) production possibilities of the unit mass are shown in figure 3. The horizontal top line ending in point S^0 represents the cold condensing state ($\beta = 0$ i.e., there is no power loss due to steam extraction). Variable temperature/pressure conditions of ambient air/water cause slight shifts in the height of the horizontal line ending in point S^0 , i.e. power loss factors change when steam is extracted. The slight shifts and changes are an argument for avoiding the use of power loss factor information in the method for assessing the quantity of cogenerated power E_{CHP} . When steam flow is extracted at pressure conditions higher than at S^0 , substitution of heat for power occurs, in principle at the rate of a kJ/kg electricity given up for one additional kJ/kg heat used. In the first step all condensing heat is recovered. When this step can be kept very short (assume S^1 just above S^0 in Figure 2, which means that the energy is at a temperature slightly above the ambient temperature), the gain in useful heat is significant because it is predominantly latent condensing heat and the loss in power is small. After recovering the latent condensing heat, only a one-to-one substitution of sensible heat remains feasible. Therefore the slope of the S points line equals -1. Two cogeneration activities are embedded in the shown Rankine steam cycle, and described by the points S^1 and S^2 .

In drawing Figure 3, the states like S^1 and S^2 are examined following the path of one kg mass fluid. In reality, a turbine in full (nominal) load processes tens to hundreds of kg/s of fluid, depending on the plant capacity. The fluid leaves the low-pressure steam turbine mainly via the exits at S^0 , S^1 and S^2 . A steam turbine has some minor steam outlets for preheating water flows and for purging. CEN/CENELEC [9] discusses the minor outlets in detail.

The method presented does not require too detailed, difficult to monitor calculations. The method is generic and encompasses all steam turbines with cogeneration activity and also other thermal power processes with CHP activity (see the example of a gas turbine further down in this section). Limiting the analysis to the major cold and hot condensers keeps the approach feasible and controllable.

In an extraction-condensing turbine, the cold condenser at S^0 can pass all the fluid at full load of the plant and requires a minimum flow during operation of the turbine. The flow over the hot condensers is physically limited and the maximum flow is designed for given maximum deliveries of useful heat. It follows that in practice the points S^1 and S^2 are virtual points, not observable by monitoring actual total flows [9]. But the observations are not necessary because one only needs the computational results with the help of σ values (σ_1 and σ_2). The merger of figures 1 and 3 is shown in figure 4. It shows graphically how the quantity of cogenerated power E_{CHP} is assessed contingent on the quantity of recovered heat Q_{CHP} .

Table 1. Numerical results of the performance during a year of an extraction-condensing steam plant with two CHP activities embedded

E-CHP calculator				
Design (tombstone) properties per major steam exhaust				
	Cold condensing S^0	Hot low back pressure S^1	Hot high back pressure S^2	
Work E kJ/kg (fig. 2)	1700	1325	1135	
Heat Q kJ/kg (fig. 2)	2300	2675	2865	
Power to heat σ (fig. 3)	0,739	0,495	0,396	
Steam flow rates kg/s	260	60	60	
Electric capacity CHP MW (fig.4)	0	79,5	68,1	
Electric capacity Condensing MW (fig.4)	442	340	340	
Electric capacity total MW (fig.4)	442	419,5	408,1	
Heat recovery capacity MW (fig.4)	0	160,5	171,9	
Operational data				
Recovered Heat GWh/y (metered)	0,0	503,0	237,6	Totals 740,6
Plant electric output GWh/y (metered)	747,9	1314,7	564,0	2626,6
CHP electric output GWh/y assessed	0,0	249,1	94,1	343,3
Condensing electric output GWh/y	747,9	1065,6	469,9	2283,3
Full load hours per exit S	1692	3134	1382	6208

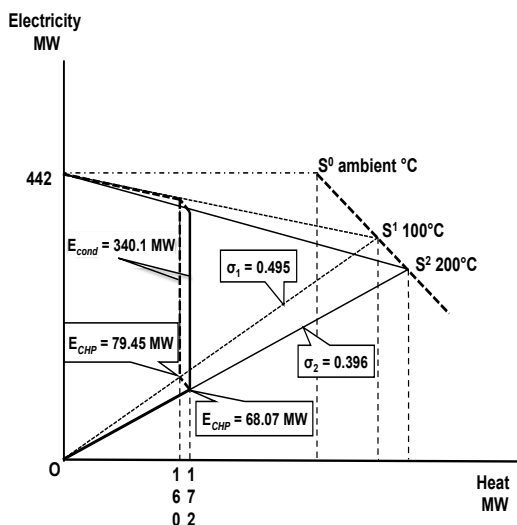


Figure 4. Electricity-Heat Production Capacities (figure 1) merged with the Roster of figure 3

The numbers in figure 4 focus on the borderlines of the production possibility sets. The method is robust for part load heat recovery operation. When yearly numbers of power plant production are reported, one often adds capacity factors or full load hours to better inform readers. Table 1 illustrates the method further with a numerical example of an E_{CHP} calculator, based on the properties of the exemplary plant as shown in figures 1 to 4.

Table 1 is composed of two parts. The top part holds the design (tombstone) parameters for describing the actual layout and capacities of power generation and heat recovery. This information is inventoried at the moment of plant commissioning or of major retrofit, and remains valid for long periods (the lifetime of the plant). The second part holds operational data and is regularly updated depending on the reporting intervals (monthly, yearly). First two rows are metered plant data on recovered heat (separately per CHP activity) and generated electricity. The numbers on the following three rows are assessed and derived from combining tombstone parameters and metered flows.

For the development and illustration of the method, the extraction-condensing cycle with two hot condensers has been employed as the reference. Not only is this an important case of cogeneration, it has proven to be the most challenging case for identifying and measuring the quantity of cogenerated electricity. Especially in the European Union, the EU Commission failed in providing a scientifically robust approach when publishing the related Directive in 2004 and 2012 [7, 8]. CEN/CENELEC neither knew how to avoid the pitfall of a circular referencing [9, 10].

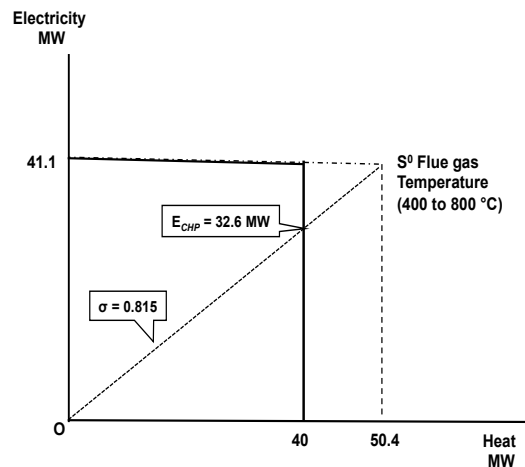


Figure 5. Electricity-Heat Possibility Set of an Open Gas Turbine with Flue Gas Heat Recovery

The method is not only valid for steam turbines, but also applicable on other cogeneration plants. This is shown for the open gas turbine with flue gas heat recovery in an added steam boiler. Because the temperature of the flue gases is in a range of 400 to 800°C, there is no power loss when their energy content is recovered. There is also but one exhaust of the heat, i.e., one CHP activity and one design power to heat ratio. The (E-Q) possibility diagram, similar to the one in figure 4, becomes very simple, as shown in figure 5.

Mostly all heat of a gas turbine equipped with a recovery boiler will be fully used. Then E_{CHP} is equal to all the electricity production of the turbine.

When the heat is not fully used, some share (for example about 20% in figure 5) is rejected to the environment. The amount of cogenerated power is calculated with the quantity of recovered heat (40 MW), multiplied by the design power to heat ratio σ (being 0.815 in figure 5), or $E_{CHP} = 32.6$ MW.

The logic applied is the same as with steam turbines. The logic is generic for all cogeneration activities, allowing the addition of the assessed E_{CHP} quantities.

CONCLUSION

The contribution builds on established know-how in thermodynamics and economics. The novelty of the presentation is the combination of solid know-how and concepts, for addressing and solving a long-standing issue in the management and regulation of CHP activities. The issue is the correct identification and accurate measurement of the quantities of cogenerated electricity E_{CHP} for the various CHP processes. The issue is of high relevance because E_{CHP} is the crucial, necessary and sufficient, indicator of CHP's merit in the energy economy. For whatever purpose (science, policy, operations, statistics) a CHP process is considered, the issue one is dealing with, i.e. the cogenerated power flows E_{CHP} , should be identified precisely and quantified accurately. Once E_{CHP} is accurately assessed, it is a sufficient indicator of qualitative and quantitative performance (and of CHP merit). E_{CHP} includes the design power to heat ratio σ of the CHP activity (the proper yardstick of thermodynamic quality) and the quantitative count of recovered heat Q_{CHP} at the thermal power process. Obviously, the prerequisite for E_{CHP} to assume the central role is the reliable measurement of its value.

The method for reliable measurement is explained and illustrated with graphs and practical examples. The method dissolves the fuss about E_{CHP} identification and measurement. It owns several valued attributes:

- Transparent by identifying CHP activities added-on or embedded in thermal power processes
- Accurate by clear definition and quantification of design power to heat ratios σ
- Generic, applicable on all CHP activities in all kinds of thermal power conversions
- Easy and cheap to apply in practice

Energy administrators and regulators can enact specific incentive regulations. Investors and operators can focus on the essential parameter σ and flows Q_{CHP} . The method supports good policies. When certified and widely adopted, it will establish a common practice with results that are comparable. As a corollary, consistent statistical data are obtained about the performance of all types of thermal power plants with cogeneration activities. Reliable E_{CHP} data are needed for effective, efficient and fair support mechanisms for CHP activities (if public authorities decide to favour CHP). This would relieve the sector from arbitrary, biased and perverse regulations, as the EU Directives on CHP entail.

REFERENCES

- [1] Danish Energy Agency (2016). Energy Statistics 2014. Available at <http://www.ens.dk>
- [2] A.Verbruggen, J.J. Klemes, M.A. Rosen (2016), "Assessing Cogeneration Activity in Extraction-Condensing Steam Turbines: Dissolving the Issues by Applied Thermodynamics", in J. of Energy Resources Technology, ASME, doi: 10.1115/1.4033424
- [3] W. Reynolds, H. Perkins, Engineering Thermodynamics, McGrawHill, New York (1977)
- [4] A. Verbruggen, P. Dewallef, S. Quoilin (2013), "Unveiling the mystery of Combined Heat & Power (cogeneration)", in Energy, Vol. 61, pp. 575-582
- [5] RAP The Regulatory Assistance Project (2011), "Electricity Regulation in the U.S.: A Guide" at <http://www.raponline.org>
- [6] UK Department for Business Innovation & Skills (2011), "Principles for economic regulation", at <http://www.bis.gov.uk>
- [7] European Union (2004), Directive 2004/8/EC of the European Parliament and of the Council of 11 February 2004 on the promotion of cogeneration based on a useful heat demand in the internal energy market and amending Directive 92/42/EEC. *Official Journal of the European Union* 21.2.2004
- [8] European Union (2012), Directive 2012/27/EU of the European Parliament and of the Council of 25 October 2012 on energy efficiency, amending Directives 2009/125/EC and 2010/30/EU and

- repealing Directives 2004/8/EC and 2006/32/EC. *Official Journal of the European Union* 14.11.2012
- [9] CEN/CENELEC (2004). Workshop Agreement. Manual for Determination of Combined Heat and Power (CHP). CWA 45547. Brussels
- [10] A. Verbruggen (2008), "The merit of cogeneration: measuring and rewarding performance", in *Energy Policy*, Vol. 36, pp. 3069-3076
- [11] C. Frangopoulos (2012), "A method to determine the power to heat ratio, the cogenerated electricity and the primary energy savings of cogeneration systems after the European Directive", in *Energy*, Vol.45, pp.52-61
- [12] D. Urošević, D. Gvozdenac, V. Grković (2013), "Calculation of the power loss coefficient of steam turbine as a part of the cogeneration plant" in *Energy*, Vol. 59, pp. 642-651
- [13] X. Ye, C. Li (2013), "A novel evaluation of heat-electricity cost allocation in cogenerations based on entropy change method", in *Energy Policy*, Vol. 60, pp. 290-295

TOPIC E:

Policy and Regulation



THE ROLE OF INTERMEDIARIES IN THE TRANSITION TO DISTRICT HEATING

R.E. Bush¹, C.S.E. Bale^{2,3}

¹ Low Carbon Technologies Doctoral Training Centre, School of Chemical and Process Engineering, University of Leeds, Leeds, LS2 9JT, UK

² School of Chemical and Process Engineering, University of Leeds, Leeds, LS2 9JT, UK

³ School of Earth and Environment, University of Leeds, Leeds, LS2 9JT, UK

Keywords: *Intermediaries, Policy, Strategic planning*

ABSTRACT

For those countries, such as the UK, in which district heating and cooling has previously played little role in the energy system, the technology often struggles to break through the numerous and complex barriers to its introduction in the context of liberalised energy markets and competition with incumbent technologies such as natural gas networks. Progress is often slow and best practice is yet to be established.

'Intermediaries' are actors who facilitate knowledge sharing and build actor networks to enable the introduction of new technologies. This paper uses a case study of the UK to explore where and how the activities of these intermediary actors are currently supporting district heating development.

An innovative method called a 'decision theatre' was used to collect empirical evidence from a range of local stakeholders involved in district heating projects. This method, which took place in the format of a group workshop, enables understanding of the interactions between stakeholders through each stage of the district heating development process.

Lessons are drawn from this case study with regard to how intermediary activities can support the development of district heating in areas with little previous history of such systems. Three geographical scales of intermediary activity are identified (local, regional and national) as having different roles in enabling delivery of new district heating projects. Interactions between the three scales and how their roles might change as the sector develops are explored. The paper will highlight implications of the study for policymakers. In particular, a role is identified for intermediaries in creating a supportive institutional and policy environment that can enable development of large-scale, strategic networks.

INTRODUCTION

A realisation about the scale of the challenge of decarbonising the heat sector has brought about an increased interest in the potential of district heating (DH) [1]. Introducing DH in countries where the technology has not previously been used brings with it a set of non-technical challenges including developing

an institutional infrastructure, market and business models that unlock the technology for deployment. In this paper we refer to these countries as 'learning countries'.

Local municipalities often seek to play a role in overcoming these non-technical barriers and enabling delivery of new schemes [2]. However, in the context of a low penetration of existing networks, they can be working with little previous experience or knowledge of what is required. The process of learning and knowledge exchange is therefore important for unlocking DH potential.

This paper will focus on the concept of 'intermediaries'. These are actors that facilitate connections between institutions involved in delivering new innovations to enable exchange of knowledge, development of skills and standards, and development of relationships between actors to support the process of innovation. Gaining an understanding of how intermediary activities are currently taking place, and where they could be improved, is critical for policy makers in learning countries that are looking to strengthen capacity of local actors to deliver DH.

A case study from the UK is used as an example of a DH learning country. It is a country with a highly centralised energy system, a liberalised energy market, and high penetration of natural gas networks for heat supply to buildings. The heat demand currently delivered by DH is only 2% [3]. This paper will analyse data from a decision theatre workshop involving a range of local stakeholders involved in DH development at the local level. It will consider where intermediary activities are taking place; who is delivering the activities; and how they could be developed further to enable successful development of more DH projects in the UK.

THEORETICAL BASIS FOR ANALYSIS

Socio-technical theory forms the theoretical basis for analysis. The theory seeks to recognise the influence of the existing system as new technologies and innovations are introduced. It considers incumbent technologies, institutional and market set ups, policy regimes and social practices [4].

The theory considers technology innovations, such as the process of delivering DH in learning countries, to take place within ‘niches’. ‘Niches’ are used to describe the idea of protected spaces where technological innovations are able to develop and learn before being embedded into the wider regime [5]. Protection within the niche can come in many forms; from financial subsidies or tax breaks, to skills development programmes or transferring of decision-making powers. In practice, technological innovations might happen in multiple niches across a country, and the experiences at each local level can be collected and shared together to contribute to innovation development across the niche as a whole [6, 7].

In this work we are considering the process of DH development in learning countries as taking place in niches. Although DH is a well-established and proven technology in many countries such as Denmark, Sweden and Finland, in ‘learning countries’ such as the UK it requires non-technical innovations to take place to enable its deployment. The term DH niche will be used to describe the delivery of a new DH project in a region of low or no deployment of DH. It could take the form of an extension of an existing scheme, but is most likely to be the delivery of a stand-alone network.

Table 1: Examples of four types of intermediary activities as reviewed by ¹Kivimaa [9] and ²Hargreaves et al [7]

Articulation of values and visions for the future¹	Building of social networks¹
Strategy development Demonstration of technology benefits Acceleration of the application and commercialisation of new technologies	Aligning interests Creation and facilitation of new networks for both learning & project delivery Finding funding sources to support activities.
Learning processes and exploration at multiple dimensions¹	Brokering and coordinating partnerships beyond the niche²
Knowledge gathering, processing & combination Communication and dissemination of knowledge Advice and support	Accreditation and setting of standards Consultation on policies Policy communication and implementation

INTERMEDIARIES

In socio-technical theory intermediaries can be defined as actors that facilitate exchange of knowledge, or use their own expertise to facilitate creation of niches and delivery of technologies. They are actors that span individual niches, networks and learning boundaries and they can undertake work at multiple levels; using their expertise to add value to project delivery within the niche and aggregating and sharing learning between niche spaces of activity [7-9]. Table 1 gives some examples of the types of activities intermediaries undertake. For a more comprehensive list of specific activities observed in studies to date, see Kivimaa [9].

Further to the practical activities that intermediaries undertake to assist in niche creation, Hodson, et al. [10] consider ‘modes’ of intermediary actors and how their scale and capacity can impact on their long-term effectiveness for enabling technology innovations to develop and transition beyond niche activities and become part of the wider regime. Figure 1 shows the two dimensions that Hodson et al [10] use to define the modes of intermediary delivery: (1) the scale and depth at which activities are embedded into institutional practice, either taking place as a stand-alone response or via an activity that is embedded within the long-term functioning of existing organisations; (2) the scale at which the priorities of intermediaries are defined, these could come from the local context of the niche, right through to a top-down national policy directive.

We apply this framework to the case study to consider the intermediary activities taking place to support DH development, and also the modes that these activities are being delivered through.

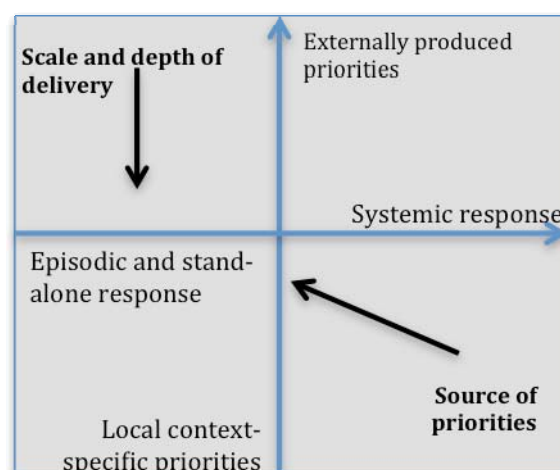


Figure 1: Modes of urban energy intermediation conceptualised by [10]. The x-axis shows the scale and depth of delivery of intermediary activities, and the y-axis shows the scale at which the priorities for intermediary activities are defined.

THE CONTEXT OF DH IN THE UK

The UK is a challenging country for DH deployment with extensive natural gas network coverage in its towns and cities. It has a highly centralised and liberalised energy system with little involvement of local or regional level actors to date [11]. Nevertheless, the publication of the UK Strategic Heat Framework [3] and action plan [12] recognised that DH would play an important role amongst the mix of technologies needed to meet future low carbon heating demand. It also recognised local authorities as having a critical role for enabling DH delivery.

The Heat Network Delivery Unit (HNDU) was formed within the Government's Department for Energy and Climate Change (DECC) in summer 2013 to support local authorities in England and Wales in taking on this new role. It seeks to tackle the issues of "capability and capacity" faced by local authorities by offering guidance, support and funding to commission studies by consultants to feed expertise into local authorities [13]. The existence of HNDU appears to have ramped up the numbers of local authority officers working on DH, but as yet most of these projects have not reached the delivery stage and DH development continues to take place within niche spaces rather than becoming part of the mainstream practice for most municipalities.

RESEARCH QUESTIONS

This work seeks to answer the following research questions:

1. Are intermediary activities taking place within the DH development process in the UK? Which actors are delivering these activities?
2. Where are they adding value to support the development of projects?
3. How could intermediary activity be strengthened for DH niche creation?

DECISION THEATRE METHODOLOGY

Data was collected for this chapter through an adaptation of a decision theatre research process; a method originally developed by Arizona State University that uses data visualisation, modelling and simulation to engage multiple stakeholders in a complex group decision process [14-16]. Use of a decision theatre research process aimed to capture rich and detailed data about the interactions and relationships between stakeholders during the process of decision making – a particularly important aspect in DH development where cooperation between local stakeholders in charge of large heat demand anchor loads and heat supply sources are crucial to enabling the viability of a project. Furthermore, this method is

valuable for the research participants themselves, allowing them to share and learn from each other and to reflect on their own work as they progress through the stages of the workshop [14].

The decision theatre research process was adapted for the purposes of this study to focus less on the use of detailed modelling that was emphasized by previous applications of the method. Instead, a fictional scenario was created and simulated through simple heat maps, qualitative information about key actors in the scenario, and basic information about the outcome of a feasibility study. This adaptation was done to steer conversations about the development process towards the relationships and interactions between various stakeholders rather than on solely technical or financial questions about the viability of a project. Using a fictionalised scenario was important because this enabled participants to draw out issues and concerns, based on their own professional experiences but in ways that did not compromise other professional relationships.

In the scenario presented to the workshop participants, three key 'stages' of a fictional DH development process were presented; namely pre-feasibility, feasibility, and delivery stages, as detailed in Figure 2. The participants were set the task of discussing how they would develop the case study example from the pre-feasibility stage through to delivery. At pre-feasibility stage, participants were presented with an example of an area-wide heat map that indicated heat demand density including a number of specific large heat demand users that might be able to act as key anchor loads for a network, as well as existing CHP plants and other potential heat sources. At the feasibility stage, participants were presented with information about a specific priority project that had been selected for further exploration with a feasibility study. Finally, at the delivery stage, the groups were presented with the information that the given project was technically and financially viable to be delivered, given the involvement of key anchor loads and heat supply sources. Participant discussions were facilitated around the key points listed in Figure 2 to explore different actor's objectives and challenges at different stages of the process, including:

- When and where actors turned to get advice and resources to support project development
- Actors' perceptions of risks,
- Differences in objectives between stakeholders,
- How available information was used to inform decision making,
- The process of stakeholder engagement and relationship building

Mixing research participants provoked vibrant decision-making situations because the different perspectives represented within the group encouraged each participant to vocalise, explain and defend their reasons for deciding to act in a particular way.

Having secured agreement in advance, group conversations and narratives were audio recorded for later analysis. Session conveners queried participant comments during each of the three stages in an effort to reveal some of the underlying decision-making rationales. In this way it was possible to gain an insight into the interests and focus of each participant and align these with their experiences of working in particular kinds of economic, political, and policy contexts. Data was transcribed and analysed for the themes and activities outlined within the analytical framework, defined in Table 1, to identify how and where intermediary activities were taking place throughout the development process stages.

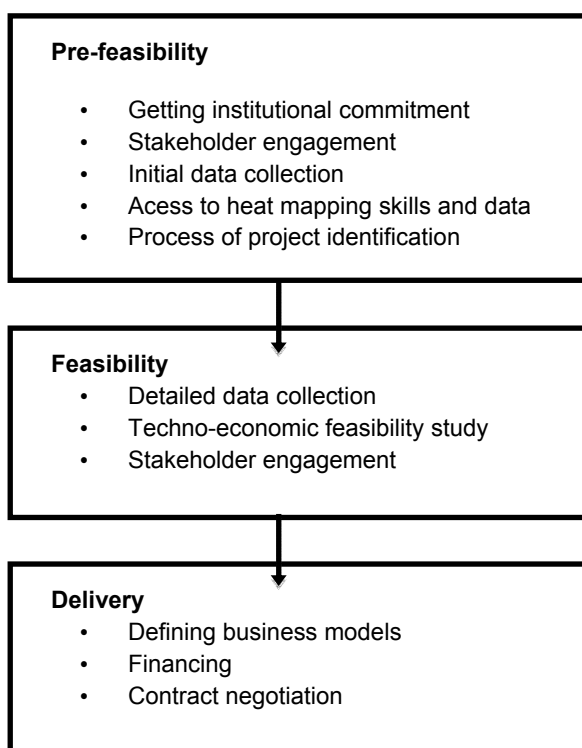


Figure 2: Outline of the three stages of the DH development process considered within the decision theatre workshop. Example activities from each stage are given. Although this diagram suggests a linear process, iterations between each of the activities often take place over time as contexts and stakeholders change.

A range of 10 stakeholders involved in local-level activities for establishing new DH networks within the UK were invited to participate and collaborate in the daylong decision theatre workshop held in Newcastle, UK during October 2014 (8 stakeholders were able to attend on the day). Stakeholder selection was focused on local-level actors to explore the experiences and learning processes of actors during DH delivery, rather than wider policy processes. The workshop was attended by 5 local authority sustainability / energy officers, a university estates energy manager, a representative of a community energy group and a local enterprise partnership representative. None of the participants had successfully completed a DH project but all were actively involved at one of the stages. The workshop was organised so that stakeholders with different kinds of organisational experience and knowledge were grouped together.

While conversations were limited to participants in the workshop, conversations were contextualised within a wider policy framework by ensuring any comments and questions needing to be addressed by national policy stakeholders such as government ministers were captured via sticky notes and pinned to their poster image. This approach allowed the participants to discuss their interactions with actors not represented in the room, and to identify issues and concerns that needed to be addressed at different scales such as through government policy measures.

RESULTS

Analysis of the decision theatre data highlighted the central role of local authorities within delivery of DH niche processes, either undertaking intermediary activities themselves or being supported by the intermediary activities of others. Activities took place at three geographical scales of engagement: locally (primarily delivered by the local authority); regionally (several local authorities working together through a local enterprise partnership); and nationally (via institutions such as trade associations, community group networks, or government programmes). Figure 3 shows examples of the range of local stakeholders involved with DH delivery and the connections where local, regional and national actors were undertaking intermediary activity.

At the local level, the local authority sustainability or energy team performed intermediary activities persuading local stakeholders of the value of DH, and building the social networks required to deliver projects. These activities were directed both externally, facilitating cooperation between local, public and private sector stakeholders, but also internally to develop local authority capacity and get corporate buy

in from across the local authority. As new actors in the energy system, these intermediary activities internally within local authorities were crucial to creating the multi-skilled team of planners, mapping specialists, lawyers, finance specialists and energy managers needed to facilitate strategic DH development. Beyond the local authority, other actors involved in intermediary activities at the local level were community energy groups, who explored opportunities to develop community owned schemes. Private sector DH companies also played an intermediary role, sharing expertise and experience from previous schemes, and offering to deliver and operate commercially attractive schemes.

At the regional level, local enterprise partnerships were sometimes undertaking intermediary activities as well. Their regional scale, joining multiple neighbouring local authorities, enabled employment of a specialist staff member for DH that would not have been possible for individual authorities acting alone. This scale of working also facilitated greater sharing and cooperation between the neighbouring local authorities working on similar challenges.

National level actors undertook intermediary activities between local actors, although none provided comprehensive coverage, or had enough capacity to meet the demands of all of the local actors. Key successes were HNDU, primarily acting as a source of funding to enable English and Welsh local authorities or regional local enterprise partnerships to buy in consultancy expertise, and also as a source of information sharing between local projects. The Core Cities group⁸, the Vanguards Network⁹ and the trade associations (Association of Decentralized Energy (ADE) and the UK District Energy Association (UKDEA)) were also cited as valuable sources of information and best practice sharing.

Evolution of intermediary roles as the niche processes develop

Table 2 gives details of the observed intermediary roles undertaken by the actors at each scale and how these vary throughout the stages of the DH development process. Most of the actors within the decision theatre are currently at stages (1) and (2) of the delivery

process, establishing conditions for successful delivery of an initial project.

This analysis of the DH development process shows the important role that intermediaries can play in delivering niche processes. The multiple scales of activity offer distinct benefits, from close connection to project delivery and alignment of interests at the local level, to sharing knowledge and pooling resource at the regional and national levels. As projects and niches develop, the role of intermediaries also develops and changes to fulfill new functions.

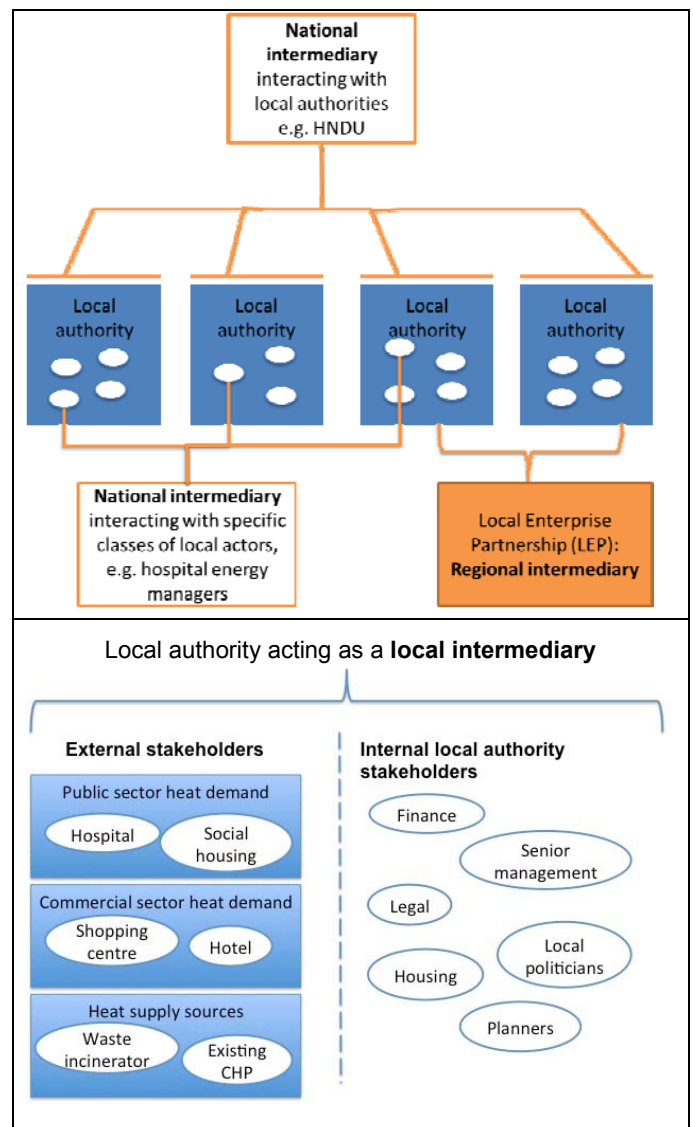


Figure 3: Illustration of the local, regional and national intermediary relationships where engagement and networks currently exist for enabling DH development in the UK. There are two types of national intermediaries represented: (1) that works with local authorities and (2) that works with other specific types of actors such as hospital or university energy managers.

⁸The Core Cities is a network formed to represent the local authorities of England's eight largest city economies outside London along with Glasgow and Cardiff, aiming to enable each city to enhance their economic performance and attractiveness as places to live, work, visit and do business.

⁹The Vanguards Network was set up by the University of Edinburgh as a forum to discuss detailed aspects of DH development for local authorities in the UK at a more advanced stage of the development process.

Table 2: Intermediary activities undertaken at the local authority, regional local enterprise partnership (LEP) and national scale (HNDU and other networks) at each stage of the DH development process.

	Intermediary activity	Who?		Comments
(1) Pre-feasibility	Increasing awareness of DH: In the context of very little existing DH, it is rare that local stakeholders had experience of DH development. Work needed to be carried out to introduce people to the technology, both internally and externally to a local authority. For example, before initial heat mapping could take place internal local authority stakeholders needed to be persuaded that this was a valid use of scarce local authority staff and budget resource.	Local authority	✓	Activities focused both internally with local authority stakeholders such as its senior management team, politicians, and finance managers, as well as externally with local stakeholders who might need to be involved to provide heat supply or large heat demand anchors. For regions where the LEP was taking an active role in facilitating DH, the pooling of resource at this stage enabled work to be undertaken on behalf of local authorities that would not have been able to take place otherwise due to lack of resources.
		LEP (regional)	✓	
		National body		
	Demonstrating the value of DH: The aims and objectives of each local actor for engaging with DH varied between individual stakeholders. Local authorities and LEPs spent time understanding the drivers and benefits sought by each stakeholder and worked to demonstrate the value that DH has to offer to each one using case studies and site visits to existing schemes from within the UK and abroad.	Local authority	✓	
		LEP (regional)	✓	
		National body	✓	
(2) Feasibility	Providing an evidence base for feasibility: This involved gathering detailed data to feed into a feasibility study; obtaining funding for a study to be carried out (primarily through HNDU funding, or alternatively by direct funding from the local authority or LEP); and the local authority or LEP commissioning consultants to undertake the study.	Local authority	✓	The involvement of consultants was important for bringing in more expertise and experience to the process, but actors expressed a worry that some consultants were bidding for work that they did not have expertise to do. HNDU was used to sense-check reports in some of these situations. HNDU played an important role consistently supporting projects right through the development process, as well as connecting and sharing information between local authorities. However, Participants expressed a desire for more opportunities to connect key peer groups, such as university or hospital finance directors or planning officers.
		LEP (regional)	✓	
		National body	✓	
	Overcoming a high perception of risk: Despite the involvement of expert consultants and techno-economic analysis of projects, the appetite to take risks to enable a projects' success was often felt to be low. Case studies were seen an important tool for achieving this. Participants talked of a "responsibility" on successful projects to share more details with others.	Local authority	✓	
		LEP (regional)	✓	
		National body	✓	
(3) Delivery	Use of the public sector estate to reduce risks: Local authorities aimed to offer an anchor load of long-term heat demand through public sector estate to increase certainty around the long-term business case for a scheme. They also considered using public sector-only access to low-interest loans to cover the upfront capital costs of schemes, therefore requiring lower rates of returns than commercial rates would require.	Local authority	✓	Emphasis transferred away from the LEP as a lead intermediary at the deliver stage and their role served more as a source of advice to the local authorities, who necessarily took a leading role for specific stakeholder negotiation, contract agreements and financing decisions. Lack of commercial experience meant that there was a perception of risk associated with taking on full local authority ownership of a scheme. However, the option of a fully private scheme, or partnership with the private sector was also associated with distrust of private sector actors.
		LEP (regional)		
		National body		
	Developing ownership models for schemes was a key point of discussion that lacked a clear vision for many actors. Local authorities were keen to maintain an element of ownership within schemes in the hope of leveraging greater benefits for the area (e.g. maintaining low heat costs for fuel poverty reduction, or generating income through scheme profits).	Local authority	✓	
		LEP (regional)	✓	
		National body	✓	

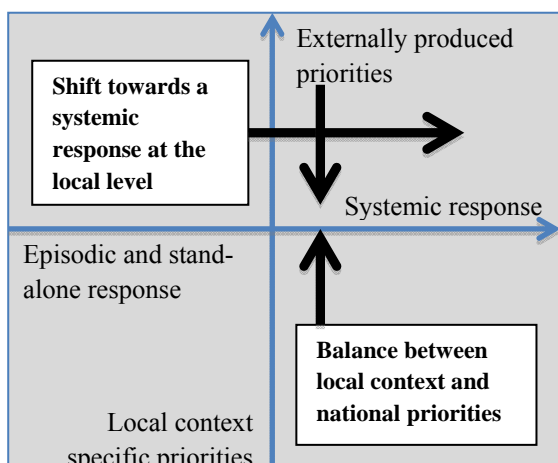


Figure 4: Analysis of the role of intermediaries for diffusion of DH niches into the mainstream energy regime

DISCUSSION

Analysis of this UK case study has shown the extensive role that intermediaries can play in niche creation throughout DH development. The multiple scales of activity offer distinct benefits, from close connection to project delivery at the local level, to sharing knowledge and pooling resource at the regional and national levels. The early stages of DH development for most areas in the UK means that most of the intermediary activities are focused at the first two stages of the development process at present, but over time this would be expected to evolve as DH becomes a more widely known and trusted option amongst local decision makers.

In this section, the two dimensions that define the modes of energy intermediaries set out by Hodson, et al. [10] are used to explore how the role of intermediary activities in niche creation could be strengthened for DH. In particular, we consider how intermediary activities and modes might transition DH development from a niche activity to becoming part of the mainstream energy regime.

The activities of local authorities were of note when focusing on the 'depth of activity', represented on the x-axis of Figure 4, who were often seeking to deliver a systemic response through delivery of local heat strategies, planning policies and sometimes municipally owned energy service companies to facilitate strategic development and growth of DH for the long term. However, the lack of top-level strategic commitment and vision from within the local authority combined with the challenges of internal capacity and access to resource were creating a serious barrier for many of the stakeholders to achieve this.

These challenges at the local level were influenced by the national level, where there was a conspicuous lack of clear strategic steer to empower local authorities and LEPs in their role as DH intermediaries. Although national policy measures highlight local authorities as having a critical role in DH delivery [12], they do not yet support this with an explicit definition of responsibilities, or sufficient resourcing and delegation of powers to enable local authorities to consistently commit to this role. The sector would benefit from further dialogue and greater clarity about what the responsibilities and powers of local authorities are in relation to DH, the extent to which they should use local authority and public sector estates to enable viability of schemes, and indeed, strive to retain ownership of new schemes.

Returning to Hodson, et al. [10] and considering the 'scale at which priorities are defined', represented on the y-axis of Figure 4, a tension highlighted in this work is the balance between local and national influence. In the context of a centralised energy system, energy policy priorities are traditionally driven at the national level. However, given that the local context is so important for DH and local authority motivations tend to adapt to this context, this local voice is an important influence over the successful implementation of national energy policies. Even at the regional scale of the LEP, the emphasis on local economic growth may mean that some of the social drivers such as fuel poverty reduction (often prioritised by local authorities) are potentially not fulfilled [17]. An increased role for local authorities as local energy intermediaries requires greater dialogue between local and national governments to ensure that local priorities and activities are integrated into the energy system and national decision making across the country. National and regional intermediary activities clearly have an important role to play in enabling this dialogue to take place.

DH development in the UK is still taking place in the context of niches with few projects successfully getting through to delivery and completion. However, even at this early stage it is apparent that a transition from niche activity to the mainstream would require both a shift towards a more systemic response, particularly at the local level, and also a greater balance and dialogue between nationally defined priorities and the voices from the local context.

CONCLUSION

This work has used the innovative methodology of a decision theatre to explore the role of intermediaries within the process of DH development in a liberalised, centralised energy system. The results illustrate the power of intermediaries in enabling niche creation for DH development.

In the UK case study explored here, intermediary activities delivered several critical functions that enabled successful delivery of DH. They increased understanding of the technology amongst local stakeholders who needed to engage with potential projects. They sought resources to buy-in specialist expertise to support inexperienced actors. They also worked to overcome perceptions of risk by sharing case studies of other projects to reassure decision makers, and committing public sector estate to projects to increase security of heat demand. Still, there was potential to strengthen their impact by increasing the capacity and resource of local actors and more consistent provision of national level activities.

Lessons from the case study presented here are applicable beyond the context of the UK. DH delivery benefited from intermediary activities taking place at multiple levels of the energy system; the local and regional level play a critical role in direct delivery of projects while the regional and national level enable sharing and pooling of experience and resources to support the local level. In particular, the local nature of DH requires empowerment of local level actors, but supported by long-term intermediary actors who can maintain dialogue between the national, regional and local levels and establish clarity over powers and responsibilities as local actors take on a new role in coordinating strategic delivery of DH.

Finally, use of the 'modes of energy intermediaries' framework has highlighted their potential of intermediary actors to support a transition beyond DH development in stand-alone niches towards becoming an integrated part of the energy system. Embedding intermediary activities systemically into the multiple levels of the energy system, particularly at the local level, offers the potential to establish the institutional infrastructure and consistent support needed to unlock the potential of DH in many countries.

ACKNOWLEDGEMENTS

The authors would like to thank Dr Katy Roelich, and Dr Jonathan Busch from the Sustainability Research Institute, University of Leeds as well as Dr Mark Powell (iBUILD project, Newcastle University) for their collaboration on delivery of the decision theatre workshop. Finally, we are particularly grateful to all the participants that took part in the decision theatre workshop.

This work was funded by the UK Engineering and Physical Sciences Research Council (EPSRC) through the University of Leeds Doctoral Training Centre in Low Carbon Technologies (Grant EP/G036608/1) and Dr Bale's fellowship (EP/K022288/1).

REFERENCES

- [1] D. Connolly, H. Lund, B. V. Mathiesen, S. Werner, B. Möller, U. Persson, *et al.*, "Heat Roadmap Europe: Combining district heating with heat savings to decarbonise the EU energy system," *Energy Policy*, vol. 65, pp. 475-489, 2// 2014.
- [2] A. Chittum and P. A. Østergaard, "How Danish communal heat planning empowers municipalities and benefits individual consumers," *Energy Policy*, vol. 74, pp. 465-474, 2014.
- [3] DECC, "The Future of Heating: A strategic framework for low carbon heat in the UK," Department of Energy and Climate Change, Ed., ed. London: DECC, 2012.
- [4] F. W. Geels, "Technological transitions as evolutionary reconfiguration processes: a multi-level perspective and a case-study," *Research Policy*, vol. 31, pp. 1257-1274, 12// 2002.
- [5] A. Smith and R. Raven, "What is protective space? Reconsidering niches in transitions to sustainability," *Research Policy*, vol. 41, pp. 1025-1036, 7// 2012.
- [6] F. Geels and R. Raven, "Non-linearity and expectations in niche-development trajectories: ups and downs in Dutch biogas development (1973–2003)," *Technology Analysis & Strategic Management*, vol. 18, pp. 375-392, 2006.
- [7] T. Hargreaves, S. Hielscher, G. Seyfang, and A. Smith, "Grassroots innovations in community energy: The role of intermediaries in niche development," *Global Environmental Change*, vol. 23, pp. 868-880, 2013.
- [8] F. Geels and J. J. Deuten, "Local and global dynamics in technological development: a socio-cognitive perspective on knowledge flows and lessons from reinforced concrete," *Science and Public Policy*, vol. 33, pp. 265-275, 2006.
- [9] P. Kivimaa, "Government-affiliated intermediary organisations as actors in system-level transitions," *Research Policy*, 2014.
- [10] M. Hodson, S. Marvin, and H. Bulkeley, "The Intermediary Organisation of Low Carbon Cities: A Comparative Analysis of Transitions in Greater London and Greater Manchester," *Urban Studies*, vol. 50, pp. 1403-1422, May 1, 2013 2013.
- [11] D. Hawkey and J. Webb, "District Energy Development in Liberalised Markets: situating UK heat network development in comparison with Dutch and Norwegian case studies," *Technology Analysis & Strategic Management*, pp. 1-14, 2014.
- [12] DECC, "The Future of Heating: Meeting the Challenge," ed. London, UK: Department of Energy and Climate Change, 2013.
- [13] DECC, "Overview of grant funding and guidance available to local authorities developing heat networks," Heat Network Delivery Unit:, London 2014.
- [14] C. L. Walsh, S. Glendinning, R. J. Dawson, K. England, M. Martin, C. L. Watkins, *et al.*, "Collaborative platform to facilitate engineering decision-making," *Proceedings of the ICE-Engineering Sustainability*, vol. 166, pp. 98-107, 2013.
- [15] C. Bale, R. Bush, K. Roelich, J. Busch, and M. Powell, "Application of a decision theatre concept to the development of an agent-based model," in *Conference on Policy Modelling in Practice*, Centre for Research in Social Simulation, London, 2014.

- [16] D. D. White, A. Wutich, K. L. Larson, P. Gober, T. Lant, and C. Senneville, "Credibility, salience, and legitimacy of boundary objects: water managers' assessment of a simulation model in an immersive decision theater," *Science and Public Policy*, vol. 37, p. 219, 2010.
- [17] R. Bush, C. Bale, and P. Taylor, "Spatial mapping tools for district heating (DH): helping local authorities tackle fuel poverty," Report for Cheshire Lehamnn Fund, Leeds2014.

CONSIDERATION OF HIGH EFFICIENT WASTE-TO-ENERGY WITH DISTRICT ENERGY FOR SUSTAINABLE SOLID WASTE MANAGEMENT IN KOREA

Geun-Yong Ham¹, Dong-Hoon Lee²

¹ Eco-energies Research Centre, Institute of Urban Science, University of Seoul

² Dept. of Energy and Environmental System Engineering, University of Seoul

Keywords: Renewable Energy, High-efficient Waste-to-Energy, District Energy, Bio-drying MBT

ABSTRACT

The global hierarchy of sustainable solid waste management is ranked with source reduction, reuse, recycle, waste-to-energy, and landfill. After adoption of the Paris Agreement, the main issue in energy usage is to reduce the greenhouse gas (GHG) emission, universally. In this context, the necessity of renewable energies were increased. However unpredictable fall in oil prices brings about the price drop of recyclables and threatens the motive of recycling activities and the frame of solid waste management hierarchy as well. In order to react properly on in the energy and waste management sectors, the current situation of Waste-to-Energy(WtE) and District Heating and Cooling (DHC) in Korea was investigated compared with the EU and considered the suggestions for improvement of WtE plants and the synergy between WtE and DHC network.

As the mixed residual waste to be treated may be increased, WtE is becoming weightier for the climate change and sustainable society. Since late 1990s, there had established directives in terms of reducing final disposal and increasing the usage of sustainable energy gained from many sources, especially from WtE as a district energy. Including Germany, Austria, the Netherlands, Denmark and Sweden which have introduced landfill bans and promoted the WtE and renewable energy usage. As a result, the WtE technology aiming at maximizing energy recovery is well developed and simultaneously the DHC system connected with WtE plant is promoted. Thus the enhancement for current WtE system and for the synergies with district energy, the changes in policy and techniques are required. In technical view, treatment of raw Municipal Solid Waste (MSW) through bio-drying MBT(Mechanical Biological Treatment) will reduce the final disposal and further produce high calorific value of Solid Recovered Fuel (SRF) by removing moisture. Burning SRF will increase the power generation efficiencies rather introducing raw MSW. Additionally, high-efficient WtE technology which applied widely through Japan, Denmark and the Netherlands also enhance the total energy recovery for securing the district energy. Eventually, combined technology between bio-drying MBT with high-efficient

WtE and DHC can reduce the GHG emission and achieve the sustainable development goals.

INTRODUCTION

The Paris Agreement (FCCC/CP/2015/L9/Rev.1) was adopted by the ministers from 195 countries universally in December, 2015, which aims to lower the rising of temperature 2°C compared with pre-industrial levels [1]. In order to support the new agreement, there has been many efforts were considered in Worldwide.

In June 2015, Korea government also set the goals of greenhouse gas (GHG) reduction by 37% compared to the 2030 BAU (Business As Usual) levels [2]. In this context, renewable energies originated from various sources solar, wind, waste, biomass and nuclear are widely applied and adopted to avoid the usage of fossil fuels. In 2013, estimated renewable energy production were 19.1% of global final energy consumption [3]. However unpredictable fall in oil prices brings about the price drop of recyclables and renewable energy.

The global hierarchy of sustainable solid waste management is ranked with source reduction, reuse, recycle, waste-to-energy (WtE), and landfill [4]. Globally, the awareness of treating waste sustainably rather than just being disposed. This means WtE is becoming weightier for the climate change and sustainable society leaving the reduction at source as the mixed residual wastes to be treated that not suitable for recycling is increased. Additionally, among the various renewable sources, energies from waste, known as WtE is the technology that producing heat, steam and electricity from the incineration plant. Energy gained from waste and biomass captured about 60% of total worldwide renewable energy production in 2015 [3], [5]. Also, solid fuel, originated from waste so called Solid Recovered Fuel (SRF) can be provided into power plant. This produced energies are supplied to adjacent residential or industrial area for district heating and cooling. But, still the collaborations between WtE and district energy in Korea are weak. In present study, the former advanced case of WtE related with district energy in Europe are analysed and compare the situation with Korea. Then, suggestions about the technology development for synergy between WtE and district energy in Korea are described.

CURRENT SITUATION OF WtE TECHNOLOGY AND DHC POLICY IN EU

Since late 1990s, the movement of changes in policies regarding with climate change had been progressed in Europe. Representatively, establishing of the EU landfill directive (1999/31/EC) [6] which sets targets for the diversion of biodegradable waste from landfills in order to reduce the impact of waste management on environment. Thereafter, the Waste Framework Directive (2008/98/EC) [4] specified the structure of the waste hierarchy and promoted high energy efficiency in WtE plants in Europe. Since the Kyoto protocol took place in 1997 and including the Paris agreement in 2015, the expansion of renewable energies usage are actively recommended. To support this, also the EU Directive on Energy from Renewable Sources (2009/28/EC) have established to set the target for all EU member States to provide a 20% of total domestic energy from renewable sources by 2020 [7]. As a result, in 2013, about 81 million tonnes of MSW were incinerated and simultaneously produced 32 TWh of electricity and 81 TWh of heat which used for district energy. Converting this generated energy to the amount of primary energy, it equates with 9 – 44 million tonnes of fossil fuels. At the same time, about 22 – 44 million tonnes of CO₂ were saved. [8]

Looking into the waste treatment in EU28 (Figure 1), less landfilling is achieved in Germany, the Netherlands, Austria, Belgium, Denmark and Sweden. These countries are commonly introduced the landfill bans and promoted to treat the MSW mainly by recycling and WtE. Further, the district energy system is well-developed in order to provide the generated steam, electricity, and hot water from WtE facilities to adjacent households, industry buildings [7], [9].

In Denmark, experiencing the oil crisis in 1970s, the long-term energy policies were needed. As a result,

'Danish Energy Agency' was established which aimed to reduce dependency on oil import and increase the reliability of supplied renewable energies. After 1980s, DHC system was actively promoted and equipped. In consequences, the large-scale DHC system 'Copenhagen Network' has been built up. 3 WtE commercial plants located in Copenhagen are providing 30% of total district heat to regions in 100-km radius [5], [10].

In Amsterdam, the Netherlands, 2 commercial WtE plants are installed. Waste is occupied 25% of total district energy sources. About 75% of total electricity consumption of city are provided from these 2 facilities and simultaneously generating the district heat which can warm the 12,000 households. Waste Fired Power Plant (WFPP) that operated since 2007 with the concept of high-efficiency incineration, is treating the 530,000 tonnes of MSW per year and showing the above 30% of electricity generating efficiencies. [5], [11]

Annually, 600,000 tonnes of MSW is treated in Sysav WtE plant located in Malmö, Sweden. Sysav WtE plant is one of the most advanced facilities for waste incineration. In total, about 1,400 GWh of heat which is equated with the heating of 70,000 households and 250,000 MWh of electricity are provided to adjacent regions. [5]

Putting all the cases in EU, following effects are expected through the synergies between WtE and District energy.

- Less dependence on primary energy and GHG emission
- Reduction in final disposal and environmental impact induced following.
- Sustainable solid waste management through less landfilling but maximizing energy recovery from

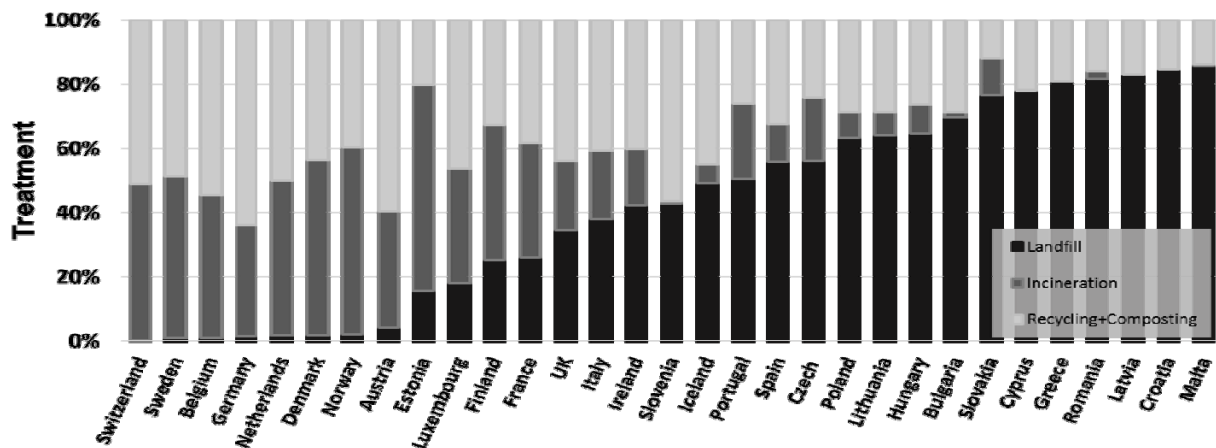


Fig. 1 Waste treatment in 31 of EU countries in 2013 (EU28 + Switzerland, Norway, Iceland)

WtE.

- By securing the district energy generated from WtE facility, the biased perception on WtE plant is changed from unpleasant facilities to fundamental infrastructure to surrounding residents.

CURRENT SITUATION OF WTE TECHNOLOGY AND DHC POLICY IN KOREA

In Figure 2, waste generation and treatment status are depicted from 1997 to 2014 in Korea [12]. The treatment by landfilling is getting reduced and the incineration is slightly increased. Comparing with the advanced countries in EU, still the landfilling ratio is quite high as about 15%. For the sustainable waste management and reducing the GHG emission, the alternatives are required. For the progress in policies, landfill taxes are required. In present, there are no specific bans on landfilling. Instead, the landfills managed by local government announced the increase of 'tipping fees'. Regardless of this, no legal regulations have existed [13].

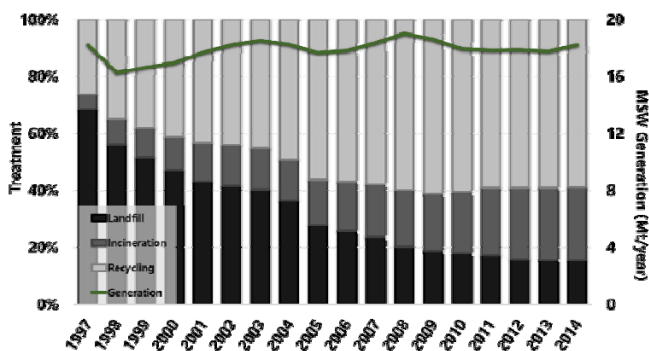


Fig. 2 Waste generation and treatment in Korea

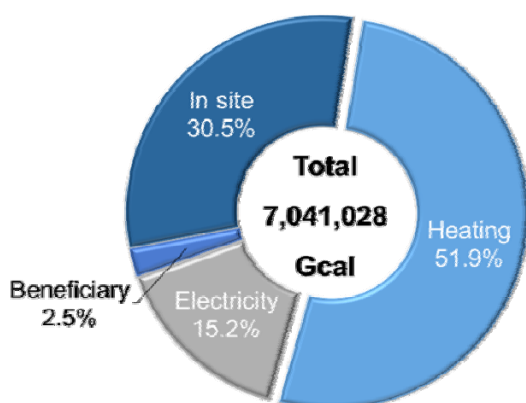


Fig. 3 Usage of waste heat in various forms from domestic resource recovery facilities in Korea, 2013

In site – consumption for maintenance of facility

In 2009, Korea government announced an 'Energy Policy Action plans of Waste and Biomass for low-carbon energy production and dissemination' [14]. The plan has established ambitiously to set the objectives for the energy recovery of 4 waste categories divided by feasible combustible wastes, feasible organic wastes, incineration waste heat, and landfill gas by 47, 26, 77 and 91% respectively until 2013, and 90, 36, 81 and 91%, respectively until 2020 against the 2007 level. As a result from an inspection by BAI (The Board of Audit and Inspection of Korea) in 2011 [15], only 4 SRF production facilities were installed and these had been much less than planned installation of 42 facilities, despite 64% of total business budget was allocated, because of an impractical introduction of SRF production technology without an operation experiences and fully established policies.

In 2014, domestic renewable energy consumption was occupied 4.1% of total energy usage and among them, 60% were originated from waste incineration which same as 53,000 TOE [16].

For district heating in Korea, few regions are equipped with district heating and cooling system. In 2014, about 84% of total production for DHC was originated mainly from LNG and coal, while the heat recovered from the waste was only 1.4% [17].

According to a report from Ministry of Environment, total 7,041,028 Gcal of waste heat was produced in 2013 at domestic incineration plant. Among them, about 67% of energies were provided to district heating system or Combined Heating and Power (CHP) facility while rest 33% was not used (Fig. 3).

In 2009, the energy recovery efficiency of incineration plant calculated by Ministry of Environment, Korea, showed 76.3% of efficiency in 22 facilities. Considering the distribution status, incineration plants which showed efficiency over 75% was 56% of total and 41% of total plants showed over 80% efficiency. But this is the theoretically calculated value, thus compared with the usage in EU and Japan technology which accomplished above 95%, there are still room for development in Korea [18], [19].

CUTTING GHG EMISSION THROUGH HIGH-EFFICIENT WTE TECHNOLOGY COMBINED WITH BIO-DRYING MBT AND THE SYNERGIES BETWEEN DHC

Considering the situation in Korea, the improvement of WtE technology as well as related policies are required for the synergies between WtE and district energy. Currently, applied bio-drying MBT and high-efficient WtE technology can be suggested in technological perspective.

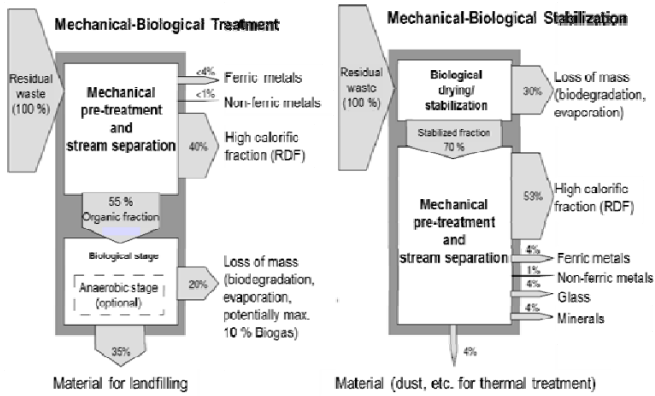


Figure 4 Fractioning of output flow of basic MBT concepts (Modified from Wagner)

- Bio-drying MBT technology

Mechanical Biological Treatment (MBT) technology was started from Germany in late 1990s as an alternative for the EU landfill directive (1999/31/EC).

Biological treatment that applied to MBT system is determined by the objective of process that related with the usage of products [20]. Applied biological treatments are composting, bio-drying, anaerobic digestion, etc. Evaluating the biological treatment technologies in different criterion – proven technique, suitable for moist MSW, demand for primary energy, and etc. Considering the overall evaluation, optimum process for moist waste treatment bio-drying and anaerobic digestion technology can be suggested [21]. Bio-drying is a drying technology that using biologically generated heat as the main heat source and by introducing the air, aerobic condition is made and evaporated vapour is discarded from reactor.

MBT with bio-drying is a little simpler in design than other process. Additionally, SRF which is produced in the end of process, can be used in power plant for heat and electricity generation. As can be seen in Figure 4, MBT process including biological treatment especially

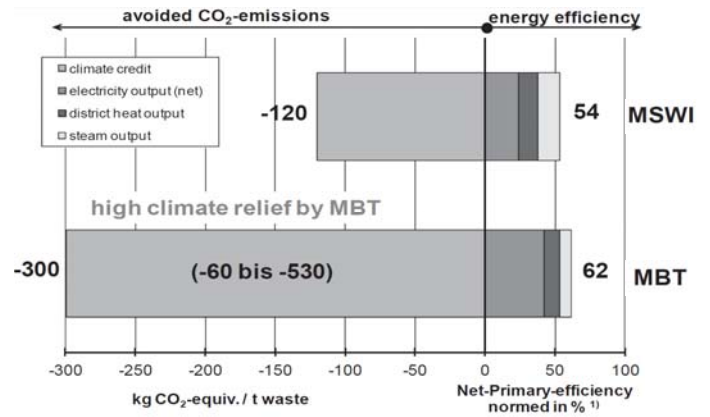


Fig. 5 Comparison of energy efficiency and GHG balance of MBT plants in 2012 (K. Ketelsen, 2015)

MSWI: MSW Incineration without SRF power plant (without SRF power plant and without climate

bio-drying, reduced the landfilling ratio markedly. Putting bio-drying process before mechanical sorting, produces 53% of high calorific fraction that is SRF. At the same time, only 4 % of total inputs are landfilled [22].

In case of Germany, where the MBT system which aims material specific waste treatment, is currently having a situation that over-capacities of solid waste treatment. During 2004 to 2008, the MBT facilities are rapidly increased in Germany. As the systems have installed, capacities were increased as well. Thus present capacities of MBT will compete with other solid waste treatment capacities. In near future, new trends of waste treatment are presented by its energy efficient waste treatment as well as the resource and energy recovery. Meaning that this will lead to decreasing treatment capacities as well as a conversion of present capacities along with a conversion of the treatment technique itself [23].

Through the MBT with bio-drying process, heating value of moist MSW is increased as the water removed.

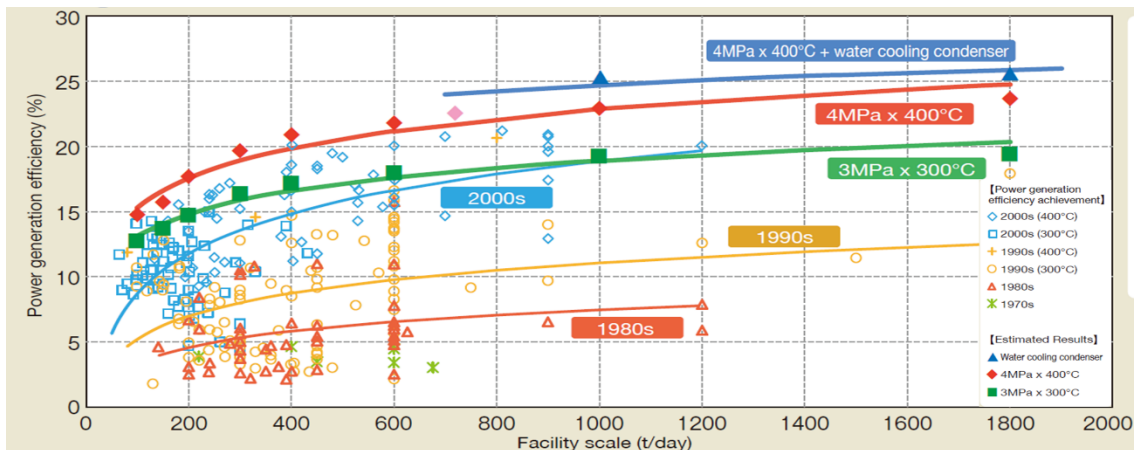


Fig. 6 Power generation efficacy achievement of waste incineration facilities and estimated results (Ministry of Environment of Japan, 2012)

Rather burning the raw MSW, energies gained from incineration of SRF that contained high calorific value are greater.

As shown in Fig. 5, energy efficiency and GHG balance in MBT and MSWI process are compared. Net primary energy efficiency was higher in MBT process as 62% than MSWI. In terms of -300 kg CO₂-equiv. / t waste were saved in MBT compared -120 kg CO₂-equiv. / t waste in Incineration plant. Especially, MBT process with bio-drying, hold a higher portion of treated waste to recovery and saved GHG emission higher [23]. To sum up this, WtE technology combined with bio-drying MBT can enhance the energy recovery efficiency by introducing the SRF that contained high calorific value and reduce the GHG emission simultaneously by providing waste heat and electricity to households or industry buildings.

- High-efficient WtE technology

As the characteristics of generated MSW are changed to high calorific value due to packing materials and also following the shift of society that is aiming at usage of valid waste heat and less GHG emission, new generation of high-efficient WtE technology is required.

Generation of energy from waste has been pioneered in Denmark and countries in Scandinavia such as Sweden, Norway and Finland, for district heating and cooling production due to their cold weather. For example, the combined heat and power plants in Denmark required a new type of boiler for high-efficiency. Thus the steam parameters were typically 40 bar, 400°C already since 2000 [10], [24].

According to the report released by ministry of Japan in 2012, the movement towards the safe and sound municipal waste incineration and high-efficiency power generation is being developed. In the past, the priority

factor in setting up waste incineration plants was antipollution control, which resulted in a significant upgrading of facilities from this perspective in Japan. However, in perspective of energy recovery, many plants now construct highly efficient electricity generation facilities with longer operating lives as demanded by greenhouse gas emission measures. Rising the temperature and steam pressure for power generation results in high efficiency are required [25], [26]. In Fig. 6, as applying high temperature and high pressure boilers, the higher power generation efficiencies can be achieved. Further technological requisites for improvement in WtE technologies are described in Table 1. Various technological requisites are widely applied to incineration facility to increase the power generation efficiency [27]. Depends on the objective of revision, various requisites can be applied. These technological alternatives also adopted to SRF power plant for maximizing the energy recovery efficiency as well. Based on this high-efficient WtE technologies, there also the movement through Japan that maximizing the energy recovery. In 2009, about 80% of total generated MSW were treated by incineration. Among them only 24.5% of plants in Japan performed energy recovery and utilisation for generated heat was also barely performed. Because most of WtE plant installed in Japan are small-scale that only aims at MSW treatment. Thus the motive for energy recovery was weak. However, counteracting on global changes, focusing on energy recovery are the main concept for the developing WtE technologies in Japan [28].

CONCLUSION

Confronting the Paris Agreement as well as Sustainable Development Goals, many environmental, economic, social strategies for proper reactions are established in worldwide. Among this, for sustainable

Table 1. Technological requisites, improvement effect for high-efficiency power generation (Japan manual)

Objective	Technological requisite	Improvement effect	Conditions for improvement effect calculation
Enhancement on heat recovery	Lowered temperature economizer	1%	Exhaust gas temperature at boiler exit 250°C → 190°C
	Lowered combustion air ratio	0.5%	MSW 300 t/d, combustion air ratio 1.8 → 1.4
Valid usage of steam	Low-temperature catalytic desulfurization	1 ~ 1.5%	Temperature at entrance 210°C → 185°C(non-reheating)
	High-efficient dry exhaust gas scrubber	3%	High-efficient dry scrubber
	No flue gas heating	0.4%	Conditions for flue gas heating 5°C, 60% → No restraint
	Waste water treatment	1%	Temperature at boiler exhaust 250°C → 190°C
Enhancement on steam turbine system	High temperature, high pressure boiler	1.5 ~ 2.5%	3MPaG × 300°C → 4MPaG × 400°C
	Extraction turbine	0.5%	Main turbine → Extraction turbine
	Cooling of Stoker	2.5%	Pressure at turbine exhaust -76kPaG → -94kPaG

waste management, WtE technologies are actively applied in many advanced EU countries targeting the waste that is not suitable for recycling to avoid landfilling and recovery of useful energy. Generated from incineration, the waste heat, steam can be used to produce thermal energy and electricity. This is a good energy source to adjacent households and industries for district heating and cooling and further for electricity. WtE technologies are introduced in Korea recent 15 years. But lack of experience and broad definitions of target wastes for energy sources, the technology and related policies are not settled completely. Benchmarking the advanced case in EU (Denmark, Sweden, the Netherlands and etc.), political and technical suggestions that are aiming at waste management for avoidance on landfills, maximizing energy recovery as district energy and reduction of GHG emission are made. For technical perspective, Bio-drying process that are maximizing the SRF production, can be applied to current MBT system in Korea which operated only by MT system. Additionally, high-efficient WtE technology is also required in current system to increase the incineration and energy recovery efficiency. Also more district energy can be secured from WtE plants when DHC system is in place. Thus when designing the new city, WtE plants are perceived as fundamental infrastructure so that the secured waste energy can be provided to residents and also the distances of wastes collection will be shortened. Finally, combining the bio-drying MBT with high-efficient WtE technology can secure more district energy and in the end, it achieve the reduction of GHG emission.

ACKNOWLEDGEMENT

This work was supported by the Korea Institute of Energy Technology Evaluation and Planning (KETEP) and the Ministry of Trade, Industry & Energy (MOTIE) of the Republic of Korea (No. 20153010102020).

REFERENCES

- [1] CAS/Paris Agreement/MTP, UNFCC December, 2015
- [2] Report of GHG reduction by 2030 (in Korean), June, 2015
- [3] REN21, Renewables 2015 Global Status Report (Annual Reporting on Renewables: Ten years of Excellence), 2015
- [4] The Waste Framework Directive (2008/98/EC)
- [5] CEWEP, ESWET, EUROHEAT&POWER, DHC+, Warmth from Waste: A Win-Win Synergy- Background paper for project development on district Energy from Waste: a common initiative, 2013
- [6] The EU landfill directive (1999/31/EC)

- [7] The EU directive on Energy from Renewable Sources (2009/28/EC_
- [8] CEWEP, Waste-to-Energy's contribution to Resource & Energy Efficiency
Available online: http://www.cewep.eu/m_1040
- [9] Waste management in EU, Eurostat, 2014
- [10] Heron Kleis, Babcock & Wilcox Vølund and Søren Dalager, Ramboll, 100 Years of Waste Incineration in Denmark, 2000
- [11] CEWEP, Energy from Waste in Amsterdam: Helps provide green certified power for the tram, metro and city, 2013
Available online:
http://www.amsterdam.nl/publish/pages/408150/aeb_brochure_uk.pdf
- [12] Ministry of Environment, Status of waste generation and treatment (1997 – 2014)
- [13] CEWEP, Landfill taxes & bans, February 2015
Available online:
<http://cewep.eu/information/data/landfill/index.html>
- [14] Ministry of Environment, Energy Policy Action plans of Waste and Biomass for low-carbon energy production and dissemination, 2009
- [15] Inspection result report of Waste-to-Energy business, BAI, 2011
- [16] Korea Energy Agency, 2014 A handbook of district energy business, 2015
- [17] Korea Energy Agency, 2014 Statistical data of renewable energy, 2015
- [18] Ministry of Environment, The operation status of resource recovery facility of MSW in 2013, 2014
- [19] Ministry of Environment, Study on improvement of energy recovery of MSW incineration facility ,2009
- [20] Juniper report, MBT: A Guide for Decision Makers – Processes, Policies & Markets, UK, 2005
- [21] K. Kanning, K. Ketelsen, MBT-Best technology for treatment of moist MSW AD and/or biodrying prior to energy recovery, Proceedings of Waste-to-Resources 2013, V International Symposium MBT and MRF, June, 2013
- [22] Wagner J, Development of Mechanical Biological Treatment of Municipal Waste in Latvia on the Basis of a Pilot-project in "Viduskurzeme" , INTECUS GmbH(2008)
http://www.zalajosta.lv/tools/download.php?file=////images/files//Joreg_Wagner_MBT.ppt
- [23] K. Ketelsen, M. Nelles, Status and new trends / perspectives of MBT in Germany, Proceedings of Waste-to-Resources 2015, VI International Symposium MBT and MRF, May, 2015

- [24] Zerowaste Europe, Denmark's transition from incineration to Zero Waste
Available online:
<https://www.zerowasteurope.eu/2014/01/the-story-of-denmarks-transition-from-incineration-to-zero-waste/>
- [25] Ministry of the Environment of Japan, Solid Waste Management and Recycling Technology of Japan Toward a Sustainable Society, 2012
- [26] S. W. Park, Energy Recovery of Municipal Solid Waste: High-Efficiency Incineration Technology, J. of Korea Society of Waste Management Vol. 31, No. 2, pp. 125-133, 2014
- [27] Ministry of the Environment of Japan: High efficiency waste power generation facility maintenance manual, 2010
- [28] T. Tomohiro, Waste-to-energy incineration plants as greenhouse gas reducers: A case study of seven Japanese metropolises, Waste Management & Research Vol. 31, No. 11, pp. 1110-1111

TOPIC F:

Open Arena, District Heating & Cooling



FEASIBILITY STUDY ON THE APPLICATION OF ADSORPTION COOLING TO DHC

J.D. Chung¹, H. Yoo²

¹ Department of Mechanical Engineering, Sejong University, Seoul 05006, Korea

² Department of Mechanical Engineering, Soongsil University, Seoul 06978, Korea,

Keywords: District Cooling, Adsorption Cooling, COP, SCP

ABSTRACT

Deployment of district cooling is one of the most interesting issues in recent integrated energy systems. While the adsorption chiller has a high potential in terms of the temperature range required for district cooling, it is not being widely used due mainly to large system size and relatively low performance. The present research conducted a feasibility study on the application of new types of adsorption chiller, which have high potential to enhance the heat transfer and reduce the system size. The proposed types are an embossed plate heat exchanger (Plate HX) type and heat pipe type adsorption chiller. The plate HX and heat pipe have a relatively high heat transfer capacity and compact size, and this study is a first attempt to apply these new type HXs of adsorption chiller, as an improved alternative to the fin-tube type heat exchanger. Deployment of district cooling is one of the most interesting issues in recent integrated energy systems. While the adsorption chiller has a high potential in terms of the temperature range required for district cooling, it is not being widely used due mainly to large system size and relatively low performance.

INTRODUCTION

Due to global warming and economic development, demand for cooling has rapidly increased. However, vapor compression refrigerators that use Freon gas have many problems, including excessive electric power consumption and environmental damage. As a result, many studies have focused on the development of eco-friendly refrigeration systems driven by heat rather than electricity [1-3].

An adsorption refrigerator is a promising alternative cooling device and also an eco-friendly refrigeration system, which can be driven by low-grade heat (60°C ~90°C) from solar energy, district heating, exhaust heat from an engine or discarded waste heat. Adsorption cooling is not being generally used yet mainly due to the system's large size and relatively low performance. Because the adsorption beds are the most important parts affecting system size and performance, many researchers have conducted the study of the adsorption beds for improvement. One of the goals has

been to optimize the shape of the heat exchanger. Various types of heat exchangers have been examined.

In the early development stages, a simple-tube type heat exchanger was used for the adsorption beds. However, due to its low system performance (COP = 0.1~0.5, SCP = 50~200 W/kg) and long cycle times (about 1,000~10,000s), the simple-tube type adsorption chiller has been rarely used in these days. To overcome the disadvantages of the simple-tube type adsorption chiller, fin-tube HXs were introduced. Fin-tube HXs with extended fin surfaces can significantly improve heat transfer capacity, which leads to increased mass transfer capacity. Most products in the market use fin-tube HX in the adsorption bed, which have relatively high performance (COP = 0.5~0.7 and SCP = 100~600 W/kg) and short cycle time (usually less than 1000s) compared to a simple-tube HX. However, the rate of improvement of system performance using fin-tube HX has apparently slowed recently, and seems to have reached near optimum.

Other types of HX with higher heat and mass transfer capacities are therefore required. Li et al. [4] reviewed on the efforts to introduce the new type of HXs in the adsorption bed such as plate-fined bed, spiral plate bed and porous bed, etc. to increase heat transfer capacity of adsorption bed. Here we introduce two types of new suggestions, i.e. an embossed plate HX type and heat pipe type adsorption chillers. A feasibility study was conducted to examine whether these two types of adsorption bed show high enough performance, compared to the fin-tube type HX applied to adsorption chiller. After that, a parametric study was conducted, from which the guideline for each parameter can be determined for the optimal design of the newly suggested adsorption chiller.

NUMERICAL METHOD

In general, two adsorption beds are used in the adsorption refrigeration system. One is for adsorption process, the other is for desorption process and vice versa. During adsorption/ desorption process, endothermic/ exothermic reaction occurs, which is to be removed by cooling and heating water. During the adsorption process, the vapor from the evaporator enters the adsorption bed, while during the desorption process, the desorbed gas is evacuated to the conden-

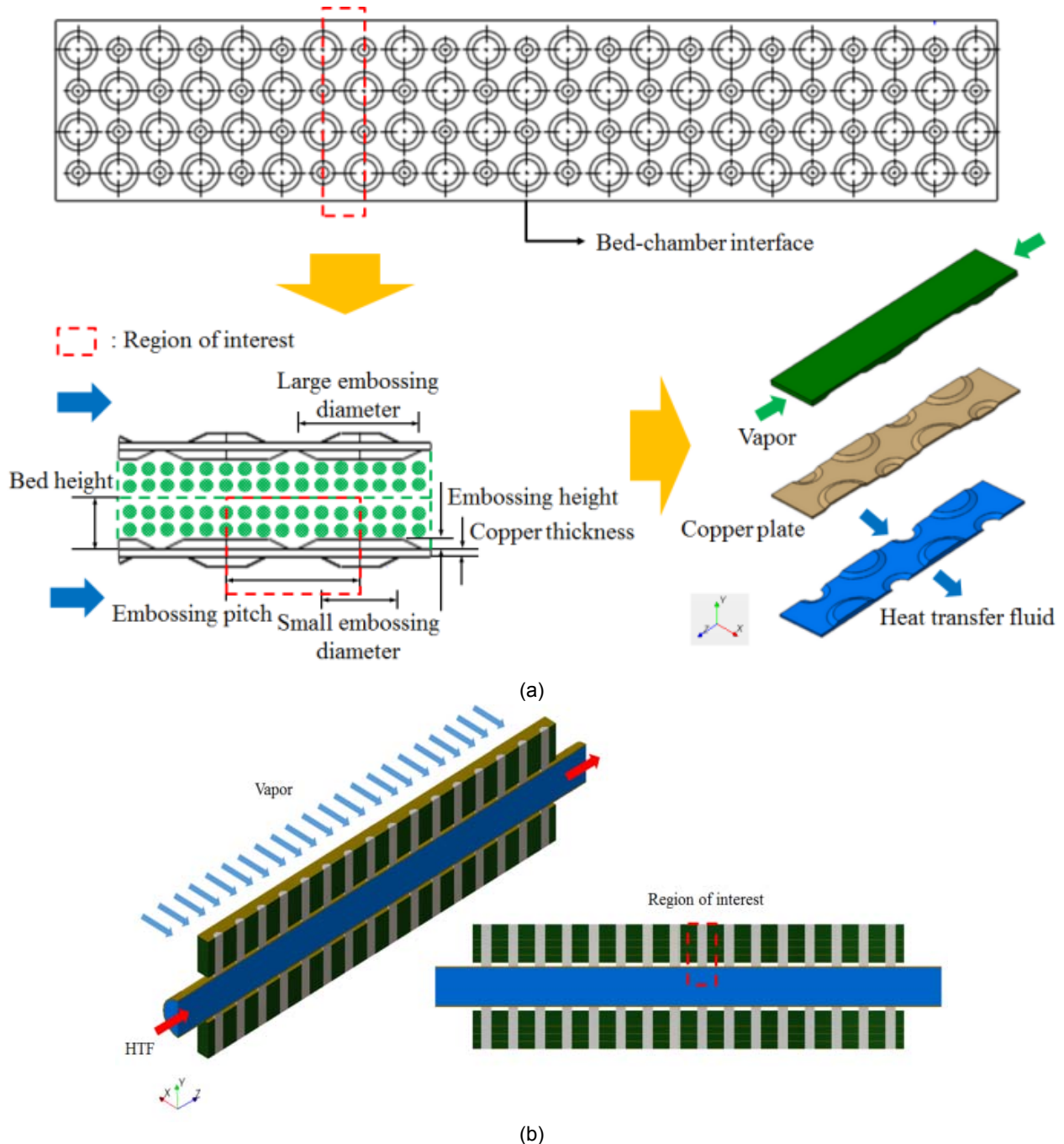


Fig. 1 Schematics of (a) plate type adsorption bed and (b) heat pipe type adsorption bed

ser. By repeating two processes in each bed, consecutive cold energy can be obtained from the evaporator. More detailed description on the system is mentioned in the resent study of Hong et al. [3].

Figure 1 shows the newly suggested two types of adsorption beds. In order to save an enormous amount of simulation time, we took one repeating section of interest to model. A three-dimensional transient model was used, and a commercial CFD program called STAR-CCM+ v7.04 was applied. Since $D/r_p^2 = 0.000368$ is larger than the critical value (0.000192) of

silica gel, the non-isobaric model and linear driving force (LDF) model were used for the inter- and intra-particle mass transfer models, respectively. The assumptions, governing equations and boundary/initial conditions are given in detail in Hong et al. [3] and Ahn et al. [5].

As the performance of an adsorption bed, coefficient of performance (COP) and specific cooling power (SCP) are used:

$$\text{COP} = \frac{Q_{eva}}{Q_{in}} \quad (1)$$

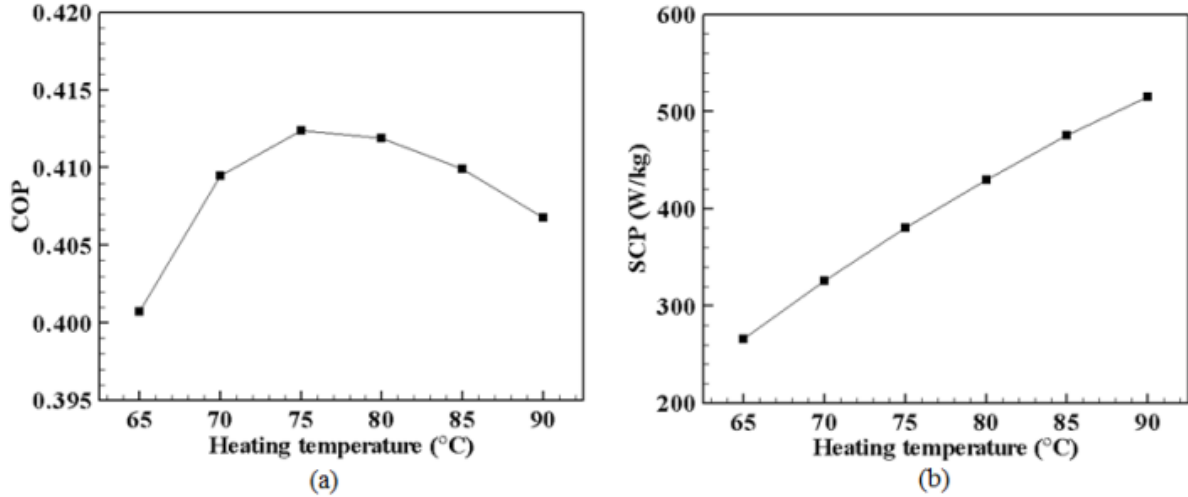


Fig. 2 Variations of (a) COP and (b) SCP with heating temperature.

$$SCP = \frac{Q_{eva}}{M_b t_{cycle}} \quad (2)$$

where Q_{eva} denotes the cooling energy obtained from the evaporator and Q_{in} denotes the input heat energy supplied to the adsorption bed during the desorption process. M_b is the total mass of the solid sorbent and t_{cycle} means cycle time.

$$Q_{eva} = L_v \int_{t_{des}}^{t_{ads}} \int_{interface} \rho_v \bar{u}_v \cdot d\bar{A} dt \quad (3)$$

$$Q_{in} = \int_{t_{ads}}^{t_{des}} \int_{A_f} \rho_f C_{p,f} (T_{f,in} - T_{f,out}) \bar{u}_f \cdot d\bar{A} dt \quad (4)$$

where L_v is approximated as follows:

$$L_v = L(T_{eva}) - C_{p,b} (T_{con} - T_{eva}) \quad (5)$$

PARAMETER STUDY OF THE PLATE HX TYPE ADSORPTION CHILLER

We conducted a parameter study on seven parameters, i.e., (1) embossing diameter ratio, (2) embossing height, (3) embossing pitch, (4) bed height, (5) plate thickness, (6) heating temperature, and (7) fluid velocity. As the typical example, Figure 2 shows the behavior of COP and SCP as a function of heating temperature. The heating temperature has been reported to have the most significant effect on the SCP of adsorption chillers [2, 6] and the result in the present study also shows it has a significant influence on SCP. Heating temperature determines the minimum value of water uptake. A large heating temperature creates a large difference in concentration between the inside and outside of a solid sorbent, which enhances the desorption rate of the adsorption bed. Therefore, SCP

is increased by increasing the difference between maximum and minimum water uptake Δq . However, if the heating temperature is too high, the input heat energy Q_{in} becomes unnecessarily large, and COP is consequently decreased after the critical point of the heating temperature (75°C). This trend is also the same in the fin-tube type adsorption chiller [2].

PARAMETER STUDY ON THE HEAT PIPE TYPE ADSORPTION CHILLER

A parametric study was conducted on six parameters affecting the system performance of a heat pipe type adsorption chiller: (1) number of layer (2) heat pipe pitch (3) fin spacing (4) heat pipe radius (5) fin width (6) hot water temperature. The level of each parameter is shown in Table. 1. The base conditions are shown in grey color. As the typical example, Figure 3 shows the behavior of COP and SCP as a function of the number of layers. When the number of layer increases, larger Q_{in} is required to heat up the extra volume of the bed during the desorption process. But, the amount of water uptake is also increased by addition of adsorbent amount. Thus, COP increases due to increased evaporation heat, that is Q_{eva} . SCP is inversely proportional to the adsorbent mass, thus SCP is decreased with increasing number of layers. The number of layers in the practical application is much larger than 7. However, due to limitation on the computer memory and calculation time, maximum 7 layers are considered in our numerical model. The performance of 7 layers (COP = 0.5204, SCP = 752.37 W/kg) turns out to be almost the same COP, while larger SCP compared to the fin-tube type adsorption bed (COP = 0.4944, SCP = 538W/kg).

CONCLUSION

In the present study, a feasibility study on two new types of HX applied to adsorption chiller, i.e. (1) plate HX type and (2) heat pipe type, and a parameter study were conducted, from which optimization guideline for each parameter was examined. All of these two types show similar COP but higher SCP, which means the new types of adsorption chiller have high potential to resolve one of the most serious disadvantages of the adsorption cooling system, i.e., system size.

Table 1 Parameters of numerical condition

Parameter	Values
Number of layer	1, 3, 5, 7
Heat pipe pitch [mm]	10, 12, 14, 16, 18
Fin spacing [mm]	0.5, 1, 2, 3
Heat pipe radius [mm]	1, 2, 2.5, 3, 3.5, 4
Fin width [mm]	4, 6, 8, 10, 12
Hot water temp. [°C]	55, 65, 70, 80, 85, 95, 100

ACKNOWLEDGEMENT

This work was supported by the Energy Efficiency & Resources (No. 20122010100120) of the Korea Institute of Energy Technology Evaluation and Planning (KETEP) grant funded by the Korea Government Ministry of Knowledge Economy.

REFERENCES

- [1] J.D. Chung, D.Y. Lee, S.M. and Yoon, "Optimization of desiccant wheel speed and area ratio of regeneration to dehumidification according to regeneration temperature", *Solar Energy* 2009, Vol. 83, pp. 625-635.
- [2] S.W. Hong, S.H. Ahn, O.K. Kwon and J.D. Chung, "Optimization of a fin-tube type adsorption chiller by design of experiment", *Int. J. Refrigeration* 2015, Vol. 49, pp. 49-56.
- [3] S.W. Hong, O.K. Kwon and J.D. Chung, "Application of an Embossed Plate Heat Exchanger to Adsorption Chiller", *Int. J. Refrigeration* 2016, Vol. 65, pp. 142-153.
- [4] X.J. Li, X.H. Hou, X. Zhang and Z.X. Yuan, "A review on development of adsorption cooling-Novel beds and advanced cycles", *Energy Conversion and Management* 2015, Vol. 94, pp. 221-232.
- [5] S.H. Ahn, O.K. Kwon and J.D. Chung, "Feasibility study on the application of a heat-pipe type adsorption chiller", *Journal of Mechanical Science and Technology* 2016, submitted.
- [6] B.B. Saha, A. Chakraborty, S. Koyama and Y.I. Aristov, "A new generation cooling device employing CaCl₂-in-silica gel-water system", *Int. J. Heat Mass Trans* 2009, Vol. 52, pp. 516-524.

SERVICE ORIENTED ARCHITECTURE ENABLING THE 4TH GENERATION OF DISTRICT HEATING

Jan van Deventer¹, Hasan Derhamy¹, Khalid Atta¹, Jerker Delsing¹

¹ Luleå University of Technology, Luleå, Sweden

Keywords: *SOA, Optimization, System of Systems, MBSE, SysML, District Heating*

ABSTRACT

The 4th Generation of District Heating (4GDH) is a complex agglomeration of heat providers, distributors, and consumers that must be automatically, continuously managed and coordinated. It is a complex system of systems; a definition which we align to Maier's architecting principles for systems-of-systems as collaborative systems. Wrapped in the idea of system of systems is the reality that the 4GDH systems' descriptions and specifications are not currently all known. Nonetheless, the transition into the 4GDH is actual. We propose the use of two frameworks to secure a smooth metamorphosis and assure systems' operation, maintenance, and evolution. The two frameworks are the Arrowhead Framework and the OPTi Framework. The first one enables system integration through Service Oriented Architecture (SOA) and the second one offers the overall system optimization with respect to all stakeholders. This paper uses the Model Based Systems Engineering (MBSE) tool SysML to model a district heating complex's structures and behaviors from the concept level down to the sensors and actuators within a district heating substation where we apply the SOA technology based on the open Arrowhead Framework. We focus on the Arrowhead Framework's core services, i.e. Service Registry, Authorization and Orchestration to clearly describe the interactions between the different service providers and consumers. Going back up from the sensors to the systems, it is clear that SOA is the architecture that will empower the 4GDH.

INTRODUCTION

District Heating is a common sense concept that becomes progressively more evident as one reflects on it. It is a centralized production of heat energy that is stored in a fluid and distributed through a network to different buildings within a district. It is a resourceful idea because the centralized production is more efficient than several distributed small ones as long as the distribution losses are small [1]. The concept becomes even more indisputable when the heat energy is a byproduct of an industrial process. For example, a paper mill, which produces paper, can sell off its incidental heat. Another great example is the Combined Heat and Power (CHP) that produces electricity from burning refuse and simultaneously

heats buildings and associated domestic hot water. This is a win-win solution for all, including the environment. And yet, it can further be improved.

In its Energy Roadmap 2050, the European Union has set itself the impressive long-term goal of reducing greenhouse gas emissions by 80-95% as compared to 1990 levels by 2050. In its commitment to reach that goal, it has considered different scenarios and their impacts. Connolly et al. assert that increased use of district heating in Europe supports the goals of the roadmap at a lower cost [2]. This continued use of district heating is accompanied with its normal evolution, which brings it to its fourth generation.

Lund et al. present an excellent review of the four generations of district heating and of the European Union's energy roadmap leading to the fourth generation [3]. They describe the trends over the generations: increase in energy efficiency, decrease in temperature of the supplied transport medium and an increasing complexity in stakeholders. The first generations period was from about 1880 to 1930 with transport medium temperatures below 200°C. The second generation from 1930 to 1980 with temperatures greater than 100°C and third from 1980 to 2020 with temperatures less than 100°C. The fourth generation should span from 2020 to 2050 with temperatures less than 70°C. The complexity increase includes an increase of different producers, which at some time might be heat consumers, as well as daily variations of heat demand.

To address this complexity increase and aim for its harmonious operation, it becomes essential to understand the district heating system. The 4GDH is made up of several heat production systems, distribution systems, and consumer systems. Each of them with their own set of sub-systems. The natural temptation is to designate the district heating concept as a system of systems, but the Maier argues that it might be a misclassification [4]. According to Maier's tenets, an equivalent term to system of systems would be "collaborative systems" where the sub-systems fulfill valid purposes in their own rights and continue to operate to fulfill those purposes if disassembled from the overall system. Additionally, the sub-systems must be managed (at least in part) for their own purposes rather than the purposes of the whole. Aligning to these views, serves not only the sub-systems, but also 4GDH and forms the point of the herewith article. Especially

when the implementation specifications of the 4GDH do not yet exist. This leads Maier to state that systems-of-systems are largely defined by their interface standards rather than their structures. He points to the Internet as a good example of collaborative systems. It is that same technology that is used here to define the interface standard of the proposed solution. This enables new emerging behaviors to surface up as the 4GDH becomes mature because the services within the architecture are loosely coupled and therefore late binding.

This article presents a systems architecture for the 4GDH knowing that the systems specifications will not all be complete for a long time. This plan of action relies on two frameworks and their related interfaces: the Arrowhead Framework and the OPTi Framework. The OPTi Framework offers a simulation platform for different components of the DH systems that can include the components of the 4GDH, which enables the optimization of the 4GDH's dynamics. The Arrowhead Framework enables system integration and collaboration through Service Oriented Architecture (SOA). We use Model Based System Engineering (MBSE) to convey how this is implemented in a structural and behavioral sense.

The structure of the article presents the two frameworks before turning to models of district heating enhanced with SOA. The models are based on uses the MBSE tool SysML. The models describe district heating's structures at the concept level down to the sensors and actuators within a district heating substation where we apply the SOA technology based on the open source Arrowhead Framework. The models additionally describe the behavior of the system with focus on service discovery, authorization, and orchestration at the lowest level to clearly demonstrate the mechanisms involved prior to scaling back up to the whole system of systems in which the OPTi Framework is an integral part.

THE FRAMEWORKS

If systems are expected to be independent, and yet be collaborative to form a system of systems, they must somehow find a benefit to co-operate. The OPTi Framework addresses the yearning for collaboration, and the Arrowhead Framework addresses the service oriented architecture to make the collaboration possible. Coincidentally, the OPTi Framework can provide services within the Arrowhead Framework. This is possible because they both have well defined interfaces.

The OPTi Framework

The OPTi Framework is the product of the European Union Horizon 2020 project OPTi, which aims to deliver

the tools to optimize district heating and cooling with full consideration of the end customers [5]. In other words, the framework is a suite of tools that offers solutions in which all stakeholders benefit. This key concept is what drives the systems to be inclined to collaborate together. The benefits include saving natural resources, assuring comfort, increasing profits and cost reductions.

One of these tools is the scalable simulation tool OPTi Sim, c.f. figure 1. It considers production, distribution, consumption, end consumers, and economics. It is also a system of systems as each sub-simulation is independent and communicates through a co-simulation router. The communication interface follows a clear standard: the open interface standard FMI (Functional Mock-up Interface) [6]. It is an independent standard that supports both model exchange and co-simulation of dynamic models using a combination of xml-files and compiled C-code. This permits each simulation tool to be developed and refined independently.

One example being addressed is the daily peak loads as demand for domestic hot water increases in the morning before work and at dinner time. The planning of production and distribution has to be done; and a good optimization should use also the buildings thermal capacitance to save resources while striving for end customer comfort. With an increase of heat suppliers, the complexity of the task becomes even more challenging. Collaborative simulation for planning will be evermore essential for the 4GDH.

Having clarified why the systems would want to collaborate, it becomes interesting to understand how they could interact with each other.

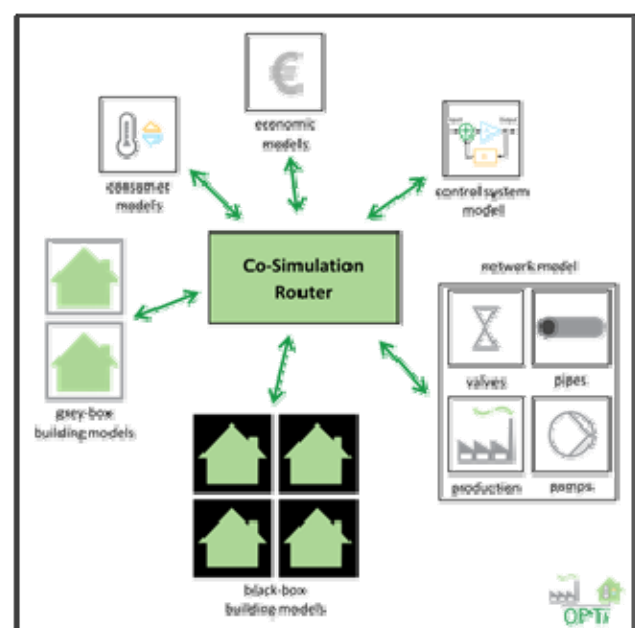


Figure 1: A block diagram depicting OPTi Sim with its different simulation engines.

STRUCTURE AND BEHAVIORAL MODELS

A short definition of Systems Engineering is: "Systems

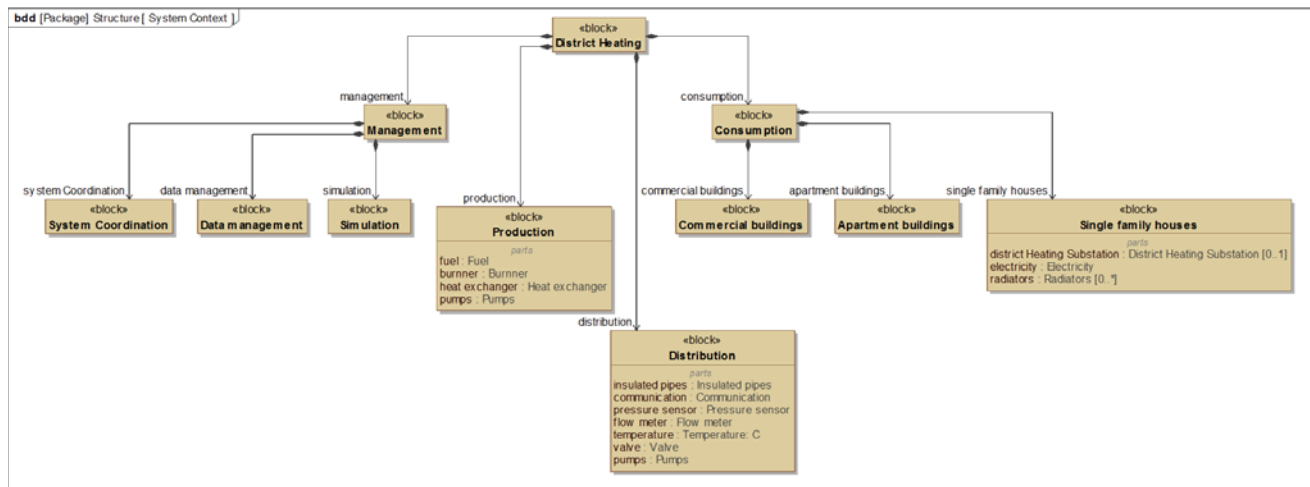


Figure 2: A block definition diagram (bdd) of district heating.

The Arrowhead Framework

The open source Arrowhead Framework is the product of another European Union project [7]. The project's vision has been to enable collaborative automation by networked embedded devices. Its grand challenges were to enable the interoperability and interchangeability of services provided by almost any device. This has been done by offering services established on the Internet Protocol Suite, which is a proven technology. It reflects the paradigm of a person, i.e., service consumer, using a web browser to address a service provider, e.g., a search engine or bank, to obtain information. The different software modules at the service providers and consumers can be updated at anytime without affecting the others as they are loosely coupled. What is clearly defined are the interface protocols themselves. Adhering to them simplifies development and insures quality.

The Arrowhead Framework proposes an assortment of services, in the form of software modules, of which three are core services. The core services are the Service Registry, Authorization and Orchestration. We describe how they interact within a district heating substation in the next section. Of the many other service modules, worth mentioning are the Historian, the Gate Keeper, and the Translator, although we do not involve them here [8]-[10]. The Historian is a data logger, while the Gate Keeper is a secure interface to the outside Internet world. The Translator is a service provider that intervenes when different component suppliers have chosen different Internet protocols, which could hinder collaboration due to dialects [11].

To elucidate how these core services are used in district heating, we employ systems engineering models.

engineering is a methodical, disciplined approach for the design, realization, technical management, operations, and retirement of a system" [12]. As systems become more complex, consistent approaches and tools are needed to manage the complexity as well as to communicate with all stakeholders. One such approach is to use models, which is referred to as Model Based Systems Engineering. Associated to this, one finds the modeling tool SysML, System Modeling Language. It is an offshoot of the Unified Modeling Language (UML) that was developed during the early 1990's and later adopted as a standard by the Object Management Group [13]. SysML uses different diagrams to represent different aspects of a system. The classification of its taxonomy of diagrams forms three groups: structure, behavior, and requirement diagrams. We shall here use structural and behavioral diagrams.

DH structural models

We begin by looking of the structure of a third generation district heating in Sweden as depicted in figure 2, which is a SysML bock definition diagram (bdd). We find the three expected sub-blocks of production, distribution, and consumption. One block that is usually not mentioned is the system management part, although it is just as essential. When models are clearly drawn, they propel the discussion of what was not initially considered. The coordination of district heating, including the billing of end customers, does exist but is often omitted. Through modeling, it is also those omissions that we are trying to capture without overwhelming the stakeholders. It is system management that we can find OPTi Sim.

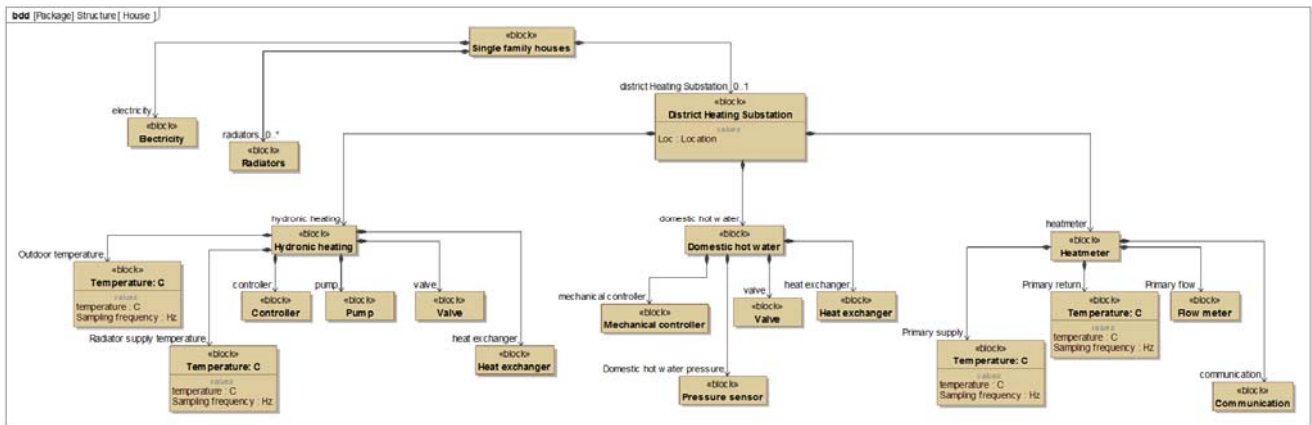


Figure 3: A block definition diagram of a single family house.

One advantage of MBSE is to go deeper into a block to further one's understanding when this is of interest. In the present case, we can dive into the consumption block and further into the single family house, whose bdd is shown in figure 3. Of interest here is the standard district heating substation, which takes a majority of the diagram.

To improve communication between the different modules within the DH substation, we added tiny web servers on several of them [14, 15]. Figure 4 shows a graphical model of a substation where the wireless servers are depicted with an "S". The energy meter, the valve on the primary circuit to the space heating heat exchanger, the temperature sensor of the supply line to the radiators, the space heating circulation pump, and the outdoor temperature sensor each have their own web servers. Similar to a search engine or a bank web server, these little web servers offer services. For example, the outdoor web server measures temperature and offers a temperature service. Those tiny web servers are dubbed Mules [16]. Figure 4 also has an access point or gateway, which is composed of a BeagleBone computer and a Mulle, as illustrated by the bdd in figure 5. The figure additionally shows the software modules of interest: the three core services, the gatekeeper service, and a district heating application. The district heating application could be the one that controls the valve on the primary circuit to the space heating heat exchangers based on outdoor temperature and supply temperature to the radiators. It could also be another application such as a building thermal analysis. One advantage with SOA is that these modules can be developed after infrastructure deployment; this being an essential key to 4GDH. This exemplifies the ideas of loosely coupled modules and late binding. Being software modules, the services can exist on any servers in contingency to a gateway malfunction thereby avoiding a single point of failure, which typifies to system fault tolerance concepts. Having an idea about the structure of the system of

systems down to a single wireless sensor server or service provider, a demonstration of how the system behaves is essential to begin to accept the SOA idea.

Among SysML's behavior diagrams are the sequence diagrams with their "swim lanes" as depicted in figure 6. We begin with a simple service discovery sequence diagram to demonstrate how SOA functions. We then present a sequence diagram with all the three core services in a local cloud. Figure 6 shows the outdoor temperature server presenting its temperature service to the service registry. It does that by POSTing, using the World Wide Web's representational state transfer (REST) style, the following message:

```
{
  "name": "temperature-em219",
  "type": "temp-json-coap.udp",
  "host": "[fdfd::df5:8c6a:5ca2:44a6]",
  "port": 5683,
  "properties": {
    "property": [
      {
        "name": "version",
        "value": "1.0"
      },
      {
        "name": "path",
        "value": "/temperature"
      }
    ]
  }
}
```

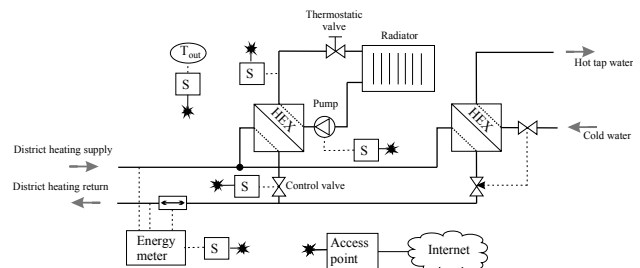


Figure 4: A district heating substation with a wireless sensor network, where each "S" is a tiny wireless server.

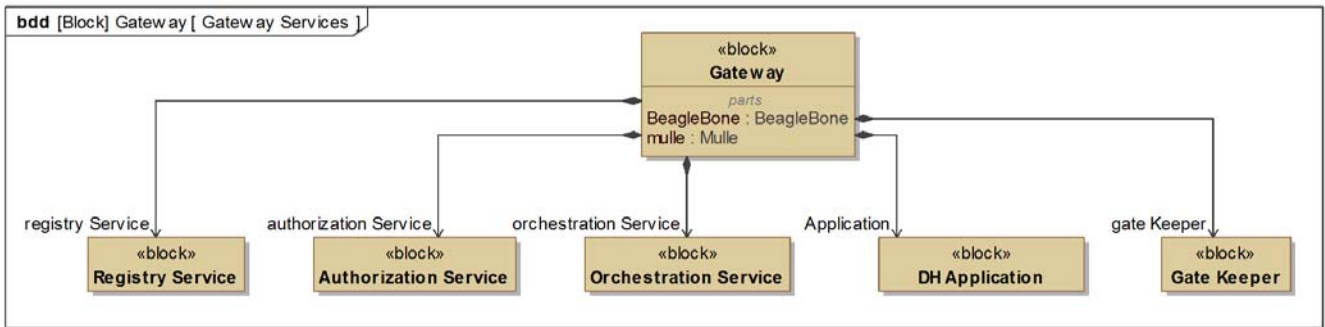


Figure 5: The gateway composed of a BeagleBone, a Mulle, along with the core services and an application.

With this posting, the service provider system tells its name, its chosen communication semantic, and the path to the service it offers. Additional services would be listed in the property array. By default or from an installation update, the service provider knows to register its services at the gateway host (host address and port).

Returning to figure 6, the service registry then builds a database of available services from all possible providers. Arrowhead's service registry is based on

DNS-SD, which is an extension to DNS. DNS, domain name system, part of the Internet Protocol Suite's application layer, provides the address at which a service is hosted. The service discovery extension, DNS-SD, provides the ability to discover services, which an application might want to use.

A service consumer, e.g., the DH application, then can ask the service registry for the desired service and receive back the address of the service provider with the path to the service of interest. The service

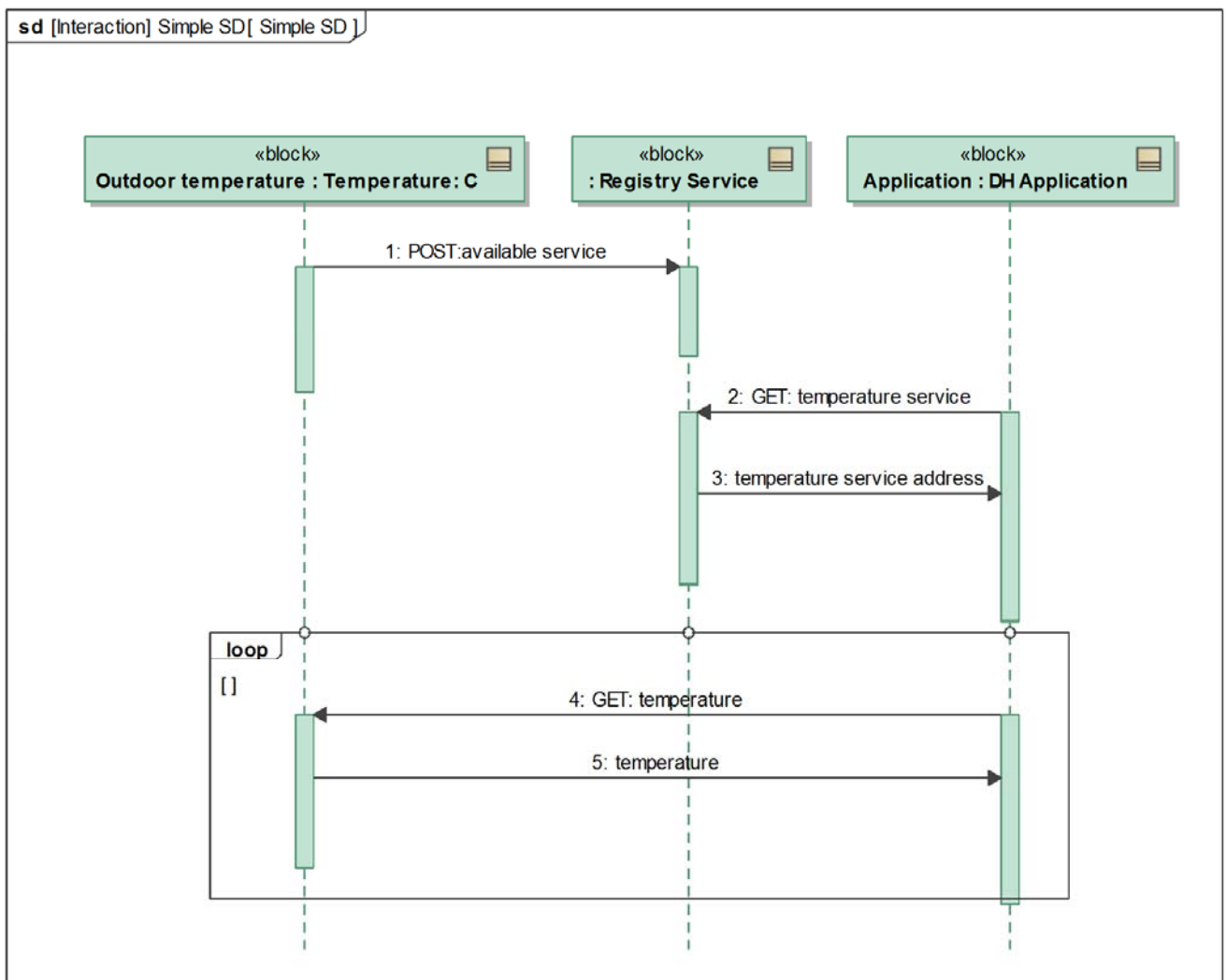


Figure 6: Sequence diagram of a service registry and discovery.

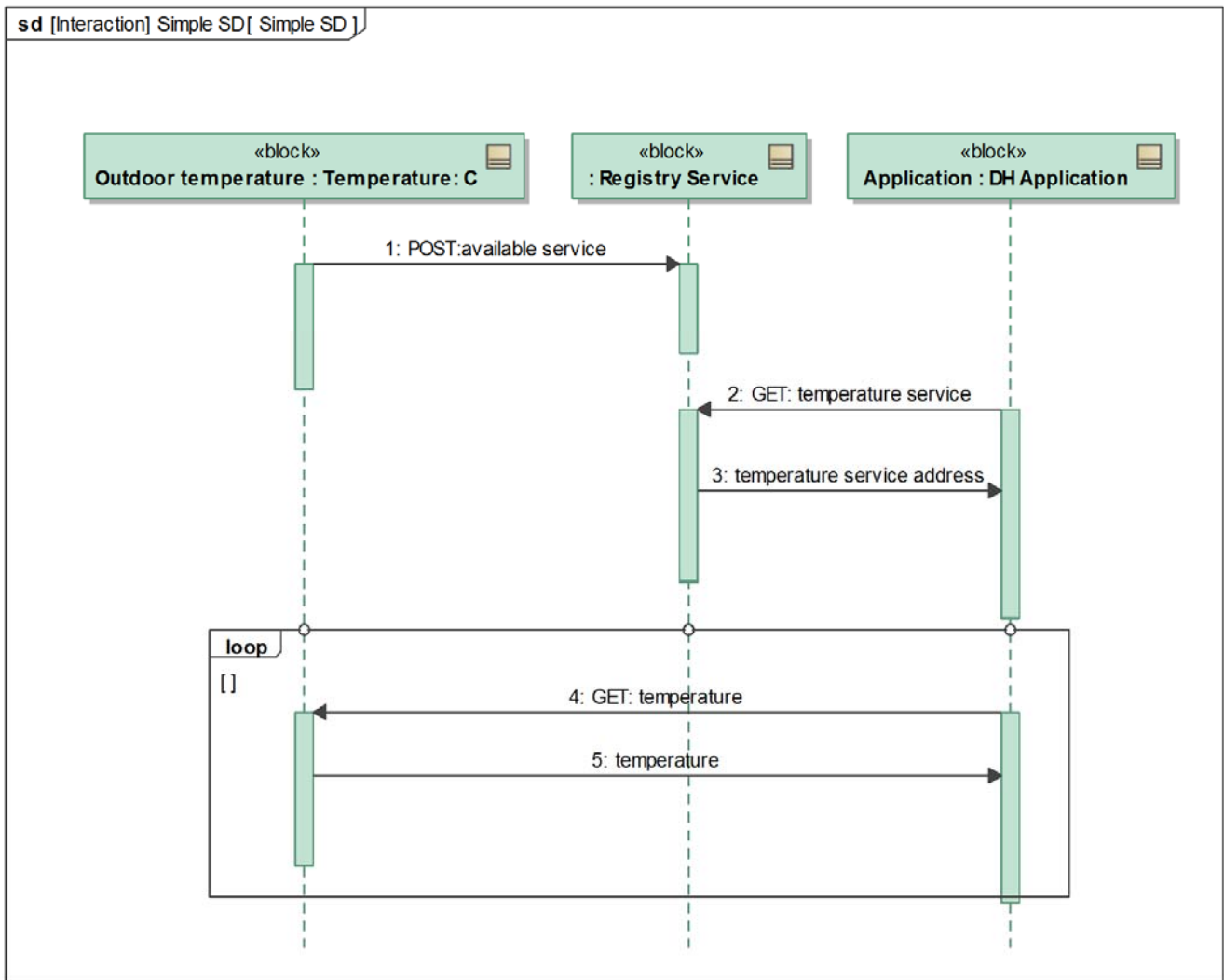


Figure 7: Sequence diagram with all three Arrowhead Framework core services.

consumer directly contacts the service provider whenever it wants the needed information, also referred to as “pulling”. The answer from the service provider is:

```

{
  e: [{
    "n": "urn:dev:mac:0024beffffe804ff1",
    "t": 1425256855,
    "u": "Cel",
    "v": 23.5
  }]
}
  
```

with its name, the timestamp of measurement, along with the unit and measured value. Alternatively, after being requested by a consumer, the service provider could “push” an update at specific time interval or upon some agreed event. The Arrowhead Framework does not restrict pull and push behaviors.

With service discovery recounted, several natural questions surface up and include the following. What is the latency in the control loop? How is security assured both for privacy protection and against tampering? How

are service selections sorted out in the case of multiple providers and how is provider drop out handled? How is the connection to the Internet handled?

The Arrowhead project has addressed such questions by first defining local clouds. The service consumers do not interact with the service providers through a cloud far away, rather through a local cloud, e.g., the gateway. This assures the low latency necessary in control application and offers some security from the outside world. Additional security is handled by the authorization service, which could use certificates or tickets. Figure 7 shows the sequence diagram using the Arrowhead Framework core services. If the service provider is power constrained, it would prefer to receive an authorization ticket with a limited lifetime to communicate with a given consumer to avoid wasting power by obtaining an authorization at each request. The logic is that the consumer obtains a ticket from the authorization service, which it passes on to the service provider. The service provider then checks if it is valid with the authorization service and if so, then will

communicate with the consumer for the lifetime of the ticket.

The third core service proposed by the Arrowhead project is the Orchestration service. Its purpose is to give some “intelligence” in the selection of service provider or recommend an alternative provider when a specific one has dropped out. If the application itself is enhanced with this ability, it does not need the orchestration, but this would mean that the application is quite specific and not general, leaving the choice to a system architect. For example, if the outdoor sensor is offline, the orchestration service could infer the outside temperature from the heat meter’s primary supply temperature or go beyond the local cloud.

The Arrowhead Framework has a collection of services such as the Gatekeeper to interact safely with the Internet or the Historian to log data. With service providers like the Gatekeeper, the Arrowhead Framework permits collaboration between local clouds to build a system of systems where the OPTi Framework entices collaboration as optimized performance benefit all stakeholders. The Gateway can then join other clouds, e.g., a district heating cloud, to provide and consume services in the same manner as is done in the local cloud. This notion ensures scalability of the systems; a concept the Internet has already proven. It also addresses possible failure points, e.g., if some parts of the communication network would be unreachable, the OPTi framework could, as a service, provide estimated values of the current state within the DH network. SOA, being based on the same architecture as the World Wide Web, empowers the transition in and evolution of the 4GDH with security and ease of maintenance.

CONCLUSION

Using MBSE and SysML, we have modeled a district heating’s structure and zoomed down into a substation. The substation incorporated very small wireless sensor and actuator nodes that were web servers offering services. Using SysML’s sequence diagrams, we have illustrated the message exchange between service providers and consumers in partnership with the Arrowhead Framework core services. The advantages with the Arrowhead Framework include properties such as loosely coupled modules (i.e. two SOA systems do not need to know about each other at design time to allow a runtime data exchange), late binding (i.e. the exchange of data between two systems is established at runtime), autonomy, pull and push behavior (i.e. data can be requested or sent without request upon predetermined conditions), several standardized SOA protocols, data structures, information semantics, and data encryption. As we zoom out from the district heating substation to the distribution network and

production plants, we use the OPTi Framework to address scalable data management, macro and micro simulations, which can be applied to manage and optimize the 4GDH while we point to new collaborative and emerging behaviors of a system of systems. We contend that the use of these two frameworks support the transition into, as well as the growth of, the 4GDH.

ACKNOWLEDGEMENT

The OPTi project has received funding from the Horizon 2020 Research Programme of the European Commission under the grant number 649796. The Arrowhead project is a part of Artemis Innovation Pilot Project. ARTEMIS stands for “Advanced Research and Technology for Embedded Intelligence and Systems”- and is the European Technology Platform for Embedded Computing Systems.

REFERENCES

- [1] S. Frederiksen and S. Werner, District heating and cooling. Lund: Studentlitteratur, 2013.
- [2] D. Connolly, H. Lund, B. V. Mathiesen, S. Werner, B. Möller, U. Persson, T. Boermans, D. Trier, P. A. Østergaard, and S. Nielsen, “Heat Roadmap Europe: Combining district heating with heat savings to decarbonise the EU energy system,” *Energy Policy*, vol. 65, pp. 475–489, 2014. [Online]. Available: <http://dx.doi.org/10.1016/j.enpol.2013.10.035>
- [3] H. Lund, S. Werner, R. Wiltshire, S. Svendsen, J. E. Thorsen, F. Hvelplund, and B. V. Mathiesen, “4th Generation District Heating (4GDH): Integrating smart thermal grids into future sustainable energy systems,” *Energy*, vol. 68, pp. 1–11, 2014. [Online]. Available: <http://dx.doi.org/10.1016/j.energy.2014.02.089>
- [4] M. W. Maier, “Architecting principles for systems-of-systems,” *Systems Engineering*, vol. 1, no. 4, pp. 267–284, 1998. [Online]. Available: [http://dx.doi.org/10.1002/\(sici\)1520-6858\(1998\)1:4\(267::aid-sys3\)3.0.co;2-d](http://dx.doi.org/10.1002/(sici)1520-6858(1998)1:4(267::aid-sys3)3.0.co;2-d)
- [5] A. Gylling, “Optimization of District Heating & Cooling Systems,” accessed 2016-04-29. [Online]. Available: <http://www.opti2020.eu>
- [6] Modelica Association Project Function Mock-up Interface, “Functional Mock-up Interface for Model Exchange and Co-Simulation v2.0,” Modelica Association, Linköping, Tech. Rep., July 2014. [Online]. Available: https://svn.modelica.org/fmi/branches/public/specifications/v2.0/FMI_for_ModelExchange_and_CoSimulation_v2.0.pdf

- [7] "Arrowhead," accessed 2016-04-29. [Online]. Available: <http://www.arrowhead.eu>
- [8] P. P. Pereira, J. Eliasson, and J. Delsing, "An authentication and access control framework for COAP-based internet of things," in IECON 2014 - 40th Annual Conference of the IEEE Industrial Electronics Society, Oct 2014, pp. 5293–5299. [Online]. Available: <http://dx.doi.org/10.1109/IECON.2014.7049308>
- [9] P. Varga and C. Hegedus, "Service interaction through gateways for inter-cloud collaboration within the arrowhead framework," 5th IEEE WirelessVitaE, Hyderabad, India, 2015. [Online]. Available: <http://www.arrowhead.eu/wp-content/uploads/2013/03/InterCloudServices.pdf>
- [10] P. Varga, F. Blomstedt, L. Ferreira, J. Eliasson, M. Johansson, and J. Delsing, "Making system of systems interoperable - the core components of the Arrowhead Technology Framework," IEEE Internet of Things Journal, vol. accepted for publication, August 2015.
- [11] H. Derhamy, J. Eliasson, J. Delsing, P. P. Pereira, and P. Varga, "Translation error handling for multi-protocol SOA systems," in 2015 IEEE 20th Conference on Emerging Technologies Factory Automation (ETFA), Sept 2015, pp. 1–8. [Online]. Available: <http://dx.doi.org/10.1109/ETFA.2015.7301473>
- [12] NASA, "NASA Systems Engineering Handbook," National Aeronautics and Space Administration, Washington D.C., Tech. Rep., Dec. 2007. [Online]. Available: <http://ntrs.nasa.gov/archive/nasa/casi.ntrs.nasa.gov/20080008301.pdf>
- [13] "Object management group," Mar. 2015. [Online]. Available: <http://www.omg.org/gettingstarted/gettingstartedindex.htm>
- [14] J. van Deventer, J. Gustafsson, J. Eliasson, J. Delsing, and H. Mäkitaavola, "Independence and interdependence of systems in district heating," in Systems Conference, 2010 4th Annual IEEE. IEEE, 2010, pp. 267–271. [Online]. Available: <http://dx.doi.org/10.1109/SYSTEMS.2010.5482342>
- [15] J. Gustafsson, "Wireless sensor network architectures as a foundation for efficient district heating," Ph.D. dissertation, Luleå tekniska universitet,, 2011. [Online]. Available: <http://pure.ltu.se/portal/files/32725662/JonasGustafsson.pdf>
- [16] EISTEC, "Mulle, Wireless Embedded Internet Systems," Mar. 2016. [Online]. Available: <http://www.eistec.se>

USING PREDICTIVE ANALYTIC SOFTWARE SOLUTION FOR IDENTIFYING EQUIPMENT FAILURE IN ADVANCE; THE UNIVERSITY OF TEXAS AT AUSTIN

A. Roberto del Real¹, B. Ho Joon Seo²

¹The University of Texas at Austin

²BNF Technology Inc.

Keywords: *Early Detection of Anomalies, Operation Excellence, Plant Health Index, Early Warning*

ABSTRACT

The University of Texas at Austin is well known for its quality of education and research. In order to maintain high standard of education, the uninterrupted and cost-effective power supply plays an important role. As a response to this, the University of Texas at Austin – Utilities and Energy Management decided to adopt predictive maintenance based innovative solution which would help them in achieving their goal of providing un-interrupted and cost effective power supply for university campus.

Technology wise Predictive Maintenance approach promises cost saving and improvement in both stability and performance over the routine or time based Preventive Maintenance. UT-UEM has deployed the Predictive Analytic Software Solution; PHI (Plant Health Index) which helps in improving Operational Excellence by early detection of any anomaly behaviours of sensors, equipment and operations of process plant. PHI also helps the analysis of the process uncertainty through statistical learning with simple to setup and easy modelling of operation history.

This paper explains how UT-UEM achieves its goals and identifies hidden problems in advance before they turn into catastrophic failure with the help of PHI. The case studies show how Predictive Analytic Software Solution helps UT-UEM by providing early warning of anomalies which could result in system and operation failures in its existing power plant systems. The studies also shows how UT-UEM identified the abnormal behaviour and hidden problems lies from sensor level to the associated equipment level for Gas Turbine, Steam Turbine and Boilers systems.

INTRODUCTION

Increase of energy consumption, issue of green policy and convergence of IT with operation has changed the circumstance of process plant operation. These days there is a lot of emphasis on reducing operating costs and process operation variability. Due to demand uncertainty and global competition from low cost source increases the process plant operators and maintenance people are trying out all possible measure to maximize operation excellence.

Process plants have been using various maintenance approaches to minimize cost and improve efficiency. The initial maintenance practice was called break down maintenance; performed only on equipment that is down, most of the time unplanned and after equipment failure, in occasions equipment was brought down on a planned basis; this type of maintenance was also called corrective.

The industry then later advanced to Preventive Maintenance approach which is a daily maintenance (cleaning, inspection, oiling and re-tightening), design to retain the healthy condition of equipment and prevent failure through the prevention of deterioration, periodic inspection or equipment condition diagnosis, to measure deterioration.

Preventive Maintenance was later changed to Proactive Maintenance defined as a plan giving a company the ability to prolong the life of machinery and prevent a complete and unexpected breakdown of production facility. A Proactive Maintenance plan allows an organization to schedule production shutdowns for repairs, inspection and maintenance.

As the industry evolved, Predictive Maintenance method became more prevalent. This is a method in which the service life of important parts is predicted based on inspection or diagnosis, in order to use the parts to the limit of their service life. Compared to periodic or preventive maintenance, predictive maintenance is condition based maintenance. It manages trend values, by measuring and analysing data about deterioration and employs a surveillance system, designed to monitor conditions through an on-line system approach that is found to be the most efficient among all the practices.

Earlier, while break down maintenance or corrective maintenance approach were used, there were large maintenance budgets to maintain a plant. Although this approach gives the best utilization of the components in a plant, the high cost incurred lead the plant operators to use the preventive maintenance approach. With preventive maintenance, the objective was to keep the plant in a good condition. In which the working components had to be often replaced with new one or refurbished parts. Although it helped to avoid major plant trips, the approach was not adequate to improve the availability, operational excellence and minimize

the maintenance cost. Proactive maintenance approach was considered an expensive maintenance approach in which the maintenance people, based on the mean time between the anomalies, were replacing the components in the plant. Necessity for cost reduction and performance improvement paved way to the predictive maintenance approach.

Predictive maintenance approach is widely used by process industry these days. It reduces unnecessary maintenance activities and improves both stability and performance with early detection of decreasing reliability of plant equipment. This is accepted by the plants as the best available practice maintenance with a low cost.

As University of Texas at Austin has the large R&D infrastructure, UT-UEM has responsibility to stably supply electricity to the campus. So, UT-UEM decided to adopt predictive maintenance based innovative solution which would help them in achieving its goal of providing un-interrupted and cost effective power supply for university campus.

BACKGROUND

PHI is the plant condition monitoring and predictive analytics solution. It provides an early warning when there is potential, hidden and functional failures for sensors, transmitter, equipment and operations of process plants before any catastrophic failure occurs.

For prediction of those failures in advance, the system uses the algorithm based on the advanced empirical models. It utilizes historical data having normal plant operation data. With the historical data, PHI designs empirical models with fault free historical normal operation data of a plant and groups correlated signal of the equipment.

With the prediction models designed by PHI, it measures discrepancies between the real-time operating condition and predicted operating condition. Then, any discrepancies in current conditions of the plant are indicated as percentage. The percentage means the plant's health condition.

When the health is seen deteriorating and needs to be analyzed, we could depend on both historical and real-time trend chart as well as track the anomalies using the success tree with plant's hierarchical chart.

In addition, it provides an alarm when the difference exceeds a certain set point determined by the viewpoint of safety and efficiency.

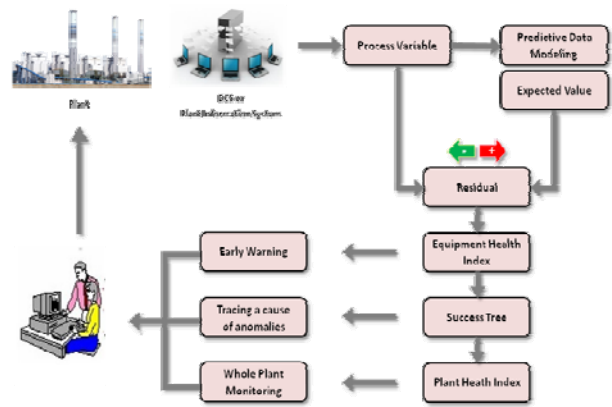


Figure 1 Diagram explaining the working of PHI

Table 1

Tag Name	Act. Value	Exp. Value	EU Range	
			Low	High
HPCompressor-Discharge_Acoustic_Dynamic_Pr_PX36A_PT809 0A	5.4	1.7	-1	10
HPCompressor-Discharge_Acoustic_Dynamic_Pr_PX36A_PT809 0B	6.5	1.7	0	10

RESULTS

PHI has been installed in UT UEM since 2013. There are several systems running in the plant located at the University of Texas at Austin campus. It is monitoring boiler 3, 7, CTG (Combustion Turbine Generator) 8, 10 and STG (Steam Turbine Generator) 7, 9.

Case 1

HP compressor discharge acoustic dynamic pressure was unstable and changing 1.7 to 10.5 (Unit: PSID) during 21:45 to 2:00 hours on 27th April 2014 (Refer Table 1). Large fluctuations in CTG10 speed and acoustic vibration levels were also observed after that the CTG10 was stopped and tripped.

The earliest indication of the problem was alerted by PHI on the 14th January 2014. Until the CTG 10 stopped and tripped, there were five (5) early warnings of the potential anomalies (Refer Figure 1).



Figure 2. Trend Analysis

To define and fix the problem, the manufacturer of the equipment was contacted to discuss reason for trip which was related to unit speed. According to GEK 112767 Volume I; the VSV system senses gas generator speed and compressor inlet temperature, and positions the VSV's. For any temperature and any speed, the VSV's takes one position and remains in that position until the NGG or T2 changes.

As a result, the T2 control logic at a steady temperature was corrected and the CTG10 has been operated with better CS (Source of Cooling) performance. The PHI system has continued to monitor the systems conditions.

Case 2

On 12th October 2015, the health index of FD Fan of the Boiler 3 has been dropped down to 25%. On 22nd November 2015, the same situation happened again. The vibration in the torque of the Boiler 3 West FD Fan was identified by PHI (Refer Figure 3). It detected the West FD Fan torque was varying.

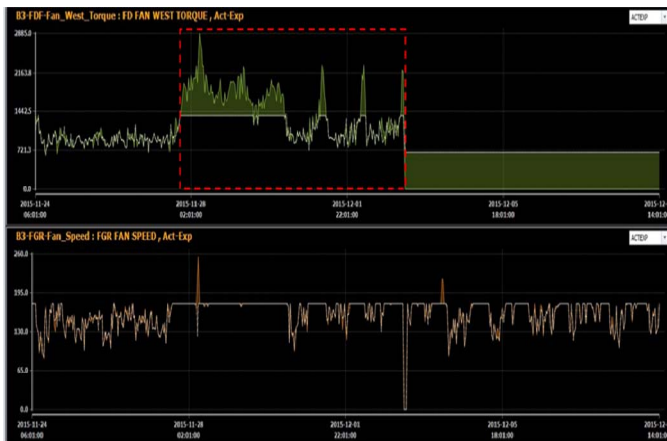


Figure 3. The vibration in the torque of the Boiler 3 West FD Fan

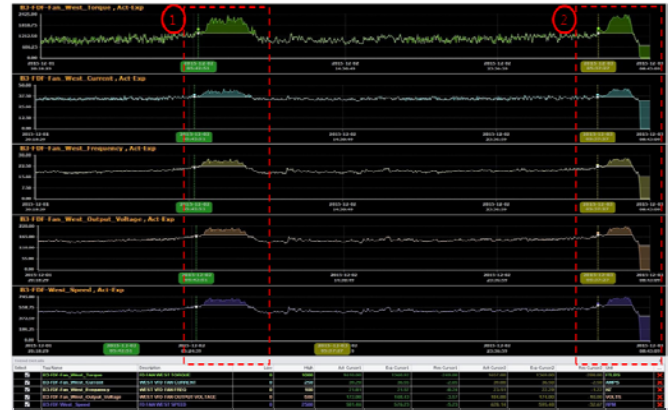


Figure 4. Discrepancies between the predicted and actual values

The same behavior was repeated on 2nd and 3rd December 2015 until the boiler 3 was shut down for repairing.

A low health index was observed on boiler 3 and after analysis it was discovered that there were variation in west fan torque and the current as shown on actual-expected trend.

This behavior alerted by PHI, but was not observed the plant HMI system and historian. There were two differential pressure transmitters which were not in the same position hence the difference in readings. Ideally the readings from both instruments should be exactly same however it was about 180% more than the other one. As s maintenance, the boiler was shutdown and calibrated the meters.

After calibration the difference in readings has been improved remarkable, there is need to calibrate those instruments for further accurate reading.

Case 3

.....do we have more cases?

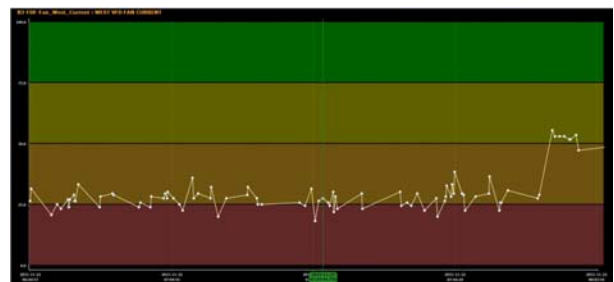


Figure 5. Alarm Trend for analyzing the problem

CONCLUSION

For achieving operational excellence of a plant, it is very important to find out hidden failures in advance, prevent catastrophic failures in advance, and improve operation and process.

As it is seen from the results obtained after implementation and use of the Plant Health Index monitoring system, the UT-UEM has adopted the advanced technology such as predictive analytics which alerts Plant operators about sensors, transmitters, equipment, and operation failures before it happens. A key difference with a more common monitoring system is that the PHI alerts on system behaviour in any condition either running at full load or partial load. PHI alarms are atypical in that they don't represent necessarily a failure condition, but a condition that is to take place if an issue is not addressed; this alone represents a considerable difference with another system that only alerts the operator when something is already in alarm. PHI shows the actual value of an instrument VS the expected value before the instrument alarm is triggered. Based on the system, UT-UEM has kept reducing unexpected equipment failures, and unplanned maintenance activities and outage time.

....do we have any saving data to prove effect of PHI?

THE INVESTIGATION OF FAILURE RATE REDUCTION IN HEAT METERS FOR DISTRICT HEATING

W. Kang¹, H-M. Choi¹, Y-M. Choi¹, C-Y. Kim¹, J-S. Lee², S-Y. Lim²

¹ Korea Research Institute of Standards and Science, Daejeon, Republic of Korea

² Korea District Heating Corporation, Seoul, Republic of Korea

Keywords: Heat meter, Failure rate, District heating, Calculation unit

ABSTRACT

A heat meter is a device which measures heat energy consumption in a heat-exchange circuit for district heating metering and billing. A heat meter typically consists of two resistance temperature sensors, volume-flow sensors and calculation units. Faults of heat meters in the district heating systems in use in Korea occur most frequently (55%) in turbine flow sensors. However, this type of fault is easy to discover and repair because it stems from visible mechanical problem. 41% of faults in heat meters are caused by temperature sensors and calculation units due to malfunctions related to signal transmission and electronic circuits which cannot easily be discovered. In the present study, in order to reduce the failure rate of heat meters in district heating systems, the major causes of common faults in temperature sensors and calculations units are investigated using failed used-heat meters. The connection conditions between temperature sensors and calculation units exposed to severe environments involving high temperatures, humidity levels and electric disturbances are revealed as significant causes of malfunctions in heat meters. A novel interface model between temperature sensors and calculation units is proposed to improve the temperature signal transmission. An accelerated reliability test at a high temperature and a high humidity level of the used calculation units was also carried out to simulate the installation environments of heat meters, such as boiler rooms in Korea.

INTRODUCTION

A heat meter is a device which measures heat energy consumption in a heat-exchange circuit for district heating metering and billing. District heating is a technology used to deliver heat energy from a central production facility to large buildings or apartment complexes [1, 2]. Recently, the demand for heat meters is increasing for efficient and economical heating. In Korea, currently 6,000 heat meters are installed and operated by the Korea District Heating Corporation (KDHC). On average, 1,500 heat meters are purchased annually to maintain district heating systems.

A heat meter typically consists of two resistance temperature sensors (PT sensors) for the supply and return through a heat exchanger, volume-flow sensors and calculation units (Figure 1). A turbine-type meter is commonly used as a volume flow sensor in Korea. The calculation units with a modem (RS 485) compute the quantity of heat which can be obtained by flow rates and the temperature difference between the two temperature sensors. The quantity of heat including the flow rates and the temperature difference by the hour is read remotely once a day through a Public Switched Telephone Network (PSTN).

The components of heat meters break down or cause failures by several reasons [3, 4]. In KDHC, the average annual failure rate was 6.8% for five years (2008 – 2011). Malfunctioning heat meters are replaced or repaired at the installation site. Flow sensors have been identified as the most common source of faults (55%), but these faults are easy to find and repair because they stems from visible mechanical issues. 41% of faults in heat meters are caused by the temperature sensors and calculation units due to malfunctions in the signal transmission and electronic circuits which are hard to find.

In present study in an effort to reduce the failure rate of heat meters in district heating systems, the major causes of common faults in temperature sensors and calculations units are investigated. In addition, a novel interface model between temperature sensors and calculation units is proposed to improve the temperature signal transmission characteristics. An accelerated reliability test at a high temperature and a high humidity level with the used calculation units was

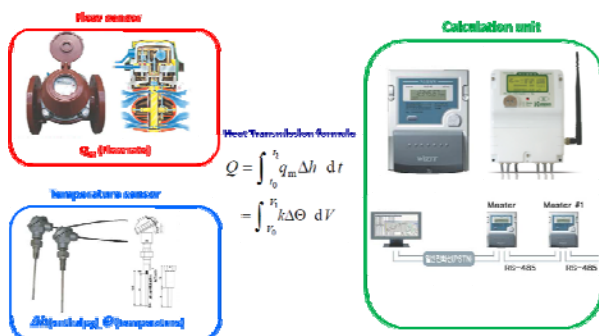


Figure 1. The components of a heat meter

also carried out to simulate the typical installation environments of heat meters such as a boiler room in Korea. Electric transient and electric magnetic tests of the heat meters were also carried to assess the vulnerability of heat meter in harsh installation environments exposed to electromagnetic noise.

FAILURE TYPES OF HEAT METERS

In order to investigate the most frequent type of failures of temperature sensors and calculation units, the replacement or repair history from 2010 to 2013 in KDHC was reviewed. Table 1 shows statistics pertaining to failure types of the temperature sensors and calculation units.

Table 1. Failure typed of temperature sensors and calculation units

Failure type	Proportion
Modem (CPU, Communication) faults	40%
Lighting (Electrical shock) damage	22%
Power supply faults	14%
Communication line faults RS485)	11%
Pulse detection & Calculation faults	6%
Data transmission malfunction	3%
Display part faults	2%

The modem part and power supply of the calculation units have been identified as the most common sources of faults. The main causes of these faults were the electrical shocks from the severe installation environments of heat meters, which operate in high-temperature and high-humidity environments such as boiler rooms as shown in Figure 2. Contact failures between calculation units and the signal lines of temperature sensors also occur frequently.

FAILURE RATE REDUCTION OF HEAT METER

To reduce these failures of heat meters in KDHC district heating systems, first, we proposed a novel interface technique between the calculation units and the signal line of temperature sensors. In the current design of a heat meter, the signal lines of the temperature sensor connected directly to the electric circuit of the calculation units. These are exposed to electro-magnetic noise and shocks (e.g., surges, lightning) due to severe installation environments such as those containing large mechanical equipment (motors) and poor electrical ground conditions. Although the replacement or repair of the heat meter is not needed, such an environment can affect the transmission of accurately measured temperatures by the temperature sensors. In order to resolve this vulnerability in the transmission of temperature signals, in the present study we designed and installed a digitized-computational interface board in a PT temperature sensor. This board converts the analog - signal of the measured temperature to a digital - signal as shown in Figure 3 and 4.

The driver in the interface board sends the temperature signals of the PT resistances by changing a single - ended signal into a differential signal, which is advantageous for long distance transmission. In the receiving parts of the calculation units, the transmitted signals can be changed back to single-ended signals.

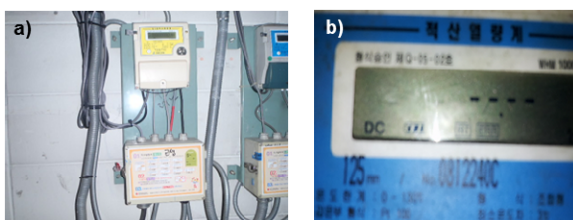


**Figure 2. a) Installation environments of heat meters
b) Electrical shock damage**

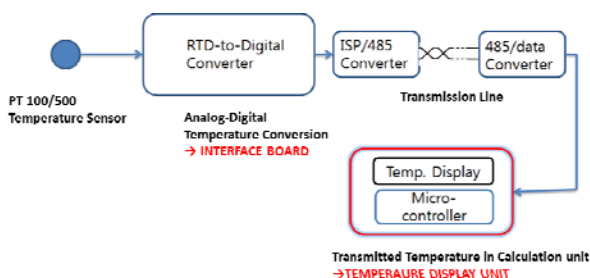


Figure 3. Proposed new interface between the temperature sensors and calculation unit

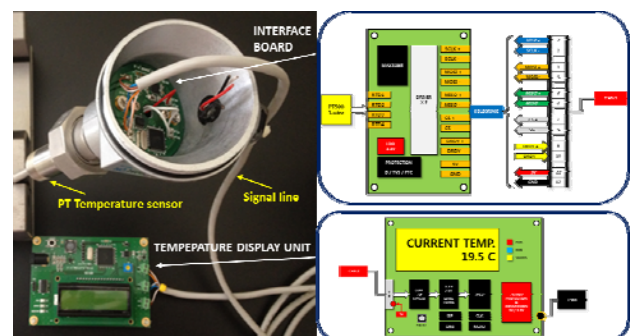


Figure 4. The interface board installed at temperature sensors and the temperature display unit.



Figure 5. Temperature and humidity chamber for accelerated reliability test

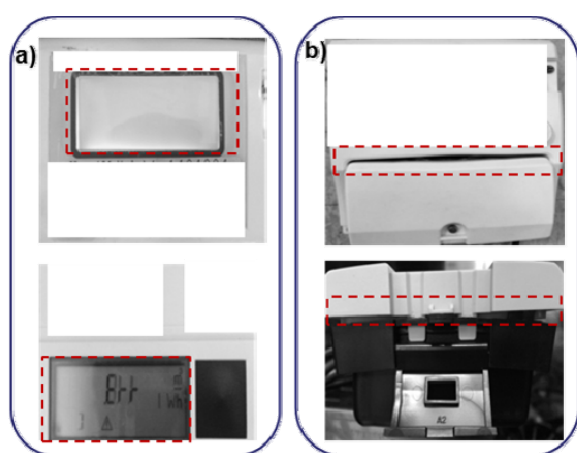


Figure 6. a) LCD failure in display units b) Gaps in the calculation units

Thus, digitized temperature signals can be stably transmitted from the temperature sensors. This will increase the reliability of long- distance transmissions within harsh environments compared to the heat meter currently in use.

For the second study regarding to the reduction of failure rate of heat meters, we investigated the durability of heat meters in the harsh installation environment such as boiler room with high temperature and humidity levels as well as electric-magnetic shocks source. These heat meters are subject to type-approval tests according to the Korea industrial standard of heat meters (KS B 50075-1, 2), which is equivalent to OIML R7 5-1,2 [5, 6]. Regarding environments with high temperatures and high humidity levels, these heat meters are exposed to cyclic damp heat in a damp heat cyclic test (section 6.9 [6]). The test conditions included a temperature of 55 °C and humidity level of 93 %. However, the installation environments of heat meters, such as boiler rooms and machine room are more severe than the test conditions in the type-approval test.

Even if a heat meter passed the damp heat cyclic test, it can still cause a malfunction in the field when used in a harsh installation environment. Thus, a durability test for similar to that of the installation locations of heat meters is required. As another metering device with a less severe installation environment compared to those of heat meters, a watt-hour meter in Korea is subject to accelerated reliability test (IEC 62059-31-1) with a temperature of 85 °C and humidity of 95% according to the own standards of Korea Electric Power Corporation. In the present study, for a proper simulation of the installation environments of heat meters, accelerated reliability test is carried out using the test condition of the watt-hour meters used in Korea which are a temperature of 85 °C and humidity level of 95%. These tests were conducted with two domestic heat meters used at KDHC. In addition, two heat meters from an overseas company were also tested for a performance comparison with domestic products. The test method involved putting four heat meters into a temperature and humidity chamber as shown in Figure 5 with a test condition of temperature of 85 °C and humidity of 95%. We stopped and measured the performance test results (e.g., permissible error of heat quantity) of the heat meters every 24 hours.

After 24 hours with tests, an operational failure occurred on a LCD display unit of two heat meters (one domestic and one foreign heat meter) as shown in Figure 6(a). The tests could not continue.

The tests for the other two heat meters were able to proceed for five days (120 hours), but showed unsatisfactory performance results with lying outside the permissible error. A gap in the appearance of the calculation units also occurred, as shown in Figure 6(b).

The accelerated reliability test results of four heat meters showed that the current standards and type-approval test conditions were not be able to guarantee the performance of heat meters in harsh installation environments such as machine and boiler rooms.

We also evaluated the durability of heat meters in harsh environments with electric-magnetic shock sources. Heat meters in Korea are subject to electric transient test including bursts (section 6.11.1), surges (6.11.2), electromagnetic field (6.12) and electrostatic discharge (6.13) in type approval tests of KS B 50075-2. Watt-hour meters had more rigorous test conditions in the standards compared to heat meters as shown in Table 2.

Table 2. Comparison test conditions for electric tests of heat meters and watt-hour meters

Test type	Test conditions	
	Heat meter	Watt-hour meter
Bursts	1.0 kV	2.0 kV
Surge transient	0.5 kV	1.0 kV
Electromagnetic field	26 –1000 MHz	1100-2000 MHz
Electrostatic discharge	Air 8 kV	Air 8 kV
	Contact 4kV	Contact 15 kV

In the present study, the electric transient and electric magnetic tests of two heat meters (one domestic and one foreign heat meter) were carried out using more rigorous standards pertaining to watt hour meters to simulate the harsh installation environments of heat meters. The test results indicated that foreign heat meter experienced a failure in the surge transient test at 1.0 kV. This demonstrated the vulnerability of heat meters in installation environments exposed to electromagnetic noise.

CONCLUSION

A heat meter is a devices which measure heat energy consumption in a heat-exchange circuit for district heating metering and billing. Recently, the demand for heat meters is increasing for efficient and economical heating in Korea. However, faults of heat meters in district heating systems in Korea have occurred at average annual rate of 6.8% for five years. 41% of faults in heat meters are caused by the temperature sensors and calculation units used in them due to signal transmission and electronic circuits malfunction which are difficult to find.

The modem part and power supply components of calculation units have been identified as the most common source of faults due to electrical shocks from the severe installation environments of heat meters, which associated with high temperature and humidity

levels, such as machine and boiler room. To reduce these failures of heat meters in KDHC district heating systems, we proposed a novel interface technique between the calculation unit and the signal line of temperature sensors, composed of a digitized-computational interface board in the PT temperature sensors for the reliable long-distance transmission of temperature signals. The accelerated reliability test results of four heat meters operating in harsh temperature and humidity conditions showed that the current standards and type-approval test conditions could not guarantee the performance of heat meters in harsh installation environments, such as machine and boiler rooms. The electric transient and electric magnetic tests of heat meters with the more rigorous standards used with watt hour meters demonstrate the vulnerability of current heat meters in installation environments exposed to electromagnetic noise.

ACKNOWLEDGEMENT

This work was supported by Korea District Heating Corporation under the project “Research on Failure Rate Reduction of User-Transaction Heat Meter”

REFERENCES

- [1] Y.Jomni, J.V. Denventer, J. Delsing, Model of a heat meter in a district heating substation under dynamic load, Proceeding for the Nordic MATLAB Conference, 2003
- [2] Y. Jomni, “Improving Heat Measurement Accuracy in District Heating Substation”, Doctoral Thesis, Department of Computer Science and Electrical Engineering, Lulea University of Technology, 2006
- [3] K. Yliniemi, J. Denvener and J. Dlesing, “Sensor faults detection in a district heating substation”, 10th IMEKO TC10 Conference, 2005
- [4] K. Yliniemi, Fault detection district heating substations”, Licentiate Thesis, Department of Computer Science and Electrical Engineering, Lulea University of Technology, 2005
- [5] OIML, Heat meters Part 1: General requirements, OIML R 75-1, 2002
- [6] OIML, Heat meters Part 2: Type approval test and initial verification tests, OIML R 75-2, 2002

EFFICIENCY OF STRAINERS

D. Waldow¹, G. Waldow¹

¹W-FILTER

Keywords: life-cycle cost, energy saving, plant efficiency, strainers

ABSTRACT

The longer the time between necessary maintenance, the more effective a plant is operating, due to less stoppage and more output. Limiting the resources carrying out the maintenance and also the handling will help to shorten also the time needed and going back to operation of the plant. Hence, the selection of strainers requires a detailed consideration of efficiency and effectiveness lowering not only operational but overall life cycle cost.

Procurement of strainers, however, is mainly based on the buying price, even though its energy cost is not only between 11% and 50% but even between 60% and 300% of its initial price.

The maintenance cost of strainers is – depending on the plant and the respective production downtime – in the range of 50% to 2000% and more of its buying price!

In this paper, we have carried out an economic analysis of strainers in the market providing an overview about the cost involved. First of all, we have set the frame work for selecting the strainers to be assessed. Having chosen three strainers from the market, we focused on the cost factors initiated by each of them: such as the energy cost of a clean strainer, pollution characteristics of the sieves that are resulting in the frequency of cleaning and its related maintenance cost.

We have compared the operating cost caused and summarized all expenditure aspects to the overall life-cycle cost of the different strainers. Enabling operators to increase their plant efficiency by considering the various aspects related to strainers.

INTRODUCTION

Despite the necessity of strainers, but due to its small quantity needed in plants and hence the resulting low investment volume, to most people involved (such as plant engineers, purchaser and valve manufacturer) the selection of strainers is rather considered as “triviality”, something “also required” or “able to supply”.

As an excuse to all parties involved, one could state, that there is:

- Rather no relevant DIN-Norms on the technical conditions or even
- Economically viable requirements on pressure loss,

- And resulting from the above neither those respective values stated in the brochures!

Table 1: example of selection parameters (i.e. car)

Brand	Price [€]	Energy cost Liter/100km	Maintenance cycle at km
X	31.000	33.5 (50%)	15 000 (2-3%)
Y	36.000	11.7 (15%)	10 000 (3-4%)
Z	37.000	8.5 (11%)	30 000 (ca 1%)

() = % of the initial price with approx. Mileage of 30.000 km/year

Providing an example: Assuming, a procurement of an i.e. car would be decided on the following offers,...

...then a decision would be done quite easily

Let us know focus on strainers, the frame-work of comparison and the various cost factors involved.

CHOOSING THE STRAINERS TO BE COMPARED

On the basis of the criteria

The following criteria of options and characteristics provided the frame for our model plant selection:

- market relevancy: nominal pressure (PN), nominal diameter (DN), construction materials,
- shape of sieves/screens (flat, curved, round, etc.)
- temperatures (from low to high temperature levels)
- connections (welded ends, flange connection)
- flow rate (from 0.5 to 6 m/s)
- sieve fineness (from 10 μ to 5 mm)

Operating conditions of the model plant:

We selected the following model plant and its technical data as a basis for the comparison of different types of strainers:

- medium water: $\gamma = 1000 \text{ kg/m}^3$
- pressure rating PN 16 (operating pressure and temperature can be neglected)
- throughput 365 m³/h = velocity of 3 m/s with
- nominal diameter DN 200, sieve fineness 0.5 mm
- pump efficiency $\eta = 0,75$
- price for electricity € 0.10/KWh

Connection of the strainers: Flange connection, even though we would have preferred the technically more correct and more cost effective connection by welded

ends. In addition, the respective list prices of the different strainers had been used for comparison.

Table 2: pipe components and its appearance

Plant component	Price Style	Energy demand Appearance	Maintenance cost
Elbow tube	known	constant	none
Shut-off valve	known	constant	yes, but low
Strainers	known	increasing	Yes, potentially high

Assumptions and experiences

Energy cost for a strainer in clean condition can exactly be determined (even by the hour).

Additional energy cost caused by the increased pressure loss, due to the growing dirt filtration, have been taken with the same amount into account as the cost in clean condition – realistically, this value increases its value 4-times at an exponential increase of the differential pressure.

We assumed that the degree of contamination is the same with all compared strainers. Hence, we have used a ratio value (W-Filter: 1) for the frequency of maintenance cycles, even though this is depending on the effective filtering area, angle of inflow and design of the sieve/screen.

The major cost factor related to a strainer is the maintenance cost and the resulting plant operation downtime. As a comparable value we have just taken €500. - per cleaning into account.

COST FACTOR

Various components and its resistances in the pipeline are slowing down the transport of liquids: whether tube, pipe elbows, valves or strainers.

And still, those components are causing different cost:

We can see out of the above, a strainer is a component, which is not expensive when procured, but will create its cost during operation. „Good“ strainers with low operating cost, can be identified even before they are purchased.

Being able to select a cost-effective strainer up-front, find the following information and formulas.

Energy cost of a clean strainer

A clean strainer comes with a given flow resistance figure (ζ) and is causing a pressure loss (Δp):

$$\Delta p = \frac{c^2 * \gamma}{2g} * \zeta [mWS] \quad (1)$$

c = flow velocity [m/s]

γ = throughput in kg/h

g = gravity = 9.81 m/s²

Overcoming the above mentioned pressure loss (Δp) a certain pump capacity (P) is required

$$P = \frac{Q * \Delta p}{\eta_p * 3600 * 102} [kW] \quad (2)$$

Q = throughput in kg/h

η_p = pump efficiency

With a given energy price (E) [€/kWh], the strainer will have a cost per hour (Kh) of:

$$Kh = P * E [€ / h] \quad (3)$$

With a plant, all operating parameters are determined – therefore, the Zeta-Value (ζ) becomes the only variable figure, that is defining whether high or low energy cost will exist in the plant.

This value, measured or calculated by the manufacturer, acts as an evaluation standard for the initial flow resistance with minimal energy requirement of a clean strainer.

Pollution of a Strainer

The dirt particles in a plant / pipeline can be classified into three categories:

- (1) particles < mesh size of the sieve: are harmless and will pass through the strainer to flow within the plant system;
- (2) particles > mesh size of the sieve: bounce off the sieve and will be collected apart from the main stream at the bottom of the strainer / sieve basket;
- (3) particles = mesh sizes of the sieve: are the ones, that will stick in the meshes of the sieve and due to the clogging of the sieve cause an increase of the pressure loss!

Flowing media will choose the lowest-resistance path between inlet and outlet of a strainer. Therefore, the dirt particles will clog the stream favorable area.

With increasing operation time, the effective filtering area not only becomes increasingly smaller, but the media stream needs to take a less favorable path through the strainer.

The increasing pressure loss is therefore not linear but exponential. Meaning, the higher the pollution level, the more increases the energy requirement / demand compared to a clean strainer.

Frequency of maintenance

There is no general valid answer to the question, whether a strainer needs to be cleaned „once a year“ or „twice a month“, as the level of dirt and hence contamination might be quite different.

Therefore, the criteria determining the need for cleaning the strainer shall be a defined value of the differential pressure itself, created by the contamination within the strainer.

Assuming, that a multiple security against destroying the sieve would determine the time for cleaning, then one would have to take into account, that such a threshold would be different at the same mesh width of the sieve of different dimensions (DN) as well as with the same dimensions (DN) with different mesh widths.

The mechanical strength of a sieve decreases with larger dimension and finer mesh width. Therefore, the usage of double-layered sieves is advisable.

Under the aspect of mechanical strength of the sieve, any brand would sustain a reference value of $\Delta p_{\max} = 400/DN$ [bar] (i.e. 2 bar with DN 200).

Taking economical operation of a plant as a measure into account, one would identify the cleaning times at an even lower Δp value. (Which plant operator would sacrifice 2 bar needed for the strainer out of the total 10 bar pump pressure and utilise the remaining 8 bar for transporting the medium through the pipeline?)

Once, the plant operator decided a particular pressure loss Δp by when the strainer needs to be cleaned, then the cleaning frequency depends on the following two factors (assuming, the same pollution level applies for all types of filters in the plant):

- Basic flow resistance ζ of a strainer in clean condition: An already high zeta-value will only allow a limited increase to the permissible resistance value and hence will require an early cleaning (short maintenance intervals);
- Time to reach maximum pollution level of a certain type of strainer: This depends on the design of the respective sieve / screen: a large sieve area is not necessarily a guarantee for longer maintenance intervals. Means, a larger sieve area will clog easier, if dirt particles are hitting in a right angle than a smaller sieve area, where the particles will hit at a flat angle. With the latter scenario, a rather “self cleaning effect” can be experienced resulting in longer maintenance intervals.

With the same amount of dirt and maximum pressure loss (Δp_{\max}), various types of filters do have different cleaning intervals = down-time of plant, production losses, maintenance cost! - summarised in Fig.1

Ensuring, that the differential pressure is increasing at a later stage, will also provide a drop of the necessary inlet pressure of the pump just before the cleaning of the sieve is required. In addition, if the maintenance interval is longer, a longer plant operation is given.

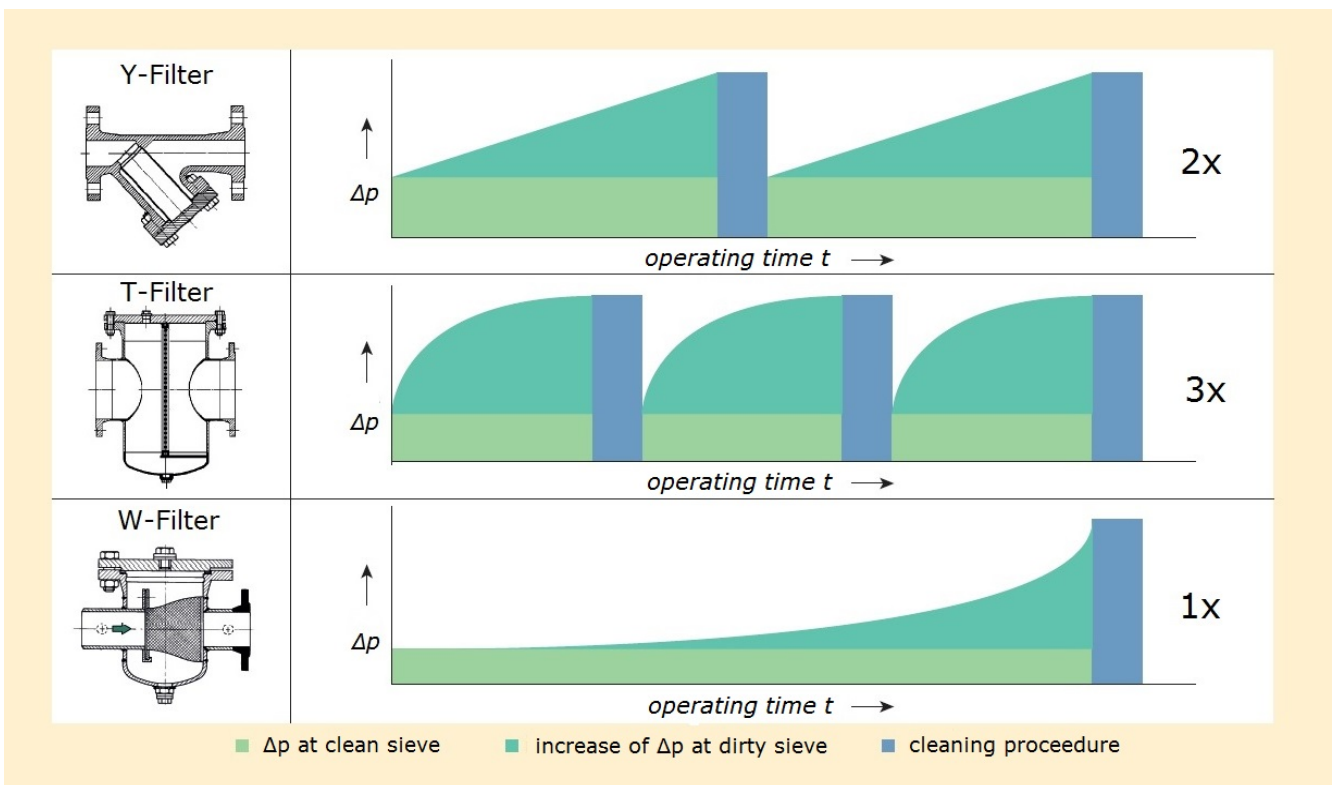


Fig. 1 cleaning intervals of different types of strainers

Maintenance cost

We just examined the frequency of cleaning – in following, we are focusing to a single cleaning cycle, irrespective of its frequency.

Undergoing the cleaning of a strainer means:

- Lock the respective pipe section,
- Drain the medium from the system/strainer,
- Dismantling of the cover flange,
- Remove the sieve / screen for cleaning,
- Remove the dirt deposit (sump) within the strainer body (if applicable),
- Installation of the sieve and cover / lid,
- Vent the strainer while refilling the pipe section with the medium.

Depending on the type of strainer, different times might be required to carry the above tasks out.

- With the larger dimension (DN), the heavy cover/lid of the i.e. Y-Filter is more difficult to handle, due to its overhead position, then the cover of a pot/basket strainer.
- After removal of a basket type sieve, an already cleaned sump is left behind in the strainer body, while the dirt is taken out together with the sieve.

The basic expenditure of this cleaning can be stated with a plant shut-down time of „only“ 1-2 hours, at around 50.- to 100.- EUR/hour plus the cost for a new cover sealing.

In plants, which are operated under temperature, the additional isolation needs to be removed and installed again. Also long cooling-off phases and required slow restarting of the plant will sum up to a 4-digit amount for cleaning.

At times, when this cleaning cycle needs to be carried out during the regular production time of a plant, the total cost incurred for cleaning will easily exceed the initial price of the strainer.

Enough reasons, selecting a strainer also with regards to its frequency of cleaning.

Comparison of operating cost

The datasheets of the three different types of strainers have acted as a basis for i.e. the cost calculation, based on the flow resistance figures (ζ -value). In addition, physical tests on the flow resistance and differential pressure have been carried out.

The flow resistance figure ζ may vary with different brands of Y-FILTER [1] due to their improvement in their flow deflection. Different ζ -values can be also found with the various T-FILTER [2] or so-called basket strainer, using a curved sieve or sieve basket.

However, no other strainer with better values than the W-FILTER [3] was identified in the market. Basically, ζ -values should be increasing the larger a strainer in its dimension is. In the brochures of various manufacturers, however, one may find discrepancies,

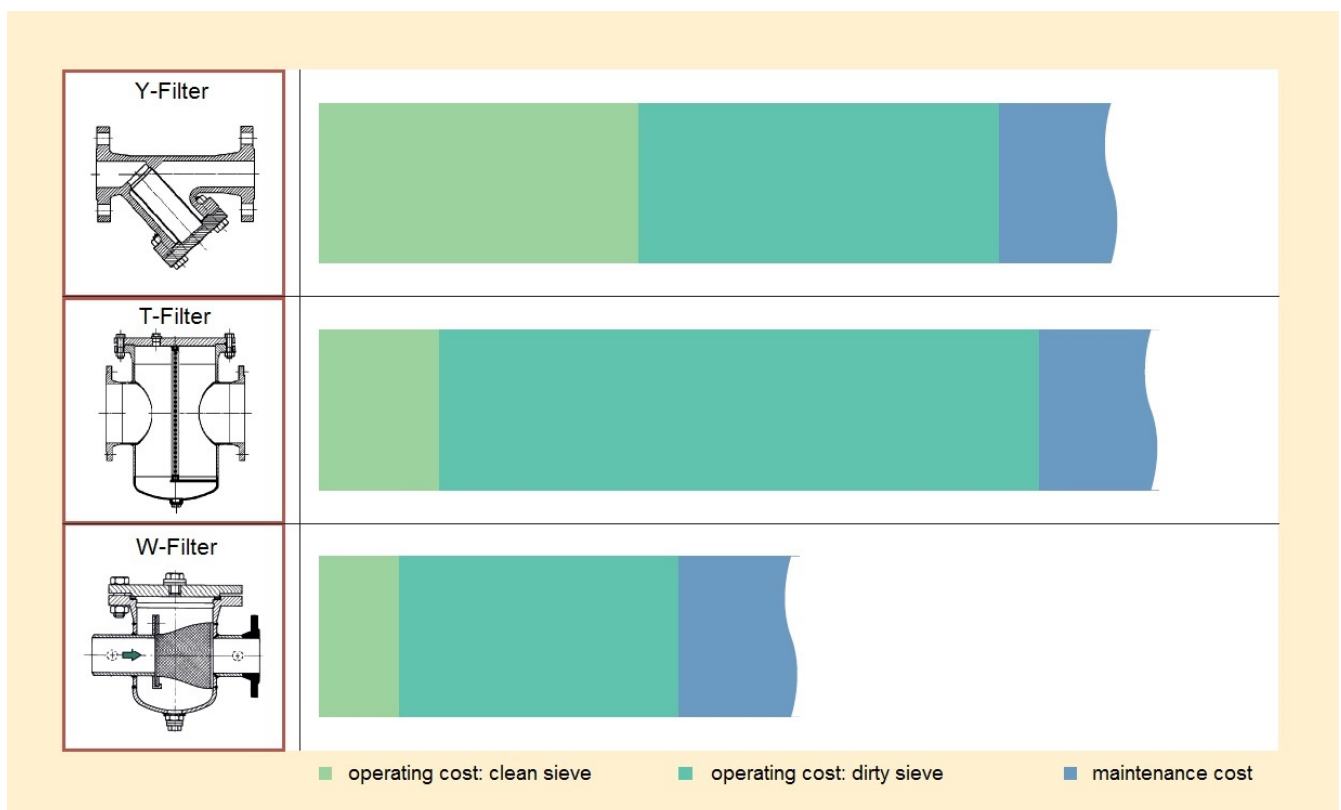


Fig. 2 calculation of operating cost

as the values may increase first and then are lower with larger diameters.

In the following figure Fig. 2 you can see the power consumption in relation to the various resistance coefficients and pressure drop of the different strainers will increase and hence result in higher operating cost. The basis is the following data: DN 200, sieve-mesh width 0.5 mm, volume stream: 365 m³/h hot water; velocity \approx 3 m/s, energy cost: 0.10 €/kWh; filter cleaning at $\Delta p = 10$ mWS \approx 1 bar; $P_{max} = 13.25$ kW:

CONCLUSION

Generally, the longer the time between necessary maintenance, the more effective a plant is operating, due to less stoppage and more output. Limiting the resources carrying out the maintenance and also the handling will help to shorten also the time needed and going back to operation of the plant.

It is well known, that a lower friction in a pipeline, resulting from a low flow resistance figure ζ , will result in less energy a pump needs to transport a medium through the plant. Therefore, a mayor focus should be on selecting components with a low ζ -value.

Total cost – life cycle cost

Ensuring the efficiency of a plant, strainers should be selected in view of operational cost and not only by price. It is experienced, that due to the casted material, dimensions \leq DN 200 of the Y-FILTER are cheaper than the others.

Taking the life-cycle cost, including higher energy consumption and maintenance/labour cost into account, the initial saving in price is negligible. See in Fig. 3 all cost components (based on the Delta-P in Fig 1) added together over the same time frame.

ACKNOWLEDGEMENT

We would like to thank KSB AG and ARI-Armaturen Albert Richter GmbH & Co. KG for their support regarding availability of their testing facilities and personnel in determining the pressure drop values.

Furthermore, thanks to Mr. Kuch (EnviCon) on the confirmation about the flow resistance figures of the Filter Type W

REFERENCES

- [1] <http://www.ari-armaturen.com/appl/files/tb/files/050001-2.pdf>, ARI Strainer 050, 050002-1.pdf, p.2.
- [2] http://www.krombach.com/cms/upload/PDF_Dateien/340a.pdf Krombach strainer Nr. 340, p.4 – (remark: the ζ -value has nowadays changed to $\zeta=3,5$).
- [3] http://www.w-filter.com/mediapool/13/138209/data/W-FILTER_Typ_W_Technical-Data_EN.pdf; W-FILTER, Filter Type W, p. 1.

Type of filter	Y-Filter	T-Filter	W-Filter
Resistance coefficient ζ (manufacturer's data)	7.22	2.80	1.70
Pressure loss Δp_o at clean screen filter ($\Delta p_o = \zeta \cdot (c^2/2g) \cdot \gamma$) [mWS]	3.32	1.29	0.78
Minimum pump capacity with $\eta_p = 0,75$ and at a clean screen filter (basic load) P_o [kW]	4.38	1.71	1.03
Maximum pump capacity P_{max} at $\Delta p = 10$ mWS [kW]	13.25	13.25	13.25
Characteristic of pollution f (angle of impact, effective screen surface, etc.)			
Required average pump capacity until cleaning of filter: $P_m = P_o + f \cdot (P_{max} - P_o)$ [kW]	8.80	9.40	5.10
Average operating cost per hour [€]	0.88	0.94	0.51

Fig. 3 total (life-cycle) cost

THE EFFECT OF CALCIUM CARBONATE FOULING IN PLATE HEAT EXCHANGERS FOR DISTRICT HEATING AND COOLING

K.S. Song¹, C.H. Baek², S.K. Choi¹, Y.C. Kim³

¹ Department of Mechanical Engineering, Graduate School Korea University, Seoul, 02841, Republic of Korea

² Department of Mechanical and Control Engineering, The Cyber University of Korea, Seoul, 03051, Republic of Korea

³ Department of Mechanical Engineering, Korea University, Seoul, 02841, Republic of Korea,

Keywords: Calcium carbonate, Fouling resistance, Pressure drop

ABSTRACT

District heating and cooling is a system for distributing heat obtained from a cogeneration plant, heat pump, and geothermal heating. It provides higher efficiency and better pollution control compared to other systems. However, if it is used for a long time, the thermal efficiency decreases because of fouling in plate heat exchangers. This is associated with additional economic loss and environmental problem. Among various fouling, calcium carbonate fouling is the main reason for the reduction in the thermal efficiency.

Therefore, in this study, the effects of calcium carbonate fouling under the various conditions are studied. Heat transfer characteristics of calcium carbonate fouling were measured by varying inlet temperature, Reynolds number, concentration and chevron angle. The tests were performed under the accelerated concentration conditions. The fouling resistance and pressure drop increased as the inlet temperature and concentration increased. However, the fouling resistance and pressure drop decreased as Reynolds number increased. The fouling resistance decreased and pressure drop increased as chevron angle increased.

NOMENCLATURE

A	heat transfer area (m ²)
β	chevron angle (°)
C_{CaCO_3}	solution concentration (wt. %)
$C_{p,c}$	cold-side constant pressure specific heat (kJ kg ⁻¹ K ⁻¹)
$C_{p,h}$	hot-side constant pressure specific heat (kJ kg ⁻¹ K ⁻¹)
Δp_R	pressure drop ratio
Δp_t	pressure drop at a given time (kPa)
Δp_0	pressure drop at clean state (kPa)
ΔT_{lm}	logarithmic mean temperature difference (°C)
m_c	cold-side mass flow rate (kg s ⁻¹)
m_h	hot-side mass flow rate (kg s ⁻¹)
Q_{avg}	average heat transfer rate (kW)
Q_c	cold-side heat transfer rate (kW)
Q_h	hot-side heat transfer rate (kW)
Re	Reynolds number
R_f	fouling resistance (W ⁻¹ m ² K)
$T_{c,in}$	cold-side inlet temperature (°C)

$T_{c,out}$	cold-side outlet temperature (°C)
$T_{h,in}$	hot-side inlet temperature (°C)
$T_{h,out}$	hot-side outlet temperature (°C)
t	time (min)
U	overall heat transfer coefficient (kW m ⁻² K ⁻¹)
U_R	heat transfer reduction ratio
U_t	overall heat transfer coefficient at the certain time (kW m ⁻² K ⁻¹)
U_0	overall heat transfer coefficient at the initial time (kW m ⁻² K ⁻¹)

INTRODUCTION

Several studies on the improvement of energy efficiency throughout many industrial fields have been conducted because the depletion of fossil fuel and development of eco-friendly energy technologies are becoming main issues. The research and development of a highly efficient heat exchanger have been required for the efficient management of energy and the recovery of waste energy. The selection of appropriate high-efficiency heat exchanger affects the efficiency of manufacturing processes and total maintenance costs. In order to solve these problems, plate heat exchangers began to use in various industrial fields. It has many advantages such as small area of installation, ease of maintenance, and high heat transfer efficiency compared to other heat exchangers. However, when it is used for a long time, the crystallization fouling that means water soluble salts become supersaturated and crystallized on heat transfer surface often causes efficiency degradation and additional pressure drop in the water heating system such as district heating and cooling. Calcium carbonate fouling is dominant at the negative effects especially. Therefore, the performance degradation of plate heat exchangers caused by calcium carbonate fouling in various operating and geometric conditions has to be studied to prevent and reduce the fouling.

Several studies have been done on the fouling for a lengthy period of time. Bott et al. studied that the crystallization fouling causes performance degradation in plate heat exchangers because insoluble salts were precipitated on the heat transfer surface in the supersaturated aqueous solution [1]. Plummer et al. studied the solubility of CaCO₃ decreased with the

increase in the water temperature continuously [2]. Yang et al. tested the calcium carbonate fouling using the mixture of calcium chloride (CaCl_2) with sodium hydrogen carbonate (NaHCO_3) [3]. Thonon et al. studied that the fouling resistance curve increased asymptotically with time and was inversely proportional to the flow rate from the experiment in accelerated concentration conditions [4].

The effects of background electrolyte on fouling were studied experimentally with slurries containing calcite (CaCO_3) particles. The background electrolyte (MgCl_2) was found to have a strong effect on the dispersion properties and fouling rate [5]. Scale formation of CaCO_3 in a plate heat exchanger was investigated in the presence of various types of added particles under isothermal conditions [6]. Pääkkönen et al. studied crystallization and particulate fouling and experimented calcium carbonate characteristics with temperature variation on the heat exchanger surface [7]. A new experimental method to visualize the fouling process of CaCO_3 was studied. It was studied how scale started initially, how scale was formed to thick layers, and how small crystal grew into a large one [8]. The effects of surface crystallization of CaCO_3 and crystallization in the bulk fluid on the fouling rate were studied [9]. The effects of calcium sulfate crystallization fouling on the performance of the plate heat exchangers with various operating and geometry conditions in accelerated concentration conditions were studied [10-12].

However, previous researches were conducted under low temperature and limited conditions. Therefore, their studies were different from the phenomenon in the actual district heating and cooling.

Even with such extensive studies on crystallization fouling in plate heat exchangers, data on the CaCO_3 crystallization fouling characteristics with the variation of operating and geometrical parameters was limited. In this study, the fouling resistance and pressure drop characteristics of plate heat exchangers were measured and analysed in accelerated concentration conditions by varying operating and geometrical parameters, such as CaCO_3 concentration, Re , inlet temperature, and chevron angle of the plates.

EXPERIMENTAL SETUP

Figure 1 is the schematic of the experimental setup used in this study. The test apparatus consisted of a heating, cooling unit, and heat exchanger section. It was similar with actual district heating and cooling system. The heating unit consisted of 500 liters of constant hot water bath, heaters with a capacity of 45 kW, and an inverter pump. The water in heating unit was heated by the heaters before it supplied to the heat exchangers. The flow rate in the heating unit was controlled by the inverter pump and measured by the volumetric flow meter. The cooling unit consisted of 500 liters of constant cold water bath, heaters with a capacity of 10 kW, an inverter pump, a chiller, and an air cooling unit. Calcium carbonate (CaCO_3) solution

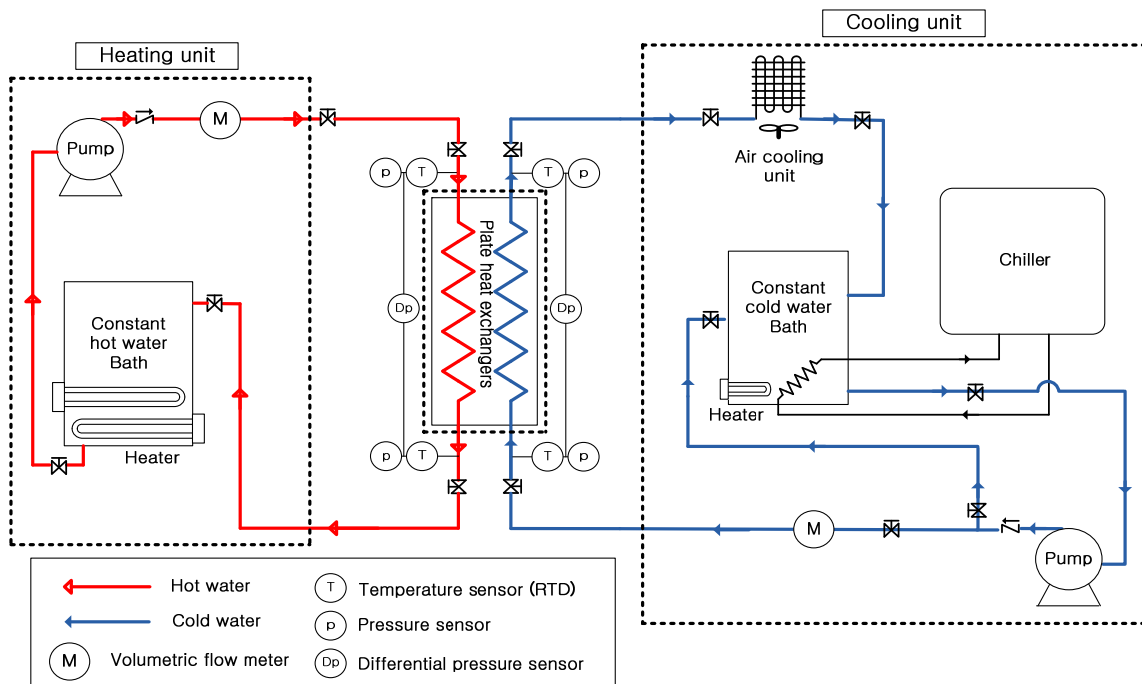


Figure 1. The schematic of the experimental setup.

was made in the constant cold water bath to study the effects of crystallization fouling.

After passing through the heat exchanger section, the heated solution was cooled using the air cooling unit and the water chiller with a capacity of 21 kW. It acts as heat supply to the consumers and heat loss in actual district heating and cooling. The heat exchanger section consisted of temperature sensors (RTD), pressure sensors and a chevron type plate heat exchanger with total four plates containing end plates. The plate contained three channels with two outer channels for the hot-side water and an inner channel for the cold-side water (solution). The heat was exchanged between the hot and cold water in the counter flow; the downward flow of the hot water and the upward flow of the cold water.

Because the solubility of calcium carbonate (CaCO_3) is significantly low and the ionic bonding force of calcium carbonate (CaCO_3) is higher than that of water molecules, it cannot be dissolved in water well. In addition, the undissolved calcium carbonate (CaCO_3) particles in the solution can affect the nucleation that accelerates crystallization of fouling. Therefore, the calcium carbonate (CaCO_3) was made by mixing two different reagents of calcium chloride dihydrate ($\text{CaCl}_2 \cdot 2\text{H}_2\text{O}$) and sodium carbonate (NaHCO_3) that have higher solubility. Equation (1) shows the chemical reaction formula that calcium carbonate (CaCO_3) was generated.



When the volumetric water flow rate and water temperature reached steady state with respective fluctuations within $\pm 0.1 \text{ m}^3/\text{h}$ and $\pm 0.5^\circ\text{C}$ compared with the setting conditions, the calcium chloride dihydrate ($\text{CaCl}_2 \cdot 2\text{H}_2\text{O}$) and sodium carbonate (NaHCO_3) reagents were mixed in the constant cold water bath. After controlling the concentration of the solution, the data measurement processes were started. When the temperature and the pressure difference of the hot and cold water with time were within $\pm 0.2^\circ\text{C}$ and $\pm 10 \text{ kPa}$ for one hour, respectively, it was considered as reached to equilibrium state. Table 1 shows the test conditions in the study. In the CaCO_3 crystallization fouling test, the CaCO_3 concentration was varied from 0.12 to 0.35 wt. % and Re was varied from 2500 to 5600. The inlet temperature of the cold-side water was fixed at 40°C and that of the hot-side water was varied from 70 to 90°C . The chevron angle of the plate heat exchanger was varied from $30/30^\circ$ to $60/60^\circ$.

DATA REDUCTION

The heat transfer rates of the hot and cold water were calculated using Equation (2) and (3), respectively

Table 2. The test conditions

Parameter	Range	Unit
Solution concentration (C_{CaCO_3})	0.12 - 0.35	wt. %
Re	2500 - 5600	-
Cold-side inlet temperature ($T_{c,in}$)	40	$^\circ\text{C}$
Hot-side inlet temperature ($T_{h,in}$)	70 - 90	$^\circ\text{C}$
Chevron angle (β)	30/30 - 60/60	$^\circ$

$$Q_h = \dot{m}_h C_{p,h} (T_{h,in} - T_{h,out}) \quad (2)$$

$$Q_c = \dot{m}_c C_{p,c} (T_{c,out} - T_{c,in}) \quad (3)$$

The energy balance between the hot and cold water was within $\pm 5\%$. The average heat transfer rate for the hot and cold water was defined as Equation (4).

$$Q_{avg} = (Q_h + Q_c) / 2 \quad (4)$$

The overall heat transfer coefficient was determined using the average heat transfer rate, heat transfer area, and logarithmic mean temperature difference as given in Equation (5). The heat transfer area A was calculated by applying the enlargement factor (Φ) proposed by Martin [13].

$$U = Q_{avg} / A \Delta T_{lm} \quad (5)$$

The logarithmic mean temperature difference was expressed by

$$\Delta T_{lm} = \frac{[(T_{h,in} - T_{c,out}) - (T_{h,out} - T_{c,in})]}{\ln[(T_{h,in} - T_{c,out}) / (T_{h,out} - T_{c,in})]} \quad (6)$$

As the CaCO_3 crystallization fouling progressed with time, the overall heat transfer coefficient decreased and the fouling resistance increased. The initial value of the overall heat transfer coefficient at clean state was defined by U_0 . The overall heat transfer coefficient at a certain time was defined by U_t . The fouling resistance (R_f) was calculated by the thermal resistance difference between the certain and initial time. In addition, the heat transfer reduction ratio (U_R) was defined as the ratio of the overall heat transfer coefficient at the certain time (U_t) to that at the initial time (U_0).

$$R_f = 1/U_t - 1/U_0 \quad (7)$$

$$U_R = U_t / U_0 \quad (8)$$

The pressure drop ratio (Δp_R) was defined by the ratio of the pressure drop at the certain time (Δp_t) to the initial pressure drop at clean state (Δp_0).

$$\Delta p_R = \Delta p_t / \Delta p_0 \quad (9)$$

RESULTS AND DISCUSSION

Reynolds number (Re)

Figure 2 shows the variation of the heat transfer reduction ratio (U_R) and pressure drop ratio (Δp_R) with time at various Reynolds number. The Re was varied from 2550 to 5597 by changing the solution flow rate with the fixed chevron angle, CaCO_3 concentration, and inlet temperatures of the hot and cold water.

The heat transfer reduction ratio and pressure drop ratio decreased with the increase of Re. In the CaCO_3 crystallization fouling in plate heat exchangers, the fouling resistance increased with time and then approached a steady value after a certain period. The increased flow velocity at the interface of the fouling layer and solution led to the higher shear force and smaller residence time of the eddy vortex on the corrugated surface resulting in lower fouling resistance. The excessive formation of deposit and decreased flow channels led to the gradual increase in the pressure drop ratio at a fouled state. However, as the Re increased, the decreased deposition rate with the decrease in the surface temperature caused the suppression of the deposit precipitation on the heat transfer surface. The removal rate increased because of the increased shear force. As the result, the equilibrium state between the deposition and removal rate was reached rapidly.

Temperature

Figure 3 shows the variation of the heat transfer reduction ratio (U_R) and pressure drop ratio (Δp_R) with time at the variation of the inlet temperature of hot-side water. The CaCO_3 concentration and Re were maintained at 0.35 wt. %, and 2550, respectively. The inlet temperature of the cold water was fixed at 40°C and that of the hot water was varied from 70 to 90°C. The decrease of hot-side water's inlet temperature means the decrease of the cold-side water's outlet temperature. Thus, the reaction rate affected by the variation of the temperature decreased because the average temperature of the plates and water decreased. The number of supersaturated ions also decreased because the solubility difference of the ions between inlet and outlet decreased with the decrease of the outlet temperature. As the results, the actual fouling on plates decreased and the heat transfer reduction ratio and pressure drop ratio also decreased.

Figure 4 shows the variation of the heat transfer reduction ratio (U_R) and pressure drop ratio (Δp_R) with time at various CaCO_3 concentrations. The Re, chevron angle, and inlet temperatures of the cold and hot-side water were maintained at 2550, 60/60°, 40°C, and 90°C, respectively.

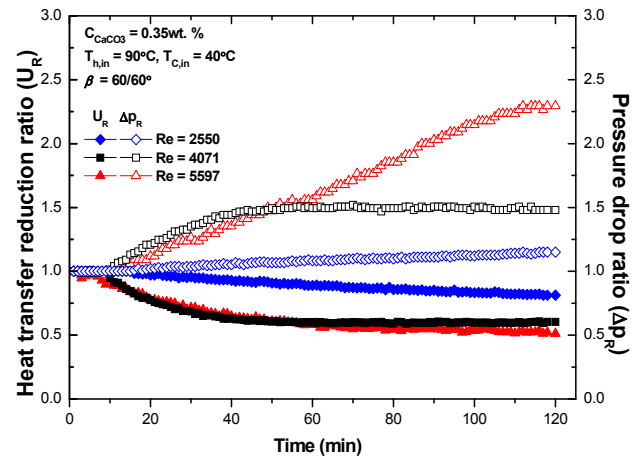


Figure 2. The effects of the Re on heat transfer reduction ratio and pressure drop ratio.

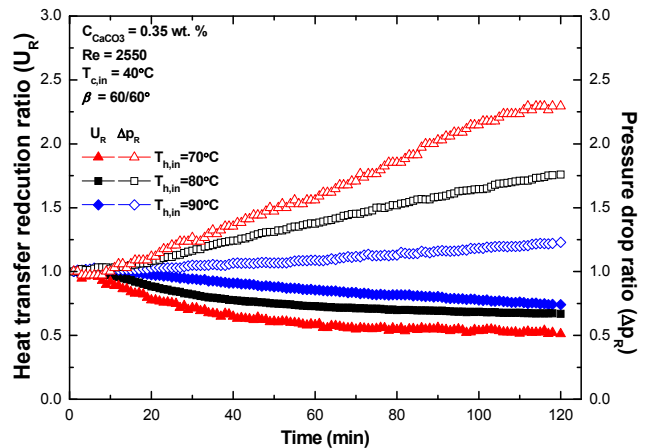


Figure 3. The effects of the temperature on heat transfer reduction ratio and pressure drop ratio.

Concentration

The heat transfer reduction ratio and pressure drop ratio increased with the increase of the concentrations. The fouling resistance increased with the increase in the CaCO_3 concentrations because the increased reaction rate with the increased number of foulant ions led to higher deposition rate. The fouling resistance was reached to the equilibrium state rapidly with the increase in the CaCO_3 concentrations because the number of foulant ions increased and the increased deposition rate at the early stage led to higher removal rate with the decreased surface temperature.

The increasing slope of the pressure drop ratio increased with the increase in the CaCO_3 concentration because the increased deposition rate led to the decreased channel diameter and the increased flow velocity.

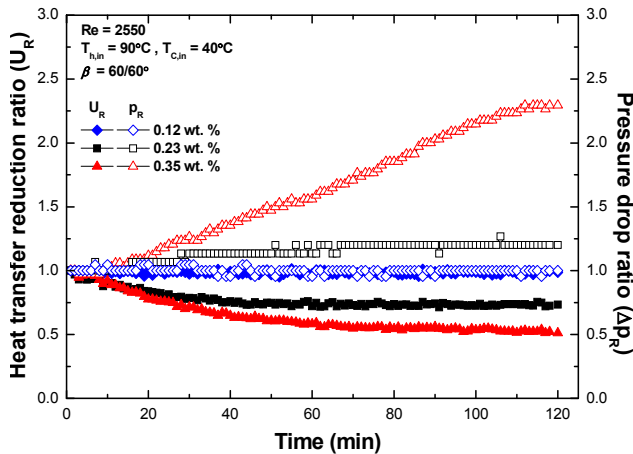


Figure 4. The effects of the concentration on heat transfer reduction ratio and pressure drop ratio.

Chevron angle

Figure 5 shows the variation of the heat transfer reduction ratio (U_R) and pressure drop ratio (Δp_R) with time at various chevron angles. The CaCO_3 concentration and Re were maintained at 0.35 wt. %, and 2550, respectively. The inlet temperatures of the hot and cold-side water were fixed at 40°C and 90°C, respectively.

The heat transfer reduction ratio and pressure drop ratio increased with the increase of the chevron angle. As the chevron angle increased from 30/30° to 60/60°, the resistance to water flow increased. As the results, actual scale and pressure drop increased. However, the fouling resistance decreased because of a higher initial overall heat transfer coefficient at the higher chevron angle.

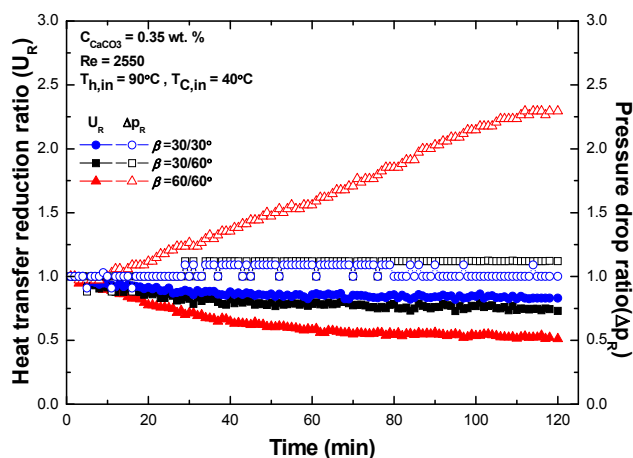


Figure 5. The effects of the chevron angle on heat transfer reduction ratio and pressure drop ratio.

Fouling visualization

Figure 6 shows the photograph of the actual fouled plate after an experiment. The water (solution) flowed upward and the fouling was accelerated as it did because of the increase of the reaction rate and supersaturated ions. The fouling around the gasket was thicker compared to other regions in the plate due to the stagnation flow effect. The hardness of the fouling was so high that it was not scratched by nails.



Figure 6. The photograph of the actual fouled plate.

CONCLUSIONS

In district heating and cooling, calcium carbonate fouling caused the negative effects such as the decrease of heat transfer efficiency and increase of the pressure drop. Therefore, the performance degradation of plate heat exchangers caused by the fouling in various operating and geometric conditions has to be studied to prevent and reduce the fouling. In this study, the fouling resistance and pressure drop characteristics of plate heat exchangers were measured and analysed in accelerated concentration conditions by varying Re , temperature, CaCO_3 concentration, and chevron angle of the plates.

The fouling resistance increased with time and then approached a steady value after a certain period in plate heat exchangers. The fouling caused the increase of the pressure drop because of the decreased flow channels. Heat transfer rate was decreased because of the dominant insulation effect of the fouling.

The heat transfer reduction ratio (U_R) and pressure drop ratio (Δp_R) decreased with the increase in the Re because of the increased shear force. Because supersaturated foulant ions increased with increase of CaCO_3 concentration, the heat transfer reduction ratio and pressure drop ratio increased with the increase in the concentration. As the inlet temperature of the hot-side water decreased, the outlet temperature of the cold-side decreased. The reaction rate and the

supersaturated ions decreased with the decreased outlet temperature of the cold-side. As the results, the heat transfer reduction ratio and pressure drop ratio decreased with the decrease in the inlet temperature of hot-side water. The heat transfer reduction ratio and pressure drop ratio increased with the increase of the chevron angle because of the increase of the flow resistance.

ACKNOWLEDGEMENT

This work was supported by the Human Resources Development of the Korea Institute of Energy Technology Evaluation and Planning (KETEP) grant funded by the Korea government Ministry of Trade, Industry & Energy (No. 20144010200770)

REFERENCES

- [1] T.R. Bott, "Aspects of crystallization fouling", *Experimental Thermal and Fluid Science* 1997, Vol. 14, pp. 356-360.
- [2] L.N. Plummer and E. Busenberg, "The solubilities of calcite, aragonite and vaterite in CO₂-H₂O solutions between 0 and 90°C, and an evaluation of the aqueous model for the system CaCO₃-CO₂-H₂O", *Geochim et Cosmochimica Acta* 1982, Vol. 46, pp. 1011-1040.
- [3] Q. Yang, J. Ding and Z. Shen, "Investigation on fouling behaviors of low-energy surface and fouling fractal characteristics", *Chemical Engineering Science* 2000, Vol. 55, pp. 797-805.
- [4] B. Thonon, S. Grandgeorge and C. Jallut, "Effects of geometry and flow conditions on particulate fouling in plate heat exchangers", *Heat Transfer Engineering* 1999, Vol. 20, pp. 12-24.
- [5] M. Riihimäki, U. Ojaniemi, T.J.H. Pättikangas, T.M. Pääkkönen, M. Manninen, E. Puhakka, E. Muurinen, C.J. Simonson and R.L. Keiski, "Fouling in high solid content suspension effect of nucleating air and background electrolyte", in *Proc. International Conference on Heat Exchanger Fouling and Cleaning VIII 2009*, pp. 192-199.
- [6] N. Andritsos and A.J. Karabelas, "Calcium carbonate scaling in a plate heat exchanger in the presence of particles", *International Journal of Heat and Mass Transfer* 2003, Vol. 46, pp. 4613-4627.
- [7] T.M. Pääkkönen, M. Riihimäki, E. Puhakka, E. Muurinen, C.J. Simonson and R.L. Keiski, "Crystallization fouling of CaCO₃-effect of bulk precipitation on mass deposition on the heat transfer surface", in *Proc. International Conference Heat Exchanger Fouling and Cleaning VIII 2009*, pp. 209-216.
- [8] W.T. Kim, C. Bai and Y.I. Cho, "A study of CaCO₃ fouling with a microscopic imaging technique", *International Journal of Heat and Mass Transfer* 2002, Vol. 45, pp. 597-607.
- [9] T.M. Pääkkönen, M. Riihimäki, C.J. Simonson, E. Muurinen and R.L. Keiski, "Crystallization fouling of CaCO₃ - Analysis of experimental thermal resistance and its uncertainty", *International Journal of Heat and Mass Transfer* 2012, Vol. 55, pp. 6927-6937.
- [10] K.S. Song, S.W. Kim, H. Kang, C.H. Baek and Y. Kim, "Effects of operating and geometric parameters on CaSO₄ crystallization fouling in plate heat exchanger", in *Proc. International Conference Heat Exchanger Fouling and Cleaning XI 2015*, pp. 226-230.
- [11] E. Lee, J. Jeon, H. Kang and Y. Kim, "Thermal resistance in corrugated plate heat exchangers under crystallization fouling of calcium sulfate (CaSO₄)", *International Journal Heat and Mass Transfer* 2014, Vol. 78, pp. 908-916.
- [12] B. Bansal, H. Muller-Steinhagen, X. D. Chen, "Performance of plate heat exchangers during calcium sulphate fouling - investigation with an in-line filter", *Chemical Engineering and Processing* 2000, Vol. 39, pp. 507-519.
- [13] H. Martin, "A theoretical approach to predict the performance of chevron-type plate heat exchangers", *Chemical Engineering and Processing* 1996, Vol. 35, pp. 301-310.

REMOVAL OF INORGANIC FOULING USING ULTRASONIC AND HYDRODYNAMIC CAVITATION

Kyoung Ho Han¹, Kwangkeun Choi², Deok-Yong Ahn³, Kyung Min Kim³, Do Young Yoon^{1,*}

¹Kwangwoon University, 20 Gwangun-ro Nowon-gu, Seoul, 139-701, Korea

²G&G InTech Co., Ltd., 120 Heungdeokjungang-ro, Giheung-gu, Yongin-si, Gyeong gi-do, 16950, Korea

³Korea District Heating Corp., 752, Suseo-dong, Gangnam-gu, Seoul, 135-220, Korea

Keywords: *Fouling, Plate type heat exchanger, Cavitation, CFD*

ABSTRACT

Fouling is the accumulation of unwanted materials such as scale on solid surfaces to the detriment of function. The fouling materials can consist of either living organisms (bio-fouling) or a non-living substance (inorganic, organic). This is one of the main problems in design and operation of heat exchanger. The heat exchange efficiency is reduced by fouling, so mechanical and chemical methods are used to remove fouling, and they may be very effective to remove fouling. But, some disadvantages are as following; time and cost expensive, toxic, harmful to plate, etc. So, a lot of researches have been studied about more effective removal methods. One of them, cavitation phenomena, can be applied to remove fouling. Generally, ultrasonic or hydrodynamic cavitator was used to produce cavitation, and the fouling was removed by some effects such as micro vibration, cavitation, etc. So, in this research, the effect of ultrasonic and hydrodynamic cavitator on the fouling removal was examined. The one is applied to direct removal, and the other is used to indirect removal of fouling, respectively. Where, direct removal means that the scale attached on the surface of plate was removed, and indirect removal means that the scale induced material such as calcium ion was removed from the system water.

As results in the case of ultrasonic unit used, we confirmed that the heat transfer coefficient was recovered to the original value. When the hydrodynamic cavitator was used, the calcium ion contained in water was reacted with alkalinity such as bicarbonate and it formed the solid particles. This reaction can be easily observed by visual inspection because when calcium ion reacts with carbonate ion it creates cloudy form. Finally, it is supposed that cavitation phenomenon is very powerful tool for fouling removal.

INTRODUCTION

By definition, the fouling is phenomena that any extraneous material is deposit at heat transfer surface of the heat exchanger; used as a term "scale". Fouling mechanisms are divided into 6 major deposit which are sedimentation fouling, inverse solubility fouling, chemical reaction fouling, corrosion product fouling and biological fouling. The major deposit material is CaCO₃ included in coolant used in heat exchanger. CaCO₃ is inorganic fouling that causes deposit at heat transfer surface by crystalizing and bonding with each other. Since the deposit materials have low thermal conductivity, growing deposit on the plate increases not

only the heat transfer thickness gradually but also the thermal resistance of heat exchanging plates between hot and cold streams. This fouling resistance diminishes eventually the heat transfer efficiency of heat exchanger. Furthermore, CaCO₃ shows fouling mechanism combined with sedimentation fouling and inverse solubility fouling that make identifying specific fouling behaviour and interaction a lot more complicated. The scale is strong bonding strength. Powerful mechanical and chemical treatment will be needed for removal of the scale [1]. If the scale is not eliminated, it interfere the flow stream as a way of generating pressure drop at the inside of tube. Therefore, flow stream is unable to maintain a stable velocity [2]. For these reason, to design heat exchanger, the effects of fouling must be taken into account [2-4]. Researches about anticipating and removing fouling technology have been conducted for the whole industry [5]. If it is hard to prevent building up the scale, it will be removed periodically by chemical or physical ways. The chemical treatment is used the most among various removal technologies because of convenient and efficient. The chemical removal process is that material reacting with the scale is injected into the pipe running coolant. The chemical means is also well known as it doesn't needed introducing additional equipment and disassembling part of pipes [6]. Chemical technology, however, has serious problems that chemical agent used in process is expensive in industrial level, causing second pollution [7]. In the mechanical removal methods, the method of scraping with a rotary brush scale accumulated inside the tube are used primarily. Mechanical removal method can reduce the use of chemical treatments. But it spends a lot of time and money than the chemical removal method, because the machine has to be operated by the hand of man. Since, moreover, the large-sized heat exchanger has the disadvantage that it is difficult to use, attempting to introduce a deletion method of replacing the chemical removal methods and mechanical removal methods [1]. According to statistics for scale removal technique using ultrasound removal techniques that can be present alternatively, about 70 papers were written in 1960 to 2010. Research of ultrasound in the 2000s, has attracted the attention so as to increase to more than three times in the 1990s [8]. It has been proven that ultrasonic removal techniques is not only effective in removing solid material remaining, but also effective in removing fouling by microorganisms [9, 10]. In addition, ultrasound causes cavitation by generating a negative pressure to the fluid inside the pipe. Cavities produced by cavitation phenomenon are known that

the cleaning effect is excellent, because they generate a supersonic [11, 12]. Among various heat exchangers, cleaning of the plate-type heat exchanger is quite cumbersome. In conventional cleaning method, the plates of the heat exchanger are cleaned with chemicals after disassembling the heat exchanger.

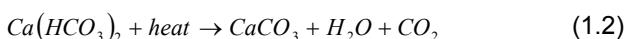
In particular, in the process of assembling the heat exchanger again, it may cause a leak. Leakage of heat exchanger reduces the heat exchange efficiency. And a heat exchanger during the washing has a disadvantage that it cannot be operated.

In this study, we have developed an ultrasonic device as a method for cleaning without having to disassemble the plate heat exchanger. And using a hydrodynamic cavitation, the study was carried out to remove scale causing substances (Ca^{2+}). Inorganic fouling removal efficiency of the heat transfer plate was evaluated from the measurement of the overall heat transfer coefficient. Additionally, we were visually checks the cleaning conditions of the heat transfer plate. In addition, the removal effect of the scale causing substances is analysed to measure the concentration of Ca^{2+} ions and X-ray diffraction spectroscopy (XRD).

MATERIALS AND METHOD

Hydrodynamic cavitation

Removal of scale causing substances using hydrodynamic cavitation is performed by converting the Ca^{2+} ions with CaCO_3 . The reason for the selection of Ca^{2+} on a scale causing materials is because Ca^{2+} ions cause the scale with the highest probability. And Ca^{2+} ions mainly react with the negative ions such as HCO_3^{2-} , CO_3^{2-} , and the reaction scheme is shown below.



In order to produce a CaCO_3 , activation energy is required, as shown in figure 1 [14]. In this study, to obtain the energy required for the reaction we used the cavitation phenomenon. When the bubble created by the cavitation is collapsed, energy of high temperature and high pressure is released to the surrounding. By using this phenomenon, we tried to convert the Ca^{2+} ions into the CaCO_3 . First, solution of Ca^{2+} was prepared to measure the efficiency of removal of Ca^{2+} from the hydrodynamic cavitation. Calcium solution is $\text{Ca}(\text{OH})_2$ saturated solution having an initial concentration of about 400 mg/L , the pH is 12. And CO_3^{2-} ions which react with the Ca^{2+} are considered as CO_3^{2-} ions contained in tap water to exist primarily in the pH.

Figure 2 shows the configuration of the hydrodynamic cavitation device. The device consists of a pressure manometer, cavitator, pump, water bath. Water bath is filled with $\text{Ca}(\text{OH})_2$ saturated solution of 100 liters. Operating conditions are inlet pressure of about 4 bar (gauge pressure) and flow rate of $3 \text{ m}^3/\text{h}$,

and was operated for 2 hours. We collected a sample every 20 minutes, and measured the pH and Ca^{2+} concentration, temperature, conductivity, SS (Suspended Solid) of the sample. After SS measurement, to analyse the components of the sediment caused by the cavitation we conducted the XRD analysis, and then confirmed whether to generate CaCO_3 .

Ultrasonic cavitation

Figure 3 shows a conceptual diagram of the scale removal experiment in the plate heat exchanger using ultrasonic cavitation.

The water bath supplies the hot water to the plate heat exchanger and the pump supplies cold water. The ultrasonic wave generator had been attached to the moving plate of the heat exchanger, and ultrasonic wave gel had been filled between the movable plate and No.1 heat transfer plate. In addition, the heat exchanger is consists of the thirty heat transfer plates, the moving plate is No.1 and the fixed plate is No.30.

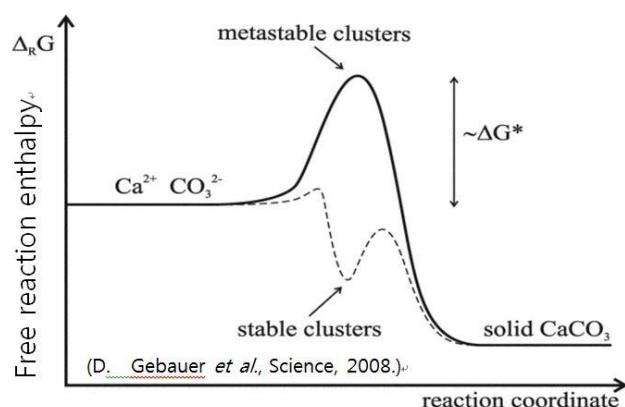


Figure 1. Free reaction enthalpy for the generation of calcium carbonate.

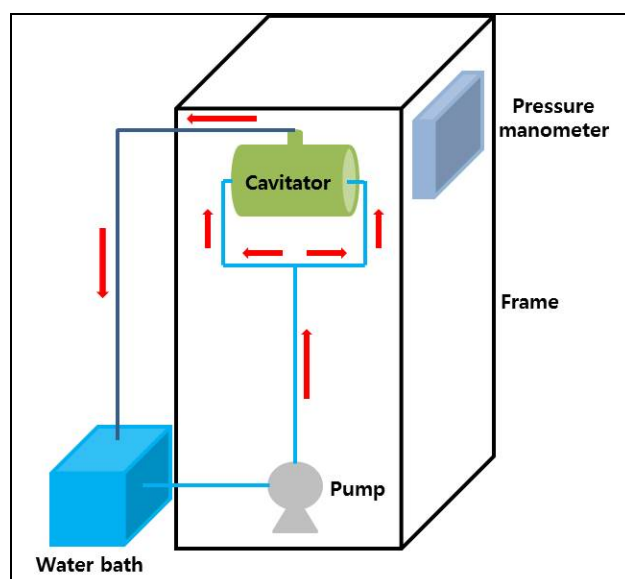


Figure 2. Experimental diagram of a cavitator.

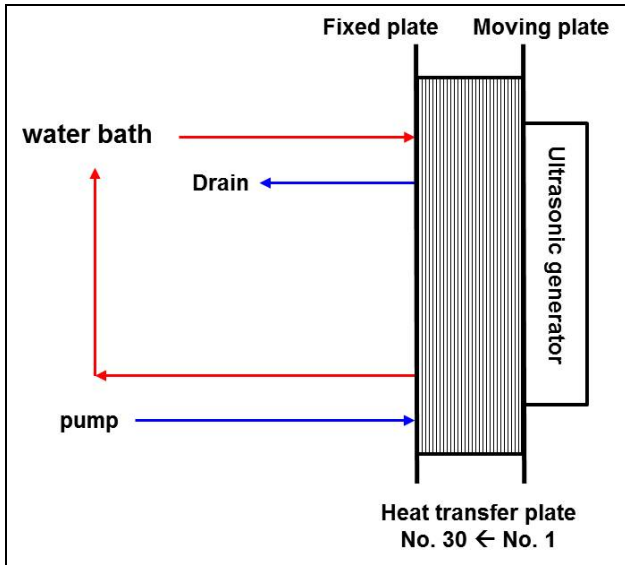


Figure 3. Conceptual diagram of a plate-type heat exchanger.

Table 1. Cases of scale removal experiment using ultrasonic cavitation

Case 1	Scale is attached for 3 hours. 1 more hour, attached before cavitator operation (totally 4 hours)
Case 2	Scale is attached for 3 hours. Perform the removal and attachment of the scale at the same time.

To measure the descaling efficiency by ultrasonic cavitation, CaCO_3 scale was deposited on the heat transfer plate that is not attached to anything. CaCl_2 and NaHCO_3 were used as a sample to attach CaCO_3 on the heat transfer plate, and their concentration is $3,000 \text{ mg/L}$ (as Ca^{2+}). Originally, in the inlet water that is used in the heat exchanger, there are scale causing ions of about 40 mg/L , but in this study, we conducted experiments to significantly increase the concentration of scale causing ions to analyze the cleaning effect in extreme conditions. Preparing a sample, and then we attached the scale by operating the heat exchanger for three hours at a flow rate of 0.3 L/min (cold water inlet) and 3 L/min (hot water inlet). After attaching the scale, we performed experiments to remove the scale for the two cases as shown in table 1.

The ultrasonic generator of 20 kHz was used to clean the heat transfer plate that is attached to the scale. Cleaning of the heat transfer plate has been going on for 23 hours, and work and rest period of the ultrasonic device was set to one to one. Operation flow rates were set to 3 L/min (hot water) and 1 L/min .

The cleaning effects using ultrasonic cavitation was evaluated from the measurement of the overall heat transfer coefficient, in this study Overall heat transfer coefficient of heat transfer plate that scale is not attached is about $0.1 \text{ J/m}^2 \cdot \text{K}$. Overall heat transfer

coefficient can be calculated from the heat transfer resistance of the solid and convective heat transfer resistance that occurs between the solid and liquid, and the bigger the value is the better heat transfer. It is expressed as follows [15].

$$U = \frac{Q}{A\Delta T_{lm}} \quad (2)$$

where, Q is heat transfer rate [J/s], A is total heat exchange area [m^2], ΔT_{lm} is Logarithmic mean temperature difference [K], It is expressed as follows.

$$\Delta T_{lm} = \frac{(T_{H,i} - T_{C,o}) - (T_{H,o} - T_{C,i})}{\ln \left(\frac{T_{H,i} - T_{C,o}}{T_{H,o} - T_{C,i}} \right)} \quad (3)$$

where subscript H is represents hot water and C is cold water, and i is inlet, o is outlet.

3. RESULTS AND DISCUSSION

3.1. Removing of Scale Causing Materials Using Hydrodynamic Cavitation

The figures 4-7 show the results for removing of the scale causing substances using hydrodynamic cavitation. Figure 4 shows the pH and temperature changes of the sample depend on operating time of the hydrodynamic cavitator. The samples were collected for 120 minutes every 20 minutes. As a result, it is showing a tendency to decrease the pH and increase in temperature as time passed. The reason for the decreasing the pH is because the OH^- ions are used continuously as the water is decomposed by the cavitation, and pH decreased approximately from 12.2 to 11.7. The temperature of the water of the bath was increased from $25 \text{ }^\circ\text{C}$ to $42 \text{ }^\circ\text{C}$, due to the heat generated from the motor of the pump. Figure 5 shows the change in the conductivity of the solution and the concentration of Ca^{2+} with time. The concentration of Ca^{2+} ions tends to decrease continuously during the experiment, and finally the concentration was reduced to 36% from 400 mg/L to 250 mg/L . Whether Ca^{2+} ions are removed can also be confirmed with the naked eye. The reason is because the calcium solution is blurred as Ca^{2+} ions are converted to CaCO_3 , it is shown in figure 6. As shown in the picture, it can be clearly observed to the colour change of the solution before and after the operating cavitator. Then, the conductivity was reduced approximately 13% as Ca^{2+} is decreased, the reason is a phenomenon that appears by decreased of positive ions and negative ions which acts as mediators of electron transfer. In this study, we operated the cavitator for 120 minutes. However, if the cavitator is operated for the longer time, it is expected that the concentration of Ca^{2+} ions can be reduced to the fresh water level.

Figure 7 shows the result of analysing the components of the precipitate by XRD method. In the result, the SS contained in the solution was confirmed

to be the all CaCO_3 as mentioned above, and other materials were not detected.

If the cavitator applied solid-liquid separation device is used as influent pre-treatment device of the heat exchanger, it is expected that the effect as the scale preventive device will be further increased.

3.2. Removing of Scale Using Ultrasonic Cavitation at Heat Transfer Plate

In this study, the cleaning effect of the ultrasonic cavitation was evaluated by measuring the overall heat transfer coefficient of the plate-type heat exchanger, the results are shown in figures 8 and 9. Figure 8 is the result for the case 1, the scale was attached for 3 hours before the experiment, after attaching the scale further for one hour, and the experiment was performed. In the graph of figure 8 to the initial driving, overall heat transfer coefficients show a very low value of 0.01 or less, it increased sharply after about 5 minutes, and for the 60 minutes when the scale is being attached it is showing a tendency to decrease slightly. In the initial experiments, the reason that the heat transfer coefficient is low is estimated to be start-up effect of the heat exchanger. Then, it became a stable after 5 minutes. Operating the ultrasonic device after 60 minutes, we observed the change characteristics of the heat transfer coefficient. The overall heat transfer coefficient is not increased for the ten minutes after the ultrasonic device is operated. Then, it showed a tendency to increase sharply at about 70 minutes. This trend is guessed that the scale should be damaged continuously by ultrasonic cavitation. Therefore the damaged scales are removed from the heat transfer plate after ten minutes. In addition, the overall heat transfer coefficient rapidly increased up to about 80 minutes, it was gradually increased thereafter. Also overall heat transfer coefficient is repeatedly increased and decreased in the process of recovery. It is estimated that because the scale that is broken away from the heat transfer plate is not well discharged from the inner of the heat exchanger. Figure 8 showed only the data up to 170 minutes to view in detail overall heat transfer coefficient of variation in the initial cleaning. However, in the actual experiment it was run for 23 hours, the ultrasonic irradiation time is 11.5 hours. Overall heat transfer coefficient finally measured is 0.1. It is similar to the heat transfer plate that scale is not attached. As a result, we confirmed that ultrasonic cavitation is highly effective in cleaning heat exchangers.

Figure 9 is the result for case 2. The scale was attached for 3 hours prior to the test, and the experiment was performed at the same time the attachment and the cleaning of the scale thereafter. In the graph in figure 9, the overall heat transfer coefficient is maintained a very low value to about 18 minutes from the initial operation and increased rapidly thereafter. After 30 minutes, it shows a tendency to continue maintain the value of 0.1 that is heat transfer coefficient of heat transfer plate that the scale is not attached. The reason why the heat transfer coefficient has a low value in the initial is seems to start-up effect

of the heat exchanger as mentioned above, or that the damage by the cavitation is being accumulated to the scale. And after 18 minutes, the reason for a sudden increase of the heat transfer coefficient is estimated that the scale accumulated the damage chips off from the heat transfer plate in chunks. After 20 minutes, Decreasing of the heat transfer coefficient seems to be because the scale is finely crushed once again by cavitation within the heat exchange. After 30 minutes, the heat transfer coefficient was maintained at a value near 0.1. In this study, we performed experiments in extreme conditions. If the cleaning device is used for the influent of the actual heat exchanger, it is expected to reduce the operation time about 75 times.

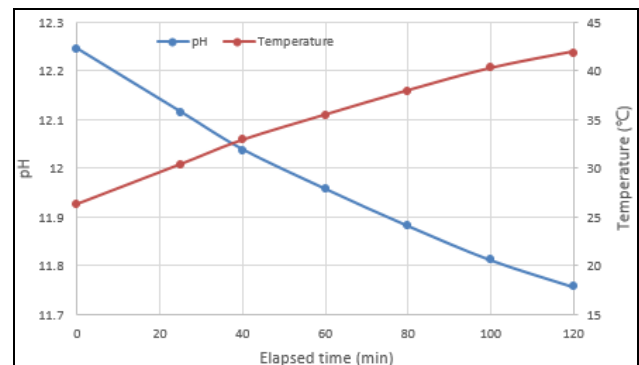


Figure 4. Characteristics of pH and temperature of the water in the bath.

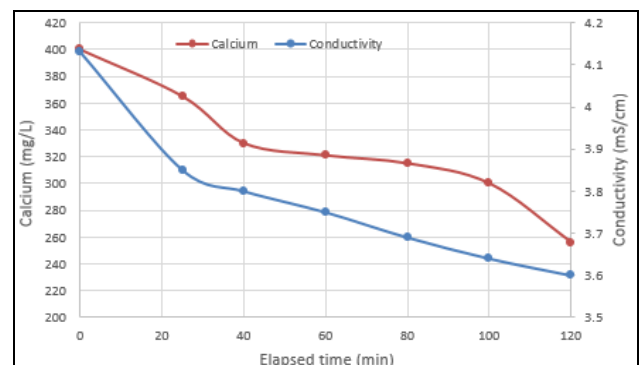


Figure 5. Characteristics of calcium ion concentration and conductivity of the water in the bath.



Figure 6. Photos of calcium carbonate generation.

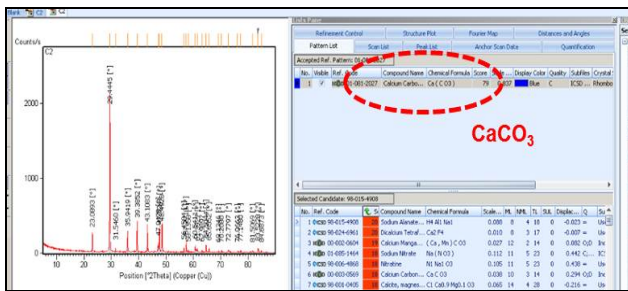


Figure 7. XRD analysis of SS (Suspended Solid) in Calcium ion Solution

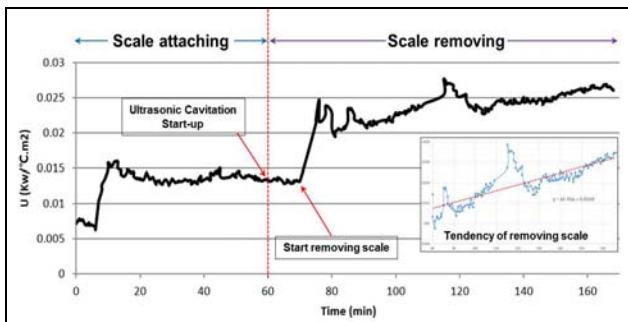


Figure 8. Overall heat transfer coefficient of case 1

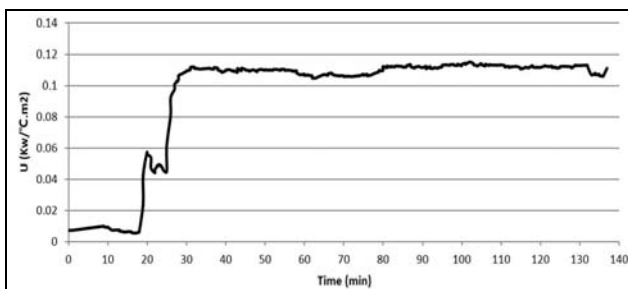


Figure 9. Overall heat transfer coefficient of case 2

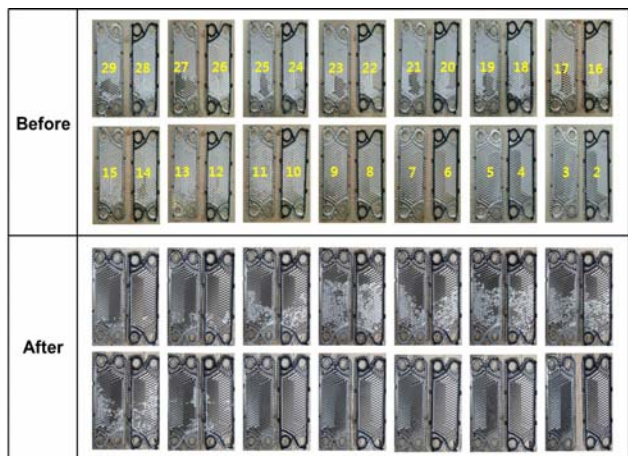


Figure 10. Comparison of heat transfer plate cleaning before and after.

3.3. Cavitation Cleaning Effect of Heat Transfer Plate

To confirm the cleaning effect of the heat transfer plate by ultrasound with the naked eye, figure 10 showed a heat transfer plate before and after cleaning. Top of the figure 10 are heat transfer plates before and after the cleaning, and the white colour of the scale can be seen attached to the heat transfer plate. The number of each picture is the number of the heating plate, the bottom of the picture is the heat transfer plate after cleaning. With the naked eye it can also be confirmed that the scale of the white that had been attached to the heat transfer plate removed so much after washing.

Compared with the results shown in figure 9, this is in good agreement with the tendency to keep the heat transfer coefficient near 0.1. In particular, the heat transfer plate of the 2 to 11 and 26 to 29 show a good cleaning effect. The reason that heat transfer plates of 2~11 were cleaned well is because the plates are located close with ultrasonic transducer. And the reason that heat transfer plates of 26~29 were cleaned well is because the plates are strongly influenced by ultrasonic waves through the fitting.

4. CONCLUSION

In this study, we carried out the experiments to remove scale causing substances using hydraulic cavitator and to remove the scale attached to the heat transfer plate of the plate heat exchanger using ultrasonic cavitation.

(1) In the experiment of removing scale causing substances (Ca^{2+}), hydrodynamic cavitator had been driven for about 2 hours. As a result, the concentration of the scale causing substance was reduced approximately 36%. if the cavitator is operated for the longer time, it is expected that the concentration of Ca^{2+} ions will can be reduced to the fresh water level. And if the cavitator applied solid-liquid separation device is used as influent pre-treatment device of the heat exchanger, it is expected that the effect as the scale preventive device will be further increased.

(2) In results of case 1, from 70 minutes the overall heat transfer coefficient was constantly increasing, and then after 23 hours it was restored up to nearly 100%. From this result, we were able to confirm that the ultrasonic cleaning device is very effective for descaling. In results of case 2, experiment was performed at the same time the attachment and the cleaning of the scale. After 30 minutes, it shows a tendency to continue maintain the value of 0.1 that is heat transfer coefficient of heat transfer plate that the scale is not attached. Therefore, when mounting the ultrasonic cleaning device in a heat exchanger, the heat transfer loss caused by the scale is expected to be significantly reduced. In addition, the ultrasonic cleaning device is expected as a very economical heat exchanger cleaning device.

ACKNOWLEDGEMENT

This work was supported by the R&D Program (No. S2137859) funded by the Small and Medium Business Administration (SMBA, Korea)

REFERENCE

- [1] Bell, K. J. and Mueller, a. C. Fouling in Heat Exchangers. *Wolver. Eng. Datab.*2001, II 46–57.
- [2] Sung, S. K., Suh, S. H. & Kim, D. W. "Characteristics of cooling water fouling in a heat exchange system", *J. Mech. Sci. Technol.*2008, Vol. 22, pp. 1568–1575.
- [3] Cho, Y. I., Fan, C. & Choi, B.-G. Theory of Electronic Anti-Fouling Technology To Control Precipitation Fouling in Heat Exchangers. *Int. Comm. Heat Mass Transfer*1997, Vol. 24, pp. 757–770.
- [4] Zhang, C. et al., "A comparative review of self-rotating and stationary twisted tape inserts in heat exchanger", *Renew. Sustain. Energy Rev.*2016, Vol. 53, pp. 433–449.
- [5] Cho, Y. I. & Choi, B. G. "Validation of an electronic anti-fouling technology in a single-tube heat exchanger". *Int. J. Heat Mass Transf.*1999, Vol. 42, pp. 1491–1499.
- [6] Tchobanoglous, G., Burton, F. L. & Stensel, H. D. *Treatment and Reuse. Wastewater Eng.* 4th edition (2003).
- [7] Chen, Y., Sun, S., Lai, Y. & Ma, C. "Influence of ultrasound to convectional heat transfer with fouling of cooling water". *Appl. Therm. Eng.*2016, Vol. 100, pp. 340–347.
- [8] Legay, M., Gondrexon, N., Le Person, S., Boldo, P. & Bontemps, A. "Enhancement of heat transfer by ultrasound: Review and recent advances", *Int. J. Chem. Eng.*2011.
- [9] Pečnik, B., Hočevár, M., Širok, B. & Bizjan, B. "Scale deposit removal by means of ultrasonic cavitation", *Wear*2016, Vol. 356-357, pp. 45–52.
- [10] Legay, M., Allibert, Y., Gondrexon, N., Boldo, P. & Le Person, S. "Experimental investigations of fouling reduction in an ultrasonically-assisted heat exchanger". *Exp. Therm. Fluid Sci*2013, Vol. 46, pp. 111–119.
- [11] Heath, D., Sirok, B., Hocevar, M. & Pecnik, B. "The use of the cavitation effect in the mitigation of CaCO₃ Deposits". *Stroj. Vestnik/Journal Mech. Eng.*2013, Vol. 59, pp. 203–215.
- [12] Prosperetti, A. Bubbles. *Phys. Fluids*2004, Vol. 16, pp. 1852–1865.
- [13] Verhaagen, B. & Fernández Rivas, D. "Measuring cavitation and its cleaning effect", *Ultrason. Sonochem.*2016, Vol. 29, pp. 619–628.
- [14] Denis Gebauer, Antje Völkel, Helmut Cölfen, "Stable Prenucleation Calcium Carbonate Clusters", *Science*2008, Vol. 322, pp. 1819.
- [15] Welty, Wicks, Wilson, Rorrer, *Fundamentals of Moementum, Heat, and Mass Transfer*, WILEY (2008), pp. 211.

*The 15th International Symposium on District Heating and Cooling
September 4-7, 2016, Seoul, Republic of Korea (South Korea).*

